Y 3. At 7:16/19/20

NUCLEAR SCIENCE ABSTRACTS

Volume 19 Number 20

Abstracts 38324–40302

October 31, 1965

MIAMI UNIVERSITY LIBRARY

UNITED STATES ATOMIC ENERGY COMMISSION
Division of Technical Information

USAEC DEPOSITORY LIBRARIES

Collections of USAEC reports are maintained in the libraries of the organizations listed below for reference use by the general public. Facilities for making photocopies are available. The USAEC also makes available through these libraries atomic energy reports of countries other than the U. S. that are abstracted in *Nuclear Science Abstracts*.

ALABAMA
Auburn, Auburn University
ARIZONA
Tucson, University of Arizona
ARKANSAS
Fayetteville, University of Arkansas
CALIFORNIA
Berkeley, University of California
Davis, University of California
Los Angeles, University of California
San Diego, Public Library
Stanford, Stanford University
COLORADO
Boulder, University of Colorado
Denver, Public Library
CONNECTICUT
New Haven, Yale University
DELAWARE
Newark, University of Delaware
DISTRICT OF COLUMBIA
Washington, Library of Congress
FLORIDA
Coral Gables, University of Miami
Gainesville, University of Florida
GEORGIA
Atlanta, Georgia Institute of Technology
HAWAII
Honolulu, University of Hawaii
ILLINOIS
Chicago, John Crerar Library
Chicago, University of Chicago
Evanston, Northwestern University
Urbana, University of Illinois
INDIANA
Bloomington, Indiana University
Lafayette, Purdue University
IOWA
Ames, Iowa State University
KANSAS
Manhattan, Kansas State University
KENTUCKY
Lexington, University of Kentucky
Louisville, University of Louisville
LOUISIANA
Baton Rouge, Louisiana State University
New Orleans, Tulane University
MARYLAND
Baltimore, Johns Hopkins University
College Park, University of Maryland
MASSACHUSETTS
Cambridge, Harvard University
Cambridge, Massachusetts Institute of Technology
MICHIGAN
Ann Arbor, University of Michigan
Detroit, Public Library
East Lansing, Michigan State University
MINNESOTA
Minneapolis, University of Minnesota
MISSISSIPPI
State College, Mississippi State University
MISSOURI
Kansas City, Linda Hall Library
Rolla, University of Missouri School of Mines and Metallurgy
St. Louis, Washington University
MONTANA
Bozeman, Montana State College
NEVADA
Las Vegas, Nevada Southern University
Reno, University of Nevada
NEW JERSEY
Princeton, Princeton University
Teaneck, Fairleigh Dickinson University
NEW MEXICO
Albuquerque, University of New Mexico
NEW YORK
Albany, The University of the State of New York
Buffalo, State University of New York at Buffalo
Ithaca, Cornell University
New York, Atomic Industrial Forum, Inc.
New York, Columbia University
New York, New York University
Rochester, University of Rochester
Schenectady, Union College
Syracuse, Syracuse University
Troy, Rensselaer Polytechnic Institute
NORTH CAROLINA
Charlotte, Public Library of Charlotte and Mecklenburg County
Durham, Duke University
Raleigh, North Carolina State College
NORTH DAKOTA
Grand Forks, University of North Dakota
OHIO
Cincinnati, University of Cincinnati
Cleveland, Public Library
OHIO (CONT.)
Columbus, Ohio State University
Toledo, University of Toledo
Youngstown, Youngstown University
OKLAHOMA
Norman, University of Oklahoma
Stillwater, Oklahoma State University
OREGON
Corvallis, Oregon State University
Portland, Reed College
PENNSYLVANIA
Philadelphia, University of Pennsylvania
Pittsburgh, Carnegie Library
University Park, Pennsylvania State University
PUERTO RICO
Rio Piedras, University of Puerto Rico
RHODE ISLAND
Providence, Brown University
SOUTH CAROLINA
Columbia, University of South Carolina
TENNESSEE
Knoxville, University of Tennessee
Memphis, Public Library
Nashville, Joint University Libraries
Oak Ridge, Oak Ridge Institute of Nuclear Studies
TEXAS
Austin, University of Texas
College Station, Texas A & M University
Dallas, Southern Methodist University
Houston, Rice University
Lubbock, Texas Technological College
San Antonio, Public Library
UTAH
Salt Lake City, University of Utah
VIRGINIA
Blacksburg, Virginia Polytechnic Institute
Charlottesville, University of Virginia
Norfolk, Old Dominion College
WASHINGTON
Pullman, Washington State University
Seattle, University of Washington
WEST VIRGINIA
Morgantown, West Virginia University
WISCONSIN
Madison, University of Wisconsin
Milwaukee, Public Library
WYOMING
Laramie, University of Wyoming

Volume 19, Number 20, October 31, 1965

NUCLEAR SCIENCE ABSTRACTS

A semimonthly publication of the USAEC Division of Technical Information, Edward J. Brunenkant, Director.
Published by the USAEC Division of Technical Information Extension, Robert L. Shannon, Extension Manager.

Nuclear Science Abstracts covers the international literature on nuclear science and technology and provides the only comprehensive abstracting and indexing of this body of information. Published twice each month since 1947, *NSA* covers technical reports of the U. S. Atomic Energy Commission and its contractors, technical reports of U. S. Government agencies and other governments, universities, industrial and research organizations, as well as patents, books, and journal literature on a world-wide basis. Nearly 300,000 abstracts have appeared in *NSA* through Volume 18. The subject matter covered in *NSA* is described in issue Number 1 and in TID-4552, *Subject Scope of Nuclear Science Abstracts*, available free from the U. S. Atomic Energy Commission, Division of Technical Information Extension, P. O. Box 62, Oak Ridge, Tennessee 37831.

Abstracts are arranged according to a number of subject categories and subcategories. Definitions of categories appear in issues Number 1 and 13. If the language of the original item is not English, the language will be indicated. Translations are not abstracted where an abstract of the original item has appeared in *NSA*.

INDEXES TO NSA

Corporate author, personal author, subject, and report number indexes appear in each issue and are cumulated quarterly, semiannually, and annually. At the end of Volume 19, report number indexes will be cumulated in two separate publications. Indexes for Vols. 1–15 will be reissued with the latest public availability known at that time. This index will not be reissued. Indexes for Vols. 16–19 will be cumulated as a separate issuance and will be reissued annually to include all volumes beginning with Volume 16.

AVAILABILITY OF PUBLICATIONS ABSTRACTED

The public availability of all U. S. Atomic Energy Commission reports is indicated in the report number indexes. The availability of other reports, when known, is also indicated. The availability of some unnumbered reports is given in the abstract.

Dissertations abstracted in *Dissertation Abstracts* and included in *NSA* are available from University Microfilms, Inc., 315 N. First Street, Ann Arbor, Michigan.

Most of the published literature abstracted in *NSA* is on deposit at the Oak Ridge Institute of Nuclear Studies Library, Oak Ridge, Tennessee, (a USAEC depository library) and is available through interlibrary loan. When requesting papers from this source, it is important that *NSA* volume and abstract number be cited.

HOW TO OBTAIN NUCLEAR SCIENCE ABSTRACTS

NSA is available on an exchange basis to universities, research institutions, industrial firms, and publishers of scientific information. Inquiries should be directed to the U. S. Atomic Energy Commission, Division of Technical Information Extension, P. O. Box 62, Oak Ridge, Tennessee 37831.

Government agencies may obtain *NSA* free of charge.

NSA is available to the general public on a subscription basis from the Superintendent of Documents, U. S. Government Printing Office, Washington, D. C. 20402, as follows:

For the 24 regular issues, $30.00 domestic, $37.00 foreign. A single issue costs $1.75, plus 25 per cent for foreign mailing. Domestic rates apply to the United States, Canada, Mexico, and Central and South American countries except Argentina, Brazil, British and French Guiana, Surinam, and British Honduras. Foreign rates apply to the countries excepted above and to all other countries throughout the world.

For the quarterly, semiannual, and annual indexes, $22.00 domestic, $25.00 foreign.

Multivolume subject and author indexes are available as follows:

Vols. 1–4 (1948–1950) Johnson Reprint Corporation, 111 Fifth Avenue, New York, N. Y. 10003, $30.00.

Vols. 5–10 (1951–1956) Superintendent of Documents, U. S. Government Printing Office, Washington, D. C. 20402, $5.25.

Vols. 11–15, Subjects, Superintendent of Documents, U. S. Government Printing Office, Washington, D. C. 20402, $19.00.

Vols. 11–15, Personal Authors, Superintendent of Documents, U. S. Government Printing Office, Washington, D. C. 20402, $14.25.

Vols. 11–15, Corporate Authors, Superintendent of Documents, U. S. Government Printing Office, Washington, D. C. 20402, $2.50.

Cumulative Report Number Index, Vols. 1–18, is available from the Superintendent of Documents, U. S. Government Printing Office, Washington, D. C. 20402, $5.75.

Annual Indexes are available separately from the U. S. Government Printing Office as follows:

Vol. 16, Subject and Authors, $9.75.
Vol. 17, Subject and Authors, $12.25.
Vol. 18, Subject and Authors, $12.50.

ACKNOWLEDGMENTS

Agreements between the United States Atomic Energy Commission and the following organizations with regard to providing continuing services and specific literature coverage for *Nuclear Science Abstracts* are gratefully acknowledged:

American Institute of Physics; Atomic Energy of Canada Limited; Atomic Energy Research Establishment, United Kingdom; European Atomic Energy Community (EURATOM); Gmelin Institute; International Atomic Energy Agency; Japan Atomic Energy Bureau — Japan Atomic Energy Research Institute; Netherlands Patent Office; Reactor Centrum Nederland.

TABLE OF CONTENTS

Volume 19, Number 20, October 31, 1965

Category	Page
BIOLOGY AND MEDICINE	4785
General	4785
Ecology	4786
Metabolism, Tissue Distribution, and Toxicology	4786
Radiation Effects	4790
Radiation Effects Therapy and Countermeasures	4803
Radiation Hazards and Protection	4806
Radiotherapy and Radiodiagnosis	4807
CHEMISTRY	4817
General	4817
Analytical Procedures	4817
Inorganic and Physical Chemistry	4821
Organic Chemistry	4835
Radiation Chemistry	4837
Radiochemistry	4844
Separation Processes and Procedures	4844
ENGINEERING	4849
General	4849
Applications of Nuclear Explosions	4850
Facilities and Equipment	4851
Heat Transfer and Fluid Flow	4852
Materials Testing	4854
Protective Structures	4855
Space Propulsion	4856
Vacuum Engineering	4856
GEOLOGY AND MINERALOGY	4857
General	4857
Natural Radioactivity and Fallout	4857
Techniques and Equipment	4860
HEALTH AND SAFETY	4862
INSTRUMENTATION	4867
General	4867
Radiation Detection	4873
Radiation Effects	4881
ISOTOPE TECHNOLOGY	4883
General	4883
Industrial Applications	4883
Power Application	4884
Separation and Production	4884
MATHEMATICS AND COMPUTERS	4886
METALS, CERAMICS, AND OTHER MATERIALS	4888
General	4888
Corrosion	4891
Fabrication	4892
Properties and Structure	4896
Radiation Effects	4906
METEOROLOGY	4911
PHYSICS	4912
General	4912
Accelerators	4917
Astrophysics and Cosmology	4919
Atomic Physics	4923
Cosmic Radiation	4929
Direct Energy Conversion	4930
Elementary Particles and Radiations	4932
Field Theory and Quantum Mechanics	4948
Geophysics	4953
Low Temperature Physics	4955
Neutron Physics	4963
Nuclear Properties and Reactions	4965
Plasma Physics and Thermonuclear Processes	4982
Shielding	4994
Solid State Physics	4996
REACTOR TECHNOLOGY	5001
General	5001
Auxiliaries and Components	5001
Criticality Studies	5004
Design and Feasibility	5006
Fuels	5007
Power and Power-Breeder Reactors	5008
Production Reactors	5012
Propulsion and Space	5012
Research and Test Reactors	5016
WASTE DISPOSAL AND PROCESSING	5018
GENERAL AND MISCELLANEOUS	5020
CORPORATE AUTHOR INDEX	INDEX-1
PERSONAL AUTHOR INDEX	INDEX-11
SUBJECT INDEX	INDEX-53
REPORT NUMBER INDEX	INDEX-133

STAFF OF NUCLEAR SCIENCE ABSTRACTS

MANAGING EDITOR

John W. Norris

ASSISTANT MANAGING EDITOR

Donald D. Davis

ASSOCIATE EDITORS

Lawrence T. Whitehead
David E. Bost
Robert C. Kelly
Lee M. Thompson

SUBJECT INDEX EDITOR

Everett J. Hoffman

EVALUATORS

William D. Matheny
John H. Mitchell
Mary H. Newman

ABSTRACTORS

F. S. Armstrong (AECL)
Jane G. Buchanan
D. Lamar Cason
Helen G. Donald
James R. Dulaney
Wells L. Green
Bernard O. Griggs
Mary Catherine Grissom
Fernando J. Hamilton
Phyllis C. Hansen
Thomas F. Heagerty
Carolyn D. Houston
Rose V. Jermain
Betty L. McDowell
Jean F. Peckham
Mona H. Raridon
Julia Redford
Lila B. Smith
Charles E. Stuber
Martha J. Thomas
Anne G. Ward
David C. West
Milton O. Whitson

SUBJECT HEADING SPECIALIST

Robert E. Upchurch

CORPORATE AUTHOR SPECIALIST

Clara L. Fox

DESCRIPTIVE CATALOGING SPECIALIST

J. Paul Meredith

SCHEDULING AND PUBLISHING COORDINATOR

Brainard L. Patton

Communication concerning the editorial policy and content of *NSA* should be addressed to the Managing Editor, *Nuclear Science Abstracts*, AEC Division of Technical Information Extension, P. O. Box 62, Oak Ridge, Tennessee 37831.

Use of funds for printing this publication approved by the Director of the Bureau of the Budget, May 20, 1963

Volume 19, Number 20 October 31, 1965

NUCLEAR SCIENCE ABSTRACTS

BIOLOGY AND MEDICINE

General

Refer also to abstracts 38722, 39265, and 39270.

38324 (JPRS-30993) STUDIES IN HYGIENE AND SANITATION. Translated from Gigiena i Sanit., No. 4, 3-6; 12-16; 28-32; 44-51; 114-16(Apr. 1965). 45p. (TT-65-31491). CFSTI, $2.00 cy.

Six articles were presented on hygiene and sanitation. A separate abstract was prepared for one. (H.G.D.)

For an abstract of the individual paper see: 38362.

38325 DENTAL LESIONS IN RAT INDUCED BY RADIOMIMETIC AGENTS. Hebborn, P.; Mishra, L. C.; Dalton, C.; Williams, J. P. G. (State Univ. of New York, Buffalo). Arch. Pathol., 80: 110-15(Aug. 1965).

Seven aromatic nitrogen mustards produced lesions of incisor teeth of adult male rats which were similar to those reported to occur after x irradiation. Tooth loss occurred 40 to 70 days after treatment and in 34% of these cases, atypical regrowth or no regeneration of incisor teeth was observed. Microscopic examination showed degeneration of odontoblasts and dentin niche formation. Body weight loss often preceded overt symptoms of incisor tooth damage and it is suggested that weight loss or death during the second or third month after treatment with radiomimetic agents may be the result of starvation due to inadequate dentition. No abnormalities were observed after treatment with triethylene melamine (TEM) or busulfan (Myleran). (auth)

38326 EPIDEMIOLOGY OF CHILDHOOD LEUKAEMIA IN NORTHUMBERLAND AND DURHAM. Knox, George (Univ. of Newcastle-upon-Tyne, Eng.). Brit. J. Prevent, Socil Med., 18: 17-24(Jan. 1964).

Progress in the understanding of the etiology of leukemia is reviewed. The survey includes 185 cases of leukemia in children under 15, in Northumberland, Durham, and on Tees-side, in the 10 years 1951 to 1960. Their distribution in space and time showed evidence of a seasonal variation with a summer peak, and a high risk in children living in the larger towns. These two factors appeared to affect different groups of cases and to be independent of each other, the seasonal variation affecting especially the lymphoblastic leukemias in younger children, the large town concentration being evident only in the myeloblastic leukemias and in the lymphoblastic leukemias of children over 6 yr old. There was, in addition, evidence of a clustering factor, a space-time interaction, affecting the lymphoblastic leukemias of young children, such that pairs of cases occurring within 60 days and within 1 km of each other were unduly frequent. The data suggest that the seasonal variation and the clustering effect may be common properties of a single factor. There were 11 children with lymphoblastic leukemia who had a history of irradiation either in utero or later. Omission both of these and of the group with abnormal karyotypes from the lymphoblastic leukemias under 6 years of age leaves a group of 68 children with 48 summer and 20 winter onsets, a ratio of 2.4:1. The children with abnormal karyotypes and those with a recorded exposure to irradiation belonged mainly to the second half of the period surveyed, but this was probably due to improved recognition of these associations. An analyses of proximity of the subjects showed that all but one of the ten children in the five close pairs had lymphoblastic leukemia, all were under 4 years old, all had summer onset, and none had been irradiated, thus affording scope for further maximization of the discrepancy. A high incidence of leukemia was seen in mongols. There was a variation between the occupation groups of younger and older affected children which was probably secondary to the urban-rural distributions. Apart from the association with mongolism there was no evidence of maternal age or birth rank variations of risk. The findings suggest further heterogeneity in the epidemiology and possibly the etiology of childhood leukemias, and particularly in the case of younger children suggest exposure to a seasonally variable factor which tends to be localized both in space and in time. (BBB)

38327 RADIOBOTANY AND ITS APPLICATION. Campo, Cesar Gomez. Ciencias (Madrid), 29: 232-6 (1964). (In Spanish)

The primary physical effect of radiations consists in a change of the energy level of the atomic electrons. The resulting ionized or excited molecules may form free radicals after a certain number of events; recombination of these radicals results in the creation of new molecules (chemical effect). Within the living cells, changes in the protoplasmic systems, such as DNA and RNA, could amplify the primary effects. In the case of plants, the detectable effects may be genetic, or hereditary, and physiological or nonhereditary. The radioinduced mutations differ from the spontaneous ones; their frequency increases linearly with the dose. At high doses the unfavorable effects, such as lethal character, sterility, and inhibition of the vegetative development, are enhanced. The differences in the radiosensitivities of various species are of great practical and theoretical interest. The effects of ionizing radiations may be applied for the improvement of the plants, for example, for preventing premature germination of stored potatoes. The higher radiosensitivity of diploid cells with respect to the tetraploid ones may be used to enhance the selection of the latter cells, after treatment with colchicine. Radioinduced mutations are especially useful for improving species with a relatively limited natural variability, in which the classical hybridization methods are not sufficient. Good practical results were obtained with the treatment of wheat, clover, barley, sunflower, peach and apple trees, mustard, and tobacco plants. At the Spanish National Institute for Agricultural Studies a ^{137}Cs source is used to irradiate growing plants in the field. (TTT)

38328 COLD SPRING HARBOR SYMPOSIA ON QUANTITATIVE BIOLOGY. VOLUME XXIX. HUMAN GENETICS.

Cold Spring Harbor, N. Y., Cold Spring Harbor Lab. of Quantitative Biology, 1964. 492p. $15.00. (CONF-640622)

Forty-five papers were presented at this symposium. Topics dealt with the genetics of human populations, of human cells in culture, and of human proteins. (C.H.)

Ecology

38329 (TID-20471) EFFECT OF CHELATES ON THE MOVEMENT OF FISSION PRODUCTS THROUGH SOIL COLUMNS. Essington, E. H.; Nishita, H. (California Univ., Los Angeles. Lab. of Nuclear Medicine and Radiation Biology). [Feb. 20, 1964]. Contract AT(04-1)-Gen-12. 39p. Dep. mn; CFSTI, $2.00 cy, $0.50 mn.

Leaching tests were conducted on columns of calcareous soil, using distilled water, mock irrigation water, and chelating agents (DTPA, CDTA, and EDDHA). The movement of the following radionuclides was studied: ^{65}Zn, ^{85}Sr or ^{90}Sr, ^{91}Y, ^{106}Ru, ^{137}Cs, ^{144}Ce, and ^{147}Pm. The results show that the radionuclides vary in their ability to be leached with chelating agents. (D.L.C.)

38330 (TID–22078) A COMPARATIVE POPULATION STUDY OF SMALL VERTEBRATES IN THE URANIUM AREAS OF THE UPPER COLORADO RIVER BASIN OF UTAH. Tanner, Wilmer W. (Brigham Young Univ., Provo, Utah). May 1965. Contract AT(11-1)-819. 40p. Dep. (mn); $2.00 (cy), 1 (mn) CFSTI.

Published as Brigham Young Univ. Sci. Bull., Biol. Ser., 7: No. 1, May 1965.

Population studies were made on small vertebrates in the uranium areas of the Upper Colorado River Basin of Utah. Four objectives were undertaken: to determine the kinds of populations of vertebrates occurring in these natural radiation areas as compared with nearby nonirradiated areas; to determine the approximate home range, seasonal distribution and migration of individuals in these areas; to establish the amount of radiation in the various areas under consideration; and to determine the degree of external morphological variation existing in populations inhabiting areas of natural radiation and to compare these with each other and with populations occurring in nearby areas having a lower surface radiation. Although the graphed data and the statistical analysis of this data show some significant variations, the great majority of the characteristics tested did not show, at the 95% level, significant variations between the populations in the areas of high and low exposure. It was found, though, that the lizard populations in the different areas varied in some characteristics. These variations were significant. Differences in the high- and low-exposure areas did not vary more than in areas with similar exposure; therefore there was insufficient evidence to establish that the variations were caused by or resulted from exposure to radiation. (P.C.H.)

38331 GROWTH RESPONSE OF TWO SEDGES INHABITING A RADIOACTIVE WASTE DISPOSAL AREA. Plummer, G. L. (Univ. of Georgia, Athens); Crossley, D. A. Jr.; Gardiner, D. A. Ecology, 46: 346-8(1965).

On White Oak Lake bed, an area contaminated with radioactive wastes, sedges (Carex frankii and C. vulpinoidea) were found to have longer inflorescences than sedges growing on nearby uncontaminated sites. This lake bed is a unique ecological system of about 48 acres, which once served as a final holding basin in the Oak Ridge National Laboratory's low-level radioactive waste disposal system. In 1955 the lake was drained, and during the spring season that followed plants and animals invaded the radioactive sediments. Soils contained ^{90}Sr, ^{137}Cs, ^{60}Co, ^{106}Ru, and other radioisotopes. The observed increase in the size of the inflorescences of the two sedges inhabiting this radioactive area is correlated with the complex interaction between various edaphic factors that contribute to plant growth and an effect of ionizing radiation. These perennial sedges tolerate a continuous dose rate generally in excess of 2 R/day at ground level. The air dose rate of γ radiation measured at 1 m above ground surface provided the best correlation with inflorescence length for the two sedge species. Although various soil factors were found to affect inflorescence length, those influences did not explain the increase in length in the radioactive areas. The variables doubtless include many more factors than radiation, however, and it is likely that other soil characteristics (nitrates and sulfates in particular) associated with inorganic constituents of industrial wastes, influence the lengths of inflorescences. The absorbed radiation dose (in rad) delivered to the plants is probably greater than the air dose measurements (in mR) would estimate. Even at minimal estimates, the dose rates on this lake bed are sufficient to induce both genetic and physiological disturbances in plants. No morphological distortions were seen in the plants; except perhaps for being larger and greener they seemed identical with controls. (BBB)

38332 THE CONTAMINATION OF GRASSLAND WITH RADIOACTIVE STRONTIUM. I. INITIAL RETENTION AND LOSS. Milbourn, G. M.; Taylor, R. (Agricultural Research Council, Wantage, Berks, Eng.). Radiation Botany, 5: 337-47(Sept. 1965).

Field experiments using ^{89}Sr applied as a spray were carried out under widely varying conditions in the U.K. to investigate the initial retention of airborne radioactive strontium on the edible herbage of permanent pastures and its subsequent loss. On average about one quarter of the deposit was initially retained on herbage edible by cattle and a similar fraction was held in the basal tissues. After contamination the levels of radioactivity in edible herbage decreased not only because of the physical decay of ^{89}Sr but also because of its removal by rain and other processes. The field loss was approximately exponential over periods of up to 9 weeks; it caused the activity in edible herbage per unit area of pasture to decrease by a factor of about two each 14 days. On account of the growth of new tissues the activity per unit weight of herbage decreased more rapidly; the half period for field loss on this basis was about 9 days. Factors that cause variation in the extent of retention and loss are discussed and the present results are compared with other findings. The effect of defoliating recently contaminated pastures was also examined; the content of ^{89}Sr on herbage which regenerated later in the season were affected to only a very small extent. (auth)

Metabolism, Tissue Distribution, and Toxicology

38333 (BNWL-SA-226) NON-EQUILIBRIUM TISSUE DISTRIBUTIONS OF URANIUM AND THORIUM FOLLOWING INHALATION OF URANIUM ORE BY RATS. Stuart, B. O.; Beasley, T. M. (Battelle-Northwest, Richland, Wash. Pacific Northwest Lab.). June 18, 1965. Contract AT (45-1)-1830. 6p. (CONF-650906-3). Dep. mn; CFSTI, $1.00 cy, $0.50 mn.

From 2nd International Symposium on Inhaled Particles and Vapours, Cambridge, Eng.

If each individual radioactive daughter comprising the uranium decay chain is considered individually, those daughter products such as ^{230}Th having unusually high pulmonary retention may contribute to a lower calculated permissible limit for uranium ore than that based solely on the levels of insoluble natural uranium. To determine whether such a lower limit is valid from a hazard viewpoint it is necessary to know whether a given daughter, ^{230}Th, does indeed have a high retention when inhaled with the parent radionuclide as a constituent of uranium ore dust. Both single and repeated exposures of rats to high grade (22% U_3O_8) pitchblende ore resulted in increasing thorium-to-uranium ratios in the lungs with increasing times post-exposure. Highly sensitive analytical procedures, allowing precise measurements on 10 μg of ore, showed significant departures from initial equilibrium levels as little as one week after three 2-hour exposures, rising to a ratio of nearly three after eight weeks. During repeated exposures occurring over two months a gradual rise in mean thorium-to-uranium ratios to 2.5 was ob-

served, in spite of the repeated deposition of fresh ore (in secular equilibrium). This ratio was found to be about nine in animals sacrificed four months after the last exposure. These data suggest a preferential retention of thorium in the lungs. Analyses of bronchial and mediastinal lymph nodes have also shown selective accumulation of thorium, while uranium initial concentrations in the kidneys were higher than those of thorium. Femurs and livers also accumulated higher thorium radioactivities. (auth)

38334 (COO-1170-1) EFFECTS OF SUBCUTANEOUS IMPLANTATION OF RARE-EARTH METALS. Talbot, Richard B.; Davison, Fred C.; Green, John W.; Reece, William O.; Van Gelder, Gary (Iowa State Univ. of Science and Technology, Ames. Inst. for Atomic Research and Iowa State Univ. of Science and Tech., Ames. Coll. of Veterinary Medicine). May 1965. Contract AT(11-1)-1170. 20p. Dep. mm; CFSTI, $1.00 cy, $0.50 mn.

Subcutaneous implantation of yttrium, cerium, praseodymium, gadolinium, dysprosium, and ytterbium pellets in C57BL mice produced a granulomatous tissue reaction in a majority of the mice examined and malignant neoplasms in three mice. The coagulation time of dysprosium, gadolinium, praseodymium, and ytterbium implanted mice was significantly longer than in control mice 6 months after implantation. Twelve months after implantation only the dysprosium and ytterbium implanted mice had elevated clotting times and at 18 months post-implantation only the dysprosium implanted mice had values longer than control values. A depression of leukocyte numbers occurred in all implanted mice at 6 months post-implantation but returned to control values at 18 months. There were no significant differences in differential leukocyte counts of treated versus control mice. There were no significant treatment differences in life spans of mice. Forty-two neoplasms were diagnosed. Three of these were positively diagnosed as injection site neoplasms produced by three different rare-earth metals. (auth)

38335 (NP-14926) BERICHT BEZUEGLICH DER ZUFUHR VON KALZIUM ALS VORBEUGUNGSMITTEL GEGEN DIE AUFNAHME VON STRONTIUM-90. (Report With Reference to the Administration of Calcium as Prophylactic Against the Uptake of Strontium-90). Seelentag, W. (Bundesgesundheitsamt, Berlin (West Germany). Institut fuer Wasser-, Boden- und Lufthygiene). May 27, 1963. 24p. Dep. mn.

A literature review is presented of the prophylactic effects of Ca against the uptake of ^{90}Sr. The topics discussed are the effectiveness of prophylactic Ca administration with respect to Sr incorporation, effects of the prophylactic administration of inactive Sr, phosphates, and other medications, evaluation of prophylactic precautions, therapeutic administration of Ca, Sr, phosphates, and other medications on the reduction of incorporated radiostrontium, pattern of Ca metabolism and results of Ca balance, and secondary effects of Ca or Sr administration. (J.S.R.)

38336 (TID-21106) INCORPORATION OF THYMIDINE INTO DNA OF ORGANS OF MICE. Hinrichs, H. Richard; Petersen, Robert O.; Baserga, Renato (Northwestern Univ., Chicago, Ill. Dept. of Pathology). [1964]. Contract AT(11-1)-1131. 30p. Dep. (mn); $2.00(cy), 1(mn) CFSTI.

Intraperitoneal injection of tritiated thymidine in doses ranging from 10 to 100 μc per adult mouse resulted in 8 to 9 per cent of the injected dose being incorporated into DNA, as measured by a modified Schmids-Thannhauser extraction procedure on homogenates of whole mouse. The remainder of the tritiated thymidine was catabolized primarily to tritiated water. The age of the animal influenced the percentage of thymidine incorporated into DNA of various organs. In adult mice injected intraperitoneally the gastrointestinal tract contained approximately 55 per cent of the total radioactivity incorporated into DNA. The carcass, including bone marrow, skin, lymph nodes, and epiphyseal cartilages, contained about 40 per cent, and all the other viscera together the remainder. The uptake of thymidine by the whole mouse was highest at midnight and lowest at noon. (40 references.) (auth)

38337 THE DEVELOPMENT OF RADIOACTIVITY IN THE THYROID AND PLASMA OF WHITE RATS MARKED WITH ^{131}I AND TREATED WITH VITAMIN B_{12}. Costiner, Emma; Niculescu-Zinca, D.; Vaisler, L. Acad. Rep. Populare Romine Studii Cercetari Endocrinol., 14: 31-4 (1963). (In Rumanian).

White rats were injected with two μC of ^{131}I. One group had received 100 μg of vitamin B_{12} each day for ten days. Each group was divided into lots of ten and sacrificed at 30-min intervals for the first four hr, and at 60-min intervals for the first four hr, and at 60-min intervals during the next 20 hr. Control rats were sacrificed at the same time. A semi-logarithmic graph was made of the fixation of ^{131}I. The curve of the intrathyroid fixation of radioiodine showed an increase in quantity during the first 12 hr in the B_{12} group, from eight to 16%. The non-B_{12} group reached 16% fixation also, but the increase was less consistent. From the 12th to the 20th hr, the curves of the B_{12} and non-B_{12} groups were almost identical. In the plasma, there was generally only a slight difference between the groups. In both, the ^{131}I level declined from one to less than 0.2% up to the ninth hr. Between the tenth and 16th hrs, the B_{12} group showed more ^{131}I than the non-B_{12} group, reaching 0.3% and 0.1% at 14 hr. From the first to the ninth hr, the ratio of red blood cells to plasma was almost equal. From the tenth to the 15th hr, it decreased in the B_{12} rats. This was interpreted as showing the presence of an increased proportion of protein-bound I in the plasma. (BBB)

38338 LABELING OF HUMAN TUMORS WITH TRITIATED THYMIDINE. Titus, Jack L.; Shorter, Roy G. (Mayo Clinic and Mayo Foundation, Rochester, Minn.). Arch. Pathol., 79: 324-8(Mar. 1965).

The uptake of tritiated thymidine by the nuclei of neoplastic tissue during in vitro incubation was studied in fresh samples of 15 human neoplasms. In the neoplastic tissue, the percentage of labeled nuclei was higher than the percentage of nuclei in mitosis. The percentage of nuclei that were labeled was greater in neoplastic tissue than in normal tissue in six instances in which comparison could be made. In four tumors, the labeled nuclei occurred in focal areas. Because labeled nuclei in radioautographs are easier to recognize than are mitotic figures, this technique may offer an additional method for the study of one aspect of the kinetics of proliferation of human tumors. (auth)

38339 THE INCORPORATION OF ^{14}C-LABELED PRECURSORS INTO THE DNA, RNA, AND PROTEINS OF L-CELL NUCLEI IN THE PRESENCE OF TRITIATED THYMIDINE. Krause, Margarida O. (Univ. of Toronto). Can. J. Biochem., 43: 1329-36(Aug. 1965).

The effects of tritiated thymidine on the incorporation of ^{14}C-labeled thymidine, uridine, phenylalanine, and lysine into nuclei of exponentially growing L-cells were studied. The incorporation of each of the ^{14}C-labeled precursors was compared in the presence and absence of ^{3}H-thymidine. Results revealed a stimulation in the incorporation of ^{14}C-thymidine, ^{14}C-uridine, and ^{14}C-phenylalanine and a depression in the incorporation of ^{14}C-lysine in the presence of tritiated thymidine. (auth)

38340 EXTRACTION RATIO AND BONE CLEARANCE OF ^{85}Sr AS A MEASURE OF EFFECTIVE BONE BLOOD FLOW. Copp, Douglas Harold; Shim, Sun Shik (Univ. of British Columbia, Vancouver, Can.). Circulation Res., 16: 461-7(May 1965).

The validity of ^{85}Sr clearance as a measure of bone blood flow depends on the consistency and completeness of removal of the isotope by bone during a single passage. This can be evaluated from the ^{85}Sr extraction ratio. A method is described for estimating this ratio using ^{85}Sr and a nondiffusible dye, Evans blue (T-1824). Both were injected simultaneously into the nutrient artery of the tibia. Blood was collected from the femoral vein during the next

5 min and the percentage of the injected dose of each substance in this blood was determined. The extraction ratio for ^{85}Sr was calculated from these data. It appeared to be sufficiently high and consistent to justify the use of initial bone clearance of ^{85}Sr as a measure of effective bone blood flow. On this basis, rates of blood flow were then determined for a number of typical bones in dogs and rabbits. The extraction ratio for ^{85}Sr removal by canine bone (0.764 ± 0.021) compared favorably with values reported for removal of bromsulfonphthalein (BSP) by liver (0.34 ± 0.12), but was not as satisfactory as those obtained for extraction of Diodrast (0.79 to 0.96) and P-aminohippurate (0.81 to 0.96) by kidney. The data for bone are remarkably consistent, and in view of this the initial (0 to 5 min) ^{85}Sr clearance should give a valid and useful measure of the effective blood flow through those regions in bone where active mineral exchange is taking place. This would be the minimal value. Total blood flow through the bone could be estimated by dividing this by the extraction ratio. (TCO)

38341 NUMERICAL DATA FOR ^{131}I UPTAKE MEASUREMENTS IN RABBITS. Oddie, T. H.; Fisher, D. A.; Epperson, D.; Criner, G.; Pirnique, F. (Univ. of Arkansas, Little Rock). Endocrinology, 77: 285-9(Aug. 1965).

Measurements of the apparent volume of distribution of ^{131}I were conducted in New Zealand white rabbits at times up to 24 hr after intravenous injection of the radioiodine dose. The average fecal content of ^{131}I at 24 hr was 17% of the 24-hr urinary content. These data with appropriate calibrations for external measurement of thyroidal radioiodine content were used to develop routine procedures for measuring thyroidal radioiodine clearance rates in rabbits. The procedures offer the advantage of minimal trauma to the animals. (auth)

38342 RENAL EXCRETION OF COLLOIDAL Au^{198}. AN EXPERIMENTAL MORPHOLOGICAL STUDY. Cruciani, V.; Gioffre, L. (Univ. of Rome). Gazz. Interu. Med. Chir., 69: 2384-92(1964).

Colloidal ^{198}Au excretion was studied in a group of 46 rats after i.p. injection. Most of the isotope was excreted via the kidneys, which showed parenchymal lesions resulting from ionizing radiation by the isotope. (Excerpta Med., Vol. 2, (July 1965))

38343 LIFE SPAN OF OVINE ERYTHROCYTES AS ESTIMATED FROM SELENIUM-75 KINETICS. Wright, P. L. (Monsanto Co., St. Louis). J. Animal Sci., 24: 546-50(May 1965).

A method is described for estimating erythrocyte life span which uses ^{75}Se labeling of the cells. A single dose containing 0.5 mC of ^{75}Se as H_2SeO_3 and 0.27 mg of selenium was administered intravenously into the jugular vein of three 12-month-old crossbred castrate rams. Three similar wethers were given orally an identical dose of ^{75}Se absorbed on cellulose in a gelatin capsule. Five ml of blood was collected at hourly intervals during the first 12 hr, at 6-hr intervals for the next 48 hr, and at weekly intervals thereafter. Aliquots of whole blood, plasma, and erythrocytes twice washed with 154mM NaCl solution were assayed for ^{75}Se in a well-type scintillation counter. The peak whole-blood and plasma concentrations of ^{75}Se were observed about 48 hr after a single oral dose; then it decreased rapidly until the third week and decreased slowly thereafter. The decrease in whole blood activity followed that of plasma until the period between 14 and 21 days, when an increase was observed. The increase in whole blood activity was due to the sharp rise in erythrocyte ^{75}Se concentration. At 170 days the radioselenium content of whole blood decreased sharply due to the decline in erythrocyte ^{75}Se. After intravenous administration there was a rapid decline in plasma ^{75}Se; 12% of the dose remained in the circulating plasma at 24 hr. Thereafter ^{75}Se blood distribution curves from intravenously treated sheep paralleled those from sheep dosed per os. The circulating erythrocytes rapidly accumulated a limited amount (0.5%) of the intravenous radioselenium dose. The accumulation of ^{75}Se by the intact erythrocytes reached a peak within 3 hr and did not rise above this level during the first 12 hr. Autoradiograms of femur demonstrated the concentration of ^{75}Se in hematopoietically active areas of the bone marrow. The route of radioselenium administration did not influence the rate of Se incorporation into newly formed erythrocytes. Radioselenium was incorporated into the globin moiety of hemoglobin, and remained in the erythrocyte for the entire life span of the cell. Estimates of the erythrocyte life span calculated from ^{75}Se turnover averaged 157 days in sheep one to two yr of age. Since ^{75}Se is a γ emitter, it can be measured directly without previous sample preparation. (BBB)

38344 TRANSFER OF RADIOACTIVE WATER, UREA AND GLYCINE BETWEEN MATERNAL AND FOETAL BODY FLUIDS IN RABBITS AND PIGS. Stanier, Margaret W. (Cambridge Univ., Eng.). J. Physiol. (London), 178: 127-40(May 1965).

The rates of transfer of water and certain solutes from fetal tissue and allantoic fluid were measured by radioactive labeling methods with THO and urea and glycine labeled with ^{14}C. The pig, whose placenta is formed from chorioallantois, and the rabbit, which has a hemoendothelial placenta, were chosen as representing anatomically one of the least and one of the most permeable types of placenta. In an assessment of validity of the radioisotope methods, radioactive solutions were injected intraperitoneally into 25 to 35 g rabbit fetuses, which with the placenta were removed from the uterus within 15 sec of the injection; a 65-day pig fetus which was examined 35 min after the injection; and a 30-g mouse, killed 5 min after the injection. The results showed that when radioactive material is injected into the peritoneum of small mammals 81 to 100% of it can be recovered, so the technique does not necessitate large losses. This makes it possible to estimate rates of movement of the radioactive material by the fall of total radioactivity in the compartment into which it is injected. All three radioactive substances quickly appeared on the maternal side of the placenta after injection into the fetal peritoneum in both species. When injected into the pig's allantoic sac, HTO was detected in maternal blood and in fetal tissue. Radioactive urea and glycine showed little or no movement from the allantoic sac. The calculated rates of movement, assuming that the label remained with the compound, from 86- and 84-day pig fetuses were 10 ml water/min and 2.4 mg urea/min; from 23- to 29-day rabbit fetuses the rates were 0.85-2 ml water/min and 0.1-0.45 mg urea/min. The rates of movement of water from the allantoic sac of pigs on the 67th and 74th days of gestation were 2 ml/min and 4.6 ml/min of which a measurable amount passed into the fetal tissue. After injection of ^{3}H-water or ^{14}C-urea into the circulation of pregnant rabbits, the specific activity of fetal tissue indicated a rapid transfer to the fetus, and equilibrium of specific activity in fetal and maternal blood was usually reached in 60 min. In every instance of injection of radioactive material into the maternal circulation, the specific activity in the fetal blood rose, at least temporarily, to a higher level than that in the maternal blood. This phenomenon has been observed also in pregnant rhesus monkeys after an injection of ^{14}C-urea. There appears to be a temporary accumulation of the isotope in the fetal blood, followed by its dispersion through the remaining fetal tissue. This could occur only if the isotope crossed the placenta very rapidly and were distributed more slowly in the fetus. (BBB)

38345 DETERMINATION OF STRONTIUM IN BONE WITH ION EXCHANGE SEPARATION-FLAME PHOTOMETRIC METHOD. Tsubota, Hiroyuki; Koyanagi, Taku (National Inst. of Radiological Sciences, Chiba, Japan). J. Radiation Res. (Japan), 5: 49-54(Mar. 1964).

A rapid and sensitive method for determining of Sr in bone was investigated. Strontium is separated from a large amount of calcium existing in bone and from interfering ions that depress the strontium emission by a cation exchanger with EDTA as an elutriant. With strontium in the effluent, EDTA solution can readily be determined by flame photometry without any treatment of effluent, when the enhancing effect of EDTA on the intensity of strontium flame emission is utilized effectively. Using this method, strontium content in bone could be determined from about 0.2g

of bone ash with the error below 10% and with the standard deviation of 3.5%. The method would be also used for the analyses of a micro amount of strontium in various calcareous materials. (auth)

38346 THE USE OF Cr-51 IN THE DETERMINATION OF RED CELL VOLUMES IN EXPERIMENTAL ANIMALS. Barnard, D. J.; Baxter, J. J. Roy. Army Med. Corps., 111: 53-60(1965).

A method of measurement of red cell volume in sheep and rabbits, using ^{51}Cr is described. Its accuracy is calculated and its limitations discussed. (Excerpta Med., Vol. 2, (July 1965)).

38347 EFFECTS OF LIPOSOLUBLE VITAMINS ON THE ^{90}Sr METABOLISM OF GROWING RATS. I. THE INFLUENCE OF VITAMIN D_3. Schmidt, B.; Lang, K. (Johannes-Guttenberg-Universitaet, Mainz). Klin. Wochschr., 42: 942-8(1964).

Biologically, ^{90}Sr is one of the most important byproducts of fallout. It has bone-seeking properties, hard beta emission, and a long physical and biological half-life. It is therefore important to obtain as much information as possible about the conditions of its absorption, metabolism, and the discrimination factor, i.e., the percentage dilution of ^{90}Sr associated with calcium after it has passed through organic membranes. Vitamin D affects the metabolism of minerals more or less directly in different places of the organism. Vitamin D_3 was therefore added in amounts of 50 to 500 and 5000 IU to a carefully weighed quantity of food (Shermann diet) contaminated with a constant amount of ^{90}Sr per gram of calcium in the food (in Sunshine units) and corresponding to 250 times of the fallout milk contamination in the year 1957. The effect of these increasing amounts of vitamin D_3 on the incorporation and retention of ^{90}Sr was studied in 400 growing rats divided in 4 groups (including the control groups). The experiment lasted 150 days and partial results were examined by sacrificing the animals in groups of five at intervals of 30 days (in the beginning also 5 and 10 days). The assays for calcium and ^{90}Sr were performed on ashed skeletons, feces, plasma, and urine. In spite of a magnitude of error reaching from 1 to 33% in the different measurements the following conclusions were reached: Physiological doses or slightly enhanced doses of vitamin D_3 caused no significant effects. High doses of vitamin D_3 caused toxic effects. This had the following consequences for ^{90}Sr metabolism: (1). The absorption of ^{90}Sr was greatly increased, as judged by the reduced excretion with the feces; while growth was delayed and food uptake insufficient. (2). Retention of ^{90}Sr in the skeleton was increased in hypervitaminosis in spite of an insufficient calcification. (3). The level of ^{90}Sr in the blood was raised due to the improved Sr absorption caused by vitamin D_3. Therefore the renal excretion of ^{90}Sr and Ca rose with increasing vitamin doses. (4). The data on mineral metabolism changed continuously with growing vitamin D_3 doses. The efficiency of discrimination by the intestinal epithelium was lowered with increasing doses of vitamin D_3. The same held true for the discrimination in the skeleton. The kidneys were injured by mineral depositions after high doses of vitamin D_3. As a consequence the discrimination efficiency decreased. (Excerpta Med., Sect. XXIII, 2: No. 6(June 1965))

38348 THE EFFECT OF TRIIODOTHYROACETIC ACID ON I^{131} INCORPORATION BY THE THYROID. Braun Cantilo, J. A.; Slepoy, A. S. S.; Hoschoian, J. C.; Andrada, J. A. (Universidad, Buenos Aires). Medicina (Buenos Aires), 24: 285-9(1964).

It has been shown that TRIAC (triiodothyroacetic acid) has an inhibitory effect upon the incorporation of iodine by the thyroid, which can be clearly seen in the radioautographic studies. At the level of 80 γ per day of TRIAC, this inhibition of complete. The action is probably due to an inhibition of the pituitary, since the thyroid can respond to a TSH stimulus. (Excerpta Med., Sect. XXIII, 2: No. 6(June 1965))

38349 GEOPHYSICAL VARIATION IN THE TOTAL BODY BURDEN OF CESIUM-137 IN JAPANESE PEOPLE AS ASSESSED BY BLOOD ANALYSIS. Yamagata, Noboru (Inst. of Public Health, Tokyo). Nature, 207: 211-12 (July 10, 1965).

Cesium-137 burdens were assessed in Japanese people by analyzing whole blood and were compared to ^{137}Cs determinations in muscle samples. Significant variations between localities were found in the blood samples, higher body burdens appearing in northern districts and near the Sea of Japan. Results indicated a 30% negative bias when muscle samples were analyzed. (H.G.D.)

38350 CHRONIC THIOURACIL FEEDING AND ACCUMULATION OF ^{131}I IN SOME ORGANS OF C_3H MICE. Casas, Carmen B.; Buso, Roberto (School of Medicine, San Juan, Puerto Rico). Nature, 207: 416-7(July 24, 1965).

Mice maintained on a 0.3 percent thiouracil (TU) diet for eleven months were injected with 336 μC ^{131}I as NaI to determine the effects of a TU diet on ^{131}I retention in muscle, liver, and intestinal tissues. Results revealed a statistically significant difference in the TU-fed animals, an increased iodine retention being noticeable in all tissues examined. The increase in retention may represent a reduced utilization of iodinated compounds or a decrease in the rate of ^{131}I excretion. (H.G.D.)

38351 ON CONTAMINATION IN ^{131}I SOLUTIONS (DISTRIBUTION AFTER INTRAVENOUS INJECTIONS IN RATS). Oppermann, W.; Ammon, J. (Universitaet, Frankfurt am Main). Naturwissenschaften, 52: 137(1965). (In German)

Exchange studies on carrier free $Na^{131}I$ solutions showed that a large part of the ^{131}I is present in solution in a chemically stable form. These compounds can be separated into two parts (a high molecular fraction and a low molecular fraction) by filtration through a membrane filter. This radioiodide solution contaminated by radiocolloid formation can be purified by distillation of the iodide. Two solutions contaminated by the formation of such radiocolloids and one solution purified by distillation were injected into rats and the distribution of the radioactivity in the thyroid, lungs, and liver were determined. The results showed that in the first hours after injection almost the same activity could be detected in the liver and lungs as in the thyroid for the first solution. In solutions two and three, however, the activity of these organs were practically nil compared to the thyroid. These results were expected on the supposition that the high molecular fraction containing the ^{131}I in a chemically stable form would be deposited as other finely distributed foreign bodies in organs belonging to the reticuloendothelial system. The consequence of this distribution on tracer studies is briefly considered. (J.S.R.)

38352 USE OF P^{32} FOR THE REGISTRATION OF CHANGES AND VARIATIONS IN THE ENAMEL SURFACE. A PRELIMINARY REPORT. Sand, H. F.; Moerch, T. Odontol. Tidskr., 72: 449-59(1964).

A method is presented, by means of which changes in the enamel surface can be registered objectively, provided the decalcification has not proceeded so far that the continuity of the enamel surface is lost. The method is based on the uptake of ^{32}P. By means of a special device, the surface activity can be determined in small selected areas of a single tooth surface. In non-treated enamel great differences in the uptake of ^{32}P were found between different teeth, in some cases also between areas of the same tooth. Both areas with early stages of caries attack (opaque spots) and artificially slightly decalcified zones took up more ^{32}P than did clinically intact enamel. The method was employed in preliminary experiments in order to assess the effect of topically applied fluoride solutions. The results obtained with ^{32}P were in agreement with the data obtained from the same material by means of the earlier methods. It appears that the proposed method makes possible a registration of changes in the enamel too small to be observed by means of the other methods. (Excerpta Med., Vol. 2, (July 1965))

38353 THE PARTITION OF TRACE AMOUNTS OF XENON BETWEEN HUMAN BLOOD AND BRAIN TISSUES AT 37 deg C. Veall, N.; Mallett, B. L. (Guy's Hospital, London). Phys. Med. Biol., 10: 375-80(July 1965).

The relative solubilities of trace amounts of ^{133}Xe at 37°C in human plasma, red blood cells, grey and white matter of the brain, and in homogenized whole brain were determined. From these data the tissue/blood partition coefficients for cortex, white matter, and whole brain were calculated as a function of hematocrit. On the basis of the measured ^{133}Xe solubilities it was estimated that the human brain consists of 60.3 ± 6.3% grey matter and the remainder white matter. (auth)

38354 A STUDY OF THE FIXATION CURVE OF I^{131} IN THE THYROID IN SUBJECTS TREATED WITH IODINATED CONTRAST MEDIA. Guinet, P.; Mornex, R.; Tourniaire, J.; Franchet-Sassolas, G.; Graber, B.; Levrat, R. (Faculte de Medicine, Lyon). Rev. Lyon Med., 13: 895-908(1964).

Sixty-two observations were made of patients receiving iodinated radiographic contrast media, subjected to a study of the thyroid fixation of ^{131}I. Thirty-seven fixation was retained, and 25 times there was a refusal curve. The analysis of this difference necessitated characterization of the different factors involved. The nature of the contrast media appeared to be important, lipiodol having an almost constantly intense and prolonged degressive action, the hydrosoluble products intended for urography and biliography having on the contrary a slight and ephemeral effect, the media used in cholecystography giving variable results. The state of the bile ducts could intervene, the refusals being rare after cholecystectomies. Finally, the thyroid functioning of the patient is not negligible, the presence of hyperthyroidism favoring the return to an appreciable fixation. In practice therefore, the benefits of a thyroid isotope exploration should not be refused for a subject having received radiological iodinated contrast media. (Excerpta Med., Sect. XXIII, 2: No. 6(June 1965))

38355 EXPERIENCES WITH THE USE OF RADIOACTIVE HYDROGEN IN INDUSTRY. Wesseldijk, A. Th. Groot (Philips Gezondheidscentrum, Eindhoven, The Netherlands). Tijdschr. Sociale Geneesk., 42: 854-7 (Nov. 6, 1964). (In Dutch)

When T_2 is inhaled, it has been found that only 0.004% remains in the body. As water, however, 99% is absorbed in the lungs. Drinking tritiated water causes an increase in the blood T activity, which reaches a maximum in 45 min; the half-life for excretion has been found to be 8.5 to 11.5 days, or 2.5 with enforced diuresis of 13 l per 24 hr. Absorption through the skin in an atmosphere of 1 μC HTO/ml is 1.6×10^4 μC/min. In the manufacture of radio valves, T_2 was chosen as an absorbate on finely divided Ti. Special precautions were taken, including nylon work clothes and rubber gloves. Medical controls were enforced. It was demonstrated with the rat that 97.5% of (accidentally) ingested Ti sponge containing T is excreted; 2.5% remains in the body, mostly in the intestinal canal where little β-ray damage can be done. From the ICRP maximum dose, it follows that a worker's daily dose should be <0.1 mC by absorption; oral uptake of the suspension thus might be 4 mC daily, an improbable figure. The danger of inhalation is greater; attempts to measure body T were made by scintillation counting of urine samples. For this the ICRP permissible concentration is 20 μC/l; the highest ever observed was 15 μC/l. Hygienic measures are reviewed; T is very difficult to remove from any surface. It is advisable to cover surfaces with polythene or filter paper. Glassblowers in the lab had excess T exposure and were made to use compressed air. (BBB)

38356 RADIOISOTOPE INDICATORS IN HEMATOLOGY. Le Bel, Etienne. Union Med. Can., 94: 63-5 (Jan. 1965).

The use of radioisotopes in iron metabolism, red cell production, the survival of red cells, white cells and platelets, and the diagnosis of spleen disorders is reviewed. (AECL)

38357 THE TOXICOLOGY OF RADIOACTIVE SUBSTANCES. Zakutinskii, D. I. pp 246-72 of Radiation Medicine. New York, The Macmillan Co., 1964.

The significance of the physico-chemical properties of radioactive substances, routes of entry of radioactive substances into the body, distribution of radioactive substances within the body, excretion of radioactive substances, and conditions influencing the action of radioactive substances treatment are discussed. (P.C.H.)

Radiation Effects

Refer also to abstract 38873.

38358 (AD-612660) A.T.D. PRESS, SPACE PHYSIOLOGY. VOLUME 3, NUMBER 183. Special Issue. (Aerospace Technology Div., Library of Congress, Washington, D. C.). Mar. 23, 1965. 17p. $1.00(CFSTI).

Topics discussed include the effects of radiation, acceleration, and vibration on the central nervous system; effects of radial accelerations on the venous blood flow in the vessels of rabbit brains; effects of prolonged accelerations on the growth of the organism and the functional condition of certain systems; effect of whole-body vertical vibration on the functional condition of the vestibular organ of guinea pigs; effects of acute whole-body irradiation by gamma rays on the functional condition of the vestibular organ of guinea pigs; combined effects of vibration and acute irradiation on the functional condition of the vestibular organ of guinea pigs; the problem of the effect of whole-body gamma irradiation on the excitability of the spinal inflex arc; effect of whole-body vertical vibration on the functional state of the spinal reflex arc; the combined effects of vibration and of ionizing radiation on the functional condition of the spinal reflex arc; the effects of repeated vibration on the oxygen tension in the brains of rats; the combined effects of whole-body vertical vibration and irradiation on the oxidative processes in the brains of rats; and the effects of whole-body vertical vibration and x rays on the nuclei of bone-marrow cells of mamals. (auth)

38359 (BNWL-SA-230) PLUTONIUM PARTICLE-INDUCED NEOPLASIA OF THE CANINE LUNG. I. CLINICAL AND GROSS PATHOLOGY. Park, J. F.; Clarke, W. J.; Bair, W. J. (Battelle-Northwest, Richland, Wash. Pacific Northwest Lab.). [June 24, 1965]. Contract AT (45-1)-1830. 20p. (CONF-650624-2). Dep. (mn); $1.00 (cy), 1(mn) CFSTI.

From 2nd International Conference on Lung Tumors in Animals, Perugia, Italy.

The pathologic effects in 32 beagle dogs that succumbed 2 to 14 months after exposure to $^{239}PuO_2$ aerosols are reviewed. One male dog, 150 days post-exposure, with a lung burden of 19 μCi, had bronchiolo-alveolar carcinomas. Inhalation of $^{239}PuO_2$ caused spontaneous death in 10 female beagle dogs 29 to 56 months post-exposure. The body burden at death ranged from 1 to 3 μCi. Cardiopulmonary insufficiency and lymphopenia were the primary clinical signs associated with severe fibrosis of the lung and bronchial lymph nodes. These organs contained 76 to 95 percent of the terminal body burden. Five of these animals showed primary pulmonary tumors. Three of the animals showed radiographic lesions suggestive of pulmonary neoplasia 4 to 9 months before death. The tumors were grossly multicentric in 2 of the 4 animals and metastases were not evident; however, microscopic examination indicated multicentric origin in 5 animals and metastases to the bronchial lymph nodes in 1 dog. Six of the 42 dogs exposed to $^{239}PuO_2$ showed bronchiolo-alveolar carcinomas, an incidence of 14 percent compared to a primary lung tumor incidence of 0.2 percent reported for canine necropsy material. (auth)

38360 (TID-21695) A COMPARISON OF X-RAY- AND ULTRAVIOLET-INDUCED ABERRATIONS IN POLLEN TUBE CHROMOSOMES OF TRADESCANTIA. Final Report. Bailey, Paul C. (Birmingham-Southern Coll., Ala. Dept. of Biology). Feb. 12, 1965. Contract AT(40-1)-3222. 25p. Dep. (mn); $1.00(cy), 1(mn) CFSTI.

Progress is reported in studies of aberrations induced in pollen tube chromosomes of Tradescantia by exposure to ultraviolet and x radiation. A survey was made of the chromosome morphology of 18 native populations of Trad-

escantia. Data are presented on the species, chromosome number for each population, place collected, total length of individual chromosomes, and length of chromosome arms of species collected in Alabama and Georgia. Results are included from a study of the number of aberrations in pollen tube chromosomes of T. paludosa exposed to 200 or 400 R x radiation with varying concentrations of lactose added to culture medium. (C.H.)

38361 (TID-21951) THE EFFECTS ON RAT BEHAVIOR OF DEVELOPMENTAL ABERRATIONS INDUCED BY IRRADIATION IN UTERO. Final Report. White, Robert K. (Texas Technological Coll., Lubbock). [1965]. Contract AT(40-1)-1982. 355p. Dep. mn; CFSTI, $7.00 cy, $1.75 mn.

Results are reported from a study in rats of the effects of in utero x irradiation of 0, 50, or 150R at 0, 4.5, 6.5, 8.5, or 9.5 day of gestation on learning ability; activity; electrocardiogram (EKG) in response to varying, empirically determined stress situations; possible differences between the sexes in general activity level, incentive motivation, emotionality, and learning; and the effects of age on learning ability. The Lashley III maze for rats was used to evaluate learning ability. Data are included from a comparison of the errors of rats, mice, and hamsters in the Lashley III maze and a study of the effects of adrenaline, phenobarbital, and chlorpromazine on two kinds of errors by rats in the Lashley III maze. A semi-automated and an automated maze recording device were developed and 5 computer programs for the IBM 1620 were developed for information retrieval from the experimental data on dependent and independent variables effecting behavior on the maze. Data are included from an extensive study of the EKG response to extreme stress in normal and irradiated animals tested on the Lashley III maze. A factor analysis was made that related the psychological and physiological findings. Follow-up studies were conducted to ascertain the influence of age at the time of testing upon radiation dose delivered in utero. A list is included of publications resulting from these studies. (C.H.)

38362 (JPRS-30993, pp 29-38) THE EFFECT OF LONG-TERM ADMINISTRATION OF SMALL DOSES OF CALCIUM-45 ON CERTAIN INDICES OF NATURAL IMMUNITY. Ternov, V. I. Translated from Gigiena i Sanit., No. 4, 47-51(Apr. 1965).

The daily introduction of ^{45}Ca into white rats in a dose one thousand times in excess of MPC of this isotope for water (0.09 microcurie/kg) clearly causes symptoms of chronic radiation injury in animals from as early as the third month on. Calcium-45 in a dose one hundred times in excess of MPC induced the first signs of radiation injuries ten and one half months after commencement of daily injection. Doses of 0.0009 microcurie/kg (ten times in excess of MPC) over the space of nine months caused only negligible functional changes involving certain natural immunity factors. Therefore, this dose is regarded as the threshold dose. (H.G.D.)

38363 THE EFFECT OF ROENTGEN RAYS ON THE DIMENSIONS OF RED BLOOD CELLS IN THE PERIPHERAL BLOOD OF MICE. Piechowska, Wanda; Pilawski, Andrzej. Acta Physiol. Polon., 16: 235-8(Mar.-Apr. 1965). (In Polish).

The experiments were performed on five groups of mice, five mice in each group. The whole-body dose of 80 kV x rays (6 ma anode current) was 50, 100, 200, 300, and 400 R to groups I through V respectively. The red blood cells of group I showed no observable change, while the remaining groups showed radiation effects that increased with dosage. These effects were in the form of enlarged average cell size. The average cell size was measured by a microscopic light-diffraction technique. (TTT)

38364 EPIDEMIOLOGICAL OBSERVATIONS ON SUSCEPTIBILITY TO CANCER IN MAN WITH SPECIAL REFERENCE TO AGE. Doll, R. (Univ. Coll. Hospital Medical School, London). Acta Unio Intern. Contra Cancrum, 20: 747-52(1964).

A review of some factors that could affect individual susceptibility to cancer is presented and data are compiled which show that susceptibility to cancer induction increases with age among adolescent and adult men. Some of this evidence was obtained from observations on persons exposed to large amounts of ionizing radiations. Data are presented for a large group of patients who were given radiotherapy for ankylosing spondylitis between 1935 and 1954. Since the results were first published in 1957, the series has been increased in size and now includes nearly 15,000 patients followed for an average of 10 yr. There are now 73 cases of leukemia diagnosed among these patients. The number of other leukemias which would have been expected in the absence of irradiation is not more than 4 or 5. (TCO)

38365 SPECTROGRAPHIC STUDY WITH ELECTRON PARAMAGNETIC RESONANCE ON THE EFFECT OF IONIZING RADIATION ON ELEMENTARY BIOLOGICAL OBJECTS. Mueller, Adolf. Akad. Wiss. Lit. (Mainz), Abhandl. Math.-Nat. Kl., No. 5, 143-261(1964). (In German).

In dried bacteriophages and their constituents (nucleic acids, proteins, nucleotides, nucleosides, nucleic acid bases, pentoses, peptides, and amino acids) radicals were induced by ionizing radiation at 100 and 300°K. The radicals were qualitatively and quantitatively measured using the EPR spectrometric method in dependence on the temperature, type of radiation, radiation dose, dose output, and time. In the spectra of all substances hyperfine structures were found. The spectra of phage proteins showed a doublet splitting that is characteristic for nonsulfur-containing proteins. Strongest structures were observed in the spectra of phage nucleic acids. The structure of the induced radicals and the reactions in which they participate were derived. Nucleic acids from bacteriophages were investigated in detail. The dependence of the radical concentration on the radiation dose followed in all substances the equation $C/C_\infty = 1 - \exp(-D/D_{37})$. Spectral and radical yields in the different constituents of the bacteriophage DNA were obtained and explained with intramolecular transition of the radical electrons from aliphatic to heterocyclic groups. The radical yield on phages with a growth capacity and the nucleic acid and protein constituents necessary for the growth were quantitatively compared with the radical yields of the chemical building blocks and with the biological inactivation. It was found that the yield was approximately 100 times greater than the yield in inactivations. (J.S.R.)

38366 SKIN CHANGES INDUCED BY UV-IRRADIATED LINOLENIC ACID EXTRACT. Waravdekar, Vaman S.; Saslaw, Leonard D.; Jones, Wallace A.; Kuhns, James G. (Armed Forces Inst. of Pathology and Veterans Administration Central Lab. for Anatomic Pathology and Research, Washington, D. C.). Arch. Pathol., 80: 91-5(July 1965).

Subcutaneous administration of an aqueous extract of ultraviolet-irradiated linolenic acid resulted in an alopecic plaque in the skin of mice. The extract induced necrosis in the epidermis; its epithelial appendages and dermis; followed by an inflammatory response, disruption of collagen; and elastic fibers. Hyperplasia of the epidermis and of the follicular sheath was quite marked about seven days after the injection. The follicular hyperplasia was followed by keratogenesis, with the formation of keratin cysts at the original follicular sites. It is presumed that these toxic properties are associated with peroxides and carbonyl compounds present in the extract. (auth)

38367 INDUCTION OF NEOPLASMS IN RAT THYROID GLANDS BY X IRRADIATION OF A SINGLE LOBE. Nichols, C. W. Jr.; Lindsay, S.; Sheline, G. E.; Chaikoff, I. L. (Univ. of California, Berkeley and Univ. of California, San Francisco). Arch. Pathol., 80: 177-83(Aug. 1965).

The induction of adenomas and papillary carcinomas is described in thyroid glands of Long-Evans rats two years after a single lobe, either the left or right, was irradiated with 1000 R of x rays. Adenomas, mainly follicular, were found in the thyroid glands of 15% of the irradiated rats, but in only 3% of the normal control rats. The development of these benign lesions was completely suppressed by feed-

ing a desiccated thyroid-containing diet. Three papillary carcinomas appeared in thyroid glands of the irradiated rats. Two of the carcinomas developed in lobes that had been shielded from the irradiation. It is inferred that these two malignant neoplasms were initiated and promoted by the TSH, but the possibility that scattered radiation also played a part in the process is not ruled out. The third papillary carcinoma was found in a radiated lobe in one of a group of rats in which benign adenoma formation had been suppressed by thyroid feeding. This carcinoma may have been initiated by radiation, but the possibility that TSH also played a role is not ruled out. Thus, the TSH or irradiation per se seems to be implicated as the agent in the development of malignant papillary neoplasms in the x-irradiated thyroid gland of the Long-Evans rat. (auth)

38368 BIOLOGICAL EFFECTS OF RADIOACTIVE PHOSPHORUS. AN ELECTROPHORETIC STUDY OF WHOLE AND DENATURED SERUM. Dragoni, G.; Zucali, R. (Universita, Milan). Arch. Sci. Med., 118: 387-95(1964).

In a study of the biological effects of radiophosphorus in rats, the electrophoretic alterations in native serum and in serum treated with formaldehyde, ammonia, and heat were examined. Electrophoretic analysis (Tiselius apparatus), of the serum of rats sacrificed at various intervals after intraperitoneal injection of 200 μC of radiophosphorus disclosed a distinct decrease in albumin and an increase in the α- and β-globulins. These changes, accompanied by alterations in the patterns of the electrophoretic tracing, were found chiefly in the first ten days after radiophosphorus treatment. No heterogeneous X-type fractions were ever found in the denatured serum on electrophoretic analysis. Denaturation did, however, cause complete aggregation of the various serum protein fractions into a single homogeneous component. Its planimetric values were decidedly below those found in denatured normal serum. (Excerpta Med., Vol. 2, (July 1965))

38369 THE EFFECT OF X-RAYS ON GONOCYTES IN THE TESTIS OF THE RAT. Sapsford, C. S. (Univ. of Sydney). Australian J. Biol. Sci., 18: 643-51(June 1965).

After treatment with x rays (300 R) at 1 or 4 days of age, the majority of gonocytes in the testes of rats failed to divide and by 8 days of age these cells, together with their nuclei and nucleoli, had markedly increased in size. A number of gonocytes still present in the testes of normal rats at 8 days of age had also undergone this generalized enlargement. Determinations of the surface areas of germ cell nuclei confirmed the occurrence of the hypertrophy of gonocyte nuclei in normal and irradiated testes, and showed that the period during which gonocyte nuclei in irradiated testes became enlarged was the same irrespective of the age of irradiation. This period coincided with the one during which gonocytes in normal testes had begun to divide. These results led to the suggestion that irradiation, while suppressing the visible manifestations of mitosis, had not similarly affected the earlier synthetic phase, and that it was the products of this synthetic phase that had caused nuclei to enlarge. An inherent incapacity to complete the final stages of mitosis could likewise have resulted in the nuclear hypertrophy observed in some gonocytes in the testes of normal rats at 8 days of age. (auth)

38370 THE SYNTHESIS OF DNA AND NUCLEAR PROTEIN BY GONOCYTES IN THE TESTES OF NORMAL AND X-IRRADIATED RATS. Sapsford, C. S. (Univ. of Sydney). Australian J. Biol. Sci., 18: 653-64(June 1965).

Investigations showed that nuclear hypertrophy in irradiated gonocytes was associated with the synthesis of both DNA and nuclear protein. Although DNA content and nuclear surface area were strongly correlated, it was found that DNA gradually became diluted as nuclei enlarged. The concentration of nuclear protein, however, remained constant, and production of this substance was regarded as being responsible for the nuclear hypertrophy. Hypertrophy of gonocyte nuclei in the testes of normal rats from 5 to 8 days of age was also found to be due to nuclear synthetic activity. At 5 days of age, enlargement, being associated with the premitotic synthetic phase of gonocytes, could be regarded as a normal process. Excessive hypertrophy of some gonocyte nuclei which took place in the 5–8 day period, however, was regarded as being abnormal. This hypertrophy was due to the accumulation of DNA and protein synthesized by nuclei that had failed to complete the division process. (P.C.H.)

38371 EFFECTS OF GAMMA RAYS ON THE RIBONUCLEIC ACID AND PROTEIN CONTENT OF AMOEBA. Skreb, Yvette; Eger, Magda; Horvat, Durda (Institut de Recherches Medicales et de Medecine du Travail, Zagreb). Biochim. Biophys. Acta, 103: 180-2(May 11, 1965). (In French)

The effects of γ radiation at 1000 R on whole ameba and ameba sectioned into nucleated and anucleated fragments were studied. The micro determination of RNA showed that the irradiation produced, in all three types of samples, a significant decrease in the RNA, a decrease that was relatively larger in the anucleated fragments. In the anucleated fragments determination of the RNA was no longer possible after 4 days. The protein concentration in the samples followed the same path as the RNA, but slower. The effects were sharply greater for the anucleated fragments. The whole living ameba showed a restoration on the fourth day. The significance of these results in comparison with the results obtained from uv radiation is discussed. (J.S.R.)

38372 EARLY LEUKAEMIAS APPEARING IN YOUNG AND YOUNG ADULT AkR MICE EXPOSED TO X RAYS. Jullien, P.; Rudali, G. (Universite de Paris). Bull. Assoc. Franc. Etude Cancer, 51: 147-52(1964).

A dose of 600 R, administered in several sessions, decreased the latency of lymphatic leukemia in AkR mice without altering the frequency. Young mice were more sensitive to this treatment than young adult animals. (Excerpta Med., Sect. XXIII, 2: No. 6(June 1965))

38373 DIFFERENTIAL ACTION OF X AND ULTRAVIOLET RAYS ON THE TARDIGRADE MACROBIOTES AREOLATUS IN THE ACTIVE AND DESICCATED STATE. May, Raoul-Michel; Maria, Monique; Guimard, Jacqueline. Bull. Biol. France Belg., 98: 349-67(1964). (In French).

Macrobiotes areolatus in dormant and active states were exposed to x and uv radiation to determine the amount of irradiation that would inhibit arousal in the first state and kill in the second state. The animals were isolated from moss and either put into a state of artificial hibernation or maintained in an active state. They were then irradiated with x-ray doses from 10,000 to 1,200,000 R. Other specimens were exposed to uv radiation for varying times, from $\frac{1}{2}$ to 6 hr. Those irradiated with x rays were observed for 25 to 30 days to ascertain the effect on their survival time. The specimens in the latent state were resistant to x rays in doses up to 300,000 R. The LD_{50} was 570,000 R one day after irradiation, and a dose of 1.2 MR completely inhibited the arousal of all the Macrobiotes exposed. The survival time for the desiccated animals in the dormant state irradiated with 300,000, 400,000, 600,000, and 700,000 R, then aroused was greatly reduced in comparison with the control group. Those irradiated with 800,000, 900,000, and 1,000,000 R succumbed on the fifth day. The Macrobiotes in an active state were at first as resistant to 200,000 R as the control group. The LD_{50} was above 540,000 R, evaluated 2 hr after irradiation. A dose of 1,200,000 R killed all the Macrobiotes within this time. The survival time of the active Macrobiotes at 200,000 R was shortened in comparison with the control group. Exposure of Macrobiotes in a dormant state to uv radiation of 2600 Å wavelength for 6 hr did not inhibit their arousal, but, when they were exposed in an active state to uv rays, all died in an asphyxiated state within $1\frac{1}{2}$ hr. The great tolerance of tardigrades to ionizing or nonionizing electromagnetic radiations makes them an ideal choice for the study of extreme conditions in outer space. (BBB)

38374 REGIONAL OXYGENATION AND THERAPEUTIC RESPONSE TO IRRADIATION. AN EXPERIMENTAL STUDY. Clapp, Paul; Charyulu, K. K. N.; Tayao, Manuel S.; Tyree, Ella B.; Nickson, James J.; Lawrence,

Walter Jr. (Sloan-Kettering Inst. and Memorial Hospital, New York). Cancer, 18: 927-36(Aug. 1965).

Observations were made on the tumor response and normal tissue tolerance to varying single doses of 250 Kv x ray administered to the VX2 carcinoma-bearing rabbit hind limb during unaltered circulation, circulatory arrest, oxygenated blood perfusion and intraarterial H_2O_2 infusion. Hypoxia produced by circulatory arrest resulted in diminished tumor response and increased tissue tolerance to irradiation. Oxygenated blood perfusion did not enhance tumor radiosensitivity. Some increased tumor response was demonstrated with hydrogen peroxide infusion but normal tissue tolerance to irradiation during this procedure was reduced markedly. When maximum tolerated and minimum effective irradiation doses were calculated for each procedure, circulatory arrest in this experimental tumor system resulted in the highest therapeutic index. These experiments lend support to the idea of a clinical trial of regional hypoxia during therapeutic irradiation of appropriate neoplasms. (auth)

38375 AUTO-IMMUNIZATION AND AUTO-ALLERGIZATION IN GUINEA PIGS INFECTED WITH TUBERCULOSIS WITH PRELIMINARY X-RAY TREATMENT. Vulchanov, V. H.; Vassilev, V. N.; Obretenova, K.; Belokonski, I. Compt. Rend. Acad. Bulgare Sci., 18: 165-8(1965).

The role of tuberculosis infection in the induction of a polyspecific auto-immunization process was investigated in guinea pigs. The serum of the animals was pre-tested for complement-fixing antibodies against lung, spleen, and brain of a normal guinea pig. Guinea pigs were exposed to 400 R x radiation and 24 hr later were infected with Mycobacterium tuberculosis, human strain. Non-irradiated guinea pigs were infected under similar conditions of dose and time. Serum samples taken from all animals on the 15th, 30th, 45th, and 60th day after infection was tested for the presence of complement-fixing antibodies against the tissue antigens. Tuberculin skin tests were also performed periodically. Results indicated that pre-treatment with 400 R x radiation produced conditions favorable for a wider spread and deeper penetration of the infection, increased the possibility of inducing auto-antigenicity, and accelerated the auto-immunization process, but inhibited delayed hypersensitivity in animals infected with tuberculosis. The induction of auto-antigenicity was ascribed to the direct action of the infection rather than to changes in immunological competence of the antibody-forming cells induced by radiation exposure. (C.H.)

38376 POLYVALENT TOLERANCE IN NEWBORN AND SUBLETHALLY IRRADIATED ADULT MICE. Rychlikova, Milena; Chutna, Jitka (Inst. of Experimental Biology and Genetics, Czechoslovak Academy of Sciences, Prague). Folia Biol. (Prague), 11: 187-93(1965).

Polyvalent tolerance was studied in non-inbred mice of H strain. Their heterogeneity is such as to permit the rejection of homografts within 24 days (with the mean survival time of 14.5 days) in all 88 control mice transplanted with skin from randomly selected donors. Polyvalent tolerance was induced in newborn H strain mice by an injection of pooled embryonic cells or by spleen cells from adult donors. By the spleen from tolerant mice, in which tolerance was elicited by embryonic or spleen cells from adult mice, polyvalent tolerance could be transferred to other newborn animals. In adult mice, polyvalent tolerance was induced by sublethal irradiation and repeated injections of embryonic or adult spleen cells. (auth)

38377 SERUM PROTEIN IN ATOMIC BOMB SURVIVORS (INCLUDING THOSE WHO SUFFERED FROM RESIDUAL RADIOACTIVITY). II. QUANTITATIVE OBSERVATION OF SERUM PROTEIN FRACTIONS BY MEANS OF FILTER PAPER ELECTROPHORESIS, AND AN ATTEMPT TO ELUCIDATE THE PHYSIOLOGICAL AND CLINICAL SIGNIFICANCE OF ELECTROPHORETIC PATTERNS. Makei, T. (and others). Hiroshima Igaku, 16: 885-914(1963).

In 100 atomic bomb survivors, γ-globulin content in serum protein averaged 24.5% (1.77 g/100 ml) in the N- and β-patterns, and 30.5% (2.2 g/100 ml) in the γ-pattern. In the β-pattern, the amount of γ-globulin was distinctly greater than normal, but that of β-globulin was almost normal. In 33 patients with cancer, both β-globulin (14.2%) and γ-globulin (27.3%, 1.9 g/100 ml) were increased. γ-Globulin was increased (24.0%, 1.7 g/100 ml) in 16 persons who had been engaged in irradiation work with radioactive rays for many years. Electrophoretic patterns were obviously changed, in that β- and γ-globulins were favorably influenced by irradiation in patients with cancer. (Excerpta Med., Vol. 2, (July 1965))

38378 HAEMATOLOGICAL FINDINGS IN THOSE WHO SURVIVED ATOMIC BOMBING IN HIROSHIMA AND NAGASAKI CITIES. OBSERVATION FOR 10 YR. Yamamoto, T. Hiroshima Igaku, 16: 1082-91(1963).

The results of hematological examinations performed by ABCC (Atomic Bomb Control Commission) on sufferers from atomic bombing in Hiroshima and Nagasaki up to 1956 are described. The incidence of leukemia was related to the distance from the explosion center and to the grade of acute symptoms due to radioactive rays. Such incidence increased at the end of 1950, and did not tend to decrease until 1956. Moderately severe iron-deficiency anemia was observed in 5% of sufferers. There was no significant difference of means of erythrocyte count, amount of Hb hematocrit, erythrocyte volume, and concentration of Hb between sufferers and non-sufferers in Hiroshima and Nagasaki. Thrombocyte count and coagulation reaction were normal in both sufferers and non-sufferers. On autopsy of sufferers, there were 6 cases of panmyelophthisis and 6 cases of hypoplastic anemia. (Excerpta Med., Vol. 2, (July 1965))

38379 STUDIES OF RADIATION INJURY TO THE KIDNEY, USING RADIOISOTOPE RENOGRAMS. THE EFFECT OF A SINGLE LARGE DOSE IRRADIATION TO THE LEFT KIDNEY. Yanagisawa, T.; Nakamura, M.; Toda, H.; Tarusawa, T.; Magaribuchi, S. Igaku To Seibutsugaku, 69: 28-32(1964).

The influence of radiation on kidney function was investigated with radioisotope renography. The left kidney of matured rabbits was irradiated with a single dose of 1000, 2000, and 5000 R, and renograms of such rabbits were taken at various times after the treatment by i.v. injection of 1 μC/2.5 kg of ^{131}I-hippuran and a pen-type renographic equipment. The renograms of the treated rabbits were compared with those of normal rabbits. It was found that the renograms of both kidneys of rabbits treated with 1000 R of x rays did not differ from those of normal animals until 3 weeks after irradiation. The animals irradiated with 2000 R showed a decrease of the C_M value (count of maximum renal ^{131}I) and delay of T_H (time required for decrease from C_M to a half of that), in both kidneys from 4 days after the irradiation. In the case of rabbits irradiated with 5000 R, the radiation injury in irradiated and non-irradiated kidneys became significant from 7 days after the treatment, although a marked decrease of C_M value in the unirradiated kidney was seen as early as 5 days after the irradiation. In these injured kidneys, differentiation of vascular, secretory, and excretory phases in renograms was not distinct. (Excerpta Med., Vol. 2, (July 1965))

38380 IMMUNITY IN EXPERIMENTAL SYPHILIS. III. ATTENUATION OF VIRULENT TREPONEMA PALLIDUM BY γ-IRRADIATION. Miller, James N. (Univ. of California, Los Angeles). J. Bacteriol., 90: 297-301(Aug. 1965).

Virulent, freshly isolated cells of Treponema pallidum strain Nichols suspended in a 50% rabbit serum-saline solution and exposed to a γ-irradiation dose of 652,800 R were rendered noninfectious without apparent loss of motility or change in observable morphological and staining characteristics. Although 5×10^7 γ-irradiated organisms failed to elicit an immobilizing antibody response in rabbits, the same organisms retained their capacity to react with classical T. pallidum-immobilizing antibody. (auth)

38381 EVIDENCE OF LYSOGENY IN DERIVATIVES OF ESCHERICHIA COLI. Frampton, E. W.; Brinkley,

B. R. (Univ. of Texas, Houston). J. Bacteriol., 90: 446-52(Aug. 1965).

Exposure of cultures of several thymine-requiring derivatives of Escherichia coli strain 15 to radiation [x rays or ultraviolet(uv)] resulted in an increased synthesis of ribonucleic acid (RNA) as measured by the incorporation of radioactive uridine. In addition to radiation, mitomycin C (5 or 25 μg/ml) or growth in the absence of thymine also stimulated RNA synthesis in cultures in which the bulk of RNA synthesis was terminated by a shift-down in growth conditions. RNA purified from x-irradiated bacteria was resolved on columns of methylated serum albumin and yielded an elution profile which appeared similar to RNA synthesized by phage-infected bacteria. Electron microscopic examination of cultures induced to lyse by exposure to uv radiation, or by growth in the presence of 5-bromouracil before exposure to radiation (x rays or uv), showed the presence of mostly incomplete phage particles. (auth)

38382 EFFECT OF IRRADIATION ON FERROKINETICS OF CROSS-CIRCULATED DOGS. Dalrymple, Glenn V.; Kundel, Harold L.; Sawyer, Donald C. (School of Aerospace Medicine, Brooks AFB, Tex.). J. Nucl. Med., 6: 292-6(Apr. 1965).

Six pairs of adult beagle dogs were cross-circulated by surgical arteriovenous anastomoses. Four of the pairs were treated as follows: following the establishment of the cross-circulation, one of the partners of each pair was irradiated with 430 rads of 2 mev x rays while the other partner was shielded. The other two pairs of dogs were cross-circulated but not irradiated. Twenty-four hours following irradiation (or cross-circulation in the case of the nonirradiated animals) radioiron ferrokinetics were performed. The expected depression of erythropoiesis occurred in the irradiated animals but not in the nonirradiated ones. Therefore, no evidence of an abscopal mechanism being responsible for radiation depression of erythropoiesis was demonstrated. (auth)

38383 SENSITIVITY OF ARTEMIA EGGS TO γ-IRRADIATION. I. HATCHABILITY OF ENCYSTED DRY EGGS. Iwasaki, Tamiko (National Inst. of Radiological Sciences, Chiba, Japan). J. Radiation Res. (Japan), 5: 69-75(Mar. 1964).

The effects of ionizing radiation on the hatchability of eggs were studied in Artemia eggs irradiated in the dry state at total γ-doses of 480 kR and 600 kR followed by soaking in 2% NaCl solution at 27°C. The delay on the development of eggs became greater as the irradiation dose increased. Radiosensitivity based on the hatchability at 72 hrs after incubation diminished with dose in a sigmoidal curve. The 50% hatching dose was about 500 kR, and the LD^{100} was 900 kR. The low radiosensitivity may be attributed to the low water content and the arrest of metabolism of the eggs. (H.G.D.)

38384 SENSITIVITY OF ARTEMIA EGGS TO γ-IRRADIATION. II. EFFECTS OF WATER CONTENT. Iwasaki, Tamiko (National Inst. of Radiological Sciences, Chiba, Japan). J. Radiation Res. (Japan), 5: 76-81(Mar. 1964).

The dependence of radiosensitivity on environmental conditions during irradiation was studied in Artemia eggs γ-irradiated at various moisture and temperature levels. Artemia eggs of various water content were irradiated and then soaked in 2% NaCl solution at 27°C. The radiosensitivity of eggs based on hatchability increased successively with an increase of water content within 5.8% to 54.0%, except that at 9.6% showed a temporary decrease. When the eggs once moistened prior to irradiation were redesiccated to the initial level of water content, their sensitivity was shown to be almost at the same level of the initial one. To test the influence of temperature, the eggs were infiltrated with moisture at 0°C and 25°C, and irradiated at low or high temperatures. There was no significant difference in sensitivity between eggs infiltrated at 0°C and 25°C. However, the sensitivity of eggs infiltrated at both temperatures, and irradiated at high temperature was found much higher than those irradiated at low temperature. Results were discussed in relation to similar ones in plant seeds. (H.G.D.)

38385 A TECHNIQUE FOR THE MICROBEAM IRRADIATION OF SINGLE CELLS IN TISSUE CULTURE. Clegg, M. D. (Oxford Univ.). J. Roy. Microscop. Soc., 83: 433-41(1964).

A technique has been developed for irradiating a particular tissue-culture cell with a microbeam of α particles and subsequently examining the same cell in the electron microscope. The methods of microbeam irradiation including source design, monitoring apparatus, and culture methods are described, together with the method of locating the particular cell irradiated when the cultures are embedded in Araldite. The block is trimmed in such a way that the position of the cells can be seen through a side-mounted low power microscope; this allows an individual cell to be observed while it is being sectioned. (Excerpta Med., Sect. XXIII, 2: No. 6 (June 1965))

38386 THE ELECTRON MICROSCOPY OF CELLS IRRADIATED WITH A MICROBEAM OF α PARTICLES. Clegg, M. D. (Oxford Univ.). J. Roy. Microscop. Soc., 83: 443-53(1964).

The effect of radiation from a microbeam of α particles directed at the cytoplasm of chick fibroblasts in tissue culture has been studied with the electron microscope. Extensive damage to all cytoplasmic inclusions was seen when the cell was irradiated with large doses (of the order of 100 α particles over an area 9 μ in diameter) and fixed within one minute after irradiation. The damage was seen throughout the entire cytoplasm of the cell and there was no apparent localization. With smaller doses (of the order of 10 α particles over areas of 3 to 6 μ in diameter) the observed damage was less severe, but nevertheless still apparent in the electron microscope. Areas of damaged mitochondria and endoplasmic reticulum were seen throughout the cell adjacent to regions which appeared completely normal. Intensification of damage in the actual irradiated area has been observed; large, multi-membranous inclusions were present in, or near this area. The nucleus, nucleoli, and nuclear membrane appeared undamaged in these cells. Possible mechanisms for the spread of damage through the cell are discussed. (Excerpta Med., Sect. XXIII, 2: No. 6(June 1965))

38387 THE EFFECT OF X-RAY IRRADIATIONS OF WEAK AND MODERATE INTENSITY ON TUMOURS OF MICE. Karrer, K.; Pape, R. Krebsarzt, 19: 405-11 (1964).

Presuming that minimal doses of x rays may inhibit the growth of tumors by indirect action, the influence of small doses of whole-body irradiation upon mice, inoculated with Ehrlich-ascites-tumor-cells either i.p., i.v., or s.c., was studied. Mice were irradiated with dosages of 1 × 3 R up to 25 × 100 R either before or repeatedly after inoculation. No significant difference could be found between the experimental group and the controls. The essential effect of tumor-inhibition by whole-body irradiation therefore seems not to occur. (Excerpta Med., Sect. XXIII, 2: No. 6 (June 1965))

38388 THE SIGNIFICANCE OF CHANGES IN PLASMA IRON CLEARANCE FOLLOWING EXPOSURE TO IONIZING RADIATION IN THE DOG. Quaife, M. A.; Odland, T. Laval Med., 35: 414-18(Apr. 1964).

Changes in the hematopoietic system are of prime importance among the parameters measured for the biological effect of ionizing radiation. Plasmairon (^{59}Fe) clearance half time was utilized as a parameter of measurement of the effect of wave and particle irradiation on the hematopoietic system of the beagle. The animals were chosen at random from the registered beagles available from the experimental animal colony. The results of the study are presented in graphic form. Preliminary evidence from this study suggests some difference in effect between the 2 radiation forms (wave or particle irradiation) in subjects succumbing to the radiation insult, with x-ray irradiation being the more damaging. (auth)

38389 THE STRENGTHENING OF THE IONIZING ACTION OF Au^{198} INDUCED BY H_2O_2. EXPERIMENTAL STUDY. Rossotto, P.; Stancanelli, V.; Georgacopulo, P.

(Universita, Ferrara, Italy). Minerva Chir., 19: 827-30 (1964).

The behavior of the respiration, aerobic and anaerobic glycolysis was studied in an experimental ascitic tumor (Yoshida's hepatoma) after introduction of ^{198}Au and H_2O_2 into the peritoneal cavity of rats. While simple introduction of H_2O_2 did not modify tumor metabolism, its association with ^{198}Au had a considerable strengthening action on the cancericide ionizing action of the radioisotope. (Excerpta Med., Sect. XXIII, 2: No. 6(June 1965))

38390 FACTORS MODIFYING MUTATION FREQUENCY PATTERNS DETECTED AFTER IRRADIATION OF DROSOPHILA MELANOGASTER MALES. Lefevre, George Jr. (Harvard Univ., Cambridge, Mass.). Mutation Res., 2: 22-8(Feb. 1965).

The frequency of sex-linked recessive lethal mutations detected in matings made immediately after irradiation of 3-day-old males which have mated twice just prior to irradiation is significantly lower than the mutation frequency observed when virgin 3-day-old males are irradiated with the same dose. A similar reduction in mutation frequency was also observed when 7-day-old premated males were irradiated, but the reduction was not so pronounced as in the case of 3-day-old males. The effect of mating prior to irradiation was simply to reduce the number of fully mature sperm present in the male in comparison with the number found in a virgin male of the same age; however, the number of immature sperm was not affected. Therefore, premating decreased the proportion of fully mature to immature sperm present in the male at the time of irradiation. The reduction in mutation frequency that is associated with premating irradiated males can be explained by the higher intrinsic mutability of fully mature as compared with less mature sperm; it cannot be explained by recovery from genetic effects of irradiation. This conclusion is supported by the fact that withholding irradiated virgin 3- and 7-day-old males from mating for 24 or 48 hr also reduced the mutation frequency, but only to a level intermediate between that observed in the first mating immediately after irradiation of virgin males of comparable age, and that observed from matings made 24 to 48 hr later, if in the meantime the males have been allowed to mate repeatedly. The change in frequency of mutations detected at successive intervals after irradiation is a dynamic reflection of the progress of spermatogenesis, as germ cells having different mutabilities because they were at different stages of development at the time of irradiation are sampled one after another. (auth)

38391 ON LETHALS AND THEIR SUPPRESSORS IN EXPERIMENTAL POPULATIONS OF DROSOPHILA WILLISTONI. Magalhaes, L. E.; Brito da Cunha, A.; De Toledo, J. S.; Toledo, S. A.; de Souza, H. L.; Targa, H. J.; Setzer, V.; Pavan, C. (Universidade de Sao Paulo, Brazil). Mutation Res., 2: 45-54(Feb. 1965).

Naturally occurring and radioinduced lethals were studied in experimental populations maintained in population cages. The populations were started with four lethals, two wild and two induced, each of them having frequency of 0.25. The lethals still had frequencies from 0.03 to 0.18 when the populations were 348 days old. Analysis of the lethals showed that all of them were able to survive in homozygous condition. The survival of the flies homozygous for the lethals was due to the presence of recessive suppressors. The proportion of the lethals accompanied by their own suppressors was measured in a sample taken when the populations were 866 days old and varied from 0 to 58.3%. The implication of the presence of suppressors regarding the behavior of lethals in populations were analyzed and the results are discussed. (auth)

38392 VISIBLE MUTATION FREQUENCIES IN DAHLBOMINUS OOGONIA PRODUCED BY ACUTE X-RAYS AND CHRONIC γ-RADIATION. Baldwin, W. F. (Atomic Energy of Canada Ltd., Chalk River, Ont.). Mutation Res., 2: 55-9(Feb. 1965).

In Dahlbominus, haploid males from unmated diploid females exhibited a small but significant difference in frequency of eye-color mutations following acute or chronic irradiation of oogonia. One experiment on quality of radiation did not show any significant difference in frequency of mutations induced by a 2 MVp and 300 kVcp radiation. (auth)

38393 GENETIC EFFECTS OF SUPRA-LETHAL X-RAY TREATMENT OF MALE MICE. Luening, K. G.; Sheridan, William; Froelen, H. (Lab. of Radiation Genetics, Stockholm and Research Inst. of National Defence, Sundbyberg, Sweden). Mutation Res., 2: 60-6(Feb. 1965).

The F_1 sons of male mice (CBA) that had been irradiated with 1092 R x rays were studied. (The fathers had received bone marrow injections following irradiation and regained fertility after some months, thus the F_1 animals had one genome irradiated in the spermatogonial stage.) Dominant lethality and dominant subviability effects were studied for each individual F_1 male in backcrosses to females of the CBA strain. The frequency of recessive lethals was estimated from the results of matings of the F_1 males with their daughters compared with crosses with daughters of other F_1 males. Three males of the total 110 tested showed semi-sterility. The suspected presence of dominant subviability mutations in 10 other males could not be verified in retests. The rate of recessive lethals was calculated to be approximately 10%. (auth)

38394 THE INDUCTION BY X-IRRADIATION OF DOMINANT LETHAL MUTATIONS IN SPERMATOGONIA OF MICE. Sheridan, William (Lab. of Radiation Genetics, Stockholm). Mutation Res., 2: 67-74(Feb. 1965).

Investigation was made of the amount of dominant lethality found among offspring of male mice after irradiation of the spermatogonia with 550 R x rays. A significantly greater rate of death was observed in the x-ray group when compared with the corresponding controls. The effects were constant and continued over a long period of time. The effect was also evident in outcrosses to another strain. No evidence of fluctuations in the results which might indicate intra-tissue selection or clustering was noted. Tests of F_1 sons of the irradiated and control groups presented no differences between the groups. There were no indications of chromosomal effects leading to semi-sterility, or dominant lethal genes with incomplete penetrance producing higher death rates. A higher rate of intra-uterine death was observed among F_1 females of the x-ray group when compared to the control. (auth)

38395 EFFECTS OF ULTRAVIOLET RADIATION ON MAMMALIAN CELLS. I. INDUCTION OF CHROMOSOME ABERRATIONS. Chu, Ernest H. Y. (Oak Ridge National Lab., Tenn.). Mutation Res., 2: 75-94(Feb. 1965).

A quasidiploid (22 chromosomes) clonal cell line of the Chinese hamster was used for investigations of the effects of uv light. The cells grown in monolayer were less than 3 μ thick, permitting ready penetration of uv light. By means of autoradiography, the average generation time was determined as 24 hr, which included 8 hr for S (DNA synthesis), 2–3 hr for G_2 (post-synthesis interphase), and 13–14 hr for G_1 (pre-synthesis interphase) and M (mitosis). Severe cellular damage was induced by uv, resulting in cell death, sterility, delay in DNA synthesis and mitosis, and chromosome aberrations. Various kinds of damage appear to depend both on wavelength and dose. All types of chromatid and chromosome aberrations were induced in the hamster cells by uv at various wavelengths. They can be induced at all stages of the cell cycle, irrespective of DNA synthesis. Within the dose-range tested, aberration frequency increased with incident uv dose. UV-induced chromosome aberrations are non-photoreactivable. Aberration frequency is wavelength-dependent and reaches a broad maximum between 2400 and 2800 Å. Thymidine analog pre-treatment of these cells significantly increases their uv sensitivity as measured by chromosome aberrations. These results suggest that DNA is a site of uv injury which leads to chromosome aberrations, but the possibility cannot be excluded that chromosomal structural proteins also play an important role in the induction of aberrations. Chromosome demolition can be induced most effectively by uv at 2800 Å, but post-treatment with a protein inhibitor (puromycin) following irradiation with uv at

2650 Å produces the same effect. The phenomenon is interpreted as the result of damage to proteins of the cell. (auth)

38396 RADIATION-INDUCED TRANSLOCATIONS IN MOUSE SPERMATOGONIA. Reddi, O. S. (Osmania Univ., Hyderabad, India). Mutation Res., 2: 95(Feb. 1965).

Young CBA male mice, known to be free of translocations, were irradiated with 700 R given to their testes in one exposure. A total of 1010 F_1 males were obtained during the post-sterile period from 100 irradiated fathers. Among the F_1 males, 5 were found to carry a translocation both by genetical (inherited semi-sterility) and cytological (19 elements at meiotic metaphase) criteria. The frequency of translocations was 0.5%. (P.C.H.)

38397 THE LOCATION OF GENES CONTROLLING RADIATION SENSITIVITY IN ESCHERICHIA COLI. Van De Putte, P.; Van Sluis, C. A.; Van Dillewijn, Jeannette; Roersch, A. (National Defence Research Council TNO, Rijswijk, Netherlands). Mutation Res., 2: 97-110(Apr. 1965).

By conjugation between Hfr and F^- strains, the location on the bacterial chromosome of various genes controlling sensitivity to ultraviolet irradiation was determined in Escherichia coli strain B, strain K12S and strain CR 34. On account of their colony-forming ability after ultraviolet irradiation, the radiosensitive mutants bearing the various markers studied appeared to fall into two classes: extremely radiation-sensitive mutants hcr^-, dar_1^-, dar_5^-, and dar_6^-; and strains B_{s-2}, dar_2^-, dar_3^-, and dar_4^- with a radiation sensitivity intermediate between that of the extremely sensitive strains and that of their corresponding wild types. Strains B_{s-2}, dar_2^-, and dar_4^- were able to propagate certain ultraviolet-irradiated bacteriophages, whereas the other mutants hcr^-, dar_1^-, dar_3^-, dar_5^-, and dar_6^- were unable to do so. According to the results of the conjugation experiments each mutant appears to belong to one of three distinct linkage groups. The markers B_{s-2}, dar_3^-, dar_2^-, and hcr^- are located in a region between the markers thr and ile; the markers dar_1^- and dar_6^- are closely linked to gal; the markers dar_4^- and dar_5^- are closely linked to his. In addition the gene phr, that controls the recovery from lethal uv damage by subsequent illumination with visible light (photoreactivation), was found to be closely linked to gal. (auth)

38398 THE RANGE OF ACTION OF GENES CONTROLLING RADIATION SENSITIVITY IN ESCHERICHIA COLI. Mattern, Ina E.; Van Winden, Maria P.; Roersch, A. (National Defence Research Organization TNO, Rijswijk, Netherlands). Mutation Res., 2: 111-31(Apr. 1965).

The range of action of the genes hcr, dar_1, dar_2, dar_3, dar_4, dar_5, and dar_6, which occur in various radiosensitive mutants of Escherichia coli, was studied. From a comparative examination of these mutants and their corresponding wild types it was deduced that all the genes must be involved in the repair of lethal uv damage in DNA. The extremely sensitive mutants hcr^-, dar_1^-, dar_5^-, and dar_6^- showed, in contrast to the wild type, neither host-cell reactivation nor uv reactivation of phage λ. The moderately sensitive mutants dar_2^- and dar_4^- showed appreciable host-cell reactivation but no uv reactivation. The moderately sensitive mutant dar_3^-, on the contrary, showed uv reactivation but no host-cell reactivation. UV irradiation of the wild type and the mutants reduced their capacity to propagate non-irradiated phage λ to the same extent. The mutants were also indistinguishable from the wild type in their ability to propagate various irradiated RNA phages; uv irradiation reduced the capacity of the strains to propagate irradiated and non-irradiated RNA phages to the same extent. The radiosensitivity of F′ particles in the various strains was studied. The F′ particles were far more radiation resistant than the survival of the cells themselves, in the wild type as well as in the sensitive mutants, and appeared to be subject to repair in the wild type. From transduction experiments with an irradiated λ_{dg} lysate, it was concluded that the processes leading to the formation of gal^+ transductants were only slightly influenced by the presence of the hcr and dar_1 genes. (P.C.H.)

38399 LACK OF INTERACTION OF X-RAY- AND NEUTRON-INDUCED CHROMOSOME BREAKS IN BARLEY. Heddle, John A. (Univ. of Tennessee, Knoxville and Oak Ridge National Lab., Tenn.). Mutation Res., 2: 149-55 (Apr. 1965). (ORNL-P-908).

Although it had been found that in Vicia faba x-ray- and neutron-induced chromosome breaks do not interact to form aberrations, it was recently reported that such interaction does occur in barley. The lack of interaction in Vicia, which had been predicted from the linear neutron kinetics for two-break aberrations, was used together with the kinetic studies to estimate the distance over which broken ends of chromosomes could rejoin. The observation that interaction did occur in barley suggested that the rejoining distance was larger in barley than in Vicia, and that, as a result, two-hit neutron kinetics would be found. Barley experiments demonstrated one-hit neutron kinetics and possible two-hit x-ray kinetics for two-break aberrations, and no quantitatively determinable interaction between x-ray- and neutron-induced chromosome breaks. The large one-hit component of the x-ray curve suggests that the rejoining distance may be even smaller in barley than in Vicia. (auth)

38400 GENETIC EFFECT OF INCORPORATED ^{14}C IN DROSOPHILA MELANOGASTER. Purdom, C. E. (Medical Research Council, Harwell, Berks, Eng.). Mutation Res., 2: 156-67(Apr. 1965).

A method is described for the quantitative incorporation of ^{14}C into Drosophila. Recessive lethal mutation frequencies were measured in successive 2-day broods for male and female flies grown on media containing ^{14}C-labeled glucose of specific activities of 0.1 and 0.05 mC/g. Although there was some evidence that incorporated ^{14}C might be excessively toxic to the developing organism, preliminary genetic results suggested that the mutagenic effect of incorporated ^{14}C was due largely to the emitted β-radiation. The possibility remained that a small transmutational genetic effect was not detectable on statistical grounds. The upper limit to such an effect in females was less than 0.01 but in males this level of effect could not be ruled out. No evidence was found for the production of mosaic mutations by the $^{14}C \rightarrow {}^{14}N$ transmutation. (auth)

38401 REVERSAL OF SOME EFFECTS OF GAMMA-IRRADIATION BY THE ETHYL ESTER OF GIBBERELLIC ACID. Mathur, P. B. (Atomic Energy Establishment, Trombay, India). Nature, 207: 212-13(July 10, 1965).

The effects of ^{60}Co gamma irradiation on sprouting retardation in potato tubers and ripening of tomato fruits were studied in tubers and fruits treated with the ethyl ester of gibberellic acid (G.A.). All irradiated, GA-treated potatoes sprouted by the 25th day of storage. Treatment with GA caused an increase in the number of buds growing on the stem-half of each tuber both in irradiated and control lots. Treatment with GA hastened the rate of ripening and increased the rate of decay both in irradiated and control tomatoes. The decay was due cheifly to fungus diseases. (H.G.D.)

38402 EFFECT OF OXYGEN PRESSURE ON RADIOSENSITIVITY OF EHRLICH ASCITES TUMOURS AT VARIOUS INTERVALS AFTER INOCULATION. van den Brenk, H. A. S.; Sparrow, Nancy (Cancer Inst. Board, Melbourne). Nature, 207: 267-70(July 17, 1965).

Experiments were designed to compare the radiosensitivity of the hyperdiploid Ehrlich ascites tumor ELD Lettré (EAT) cell x-irradiated in vitro in the presence of either nitrogen at 1 atmosphere or oxygen at 5 atmospheres absolute pressure (HPO). The method was essentially that described by Deschner and Gray. The results obtained show that the incidence of chromosome aberrations in the hyperdiploid Ehrlich ascites tumor, induced by ionizing radiation in vitro and measured after incubation of the cells in recipient mice for varying times, is highly dependent on the post-inoculation period. In both HPO (5 atmospheres absolute) and in N_2, respectively, the aberration coefficient rises to a peak value and then rapidly decreases as a curvilinear effect. HPO treatments delay division by an addi-

tional ~2 h. The mean oxygen effect factor ranged from 3.7 to 3.2 for 8 hrs to 24 h. A higher oxygen effect factor was noted for cells irradiated during DNA synthesis (S phase). An estimate of the ratio (E_2) of oxygen effect factors for cells in DNA synthesis to that for G_1 cells is 1.4. The oxygen effect factor for X-irradiation in HPO was ~2.3 minimum for cells considered to be mostly in the presynthetic G_1 phase, and ~3.3 for cells in DNA synthesis (S phase). (H.G.D.)

38403 GROWTH OF MAMMARY TUMOURS IN F_1 HYBRIDS. Wallace, A. C. (Univ. of Western Ontario, London). Nature, 207: 309(July 17, 1965).

The decreased incidence of tumor transplant takes in F_1 hybrids was investigated under conditions of low x-radiation dosage. A mammary carcinoma and a mammary adenocarcinoma were irradiated and transplanted into mice. The incidence of successful takes was essentially the same with both tumors and at low and high doses. Results suggest that reduced frequency of takes is not invariable in F_1 hybrids even when very low doses of viable cells are used. (H.G.D.)

38404 SERUM PROTEIN FORMATION OF DONOR TYPE IN RAT-INTO-MOUSE CHIMAERAS. Phillips, Mildred E.; Thorbecke, G. J. (New York Univ., New York). Nature, 207: 376-8(July 24, 1965).

Immunoelectrophoresis and autoradiography were used to demonstrate ^{14}C-amino-acid incorporation into individual serum proteins in a study of an effort to identify the donor serum proteins in rat-into-mouse chimeras. The rat-into-mouse chimeras were produced by intravenous injections of Sprague-Dawley rat bone marrow into CBA or A mice within 4 hrs after 750 to 1000 R doses of whole-body x radiation. Serum samples were prepared from mouse liver and spleen at intervals of 3 to 7 weeks post-irradiation. Sera from mice obtained during the first week following irradiation were found to contain rat hemoglobin-hoptoglobin complex: transferrin appeared in samples taken 2 to 3 weeks after exposure: and γ_1 and γ_2-globulin were demonstrable and α_2-macroglobulin six to seven weeks later. The analysis of tissue culture fluids from liver did not reveal the presence of any specific rat serum protein synthesis, whereas mouse serum proteins were actively synthesized by the livers of most chimeras studied. (H.G.D.)

38405 CELL CYCLE OF MOUSE EMBRYONIC TISSUE UNDER CONTINUOUS GAMMA-IRRADIATION. Wimber, Donald E.; Lamerton, Leonard F. (Royal Cancer Hospital (Surrey Branch), Belmont, Sutton). Nature, 207: 432-3(July 24, 1965).

The cell cycle was studied in the tip of the tail of the embryonic mouse at the 12th to 18th day of gestation in controls and in animals exposed chronically for 5 days to γ radiation at 50 rads/day. Data were similar for both irradiated and control groups. Results showed a cycle time of about 8.5 hrs, one of the shortest times yet observed in mammals. An analysis of the cycle for both series indicated an S period of 6.5 hrs, a G_2 + m/2 of 1 hr, and a G_1 + m/2 of 1 hr, where m represents the duration of mitosis. (H.G.D.)

38406 INFLUENCE OF RADIATION ON OVARIAN MATURATION AND HISTOLYSIS OF PUPAL FAT BODY IN DIPTERA. Monro, J. (Univ. of Adelaide); Bailey, P. T. Nature, 207: 437-8(July 24, 1965).

The effects of x radiation on ovarian development and histolysis of the pupal fat body was studied in Sacus to tryoni that were treated in the pupal stage with 8,000 R of gamma radiation given to: the whole body, the anterior third of the body, or the posterior third of the body. Results were interpreted to mean that radiation blocked an abdominal stimulus, thus indirectly preventing ovarian development. Radiation did not act hormonally and the contention was supported that it directly damaged the ovarian nurse cells, which in turn probably reduced demand on the pupal fat-body and delayed its histolysis. (H.G.D.)

38407 AN IN VIVO CELL SURVIVAL SYSTEM BASED ON THE RECOVERY OF RAT GROWTH CARTILAGE FROM RADIATION INJURY. Kember, N. F. (Royal Free Hospital, London). Nature, 207: 501-3(July 31, 1965).

An in vivo system is described for use in studies of radiation injury and recovery. The system is based on the recovery of the epiphyseal cartilage plate of rats. A dose of approximately 2,000 rads x radiation kills a large proportion of the cells in the cartilage plate but after 10 to 15 days the few surviving cells form cloves that are readily visible in the matrix. These cloves enlarge and coalesce to repopulate the cartilage plate so that the mechanism of endochondral ossification is restored. The number of cloves that arise from cells surviving a given radiation dose can be easily counted 3 to 4 weeks after irradiation. The method gives valid results in studies of dose fractionation and cell survival after acute irradiation. (C.H.)

38408 GENETIC PROPERTIES OF EXOGENOUS DEOXYRIBONUCLEIC ACID AT VARIOUS LEVELS OF DEGRADATION IN DROSOPHILA MELANOGASTER. Fahmy, O. G.; Fahmy, Myrtle J. (Royal Cancer Hospital, London). Nature, 207: 507-10(July 31, 1965).

Homologous DNA extracted from adult Drosophila melanogaster was exposed in the gel state to about 230,000 R γ radiation and immediately injected around the testes of male Drosophila melanogaster. The genetic effects were compared with those obtained using untreated DNA and DNA degraded by ultrasonic treatment. Results showed that DNA at various levels of degradation was decisively active as regards the induction of small chromosome deletions, weakly active for the recessive visibles, but completely inactive for the recessive lethals. Evidence was found that DNA mutagenicity could be produced indirectly through its passive conveyence by the sperm during fertilization and the subsequent induction of mutation in the course of chromosome replication at cleavage. Mutants occurred in the maternal X-chromosome when treatment was restricted to the paternal germ line. Degradation of DNA by γ radiation or ultrasonics did not alter the type of mutations induced, but only increased the mutagenic efficiency as regards the induction of small chromosome deletions. (C.H.)

38409 POTENTIATING EFFECT OF NEONATAL THYMECTOMY ON X-RAY-INDUCED INTERCAPILLARY GLOMERULOSCLEROSIS. Guttman, Paul H.; Bailey, Donald W. (Univ. of California, San Francisco). Nature, 207: 539-40(July 31, 1965).

X irradiation (150 to 900 rads) accelerates the course of intercapillary glomerulosclerosis (IGS), a naturally occurring progressive ageing process in mice, rats, and hamsters. This acceleration effect occurs only in kidney tissue that is directly irradiated and is preceded by a latent period, the duration of which is dependent on age of the animal at exposure. The possibility that an immune mechanism might be involved in the pathogenesis of IGS was investigated using the effects on neonatal thymectomy on the course of x-ray-induced IGS in mice. Results showed that neonatal thymectomy potentiates the effect of x radiation for the development of IGS. There was indication that the immune mechanism in the animals was altered by neonatal thymectomy. (C.H.)

38410 RESTORATION OF IRRADIATED ALGAE AFTER A PERIOD OF DARKNESS. Marcenko, Elena. (Inst. Rudjer Boskovic, Zagreb). Nature, 207: 542-3 (July 31, 1965).

The effects of light and darkness on the survival of Micrasterias truncata after exposure to ^{60}Co γ radiation were studied. Results indicate that treatments that retard growth during the period immediately after γ irradiation increase the survival of algae. (C.H.)

38411 RETARDED EMBRYO SAC DEVELOPMENT IN IRRADIATED CLONES OF MALUS SILVESTRIS HORT. cv. GOLDEN DELICIOUS. Barritt, B. H.; Eaton, G. W. (Univ. of British Columbia, Vancouver). Nature, 207: 546(July 31, 1965).

Seven apple clones, of the Golden Delicious variety, were propagated from buds exposed to 5000 R γ radia-

tion. Pollen abortion was 4.9% in a typical clone and varied in irradiated clones from 10.4% to 84.8%. Blossoms collected at anthesis were examined for embryo sac development. Results suggest that irradiation resulted in retardation of female gametophyte development. A close association was noted between pollen abortion and retardation of embryo sac development. (C.H.)

38412 INFLUENCE OF WATER CONTENT ON THE DELAYED EFFECT OF IRRADIATED WHEAT SEEDS. Mostafa, I. Y. (Atomic Energy Establishment, Cairo). Naturwissenschaften, 52: 131-2(1965).

To investigate the correlation between water content and the delayed effect of radiation, wheat seeds were allowed to attain different water contents by storage for various lengths of time in desiccators containing different vapor pressures. The seeds were then irradiated with 20 kR γ rays and immediately returned to the desiccators for storage. The samples were then germinated and the effect of water content on the delayed effect was evaluated by the seedling height. The results showed that for dry seeds the damage was a very effective function of storage time, but for moist seeds there was a relatively small effect. Storing moist seeds under moist conditions stopped the increase in injury that occurs in storage. At higher relative humidities the effect was completely eliminated and even a growth stimulation was observed. Moist seeds stored under dry conditions have a considerable increase in the radiosensitivity, but dry seeds stored under humid conditions have only a slight but insignificant recovery. (J.S.R.)

38413 ON THE RADIOMIMETIC EFFECT OF IRRADIATED DESOXY-RIBONUCLEIC ACID (DNA_m) ON DROSOPHILA MELANOGASTER. Parkash, Om (Universitaet, Vienna). Naturwissenschaften, 52: 142(1965).

The mutagenic effect of DNA irradiated with a dose of 100,000 R at a rate of 625 R/min on Drosophila melanogaster was investigated. The males from the larva that had grown on irradiated DNA were tested for the presence of sex linked recessive lethals. A sex linked recessive lethal rate of 5.7% was found, and an autosomal recessive lethal rate of 9.6%. In addition a number of visible mutations concerning the eye color, body color, and body size, abdominal malformation, and wing size and form were also detected. The results showed a 30-fold increase for the sex linked lethals and 60-fold increase for the autosomal lethals. (J.S.R.)

38414 THE EFFECTS OF IONIZING RADIATION EMITTED FROM Co^{60} UPON THE FATE OF RETICULOCYTES IN THE PERIPHERAL BLOOD IN RATS. I. THE RELATIONSHIP BETWEEN CHANGES IN IRRADIATION DOSES AND RETICULOCYTE COUNTS. Kumagai, Y. (Nihon Univ., Tokyo). Nichidai Igaku Zasshi, 23: 403-12(1964).

Studies were made on the fate of reticulocytes in the peripheral blood following an external irradiation of rats with γ rays emitted from ^{60}Co. Blood-smear preparations were doubly stained by Schilling's brilliant cresyl blue and Giemsa's method, and a few drops of acetic acid solution were placed on the preparations to allow reticulocytes to be stained more distinctly. Irradiation with 50 R produced a marked increase in reticulocyte counts in about a week. Following irradiation with a dose of 600 R there was a sudden decrease in reticulocyte counts and in red cell counts. After irradiation with 200 to 400 R reticulocyte and red cell counts underwent a temporary decrease, and then returned to the normal values. Thus, the reticulocyte counts varied according to the irradiation dose. (Excerpta Med., Vol. 2, (July 1965))

38415 A CONVENIENT ^{137}Cs UNIT FOR IRRADIATING CELL SUSPENSIONS AND SMALL LABORATORY ANIMALS. Cunningham, J. R.; Bruce, W. R.; Webb, H. P. (Univ. of Toronto). Phys. Med. Biol., 10: 381-4(July 1965).

A ^{137}Cs unit for irradiating cell suspensions and small laboratory animals is described. A 25 cm diameter × 4 cm high container is placed in an opening in a lead drawer and is moved midway between two 1000 Curie ^{137}Cs sources. Lead compensating filters above and below the capsule hold the field to 116 ± 4 rads/min within the container and the lead shielding of the unit is sufficient to permit its use in an unshielded laboratory. (auth)

38416 FAR-RED-INDUCED MITOTIC DELAY AND THE APPARENT INCREASE OF X-RAY INDUCED CHROMATID ABERRATIONS IN TRADESCANTIA MICROSPORES. Ma, Te Hsiu; Wolff, Sheldon (Oak Ridge National Lab., Tenn.). Radiation Botany, 5: 293-8(Sept. 1965). ORNL-P-461).

Experiments were carried out showing that far-red radiation given in conjunction with x-rays to Tradescantia microspores, induces a mitotic delay that shifts the arrival of cells at metaphase. Since S and G_2 are parts of the cell cycle that are not uniformly sensitive to x-rays, the shifts can lead to an apparent synergistic effect of far-red radiation and x-rays in the induction of chromatid aberrations. This is only true, however, if cell samples are taken at a fixed time after x-irradiation. When many samples are taken at successive times to characterize the changes in sensitivity, the apparent synergism is seen to be merely a reflection of the shift. The use of far-red radiation to delay mitosis and, thus, to allow a recovery from x-ray-induced pycnosis has allowed the characterization of the changes in radiation sensitivity as the cells progress through the cell cycle towards metaphase. There are two peaks of sensitivity. The one closer to metaphase is usually not seen because of the radiation-induced pycnosis. (auth)

38417 RADIATION-INDUCED INCREASE IN H^3-VALINE INCORPORATION BY THE CHROMOSOMES OF VICIA FABA. Alvarez, M. R. (Brookhaven National Lab., N. Y.). Radiation Botany, 5: 299-305(Sept. 1965). (BNL-8791)

Germinating seeds of Vicia faba were divided into three groups. Group 1 was irradiated with 1000 R of x-rays while immersed in an H^3-valine solution and remained in the isotopic solution during the post-irradiation period in which chromosomal restitution is known to occur. Group 2 was irradiated with an equal dose while immersed in water and transferred to an H^3-valine solution after the restitution period. Group 3 served as a control and was immersed in tritiated valine for a period of time equal to the restitution period but was not irradiated. Grain counts were made over interphase nuclei before the initiation of cell divisions in the primary root tip and compared between irradiated and non-irradiated cells. Grain counts over the chromosomes and over the cytoplasm were scored at the first mitotic divisions (X1) of the cells of the primary root and compared among the three treatments. Germinating seeds were also irradiated with x-ray doses ranging from 300 to 1000 R while immersed in H^3-valine and remained in the isotopic solution during the restitution period. Grain counts over X1 metaphase chromosomes were scored and a dose response curve was constructed. Chromosomes from tissue irradiated with 1000 R while immersed in the tritiated valine solution and which remained immersed during the restitution period (Group 1) showed an approximately 2.5 times greater labeling than those from non-irradiated controls (Group 3). Grain counts over chromosomes from tissue irradiated with 1000 R and transferred to the H^3-valine solution after the restitution period (Group 2) were not significantly different from the non-irradiated controls. The level of cytoplasmic labeling did not change significantly after irradiation with 1000 R of x rays. Grain counts over chromosomes from tissue exposed to doses ranging from 300 to 1000 R increased exponentially with dose. (auth)

38418 GROWTH INHIBITION IN CEREAL SEEDLINGS INDUCED BY GAMMA IRRADIATION AT DIFFERENT OXYGEN TENSIONS. Dumanovic, J. (Inst. for Application of Nuclear Energy in Agriculture, Veterinary Medicine and Forestry, Belgrade); Ehrenberg, L. Radiation Botany, 5: 307-19(Sept. 1965).

The reaction of barley and rye seeds to anaerobic and aerobic γ-irradiation was studied, with special emphasis on such properties where the action of neutrons was found qualitatively different from that of (aerobic) γ- or x-irra-

diation. The reaction of anaerobic γ-irradiation was found similar to that of neutrons, and unlike that of aerobic γ-irradiation, in the following respects: a more linear dose dependence of the radiation induced growth inhibition of seedlings; a relatively greater inhibition of root growth; a smaller variation of seedling heights; the coefficient of variation of seedling height following anaerobic γ-irradiation or neutron irradiation is equal to that of the unirradiated control samples; after aerobic γ-irradiation (in air or in high pressure oxygen) the coefficient of variation at 50 per cent growth reduction is 2 to 3 times the control value; and no influence of the water content of the seeds on their radiation sensitivity, within the range of water contents investigated (6–20%) (indicated in comparison of different experiments). The findings are discussed in the light of investigations of especially Howard-Flanders and Caldecott, demonstrating that in the absence of oxygen, the γ-irradiation is active exclusively through high LET segments of the total track length. RBE of fission neutrons relative to anaerobic γ-radiation is found to be around 50. (auth)

38419 GENETIC VARIABILITY IN QUANTITATIVE CHARACTERS INDUCED BY THERMAL NEUTRON TREATMENT OF DIPLOID, TETRAPLOID, AND HEXAPLOID OAT SEEDS. Gonzalez, C.; Frey, K. (Iowa Agricultural and Home Economics Experiment Station, Ames). Radiation Botany, 5: 321-35(Sept. 1965).

Seed lots from five oat varieties were treated with thermal neutron irradiation, to provide materials for comparing the relative magnitude of variability and the types of mutations induced at different ploidy levels. Forty lines were derived from each irradiated population, and a like number from check populations, in a replicated experiment. Plants were measured for heading date, plant height, number of branches per panicle, flag-leaf length, weight per 100 seeds, seeds, groat width, and groat length. Irradiation caused a significant shift in the population means, and variability was increased for most of the attributes. In general, variability was shifted in both plus and minus directions from the check population means. At the hexaploid level, the mean induced variability from all attributes as measured by genetic coefficients of variation was as great as or greater than that at the tetraploid and diploid levels. Comparisons of the characteristics of the seed-attribute frequency distributions from irradiation derived and check populations tended to show that: mutations occurring in diploid lines produce more discrete expression than those occurring in hexaploids; and a larger portion of hexaploid than diploid lines carry mutations which show some degree of expression. The presence or magnitude of genetic variability induced was influenced by the attribute studied, and the genotype treated. No genetic variability was induced for number of branches (except in Pusa variety) and for flag-leaf length; among the hexaploid varieties, Pusa showed nearly twice as much relative variability as the other two varieties. The genetic correlations indicated that the types of mutations induced by irradiation in hexaploids are similar to those induced in diploids; thus, induced genetic variability in hexaploids should be as heritable as that in diploids. Thermal neutron irradiation increased sterility in two of the treated populations. However, there was no evidence that sterility contributed to the apparent induced variability. Intrapopulation correlations, calculated between groat width and sterility, were not significant. (auth)

38420 THEORETICAL STUDIES ON THE METHODOLOGICAL PROCEDURES OF RADIATION BREEDING. VI. APPLICABILITY OF THE ONE-PLANT-ONE-GRAIN METHOD ETC. TO BREEDING IN CASE OF INCLUDING TWO OR MORE GENE MUTATIONS IN AN X_2-PLANT. Yoshida, Yoshio (Kyushu Agricultural Experiment Station, Chikugo, Japan). Radiation Botany, 5: 349-55(Sept. 1965).

Let k be the number of desirable mutated recessive characters in one X_2-plant when monogenic mutation corresponds to the occurrence of one mutated character. Whether or not the superiority of the one-plant-one-grain method (method C), the one-plant-two-grain method (method D) and the one-plant-three-grain method (method E) established for k = 1 holds for k = 2 – 4, is examined from a theoretical point of view. It is made clear that the efficiency of methods C, D and E decreases with the increase of k. When k = 2 and 3, those methods, with dense planting in X_1, will be useful. But methods employing four or more X_2-seeds from an X_1-ear will be rather inefficient when k = 2 but may be useful in some cases for k = 3. When k = 4, the efficiency of selecting a desirable mutant varies little for any number of X_2-seeds taken from an X_1-ear. Since most gene mutations correspond to k = 1, breeders must not have a doubt for the superiority of methods C, D and E when major gene mutation is applied to the practice of radiation breeding. (auth)

38421 BIOLOGICAL EFFECTS OF IONIZING RADIATION. Avargues, M. Rev. Hyg. Med. Sociale, 17: 202-14(1964).

A review is presented on the biological effects of external or internal or cutaneous radiation exposure. The basic underlying mechanisms and the general characteristics of its effects of living material are defined. (TCO)

38422 INFLUENCE OF POST-RADIATIONAL INCUBATION CONDITIONS ON X-RAY SURVIVAL OF DIPLOID YEAST. Bacchetti, Silvia; Elli, Raffaella; Falchetti, Roberto; Mauro, Francesco (Universita, Rome and Centro Nazionale per la Radiobiologia Applicata a Problemi Agricolo-Alimentari (CNR), Rome). Ric. Sci. Rend., Sez. B, 6: 39-40(Jan.-Mar. 1965). (In Italian).

Irradiation experiments were performed on diploid yeast cells to investigate the survival variations in different incubation conditions of the cells after x ray treatment. Restoration of cell viability occurs upon delayed plating when the cells are stored in suitable environmental conditions during the interval between irradiation and plating. X rays (180 kvp) at a dose rate of about 1000 R/min were used. The survival variations upon delayed plating observed included: after a single dose of 30 kR, an initial decrease, then a further increase up to a constant value higher than the survival value observed immediately after the irradiation; after a single dose of 60 kR, a continuous increase of the survival up to the constant value without any marked initial decrease. These survival kinetics, therefore, show the occurrence of the restoration of cell viability, that is of the recovery of the cells from x ray lethal damage. The general trend of this phenomenon seems to be not depending on the different conditions of incubation (as temperature and medium composition) and growth (growth phase and reproductive synchrony of the cells), which affect only the time interval necessary to the restoration. Only the incubation of resting cells in complete growth medium seems to reduce the initial survival decrease after the dose of 30 kR. Experiments carried out on cells irradiated with two fractions of dose (30 kR + 30 kR = 60 kR), split by a period of time sufficient to obtain a complete recovery from sublethal damage (already observed in diploid yeast show that the survival variations of these cells upon delayed plating are similar to those of cells irradiated only with a single dose of 30 kR, corresponding to the 2nd fraction. (tr-auth)

38423 EFFECT OF RADIATION OF γ ^{60}Co ON VITAMIN CONTENT IN FLOUR. Wozniak, Jan. Roczniki Panstwowego Zakladu Hig., 16: 183-8(1965). (In Polish).

Investigations on the effect of ^{60}Co γ radiation on vitamin B_1, B_2 PP and tocopherols in whole rye flour were performed. Determinations were made directly after exposure of the flour samples to different doses of radiation and after 40 days of storage. Fluorometric method was applied for vitamin B_1 and B_2 determination. Bromocyanic method for vitamin PP was used. Total tocopherol content was determined with modified Emmeric-Engel method. Thiamine was mostly susceptible to radiation while niacin appeared to be of doubtful susceptibility. After radiation in doses of 1.6×10^5R the highest loss of thiamine consisted of 21% after 39 days of storage, while only 7% of tocopherols was lost after 40 days storage. Lower doses of radiation did not reveal any loss of tocopherols. A connection was observed between the loss of thiamine and tocopherols and intensity

of oxidative process in fats of flour radiated with doses of 1.6×10^5R. (auth)

38424 STUDIES ON THE EFFECT OF IONIZING RADIATION UPON THE MITOCHONDRIAL STRUCTURE AND FUNCTION. I. EARLY POST-IRRADIATION STRUCTURAL AND FUNCTIONAL CHANGES OF LIVER MITOCHONDRIA IN WHOLE BODY IRRADIATED MICE. Yang, Fu-yu; Lin, Zhi-huan; Li, Jin-zhao; Li, Sheng-guang (Inst. of Biophysics, Academy of Sciences, Peking). Shih Yen Sheng Wu Hsueh Pao, 9: 261-9(1964).

White male mice about 2 months old received 700 R of x rays at a dose rate of 37.5 R/min. The characteristics of swelling and the degree of coupling of oxidative phosphorylation, respiratory control, and P/O ratios of mitochondria in early post-irradiation stages were then examined. The spontaneous swelling of liver mitochondria isolated from mice 30 mins and 1 hr after exposure was markedly increased. This returned essentially to normal within 4 hours. The thyroxine or Ca^{++} induced mitochondrial swelling ½ hr also increased after exposure; again this change was not observed 4 hr after irradiation. The initial optical density per mg liver mitochondrial protein of normal and irradiated animals was approximately identical. On account of these observations it may be suggested that a slight alteration in structural integrity is involved in the early post-irradiation stage. Concurrent with the investigation on the characteristics of mitochondrial swelling, the biochemical integrity of mitochondria, respiratory control index and P/O ratios following irradiation were also determined. The respiratory control index of mitochondria fell 30 min after exposure and reached a minimum 1 hour after irradiation. A slight depression of P/O ratios appeared only 1 hour after irradiation. Within 4 hours both had recovered to control values. Besides the changes of swelling pattern, parallel with the biochemical lesion, decrease and subsequent increase in the protein content of the mitochondrial suspension per gm of fresh liver tissue were noted. From the results it appears that the mitochondria of mouse liver are transiently damaged both structurally and functionally by irradiation in vivo, but they are soon restored almost to pre-irradiation levels. (Excerpta Med., Sect. XXIII, 2: No. 6(June 1965))

38425 PROLONGATION OF RENAL HOMOGRAFT FUNCTION BY LOCAL GRAFT RADIATION. Kauffman, H. Myron Jr.; Cleveland, Richard J.; Dwyer, James J.; Lee, H. M.; Hume, David M. (Medical Coll. of Virginia, Richmond). Surg. Gynecol. Obstet., 120: 49-58(Jan. 1965).

Local graft irradiation, as the sole method of immunosuppression, was employed in mongrel dogs receiving kidney homografts. Although there were no permanent survivors, significant prolongation of functional survival was achieved without either hematopoietic depression or generalized immune system suppression. Local irradiation of the donor kidney was performed with 2000-kv x rays at a dose rate of 100 R/min to doses of 150 or 200 R/day. Some animals were sacrificed after 30 days, and the kidney was examined grossly and histologically. Treated animals were divided into six experimental groups according to radiation dose and day of administration of the first dose of radiation. Doses were given at 2- or 3-day intervals until the animal received 6 doses or died. Dogs given 150 R beginning on the day of transplantation, showed a mean survival time of 23.4 days compared with 9.9 days for the control group, and this was considered to be highly significant. None of the other treated groups had prolongation of the mean survival time. Transplants functioning over 20 days were considered as having prolonged survival. Eleven out of 47 treated animals survived over 20 days. The highest percentage of 20-day survivors was obtained in the groups which received the first dose of radiation on the day of transplantation (day 0). This was 36.3% for 150 R and 28.5% for 200 R. Another criterion used for assessment of the effect of local radiation on function of kidney homografts was measurement of the animal's blood urea nitrogen. The ability of local radiation to reverse blood urea nitrogen elevations was found. (TCO)

38426 PATHOLOGICAL EFFECTS OF RADIATION INJURIES. Grigar'yan, M. S. Tr. Evevansk. Zootekhn. Vet. Inst., No. 25, 73-9(1962). (In Russian)

Studies of histamine-histaminase levels in the blood of irradiated animals showed an initial increase followed by a drop. In animals demonstrating a progressive drop in the histamine level, radiation sickness is usually lethal; while in animals with tendencies to blood level normalization, a higher percentage survives. Blood histaminase activity was strongly reduced by irradiation; pain reduced it still further. Changes in general protein and serum protein levels appeared at early stages of sickness. Pain during sickness raised the level of serum protein, but it remained below normal. (R.V.J.)

38427 RADIATION EFFECTS ON SULFHYDRYL (SH) GROUP OF ALBUMIN BLOOD STRUCTURES. Grigor'yan, M. S.; Aralova, G. A. Tr. Erevansk. Zootekhn. Vet. Inst., No. 25, 81-4(1962). (In Russian).

Studies of radiation effects on sulfhydryl groups (SH) in blood albumin showed that the SH level in pigs varies from 1.20 to 1.70 mg % and in rabbits from 0.58 to 1.71 mg %. Pain before exposure generally lowered the SH level. During radiation sickness the SH level in albumin is depressed, rising as the clinical picture improved. The radiosensitivity of SH groups during pain varied, in some animals the level was depressed and in some, increased. (R.V.J.)

38428 THE INFLUENCE OF IONIZING RADIATION ON THE ANTITUMORAL EFFECTS OF KRUTSIN ANTIBIOTIC. Kolomina, S. M.; Roskin, G. I. Vestn. Mosk. Univ., Ser. VI: Biol., Pochvoved, No. 4, 10-17(1964). (In Russian)

Clinical studies indicated that the antibiotic cruzine (from Trypanosoma cruzi) is nontoxic and acts selectively on malignant neoplasms. The potential synergistic effect of this antibiotic, used jointly with x radiation was investigated in 239 male mice. Sarcoma 180 from donor mice was subcutaneously grafted on the experimental animals. One group of mice was treated with 20 to 25 units of cruzine per day and by localized irradiation of the tumor, while the three control groups were exposed to one, the other, or none of these agents. The animals were shielded, except at the site of the tumor during the 60 to 90 R/minute irradiation which was repeated in 48 hour intervals. The results indicated that the joint use of cruzine and x radiation in total doses of 600, 800, and 1000 R exerts a more marked antitumoral action than either the antibiotic or the radiation alone. (TTT)

38429 ON THE FORMATION OF TOXIC (HEMOLYTIC) LIPIDS IN ANIMALS SUFFERING FROM RADIATION INJURIES. Kakushkina, M. L. Vestn. Mosk. Univ., Ser. VI: Biol., Pochvoved., No. 5, 11-17(1964). (In Russian)

The toxic compounds formed in animals exposed to ionizing radiation were evaluated on the basis of the hemolytic (cytotoxic) factor which is represented by an unsaturated fatty acid. In order to clarify the problem whether this hemocytologic factor pre-exists in vivo in the tissues or is formed in the irradiated animals during the testing process, its condition of formation was investigated, attempting to determine also the effect of the amino mercaptan type radioprotective compounds on the activity of the hemolytic products. Rabbits were exposed to 100 and 300 R of γ radiation; in order to eliminate the effect of foodstuffs, the irradiated animals were not fed. The hemocytotoxic factor was determined by means of a modified arythrogram method. It was found that the activity of the hemotoxic compounds in the liver of the exposed animals was increased. These compounds could be found in the lipid fraction of the tissue after precipitation of the phospholipids. The hemotoxic activity which is enhanced by the oxidation of the lipids, was recorded without autolysis of the tissue. The phospholipids were found to possess antihemolytic properties, as compared with the hemotoxic compounds. Cysteamine exerts a protective action against the toxic effect of the liver lipids. (TTT)

38430 ON THE EFFECTS OF IONIZING RADIATION ON GLADIOLAS. Dryagina, I. V. Vestn. Mosk. Univ., Ser. VI: Biol., Pochvoved., No. 5, 46-56(1964). (In Russian)

Following up previous studies on the effect of ionizing radiation on bulbs, it was found in experiments carried out with gladiolus bulbs planted in a γ field that exposure to 10 kR results in a depression of the growth rate with respect to the unirradiated plants. Great differences were observed in the radiation sensitivity of the various subspecies of gladiolus. The bulbs withstood chronic exposure in the γ field much better than a single high dose; a total dose of 74.8 kR was tolerated without any marked lowering of the germinating ability. The radiation reduced the number of new bulbs formed both during the year of exposure and during following years. The irradiation had a harmful effect on the normal course of physiological and biological processes, interfering with the activity of the oxidation-reduction ferments, photosynthesis, and respiratory processes. Doses up to 5 kR changed only the shape of the plant, causing the formation of double-petal, stamen-free blooms and changes in the coloration of the petals. (TTT)

38431 REACTIVE CHANGES IN THE ORGANS OF THE EAR, NOSE AND THROAT OF RABBITS WITH ACUTE RADIATION SICKNESS COMPLICATED BY BLOOD LOSS. Filatov, V. F. Vestn. Oto-Rino-Laringol., 6: 81-6(1964).

The dynamics of the distribution of ^{32}P in the organs of the ear, nose, and throat and the ability of the tissues to adsorb a dye (neutral red) 3, 5, and 7 days after irradiation and after a combination of irradiation and blood loss were investigated in 62 male rabbits. The experimental method is described. After three days nearly all the organs tested reacted to irradiation by an increase in the accumulation of ^{32}P, but later, despite the fact that the activity of the blood remained low, there was a decrease in the accumulation of ^{32}P by the salivary gland, and the content of ^{32}P in the inferior nasal concha (in 9%) fell below the control-value. After 7 days a considerable decrease in the activity of most organs was observed. The increased accumulation of ^{32}P in the organs and the decrease in its blood concentration in the irradiated animals demonstrates the injurious action of radiation on the organs of the ear, nose, and throat. Acute blood loss by irradiated animals led to an increase in the ^{32}P content in the organs of the ear, nose, and throat, and prolonged the period of decrease in the sorptive properties of the tissues in relation to ^{32}P to 7 days, while the quantitative accumulation of ^{32}P by these animals did not fall below the normal value in the individual organs, as was found in the animals subjected to irradiation only. Blood loss evidently caused changes in tissue metabolism, altered their reactivity, mobilized their protective and compensatory powers, and thus delayed the manifestations of the injurious action of radiation. (Excerpta Med., Vol. 2, (July 1965))

38432 BIOLOGICAL EFFECTS. Demin, N. N.; Lebedinskii, A. V. pp 116-22 of Radiation Medicine. New York, The Macmillan Co., 1964.

The biological effects of radiation on separate components of living materials are discussed. (P.C.H.)

38433 THE PATHOLOGY OF RADIATION SICKNESS. Gorizontov, P. D. pp 123-228 of Radiation Medicine. New York, The Macmillan Co., 1964.

Information is included on: development of acute radiation sickness; pathogenesis; nervous system; metabolism; problem of toxemia; blood system; hemorrhagic syndrome; cardiovascular system; respiratory organs; gastrointestinal tract, liver, and kidneys; endocrine glands; and reaction of the organism. (P.C.H.)

38434 INFECTION AND IMMUNITY IN IRRADIATED ANIMALS. Klemparskaya, N. N.; Petrov, R. V. pp 229-45 of Radiation Medicine. New York, The Macmillan Co., 1964.

The process of infection, endogenous infection, exogenous infection, and immunological response of the irradiated animal are discussed. (P.C.H.)

38435 REMOTE AFTER-EFFECTS OF IONIZING RADIATION. Zakutinskii, D. I. pp 273-80 of Radiation Medicine. New York, The Macmillan Co., 1964.

Late effects of radiations and radioisotopes in animals are discussed. These late effects may affect the response to various external stimuli such as chemical substances, physical factors, and infectious agents. Changes in vascular permeability reproduction, and sexual function are also discussed. (P.C.H.)

38436 THE PATHOLOGICAL ANATOMY OF RADIATION DAMAGE. Krayevskii, N. A. pp 316-47 of Radiation Medicine. New York, The Macmillan Co., 1964.

The pathology and anatomy of radiation sickness in animals is discussed. Studies of the pathological and anatomical changes occurring during the course of the whole disease show that all vital functions are profoundly disturbed, and that many morphological changes occur that affect chiefly the hemopoietic tissue and the gastrointestinal tract, and that a hemorrhagic diathesis develops. Also, during the whole course of the disease as far as its rate of development is concerned, the widespread nature of the damage, and the varied interrelations of the symptoms all indicate a profound impairment of nervous activity and very great changes in its trophic function. The pathological and anatomical changes caused by contamination with radioactive substances are more varied than those that are due to externally applied radiation. (P.C.H.)

38437 BIOLOGICHESKOE DEISTVIE NEITRONNOGO IZLUCHENIYA. (Biological Effects of Neutron Radiation). Gorodetskogo, A. A. (ed.). Kiev, Naukova Dumka, 1965. 104p. (In Russian).

Fourteen sections are included; separate abstracts were prepared for each. (P.C.H.)

For abstracts of individual sections see: 38438, 38439, 38440, 38441, 38442, 38443, 38444, 38445, 38446, 38447, 38448, 38449, 39042, and 39043.

38438 THE RBE OF FAST NEUTRONS. Gorodetskii, A. A.; Kirichinskii, B. R.; Chebotarev, E. E. p.3-13 of Biologicheskoe Deistvie Neitronnogo Izlucheniya. Kiev, Naukova Dumka, 1965. (In Russian).

Three groups of rats were exposed to fast neutrons. The animals were irradiated in the horizontal channel of a VVR-M reactor where the gamma radiation background was 15%. The duration and intensity of radiation was the same for all three groups. However, the first group of rats was irradiated in containers which allowed complete freedom of movement. The second group was placed so that the longitudinal axis of the body was parallel to the neutron beam, and the third group was placed with the longitudinal axis at right angles to the beam. After one month, mortality for the first group was 56.5%, for the second group – 10%, and for the third group – 83%. The difference in mortality percentages was attributed to the fact that the intensity of a neutron beam quickly dissipates even after passing through relatively thin layers of biological tissue. The results indicate the need for fixing animals in a rigid position to obtain consistent results when determining the RBE of various types of radiation. The physical conditions of radiation exposure, such as temperature, humidity, and atmosphere, must also be constant, as well as the time of day when irradiation takes place. Finally, the family and species of animal and the test for determining radiation injury must be controlled. (ATD)

38439 IRRADIATION OF ANIMALS WITH FAST NEUTRONS AND MEASUREMENTS OF TISSUE DOSES IN A NUCLEAR REACTOR. Kirichinskii, B. R.; Levchuk, Yu. N.; Pasechnik, V. M.; Tatsii, Yu. A. p.14-23 of Biologicheskoe Deistvie Neitronnogo Izlucheniya. Kiev, Naukova Dumka, 1965. (In Russian).

Requirements for irradiating biological objects with fast neutrons are listed. A system for shifting biological preparations in the reactor is illustrated. It was observed that there is no direct relationship between the reactor power and tissue dose. When animals are irradiated with fast neutrons, the final biological effect depends on the distribution of absorbed radiation in the organs and tissues. Determination of the relative depth distribution of the dose can be easily determined by a method based on the deceleration of neutrons in hydrocarbon materials. Materials and principles applied to making tissue equivalent phantoms and measuring radiation doses in them are discussed. (ATD)

38440 THE EFFECT OF NEUTRON RADIATION ON SOME PHYSICAL AND CHEMICAL PROPERTIES OF THE BLOOD. Chebotarev, E. E.; Kirichinskii, B. R.; Shur'yan, I. M. p.24-9 of Biologicheskoe Deistvie Neitronnogo Izlucheniya. Kiev, Naukova Dumka, 1965. (In Russian).

Research on the physical and chemical properties of the blood of neutron irradiated animals included studies of the average diameter of erythrocytes, the hemolytic stability of erythrocytes, and the morphological composition of the peripheral blood. White rats weighing 130–150 g were irradiated with fast neutrons (doses of 400 and 500 Rad) and then examined periodically for a month after irradiation. The average diameter of erythrocytes was measured optically (by the diffraction method) on a special unit equipped with a camera. The diameter of erythrocytes was found to decrease at first and then increase. Anisocytosis, which is especially clear on photographs of diffraction patterns, was usually observed at the peak of radiation sickness. Comparison was made of the hemolytic stability of the erythrocytes of white rats irradiated with x rays (dose 600 R) and neutrons (comparable dose). Neutrons caused changes in the morphological composition of the peripheral blood. The content of hemoglobin, erythrocytes, reticulocytes, and leukocytes had dropped considerably by the 8th–12th day after irradiation; none had returned to the initial level 50 days after irradiation. Cells with qualitative degenerative changes were also found. It was concluded that LD_{50} of neutron and x radiation cause the same type of changes in the peripheral blood and in the kinetics of hemolysis of erythrocytes. Some differences were noted in the degree and depth of the reactions investigated, in the periods of approach of these changes, and in the severity of radiation sickness. Neutron irradiated animals showed more severe damage to the gastrointestinal tract, earlier occurrence of rhinitis and conjunctivitis, and sharper weight loss. (ATD)

38441 PECULIARITIES OF THE EFFECTS OF NEUTRON AND X RADIATION ON THE HEMATOPOIETIC AND CARDIOVASCULAR SYSTEMS. Shur'yan, I. M.; Ryabova, E. A.; Rudakov, N. P. p.30-42 of Biologicheskoe Deistvie Neitronnogo Izlucheniya. Kiev, Naukova Dumka, 1965. (In Russian).

The comparative effects of x rays and neutrons in biologically equivalent doses on the hematopoietic and cardiovascular system of 200 rats were studied. The 200 rats weighed an average of 140 g. Irradiation took place in the horizontal channel of a nuclear reactor. In the first series of tests, rats were exposed to 400-Rad doses (reactor power, 4.0 Mw) of fast neutrons and 600-R doses of x rays with a radiation duration of 23.6 min. In the second series, animals were irradiated with a fast neutron dose of 175 Rad (reactor power, 8 Mw), in the third series, with 200 Rad (10 Mw), and in the fourth series, with 800 R. The morphological content of peripheral blood, erythrocyte resistance, and electrocardiograms were studied 3 times before and 4, 8, 12, 16, 20, 24, and 30 days after irradiation. It was concluded that fast neutrons differed from x rays in their biological effects, evoking more severe changes in the content of the blood (reticulocyte content, general leukocyte quantity, absolute number of lymphocytes and neutrophiles, and thrombocyte quantity). Recovery from the effects of neutrons took longer than recovery from x rays. The blood indexes of irradiated animals were not normalized even after a month. Erythrocyte stability was more sharply lowered, equilibrium processes were more noticeably altered, and qualitative changes in erythropoiesis were greater as a result of neutron irradiation. Finally, fast neutrons not only evoked dystrophic changes in the cardiovascular system as did x rays, but produced injuries to cardiac muscle. Data are tabulated. (ATD)

38442 THE EFFECTS OF NEUTRON IRRADIATION ON THE FUNCTIONAL CONDITION OF THE THYROID GLAND. Sivachenko, T. P. p.43-51 of Biologicheskoe Deistvie Neitronnogo Izlucheniya. Kiev, Naukova Dumka, 1965. (In Russian).

The effects of fast neutrons in doses of 175, 200, and 300 Rad on the functional state of the thyroid gland of 144 white rats were investigated. The animals were irradiated in the horizontal channel of a nuclear reactor specially constructed for the irradiation of biological objects. Thermal neutrons were absorbed by a special filter and background gamma radiation did not exceed 20%. To assess the condition of the thyroid gland, oxygen consumption, the accumulation of iodine-131 in the thyroid 2–24 hr after administration, in urine after 1 day, and the amount bound to blood serum protein were tested. Iodine was injected interperitoneally. It was concluded that the effects of neutrons should be determined 3, 6, and 9 months after irradiation because other investigations have shown that more pronounced changes occur in the organism long after exposure. One observer noted that mice that were still alive a month after exposure to neutrons ($LD_{50/30}$) died much later. The results indicated that the thyroid gland is extremely sensitive to fast neutrons and that functional shifts depend on the radiation dose and the time the organ is examined. A neutron dose of 300 Rad inhibits the functional state of the thyroid 1 day after exposure while doses of 175 and 200 Rad increase its activity after 1 and after 10 days. It was noted that thyroid activity was lowered 30 days after exposure to 200 Rad. Data are tabulated. (ATD)

38443 THE FUNCTIONAL STATE OF THE ADRENAL CORTEX DURING IRRADIATION WITH FAST NEUTRONS. Sivachenko, T. P. p.52-8 of Biologicheskoe Deistvie Neitronnogo Izlucheniya. Kiev, Naukova Dumka, 1965. (In Russian)

The effects of neutron irradiation on the functional condition of the adrenal cortex was studied by determining the amount of ascorbic acid in the adrenals, eosinophils in the blood, and 17-ketosteroids in the urine. Male white rats weighing 120–150 g were irradiated with neutrons (doses 175, 200, and 300 Rad) and then examined one day and ten days after irradiation. Experiments showed that irradiation with fast neutrons alters the content of ascorbic acid and dehydroascorbic acid in adrenal tissue. Other indications of stimulation of the adrenal cortex in the first days after irradiation were a decrease in the amount of ACTH, an insignificant increase of steroids in the urine, and a decrease in the amount of eosinophils. Ten days after irradiation, however, depression of the activity of the adrenal cortex was noted, the content of ascorbic acid had been restored, and the amount of steroids had decreased. However, the number of eosinophils had not returned to the initial level at the end of the experiment. It was concluded that the adrenal cortex reacts to LD_{50} neutron irradiation and lethal doses (300 Rad). (ATD)

38444 MORPHOLOGICAL CHANGES IN SOME ORGANS OF WHITE RATS DUE TO NEUTRON IRRADIATION. Sivachenko, T. P.; Estrin, I. M. p.59-61 of Biologicheskoe Deistvie Neitronnogo Izlucheniya. Kiev, Naukova Dumka, 1965. (In Russian)

Morphological changes in selected organs of white rats were studied after various doses of neutron irradiation. Thirty-two male white rats, weighing 110–140 g, were irradiated with fast neutrons in a specially equipped nuclear reactor (lethal dose–300 Rad; sublethal doses–175 and 200 Rad). Symptoms of radiation sickness in rats subjected to a sublethal radiation dose (200 Rad) included noticeable sluggishness, diarrhea, and in half the animals, rhinitis, conjunctivitis, and loss of weight. Adynamia, loss of appetite, and then diarrhea and weight loss preceded the death (on the 9th day) of animals exposed to a lethal radiation dose. Macroscopic examination showed irregular blood supply in internal organs and some focal hemorrhages in subcutaneous tissue and the lungs. Changes in brain tissue, bone marrow, lymph system, spleen, lungs, gastrointestinal tract, lives, testes, and pituitary, adrenal, and thyroid glands are described. The results indicated that, in general, changes in several organs of rats subjected to neutron irradiation correspond to changes during other types of irradiation. Unusual changes with neutron irradiation are proliferation of cells in the interalveolar septa of the lungs and proliferation of Kupffer cells in the liver. In both cases metabolic disturbances may be responsible for the changes. (ATD)

38445 SEROLOGICAL AFFINITY OF PERFRINGENS RADIATION MUTANTS. I. STUDIES OF ANTIGEN STRUC-

TURE BY THE AGGLUTININ ADSORPTION METHOD. Pasechnik, A. M.; Tulina, G. G. (Inst. of Microbiology, Academy of Sciences, Ukrainian SSR). p.62-7 of Biologicheskoe Deistvie Neitronnogo Izlucheniya, Kiev, Naukova Dumka, 1965. (In Russian)

Variations in the antigen characteristics of radioinduced mutants in type B Cl. perfringens were determined by cross agglutination and agglutinin adsorption reactions. Castellani analyses of 5 strains with various antigen characteristics showed that the strains of one serological group could be divided into 4 subtypes. (R.V.J.)

38446 ACTIVITY OF α TOXIN OF CL. PERFRINGENS TYPE A RADIATION MUTANTS. Matveeva, M. D.; Gornaya, M. S. (Inst. of Microbiology, Academy of Sciences, Ukrainian SSR). p.68-73 of Biologicheskoe Deistvie Neitronnogo Izlucheniya. Kiev, Naukova Dumka, 1965. (In Russian)

Studies of high-activity mutants 1032, 1038, and 1066 induced in type-A Cl. perfringens by gamma-neutron irradiation showed that Martin boullion with dextrin is the most favorable medium for α and θ toxin formation. The high toxin activity continued throughout the experiment. (R.V.J.)

38447 EFFECTS OF IONIZING RADIATION ON THE ANTIGENIC AND IMMUNOGENIC PROPERTIES OF PERFRINGENS BACTERIA TOXINS. I. RESISTANCE OF Cl. PERFRINGENS TOXINS TO IONIZING RADIATION. Gornaya, M. S.; Pasechnik, A. M. (Inst. of Microbiology, Academy of Sciences, Ukrainian SSR). p.74-7 of Biologicheskoe Deistvie Neitronnogo Izlucheniya. Kiev, Naukova Dumka, 1965. (In Russian)

Effects of various doses of gamma radiation on the antigenic and immunogenic properties of type-A (VR6K strain) and type-B (strain 5) Cl. perfringens toxins and of fast-neutron induced mutants (1032 and 2359) were investigated. Toxin solutions (5 to 6 ml) were exposed to 5.5, 6.0, 7.5, and 8.0 MR of ^{60}Co gamma radiation at 118 and 1400 R/sec. All white mice injected with toxins exposed to 7.5 and 8.0 MR perished within a few hours. (R.V.J.)

38448 EFFECTS OF IONIZING RADIATION ON TOXIN PRODUCTION OF CL. PERFRINGENS TYPE A BACTERIA. Matveeva, M. D. (Inst. of Microbiology, Academy of Sciences, Ukrainian SSR). p.78-83 of Biologicheskoe Deistvie Neitronnogo Izlucheniya. Kiev, Naukova Dumka, 1965. (In Russian)

Studies of gamma-neutron and gamma irradiated type-A Cl. perfringens showed that variations in α-toxin formation depend on the doses and on the properties of various strains. In most cases toxin formation was inhibited by γ-neutron exposures between 0.45×10^6 to 0.9×10^6 Rad and γ exposures from 0.5×10^5 to 0.1×10^7 Rad. An increased toxin formation in type-A Cl. perfringens (strain BP6K) was observed with γ-neutron doses from 0.15×10^6 to 0.25×10^5 Rad and γ doses of 0.3×10^5 Rad. (R.V.J.)

38449 THE EFFECT OF FAST NEUTRONS ON THE CULTURE AND MORPHOLOGICAL CHARACTERISTICS OF BACILLUS MESENTERICUS. Balkasheva, L. U.; Palchevskaya, A. E.; Goncharenko, S. V. p.84-90 of Biologicheskoe Deistvie Neitronnogo Izlucheniya. Kiev, Naukova Dumka, 1965. (In Russian)

Results are presented of a study on the cultural and morphological properties of variants of Bacillus mesentericus No. 10, which were isolated during irradiation with fast neutrons. A suspension of the bacteria was irradiated with fast neutrons (doses of 50–1000 Rad) and cultured on various media. Then the growth of colonies was examined. It was found that morphological changes were caused by lower doses of neutrons than by other types of radiation (for instance, ^{60}Co gamma radiation). In most cases no essential differences were noted in the behavior of cultures grown on milk and carbohydrate media. The initial strain of Bacillus mesentericus No. 10 is characterized by grayish-white colonies with a convoluted surface, convex center, and uneven edges. As a result of irradiation of the initial strain of the bacteria with ^{60}Co gamma rays and fast neutrons, the following morphological variants were isolated: smooth variant—with green scalloped edges; flat wrinkled variant—with flat, concave center surrounded by wrinkled area; pigment variant—green and orange colonies with powdery white deposit on the surface; and mucous variant—with flat green center and mucous edges. (ATD)

Radiation Effects Therapy and Countermeasures

38450 (USNRDL-TR-851) THE INFLUENCE OF AET AND HYPOXIA ON RECOVERY FROM RADIATION INJURY IN MICE. Ainsworth, E. J.; Phillips, T. L.; Kendall, K. (Naval Radiological Defense Lab., San Francisco, Calif.). May 20, 1965. 20p.

Aminoethylisothiouronium bromide-hydrobromide (AET) and hypoxia appear to act as radiation dose reducers. Studies were conducted in mice, using the split-dose technique, to determine the influence of these protectants on initial injury and subsequent recovery from sub-lethal 250 kvp x ray exposure. The results demonstrate that recovery from theoretically equivalent doses of irradiation is slower in protected mice than in non-protected mice. This would suggest that the initial injury in the protected and non-protected groups is not equivalent. (auth)

38451 IMMUNOLOGIC ROLE OF THE THYMUS IN RADIATION CHIMERAS. Miller, J. F.A. P.; Leuchars, E.; Cross, A. M.; Dukor P. (Royal Cancer Hospital, London). Ann. N. Y. Acad. Sci., 120: 205-17(1964).

Mice of the CBA and C57BL strains were thymectomized at two months of age, subjected to a lethal dose of whole-body irradiation, and protected with marrow, fetal liver, or spleen cells from syngenic adult donors. Thymectomized mice protected with marrow showed some trophic disturbances, such as loss of body weight between 30 and 70 days postirradiation, but thereafter recovered. Sham-thymectomized controls showed no such disturbances. The lymphocyte population of the blood and tissues of thymectomized, irradiated mice was diminished in contrast to that of controls. Sham-thymectomized, irradiated mice, protected with either marrow, fetal liver, or spleen cells, were capable of rejecting allogenic skin grafts within 20 days when grafted four weeks after irradiation. Thymectomized, irradiated mice, however, protected with either fetal liver cells or with doses of up to 40 million marrow cells, never recovered the capacity to reject allogenic skin grafts. Such mice, protected with spleen cells from normal adult donors, but not from donors thymectomized at birth, could reject skin grafts within normal periods of time. Implanting either syngenic or allogenic thymus tissue subcutaneously or under the renal capsule enabled thymectomized, irradiated mice to recover practically normal immune functions. Mice bearing allogenic thymus implants rejected thymus-donor type skin as a second-set response and showed evidence of having rejected the thymus graft. Thymus tissue enclosed in cell-impenetrable diffusion chambers implanted into the peritoneal cavity of thymectomized, irradiated mice also enabled such mice to recover immune capacity. It was concluded that marrow cell suspensions lack adequate numbers of immunologically competent cells but contain precursor cells which mature to immunocompetent cells under the influence of a humoral thymus mechanism. (Excerpta Med., Vol. 2, (July 1965))

38452 PRINCIPLES AND POSSIBILITIES OF BIOLOGICAL-CHEMICAL RADIOPROTECTION FROM THE ACTION OF EXTERNAL RADIATION. Langendorff, H. (Universitaet, Frieburg i. B.). Arzneimittel-Forsch., 15: 463-72(May 1965). (In German)

This review considers the theoretical and practical aspects of protection against the effects of external radiation, especially with chemical agents. While many protective substances have a good effect on survival rates in laboratory animals exposed in toto to radiation and on the recovery potential of cells and tissues even with high doses of short-term radiation, the same is not true to the same

degree in case of protracted irradiation with low doses or fractionated irradiation with short intervals between exposures. The cause for this reduced efficacy of protective agents in protracted exposure must be the relatively short duration of activity of most of the known protective agents. One of the explanations for their reduced efficacy in fractionated irradiation may be the fact that recovery has its locus of action in the same reactive system as the administered protective substance so that an additive effect cannot be expected. Maximum resistance to irradiation obtainable with a protective agent, for which the dose reduction factor is the conventional measure, only under exceptional circumstances surpasses the value 2. The ascertained dose reduction factors usually lie below this value. At this time it is not possible to say which factors decisively prevent a further increase in the dose reduction factors. Individual observations in humans indicate that here, too, administration of protective agents can lead to increased resistance to high-energy irradiation. However, the data available are not sufficient to permit far-reaching conclusions. Also discussed are problems of chemotherapy of irradiation lesions. There are few available data on experimental and clinical observations, but the possibility of chemotherapeutically treating irradiation lesions does exist. The observation is mentioned that NaCN or K_2SO_3 can increase the survival rate of female mice even when these substances are administered 30 min. after exposure to radiation. A similar effect can be observed when Na thioglycolate, 2-aminothiazoline, or 2-iminothiazoline-4-carboxylic acid are administered to mice after exposure to a supralethal dose. With thiazolidine-4-carboxylic acid, 30% of the irradiated animals survived exposure to 800 R. This result provides evidence for the possibility of influencing the pattern of radiation effects with chemicals, even when administered after the exposure. (BBB)

38453 FIRST RADIOBIOLOGICAL AND PHARMACODYNAMIC STUDIES ON THE RADIOPROTECTIVE EFFECT OF MORPHINE. Stuart, C.; Cittadini, G.; Cappelli, B. Romano, E. (Universita, Siena, Italy). Boll. Soc. Ital. Biol. Sper., 40: 543-5(1964).

Morphine exerts a highly significant radioprotective action in mice against the lethal effects of whole-body x irradiation with 700 R. The probable mechanism of action of this drug is that of an effect on pulmonary ventilation, or a decrease in tissue metabolism resulting in a negative influence on the oxygenation of the tissues so that they become less vulnerable to radiation. (Excerpta Med., Sect. XXIII, 2: No. 6(June 1965))

38454 STUDY OF THE MECHANISM OF IMMUNOLOGICAL UNRESPONSIVENESS INDUCED BY THE TRANSPLANTATION OF HOMOLOGOUS SPLEEN CELLS TO SUBLETHALLY IRRADIATED ANIMALS. Shevelev, A. S. (Dept. of Microbiology, Roentgenology and Radiology, Faculty of Medicine, Smolensk, USSR). Folia Biol. (Prague), 11: 177-86(1965).

The transplantation of spleen cells from C57BL/6 mice to CBA recipients irradiated with a dose of 500 R was followed by marked inhibition of antibody formation. This was even more pronounced after the administration of parental strain spleen cells to F_1 (C57BL/6 × CBA) hybrids irradiated with 500 R. The mechanism of the induction of immunological unresponsiveness on these two systems was studied. Evidence is submitted showing that the development of unresponsiveness in the parental strain–F_1 hybrid system (as distinct from the C57BL/6–CBA system) is determined by the reaction of the transplanted cells against the host and is an early sign of this reaction. In addition to nonspecific inhibition of the primary antibody formation reaction, still more pronounced inhibition and reversal of the secondary immune reaction occurred, up to complete absence of antibody formation (if the first dose of antigen was administered immediately after transplantation of the spleen cells). This state is termed histoimmune shock. In both genetic systems, sublethal irradiation provided optimal conditions for the induction of histoimmune shock. Findings are submitted indicating that homologous disease can be prevented in sublethally irradiated F_1 hybrids by means of the immune reaction between the spleen cells of donors of the two parental strains immunized with cells of the other parental strain. Manifest histoimmune shock occurred in surviving recipients. (auth)

38455 SENSITIZATION OF THE CAPACITY OF ESCHERICHIA COLI B FOR PHAGE T3 TO X-RAYS BY IODOACETAMIDE. Hercik, F.; Holzmannova, Alice (Inst. of Biophysics, Czechoslovak Academy of Sciences, Brno). Folia Biol. (Prague), 11: 243-5(1965).

Contact of E. coli B with iodoacetamide (0.001 M) during x irradiation (120–240 kRad) did not sensitize colony formation. Under the same conditions, the capacity of irradiated E. coli B cells for phage T3 was sensitized, however. (auth)

38456 THE EFFECTS OF VARIOUS DRUGS ON RADIATION DAMAGE. Noda, Y. (Kyoto Prefecture Medical Univ.). Furitsu Ikadaigaku Zasshi, 72: 321-50 (1963).

Four groups of mice were injected intraperitoneally with 0.2 and 2.0 mg of glucuronic acid, and 5 and 50 R of cobalt-chlorophyll daily for 30 days after whole-body x irradiation of 700 R. Body-weight changes and mortality rates of these mice were examined. Both the drugs, glucuronic acid and cobalt-chlorophyll, showed protective effects against post-irradiation weight-loss of the mice. Mortality rates were 70% in a control group, 55% in the 2.0 mg glucuronic-acid group, 45% in the 5 R and 25% in the 50 R of cobalt-chlorophyll groups; no protective effect was noted in the 0.2 mg glucuronic acid group. The protective effects of rubraferate, vitamin B_{12}, and cobalt-chlorophyll against radioinduced anemia were examined, using guinea-pigs. Rubraferate showed a greater protective effect than vitamin B_{12} against radioinduced anemia and leukopenia. Intraperitoneally-injected cobalt-chlorophyll showed marked efficacy in prophylaxis and treatment of radioinduced leukopenia. (Excerpta Med., Vol. 2, (July 1965))

38457 THE PROTECTIVE ROLE OF FOOD AND VITAMINS IN RADIATION INJURIES. Perepelkin, S. R. (Inst. of Medicine, Moscow). Gigiena i Sanit., No. 3, 48-56(Mar. 1965). (In Russian).

Dogs and rats were exposed to single general irradiation with x rays in doses of 350, 400, 500, 600, or 700 R respectively. Rats were also exposed to general irradiation with sublethal doses. In the course of the radiation sickness the animals were given 5 different diets: physiological, meat, milk and eggs, liver and vivarium diets, differing one from the other in the quantity and quality of the administered proteins and animal products. The milk and egg diet had the most favorable effect on the radiation sickness. A weaker protective effect was noted in case of liver ration and to a still lesser extent in case of the physiological one. The least significant curative and preventive effects were obtained with the meat and vivarium rations. The enrichment of the food with vitamins C, P, and those of the B group (B_1, B_2, PP, B_8, folic acid) alleviated the gravity of the radiation sickness especially in the use of physiological and meat diets. The complex of vitamins C, P and PP produced a somewhat weaker effect. The complication and the improvement of the course of the disease, caused by ionization radiations, depended considerably on the features of the diet provided. (auth)

38458 STUDIES ON CHEMICAL PROTECTION AGAINST RADIATION. I. THE PROTECTIVE EFFECT OF OROTIC ACID AGAINST X-RADIATION DEATH IN MICE. Morita, Kazuo (Sapporo Medical Coll.). J. Radiation Res. (Japan), 5: 35-8(Mar. 1964).

An experiment was carried out to determine the protective effect of orotic acid (uracil-4-carboxylic acid) against x rays. Orotic acid in dose of 0.05, 0.1, 1.0, 1.7 and 10 mg per mouse was given intraperitoneally to mice before or after a single dose whole-body x-irradiation of 700 R or 550 R, after which the 30-day survival rate was observed. As a result it was concluded that it would be difficult to state thar orotic acid has a protective effect against x-irradiation. It may be added that even if a protective effect exists it would be slight. (auth)

38459 EFFECT OF HALOGENATED PYRIMIDINES ON RADIOSENSITIVITY OF MOUSE STRAIN L CELLS AND THEIR RADIORESISTANT VARIANT. Aoyama, Takashi (Kobe Medical Coll., Japan); Kondo, Teruo; Horikawa, Masakatsu; Sugahara, Tsutomu J. Radiation Res. (Japan), 5: 39-48(Mar. 1964).

Incorporation of halogen analogs of pyrimidine into DNA of the mouse strain L cells enhanced their sensitivity to x irradiation. The maximal radiosensitization was obtained either with 72 hrs incubation in the presence of BUdR alone, or 24 hours' incubation in the presence of BUdR and aminopterin given prior to x irradiation. The replacement of thymidine by BUdR in these optimal conditions was approximately 30%, and a further increase of the replacement up to 50% did not intensify the radiosensitivity. These results may support the view that BU-labeling to single strand of DNA double helix is sufficient to confer significant radiosensitivity. The radiosensitivity of the resistant Ly cells was restored by BUdR incorporation up to the same level as that of untreated original cells. These observations would contribute to some extent towards the improvement of radiotherapy. (auth)

38460 THE EFFECT OF CHEMICAL RADIOPROTECTIVE SUBSTANCES ON DAMAGE TO THE DNA OF THE INTESTINAL WALL BY NITROGEN MUSTARD AND DEGRANOL. Jeney, A.; Kovacs, P.; Hernadi, F. Kiserl. Orvostud., 16: 543-6(1964).

Nitrogen mustard and degranol caused a considerable reduction of the DNA content of the intestinal wall of rats, related to the dry substance. This reduction was favorably influenced by various chemical radioprotective substances (AET, cysteine, penicillamine). This reduction of the toxicity of radiomimetic drugs may permit a wider therapeutic use of such substances. (Excerpta Med., Sect. XXIII, 2: No. 6 (June 1965))

38461 INFLUENCING RADIATION EFFECTS IN MAN AND ANIMALS. Ladner, H.-A. Med. Welt, 65: 106-10(1965).

Pyridoxal-5'-phosphate, the active form of vitamin B_6, influences radiation effects (including combined damage) in man and animals. In dogs therapeutic splenectomy after a lethal dose of irradiation also influences radiosensitivity, which appears interesting for surgical transplantation. (Excerpta Med., Vol. 2, (July 1965))

38462 PHOTODYNAMIC ACTION AND POST-IRRADIATION MODIFYING EFFECTS OF METHYLENE BLUE AND ACRIDINE ORANGE IN BARLEY AND VICIA FABA. Kumar, Sushil; Natarajan, A. T. (Indian Agricultural Research Inst., New Delhi, India). Mutation Res., 2: 11-21 (Feb. 1965).

Methylene blue was demonstrated to be a potent chromosome-breaking agent in the presence of light and oxygen, using Hordeum vulgare and Vicia faba as test systems. Damage caused by methylene blue differed from that caused by acridine orange, quantitatively and qualitatively. Both caused mitotic inhibition. The distribution of chromosome breaks resulting from methylene blue treatment was nonrandom, and centromeres and some other sites were affected preferentially. A possible mechanism of these localized effects is discussed. Post-treatments with methylene blue and acridine orange in the dark without oxygen, modified the radioinduced two-break chromosome aberrations by a factor of 1.5 and 1.3, respectively. The post-treatment of irradiated seeds by methylene blue increased chlorophyll mutation frequency by a factor of 5 in a segregating X_2 population. No modifying effect was found with acridine orange. (auth)

38463 THE ROLE OF OXYGEN IN DETERMINING INITIAL RADIOSENSITIVITY AND POST-RADIATION RECOVERY IN THE SUCCESSIVE STAGES OF DROSOPHILA SPERMATOGENESIS. Sobels, F. H. (Rijksuniversiteit, Leiden). Mutation Res., 2: 168-91(Apr. 1965).

The role of oxygen in determining radiosensitivity to the induction of premutational damage, and in processes of post-radiation repair was studied in different stages of spermatogenesis by comparing the effect of post-treatment with N_2 to that with O_2 after x-irradiation of Drosophila males in either N_2 or O_2. Recessive lethals were scored in a ring-X chromosome in 4–5 successive two-day broods. After irradiation in N_2, it was found that post-radiation recovery in sperm is favored by N_2, but in early spermatids and spermatocytes by O_2. In late spermatids and spermatogonia no significant post-radiation modifications were observed. Post-radiation recovery by N_2 in mature sperm was further confirmed by results obtained from sperm, treated in the inseminated females. The results for early spermatids and spermatocytes indicate that a repair system which has been rendered ineffective by anoxia can be regenerated to normal functioning by post-treatment with O_2. The time of mutation fixation in early spermatids could not be established definitely, but indications were obtained that in N_2 fixation does not occur within 25 min, whereas after 50 min the reversibility of the pre-mutational lesions is strongly decreased. In contrast to the observations after irradiation under anoxia, no post-radiation modification of the mutation frequencies by N_2 or O_2 was found after irradiation in O_2 for sperm, spermatids, or spermatocytes. Only in spermatogonia post-treatment with O_2 lowered the mutation frequency, as compared to that after N_2 post-treatment. It was concluded that radiation in O_2 produces more irreparable damage than radiation in N_2. (P.C.H.)

38464 CYSTEAMINE-INDUCED INCREASE OF CELLULAR GLUTATHIONE-LEVEL: A NEW HYPOTHESIS OF THE RADIOPROTECTIVE MECHANISM. Revesz, Laszlo; Modig, Hans (Karolinska Inst. Medical School, Stockholm). Nature, 207: 430-1(July 24, 1965).

Tissue cultures of ELD ascites tumor cells were grown on media supplemented with various amounts of cysteamine, and the contents of acid-soluble non-protein-bound sulfhydryl groups (NPSH) and glutathione (GSH) were determined. NPSH in the cells increased in a direct relationship to the amount of cysteamine in the medium in an approximate ratio of 2 to 10-fold. About 37% of the increase in NPSH was attributable to a rise of the GSH level. Release of intracellular GSH was determined to be a significant factor in the radioprotective action of cysteamine. Hence, it is suggested that compounds that can induce an increase of intracellular GSH be included in the search for potential radioprotectors. (H.G.D.)

38465 REACTIVATION OF RADIATION-KILLED E. COLI WITH RIBONUCLEASE. Bhattacharjee, S. B. (Saha Inst. of Nuclear Physics, Calcutta). Nature, 207: 431-2(July 24, 1965).

Escherichia coli B cells were grown on plates to which ribonuclease was added prior to or following ultraviolet or x irradiation. The presence of ribonuclease during irradiation did not influence the percentage of survivors, but the presence of ribonuclease after irradiation and during incubation increased survivor ratios to a very high rate. (H.G.D.)

38466 CONTRIBUTION TO THE STUDY OF THE RADIOPROTECTIVE PROPERTIES OF 2-MERCAPTOBENZOTHIAZOLE. Lopez Zumel, M. C.; Bernard, Y.; Rinaldi, R. Rev. Espan. Fisiol., 20: 121-7(1964).

In order to determine the radioprotective properties of 2-mercaptobenzothiazole (MBT) under specific conditions, the following were studied: a) Radioprotection due to the substance, its distribution in the tissues, and hypothermia in mice. b) Radioprotection in vitro against a bilirubin solution. Results confirmed a survival of 70% of the animals, and showed that MBT is inactive in vitro. Rapid diffusion of the substance and its complete elimination in 24 hours was noted as well as hypothermia 50 minutes after the injection. (Excerpta Med., Sect. XXIII, 2: No. 6 (June 1965))

38467 THE PROTECTIVE EFFECT AGAINST X-RAY LESIONS OF GLYCINE ON SOME ENZYME SYSTEMS. Capalna, S.; Chizari, E.; Stefan, M.; Petec, G. Rev. Roumaine Physiol., 1: 263-9(1964).

A study was made of the effect of x rays (500 R/hour) on the activity of various enzymes (catalases, ATP-ase, pyrophosphatase, and glutaminase) from livers and

spleens of rats, with and without protection by glycine. Administration of glycine prior to irradiation had a greater protective effect on the catalases than administration after irradiation. The protective action of glycine was attributed to the manifold effects of the amino acid in intermediate metabolism, especially by biosynthesis of the porphyrin nucleus, i.e., the prosthetic part of the catalases. It was found that the radioprotective effect of glycine on ATP-ase, pyrophosphatase, and glutaminase was less pronounced than on the catalases. (Excerpta Med., Sect. XXIII, 2: No. 6(June 1965))

38468 TREATMENT OF X-RAY-IRRADIATED SKIN WITH LOCAL APPLICATION OF AN ANABOLIC STEROID. Picha, E. I. (Universitaet, Vienna). Wien. Med. Wochschr., 114: 811-13(1964).

A report is given on 100 women treated with radiotherapy. The consequent dermal reactions were favorably influenced by a cream containing 0.5% of methandrostenolone as anabolic agent, 0.1% hexachlorophene as disinfectant, and an oil-water emulsion as a carrier, with the consistency of thick cream. Prophylactic use when irradiation is started appears to be especially promising. The favorable effect of the cream is in the main attributed to the anabolic steroid. (Excerpta Med., Sect. XXIII, 2: No. 6 (June 1965))

38469 THE EFFECT OF CYSTEAMINE AND AET ON THE OXYGEN CONSUMPTION AND BODY TEMPERATURE OF MICE. Locker, A.; Pany, J. E. Z. Ges. Exptl. Med., 138: 331-7(1964).

Both cysteamine and AET depressed the oxygen uptake of the mouse, the effect being strongest during the 15 minutes following intraperitoneal injection. The increased oxygen uptake observed after high doses of cysteamine was correlated with the increased motor activity caused by the high doses of the drug. With AET the initial depression of O_2 consumption was reversed in time, but the responses were dose dependent. Both compounds reduced body temperature linearly with dose. These results are discussed in relation to the radiation protective action of the drugs. (Excerpta Med., Sect. XXIII, 2: No. 6(June 1965))

38470 RADIATION MEDICINE. Burnazyan, A. I.; Lebedinskii, A. V. (eds). A Pergamon Press Book. International Series of Monographs on Nuclear Energy. Division III. Biology. New York, The Macmillan Co., 1964. 375p. $12.00.

Translated by Harry Asher from Radiatsionnaya Meditsina.

Information is included on the diagnosis and therapy of various forms of illness and disease related to radiation damage. Nine chapters are included; separate abstracts were prepared for each. (P.C.H.)

For abstracts of individual chapters see: 38357, 38432, 38433, 38434, 38435, 38436, 38471, 38472, and 38481.

38471 SIGNS, SYMPTOMS AND TREATMENT OF RADIATION SICKNESS. Kurshakov, N. A.; Glazunov, I. S. pp 281-305 of Radiation Medicine. New York, The Macmillan Co., 1964.

Radiation sickness occurs either when the penetrating radiation is applied from outside or when the radioactive substances enter the body, usually through the respiratory passages. The disease may be either acute or chronic. The four different periods that may be distinguished in radiation sickness are discussed. Treatment of the disease including diet and drugs and diagnosis of chronic radiation sickness are briefly described. (P.C.H.)

38472 CHEMICAL PROTECTION AGAINST IONIZING RADIATION. Romantsev, E. F. pp 306-15 of Radiation Medicine. New York, The Macmillan Co., 1964.

The protective effects of sulfur-containing amonoacids, aminothiols, amines containing no SH-groups, methaemoglobin producers (cyanides, azides, and nitrides) vitamins, aminosugars, alcohols, fatty acids, and other compounds against radiation effects in animals are discussed. (P.C.H.)

Radiation Hazards and Protection

See also HEALTH AND SAFETY.

38473 (NP-14923) GUTACHTEN UEBER DEN UMGANG MIT NATRIUMDIURANAT FUER DAS EINFAERBEN VON ZAHNMASSEN. (Expert Opinion on the Alloying With Sodium Diuranate for the Coloring of Artificial Teeth). Seelentag, W. (Bundesgesundheitsamt, Berlin (West Germany). Institut fuer Wasser-, Boden- und Lufthygiene). Apr. 7, 1962. 30p. Dep. mn.

The dangers resulting from the use of sodium diuranate as the coloring agent in the preparation of artificial teeth were investigated. The report of the Battelle Institute on this subject was summarized as an introduction to the calculation of the dose output from teeth containing uranium. Porcelain teeth containing uranium were experimentally tested, and the radiation charge emitted was biologically evaluated. It was concluded that no injury would result. (J.S.R.)

38474 ASSESSMENT OF AVERAGE OCCUPATIONAL EXPOSURE TO IONIZING RADIATION. Prpic, B.; Cerovac, H.; Despotovic, Lj. Arhiv Hig. Rada Toksikol., 14: 245-9(1963).

The occupational exposure to ionizing radiation 654 persons in 42 different establishments was monitored by film dosimetry over a three-year period, and the annual average accumulated dose calculated for certain professional groups (nurses, radiotherapists, doctors, medical assistants, technicians, x-ray attendants, etc.). These were classified according to their degree of exposure. It was found that protective measures led to a reduction of the doses accumulated during the period, and the importance of training personnel exposed to radiation in the various forms of protection available is therefore stressed. (auth)

38475 INDIVIDUAL PROTECTION AGAINST RADIOACTIVITY IN TIMES OF WAR. Kluchert, W. Berl. med. Rundschau, 4: 19-20(1964).

Under normal conditions masks and protective clothing prevent penetration of the body by radioactive aerosols or fluids. After detonation of atom bombs or belligerent use of radioactive substances such masks and protective clothing should be improvised. Instead of masks wetted cloth, cotton wool, bandages etc. can be used. For protective clothing the material should consist of leather, rubber, synthetic rubber etc. Solid shoes, covered by cloth protect the feet. The hands and the neck can be protected by gloves and a high collar. The population should leave the contaminated area as speedily as possible, perpendicular to the prevailing direction of wind. They should go to a center for treatment, where bathing rooms for decontamination are available. Water is often sufficient for removing radioactive pollution. (Excerpta Med., Vol. 2, (July 1965))

38476 WORK HAZARD AND REQUIRED TIME OF HOSPITALIZATION IN INTRAPERITONEAL ADMINISTRATION OF COLLOIDAL ^{198}Au. Vebersik, V. Casopis Lekaru Ceskych, 104: 124-9(1965).

The hazards involved in work with short-term isotopes used for therapeutic purposes are discussed, with special reference to the intraperitoneal administration of colloidal ^{198}Au. Extreme views regarding the period of necessary hospitalization and investigations of decisive circumstances form the basis of a reflexion on the real character of residual activity of 1 mC for ^{198}Au. Basic conditions regarding the technique of administration are described and dosimetric nomograms are recommended. (Excerpta Med., Vol. 2, (July 1965))

38477 MEASUREMENT OF RADIATION IN TRAUMATOLOGIC INTERVENTION. Gesztessy, Akos; Nikl, Istvan; Pota, Laszlo (MAV Korhaz es Koezponti Rendeloe, Budapest). Magy. Radiol., 17: 169-78(June 1965). (In Hungarian).

Extensive dose measurements were conducted on surgical and x-ray personnel in the accident clinic of a hospital to

determine the amounts of radiation reaching various parts of the body in various orthopedic procedures. Three specific areas of treatment of traumatic injuries were investigated: fixation by nails of the broken neck of the femur, detection and removal of foreign bodies, and control x-ray examination of bedridden patients in traction. About 50 small dosimeters utilized for the measurements were distributed and affixed to the staff at various sites. It was found impractical and time consuming to distribute, affix, and record the instruments in actual emergencies; therefore, phantoms representing portions of the human body were used for the measurements and various operations were performed on them. The doses recorded on the hands and fingers of the operating personnel were much higher than expected. In the femur operation measurements ranged from 1.1 to 129.8 mR during a total operating time of 4 hr 25 min, and from 1.5 to 141.5 mR over 6 hr 44 min. In procedures involving location of foreign objects some measurements on fingertips ranged as high as 3785.0 mR over an exposure period of 4 hr 57 min. The x-ray tube was operated at 64 kv-1.5 ma or 70 kv-2.0 ma. It was concluded that measurement techniques of this nature should be conducted to determine what protective measures are indicated for operating room personnel. (BBB)

38478 LESIONS FROM ATOMIC AND THERMONUCLEAR ARMS. THE PRESENT STATE OF KNOWLEDGE. Carro, Amigo S. Med. Cir. Guerra, 26: 575-81(1964).

After a brief historical introduction to the subject a short study is made of the various types of weapons, both of fission and of fusion, formed by atomic and thermonuclear bombs, as well as of the different explosions, according to the ambient medium in which they are effected, mention being made also of the so-called ballistic projectiles with a nuclear head, according to their range. A clinical study of the lesions caused is made by classifying them into 4 groups: mechanical, luminary, thermal, and radioactive; the last 2 groups are mainly considered on account of their greater interest. Further, the factors influencing the gravity of these lesions were studied. Some of the detectors and devices for measuring radioactivity currently employed are mentioned, and the fundamental norms to be taken into account in protection, as well as medical and sanitary aids are given. It is stated that the wounded should be treated with priority. (Excerpta Med., Vol. 2, (July 1965))

38479 HYGIENIC ASPECTS OF WORK WITH IONIZING RADIATION. Spaander, J. Ned. Tijdschr. Geneesk., 108: 1986-91(1964).

The use of radioactive substances in medicine gives rise to questions about radiation protection. The policy of the I.C.R.P. in giving maximum permissible levels for internal and external radiation is explained. This policy is based upon biological considerations by which the effects of ionizing radiations on living cells and tissues can be explained. In particular, the relation between atoms, macro-molecules (like DNA), viruses, bacteria, and other living organisms, including vertebrates and man, and ionizing radiation is discussed. In addition to the somatic effects, the genetic problems are mentioned. According to law in the Netherlands, radioactive substances may only be utilized by licensed persons working in well-equipped laboratories. Some explanation of this is given. (Excerpta Med., Vol. 2, (July 1965))

38480 RADIOPROTECTION WITH NEUTRON GENERATORS. Schwanecke, R. Zentr. Arbeitsmed. Arbeitssch., 15: 1-7(1965).

Three types of neutron accelerator sources known to be in use in the Darmstadt region and the type of radiation produced are discussed. Reference is made to the literature containing simple calculations for screening. (Excerpta Med., Vol. 2, (July 1965))

38481 THE PHYSICS AND DOSE MEASUREMENT OF PENETRATING RADIATIONS. Shtukkenberg, Yu. M. pp 1-115 of Radiation Medicine. New York, The Macmillan Co., 1964.

Structure of the atom, interaction of radiation with matter, dose measurements of ionizing radiations, and contamination from atomic explosions are discussed. (P.C.H.)

Radiotherapy and Radiodiagnosis

38482 RADIATION SAFETY. Boeker, Elisabeth H. (Radiological Health Lab., Rockville, Md.). Am. J. Nursing, 65: 111-16(Apr. 1965).

Hazards to nurses caring for patients being treated with sealed or unsealed sources of radioisotopes are reviewed, and recommendations are made for reducing their exposure to radiation. Nurses may be exposed to radiation in caring for patients being treated with Ra or assisting with the administration of radioisotopes. Hazardous practices which may add further to a nurse's exposure to radiation are assisting patients during fluoroscopic examinations or holding patients for diagnostic x rays without the protection provided by wearing lead aprons and lead gloves. Time, distance, and shielding are the factors to be considered by nurses in establishing protective procedures to reduce exposure to external radiation. Exposure time can be reduced further if the physician prepares the patient before he removes the implant from the container, and then rapidly transfers the applicator directly from the shielded container to the patient. Radioactive materials should be kept in a separate place with containers and work areas clearly marked. Liquid radioisotopes should be placed on a tray covered with absorbent paper so that if a spill occurs, the material will be confined to the tray. Long-handled forceps should be used for handling radioisotopes emitting γ radiation. Hospital radiation safety programs are discussed. (TCO)

38483 AN AUTOMATIC APPLICATION UNIT FOR INTRACAVITARY RADIOTHERAPY. Unnerus, C.-E.; Nieminen, T.; Rekonen, A.; Vauramo, E. (Univ. Center Hospital, Helsinki). Ann. Chir. Gynaecol. Fenniae, 53: 480-4(1964).

A new type of therapeutic apparatus for intracavitary cancer therapy has been constructed. Radiocobalt ^{60}Co was used as the source of radiation. The activity of the source in the initial phase was about 30 C. This method gave better control of dosage distribution that the present methods and allowed convertion of dosage distribution rapidly by a quick control method. The apparatus, which can be moved in different directions, permits very good radioprotection of the nursing staff. Fractionation of the patient's treatment can be improved. The treatment times, a few minutes duration, reduce the radiation strain on the patient per application. Remote control of the applicators is another advantage. (Excerpta Med., Sect. XXIII, 2: No. 6(June 1965))

38484 EFFECT OF X-RAY IRRADIATION OF LARYNGEAL CANCER ON THE FUNCTION OF THE THYROID GLAND: EXPERIMENTAL OBSERVATIONS. Koulumies, Marja; Voutilainen, Antero; Koulumies, Rolf (Univ. Central Hospital, Helsinki). Ann. Med. Internae Fenniae, 53: 89-96(1964).

Thyroid function, as measured by ^{131}I uptake of the gland, was investigated before and after radiotherapy in the neck region of 118 patients with cancer of the larynx. In radical radiotherapy of laryngeal carcinoma the dose directed to the tumor is about 5000 rad over a month. The radiation field includes the thyroid gland owing to its anatomical location; the gland lies 3 to 4 cm to the caudal side of the horizontal plane of the vocal chords. The radiation dose received by the thyroid gland therefore approaches the tumor dose. Previous studies show that to reduce the function of the thyroid gland, e.g. in the treatment of thyrotoxicosis, ^{131}I is required in doses of 10 to 15 mC, equivalent to a radiation dose of 10,000 rad. In most of the 118 patients studied the radioiodine tests carried out prior to treatment were normal. Subsequent to radiotherapy, the ^{131}I uptake diminished in 15 cases, increased in ten, and remained unchanged in one case among the patients who were not operated upon; the post-therapeutic uptake of the operated patients was lower than prior to irradiation in

seven cases and an increase was seen in one case only. The uptake displayed a slight decreasing tendency immediately after radiotherapy. In four cases there was a marked increase of uptake, which suggests thyroid stimulation. When the second radioiodine tests were conducted after 2 to 3 months, most revealed augmented uptake, that is, restoration of the initial values, and at the later examinations nearly normal levels were seen. Also, uptakes higher than usual, taken as an indication of toxicity, had gone down to close to normal levels, whereas initially low uptake values tended to increase and remain at an elevated level. Irradiation thus normalized the function of the thyroid and did not exert any detrimental effect on the normal thyroid function. After radiotherapy, low PBI (protein-bound I) values were recorded in 50% of the cases, and elevated initial values fell to normal levels. Total blood cholesterol values decreased after radiotherapy in about 68% of the cases, followed by a slight increase as a general trend. Thyroid antibodies were found prior to radiotherapy in four cases out of 118 (in 3.3%), after radiotherapy they were found in ten cases (13.2%). These studies show that the thyroid gland is rather resistant to ionizing radiation. The function of the gland does not seem to be disturbed, at least not permanently, even after it is subjected to a radical dose for destruction of a malignant tumor. However, the slight increase of autoantibody incidence may reflect some damage to the gland by irradiation. (BBB)

38485 TRACER STUDIES ON A TRANSPLANTABLE HAMSTER MELANOMA. Potts, Albert M. (Univ. of Chicago). Arch. Ophthalmol., 72: 359-64(Sept. 1964).

Some exploratory studies on radionuclide-containing compounds that might be used for radiodiagnosis or therapy of ocular tissues are reported. An attempt to utilize radioactive tracers for diagnosis of ocular tumors was based on external counting of the suspected eye after administration of ^{32}P and depended upon greater incorporation of isotope in the phosphorylated compounds of rapidly growing tumor tissue than in normal ocular tissue. If a compound could be found that would combine specifically with a unique component of a tumor, and if this compound could be labeled with a γ-emitting isotope, it would provide an ideal diagnostic aid. The same compound with a short range β-emitting isotope could provide a potentially effective therapeutic agent. Since the phenothiazine tranquilizers combine specifically with uveal pigment, they might possibly be used for diagnosis and treatment of pigmented tumors arising in the uveal tract. Thus, ^{35}S-labeled chlorpromazine and prochlorperazine were tested, as well as diiodofluorescein (DIF), reported to localize in human melanomas, and iodoxuridine (IDU) which might be expected to be incorporated selectively into the nucleic acid of rapidly growing tissues. Both of the latter compounds were ^{125}I labeled; ^{125}I is particularly advantageous for use in the eye because of its longer half-life and weaker photon relative to ^{131}I. The test object was the transplantable melanoma of the Syrian golden hamster, which is transplantable to the uvea. The experiments describe the storage of labeled prochlorperazine, chlorpromazine, IDU, and DIF in this transplantable melanoma. With prochlorperazine the eye tumor counted 50% or more higher than the control, an effect which would have shown equally well with a γ-emitter and external counting. With chlorpromazine and the ocular melanomas, concentration in the eye tumor was low compared to the control. However, because the concentration of chlorpromazine is less than that of prochlorperazine in normal uvea, the differential between tumor and nontumor eye was less. With IDU and DIF there was no marked concentration in uveal tissue and no higher content in normal iris and ciliary body as compared to tumor, but the extra mass of tumor resulted in much higher counts in the tumor eye. Whether any of the three types of substance used have a theoretical basis for usefulness in tumor detection or therapy by virtue of selective storage in tumor tissue is discussed. (BBB)

38486 POSTRADIOTHERAPY CRANIAL SARCOMA AFTER TREATMENT OF RETINOBLASTOMA. Dollfus, M. A.; Delthil, S.; Haye, C. Bull. Soc. Ophthalmol. France, 62: 233-6(Apr. 1962). (In French).

A 16-month old infant with a retinoblastoma in the right eye underwent enucleation. The left eye, showing the presence of a supranasal tumor, was treated by surface diathermal congulation. A massive relapse prompted treatment by radiotherapy. A first series of penetrating radiation was applied during a period of 10 days over anterioposterior and lateral fields with 2200 R each. A second series of 4000 R in seven days was applied a month later, because of continued tumor growth. A third irradiation series was given a month later. Finally, two more treatments were given totaling 4000 R, so that the total orbito-ocular dosage received was 16,000 R (8150 R anterioposteriorly and 7850 R laterally). Ten years later, atrophy of the left eyeball was pronounced and cutaneous telangiectasia was present with atrophy of the part of the head included in the field of irradiation. The right orbital cavity was normal. Four years later, the patient developed a painless, subcutaneous swelling in the frontal-temporal area. Histological examination of a biopsy revealed a typical fibrosarcoma. Under the influence of x-ray therapy, the swelling disappeared almost completely. The causal relation between the secondary tumor and radiotherapy was probable since it appeared in the field of irradiation. These observations indicate the usefulness of treating retinoblastomas with a combination of chemotherapy and irradiation to reduce the dose necessary and possible development of secondary neoplasms. (BBB)

38487 RADIATION THERAPY OF CANCER. Stein, Justin J.; Baker, Sol R. (Univ. of California, Los Angeles). Calif. Med., 102: 370-5(May 1965).

Many aspects of radiotherapy are reviewed: radiobiologic principles, radiosensitivity of various cells and tumors, dose measurement and fraction, equipment and sources (especially megavoltage devices), and clinical results. Although some malignant tumors are considered to be relatively radioresistant, it is not always possible to predict what the radiation response will be until it is tried. Once a full course of radiation has been given, only under very special circumstances can adequate additional radiation be administered. Excessive radiation therapy will produce complications of varying degrees of severity, yet the radiation therapist must take certain calculated risks when treating radiocurable malignant tumors. Research in radiobiology with respect to fractionation, dose rate, and cell survival done during the past ten years is considered. The results of these studies, both clinical and experimental, concerning the dose-time relation offer improvement in radiation treatment methods. The use of ^{32}P, ^{60}Co, ^{90}Sr, ^{131}I, ^{137}Cs, ^{182}Ta, ^{198}Au, ^{192}Ir, and ^{226}Ra in therapy is considered. The physical advantages and qualities of megavoltage therapy as compared with conventional x-ray therapy (200 to 300 kv) in the treatment of cancer are reviewed. The usefulness of megavoltage in cancer therapy has been clearly established. An increasing number of reports indicating an improved five-yr survival for patients with certain types of tumor following the use of megavoltage therapy, and other factors such as ease of administration and tolerance by the patient, demonstrate that all well-equipped radiation therapy treatment centers should have some type of megavoltage equipment available. The major uses of megavoltage therapy are in the treatment of cancer in the head and neck, esophagus, brain, lungs, bladder, and ovaries. The question of whether radiation alone can be curative is examined, and it is concluded that in some circumstances and at some sites radiation can produce curative results. It is concluded that no other method of therapy has produced more consistent palliation in a greater number of cases of various types of cancer with less mortality and morbidity than has radiation. (BBB)

38488 RADIATION-INDUCED CHANGES IN THE CYTOPLASMIC ACRIDINE ORANGE STAINING OF EXFOLIATED CELLS. Seydel, H. Gunter. (Wayne State Univ., Detroit and Detroit Memorial Hospital). Cancer, 18: 937-41(Aug. 1965).

Smears of exfoliated cells from 27 patients undergoing radiotherapy for malignancies of the uterus and oral cavity were examined using acridine orange stain. A progressive change in RNA was found which led to a change of the cytoplasmic fluorescence from red to brown and green. This

suggests that acridine orange stained smears may be of value in predicting the effect of radiation therapy upon primary tumors. Most patients who exhibited more than 40% damaged cells after 4,000 R radiation dose showed no evidence of local recurrence 8 to 26 months after radiation therapy. (auth)

38489 CEREBRAL CIRCULOGRAPHY WITH RADIOISOTOPES. Kvicala, V.; Boucek, J.; Klan, V.; Vitkova, S. Casopis Lekaru Ceskyde, 104: 64-8(1965).

A method for examining cerebral circulation is described, which depends on intravenous administration of ^{131}I serum-albumin. The patient has 2 leads fixed in symmetrical position over both temporal areas and directly recording ammeters register the rise and fall of activity. The normal curve is determined by the condition of the cerebral vessels but the extracerebral cardiovascular apparatus also has some effect on the curve. Broader curves with slow rise and fall were found in atherosclerosis. Comparison of curves from the right and left half of the head showed that the curves are higher on the side of glioblastoma and arteriovenous aneurysm, lower over meningiomas, malacia, and hematoma. (Excerpta Med., Vol. 2, (July 1965))

38490 USE OF RADIOIODINATED FATTY ACID FOR PHOTOSCANS OF THE HEART. Evans, J. R.; Gunton, R. W.; Baker, R. G.; Beanlands, D. S.; Spears, J. C. (Univ. of Toronto). Circulation Res., 16: 1-10(1965).

Radioiodinated fatty acid bound to albumin (RIFA) was given by intravenous injection to dogs and moribund human subjects in order to label heart muscle. Photoscans of the thorax of dogs given RIFA revealed concentration of radioactivity in the ventricular region of the heart due to incorporation of the labeled fatty acid into myocardial triglyceride and phospholipid. Photoscans of the thorax following intravenous injection of radioiodinated serum albumin or $Na^{131}I$ showed a different density pattern in the region of the heart due to radioactivity in blood within the cardiac chambers. Areas of myocardial infarction were detected in photoscans of the thorax in 11 of 14 dogs in which one coronary artery was ligated. At necropsy the concentration of radioactivity was much higher in healthy myocardium than in infarcted muscle. The same distribution of radioactivity was observed in hearts from three human subjects with myocardial infarction given RIFA shortly before death. It is proposed that areas of myocardial infarction might be demonstrated during life by photoscans of the thorax following intravenous injection of RIFA. (Excerpta Med., Vol. 2, (July 1965))

38491 CEREBRAL BLOOD FLOW DETERMINED BY SATURATION AND DESATURATION WITH KRYPTON^{85}: AN EVALUATION OF THE VALIDITY OF THE INERT GAS METHOD OF KETY AND SCHMIDT. Lassen, N. A.; Klee, A. Circulation Res., 16: 26-32(1965).

Cerebral blood flow was studied in 11 subjects using the ^{85}Kr method during a 10-min saturation period followed by a 10-min desaturation period. The calculated cerebral blood flow averaged 8.5% higher during desaturation than during saturation for the eight cases with blood flow values in the normal range. At higher flow (1 case) the deviation was less pronounced, while at lower flows (2 cases) the percentage difference increased. It is suggested that this systematic difference is due to the failure, at 10 min of reaching equilibrium between average tissue and mixed venous blood in the human brain. The studies disclose a systematic error inherent in the Kety-Schmidt technique. According to observations in the literature this error is, however, not of such magnitude that it affects seriously the method as applied to the brain. Employing an inert gas saturation period of 10 min, an overestimation of the flow by about 10% probably occurs in normal subjects, while at subnormal flow levels the magnitude of this error increases somewhat. The error mentioned may be counteracted by prolonging the saturation period to 15 or 20 min and by extrapolation of the curves to infinity. (Excerpta Med., Vol. 2, (July 1965))

38492 THYROID FUNCTION IN PATIENTS WITH ADVANCED CANCER OF THE PORTIO. EFFECTS OF RADIUM THERAPY. Boemi, P.; Anzalone, G. (Universita, Catania, Italy). Clin. Ginecol., 6: 185-94(1964).

Thyroid function was investigated after radium therapy in women with epitheliomas of the vagina in the 3rd and 4th stages. In women over the age of 65 years, the ionizing radiations caused an increase of the basal metabolic rate and a drop of the blood cholesterol; in women under 65 years of age, both the basal metabolic rate and the blood cholesterol increased. An explanation is proposed, and it is concluded that the thyroid gland reacts actively against the ionizing stimulus, thus showing a good functional capacity even in very old women. (Excerpta Med., Sect. XXIII, 2: No. 6(June 1965))

38493 THE USE OF RADIOISOTOPES FOR MEDICAL DIAGNOSIS. Combrisson-Le Bolloc'h, A. Concours Med., [No.] 26, 5-40(1964).

A brief review is presented of the principles involved in tracer studies and chemical and isotope methods for the identification and determination of atoms and molecules of interest in medical diagnosis. Applications of radioisotopes in hematological studies are discussed in detail. Topics covered include the measurement of total blood volume, plasma volume, and erythrocyte volume; the use of blood volume measurements in medical and surgical practice; methods of labeling blood cells; survival studies for erythrocytes, leukocytes, and platelets; methods of labeling developing and mature populations of blood cells; iron metabolism; and methods for studying the metabolism of vitamin B_{12}. (TCO)

38494 RADIATION SENSITIVITY OF MALHERBE'S CALCIFYING EPITHELIOMA. Born, W.; Parra, C. (Albert-Ludwigs-Universitaet, Freiburg i. B.). Dermatol. Wochschr., 150: 408-14(1964).

A calcifying Malherbe epithelioma was found to be sensitive to radiation, and so was a recurrence 10 yr later. These tumors are relatively rare, and are usually described as being radioresistant. In view of the repeated observation of good results with x rays and gamma radiation, radiological treatment is indicated in suitable cases. (Excerpta Med., Sect. XXIII, 2: No. 6(June 1965))

38495 EXPOSURE OF THE POPULATION OF UPPER AUSTRIA TO RADIATION AND ITS RELATIONSHIP TO THE MORBIDITY STATISTICS. Jarosch, K. Deut. Z. Ges. Gerichtl. Med., 55: 148-55(1964).

The increasing use of radiation in medical science and technology makes it likely that in the future difficult problems will arise in the assessment of radiation damages and in penal procedure. Assessment is based on general and individual exposure to radiation. Burns due to x rays, acute radiation sickness, chronic radiation syndrome, relationships between malignant tumors and ionizing rays, and fetal damage, are widely known radiation problems. The possibility of criminal use of ionizing rays, in the form of radioactive substance, should also be taken into account. The radiation effect can either be external or internal. These are new problems in forensic medicine. (Excerpta Med., Sect. XXIII, 2: No. 6(June 1965))

38496 RADIO-IODINE AND THYROID EXPLORATION. Perez, R. Gaz. Med. France, 71: 2503-18(1964).

Of the radioactive isotopes of iodine used for diagnosis of thyroid diseases, ^{125}I is hardly used on account of its long half-life (60 days); ^{132}I has a very short half-life (2.3 hours) and is used in children only; ^{131}I has a half-life of 8.04 days and is used in all other cases, i.e., almost exclusively for thyroid exploration. A detailed description is given of the technique and the data obtained, in the form of measurement of the total activity on the thyroid, determination of the isotope in the urine, and determination of hormonal iodine in the plasma. Gammagraphy (scintigraphy) permits a distinction of cold or hot nodules in more or less normally accumulating thyroids and thus helps in the diagnosis of possibly malignant tumors and toxic adenomas. For treatment of thyroid cancer and its metastases with radioactive iodine the accumulation properties are decisive: papillary carcinomas rarely accumulate iodine, vesicular carcinoma in 75% of cases, and plastic carcino-

mas never. (Excerpta Med., Sect. XXIII 2: No. 6(June 1965))

38497 TREATMENT OF THYROID DISEASES WITH RADIO-IODINE. Tubiana, M. Gaz. Med. France, 71: 2521-36(1964).

Hyperthyroidism is treated with 1 mC of ^{131}I per 10 g of thyroid weight, amounting to 8,000 to 10,000 rad. The effect appears after 15 to 18 days at the earliest, usually after 4 weeks, when the patient's general condition and restlessness improve. After 6 weeks the sensitivity to heat diminishes, weight increases and the pulse frequency becomes normal. Regression of exophthalmus takes the longest time, and occurs in only 20% of cases. If hyperthyroidism causes disturbances of menstruation (frequent and slight bleeding) these are also corrected. Treatment with radioactive iodine is mainly indicated in patients over 40, and in exceptional cases also in patients from 20 to 40 yr of age. Below the age of 20 other therapeutic methods should be used. A single therapeutic course was effective in 55 to 60% of cases, and two courses and more were required in some cases. In 65% results were very good, in 20% satisfactory. Permanent myxoedema was seen in 5 to 10%. The recurrence rate was less than 5%. The advantages and disadvantages are compared with those of other methods. The risks of carcinogenesis, increase in leukemia rate, and genetic damage due to treatment with radioactive iodine are considered negligible. At the present annual consumption of 70 C of ^{131}I the exposure of the French population of 50 million people is some 0.03 rad for 30 yr (a generation). Contraindications are pregnancy and nodular goiter, as in the presence of cold nodules a malignant goiter may be overlooked, while toxic adenomas must be treated with a high dose of radioactive iodine. In cardiac thyreosis treatment with radioactive iodine has sometimes yielded such spectacular results that some cardiologists prescribe ^{131}I even in non-thyreogenic cardiac insufficiencies, as a reduction of the basal metabolism decreases cardiac stress. Malignant goiter can be treated with ^{131}I in only a quarter of cases, as in the majority iodine is not, or insufficiently, stored. First an exact study should be made with radioactive iodine tests, scintigraphy, and histological verification of the diagnosis. To obtain optimal storage of the iodine in the tumor tissue, pretreatment with TSH is followed by oral administration of 100 mC every 3 months. The consequent athyreosis is treated by substitution of thyroid hormone up to 14 days prior to the next treatment. The results are reported. (Excerpta Med., Sect. XXIII, 2: No. 6(June 1965))

38498 ORGANIZATION AND EQUIPMENT OF A RADON LABORATORY. Gusarov, I. I. Gigiena i Sanit., No. 3, 87-90(Mar. 1965). (In Russian)

Descriptions are given for construction of a therapeutic laboratory for treating patients with radioactive baths. The laboratory was designed for 6 to 12 bubbling tanks with 30 mg radium per tank. It is capable of serving cities with 100,000 to 500,000 population. The main source of γ radiation is the radium in the tanks and bottles with concentrated radon solution. Safety measures for the personnel and for transportation of containers with radioactive solutions are considered. (R.V.J.)

38499 THE MODE OF ACTION OF HIGH-ENERGY RADIATION. Pohlit, W. (Max-Planck-Institut fuer Biophysik, Frankfurt am Main). Internist, 5: 263-71(1964).

By means of diagrams, the mode of action of high-energy radiation is explained for the non-specialized reader. Starting with the scattering and absorption of photons in matter, an explanation is given of the Compton Effect, and the development and operation of the betatron and ultrahard x rays. The depth-dose curves of high-energy secondary radiation and fast electrons are shown. In the future radiotherapeutic possibilities may be enlarged by the use of heavy proton nuclei, which penetrate matter without appreciable scattering. (Excerpta Med., Sect. XXIII, 2: No. 6(June 1965))

38500 THE CASE FOR HYPERBARIC OXYGEN RADIOTHERAPY. Wildermuth, Orliss (Swedish Hospital, Seattle). J. Am. Med. Assoc., 191: 986-90(Mar. 22, 1965).

The radiobiologic basis, practical aspects, and possible future applications of high-tension oxygen in radiotherapy are reviewed. Clinical experience indicates that it is possible and within human tolerance to subject patients to hyperbaric oxygenation during the course of radiation therapy. The author has substantiated this experience and also demonstrated its practicability and applicability to be within the financial framework of clinical radiation therapy in a private hospital. In addition to the cancers with a growth pattern and histological configuration resulting in anoxia, there are other areas in radiation therapy of malignant disease in which an oxygen effect has been indicated. Thus, malignant melanoma, a deadly tumor with an unpredictable course, when irradiated is estimated to have a regression rate of 25%. Studies indicate that melanin, when irradiated, assumes a paramagnetic configuration resembling that of oxygen. It is possible, therefore, that the unpredictable radiation responses of the malignant melanoma could result from the protection of the tumor from radiation effects by the ion-scavenging pigment, melanin. Flooding the tumor site with oxygen, under hyperbaric conditions, might overcome the protective effect of melanin. In many areas where cancers grow the surrounding tissues are so sensitive to radiation that even modest doses cannot be tolerated. Cancers of pancreatic origin have a sensitivity to acceptable doses of radiation when treated in areas of metastasis such as in the chest or supraclavicular areas. By the use of the radiation potentiation effect of hyperbaric oxygen, they can be irradiated with doses that should be effective and tolerated in the upper abdomen. It is concluded that hyperbaric oxygenation is potentially one of the most important advances in radiation therapy of cancer. It has even a greater potential for cure of cancer than the introduction of supervoltage (^{60}Co) radiation therapy. (BBB)

38501 BRAIN SCANS IN DIAGNOSIS OF CEREBROVASCULAR DISEASE: SCANNING WITH CHLORMERODRIN Hg-203. Waxman, Herbert J.; Ziegler, Dewey K.; Rubin, Sidney (Univ. of Kansas, Lawrence). J. Am. Med. Assoc., 192: 453-6(May 10, 1965).

Chlormerodrin-^{203}Hg brain scans were done in 27 patients with neurologic symptoms. The technique required the intramuscular injection of 1 ml of sodium meralluride the night before the administration of chlormerodrin-^{203}Hg, to bind the sites of action in the renal tubules so that renal radiation is reduced. On the following day 750 μC of chlormerodrin-^{203}Hg was given intravenously. After four hr, radioactive emission from the cranial cavity was measured and recorded by dot scan and photoscan, using a large scanner. The skull was scanned in the anterior position and in either a right or left lateral projection, depending upon the localization of the greater intensity of radioactivity. The tests were conducted at various periods after cerebrovascular accidents; infarctions, hemorrhages (both intracerebral and subdural), and insufficiencies were represented. A high degree of correlation was obtained between the brain scan and other methods of clinical evaluation. In only one case of infarction of the hemisphere did the scan show a site other than that suspected clinically (a false-positive localization). Thus 17 out of 20 cerebral infarcts were accurately located by the scan. Most showed such a high differential from the surrounding tissues that the lesion was evident even on casual observation. Positive scans were obtained over a range of 4 to 53 days after the clinical onset of the illness. Scans four hr postinjection produced the most satisfactory record. However, in two elderly patients the blood had not sufficiently cleared the radioactive material for a lesion to be shown at two hr. Brain pathology was demonstrated by the scan in some cases that could not be demonstrated by the arteriogram. Confirmation of the nature of the lesions and their locations was obtained in three patients after craniotomy, and scan demonstrated the proper location in all of these patients. It is proposed that in cases of alteration of consciousness or atypical stroke, brain scanning may offer a facile method in helping define the lesion, thus obviating more dangerous procedures, such as an emergency cerebral arteriogram. The uptake of radioactive substances by infarcted brain tissue may be explained by two possible mechanisms. In infarct due to an occluded vessel radioactive uptake would

occur, presumably, not in the center of the lesion which would be totally anemic, but rather in the periphery. In these areas, moderate ischemia, resulting in altered capillary permeability and breakdown in the blood-brain barrier, would permit leakage of the radioactive material into the brain substance. If the lesion is due to transient interruption of blood flow from disturbances in the cardiovascular physiology, such as shock, restoration of the normal circulation results in a hemorrhagic infarct, capillary damage in the area of infarction allowing transudation of the radioactive substance into brain tissue. Accumulation of radioactive material near subdural hematomas may be due to either diffusion into the cavity itself or concentration in cerebral material compressed beneath the actual lesion. (BBB)

38502 CESIUM-131 UPTAKE AND DISTRIBUTION IN THE HUMAN HEART: AN ANALYSIS OF CARDIAC SCANS IN 104 PATIENTS. Himes, George E.; Worth, Leonard V.; Smith, Robert M. (Flint Osteopathic Hospital, Mich.). J. Am. Osteopath. Assoc., 64: 575-90(Feb. 1965).

Cesium-131 was used to scan patients whose hearts were considered normal after evaluation by other methods. An empiric dosage of sterile ^{131}Cs acetate, 1.25 mC for patients of 175 lb or more in weight and 1 mC for smaller patients, was injected into an antecubital vein. Two hr after injection the patient was scanned with a 3 by 2 in. Tl-activated NaI crystal and 19-hole focusing collimator. The count rate differential setting was set for the sharpest background cutoff, using a phantom made of sterile agar into which ^{131}Cs had been mixed in the liquid state and which was then molded roughly in the shape of the heart. A whole-body radiation exposure of 341 Mrad in a man weighing the standard 70 kg was calculated. It was noted that in active, ambulatory patients the concentration of ^{131}Cs in heart is less than in the patient on bed rest. Accordingly, scans in the latter were started 1½ hr after injection instead of 2 hr. The lean, muscular patient showed a higher concentration than did obese patients. One mC produced satisfactory scans in patients weighing under 85 kg, and was calculated to give a dose of 12 μC/kg. No detectable unfavorable reaction to the ^{131}Cs was seen in any of the patients. The scans showed the ventricular walls very well, the wall of the left ventricle and interventricular septum showing up much better than the wall of the right ventricle. The atria were seen in cardiac enlargement, since the mass of the atrial musculature was increased, resulting in a greater concentration of Cs. That Cs is rapidly and efficiently removed from the circulating blood was shown by the cold areas on the scans of the area occupied by the great vessels. Blood drawn at 15 and 30 min following the injection of Cs and showed extremely low counting rates. Counting of the separated plasma and red cells showed nearly all the activity to be in the plasma. Uptake of Cs by the liver was demonstrated on the scans as an area of increased uptake below and to the left of the heart. An area of acute infarction of the myocardium could not be distinguished from healing or healed infarction, fibrosis, or scar tissue. Since the damaged tissue does not contain a significant amount of active functional muscle fibers, the concentration of ^{131}Cs is so low that the area appears cold on the scan. In patients showing evidence of old infarction or who had previously had a recognized infarction, cold areas corresponding to the infarct, as indicated by the electrocardiogram, were always found. All patients with defects of the atrioventricular and right and left bundle branch conduction mechanisms demonstrated on electrocardiograms exhibited cold defects in the upper or basal areas of the ventricles along the area of the interventricular septum, although none of these patients has had an episode of clinical infarction. These studies suggest that infarction of a subclinical type, size, or location may occur earlier than has been previously thought and that the damage it leaves may not be detectable by any means other than autopsy or a technique such as scanning. It was not possible to measure the actual concentration of ^{131}Cs in the heart at autopsy so that the cold and cool areas could be examined by histologic sections. (BBB)

38503 ABSORBED RADIATION DOSE AND EXCRETION OF CESIUM-131 IN HUMANS. Himes, George E. (Flint Osteopathic Hospital, Mich.). J. Am. Osteopath. Assoc., 64: 724-8(Mar. 1965).

In 55 patients in which the isotope was used for cardiac scanning, data were collected on the effective half-life, absorbed dose of radiation, and excretion rates of ^{131}Cs. Cesium-131 is an excellent material for cardiac scanning, since a very low amount of radiation is absorbed, a dose about $\frac{1}{20}$ that received in diagnostic x-ray studies of the gastrointestinal tract. In calculating the dose of radiation absorbed by these patients a correction was made of the physical half-life from 10 days to 9.71 days. This was determined on each isotope lot by the actual counting of an aliquot of material at the same time each day. The effective half-life for each patient was determined by adding the percentage of the dose excreted in urine and/or feces plus 10% for decay for each day following dosage. With the intravenous dose used (1.25/mC) the absorbed dose is about 170 Mrad. In five patients, very low count rates over the liver or sacrospinalis muscles were found after 4 days. The count rate over the heart was 1.4 times the background radiation in the room. The calculated dose of absorbed radiation was lowest in those patients with the highest ^{131}Cs excretion rates. Differences in absorbed dose in patients with similar excretion rates were due to the differences in the concentration of the ^{131}Cs (in μC/g) of tissue, hence were due to actual variations in body weights. Early in the study the extreme variability of excretion rates in the urine was puzzling. A review of the charts revealed that patients who were receiving thiazide diuretics had the highest rates of Cs excretion in the urine. This is explained by the chemical behavior of Cs, which is like that of K. Chlorothiazide and related diuretics cause increased secretion of K in the distal tubule in exchange for Na. In patients taking thiazide diuretics, the average Cs excretion in the urine was four times that of the other patients; excretion rates in the stool were higher in patients not taking thiazide diuretics (intestinal secretions are rich in K). It seemed probable that Cs is similarly metabolized and would thus normally appear in greater quantity in the feces than in the urine. There is diversion of the Cs from gastrointestinal secretion due to increased excretion in the urine caused by the thiazide diuretics. The results show that absorption of radiation can be reduced further by the administration of a thiazide type of diuretic and, probably, by catharsis after the scan. (BBB)

38504 TUMORS OF THE BLADDER. (3) RADIOTHERAPY. Holden, H. (Peter MacCallum Clinic, Launceston, Australia). J. Coll. Radiologists Australasia, 8: 200-4(Oct. 1964).

The use of γ radiation, from both Rn and ^{60}Co, to treat 68 patients with bladder cancer is described, with data on technique, dosage, results, and incidence of complications and their treatment. Tumors too large for fulguration or with minimal evidence of infiltration and not more than 3.5 cm in dia were treated by radon seed implantation (three cases). Cobalt-60 arc therapy was used in early cases and in late cases where tumors were localized, and also in those patients whose girth was too great for fixed fields. Fixed fields were used in late cases. Radon seed implantation techniques used a dose of 6000 rad delivered at a depth of 0.5 cm by permanent implantation. Cobalt-60 beam radiation therapy was delivered over 280° arc with the patient lying supine to deliver a mean dose of 6000 rad to the tumor volume in 35 to 40 days. The minimum tumor dose was 4360 rad, and the maximum 6600 rad. The fixed field technique used five fields to deliver a mean dose of 6000 rad to the tumor volume, which often included the entire bladder. Following irradiation, two patients with residual tumor in the bladder were submitted to cystectomy. In one patient the obstructed ureter was reimplanted into the bladder at the time of radon seed implantation. Sudden renal failure during irradiation occurred in one patient and a bilateral ureteric transplant into the sigmoid colon was performed. Three patients required ureteric transplants after irradiation treatment. Only 12 cases were

available for assessment at five yr, only five were alive at five yr. Radical treatment of an advanced tumor produced death from uremia with alarming rapidity. Fifteen patients died from uremia within seven months from commencement of treatment, and although tumor could be eliminated from the bladder, the stress of the treatment superimposed on previous renal damage often resulted in fatal complications. Accurate assessment of renal function is an essential prerequisite to treatment, and the extent of the tumor must be accurately determined in planning such treatment. To assess renal impairment, a systematic study with radioiodinated hippuran excretion renogram was undertaken. Results of renograms obtained in patients with a bladder cancer before and after treatment with ^{60}Co beam rotation are shown. Renal impairment is revealed by this test earlier and more accurately than by other renal function tests, including the excretion pyelogram. (BBB)

38505 RADIOISOTOPES AND THEIR MEDICAL APPLICATIONS. Blanquet, M. P. (Hopital St. Andre, Bordeaux). J. Med. Bordeaux Sud-Ouest, 141: 1598-1612(Oct. 1964). (In French).

Various medical applications of radioisotopes are reviewed, with emphasis on diagnostic rather than therapeutic applications. Their possible uses and limitations in detecting diseases of the thyroid, liver, kidney, blood, heart, and nervous system are discussed. Functional examinations of the thyroid are effected by the administration of radioiodine as a tracer in about 50-μC doses. By this technique, the uptake of ^{131}I by the thyroid, the concentration of radioactive hormones in the circulation, and scintigraphic patterns of the thyroid can be determined. Hepatography can be accomplished through the injection of ^{198}Au, but because of its tendency to fix in the Kupffer cell system of the liver, false-positive diagnoses of metastases often occur. For the examination of the hepatic cell, Rose Bengal labeled with ^{131}I provides an excellent tracer. However, the length of time required for the examination limits its effectiveness. The utilization of radioisotopes to investigate renal function is discussed. Other clinical tests employing radioisotopes to investigate blood volume, extracellular fluid space, anemias, iron metabolism, cardiovascular disorders, and neurologic diseases are described, with reference to use of ^{24}Na, ^{42}K, ^{45}Ca, ^{51}Cr, ^{58}Co, ^{59}Fe, ^{68}Ga, ^{74}As, and ^{206}Bi. Some examples of the results of these tests in various disorders are illustrated. (BBB)

38506 INTERNAL DOSE CALCULATION FOR ^{99m}Tc. Smith, E. M. (Public Health Service, Bethesda, Md.). J. Nucl. Med., 6: 231-51(Apr. 1965).

The total local energy deposited per distintegration, $\bar{E}_\delta$ for ^{99m}Tc is 14 kev per disintegration. The specific gamma-ray constant, Γ, for ^{99m}Tc is 0.72 R-cm^2/mc-hr; however, 29 per cent of this value is due to K_α and K_β x rays which make up only 1.2 per cent of the total photon energy emitted by ^{99m}Tc. Standard methods of calculating the gamma component of the absorbed dose for ^{99m}Tc using the geometrical factor and Γ yield results which underestimate the absorbed dose by 16 to 30 per cent compared to calculations based on Monte Carlo techniques which take into account the energy dependence of μ_{air} and the inflated value of Γ. The Monte Carlo technique was used in making the absorbed dose estimates presented. Absorbed dose estimates were made for ^{99m}Tc as TcO_4^- for brain scanning, as compared to ^{131}I labeled serum albumin and ^{203}Hg and ^{197}Hg labeled Neohydrin; ^{99m}Tc labeled serum albumin for placental scanning, as compared to ^{131}I labeled serum albumin; and the ^{99m}Tc sulfur colloid for liver and bone marrow scanning as compared to colloidal ^{198}Au, colloidal ^{199}Au and ^{131}I aggregated albumin. Some of the biological problems encountered in calculating the absorbed dose are discussed. (auth)

38507 PURIFICATION OF RADIOACTIVE SODIUM O-IODOHIPPURATE USING GEL FILTRATION WITH DEAE-SEPHADEX. Brown, Donald W.; Phelps, Norma J.; Palmer, Darwin L. (Univ. of Colorado, Denver). J. Nucl. Med., 6: 287-91(Apr. 1965).

A simple method of separating radioactive impurities from ^{131}I-labeled o-iodohippurate using gel filtration with DEAE-Sephadex is presented. (auth)

38508 TUMOR SCANNING WITH RADIOACTIVE ^{131}CESIUM. Charkes, N. David; Sklaroff, David M.; Gershon-Cohen, J.; Cantor, Robert E. (Albert Einstein Medical Center, Philadelphia). J. Nucl. Med., 6: 300-6 (Apr. 1965).

Fourteen patients with cancer were scanned 10 minutes to 48 hours after injection of radioactive ^{131}Cs, and satisfactory scans of the tumors were obtained in seven. Positive scans were obtained in large, superficial tumors, in a pulmonary lymphoma, and in a carcinoma of the upper third of the esophagus. The negative scans were all in abdominal tumors. Correlations were made with data obtained from external counting and by well scintillation counting of biopsy specimens. Two modes of uptake suggested include early uptake due to vascularity and probably not proportional to stable cesium content; and a later uptake based upon greater alkali metal content of tumors than of normal tissue. (auth)

38509 SEVERE RADIOINDUCED HEMOLYSIS IN HEREDITARY DEFICIENCY OF REDUCED GLUTATHIONE IN BLOOD CELLS. Waller, Hans Dierck; Gerok, Wolfgang (Medizinische Universitaetsklinik Tuebingen, Ger.). Klin. Wochschr., 42: 948-54(Oct. 1, 1964). (In German).

Clinical and biochemical data are presented and a detailed case report is given of a 51-yr-old woman, suffering from carcinoma of the uterine cervix, who developed severe hemolysis during a combined treatment of x-ray and Ra radiation. This hemolysis, caused by irradiation, was produced by a low level of reduced glutathione (GSH) in the red cells. All enzymes of the red cells involved in the reducing reactions of GSH showed normal activities. Thus a defect in GSH synthesis is most likely. The results of the amino acid chromatography were in accordance with this hypothesis. In the erythrocytes the GSH content amounted only to 50% that of normal individuals; beside this, an instability of GSH to a varying degree was found as well as increased Heinz body formation after incubation with acetylphenylhydrazine. Glycolysis and ATP content of the red cells were within normal limits; cold agglutinin and Coombs tests were negative. The investigation of other members of the same family showed the same diminution of GSH in the red cells. Most likely this inborn metabolic disorder is inherited in an autosomal recessive way. The radiation-induced hemolysis was treated successfully by blood transfusions and adrenal steroids. Six months after the onset of the hemolysis, red cell count and hemoglobin were compensated without further therapy, whereas leucocytes and blood platelets were still diminished. (BBB)

38510 GAMMA-ENCEPHALOGRAPHY WITH Hg^{203}-NEOHYDRIN. Bernier, J.-P.; Heon, M.; Plamondon, C. Laval Med., 35: 1077-83(1964).

A preliminary report is given on gamma encephalography with ^{203}Hg-neohydrin. Visualization is good if flat scanning is done, using a detector with an NaI crystal of two inches in diameter. Detection of a lesion and its localization are more important than exact determination of its outline. Therefore definition of the detector can be sacrificed for sensitivity if necessary. (Excerpta Med., Vol. 2, July 1965))

38511 TREATMENT OF HAEMANGIOMAS OF THE SKIN. Panzner, R. (Universitaet, Halle/Saale, Ger.). Med. Klin. (Munich), 59: 1783-5(1964).

For treatment of hemangiomas many therapeutic possibilities are available. Results are reported for 700 hemangiomas treated during a period of 10 yr. Simple and small cavernous hemangiomas, up to a diameter of 1 cm, were treated with frozen CO_2. In 92% of the cases where follow-up was possible, good to satisfactory results were obtained. The method is very inexpensive and safe. Larger cavernous hemangiomas were treated by excision. The operation is radical and safe. Radiotherapy is not recommended. Personal follow-up studies showed that in some 50% of cases late results were poor. A benign change of the skin such as a hemangioma does not require x ray therapy, and

ionizing rays should no longer be used for treatment of hemangiomas, as some cases of manifest radiation damage were seen. (Excerpta Med., Sect. XXIII, 2: No. 6(June 1965))

38512 INDICATIONS AND EFFECTS OF ADDITIONAL ANTIBIOTIC TREATMENT IN RADIOTHERAPY. Kleibel, F. (Universitaet, Heidelberg). Med. Welt, [No.] 47, 2536-41(1964).

The importance and genesis of inflammatory complications in tumoral diseases are discussed. Control of inflammation with antibiotics and corticosteroids is described. Sixty-one patients with carcinoma and secondary inflammations were treated with dimethylchlorotetracycline. The secondary inflammations were either caused by the tumor, by irradiation, or by radiomimetic drugs. In toxic damage to the bone marrow and protracted glucocorticoid therapy with large doses, dimethylchlorotetracycline was given for protection. The antibiotic effect was always good and some radioprotective effect was obtained. Serious side-effects were not seen and the antibiotic was not discontinued prematurely on account of undesirable reactions. (Excerpta Med., Sect. XXIII, 2: No. 6(June 1965))

38513 SURGICAL MANAGEMENT OF POSTRADIATION ULCERATIONS AND SCARS OF THE SKIN. Kulakowski, A. Nowotwory, 14: 357-66(1964).

Causes and pathological appearances of radiological ulceration of the skin, and factors influencing the healing of these lesions, are discussed. Principles of general and topical treatment of postradiation ulcerations and scars are presented. Tactical and technical problems of surgical management of ulcerations are discussed in detail and illustrated by a number of cases. (Excerpta Med., Sect. XXIII, 2: No. 6(June 1965))

38514 SOME PROBLEMS OF RADIATION PROTECTION ASSOCIATED WITH THE GYNAECOLOGICAL APPLICATION OF BRACHYCURIE THERAPY. Kuhn, E.; Keller, G. Orv. Hetilap., 105: 2427-9(1964).

Measurements of radiation level were carried out in the gynaecological department engaged in brachycurie therapy. The department was well equipped for this purpose with radioprotective devices. Purposeful modification of the radioactive preparations, their careful application, the proper care and placement of the active patient, in advance planning and organization up to the smallest detail of department routine resulted in significant reduction of the radiation exposure of personnel. By such means it became possible to keep the radiation exposure of nursing and medical staff under the permissible maximum radiation level. Exchange of personnel, and the employment of nulliparous young women should be avoided. (Excerpta Med., Sect. XXIII, 2: No. 6(June 1965))

38515 RADIOACTIVE COLLOID TREATMENT OF MALIGNANT EFFUSIONS. Sklaroff, David M. (Albert Einstein Medical Center, Philadelphia). Penn. Med. J., 68: 41-3(Jan. 1965).

Indications for, mode of action, biological and physical properties, contraindications, side-effects and hazards, and clinical results in the use of ^{32}P, ^{90}Y, and ^{198}Au to treat malignant infusions are reported. The two primary indications for intracavitary instillation of these radioisotopes are for the suppression of pleural and peritoneal fluid accumulation due to metastatic malignancy and destruction of spilled tumor cells. The injected radioisotope produces its result locally, either by inhibiting the fluid inflow or by enhancing reabsorption. It achieves this through its lethal effect on the serous carcinosis (free cancer cells, serosal implants, or both), its alteration of the normal serous membrane with its important lymphatic and vascular channels, its tendency to promote adhesions, or a combination of these factors. Gold-198 has a half-life of 2.7 days, a single γ ray of 412 kv, and a β ray of 960 kv; ^{32}P has a half-life of 14.3 days, no γ emission, its maximum β energy of 1700 kv (almost twice that of ^{198}Au, and the depth of penetration of the β particle into the tissue is correspondingly greater). The half-life of ^{90}Y is 2.4 days. Like ^{32}P, it emits no γ rays, and its maximum β energy of 2260 kv is 33% higher than that of ^{32}P. After intracavitary injection, a small amount of ^{198}Au slowly finds its way into the blood stream. The estimated β surface doses (assuming an area of 30,000 cm^2 for the average peritoneum) is 4500 rad for 150 mC of ^{198}Au. Because of the smaller area of pleural serosa, the β dose would be several times greater in intrapleural administration. Similarly, radioactive colloidal chromic phosphate, is rapidly removed from the effusions, but it has these advantages over ^{198}Au: it is safer to handle, due to the absence of γ radiation; it is more economical, since its use precludes hospitalization; and it has a more penetrating β particle. The ^{90}Y β ray is the most penetrating of any in these colloids (11 mm). In the injected cavity, aggregates of the complex precipitate in the serosal surfaces, its isotope thus being brought into intimate contact with the wall of the cavity, upon which its intense β rays can exert their effect. No radiation damage is sustained by distant tissues. Suggested doses for the three isotopes in various cavities are tabulated. When a radioisotope is injected into the pleural or peritoneal cavity, two dangers must be avoided: injecting it into the subcutaneous tissue, where it would cause a severe local radiation reaction, and injecting it into an underlying viscus. Both accidents have occurred when little fluid or many adhesions were present. Also described are the equipment and methods of administration. Because of the danger of radionecrosis, the presence of loculated areas in the abdomen is a contraindication, as are symptoms of intestinal obstruction. Because spillage and contamination are likely, administration should not be made in exposed cavities. As to side-effects and hazards, no deleterious effects on the patients' general condition, or on liver, blood, or bone marrow were seen. Occasional nausea is easily controlled with antiemetics. Radiation exposure during administration of ^{198}Au can be kept as low as 5 to 10 mrad. Personnel attending a patient who receives 100 mC can usually remain within three ft of him for 20 hr during a week without exceeding tolerance. Except for accidental spillage during administration, no radiation danger to attending personnel exists when the β-emitting isotopes are used. Clinical results showed that slightly more than 50% of patients with malignant pleural and peritoneal effusions benefit by intracavitary injections of radioisotopes, the results with the three used showing no statistically significant differences. (BBB)

38516 MEDICAL RADIOISOTOPE SCANNING. Mallard, John R. (St. Thomas's Hospital, London). Phys. Med. Biol., 10: 309-34(July 1965).

The use of radioisotope scanning in diagnostic radiology is discussed. Information is given on: principles of the technique; moving detector scanners; stationary detector scanners; clinical applications of scanning; and intercomparisons of isotopes and scanning machines. 124 references are included. (P.C.H.)

38517 NEUTRON MEASUREMENTS RELATING TO PATIENTS TREATED WITH X-RAYS FROM 70-Mev SYNCHROTRON. Adams, Gail D.; Paluch, Ilga R. (Univ. of California, San Francisco). Phys. Med. Biol., 10: 335-44 (July 1965).

An attempt was made to estimate the flux and spectrum of neutrons under three circumstances found in connection with the use of x-rays from a 70-Mev synchrotron in cancer therapy: neutrons generated within the synchrotron structure and appearing in the air space generally occupiable by the patient; neutrons generated by tissue phantoms and contributing to the general background; and neutrons present within a water phantom. The flux and spectrum information was converted to appropriate absorbed dose rates and found to be insignificant compared with the dose rate from photons. The method of threshold detector foils was used but only phosphorus was really useful, so that spectrum information in the end had to be assumed. Two difficulties are encountered with the lower energy threshold detectors: natural radioactivity, causing a high background; and photofission, which usually overwhelms the neutron fission to be measured. The neutron dose to the fetus of a pregnant woman treated for lung cancer was evaluated and found to be less than from photons. (auth)

38518 COMPUTER OPTIMIZATION OF 4 Mev TREATMENT PLANNING. Hope, C. S.; Orr, J. S. (Western Regional Hospital Board, Glasgow). Phys. Med. Biol., 10: 365-73(July 1965).

The place of optimization in treatment planning is discussed and the difficulties examined. A model computer program for optimizing two or three field treatments is described in which dose gradients are represented by vectors. Three criteria—uniformity, tumor dose, and integral dose—are used in the program to select the optimum. (auth)

38519 LATE CHANGES OF THE LARYNX AFTER RADIUM IRRADIATION OF CARCINOMA OF THE VOCAL CORD. Minnigerode, B. Pract. Oto-Rhinolaryngol., 26: 409-17(1964).

Independent of the applied radiation dose, late lesions can be observed in 19.8% of the cases following radiotherapy of carcinoma of the vocal cord; they can be the delayed result of an acute radiation lesion or they can develop without a previous acute lesion. As differences in degree of the same pathological-anatomical processes, late lesions occur in the form of fibrinous chorditis, fibrino-ulcerous chorditis, radioinduced dystrophia of cartilage, and persisting fistulae in the region of the operative scar on the skin of the neck. Based on experience with 293 cases of carcinoma of the vocal cords treated by radiotherapy, the clinical and pathological-anatomical manifestations as well as the frequency of the individual lesions are described and suggestions for their interpretation and treatment are made. (Excerpta Med., Vol. 2, (July 1965))

38520 A COMPARATIVE STUDY OF RADIONEPHROGRAPHY AND EXCRETION UROGRAPHY. Gotta, H.; Olivari, A.; Pecorini, V.; Garcia del Rio, H.; Chwojnik, A. Prensa Med. Arg., 51: 853-8(1964).

A comparative study of the relation between radioisotope renography (RR) and excretory urography (EU) was performed on 200 patients. The RR's were classified into four groups: I: normal, II: subnormal, III: obstructive pattern and IV: renal failure pattern, and the EU's as A: normal, B: subnormal, C: uronephrosis, ptosis or lithiasis and D lack of pyelocalycial image. Of 47 bilateral normal RR's 38 normal, EU-wise, were found; for the remaining 153 abnormal cases, only 49 showed an equivalent diagnostic pattern by the two methods. On the whole, the general diagnostic correlation was 43%, showing higher values in the normal group (80%) than in the abnormal one (32%). There was thus no absolute correlation between RR and EU. Disturbance in renal function has a different effect on the two methods: renal failure and obstructive uropathy can be detected earlier by means of RR. The RR and the EU are procedures which do not substitute but supplement each other. The RR mainly provides information on kidney function and its excretion dynamics with the advantages of continuous recording over the interrupted serial information afforded by EU. (Excerpta Med., Vol. 2, (July 1965))

38521 IS Ir^{192} ABLE TO REPLACE RADIUM? Pierquin, B. Presse Med., 73: 69-72(1965).

A comparative study between the conditions of use of radium and of iridium-192 suggested that considerable advantages may be obtained by the replacement of radium with iridium-192. While the future of endo- and plesiocurietherapy appeared to be using limited radium, a new development in the clinical indications of endo- and plesiocurietherapy is possible using iridium-192. (Excerpta Med., Vol. 2, (July 1965))

38522 A CONTRIBUTION TO THE STUDY OF DEEP POSTRADIOTHERAPEUTIC DIGESTIVE STENOSES: IN REGARD TO FIVE OBSERVATIONS. Belotte, J.; Gary-Bobo, J.; Pourquier, H.; Pages, A. (Clinique Saint-Eloi, Montpellier, France). Presse Med., 73: 851-6(Mar. 24, 1965). (In French).

Five cases of anatomical modifications of the digestive tube after deep localized irradiation of gynecologic tumors are described. Observation I: A woman, 52, received 5800 R for epithelioma of the uterus. Six months later she developed a genital hemorrhage and diarrhea, and then an alternation of constipation and diarrhea. A blockage was found in the large intestine. It was diagnosed as a secondary neoplasic invasion. The patient died a year later. Observation II: A woman, 32, received 2000 R preoperatively and 3000 R postoperatively for a vaginal epithelioma and pelvic lymphadenectomy. Eight months later she was hospitalized, suffering from moderate lymphedema and hydronephrosis. She was treated, but relapsed in six months. It was believed the rectosigmoidal modifications were secondary results of the pelvic irradiation. Observation III: A woman, 51, had received radiosurgical treatment for cancer of the uterus, Curie-therapy and hysterectomy, and deep radiotherapy. Eight years later she suffered with constipation, diarrhea, and a subocclusion of the intestine. Following two operations, she had persistent pain in the left iliac region. The normal sigmoid was absent. The neoplasia of the patient was controlled, but problems with the intestinal passage persisted. The diagnosis was postradiotherapeutic sclerosis. Observation IV: A woman received 3500 R before and 2500 R after receiving 10,300 mg-hr radium for uterine cancer. One year later she had trouble with intestinal passage. Seven months after that, a cutaneous sclerosis developed at the four radiation portals on the abdomen. There was, also, a stenosis of the descending sigmoid. A histological examination confirmed parietal sclerosis. The condition was controlled. Observation V: A man, 52, received deep roentgentherapy for testicular cancer and later x-ray treatment for localized metastases. Two years later, he was hospitalized for dorsolumbar pain. It was discovered his stomach had profound adhesions and sclerosis as a result of the radiotherapy. He died within two years. (BBB)

38523 RADIATION PROTECTION IN MEDICAL RADIOLOGY. Schinz, H. R.; Wideroee, R. Radiol. Clin. Biol., 34: 32-60(1965).

After review of the present maximum permissible body dose and the genetically desirable yearly dose for the total population, the physical basis of radiation damage in therapy and diagnostics are discussed. A judicious procedure for radiation diagnosis of patients is indicated. Radiation protection for patients, doctors, and technicians requires not only well screened apparatus and devices that are as free from scattering radiation as possible, but also discipline in the application of x radiation. (tr-auth)

38524 QUANTITY AND QUALITY OF SCATTERED X RAYS. Wachsmann, F. (Universitaet, Erlangen, Ger.). Radiol. Diagn., 6: 369-78(1965). (In German).

The theoretical foundations of scattered x rays in matter and the practical measurements with various materials, i.e., materials of low atomic number, building materials, and metals are discussed. These measurements are performed within the energy range of 15 kv–17 Mev. The quantity of the scattered rays expressed in percentage of the incident radiation as well as the quality expressed in mm HVL depend to a large degree on the kind of the scattering material and on the hardness of primary radiation. Conclusions are made with regard to the improvement of the radiation climate, especially in small diagnostic rooms. (auth)

38525 ISOTOPIC METHODS FOR THE DETERMINATION OF BLOOD VOLUME. Eich, Glen B. (Immanuel Hospital, Omaha). Radiol. Technol., 36: 316-20(Mar. 1965).

The use of ^{32}P, ^{51}Cr, ^{59}Fe, and ^{131}I-serum albumin (RISA) in measuring blood volume is discussed, and it is shown that only two of these isotopes have proven to be reliable tags for their respective carriers. Radioactive $Na_2{}^{51}CrO_4$ preferentially labels red blood cells, and this tag is quite stable, with little elution in the first 24 hr. Also, the bond between radioiodine and albumin is stable. The possibility of simultaneous methods for the independent measurement of red cell mass and plasma volume using these isotopes is discussed. A problem exists in that the major energies of these two isotopes are close: 0.32 Mev for ^{51}Cr and 0.36 Mev for ^{131}I. However, with the use of a pulse height analyzer and the usual isotope dilution methods, consecutive ^{51}Cr and ^{131}I red cell and plasma volumes may be measured.

For the consecutive measurement of ^{51}Cr red cell mass and RISA plasma volume, the ^{51}Cr cell volume is determined by the isotope dilution principle. The patient's whole blood (20 ml) is incubated with 100 μC of ^{51}Cr in acid citrate dextrose solution and the tagging process is stopped with ascorbic acid. After 15 ml of labeled whole blood is returned to the patient, and allowing 20 min for adequate mixing, a single sample of blood is withdrawn from the patient. One ml aliquots are then counted with the pulse height analyzer at the ^{51}Cr level on integral setting. Immediately after withdrawing the ^{51}Cr sample, 20 μC of RISA is given the patient intravenously, and after allowing 15 min for intravascular mixing, another sample is removed. One-ml samples of ^{51}Cr whole blood and plasma are also counted at the RISA setting, and these values are subtracted from the RISA counts to obtain net counts due to RISA alone. Some disease states which may be associated with considerable changes in either red cell mass or plasma volume, with or without parallel changes in the other, are: emphysema, polycythemia vera, congestive heart failure, tuberculosis, hemorrhage, relative polycythemia, cirrhosis, pregnancy, and acute glomerular nephritis. Only blood volume studies can distinguish these situations from normal. (BBB)

38526 CLINICALLY USEFUL CALCULATIONS OF THE DOSE DISTRIBUTION FROM MULTIPLE RADIATION SOURCES. Adams, Robert M.; Peterson, Mary; Collins, Vincent P.; Hudgins, Philip T.; Gibbs, Priscilla. Radiology, 85: 361-4(Aug. 1965).

The use of an electronic digital computer for dosimetry of intracavity radium is discussed. It is possible, using the computer, to compute the value of the dose rate at points on a 1 cm or even a 0.5 cm grid in a 20 × 20 cm tube about the radium applicator. The printed values can be plotted on a set of parallel planes and various isodose curves found on each plane by interpolation. Other functions of the computer are also described. (P.C.H.)

38527 MANDIBULAR RADIONECROSIS. Jucker, C.; Ferrari Parabita, G.; Preda, G. Riv. Patol. Clin., 18: 919-45(1963).

The histological and radiological characteristics of radionecrosis are reviewed. The factors involved are: absorption of radiation by the bone (with supervoltage radiations, the osseous absorption is less than with 200 kv); the condition of the irradiated osseous tissue and the state of the teeth (infections and dental caries favoring radionecrosis); and the characteristics of the radiotherapeutic technique employed (interstitial radium therapy, radiotherapy, whether conventional, cobalt therapy or betatron). Prevention is considered the best defence against radionecrosis and it is advisable to extract the dental pieces present in the field of irradiation before the radiological treatment. Interstitial radiotherapeutic methods are preferable, since they cause fewer accidents. The risk diminishes also with the use of high energies. The collaboration between radiotherapist and odontostomatologist is considered indispensable. (Excerpta Med., Vol. 2, (July 1965))

38528 THE EFFECT OF RADON INHALATION ON SOME CHRONIC DISEASES OF THE NOSE AND THE PARANASAL CAVITIES IN THE RESORT MOMIN PROHOD. Simeonov, K.; Agopian, K. Sb. Tr. Visshiya Med. Inst. I. P. Pavlov, [No.] 18, 25-9(1964). (In Russian).

For a period of two years over 1400 patients were examined. At the end of the treatment all patients, except those with hyperplastic polypous alterations of the nasal cavity, reported that subjective complaints disappeared. In patients with hyperplastic polypous formations the complaints were aggravated during the course of the treatment, but a month later, after the cessation of the treatment, they felt very well for a period of 6 to 9 months. Morphologic examination of the polypous masses after inhalatory treatment showed that dystrophic and necrotic changes occurred in the polypous tissue, possibly due to the action of radonic substance, containing radon, in the inhalated water. (Excerpta Med., Sect. XXIII, 2: No. 6(June 1965))

38529 CLINICAL AND ROENTGENOLOGICAL OBSERVATIONS ON THE FUNCTIONAL CONDITION OF THE GASTROINTESTINAL TRACT OF PATIENTS WITH THYROTOXICOSIS BEFORE AND AFTER TREATMENT WITH I^{131}. Gezentsvei, Z. A.; Petrova, M. M.; Kurbatova, L. I. Terapevt. Arkh., 36: 30-6(1964).

Disorders of the gastrointestinal tract, such as changing appetite, gastralgia, sometimes vomiting, and frequent stools, occur in patients with thyrotoxicosis. Decreased gastric secretory activity and marked disturbances of peristalsis in the form of hyperkinesis of the whole gastrointestinal tract were noted in patients before treatment with ^{131}I. Treatment with ^{131}I resulted in a marked tendency towards normalization of the gastric secretory activity and decreased hypermobility of the gastrointestinal tract, and especially in functional normalization of the large intestines. (Excerpta Med., Vol. 2, (July 1965))

38530 RADIO-PYELOGRAPHY. Tsuchida, S. (and others). Tohoku J. exptl. Med., 82: 316-26(1964).

A new and simple method, radiopyelography, was devised for examination of the renal pelvis and calyx dynamics. This method proved to be useful for recording the excretory function of the renal pelvis and calyx. The changes in radioactivity of ^{131}I-labeled hippuran following injection into the renal pelvis were recorded with a scintillation detector ratemeter and recorder. The graphic record was named the radiopyelogram. The radiopyelogram gave a constant curve in normal cases, but in patients with disorders of the upper urinary tract some changes in its figure were demonstrated. The basic pattern of the radiopyelogram was represented in a logarithmic formula as a function of outflow of urine, capacity of the renal pelvis and time course. Radiopyelography is useful in the analysis of radiorenograms of patients with disorders of the upper urinary tract. (Excerpta Med., Vol. 2, (July 1965))

38531 THE LATE BLADDER CHANGES CAUSED BY RADIOTHERAPY OF UTERINE CARCINOMA. Holtorff, J.; Moench, L. (Akademie "Carl Gustav Carus", Dresden). Wiss. Z. Humboldt-Univ. Berlin, Math.-Naturw. Reihe, 12: 163-8(1963). (In German).

Often the gynecologist or radiologist remains unaware of the eventual result of tumor irradiation because a certain number of the patients treated become unavailable for follow up studies. Bladder injuries may appear at any time from 1 month to many yr after irradiation of uterine tumors. Injuries produced in the urinary system after combined Ra and x irradiation treatment in 200 patients were studied by means of urological tests from 1 to 12 yr after the treatment. In ~50% of the cases bladder injuries consisting of atrophic mucosa, teleangiectasis, scarification, inflammation, ulcers, and bladder rigidity were observed. However, injuries were severe enough in only 15% to require special or immediate treatment. In general, the prognosis for late developing bladder injuries is favorable, but damage to the bladder walls caused by irradiation should not be underestimated. Two illustrative cases are described. In both, severe bladder hemorrhage suddenly appeared 9 or 10 yr after irradiation. In both cases the injuries to the bladder consisted of irradiation cystitis, and the patients died. (BBB)

38532 UROLOGICAL INJURIES AFTER TREATMENT OF CARCINOMA OF THE UTERINE NECK (RESULTS OF CONTROL STUDIES). Guenther, Horst (Landesfrauenklinik der Medizinischen Akademie, Magdeburg, Ger.). Wiss. Z. Humboldt-Univ. Berlin, Math.-Naturw. Reihe, 12: 179-81(1963). (In German).

Out of 261 patients who showed evidence of recurrence of carcinoma of the neck of the uterus after x irradiation with 4000 to 4500 R, 73% showed no urinary tract damage. Slight urinary tract damage was observed in 18%, and 9% had severe urinary tract damage. The symptoms of injury appeared within 6 months to 6 yr after irradiation. The relatively slight injuries observed consisted of unilaterally or bilaterally impaired excretion of dye, bulbous edema of the trigonoma vesica, irradiation cystitis, fibrotic or hemorrhagic trigonomal cystitis, and nonspecific irradiation ui-

cer. The severe irradiation injuries consisted of ureteral atonia, ureteral scarification, narrowing of the ureteral lumen, contracted bladder, cystitis, kidney blockage, and hydronephrosis. For these injuries the value of 9% incidence lies within the lower portion of the range of severe urinary tract damage reported from other clinics. (BBB)

38533 AUTORADIOGRAPHY OF THE THYROID. Vickery, Austin L. Jr. (Massachusetts General Hospital, Boston). p.207-25 of The Thyroid (International Academy of Pathology Monograph No. 5), Edited by J. Beach Hazard; David E. Smith. Baltimore, Williams & Wilkins, 1964.

Detailed directions, with many illustrations, for autoradiographic techniques used to study radioiodine uptake in human thyroid glands are presented. The theory and principles of autoradiography are reviewed. Although ^{131}I has proved useful in thyroid autoradiographic studies, its relatively high-energy β particles have too long a range for critical cytologic localization. Since the range of β particles is an exponential function of their energy, the weaker β rays have the desirable features of very short paths which produce better resolution. Iodine-125, a 60-day half-life isotope with a very low energy β-like component (21 kev compared to 187 kev for ^{131}I, was found to be highly superior to ^{131}I in experimental studies requiring high degrees of resolution. It also emits γ rays, actually in higher proportion than does ^{131}I, so that counting of ^{125}I radioactivity is more efficient. The concentration of radioiodine in thyroid tissue high enough to give a positive autoradiograph depends to a large extent on the method used. A rough screening procedure on surgical thyroids (by weighing samples of the gland, measuring radioactivity in a well-type counter, and calculating $\mu C/g$) showed that 1 $\mu C/g$ of tissue is about the min activity for the conventional microautoradiographic use, but that autoradiographs of histologic sections made with the simple contact film method can be obtained from 0.1 $\mu C/g$ or less. Factors such as section thickness, type of emulsion, and exposure time are considered. In general, highest resolution in autoradiography requires the thinnest sections and emulsions. Also considered are gross autoradiographs, which are of value in clinical correlations, such as thyroid scintograms, and in situations in which only coarse localization of radioactivity is required. The four general types of microautoradiographs, which utilize microtome-cut histologic sections but differ in methods of photographic emulsion application, are outlined. Whichever technic is used, stripping or dipping, the principle is the same: emulsion is on the top of the histologic section, producing a slide-tissue photographic emulsion sandwich effect. Preferred is the liquid emulsion method, because of its superior staining qualities, ease of preparation, and versatility of application and it is recommended as the one of choice for routine microautoradiography. Types of technical errors are described. These techniques have a wide range of applicability which includes comparative studies of radioiodine uptake and histochemical observations on enzymatic activity; measurements of cell turnover times with ^{3}H-labeled thymidine in various experimental thyroid states; and observations on sites of tissue localization of ^{35}S-labeled thiouracil compounds. (BBB)

38534 DOSISVERTEILUNG UND DOSISERMITTLUNG BEI DER PENDELBESTRAHLUNG (200 kv BIS 17 Mev). ROENTGENSTHAHLEN UND SCHNELLE ELEKTRONEN. (Dose Distribution and Dose Determination in Pendulum Irradiation (200 kv at 17 Mev). X-Rays and Fast Electrons). Keller, Hans Ludwig. Munich-Berlin, Urban and Schwarzenberg, 1964. 242p.

Graphs and tables to be used by the radiologist in the determination of the dose distribution and dose rate in pendulum irradiation with both x rays and fast electrons are compiled. The principles used in the compilation of the table and the methods for their application are discussed. (J.S.R.)

CHEMISTRY

General

Refer also to abstract 39265.

38535 (RFP-508) HANDLING AND MEASUREMENT OF PLUTONIUM SHIPMENTS. Byrne, J. T. (Rocky Flats Div., Dow Chemical Co., Golden, Colo.). [1965]. Contract AT(29-1)-1106. 32p. (CONF-650803-5). Dep. mn; CFSTI, $2.00 cy, $0.50 mn.

From IAEA Symposium on Nuclear Materials Management, Vienna.

Recent studies on the measurement problems associated with handling and shipping plutonium are summarized. Factors affecting the stability of plutonium in the forms of metal, nitrate solution, and oxide were identified and current procedures evaluated. Conditions which lead to gas evolution, hydrogen ion consumption, and precipitation in plutonium nitrate solutions were defined. With proper control of these effects, nitrate shipments can be made with average shipper-receiver differences under 0.2% and a standard deviation of under ±0.3%. Compositions in the range of 50–250 g/l plutonium, 2–10N nitric acid, and up to 5000 ppM metallic impurities were tested. Procedures for bulk measurements (both weight and volume), complete transfer, sampling, and analysis of plutonium nitrate in batches up to 10 liters are available. The major contributor to shipper-receiver differences in shipments studied was the analytical determination of plutonium in solution. Smallest differences are observed when the same analytical method is used for both shipper and receiver measurements. Plutonium oxide cans may pressurize during shipment, if the oxide is low-fired, causing loss of material when the can is opened. However, properly prepared oxide can be shipped in batches of 2–12 kg with a measured loss less than 0.2%. Procedures for blending, sampling, and transferring were tested. Calorimetric assay of the plutonium can eliminate sampling errors and reduce analytical cost. Metal shipments have presented little problem in measurements. Oxide formation due to self-heating and atmospheric corrosion is controlled by proper packaging. The cost of shipping plutonium depends upon the form and size of the shipment. Factors affecting the shipping cost are evaluated. (D.L.C.)

Analytical Procedures

See also Separation Processes and Procedures.

Refer also to abstract 38769.

38536 (ACF-6) ELECTRON MICROPROBE DATA QUANTIFICATION. An Analytical Chemistry Evaluation. Allen, J. D.; Sandoval, Jacob (ACF Industries, Inc., Albuquerque, N. Mex.). June 1, 1965. Contract AT(29-1)-1352. 19p. (ACF-413-244) Dep.(mn); $1.00(cy), 1(mn) CFSTI

A comparative study of several methods for data quantification incorporating absorption and fluorescence corrections was conducted. The basic differences in the methods are found in their complexity and their mode of presenting and manipulating the variable parameters concerning the absorption and fluorescence phenomena. Although the mathematical models for these quantification procedures are based on consideration of binary alloy systems, sufficient information is available to allow investigation of ternary systems using the same basic parameters. Four data correction procedures were examined for the analysis of nickel, iron, and chromium in stainless steel. For the concentration ranges, nickel 0.5–13%, iron 69–85% and chromium 5–24%, the relative errors in the corrected data (compared to certified chemical values) were generally less than four percent of the amount present. It appears, therefore, that the selection of a particular correction technique is essentially one of operator preference. The determination of light elements in heavy matrices (e.g., silicon in steel, aluminum in aluminum bronze) or light elements in the presence of alloying quantities of heavy elements (e.g., aluminum in copper and zinc bearing 7079 alloy) must be undertaken with caution. Examination of data quantification in these types of analyses indicated that poor accuracy is achieved because of the large value of the absorption correction, inaccurate values of the absorption coefficients, and limited knowledge of the fluorescence parameter associated with elements emitting long wavelength radiation. (auth)

38537 (ACF-7) A CRITICAL EVALUATION OF NITROGEN IN 304 ELC STAINLESS STEEL USING THE PLATINUM FLUX TECHNIQUE. Curry, Kenneth J. (ACF Industries, Inc., Albuquerque, N. Mex.). Apr. 28, 1965. Contract AT(29-1)-1352. 7p. (CONF-650438-1). Dep. mn; CFSTI, $1.00 cy, $0.50 mn.

From Analytical Chemistry Conference, Albuquerque, N. Mex.

The nitrogen contents obtained by inert gas fusion chromatography with and without platinum flux and the Kjeldahl method are compared. The nitrogen content obtained by the platinum flux technique agreed with the Kjeldahl values within 0.001% of the amount present. (W.L.G.)

38538 (ADR-08-13-63.1) DETERMINATION OF ORGANIC RESIDUE FROM SOLVENTS BY RADIOISOTOPIC METHOD. Masek, John G. (Grumman Aircraft Engineering Corp., Bethpage, N. Y.). Oct. 28, 1963. 30p.

A radioisotopic method was developed for evaluating organic residue and contamination left by proprietary solvents. Freon T. F., evaluated with this technique, left an organic residue on aluminum that outgasses when exposed to a vacuum. (auth)

38539 (APDA-168) THE DETERMINATION OF OXYGEN IN SODIUM METAL. Boltz, D. F.; Kermoshchuk, J. O.; Meacham, S. A. (Atomic Power Development Associates, Inc., Detroit, Mich.). July 2, 1965. Contract AT(11-1)-865. 34p. Dep. mn; CFSTI, $2.00 cy, $0.50 mn.

A method for the determination of oxygen in sodium metal was modified and refined to increase the sensitivity and reliability. Sodium metal is separated from the insoluble residues, which should include all chemical compounds containing oxygen, by amalgamation and extraction with mercury. The oxygen-bearing residue is dissolved in deionized water, titrated with sulfuric acid in the presence of excess sodium hydroxide using a modified methyl red indicator, and the oxygen concentration is calculated from the total alkalinity. The combining weight of oxygen in sodium monoxide is 8, in sodium hydroxide it is 16, and in sodium carbonate it is 24 if all the combined oxygen is considered. However, it is conventional to report oxygen concentrations in sodium calculated on the basis that all of the alkalinity in the insoluble residue is due to sodium monoxide. The effect of the presence of sodium carbonate and sodium hydroxide on the validity of the analytical results is also reported. The recommended procedure, based on the principles of the Pepkowitz and Judd method, is applicable to the determination of 10 to 100 ppM of oxygen in metallic sodium with a relative standard deviation of approximately 10 per cent. (auth)

38540 (CEA-Note-397) DETERMINATION DE L'URANIUM LIBRE DANS LES ALLIAGES UC–U ET UC–U–C. (Determination of the Free Uranium in UC–U and UC–U–C Alloys). Baudin, G.; Besson, J.; Blum, P.; Spitz, J. (Commissariat a l'Energie Atomique, Grenoble (France). Centre d'Etudes Nucleaires). 1962. 16p. Dep.(mn).

A method based on the analysis of gases released by acid attack on UC–U and UC–U–C alloys was studied. The operational conditions and the range of applicability of the

method are determined. The method is easily performed but necessitates an apparatus for the determination of gases. It is principally valuable for the determination of low quantities of free uranium and it presents clear advantages over the method by the determination of the total and free carbon in the case of alloys in the equilibrium. (J.S.R.)

38541 (K-L-6057) MASS SPECTROMETRIC ANALYSIS OF BORON TRIFLUORIDE. Horton, J. C. (Oak Ridge Gaseous Diffusion Plant, Tenn.). June 11, 1965. Contract W-7405-eng-26. 5p. (CONF-651004-1). Dep. mn; CFSTI, $1.00 cy, $0.50 mn.

For presentation at 9th Conference on Analytical Chemistry in Nuclear Technology, Gatlinburg, Tenn.

A mass spectrometer and an analytical method for measuring the abundance of the boron isotopes in boron trifluoride are described. Heretofore, "memory" has prevented rapid measurements of isotopically different samples; a system was devised that reduces memory to an acceptable level at which a correction factor can be accurately determined and applied. (auth)

38542 (LA-DC-6938) METHODS FOR THE DETERMINATION OF PLUTONIUM IN SPENT REACTOR FUELS, PLUTONIUM METAL, ALLOYS AND COMPOUNDS. Metz, Charles F.; Waterbury, Glenn R. (Los Alamos Scientific Lab., Univ. of California, N. Mex.). [1965]. Contract W-7405-eng-36. 27p. (CONF-650803-6; SM-67/33). Dep. mn; CFSTI, $2.00 cy, $0.50 mn.

From IAEA Symposium on Nuclear Materials Management, Vienna.

A review is presented of the analytical methods for Pu which are most widely used in the U. S. in Pu production processes and in research and development programs on Pu metal, alloys, and compounds. (D.L.C.)

38543 (MCW-1492) PROCESS DEVELOPMENT QUARTERLY PROGRESS REPORT, JANUARY-MARCH 1965. (Mallinckrodt Chemical Works, Weldon Spring, Mo. Uranium Div.). May 1, 1965. Contract W-14-108-eng-8. 24p. Dep. mn; CFSTI, $1.00 cy, $0.50 mn.

Progress is reported on development of methods for (a) determination of Ca in U ore concentrates by x-ray-fluorescence, (b) electrolytic preparation of U metal from UO_2, (c) spectrochemical determination of U in electrolytes, (d) gas-flow proportional counting analysis, and (e) spectrochemical determination of impurities in Th compounds. Separate abstracts were prepared for each topic except (a) and (d). (J.R.D.)

For abstracts of individual papers see: 38544, 38545, and 39099.

38544 (MCW-1492, pp 13-19) A SPECTROCHEMICAL METHOD FOR THE DETERMINATION OF URANIUM IN ELECTROLYTE. Nelms, J. R.; Vogel, R. S. (Mallinckrodt Chemical Works, Weldon Spring, Mo. Uranium Div.).

A spectrochemical method for the determination of U in electrolyte in the range between 1 and 50% U is presented. At midrange, the over-all precision of a determination is ±2.0% absolute at the 95% confidence level. A determination can be completed within ½ hr after receipt of a sample. The method is characterized by a high degree of freedom from matrix effects. (J.R.D.)

38545 (MCW-1492, pp 23-8) A SPECTROCHEMICAL METHOD FOR THE ROUTINE DETERMINATION OF IMPURITY ELEMENTS IN HIGH-PURITY THORIUM COMPOUNDS. Nelms, J. R.; Vogel, R. S. (Mallinckrodt Chemical Works, Weldon Spring, Mo. Uranium Div.).

A spectrochemical method was developed for the determination of trace elements in high-purity Th compounds. The method is based on a carrier-distillation technique using gallium oxide as the carrier. The method is calibrated for 21 elements of current interest. (J.R.D.)

38546 (RFP-552) TECHNICAL SERVICES QUARTERLY PROGRESS REPORT FOR DECEMBER 1964-FEBRUARY 1965. (Rocky Flats Div., Dow Chemical Co. [Denver], Colo.). June 24, 1965. Contract AT(29-1)-1106. 13p. Dep. mn; CFSTI, $1.00 cy, $0.50 mn.

Information is included on: in vivo Pu measurements; ion exchange procedure for Pu bioassay; miniature wound counters; alpha counting by liquid scintillation method; dimethylglyoxime determination of Ni in Pu; volumetric determination of Pu in plutonium fluoride; spectrophotometric determination of Np in Pu-Np alloys; spectrographic determination of impurities in Pu; determination of F in Pu metal and solutions; spectrophotometric determination of Fe in Pu; solid analysis by spark source mass spectrometry; gas analysis using a double focusing mass spectrometer; analysis of bake-out over atmosphere; closure weld test; oxygen analysis by neutron activation; and drop tests on the Types F and G shipping containers. (P.C.H.)

38547 (TID-21475) NONDESTRUCTIVE ASSAY OF NUCLEAR FUELS. Final Report. McGonnagle, Warren J.; Nydegger, Raymond R.; Basdekas, Demetrios L. (Southwest Research Inst., San Antonio, Tex.). May 26, 1964. Contract AT(11-1)-1321. 84p. Dep. mn; $3.00 cy; $0.75 mn.

A feasibility study was conducted of various nondestructive methods for determining the fissionable material content of both irradiated and unirradiated nuclear fuels. The Compton magnetic spectrometer was evaluated and found to be too inefficient for fuel assay on a production line basis. The use of solid-state detectors in gamma-ray spectrometry was evaluated. X-ray transmission, neutron transmission, induced fission, and activation analysis of fission products were also evaluated. Analysis of scrap is considered. (D.L.C.)

38548 (UCRL-14166-T) A PROPOSED STANDARD FOR THE TITRATION OF AQUEOUS SOLUTIONS OF BORON. A Preliminary Report. Rigdon, L. P.; Colman, D. M. (Lawrence Radiation Lab., Univ. of California, Livermore). May 21, 1965. Contract W-7405-eng-48. 7p. (CONF-650639-1). Dep. mn; CFSTI, $1.00 cy, $0.50 mn.

From Analytical Chemistry Conference, Lewiston, N. Y.

The compound tetramethylammonium octahydrotriborate is proposed as a standard for titrating aqueous solutions of boron. It meets the requirements of being non-hygroscopic, having a long shelf life, stoichiometry, and ease in handling. Therefore, it is proposed that this material be used as a standard instead of boric acid or boric oxide to standardize the base used for titrating boric acid solutions. (auth)

38549 DETERMINATION OF NIOBIUM, TANTALUM, AND URANIUM IN NIOBIOTANTALATES BY MEANS OF X RAY FLUORESCENCE SPECTROMETRY. Latorre, C. O.; Bermudez Polonio, J. (Junta de Energia Nuclear, Madrid). Anales Real Soc. Espan. Fis. Quim. (Madrid), Ser. B, 61: 667-72(Apr. 1965). (In Spanish).

A simple and quick procedure was developed for determining niobium, tantalum, and uranium employing the internal standard technique. Zinc served as internal standard for tantalum and molybdenum for niobium and uranium. The precision of the method is about five per cent. Time consumption for each sample, excluding grinding time, is about 45 min. (auth)

38550 THE DETERMINATION OF SODIUM IN HEAVY FUEL OILS BY NEUTRON-ACTIVATION ANALYSIS. Caddock, B. D.; Deterding, J. H. (Shell Research Ltd., Chester, Eng.). Analyst, 90: 437-9(July 1965).

Neutron activation analysis was used for determining sodium in heavy fuel oils. It was found to be especially suitable for measurements on large numbers of samples. The procedure is given, and experimental work done in order to determine the sensitivity and precision of the method and its freedom from interferences is described. (auth)

38551 ARSENATE-IODOMETRIC DETERMINATION OF YTTRIUM. Shakhtakhtinskii, G. B.; Aslanov, G. A.;

Veliev, B. S. Azerb. Khim. Zh., No. 5, 97-102(1964). (In Russian)

An arsenate-iodometric method for the determination of yttrium was developed. It was established that with this method Y can be determined in a wide concentration interval with sufficient accuracy in only 20 to 30 min. (tr-auth)

38552 METHODS FOR RECORDING H^3. Ritzl, F. (Kernforschungsanlage, Julich, Ger.). Elektromedizin, 9: 207-10(1964).

The various methods of recording tritium including counting with the flow counter tube, the gas counter tube, the ionization chamber, and the liquid scintillation counter, are compared and evaluated. The individual measuring methods have their specific fields of application. In particular the tritium counting in the liquid scintillation counter is discussed. Various proved methods of counting samples soluble in fat, watery samples, protein-containing samples, and suspensions are described. The background effects in the various methods are discussed. (Excerpta Med., Sect. XXIII, 2: No. 6(June 1965))

38553 CHEMICAL SEPARATION AND SPECTROGRAPHIC DETERMINATION OF TRACE AMOUNTS OF RARE EARTHS IN SAP MATERIAL. PART II. Cerrai, E.; Hainski, Z.; Rossi, G.; Trucco, R. (CISE, Segrate, Italy). Energia Nucl. (Milan), 12: 406-12(Aug. 1965).

The technique of chemical separation and spectrographic determination of rare earths in SAP materials described previously, was transferred to a routine analysis procedure. When the solutions coming from the separation were dried in a beaker, the spectrographic method showed that a loss of rare earths up to 60% was possible. This difficulty was overcome by keeping the solutions in sealed vials until they were analyzed. In the latter case results obtained with standard solutions were satisfactory. By use of a rotating graphite disk method, the following limits of detection were reached: 0.120 ppm Sm, 0.005 ppm Eu, 0.017 ppm Gd, 0.024 ppm Dy, and 0.06 ppm Er, by processing a 1 g sample. (auth)

38554 A CHROMATOGRAPHIC METHOD OF DETERMINING URANIUM AND PLUTONIUM IN THE AIR. Pomytkin, V. F.; Vorobev, A. M.; Bokova, G. B.; Fomicheva, V. I. Gigiena i Sanit., No. 3, 65-6(Mar. 1965). (In Russian)

The content of Pu and U in aerosols was determined by collection on filters, dissolution in HCl, and sorption of trivalent plutonium and hexavalent uranium from the HCl on anion resins. After filtering, eluting, and drying the solution the content of Pu or U was determined from the α activity using a β detector equipped with a scintillation transducer. The threshold of the method using scintillation attachment was 2×10^{-12} C. The order of error was ~20% for the low concentrations (10^{-11} to 5×10^{-12} c) of Pu and U in the specimen. (R.V.J.)

38555 A RAPID METHOD FOR DETERMINATION OF PLUTONIUM IN URINE. Silker, W. B. (General Electric Co., Richland, Wash.). Health Phys., 11: 965-6 (Sept. 1965). (HW-SA-3760).

A rapid method for the determination of Pu in urine is described. The direct removal of Pu from the urine by ion exchange eliminates time-consuming preparation of samples. Application of the procedure to a spiked water sample yielded a Pu recovery of 90%. (C.H.)

38556 INTERLABORATORY STUDY OF STRONTIUM-90 MEASUREMENTS IN MILK—AUGUST 1963. Rosenstein, Marvin; Hahn, Paul B.; Goldin, A. S. (U. S. Department of Health, Education, and Welfare, Winchester, Mass.). Health Phys., 11: 966-70(Sept. 1965).

The results of an interlaboratory comparison of results of milk analysis for ^{90}Sr indicated that the internal precision for each laboratory was satisfactory in comparison with the selected limits of reproducibility. Agreement of the laboratory results with the known value, within appropriate limits, was satisfactory in eight of the eleven cases. Corrective action taken by the three laboratories whose original results were not acceptable appears to have been successful. The value of such intercomparisons on samples of known concentration is evident, since acceptable internal precision is not sufficient to establish the accuracy of a procedure. Agreement with true values must also be demonstrated. It is of interest to note that acceptable results were obtained by laboratories using all three of the basic radiochemical procedures. Biased results appeared to originate from local technique or calibration rather than from inherent shortcomings of the methods. (auth)

38557 OBSERVATION OF GAMMA-EMITTING NUCLIDES WITH INTERMEDIATE HALF LIVES IN RAIN WATER (OCTOBER 1961 TO DECEMBER 1962). Watanabe, Hironobu; Yamashita, Mikio; Tsubota, Hiroyuki (National Inst. of Radiological Sciences, Chiba, Japan). J. Radiation Res. (Japan), 5: 12-22(Mar. 1964).

Rain water radioactivity in each rain fall was analyzed by gamma-ray spectrometric method for the gamma-emitting nuclides with intermediate half lives during the period from October 1961 through December 1962. The gamma-ray spectra observed were generally featured with three predominant photopeaks at around 0.14 Mev, 0.5 Mev and 0.75 Mev, which mostly attributed to (^{141}Ce, ^{144}Ce), (^{103}Ru, $^{106}Ru-^{106}Rh$) and ($^{95}Zr + ^{95}Nb$) respectively in comparatively younger fallout. Analytical data were presented together with graphical explanations. Decay rate of the 0.14 Mev peak observed in samples from March through July 1962 revealed that there was little influence of fallout due to the Pacific Test Series in the same period. A clear peak of $^{95}Zr + ^{95}Nb$ in the cumulative deposition was shown in early summer with a maximum value of about 200 $m\mu c/m^2$, probably due to frequent rain falls in this period. The data presented could be useful to estimate approximately the fallout deposition of gamma-emitters with intermediate half lives in other areas in this country with some assumptions. (auth)

38558 APPLICATION OF NEUTRON ACTIVATION ANALYSIS FOR DETERMINING PROPERTIES OF ORGANIC MATERIALS. Rakovic, Miloslav (Karlov Inst., Prague). Jaderna Energie, 11: 182-3(May 1965). (In Czech)

Neutron activation analysis was used to determine elements bound in organic compounds as well as to determine trace impurities. It is especially convenient that in the activation of organic samples the level of activity was usually lower than with samples of inorganic materials. Also, self absorption of neutrons (self shielding) was usually not a source of error. With low levels of total activity, it is possible, as a rule, to carry out the determination nondestructively, i.e., without chemical dissolution of the sample and separation of the individual elements. However, organic materials may suffer chemical changes from the effects of the radiation. Therefore, some authors prefer the direct method to the nondestructive method. (28 references). (TTT)

38559 SPECIAL METHODS OF STABLE ISOTOPE ANALYSIS. Mueller, G. (Institut fuer Stabile Isotope, Leipzig). Kernenergie, 8: 265-83(May 1965). (In German).

A survey of analytical techniques is presented, covering gravimetry, densimetry, viscosimetry, ebulliometry, katharometry, refractometry, interferometry, tensiometry, kryometry, electrochemical methods, gaseous chromatography, spectroscopy, activation analysis, and nuclear resonance spectroscopy. 240 references. (D.C.W.)

38560 THE RAPID RADIOCHEMICAL DETERMINATION OF I^{131} IN LIQUID MILK. Iwashima, I.; Yamagata, N. (Inst. of Public Health, Tokyo). Koshu Eiseiin Kenkyu Hohoku, 13: 126-8(1964). (In Japanese).

A method has been devised for the rapid radiochemical determination of ^{131}I in fresh cow's milk containing more than 10 $\mu\mu c/l$. The first step was separation of iodine by a strong base anion exchanger such as Dowex 1-X8 in chloride form, the second was elution of iodine with 1M aqueous solution of perchloric acid, and the third was precipitation as silver iodide with silver nitrate solution and ammonium hydroxide. The precipitate was washed with water and then with ethanol, and the radioactivity of iodine was counted with a low-background beta counter. The re-

covery of iodide-iodine in milk was almost complete, and decontamination from other radioisotopes with satisfactory. About 2 hr were required for the complete processing before the counting. (Excerpta Med., Sect. XXIII, 2: No. 6 (June 1965))

38561 SIMPLE ACTIVITY MEASUREMENTS OF DOUBLY LABELED SUBSTANCES ON CHROMATOGRAMS. Wenzel, Martin (Freie Universitaet, Berlin). Naturwissenschaften, 52: 129(1965). (In German)

A method is proposed for the measurement of the activity of samples labeled with ^{3}H and ^{14}C or ^{14}C and ^{32}P. The method employs a counter tube with and without a window; the window absorbs the ^{3}H activity. The results of measurements made showed that the error width of the activity determinations in the simultaneous presence of ^{3}H and ^{14}C is relatively high for ^{3}H but still satisfactory. In samples containing both ^{14}C and ^{32}P the accuracy was significantly improved. (J.S.R.)

38562 THE CONCENTRATION OF SOME ELEMENTS IN THE ENAMEL OF UNERUPTED (IMPACTED) HUMAN TEETH. Lundberg, Max; Soeremark, Rune; Thilander, Holger (Univ. of Umea, Sweden). Odontol. Revy, 16: 8-11(1965).

The concentrations on the basis of dry weight of Na, Zn, Mn, Rb, Sr, Au, and Cd in enamel from impacted human bicuspids were studied. The values were obtained from ten maxillary and mandibular impacted bicuspids from 14- to 25-yr old patients. The concentrations were determined by means of thermal neutron activation analysis of the enamel samples. Standards and samples of enamel were irradiated simultaneously in an aluminium can by thermal neutrons for about 20 hr at a flux of about 2×10^{12} neutrons cm^{-2} sec^{-1}. When the irradiation was completed, the samples were dissolved in N HCl containing 0.3% H_2O_2, and the solution was subjected to chemical group separation. After the radioactive elements had been collected on various ion exchange columns, the ion exchange resins were dried, homogenized, and transferred to polyethylene tubes for counting with a 3 × 3 in. well-type NaI scintillation crystal. The following values were found (as ppM): Zn 215, Mn 1.12, Sr 83, Rb 73, Au 0, and Cd 0. The Na content was 0.97%. In addition to these values for impacted teeth, values are also given for enamel composition of erupted teeth. There is no pronounced difference in the concentrations of Na between the erupted and the impacted teeth, and about the same amount of Zn and Sr was found in both erupted and unerupted teeth. Most of the Zn and Sr is deposited before eruption. Higher concentrations of Mn and Rb were found in the impacted teeth; this is surprising and cannot be explained at present. No Au was found in the impacted teeth. Obviously the incorporation of Au takes place after eruption. (BBB)

38563 BEHAVIOR OF THE ORGANIC LIQUID PHASE IN TBP-KEROSENE EXTRACTION. Iwase, Eiichi; Isono, Toshiaki (Inst. of Physical and Chemical Research, Tokyo). Rika Gaku Kenkyusho Hokoku, 36: 117-20(1960). (In Japanese).

When a kerosene solution of TBP (tributyl phosphate) was used for the extraction of uranium tetrachloride from its aqueous solution containing hydrochloric acid, the formation of three liquid layers (two organic and one aqueous) was observed in a certain concentration range of uranium tetrachloride and hydrochloric acid. To investigate this further, distribution of the acid between the two organic layers as well as their specific gravity and volumes were measured. It was found that the lower organic layer consisted mainly of TBP and the upper organic one of kerosene. The fact that a single organic layer separates into two may be due to the low solubility of the TBP acid complex in kerosene. The separation of kerosene proceeded much more completely when sulfuric acid was used than hydrochloric acid. (BBB)

38564 TECHNIQUES FOR MEASURING THE ORGANIC CONTENT OF VACUUM ATMOSPHERES. Laurenson, L. (Edwards High Vacuum International Ltd., Crawley, Sussex, Eng.). Vide, 20: 211-21(May-June 1965). (In French and English).

The techniques used for measurement of organic vapors present in a vacuum system are reviewed. The methods varied from direct measurements, by weight or volume, of back-streaming pump oil to the conversion of organic vapors into another form which is then measured. Organic vapors were changed into polymer films by the interaction of electrons with organic molecules while they were adsorbed on a glass surface. The thickness of the resultant polymer films was measured by interferometry. The technique and the results obtained from three typical vacuum systems are discussed. For example an ultrahigh vacuum system constructed of stainless steel gave a polymer growth rate of only 5 Å/hr after baking but could give the high level of 200 Å/hr during baking. The secondary emission of an electron bombarded Cu-Be target was reduced by the presence of adsorbed organic vapors and this effect is discussed as a method of detecting contaminant vapors. (auth)

38565 USE OF NEUTRON MULTIPLIERS AND GENERATORS IN NEUTRON ACTIVATION ANALYSIS. Leipunskii, D. I. Zavodsk. Lab., 31: 695-9(1965). (In Russian)

Neutron activation analysis using neutron multipliers and generators is reviewed. The greatest analysis sensitivity was realized by specimen irradiation in a reactor with a neutron flux density to $\sim 10^{14}$ n/cm^2 sec. Tabulated data are given on neutron flux densities from neutron sources with thermal and fast neutrons of >1 Mev. The sensitivity of neutron activation analysis in specimen irradiation in neutron multipliers with thermal neutron densities of 5×10^{6} and fast neutron densities of 10^{5} n/cm^2 sec and in neutron generators with 14-Mev neutrons and flux densities of 10^{8} n/cm^2 sec was also tabulated. (R.V.J.)

38566 QUANTITATIVE ANALYSIS OF COMPLEX γ SPECTRA OF RADIOACTIVE METALS AND ALLOYS. Yanshkevich, V. A.; Ivanov, L. I. (Baikov Inst. of Metallurgy, USSR). Zavodsk. Lab., 31: 699-702(1965). (In Russian)

A system of linearly approximate equations were developed for the case of Gauss distribution of errors and were applicable for complex gamma spectra of mixed radioisotopes. A probable solution of the system of equations was suggested for practical use in activation analysis of metals and alloys. The method was used in the spectral analysis of Tr + 39% Nb alloy carried out with a multichannel analyzer and a two-window method. (tr-auth)

38567 COMPLEX FORMATION OF THORIUM WITH 8-HYDROXYQUINALDOXIME AND CAPROIC ACID. Rudenko, N. P.; Kremenskaya, I. N.; Avilina, V. N. Zh. Neorgan. Khim., 10: 1160-5(May 1965). (In Russian)

The extraction of Th with chloroform in the presence of 8-hydroxyquinaldoxime, caproic acid, and their mixtures was investigated using the radioactive isotope of Th (UX_1). It was established that in perchlorate solutions at pH = 3.1 Th forms two compounds with 8-hydroxyquinaldoxime in which the molar ratios Th : OXM are 1 : 1 and 1 : 3. It was found that in chloroform solutions, complex compounds with the same ratio of reagents were extracted. The ratio of the reagents in mixed complex compounds Th : OXM : caproic acid was determined to be equal to 1 : 2 : 2 by the method of ternary colored systems using the triangular diagrams. Spectrophotometric studies were made of the reagent 8-hydroxyquinaldoxime; its molar absorption coefficient was determined to be $\sigma = 48622 \pm 470$. The distribution coefficients of the oxime between chloroform and perchlorate acid solutions at $\mu = 0.2$ mole was determined as $D_{HIA} = 22.9$ at $t = 20 \pm 1°C$. The dissociation constants of 8-hydroxyquinaldoxime were calculated, using the distribution method, to be $pK_1 = 1.56 \pm 0.1$ and $pK_2 = 9.04 \pm 0.1$. (tr-auth)

38568 ACTIVATION ANALYSIS APPLICATIONS OF AN ON-LINE DIGITAL COMPUTER. Cohan, Morton D. (Armed Forces Radiobiology Research Inst., Bethesda, Md.). 7p. (CONF-650405-12). Gmelin, AED-CONF-65-040-7.

From International Conference on Modern Trends in Activation Analysis, College Station, Tex.

A general-purpose digital computer is being used as the memory and control element of an on-line data acquisition system in activation analysis. The computer configuration includes a central processor with 8192-word memory, a magnetic tape control unit, one magnetic tape unit, a typewriter, a paper tape reader and punch, a digital graph plotter, and a priority interrupt system. The interface system between the computer and the experimenter is composed of a digital multiplex register, and EOM decoder, a group enable unit, a program selector board, an output multiplex, spectrum ADC, scalers, and analog voltage ADC. (M.C.G.)

38569 PRECISION ANALYSIS WITH 14-Mev NEUTRONS. Mott, William E.; Orange, John M. (Gulf Research and Development Co., Pittsburgh). 26p. (CONF-650405-6). Gmelin, AED-CONF-65-040-15.

From International Conference on Modern Trends in Activation Analysis, College Station, Tex.

As part of a program to develop, for routine industrial use, a series of analytical methods based on activation with 14-Mev neutrons, an extensive study was made of the factors affecting precision. Both the comparator and the indirect flux monitoring methods of analysis were studied. In each case the precision was found to be limited by conditions inside, rather than outside, the accelerator, viz., by variations in deuteron flux over the beam area and by inhomogeneities in the density of tritons in the target. Observed fractional standard deviations (root-mean-square errors) consistently agreed with the expected values (from counting statistics), which in some analyses were frequently as low as 0.3%. (auth)

38570 A QUANTITATIVE POWDER METHOD FOR THE SPARK SOURCE MASS SPECTROGRAPH. Whitaker, H. H. (Radio Corp. of America, Princeton, N. J.). 13p. (CONF-650311-2). Gmelin, AED-CONF-65-025-10.

From Conference on Analytical Chemistry and Applied Spectroscopy, Pittsburgh.

A powder method was developed for determining quantitatively the content of rare earths in insulating powders. The method involves pulverizing the sample, mixing with silver powder, briquetting into bars, and sparking in the spark source mass spectrograph. The precision of the method is about 10%, standard mean deviation. Indications are that this method could be applied to other impurities in insulating material and extended to other powdered materials. (auth)

38571 CONTRIBUTION TO THE QUANTITATIVE X-RAY SPECTROSCOPIC DETERMINATION OF TRACES OF ELEMENTS, USING DIRECT ELECTRON EXCITATION. Toussaint, C. J.; Vos, G. (EURATOM-CCR, Ispra, Italy). 26p. (CONF-650311-4). Gmelin, AED-CONF-65-025-6.

From Conference on Analytical Chemistry and Applied Spectroscopy, Pittsburgh.

An x-ray spectrographic method using direct electron excitation for the quantitative determination of traces of a number of elements in different matrixes is described. Calibration curves and limit of detection are reported for: Zn, Cu, Si, and Mg in aluminum; Co in low-alloy steel; P in bronze; and Na in a graphite matrix. The results are compared with those obtained by other methods. Further improvements for decreasing the limit of sensitivity of the low atomic number elements are discussed. (auth)

38572 DEVELOPMENTS IN APPLIED SPECTROSCOPY. VOLUME 4. Proceedings of the Fifteenth Annual Mid-America Spectroscopy Symposium Held in Chicago, Illinois, June 2-5, 1964. Davis, Elwin N. (ed.). A Publication of the Chicago Section of the Society for Applied Spectroscopy. New York, Plenum Press, 1965. 546p. $18.50. (CONF-640612)

Proceedings of the Fifteenth Annual Mid-America Symposium on Spectroscopy held in Chicago on June 2–5, 1964 are presented. The 45 papers cover the following subject areas: x-ray spectroscopy (9 papers); infrared and Roman spectroscopy (8 papers); ultraviolet and visible spectroscopy (4 papers); gas chromatography (11 papers); and NMR, emission, flame, and atomic absorption spectroscopy (13 papers). (F.J.H.)

38573 IMPROVEMENTS IN THE HYGROMETRIC MEASUREMENT OF THE URANIUM HEXAFLUORIDE CONTENT OF GASES. Saha, Bijay (to Commissariat a l'Energie Atomique). British Patent 996,458. June 30, 1965. Priority date Aug. 3, 1961, France.

A process is described for measuring the UF_6 content of a noncondensable gas (a gas that does not solidify or liquefy at the operating temperature at which the process is carried out, e.g. nitrogen) by means of a dew-point hygrometer. The stainless steel, dew-point hygrometer used in the apparatus is provided with a gold mirror and Pyrex windows to protect the lamp that illuminates the mirror and the photo-resistant cell. The apparatus is passivated with ClF_3 or F_2; and subsequently, the UF_6-containing gas is analyzed in the presence of an amount of ClF_3 or F_2 of from two to ten times the UF_6 content of the gas. (B.L.M.)

Inorganic and Physical Chemistry

38574 (ANL-7008) INVESTIGATION OF FUSED-SALT PROCESSES FOR THE PREPARATION OF URANIUM SULFIDES. Messier, D. R. (Argonne National Lab., Ill.). Mar. 1965. Contract W-31-109-eng-38. 12p. Dep. mn; CFSTI, $1.00 cy, $0.50 mn.

Attempts were made to prepare uranium monosulfide by two fused-salt processes. The first consisted of bubbling a H_2-H_2S stream through molten alkali halides containing dissolved UF_4. In the second, UF_4 or UCl_4 with various sulfides were electrolyzed in fused chloride media. Mixtures of UOS and UO_2 were obtained by the bubbling method under uncontrolled drying conditions. No product was obtained when careful drying was done. Under the driest electrolysis conditions, UOS was obtained. It was concluded that the monosulfide cannot be produced by the gas reaction method, and that improved experimental conditions would be necessary for success with the electrolytic method. (auth)

38575 (BNL-9343) SOLID-STATE ELECTROMOTIVE FORCE TECHNIQUES. THE FREE ENERGY OF FORMATION OF $NiCl_2$, $CoCl_2$, AND SEVERAL DOUBLE SALTS OF KCl. Egan, J. J. (Brookhaven National Lab., Upton, N. Y.). [1963]. Contract AT-30-2-GEN-16. 7p. (CONF-650704-11). Dep. mn; CFSTI, $1.00 cy, $0.50 mn.

From IAEA Symposium on Thermodynamics, Vienna.

Cells were operated to obtain the free energies of formation of $KMgCl_3$, $KCaCl_3$, K_2SrCl_4, KSr_2Cl_5, and K_2BaCl_4 at 450 and 550°C, and of $CoCl_2$ and $NiCl_2$ at 400 and 450°C. The results for the double salts show that the stability decreases from $MgCl_2$ to $BaCl_2$, and that K_2BaCl_4 is unstable below 500°C. (D.L.C.)

38576 (CONF-650425-2) MOESSBAUER PARAMETERS FOR METAL-ORGANIC (Fe,Sn) COMPOUNDS. Herber, R. H. (Rutgers-The State Univ. of New Jersey, New Brunswick. School of Chemistry). [1965]. Contract AT(30-1)-2472. 28p. Dep. mn; CFSTI, $2.00 cy, $0.50 mn.

From Panel on the Uses of the Moessbauer Effect in Chemistry and Solid State Physics, Vienna.

The isomer shift and quadrupole splitting parameters reported in the literature were tabulated. The isomer shifts for organo-iron compounds were tabulated as shifts from the center of the sodium nitroprusside spectrum. This calculation made use of shifts, which were thought to be the best currently accepted values for a room-temperature nitroprusside absorber and a room-temperature source (in mm sec^{-1}). The isomer shifts for organo-tin compounds were recalculated as shifts from the center of the SnO_2 spectrum. (F.J.H.)

38577 (CONF-650425-3) INTERMOLECULAR BONDING EFFECTS IN Sn^{119m} MOESSBAUER SPECTROSCOPY. Herber, R. H.; Stoeckler, H. A. (Rutgers-The State Univ. of New Jersey, New Brunswick. School of Chemistry). [1965]. Contract AT(30-1)-2472. 16p. Dep. mn; CFSTI, $1.00 cy, $0.50 mn.

From Panel on the Uses of the Moessbauer Effect in Chemistry and Solid State Physics, Vienna.

It was shown that 6 coordination was neither a necessary nor a sufficient condition for the observation of measurably large Mössbauer resonance effects at room temperature as was previously presented. From a consideration of melting points and heat of phase transition for organometallic solids as compared to pure metals it was found that the intermolecular forces between molecular units was much smaller than the interatomic forces in a metallic lattic. Moreover the molecular weight of the compound was insufficient by large to reduce the recoil energy to values less than the natural line width of the Mössbauer nuclide. The number of lattice vibrational states that can be populated at a given experimental temperature is larger than it is in the case of metallic lattice. For this reason, even lower temperatures are required to observe measurably large resonance effects in the case of molecular solid organo-tin absorbers than is required of the simple metallic tin lattice. The presence of strong intermolecular bonds reduces the density of vibrational states and thus increases the recoil-free fraction, which is observed at a given temperature. (F.J.H.)

38578 (IA-1014) A STUDY OF THE INTERACTION BETWEEN LANTHANIDE AND NITRATE IONS. Abrahamer, I.; Marcus, Y.; Eliezer, I. (Israel Atomic Energy Commission, Yavne. Soreq Nuclear Research Center). Feb. 1965. 30p. Dep. mn.

The interactions between lanthanide and nitrate ions in aqueous solutions and in some organic solvents were investigated. Densities, visible spectra, magnetic susceptibilities, NMR spectra, and the water content of hydrates and TIOA extracts were measured. The results are discussed in terms of inner and outer sphere complexes. (auth)

38579 (JUL-238-PC) SELBSTDIFFUSION IM FLUESSIGEN AMMONIAK. (Self-diffusion in Liquid Ammonia). Dorfmueller, Th. (Kernforschungsanlage, Juelich (West Germany). Institut fuer Physikalische Chemie). Mar. 1965. 79p. Dep.(mn).

The self-diffusion in liquid ammonia was measured by simultaneous isotopic labelling with duterium and with $^{15}N(^{14}NH_2D$ and $^{15}NH_3)$. The capillary method was used. The diffusion coefficients were determined using the solution of the two Fick laws. Measurement temperatures could be maintained from −60 to +20°C with the deviation of ±0.05°C. The expressions for the temperature dependency at the saturation pressure of the ammonia from 20 to 8 torr was obtained. The maximum error of the individual measurements were estimated at ±2.5°. The measurement results are discussed on the basis of several hydrodynamic and kinetic theories. The pressure dependence of the diffusion coefficient, the relation between the activation energy for diffusion, viscosity, and dipole relaxation, the relation between the activation energy of the diffusion and the H binding energy, and the isotopic effects are described and discussed. (J.S.R.)

38580 (LA-3303) THE SOLUBILITY OF SELECTED ELEMENTS IN LIQUID PLUTONIUM. IV. EVALUATION OF SAMPLING TECHNIQUES. Bowersox, D. F.; Leary, J. A. (Los Alamos Scientific Lab., Univ. of California, N. Mex.). Mar. 22, 1965. Contract W-7405-eng-36. 5p. Dep. mn; CFSTI, $1.00 cy, $0.50 mn.

Quench cast, filtered, and unfiltered thief samples were taken from liquid Pu saturated with W over the temperature range 700 to 925°C., and the results were evaluated. The three methods were in agreement when saturation was approached from a lower temperature. Only the filtered samples were reliable when saturation was approached from a higher temperature. (auth)

38581 (NAA-SR-11401) KINETICS OF THE REACTION OF URANIUM MONOCARBIDE WITH WATER. Colby, L. J. Jr. (Atomics International, Canoga Park, Calif.). July 25, 1965. Contract AT-11-1-GEN-8. 16p. Dep. mn; CFSTI, $1.00 cy, $0.50 mn.

The rate of hydrolysis of uranium carbide from 30 to 86.2°C was measured by a constant volume technique. An activation energy of 17.6 kcal/mole of UC was obtained from an Arrhenius plot of the data. The hydrolysis reaction rate at 70°C was found to be proportional to the square root of the water concentration when 2-propanol was used as a diluent. It is, therefore, postulated that the rate-determining step in the hydrolysis of uranium carbide involves the breaking of an O−H bond. (auth)

38582 (ORNL-P-1428) THE CHEMISTRY AND THERMODYNAMICS OF MOLTEN SALT REACTOR FLUORIDE SOLUTIONS. Baes, C. F. Jr. (Oak Ridge National Lab., Tenn.). [1965]. Contract W-7405-eng-26. 34p. (CONF-650704-6). Dep. mn; CFSTI, $2.00 cy, $0.50 mn.

From IAEA Symposium on Thermodynamics, Vienna.

As a result of the chemical development work done for the Molten Salt Reactor Experiment, considerable chemical and thermodynamic information has been acquired on 2 $LiF-BeF_2$ and its solutions with actinide, lanthanide, and structural metal fluorides. A review is presented of this information. The data were obtained mainly by measurements of heterogeneous equilibria. The results of these measurements give direct information about such important chemical problems as: (1) the corrodibility of structural metals and the reducibility of the structural metal ions, Ni^{2+}, Fe^{2+}, Cr^{2+}; (2) reactions with water vapor to form oxide and hydroxide ions, and the removal of these ions; (3) the precipitation and solubility of the oxides of beryllium, uranium, zirconium, thorium, and the rare earths; (4) the stability of uranium(IV) toward reduction to the trivalent state and possible subsequent disproportionation; and (5) the solubilities and solid solution formation of rare earth fluorides. Equally important has been the wider usefulness of this information when the methods of thermodynamics are brought to bear. Thus the data obtained could be used to: (1) correlate, revise, and extend existing thermochemical data on fluorides and oxides; (2) determine activity coefficients of the components LiF, BeF_2, UF_4, and NiF_2 in these molten salt solutions; (3) calculate electrode potentials involving a variety of solute ions; and (4) estimate solubilities and reactivities of compounds not directly investigated. (D.L.C.)

38583 (SC-DC-65-1480) THE COMBUSTION OF METALS. First Semi-Annual Progress Report, July 1, 1964–December 31, 1964. Hansel, James G.; Zwillenberg, Melvin; Mellor, Arthur M.; Sullivan, H. F. (Princeton Univ., N. J. Guggenheim Labs. for the Aerospace Propulsion Sciences). Feb. 17, 1965. Contract AT(30-1)-3451. 38p. Dep. mn; CFSTI, $2.00 cy, $0.50 mn.

For Sandia Corp., Albuquerque, N. Mex.

Effort was devoted to the construction of the necessary experimental apparatus, an experimental method for measuring the metal flame temperature, and the performance of initial experiments with Al, Ta, and Zr. (W.L.G.)

38584 (SC-RR-65-219) KINETICS OF THE REACTIONS BETWEEN FOUR VALENT URANIUM AND THE VARIOUS VALENCE STATES OF NEPTUNIUM. Wear, J. O.; Shastri, N. K.; Amis, E. S. (Sandia Corp., Albuquerque, N. Mex.). May 1965. Contract AT(29-1)-789. 67p. Dep. mn; CFSTI, $3.00 cy, $0.75 mn.

The kinetics of the oxidation of U(IV) by various valence state of neptunium in aqueous-perchlorate and aqueous-chloride media are presented. The work of Sullivan et al. on the Np(VI) - U(IV) reaction in aqueous-perchlorate medium is reviewed. Original data and interpretations are presented for the following systems: $Np(V)-U(IV)-ClO_4^- - H_2O$; $Np(V)-U(IV)-Cl^- - H_2O$; $Np(IV)-U(IV)-ClO_4^- - H_2$); and $Np(IV)-U(IV)-Cl^- - H_2O$. The specific velocity constants and activation energies were determined for all of the paths involved in the various mechanisms. The Np(V) - U(IV) system is explained by use of the Np(IV) - U(IV) system with very good agreement. (auth)

38585 (SC-TM-64-1677) STRUCTURE AND ELECTRICAL PROPERTIES OF VACUUM-DEPOSITED CdS THIN FILMS. Terry, L. E.; Komarek, E. E. (Sandia Corp., Albuquerque, N. Mex.). Nov. 1964. Contract AT(29-1)-789. 37p. Dep. mn; CFSTI, $2.00 cy, $0.50 mn.

The effects of condensation rate, substrate temperatures, and post-deposition treatment on the electrical and structural properties of CdS were investigated. Rates from 1 to 200Å/sec and substrate temperatures from 40 to 275°C were studied. X-ray diffraction and reflection electron diffraction indicated that the films are highly orientated in the hexagonal phase with the "C" axis perpendicular to the substrate. Post-deposition treatments of vacuum and/or air bake at 400°C for 1 hour had no apparent effect on the orientation. At rates of 1 to 7Å/sec the film resistivity increased from 1 to $10^5\Omega$-cm with an increase in substrate temperature from 40 to 275°C. Hall mobility increased in an orderly fashion from 1 to 15 cm^2/v-sec over this same substrate temperature range. Films formed on 200°C substrates at increasing rates had resistivity decreasing to 10Ω-cm at a rate of 200Å/sec. (auth)

38586 (UCRL-11957) MEASUREMENTS OF THE THERMODYNAMIC STABILITIES OF THE NIOBIUM AND TANTALUM OXIDES USING A HIGH-TEMPERATURE GALVANIC CELL. Worrell, Wayne L. (Lawrence Radiation Lab., Univ. of California, Berkeley). June 1965. Contract W-7405-eng-48. 22p. (CONF-650704-5). Dep. (mn); $1.00(cy), 1(mn) CFSTI.

From IAEA symposium on Thermodynamics, Vienna.

Thermodynamic data for $Nb_2O_{4.8}$, NbO, and Ta_2O_5 were obtained from six different galvanic cells operating between 1030 and 1300°K. The electrolyte used is a solid-solution of either ThO_2 (94 wt %)-Y_2O_3 or ThO_2 (98.6 wt %)-CaO which remains an ionic conductor at lower oxygen activities and higher temperatures than the more commonly used zirconia-based electrolytes. The $YFeO_3$ phase was detected on the surface of the ThO_2-Y_2O_3 electrolyte where it had been in contact with the Fe, $Fe_{0.95}O$ electrode. More stable readings were obtained using the ThO_2-CaO electrolyte with the Fe, $Fe_{0.95}O$ electrode. A comparison between the temperature variation of the Gibbs energy of formation of $Nb_2O_{4.8}$ obtained in this study and that of Nb_2O_5 from calorimetric data indicates that the homogeneity range of the pentoxide increases with increasing temperature. Two independent Gibbs-energy-of-formation equations were determined for NbO. Values from the two equations differ by 600 calories, but the data from one of the NbO cells is suspected of containing a systematic error. There is considerable disagreement between the enthalpy and entropy values for NbO obtained in this study and those calculated from thermal data. It is suggested that this difference may indicate a homogeneity range for NbO. The thermodynamic stability of Ta_2O_5 obtained in this study is in excellent agreement with the thermal data. The effect of the solubility of oxygen in niobium and tantalum on the results for NbO and Ta_2O_5 is discussed. (auth)

38587 (UCRL-11986) THE KINETICS OF THE CHLORINATION OF UCl_4 BY Cl_2 (thesis). Camahort, Jose Luis (Lawrence Radiation Lab., Univ. of California, Berkeley). May 20, 1965. Contract W-7405-eng-48. 116p. Dep. mn; CFSTI, $4.00 cy, $0.75 mn.

The kinetics of the chlorination by Cl_2 gas of UCl_4 dissolved in the LiCl–KCl eutectic melt was studied. The solubility of Cl_2 gas in the uranium-free salt was measured; the results showed that Cl_2 is essentially insoluble in the LiCl–KCl melt. Henry's Law constants at 400 and 500°C are less than 4×10^{-9} moles/(cm^3) (atm). The equilibrium of the reaction $UCl_4(l) + Cl_2(g) = UCl_6(l)$ in the fused salt was studied by sparging a 2 wt % UCl_4 solution with pure Cl_2 gas at 400–600°C. The reaction was found to be reversible and endothermic, with a heat of reaction of 5.4 kcal/mole. The kinetics of the reaction was investigated using a wetted-rod apparatus at 400–700°C. Theoretical and experimental results show that the chlorination reaction is essentially a liquid phase process, with diffusion-chemical equilibrium control. The experimental rates at 400 and 450°C are greater than the predicted values for an infinitely fast reaction, but at the higher temperatures (≥500°C) the experimental values become less than the theoretical predictions. This uncommon behavior tends to rule out any reaction rate control of the overall process. It may be caused by an unknown interfacial resistance, a much lower diffusivity of UCl_6 than UCl_4 in the salt, or a sudden shift in the equilibrium during the sample collection. (D.L.C.)

38588 (UCRL-12496) CHEMICAL BONDING AND THE SULFUR K-X-RAY SPECTRUM. Wilbur, D. W.; Gofman, J. W. (Lawrence Radiation Lab., Univ. of California, Livermore). July 20, 1965. Contract W-7405-eng-48. 19p. (CONF-650810-1). Dep. mn; CFSTI, $1.00 cy, $0.50 mn.

From Annual Conference on Applications of X-Ray Analysis, Denver.

The sulfur K_β intensities and K_α energies were studied in a series of sulfur compounds in an attempt to better understand their relationship to each other and to the chemical state of the sulfur atom, particularly its charge. The two parameters display an approximately linear relationship for compounds involving sulfur in three or more bonds, thus showing at least some agreement concerning the charges on these atoms. For lower valence states no obvious relation was found. A plot of the relationship between K_α energy and K_β intensity was prepared. This relationship should be independent of the spectrometer employed and hopefully can be used to empirically relate uncertain chemical states to known ones. (auth)

38589 (UCRL-14186) A LOW-DENSITY, LOW-PRESSURE SOLID EXPLOSIVE. Archibald, Paul B. (Lawrence Radiation Lab., Univ. of California, Livermore). May 25, 1965. Contract W-7405-eng-48. 8p. Dep. mn; CFSTI, $1.00 cy, $0.50 mn.

A new detonable system based on low concentrations of crystalline PETN deposited in a porous low-density substrate was demonstrated. Stable detonation waves propagating in ¾-in.-diameter rate sticks at 1.5 mm/μsec were measured. The detonation velocity can be varied by changing the PETN concentration. At a concentration of 0.09 g of PETN per cc, a detonation velocity of 2.05 mm/μsec was measured. Under these conditions, calculations indicated a CJ pressure of 3 kilobars and a gamma of 1.7. (auth)

38590 (UCRL-16050) STUDIES OF ATOMIC HYDROGEN AT LOW PRESSURES. Rony, Peter R. (Lawrence Radiation Lab., Univ. of California, Berkeley). Apr. 20, 1965. Contract W-7405-eng-48. 222p. Dep. mn; CFSTI, $6.00 cy, $1.25 mn.

Gas- and surface-phase kinetics of atomic hydrogen at low pressures are considered. The theoretical description of diffusion and flow tubes was extended to the following situations: a discharge zone of finite length, discharge-zone walls inactive catalytically, an end-plate sink composed of two or more catalytic materials, and atom-recombination coefficients on the discharge- and reactor-zone walls differing in magnitude. The dimensionless groups characterizing the rate processes within the system were systematized, and practical examples illustrating the use of the theoretical solutions are given. After a description of a simple water-cooled Wrede-Harteck gage capable of detecting atom concentrations of less than 0.06% at 75 mtorr, it was experimentally shown that the device may not be absolute, is sensitive to the presence of H_2O and HCl, is susceptible to thermal effusion problems, and cannot discriminate between atomic hydrogen or atomic oxygen. The presence of small amounts of H_2O did not influence the yield of atomic hydrogen from a microwave or electrodeless discharge at 75 mtorr. This result is independent of the measurement technique, the source of hydrogen, the source of water, and the discharge power. Small amounts of O_2 stoichiometrically increased the yield of atomic hydrogen from the low-pressure discharge by a ratio of at least two atoms of hydrogen per molecule of oxygen. Molecular nitrogen had a similar but a smaller effect. A cyclotron-resonant microwave discharge is a convenient method for producing an electrical discharge in the low-pressure system with a microwave power as low as 250 mw. The intensity of the Balmer lines or color of low-pressure hydrogen discharges is not a reliable qualitative indication of the atomic-hydrogen yield. The location of an active catalytic probe affects the atom-concentration

level throughout a diffusion tube or flow tube at low pressures. Studies with Teflon or copper probes indicated that both have recombination coefficients below 10^{-3}. In order for an isothermal calorimeter to be used for the measurement of absolute atom concentrations in a low-pressure system, most of the atoms produced must recombine on the calorimeter, both the diffusive and convective flux of atoms must be known, the presence of the atoms must not alter the rate of heat loss from the calorimeter, and the thermal-accommodation coefficient of the recombination energy must be equal to unity. (auth)

38591 (UCRL-16113) REACTION DISTRIBUTION IN A POROUS ANODE (thesis). Alkire, Richard Collin (Lawrence Radiation Lab., Univ. of California, Berkeley). June 1965. Contract W-7405-eng-48. 70p. Dep. mn; CFSTI, $3.00 cy, $0.75 mn.

An experimental technique was developed for measuring the reaction distribution within flooded porous electrodes in which there is no bulk flow of electrolyte in the pores. A porous metal anode is dissolved electrolytically forming soluble reaction products. The porosity of the electrode, uniform prior to electrolysis, is determined after electrolysis by a microscopic examination. The change in porosity distribution is equivalent to the time-average reaction distribution during electrolysis. The design of the experiment is such that electrolysis proceeds in a manner which is well characterized. The acid copper system was used for study. Six experiments were conducted to investigate the capabilities and limitations of the method. It was found that reaction distributions can be determined which are in qualitative agreement with present theories. (auth)

38592 (UCRL-16150) VAPOR PRESSURE AND HEAT OF SUBLIMATION OF CERIUM(III) FLUORIDE (thesis). Lim, Mahn Jick (Lawrence Radiation Lab., Univ. of California, Berkeley). May 20, 1965. Contract W-7405-eng-48. 26p. Dep. mn; CFSTI, $2.00 cy, $0.50 mn.

The vapor pressure of CeF_3 was measured in the temperature range 1370°K to 1685°K by the torsion-effusion method. The vapor pressure of CeF_3 in atmospheres is given in the experimental range by the expression $\log_{10} P = -(1.983 \pm 0.013) \times (10^4/T) + 8.816 \pm 0.086$, where the quoted errors are the standard deviation from the least-squares fit. Extrapolations yield a calculated normal boiling point of 2472°K and a heat of sublimation at 298.15°K of 99.51 ± 0.25 kcal/mole by the third-law method and 99.29 ± 0.58 kcal/mole by the second-law method. (auth)

38593 (ORNL-tr-674) NEW REACTION FOR PRODUCING STRONTIUM. Matignon, Camille. Translated by Martha Gerrard (Oak Ridge National Lab., Tenn.), from Compt. Rend., 177: 1116-18(1923). 2p. Dep. mn; JCL, $1.10 fs, $0.80 mf.

Approximate calculations were made for the pressure of Sr produced by the reaction $\frac{3}{2}$ SrO + $\frac{1}{2}$ Si → $\frac{1}{2}$ SiO_2SrO + Sr vapor, relative to the pressure of Ba produced by the same reaction. Tests were made at 1200°C, and the results show that the Sr production is possible but much slower than for Ba. (D.L.C.)

38594 CONTRIBUTIONS TO THE SPECTROPHOTOMETRIC STUDY OF THE U(VI)-PYRIDYL-AZO-RESORCINOL SYSTEM. Vasilescu, C.; Negoiu, M.; Ulariu, A. Analeli Univ. Bucuresti, Ser. Stiint. Nat., 13: No. 41, 45-53(1963). (In Rumanian)

The U(VI)-pyridyl-azo-resorcinol system was studied spectrophotometrically. The formula of the complex combination formed in aqueous solution at pH = 7.8 was determined and verified electrolytically. The formula corresponds to a non-ionogenic complex combination. The stability constant of the combination was determined using the method of continuous variation of series of non-equimolecular solutions and the method of continuous variation of series of isomolecular solutions. The two methods lead to perfectly comparable results; the values obtained were 3.18×10^{-6} by the first method and 3.08×10^{-6} by the second method. (tr-auth)

38595 EFFECT OF Y^{+3} ON THE REDUCTION OF Sm^{+3} IN CaF_2. O'Connor, J. R.; Hilton, R. M. (Massachusetts Inst. of Tech., Lexington). Appl. Phys. Letters, 7: 53-4 (Aug. 1, 1965).

Further data are reported confirming a definite interaction between Y and rare earth ions during photochemical reduction processes. Several CaF_2 crystals were grown by the Bridgman method under high vacuum. The starting material was either pure commercial fluorite containing a trace amount of Y^{3+} or was additionally doped with YF_3. The crystals showed no optical absorption until after the addition of SmF_3, when weak spectra due to Sm^{3+} and Sm^{2+} was observed. Bleaching effects were observed at room temperature. Absorption bands due to Y^{2+} were found to decrease at a slow rate. Similar results are obtained when Sm^{3+} is replaced by either Dy^{3+} or Tm^{3+}. It is suggested that the effect of Y^{3+} on the photochemical reduction of rare earths is due to ion-pairing. (J.F.P.)

38596 CATALYTIC DEUTERIUM EXCHANGE REACTIONS WITH ORGANICS. XII. FURTHER STUDIES IN PLATINUM CATALYST PREPARATION—THE PROCESS OF SELF-ACTIVATION. Garnett, J. L.; Sollich, W. A. (Univ. of New South Wales, Kensington, Australia). Australian J. Chem., 18: 993-1002(July 1965).

A new process for the activation of platinum oxide, termed self-activation, is described. This procedure involves the reduction of platinic oxide with an organic compound such as benzene, naphthalene, or n-octane. The potential of the resulting catalyst in deuterium exchange reactions was evaluated. A comparison was made in the properties of prereduced catalysts prepared by a self-activation procedure and catalysts activated conventionally with hydrogen gas. For high-temperature exchange reactions (>90°), the former catalysts are to be preferred since higher final activities of up to 300% may be achieved. The kinetics of self-activation suggest that catalyst deactivation by reagents may be due to modification of active sites. With aromatic compounds, it is proposed that this deactivation occurs through a π-complex interaction. Isotope distribution studies in the labeled benzenes indicate that self-activated, prereduced catalysts, by comparison with hydrogen-activated catalysts, exhibit relatively low M values in relation to their activities. Distribution data are consistent with the explanation that catalyst deactivation by benzene is a process involving the generation of new types of active sites which are more numerous but of lower activity than the original sites. Attempts to stabilize prereduced catalysts by chemical methods were unsuccessful. (auth)

38597 CATALYTIC DEUTERIUM EXCHANGE REACTIONS WITH ORGANICS. XIII. CHARACTERISTIC REACTIONS OF THE GROUP VIII TRANSITION METALS. Garnett, J. L.; Sollich, W. A. (Univ. of New South Wales, Kensington, Australia). Australian J. Chem., 18: 1003-8 (July 1965).

Activation procedures and hydrogen exchange reactions with six Group VIII transition metal catalysts (Pt, Pd, Ru, Rh, Ir, Ni) are reported for three characteristic reaction systems: deuterium oxide/benzene; deuterium oxide/naphthalene, and deuterium oxide/n-octane. Results of these exchange reactions indicate that both π-complex adsorption and the dissociative π-complex substitution mechanism previously established for platinum are applicable to other Group VIII transition metal catalysts. For general catalytic labeling with isotopic hydrogen, platinum was found to be the most efficient of the catalysts investigated. (auth)

38598 REACTIONS OF $A^{III}B^{VI}$ LANTHANUM AND GALLIUM SELENIDES. Efendiev, G. Kh.; Karaev, Z. Sh.; Nasibov, I. O. Azerb. Khim. Zh., No. 5, 103-7(1964). (In Russian)

By different physical-chemical methods of analysis it was established that in the $La_2Se_3-Ga_2Se_3$ section of the La–Ga–Se system chemical compounds with the composition $LaGaSe_3$ were formed. La selenogallate appears to be a thermally stable compound and in vacuum (approximately

10^{-3} mm) did not decompose at the temperature of fusion (1120°C). $LaGaSe_3$ was not soluble in water. At room and at higher temperatures (up to 200°C.) it did not react with atmospheric oxygen. It dissolves comparatively slowly in H_2SO_4–HCl. HNO_3 reacted somewhat more strongly with $LaGaSe_3$ with the result that elementary Se was precipitated. Alkalis, weak acids, and organic solutions did not dissolve $LaGaSe_3$. The La and Ga selenides to some extent (at 20 mol %) dissolved in each other with the result that in the La_2Se_3- and Ga_2Se_3-rich areas of the system solid solutions were formed. The electric conductivity of the alloys of the La_2Se_3–Ga_2Se_3 system increased in relation to the temperature (the measurement was made at 160°C). (tr-auth)

38599 SOME OBSERVATIONS ON THE REACTION OF POLYMER CARBONS WITH CARBON DIOXIDE. Bregazzi, M.; Greenhalgh, E.; Sutherland, J. W.; Tucker, Dorothy J. (Morganite Research and Development Ltd., London). Carbon, 3: 73-85(July 1965).

The reaction of carbon dioxide with pyrolyzed polymer carbons having different structures was studied in the temperature range from 750 to 850°C and in the pressure range from 1 to 12 cm Hg. The kinetics were followed gravimetrically using a sensitive microbalance. A static system was used throughout. The carbons were characterized by electron microscopy, electron diffraction, x-ray diffraction, chemical analysis, and physical adsorption techniques. The two polymer materials chosen (polyvinyl chloride, and polyvinylidene chloride) produced two carbons having extreme structures (graphitizable and non-graphitizable, respectively). The samples used were heat treated to 2500°C. Two distinct activation energies were found and these were identical for both materials. The high value (85 kcal $mole^{-1}$) was always found with well outgassed samples, and the low value (69 kcal $mole^{-1}$) with those which were poorly outgassed or highly oxidized. A reaction scheme was postulated, which fits all the facts. The two activation energies were explained in terms of the intercalation of oxygen, water vapor, and possibly carbon dioxide. (auth)

38600 CHELATING FUNCTION OF LANTHANUM AND NEODYMIUM WITH N,N'-DIMETHYL-N,N'-DINITROSO-TEREPHTHALAMIDE (NTA). Su, Chiang. Chung-Kuo K'o Hsueh Yuan Ying Yung Hua Hsueh Yen Chiu So Chi K'an, No. 6, 19-24(1962).

The pH and conductometric methods were used to investigate the composition and properties of the lanthanum and neodymium (N,N'-dimethyl-N,N'-dinitrosoterephthalamide) complex systems as follows: $La(NO_3)_3$-Na_3X-H_2O, $La(NO_3)_3$-Na_2HX-H_2O, and $Nd(NO_3)_3$-Na_2HX-H_2O. The pH values and resistance changes were determined in test solutions. pH values of the test solutions were controlled by adding 0.1156 N NaOH at various α values (α = $NaOH/R^{3+}$). Mechanisms of the chelating reactions are discussed. The complex Na[R(OH)X] having a property different from the properties of La and Nd in NTA is considered suitable for use in La separation. (ATD)

38601 DETERMINATION OF SOLUBILITIES OF PRASEODYMIUM OXALATE AND NEODYMIUM OXALATE IN N,N'-DIMETHYL-N,N'-DINITROSOTEREPHTHALAMIDE (NTA) AT 25C. Su, Chiang; Pai, Yun-chi. Chung-Kuo K'o Hsueh Yuan Ying Yung Hua Hsueh Yen Chiu So Chi K'an, No. 6, 25-8(1962).

The solubilities of praseodymium oxalate and neodymium oxalate in N,N'-dimethyl-N,N'-dinitrosoterephthalamide. Praseodymium oxalate and neodymium oxalate were prepared with 99% pure praseodymium and neodymium oxides. The oxides were prepared by an ion-exchange method. Solubility determination was carried out by checking the pH values of filtrates and rare earth contents at 25°C. Oxalate precipitation was developed by the addition of perchloric acid and oxalic acid to the filtrate. The neodymium content was determined by weighing the calcinated oxalate oxides and praseodymium oxalate content was determined by dissolving oxalates in sulfuric acid and titrating the solution with 0.1042 N potassium permanganate. The solubilities of praseodymium and neodymium oxalates were determined in 0.5 M solution at 25°C at various pH values. Solubilities of oxalates were found to increase slightly with the increasing pH value at pH < 6. Solubility of praseodymium oxalate increases rapidly with the increasing pH value at pH 6-7. Neodymium oxalate has a higher solubility at pH 6-7 than praseodymium oxalate. It was also found that the solubility of neodymium oxalate in a Na_2HX solution increases as concentration of the solution is increased. The stability constants of the neodymium complexes were calculated. (ATD)

38602 CONTRIBUTION TO THE STUDY OF COMPLEXES OF PENTA- AND TETRAVALENT PROTACTINIUM. Guillaumont, Robert (Institut du Radium, Arucil, France). Compt. Rend., 260: 4739-41(May 3, 1965). (In French).

The composition of some complexes of penta- and tetravalent Pa existing in aqueous medium with an ionic force 3 was established. The formation constants beginning with $PaO(OH)^{2+}$ and Pa^{4+} are given. (tr-auth)

38603 A NEW OXYBROMIDE OF PENTAVALENT URANIUM. Levet, Jean-Claude (Faculte des Sciences, Rennes, France). Compt. Rend., 260: 4775-6(May 3, 1965). (In French).

The reaction of HBr gas with the amorphous oxide UO_3 led at −20°C to the hydrate $UO_2Br_2 \cdot H_2O$ and at 250°C to the oxybromide of pentavalent uranium, UO_2Br. Its properties are given. (tr-auth)

38604 RELATION BETWEEN THE MODIFICATIONS OBSERVED IN ZIRCONIA DURING ELECTROTRANSPORT TESTS AND DURING THE OXIDATION OF ZIRCONIUM. Beranger, Gerard; Lacombe, Paul (Ecole des Mines, Paris). Compt. Rend., 260: 5278-81(May 17, 1965). (In French).

An attempt is made to interpret the changings in the color of zirconia layer formed during the oxidation of Zr by comparing them to observations made on zirconia exposed to the action of a continuous electric current at high temperature. This treatment leads to the creation of new anionic gaps. (tr-auth)

38605 THE THERMOELECTRIC PROPERTIES OF BORON CARBIDE AT HIGH TEMPERATURES. Vuillard, Guy; Luque, Albert (College Scientifique Universitaire, Orleans, France and Office National d'Etudes et Recherches Aerospatiales, Chatillon-sous-Bagneux, France). Compt. Rend., 260: 5282-5(May 17, 1965). (In French).

The boron carbide is a refractory substance very resistant to oxidation. The compound with the formula B_4C is a semiconductor of the P type in which the Seebeck coefficient and the factor of merit increase constantly from room temperature up to above 1000°C. The resistivity, too large, is the weak point of this thermoelectric component. A wide interval of solid solutions makes it possible to vary extremely the composition and characteristics of the boron carbide. (tr-auth)

38606 THE HYDROLYSIS MECHANISM AT HIGH TEMPERATURE OF URANIUM MONOCARBIDE. Besson, Jean; Moreau, Claude; Phillippot, Joseph (Centre d'Etudes Nucleaires, Grenoble, France). Compt. Rend., 260: 5286-9(May 17, 1965). (In French).

The reaction of water vapor on uranium monocarbide was studied at 1055°C under a pressure p between 5 and 60 mm of Hg; the velocity constants relative to the growth of the two layers of products formed obey the following relations, respectively: for the external layer (UO_2), $k = ap/(1 + bp)$, for the subjacent layer ($UO_2 + C$), $k' = cp^{1/2}$. These relations define usefully the reaction mechanism. (tr-auth)

38607 COMPLEX FORMATION BETWEEN URANYL IONS AND β-RESORCYLIC ACID. Desai, M. N.; Desai, B. M. (Gujarat Univ., Ahmedabad, India). Current Sci. (India), 34: 244-5(Apr. 20, 1965).

Formation of a deep orange-colored, water-soluble complex between uranyl ions and β-resorcylic acid with maximum absorption in the range from 454 to 478 mμ was observed. The color attained maximum intensity at pH 4.2. The composition of the complex was determined by the

molar-ratio method and slope-ratio method employing spectrophotometric data. The curves of absorbance vs wavelength for 1:1, 1:2, and 1:3 ratios of U to β-resorcylic acid at pH 4.2 were practically identical in shape, suggesting that the acid formed only one complex in solution with uranyl ions under the conditions of the study. Absorbance values (at pH 4.2), when plotted against the ratios of concentrations of uranyl ion to the total concentration of reagent, showed a maximum at the ratio of 0.5, indicating the formation of a 1:1 complex. Each curve had a broad maximum as expected for appreciable dissociation. The slope-ratio method also suggested the formation of 1:1 complex, as did the molar-ratio method. On mixing a solution of uranyl nitrate and β-resorcylic acid, the pH decreased, indicating the displacement of phenolic proton of the resorcylate by uranyl ion. (BBB)

38608 POTENTIAL OF Pd-D/D^+ ELECTRODE AND ION PRODUCTS OF HDO. Shiratori, H. Denki Kagaku, 31: 904-6(1963). (In Japanese)

The anomaly of palladium–hydrogen electrodes in aqueous solution was studied. The potential of the Pd–D electrode and the ion products of HDO were studied. From the viewpoint of thermodynamic properties, the reactions of hydrogen and deuterium on palladium electrodes were similar. There also existed two reactions: $2D^+ + 2e \rightarrow D_2$ (β alloy electrode reaction) and $D^+ + e \rightarrow D$ (α alloy electrode reaction), the former was the deuterium electrode reaction and the latter the anomalous reaction of deuterium. In order to prevent effects from the varying amount of deuterium contained in palladium on the electrode potential, α and β biphase coexistent Pd–D alloy electrodes were used. Saturated mercurous chloride electrodes were used as reference electrodes. The electrode potential of (α + β) Pd–D/D^+ and (α + β) Pd–H/H^+ in both solutions was measured. There was a potential difference of 63.64 mv at 25°C between these electrodes against the saturated mercurous chloride electrode. A standard electrode potential of 0.02860 V was obtained for (α + β) Pd–D/D^+, this value agreed with the theoretical value. The curve of heavy water concentration-electrode potential appeared to be in linear relation, but the only bending point was found when D_2O equaled 50%. It was assumed that Pd–D alloy electrode and Pd–H alloy electrode in mixed solution are similar, and that the D^+ electrode reaction is also reversible. The first ion product $[\alpha H^+ \times \alpha_9 D^-]$ of HDO at 25°C was measured to be 0.67×10^{-14}. The second ion product $[\alpha D^+ \times \alpha OH^-]$ was 0.90×10^{-14}. (F.J.H.)

38609 DETERMINATION OF THE SPECIFIC ACTIVITY OF IODINE-131 WITHOUT CARRIER ISOTOPE. Constant, R. (Centre d'Etude de l'Energie Nucleaire, Mol, Belg.). Intern. J. Appl. Radiation Isotopes, 16: 447(July 1965).

A method is proposed for the determination of the specific activity of ^{131}I that is based on a photometric determination in the uv of the triiodide ion. The conditions for the formation of this ion and the formula for calculating the specific activity of the solution 6 hours after the end of irradiation are given. Application of the method to numerous samples and controls showed a sufficient precision when the solutions contained sufficient thiosulfate. (J.S.R.)

38610 RESEARCH ON THE SYSTEM LiF–ZrF_4. Korenev, Yu. M.; Novoselova, A. V.; Glinskii, K. K.; Shornikov, V. V. (Moscow State Univ.). Izv. Akad. Nauk SSSR, Neorgan. Materialy, 1: 201-3(1965). (In Russian).

The system LiF–ZrF_4 was investigated by the differential thermal and x-ray analyses. Differential thermal analysis was carried out with a pyrometer with platinum–platinum-rhodium thermocouples. The temperature was measured with an accuracy of ±5°C. The three compounds Li_4ZrF_8, $LiZrF_7$, and Li_2ZrF_6 were observed. (CFSTI)

38611 SYNTHESIS AND PROPERTIES OF LANTHANUM BORATES. Isupova, E. N.; Lileev, I. S. (Grebenshchikov Inst. of Chemistry, Academy of Sciences, USSR). Izv. Akad. Nauk SSSR, Neorgan. Materialy, 1: 222-6(1965). (In Russian).

Studies were made on the synthesis and chemical stability of lanthanum borates. Lanthanum meta- and orthoborates $La(BO_2)_3$ and $LaBO_3$ were produced by reactions in La_2B_3–B_2O_3 at 1100 to 1300°C. Exchange reactions between lanthanum sulfate and sodium borates (meta-, ortho-, and tetraborates) at 900 and 1000°C also produced $La(BO_2)_3$ and La BO_2 systems. It was found that lanthanum ortho-borate, $LaBO_3$, does not decompose in cold or boiling water or sodium hydroxide (6N and 12N) solutions, however, lanthanum metabromate $La(BO_2)_3$ was completely decomposed by alkali. (R.V.J.)

38612 LANTHANUM GERMANATES. Kornilova, E. E.; Prikhod'ko, N. E.; Lileev, I. S. (Inst. of Chemistry of Silicates, Academy of Sciences, USSR). Izv. Akad. Nauk SSSR, Neorgan. Materialy, 1: 227-31(1965). (In Russian).

Phase studies were made of systems of lanthanum oxides (99.9% pure) with germanium dioxides sintered at 1100 to 1300°C. Compounds of lanthanum meta-, pyro-, and oxy-ortho germanates were prepared by sintering at temperatures below the temperatures required for preparation by smelting. Lanthanum metagermanate melted into pyrogermanate and germanium dioxide at 1300°C. Lanthanum germanate melting points, density, and refractive indicies were found. (R.V.J.)

38613 LANTHANUM SILICIDES AND THEIR CRYSTAL STRUCTURE. Gladyshevskii, E. I.; Dvorina, L. A.; Kulikova, A. A.; Verkhoglyadova, T. S. (Lvov State Univ. and Inst. of Problems in Study of Materials, Academy of Sciences, USSR). Izv. Akad. Nauk SSSR, Neorgan. Materialy, 1: 321-5(1965). (In Russian).

X-ray structure analysis of La–Si systems prepared by melting the components in an arc furnace and by a reduction of La_2O_3 by silicon powder indicated the presence of $LaSi_{2-n}$ (with the structure type a-$GdSi_2$, a = 4.272, b = 4.184, and c = 14.02 Å) and La_2Si_2 (structure type U_3Si_2, a = 7.87 and c = 4.50 Å) in addition to the previously known silicides $LaSi_2$, LaSi, and La_5Si_3. (R.V.J.)

38614 LANTHANUM SELENIDES. Yarembash, E. I.; Vigileva, E. S.; Eliseev, A. A.; Reshchikova, A. A. (Kurnakov Inst. of General and Inorganic Chemistry, Academy of Sciences, USSR). Izv. Akad. Nauk SSSR, Neorgan. Materialy, 1: 330-6(1965). (In Russian).

The results of chemical, physical, x-ray, and differential thermal analyses of lanthanum selenides LaSe, La_2Se_4, La_3Se_2 and $LaSe_2$ were tabulated. The existence of lanthanum selenide La_4Se_7 was found and it is shown that its structure is homologous to lanthanum disilenites. Monocrystals of $LaSe_2$, with p- and n-conductivity were prepared. At room temperature the thermal-electromotive force of $LaSe_2$ exceeded 200 $\mu v\text{-degrees}^{-1}$, and the specific electric resistance $\rho \sim 10^4$ ohm·cm. Postulations were made about the existance of a phase with Th_3P_4 structure and the lattice ordering resulting in production of lanthanum selenides with rational and irrational stoichiometry. (R.V.J.)

38615 THE PHASE COMPOSITION OF CaF_2–YF_3, SrF_2–YF_2, AND BaF_2–YF_3. Sobolev, B. P.; Ippolitov, E. G.; Zhigarnovskii, B. M.; Garshina, L. S. (Kurnakov Inst. of General and Inorganic Chemistry, Academy of Sciences, USSR). Izv. Akad. Nauk SSSR, Neorgan. Materialy, 1: 362-8(1965). (In Russian).

The influence of alkaline earth and rare earth ion radius ratios on the stability of anomalous solid solutions of CaF_2–YF_3, SrF_2–YF_3, and BaF_2–YF_3 was analyzed. The stability limits of fluoride structure solid solutions varied very slightly with changes in alkaline earth radii and were equal to 37.4 ± 0.5, 38.0 ± 0.5, and 40 ± 1 mole % YF_3 for CaF_2–YF_3, SrF_2–YF_3, and BaF_2–YF_3, respectively. The solid solutions of these systems had the elementary cell parameters 5.535, 5.700, and 5.896 Å, respectively. The CaF_2–YF_3 system formed two compounds $CaF_2 \cdot 2YF_3$ and $2CaF_2 \cdot 5YF_3$. The SrF_2–YF_3 system formed one compound $SrF_2 \cdot 2YF_3$ with a hexagonal structure and parameters $a_0 = 6.916$ and $c_0 = 7.057$ Å. The $2CaF_2 \cdot 5YF_3$ and $SrF_2 \cdot 2YF_3$ nonequilibrated crystallization formed metastable solid solutions with YF_3 expanding to 80 mole % YF_3. (R.V.J.)

38616 SAMARIUM PYROPHOSPHATES. Tananaev, I. V.; Shevchenko, G. V. (Kurnakov Inst. of General and Inorganic Chemistry, Academy of Sciences, USSR). Izv. Akad. Nauk SSSR, Neorgan. Materialy, 1: 369-73(1965). (In Russian).

Reactions of $Sm(NO_3)_3$ with lithium, sodium, and potassium pyrophosphates in solution produced a normal samarium pyrophosphate $Sm_4(P_2O_7)_3 \cdot 14H_2O$, which, on increasing the alkali metal pyrophosphate concentration, formed a binary pyrophosphate $MSmP_2O_7 \cdot 4H_2O$ (M = Li, Na, K). The thermographic and roentgenographic data on the various pyrophosphates are included. (R.V.J.)

38617 ON THE ORTHONIOBATES OF YTTRIUM SUBGROUP ELEMENTS. Sanatina, V. N.; Krylov, E. I. (Kirov Ural Polytechnic Inst., Sverdlovsk, USSR). Izv. Akad. Nauk SSSR, Neorgan. Materialy, 1: 380-2(1965). (In Russian).

The thermal stability of Ga, Dy, Ho, Er, Yb, and Lu niobates was studied. It is shown that all these salts are stable in a $\sim 10^{-4}$ mm Hg vacuum at 1200°C. Differential thermal analysis of the oxide mixture ($La_2O_3 : Nb_2O_5 = 1:1$ and $Lu_2O_3 : Nb_2 = 1:1$) showed that at 1190°C and 1050°C in lanthanum and lutetium orthoniobates were produced. The $LuNbO_4$ is diamagnetic and $GdNbO_4$, $DyNbO_4$, $HoNbO_4$, $ErNbO_4$, and $YbNbO_4$ are paramagnetic. The Curie-Weis law holds for the temperature dependence χm^{-1}. (R.V.J.)

38618 INFRARED ABSORPTION OF $PrTe_2$. Zorina, E. L.; Yarembash, E. I. (Kurnakov Inst. of General and Inorganic Chemistry, Academy of Sciences, USSR). Izv. Akad. Nauk SSSR, Neorgan. Materialy, 1: 446(1965). (In Russian).

The infrared absorption spectra of $PrTe_2$ was determined using a wavelength of 0.67 to 2.5μ. The constructed curve showed two boundaries at 1.288 ev and 1.02 ev, which are related to direct and indirect transitions. A comparably small penetration magnitude (20%) in a 0.7 mm thick specimen indicated comparatively low absorption coefficients in indirect transitions and large in direct transitions (at penetration up to 10%). (R.V.J.)

38619 YTTRIUM PHOSPHATES. Tananaev, I. V.; Dzhabishvili, N. A. (Kurnakov Inst. of General and Inorganic Chemistry, Academy of Sciences, USSR). Izv. Akad. Nauk SSSR, Neorgan. Materialy, 1: 514-19(1965). (In Russian).

Formation of yttrium phosphate compounds in YCl_3 - H_3PO_4(NaH_2PO_4, Na_2HPO_4, and $NaPO_4$)$-H_2O$ systems at 25°C was studied by solubility, electric conductivity, and pH methods. It was shown that only the $YPO_4 \cdot 2H_2O$ compound precipitates in $YCl_3-H_3PO_4(NaH_2PO_4)-H_2O$ systems. A mixed salt $2YPO_4 \cdot Na_2HPO_4 \cdot 4H_2O$ was separated from systems with Na_2HPO_4 in addition to the mean yttrium phosphate. The basic salt $9YPO_4 \cdot Y(OH)_3 \cdot 27H_2O$ formed in the system with Na_3PO_4 at the beginning of the reaction. However, as the reaction with trisubstituted sodium biphosphate continued the basic salt transformed into mean yttrium phosphate $YPO_4 \cdot 2H_2O$, which, with saturation of the precipitant, formed the mixed salt $2YPO_4 \cdot Na_3PO_4 \cdot 5H_2O$. (R.V.J.)

38620 INVESTIGATION OF YTTRIUM CHLORIDE REACTIONS WITH POTASSIUM PHOSPHATES. Tananaev, I. V.; Dzhabishvili, N. A. (Kurnakov Inst. of General and Inorganic Chemistry, Academy of Sciences, USSR). Izv. Akad. Nauk SSSR, Neorgan. Materialy, 1: 520-4(1965). (In Russian).

Studies were made of solubility, electric conductivity, and pH of $YCl_3-K_xH_{3-x}PO_4-H_2O$ systems (where x = 1, 2 and 3) at 25°C. Chemical and thermographic analysis were made of the separate systems. It was found that $YPO_4 \cdot 2H_2O$ precipitates from a system with KH_2PO_4 while the mixed salts $5YPO_4 \cdot 2K_2HPO_4 \cdot 9H_2O$ and $5YPO_4 \cdot 2K_3PO_4 \cdot 10H_2O$ were formed in systems with K_2HPO_4 and K_3PO_4, respectively. (R.V.J.)

38621 SYNTHESIS OF DIVALENT RARE EARTH SILICATES. Bondar, I. A.; Toropov, N. A.; Koroleva, L. N. (Grebenshchikov Inst. of Chemistry of Silicates, Academy of Sciences, USSR). Izv. Akad. Nauk SSSR, Neorgan. Materialy, 1: 561-8(1965). (In Russian).

Preparation of ten silicates of divalent samarium, europium, and ytterbium is described. Crystal, optical, and x-ray diffraction analysis indicated similar crystal structure for Sm, Eu, Yb, Ca, and Sr silicates. (R.V.J.)

38622 INFRARED SPECTRA AND STRUCTURE OF SILICATES WITH DIVALENT RARE EARTH CATIONS. Tenisheva, T. F.; Lazarev, A. N. (Inst. of Chemistry of Silicates, Academy of Sciences, USSR). Izv. Akad. Nauk SSSR, Neorgan. Materialy, 1: 569-75(1965). (In Russian).

Spectrometers were used to investigate the structure of compounds with Sm^{2+}, Eu^{2+}, and Yb^{2+} cations. The infrared spectra of the divalent rare earth cations confirmed the existence of the 3:1, 2:1, 3:2, and 1:1 compounds in the $YbO-SiO_2$ and $EuO-SiO_2$ system and 2:1 and 1:1 compounds in the $SmO-SiO_2$ system. The isostructure of Yb^{2+} silicates and the corresponding calcium silicate were identical to the structure Sm^{2+} and Sr^{2+} silicates while Eu^{2+} silicates occupied an in-between position. Partial interpretation of the spectra is given for complex ion-reagent oscillation frequencies and it is shown that the lattice oscillation frequencies of the compounds examined do not exceed 400 cm^{-1}. (R.V.J.)

38623 NUCLEAR MAGNETIC RESONANCE STUDIES OF THE URANYL-CITRATE SYSTEM IN DEUTERIUM OXIDE AT LOW pD. Bramley, Richard; Reynolds, William F.; Feldman, Isaac. (Univ. Coll., London and Univ. of Rochester, N. Y.). J. Am. Chem. Soc., 87: 3329-32(Aug. 5, 1965).

Nuclear magnetic resonance spectra of uranyl nitrate–citric acid mixtures in D_2O having citric acid concentrations 0.1M and higher, showed that a uranyl–citrate complex exists at unexpectedly high acidity. This "high-acidity" species is different from the dimer existing in H_2O solution at lower concentration (0.01M and less) and higher pH (>2). From the line width broadening of citric acid transitions in the presence of uranyl nitrate, an average lifetime of the order of 0.006 sec was calculated for the "high-acidity" complex species. From the mean chemical shift of the methylene protons, a value of 3.16 ± 0.08 was obtained for the logarithm of the stability constant of this complex under the assumption that it is the monomer $UO_2D_2Citrate^+$. A calculation is presented relating the low-field shift of the methylene deuterons to the electrostatic field and the magnetic anisotropy of the uranyl entity in the complex. (auth)

38624 PREPARATION AND PROPERTIES OF MONO-ALKALI XENATES. Spittler, T. M.; Jaselskis, Bruno (Loyola Univ., Chicago). J. Am. Chem. Soc., 87: 3357-60 (Aug. 5, 1965).

Monosodium, -potassium, -cesium, and -rubidium xenates were prepared by lyophilization of 0.1M xenon trioxide and alkali hydroxides in 1:1 ratio. The existence of alkali xenates was confirmed by infrared spectroscopy, x-ray powder diffraction patterns, and determination of the oxidation equivalent by the "hi–lo" titration method. Sodium xenate has an apparent formula weight of 247 ± 4. Sodium xenate is more stable than xenon trioxide and less stable than sodium perxenate. At room temperature, sodium xenate does not react readily with anhydrous methyl alcohol. The salt of sodium xenate is stable under anhydrous conditions, otherwise it disproportionates to xenon(0) and xenon (VIII). (auth)

38625 ALKALI FLUORIDE COMPLEXES OF TETRAVALENT PROTACTINIUM. Asprey, L. B.; Kruse, F. H.; Penneman, R. A. (Los Alamos Scientific Lab., N. Mex). J. Am. Chem. Soc., 87: 3518(Aug. 5, 1965). (LA-DC-7144).

Alkali fluoride complexes of tetravalent protactinium were prepared by two methods: vacuum heating of PaF_4 with alkali fluoride, and hydrogen reduction of pentavalent protactinium compounds, which was the method yielding purer preparations. X-ray powder data for $7RbF \cdot 6PaF_4$ are presented. (M.C.G.)

38626 γ-RADIATION-INDUCED EXCHANGE OF DEUTERIUM WITH SILICA SURFACES. Kohn, Harold W. (Oak Ridge National Lab., Tenn.). J. Am. Chem. Soc., 87: 3521-2(Aug. 5, 1965). (ORNL-P-1359)

Direct isotopic exchange radiolysis of silica gel was studied. Samples of silica gel were irradiated with ^{60}Co γ rays or 2-Mev electrons and their isotopic exchange with deuterium, $SiO_3/_2OH + D_2 \rightarrow SiO_3/_2OD + HD$, studied. (M.C.G.)

38627 ISOTOPIC EXCHANGE OF A HYDRIDOPLATINUM(II) COMPLEX WITH DEUTERIUM OXIDE. Falk, Charles D.; Halpern, Jack (Univ. of Chicago). J. Am. Chem. Soc., 87: 3523-4(Aug. 5, 1965).

A kinetic study was made of a substitution reaction of a square-planar complex, involving the isotopic exchange trans-$PtHCl(PEt_3)_2 + D_2O \rightarrow$ trans-$PtDCl(PEt_3)_2 + HDO$. Samples of the reaction mixture were removed periodically, added to benzene, freeze-drying the resulting mixture, and extracting the solid residue with benzene. The infrared spectra of the benzene solutions were recorded and the isotopic exchange determined by the decrease in absorbance of the Pt-H stretching band. Isotopic exchange was found to be very slow in the absence of added acid, but was markedly accelerated by DCl. (M.C.G.)

38628 SINGLE-CRYSTAL GROWTH OF THORIUM DIOXIDE FROM LITHIUM DITUNGSTATE SOLVENT. Finch, C. B.; Clark, G. Wayne (Oak Ridge National Lab., Tenn.). J. Appl. Phys., 36: 2143-5(July 1965). (ORNL-P-699)

Single crystals of ThO_2 were grown from molten $Li_2O \cdot 2WO_3$ solvent at 1225 to 1300°C. Growth occurred primarily by solution transfer from ThO_2 nutrient at 1250 to 1350°C to seeds in regions 20 to 75° cooler. The resulting crystals, optically transparent octahedra up to 3 mm on edge, contain <500 ppm W and <50 ppm Li as major impurities. The method was also used to prepare ThO_2 crystals containing limited amounts of several lanthanide ions. Increased growth rates were obtained by adding 1 wt % B_2O_3 to the $Li_2O \cdot 2WO_3$ solvent. (auth)

38629 STUDY OF COLLISION NARROWING BY COMPARISON OF MOLECULAR-BEAM AND GAS-PHASE NUCLEAR RESONANCE SPECTRA. Crapo, L. M.; Flynn, G. W. (Harvard Univ., Cambridge, Mass.). J. Chem. Phys., 43: 1443-50(Sept. 1, 1965).

The second moments of molecular-beam nuclear resonance curves were compared through a simple motion-narrowing theory with linewidths from gas-phase NMR data for CF_4, SiF_4, SF_6, CH_3F, CF_3H, and CH_2F_2 at 300°K. From this comparison the average number of collisions necessary for these molecules to change their angular momentum was estimated to be on the order of three. (auth)

38630 TOTAL CROSS SECTIONS FOR IONIZATION AND ATTACHMENT IN GASES BY ELECTRON IMPACT. I. POSITIVE IONIZATION. Rapp, Donald; Englander-Golden, Paula (Lockheed Missiles and Space Co., Palo Alto, Calif.). J. Chem. Phys., 43: 1464-79(Sept. 1, 1965).

The total ionization cross sections of He, Ne, Ar, Kr, Xe, H_2, D_2, N_2, O_2, CO, NO, CO_2, N_2O, and CH_4 were measured from threshold to 1000 ev in a total ionization tube. More limited measurements were performed in C_2H_4 and SF_6. Great care was taken to assure complete collection of electron and ion currents, and the absence of spurious instrumental errors. A method was devised for obtaining absolute cross sections of gases relative to H_2, and a McLeod gage was used to obtain the absolute cross section in H_2. The cross sections in NO and O_2 could not be obtained by this method, and an approximate correction to direct McLeod gage readings was used for these gases. It is believed that the results are as accurate as is possible with the present method. It is difficult to explain the differences found between cross sections measured by various investigators. McLeod gage errors appeared to account for most of the difference in absolute magnitude. (auth)

38631 TOTAL CROSS SECTIONS FOR IONIZATION AND ATTACHMENT IN GASES BY ELECTRON IMPACT. II. NEGATIVE-ION FORMATION. Rapp, Donald; Briglia, Donald D. (Lockheed Missiles and Space Co., Palo Alto, Calif.). J. Chem. Phys., 43: 1480-9(Sept. 1, 1965).

Absolute total cross sections for negative-ion formation in several gases (CO, NO, O_2, CO_2, N_2O, SF_6, D_2, HO, and H_2) by electron impact were measured in a total ionization tube. Both dissociative attachment and ion-pair formation were measured, with careful attention paid to complete collection of the negative ions. Possible errors due to scattered electrons and energy spread are discussed. (auth)

38632 ISOTOPE EFFECTS ON VIBRATIONAL TRANSITION PROBABILITIES. III. IONIZATION OF ISOTOPIC H_2, N_2, O_2, NO, CO, AND HCl MOLECULES. Halmann, M.; Laulicht, I. (Weizmann Inst. of Science, Rehovoth, Israel). J. Chem. Phys., 43: 1503-9(Sept. 1, 1965).

Franck–Condon factors are given for the normal and stable isotope-labeled molecules for transitions to spectroscopically known ionic states. Appreciable isotope effects on Franck–Condon factors were found in several transitions, and were related both to the differences in internuclear separation associated with different levels and to differences in reduced masses. Isotopic substitution by a heavier element resulted in a shift in the transition probability towards higher vibrational levels. Therefore an inversion in the ratio of ionization efficiencies of light and heavy molecules is predicted. (auth)

38633 CONCENTRATION DEPENDENCE OF THE THERMAL-DIFFUSION FACTOR FOR $^3He-^4He$ AND H_2-D_2. Paul, R.; Howard, A. J.; Watson, W. W. (Yale Univ., New Haven). J. Chem. Phys., 43: 1622-6(Sept. 1, 1965).

The thermal-diffusion factors of $^3He-^4He$ and H_2-D_2 systems were determined with high precision at several different compositions and at a fixed mean temperature, T = 160°K, using a four-tube swing separator for $^3He-^4He$ mixtures, and a simple two-bulb apparatus in the case of H_2-D_2. The results indicated that the thermal-diffusion factor increased in magnitude with the increasing concentrations of the lighter component, as anticipated from theory. Detailed theoretical calculations on the Chapman-Cowling first approximation and the Kihara first and second approximations were carried out, and comparisons made with the experimental results in both the cases. Good agreement between the Chapman-Cowling first approximation and the experimental results was obtained, though Kihara approximations also could be fitted within the experimental uncertainty of the data in both the systems studied. (auth)

38634 TIME-RESOLVED SPECTROSCOPY OF EUROPIUM CHELATES. Bhaumik, M. L.; Nugent, L. J. (Electro-Optical Systems, Inc., Pasadena, Calif.). J. Chem. Phys., 43: 1680-7(Sept. 1, 1965).

Time-resolved fluorescence spectra of several europium chelates were measured using the stroboscopic time-resolution technique. For each of the β-diketone chelates, where the ligand triplet levels were in general above the $^5D_1$ level of Eu^{3+}, the spectra provided evidence that the Eu^{3+} $^5D_0$ state was populated by nonradiative energy transfer from the higher-lying $^5D_1$ state. The relaxation time for energy decay from the $^5D_1$ state was measured both in the microcrystals and in solution to be of the order of a few microseconds. Since this was shorter than the corresponding relaxation time of Eu^{3+} in systems where there were no vibrational frequencies near 1760 cm^{-1}, the $^5D_1-^5D_0$ energy separation, it is suggested that the ligand

$$>C=O \text{ and } >C=C<$$

stretching vibrations and the bending vibration of coordinated water molecules make important contributions to the relaxation process. On the other hand, complete nonradiative degradation to the molecular environment from the $^5D_0$ and the $^5D_1$ energy levels appeared to be more strongly influenced by higher-energy molecular vibrations such as the C–H, and O–H stretches. Variations with temperature in the relaxation time from the $^5D_1$ energy-level were mainly accounted for by the temperature dependence of the rate of energy degradation from the $^5D_1$ level to the

environment, and it is suggested that the $^5D_1 \rightsquigarrow {}^5D_0$ relaxation process was temperature insensitive between 300 and 77°K. In general, the nonradiative energy-transfer processes in Eu^{3+} appeared to be dominated by interactions with molecular vibrations, and to a smaller extent by crystal lattice modes, rather than by other possible relaxation mechanisms. (auth)

38635 EXCHANGE AND RELATIVISTIC EFFECTS ON PI BONDING IN THE URANYL ION. Newman, John B. (Johns Hopkins Univ., Baltimore). J. Chem. Phys., 43: 1691-4(Sept. 1, 1965).

Overlap integrals for the uranyl ion were calculated using Hartree-Fock-Slater and Hartree relativistic U^{5+} 5f and 6d wavefunctions. Earlier primary overlap calculations by Belford and Belford, using solutions that were approximately Hartree functions, gave π larger than σ overlaps. Exchange effects tended to equalize the σ and π overlaps, and a case was found where the σ overlaps exceed the π values. The relativistic effects were indirect and more pronounced for the 5f orbital. They tended to equalize the σd and πf overlaps, and to increase the πd value, which nevertheless remained the largest. These results were indicative of a uranyl structure having strong πd, and weak σf primary bonds, and having at most weak 5f orbital involvement in the secondary bonding. Thus, the overlap results obtained using exchange and relativistically corrected uranium wavefunctions supported the view of uranyl complex structures as proposed by Belford and Belford and by Coulson and Lester. (auth)

38636 FLUORESCENCE OF TRIVALENT EUROPIUM IN D_2O–H_2O MIXTURES. Gallagher, P. K. (Bell Telephone Labs., Inc., Murray Hill, N. J.). J. Chem. Phys., 43: 1742-4(Sept. 1, 1965).

The absorption and emission spectra and fluorescent lifetimes of solutions of europium(III) chloride in D_2O–H_2O mixtures were measured. The lifetime of the most deuterated solution, 99.6%, was found to be 3.9 msec while that of the undeuterated solution was 0.12 msec. The decay curves of intermediate solutions exhibited two portions having lifetimes essentially equal to the end members. These results are discussed and compared with those of previous investigators. (auth)

38637 ION-MOLECULE INTERACTION IN THE CATHODE REGION OF A GLOW DISCHARGE. Shahin, M. M. (Xerox Corp., Rochester, N. Y.). J. Chem. Phys., 43: 1798-1805(Sept. 1, 1965).

Studies of the ions arriving at the cathode of a glow discharge in nitrogen were made by the use of a quadrupole mass spectrometer. Detailed investigation of the dependence of the relative intensities of the two major ions N_2^+ and N^+ on the discharge conditions indicated that the latter species mostly originate within the cathode dark space, probably through the reaction $N_2^+ + N_2 \rightarrow N^+ + N + N_2$. Calculation of the reaction time, with due allowance for the resonance charge exchange of N_2^+ ions, permitted the treatment of the data to yield a value of 7.4×10^{-11} cc/sec for the rate constant of this reaction, at ion energies above the minimum of 17.4 ev required for this process. (auth)

38638 ENDOR OF FREE RADICALS IN SOLUTION. Hyde, James S. (Varian Associates, Palo Alto, Calif.). J. Chem. Phys., 43: 1806-18(Sept. 1, 1965).

Electron nuclear double resonance techniques were used on six free radicals in solution. Polar and nonpolar solvents were employed, and both neutral and ionic radicals investigated. The instrumentation is described. Features of the instrument include: pulsed nuclear r-f magnetic fields, r-f fields as high as 40 G in the rotating frame, and provision to observe changes in the EPR spectrum caused by nuclear resonance with the ordinary EPR spectrum subtracted (ENDOR-induced EPR). ENDOR mechanisms and adjustment of experimental conditions to achieve optimum signal intensity are discussed. It was established that successful ENDOR experiments can be performed on a large number of free radicals in solution, resulting in improved resolution, simplification of spectra, and more accurate hyperfine splittings. (auth)

38639 ISOTOPIC EFFECTS IN LIQUID HYDROGEN. Reed, Robert D. (LTV Research Center, Dallas); Henderson, Douglas; Chen, Ru-yong. J. Chem. Phys., 43: 1836-8(Sept. 1, 1965).

Calculations of the thermodynamic properties of all of the isotopically substituted forms of hydrogen are presented. It was assumed that the potential between two hydrogen molecules is satisfactory represented by the Lennard-Jones 6:12 potential $U(r) = 4\epsilon - \{(\sigma/r)^{12} - (\sigma/r)^6\}$. The primary dependence of the thermodynamic properties on the mass of the molecule was investigated. The same values of ϵ and σ were used for all the isotopes. Secondary quantum effects caused by rotations, small changes in the potential parameters, and quantum statistics were not considered. The experimental critical constants given for DT and T_2 are estimates based on the law of corresponding states since experimental values are unavailable. Only for the critical temperature is the agreement satisfactory. However, the critical constants predicted by the quantum cell model show about the same errors as do those predicted by the classical cell model. (F.J.H.)

38640 REPORT ON THE CHEMISTRY OF THE ELEMENTS NIOBIUM AND TANTALUM. XLVII. NIOBIUM FLUORIDE. Schaefer, H.; Schnering, H. G.; Niehues, K.-J.; Nieder-Vahrenholz, H. G. (Universitaet, Muenster, Ger.). J. Less-Common Metals, 9: 95-104(Aug. 1965). (In German).

NbF_5 was obtained by reaction of K_2NbF_7 with AlF_3. NbF_5 and TaF_5 formed a complete solid solution with almost ideal behavior. NbF_4 was formed at ~350°C by reduction of NbF_5 with Nb. NbF_4 disproportionated under suitable conditions to $NbF_{2.5}$ and NbF_5. NbF_4 crystallized in the tetragonal SnF_4-type. "NbF_3" apparently always contains more or less oxygen. A wide $Nb(O,F)_3$– mixed crystal range exists. $NbF_{2.5}$ was formed by Nb + NbF_5 at ≧ 700°C. It can be obtained in crystals by chemical transport. The compound crystallized cubically with a structure, which can be described by the formula $[Nb_6F_{12}]F_{6/6}$. Thus the already known Nb_6-octahedron acted as structure element. (auth)

38641 STUDIES ON THE STABILITY OF BERYLLIUM CHELATES OF CATECHOLDISULPHONIC AND CHROMOTROPIC ACIDS IN AQUEOUS SOLUTIONS. Dubey, S. N.; Mehrotra, R. C. (Univ. of Rajasthan, Jaipur, India). J. Less-Common Metals, 9: 123-32(Aug. 1965).

The complexation reactions of beryllium with the disodium salts of catecholdisulfonic and chromotropic acids were studied by potentiometric and conductometric methods. In the acidic range, the formation of mono-derivatives only was indicated in both the systems even in the presence of a large excess of chelating agents. The equilibrium constants "K" of the reaction, $Be^{2+} + H_2A^{2-} \rightleftharpoons BeA^{2-} + 2H^+$, and the logarithms of the formation constant (K_1) of the complex anion $[BeA^{2-}]$ in catecholdisulfonic and chromotropic acids systems were found to be 9.33×10^{-8} and 13.23, and 2.95×10^{-5} and 16.43, respectively. The logarithms of the formation constants (log K_n) in both the systems for 1 : 1 and 1 : 2 complexes were also determined by the alternative methods to be 13.52 ± 0.12; 12.54 ± 0.14 and 16.89 ± 0.09; 15.91 ± 0.11, respectively. (auth)

38642 THE THERMODYNAMICS OF THE YTTRIUM–HYDROGEN SYSTEM. Yannopoulos, L. N.; Edwards, R. K.; Wahlbeck, P. G. (Illinois Inst. of Tech., Chicago). J. Phys. Chem., 69: 2510-15(Aug. 1965). (COO-1029-5).

Isothermal equilibrium hydrogen pressure measurements were carried out as a function of composition for the yttrium-hydrogen system in the temperature ranges 250 to 350° and 650 to 950°C, up to a pressure of 1 atm. The existence of three solid solution phases in this system is indicated by the data. The primary solid solution range extends to about $YH_{0.85}$. The other two solid solution phases can be described as yttrium hydride phases deficient in hydrogen with respect to YH_2 and YH_3. The phase boundaries were evaluated in the temperature ranges 650 to 950 and 250 to 350°C, respectively. The experimental relative partial molal and integral thermodynamic quantities were calculated. (auth)

38643 CALCULATION OF THE HALL EFFECT IN IONIC SOLUTIONS. Friedman, Harold L. (IBM Watson Research Center, Yorktown Heights, N. Y.). J. Phys. Chem., 69: 2617-27(Aug. 1965).

The theory of electrical conductance in ionic solutions previously reported was extended to apply to the transport in combined electric and magnetic fields. Calculations were made with the brownon model, essentially the model used in the Debye-Hückel-Onsager conductance theory. General expressions and numerical results were obtained for the ideal and limiting-law terms of the Hall conductance. The calculations indicate that the effect is large enough to be measurable, at least for solutions of the more mobile ions. For symmetrical electrolytes the limiting-law term opposes the ideal term in the Hall conductance, while for unsymmetrical electrolytes it may either aid or oppose the ideal term. (auth)

38644 VAPORIZATION, THERMODYNAMICS, AND DISSOCIATION ENERGY OF LANTHANUM MONOSULFIDE. Cater, David E. (Univ. of Iowa, Iowa City); Lee, Thomas L.; Johnson, Ernest W.; Rauh, Everett G.; Eick, Harry A. J. Phys. Chem., 69: 2684-9(Aug. 1965).

The congruent vaporization of lanthanum monosulfide was studied over the temperature range 2012 to 2490°K by the effusion technique with the aid of vacuum balance and mass spectrometer. The principal vapor species is LaS, and calculation shows that 3 to 10% of the vapor is La + S. The vapor pressure of solid LaS is given by log P_{atm} = $7.365 - 2.873 \times 10^4/T$. The heat and entropy of sublimation at 2240°K are ΔH°_{2240} = 131.5 ± 1.0 kcal/mole and ΔS°_{2240} = 33.5 ± 0.6 eu. Estimated thermal data yield ΔH°_{298} = 141.4 ± 2.0 and ΔH°_0 = 141.7 ± 2.0 kcal/mole. The dissociation energy of gaseous LaS is 137 ± 6 kcal/mole or 5.9 ± 0.2 ev. The quoted uncertainty for ΔH°_{2240} is the statistical standard deviation; the other uncertainties are estimated limits of accuracy, and the values apply if the ground state of LaS(g) is $^4\Sigma$. The lattice parameter of LaS at room temperature is 5.854 ± 0.002 Å. The melting point of LaS is at least as high as 2327 ± 20°. (auth)

38645 DISSOCIATION CONSTANT OF ACETIC ACID IN DEUTERIUM OXIDE FROM 5 TO 50°. REFERENCE POINTS FOR A pD SCALE. Gary, Robert; Bates, Roger G.; Robinson, R. A. (National Bureau of Standards, Washington, D. C.). J. Phys. Chem., 69: 2750-3(Aug. 1965).

Electromotive force measurements of a cell without liquid junction were used to determine the dissociation constant of acetic acid in deuterium oxide from 5 to 50°. The enthalpy, entropy, and heat capacity changes on dissociation of acetic acid were calculated. Values of $-\log (a_D + \gamma_{Cl^-})$ and the conventional pa_D values for the equimolal (0.05 m) acetic acid-sodium acetate buffer solutions have been determined. These provide a second fixed point for standardizing the pD scale, supplementing data for the equimolal mixture of KD_2PO_4 and Na_2DPO_4 established previously. (auth)

38646 DIFFUSION IN DEUTERIO-NORMAL HYDROCARBON MIXTURES. Birkett, J. D.; Lyons, P. A. (Yale Univ., New Haven). J. Phys. Chem., 69: 2782-3 (Aug. 1965). (TID-21729).

Tracer diffusion coefficients were measured for benzene, cyclohexane, isooctane, and n-heptane using the Rayleigh interferometric procedure. The results were corrected for the difference in viscosity relative to pure undeuterated hydrocarbon. All the values (except for benzene) were consistent with precise binary diffusion data. Within the experimental error, which would appear to be about ±1%, the corrected quantities are independent of the concentration of the deuterated species. Data are tabulated. (P.C.H.)

38647 ZIRCONIUM COMPOUNDS AND THEIR USES. Kokube, Taiitiro. Kogyo Reametaru, No. 24, 53-8(1963). (In Japanese)

Several industrial methods for the preparation of zirconium compounds and their main applications are described. Na_2ZrO_3 was obtained through fusion of zircon and soda. It is used as refractories of medium grade and also as a grinding agent and chamoising agent for white leather. $ZrOSo_4$ was obtained through treatment of Na_2ZrO_3 with sulfuric acid. In addition to its use as materials for the preparation of various zirconium compound, it is also used as specific chamoising agent for white leather and is particularly suitable for thin textiles. It is also a good agent for treating woolen goods. $ZrOCl_2 \cdot 8H_2O$ was obtained through concentration of sodium zirconate or sodium zirconium silicate in hydrochloric acid. Zirconium oxychloride can be used not only as starting material for organic and inorganic zirconium compounds, but also as waterproofing agent, dark-red dyestuff, and catalyst for the preparation of butadiene and various adhesives for the formation of zirconium anhydride refractories. Zirconium acetate was obtained through dissolution of zirconium hydroxide in acetic acid. Zirconium acetate is applied in making a perpetual waterproofing agent for cellulose and as a catalyst for silicon waterproofing agent. Recently, it was used as an additive in heavy oil in order to protect vanadium from precipitation on the inner walls of the tube in the heavy oil boiler. Zirconium soap was made by the double decomposition reaction of the water-soluble zirconium salt of zirconium oxychloride or sodium zirconium sulfate with fatty sodium, or by the fusion of aliphatic acid with insoluble carbonate. It is mainly used as catalyst, oil additive, stabilizing agent for milk sap, dryer for printing ink, dryer for various coatings, water-proof agent, etc. Zirconium dioxide was obtained through a wet process, i.e., through calcining the insoluble zirconium hydroxide, which was previously obtained by alkalifying the aqueous solution containing zirconium sulfate and zirconium oxychloride. It is mainly employed in the fabrication of refractory, as special porcelain, catalyst, grinding material, milk agent, optical glass, additive for rubber, etc. (NFSAIS)

38648 LUMINESCENCE FROM IONIZED F-AGGREGATE CENTERS IN ALKALI HALIDE CRYSTALS. Schneider, I.; Kabler, M. N. (Naval Research Lab., Washington, D. C.). Phys. Letters, 17: 213-14(July 15, 1965).

The absorption and emission spectra of ionized F-aggregate centers in additively colored KCl and KBr were measured. The spectra are shown and the data on all bands studied, including the overlapping bands, are tabulated. It was found that the luminescence from an ionized F-aggregate is characterized by a relatively small Stokes shift. The small Stokes shifts, the occurrence of 0–0 transition, and the close correspondence between the emission and absorption band half-widths are viewed as evidence that the ground and excited electronic states of the various centers are localized within the halide ion vacancies throughout the de-excitation process. (L.B.S.)

38649 FERROMAGNETIC AND PARAMAGNETIC RESONANCE IN EuS. Von Molnar, S.; Lawson, A. W. (Univ. of California, Riverside). Phys. Rev., 139: A1598-1602 (Aug. 30, 1965).

Ferromagnetic and paramagnetic resonance was observed in single crystals of EuS. A standard microwave spectrometer, operating near 22 Gc, was used to measure the power absorption at 1.4 and 300°K. The resonance line width, 75 Oe at 1.4°K, was found to be approximately 1200 Oe at room temperature. An upper limit of 30 Oe established for the magnitude of the magnetocrystalline anisotropy field, in contrast to the value of −190 Oe found for EuO. The paramagnetic line width is explained solely on the basis of spin-spin interactions. The anisotropy results are understood in terms of crystal-field perturbations of the magnetic Eu^{2+} ion. (auth)

38650 PARAMAGNETIC RESONANCE OF TRIVALENT HOLMIUM IONS IN CALCIUM TUNGSTATE. Kirton, J. (Royal Radar Establishment, Malvern, Worcestershire, Eng.). Phys. Rev., 139: A1930-3(Sept. 13, 1965).

Paramagnetic resonance was observed in calcium tungstate containing trivalent holmium ions in sites with tetragonal symmetry. The observed spectrum was fitted to the spin hamiltonian $\mathcal{H} = g_{||}\beta H \cos\theta S_Z + \Delta_x S_x + \Delta_y S_y + AS_x I_x$ with A = 0.299 cm^{-1} and $g_{||}$ = 13.691. The distortion

parameter $\Delta = (\Delta_x^2 + \Delta_y^2)^{1/2}$ did not possess a unique value and consequently the absorption line shape was asymmetric, the value of Δ corresponding to the peak intensity being 0.03 cm^{-1}. These results for Ho^{3+} are contrasted with those published for Tb^{3+} in $CaWO_4$ and attention is drawn to the differences in line shape in the two cases. It is found that the lowest level in $CaWO_4/Ho^{3+}$ is of the type $\psi = \phi|\pm 7\rangle + \chi|\pm 3\rangle + \Psi|\ 1\rangle + \Omega|\mp 5\rangle$. The results of paramagnetic-resonance measurements on all trivalent rare-earth ions in tetragonal sites in $CaWO_4$ are summarized. (auth)

38651 MOESSBAUER EFFECT IN FERROELECTRIC $BaTiO_3$. Bhide, V. G.; Multani, M. S. (Inst. of Science, Bombay). Phys. Rev., 139: A1983-90(Sept. 13, 1965).

The Mössbauer effect for ^{57m}Fe in the $BaTiO_3$ lattice was studied from 300 to 1200°K with particular emphasis on the region near the Curie temperature. The Mössbauer probe seems to serve as a useful tool for the study of ferroelectrics. The electric-field gradient as seen by the probe at room temperature is -0.52×10^{14} esu cm^{-3} and is closely proportional to P_s^2 as the spontaneous polarization P_s varies with temperature. The strength of the resonant absorption was also determined as a function of temperature in the region above T_c. Much above T_c these measurements are compatible with a Debye temperature of 450°K. However, as the Curie temperature is approached, the Lamb-Mössbauer factor decreases appreciably. These results are discussed in the light of Cochran's theory of ferroelectricity. From the isomer shift at room temperature (0.50 ± 0.02 mm/sec with respect to 310 stainless steel) the over-all degree of ionicity is estimated to be 60 ± 20%. The temperature shift shows a discontinuity at T_c and is attributed to the change in covalent binding. (auth)

38652 OPTICAL-ABSORPTION INTENSITIES OF RARE-EARTH IONS IN CRYSTALS: THE ABSORPTION SPECTRUM OF THULIUM ETHYL SULFATE. Krupke, William F. (Aerospace Corp., El Segundo, Calif.).; Gruber, John B. Phys. Rev., 139: A2008-16(Sept. 13, 1965).

Absolute intensities of the electronic transitions occurring in the absorption spectrum of thulium ethyl sulfate were measured at 4.2 and 23°K. In addition, absolute intensities due to vibronic and electronic transitions were measured at 300°K. The oscillator strengths of electric-dipole transitions between individual crystalline Stark-split components which were observed at 23°K are compared with theoretical calculations and the results are discussed. The total electric-dipole oscillator strengths measured at 300°K are compared with theoretical calculations and also with the low-temperature results. The observed intensities, which vary as much as 40-fold between 38,000 cm^{-1} and 15,000 cm^{-1}, can be accounted for by using only several phenomenological parameters. Interpretation of the parameters is discussed in terms of excited-electronic-state wave functions and their admixture into the ground-state electronic configuration. (auth)

38653 MOESSBAUER-EFFECT STUDY OF RELAXATION EFFECTS IN IRON-DITHIOCARBAMATES. Wickman, H. H.; Trozzolo, A. M. (Bell Telephone Labs., Murray Hill, N. J.). Phys. Rev. Letters, 15: 156-8 (July 26, 1965).

The Mössbauer effect was observed in iron dithiocarbamates at absorber temperatures of 1.8, 4.2, 77 and 300°K. An asymmetric quadrupole pattern resulting from the addition of a time-independent axially symmetric electric-field gradient colinear with the fluctuating internal field was established. The results were compared with relaxation spectra calculated using solutions of the modified Bloch equations. (D.C.W.)

38654 INVESTIGATION OF CONTACT INTERACTIONS OF METAL BORIDES WITH GRAPHITE AT HIGH TEMPERATURES IN VACUUM. Burykina, A. L.; Evtushok, T. M. (Inst. of Problems in Metallography, Academy of Sciences, Ukrainian SSR). Poroshkovaya Met., Akad. Nauk Ukr. SSR, No. 6, 75-8(June 1965). (In Russian).

Contact reactions of compacted and powdered borides (TiB_2, ZrB_2, HfB_2, NbB_2, Mo_2B_5, and W_2B_5) with graphite and graphite powder were investigated at 2200°C in vacuum. The results of metallographic and chemical analyses and microhardness measurements showed that hafnium, niobium, tantalum, and tungsten borides remain stable at 2200°C for periods to 5 hr. Molybdenum boride is stable up to the melting point. After 5 hr at 2200°C, zirconium boride reactions with graphite powder resulted in some loss of weight and microhardness; reactions of ZrB_2 powder with compacted graphite resulted in an increase in graphite microhardness and a change in the chemical composition of the boride. (R.V.J.)

38655 EPR AND ENDOR OF Tb^{4+} IN THORIA. Baker, J. M.; Chadwick, J. R.; Garton, G; Hurrell, J. P. (Oxford Univ.) Proc. Roy. Soc. (London), Ser. A, 286: 352-65(July 20, 1965).

EPR and endor spectra were measured in ThO_2 containing Tb^{4+}. The crystalline electric field was cubic, and the splittings very large compared with other S state ions. The values of the parameters in the standard cubic spin-Hamiltonian were: $g = 2.0146 \pm 0.0004$, $60B_4 = -2527.53 \pm 0.10$ Mc/s, $1260B_6 = -24.84 \pm 0.04$ Mc/s, $A = -73.891 \pm 0.023$ Mc/s, $B = +6.194 \pm 0.038$ Mc/s, and $\mu_N(^{159}Tb) = +1.994 \pm 0.004$ nuclear magnetons. There were also additional small high-order terms. There were very marked differences between these parameters and those for the other S state ions Gd^{3+} and Eu^{2+}. In addition to the much larger $60B_4$, the g value was in excess of the free spin value; at the nucleus, the electrons produced a smaller magnetic field (proportional to A/g_1) and a larger electric field gradient (proportional to B/Q) than they did in Gd^{3+} and Eu^{2+}. These differences were probably due to covalent bonding. The value of the nuclear moment of ^{159}Tb was used to obtain a value of $\langle r^{-3} \rangle = 8.23$ au for Tb^{3+} from the known hyperfine structure in Tb^{3+}. (auth)

38656 PREPARATION AND SOME PROPERTIES OF PENTAVALENT PLUTONIUM NITRATE SOLUTIONS. Gel'man, A. D.; Zaitseva, V. P. Radiokhimiya, 7: 49-55 (1965). (In Russian).

Studies were made to select a method and to determine conditions for preparation of relatively concentrated solutions of pure pentavalent plutonium. Under appropriate experimental conditions $2 \cdot 10^{-2}$ M Pu(V) nitrate solutions were obtained by reduction of hexavalent plutonium with hydrogen peroxide. Continuous pH control was necessary because addition of hydrogen peroxide to hexavalent plutonium increases the acidity of the solution as the reduction proceeds. A calibration curve was obtained for the optical density of Pu(V) nitrate solutions as a function of the concentration of Pu(V) in solution. Spectrophotometric study of Pu(V) nitrate solutions in the pH 2–6 range showed analogous spectra thus indicating no complexation and no hydrolysis. Solutions where pH = 4–6 can be stored over long periods of time without oxidation of Pu(V). At pH > 3 Pu(V) was detected only after a month of storage. (ATD)

38657 REACTION OF VARIOUS URANIUM OXIDES WITH SULFURIC ACID. Kuz'micheva, E. U.; Dunaeva, K. M.; Kovba, L. M.; Ippolitiva, E. A. Radiokhimiya, 7: 78-83(1965). (In Russian).

Changes in composition and structure produced by sulfuric acid treatment of uranium oxides obtained under various conditions were investigated. The analyses of the obtained preparations were carried out by two methods: heating at 720°C in air to constant weight and heating at 800°C in a hydrogen stream. X-ray powder diffraction studies were conducted in order to establish the phase composition. It was found that the amount of uranium that passes into solution decreases with an increase in the temperature under which the oxides were obtained. Rhombic oxides $U_3O_{8\pm x}$ were obtained by heating hydrated uranium peroxide above 500°C. Hydrogen reduction of uranium oxides at 500–1000°C produced cubic UO_{2+x} oxides with a uranium dioxide structure. Oxidation of UO_2 at 250°C produced an oxide with the composition $UO_{2.337}$, which has a tetragonal face-centered unit cell. Treatment of U_3O_8 with sulfuric acid produced first a U_3O_8-x phase and then a hexagonal $UO_{2.5\pm x}$ phase. Cubic oxides that contain more oxygen than is rep-

resented by the formula $UO_{2.00}$ change their composition during acid treatment to approach $UO_{2.00}$. Tetragonal oxides are practically insoluble in sulfuric acid. (ATD)

38658 PREPARATION OF Sr, Ca, AND Mg ACCELERATOR TARGETS. Sauer, J. M. (Univ. of Washington, Seattle). Rev. Sci. Instr., 36: 1374(Sept. 1965).

A technique is described whereby metallic, isotopically enriched Sr, Ca, and Mg accelerator targets may be prepared starting either from the metal oxide or carbonate by simultaneous reduction of the oxide to metal using aluminum metal and evaporation of the resulting metal in vacuum. (C.E.S.)

38659 PREPARATION OF URANOUS SALT BY WAY OF INTERMEDIATE FORMATION OF URANYL SULFIDE. Iwase, Eiichi; Matsuda, Kiyoshi (Inst. of Physical and Chemical Research, Tokyo). Rika Gaku Kenkyusho Kohoku, 36: 114-16(1960). (In Japanese).

A method is described for the preparation of uranous sulfate or chloride from a uranyl salt by the action of hydrogen sulfide or alkali sulfide. An aqueous solution of the uranyl salt is treated with ammonium sulfide or sodium sulfide, and is heated so that the uranyl sulfide formed as a suspension decomposes into uranium dioxide and sulfur, which are separated from the mother liquor by filtration. The resulting uranium dioxide is then converted to the uranous ion by treatment with an acid such as sulfuric acid or hydrochloric acid, from which the sulfur is removed by filtration. Alternatively, the original solution is first treated with ammonia or sodium hydroxide, and the hydrogen sulfide is bubbled into the solution. The uranyl sulfide formed is treated by the same procedure. The pH of aqueous solution of uranyl salt (containing less than 0.1% of the salt in solution) is adjusted to 9 with ammonia. The solution is then saturated with hydrogen sulfide and heated at about 80°C for 30 min. Sulfuric acid is added to the solution and then sulfur is separated from the uranous sulfate solution by filtration. The yield of uranous sulfate is ~90%. (BBB)

38660 THERMAL DECOMPOSITION AND AIR-OXIDATION OF SOME URANIUM COMPOUNDS. Kobayashi, Ichiro (Inst. of Physical and Chemical Research, Tokyo). Rika Gaku Kenkyusho Hokoku, 36: 710-13(1960). (In Japanese).

The thermal decomposition of some uranium compounds and oxidation of uranium dioxide in air were studied by thermogravimetric and x-ray powder diffraction methods. Thermogravimetric curves showed that uranyl oxalate, uranyl acetate, uranyl tartrate, ammonium diuranate, hydrated uranium trioxide, uranyl sulfate, and uranyl nitrate have the compositions $UO_2C_2O_4 \cdot 3H_2O$, $UO_2(CH_3CO_2) \cdot 2H_2O$, $UO_2C_4H_4O_5 \cdot H_2O$, $(NH_4)_2U_2O_7 \cdot 2H_2O$, $UO_3 \cdot 2H_2O$, $UO_2SO_4 \cdot 3H_2O$, and $UO_2(NO_3)_2 \cdot 6H_2O$, respectively. The uranyl salts of carboxylic acids have a tendency to form uranium dioxide in the course of thermal decomposition and this tendency is especially marked in the case of uranyl tartrate, at least as observed in the present investigation. Amorphous uranium trioxide, resulting from the thermal decomposition of uranyl nitrate, changes to the crystalline form in the temperature range 400 to 450°C. The oxidation of uranium dioxide in air proceeds in two steps as was reported previously. (BBB)

38661 ON THE REACTION BETWEEN URANIUM OXIDES AND CARBON TETRACHLORIDE. Iwase, Eiichi; Nishiyama, Seijiro; Kobayashi, Ichiro; Matsuda, Kiyoshi (Inst. of Physical and Chemical Research, Tokyo). Rika Gaku Kenkyusho Hokoku, 36: 714-19(1960). (In Japanese).

An attempt was made to react uranium oxides and carbon tetrachloride vapor at 350-450°C with the object of preparing uranium tetrachloride. When U_3O_8 or UO_3 was used as the starting substance, brown prismatic crystals were obtained as intermediate products during these reactions, while UO_2 did not give such products. These intermediate products were examined by chemical analysis, microscopic observations, and x-ray diffraction. Their chemical compositions were determined to be $2UCl_4 \cdot UO_2Cl_2$ or $3UCl_4 \cdot 2UO_2Cl_2 \cdot UOCl_2$. (BBB)

38662 USE OF Mg-Al ALLOY FOR THE REDUCTION OF UO_2Cl_2 AND OF $FeCl_3$ IN AQUEOUS SOLUTIONS. Iwase, Eiichi; Kobayashi, Ichiro; Isono, Toshiaki (Inst. of Physical and Chemical Research, Tokyo). Rika Gaku Kenkyusho Hokoku, 36: 720-2(1960). (In Japanese).

A method is presented for preparing uranous chloride of high purity, whereby Mg-Al alloy is used as the reducing agent and tributyl phosphate-kerosene as the extraction solvent. Uranyl chloride in a HCl solution is reduced to UCl_4 with Mg-Al alloy; the amount of uranous ion at the end of the run is titrated with a $K_2Cr_2O_7$ solution and the reduction rate of uranyl ion is calculated. The results of the experiments showed that: the Al alloys, with Mg as high as 10-15%, appear to be more effective than Al, Mg, or their simple mixtures for promoting the reducing reaction, the intensified action of these Al-Mg alloys in the reduction of UO_2^{2+} is also found in reduction of Fe^{3+}, and the amount of hydrogen evolved per minute is related to the rate of reduction of uranyl or ferric ions in these reactions. (BBB)

38663 THE MICROWAVE ROTATION SPECTRA OF GeS. Hoeft, J. (Freie Universitaet, Berlin). Z. Naturforsch., 20a: 826-9(June 1965). (In German).

The rotational transitions $J = 0 \rightarrow 1$ and $J = 2 \rightarrow 3$ of GeS were measured in the frequency ranges of 10.7 to 11.4 and 32.1 to 34.1 GH_2 at temperatures between 450 and 650°C. The total of 39 lines could be associated with eight isotope combinations of GeS with natural abundances between 0.9 and 34.7%. The rotation constants, quadrupole coupling constants, internuclear distances, and mass ratios of the isotopes are given for line frequencies. (tr-auth)

38664 ELECTRON PARAMAGNETIC RESONANCE OF Eu^{2+} IN CdF_2. Glaeser, H. J.; Geist, D. (Technische Hochschule, Clausthal, Ger.). Z. Naturforsch., 20a: 842-4(June 1965).

Equations are obtained for line positions of the EPR-spectra of Eu^{2+} ions in CdF_2 for magnetic dipole transitions $\Delta M = \pm 1$, $\Delta M = 0$, which explain the angular variation. The spectra of Eu^{2+} and Mn^{2+} in CdF_2 for H II [100] direction are shown. The EPR constants are tabulated and compared with other values for Eu^{2+} ion in alkaline earth fluorides having the same lattice structure. (L.B.S.)

38665 ON THE POSSIBILITY FOR SIMULTANEOUS MEASUREMENT OF ION DIFFUSION COEFFICIENTS AND ION MOBILITY BY USE OF RADIOACTIVE ISOTOPES. Lengyel, S. (Lorand Eoetvoes Univ., Budapest). Z. Physik. Chem. (Leipzig), 228: 393-407(1965). (In German)

The possibility exists of measuring simultaneously the diffusion coefficients and the mobilities of ions. The method is based on the measurement of the concentration distribution of a radioactive isotope along a capillary tube containing a solution through which electrical currents flow. (tr-auth)

38666 ACETIC COMPOUNDS OF TRIVALENT CERIUM. Pospelova, L. A.; Zaitzeva, T. F. (Kurnakov Inst. of General and Inorganic Chemistry, Academy of Sciences, USSR). Zh. Neorgan. Khim., 10: 1097-1106 (May 1965). (In Russian)

Acetate compounds of trivalent cerium were synthesized. They were $(NH_4)_2[Ce(CH_3COO)_5] \cdot 3H_2O$, $K_2[Ce(CH_3COO)_5] \cdot H_2O$, $Cs_2[Ce(CH_3COO)_5] \cdot 4H_2O$, $K_3[Ce(CH_3COO)_6] \cdot 5H_2O$, and $(NH_4)_3[Ce(CH_3COO)_6] \cdot H_2O$. It was shown that all these compounds could be arranged in a genetic series similar to the Werner-Miolatti classical series: $[Ce(CH_3COO)_3] \cdot H_2O$; $(CN_3H_6)[Ce(CH_3COO)_4] \cdot H_2O$; $(NH_4)_3[Ce(CH_3COO)_5] \cdot 3H_2O$; $K_2[Ce(CH_3COO)_5] \cdot H_2O$. Crystallographic and thermogravimetric studies were made of all of the compounds synthesized. Measurements of the pH value and the molar electroconductivity of the acetocerates were measured in water and methyl alcohol. Hypotheses on the coordinate number of Ce(III) in acetate complexes and methods for the joining of the acetate group to Ce are discussed. (tr-auth)

38667 ZIRCONIUM REACTIONS WITH CERTAIN COMPLEXING AGENTS. Knyazeva, E. M.; Luk'yanov, V. F. Zh. Neorgan. Khim., 10: 1107-9(May 1965). (In Russian)

The interaction of zirconium with a series of complexing

agents was investigated in strong acid media (0.5 to 2N $HClO_4$, HCl, and HNO_3) by the metal indicator method. It was found that the greatest stability was obtained with compounds of zirconium with 1,2-diamine cycloheptane-tetracetic acid and the least stability with nitrilotriacetic acid. The stoichiometric coefficients of the reaction were found by the isomolar series method. In all cases they had the ratio of zirconium : complex = 1 : 1. (tr-auth)

38668 REACTIONS OF SODIUM METAPHOSPHATE WITH CERIUM, NEODYMIUM, AND SAMARIUM OXIDES. Berul, S. I.; Voskresenskaya, N. K. (Kurnakov Inst. of General and Inorganic Chemistry, Academy of Sciences, USSR). Zh. Neorgan. Khim., 10: 1110-20(May 1965). (In Russian)

In the system CeO_2–$NaPO_3$, compounds were formed containing trivalent cerium; NaCe diphosphate, the composition of which is $Na_6Ce_2(P_2O_7)_3$ and a monophosphate $(CePO_4)_2 \cdot Na_2O$. The infrared spectra showed that at first the ion P_2O_7 was absent from the compounds and then the ion PO_4^{3-}. It is probable that Ce^{3+} enters into the complex anions. The composition, representing the monophosphate $Na_3PO_4 \cdot 2CePO_4$, disproportionates to the basic Na–Ce monophosphate and (from the index of refraction) to the diphosphate on (from the ir spectra) to compounds with the ion $P_2O_7^{4-}$. The liquidus diagrams of the system CeO_2–$NaPO_3$ have short branches of $NaPo_3$, eutectic at concentrations of 0.3 mol % (CeO_2) different from the nonstable branches CeO_2 and other eutectics from highly stable branches of Na–Ce diphosphates which extend to a very great measure to points satisfying the composition of this compound. Na–Ce diphosphate melt above 700°C forming viscous liquids. The primary Na–Ce monophosphate fuses near 600°C. Two analogous compounds were found in the system Nd_2O_3. In the system with Sm_2O_3 compounds analogous to Na–Ce diphosphate were found. (tr-auth)

38669 HEAVY LANTHANIDE FORMATES. Shklover, L. P.; Piyushchev, V. E.; Kuznetsova, G. P.; Trushina, T. A. Zh. Neorgan. Khim., 10: 1121-5(May 1965). (In Russian)

By the interaction of HCOOH and the hydroxides of Tm, Yb, and Lu, lanthanide formates with the composition $Me(HCOO)_3 \cdot 2H_2O$ were formed, where Me = Tm, Yb, and Lu. Tm formate and Lu formate were obtained for the first time. By desiccation of the dihydrides at 80 to 90°C, hydrous formates of Yb and Lu were prepared. The data of the elementary analysis confirmed the results of thermogravimetric and infrared spectral analyses. The possibility of dehydration of $Tm(HCOO)_3 \cdot 2H_2O$ under analogous conditions was established by the method of thermogravimetric analysis. The density of Yb and Lu formates and their dihydrides was determined by the pycnometric method. The solubility of the latter in water at 25, 40, and 50°C was measured by the isothermal method. The thermal stability of the formates Tm, Yb, and Lu was determined using the methods of isothermal dehydration, thermal analysis, and thermogravimetric analysis, and the decomposition scheme of their oxides was determined. (tr-auth)

38670 COMPLEXING IN THE SCANDIUM–DIANTIPYRILMETHANE–IODIDE SYSTEM. Zhivopistsev, V. P.; Kalmykova, I. S. Zh. Neorgan. Khim., 10: 1126-30(May 1965). (In Russian)

The process of the complex formation in the system Sc–diantipyrilmethane–iodide was determined at pH 2. The equilibrium displacement measure was used to establish the composition of the complex cation $(ScD_3)^{3+}$ and its instability constant was determined as 2.48×10^{-5}. The ternary system Sc–diantipyrilmethane–iodide was investigated. The composition of the compound extracted from acid media (0.5 to 2N H_2SO_4) in dichlorethane of the ternary complex $(ScD_3)I_3$ was determined by the method of physical chemical analysis. Complexes of this composition were produced by decantation of alcohol solutions of the components as well as by processing with acetone of the second organic phase, originating under the given conditions by extraction of the complex of Sc with chloroform. (tr-auth)

38671 COMPLEXING OF 2-HYDROXYETHYLIMINODIACETIC ACID WITH RARE EARTH ELEMENTS. Dyatlov, N. M.; Temkina, V. Ya.; Belugin, Yu. F.; Lavrova, O. Yu. Bertina, L. E.; Iozefovich, F. D.; Kalmykova, N. N.; Zhirov, E. P. Zh. Neorgan. Khim., 10: 1131-7(May 1965). (In Russian)

The dissociation constants of β-hydroxyethyliminodiacetic acid were determined. The successive instability constants of the rare earth complexes with β-hydroxyethyliminodiacetic acid were calculated. The efficiency of the utilization of β-hydroxyethyliminodiacetic acid as a complexing reagent was found by chromatographic partition of Dy mixtures with Y. (tr-auth)

38672 SCANDIUM OXALATE-CARBONATE COMPOUNDS. Fedorov, I. A.; Balakaeva, T. A. Zh. Neorgan. Khim., 10: 1258-9(May 1965). (In Russian)

Mixed oxalate-carbonate compounds of Sc were synthesized for the first time. It was found that the composition of the oxalate-carbonate obtained depends on the cation used and the number of carbonate bonds. The following salts were obtained in solid form: $K_6[Sc_2(C_2O_4)_3(CO_3)_4] \cdot 6H_2O$, $Na_6[Sc_2(C_2O_4)_3(CO_3)_4] \cdot 8H_2O$, $(CH_5N_3H)_2[Sc_2(C_2O_4)_3CO_3] \cdot 3H_2O$, $(CH_5N_3H)_4[Sc_2(C_2O_4)_3 \cdot (CO_3)_2] \cdot H_2O$, $(CH_5N_3H)_5[Sc(CO_3)_4] \cdot 4H_2O$. For the first two compounds the molecular electric conductivity was determined; on the basis of which an hypothesis on the complex structure of this compound was made. (tr-auth)

38673 MASS-SPECTROMETRIC STUDY OF EVAPORATION OF LANTHANUM HEXABORIDE. Torshina, V. V.; Smolina, G. N.; Dobyrin, S. Ya. Zh. Neorgan. Khim., 10: 1275-6(May 1965). (In Russian)

The sublimination energy of lanthanum hexaboride was determined as equal to 105 ± 12 kcal/g-atm. It was found that the evaporation of LaB_6 occurs in the form of La compounds with boron, the composition of which was not established, but the dissociation energy for La and B is 5.7 ev. The mass spectra of LaB_6 vapor was studied and the potentials for the appearance for La and B ions (11.3 and 14.0 ev, respectively) were determined for the ionization of the vapor by electron collision. (tr-auth)

38674 RUBIDIUM AND CESIUM. Perel'man, F. M. International Series of Monographs on Nuclear Energy. Division VIII. Materials. Volume 2. New York, The Macmillan Co., 1965. 160p. $12.00.

Translated by R. G. P. Towndrow from Rubidii i Tsezii.

The properties of cesium and rubidium are discussed. Topics covered include: the discovery and natural occurrence of cesium and rubidium; properties of cesium and rubidium and their compounds; systems formed by rubidium and cesium salts; the analytical chemistry of cesium and rubidium; the extraction of cesium and rubidium from minerals and ores; and the preparation of the metals and various compounds of cesium and rubidium. (F.J.H.)

38675 A HIGH TEMPERATURE ISOTHERMAL CALORIMETER. Lacher, J. R.; Gottlieb, H.; Fowell, P.; Park, J. D. (Univ. of Colorado, Boulder). Vienna, International Atomic Energy Agency, 1965, Preprint No. SM-66/90, 17p. (CONF-650704-31). ORINS.

From IAEA Symposium on Thermodynamics, Vienna.

A calorimeter is described, which operates isothermally. Since there are no temperature differences between the calorimeter and its surroundings, no corrections due to heat loss by radiation and conduction are to be applied. The heat supplied to the calorimeter by the chemical reaction is substituted directly by electrical heating. The calorimeter was used to measure heats of reactions involving gases. The catalyst chamber consists of a cylinder constructed of annealed tantalum, which was found to be completely resistant to corrosion at 250°C. The chamber is closed with a Teflon plug and surrounded by a tantalum heat exchanger for removing exit gases. The reacting gases are led to the catalyst chamber in tantalum tubes. The chamber is suspended from a circular plate into a quart Dewar filled with a volatile liquid. For operation at 250°C tetra-2-ethybutyl silicate (b.p. 320°/630 mm) is suitable. As a chemical reaction takes place, the heat is transferred to this liquid. Also contained in the Dewar is a sintered brass frit, through which pure hydrogen may be passed to cool the volatile liquid by evaporation. An electrical heater

is also located in this liquid. In a run, cooling hydrogen is passed through the frit at a constant rate for several days. During this time electrical heating is supplied at a constant rate just sufficient to balance the cooling (5 to 10 cal/min). The balance is read on a differential platinum thermometer extending both in the calorimeter and the surrounding air space. The gaseous reactants are then led to the catalyst chamber at controlled rates. The electrical heat input is reduced so that the total heat again balances the cooling and the calorimeter is again at the same temperature as its surroundings. The reduction of the rate of electrical heating thus corresponds to the rate of evolution of heat by the reaction. The rate of formation of products is measured. The results obtained on the hydrogenation of alkyl halides are summarized. (auth)

38676 THERMODYNAMIC PROPERTIES OF HEXAVALENT URANIUM COMPOUNDS. Cordfunke, E. H. P. (Reactor Centrum Nederland, Petten, Netherlands). Vienna, International Atomic Energy Agency, 1965, Preprint No. SM-66/7, 18p. (CONF-650704-14). ORINS.

From IAEA Symposium on Thermodynamics, Vienna.

Recent experimental work on the thermodynamic and thermal properties, including phase diagrams, of a number of hexavalent uranium compounds is described and discussed in relation to practical applications. Thermodynamic data are given on such systems as $UO_3-U_3O_8$, UO_3-H_2O, and $UO_2(NO_3)_2-H_2O$ based on calorimetric measurements as well as on vapor pressure measurements. Finally, data of some other materials, including the hydrates of uranium peroxide and UO_2Cl_2, are discussed. Although many of the thermodynamic data are consistent, a number of inconsistencies still remain to be resolved. On this basis suggestions are given for future work. (auth)

38677 SOME KEY THERMOCHEMICAL DATA FOR PLUTONIUM COMPOUNDS. Rand, M. H. (Atomic Energy Research Establishment, Harwell, Berks, Eng.). Vienna, International Atomic Energy Agency, 1965, Preprint No. SM-66/31, 13p. (CONF-650704-19). ORINS.

From IAEA Symposium on Thermodynamics, Vienna.

The key data for thermochemical calculations involving plutonium compounds are discussed. The problems involved in determining reliable standard entropies for plutonium compounds are emphasized, and it is suggested that much more use will have to be made of accurate measurements of equilibria involving the gaseous plutonium species whose standard entropies are known (namely Pu(g) and $PuF_6(g)$) to obtain entropies of condensed phases. A number of equilibria, which could be of use for this purpose, are discussed. The data for the plutonium carbides were critically assessed. (auth)

38678 MASS TRANSFER ALONG A TEMPERATURE GRADIENT. Lidiard, A. B. (Atomic Energy Research Establishment, Harwell, Berks, Eng.). Vienna, International Atomic Energy Agency, 1965, Preprint No. SM-66/30, 25p. (CONF-650704-18). ORINS.

From IAEA Symposium on Thermodynamics, Vienna.

The processes of mass transfer in solids subjected to a temperature gradient are reviewed. The phenomenological description of these processes depends on a knowledge of parameters called "heats of transport" as well as (chemical) diffusion coefficients. The description of the Soret effect and the influence of a temperature gradient on chemical diffusion are discussed in these terms. Simple kinetic arguments often led to the supposition that heats of transport are largely independent of temperature and equal to or less than the heats of activation for the relevant atomic displacement jump. Recent experimental studies on heats of transport of interstitial solutes in metals and intrinsic heats of transport in pure metals and ionic crystals, which showed that these expectations are wrong, are reviewed. Heats of transport in these systems show an unexpected temperature dependence and their magnitude may be greater than the corresponding heats of activation. (auth)

38679 VAPORIZATION IN THE LITHIUM FLUORIDE–BERYLLIUM FLUORIDE SYSTEM. Buechler, A.; Stauffer, J. L. (Arthur D. Little, Inc., Cambridge, Mass.). Vienna, International Atomic Energy Agency, 1965, Preprint No. SM-66/26, 22p. (CONF-650704-17). ORINS.

From IAEA Symposium on Thermodynamics, Vienna.

The sublimation of pure lithium fluoride was re-examined. From the temperature dependence of the Li^+, Li_2F^+, and $Li_3F_2^+$ ion intensities the following heats of sublimation at 1000°K were obtained: for $LiF(c) \rightarrow LiF(g)$, 64.8 ± 2 kcal/mole; for $2LiF(c) \rightarrow Li_2F_2(g)$, 68.3 ± 2 kcal/mole; and for $3LiF(c) \rightarrow Li_3F_3(g)$, 73.9 ± kcal/mole. For studies of the mixed system, a twin-crucible Knudsen effusion cell was designed, which permitted the comparison, in a single experiment, of the mass spectra of a solution and of one of its components. With this crucible design it was possible to obtain the activities of LiF and BeF_2 in solution, the composition of the vapor, and the heats of formation of the mixed species $LiBeF_3(g)$ and $Li_2BeF_4(g)$. The $LiF-BeF_2$ melt in equilibrium with excess solid LiF was studied in the temperature range from 748 to 987°K, corresponding to melts containing from 66 to 79% LiF. At 900°K the ions observed, in order of abundance, were BeF_2^+, BeF^+, Li^+, $LiBeF_2^+$, Li_2F^+, LiF^+, $Li_2F_2^+$, and $Li_2BeF_3^+$. Comparison of this mass spectrum with that of pure LiF(c) showed that most of the Li^+ intensity was contributed by the dissociative ionization of the mixed dimer $LiBeF_3(g)$, which is thus the major lithium-containing species in the vapor above the $LiF-BeF_2$ system. For the reaction $LiF(c) + BeF_2(g) \rightarrow LiBeF_3(g)$, $\Delta H_{900} = 4 \pm 2$ kcal/mole was obtained. Comparison of the mass spectrum of the same melt with that of pure $BeF_2(l)$ showed strong negative deviations from ideality for the activity of BeF_2 in the melt. The mass spectrum of a solution containing 67% BeF_2–33% LiF was also examined. The results obtained confirmed the identification of the Li_2BeF_4 molecule as the precursor of the $Li_2BeF_3^+$ ion. The BeF_2 activity in the 67% BeF_2 solution showed a positive deviation from ideality. (auth)

38680 THE PREPARATION AND THERMODYNAMICS OF EUROPIUM DICARBIDE. Gebelt, R. E.; Eick, H. A. (Michigan State Univ., East Lansing). Vienna, International Atomic Energy Agency, 1965, Preprint No. SM-66/58, 24p. (CONF-650704-24). ORINS.

From IAEA Symposium on Thermodynamics, Vienna.

Europium dicarbide was prepared by the reaction of europium metal and graphite in a stainless steel bomb. Chemical analysis indicated an average composition of the product of $EuC_{1.87} \pm 0.07$. X-ray powder diffraction analysis showed the compound to be of body-centered tetragonal symmetry, space group D_{4h}^{17}-I4/mmm, with lattice parameters: $a_0 = 4.045$ and $c_0 = 6.645$ Å. Vapor phase chromatographic analysis indicated that 98% of the gaseous product of acid hydrolysis of europium dicarbide is the hydrocarbon, acetylene. These analytical data, together with the lattice parameters, indicated that europium dicarbide resembles alkaline earth dicarbides more than it resembles the other lanthanon dicarbides. The vaporization of europium dicarbide over the temperature range 1130 to 1600°K was investigated by the Knudsen effusion method. The effusate was either collected and analyzed chemically or observed with a time-of-flight mass spectrometer. The data presented are based predominantly on the mass spectrometric observations since they yielded more reproducible data than the collection technique. Gaseous europium dicarbide and europium, in concentrations of 1 and 99% respectively, were found in the effusate. Instrumental limitations prevented determination of the concentration of the gaseous dicarbide as a function of temperature. Calibration of the mass spectrometer with silver permitted the calculation of the pressures corresponding to the observed ion intensities. An empirical equation, fitted to the data for europium by the method of least squares, gave: $\log P_{(atm)} = (-11163 \pm 310/T) + 4.027 \pm 0.385$. From the second law of thermodynamics for the reaction, $EuC_2 \rightleftharpoons Eu_{(g)} + 2C_{(graphite)}$, the following values were calculated: $\Delta H_{298}^0 = 51.09 \pm 1.42$ kcal/mole and $\Delta S_{298}^0 = 18.43 \pm 1.75$ e.u. Values of the free energy function for $EuC_2(s)$ were estimated and combined with published data to yield, for the same reaction from the third law of thermodynamics, the value $\Delta H_{298}^0 = 51.22 \pm 0.80$ kcal/mole. The enthalpies obtained for the dissociation reaction were combined with published

data on the enthalpy of vaporization of europium to yield the following value for the standard enthalpy of formation of EuC_2: $\Delta H_{f(298)} = -9.17 \pm 1.15$ kcal/mole. (auth)

38681 A STUDY OF CATION DIFFUSION IN STOICHIOMETRIC UO_2 USING α-RAY SPECTROMETRY. Alcock, C. B.; Hawkins, R. J.; Hills, A. W. D.; McNamara, P. (Imperial Coll. of Science and Tech., London). Vienna, International Atomic Energy Agency, 1965, Preprint No. SM-66/36, 23p. (CONF-650704-23). ORINS.

From IAEA Symposium on Thermodynamics, Vienna.

Diffusion of the uranium ion in single crystals and polycrystalline samples of uranium dioxide was studied in the temperature range from 1450 to 1700°C. The stoichiometry of the uranium dioxide was maintained with a hydrogen atmosphere. Results calculated from the decrease in surface activity agreed with those of Auskern and Belle, but comparison between the α-spectra for single crystals and polycrystals showed that grain boundary diffusion occurred. The energy spectra of the α particles emerging from the diffused sample were analyzed using an ionization chamber or a solid-state detector in conjunction with a pulse analyzer. A mathematical treatment is presented for analyzing the spectra obtained from a total free surface (or "2π" count) and a collimated count. These treatments were extended to allow for the effect of instrumental error. Results obtained from the decrease in surface activity are of the order: $D = 1.2 \exp(-108{,}000/RT)$ cm^2/sec. Results obtained from analysis of the concentration profile give: $D = 4 \times 10^{-7} \exp(-70{,}000/RT)$ cm^2/sec. The grain boundary diffusion coefficient exceeded the volume diffusion coefficient by a factor of about 10^5. (auth)

38682 THERMODYNAMIC DATA FOR PLUTONIUM OXIDES. Markin, T. L.; Rand, M. H. (Atomic Energy Research Establishment, Harwell, Berks, Eng.). Vienna, International Atomic Energy Agency, 1965, Preprint No. SM-66/32, 13p. (CONF-650704-20; AERE-R-4724). ORINS.

From IAEA Symposium on Thermodynamics, Vienna.

Thermodynamic data were obtained for plutonium oxides with O/Pu ratios between 1.53 and 2.00 at temperatures between 700 and 1140°C, using a high temperature galvanic cell, containing solid electrolytes reversible to oxygen ions only and employing two reference electrodes (Ni–NiO and Fe–wustite). A large change in $\Delta\bar{G}_{(O_2)}$ occurred between PuO_2 and $PuO_{1.9}$ and the thermodynamic data were sufficiently precise to give reliable values of $\Delta\bar{H}_{(O_2)}$ and $\Delta\bar{S}_{(O_2)}$ for all compositions between $PuO_{1.82}$ and $PuO_{1.98}$ for 700° < t < 1140°C. The plutonium–oxygen phase diagram was recently re-investigated for O/Pu ratios between 1.50 and 2.00 at temperatures between 25 and 900°C, using a high temperature x-ray powder diffraction camera. A phase diagram is suggested, which attempts to summarize the work of the several investigators. The thermodynamic data, obtained from emf cell measurements, agreed with the suggested phase diagram, of which it is entirely independent, extremely well, and an extrapolation of the thermodynamic data from 700°C to room temperature was made that is consistent with the suggested phase diagram. For the reaction $2\langle Pu_2O_3\rangle + O_2 \rightarrow 4\langle PuO_2\rangle$, an estimated value of ΔCp was taken from the value for the corresponding cerium oxide reaction. The partial molar heats and entropies were calculated for the several phase regions and $\Delta\bar{S}_{(O_2)}$ and $\Delta\bar{H}_{(O_2)}$ for the entire region from $\langle Pu_2O_3\rangle_{Hex}$ to $\langle PuO_2\rangle$, was integrated and the heats of formation and standard entropies calculated for $\langle Pu_2O_3\rangle_{Hex}$ and $\langle PuO_{1.61}\rangle$. (auth)

38683 THERMODYNAMICS OF FUSED SALTS AND FUSED SALT MIXTURES. Kleppa, O. J. (Univ. of Chicago). Vienna, International Atomic Energy Agency, 1965, Preprint No. SM-66/89, 29p. (CONF-650704-30). ORINS.

From IAEA Symposium on Thermodynamics, Vienna.

Ionic liquids available for technological applications at elevated temperatures are reviewed. To a first approximation the behavior of ionic liquids may be described in terms of simple models that incorporate features known from the chemistry of ionic solids. This forms the background for the corresponding states approach, which has had considerable success in rationalizing the thermodynamic properties both of pure ionic liquids and of mixtures formed by them. Simple fused salt mixtures may be classified according to the following scheme: mixtures of salts with similar charge structure containing a common ion, mixtures of salts with different charge structure but with a common ion, and mixtures of salts containing two different cations and two different anions (reciprocal systems). The way in which thermodynamic properties of each type of mixed system depend on the size, charge, and structure of the participating ions is discussed and in rationalizing the behavior of fused salt systems are reviewed. (auth)

38684 IMPROVEMENTS IN OR RELATING TO CARBON ARTICLES. Jenkins, Mansell John; Schofield, Philip (to United Kingdom Atomic Energy Authority). British Patent 992,085. May 12, 1965. Filed Mar. 14, 1963.

A process for reducing the porosity of carbon articles includes incorporating in the article a resin formed by heat-treating a mixture of phenol and hexamethylene tetramine and heating the article to carbonize the resin. The resin may be incorporated by impregnation of the article with liquid resin or by binding a mass of loose particles of carbonaceous material of low volatile content with liquid or solid resin and then forming the article. The carbon article is heated to 350°C at a rate not exceeding 10°C/hr to polymerize the resin and then to 1000°C at a rate not exceeding 6°C/hr to form the carbon article. If the article is to be graphitized, the temperature is raised to 1500°C at a rate of 30°C/hr and then to 3000°C at a rate of 140°C/hr. (B.L.M.)

38685 PROCESS AND APPARATUS FOR THE PREPARATION OF URANIUM AND PLUTONIUM NITRIDES. Anselin, Francois; Pascard, Roger (to Commissariat a l'Energie Atomique). British Patent 997,446. July 7, 1965. Priority date July 4, 1962, France.

A process for the preparation of U and Pu nitrides consists in carrying out the nitriding operation on the U or Pu in massive form at a temperature of 400°C after the massive form of metal has been previously subjected to a surface hydriding to facilitate the initiation and development of the nitriding operation towards the center of the metal. The hydriding of the metal is carried out by contacting the metal in massive form at 230°C with H_2 in an air-tight vessel. The vessel for both the hydriding and nitriding operations is composed of metal, closed by a detachable cover fitted with a sealing gasket, and cooled by the circulation of a cooling liquid. Means are providing for evacuating the vessel, supplying both hydrogen and nitrogen for the appropriate operation, and bringing the vessel to the temperature necessary for both operations. After nitriding the massive U, dissociation at a temperature of at least 800°C produces the mononitride. (B.L.M.)

38686 METHOD OF CARRYING OUT CHEMICAL-METALLURGICAL PROCESSES WITH USE OF THE HEAT, WHICH IS PRODUCED IN A NUCLEAR REACTOR. Maennich, Oscar. German Patent 1,194,994. June 16, 1965. Filed June 9, 1958.

Method of carrying out chemical-metallurgical processes with use of the heat, which is produced in a nuclear reactor is discussed. Nuclear heat was provided by a nuclear reactor consisting of a central critical core portion and an adjacent subcritical core portion in which the chemical-metallurgical processes took place. The normally subcritical portion of the core, which contained the reaction mass, was brought to criticality by starting the central core portion, which was operated as a power reactor, and of controlling the reaction temperature by means of neutron absorbing control rods arranged in the normally subcritical portion of the core. (Gmelin Inst.)

Organic Chemistry

38687 (EUR-2423.e) THE FLUORESCENCE OF p-HYDROXYDIPHENYL IN AQUEOUS SOLUTION. Scoppa, P.; Gerbaulet, K. (European Atomic Energy Community, Ispra (Italy). Joint Nuclear Research Center). 1965. 20p. Dep. mn.

p-Hydroxydiphenyl shows fluorescence not only in the known alkaline pH range, but also in the neutral and acidic range. The characteristics of the excitation-fluorescence spectra as well as their modification by several factors, are described. (auth)

38688 NICKEL-CATALYSED HYDROGEN EXCHANGE OF ALKYLAROMATIC HYDROCARBONS AND TOLUIC ACID DERIVATIVES WITH DEUTERIUM OXIDE. MacDonald, C. G.; Shannon, J. S. (Commonwealth Scientific and Industrial Research Organization, Chatswood, New South Wales, Australia). Australian J. Chem., 18: 1009-21(July 1965).

The selective hydrogen exchange of alkyl groups of some alkylaromatic hydrocarbons and toluic acid derivatives was achieved by allowing these compounds to react with deuterium oxide over nickel on kieselguhr at 99°. The observed deuterium distributions and the results of catalyst poisoning experiments can be interpreted in terms of initial π-bonding of the substrates to the catalyst followed by dissociative adsorption at a benzylic carbon atom and transfer of adsorption through the alkyl group by an α-β process. Some nitro- and halo-toluenes underwent little or no exchange. (auth)

38689 THE DEUTERATION OF SOME N-METHYL-4-PYRIDONES. Beak, Peter; Bonham, James (Univ. of Illinois, Urbana). J. Am. Chem. Soc., 87: 3365-71(Aug. 5, 1965).

In contrast to other α,β-unsaturated carbonyl systems N-methyl-4-pyridone, 3,5-dimethyl-N-methyl-4-pyridone, and 3,5-dibromo-N-methyl-4-pyridone substituted deuterium for protium at the β-(2 and 6)-position in basic deuterium oxide at 100°C. A mechanistic proposal, supported by kinetic data, is given for these substitutions. (auth)

38690 NITROGEN ISOTOPE EFFECTS IN THE DECOMPOSITION OF DIAZONIUM SALTS. Brown, L. L.; Drury, J. S. (Oak Ridge National Lab., Tenn.). J. Chem. Phys., 43: 1688-91(Sept. 1, 1965). (ORNL-P-929).

Nitrogen isotope effects produced on fractionally decomposing C_6H_5NNCl, $C_6H_5NNBF_4$, m-$ClC_6H_4NNBF_4$ and o-, m-, and p-$CH_3C_6H_4NNBF_4$ were measured as a function of temperature. Between 5 and 70°C the data were well represented by the least-squares equation, $\log (k^{14}/k^{15}) = 6.949/T - 0.002528$. The experimental results agreed well with those predicted from spectroscopic data. The data were consistent with the model in which decomposition occurred through the rupture of a single C–N bond. The observed isotope effect was insensitive to the nature and position of substituents on the aromatic ring and to the anion of the salt. The difference in the activation energy for the decomposition of the ^{14}N- and ^{15}N-labeled diazonium salts was 32 cal $mole^{-1}$ deg^{-1}. (auth)

38691 LIQUID SCINTILLATORS. XIII. STERIC INHIBITION OF RESONANCE IN LIQUID SCINTILLATORS. Taber, Richard L.; Daub, Guido H.; Hayes, F. Newton; Ott, Donald G. (Colorado Coll., Colorado Springs). J. Heterocycl. Chem., 2: 181-7(June 1965). (LA-DC-7179).

Biphenyl systems in which free rotation about the 1,1′-biphenyl bond is hindered by bulky groups in the 2,2′-positions showed that the covalent bond order of the 1,1′-bond will be at a maximum when the two benzene rings lie in the same plane. Accordingly, the synthesis of some 2″,3′-substituted p-quaterphenyls was carried out to study the effect of steric inhibition of resonance across the 1″,4′-p-quaterphenyl bond on the scintillation properties of the molecule. 2″,3′-Dimethyl-p-quaterphenyl(I) was prepared via the Ullmann coupling of 4-iodo-3-methylbiphenyl, available in four steps from o-acetotoluidide, which was converted to N-chloro-o-acetotoluidide. The chloramide was allowed to react with benzene in the presence of anhydrous $AlCl_3$ to give 4-acetamido-3-methylbiphenyl, which, on hydrolysis with 20% HCl, gave 4-amino-3-methylbiphenyl hydrochloride, the diazonium salt of which was allowed to react with potassium iodide to give the starting iodo compound. The preparation of 2″,3′,5′,6″-tetramethyl-p-quaterphenyl(II) was accomplished by a similar route. The compounds 6,7-diphydro-6-methyl-3,9-diphenyl-5H-dibenzo[c,e]azepine(III), 5,7-dihydro-3,9-diphenyldibenzo[c,e]thiepin(IV), 5,7-dihydro-3,9-diphenyldibenzo[c,e]selenepin(V), and 6,6-dicarbethoxy-6,7-dihydro-3,9-diphenyl-5H-dibenzo[a,c]cycloheptene(VI) were prepared. All six compounds were screened as potential primary liquid scintillation solutes, and compared with 2,7-diphenylfluorene(VII), 9,10-dihydro-2,7-diphenylphenanthrene(VIII), and 5,7-dihydro-3,9-diphenyldibenz-[c,e]oxepin(IX). The relative pulse heights of I, VI, VII, VIII, and IX at 3mM in toluene gave a linear relation when plotted against the $\cos^2$ of the respective estimated angles of torsion about the 1″,4′-bound in the p-quaterphenyl system. The azepine III, thiepin IV, senenepin V, and tetramethyl-p-quaterphenyl II were very poor scintillators in toluene solution. These results may be explained in terms of scintillation quenching due to the presence of the respective hetero atom. This hypothesis was substantiated with the azepine by an experiment in which a good scintillator, I, had a relative pulse height of less than 0.1. (BBB)

38692 KINETIC HYDROGEN ISOTOPE EFFECTS IN THE IONIZATION OF SOME KETONIC SUBSTANCES. Bell, R. P.; Crooks, J. E. (Physical Chemistry Lab., Oxford). Proc. Roy. Soc. (London), Ser. A, 286: 285-99 (July 20, 1965).

The kinetic hydrogen isotope effect was measured for the water-catalyzed bromination of acetylacetone, monobromoacetylacetone, ethyl acetoacetate, ethyl α-bromoacetoacetate, ethyl α-methylacetoacetate, ethyl malonate, ethyl monobromomalonate, and methyl methylmalonate and for the bromination of ethyl α-methylacetoacetate catalyzed by six basic anions. All these reactions were of zero order with respect to bromine, so that the process studied was the rate of transfer of a proton or deuteron from the organic molecule to the catalyst. For ethyl α-methylacetoacetate there was correlation between the basic strength of the catalyst, the rate of proton transfer, and the magnitude of the isotope effect. Various possible explanations were considered for the variation in isotope effect, and it was concluded that current interpretations in terms of a three-center model of the transition state are inadequate. The isotope effect also varies considerably with the nature of the organic molecule, but is not in general related to its reactivity. There is, however, a correlation between the magnitude of the isotope effect and the exponent β of the Brönsted relation between basic strength and catalytic power, suggesting that both quantities depend on the position of the proton in the transition state. (auth)

38693 CATALYTIC ISOTOPIC ISOMERIZATION OF DEUTERATED TOLUENE-d_1 ON PLATINUM BLACK. Hirota, Kozo; Ueda, Tomiko (Inst. of Physical and Chemical Research, Tokyo). Tetrahedron Letters, No. 28, 2351-6(July 1965).

Toluene-d_1, deuterated at a ring hydrogen, changes into its isotopically isomeric species if platinum or nickel is used as the catalyst. Results on platinum catalysis, as well as results on the exchange reaction (II) of toluene-d_1 with H_2O, which are compared with those of the reaction (I), are reported. Ortho- and meta-deuterated toluenes were prepared respectively from corresponding tolylmagnesium bromide by the reaction with deuterium oxide. From analysis on the product in the reaction (II), it was found that deuterium atoms were transferred from the meta position to the other ring positions and also to the methyl position; also that concentration of d_1 decreased markedly, as expected, by the dilution effect of water. Nevertheless, in spite of the decrease of mean deuterium content, concentration of d_2 and d_3 species increased, though slightly, in the products. However, the result of the reaction (I) included several important differences from that of reaction (II): total deuterium content did not change practically, even though d_0 and d_2 species were produced markedly, and also d_3 species to some extent; all the runs showed that reactivity of hydrogen at the methyl and ortho position was negligibly small, compared to that of the other positions. Thus, reaction (I) seemed to be a kind of isotopic isomerization superposed by self-exchange reaction. The peculiar

activity of ortho position suggested that scission of C–H (or C–D) bond at this position is more difficult than at the other positions, considering that this tendency could not be observed in reaction (II). Toluene molecules probably are not adsorbed with the benzene ring parallel to the platinum surface. Due to steric hindrance of the methyl group, adsorption will not occur at the ortho position to the surface. It is possible that bond scission of ring hydrogen does not occur in reaction (II) due to the poisoning effect of water. However, exchange of methyl hydrogen is explained by its scission of C–H bond, followed by indirect addition of deuterium via water, for energetic reasons. (BBB)

Radiation Chemistry

See also BIOLOGY AND MEDICINE — Radiation Effects.

Refer also to abstract 39091.

38694 (BNL–9200) THE ROLE OF OXYGEN IN SOLID STATE POLYMERIZATION. I. ACRYLAMIDE AND ITS SOLID SOLUTIONS. Adler, George (Brookhaven National Lab., Upton, N. Y.). [May 18, 1965]. Contract AT(30-2)-Gen-16. 25p. Dep. mn; CFSTI, $1.00 cy, $0.50 mn.

It is shown that the presence of oxygen has little effect on the ESR spectrum of acrylamide. On the other hand, the spectrum of propionamide is markedly changed and shows sharply increased decay rates with oxygen. The behavior of solid solutions of the two is intermediate and depends on the relative concentrations of the two materials. The polymerization is markedly decreased in the solid solutions when oxygen is present. The polymerization data are thus consistent with those derived from the ESR spectra. These effects are interpreted in terms of the crystal structure of the materials and the polymerization mechanism. (auth)

38695 (KFK-317) DURCH GAMMA-STRAHLUNG INDUZIERTE REAKTIONEN DES TETRACHLORKOHLENSTOFFS, CHLOROFORMS UND METHYLENCHLORIDS MIT CYCLOALKENEN. STRAHLENCHEMISCHE SYNTHESE ^{14}C-MARKIERTER TRICHLORMETHYLCYCLOALKANE. (Gamma-Ray-Induced Reactions of Carbon Tetrachloride, Chloroform, and Methylene Chloride with Cycloalkenes. Radiochemical Synthesis of ^{14}C-Labeled Trichloromethylcycloalkane). Schwarz, Alexander (Kernforschungszentrum, Karlsruhe (West Germany). Institut fur Radiochemie). Feb. 1965. 82p. Dep.(mn).

The reactions between cyclohexenes or cyclopentenes and carbon tetrachloride, chloroform, and methylene chloride under the effect of gamma radiation were investigated. The cycloalkene derivatives formed were identified, their yield was determined in dependence on the dose and composition of the mixture, and the results obtained were compared with those found by other authors in the decomposition of cycloalkenes with halogen hydrocarbons in the presence of peroxides. The possibility of the radiochemical labeling of trichloromethylcycloalkane by decomposition of ^{14}C-labeled carbon tetrachloride with cyclohexane or cyclopentene was investigated. In cyclohexane–carbon tetrachloride mixtures the principle product was trichloromethylcycloalkane, but in cyclopentene–carbon tetrachloride solutions two new substances, trichloromethylcyclopentane and 1-chloro-2-trichloromethylcyclopentane, were formed in large amounts. Compounds labeled in the methyl group were prepared for the first time by the use of ^{14}C-labeled carbon tetrachloride. The labeled compounds formed were trichloromethylcyclohexene and -cyclopentane and 1-chloro-2-trichloromethylcyclopentane. The radiolysis of cyclohexene–chloroform and cyclopentene–chloroform mixtures offered a new way for the preparation for the preparation of dichloromethylcyclohexenes and cyclopentanes which could not be prepared by other methods. In the radiolysis of cyclohexene–methylene chloride and cyclopentene–methylene chloride mixtures, the formation of chloromethylcyclohexene or -cyclopentene were established. Both compounds were formed however in very small quantities. The most important radiolysis products found in the systems investigated were identified and their G values were measured in dependence on the length of irradiation and the composition of the mixture. (tr-auth)

38696 (MIT–2909-4) EFFECTS OF GAMMA-IRRADIATION AND ADDITIVES ON THE GROWTH OF POTASSIUM CHLORIDE CRYSTALS FROM AQUEOUS SOLUTIONS. Final Report. Botsaris, Gregory D.; Mason, Edward A.; Reid, Robert C. (Massachusetts Inst. of Tech., Cambridge. Dept. of Chemical Engineering and Massachusetts Inst. of Tech., Cambridge. Dept. of Nuclear Engineering). Apr. 1965. Contract AT(30-1)-2909. 477p. Dep. mn; CFSTI, $7.77 cy, $2.00 mn.

Theories and previous experiments on crystal growth and impurity incorporation are reviewed. Single KCl seed crystals were grown from aqueous solutions under conditions of constant temperature, supersaturation, and impurity concentration, and growth rates normal to the (100) faces were calculated. The incorporation of Pb^{2+} and other ionic impurities in growing KCl crystals was also studied. The experiments were run in the absence and presence of a gamma-ray field. The results show that at certain lead concentrations, irradiation decreased the growth rate and dislocation density in the crystals. The distribution coefficients of impurities between crystal and solution were found to be greater than unity at very low concentrations. Mechanisms of diffusion in the crystal are discussed. (D.L.C.)

38697 (ZFK-RN-17(p.139-64)) K VOPROSU O RADIATSIONNOI USTOICHIVOSTI NEKOTORYKH IONOOBMENNYKH SMOL. (On the Radiation Stability of Certain Ion-Exchange Resins). Alekseev, B. A.; Novikov, P. D. (Institut Atomnoi Energii, Gosudarstvennyi Komitet po Ispol'zovaniyu Atomnoi Energii SSSR, Moscow).

A review of previous work on the radiation stability of ion-exchange resins is presented. The preparation of samples of anion resins for irradiation, the conditions of irradiation in the IRT reactor, and results of measurements of the stability of the anionites EDE-10P, AM, and AV-17 are described. Detailed results of the performance of the nonirradiated resins and the resins irradiated to various integral doses are presented. (M.J.T.)

38698 (ZFK-RN-17(p.199-207)) NEKOTORYE ZAMECHANIYA O RAZLOZHENII VODY V REAKTORE. (Some Remarks on Decomposition of Water in a Reactor). Bebemel, I.; Kiotan, I.; Purika, I. (Institutul de Fizica Atomica, Academia R.P.R., Bucharest).

Results are summarized on studies of water decomposition in a reactor. The rate of decomposition was measured for various reactor power levels, and, thus, for various flux levels of gamma radiation and fast neutrons. The volume of product gases as a function of time and power is given. A method of differentiating between the effects of neutrons and of gamma radiation is presented. The various chemical reactions and their mechanisms occurring in the decomposition of water are discussed in detail, and the roles of various impurity ions — Cu^{2+}, Fe^{2+}, NO_3^-, and SO_4^{2-} — are considered. (M.J.T.)

38699 INVESTIGATIONS IN THE FIELD OF RADIATION-INDUCED SOLID STATE POLYMERIZATION. I. CETYL METHACRYLATE. Hardy, Gy.; Nyitray, K.; Kovacs, G.; Fedorova, N. (Research Inst. for the Plastics Industry, Budapest). Acta Chim. Acad. Sci. Hung., 43: 121-8(1965).

Kinetics of solid state polymerization of cetyl methacrylate were examined from 60 to −195°C. In the liquid phase (60,40, and 20°C) the usual linear relation was obtained with an overall activation energy of 2.5 kcal/mole. The measured values of polymerization rates were proportional to the square roots of the dose rates. Near the melting point (10°C) the curves of polymerization rate vs temperature showed a sudden rise reaching a value higher than that observed at 60°C. The activation energies also changed rapidly in this section. The polymerization rate was proportional to the 1.2th power of the dose rate. In the solid state, farther from the mp (at −21, −78, and −195°) the

polymerization rate increased linearly as the temperature was decreased. The overall activation energy of the process was −0.7 kcal/mole; the polymerization rate is proportional to the dose rate. In the liquid state, the degree of polymerization decreased with temperature. This meant that the rate of propagation decreased with the temperature more rapidly than the rate of chain termination. Near the mp the degree of polymerization rose suddenly. This meant that the rate of propagation increased as the result of an increase of the main free paths of the closely packed vinyl groups, prearranged in a favorable way in the crystal lattice. In the solid state, the degree of polymerization was practically independent of the temperature and of the dose rate. This suggested that the chain length was mainly determined by the properties of the crystal structure; chains could propagate until they reached a defect, or a microcrystalline border surface. The mechanism of the solid state polymerization was probably anionic, although radical inhibitors were found to be very effective. Measurements of the thermal effect showed that the process was true solid-state polymerization. (BBB)

38700 NEUTRON-INDUCED REACTIONS IN AROMATIC PHOSPHORUS COMPOUNDS. Wheeler, O. H.; Facetti, J. F.; Santos-Sanchez, M. (Puerto Rico Nuclear Center, Mayaguez). Acta Cient. Venezolana, 15: 248 (Nov. 1964–Jan. 1965).

The chemical nature of the ^{32}P formed in the reaction of triphenyl phosphine, triphenyl phosphine oxide, and tetraphenyl phosphonium chloride with thermal neutrons was investigated. The irradiated products were separated into fractions of inorganic phosphorus. Only small amounts of inorganic phosphorus were formed from triphenyl phosphine and its oxide. The water-soluble ^{32}P fractions were analyzed by precipitation techniques, and the neutral fraction by vapor-phase chromatography. (BBB)

38701 ULTRAVIOLET LIGHT-INDUCED CHANGE IN COLLAGEN MACROMOLECULES. Fujimori, Eiji (Tokyo Univ.) Biopolymers, 3: 115-19(1965).

Irradiation of a collagen solution with uv light of 2537 Å increased its viscosity. A solution of 0.184% rat tail tendon collagen in 0.05% acetic acid in a shallow dish was exposed to a 15-w germicidal lamp at a distance of 5 cm, the solution being maintained at 4°C during irradiation. Aliquots were removed periodically for measurements with a capillary viscometer at 20°C. An intrinsic viscosity of 5.1×10^3 ml/g, was obtained for collagen irradiated for 15 min, for which an axial ratio of about 400 was calculated. Comparison of this value to that of native collagen (180 to 200) indicates that the collagen underwent photopolymerization when irradiated with uv light. Since the rotary diffusion constant of a molecule is particularly sensitive to a change in molecular length, the method of flow birefringence was also applied. The results showed a greater variation in rotary diffusion constants with different flow gradients in irradiated collagen than in native collagen than in native collagen. This variation is a sensitive test for polydispersity. The presence of larger molecules was indicated by the lower values obtained for the rotary diffusion constants at the low flow gradients. At high gradients, the rotary diffusion constants were close to the value for the monomer. These results indicated that irradiation of native collagen for 15 min produced molecules as large as dimers. Also demonstrated was the inhibition of formation of native-type fibers (obtained by the addition of 0.1M citrate buffer to an 0.18% collagen solution in 0.06% acetic acid) by turbidity measurements made with a nephelometer after the solutions were allowed to stand at 20°C, for a few hours. Thus, ten-min irradiation inhibited fibril formation. This inhibition occurred before the molecular length of the collagen molecule was appreciably altered. The major rigid portion of the molecule seemed to remain unchanged to a certain extent, since the optical rotatory properties showed very little change after irradiation, and the irradiated collagen was still capable of forming a segment-long-spacing (SLS) type of ordered aggregates upon the addition of ATP. This indicates that a part of the peptide extending from the triple-helix body is modified by uv light. Longer irradiation led to new cross-linkages. Peptides rich in tyrosine and possibly phenylalanine are capable of undergoing photochemical change. The initial formation of free radicals could be responsible for the aggregation of the protein molecules. Transient species corresponding to the hydrated electron and benzyl or phenoxyl radicals have been found as primary photochemical products of aromatic amino acids. Thus, photoejection of an electron producing free radicals and hydrated electrons may be a primary reaction in irradiated proteins containing aromatic amino acids. Permanent photochemical changes would follow in the subsequent steps. (BBB)

38702 RADIOFORMATION OF ASPARTIC ACID IN AQUEOUS SOLUTIONS OF ALANINE. Mehran, A.-R.; Pageau, R. (University Laval, Quebec). Can. J. Biochem., 43: 1359-66(Aug. 1965).

Aspartic acid was found to be present in 0.1 M aqueous solutions of alanine irradiated with gamma rays from cobalt-60 under three different experimental conditions: in the presence of air; in a nitrogen atmosphere; and in the presence of nitrogen plus CO_2. Although the presence of oxygen and CO_2 in the solutions was necessary for the formation of appreciable quantities of aspartic acid, small quantities of it may be formed in their absence. Addition of CO_2 to the nitrogen atmosphere favored formation of aspartic acid at the lowest levels of irradiation, but the amount decreased rapidly with higher levels. Degradation of alanine was less in the presence of oxygen than under the other two experimental conditions. Addition of CO_2 to the nitrogen atmosphere had no effect on the degradation of alanine. Two possible mechanisms to explain the radiochemical degradation of alanine with formation of aspartic acid are proposed. (auth)

38703 THE ACTION OF SECONDARY ELECTRONS IN SYSTEMS OF RADIATION CHEMISTRY. Man-wei Chang. Hua Hseuh Tung Pao, No. 3, 26-35(Mar. 14, 1965). (In Chinese)

The production and energy distribution of the secondary, tertiary, and multistage electrons, the so-called δ electrons, are reviewed. The quasi-theoretical equation for the energy of the thermal electrons was analyzed on the basis of Platzman's and Elkmoss and Magee's findings. In order to develop a proper framework for the understanding of radiation-chemistry systems, a brief historical sketch of the subject is followed by a more detailed review of the following topics: secondary electrons and reionization and excitation effects; selective absorption of secondary electrons; and the ultimate fate of under-excited electrons. It was concluded that the current thinking concerning secondary electrons seemed to indicate that the electrons escaping from the influence of the mother ion become solvated, as proposed by Platzman, in preference to the assumption that the secondary electrons are recaptured by another ion within a very short period of time. (TTT)

38704 RECOIL TRITIUM REACTIONS WITH ETHYL CHLORIDE. Tang, Yi-Noo; Rowland, F. S. (Univ. of Kansas, Lawrence and Univ. of California, Irvine). J. Am. Chem. Soc., 87: 3304-11(Aug. 5, 1965).

The substitution of energetic tritium atoms for H atoms in ethyl chloride led to excited $C_2H_4TCl^*$ molecules, which exhibited pressure and phase dependence of yields, consistent with unimolecular decomposition of the primary product. The most important unimolecular reaction for $C_2H_4TCl^*$ was the elimination of HCl with the formation of C_2H_3T, while 15 ± 5% of the decomposing molecules reacted by C−Cl bond break. The substitutions of energetic tritium atoms for Cl to form $C_2H_5T^*$, for CH_3 to form CH_2TCl^*, and for CH_2Cl to form CH_3T^* were observed, and each of these products also underwent unimolecular decomposition reactions. The primary yields of hot tritium reactions with ethyl chloride were estimated in the ratios: HT, 100; C_2H_4TCl, 56; C_2H_5T, 10; CH_3T, 7; CH_2TCl, 3. The replacement of Cl in ethyl chloride was 0.7 times as likely as the replacement of Cl in methyl chloride, confirming that C−T bond formation was more difficult with C_2H_5 than with CH_3. (auth)

38705 HYSTERESIS STUDIES OF REACTOR-IRRADIATED SINGLE-CRYSTAL BARIUM TITANATE. Glower, D. D.; Hester, D. L. (Sandia Lab., Albuquerque, N. Mex.). J. Appl Phys., 36: 2175-80(July 1965).

Nuclear reactor irradiation of single-crystal $BaTiO_3$ causes an increase in the coercive field (E_c) and a decrease in the remanent polarization (P_r). The magnitude of these changes, for a particular level of irradiation, depends upon the polarization state of the crystal during irradiation; crystals in the polarized state during irradiation are more resistant to radiation damage than are virgin crystals. The radiation damage rate is only slightly dependent upon crystal thickness. The magnitude of the change in P_r depends significantly, for irradiation levels below 10^{18} nvt (E > 0.1 Mev) fast neutron flux and the associated 10^{19} rad (H_2O) gamma dose, upon the particular loop for which data are reported; the first loop after irradiation indicates a damage accumulation but this damage is annealed by an external field in approximately 70 consecutive loops. The coercive field is relatively insensitive to irradiation until the total accumulated exposure mentioned above, but E_c increases in an asymptotic manner at levels which are about a factor of two or three greater. The changes in E_c and P_r are interpreted in terms of a radiation damage model involving a buildup of a space charge (with associated strain) due to the trapping of ionized carriers in the domain walls of the crystals. (auth)

38706 ESR STUDY OF FREE-RADICAL PRODUCTION IN THE IRRADIATION OF ADDITIVE-CONTAINING POLYMETHYLMETHACRYLATE. Atwater, H. A. (Pennsylvania State Univ., University Park). J. Appl. Phys., 36: 2220-4(July 1965).

The free-radical density produced in polymethylmethacrylate under x and γ irradiation was measured as a function of the amount and kind of organic additive substances present in the polymer. The ratio of radical density produced in the pure polymer by a given radiation dose to that produced in polymers containing additives exhibits a strong dependence upon radiation dose, unlike the similarly defined ratio for the protection against radiation damage by polymer chain scission. The time rate of decay of free-radical density was also found to depend upon the additives present. The existence of a radiation-dependent free-radical annihilation process is postulated. (auth)

38707 RADIOLYSIS OF BINARY PARAFFIN–OLEFIN SOLUTIONS. II. EFFECTS OF DEUTERIUM ISOTOPIC SUBSTITUTIONS. Yang, John Y.; Marcus, Inge (North American Aviation Science Center, Thousand Oaks, Calif.). J. Chem. Phys., 43: 1585-90(Sept. 1, 1965).

The effects of deuterium isotopic substitutions on product distributions in the radiolysis of paraffin-olefin solutions were studied. The total hydrogen yield was apparently not affected by deuterium substitution in the olefin. However, the isotopic compositions of hydrogen from mixtures containing deuterated components were typically those expected by hydrogen abstraction involving large isotope effects. Product distributions of dimers from irradiations of cyclohexane-cyclohexene, cyclohexane-cyclohexene-d_{10}, cyclohexane-d_{12}-cyclohexene, cyclohexane-d_{12}-cyclohexene-d_{10}, cyclopentane-cyclohexene, and cyclopentane-cyclohexene-d_{10} solutions were found to be highly affected by deuterium substitutions in the olefin but scarcely changed by similar substitutions in the paraffin. Such observations were rationalized by the proposal that physical interactions may take place by positive charge transfer from saturated hydrocarbon ions to the olefin, but that the resulting dimer product distributions were governed primarily by subsequent radical scavenging and abstraction reactions. Differences in dimer product yields observed in the various deuterated-vs-nondeuterated mixtures were explained by changes in the relative importance of two different reaction sequences each initiated by the olefin positive ion. (auth)

38708 THE RADIATION-INDUCED ADDITION REACTION OF ALCOHOLS TO 1,2-DICHLOROTETRAFLUOROCYCLOBUTENE AND 1,2-DICHLOROHEXAFLUOROCYCLOPENTENE. Muramatsu, Hiroshige; Inukai, Kan; Ueda, Teruo (Government Industrial Research Inst., Nagoya, Japan). J. Org. Chem., 30: 2546-9(Aug. 1965).

Alcohols containing polyfluorocycloalkyl or polyfluorocycloalkenyl groups were synthesized by the addition reaction of alcohols, such as methanol, ethanol, and 1- and 2-propanol, to 1,2-dichlorotetrafluorocyclobutene and 1,2-dichlorohexafluorocyclopentene under γ irradiation. While only the polyfluorocyclopentenylcarbinols were obtained in the addition to the halocyclopentene, the addition of alcohols to the halocyclobutene gave both the 1:1 adduct and the dehydrochlorinated 1:1 adduct, whose molar ratio varied markedly with the structure of the alcohols. (auth)

38709 RADIATION CHEMISTRY OF SOME CYCLIC FLUOROCARBONS. MacKenzie, D. R.; Bloch, F. W.; Wiswall, R. H. Jr. (Brookhaven National Lab., Upton, N. Y.). J. Phys. Chem., 69: 2526-30(Aug. 1965). (BNL-8659).

Radiolysis experiments were carried out on a series of highly purified cyclic fluorocarbons-hexafluorobenzene, perfluorobiphenyl, and perfluoronaphthalene, and their saturated analogs perfluorocyclohexane, perfluorobicyclohexyl, and perfluorodecalin (perfluorodecahydronaphthalene). Irradiations were done in nickel cells using a 1.5-Mev Van de Graff electron beam. Temperatures were chosen so that materials were irradiated in the liquid phase and were room temperature where possible, otherwise around 100°C. Radiation doses were of the order of 10^9 rads. Radiation stability of the aromatic compounds was less than that of the corresponding hydrocarbons, whereas the alicyclic fluorocarbons were more stable than their hydrocarbon analogs. Total G values for destruction of starting material ranged from 1.3 to 2.4 and were very similar for aromatic and alicyclic compounds. The aromatic fluorocarbons under irradiation yielded polymeric material almost exclusively. Only traces of gaseous and low molecular weight compounds were formed. Polymeric material was colored yellow to dark brown depending on the dose. Radiolysis of the alicyclic fluorocarbons caused appreciable breakdown into gases and products of lower molecular weight than the starting material, as well as polymer formation. Polymeric material was colorless. No free fluorine was detected in any of the irradiations. (auth)

38710 RADIOLYSIS OF HEAVY WATER IN THE pD RANGE 0–14. Hayon, E. (C.E.N., Saclay, France). J. Phys. Chem., 69: 2628-32(Aug. 1965).

Radical and molecular yields from various systems irradiated with ^{60}Co γ rays in heavy water in the pD range 0–14 were determined and compared with data obtained in light water. Radical yields were found to increase in acid and alkaline solutions as compared to neutral solutions. This was interpreted as due to scavenging in the spurs of the radicals $(D_2O)^-$ and OD by D^+ and OD^- ions, respectively. This is similar to the conclusions reached regarding H_2O. At all pH values, the values of G_{D_2}, and $G_{D_2O_2}$ were lower in D_2O than those of G_{H_2} and $G_{H_2O_2}$ in H_2O, while the yields of G_{Red} and G_{OD} were only slightly lower in D_2O than the corresponding yields in H_2O. (auth)

38711 THE RADIATION-INDUCED CIS-TRANS ISOMERIZATION OF POLYBUTADIENE. IV. Golub, Morton A. (Stanford Research Inst., Menlo Park, Calif.). J. Phys. Chem., 69: 2639-45(Aug. 1965).

Polybutadiene in the solid state undergoes a marked radioinduced loss of unsaturation in addition to the previously investigated cis-trans isomerization. The latter reaction was reinvestigated, and the former reaction studied for the first time, with the help of cis-polybutadiene-2,3-d_2 which provided unambiguous spectroscopic evidence for these reactions. Use of the deuterated polymer also revealed that double-bond migration and formation of conjugated triene structures occur to a negligible extent in irradiated polybutadiene. G values for the loss of double bonds in films irradiated with electrons under nitrogen or with γ rays in vacuo are 13.6 and 7.9, respectively, while the initial G values for cis-trans isomerization, using either radiation, was redetermined as 7.2. The decrease in unsaturation is attributed to a chain cyclization, but the

relative contributions of free radicals and carbonium ions to this process have not yet been established. Other radioinduced processes in polybutadiene are cross linking and evolution of hydrogen (G values of about 0.9 and 0.45, respectively). (auth)

38712 THE RADIATION CHEMISTRY OF CYCLOPENTANE. Hughes, B. Mason; Hanrahan, Robert J. (Univ. of Florida, Gainesville). J. Phys. Chem., 69: 2707-14(Aug. 1965).

The products of the radiolysis of pure liquid cyclopentane were found to be hydrogen, methane, ethane, propylene, propane, cyclopropane, C_4's, n-pentene, n-pentane, cyclopentene, and bicyclopentyl. The G value of the major products are: hydrogen, 5.20; ethylene, 0.40; n-pentene, 0.62; cyclopentene, 3.10; bicyclopentyl, 1.22. The total G value for radical production was determined to be 6.40 using HI as a scavenger. Hydrogen production was shown to be temperature dependent when scavengers were present at concentrations between 1 and 10 mM. The reaction scheme is similar to that of cyclohexane except for the occurrence of greater C–C bond rupture and ring cleavage. The latter effects can be attributed to strain in the C_5 ring. (auth)

38713 EFFECTS OF EXPERIMENTAL PARAMETERS ON (n,γ)-ACTIVATED REACTIONS OF BROMINE WITH LIQUID CYCLOHEXANE. Merrigan, Joseph A.; Rack, Edward P. (Univ. of Nebraska, Lincoln). J. Phys. Chem., 69: 2795-9(Aug. 1965).

Studies were made on the effects of various experimental parameters on the reactions of ^{80m}Br and ^{82}Br, activated by the (n,γ) reaction, with liquid cyclohexane. The determinations of bromine organic retentions (percent of radiobromine stabilized in organic combination) were found to be complicated by postactivation thermal reactions which occurred readily during and after thermal neutron irradiations. However, a general increase in both organic retentions with length of irradiation was found. Reasons for this are discussed. (P.C.H.)

38714 THE RADIOLYSIS OF MONODISPERSE COLLOIDAL SULFUR. Johnston, F. J. (Univ. of Georgia, Athens). J. Phys. Chem., 69: 2805-6(Aug. 1965).

Colloidal sulfur systems were irradiated in a ^{60}Co source at dose rates that varied from 2.90 to 2.75×10^{19} ev/ml hr. The observed particle size-dose relations indicated that a complex mechanism is involved and that there is an increasing reactivity of the colloidal material with a decrease in particle size. (P.C.H.)

38715 EVIDENCE FOR BROMINE-82m ISOMERIC TRANSITION ACTIVATED REACTIONS IN SATURATED HYDROCARBONS AND ALKYL HALIDES. Merrigan, Joseph Andrew; Rack, Edward Paul (Univ. of Nebraska, Lincoln). J. Phys. Chem., 69: 2806-7(Aug. 1965).

Organic retentions of ^{80m}Br and ^{82}Br in solid saturated hydrocarbons and alkyl halides produced in 3-sec thermal neutron irradiations at –196°C were studied. Unusual and totally unexpected results were that neither ^{80m}Br nor ^{82}Br organic retentions were over 1% in saturated C_6 hydrocarbons and CCl_4 when the samples were kept frozen and extracted directly from the frozen state into organic and inorganic phases. When the samples were melted and maintained at 25°C for 10 min immediately following irradiation, ^{82}Br organic retentions increased markedly while those of ^{80m}Br remained below 1%. Since the changes in ^{82}Br organic retentions only occurred when samples were liquefied immediately after irradiation, it was concluded that the ^{82m}Br (isomeric transition) ^{82}Br reaction produced ^{82}Br retention changes. (P.C.H.)

38716 γ-RADIOLYSIS OF METHANOL. Ladygin, B. Ya.; Saraeva, V. V. Kinetika i Kataliz, 6: 221-8(Mar.-Apr. 1965). (In Russian).

In the radiolysis of methanol by ^{60}Co γ radiation, the yields of hydrogen and methane and the sum of the yields of ethylene glycol and formaldehyde increased with increasing temperature. The activation energy observed for the process was 0.65 kcal/mol. The yields of dimethyl ether and formaldehyde decreased with increasing temperature. The introduction of some compounds during the exposure of methanol significantly increased the yield of the formaldehyde. The results obtained were interpreted on the basis of the introduction of diffusion processes. (tr-auth)

38717 KINETICS OF HYDROGEN ADSORPTION OF Al_2O_3 DURING γ IRRADIATION. Kolbanovskii, Yu. A.; Pepelyaev, Yu. V. (Topichiev Inst. of Petroleum-Technological-Chemical Synthesis, Academy of Sciences, USSR). Kinetika i Kataliz, 6: 237-43(Mar.–Apr. 1965). (In Russian)

The kinetics of the radioinduced chemisorption of hydrogen on γ-Al_2O_3 was investigated; equations satisfactorily describing the process were derived. The number of active centers of the surface was determined with respect to the chemisorption. Hypotheses on the mechanism of the process at T ~ 300°K are expressed. (tr-auth)

38718 COMBINED RADIOCHROMATOGRAPHY TECHNIQUE USED IN INVESTIGATIONS ON THE MECHANISM OF HETEROGENEOUS CATALYTIC REACTIONS. Semenenko, E. I.; Roginskii, S. Z.; Yanovskii, M. I. (Inst. of Chemical Physics, Academy of Sciences, USSR). Kinetika i Kataliz, 6: 320-8(Mar.–Apr. 1965). (In Russian)

A combined radiochromatographical method for the chromatographic investigation of the mechanism of heterogeneous catalytic reactions is described. The realization of the microcatalytic synthesis of labeled and nonlabeled compounds (of the order of mg) and the possibility of their introduction into catalytic reagents is described. The advantages of the method seemed to be its speed, low consumption of catalyst and primary materials, and the ease of production of a large number of compounds, the synthesis of which under usual conditions offer great difficulties. The possibilities of the new method are illustrated by examples of the investigation of the reaction mechanism of dehydrogenation and isomerization of butylene and divinyl. (tr-auth)

38719 ON THE KINETICS OF DESTRUCTION OF FREE RADICALS BY IONIZING RADIATION. Tikhomirov, L. A.; Buben, N. Ya. (Inst. of Chemical Physics, Academy of Sciences, USSR). Kinetika i Kataliz, 6: 329-31(Mar.–Apr. 1965). (In Russian)

The kinetics of the decrease of paramagnetics particles by irradiation of stable radicals (2,2,6,6-tetramethylpiperidine nitrogen oxide) with fast electrons was investigated by the electron spin resonance method. It was established that the destruction of the radicals originates through first order reactions at a constant velocity k proportional to the size of the dose. At temperature intervals from 100 to 300°K an increase in k with the activation energy of 0.4 kcal/mol. was observed. (tr-auth)

38720 NITROUS OXIDE AS A SCAVENGER IN THE RADIOLYSIS OF WATER. Head, D.; Walker, D. C. (Univ. of British Columbia, Vancouver). Nature, 207: 517-18(July 31, 1965).

Nitrous oxide is widely used as a specific scavenger for the solvated electron in the radiolysis of liquid water. Variations in rate constants of the reactions involved were studied for various concentrations of N_2O in pure water at natural pH irradiated with ^{60}Co γ radiation. Reaction mechanisms are discussed. (C.H.)

38721 α-DEHYDRO DIMER—A MAJOR PRODUCT IN IRRADIATED METHYL LAURATE. Macfarlane, J. J. (C.S.I.R.O., Ryde, New South Wales); Sweeting, J. W. Nature, 207: 520-1(July 31, 1965).

The wholesomeness of some foods after radiation processing has been found to be affected by radiation effects on lipid components. Results are reported from a study of the effects of 40 Mrads of γ radiation on methyl laurate. Analysis of the residue by gas chromatography showed that the major component was the α-dehydro dimer, n-docosane-11, 12-dimethyl carboxylate (DDMC), $CH_3(CH_2)_9$-$CH(COOMe)CH(COOMe)(CH_2)_9(CH_3)$. (C.H.)

38722 FIXATION OF CARBON-11 IN THE CELLS OF PROTON-IRRADIATED BLOOD. Larsson, Boerje; Graffman, Sten; Jung, Bo (Univ. of Uppsala). Nature, 207: 543-4(July 31, 1965).

Carbon-11 was produced during the exposure of citrated whole blood to 185-Mev protons. The radioactivity of whole blood, blood cells, and supernatant was followed during the course of a step-wise washing procedure after irradiation. It was concluded that ^{11}C is fixed in the body of blood cells during proton irradiation to such an extent as to be of practical importance for labeling purposes. (C.H.)

38723 A REPORT ON INTERCOMPARISON BY MAILED DOSEMETERS OF HIGH ENERGY ELECTRON BEAMS. Laughlin, John S. (Memorial Hospital and Sloan-Kettering Inst., New York); Shalek, Robert J.; Ovadia, Jacques; Holt, J. Garrett. Phys. Med. Biol., 10: 429-30(July 1965).

The use of mailed dosimeters is reported and procedures for high energy radiation dose standardization in use in the U.S.A. is discussed. Three institutions carried out dose intercomparisons by the mailed exchange of ferrous sulfate and lithium fluoride dosimeters. The results indicated substantial agreement between the methods and gave encouragement to the possibility of using ferrous sulfate, and potentially also lithium fluoride, for mailed intercomparisons. (P.C.H.)

38724 INFLUENCE OF THE STRUCTURE OF HYDROCARBONS ON THE FORMATION OF RADICALS IN LOW-TEMPERATURE γ-RADIOLYSIS IN THE SOLID PHASE. Lependina, O. L.; Polak, L. S. (Inst. of Petroleum Chemical Synthesis, Academy of Sciences USSR). Petrol. Chem. (USSR) (English Transl.), 2: 46-9(1963).

The stabilized free alkyl radicals obtained by the action of ionizing radiation at low temperatures on solid hydrocarbons were studied by electron spin resonance (ESR). The ratio between the probabilities of rupture of the various C–H bonds in the radiolysis of hydrocarbons in the solid phase was investigated from the ESR spectra of irradiated isomeric dodecanes. The isomeric dodecanes investigated were 5-methylundecane, 4-ethyldecane, 4-ethyl-5-methylnonane, and 4,5-diethyloctane. After irradiation, all the dodecane isomers had poorly resolved 8-component ESR spectra. The positions of the main peaks of the spectra of 4,5-diethyloctane, 4-ethyl-5-methylnonane, 4-ethyldecane, and 5-methylundecane coincided. All four spectra had similar widths of the order of 120 Oe and resolutions of ~17 Oe. The distribution of the intensities of the components was close to the binomial distribution (1 : 7 : 21 : 35 : 35 : 21 : 7 : 1) and showed that in these four spectra the hyperfine structure of a single type of radical was involved. The spectrum of n-dodecane differed sharply from the spectra of the isomers both in the number of components (13 for n-dodecane, 8 for each of the isomers) and in the position of the main lines of the hyperfine structure. Chemically, n-dodecane differed from its isomers by the absence of a tertiary carbon atom. The similarity of the isomers of dodecane between themselves and their marked difference from the spectrum of n-dodecane suggested that in these isomers an atom of hydrogen is probably split off from tertiary carbon atoms. In n-dodecane, apparently detachment of hydrogen atoms took place both from a primary C atom and from a secondary C atom, which explained the observed occurrence in its ESR spectrum of a number of spectra of different radicals. It was concluded that when a tertiary carbon atom is present in the molecule the formation of radicals on γ irradiation in the solid phase takes place predominantly by the rupture of the C–H bond at the tertiary carbon atom. (BBB)

38725 THE PRODUCTION OF STEREOSPECIFIC POLYMERS BY THE γ-IRRADIATION OF INCLUSION COMPOUNDS. Glavati, O. L.; Polak, L. S. (Inst. of Petroleum Chemical Synthesis, Academy of Sciences USSR). Petrol Chem. (USSR) (English Transl.), 2: 201-9(1963).

Some features and kinetics of the radioinduced polymerization of inclusion compounds were studied using dimethylbutadiene and cyclohexa-1,3-diene, which readily form inclusion compounds with thiourea, as examples. Irradiation of the complexes using a ^{60}Co source was carried out at doses of from 5.6×10^{9} to 1.13×10^{20} ev/g. The following analyses of the samples were carried out: powder x-ray diagrams, infrared spectra of films of the polymers formed by evaporating their solutions in tetralin, viscosities in solution in tetralin at 150°C, solubilities, and mp by the capillary method. Comparison of the infrared spectra of polydimethylbutadiene obtained at –78°C under homogeneous conditions with the polymer obtained under otherwise the same conditions in an inclusion compound showed that the latter completely lacks the band at 901 cm^{-1} corresponding to the vinyldiene structure; thus the polymer was constructed completely on the 1,4 pattern while in the polymer obtained by radioinduced polymerization there were some links added in the 1,2 position. The curve for dependence of the yield of polymer on the dose at 0°C indicated that the yield of polymer at first rises rapidly with the dose. At a dose of 4.5×10^{19} ev a break in the curve was found and the yield rose more slowly. It was possible to distinguish three sections of the curve with successively decreasing rates of polymerization. The yield did not depend on the temperature below the mp of the dimethylbutadiene. Above it, the velocity of the reaction depended on the temperature in a manner corresponding to a small energy of activation of ~0.3 kcal/mole. Study of dependence of the characteristic viscosity on the dose and temperature showed that an increase in the dose led to a decrease in the molecular weight, probably due to the fact that at small doses the polymerization took place predominantly in long chains of molecules, and then in the shorter chains. At a dose of $\sim 3.4 \times 10^{19}$ ev the characteristic viscosity ceased to change, probably associated with the fact that polymerization took place with equal probability for all chains of molecules of the monomer. The radiation-chemical yield at 0°C for a dose of about 5.6×10^{18} to 1.0×10^{19} ev/g was 3.3×104 molecules of monomer per 100 ev. It was concluded that radioinduced polymerization carried out in inclusion compounds possesses certain advantages with respect to ordinary radiation polymerization: the possibility of obtaining polymers with a highly regular structure; the absence of the main disadvantage of radioinduced polymerization, i.e., the dependence of the yield and molecular weight on the intensity of irradiation; and the possibility of obtaining under definite conditions polymers with a narrow fractional composition. For dimethylbutadiene, the process could be carried out on an industrial scale. (BBB)

38726 RADIATION-THERMAL CRACKING OF PETROLEUM HYDROCARBONS. II. RADIATION-THERMAL CRACKING IN A UNIFORM TEMPERATURE AND DOSE FIELD OF γ-RADIATION AT PRESSURES OF 1–30 ATM. Topchiev, A. V.; Polak, L. S.; Timofeev, T. D. (Inst. of Petroleum Chemical Synthesis, Academy of Sciences, USSR). Petrol. Chem. (USSR) (English Transl.), 3: 41-54(1964).

Earlier investigations of the radiation-thermal cracking (RTC) of n-heptane and petroleum in a field of nonuniform temperature and irradiation with electrons at 800 kev were continued. These conditions permitted experiments to be carried out only at vapor pressures of 1 atm. In the present RTC experiments, fields were uniform with respect to temperature and dose (created by γ irradiation), and the influence of changes of pressure from 1 to 30 atm on the RTC process was followed. As was shown previously, the yield of RTC products rises almost linearly with the dose rate over a wide range. The dose rate used in these experiments was $\sim 10^{14}$ ev/sec-cm^3 as compared with $\sim 10^{16}$ ev/cm^3-sec for 800-kev electrons. The volume of gas evolved, the amount of raw material passed, and the amount of liquid product obtained were recorded. Together with each RTC experiment, a pure thermal cracking (TC) experiment without irradiation was carried out under the same conditions. The yield of gaseous products (in cm^3 per g of raw material fed) in RTC and TC at atmospheric pressure as a function of the temperature in the range from 450 to 600°C showed that the superiority of RTC to TC was slight and was somewhat less than that obtained previously with electrons. This may be due to the lower dose rate. At temperatures close to the temperature of thermal cracking, the yield of gaseous products using the ^{60}Co source, with a uniform

field, was approximately twice as great as with the electron source used previously. The composition of the gaseous products approximated, with an increase in the temperature, the composition of the gases from thermal cracking. However, if the yield of gaseous products per gram of raw material fed was considered, the yield of the individual gases in RTC exceeded their yield in TC; thus, at 600°C the yields of ethylene in cm^3/g of raw material fed were, respectively, 61.0 and 54.5. The iodine numbers, the contents of sulfonatable hydrocarbons, and the refractive indices of the liquid products of RTC were somewhat higher than for TC. An investigation of the influence of the pressure on the RTC process was carried out in the range from 1 to 30 atm at various temperatures from 450 to 600°C with gasoline having a bp of 140°C. As the pressure increased the total yield of gaseous products increased. However, their rate of formation fell on passing from 1 to 5 atm and then remained almost constant up to a pressure of 30 atm at which a slight tendency for the rate to increase could be seen. In the gaseous products at 450°C, a slight rise in the content of unsaturated compounds was first found, and then, beginning at ~10 atm, it remained practically constant. The absolute yield of unsaturated compounds in RTC exceeded that in TC and increased with the pressure. Although at 450 and 500°C, a rise in the pressure led to an increase in the yield of gaseous radiation-thermally cracked products, at 550 and 600°C a slight tendency to fall was found. The yields of gaseous products and, in particular, of olefins in radiation-thermal cracking under the conditions of these experiments exceeded the yields in thermal cracking. The radiation-chemical yields at various pressures and temperatures of the process are given, showing that the radiation-chemical yields fall with increased pressure. (BBB)

38727 REACTIONS OF SOME HYDROCARBONS WITH CARBON DIOXIDE UNDER THE INFLUENCE OF RADIATION. Kalyazin, E. P.; Makrov, V. I. (Moscow State Univ.). Petrol. Chem. (USSR) (English Transl.), 3: 95-102(1964).

The reaction of n-neptane, n-nonane, or cumene with carbon dioxide under the action of x and γ rays was studied, as well as the influence on the reaction of a number of factors, including: intensity of radiation, temperature, and ratio of the components. For n-neptane saturated with carbon dioxide at atmospheric pressure and room temperature under the action of γ radiation, the yields of acids, esters, and carbonyl compounds were, respectively, 0.43, 0.050, and 0.0075 moles per 100 ev. No dialkyl peroxides were found. Yields of reaction products were independent of the dose rate over the range from 3.8×10^{16} to 1.1×10^{14} ev/ml-sec. Study of the temperature dependence of the yield of acids and carbonyl compounds for n-heptane, n-nonane, and cumene under the action of x irradiation showed that temperature had no effect on the reactions over the range from –77 to + 145°C. Dependence of the yield of acids and carbonyl compounds under the action of γ radiation in heptane on the concentration of carbon dioxide over the range from 6×10^{-4} to 8.9M was also determined. Maximum yield of acids (0.9) was obtained at a concentration of CO_2 of 2M, and the maximum yield of carbonyl compounds (0.29 at 8.9M. A linear dependence of the yield on the concentration was seen. Hypotheses on the mechanism of the formation of the reaction products were advanced, but it did not appear possible to establish unambiguously the mechanism of the radiation carboxylation of hydrocarbons. (BBB)

38728 THE PULSE RADIOLYSIS OF AQUEOUS SOLUTIONS OF SOME INORGANIC COMPOUNDS. Baxendale, J. H. (University, Manchester, Eng.); Fielden, E. M.; Keene, J. P. Proc. Roy. Soc. (London), Ser. A, 286: 320-36(July 20, 1965).

The reactions of the hydrated electron, e^-_{aq}, with a variety of inorganic metal ions, complex metal ions, and anions were investigated with pulses of 4-Mev electrons. Absolute rate constants were measured in each case and some temperature coefficients were also determined. Absorption spectra of transient species produced by the pulse were obtained. Some of these species were unstable valency states produced by reduction with e^-_{aq}, e.g., Ni^+, Cr^V; others were the result of oxidation by OH, e.g., Cu^{3+}. Rate constants for the reactions $OH + Cu^{2+}$ and $H + MnO_4^-$ were obtained. (auth)

38729 TRAPPED HOLE CENTER CONTAINING FLUORINE IN MAGNESIUM OXIDE. Wertz, John E.; Auzins, Peteris V. (Univ. of Minnesota, Minneapolis). Phys. Rev., 139: A1645-7(Aug. 30, 1965).

An intrinsic defect center readily induced in MgO by ionizing radiation is the positive hole localized on an oxygen atom adjacent to a positive ion vacancy (V_1 center). This has a tetragonal symmetry axis along [001] or equivalent directions. A similar ESR spectrum but with each line a hyperfine doublet was identified earlier as arising from the center $O^- - [=] - H^+O$ (V_{OH} center). A similar ESR spectrum of a trapped hole center (V_F) with smaller (anisotropic) hyperfine splitting than V_{OH} is described. It is best observed in single crystals, but it may be induced in powdered MgO by fluorine doping and heating. It thus appears that fluorine is the nucleus responsible for hyperfine splitting. The contact and dipolar splitting constants are, respectively: a = 0.08 G, b = 0.33 G. The proposed model for the V_F center is $O^- - [=] - F^+$ (only deviations from normal site symmetry are shown). (auth)

38730 ELECTRON SPIN RESONANCE OF NO_3^{2-} IN THE IRRADIATED $Ba(NO_3)_2$ SINGLE CRYSTAL. Zdansky, K.; Sroubek, Z. (Inst. of Radio Engineering and Electronics, Czechoslovak Academy of Sciences, Prague). Phys. Status Solidi, 10: 571-4(Aug. 1, 1965).

Electron-spin resonance measurements are made on a single crystal of $Ba(NO_3)_2$ which has been x irradiated at 90°K. The NO_3^{2-}-spectrum, with a hyperfine structure arising from a single nitrogen nucleus, is observed at 90°K. The directions of the principal axes of the g tensors and hyperfine tensors and their eigenvalues are determined. The partially resolved super-hyperfine structure assigned to an interaction with three Ba nuclei is also observed and compared with the super-hyperfine structure of the NO_3^{2-} spectrum in $Pb(NO_3)_2$. (auth)

38731 BEHAVIOR OF PENTAVALENT PLUTONIUM NITRATE SOLUTIONS. Gel'man, A. D.; Zaitseva, V. P. Radiokhimiya, 7: 56-68(1965). (In Russian).

The cause of instability of Pu(V) in dilute nitric acid solutions and the conditions under which these solutions are most stable were determined. Pentavalent plutonium solutions were obtained by reduction of Pu(V) nitrate solutions with hydrogen peroxide at pH = 3-4. A pentavalent plutonium solution having pH = 4 and containing ~5 g/l of plutonium was used as a stock solution for further preparations. It was found that in the pH 2-6 range disproportionation of Pu(V) is not a major factor in determing the stability of Pu(V), while oxidation and reduction by radiolysis products is quite significant. The instability of Pu(V) solutions due to oxidation and reduction by the radiolysis products of water can explain the increase of the stability of Pu(V) solutions as its concentration in the solution decreases; lowering the plutonium concentration in the solution decreases the concentration of the radiolysis products and also decreases the rates of reduction, oxidation, and disproportionation reactions. Pentavalent plutonium solutions may be stabilized by lowering the temperature, taking up the radiolysis products and by storage of Pu(V) in the form of its compounds. (ATD)

38732 CHEMICAL REACTION BY IONIZING RADIATION. IV. CHLOROFORM-DYE TWO PHASE SYSTEM DOSIMETER. Ishikawa, Sumio (Inst. of Physical and Chemical Research, Tokyo). Rika Gaku Kenkyusho Hokoku, 36: 328-34(1960). (In Japanese).

The use of the chloroform-dye system for measuring x-ray doses was investigated. (BBB)

38733 SOME PHYSICAL PROPERTIES OF POLYVINYL CHLORIDE-STYRENE GRAFT COPOLYMERS PREPARED BY γ-IRRADIATION. Takamatsu, Toshiaki

(Inst. of Physical and Chemical Research, Tokyo). Rika Gaku Kenkyusho Hokoku, 36: 646-51(1960). (In Japanese).

The preparation of polyvinyl chloride-styrene graft copolymers by γ irradiation and some physical properties of the copolymers obtained are discussed. The physical properties measured were specific gravity, flow temperature, intrinsic viscosity, dielectric constant and loss, and ir absorption spectrum. They were examined as functions of the degree of grafting, and as functions of temperature. The results of dielectric measurements indicate that as the degree of graft increases, the hindrance of the molecular motion of the polyvinyl chloride increases, probably due to the steric hindrance of phenyl groups of polystyrene branches which have been grafted to the main chain polymer. (BBB)

38734 RADIATION-INDUCED GRAFT COPOLYMERIZATION. I. GRAFTING IN MONOMER VAPOR. Shinohara, Kenichi; Takamatsu, Toshiaki (Inst. of Physical and Chemical Research, Tokyo). Rika Gaku Kenkyusho Hokoku, 36: 652-7(1960). (In Japanese).

When polymer films were irradiated in the presence of monomer vapor, graft copolymers were produced. The polymers studied were high pressure and low pressure polyethylene, polyvinyl chloride, and polytetrafluoroethylene. As monomers, styrene and acrylonitrile were used. The method offers a good technique for graft copolymer formation. Special features of the process were: only a small amount of homopolymer is produced, the separation and purification of graft copolymer can be done easily, comparative or even a higher degree of graft can be obtained for the same radiation dose compared with other methods of grafting, and the expenditure of the monomer is small in the process of grafting. (BBB)

38735 THE CONCENTRATION DEPENDENCE OF KI-Tl PHOTOLUMINESCENCE AND RADIOLUMINESCENCE YIELD. Kink, R. A.; Liid'ya, G. G.; Maaroos, A. A.; Soovik, T. A. Tr. Inst. Fiz. i Astron., Akad. Nauk Est. SSR, No. 26, 216-19(1964). (In Russian)

Experiments were carried out to determine the influence of the radiation-generated excitons (e x mechanism) or electron-hole formation (e p mechanism) on the radioluminescence of KI-Tl phosphors as a function of the activator concentration. The luminescence yield was determined at various Tl concentrations by optically creating the excitons or electron–hole pairs and also by employing α particles for excitation. The Tl concentration was determined polarographically; at low concentrations, the 4.35ev absorption band of Tl was used. The quantum yield of the luminescence of the crystals was determined by means of a vacuum monochromator. Examination of the concentration dependence of the energy yield revealed that within broad limits the relation between the activator concentration and the exciton yield may be described by a line with a slope <1. At activator concentrations $>10^{-1}$ mole % the yield increase was slowed down. The electron–hole pair luminescence yield increased rapidly with the concentration only in the $<5 \times 10^{-3}$ mole % range. The fluxes studied were in the range of 10^9 quanta/cm^2 sec. The difference in the behavior may be due to the fact that the ratio of effective capture at luminescence centers and the competing defects where nonradiative recombination of the charge or nonradiative annihilation of the excitons takes place was lower for excitons than for the electron–hole pairs. Tests were also carried out with the 5.15-Mev α particles of ^{239}Pu. The results obtained did not agree with these findings. (TTT)

38736 THE ROLE OF HO_2 RADICALS IN THE BLEACHING OF AQUEOUS DYE SOLUTIONS BY ^{60}Co γ RADIATION. Rakintzis, Nikolaus (Kernforschungszentrum Dimokritos, Athens); Papaconstantinou, Elias; Schulte-Frohlinde, Dietrich. Z. Physik. Chem. (Frankfurt), 44: 257-69(Mar. 1965). (In German).

The radiochemical bleaching of seven dyes in the presence and absence of 2,5-dichlorhydroquinone was investigated in the presence of atmospheric oxygen. In the presence of hydroquinone the bleaching occurred through HO_2 radicals. These conclusions could be verified by comparison with the effect of chemical HO_2 radicals prepared by the reaction $Ce^{4+} + H_2O_2 \rightarrow Ce^{3+} + H^+ + HO_2$. HO_2 radicals scarcely attacked Safranine T and neutral red, but methylene blue, acridine orange NO, and the indigo dyes investigated were bleached by HO_2 radicals. The G value of the bleaching by HO_2 radicals depended very strongly on the dye concentration. The origin of the concentration dependence was the disproportionation of the HO_2 radicals concurrent with the dye bleaching. (tr-auth)

38737 APPLICATION OF SCINTILLATION GRANULES FOR MEASURING β RADIATION FROM RADIOACTIVE ISOTOPES. Tsirlin, Yu. A.; Gel'fman, A. Ya.; Bykovets, N. P.; Solomonov, V. M. (All-Union Research Inst. of Monocrystals Scintillation Materials and Especially Pure Chemical Substances, USSR). Zavodsk. Lab., 31: 704-6 (1965). (In Russian).

Beta emission from radioactive isotopes in various solutions was measured by plastic scintillation granules. A granular suspension was added to the investigated solution. The counting rate of the suspension was compared with the counting rate of a standard preparation. (R.V.J.)

38738 RADIATION EFFECTS ON THE DISINTEGRATION RATE OF ALUMINATE SOLUTIONS. Koryukov, V. N.; Kuznetsov, S. I.; Derevyakin, V. A. (Kirov Ural Polytechnic Inst., USSR). Zh. Prikl. Khim., 38: 1122-5 (May 1965). (In Russian)

The maximum disintegration rate acceleration by ultraviolet, x, and γ radiation was obtained using aluminate solution seeded before or during the course of disintegration. Irradiation increased the amount of alumina obtained by 2 to 8%. The impure industrial aluminate solutions responded better to the radioinduced disintegration than the synthetic solutions. Increased radiation intensity increased the rate of disintegration, moreover, the wavelength was important. Radiation disintegration of aluminate solutions produced a finer grain alumina. (R.V.J.)

38739 PROCESS FOR THE PRODUCTION OF SHAPED ARTICLES OF VINYL CHLORIDE POLYMERS. (to the Dow Chemical Co.). British Patent 996,641. June 30, 1965. Priority date July 16, 1962, United States.

A process for the production of shaped articles includes shaping at elevated temperatures a uniform mixture of a polymer of vinyl chloride and one or more monoethylenically unsaturated monomers that are compatible with the polymer and subjecting the shaped article to high energy ionizing radiation. The radiation dose employed is less than that required for the complete conversion of the monomer and is 0.1 to 6 megarad. The shaped mixture is maintained at a temperature of from 10° to 100°C during the radiation treatment. Subsequent to the radiation treatment, the shaped mixture is subjected to a heat treatment that is carried out at not more than 30°C above the second order transition temperature of the vinyl chloride polymer, preferably at a temperature of from 50° to 100°C. (B.L.M.)

38740 COMPOSITIONS OF VINYL CHLORIDE POLYMERS. (to the Dow Chemical Co.). British Patent 996,642. June 30, 1965. Priority date July 16, 1962, United States.

A process is described for the production of shaped articles composed of an intimate mixture of 70 to 95% by weight of a polymer of vinyl chloride and 5 to 30% by weight of styrene. The shaped articles are subjected to a dose of high energy ionizing radiation sufficient to induce complete conversion of the styrene to the polymer. The articles are then heated to about 100°C for about 30 minutes. The articles produced by this process have exceptionally good impact and flexural strengths. (B.L.M.)

38741 PROCESS FOR THE PRODUCTION OF SHAPED ARTICLES. (to the Dow Chemical Co.). British Patent 996,643. June 30, 1965. Priority date July 16, 1962, United States.

Radioinduced graft polymerization of one or more monoethylenically unsaturated monomers, at least one of which is capable of thermal homopolymerization, on vinyl chloride polymers for the production of shaped articles is described. Products with improved clarity and physical properties

were obtained by this method. Maximum results were obtained using high-energy radiation in a field of about 50,000 rads per hr. A thermal homopolymerization inhibitor is added to the mixture before the mixture is shaped. (M.C.G.)

38742 IMPROVEMENT OF THE ACTIVITY OF PLATINUM HYDROGENATION CATALYSTS BY HIGH ENERGY IRRADIATION. Graham, Donald P. (to E. I. du Pont de Nemours and Co.). U. S. Patent 3,189,560. June 15, 1965. Filed Jan. 12, 1961.

A process is described for increasing the activity of a hydrogenation catalyst in which the catalyst consisting of Pt-metal supported on activated carbon is irradiated with 3 to 8 mev of beta radiation in dosage of 5,000 to 20,000 wsec/cm^2. (B.L.M.)

Radiochemistry

See also Separation Processes and Procedures.

38743 (NP-15262) PREPARACION DEL FERROCIANURO DE POTASIO MARCADO CON ^{59}Fe. Informe No. 145. (Preparation of Potassium Ferrocyanide Labeled With ^{59}Fe. Report No. 145). Marques, Roberto O. (Comision Nacional de Energia Atomica, Buenos Aires (Argentina)). 1965. 7p. Dep. mn.

^{59}Fe labeled potassium ferrocyanide was prepared by reduction of $^{59}FeCl_3$ and treatment with potassium cyanide. The chemical yield was higher than 90%. To test its radiochemical purity a method was developed for separating, by paper chromatography and electrophoresis, the possible active impurities: ferricyanide, and ferric and ferrous ions. Ferro and ferricyanide were separated from ferric and ferrous ions by ascending cromatography using as a solvent methil ethil ketone-hydrochloric acid (92 : 8). By electrophoresis ferrocyanide was separated from ferricyanide and ferrous or ferric ions. The radiochemical purity, as tested by these methods, was greater than 99%. (auth)

38744 (PHS-999-RH-12) RADIOACTIVE DECAY CORRECTION FACTORS. Falter, Kenneth H. (Public Health Service, Washington, D. C. Div. of Radiological Health). 1965. 212p. Free (Public Health Service, Washington, D. C.).

Tables of correction factors for radioactive decay are presented which facilitate the task of calculating the activity of a radioactive nuclide at a given time, given its activity at any other time. Tables are included for those nuclides which are commonly measured, those used as standards, and those used as tracers. In addition, the thorium, neptunium, uranium, and actinium decay series are included. Tables giving the fractional ingrowth of yttrium-90 into strontium-90 and of radon-222 into radium-226 are also presented. (auth)

38745 (Y-1484) THE PREPARATION OF RADIOACTIVE PHOSPHOROUS-32 SOURCES ON METAL PLATES. Dietrich, W. C.; Barringer, R. E. (Union Carbide Corp., Oak Ridge, Tenn. Y-12 Plant). May 3, 1965. Contract W-7405-eng-26. 14p. Dep. mn; CFSTI, $1.00 cy, $0.50 mn.

A technique was developed for adhering phosphorous-32 to a tantalum or aluminum metal supporting plate. An aqueous radioactive solution was incorporated into a proprietary cement thinner (Sauereisen 14) and a measured quantity deposited on a metal plate. After drying and baking thoroughly, a uniform, hard, and tenacious radioactive source was produced. (auth)

38746 OBSERVATIONS CONCERNING THE UNSTABLE BEHAVIOR OF ^{14}C-PHENYLETHYLAMINE CARBAMATE IN LIQUID SCINTILLATION MIXTURES. Georgi, P.; Lober, M. (Ernst-Moritz-Arndt-Universitat, Greifswald, Ger.). Acta Biol. Med. Ger., 14: 91-2(1965). (In German)

Measurement of the activity of the ^{14}C-carbamate showed a steady decrease of the count yield; after 24 hr the count rate decreased to zero. This behavior was not noted in the benzoic acid standard and it was assumed that $^{14}CO_2$ was being lost from the scintillator solution. The gas could be completely picked up with phenylethylamine in a closed system. The observation was made with a dioxane-naphthalene-PPO-POPOP and a PPO-POPOP-toluene system. With hyamine hydroxide, there was no loss of CO_2 over the whole observation time. This base had several drawbacks, however: it was pipetted without precision because of its low surface tension, and it had a greater quenching effect on scintillation in both systems. Phenylethylamine carbamate could be used if it were undiluted; within the first 10 min the loss was less than 5%. It was necessary on radioprotective grounds that these studies be carried out in well-ventilated areas, e.g., in a hood. The studies were carried out with the lowest possible activities, ~10 nC per measurement. Other bases will be tested for such studies in this regard. (BBB)

38747 NEW APPROACH TO THE PREPARATION OF ^{35}S-LABELED CYSTINE. Fojtik, A.; Spurny, Z.; Brdicka, R. (Inst. of Physical Chemistry and Inst. of Nuclear Research, Czechoslovak Academy of Sciences, Prague). Collection Czech. Chem. Commun., 30: 892-3(Mar. 1965).

A method for the production of cystine-^{35}S by exposing it to a neutron flux is described. The neutron irradiation converts the cystine into cysteine; this is reoxidized to cystine-^{35}S by cystine disulfoxide. The product yield is 15% with a specific activity of 1.08×10^{-2} mC/g. (tr-auth)

38748 RADIOSYNTHESIS OF CARBON-14-LABELED 4-DIMETHYLAMINO-3,5-XYLYL METHYLCARBAMATE. Williams, Elinor A.; Meikle, Richard W.; Redemann, Carl T. (Dow Chemical Co., Walnut Creek, Calif.). J. Agr. Food Chem., 13: 210-13(May-June 1965).

Zectran, 4-dimethylamino-3,5-xylyl methylcarbamate is a highly active material for control of mollusks and a large number of arthropod pests of plants. Its potential use on food crops necessitated a study of its metabolism in both plants and animals. The synthesis of this compound labeled with ^{14}C in both the ring and the carbamate functional group was undertaken. The preparation of 4-dimethylamino-3,5-xylyl methyl carbamate-carbonyl-^{14}C; 4-dimethylamino-3,5-xylyl-1-^{14}C methylcarbamate; and 4-dimethylamino-3,5-xylyl-α^3,3-$^{14}C_2$ methylcarbamate are described. In the first of these three forms, the carbonyl group was labeled, in 46% yield based on radioactivity, by the conversion of acetic anhydride-1,1-^{14}C to methyl isocyanate and reaction of this with 4-dimethylamino-3,5-xylenol. For the second form, the 1-position in the ring was labeled in 3% yield by the addition of carbon dioxide-^{14}C to the di-Grignard reagent of 1,5-dibromo-2,4-dimethylpentane and catalytic conversion to 3,5-xylenol. This was followed by nitrosation, hydrogenation, methylation, and reaction with methyl isocyanate. The di-Grignard reagent was prepared by a seven-step synthesis starting with diethyl malonate. Both the 3-position in the ring and the 3-methyl group were labeled in 10% yield by the reaction of acetaldehyde-1,2-^{14}C with ethylacetoacetate and conversion to 3,5-xylenol. The reaction sequences for the preparation of these three labeled forms of Zectran are shown, and the detailed data for conducting the syntheses, as well as analytical results, are provided. (BBB)

38749 A NOMOGRAM FOR THE ESTIMATION OF MICROCURIES AND MILLIMICROGRAMS FROM CPM. Prasad, K. N.; Cotzias, G. C. (Brookhaven National Lab., Upton, N. Y.). J. Nucl. Med., 6: 297-9(Apr. 1965). (BNL-8483).

A nomogram is presented which permits estimation of dpm and microcuries from cpm and efficiency of the counter; and of millimicrograms from cpm and specific activity. (auth)

Separation Processes and Procedures

See also Analytical Procedures.

ISOTOPE TECHNOLOGY — Separation and Production

Refer also to abstracts 40112, 40113, 40128, and 40177.

38750 (HW-81166) THE DISTRIBUTION OF Am^{3+} BETWEEN XYLENE–DBBP SOLUTIONS AND NITRATE

SOLUTIONS. Sheppard, J. C. (General Electric Co., Richland, Wash. Hanford Atomic Products Operation). Mar. 1964. Contract AT(45-1)-1350. 9p. Dep. mn; CFSTI, $1.00 cy, $0.50 mn.

The distribution of ^{241}Am between xylene–dibutylbutylphosphonate (DBBP) and solutions of nitric acid and metal nitrates was studied. The DBBP and nitric acid dependences of the ^{241}Am distribution were determined. The total nitrate ion and hydrogen ion concentrations are shown to have a strong influence on the distribution coefficients, and the distribution is determined by a competition between ^{241}Am and nitric acid for free DBBP. A formal equation is given for the distribution with sodium, aluminum, and magnesium nitrates. (D.L.C.)

38751 (HW-82103) LABORATORY STUDIES ON THE USE OF URANIUM(IV) AS A PLUTONIUM REDUCTANT IN A PUREX PROCESS Mendel, J. E. (General Electric Co., Richland, Wash. Hanford Atomic Products Operation). June 1965. Contract AT(45-1)-1350. 14p. Dep. mn; CFSTI, $1.00 cy, $0.50 mn.

A flowsheet was proposed for a plant production test of uranium(IV)-hydrazine instead of ferrous sulfamate-sulfamic acid as partitioning agent in HAPO Purex partition column. In this flowsheet, an aqueous stream containing uranium(IV) is contacted with Purex solvent and both phases are introduced into the 1BX column at the feed point. Hydrazine is added to the 1BX column feed accumulation tank to destroy nitrite present in the organic feed stream. A hydrazine-nitric acid stream is introduced at the top of the 1BX column instead of the usual ferrous sulfamate-sulfamic acid stream. The solvent phase leaving the 1BS column is routed to the 1BX feed tank instead of to the co-decontamination cycle. Otherwise, the stream compositions and flows remain as at present. Laboratory studies indicated that satisfactory operation of the 1B column should be obtained with the proposed flow sheet. Uranium(IV) was shown to be adequately stable in Purex solvent to allow reasonable hold-up time in the vessel in which the feed stream is made up. Plutonium reduction was sufficiently rapid and complete under 1BX extraction conditions to assure adequate separation of plutonium from the product uranium stream. Although some re-oxidation and re-extraction of plutonium in the 1BS column (scrub section) was anticipated, the results indicate that the plutonium reflux will be no greater than that which occurs with the present flowsheet. Extraction of uranium (IV) in the 1BS column should be adequate to insure acceptably low uranium in the product plutonium stream, particularly if high acidity (4M HNO_3) is maintained through addition of the 1BXP-HNO_3 stream. (auth)

38752 (LA-DC-6947) PRACTICAL APPLICATION OF THERMODYNAMICS TO PLUTONIUM PROCESS REACTIONS AT HIGH TEMPERATURE. Leary, J. A.; Mullins, L. J. (Los Alamos Scientific Lab., Univ. of California, N. Mex.). June 11, 1965. Contract W-7405-eng-36. 18p. (CONF-650704-9). Dep. mn; CFSTI, $1.00 cy, $0.50 mn.

From IAEA Symposium on Thermodynamics, Vienna.

The important high temperature reactions for processing Pu involve equilibria between liquid metal and fused salt phases. Estimates are made of equilibrium concentrations for the following processes: fused salt extraction, electrorefining, bomb reduction, and oxide drossing of liquid Pu fuels. Container materials for Pu are considered briefly. (D.L.C.)

38753 (LA-DC-7013) KINETIC STUDIES ON EXTRACTION OF EUROPIUM BY LITHIUM AMALGAM AND COMPARISON TO REMOVAL BY ELECTROLYSIS. Onstott, E. I.; Goddard, John F. (Los Alamos Scientific Lab., Univ. of California, N. Mex.). [1964]. Contract W-7405-eng-36. 9p. (CONF-650804-4). Dep. mn; CFSTI, $1.00 cy, $0.50 mn.

From 5th Rare Earth Research Conference, Ames, Iowa.

Extraction of Eu by saturated lithium amalgam from aqueous lithium citrate electrolytes containing a preponderance of Gd proceeds linearly with time after an initial much more rapid extraction of a fraction of the Eu present in the electrolyte. When ammonium ion is substituted for lithium ion in the electrolyte, the initial rapid extraction of Eu is reduced by a factor of two to three, but subsequent steady-state extraction is virtually nil. The amount of Eu in the initial faster reaction depends on the method of contacting the phases. About twice as much Eu is extracted when the amalgam is dumped into the electrolyte compared to the reverse procedure of adding the electrolyte to the amalgam. Removal of Eu by electrolysis from aqueous lithium citrate electrolytes containing a preponderance of Gd starting with pure mercury (lithium amalgam cathode method) is linear with time at constant current density for short electrolysis times. The rate of removal increases as the current density is increased. No initial very rapid removal of Eu by electrolysis is observed. When ammonium ion is substituted for lithium ion in electrolytes, the removal of Eu by electrolysis is a factor of about 1500 slower than with lithium ion present and ammonium ion absent. (auth)

38754 (NAA-SR-10737) ELECTROLYSIS OF URANIUM CARBIDE IN FUSED SALT USING MOLTEN METAL CATHODES. Iverson, M. L.; Sullivan, R. J. (Atomics International, Canoga Park, Calif.). June 30, 1965. Contract AT(11-1)-Gen-8. 22p. Dep. mn; CFSTI, $2.00 cy, $0.50 mn.

Uranium carbide was anodized in fused LiCl–KCl eutectic containing UCl_3 to give deposits of uranium and uranium intermetallic compounds in liquid metal cathodes. The cathode current efficiencies found for the metal cathodes, lead, zinc, bismuth, and cadmium, decreased in the order given and ranged from 0.1 to 91%. The anode efficiencies varied in approximately the same manner and ranged from 1 to 93%. Under similar conditions, uranium anodes gave higher yields and this difference was attributed to a greater loss of current through U^{+3}/U^{+4} cycling with uranium carbide anodes. The current efficiency decreased markedly with the increase in UCl_3 beyond an optimum concentration. This decrease in yield was attributed to a greater current loss through U^{+3}/U^{+4} cycling at higher UCl_3 concentrations. (auth)

38755 (ORNL-3611) STATUS AND PROGRESS REPORT FOR THORIUM FUEL CYCLE DEVELOPMENT FOR PERIOD ENDING DECEMBER 31, 1963. Wymer, R. G.; Douglas, D. A. Jr. (comps.) (Oak Ridge National Lab., Tenn.). July 1965. Contract W-7405-eng-26. 169p. Dep.(mn); $5.00(cy), 4(mn) CFSTI

Demonstration of a Th fuel cycle process (Kilorod Program) including remote fabrication of ThO_2–$^{233}UO_2$ fuel elements by sol-gel vibratory compaction was achieved during the period. 720 fuel rods containing 3 wt% $^{233}UO_2$–97 wt% ThO_2 were prepared in a program to produce 1000 such rods. Results obtained during the demonstration are presented. Design and development of a facility to evaluate Th fuel cycles are described. Work on improvement of sol-gel process flowsheets for Th and Th–U oxide and carbide production is reported along with development of remote Th–^{233}U fuel fabrication, and irradiation testing of mixed Th and U oxides, carbides, and Th alloys. Results of studies concerning sol-gel processing of U–Th carbide are reported. (J.R.D.)

38756 (RFP-488) VOLUMETRIC CALIBRATION OF PROCESS VESSELS USING DIGITAL COMPUTER TECHNIQUES. Doher, L. W.; Schulz, J. A. (Rocky Flats Div., Dow Chemical Co., [Denver], Colo.). July 1, 1965. Contract AT(29-1)-1106. 67p. Dep. mn; CFSTI, $3.00 cy, $0.75 mn.

A procedure for accurately and speedily calibrating tanks used for the chemical processing of nuclear materials is described. The procedure features the use of precalibrated vessels certified to deliver known volumes of liquid, calibrated linear measuring devices, and a digital computer for manipulating data and producing printed calibration information. Calibration records of the standards are traceable to primary standards. Logic is incorporated in the computer program to accomplish curve fitting and perform the tests to accept or to reject the calibration, based on statistical, empirical, and report requirements. This logic is believed to be unique. (auth)

38757 (SGAE-CH-17/1965) DIE ISOLIERUNG VON TRAGERFREIEM STRONTIUM-89 UND BARIUM-140 AUS KURZZEITIG BESTRAHLTEM URAN DURCH IONENAUSTAUSCHCHROMATOGRAPHIE. (The Isolation of Carrier-Free Strontium-89 and Barium-140 from Short-Time Irradiated Uranium by Ion Exchange Chromatography). Titze, H. (Oesterreichische Studiengesellschaft fuer Atomenergie G.m.b.H., Seibersdorf. Institut fuer Chemie). 1965. 14p. Dep.(mn).

Carrier-free ^{89}Sr and ^{140}Ba were obtained from short-time irradiated U by an ion exchange method. Uranium and a large part of the fission products formed were separated by double anion exchange on the basis of their tendency to form chloride complexes in hydrochloric acid solutions. The earth alkali metals and rare earths remaining in solution were chromatographed on a cation exchange column with lactate buffer as the complexing reagent. The purity of the ^{89}Sr and ^{140}Ba fractions were proved by the elution curve and the γ spectra. (tr-auth)

38758 (Y-KA-7) NUCLEAR MATERIALS MANAGEMENT IN A RECOVERY FACILITY FOR UNIRRADIATED ENRICHED URANIUM. Jasny, George R. (Union Carbide Corp., Oak Ridge, Tenn. Y-12 Plant). June 28, 1965. Contract W-7405-eng-26. 15p. (CONF-650803-3). Dep. mn; CFSTI, $1.00 cy, $0.50 mn.

From IAEA Symposium on Nuclear Materials Management, Vienna.

A discussion is presented of several aspects of a "total" nuclear material control program which was developed in a large facility at Y-12 for the reprocessing of unirradiated, highly enriched uranium scrap. Facilities design, physical measurements of inputs, outputs, and inventories, measurement of losses and discards, control of quality of measurements, accounting records system, training and motivation of personnel, and costs are covered in the discussion. (D.L.C.)

38759 (ZFK-RN-17(p.95-117)) VOPOOCHISTKA I VODOPODGOTOVKA NA ISSLEDOVATEL'SKIKH YADERNYKH REAKTORAKH. SOOBSHCHENIE II. (Water Purification and Treatment for Nuclear Research Reactors. II.). Alekseev, B. A.; Babulevich, E. N.; Chernorotov, E. S. (Institut Atomnoi Energii, Gosudarstvennyi Komitet po Ispol'zovaniyu Atomnoi Energii SSSR, Moscow).

The performance of filters using mixtures of cation and anion exchange resins was measured for various mixtures. The use of noncorrosive material for the supporting layer in ion-exchange filters of the primary coolant loop is discussed. Results of a study of the distribution of sorbed material as a function of height of the filtering layer are presented. (M.J.T.)

38760 (ZFK-RN-17(p.127-38)) OPYT EKSPLUATATSII IONOOBMENNOGO FIL'TRA REAKTORA "EVA". (Operation of Ion-Exchange Filter for EWA Reactor). Bergushevski, Z.; Zharnovetski, K.; Kostyrko, A. (Polish Academy of Sciences, Warsaw. Inst. of Nuclear Research). Dep.(mn).

Experiments were performed on the first loading of the ion-exchange filter. Two resins, the cationite MK-3 and the anionite Imak-S4, suffered no significant damage and maintained their specific operating capacity as well as their physical properties. Regeneration was carried out easily and efficiently, and the columns prepared after regeneration proved entirely satisfactory. (M.J.T.)

38761 (CEA-tr-A-1809) ETUDE FONDAMENTALE DU PROCEDE D'EXTRACTION EN TECHNIQUE NUCLEAIRE. (Fundamental Study of the Extraction Process in Nuclear Technology). Knoch, W; Lindner, R. Translated into French from Z. Elektrochem., 64: 1020-1(1960). 11p. Dep.(mn); $1.10(fs), $0.80(mf) JCL.

The partician coefficients of U(IV), Pu(IV), Zr, and (RuNO)(III) between nitric acid aqueous solutions with variable molarity and solutions of tertiary amine (triisooctylamine and trilaurylamine) in kerosene and xylene were measured. In order to study the kinetics of the extraction process, the self diffusion of ^{239}Pu and ^{233}U in nitric aqueous solutions and in solution of tributylphosphate (TBP) in equilibrium and the self diffusion of ^{106}Ru in nitric acid aqueous solutions were measured. The purpose of these tests was to obtain precise knowledge on the formation and the dimension of the anionic complexes and on the radiocolloids. It was established that the mass transfer of the dispersed phase (falling drop by drop) in the continuous phase is made by double film diffusion. The total film coefficient of U(IV) and of Pu(IV) in the system HNO_3 (aqueous solution)/TBP (20%) was measured and compared to the self diffusion coefficient. (tr-auth)

38762 ON THE RELEASE OF METALLIC IMPURITIES FROM GRAPHITE AT TEMPERATURES ABOVE 1750 deg C. George, D. W. (Univ. of Sydney). Carbon, 3: 43-52(July 1965).

The release of metallic impurities from the surface of graphite at temperatures from 1750 to 2250°C in the presence of a high pressure inert gas (Ar and He) was studied. The impurities were identified by their characteristic radiation and their relative concentrations were measured spectroscopically. Electrical measurements, based on the electric fields produced by ionized impurities, confirmed the release of the impurities at temperatures as low as 1750°C. From Arrhenius-type plots of the spectroscopic and electrical data, mean energies of release for Ca, Ba, Sr, and Al atoms, were found to lie between 2.5 and 5.5 ev. (auth)

38763 OXIDATIVE EXTRACTION SEPARATION OF RUTHENIUM FROM SOLUTIONS OF ITS COMPOUNDS. Bezdek, M.; Mencl, J. (Inst. for Nuclear Research, Czechoslovak Academy of Sciences, Rez). Collection Czech. Chem. Commun., 30: 711-23(Mar. 1965). (In German).

The oxidizability of Ru(IV) nitrate, nitroso-Ru(III) nitrate, nitronitroso-Ru(III) nitrate, and nitroso-Ru(III) chloride with Ce^{4+} and periodate ions was investigated. The pattern and the yield of the oxidation of the Ru to RuO_4 were determined by radiometric measurement of the Ru distribution (^{106}Ru) between the aqueous phase and tetrachloromethane in relation to the oxidation time, solution acidity, ion strength of the aqueous phase, and molar ratio of the oxidation medium and the Ru. The oxidation and extraction were carried out, for the most part, in solutions with a Ru concentration of 10^{-4} to 10^{-5}M at room temperature (24 ± 2°C). (tr-auth)

38764 EXTRACTION OF NITROSORUTHENIUM(III) COMPLEXES FROM A NITRATE MEDIUM WITH 30 PER CENT TRIBUTYLPHOSPHATE. EFFECT OF COMPLEXING REAGENTS AND ACID DEFICIENCY. Brutovsky, M.; Sraier, V. (Inst. for Nuclear Research, Czechoslovak Academy of Sciences, Prague). Collection Czech. Chem. Commun., 30: 802-10(Mar. 1965). (In German).

The effect of a series of complexing reagents on the extraction of nitrosoruthenium(III) complexes with TBP from a medium of 0.5 to 5.0M HNO_3 was investigated. The value of the distribution ratio of the nitroso-Ru(III) complex in extraction with the same reagents from an aqueous uranyl nitrate solution was investigated in rotation to the acid deficiency, the aging time of the hydrolyzed solution, pH value, and the temperature. The efficiency of the washing out of Ru with aqueous solutions of various pH values from 0.3M $UO_2(NO_3)_2$ in TBP was determined in relation to the volume ratio of both phases. (tr-auth)

38765 SEPARATION AND PURIFICATION OF SAMARIUM BY DISTILLATION OF THE HALOGENIDES. Schiffmacher, Gerard (Laboratoire des Terres rares, Bellevue, France). Compt. Rend., 260: 5049-50(May 10, 1965). (In French).

It was indicated in a previous article (Compt. Rend., 260: 182(1965)) that the vapor pressures calculated for the divalent halogenides of Sm, Eu, and Yb are less than those of their trivalent halogenides which are, from the point of view of the vapor pressure, in the normal series of the rare earth halogenides. The problem was to obtain the formation of a divalent halogenide before the distillation separation. In the case of europium, the bromide was the most inter-

esting because the divalent bromide was stable at distillation temperature. Europium thus can be separated from the other rare earths and also from samarium which has a stable trivalent bromide. (tr-auth)

38766 CHARACTERISTICS AND DESIGN OF A CO-CURRENT DISTILLATION COLUMN. Angelino, G. C.; Brigoli, B.; Silvestri, M. (CISE, Segrate, Italy). Energia Nucl. (Milan), 12: 353-64(July 1965).

The application of co-current two phase flow, as a contacting medium for the separation of the components of a mixture, was performed in a new type of distillation column. Efficiency, pressure drops, and equilibrium time determinations are presented for the operation of the column with the steam-water system using deuterium oxide tracer. (auth)

38767 THE SEPARATION EFFICIENCY IN THE DIFFUSION OF NONISOTOPIC GASEOUS MIXTURES. Fiocchi, R. (Universita, Milan). Energia Nucl. (Milan), 12: 372-7 (July 1965). (In Italian).

The theory recently established by Breton and Massignon and used by them for calculating heavy isotope separation was applied to the separation by diffusion through porous barriers of non-isotopic gaseous mixtures. It was evident from comparison with the theory of Present and de Bethune that the representation of the porous barrier as a pack of spherical particles, which is more adherent to the structure of the actual barriers, gives results that are in better agreement with the experimental data than those obtainable through the capillary representation of the barrier. (auth)

38768 TUFF AS CATION EXCHANGER FOR THE REMOVAL OF Cs^+ AND Sr^{++} FROM AQUEOUS SOLUTIONS. PART I. BATCH TESTS. Boenzi, D.; Blanca, G. (CNEN, Casaccia, Italy). Energia Nucl. (Milan), 12: 413-21(Aug. 1965).

Experimental methods used to determine the cation-exchange properties of neapolitan yellow tuff with a view to its potential use in the treatment of water are described, with special reference to radioactively contaminated water. A description is given of the mineralogical and chemical composition of the material and then of results of research on its exchange capacity, the distribution coefficients for Cs^+ and Sr^{2+}, and the rate at which exchange equilibrium between solution and sample is reached in batch tests. The influence exerted by the pH of the contact solutions, by the presence in the latter of interfering ions (e.g., Na^+ and Ca^{2+}) and by particle size on the exchange properties of both the material as such and of that material considered under different forms (sodium, potassium, and calcium salts) is illustrated. A description of the effect of gamma irradiation and heat treatment on the cation exchange properties of tuff is given. (auth)

38769 INSTALLATION FOR PURIFICATION OF ARGON FOR GLOVE BOXES. Aubecq, Maurice (Universite de Grenoble, France); Flipot, A. Jean. Ind. At., 9: 83-9(1965). (In French)

Certain manipulations of highly reactive metals and, in particular, certain processes for fabricating combustible elements must be performed in an argon atmosphere extremely pure. The practical possibilities of an installation for the purification of argon, based on the chemical combination of the impurities are described. The economy effectuated by replacing the alloy of titanium and zirconium (50-50 atomic weight) by titanium sponge is stressed. The influence of the temperature of the titanium charge on the elimination of the nitrogen is also examined. The operating safety of the installation has been scrupulously perfected. (auth)

38770 ANION-EXCHANGE BEHAVIOR OF SCANDIUM, RARE EARTHS, THORIUM AND URANIUM IN MAGNESIUM NITRATE SOLUTION. Hamaguchi, Hiroshi; Hikawa, Ikuko; Kuroda, Rokuro (Tokyo Univ.). J. Chromatog., 18: 556-63(June 1965).

Adsorption of scandium, rare earths, thorium, and uranium in magnesium nitrate solution was demonstrated with a strongly basic anion exchanger. The adsorbability of these metals increased sharply with increasing concentration of magnesium nitrate solution. Fractionation of the lighter rare earths was possible in a 3M magnesium nitrate solution. The distribution coefficients were found to decrease within the cerium group, reaching a minimum near gadolinium, to increase slightly with further increases in atomic number. Sufficiently large diffferences in adsorbability to permit the separation of scandium and thorium/or uranium were found and selected pairs of the lighter rare earths were also found to be separable with relatively short columns. (auth)

38771 ION EXCHANGE IN FUSED SALTS. I. CHROMATOGRAPHIC BEHAVIOUR OF VARIOUS METAL CATIONS IN FUSED SALTS ON γ-ALUMINA AND SYNTHETIC INORGANIC ION EXCHANGE MATERIALS. Alberti, G.; Conte, A.; Allulli, S. (Universita, Rome). J. Chromatog., 18: 564-71(June 1965).

Chromatographic adsorption on γ alumina and synthetic inorganic ion exchange materials of various metal cations dissolved in a fused lithium nitrate–potassium nitrate eutectic was studied. The results obtained seemed to confirm that metal ions are adsorbed by ion exchange, although other mechanisms, e.g., oxide precipitation, or formation of insoluble phosphates, are possible. A relationship between the adsorption of the metal ions tested, the solubility of their oxides and the ionic potentials was found. Some conflicting results of other authors are discussed. (auth)

38772 PROMETHIUM PREPARED IN PURE FORM. Droessmar, F. Naturw. Rundschau, 18: 158(Apr. 1965). (In German).

Pure Pm was prepared, starting with a sample of 60 mg ^{147}Pm mixed with 50 mg Sm, 40 mg Nd, and 7 mg ^{241}Am. The other elements were separated by ion exchange, Pm was precipitated with HF as the rose-violet trifluoride (PmF_3), washed, centrifuged, and dried for 48 hr over P_2O_5. The fluoride was then placed in the inner part of a Ta crucible with ten times its weight of Li in the outer part, and heated in high vacuum to 1090°C. On cooling for 1 hr Pm fused with Ta wires separated. The history of early attempts to isolate this element from natural sources and to prepare it from Pr and Nd is given, together with an account of the successful preparation. The physical properties of the material and its isotopes are reviewed and estimates of production (USA, 1959: 650 g) are presented. Several examples of its possible use are envisioned: in control instruments in aircraft; for thickness measurements in the metal, plastic, and cigarette industries; and also in batteries in satellites and space probes. (BBB)

38773 REMOVAL OF TRITIUM FROM ^3He BY ADSORPTION ON CHARCOAL. Akhtar, Sayeed; Smith, Hilton A. (Univ. of Tennessee, Knoxville). Rev. Sci. Instr., 36: 1250-1(Aug. 1965). (TID-21637)

The possibility of removing tritium from ^3He by passage over activated charcoal cooled to −196°C was investigated. The results indicate that the tritium content can be reduced to a level at least ten times as low as that obtained by other techniques. (D.C.W.)

38774 SEPARATION OF STRONTIUM FROM YTTRIUM ($^{90}Sr/^{90}Y$) USING ANION EXCHANGER SULFATE. Ziegler, Max; Rittner, Walter (Universitaet, Gottingen, Ger.). Z. Anal. Chem., 211: 170-3(1965). (In German).

Selective "precipitating sorption" of strontium as $SrSO_4$ on Dowex-I-sulfate in a column operation, using aqueous methanol solution (1 : 1), permits the isolation of pure ^{90}Y, produced by the beta decay of ^{90}Sr. The effect of separation may be controlled by determination of the half life of ^{90}Y. Taking into account the velocity of formation, ^{90}Y can be obtained several times depending on the length of the ion exchange column. (auth)

38775 PAPER ELECTROPHORETIC SEPARATION OF THORIUM, PROTACTINIUM, AND URANIUM. Merz, E. (Kernforschungsanlage, Juelich, Ger.). Z. Anal. Chem., 211: 331-4(1965). (In German).

A simple electrophoretic procedure for the separation and determination of thorium, protactinium, and uranium

is described, based on the different migration velocities of the oxalate complexes of the three elements in an electric field. Their quantitative separation was achieved using a 0.12M ammonium oxalate electrolyte applying a potential gradient of 16 v/cm for two hr. The anionic migration of the metal oxalate complexes increased in the order Th, Pa, and U. (auth)

38776 METHOD FOR DECONTAMINATING NUCLEAR FUELS. (to U. S. Atomic Energy Commission). British Patent 997,423. July 7, 1965. Priority date June 19, 1963, United States.

A process is described for the separation and decontamination of neutron-irradiated fuel values from an aqueous acidic solution containing the values together with ruthenium in the form of nitrosylruthenium complexes by contacting the aqueous solution with an organic solvent or cation exchange material to preferentially extract at least one of the nuclear fuel values. At least one mole of barbituric acid per mole of ruthenium is added to the solution to maintain the Ru in solution, and the solution is digested for at least one hour at a temperature between 90 to 100°C prior to extraction. The process is particulary applicable to the separation of U and Pu from Ru by the extraction of the U or Pu values with TBP. (B.L.M.)

38777 PLANT FOR LIQUID-LIQUID EXTRACTION BY THE COUNTER-CURRENT FLOW PROCESS. Faugeras, Pierre; Minart, Paul; Pouchot, Pierre; Talmont, Xavier. (to Commissariat a l'Energie Atomique). British Patent 997,712. July 7, 1965. Priority date May 19, 1961, France.

A plant for liquid-liquid extraction by counter-current flow process includes a number of stages arranged in a cascade. Each stage includes an ejector nozzle that simultaneously effects the mixing of the liquid phases and the injection of these phases into a separator after they are mixed. The separators constituted by a cyclone are fitted with automatic means to regulate the outflow rates of the fluid. The plant is provided with means for putting at least one of the fluids that are fed into the ends of the plant under a pressure that is sufficient to provide all the energy necessary for the operation of the ejector nozzles. The ejector nozzle and the cyclone combination provide rapid mixing and separating of the phases, of the order of one minute for both operations, that is very advantageous from the point of view of criticality and of limiting the degradation of the solvent under the action of radiation from an irradiated solution being treated. The use of the ejector nozzle both as a mixer and as a driving element eliminates the need for any movable stirring device and all moving machinery such as circulation pumps usually necessary at each stage. (B.L.M.)

38778 METHOD OF REPROCESSING A NITRIC ACID SOLUTION CONTAINING MOLYBDENUM, CESIUM, AND ZIRCONIUM COMPOUNDS AFTER EXTRACTION OF URANIUM AND PLUTONIUM FROM IRRADIATED URANIUM–MOLYBDENUM ALLOYS. Lefrevre, Jean; Raggenbass, Andre (to Commissariat a l'Energie Atomique). German Patent 1,189,536. Mar. 25, 1965. Priority date Mar. 30, 1962, France.

The solution was concentrated by evaporation in succeeding steps whereby phosphoric acid was continuously added and the amount of nitric acid was kept constant at 3N. The precipitate obtained was separated and treated with a base until the Cs component was dissolved. The Zr component remaining in the form of insoluble zirconium hydroxide, was separated. The Cs solution was acidified by cesium phosphorus molybdate precipation. (Gmelin Inst.)

ENGINEERING

General

Refer also to abstracts 39270 and 40203.

38779 (LA-DC-7158) BEHAVIOR OF PERLITE IN COMPRESSION. Novak, J. K. (Los Alamos Scientific Lab., Univ. of California, N. Mex.). [nd]. Contract W-7405-eng-36. 23p. (CONF-650802-4). Dep. mn; CFSTI, $1.00 cy, $0.50 mn.

From Cryogenic Engineering Conference, Houston, Tex.

The possibility of compaction of insulation due to thermal cycling has become a problem for designers of large perlite-insulated dewars. A qualitative study of perlite fluidity was done, and the results indicated that perlite insulation will compact rather than flow. A model was proposed for describing this compaction. Measurements were made of the pressure required to compress perlite in closed cylinders, and these results were applied to the compaction model to calculate an upper limit on the forces and pressures to be expected in large perlite insulated dewars as a function of the number of thermal cycles experienced. (auth)

38780 (LA-DC-7206) STATUS REPORT ON THEORY AND EXPERIMENTS ON HEAT PIPES AT LOS ALAMOS. Cotter, T. P.; Deverall, J.; Erickson, G. F.; Grover, G. M.; Keddy, E. S.; Kemme, J. E.; Salmi, E. W. (Los Alamos Scientific Lab., Univ. of California, N. Mex.). [1965]. Contract W-7405-eng-36. 12p. (CONF-650908-1). Dep. mn; CFSTI, $1.00 cy, $0.50 mn.

From International Conference on Thermionic Electrical Power Generation, London.

A survey of the experiments on the characteristics of heat pipes is presented. The status of corrosion studies at elevated temperatures is reviewed. A quantitative engineering theory for the design and performance analysis of heat pipes is given. (auth)

38781 (N64-25903) ELECTROMAGNETIC ALKALI METAL PUMP RESEARCH PROGRAM. Quarterly Progress Report No. 3, December 27, 1963-March 27, 1964. Verkamp, J. P. (ed.) (General Electric Co., Cincinnati, Ohio. Space Power and Propulsion Section). May 22, 1964. Contract NAS 3-2543. 129p. (NASA-CR-54036) CFSTI, $10.10 cy.

Activities in programs to determine the feasibility of using electromagnetic (EM) pumps in space electric powerplants, to establish the bases for selecting pumps for specific applications, and the bases for the design of EM pumps applicable to space powerplants, to select pumps for construction and testing, and to establish a test program for the selected pumps are reported. Program results indicate that the design approach being developed will produce pumps with about one-tenth the weight of previous pumps, and that a boiler feed EM pump for the turboelectric powerplant could be competitive in weight with a canned motor-jet injector pump for the same application. A single-phase induction pump was developed that is particularly well suited to high-temperature primary coolant application. (auth)

38782 (ORNL-TM-1170) MOTION OF PARTICLES IN FLUIDIZED BEDS AND IMPLICATIONS FOR THE PREPARATION OF COATED NUCLEAR FUEL PARTICLES. Pilloton, R. L.; Carpenter, J. A. (Oak Ridge National Lab., Tenn.). Aug. 1965. Contract W-7405-eng-26. 27p. Dep. mn; CFSTI, $2.00 cy, $0.50 mn.

The improvement of the fluidized-bed coating of nuclear fuel particles as a step toward the economical refabrication of fuel in the Thorium-Uranium Recycle Facility is being sought. The motion of particles in glass apparatus that simulated the geometry of coating equipment when the particles were fluidized by air introduced through single or multiple inlets, was observed. A constant pattern of particle circulation with an upward flow in the center and a downward flow at the periphery was found. Since in actual coating furnaces particles would be coated mostly at the lower part of the bed where the coating gas is introduced, the cycling time of the particles is an indication of the coating efficiency. Therefore, the velocity of the particles and the resulting cycling time were measured under various conditions. The downward particle velocity at the periphery increased with increasing gas flow and decreased with increasing bed charges. Furthermore, there was an optimum ratio of central to peripheral gas flow in the case of multiple-inlet gas distributors. These observations can be used to improve the design of coating furnaces. An apparatus was designed to determine the height of a fluidized bed in a glass column through the attenuation of a beam of light. (auth)

38783 HIGH-FREQUENCY SKYWAVE COMMUNICATION SYSTEM PERFORMANCE IN A NUCLEAR ENVIRONMENT. Barrios, Arthur A. (Communication Systems Inc., Paramus, N. J.). IEEE (Inst. Elec. Electron. Engr.) Trans. Military Electron., 9: 125-30 (Apr. 1965).

A model is described which can be used to predict the performance of h-f skywave circuits in a nuclear environment. The model may aid communication planners and designers to predict the expected magnitudes and durations of the h-f degradation parameters. Probability distribution curves and nomographs, derived from disturbed ionosphere data, include signal-to-noise ratio, reliability and distance, teletype error rate, multipath fading, and time parameters. The nuclear environment considered is that existing after a high-altitude nuclear burst. The degree of severity and duration of this environment are determined by various combinations of burst yields and altitudes. Although much attention has been paid to the immediate blackout effects caused by the high ionization levels induced by early nuclear radiations, little study has been made of the delayed degradation effects on h-f system performance for various intervals. The effects of h-f system parameter degradation are examined in terms of a natural, localized, ionospheric disturbance that is similar to that produced by a nuclear burst. While the mechanisms that produce natural and nuclear ionospheric disturbances are somewhat different, the end effects on the propagation parameters can be assumed to be the same in magnitude. The degradation parameters are defined within the context of statistical formats. Using these formats, the performance of h-f radio circuits in an area of interest are predicted in terms of circuit reliability, expected degradation time, and performance levels. The model presented is representative of a wide range of nuclear disturbance possibilities and should be useful in a computer simulation program. (BBB)

38784 PROCEEDINGS OF THE CONFERENCE ON THE ROLE OF SIMULATION IN SPACE TECHNOLOGY, AUGUST 17-21, 1964 [Blacksburg, Va.]. Virginia Polytechnic Institute Engineering Extension Series Circular No. 4, Parts A, B, C, and D. Virginia Polytech. Inst., Eng. Ext. Ser. Circ. Pts. A, B, C, D, ([1964]). (CONF-640806(Pts. A, B, C, D)).

Twenty-five papers are presented on the role of simulation in space technology. Topics covered include: vacuum technology, electromagnetic radiation in space, ionizing particle radiations effects and simulation consideration, needs for meteoroid penetration scaling laws and the potentials of simulation techniques, reasons for simulation of magnetic fields and methods available, hypersonic flight simulation, convective and radiative heat transfer during reentry and advanced techniques for their simulation, evaluation of materials in entry heating simulation, problems in simulating detection of space vehicles and communication with them during atmospheric entry, flight reentry experiments, computers for simulation of space vehicle systems, existing and planned simulators for space research, visual and motion simulation techniques,

dynamic simulators for tests of space vehicle altitude control systems, structural dynamics, principles and practices for simulation of structural dynamics of space vehicles, models for orbiting effects of ground winds on space vehicles erected on the launch pad, simulation of structural dynamics of space vehicles during launch, simulation of the structural dynamics of spacecraft during lunar landing, simulation in aeronautical and space technology, physiological aspects of sensory deprivation, effect of low-gravity on physiological processes, effect of high-gravity on physiological performance, and closed atmospheres. Separate abstracts were prepared for two papers. (F.J.H.)

For abstracts of individual papers see: 38842 and 39059.

38785 IMPROVEMENTS IN FLUID SEALING MEANS BETWEEN CO-AXIAL TUBES. (to Commissariat a l'Energie Atomique). British Patent 996,508. June 30, 1965. Priority date Nov. 13, 1962, France.

A sealing means adapted to prevent the flow of a fluid under pressure in the annular space formed between two coaxial tubes capable of being displaced axially relatively to one another is particularly applicable to use between the inner guide tube of a reactor and an outer tube that is filled with a gas under pressure. A sealing-tight sleeve made of an elastic material is fixed within the annular space to one of the tubes and comprises upstream, in relation to the direction of flow of the gases in the tubes, a convexly or concavely barrelled portion that bears elastically on the other tube. The barrelled portion slides freely on the tube on which it bears. The zones at which the sleeve is fixed on the first tube and bears on the second tube extend over the entire periphery of the sleeve. A centering device provided in the sealing means consists of a circumferential bead projecting from the surface of one tube and capable of sliding in contact with the surface of the other tube. (B.L.M.)

Applications of Nuclear Explosions

Refer also to abstract 39889.

38786 (LA-DC-7111) PRODUCTION OF HEAVY NUCLIDES BY MULTIPLE NEUTRON CAPTURE IN NUCLEAR EXPLOSIONS. Bell, George I. (Los Alamos Scientific Lab., Univ. of California, N. Mex.). [1965]. Contract W-7405-eng-36. 5p. (CONF-650706-18). Dep. mn; CFSTI, $1.00 cy, $0.50 mn.

From International Conference on the Study of Nuclear Structure with Neutrons, Antwerp.

The production of heavy nuclides by neutron capture in nuclear explosions is discussed. Results are reported in a table for a neutron energy of 20 kev where the s and p wave contributions to capture are comparable. In the table one observes even-odd fluctuations for each Z chain. Averaging over even-odd pairs, one sees that (1) the Np cross sections are largest followed by Pa and U in that order, and (2) the cross sections for each Z decrease as A increases. (M.O.W.)

38787 (PNE-102F) ISOTOPE PROGRAM. Final Report. Nathans, Marcel W. (Lawrence Radiation Lab., Univ. of California, Livermore). Jan. 1965. Contract W-7405-eng-48. Project GNOME. 120p. Dep. mn; CFSTI, $4.00 cy, $0.75 mn.

The purpose of the isotope program in Project Gnome was to study the distribution and the disposition of a number of nuclides following a nuclear detonation in a salt medium as well as the means by which those nuclides might be recovered. The results of this study are to be applicable to a future experiment in which one or more useful isotopes are to be produced. The results of gas and water analyses show that less than one percent of the tritium originally introduced was present in the condensable portion (as HTO), the rest being gaseous. Water leaching of solid samples removes a large fraction of alkali and alkaline earth fission products, but less than a few tenths of a percent of the heavy-element alpha activity. The latter is solubilized with varying efficiency by strong acids. Hydrochloric and nitric acids are about equally effective, but sulfuric acid much less so. The leaching efficiency is primarily determined by the strength of the acid, the acid-to-sample ratio, and the duration of contact. Kinetic studies show that at least two rate laws are simultaneously obeyed, suggesting that alpha activity is associated with at least two chemical species. Although a good correlation between the plutonium and iron contents of the samples was established, iron is not the primary cation with which plutonium is associated. The association is more likely to be with olivine-type minerals, $M^{II}_2SiO_4$, which are formed from the interaction of the impurities in the medium with each other and with the contents of the shot room. Fractionation of fission products and several of the heavy elements has been considerable. Some of the fractionation data have made it possible to reconstruct an approximate time sequence of events. (auth)

38788 (PNE-501F) STEM DESIGN AND SHOTCRETE, GROUT, AND CONCRETE SUPPORT. Project Pre-SCHOONER. Saucier, Kenneth L. (Army Engineer Waterways Experiment Station, Vicksburg, Miss.). Nov. 1964. Contract AT(29-2)-752. 50p. Dep. mn; CFSTI, $0.50 cy, $0.50 mn.

Project Pre-SCHOONER consisted of four 20-ton chemical-explosive detonations in hard, dry rock at scaled depths of burst of 135, 160, 185, and 210 ft/kt$^{3.4}$. The primary purpose of the project was to increase the knowledge of crater dimensions in hard, dry rock as a function of depth of burst and type of explosive. A description is given of the following work performed for the project: (a) the design and placement of grout mixtures used in grouting satellite holes surrounding each ground zero location, (b) the design and supervision of the placement of a shotcrete mixture used in lining the walls of each of the shot cavities, and (c) the design and supervision of the placement of a concrete mixture used in stemming the access holes to each of the shot cavities. (auth)

38789 (PNE-601F) APPARENT CRATER STUDIES. Spruill, Joseph L. (Army Engineer Nuclear Cratering Group, Livermore, Calif.). Mar. 1965. Project DUGOUT. 66p. Dep. mn; CFSTI, $3.00 cy, $0.75 mn.

Dimensions and geometry of the Dugout crater, produced by the detonation of a row of five 18,144-kg nitromethane charges in basalt, were analyzed. The linear portion of the crater was 41.6 meters wide and 10.7 meters deep, 36% wider, and 53% deeper than the Pre-Schooner Alfa crater, which was produced by the detonation of an identical charge at the same depth. Lips on the sides of the crater were massive, and were about twice as high as those of the Alfa crater; on the ends of the crater the lips were slightly smaller than the Alfa crater lip. The volume per charge of the linear section of the crater was 70% greater than the volume of the Alfa crater. The greatest range of the rock missiles perpendicular to the row of charges was 2.5 times the greatest missile range from the Alfa detonation. To the ends of the row, rock missile ranges were about the same as for the Alfa detonation. The average cross section of the linear section of the Dugout crater was a hyperbola. Factors for the enhancement in row charge crater dimensions over those of the comparable single charge crater were generally larger than those developed from the Pre-Buggy II row charges in alluvium. (auth)

38790 (PNE-608F) CLOSE-IN AIR BLAST FROM A ROW CHARGE IN BASALT. Vortman, L. J. (Sandia Corp., Albuquerque, N. Mex.). May 1965. Contract [AT (29-1)-789]. Project DUGOUT. 72p. Dep. mn; CFSTI, $3.00 cy, $0.75 mn.

Close-in air blast measurements were made on the Dugout shot (a row of five 18,000-kg high-explosive charges placed 17.9 meters below the surface in basalt). Major constituents of the blast wave were the ground-shock-induced pulse and the pulse from venting gases. The ground-shock-induced pulse was the dominant one at all stations. The pulse from venting gases was superimposed on the negative phase following the ground-shock-induced

pulse; as a result, the positive pressures were less than they otherwise would have been. The ground-shock-induced overpressures perpendicular to the row were slightly more than twice those along the axis of the row. Perpendicular to the row, they were 3.3 times single charge values but only 1.4 times single charge values off the end of the row. A third constituent of the blast wave precedes the ground-shock-induced pulse. Its timing indicates it is associated with a seismic wave. A subsequent experiment has shown that air pressure induced by the ground wave was measured. (auth)

38791 (TEI-857) POTENTIAL APPLICATIONS OF NUCLEAR EXPLOSIVES IN DEVELOPMENT AND MANAGEMENT OF WATER RESOURCES — PRINCIPLES. Piper, Arthur M.; Stead, Frank W. (Geological Survey, [Menlo Park, Calif.]). Mar. 1965. 132p. Dep. mn; CFSTI; $4.00 cy; $1.00 mn.

Underground nuclear explosions can be used to modify the natural environment of water in such a way that water supplies are increased. After a discussion of the characteristics of such explosions, their effects on water environments are considered. An attempt is made to develop general criteria by which favorable areas and sites can be identified. (D.L.C.)

Facilities and Equipment

Refer also to abstract 39113.

38792 (JUL-250-RW) DISASSEMBLY AND SAMPLING OF GRAPHITE BALL FUEL ELEMENTS. Erfurth, H.; Stockschlaeder, F.; Ullrich, M. (Kernforschungsanlage, Juelich (West Germany). Institut fuer Reaktorwerkstoffe). Apr. 1965. 14p. Dep. mn.

In the scope of the THTR postirradiation examination program, irradiated ball-type fuel elements must be examined and prepared for advanced experiments. This requires a controlled breaking-open of the graphite shell for taking samples of definite size and dimensions from the inner and outer parts of the fuel element. Two special pieces of equipment are described which were developed and constructed for this purpose. They emphasize avoiding contamination of the neighboring equipment of the box, and diminishing the inevitable cross-contamination of the surfaces of the samples themselves by means of a suitable ventilation procedure. (auth)

38793 (JUL-251-RW) DESIGN AND PROCEDURES FOR HANDLING HIGH-LEVEL ALPHA-GAMMA BOXES AT THE LABORATORY FOR RADIOACTIVE SOLIDS AT KFA JUELICH. Herren, M. (Kernforschungsanlage, Juelich (West Germany). Institut fuer Reaktorwerkstoffe). Apr. 1965. 20p. Dep. mn.

Four concrete hot cells with sufficient shielding for 10^4 curies of a 1 Mev gamma emitter are designed for experiments on humidity-sensitive, very dusty, or alpha-gamma emitting reactor fuel materials. A discussion is presented of problems arising by (1) transfer operations of experimental materials and wastes into and out of boxes, and of boxes themselves into and out of the cells; (2) exchange, repair and maintenance of box equipment, and (3) plastic bagging techniques. (auth)

38794 (JUL-252-RW) IMPROVING ECONOMY WITH THE USE OF STANDARDIZED, MOVABLE, IN-CELL BOXES, AND THE DECONTAMINATION OF THEIR EQUIPMENT AT THE CENTRAL DECONTAMINATION FACILITY. Brinkmann, G.; Schenk, W.; Schulz, W.; Stockschlaeder, F. (Kernforschungsanlage, Juelich (West Germany). Institut fuer Reaktorwerkstoffe). Apr. 1965. 15p. Dep. mn.

When a nuclear research center has several hot laboratories, all of which use in-cell boxes, it is desirable to standardize the cells and boxes as far as possible in order to achieve maximum economy, efficiency, and convenience. A discussion is presented of the principles of planning which are laid down at KFA-Jülich, in connection with the construction of several plants. The advantages and the conditions which must be observed during planning are described. The decontamination facility is discussed as an important part of the entire box-exchange system. In addition are described some of the more interesting points of equipment and techniques, especially a new manipulator exchange technique. (auth)

38795 (JUL-253-RW) DISASSEMBLY OF TEST IRRADIATIONS AND FUEL ELEMENTS IN SMALL CAST IRON, ALPHA-GAMMA-CELLS AND THEIR SUBSEQUENT HANDLING. Schmiddem, P. J.; Stephan, W.; Zamja, K. (Kernforschungsanlage, Juelich (West Germany). Institut fuer Reaktorwerkstoffe). Apr. 1965. 20p. Dep. mn.

Three fairly small alpha-gamma cells, made from cast iron blocks, are being built for disassembling of test irradiations and fuel èlements. Aside from disassembly equipment, the cells will enable the usual critical evaluation of the performance of the fueled section. The cells use gas-tight stainless steel boxes with double-cover alpha-gamma locks between boxes and to the outside. Special gas-tight, extended reach manipulators of a shortened design with a shielded through-wall plug are used. These manipulators are gas-tight and do not require plastic bootings for sealing to the boxes. Some equipment (periscope, dimensional measurement, gamma-scan) is of special design in order to save space in the narrow boxes. (auth)

38796 ARC HEATERS FOR PLASMA CHANNELS. Peters, Th. (DVL-Institut fuer Plasmadynamik, Stuttgart). Raumfahrtforschung, 9: 1-6(Jan.-Mar. 1965). (In German).

Different types of arc heaters for application in plasma-wind tunnels are described. Most of the arc heaters produce jets with non-uniform temperature profiles. To obtain more uniform profiles, a plenum chamber is usually needed. As this chamber has to be cooled intensively, high cooling losses occur. To avoid these losses, experiments are discussed in which the arc obtains turbulent motion due to the application of an external alternating magnetic field. Furthermore, an arc discharge is described in which the self-magnetic acceleration effect inside an expanding supersonic plasma jet becomes effective. (auth)

38797 IMPROVEMENTS IN OR RELATING TO CONVEYOR SYSTEMS FOR PACKAGE IRRADIATION PLANTS. Grant, John (to United Kingdom Atomic Energy Authority). British Patent 996,775. June 30, 1965. Filed Nov. 12, 1962.

A monorail conveyor system suitable for use in a package irradiation plant includes two discrete substantially parallel tracks with carriers suspended from the tracks. Means are provided for moving the carriers at spaced intervals along the tracks. A further section of conveyor track is transversely movable relative to the fixed track, and means are provided for aligning the movable track with either fixed track. A first rotatable arm abuts a carrier during part of the revolution of the arm, and a second rotatable arm abuts the movable track during part of the revolution of the arm. The arms and the carrier moving means are interconnected so that a carrier is transferred from one fixed track to the movable track by the rotation of the first arm, the movable track is moved from alignment with one fixed track to the other track, and the carrier is transferred from the movable track to the other fixed track by the continued rotation of the first arm. Rotation of the second arm serves to return the movable track into alignment with the fixed track so that the spacing of the carriers on the parallel tracks remains uniform. An endless chain comprises the moving means for the carriers. (B.L.M.)

38798 CONTROL APPARATUS FOR HANDLING DEVICE. Moulin, Maurice (to Commissariat a l'Energie Atomique). British Patent 997,064. June 30, 1965. Priority date July 18, 1962, France.

A control apparatus is provided for a handling device in which the system for the attachment and detachment of the load is provided with a safety program and is driven by a cable operated by a winch. The apparatus includes, between the winch and the handling device, a system of control of a succession of raisings and lowerings of the cable according to the cycles of the program. Means are also provided for control of stopping the winch and initiation of the program.

The end of the program causes the starting of the winch, and the program can be stopped in a specific zero position to cause the restarting of the winch. The program control system includes a link-crank system for the successive liftings and lowerings of the handling device according to the number of cycles in the program. (B.L.M.)

38799 DEVICE FOR MEASURING THE RADIOACTIVITY OF A PLURALITY OF INDIVIDUAL SAMPLES. Packard, Lyle E.; Scott, William; Mason, Emerson B.; Soderquist, Charles E. (to Packard Instrument Co.). German Patent 1,192,329. May 6, 1965. Priority date Apr. 10, 1959, United States.

The mechanical construction of the sample changer is described. It consists of a circular plate on which the samples are arranged in successive positions along a circular arc. In order to reduce the background the counter is mounted in the center of the circular plate, which is rotated about its central, circular axis. A transport member rotated about an axis vertical to the axis of the sample holder between two end positions is provided for transferring the samples successively from the circular sample holder to the counter. (Gmelin Inst.)

38800 TURNTABLE-TYPE DRIER FOR GRANULAR MATERIAL. Plumb, Geoffrey Richard; Hadfield, Timothy J. (to United Kingdom Atomic Energy Authority). U. S. Patent 3,193,945. July 13, 1965. Priority date Mar. 28, 1961, Great Britain.

A turntable type drying apparatus is described for particular application to the drying of radioactive and/or toxic materials. The material may be fed to the turntable as powdered, granular, or gelatinous material in solid or slurry form and is fed to the table in a first position and removed from the table at a second position angularly spaced from the first position. A sealed casing envelopes the table with a series of windows of heat transmitting material positioned in the upper part of the casing. The windows are so spaced about the circumference of the table between the first and second positions to direct heat from infrared heaters disposed above the casing through the windows to dry the material on the table. A roller that is rotatable about its axis is disposed between the table and the feeding means to distribute the material fed to the table. Scrapers are provided between the casing and the faces and side edges of the table to divert the dried material to the removal means. (B.L.M.)

Heat Transfer and Fluid Flow

See also PHYSICS — General.

38801 (ACNP-65004) STEAM SEPARATION TECHNOLOGY. Quarterly Progress Report, April 1, 1965–June 30, 1965. (Allis-Chalmers Mfg. Co., Milwaukee, Wis. Atomic Energy Div.). July 9, 1965. Contract AT(11-1)-1186. 75p. (EURAEC-1417). Dep. mn; CFSTI, $3.00 cy, $0.75 mn.

Work Performed Under United States–Euratom Joint Research and Development Program.

Steam–water testing of the upcomer separator verified the performance predicted from the air–water tests. Using the separator cross sectional area of 1.75 sq ft, a maximum steam release rate of 50,000 lb/hr was achieved. At a water flow rate of 1900 gpm (approximately 780,000 lb/hr total) the pressure drop was slightly less than 2 feet of water and carryunder was less than 2 per cent by volume. Higher steam and water flow rates could probably have been attained if more driving head was available. Separator operation was stable and satisfactory in all respects. Testing of the small horizontal separator further verified the analytical technique for calculating separating length. It also demonstrated that the centrifugal separator can be operated satisfactorily in the horizontal position. (auth)

38802 (APED-4827) MAXIMUM TWO-PHASE VESSEL BLOWDOWN FROM PIPES. Moody, F. J. (General Electric Co., San Jose, Calif. Atomic Power Equipment Dept.). Apr. 20, 1965. 30p. (65APE4).

A theoretical model is proposed for maximum two-phase flow from a constant area, adiabatic pipe with friction. Graphs are given for maximum steam/water flow rate in terms of pipe geometry and entrance stagnation properties. The proposed model is used to obtain theoretical blowdown transients from saturated water systems initially at 1000, 1250, and 2000 psia. Estimated pipe flow rates and blowdown transients are compared with steam/water data. Reasonable agreement is shown. (auth)

38803 (BAW-1280-26) SODIUM-HEATED STEAM GENERATOR DEVELOPMENT. Progress Report No. 24. Probert, Paul (Babcock and Wilcox Co., Barberton, Ohio. Boiler Div.). Apr. 1965. Contract AT(11-1)-1280. 54p. Dep. mn; CFSTI, $3.00 cy, $0.50 mn.

Some background information is presented on the various phases of the work, and the present status of each phase is summarized. The preliminary design of the Full-Size Steam Generator is complete. The preliminary design of the Prototype Steam Generator is approximately 95% complete. The analysis of sodium-water reaction problems in B&W Full-Size and Prototype Steam Generator is reported. (D.L.C.)

38804 (BNL-8185) NUMERICAL CONTINUATION BACKWARDS IN TIME FOR SOLUTIONS OF THE HEAT EQUATION AND NUMERICAL CONTINUATION OF SOLUTIONS OF LAPLACE'S EQUATION IN A HALF-SPACE. Cannon, J. R. (Brookhaven National Lab., Upton, N. Y.). [nd]. Contract AT(30-2)-Gen-16. 28p. Dep.(mn); $2.00 (cy), 1(mn) CFSTI.

A numerical scheme using explicit solutions of the heat equation is used to produce continuation, backward in time, of solutions of the heat equations in an infinite space of arbitrary dimension. Under certain a priori restrictions on the class of solutions, explicit a priori and a posteriori estimates of error are given. As a corollary of the analysis of the heat equation, numerical continuation of solutions of Laplace's equation in the half-space is also carried out. (T.F.H.)

38805 (BNWL-C-3) HANFORD STUDIES EXECUTED FOR THE USAEC-AECL COOPERATIVE PROGRAM ON DEVELOPMENT OF HEAVY WATER MODERATED POWER REACTORS. Monthly Progress Report, December 1964. Albaugh, F. W. (Battelle-Northwest, Richland, Wash. Pacific Northwest Lab.). Jan. 14, 1965. Contract AT(45-1)-1830. 4p. Dep. mn; CFSTI, $1.00 cy, $0.50 mn.

A summary is presented of a brief study of fluid mixing in multirod bundles at burnout. The burnout data for 19-rod bundles were compared with data obtained for various test sections. Burnout curves were established, and a correlation of enthalpy influenced by mixing was derived for 19-rod bundles. It is concluded that small rod spacing restricts flow mixing and leads to low burnout heat fluxes. (D.L.C.)

38806 (GEAP-4908) TRANSITION BOILING HEAT TRANSFER PROGRAM. Tenth Quarterly Progress Report, April–June 1965. (General Electric Co., San Jose, Calif. Atomic Power Equipment Dept.). July 1, 1965. Contract AT(04-3)-189. 33p. (EURAEC-1443). Dep. mn; CFSTI, $2.00 cy, $0.50 mn.

Work Performed Under United States–Euratom Joint Research and Development Program.

A test series was carried out to determine the effect of oscillating the inlet water flow to the heated section on transition boiling. Test conditions were at 0.5 and 1.0 million lb/h-ft^2, with flow variations of 0, 2.5, 7.5, and 15% at four frequencies from 0.25 to 3.0 cps. The size of the transition boiling region was increased by as much as seven times that for steady flow. Transition boiling temperature fluctuations were also larger and occurred at the forcing frequency. It is concluded that transition boiling heat transfer behavior is dependent upon the magnitude of flow variations. A sequence of motion picture frames taken of a steam-blanketed heated rod by means of its own incandescent light is included. (auth)

38807 (NYO-2404-70) EFFECTS OF ELECTRICAL FIELDS ON BOILING HEAT TRANSFER. Quarterly Progress Report, January 1–March 31, 1965. Nichols, Charles

R.; Spurlock, Jack M.; Markels, Michael Jr. (Atlantic Research Corp., Alexandria, Va.). Contract AT(30-1)-2404. 29p. Dep. mn; CFSTI, $2.00 cy, $0.50 mn.

Additional tests were conducted on the forced convective boiling of water at pressures of 115 and 1500 psia and a-c fields of up to 2000 v. The results at 115 psia and 2000 v indicate improvements in burnout heat flux over that for 1000 v. Some of the tests at 115 psia gave burnouts with and without hydrodynamic instabilities. (D.L.C.)

38808 (NYO-3114-8) TWO-PHASE FLOW AND BOILING HEAT TRANSFER. Interim Report. THE RISE VELOCITY OF CYLINDRICAL BUBBLES IN INCLINED TUBES. Runge, D. E.; Wallis, G. B. (Thayer School of Engineering, Dartmouth Coll., Hanover, N. H.). June 1965. Contract AT(30-1)-3114. 33p. (EURAEC-1416). Dep. mn; CFSTI, $2.00 cy, $0.50 mn.

Work Performed under United States–Euratom Joint Research and Development Program.

A study was made of the effects of tube inclination on the buoyant bubble rise velocity through stagnant liquids. The effects of bubble length and tube material were determined for glycerin and water. The ratio of V_α/V_∞ vs α (degrees from vertical) is plotted for various ranges of inverse viscosity numbers and Eötvös numbers. The possible correlation of the results is considered. (D.L.C.)

38809 (NYO-3304-3) INVESTIGATION OF BOILING FLOW REGIMES AND CRITICAL HEAT FLUX. Final Report. Dynatech Report No. 517. Suo, M.; Bergles, A. E.; Doyle, E. F.; Clawson, L.; Goldberg, P. (Dynatech Corp., Cambridge, Mass.). Mar. 1, 1965. Contract AT(30-1)-3304. 110p. Dep. mn; CFSTI, $4.00 cy, $0.75 mn.

A program is being conducted to investigate the mechanism of the critical heat flux condition from the standpoint of flow regimes. Available data for adiabatic steam–water flow were utilized to construct a flow regime map for the anticipated test conditions. An analysis indicated that the test section should be free of system hydrodynamic instability. The experimental facility was extensively modified so that it would be suitable for obtaining flow regime and critical heat flux information. Flow regime data were obtained for an 8-foot-long, 0.4-inch-diameter heated tube at 1000 psia over a range of flow rates and inlet subcoolings. By means of an electrical resistance probe, the flow regimes of bubbly and slug flow were reasonably well delineated. These data are compared with the adiabatic predictions. Critical heat flux data were also obtained and were found to be in agreement with available data. For the entire range of test conditions, the flow was found to be stable as predicted. (auth)

38810 (RL-SA-31) PRESSURE DROP CHARACTERISTICS OF TWO ECCENTRICALLY POSITIONED ORIFICES IN SERIES. I. EFFECT OF ECCENTRICITY, SPACING OF ORIFICES AND OF THE ORIFICE TO PIPE DIAMETER RATIO (thesis). Agar, James Darrel (General Electric Co., Richland, Wash. Hanford Atomic Products Operation). June 4, 1965. Contract AT(45-1)-1350. 96p. Dep. mn; CFSTI, $3.00 cy, $0.75 mn.

Submitted to Univ. of Washington, Seattle.

This investigation was conducted to determine the pressure drop characteristics of cold water flow through two eccentrically positioned orifices in series. The system parameters of flow, orifice spacing, orifice diameter to flow channel diameter ratio, and the degree of orifice eccentricity were included in the investigation. The flow channel was limited to a 1½ inch inside diameter, stainless steel pipe. (auth)

38811 (SAN-409-24) HIGH ACCELERATION FIELD HEAT TRANSFER FOR AUXILIARY SPACE NUCLEAR POWER SYSTEMS. Quarterly Technical Report, March 1-May 31, 1965. Poppendiek, H. F.; Greene, N. D.; Sabin, C. M.; Feigenbutz, L. V.; Schwartz, P. E.; Connelly, D. J. (Geoscience Ltd., Solana Beach, Calif.). Contract AT (04-3)-409. 17p. Dep. mn; CFSTI, $1.00 cy, $0.50 mn.

Research on high-temperature liquid metals is described. Information on experimental and predicted vaporization lifetimes for potassium droplets on a heated tantalum surface is presented. Also vaporization lifetime measurements for Freon 114 drops are shown and compared to the earlier results for Freon 11. Results of an accuracy analysis for the previously reported forced flow boiling potassium conductance measurements are also presented. (auth)

38812 (UCRL-11951) AXIAL DISPERSION IN LIQUID FLOW THROUGH PACKED BEDS. Miller, Steven Frank; King, C. Judson (Lawrence Radiation Lab., Univ. of California, Berkeley). May 24, 1965. Contract W-7405-eng-48. 44p. Dep. mn; CFSTI, $2.00 cy, $0.50 mn.

Step-function injection and purging of a dilute salt tracer in water was used to measure axial dispersion for low Reynolds number liquid flow through beds of uniform sized, random packed glass spheres. The resultant data and those of several previous studies are coordinated and interpreted in terms of Reynolds number, Schmidt number, and Peclet number. (auth)

38813 (UCRL-12204, pp 48-59) FLUID AND HYDRODYNAMICS. (Lawrence Radiation Lab., Univ. of California, Livermore).

A brief discussion of each of the following is included; similarity solutions in 1-D hydrodynamics, numerical treatment of turbulent flows, Lagrange representation with time-independent mass density, numerical simulation of the earth's atmosphere, model atmosphere, evaluation of spectral versus grid methods of hemispheric numerical weather prediction, propagation of water waves on sloping beaches, a zonal two-dimensional weather calculation, and atmospheric model in FORTRAN. (M.O.W.)

38814 BURNOUT CORRELATIONS FROM THE RUSSIAN LITERATURE. Wiley, John S. Power Reactor Technol., 7: No. 3, 223-36(Summer 1964).

Burnout correlations for subcooled water in tubular and rod-cluster geometries, and for net boiling in tubular geometry, are surveyed. Results obtained by Russian, British, and American investigators are compared and evaluated. 27 references. (T.F.H.)

38815 IMPROVEMENTS IN AND RELATING TO WATER TUBE STEAM GENERATORS. Bell, Alan; Lawrence, Arthur (to Foster Wheeler Ltd.). British Patent 991,911. May 12, 1965. Filed Dec. 11, 1961.

A water tube steam generator is described in which the heating fluid circulating through the upright cylindrical shell can be the primary coolant from a nuclear reactor. The shell contains a co-axial downcomer and risers connected at their lower ends to the downcomer and communicating with a steam and water drum at the upper end of the downcomer. Each riser includes an inlet tube and an outlet tube joined by a cluster of substantially straight intermediate tubes of smaller diameter having at each end a circular or polygonal header. The clusters are distributed over the cross section of the shell so as to form an annular composite bundle closely surrounding the downcomer and occupying the greater part of the volume of the shell. If the outlet tubes of the risers are connected to an annular collecting riser surrounding the downcomer at its upper end. This arrangement contributes to the compactness of the generator, and all circulation needs can be satisfied with only one piercing of the upper end of the shell. (B.L.M.)

38816 IMPROVEMENTS IN AND RELATING TO WATER TUBE STEAM GENERATORS. Bell, Alan; Lawrence, Arthur (to Foster Wheeler Ltd.). Britsh Patent 991,912. May 12, 1965. Filed Dec. 11, 1961.

A steam generator includes a cylindrical shell through which a heating fluid that may be the primary coolant from a reactor is circulated and a steam and water drum surmounting the shell. The shell contains a co-axial downcomer and steam generator tubes in the form of risers connected at their lower ends to the downcomer and at their upper ends to an annular collecting riser surrounding the downcomer and leading to the steam and water drum. The drum may be either spherical or cylindrical in shape and contains means for separating water from the steam gen-

erated within the risers. The drum is connected with superheater tubes within the shell by an annular passage surrounding the annular riser for passage of dewatered steam to the shell. (B.L.M.)

38817 IMPROVEMENTS IN AND RELATING TO WATER TUBE STEAM GENERATORS. Bell, Alan; Lawrence, Arthur (to Foster Wheeler Ltd.). British Patent 991,913. May 12, 1965. Filed Dec. 11, 1961.

In a steam generator of the type described in Brit. Pat. 991,912, the superheater tubes line the shell, surround the steam generating tubes, receive the dewatered steam from the steam and water drum surmounting the cylindrical shell, and pass the steam downwards to a final steam outlet. The water separating means comprises centrifugal separators for separating the bulk of the water from the steam and driers for removing further water from the steam. The water seaparating means are enclosed by a baffle that defines with the drum a passage for the dewatered steam on its way to the superheating tubes. The final outlet for the steam is an extension of the tube forming the downcomer and when the downcomer is free to expand and contract independently of the shell. A flexible seal is provided between the outlet and the shell. (B.L.M.)

38818 IMPROVEMENTS IN OR RELATING TO THERMAL EXCHANGE. Le Foll, Jean; Houseaux, Oscar (to Commissariat a l'Energie Atomique). British Patent 997,664. July 7, 1965. Priority date July 6, 1960, France.

A heat exchange apparatus includes a tubular member arranged to be disposed in a flow of cooling fluid and provided with a number of external heat-exchange fins of substantially square cross section. Each fin is disposed at an angle to the longitudinal axis of the member and defines elementary channels between the fins. Each fin is provided with a fluid deflector at the mid-point of at least one side of the square. (B.L.M.)

38819 IMPROVEMENTS IN OR RELATING TO THERMAL EXCHANGE. (to Commissariat a l'Energie Atomique). British Patent 997,665. July 7, 1965. Priority date July 6, 1960, France.

A heat exchanger apparatus includes a tubular member provided with a number of external heat-exchanger fins that extend obliquely with respect to the longitudinal axis of the member and are arranged in sets along the member. Adjacent sets of fins have opposite angles of inclination to the longitudinal axis of the member to form a number of substantially V-shaped arrays. The fins are shaped so that when the tubular member is arranged in a flow of cooling fluid the height of each fin increases from its upstream to its downstream edge in the direction of flow. The fins are substantially trapezoid in shape and are thicker at the portion adjacent to the tubular member than at the outer edge. Deflector members are provided adjacent to the fluid inlet zones for directing fluid into the elementary channels defined by the fins. (B.L.M.)

38820 HEAT EXCHANGERS. Bell, Alan (to Foster Wheeler Corp.). U. S. Patent 3,183,969. May 18, 1965. Filed Feb. 28, 1962.

A tube and shell type heat exchanger has a cylindrical shell containing three assemblies or bundles of tubes that may be straight, U-tubes, or flat coils. The tubes in each assembly are arranged close to each other in parallel planes so that the tube bundles form parallelepipeds. The assemblies are juxtaposed so that the cross section of the three assemblies is a hexagon circumscribed by the cylindrical shell. The three tube bundles can be connected in series or in-parallel. The shell can be unobstructed internally except for the tube bundles or it can be baffled or otherwise partitioned to provide compartments housing the bundles and defining a long path for the heat exchanger medium through the shell. The compartments may also be connected in series, and one fluid circulates through the tube assemblies in series while another fluid circulates through the compartments in series. The tube assemblies and compartments are arranged for counter-current flow of the heat exchanging fluids. (B.L.M.)

38821 HEAT EXCHANGER. Ammon, Johannes H. (to The Babcock and Wilcox Co.). U. S. Patent 3,187,807. June 8, 1966. Filed May 3, 1961.

A heat exchanger that utilizes liquid metal as a source of heat interchange includes a vertically elongated pressure vessel of circular cross section. The interior of the vessel is divided into a centrally disposed inner chamber and an annular shaped outer chamber by a dependently supported tubular shaped baffle. Communication is provided between the two chambers at the lower end of the vessel by positioning the baffle above the bottom of the vessel. A number of tubes are disposed in the vessel with the first portion of each tube located in the inner chamber and the second portion located in the outer chamber. The portions of the tubes in the outer chamber form a number of separate vertically extending tube banks, each of which is made up of a number of horizontally spaced vertically extending tube platens arranged in a single vertical plane. The tubes in each platen are vertically spaced and extend horizontally back and forth across the platen joined by reverse bends. The second portions of the tubes forming the tube banks are arranged in counter-flow heat transfer relationship with the heating fluid flowing downwardly and the fluid to be heated flowing upwardly within the outer chamber. Another baffle is positioned between the first baffle and the pressure vessel to form the radially outer boundary of the outer chamber and to form in combination with the pressure vessel walls a thermal barrier space between the outer chamber walls and the pressure vessel walls. (B.L.M.)

Materials Testing

Refer also to abstract 40113.

38822 (BNWL-SA-2) SMALL SPECIMENS, SUITABLE FOR IRRADIATION DAMAGE STUDIES ON REACTOR STRUCTURAL MATERIALS. Hoagland, R. G. (Battelle-Northwest, Richland, Wash. Pacific Northwest Lab.). Jan. 4, 1965. Contract AT(45-1)-1830. 17p. (CONF-650114-1). Dep. mn; CFSTI, $1.00 cy, $0.50 mn.

From American Society for Testing Materials Meeting, Washington, D. C.

The feasibility and techniques involved in using double cantilever beam specimens for studying the effects of hot water irradiations on the fracture behavior of candidate reactor materials is discussed. (W.L.G.)

38823 (BNWL-SA-97) HIGH VOLUME NONDESTRUCTIVE TEST APPLICATIONS AT THE HANFORD ATOMIC PRODUCTS OPERATION. Worlton, D. C. (Battelle-Northwest, Richland, Wash. Pacific Northwest Lab.). [Mar. 11, 1965]. Contract AT(45-1)-1830. 29p. (CONF-650509-5). Dep. (mn); $2.00 (cy), 1 (mn) CFSTI.

From IAEA Symposium on Nondestructive Testing in Nuclear Technology, Bucharest.

The transition from laboratory to field use is discussed from eddy current and ultrasonic testing methods in two fields: inspection of thin-wall tubing, and automatic fuel testing. (D.L.C.)

38824 (GEAP-4474) EXPERIMENTAL AND ANALYTICAL PROGRAM RECOMMENDATIONS—REACTOR PIPE RUPTURE STUDY. Klepfer, H. H. (comp.) (General Electric Co., San Jose, Calif. Atomic Power Equipment Dept.). Jan. 1965. Contract AT(04-3)-189. 88p.

Investigations conducted under Phase I of the AEC Pipe Rupture Study delineated areas of uncertainty in assessing the likelihood of pipe ruptures. A three-year research and development program is recommended as Phase II of the Pipe Rupture Study: To conduct analytical (30%) and experimental (70%) work to permit a more firmly supported assessment of piping reliability. To combine the results of this program with available data in an attempt to evaluate the mathematical probability of occurrence of various size pipe ruptures. To recommend any changes or additions to existing codes, standards, or procedures which will improve the reliability of nuclear plant piping. Program requirements, recommended programs, and the relevance of each

of the Phase II objectives were defined for the ten tasks: reliability engineering, stress analysis, fracture mechanics, fatigue, localized corrosion cracking, impact erosion by wet steam, quality assurance procedures, operational surveillance development, creep-fatigue, and large-scale test facility. A time sequence was established for the recommended program. (auth)

38825 (NP-15176) THE NONDESTRUCTIVE TESTING OF FUEL ELEMENTS BY MEANS OF COMPTON RECOIL SPECTROMETRY. Final Report. [Weinzierl, P.] (Oesterreichische Studiengesellschaft fuer Atomenergie, G.m.b.H., Seibersdorf. Physik-Institut). Dec. 1964. IAEA Contract 180/RB. 41p. Dep. mn.

For nondestructive routine determination of nuclear fuel burnup a high resolution Compton-γ-spectrometer using a semiconductor detector was developed. The method is based on a measurement of the intensity of the ^{137}Cs 661 kev γ line, which is hidden in the complex fission product spectrum. Because of the long half life (30 y) the information obtained is independent of a knowledge of irradiation history within usual reactor operation times. The equipment developed is transportable, the spectrometer itself has a size of only $40 \times 40 \times 20$ cm. In routine operation a resolution of 13-15 kev (fwhm) was obtained. The method was shown to be reliable within 15% (standard deviation) or even less. A measurement of one fuel element takes typically 20 minutes. (auth)

38826 THE ROLE OF VARIABLE PARAMETERS IN THE CONTINUOUS X-RAY DIFFRACTION ANALYSIS OF STRUCTURAL CHANGE PHENOMENA. Szanto, Istvan (Research Inst. for Engineering Physics, Budapest). Magy. Tud. Akad. Muszaki Tud. Oszt. Kozlemenyei, 34: 435-41 (1965). (In Hungarian)

The most important parameter in the continuous recording of x-ray diffraction analysis data is time, or the rate of change of the observed phenomena, which may include kinetics of annealing of stresses, polygonization, grain boundary migration, or crystal growth. The rate may be exponential, being different at the start and at the end of the process. The events may be classified in 3 groups according to duration, requiring hours, minutes, or seconds; the recording will vary accordingly. In the first case the step-by-step (SBS) counting method is used; in the second case, SBS counting is combined with the autodiffractogram or rate measuring method. A special variation of SBS counting is used in the third case, determining the pulse density, which is proportional with the intensity at a chosen point of the background. This pulse density is the ratio of X-ray photons captured in unit time per unit surface area of a G-M counter. (TTT)

38827 REPORT ON THE RESEARCH ON THE MECHANISM OF FLAME PROPAGATION IN DUST CLOUDS. Leuschke, Guenter (Bundesanstalt fuer Materialpruefung, Berlin). Staub, 25: 180-6(May 1965). (In German)

The processes of ignition propagation in burning dust–air mixtures are more manifold than in gas–air mixtures. It was assumed previously that the light and heat radiation of the combustion process plays a part in the transportation of energy. The possibility of ignition propagation by the radiation emitted with dust combustion is shown. Tests also showed that the flame propagation in dust–air mixtures can occur through the interaction of several phenomena. The possibility that rapidly moving particles can act as ignition carriers is discussed. In experiments with Ti particles it is shown that burning dust particles suddenly explode and the particle fragments can fly apart with great speed. (tr-auth)

38828 KERNTECHNIK IM BAUWESEN. (Nuclear Technology in Construction). Pohl, Erwin. Berlin, Veb Verlag fuer Bauwesen, 1964. 216p.

The nondestructive testing techniques possible with nuclear technology makes possible a greater knowledge of the quality of construction materials to give greater economy and safety in construction. The methods used in practice and the methods being developed for the application of radioactive preparations to the determination of the properties of construction materials are discussed. The structure of the atom, nuclear physics, and the detection of energetic radiation are briefly described. The use of concrete as a shielding material, the use of sealed and open radioactive preparations in construction work, and measurements with neutrons are considered. Examples of utilization of each of these are given. (J.S.R.)

38829 AN INTRODUCTION TO INDUSTRIAL RADIOLOGY. Rockley, J. C. London, Butterworths, 1964. 242p. $10.75.

The specialized techniques in industrial radiology are discussed under the following headings: the nature, properties, and detection of x rays and γ rays; the production of x radiation; γ sources for industrial radiography; the photographic aspects of radiography; special photographic processes; practical radiography, setting-up and selection of aspect; radiographic quality and the selection of exposure conditions; interpretation and reporting; fluoroscopy and related techniques; and protection against radiation hazards and installation of radiographic equipment. (F.J.H.)

38830 DIMENSIONAL INSPECTION BENCH FOR PARTS HAVING CYLINDRICAL BODIES. Brebant, Charles (to Commissariat a l'Energie Atomique). British Patent 991,516. May 12, 1965. Priority date Apr. 27, 1962, France.

A dimensional inspection bench is described that provides the possibility of checking the dimensions of parts having preferably a circular cross section with a precision of a few hundredths of a millimeter and that is particularly applicable to the testing of fuel elements in totally enclosed fuel cells. The bench measures and checks the variations between an actual curve and a theoretical curve traced on the surface of the cylindrically bodied part. The bench includes a rotary support for the part and a measuring head. The head and support are movable relatively to each other parallel to the axis of rotation of the support. The measuring head includes a frame that supports two systems: first, one moving system mounted to rotate about a first shaft carried by the frame and located in a plane passing through the theoretical curve traced on the surface of the body; and second, another moving system mounted to rotate about a second shaft carried by the first moving system and orientated at right angles to the first shaft in the same plane. A detector element is carried by the second moving system for the purpose of following the actual curve by contact with the part. Means are provided for measuring the angular deviations of the moving systems with respect to reference positions defined by the theoretical curve. (B.L.M.)

38831 DEVICE FOR THE IRRADIATION OF AN OBJECT WITH CHARGED PARTICLE BEAMS. Knowlton, James Albert Jr.; Arndt, Richard Harold (to General Electric Co.). German Patent 1,188,225. Mar. 4, 1965. Priority date June 20, 1960, United States.

The device consists of an object disposed in front of one or more accelerator tubes and means for the linear deflection of the particle beam across the beam exit window. Further means are provided for influencing the beam in such a way that the density distribution of beam becomes unequal in the plane of the window so that the density distribution of a cross section of the beam in the plane of the object to be irradiated becomes equal. The density distribution of beam preferably has two maxima in the plane of the beam exit window bordering the central axis of the beam. (Gmelin Inst.)

Protective Structures

38832 (ORNL-TM-1155) MECHANIZED DURABILITY TESTS OF A SIX-FOOT PUNKAH-PUMP. Kearny, Cresson H. (Oak Ridge National Lab., Tenn.). July 1965. Contract W-7405-eng-26. 18p. Dep. mn; CFSTI, $1.00 cy, $0.50 mn.

In order to test and to improve the durability of a six-foot manually operated punkah-pump for shelter ventilation, motor-powered durability tests were conducted. This model pump, in a previous volumetric test in December 1964, transferred more than 5000 cfm into the 500-person

belowground shelter room at the Protective Structures Development Center, Fort Belvoir, Virginia, when operated by a single man. This model ventilating pump was tested at ORNL for more than 1000 hours. The testing indicated that this pump is dependable for at least six weeks of continuous use, provided modifications of the flap-valves and pulleys are incorporated. These modified parts were supplied to the Protective Structures Development Center for possible future tests with their six-foot punkah-pump. The modified punkah-pump, like other manual shelter-ventilating pumps, needs further realistic manual testing operated by average people during a shelter test of more than two weeks duration. (auth)

38833 VENTILATING SYSTEM FOR FALLOUT SHELTER. Solzman, Isel I. U. S. Patent 3,191,517. June 29, 1965. Filed Oct. 27, 1961.

A ventilating system is described for a personnel radiation fallout shelter adapted to house a number of people for an extended period of time. The shelter is provided with one or more conventional air compressor systems driven by gasoline or diesel engines to provide power. These compressor systems include air accumulators of either the permanently installed or mobile type. Compressed air from these systems is used in combination with suitable air motors to operate the shelter ventilating system and other equipment. The air may also be released directly into the shelter for breathing if necessary. (B.L.M.)

Space Propulsion

See also REACTOR TECHNOLOGY — Propulsion and Space.

38834 (N64-29495) ION ROCKET SYSTEM RESEARCH AND DEVELOPMENT. Quarterly Report. Reid, G. C.; Barcatta, F. A.; Sohl, G.; Speiser, R. C. (Electro-Optical Systems, Inc., Pasadena, Calif.). Sept. 20, 1964. Contract NAS3-5250. 63p. (NASA-CR-54026; EOS-4920-Q-2). CFSTI, $6.60 cy.

Work performed on an electron bombardment Cs ion rocket system is reported. A long duration engine system test is described including operating parameters during the run and analyses of components upon termination of the test. A new permanent magnet engine is reported, and the results of plasma distribution studies and autocathode tests are discussed. (auth)

38835 (N65-27619) SPACE ELECTRIC POWER SYSTEMS STUDY—D-C TO D-C CONVERTERS FOR NUCLEAR-THERMIONIC ENERGY SOURCES. Swiderski, E. F.; Jessee, R. D.; Gerecke, G. E. (Westinghouse Electric Corp., Lima, Ohio. Aerospace Electrical Div.). May 1965. Contract NAS3-6011. 175p. (NASA-CR-54415; WAED-65.28E). CFSTI, $5.00 cy, $1.00 mn.

The results of a study of d-c to d-c converters used in a 3.25 megawatt power system for space ion thrustor electric propulsion are presented. A 30-kw converter using silicon controlled rectifiers in the inverter circuit and silicon diodes as rectifiers was compared to a 30-kw converter using vapor tube thyratrons in the inverter circuit and gas tube diodes as rectifiers. The converters operated from a 150 volt nuclear-thermionic source and provided a 5000 volt output. Considering effects of thermal radiators, source weight penalties, nuclear radiation shielding, transmission line conductors and their cooling requirements, the vapor and gas tube switching device converter system weighs less than the power silicon semiconductor converter system. Therefore, the vapor and gas tube converter was selected for further study. Weight, volume, and power losses were determined for 30-kw converters using these devices when operating in 6 groups of 17 converters each. The input voltages were 50 and 100 volts. The output remained at 5000 volts. (auth)

38836 (NASA-SP-79) ELECTRICAL POWER GENERATION SYSTEMS FOR SPACE APPLICATIONS. (National Aeronautics and Space Administration, Washington, D. C. and Department of Defense, Washington, D. C.). 1965. 42p. $1.00(CFSTI).

Solar, chemical, and nuclear power plants for space uses are described. A chronology of flight requirements and missions is given. Safety, reliability, and program integration (between NASA, AEC, and DOD) aspects of the development effort are discussed. (T.F.H.)

38837 ABOUT SOME NEW ASPECTS OF PHOTONIC PROPULSION. Peschka, W. (DVL-Institut fuer Energiewandlung und Elektrische Antriebe, Stuttgart). Raumfahrtforschung, 9: 26-30(Jan.-Mar. 1965). (In German)

Through recent developments in the field of space technology, photonic propulsion in a certain way seems to be realizable. For example plasma reactors which are magnetically encapsulated could be used as light sources for photonic propulsion. A survey is given of these problems, and some special features are discussed in more detail. (auth)

38838 THE OPERATION OF AN ELECTRON BOMBARDMENT ION SOURCE WITH VARIOUS GASES. Reader, Paul D. (Lewis Research Center, Cleveland). pp 925-35 of First International Conference on Electron and Ion Beam Science and Technology. New York, John Wiley and Sons, Inc., 1965.

The performance of an electron bombardment ion source was evaluated with krypton, argon, nitrogen, helium, and hydrogen. The study was made with an existing 10-cm thrustor that had been thoroughly investigated with Hg as the propellant. Results indicate that gases with atomic weights greater than that of argon can be ionized in a conventional ion source at mass utilization efficiencies of at least 50%. It is anticipated that the mass utilization of any of the gases tested could be improved by careful attention to flow and geometric configurations. (A.G.W.)

Vacuum Engineering

38839 (RFP-672) AN ELECTRIC DISCHARGE AS A TRAP FOR DIFFUSION PUMP VACUUM SYSTEMS. Adams, R. O. (Rocky Flats Div., Dow Chemical Co., [Denver], Colo.). [1965]. Contract AT(29-1)-1106. 12p. Dep. mn; CFSTI, $1.00 cy, $0.50 mn.

An electric discharge is used as a trap for a diffusion pump with DC-704 silicone pump fluid. The discharge cracks the pump fluid vapor thus taking it out of the system. In the process much hydrogen and some other lighter gases are evolved. (auth)

38840 ADHESION OF POLISHED QUARTZ CRYSTALS UNDER ULTRAHIGH VACUUM. Smith, H. I. (Device Development Corp., Waltham, Mass.); Gussenhoven, M. S. J. Appl. Phys., 36: 2326-7(July 1965).

The observation of a strong adhesion between optically polished single-crystal quartz surfaces at ultrahigh vacuum is reported. The pyrex vacuum system is described. Adhesion of optical flats is generally attributed to surface tension of a thin film of adsorbed water between the surfaces. The optical contact experiments carried out at ultrahigh vacuum where liquid films could be readily eliminated showed that additional forces contribute to the adhesion. The adhesion was most likely due to van der Waals forces or, more specifically, London dispersion forces. (M.J.T.)

38841 ULTRAHIGH VACUUM GATE VALVE. Sheffield, James C. (Knolls Atomic Power Lab., Schenectady, N. Y.). Rev. Sci. Instr., 36: 1269-70(Aug. 1965).

An ultrahigh vacuum valve with a thickness of only 15.87 mm is described in which a copper seat is used. A simpler version of the valve for higher pressure applications is described in which an O-ring seat is used. (D.C.W.)

38842 VACUUM TECHNOLOGY. Santeler, Donald Virginia Polytech. Inst., Eng. Ext. Ser. Circ., Pt. A, I.1-21 ([1964]).

The development of vacuum technology for space simulation and the production of electronic thin films is discussed. The limits of vacuum, molecular flow, gas flow in short tubes, flow through restrictions, approaches to zero pressure, pumps and pumping problems, measuring vacuums, a typical vacuum system, economics, and methods for simulating the void of space and thin-film deposition are discussed. (F.J.H.)

GEOLOGY AND MINERALOGY

General

Refer also to abstract 39265.

38843 (BNWL-SA-135) PROBLEMS ASSOCIATED WITH THE EXTENSION OF THE STRATIGRAPHIC UNITS OF SOUTH-CENTRAL WASHINGTON. PART I. THE LATE BASALT FLOWS, ELLENSBURG AND LOWER RINGOLD FORMATIONS. Brown, R. E.; Brown, D. J. (Battelle-Northwest, Richland, Wash. Pacific Northwest Lab.). [Apr. 5, 1965]. AT(45-1)-1830. 11p. (CONF-650432-3). Dep. (mn); $1.00(cy), 1(mn) CFSTI.

From 53rd General Conference of Pacific-Northwest Trade Assn., Portland, Ore.

A summary is presented of recent work on the geology and stratigraphic problems at Hanford. After a description of the regional setting, the base of the Ellensburg Formation and the top of the Yakima basalt are discussed. The relationship between the Ringold Formation and the older Ellensburg Formation is considered. (D.L.C.)

38844 (BNWL-SA-140) PROBLEMS ASSOCIATED WITH THE EXTENSION OF THE STRATIGRAPHIC UNITS OF SOUTH-CENTRAL WASHINGTON. PART II. THE POST BASALT SEDIMENTS. Brown, D. J.; Brown, R. E. (Battelle-Northwest, Richland, Wash. Pacific Northwest Lab.). Mar. 26, 1965. Contract AT(45-1)-1830. 9p. (CONF-650432-2) Dep. (mn); $1.00 (cy), 1 (mn) CFSTI.

From 53rd General Conference of Pacific-Northwest Trade Assn., Portland, Ore.

There are four distinct stratigraphic units within the Pasco Basin which if interpreted on the basis of recent field evidence and described properly could be traced over most of Southeastern Washington. At the present time these post-basalt sediments are described in the literature in such a way as to make extensive correlations impossible. Some descriptions overlap more than one unit whereas others describe only a part of the unit. It is proposed that all interested geologists in the Pacific Northwest now consider reconciling the differences which exist in the names and descriptions of those sedimentary deposits in light of this new evidence. (auth)

38845 (RME-4584) GEOLOGY OF THE CUZCO-ANTA-URUBAMA AREA, CUZCO DEPARTMENT, PERU. Gabelman, John W.; Jordan O., Victor (Division of Raw Materials (AEC), Washington, D. C.). June 1964. 100p. Dep. mn; CFSTI, $3.00 cy, $0.75 mn.

The geological features of the Cuzco-Anta-Urubamba area that were recognized provide a key for interpreting the stratigraphic, structural, and mineralogical characteristics of the entire region. Tectonically the area lies inside the arc formed by the cordilleras Vilcanota and Vilcabamba where the mountain front is topographically, and probably structurally, offset, or where two independent uplifts meet. In this area readily recognizable small fault blocks with good physiographic expression have risen or subsided, localizing mineral deposits. Selectively the area is perhaps the most complexly faulted part of the region. It is unique for the variety and number of breccia pipes whose possible origins range from salt intrusives to volcanic explosions. For at least 50 km in any direction the region lacks known significant mineral deposits, although the study indicated that the area was subjected to low-temperature epithermal solutions with a surprisingly large volume of alteration products. The very low ratio of metal to alteration products indicates that some metal deposits should exist and could contain Cu, U, or Se. (P.C.H.)

38846 (ORNL-tr-698) CONTRIBUTION TO THE REVERSAL OF PLEOCHROIC HALOS. Weber, Maximilian. Translated for Oak Ridge National Lab., Tenn. from Centr. Mineral., Geol., 388-92(1923). 8p. Dep. mn; JCL, $1.10 fs, $0.80 mf.

A cordierite gneiss shows a biotite adjoined by a larger cordierite crystal; a large rounded zircon projects into both sides of the biotite-cordierite boundary. The zircon produced in the biotite ~1/4 of a uniform pleochroic halo with a disk shape, and in the cordierite ~3/4 of a reversed halo. Possible causes of the reversal are discussed. It is concluded that the reaction rate of the host mineral should be considered in cases of reversal of pleochroic halos. (D.L.C.)

38847 VARIATIONS IN THE S^{33}, S^{34}, AND S^{36} CONTENTS OF METEORITES AND THEIR RELATION TO CHEMICAL AND NUCLEAR EFFECTS. Hulston, J. R.; Thode, H. G. (McMaster Univ., Ontario). J. Geophys. Res., 70: 3475-84(July 15, 1965).

The isotopic ratios $^{33}S/^{32}S$, $^{34}S/^{32}S$, and $^{36}S/^{32}S$ of the different forms of sulfur in a number of meteorites were studied. The results obtained indicate that chemical fractionation processes have occurred in some meteorites, but that the isotopic composition of the total sulfur is remarkably constant from meteorite to meteorite. Variations in the ^{33}S, ^{34}S, and ^{36}S abundances and the relation between them indicate isotopic fractionation in chemical and physical processes. There is no evidence of variations due to inhomogeneities in the processes of nucleosynthesis. (auth)

38848 RARE-EARTH DISTRIBUTIONS IN SOME ROCKS AND ASSOCIATED MINERALS OF THE BATHOLITH OF SOUTHERN CALIFORNIA. Towell, David G.; Winchester, John W.; Spirn, Regina Volfovsky (Massachusetts Inst. of Tech., Cambridge). J. Geophys. Res., 70: 3485-96 (July 15, 1965).

The rare-earth and yttrium abundances in four whole-rock samples and eight associated mineral fractions from the batholith of Southern California were determined by means of neutron activation and partition chromatography. It is shown that, on a whole-rock basis an increase in total rare-earth content in the sequence gabbro-tonalite-granodiorite-quartz monzonite is paralleled by an increase in relative fractionation favoring the lighter rare earths. In the same sequence, there is an apparently systematic, increased relative removal of Eu which is attributed to the existence of Eu(II). Analyses of feldspar, pyroxene, amphibole, mica, and apatite mineral fractions also indicate that divalent Eu was an important constituent during the evolution of the rocks studied. The feldspar mineral fractions were invariably enriched in Eu relative to the adjacent rare earths, whereas the ferromagnesian minerals were relatively depleted. (auth)

Natural Radioactivity and Fallout

See also HEALTH AND SAFETY.

Refer also to abstracts 38347 and 39774.

38849 ISOTOPIC COMPOSITION OF URANIUM IN ZIRCON. Doe, Bruce R.; Newell, Marcia F. (Geological Survey, Denver and Washington, D. C.). Am. Mineralogist, 50: 613-18(May-June 1965).

Twenty analyses were made of the isotopic abundances of ^{238}U, ^{235}U, and ^{234}U in 13 selected zircon samples by mass spectrometry. Five samples were checked for $^{238}U/^{234}U$ by alpha spectrometry. Variations in $^{238}U/^{235}U$, did not exceed 0.5% of the ratio. The range in $^{235}U/^{234}U$ was about 9%. Variations in $^{235}U/^{234}U$ could not be correlated with age, grain size, per cent discordance in the isotopic ages, type of discordance (positive or negative), uranium content, or radiation damage. The ratio, $^{235}U/^{234}U$, for two of four samples could not be reproduced within analytical uncertainties, suggesting lack of sample homogeneity or problems arising from chemical procedures. The range in $^{238}U/^{234}U$ was not large enough to account for discordant U-Pb ages in zircons by radioactive disequilibrium between

^{238}U and ^{234}U. Most zircon concentrates were obtained from surface rocks that were at least incipiently weathered. Use of $^{235}U/^{234}U$ as a weathering indicator led to the conclusion that incipient weathering has little or no effect on zircons. (auth)

38850 Sr^{90} CONTENT OF HUMAN BONES IN FINLAND, 1960-1962. Salo, K.; Uotila, U.; Alha, A.; Tamminen, V.; Lindfors, R.; Laiho, K. (Univ. of Helsinki). Ann. Acad. Sci. Fennicae, Ser. A V, 110(1964).

The ^{90}Sr content of human bones in Finland in 1960 to 1962 was studied. The material was collected in medico-legal autopsies and consisted mostly of tibias. In the adult group the mean ^{90}Sr content increased from 0.66 pc/g Ca in 1960 to 0.77 pc/g Ca in 1961 and to 0.90 pc/g Ca in 1962. The age group 6 to 20 years showed decreased activity from 1960 (1.60 pc/g Ca, 3 cases) to 1961 (1.04 pc/g Ca) and to 1962 (1.21 pc/g Ca). A similar trend was present in the age group 0 to 5 years (1960, 3.16 pc/g Ca; 1962, 2.14 pc/g Ca), whereas the newborn showed the opposite tendency (1961, 1.46 pc/g Ca; 1962, 1.99 pc/g Ca). Significant differences could not be seen in the ^{90}Sr content in the material from North and South Finland. (Excerpta Med., Sect. XXIII, 2: No. 6(June 1965))

38851 ON THE DISTRIBUTION OF RARE AND DISPERSE ELEMENTS IN SUBTERRANEAN BULGARIAN SALT WATER. Pentcheva, E. (Geologic Inst., Bulgarian Academy of Sciences, Bucharest). Compt. Rend. Acad. Bulgare Sci., 18: 149-51(1965). (In French).

Among the elements discovered in the subterranean salt waters of Bulgaria were Li, Sr, Ba, Rb, and Cs. The greater concentration of rare alkaline earth elements was found in the north. The amount of Li in the waters varied from several tenths to 22.4 mg/kg, and increased in direct proportion to the rate of mineralization and the contents of Na and K. The abundance of Rb and Cs varied from 0.5 to 0.8 mg/kg for Rb and from 0.005 to 0.3 mg/kg for Cs. The gases richest in He in Bulgaria were found to be released by the strata containing the largest concentrations of rare alkaline earth elements. The amounts of Sr found in the waters varied from several hundredths to several tenths mg/kg, and was generally greater than that of Ba in the same strata. It was found to increase in direct proportion to the rate of mineralization and the content of Ca. The amount of Ba varied likewise from several hundredths to several tenths mg/kg. Furthermore, Ba is one of the elements that is practically immobile in sedimentary deposits. Its concentration increased as the concentrations of the more mobile Sr increased. (BBB)

38852 STUDIES ON THE RADIOACTIVE CONTAMINATION OF THE ATMOSPHERIC PRECIPITATION OF BUDAPEST WITH SPECIAL REGARD TO RADIOACTIVE STRONTIUM. Bakacsne Polgar, E.; Kurczne Csiky, I. Egeszsegtudomany, 8: 371-8(1964).

For an appropriate evaluation of the radiation load produced by rainfall not only the determination of the total beta-activity but also the relative amount of the individual radioisotopes, particularly that of ^{90}Sr are needed. The procedure of separation of pure beta-emitting ^{90}Sr is quite laborious. A routine method for the separation of radioactive Sr and Ba has been developed. This procedure has been improved further and used for the determination of the average monthly ^{90}Sr and ^{89}Sr content of the rainfall. Experiments for the routine separation and analysis of yttrium are in progress. Systematic studies carried out in Budapest since Oct. 1962 yield data essentially similar to those known internationally. The total beta-activity and the radioactive Sr content of the rainfall has exhibited a decreasing tendency since the stop of atom-bomb experiments. (Excerpta Med., Sect. XXIII, 2: No. 6(June 1965))

38853 ON THE ROCK AGE OF THE VINDHYAN SYSTEM (INDIA) ACCORDING TO GLAUCONITES. Tugarinov, A. I.; Shanin, L. L.; Kazakov, G. A.; Arakelyants, M. I. (Inst. of Geochemistry and Analytical Chemistry, Moscow). Geokhimiya, No. 6, 652-60(June 1965). (In Russian).

On the basis of absolute age determination by the K/Ar method for 15 samples of unaltered glauconites from four horizons of the Vindhyan system, age characteristics of the sedimentation time of the Upper Precambrian in India were obtained. It was established that the age of the Guddapakhi series is on the order of 1330 ± 40 to 1470 ± 40 million years; Somri, 1170 ± 35 to 1070 ± 35 million years, and Keimur, 945 ± 35 to 890 ± 30 million years. A comparison of absolute age measurements of the Guddapakhi series sedimentation according to glauconite and to lead from sedimentary rocks showed their close conformity. The age of pegmatites (900 to 1000 million years) interrupting the crystalline rocks of the Sausarsk series was studied and it was found that the series Aravalli and Daly cannot be the lower limit of the Vindhyan system age. The general position of the Vindhyan system corresponds to the geochronological extent of the lower, the middle, and, perhaps, of the lower parts of the Upper Rhifean of the territory of USSR, to the Sinian system and to the Khuta series of China. The history of the Rhifean found in measuring the absolute age of glauconite indicated epeirogenic movements, which led to the beginning of the Upper Rhifean (900 million years), to the uplift of the entire Indian shield, and in the Middle Rhifean (1400 million years) raised to the surface the whole southern half on which from this moment the sedimentation ceased. (auth)

38854 AGE EFFECT IN THE ISOTOPIC COMPOSITION OF CARBON OF STALACTITE ANNULATIONS OF THE CRIMEA HIGHLANDS. Galimov, E. M.; Grinenko, V. A. (Gubkin Inst. of Chemical Oil and Gas Industry, Moscow and Vernadskii Inst. of Geochemistry and Analytical Chemistry, Moscow). Geokhimiya, No. 6, 661-7(June 1965). (In Russian).

The isotopic carbon composition in sequential stalactite layers from karst caves was determined to verify the assumption that the $\delta\ ^{13}C$ variations in secondary calcite were due to change in the isotopic composition of soil carbon dioxide. In all cases a lesser enrichment in ^{13}C was detected in the outer stalactite layer. A correlation of the structure and isotopic composition of stalactite annulation carbon with the geological history of the region allowed the conclusions to be drawn about the geological age of stalactites and also about the fact that the isotopic composition of stalactite carbon may be used to obtain data on the change of soil-climatic conditions. (auth)

38855 BIOGENIC MIGRATION OF URANIUM IN THE LAKE ISSYK-KUL. Kovalski, V. V.; Vorotnistskaya, I. E. (Vernadskii Inst. of Geochemistry and Analytical Chemistry, Moscow). Geokhimiya, No. 6, 724-32(June 1965). (In Russian).

The role of living organisms in uranium migration in the lake Issyk-Kul and the connection of uranium food chains with the level of its content in fishes inhabiting the lake was studied. Various stages of the biogenic uranium migration were investigated: water silts, benthos algae and higher plants, plankton, benthos animal organisms, and fishes. The uranium content was determined by the extraction-luminescent method. The chief uranium concentrator in the lake was algae of the charophytes family; in this connection an exceptional polymorphism was observed. It was shown that the chief enrichment of silts in uranium was genetically connected with its accumulation by charophyte algae during their life time, since the greatest uranium amount was contained in silts, underlying the charophyte algae and since uranium was not washed off the algae, which died. The uranium content and its accumulation gradient decreased with the complication of organism structure in the chain: algae → animal organisms of the benthos fishes. In uranium passing through the food chain a gradual decrease in uranium concentration was observed. (auth)

38856 ^{90}YTTRIUM CONCENTRATION IN MILK. Murthy, G. K. (Robert A. Taft Sanitary Engineering Center, Cincinnati). J. Dairy Sci., 48: 609-11(May 1965).

The concentration of ^{90}Y and its ingrowth pattern in milk contaminated with fallout were investigated. Fresh raw whole milk samples collected from individual cows were processed and analyzed for ^{90}Y and ^{90}Sr, according to an ion exchange procedure, at various times after milking.

At the time of morning milking the ^{90}Y concentration was about 15% of the ^{90}Sr concentration present in milk. Extrapolation of the curve to zero ^{90}Y concentration gave a time of negative 16 hr, the time of evening milking the previous day. From this time on, the rate of ingrowth of ^{90}Y followed exponentially, with a physical half life of 64.2 hr. This suggested that any ^{90}Y activity in milk originated from ^{90}Sr in milk at the time of secretion into the udder. To test the feasibility of utilizing the ^{90}Y ingrowth curve, in analyzing market milk stored for shorter periods than the customary 8 to 12 days, a study was made of raw milk samples collected at a milk plant on different days. An estimate of the true age (time of secretion in udder) of milk was computed by adding 16 hr to the observed age. When the milk samples were analyzed for ^{90}Y and ^{90}Sr, the results showed no significant differences in ^{90}Sr and ^{90}Y values, indicating that analyses of milk samples stored for shorter intervals provide satisfactory results. Any discrepancy may be due to errors in estimating the age of milk, especially when it is less than about four days old, during which period the rate of ^{90}Y ingrowth is rapid. However, in processed milk, usually four or five days old by the time it reaches the lab, errors in estimating the age of milk are considerably reduced and milk may be analyzed after shorter intervals of storage with satisfactory results. (BBB)

38857 ENVIRONMENTAL BEHAVIOR OF NUCLEAR DEBRIS. Straub, Conrad P. (Dept. of Health, Education, and Welfare, Cincinnati); Carter, Melvin W.; Moeller, Dade W. J. Sanit. Eng. Div., Am. Soc. Civil Engrs., 90: 25-40 (Dec. 1964).

Since the early 1950's, the Public Health Service, the Atomic Energy Commission, its contractors, and other groups have collected considerable data on the levels of radioactive materials in the United States environment resulting from fallout from nuclear detonations. A review of these data on a global scale confirms the latitudinal banding of debris from nuclear testing and the value of surface air measurements in tracing the movement of such materials through the atmosphere. Although not seeming to follow any systematic pattern on a gross basis, levels of Sr-90 and Cs-137 in milk appear to be readily interpretable when considered in the light of weather patterns and total precipitation. Similarly, seasonal patterns show a close correlation with dairy practices, the time spent on open pasture having a direct influence on levels of both short and long-lived radionuclides in milk. As has been observed in essentially all areas of environmental health, this review again confirms the interrelationship of the various phases of the environment and substantiates the fact that an understanding of any one transport mechanism requires some knowledge and appreciation of all transport mechanisms. By using the data provided by one series of environmental measurements (such as those in air), public health officials can take steps to intercede in alleviating and even preventing the next step in the transport cycle. Action of this type can be quite significant in reducing human intake and resulting exposure in times of emergency. (auth)

38858 SECRETION OF GAMMA RADIOACTIVITY IN MILK IN RELATION TO CONTAMINATION OF FEEDS IN SPRING 1962. Pfau, Alexander; Hoeck, Helmuth (Max-Planck-Institut fuer Tierzucht und Tierernaehrung, Mariensee/Trenthorst, Ger.). Milchwissenschaft, 17: 673-7 (Dec. 1962). (In German).

From January to June 1962, the total γ activity was measured in fresh pooled milk samples, and the natural ^{40}K content calculated on the basis of flame-photometric determinations of potassium. The artificial γ activity tended to increase during April, May, and June. In June 1962, the ^{137}Cs activity was estimated to be at 140 pC/l, and the ^{90}Sr content at 49 pC/l. The γ-spectrometric measurements of rain water, pasture grass, and water used for cattle showed energy maxima at 0.14 Mev (^{144}Ce), 0.51 Mev ($^{106}Ru-^{106}Rh$), and 0.76 Mev ($^{95}Zr-^{95}Nb$). Moreover, measurements of pasture grass and water for cattle indicated the γ line of ^{40}K at 1.46 Mev. Milk ash displayed clearly delineated γ-energy maxima only at 0.66 Mev (^{137}Cs), and 1.46 Mev (^{40}K). A significant result obtained in these studies was demonstration of the artificial contamination of water pumped up from a depth of 5 m at the Research Station in Mariensee. Measurements of total radioactivity supplied to the cow through the feed and that secreted with the milk during the second quarter of 1962 were used as the basis for estimating a filtration efficiency of 0.5% for the cow. The levels of ^{137}Cs and ^{90}Sr found in milk in June 1962, were about $\frac{1}{10}$ and $\frac{1}{2}$, respectively, the maximum allowable limits provided by the International Commission on Radiological Protection. (BBB)

38859 THE NUCLEAR METALS: THORIUM AND THE RARE EARTHS. Mining Ann. Rev., 63(May 1965).

Production and uses of Th and rare earths are reviewed. An approximate assessment of world reserves (capable of being economically processed) of Th is 945,000 tons. The main deposits are found in India, Canada, Brazil, and the United States. Long-term forecasts indicate that, as low-grade U ore becomes exhausted and as the price of U increases, both the fast breeder reactor and reactors on the Th and U cycle may become more competitive with U. As a probable trend, other processes for producing ^{233}U or ^{239}Pu from Th and U by other nuclear reactions might become available and competitive, thus limiting the demand for the latter metals. That there is much support at present for the future development of reactors employing Th is evident from plans in the U.K., U.S.S.R., France, Germany, and the U. S. In 1962 Brazil prohibited the export of thorium ores, and proceeded to develop these resources, which are considerable, and plans to produce its own nuclear fuel via Th (^{233}U) to produce power to 300 Mw by 1969. Although monazite is still used as a raw material, a high grade bastnaesite mined in the U. S. may come to be preferred as a rare earth source. A marked increase in the production of rare earths with emphasis on the Ce group occurred in 1964. Much research is being conducted to evolve new processes for the extraction and separation of the rare earths. The uses of the rare earth elements are summarized in a table. (BBB)

38860 A BRIEF REPORT ON MEASUREMENTS OF AMBIENT RADIOACTIVITY AND RADIOACTIVITY OF FOOD IN AUSTRIA DURING 1963. Vychytil, P. Mitt. Oesterr. Sanitaetsverwalt., 65: 324-5(1964).

During 1963, the total beta activity of the air was comparable to that in the spring, but the activity of the precipitation and deposits of total beta activity and ^{90}Sr activity of the soil increased. Contamination of food, especially with ^{90}Sr, also increased, but the activity of the drinking-water (except for water from cisterns) was extremely low. (Excerpta Med. Sect. XXIII, 2: No. 6(June 1965))

38861 PRESENT STATUS OF RADIOACTIVE FALLOUT. Toke, T. (St. Paul's Univ., Tokyo). Sci. World, 8: 7-11(1964).

A discussion is presented of the estimated total doses that will be received by human populations as a result of nuclear weapons tests, and of the projected risks involved. First, an estimate is made of the quantity of fission products and induced activities injected into the atmosphere up to the end of 1962. The total power of nuclear explosions from the testing conducted by the Soviet Union and U.S.A. in 1962 was estimated by the Japanese Meteorological Agency to be from 190 to 240 Mt, and the estimate of the fission-fusion ratio from these tests was 0.2. The quantity of ^{90}Sr injected into the stratosphere in this period is estimated to be about 4 mC. The amount of ^{90}Sr released in 1961 and 1962 would be comparable to that released prior to 1959. For the estimation of ^{137}Cs, 1.7 mC is assumed to be injected into the stratosphere per 10 Mt of fission energy. The total amount of ^{14}C produced by nuclear testing in 1961 and 1962 is estimated to be 6.4×10^{28} atoms. Figures are also derived for cumulative deposits of the major radionuclides in fallout, following which dietary levels are estimated and transfer factors (diet to human tissues) are considered. The body dose of ^{90}Sr is considered to be 2.7, 1.4, and 0.7 mRem/yr respectively to bone cells, cells lining bone surfaces, and bone marrow. For ^{137}Cs the dose rate to bone cells, cells lining bone surfaces, bone marrow, and gonads per pC/g potassium of mean value for a whole body is taken as 0.044, 0.036,

0.026, and 0.020 mRem/yr, respectively. The annual dose from ^{14}C is 1.6, 1.18, 0.7, and 0.7 mRem/yr respectively for the bone cells, cells lining bone surface, bone marrow, and gonads. Finally, contribution of the external exposure from fallout deposit to the dose commitment is estimated. A table shows an estimate of the dose commitment for the human body under the conditions of tests ending in 1962 and continued testing. These doses are average doses which take into account the population distribution, fallout pattern, and dietary habits. Comparative risk due to fallout from a finite period of testing is estimated by a comparison of the dose commitment with the total dose delivered by natural sources over the same period, and for continued testing the comparative risk is equivalent to the ratio of the dose commitment per year of testing to natural sources. A table shows the results obtained, assuming that the nuclear tests were carried out only during the nine-yr period from 1954 to 1962, and the human body receives the annual dose of 100 mRem/yr from natural sources. The comparative risks due to nuclear tests up to 1962 range from 30 to 100% for human gonads and bone. These values indicate the levels which will be reached in equilibrium if nuclear testing should continue to be carried out at the mean rate of the above-mentioned nine-yr period. For the last two years of the period during which three mC of ^{90}Sr per yr was injected into the environment, the comparative risks for this period would be estimated to be over 90% for all human organs. The warning levels, which are about one-tenth of the maximum permissible level for population, have recently been reached in several countries. (BBB)

38862 A COMPARISON OF FALLOUT β ACTIVITY IN THE PRECIPITATION AND THE TOTAL β ACTIVITY IN THE MILK IN THE GREIFSWALD DISTRICT DURING 1963. Loscher, J.; Riemer, F. (Ernst-Moritz-Arndt-Universitaet, Greifswald, Ger.). Z. Ges. Hyg. [Ihre Grenzgebiete], 10: 779-81(1964).

Rainfall quantities, as well as their beta-fall-out activity and the total beta activity detected in the milk during the period from January-December 1964 in the Greifswald area of Germany are reported. The correlations of these three parameters are discussed. (Excerpta Med., Sect. XXIII, 2: No. 6(June 1965))

38863 ASSAY OF STRONTIUM-90 IN HUMAN BONE IN THE UNITED KINGDOM. Results for 1964. Part I. Monitoring Report Series No. 10. (Medical Research Council London (England)). 1965. 17p. BIS, $0.30 cy; HMSO, 1s. 9d.

Data are presented on the content of ^{90}Sr in samples of human bone collected in Great Britain during the first half of 1964. Values for infants and children in the 0 to 4 year age group were considerably higher than those for the first half of 1963. There was also an increase over the values for the last half of 1963. (C.H.)

Techniques and Equipment

38864 (SC-R-65-904) FOUR PAPERS CONCERNING RECENT WORK ON GROUND MOTION MEASUREMENTS. Perret, W. R.; Wistor, J. W.; Hansen, G. J.; Palmer, D. G. (Sandia Corp., Albuquerque, N. Mex.). July 1965. Contract AT(29-1)-789. 73p. Dep. mn; CFSTI, $3.00 cy, $0.75 mn.

The papers were presented at a meeting held in Port Hueneme, Calif., on Feb. 16 and 17, 1965. The intent of the papers was to re-examine earlier earth stress observations, to discuss new instruments and data processing components, and to examine data acquisition and conditioning equipment for stress or motion induced in earth by large explosions. Separate abstracts were prepared for all the papers. (D.L.C.)

For abstracts of individual papers see: 38865, 38917, 38918, and 38919.

38865 (SC-R-65-904, pp 3-22) GROUND MOTION MEASUREMENTS. Perret, W. R. (Sandia Corp., Albuquerque, N. Mex.).

A discussion is presented of some types of measurements made in large explosions and of the reasons and practical factors influencing instrumentation. It is shown that measurement of stress, acceleration, or velocity in soils or rock is reliable, while the reliability of strain measurements is marginal. The problem of gage-environment mismatch is probably not so serious as has been generally considered. Hysteresis in stress-strain diagrams is useful for study of energy dissipation in the earth. (D.L.C.)

38866 AN EVALUATION OF THE U^{234}/U^{238} METHOD AS A TOOL FOR DATING PELAGIC SEDIMENTS. Ku, Teh-Lung (Columbia Univ., Palisades, N. Y.). J. Geophys. Res., 70: 3457-74(July 15, 1965).

The possibility of using the 15% excess ^{234}U activity in oceanic uranium for dating pelagic sediments in the age range 100,000 yr to more than 1 Myr was explored. Results from a series of analyses of bulk samples, mechanical separates, and acid leach fractions indicate that separation of authigenic uranium from detrital uranium by either mechanical or chemical means is impractical. Measurements on totally dissolved samples reveal that the sediments do not form a closed system; post-depositional migration of ^{234}U in the sedimentary column takes place. Based on the experimental data obtained from three red-clay cores with sedimentation rates ranging from 2 to 6 mm/1000 yr, a model depicting diffusion of the ^{234}U generated within the sediments is proposed. The diffusion equation includes three parameters: sedimentation rate, diffusion coefficient for ^{234}U, and fraction of the internally produced ^{234}U subject to mobility. If the amount of ^{234}U lost from these cores is typical, a sizeable part of the ^{234}U excess in the sea must be from this source. (auth)

38867 GAMMA-GAMMA LOGGING OF SOFT RADIATIONS. Kalitiuk, Ryszard. Przeglad Geofiz., 13: 208-13 (May 1965). (In Polish).

The gamma-gamma logging of soft radiations is a variety of the common gamma-gamma logging. The measurement of a phenomenon consists in using the existing relation between photoelectric observation of multiply spread gamma quanta and atomic number Z of the atoms in the environment. Isotopes emitting gamma rays of low energy are used as radiation sources. Theoretical and interpretative bases for prospecting and determining the grade of heavy metal ore deposits are given. In addition, factors influencing quantitative interpretation are discussed. (auth)

38868 HELIUM–URANIUM RATIOS FOR PLEISTOCENE AND TERTIARY FOSSIL ARAGONITES. Fanale, F. P.; Schaeffer, O. A. (Brookhaven National Lab., Upton, N. Y.). Science, 149: 312-17(July 16, 1965). (BNL-8939).

Uranium : helium ages were compared with $^{230}Th : ^{234}U$ ages and stratigraphic ages for selected Pleistocene and tertiary shells and corals. Agreement was good except for those fossils for which independent criteria (for example, aragonite : calcite, $^{226}Ra : ^{230}Th$, or $^{234}U : ^{238}U$ ratios) indicated a chemically open system. Certain of the tertiary samples yielded erroneously low ages, which probably resulted from secondary addition of uranium. The helium geochronometer appeared to yield reliable minimum ages and may be applicable to direct dating of aragonitic fossils, especially those of Pleistocene age, when used in conjunction with other isotopic and geologic information. (auth)

38869 CONVENIENT CADMIUM-METAL STANDARD FOR CHECKING NEUTRON, SOIL MOISTURE PROBES. Bowman, D. H.; King, K. M. (Ontario Agricultural Coll., Guelph). Soil Sci. Soc. Am. Proc., 29: 325-7(May-June 1965).

A convenient standard was devised for checking the calibration of a neutron-scattering soil moisture depth probe at five fixed points. For a calibration check the probe was placed into one of five waterproof steel tubes immersed in water. Fixed points were obtained by attaching different amounts of cadmium sheet metal to the outside of the tubes to absorb different amounts of the thermal neutrons scattered back by the water. Cadmium-metal standards were applicable as well to surface probes. (auth)

38870 AN INJECTION PROBE FOR RAPID PLACEMENT OF RADIOISOTOPES IN SOIL. Loewenstein, H.

(Univ. of Idaho, Moscow). Soil Sci. Soc. Am. Proc., 29: 328-9(May-June 1965).

Numerous time-consuming injections of radioisotopes in soil were required in certain studies utilizing tracer techniques. The injection probe described retained desirable features of earlier models, but allowed placement of the tracer to proceed at a greatly accelerated rate. (auth)

38871 RADIOACTIVE WELL LOGGING METHOD. Tittle, Charles W. (to Schlumberger Ltd.). U. S. Patent 3,184,598. May 18, 1965. Filed May 17, 1954.

Method and apparatus are described for making a radiological survey of an extensive heterogeneous material by alternately bombarding the material with fast neutrons and detecting the gamma rays emitted by such material. The method is described with particular application to well-logging for obtaining data of value for estimating the concentration of oxygen in formations. A source of pulsed fast neutrons of about 11 Mev and a gamma-ray detector are moved along a borehole. Only gamma rays having energies of about 1.6 to 6.13 Mev detected during time intervals between the neutron pulses after substantial disappearance of the primary pulsed neutrons are detected. (B.L.M.)

HEALTH AND SAFETY

See also BIOLOGY AND MEDICINE — Radiation Hazards and Protection
GEOLOGY AND MINERALOGY — Natural Radioactivity and Fallout

Refer also to abstracts 38329, 38473, 38546, 40062, and 40119.

38872 (AEET/HP/TH-15) MAXIMUM PERMISSIBLE CONCENTRATIONS OF FISSION PRODUCT MIXTURES IN AIR AND WATER FOR OCCUPATIONAL EXPOSURES. Iyer, M. Ramakrishna; Krishnamurthi, T. N. (Atomic Energy Establishment, Trombay (India). Health Physics Div.). 1963. 45p. Dep. mn.

Maximum Permissible Concentrations of uranium-235 fission product mixtures in air and water, for a 40 hour week occupational exposure, were calculated for irradiation times of 10^6, 10^7, and 10^8 seconds and decay times from 10^3 seconds to 10^8 seconds. In the calculations the thermal neutron flux was taken as $10^{12}n/cm^2/sec$. All the fission products (83) for which Maximum Permissible Concentrations are listed by ICRP have been taken into account in the computations. MPC's have been calculated for 21 organs, out of which the results for the nine most radiosensitive organs are presented. The lowest value of MPC for any of the organs in air and water are plotted as a function of cooling time for the three irradiation times. MPC of the fission product mixture varies from 1.8×10^{-7} uc/cc to 1.6×10^{-9} uc/cc in air and from 1.2×10^{-3} uc/cc to 2.2×10^{-5} uc/cc in water during the course of the irradiation and decay history considered. The most critical organ for the fission product mixture for the different cases are presented. (auth)

38873 (BNL-9331) H^3THYMIDINE (H^3TdR) INCORPORATED INTO DNA; DOSIMETRIC AND RADIOBIOLOGICAL CONSIDERATIONS. Bond, V. P.; Feinendegen (Brookhaven National Lab., Upton, N. Y.). [1965]. Contract AT(30-2)-Gen-16. 35p. (CONF-650302-23). Dep. mn; CFSTI, $2.00 cy, $0.50 mn.

From IAEA Symposium on Personnel Dosimetry for Accidental High-Level Exposure to External and Internal Radiation, Vienna.

The literature is reviewed and experimental data are presented to determine whether observed effects from intranuclear ^3H could be accounted for on the basis of calculated absorbed dose in rads to the cell nucleus, or whether additional factors inherent in the presence of ^3H in the DNA molecule are involved. Results are discussed in terms of radiobiology and radiation protection. The degree of early somatic biological effect from intranuclear ^3H appeared to be that anticipated on the basis of calculated absorbed dose to the cell nucleus, at least down to doses of 5 rads or less. Consequently: the absorbed dose concept held down to the order of 10^{-11} grams or less, somatic effects being predictable on this basis; the distribution of ^3H atoms incorporated into DNA as ^{3}HTdR (and ion pairs from the beta particles) was random as far as dose calculations for the purpose of predicting somatic effects were concerned; every part of the cell nucleus lay within one ^3H beta range of some part of a chromatid, and the nucleus contained no contiguous insensitive volume of a radius exceeding the effective range of ^3H beta rays (1 to 2 μ); and the origin of ^3H beta tracks in, or their close juxtaposition to, the DNA molecule does not appear to enhance the degree of somatic effect. Transmutation effects of the disintegrating ^3H nuclide in DNA seemingly produced genetic mutations in microorganisms. It is concluded that the biological effects of ^{3}HTdR can be approximated closely from the absorbed dose to the nucleus. (H.G.D.)

38874 (BNWL-SA-53) EVALUATION OF EXPOSURE FROM MULTIPLE ENVIRONMENTAL SOURCES IN THE ENVIRONS OF THE HANFORD PLANTS. Foster, R. F.; Wilson, R. H. (Battelle-Northwest, Richland, Wash. Pacific Northwest Lab.). [June 8, 1965]. Contract AT(45-1)-1830. 21p. (CONF-650616-4). Dep. (mn); $1.00(cy), 1(mn) CFSTI.

From Health Physics Society, Annual Meeting, Los Angeles.

The people that live near the Hanford Atomic Energy site can acquire radioactive materials by several different environmental pathways that begin with the release of reactor effluent to the Columbia River, the release of stack gases to the atmosphere, and world-wide fallout. In 1964 the radiation dose received by the vast majority of the local residents, from all of the sources combined did not exceed ten per cent of the appropriate limits. Except for the dose to the GI tract from drinking water, the exposure resulting from world-wide fallout was at least as great as that which could be attributed to the Hanford Plants. For the relatively few people who eat large numbers of fish caught from the Columbia River immediately below the Hanford reservation, ^{32}P is an important source of exposure. In 1964 the hypothetical individual who had the maximum credible intake of ^{32}P and other nuclides of Hanford origin, could have taken in about 25 per cent of the permissible annual intake of bone-seeking radioisotopes. (auth)

38875 (HASL-160) CONTROL OF LIQUID HYDROGEN HAZARDS AT EXPERIMENTAL FACILITIES—A REVIEW. Weintraub, A. A. (Health and Safety Lab., New York Operations Office (AEC), N. Y.). May 1965. 257p. Dep. mn; CFSTI, $6.00 cy, $1.25 mn.

The hazards of liquid hydrogen at experimental facilities are described and current techniques are presented for their control. As background, the uses of hydrogen, its general properties, and the design and materials for liquid hydrogen systems are discussed. Flame propagation, deflagration and detonation, ignition in free space and under confined conditions are considered under fire and explosion hazards. The techniques of hazard control are examined in relation to hydrogen detection systems, ventilation, liquid hydrogen dump systems, flaring, ignition sources, explosion suppression, inerting, fire control, and personnel exposures. Storage, transfer, and transportation are also discussed. Case histories of hydrogen accidents are included. Two of the liquid hydrogen safety guides, cited among the 60 references, are reproduced. (auth)

38876 (NP-14927) STRONTIUM-90-BILANZ FUER DAS JAHR 1961/62. (Strontium-90 Balance for the Year 1961/62). (Bundesgesundheitsamt, Berlin (West Germany). Institut fuer Wasser-, Boden- und Lufthygiene). Jan. 31, 1963. 40p. Dep. mn.

The ^{90}Sr activity of the soil, fallout, cistern water, milk, foods, and the human skeleton measured in Germany is reported. A biological evaluation of the ^{90}Sr content of the human skeleton was made. The conclusions and recommendations from Vol. 1 of "^{90}Sr in Man and His Environment" are translated in the appendix. (J.S.R.)

38877 (NP-15183) BACKGROUND MATERIAL FOR THE DEVELOPMENT OF RADIATION PROTECTION STANDARDS. PROTECTIVE ACTION GUIDES FOR STRONTIUM-89, STRONTIUM-90 AND CESIUM-137. Report No. 7. (Federal Radiation Council, Washington, D. C.). May 1965. 44p. GPO, $0.30 cy.

Information is presented for guidance in situations involving contamination of the environment by ^{89}Sr, ^{90}Sr, and ^{137}Cs. Both acute localized contamination, in which prompt action will be necessary to avoid exposure of the population, and a widespread, generally-increasing low-level of contamination, such as from stratospheric fallout, that causes a continuous intake of radioactive materials by large numbers of people for a period of years are considered. The transmission of radioactive material from the atmosphere

through food chains to man is outlined and biological risk, dosimetry, and protective measures are discussed. It is concluded that in the event of an acute contaminating event protective actions taken within 2 days will avert 90% of the projected intake, while protective actions initiated at approximately 2 weeks following the contamination will avert 50% of the projected intake. A review of data on radioactivity in food from stratospheric fallout in the U. S. in 1965 led to the conclusion that the health risk from radioactivity in food over the next several years will be too small to justify protective actions to limit the intake of radionuclides either by diet modifications or by altering the normal distribution and use of foods, particularly milk and dairy products. (C.H.)

38878 (ORNL-P-1405) BETA-TYPE ABSORBED DOSE FROM NON-BETA-EMITTING RADIONUCLIDES. Harris, C. Craig (Oak Ridge National Lab., Tenn.). [1964]. Contract W-7405-eng-26. 4p. (CONF-650313-3). Dep. mn; CFSTI, $1.00 cy, $0.50 mn.

From Symposium on Nuclear Medicine, Philadelphia.

The equations of Loevinger et al for estimating the amount of local energy deposition from the electron capture and gamma ray conversion processes from decay-scheme data were used to derive values for the total energy deposition from Auger electrons, conversion electrons, x-rays, and Kx-rays below 11.3 kev. Values in kev per disintegration are reported for ^{131}Cs, ^{51}Cr, ^{57}Co, ^{197}Hg, ^{75}Se, ^{85}Sr, ^{87}Sr, and ^{99}Te. In view of previously published data, mercury-197 and ^{75}Se proved to be particularly interesting, yielding values of 80 kev and 19.2 kev respectively. (H.G.D.)

38879 (RFP-566) PRELIMINARY STUDIES ON REACTIONS OF BURNING PLUTONIUM IN VARIOUS SOLVENTS. Pitts, S. H. Jr. (Rocky Flats Div., Dow Chemical Co., Denver, Colo.). July 19, 1965. Contract AT(29-1)-1106. 11p. Dep. mn; CFSTI, $1.00 cy, $0.50 mn.

Experiments were made by igniting plutonium coupons (0.06 by 0.2 by 0.5 inch), dropping them into the solvents, and recording the temperature, pressure, light intensity, and light duration of the resulting reaction. The plutonium–carbon tetrachloride reaction was consistently the most vigorous. Burning plutonium was extinguished in 1,1,1-trichloroethane, perchloroethylene, 1,1,2-trichloroethylene, chloroform, methanol, and water. The inactivity of inhibited 1,1,1-trichloroethane was found to be due to the compound alone and not the inhibitors. This study suggests that 1,1,1-trichloroethane would be a safer solvent to use for plutonium degreasing. Independent studies have shown this solvent to also be less corrosive to plutonium. (auth)

38880 SUPPORT OF NEW LABORATORY SERVICES BY THE DIVISION OF RADIOLOGICAL HEALTH. McMartin, Howard L. (Public Health Service, Washington, D. C.). Am. J. Public Health, 55: 911-14(June 1965).

The Division of Radiological Health of the U. S. Public Health Service has as a primary responsibility the strengthening of the role of the state and local health departments in the field of radiological health. This comprehensive radiological health plan should include provisions for the adequate surveillance of radiation levels in air, water, food, and milk. To handle the radiation problems, new methods and procedures, new and expensive equipment, and special training are needed to develop radioanalytical competence. A chief goal of the Public Health Service is to develop adequate competency in the states to permit them to handle their own problems of radiation control. As of June 30, 1963, less than half of the states had equipment or trained personnel capable of doing radioanalytical work. Most state and local radiological health programs have come into being in the past five years. The Division has been providing them with services and resources to help them during the first years in program development. This is in the form of financial assistance, assignment of personnel to bolster their staff, consultation through the regional and headquarters offices on technical and administrative matters, provision for training through the use of short courses, as well as funds to universities and individuals for long-term training in the field of radiological health. The Division, to maintain high standards of lab analysis, has established an Analytical Quality Control Service, at Northeastern Radiological Health Lab at Winchester, Mass. This service will assure that all analytical results are within acceptable limits of accuracy, and assist state laboratories and other public health agencies in conducting radionuclide analysis. (BBB)

38881 THE RESULTS OF RADIOACTIVITY MEASUREMENTS OF DUST AND RAINFALL IN WESTERN SLOVAKIA IN 1961-1963. Petrasova, M.; Csupka, S.; Carach, J. Cesk. Hyg., 9: 595-600(1964).

The results of radioactivity measurements of dust and rainfall in Western Slovakia in 1961-63 are published. The average activity of dust fall in March–August 1961 was 1.82 mC per km^2, in September–December 134.43 mC per km^2. An outstanding increase by 2 Rads in average occurred during October 1961 after the tests of megaton nuclear weapons. There was a spring increase of dust fall radioactivity (May 1962 and May, June 1963) and the influence of the dry period was noted on the outstanding decrease of activity and its increase during showers when the level of activity in troposphere is stabilized. (Excerpta Med., Vol. 2, (July 1965))

38882 CONSUMPTION AND INSPECTION OF WATER AND FOOD IN THE EVENT OF A NUCLEAR CONFLICT. Rocquet (Service de Sante des Armees). Gaz. Med. France, 17: 2253-6(June 10, 1964). (In French).

The norm of consumption of irradiated water for a human being can be determined by knowing the physical and biological half time periods of the radioelements, the fraction fixed by an organism, and the quantity of water normally consumed by an individual. The most important cause of radioactive contamination will be non-fissioned elements from the bomb, radioelements produced by fission, and radioelements produced by neutron activation of certain soil elements. Knowing the radioactive periods of the isotopes will make possible the use of some food that was exposed. Food close to an explosion would most likely be unfit for consumption. This food would become radioactive from exposure to ^{24}Na, ^{42}K, ^{32}P, and ^{35}S. Fresh foods become contaminated by metabolically active fission products (^{131}I, ^{89}Sr, ^{90}Sr, ^{137}Cs). A radiochemical analysis of contaminated fresh food should be made before consumption. Water contamination surpassing admissible levels would probably be rare, but decontamination of large quantities of water would be difficult. Water purification installations could not remove more than 70% of the radioactivity. If all the available water is contaminated, filtering through a sock filled with soil (not surface soil) will remove 50 to 70% of the radioactivity. Food and water in containers will be the least affected by radioactivity. (TCO)

38883 DATA ON THE RATE OF AIR EXCHANGE IN PREMISES WITH POWERFUL γ-INSTALLATIONS. Sobol, N. V.; Breger, A. Kh.; Petushkov, A. A. (Inst. of Industrial Hygiene and Occupational Diseases, Academy of Medical Sciences, USSR and Karpov Inst. of Physics and Chemistry, Moscow). Gigiena i Sanit., No. 3, 42-8(Mar. 1965). (In Russian)

The authors carried out experiments which confirmed the correctness of the existing theoretical principle of calculating the rate of air exchange and expenditure. On the basis of the formula obtained nomograms were drawn to determine the air expediture and the rate of air exchange required in case of different values of gamma-activity of the source and the size of the room. (auth)

38884 THE EFFECT OF IONIZING RADIATION ON THE AIR CONTENT OF INDUSTRIAL PREMISES. Dmitriev, M. T. (Scientific-Research Inst. of Hydrometeorological Equipment, Moscow). Gigiena i Sanit., No. 4, 39-44(Apr. 1965). (In Russian).

A study was made of processes leading to the production of nitrogen oxides and ozone in the air under the action of ionizing radiation and neutrons. A comparison of the data obtained with concentrations of nitrogen dioxide and ozone gases, formed in the air under natural conditions, made it

possible to set the maximum permissible doses of ionizing radiation and that of the integral neutron current in the air of industrial premises. The standard values of ventilation required in industrial premises containing radioactive isotopes are given. (auth)

38885 PHILOSOPHICAL INFLUENCES ON RADIATION PROTECTION STANDARDS. Taylor, Lauriston S. (National Bureau of Standards, Washington, D. C.). Health Phys., 11: 859-64(Sept. 1965).

Radiation protection philosophies and practical developments derive from a mixture of technical facts and numerous non-technical influences involving judgment and educated opinion. Various technical developments and various segments of our society each exert their own influence on our radiation protection standards. A complex of national and international bodies, each having its own special interests, has served to complicate, rather than simplify, the philosophical approach to the problem of maximizing man's protection against the hazards of radiation. Whether this redundancy of radiation-standards-making activity is necessary or even good is still an open question. (auth)

38886 GUIDES, STANDARDS AND REGULATIONS FROM THE FEDERAL RADIATION COUNCIL POINT OF VIEW. Palmiter, C. C.; Tompkins, P. C. (Federal Radiation Council, Washington, D. C.). Health Phys., 11: 865-8(Sept. 1965).

The Federal Radiation Council, established in 1959, advises the President with respect to problems in which radiation is a factor and recommends to the President guidance for Federal agencies in their radiation protection programs. In the development of radiation protection guidance it is necessary to consider the balance between the need for radiation programs and the possible effects on the health of the individual and the public. This involves fundamental determinations of public policy influencing national security, economics and other factors. In a specific case where this balance is achieved, the guide which is developed does not, and cannot, set a line which is safe on one side and dangerous on the other. Guidance for protective programs to reduce exposure from radioactive materials after they are in the environment must consider any health benefit associated with the available reduction in exposure and the over-all impact on the program. The decision to implement a protective action program must consider such factors as the resulting exposure if no action is taken, how much exposure can be reduced by taking the action, the difficulty of making the action effective, and possible risks to health, direct or indirect, that may be associated with the action itself. Judgment and discretion in the application of any radiation protection guidance are necessary to assure in a reasonable manner the attainment of the goal of protecting man and also realizing the benefits from the uses of ionizing radiation. (auth)

38887 GUIDES, STANDARDS AND REGULATIONS FROM STATE HEALTH DEPARTMENT POINT OF VIEW. Davies, Sherwood (New York State Department of Health, Albany). Health Phys., 11: 869-73(Sept. 1965).

Health is an almost exclusive responsibility of the states. Over 90 per cent of all radiation sources are subject to exclusive jurisdiction of the states. Since 1953 the New York State Health Department has been developing a comprehensive radiation control program. This program includes environmental surveillance, surveys of facilities using x ray, and radioactive materials, and surveys of nuclear facilities. (auth)

38888 PUBLIC HEALTH RADIATION SURVEILLANCE. Terrill, James G. Jr. (U. S. Department of Health, Education, and Welfare, Washington, D. C.). Health Phys., 11: 917-33(Sept. 1965).

A basic public health outlook on environmental monitoring is presented. The public health significance, scope, and need for environmental monitoring, certain controlling criteria on acceptability of data, pertinent statutory requirements and a description of air and milk data provide a background for commenting on the future. (auth)

38889 ANALYTICAL RADIOCHEMISTRY IN HEALTH PHYSICS. Goldin, A. S.; Kahn, B. (Northeastern Radiological Health Lab., Winchester, Mass. and Robert A. Taft Sanitary Engineering Center, Cincinnati). Health Phys., 11: 935-44(Sept. 1965).

An important phase of health physics is the utilization and development of chemical and instrumental techniques for the accurate measurement of the radionuclide content of various type of samples. This paper describes broadly the newer developments in these techniques, including the utilization of standards and the validation of analytical results (quality control). Advantages and deficiencies of the various techniques are noted and predictions of future developments are made, based on present needs and promising discoveries and applications. (auth)

38890 WHOLE-BODY COUNTING. Roesch, W. C. (General Electric Co., Richland, Wash.). Health Phys., 11: 945-8(Sept. 1965). (HW-SA-3601).

Applications of whole-body counting of radioactivity in man are discussed. These include studies on fallout fission product metabolism, in radiation protection programs at radiation installations, and in biological research and medical studies. (C.H.)

38891 EXTERNAL GAMMA EXPOSURE TO MAN FROM THE FISSION PRODUCTS DISPERSED IN THE ATMOSPHERE. Havlovic, Vratislav (Charles Univ., Prague). Health Phys., 11: 971-3(Sept. 1965).

A method is described for estimating the external γ dose to man from radioactive aerosols containing fission products of nuclear explosions dispersed in the atmosphere. Calculations of the external γ dose to which man was subjected in 1957, 1958, 1959, and 1960 are included. (C.H.)

38892 PENETRATION OF RADIATION FROM NUCLEAR WEAPONS: APPLICABILITY TO THE HIROSHIMA AND NAGASAKI SURVEY. Ritchie, H.; Hurst, G. S. Hiroshima Igaku, 16: 602-21(1963).

Some of the energy from the atomic bomb takes the form of γ rays and neutrons which traverse the air for a long distance from the explosion site, resulting in extensive biological damage. In this connection, vital physical data on shielding against radiation from nuclear weapons are given, viz. dosimetric data, study of distribution of neutrons and γ rays, and spectrum of fast neutrons. (Excerpta Med., Vol. 2, (July 1965))

38893 A NEW METHOD OF INTEGRAL DOSE MEASUREMENT WITH A PLASTIC SCINTILLATOR PHANTOM. Murai, Takeo; Nakamura, Tadashi; Yamamoto, Akira (Tokyo Medical and Dental Univ.). J. Radiation Res. (Japan), 5: 23-35(Mar. 1964).

The plastic scintillator emits fluorescent light of which the quantity is proportional to the absorbed radiation dose in it. And it can be believed that in this phenomenon the energy dependence does not exist. Based upon the above characteristics of the plastic scintillator a new method of the integral dose measurement was developed. A cuboid plastic scintillator of $28 \times 28 \times 15$ cm in size was used as a phantom. It was irradiated by x rays and fluorescent light from the phantom was measured as a direct current using a photomultiplier, thus the integral dose in the phantom was obtained. Results were compatible with those obtained by Bewley and his co-workers. (auth)

38894 FALLOUT RADIOACTIVITY IN DIET AND EXCRETA. THE LEVELS AT TOKAI DISTRICT, JAPAN IN 1962 TO 1963. Fujita, Minoru; Akaishi, Jun; Iwamoto, Junko; Yabe, Akira; Ichikawa, Yoshiko; Okamoto, Toshio; Fukuda, Hiroshi (Japan Atomic Energy Research Inst., Tokyo). J. Radiation Res. (Japan), 5: 56-68(Mar. 1964).

The levels of fission products such as ^{90}Sr, ^{137}Cs, ^{95}Zr, ^{95}Nb, ^{103}Ru and ^{106}Ru in diet and excreta were examined. The experiment started in May, 1962 and ended in February, 1963. During the period, seven intermittent samplings of excreta and diet were made. In each sampling, excreta were collected over five consecutive days from four normal human subjects who took the same diet at that time. An exact duplicate of the diet was collected at

the same time. A large NaI(Tl) crystal scintillator and a 100 channel pulse height analyzer were used to determine the radioactivities of γ-emitters in ashed samples, but ^{90}Sr and ^{137}Cs were analyzed radiochemically. In general, the value of ^{95}Nb in the diet was highest among all the radioactive fission nuclides, reaching about 60 $\mu\mu$c/day/person in February, 1963. The level of ^{90}Sr in the diet varied between 7.0 and 13 $\mu\mu$c/day/person during the period, and that of ^{137}Cs changed between 13 and 35 $\mu\mu$c/day/person. However, about 1 $\mu\mu$c of ^{90}Sr was always found in 24-hr urine samples, irrespective of the contents in the diet. The activities of ^{137}Cs in the same urine specimens, in contrast to ^{90}Sr, changed between 10 and 31 $\mu\mu$c corresponding to the contents in the diet. During the period examined, the levels of ^{137}Cs and ^{95}Zr + ^{95}Nb in the diet varied according to the changes of the dry fallout in the atmosphere. The amount of stable potassium and calcium in the diet and excreta were also examined. (auth)

38895 ZINC-65 AND OTHER FALLOUT NUCLIDES IN MARINE ORGANISMS OF THE CALIFORNIA COAST. Nagaya, Yutaka (Maritime Safety Agency, Tokyo); Folsom, Theodor R. J. Radiation Res. (Japan), 5: 82-9(Mar. 1964).

Measurements were made of several fallout nuclides in selected organisms of the California coast. Hagfish and amphipod were noticeably free from ^{95}Zr and contained small amounts of ^{137}Cs (average 1.2 and 32 $\mu\mu$c/kg-wet). Mussel, a filter feeder, contained less ^{137}Ca but its ^{65}Zn and ^{54}Mn concentrations were remarkable (average 50.2 and 24.5 $\mu\mu$c/kg-wet). Zinc-65 concentration in amphipod is about 5 times that of mussel, but it did not contain ^{54}Mn. (auth)

38896 AN APPARATUS FOR THE COLLECTION OF SAMPLES OF AEROSOLS ON MEMBRANE FILTERS. Havlovic, Vratislav; Santholzer, Vilem. (Charles Univ., Hradci Kralove, Czechoslovakia). Jaderna Energie, 11: 102-3(Mar. 1965). (In Czech).

The apparatus uses a membrane filter with a pore size 1.2 μ. Curves are given showing flow rate and pressure drop as a function of time. Results of collections of activity from June 1963 through June 1964 are shown. These data were used to calculate the rate of dry deposition of activity, V, and a cleansing factor, W, based on the activity in rain water. During the course of the period tested, V fell from 0.6 cm/sec to 0.4 cm/sec while the factor W was of the order of 1000 to 2000. These figures are given as examples of the way in which such equipment can be used to predict the long-term nuclear fallout on the earth's surface. (TTT)

38897 METHODS OF CALCULATION IN NEUTRON DOSIMETRY. Nachtigall, D. (Kernforschungsanlage, Julich, Ger.). Kerntechnik, 7: 285-8(June 1965). (In German).

Methods for calculating the first collision energy dose of monoenergetic fast neutrons, of the first collision energy dose of continuous spectra of fast neutrons, the energy dose in large objects, and the dose equivalence of neutrons are given and illustrated with examples. (J.S.R.)

38898 ROYAL ORDER OF 28 FEBRUARY 1963 CONCERNING THE PROTECTION OF THE PUBLIC AND WORKERS AGAINST IONIZING RADIATIONS. Moniteur Belge (Brussels), No. 98, 5206-86(May 16, 1963).

The scope includes definition of terms, inspection of working conditions, and medical examinations, education of the worker and his duties, general safety provisions and measures, radioactive waste, the medical use of unsealed isotopes, the storage and use of radioactive materials for use in medicine, transport of radioactive substances, and nuclear propulsion. Special provisions are given concerning the theft or loss of radioactive substances, accidents and contamination, decontamination and handling of corpses. Provisions concerning environmental monitoring are made. Approval of experts, institutes and physicians and responsibility are discussed. (auth)

38899 DETECTION OF NUCLEAR FISSION PRODUCTS FROM THE CHINESE NUCLEAR WEAPON TEST IN THE LOWER TROPOSPHERE BETWEEN 3000 AND 700 m NN. Reiter, R. (Fraunhofer-Gesellschaft, Garmisch, Ger.). Naturwissenschaften, 52: 128-9(1965). (In German)

Continuous measurements of the specific nuclear fission product of the radioactivity of the air carried out at 3 geophysical stations of the Garmisch Institute made possible the detection of the passage of nuclear fission products from the October 15, Chinese Nuclear Weapon Test and the study of the exchange processes between 3000 and 700 m NN. The inflow of the nuclear fission products was in clouds. At 3000 m two concentrated and several diluted clouds were noted. (J.S.R.)

38900 . FILTRATION MATERIALS FOR RESPIRATORS PROTECTING AGAINST RADICACTIVE AEROSOLS. Spurny, K. Pracovni. Lekar., 17: 22-4(1965).

By means of radioactive labeled NaCl aerosol with a medium size of particles r = 0.3 μ, it was found that the effective absorption of submicronic particles by the Lepestok filter (chlorated PVC) is greater than 99.99%. It seemed advantageous to use respirators with this kind of filter while working with radioactive isotopes. (Excerpta Med., Vol. 2, (July 1965))

38901 STRONTIUM-90 IN THE BALTIC SEA. Paakkola, O.; Voipio, A. (Inst. of Radiation Physics, Helsinki). Suomen. Kemistilehti, 38: B11-B17(1965).

Samples (48) collected during the years 1959–1963 from 9 sampling stations were analyzed. The ^{90}Sr activity in the surface water varied from 0.24 to 1.8 pC/l and in the bottom waters from 0.05 to 0.41 pC/l. The ratio of ^{90}Sr to Ca was calculated. ^{90}Sr values were compared with the fallout rate in the Northern Hemisphere and with the level of the ^{90}Sr content of the Finnish milk. The correlation between ^{90}Sr and salinity is discussed. A detailed procedure for the determination of ^{90}Sr in brackish waters is appended. (Excerpta Med., Vol. 2, (July 1965))

38902 METHODS PREVENTING THE DIFFUSION OF RADIOACTIVE MATERIALS FROM NUCLEAR REACTORS AND HOT LABORATORIES. Pelser, J. Water, Bodem, Lucht, 54: No. 4, 67-73(1964).

Methods employed for the safe operation of nuclear reactors and hot laboratories by preventing release of radioactive materials are reviewed. In the case of nuclear reactors leakage of the fuel cladding, the primary cooling circuit, and the containment have to be prevented. The disposal of gaseous radioactive waste is an important problem. In hot laboratories a good ventilation system is necessary; several precautions are required for the handling of solid, liquid, and gaseous radioactive waste. (J.V.E.)

38903 METHODS FOR SURVEYING THE AIR CONTAMINATION BY RADIOACTIVE AEROSOLS. Sivintsev, Yu. V.; Khovostov, Kh. Kh. pp 165-86 of Predel'no Dopustimye Kontsentratsii Atmosfernykh Zagryaznenii. Moscow, Medgiz, 1962. (In Russian)

In view of the potential danger presented by the absorption of ionizing radiation in the tissue and the absence of a clear threshold effect, the ICRP recommended in 1958 that the maximum permissible professional exposure be lowered from 600 to 200 rem. As a result of this, new, lower MPC values were established in 1960 for the various radioisotopes, reducing especially the permissible values for the α-active aerosols with a high specific activity: for ^{210}Po – 1×10^{-16}, for ^{226}Ra – 3×10^{-16}, and for ^{239}Pu – 2×10^{-17} C/l. These values present the problem of determining the concentration of long-half-life radioactive aerosols in the important concentration range from 10^{-14} to 10^{-17} C/l. As these activities lie below the sensitivity of current radiometric methods, the measurements require a concentration of the low contents by using large volumes of air; however, this is rendered difficult by the relatively high background activity of the air caused by the atmospheric nuclear weapons testing. In order to yield reliable data, the activity of the sample on the filter paper must exceed the background level by at least a factor 2, requiring the passage of at least 1 m^3 of air through the filter. This is sufficient for measurements in the 10^{-13} C/l range, of interest for thoron and radon fission products; for true contaminants, 20 to

2000 m^3 of air must be sampled. The specifications require a pumping rate of 7 to 10 l/min/cm^2 of filter, or 80 to 120 l/min for the usual 12 cm^2 filter paper. It was found that ventilating systems with flow rates from 50 to 100 m/hr are useful for such analyses. The energy spectra of the β active materials must also be taken into account. (TTT)

38904 UMWELTRADIOAKTIVITÄT UND STRAHLENBELASTUNG. Bericht IV/64. (Environmental Radioactivity and Radiation Burden. Fourth Quarterly Report, 64). Bad Godesberg, Bundesminister fuer Wissenschaftliche Forschung, 1965. 179p. DM 8,--.

The results of measurements on the radioactivity in air, water, earth, and foods and the radiation burden of the population in the West German Republic are reported for the fourth quarter of 1964. Data are tabulated. (J.S.R.)

38905 SOURCE OF RADIATION FOR MEASURING PURPOSES. Siering, Richard (to Phywe AG). British Patent 990,665. Apr. 28, 1965. Filed Sept. 23, 1963.

A source of radiation for measuring purposes that is suitable for classroom lecture work consists of two cylindrical vessels of radiation shielding material. Each cylinder has walls of at least 10 mm thickness, and each cylinder is closed at one end. The base of the inner cylinder carries the radioactive preparation, and the outer cylinder serves to close the inner cylinder's open end. (B.L.M.)

38906 ATMOSPHERIC FALL-OUT COLLECTOR. Blondeau, Emile; Doury, Andre; Francois, Henri (to Commissariat a l'Energie Atomique). British Patent 996,864. June 30, 1965. Priority date Dec. 5, 1962, France.

An apparatus provides a collector for atmospheric dust, particularly radioactive fallout, that includes an adhesive surface for retaining dry particles and a cover for the adhesive surface controlled by means responsive to atmospheric precipitation. The adhesive surface is exposed when precipitation is not occurring and is covered when precipitation is occurring. When the cover is in position over the adhesive surface, means connected to the cover control mechanism serve to guide the precipitation toward a receptacle. (B.L.M.)

38907 METHOD FOR THE RECOVERY OF DEUTERIUM OXIDE AND TRITIUM FROM THE AIR OF CLOSED ROOMS OF NUCLEAR REACTOR INSTALLATIONS AND DEVICE FOR ITS ACCOMPLISHMENT. Ziegler, Albert; Meyer, Peter-Juergen (to Siemens-Schuckertwerke AG). German Patent 1,194,995. June 16, 1965. Filed Aug. 16, 1962.

The method consists of repeatedly drying and saturating the air by spraying with non-irradiated light or heavy water until the tritium content is reduced below a predetermined level. (Gmelin Inst.)

38908 SHIELDED CONTAINERS FOR NUCLEAR FUEL ELEMENTS. Ashcroft, David John (to United Kingdom Atomic Energy Authority). U. S. Patent 3,179,243. Apr. 20, 1965. Priority date May 24, 1960, Great Britain.

A shielded container for the temporary storage of irradiated fuel elements includes two mating parts of tubular form. The first part has a closed lower end and an upper open one, and the second part insertable into the first part has an open lower end and a closed upper one. A fuel supporting magazine is demountably located in the first part, and an opening in the side wall of the first part is of a size and form to allow sideways removal of the magazine. The opening is normally closed by the wall of the second part when the second part is inserted into the first. The closed end of the second part defines a port aligned with the magazine for the endwise entry of fuel into the magazine. A sealing joint member is provided between the lower end face of the wall of the second part and the closed lower end of the first part. (B.L.M.)

38909 APPARATUS FOR WIPE TESTING RADIOACTIVE SOURCES. Noble, Robert C.; Broyles, Leland E.; Sandeen, Charles R. U. S. Patent 3,191,037. June 22, 1965. Filed Feb. 4, 1963.

An apparatus for leak testing radioactive sources sealed in stainless steel capsules provides a complete 360° wipe and variable wipe pressure. The apparatus, which is secured between the storage container and the projector head, consists essentially of a special doughnut or gauze-covered ring through which the source is reciprocated by use of the source control cable. The gauze is then removed and tested for the presence of contamination. (A.G.W.)

INSTRUMENTATION

General

Refer also to abstracts 39270 and 39690.

38910 (CERN-6-11(p.43-56)) AUTOMATIC ANALYSIS OF PHOTOGRAPHIC DATA IN BIOLOGY. Butler, J. W.; Butler, Margaret K.; Stroud, Agnes (Argonne National Lab., Ill.).

Photographs of chromosomes in individual cells are analyzed by flying-spot devices, and are thereby classified by size and configuration. The data obtained in this analysis are prepared in a form suitable for computer calculations. (T.F.H.)

38911 (LA-DC-7004) APPLICATION OF MINIATURE INTRINSIC THERMOCOUPLES FOR REACTOR TRANSIENT DIAGNOSTICS. Morrison, Roderick G. (Los Alamos Scientific Lab., Univ. of California, N. Mex.). [nd]. Contract W-7405-eng-36. 3p. (CONF-650602-16). Dep. mn; CFSTI, $1.00 cy, $0.50 mn.

From American Nuclear Society 11th Annual Meeting, Gatlinburg, Tenn.

A technique was developed using small thermocouple leads to better understand the behavior of coated particle fuels when subjected to rapid nuclear transients. An experiment was conducted using this technique. The procedure and results are presented. (M.O.W.)

38912 (LA-DC-7025) THE RESPONSE OF PRESSURE TRANSMISSION LINES. Watts, Geoffrey P. (Los Alamos Scientific Lab., Univ. of California, N. Mex.). [1965]. Contract W-7405-eng-36. 11p. (CONF-651002-5). Dep. mn; CFSTI, $1.00 cy, $0.50 mn.

For Presentation at Instrument Society of America, 20th Annual Conference, Los Angeles.

Due to environmental factors, it is often necessary to separate a pressure transducer from the region in which pressure is to be measured. Pressure lines are then required to transmit the pressure to the pressure transducer. Equations describing the response of pressure lines have been derived by Iberall, and are sufficiently complicated that they have never had wide use. A digital computer code was devised which calculates pressure line response using Iberall's equations. Laboratory experiments were conducted using condenser microphones to measure the response of $\frac{1}{4}$ inch and $\frac{3}{4}$ inch outside diameter tubes containing atmospheric air. Frequency response data obtained in the 10 to 2000 cps region. Reynolds numbers in the tubes were held below 2000. The experimental and calculated results agree to within the experimental accuracy for 4 and 8 foot long tubes. Considerable error is evident, however, when tubes as short as 6 inches are used. (auth)

38913 (LA-DC-7071) VERSATILE HIGH TEMPERATURE THERMAL ANALYSIS APPARATUS. Rupert, George N. (Los Alamos Scientific Lab., Univ. of California, N. Mex.). [1963]. Contract W-7405-eng-36. 2p. (CONF-650914-1). Dep. mn; CFSTI, $1.00 cy, $0.50 mn.

From 1st International Conference on Thermal Analysis, Aberdeen, Scotland.

An apparatus was developed for the use of the classical methods of thermal analysis and differential thermal analysis at 1000 to 3000°C. Its operation is described. Display techniques are described for thermal analysis, differential thermal analysis, derivative thermal analysis, and thermal derivative thermal analysis. (D.L.C.)

38914 (SC-DC-65-1332) MODULATOR MATERIALS STUDY PROGRAM. Final Report. McQuistan, Richmond B. (Honeywell, Inc., Minneapolis, Minn. Aeronautical Div.). July 1963. For Sandia Corp., Albuquerque, N. Mex. Contract AT(29-1)-789. 71p. Dep.(mn); $3.00 (cy), 2(mn) CFSTI.

The fabrication and electro-optical properties of Ge- and Si-junction i-r modulators are investigated theoretically and experimentally. The factors studied include figures of merit, operation mechanisms, and the effects of fabrication procedures on the characteristics (particularly on the relation between frequency bandwidth and minority carrier lifetime). (T.F.H.)

38915 (SC-DC-65-1419) ACCEL: AUTOMATED CIRCUIT CARD ETCHING LAYOUT. Fisk, C. J.; Isett, D. D. (Sandia Corp., Albuquerque, N. Mex.). Apr. 1965. Contract AT(29-1)-789. 13p. Dep. mn; CFSTI, $1.00 cy, $0.50 mn.

The feasibility of computer-controlled production of printed circuit boards was studied. The computer operations include conversion of engineering design into computer input data, editing data for validity, retention in a computer-accessible library of the dimension and performance characteristics of a standard set of components, method for handling nonstandard data, positioning the components on the board layout, and making the electric connections by routing paths connecting like electric nodal points. Subroutines were written for the SC 4020, a magnetic tape-to-microfilm converter. The design limitations for which programs are being developed are given. Principles of the various computer operations are described. (M.J.T.)

38916 (SC-DC-65-1589) APPLICATION OF ELECTRON MICROSCOPY IN DIMENSIONAL METROLOGY. Estill, W. B.; Moody, J. C. (Sandia Corp., Albuquerque, N. Mex.). [July 20, 1965]. Contract AT (29-1)-789. 19p. (CONF-651002-3). Dep. mn; CFSTI, $1.00 cy, $0.50 mn.

For presentation at Instrument Society of America, 20th Annual Conference, Los Angeles.

The amount of plastic deformation caused by a Talysurf stylus as it is traced across a thin gold film can be determined by the use of electron microscopy. In this experiment, variables were introduced that caused changes in the magnitude of plastic deformation from 50 to 490 Å. The study indicated that the damage to a thin film of soft gold can probably be limited to about 100 Å if appropriate precautions are taken. (auth)

38917 (SC-R-65-904, pp 23-48) AN EXTENDED RANGE VELOCITY GAGE FOR MEASUREMENTS IN HIGH SHOCK ENVIRONMENTS. Wistor, J. W. (Sandia Corp., Albuquerque, N. Mex.).

The development of a high-range velocity gage for use in structure and free field measurements is described. The gage is a highly overdamped, low-natural-frequency accelerometer operating in the "velocity" portion of its response spectrum. Two models, DS and DX, are described. The Model DX was designed to measure ground motions in the vicinity of subsurface explosions. (D.L.C.)

38918 (SC-R-65-904, pp 49-58) ELECTRONIC INTEGRATORS FOR INSTRUMENTATION APPLICATIONS. Hansen, G. J. (Sandia Corp., Albuquerque, N. Mex.).

Compensated electronic integrators for accelerometers and velocity gages allow integrated velocities and displacements to be immediately available after an event. The circuits and their operation in single and double integrators are described. Typical instrumentation results from displacement sled tests are shown, and electronic and computer integrations are compared. (D.L.C.)

38919 (SC-R-65-904, pp 59-74) INSTRUMENTING NUCLEAR EXPLOSIONS. Palmer, D. G. (Sandia Corp., Albuquerque, N. Mex.).

Some possible effects of nuclear explosions and environments on instrumentation packages are described. The elements of a general instrumentation system and the economic factors affecting design are discussed. Sensor characteristics, remote calibration, and telemetry cables are considered. (D.L.C.)

38920 (TID-22019) AN EVALUATION OF A FAST COMPLEMENTARY, HYBRID BISTABLE MULTIVIBRATOR. Scientific Report No. 18. Barnett, T. O.; Pierce,

J. F. (Tennessee Univ., Knoxville. Dept. of Electrical Engineering). Apr. 15, 1965. Contract W-7405-eng-26, Subcontract 2160. 63p. Dep. mn; CFSTI, $3.00 cy, $0.75 mn.

For Oak Ridge National Lab., Tenn.

A high-speed common-base transistor, tunnel-diode bistable multivibrator was analyzed. Emphasis was placed on the suitability of the circuit for high-speed scaling-system applications. A steady-state analysis, a transient analysis, and an experimental evaluation of the circuit are given. The characteristics of the circuit tested were triggering resolution, five nanoseconds; stage delay, five nanoseconds; triggering sensitivity, 0.5 volt; and temperature stability range, 25 to 100°C. The output pulse produced by the circuit provided marginal triggering of an identical stage. The results indicated that the bistable circuit met all of the requirements of a useful, high-speed scaling-system element except for the capability of triggering an identical circuit reliably. An interstage pulse amplifier is apparently necessary to produce an adequate trigger pulse. (auth)

38921 (UCRL-11623) ULTRACENTRIFUGE PHOTOELECTRIC SCANNER, MULTIPLE CELL. Lamers, Kenneth W. (Lawrence Radiation Lab., Univ. of California, Berkeley). Apr. 1, 1965. Contract W-7405-eng-48. 130p. Dep. mn; CFSTI, $4.00 cy, $1.00 mn.

A description is given of the modifications for conversion of an electromechanical scanner to multiple-cell operation, and instructions are given. The scanner is used for displaying optical density changes that take place when a light-absorbing material such as virus, protein, or nucleic acid is sedimenting in the centrifugal field of an ultracentrifuge—that is, a high-speed centrifuge employing an optical system. These materials absorb some of the light transmitted by the optical system, thereby projecting a pulsating image that varies in intensity with distance from the center of rotation. This image is scanned by a photomultiplier and compared with the pulsating image of a reference cell in order to compensate for nonuniform illumination and other optical imperfections. Circuitry separates the reference and sample pulses, subtracts their logarithmic equivalents, and displays the subtraction on a chart recorder. The chart moves in synchronism with the scanner, and optical density (concentration) is therefore displayed as a function of radius. The system includes additional features such as: (a) an internal calibration that permits measurements of absolute density; (b) a monochromator to facilitate spectral analysis, a powerful tool for disclosing the radial distribution of components responsive to different wavelengths; and (c) derivative of the function, which is displayed in time coincidence. The system described is an improved version of an earlier model in that it is designed (a) for two double-sector cells separated 180 deg, with sector separation 2.5 deg at each cell, or (b) for two single-sector cells, also separated 180 deg. Single-sector cells are 4 deg; this permits longer slits and increases illumination proportionately. Other modifications improve basic performance over that of the earlier version. (auth)

38922 (AAEC/Trans-18) THE DETERMINATION OF THE SPECIFIC CONDUCTANCE OF REFRACTORY MATERIALS IN VACUUM UP TO 2200 deg C. Lulichev, A. N.; Chuprinin, F. I.; Kovalenko, S. I. Translated by H. J. de Bruin (Australian Atomic Energy Commission Research Establishment, Lucas Heights) from Zavodsk. Lab., 23: 931(1957). 4p. Dep. mn; CFSTI, $1.00 cy, $0.50 mn; JCL, $1.10 fs, $0.80 mf.

An apparatus for measuring the electric resistivity of refractory ceramics in a vacuum up to temperatures of 2200°C is described. (W.L.G.)

38923 (UCRL-Trans-1228) ON THE COMBINATION OF THE PHASE CONTRAST PROCESS WITH FLUORESCENCE MICROSCOPY. Gabler, F.; Herzog, F. Translated by Joseph L. Zygielbaum (Data Dynamics, Inc., Monterey, Calif.), from Appl. Opt., 4: 469-72(1965). 15p. Dep. mn; JCL, $1.60 fs, $0.80 mf.

After discussion of several technical problems regarding instrumentation of fluorescence microscopy and of the ways how to solve them, a device is described which makes it possible to examine fluorescent specimens both in positive and negative phase contrast (so-called simultaneous contrast fluorescence). Furthermore, light filtration and the relating questions are briefly mentioned. Finally, the resulting effects and the manifold fields of application of this new device are demonstrated with the aid of two examples and its advantages are discussed. (auth)

38924 ESONE—A NUCLEAR ELECTRONICS SYSTEM. Becker, W. (Euratom-Kernforschungszentrum, Ispra, Italy); Stuckenberg, H.-J.; Zander, K. Atomwirtschaft, 10: 298-302(June 1965). (In German).

ESONE (European System of Nuclear Electronics) constitutes a system of electrical and mechanical reference parameters for application to nuclear electronic equipment including all associated logical connections and instrumentation for automation and programming. The principles set up undertake to establish a practicable system not only for mechanical dimensions but also for electrical supply and control voltages, for plug-and-socket connections, etc. The adoption on a voluntary basis at numerous nuclear research centers within the Euratom countries won for this system a supranational area of validity. The origin, structure, and recommended parameters of the system are discussed. The objective of such system is to make electronic equipment of different origins interchangeable and usable together, without any need generally of an additional electrical or mechanical adaptation of the various units. (auth)

38925 THE UTILIZATION OF MASS SPECTROMETRY IN NUCLEAR SCIENCE. Nater, K. A. Atoomenergie Haar Toepassingen, 7: 73-81(Apr. 1965). (In Dutch)

After a description of the various types of mass spectrometers, a number of mass spectrometric techniques used in nuclear science are discussed. These include gas analysis, the determination of isotopic ratios in solids, trace analysis, and the determination of thermodynamic data. (tr-auth)

38926 PERFORMANCE OF A BENNETT RADIO-FREQUENCY MASS SPECTROMETER. Ryan, K. R.; Green, J. H. (Univ. of New South Wales, Australia). J. Sci. Instr., 42: 455-60(July 1965).

An improved Bennett-type r-f mass spectrometer is described. Characteristics of the ion source, sensitivity and resolution, and the dependence of the collected ion current on various factors are described. (auth)

38927 KINETIC ENERGY OF FRAGMENT IONS USING A RADIO-FREQUENCY MASS SPECTROMETER. Ryan, K. R.; Green, J. H. (Univ. of New South Wales, Australia). J. Sci. Instr., 42: 461-4(July 1965).

The possible methods of measuring excess kinetic energy of fragment ions using an r-f mass spectrometer are discussed. Retarding potential analysis before mass analysis is examined experimentally. Fragment ions from the simple molecules N_2, CO and CO_2 were examined in this way. It is concluded that the instrument can detect the presence of fragments with excess initial kinetic energy and that the results obtained are qualitatively similar to those obtained using magnetic deflection instruments. (auth)

38928 MONOCHROMATIC PHOTOGRAPHY IN THE EXTREME ULTRAVIOLET. Burton, W. M. (United Kingdom Atomic Energy Authority, Abingdon, Berks, Eng.). J. Sci. Instr., 42: 477-9(July 1965).

A pinhole camera with a thin aluminium filter can be used for broadband photography in the wavelength region below 800 Å. Two developments of this instrument are described which result in improved wavelength resolution. The first uses a camera with a reflection filter to provide sensitivity only in the waveband from 170 to 800 Å. The reflection filter consists of two mirrors used at 10° grazing angle to reject short wavelength radiation. The second instrument combines a pinhole camera with a plane diffraction grating used at grazing incidence to

give increased wavelength resolution. This instrument was used to obtain monochromatic photographs of a helium plasma in spectral line radiation at 304 and 256 Å. (auth)

38929 A MAGNETIC VELOCITY SELECTOR FOR HYDROGEN ATOM BEAMS USING AN UNFOLDING TECHNIQUE. Fluendy, M. A. D. (Harvard Univ., Cambridge, Mass.). J. Sci. Instr., 42: 489-91(July 1965).

A velocity selector for hydrogen atom beams using an inhomogeneous magnetic field is described. The transmission intensity as a function of field strength is calculated from the geometry of the system. The resulting Fredholm equation is then solved numerically to yield the intensity-velocity distribution in the beam. (auth)

38930 CYLINDRICAL GEOMETRY SPUTTERING APPARATUS. Sinclair, W. Robert; Peters, F. G. (Bell Telephone Labs., Inc., Murray Hill, N. J.). J. Vacuum Sci. Technol., 2: 178-81(July-Aug. 1965).

A cylindrical geometry sputtering apparatus and associated fixtures were described which feature ease of construction and use. Because of the high symmetry of the apparatus, films can be deposited simultaneously on different substrates at different temperatures and meaningful comparisons made between results. Films can be deposited onto substrates that are electrically floating, and it is pointed out that this is valuable in reactive sputtering in oxygen as it minimizes damage to sensitive electronic structures which can be caused by anionic bombardment. The planarity of the sputtered films and the rate of deposition are discussed. (auth)

38931 TUNNELING IN III-V COMPOUND p-n JUNCTIONS. Shewchun, John (Brown Univ., Providence); Williams, Robert M. Phys. Rev. Letters, 15: 160-3 (July 26, 1965).

Measurements were made near 1°K around zero bias in GaAs, GaP, and InP p-n junctions. At least three separate effects were observed which lead to bell-shaped resistance-voltage curves. Spike structure was found in GaP, but not in InP. It was found that for GaP and InP, the incremental zero-bias resistance exhibits a three-segment logarithmic temperature dependence. (D.C.W.)

38932 MULTICHANNEL TIME-DELAY ANALYZER (REVIEW). Firsov, E. I.; Chernyavskii, A. F.; Shushkevich, S. S. (Belorussian State Univ., USSR). Pribory i Tekhn. Eksperim., No. 2, 5-14(Mar.-Apr. 1965). (In Russian).

A review on the measurement of the duration of brief physical phenomena using multichannel analyzers is presented, covering both instrumentation and methods. (D.C.W.)

38933 SUPERCONDUCTING PSEUDO-HELMHOLTZ COIL. Sampson, W. B. (Brookhaven National Lab., Upton, N. Y.); Kruger, P. Gerald. Rev. Sci. Instr., 36: 1081-3(Aug. 1965). (BNL-9130)

The field distribution along the axis of a Nb_3Sn superconducting pseudo-Helmholtz coil, or "split pair," was measured for various spacings between the two coils. The results agree well with the classically calculated field distribution, and no current degradation effects that could be attributed to the multiple coil arrangement were observed. A maximum field of 58 kgauss was obtained in the region between the coils with the fields adding and a maximum field gradient of 26 kgauss cm was achieved with the coils powered in opposition. (auth)

38934 DESIGN OF EFFICIENT FLUX CONCENTRATORS FOR PULSED HIGH MAGNETIC FIELDS. Wilson, M. N.; Srivastava, K. D. (Rutherford High Energy Lab., Chilton, Berks, Eng.). Rev. Sci. Instr., 36: 1096-1100 (Aug. 1965).

The design of flux concentrators to produce pulsed high magnetic fields is discussed with special attention to the problem of energy transfer efficiency. A flux concentrator is described which produces a peak field of 300 kgauss in a cylindrical volume 2.0 cm in diameter and 3.5 cm in length. Energy storage is by means of a 440 μF capacitor bank, and the pulse length is 120 μsec. (auth)

38935 DESIGN OF HIGH FIELD MAGNET COILS FOR LONG PULSES. Gersdorf, R.; Muller, F. A.; Roeland, L. W. (Universiteit, Amsterdam). Rev. Sci. Instr., 36: 1100-9(Aug. 1965).

Magnet coils are investigated which can produce magnetic fields of 15 to 40 Mamp/m (200–500 kgauss) during working times of the order of 0.1 sec. These fields are suited for measurements in highly conducting materials. The coils are precooled to 20 or 77°K, and the Joule heat is not removed during the pulse. The thermal limitations of this method are reviewed. Plots are given for the optimum dimensions and current densities for coils producing a specified field during a specified time, minimizing the necessary power supply. Details of a magnet constructed along these lines are given. The maximum field produced by this coil, 16 Mamp/m (200 kgauss) during 0.3 sec, however, proved to be determined by mechanical instabilities. These problems are reviewed. Calculations of the Lorentz force and the internal stresses resulting from it were carried out taking the elastic and plastic properties of copper and insulation into account. It is shown theoretically that a magnet stable to 35 Mamp/m (440 kgauss) can be built from hard-drawn copper if a reinforcing steel cylinder is used at a certain radius inside the coil. (auth)

38936 X RAY LUMINESCENCE SAMPLE COMPARTMENT WITH AUTOMATIC SHUTTER. Bodi, Lewis J.; Cosgrove, James F.; McIntosh, Gardiner (General Telephone and Electronics Labs., Bayside, N. Y.). Rev. Sci. Instr., 36: 1112-13(Aug. 1965).

A sample compartment is described which, with a standard x-ray generator, allows routine observation of phosphor response to x rays. A unique feature is an automatic shutter which permits safe sample transfer while the x-ray tube is excited. Some experimental results are provided. (auth)

38937 FOCUSED SLOW ION BEAM FOR STUDY OF ELECTRON EJECTION FROM SOLIDS. Hagstrum, H. D.; Pretzer, D. D.; Takeishi, Y. (Bell Telephone Labs., Murray Hill, N. J.). Rev. Sci. Instr., 36: 1183-91(Aug. 1965).

Advances are reported in the operation of the ion lens system used in studies of electron ejection by slow ions which make it possible to conduct the experiment with ion energies as low as 4 ev. Ejected electrons may be retarded by as much as 20 ev in the presence of this beam. Significant differences in electron kinetic energy distributions for ion energies differing by as little as 1 ev in the lower energy range are observed. Electrode arrangements and circuit innovations including amplifier calibration and negative feedback stabilization of the ion beam are discussed. Criteria for proper lens performance are given, and experimental data illustrating the meeting of these criteria are presented. Examples of lens failure are also shown. (auth)

38938 HYDROGEN–OXYGEN VERTICAL BRAZING FURNACE. Eldredge, Arnold L. (Stanford Univ., Calif.). Rev. Sci. Instr., 36: 1207-9(Aug. 1965).

A hydrogen–oxygen vertical flame furnace designed for brazing together the copper pieces of the accelerator structure for the Stanford two-mile linear electron accelerator is described. The furnace features a moving ring burner and a water-cooled cylinder that has a reducing atmosphere to protect the surface while it is being brazed and to cool it after brazing. (D.C.W.)

38939 HIGH TEMPERATURE PULSED LIGHT SOURCE. Nodwell, R. A.; Irwin, J. C. (Univ. of British Columbia, Vancouver). Rev. Sci. Instr., 36: 1242(Aug. 1965).

A light source developed for use in absorption spectroscopy in plasma is described. It consists essentially of a spark gap mounted on a 1.6 μF, 20-kv low-inductance capacitor. The discharge is oscillatory with a period of 2 μsec, and the main light pulse is approximately 2 μsec in duration. (D.C.W.)

38940 ION BEAM ELECTROGRAPHY. McClure, Richard J. (Bell and Howell Research Center, Pasadena, Calif.). Rev. Sci. Instr., 36: 1246-7(Aug. 1965).

The properties of several materials for collecting charge patterns produced by ions in mass spectrometers were investigated. The materials included Mylar bonded by epoxy resin to a glass plate, Mylar as before but coated with a light-transmitting layer of aluminum on the reverse side, Mylar as before but aluminized to opaqueness on the reverse side, and Saran film backed by an aluminum sheet. The images obtained were compared with images on conventional Ilford Q-2 plates. (D.C.W.)

38941 FOCUSED HEAT SOURCE FOR X RAY DIFFRACTOMETER. Moss, Marvin; Smith, Douglas L. (Sandia Lab., Albuquerque, N. Mex.). Rev. Sci. Instr., 36: 1254-5(Aug. 1965).

A furnace developed for rapidly heating samples to moderately high temperatures on an x-ray diffractometer is described. The sample is heated from below by an internally focused projection lamp which rotates with the sample. (D.C.W.)

38942 QUICK CLOSING LIGHT SHUTTER. Dike, R. S.; Kemp, E. L. (Los Alamos Scientific Lab., N. Mex.). Rev. Sci. Instr., 36: 1256-7(Aug. 1965). (LA-DC-6948)

A light shutter developed for the investigation of the light spectra of theta pinch plasmas is described. (D.C.W.)

38943 ELECTRON COLLISION CROSS SECTION PLOTTER. Briglia, Donald D.; Rapp, Donald (Lockheed Missiles and Space Co., Palo Alto, Calif.). Rev. Sci. Instr., 36: 1259-60(Aug. 1965).

A semiautomatic data recording system for electron collision cross section measurements is described in which the proportionality of the cross section to the ratio of the ion current to the electron current is used. The plotter can be adapted to provide digitized data for the preparation of tables of cross section data. (D.C.W.)

38944 LOW LEVEL SECOND HARMONIC DETECTION SYSTEM. Thomas, D. E.; Rowell, J. M. (Bell Telephone Labs., Inc., Murray Hill, N. J.). Rev. Sci. Instr., 36: 1301-6(Sept. 1965).

A second harmonic detection system suitable for detailed study of current-voltage characteristics, particularly tunneling characteristics of superconductor and semiconductor junctions, is described. The system is capable of detecting second harmonic voltage changes as low as 10^{-9} v which allows the fundamental signal level to be $\leq kT$ at a junction temperature of 1°K. A selection-rejection impedance transformation reactance network which is the heart of the system is described. The quantitative relation between second harmonic voltage and second derivative of current with respect to voltage are given. The capabilities of the system are illustrated by a photograph of an X-Y recorder tracing of second harmonic voltage vs d-c bias voltage for an Al-I-Pb tunnel junction. (auth)

38945 STABLE CURRENT REGULATOR FOR SUPERCONDUCTING SOLENOIDS. Fietz, W. A. (Cornell Univ., Ithaca, N. Y.). Rev. Sci. Instr., 36: 1306-9(Sept. 1965).

A zero to twenty-five ampere controller for use with a superconducting solenoid is described. The controller drift is less than one part in 10^6 per hour and the low frequency peak-to-peak noise is less than one part in 10^6 of the maximum current output. In addition, the controller contains circuitry to maintain the solenoid terminal voltage at a value which may be programmed as a decreasing function of solenoid current in order to vary the magnetic field to any desired value without exceeding the allowable terminal voltage of the solenoid. (auth)

38946 RIGID-TAIL HELIUM CRYOSTAT FOR X RAY DIFFRACTION STUDIES OF CRYSTALLIZED GASES. Peterson, O. G.; Simmons, R. O. (Univ. of Illinois, Urbana). Rev. Sci. Instr., 36: 1316-18(Sept. 1965). (COO-1198-250).

A rigid-tail cryostat suitable for x ray back-reflection diffraction studies requiring temperature control within a few hundredths of a degree for extended time intervals in the range above 2.3°K is described. The specimen chamber permits the growth, visual study, thermal etching, and annealing of crystallized gases. It may also be pressurized to 20 atm for x ray studies of compressibility. (auth)

38947 EVACUATE-BACK FILL GLOVE BOX. Wanser, R.; Uhlmann, D. R. (Harvard Univ., Cambridge, Mass.). Rev. Sci. Instr., 36: 1365-6(Sept. 1965).

A glove box is described whose chamber may be evacuated into the range of 10^{-6} mm Hg and subsequently backfilled with a dry gas. Essential features include caps for evacuating simultaneously both sides of the gloves and quick disconnecting fittings for ready accessibility to the box. Slight modification of design permits wide variation in box geometry. (auth)

38948 EFFECT OF BULK DENSITY AND OF HYDROGEN IN FORMS OTHER THAN FREE WATER ON THE CALIBRATION CURVE OF THE NEUTRON MOISTURE METER. Marais, P. G.; De V. Smit, W. G. (Western Province Fruit Research Inst., Stellenbosch, Republic of South Africa). S. African J. Agr. Sci., 5: 225-38(June 1962).

The use of neutrons for measuring soil moisture is based on the fact that hydrogen is more effective in slowing down fast neutrons than other elements present in the soil. However, in organic soils, or soils rich in clay minerals such as kaolinite the presence of H in forms other than free water should be considered when the neutron moisture meter is calibrated. This aspect of the neutron moisture meter was investigated by studying the effects of the bulk density of several different soil types and of peat moss on the calibration curve of the neutron moisture meter, and the contribution to this effect of the presence of H in forms other than free water. It was found that the calibration curve of the neutron moisture meter therefore depends on the bulk density, or compaction, of the soil and it is essential for the meter to be calibrated at a specific bulk density. Investigations showed that it is possible to determine a correction factor enabling the meter to be used at other bulk densities. A linear relation exists between the counting rate of the neutron moisture meter and the moisture content of the soil. However, the slopes of regression lines obtained with different soils, or groups of soils differed markedly, showing that a single calibration curve cannot be used for all soil types. Differences in the slopes of these lines reflects the presence in soils of elements with large cross sections for slow neutrons. (TCO)

38949 ENERGETIC ELECTRON BEAMS AND COLD CATHODE BOUNDARY CONDITIONS. Muly, Emil C.; Litton, James Jr. (Martin Co., Baltimore). pp 133-57 of First International Conference on Electron and Ion Beam Science and Technology. New York, John Wiley and Sons, Inc., 1965.

Screen mesh cathodes used to produce electron beams operating in the electron-beam mode discharge (EBMD) were investigated. Several variations of spherical geometries were studied. A cylindrical cathode designed to function both as a EBMD cathode and a microwave resonant cavity was used to measure average electron density in the cavity. Measurements were made for varying operating pressures and different screen-mesh transparencies. (A.G.W.)

38950 SOME OBSERVATION ON THE FORMATION OF TRACKS IN THIN, SUPPORTED METAL FILMS PRODUCED BY AN ELECTRON BEAM. Einstein, P. A. (Vickers Research, Ltd., Sunning Hill, Berks, Eng.). pp 205-19 of First International Conference on Electron and Ion Beam Science and Technology. New York, John Wiley and Sons, Inc., 1965.

The formation of tracks in thin metal films of the order of 1000 Å, supported on a substrate of thermally poorly conducting material such as silica or glass, was studied using a simple two-stage experimental electron-beam machine. The nature of the heat source is discussed and calculated temperature distributions are given. In the formation of tracks, metal evaporation plays only a minor role; it appears that metal removal is linked inversely with the melting point of the metal. In general the beam diameter should be chosen to coincide with the dimension

of the heat source. It was shown that it should be possible to cut resistive circuits in times of the order of 1 sec. (A.G.W.)

38951 IMPROVEMENTS IN LIGHT PROJECTORS. Lenze, Eberhard (to Trilux-Lenze K.G.). British Patent 990,675. Apr. 28, 1965. Priority date Feb. 26, 1960, Germany.

A light projector is described that has a cavity within the body to receive from the outside a radioactive luminescent light source. The reflector is in spaced relationship to the cavity, and the body is of transparent filling material filling the reflector and acting as a radioactive radiation guard after the light source is in the cavity. A part of the body surface has reflecting properties and follows the shape of the reflection surface of the reflector. The remaining surface of the body acts wholly as a light emitting surface. The body of filling material is formed of plies of transparent material with the plies closest to the source formed of substantially radiation resistant material of high mechanical strength. The cavity is spherical in shape and is divided into cells. The reflector may have either a form of a paraboloid of revolution or an elliptical cylinder. The light source consists of either a physical or chemical combination of a luminescent substance with a radioactive isotope. The body of the projector is made pressure tight so that the radioactive isotope may even be a gas such as krypton-85, either alone or in combination with a solid radioactive isotope. (B.L.M.)

38952 APPARATUS FOR MEASURING VERY THIN FILM THICKNESSES. (to the Boeing Co.). British Patent 996,777. June 30, 1965. Priority date Nov. 20, 1961, United States.

An apparatus is described that uses the beta-radiation backscatter technique to determine the thickness of very thin films or coatings. The apparatus includes a member of radiation shielding material having a surface for supporting the coated specimen in abutting relationship. Radiation from a source is directed through an opening in the supporting surface onto the coating of the specimen. Radiation detecting means are provided for indicating or measuring the radiation backscattered from the coated specimen through the opening. The opening, the source, and the detecting means are arranged in a substantially straight line; however, the source retaining means are arranged to allow the backscattered radiation to reach the detector. (B.L.M.)

38953 STANDARDIZATION OF RADIATION-ABSORPTION TYPE DENSITY GAUGES. (to Electronic Automation Systems Inc.). British Patent 997,579. July 7, 1965. Priority date May 14, 1962, United States.

A method is described for calibrating a gage for decay of source output radiation in which the gage is an electrically balanced density gage of the radiation-absorption type for continuously indicating the density of material moving from a production line. The apparatus includes a radiation source and a detector spaced with respect to each other and the production line for producing a measuring signal in response to unabsorbed radiation that has passed through the material. Sequential standardization steps for the gage are: (1) adjusting the gage according to the radiation received by the detector with the production line empty for zeroing the meter, (2) adjusting the sensitivity of the meter, (3) adjusting the meter gage according to the radiation received by the detector with a standard of known density in the production line, (4) adjusting the meter input according to the radiation received by the detector for the material having a known deviation in density from the standard for producing full scale deflection of the meter, and (5) separately modifying the empty production line zeroing adjustment for directly producing full scale deflection of the meter. (B.L.M.)

38954 METHOD AND SYSTEM FOR ELECTRON IRRADIATION OF MATERIALS. Lawton, Elliott J.; Gurewitsch, Anatole M. (to General Electric Co.). U. S. Patent 3,176,129. Mar. 30, 1965. Filed Oct. 23, 1961.

An electron beam generator system for uniform irradiation of materials includes an electron gun for producing the electron beam and a vacuum tight electron transmissive window between the gun and the materials. Means are provided for applying a bias voltage to the grid electrode of the gun for producing space charge limited operation of the gun. The electron beam is accelerated with a voltage whose magnitude varies as a function of time during substantially the entire period of operation. A variable voltage is applied to the grid electrode for causing the magnitude of the beam current to vary during the same period and in proportion to the magnitude of the acceleration voltage. (B.L.M.)

38955 SERIALOGRAPH WITH SPACED CARRIERS FOR MOVABLE X-RAY FILM CASSETTES IN SHIELDED TRAYS. Jimenez, Roberto J. U. S. Patent 3,188,466. June 8, 1965. Filed Jan. 31, 1962.

A portable, inexpensive serialograph capable of taking a plurality of x rays in a given sequence at desired intervals includes a frame that has at least two substantially parallel spaced-apart walls. On the lower wall a cassette is positioned for shifting movement. The upper wall is provided both with a parallel grid through which the cassette is exposed and with shielded portions. The cassette is manually shifted between positions where exposures can and cannot be made. A third wall on which a cassette may be placed may be positioned below the first two walls. In this case the cassette on the intermediate wall is held by a tray that also carries a shield. Thus a pair of cassettes may be located one above the other, an exposure may be made on the cassette on the tray, the tray may be shifted, and an exposure may be made on the lower cassette. (A.G.W.)

38956 COIN IDENTIFICATION APPARATUS UTILIZING RADIATION BOMBARDMENT. Hansen, Carl Woodrow; Clack, Peter J. (to Lab. for Electronics, Inc.). U. S. Patent 3,188,471. June 8, 1965. Filed Jan. 23, 1961.

An apparatus for identifying preselected coins by a determination of their atomic number and their weight per unit area is intended for use in vending machines and pass meters. A source of β and x radiation is located to one side of the path of travel of a coin. A β-ray detector is located on the same side and shielded from the source to detect backscattered β rays. An x-ray detector is located on the opposite side of the path of travel to detect transmitted radiation. Signaling devices indicating acceptance or rejection of any selected coin may be provided. (A.G.W.)

38957 METHOD AND APPARATUS FOR DETERMINING SATELLITE ORIENTATION UTILIZING SPATIAL ENERGY SOURCES. Whipple, Elden C. Jr. (to National Aeronautics and Space Adm.). U. S. Patent 3,188,472. June 8, 1965. Filed July 12, 1961.

A device for determining the orientation of a space vehicle includes particle traps sensitive to electrons, ions, or light radiation secured to the outer surface of the vehicle. The traps are simple, relatively substantial structures including a plate and two grids, electrically connected in different manners to produce output signals indicative of either the velocity vector, the solar vector, or the magnetic field intensity vector. Satellite orientation can be determined from information from any two types of traps, but the inclusion of all three provides a desirable flexibility and reliability. (A.G.W.)

38958 MASS SPECTROMETER WITH MEANS TO IMPRESS A FLUCTUATING COMPONENT UPON THE ION STREAM AND MEANS TO DETECT THE SAME. Field, Frank H. (to Esso Research and Engineering Co.). U. S. Patent 3,191,027. June 22, 1965. Filed Aug. 24, 1962.

The mass spectrometer patented has a retarder electrode placed in the analyzer between the ion source and the collector. The potential on this electrode is generally slightly higher than the potential of the ion source, but the voltage is varied periodically by an amount on the order of 0.1-1.0 volts. The number of ions that can pass through the slit in the electrode changes inversely with the changing voltage. Thus the ion current through the analyzer

consists of a constant component of broad energy spread and a modulated fluctuating component of energy spread equal to the voltage variation applied to the retarder electrode. The detecting portion of the system is constructed to be sensitive only to the narrow-energy-range fluctuating component. (A.G.W.)

38959 RETRACTABLE MOUNT FOR RADIATION THICKNESS GAUGE. Cherkas, Paul (to Lab. for Electronics, Inc.). U. S. Patent 3,191,034. June 22, 1965. Filed Nov. 29, 1960.

A track and carriage arrangement for movably supporting the measuring head of a radiation thickness gauge is patented. The track consists of a pair of parallel members formed of cold rolled bar stock secured to a suitable frame. The carriage consists of a box-like frame constructed to fit over the track and including ball bearings arranged to contact the tracks. Preferably the tracks are formed of hexagonal stock, and the carriage includes eight bearings mounted so as to keep the carriage firmly in contact with the track whether or not the plane defined by the track is horizontal. The track members are secured to opposite ends of distributed spacer rods, which may be adjusted after installation to provide curvature in the track. (A.G.W.)

38960 ENERGY TRANSFER CIRCUITS PARTICULARLY FOR THE TRANSFER FROM AN INDUCTIVE STORE TO AN INDUCTIVE LOAD. Carruthers, Robert; Smart, David Lorimer (to United Kingdom Atomic Energy Authority). U. S. Patent 3,191,074. June 22, 1965. Priority date Mar. 25, 1959, Great Britain.

An energy transfer circuit includes a storage inductor, a source for charging the storage inductor, a switch for short-circuiting the storage inductor after charging, an inductive load, and a capacitor. The inductive load and the capacitor can be connected selectively in parallel with the storage inductor to form a resonant circuit for transferring energy to the inductive load without substantial loss. The capacitor may also be used to establish an initial current in the inductive load. (A.G.W.).

38961 D. C. AMPLIFIERS. Fowler, Eliot Patrick (to United Kingdom Atomic Energy Authority). U. S. Patent 3,191,126. June 22, 1965. Filed Feb. 16, 1962.

A d-c amplifier includes means for modulating a d-c input signal, an a-c amplifier for amplifying the modulated input signal, means for applying the a-c output of the amplifier to drive the modulating means whereby the circuit oscillates for a given polarity of input only, means for defining the oscillation frequency, and non-phase-sensitive rectifying means connected to the output of the a-c amplifier for producing a d-c voltage. The a-c amplifier may be tuned to constitute the means for defining the oscillation frequency. The modulating means may be a transistor chopper. A negative feedback connection may be provided between the d-c output of the amplifier and the input of the modulating means. The amplifier is particularly suitable for use in voltage converters. (A.G.W.)

38962 MASS SPECTROMETER ION COLLECTOR WITH A SECONDARY PARTICLE COLLECTING ELECTRODE EXTENDING OVER THE COLLECTOR. Green, Brian Noel (to Associated Electrical Industries Ltd.). U. S. Patent 3,192,383. June 29, 1965. Priority date Dec. 22, 1961, Great Britain.

Ion collecting apparatus for a mass spectrometer includes a collector member with a layer of photosensitive material that is sensitive to ions and an electrode extending over the sensitive surface and spaced from it. A potential positive with respect to the sensitive layer can be applied to the electrode so that the electrode attracts negatively charged secondary particles emitted from the sensitive layer when primary ions strike the sensitive layer. The surfaces of the electrodes define a slit extending through the electrode to allow the passage of primary ions to the sensitive layer. (B.L.M.)

38963 MASS SPECTROMETER ELECTROSTATIC ANALYSERS. Wildig, Edward (to Associated Electrical Industries Ltd.). U. S. Patent 3,192,384. June 29, 1965. Priority date Sept. 15, 1961, Great Britain.

An electrostatic analyzer for a mass spectrometer includes a chamber adapted to be evacuated and two superposed electrostatic plates located within the chamber and defining a gap between their adjacent surfaces for the passage of ion beams. Means are provided for connecting the two plates to suitable sources of potential so as to produce an electric field between the two plates. The upper deflecting plate is supported from the lower deflecting plate so as to prevent relative movement between the adjacent central regions of the deflecting plates, but to permit longitudinal movement between the remaining adjacent regions of the plates. (B.L.M.)

38964 X-RAY TUBE WITH ADJUSTABLE ELECTRON BEAM CROSS-SECTION. Foster, Leigh Curtis (to Zenith Radio Corp.). U. S. Patent 3,192,425. June 29, 1965. Filed Mar. 6, 1961.

An x-ray generator includes an electron gun for projecting an electron beam along a given path. The gun includes an electron emissive cathode located coaxially with the path and a heater for the cathode. The anode structure has a conductive cylindrical portion positioned axially with the path and spaced from the cathode. The cylindrical portion has a radius small compared to the cathode and supports at its end remote from the cathode a target portion constructed of a material that radiates x rays when bombarded by electrons. The target is disposed across the path of the electron beam. Focusing means are provided in the region between the cathode and the cylindrical portion to form electrons emitted from the cathode surface into a converging beam of substantially circular cross section focused on the target and to establish the cylindrical portion and the target at approximately the same operating potential. The spacing of the target from the open end of the cylinder is greater than the depth of penetration of the focusing field into the anode cylinder. Adjustable magnetic means are supported outside the anode cylinder for establishing a magnetic beam shaping field about the beam path to selectively shape the beam into any of a number of predetermined different non-circular beam cross sections at the target. (B.L.M.)

38965 THICKNESS MEASUREMENT USING ALPHA PARTICLES. Anderson, Herbert L. U. S. Patent 3,193,680. July 6, 1965. Filed Oct. 6, 1960.

A method and apparatus are provided for measuring the thickness of a substance by determining the shift in the energy spectrum of alpha particles passing through the substance to indicate its thickness. The apparatus includes the alpha source and a semiconductor junction diode detector positioned on either side of the substance. Electrical integrating and comparing means are employed to determine the thickness of the substance by comparison with the energy transmitted by standard thickness substances. (B.L.M.)

38966 MEASURING SYSTEM USING THE RESONANT ABSORPTION OF GAMMA RAYS. Reiffel, Leonard (to IIT Research Inst.). U. S. Patent 3,193,683. July 6, 1965. Filed May 23, 1960.

A measuring system is described that employs the resonant absorption of gamma rays and that is applicable to the measurement of velocity or a quantity functionally related to velocity, such as distance or acceleration. The system is also useful for the measurement of stress and of magnetic fields. The system includes a gamma source, a resonant absorber, and a detector. The difference between the effective frequency and the mid-frequency of the narrow frequency range is effected by certain parameters including the relative temperature and magnetic field strengths of the emitter and absorber, relative speeds of movement of the emitter and absorber, and relative stress conditions in the absorber and emitter. Three of these parameters are substantially constant, the variable being measured is a function of the other parameter. (B.L.M.)

38967 MAGNETIC MOMENTUM ANALYZING SLIT WITH CURRENT CONDUCTING STRIPS SECURED TO THE MAGNETIC POLES. Ballam, Joseph; Chu, Eu-Lang (to U. S. Atomic Energy Commission). U. S. Patent 3,201,585. Aug. 17, 1965.

An improved device is designed for isolating particles of a given momentum range from a particle beam. The device employs a conventional arrangement of C-type magnets providing fields oriented at right angles in a rectangular aperture. The improvement comprises the disposition of strip or sheet conductors on magnet pole faces which are energized with direct current to provide magnetic fields of the C-type magnets in the aperture providing in effect a larger aperture for transmitting particles of a desired momentum range. (AEC)

Radiation Detection

Refer also to abstracts 39419, 40122, and 40256.

38968 (AEET/HP/D-1) A COUNTER FOR FAST NEUTRON DOSIMETRY. Murthy, K. B. S.; Muthukrishnan, G.; Sunta, C. M. (Atomic Energy Establishment, Trombay (India)). Oct. 1964. 28p. (CONF-803-6) Dep. mn.

From International Symposium on the Dosimetry of Irradiations From External Sources, Paris, Nov. 1964.

A proton recoil proportional counter designed for the purpose of fast neutron dosimetry is described. The energy response of the counter is made such that the counting efficiency varies as inverse of the current values of the maximum permissible flux (MPF) of fast neutrons of energies up to 14 Mev. This counter thus gives a fixed number of counts per maximum permissible flux of fast neutrons irrespective of their energy. The design of the counter is based on the principle of Hurst, Ritchie and Wilson. Thick and thin layers of polythene and a commercial fuel gas Burshane are used as proton radiators. The combination of proton radiators that was found to best approximate the required energy response is: (1) 80% of the solid radiator area occupied by 0.02 mm thick polythene, (2) 20% of the solid radiator area occupied by 2.0 mm thick polythene, and (3) Burshane gas at a pressure of about 16 cms of Hg. The energy response of the counter was verified with monoenergetic neutrons using Van de Graaff accelerator and cascade generator. The observed response is found to be very close to the required response. Response to composite spectrum of fast neutrons was verified with Ra–Be source. The sensitivity was found to be 34 cpm/MPF for counters with diameter 3.6 cms and length about 25 cms. Using Burshane and argon, the proportional counters with required response could be operated at much lower voltage as compared to counters using methane, which is of convenience in making a portable dosemeter. The counter is found insensitive to gamma rays. Its thermal neutron sensitivity also is negligible. (auth)

38969 (ANL-6949) THEORETICAL ESTIMATES OF PILE-UP DISTORTION. Gold, Raymond (Argonne National Lab., Ill.). Mar. 1965. Contract W-31-109-eng-38. 40p. Dep. mn; CFSTI, $2.00 cy, $0.50 mn.

An analysis of pile-up distortion for a (pulse) detector is formulated by means of probability generating functions. Solutions are determined in the form of integral representations. Several important special cases, which are of interest in experimental applications, are treated. The representations for these special cases were evaluated, and numerical results are presented in both graphical and tabular form. The results of the present method are compared with other estimates of pile-up distortion. (auth)

38970 (BNL-9236) ON GETTING RESULTS FROM AN HPD SYSTEM. Hough, P. V. C. (Brookhaven National Lab., Upton, N. Y.); Powell, B. W. (European Organization for Nuclear Research, Geneva (Switzerland)). May 27, 1965. Contract AT(30-2)-Gen-16. 41p. (CONF-650510-10). Dep. (mn); $2.00(cy), 1(mn) CFSTI.

From Purdue Conference on Instrumentation for High Energy Physics, Lafayette, Ind.

Evidence is presented to show that HPD measurements at CERN have reached equality with and now surpass CERN hand data in reliability. Perhaps the most direct and incisive test for correct measurement is provided by a three-view geometry diagnostic; its use for the study of performance of this (and any) analysis system is described. Various other problems connected with the development and use of the HPD system are discussed briefly. (auth)

38971 (CERN-65-11) PROGRAMMING FOR FLYING-SPOT DEVICES. A Conference held at The Centro Nazionale Analisi Fotogrammi, I.N.F.N., Bologna on 7-9 October, 1964. Moorhead, W. G.; Powell, B. W. (eds.) (European Organization for Nuclear Research, Geneva (Switzerland)). Mar. 26, 1965. 277p. (CONF-641023). Dep. (mn).

Twenty-one papers are included; separate abstracts have been prepared for all. (T.F.H.)

For abstracts of individual papers see: 38910, 38972, 38973, 38974, 38975, 38976, 38977, 38978, 38979, 38980, 38981, 38982, 38983, 38984, 38985, 38986, 38987, 38988, 38989, 38990, and 38991.

38972 (CERN-65-11(p.7-13)) EXPERIENCE WITH THE SPASS SYSTEM. Deutsch, M. (Massachusetts Inst. of Tech., Cambridge).

The system described utilizes a programmed track-following method for analyzing spark-chamber photographs. Operating experience with the system is described. (T.F.H.)

38973 (CERN-65-11(p.15-23)) LIST PROCESSING TECHNIQUES IN THE AUTOMATIC ANALYSIS OF SPARK CHAMBER DATA. Clark, D. D. (Argonne National Lab., Ill.).

The program LINK, in Fortran for the IBM 3600, is used to analyze and reconstruct events starting from spark-position data gathered by flying-spot searches of spark-chamber photographs. (T.F.H.)

38974 (CERN-65-11(p.25-33)) THE AUTOMATIC ANALYSIS OF 200,000 SPARK CHAMBER PICTURES USING THE CERN HPD. Blackall, P. M.; Powell, B. W.; Zanella, P. (European Organization for Nuclear Research, Geneva (Switzerland)).

Automatic scanning and measurement methods for the photographs from a π-p spark chamber experiment at the CERN PS are described. The photographs (200,000) are analyzed by machine and by hand, and the results are compared. (T.F.H.)

38975 (CERN-65-11(p.35-41)) A PROGRAM FOR CALIBRATING THE FLYING-SPOT CATHODE RAY TUBE FOR CHLOE. Royston, R. J.; Butler, J.; Pennock, P. (Argonne National Lab., Ill.).

The calibration of a flying-spot CRT track-analyzing instrument in the CHLOE flying-spot system is carried out by scanning a suitable photograph, which is also measured on an accurate conventional measuring table. The CHLOE output is then processed by a program that identifies and measures the positions of the calibration marks. These marks are then compared with their measured positions, and a correction function is computed by means of a fitting procedure. (T.F.H.)

38976 (CERN-65-11(p.57-69)) SPARK CHAMBER PHOTOGRAPH ANALYSIS USING LUCIOLE. Head, A. E.; Wilson, J. A. (European Organization for Nuclear Research, Geneva (Switzerland)).

Luciole is a device that generates a flying spot of light to scan spark-chamber film, and to feed digitized data on-line to large computer. The operation and accuracy of Luciole are outlined. (T.F.H.)

38977 (CERN-65-11(p.71-9)) PROGRAM DEVELOPMENTS IN THE CERN FSD SPARK SYSTEM. Blackall, P. M.; Zanella, P. (European Organization for Nuclear Research, Geneva (Switzerland)).

The use of the CERN HPD flying-spot digitizer system in the analysis of spark-chamber photographs is described. (T.F.H.)

38978 (CERN-65-11(p.81-90)) A PRECISION ENCODING AND PATTERN RECOGNITION SYSTEM (PEPR). Pless, I.; Rosenson, L.; Bastien, P.; Wadsworth, B.; Watts, T.; Yamamoto, R. (Massachusetts Inst. of Tech., Cambridge); Alston, M. H.; Rosenfeld, A. H.; Solmitz, F. T. (Lawrence Radiation Lab., Univ. of California, Berkeley); Taft, H. D. (Yale Univ., New Haven, Conn.). (CONF-550-98).

From The International Conference on High-Energy Physics, Dubna, USSR, Aug. 1964.

The operation of the PEPR flying-spot analyzer for bubble-chamber tracks is described. (T.F.H.)

38979 (CERN-65-11(p.91-5)) THE CERN PICTURE NUMBER FINDING ROUTINE. Rosenblum, M. (European Organization for Nuclear Research, Geneva (Switzerland)).

The picture-number-finding routine, a FAP subroutine of the CERN HAZE program, is written for locating and reading the picture number on bubble-chamber pictures. (T.F.H.)

38980 (CERN-65-11(p.97-113)) THE STATUS OF HPD PROGRAMS AT BROOKHAVEN NATIONAL LABORATORY. Abrams, K.; Cockrill, J.; Connolly, P.; Crennell, D.; Hough, P.; Potter, L.; Stonehill, D.; Strand, R.; Thompson, W. (Brookhaven National Lab., Upton, N. Y.).

Computer programs used with an HPD flying-spot analysis system are reviewed and described. (T.F.H.)

38981 (CERN-65-11(p.115-21) CERN VERSION OF FILTER. Krischer, W.; Moorhead, W. G.; Seyboth, P. (European Organization for Nuclear Research, Geneva (Switzerland)).

FILTER is a routine of about 2000 FAP instructions. The purpose of FILTER is to scan and improve the "road" parameters in flying-spot searches of photographs of particle tracks, to separate interesting tracks from other tracks and noise, and to compute master points for a spatial reconstruction program. The FILTER flowsheet is outlined. (T.F.H.)

38982 (CERN-65-11(p.123-37)) EXPERIENCE WITH THE CERN HAZE PROGRAM. Howie, J. M. (European Organization for Nuclear Research, Geneva (Switzerland)).

The operations and efficiency of the HAZE program are outlined. HAZE is used for flying-spot analysis of bubble-chamber photographs of particle tracks. (T.F.H.)

38983 (CERN-65-11(p.139-43)) THE POST FILTER ROUTINE OF CERN HAZE. Hanerfeld, H. (European Organization for Nuclear Research, Geneva (Switzerland)); Seyerlein, J. (Max-Planck-Institut fuer Physik und Astrophysik, Munich (West Germany)).

A routine is described for use with the flying-spot particle-track analyzing program HAZE. The routine is intended to increase the accuracy of tracks reconstructed by the THRESH program from HAZE output, and to enable THRESH to calculate those tracks for which the FILTER code finds only one or two average points. Several sections of the routine are explained. (T.F.H.)

38984 (CERN-65-11(p.145-52)) THE FORTRAN DIAGNOSTIC ROUTINE USED WITH CERN HAZE. Luvisetto M. L. (European Organization for Nuclear Research, Geneva (Switzerland)).

The diagnostic routine used in the CERN HAZE program for following particle tracks in photographic film is described. (T.F.H.)

38985 (CERN-65-11(p.153-72)) PRELIMINARY REPORT ON AN "INTEGRAL" FILTER TECHNIQUE FOR THE HPD. Webre, N.; Burd, D.; Garder, L.; Tycko, D.; Zaslavsky, B. (Columbia Univ., New York).

A computer program technique for flying-spot analysis of particle tracks in photographs is described, in which a conformal mapping is used to transform curved tracks into straight lines. (T.F.H.)

38986 (CERN-65-11(p.173-81) HPD PROGRAMMING AT THE RUTHERFORD LABORATORY. Burren, J. W.; Gardner, J. W.; Mitchell, M. J. (National Inst. for Research in Nuclear Science, Chilton (England). Rutherford High Energy Lab.); Turnill, M. C. (Imperial Coll. of Science and Tech., London (England)).

Computer techniques for following particle tracks in photographs using flying-spot devices and the ORION computer are described. The overall method used consists of "gating" a road for a number of scan lines, and then "filtering" the histograms produced by the gating process. (T.F.H.)

38987 (CERN-65-11(p.207-16)) CONTROL OF THE HPD BY A SMALL COMPUTER. Leblond, Ph. (College de France, Paris).

The use of a CDC 160A computer to control the operation of an HPD flying-spot particle-track analyzer is described. The computer also carries out a few coarse grating operations on the measured tracks before recording them. (T.F.H.)

38988 (CERN-65-11(p.183-206)) RESULTS OBTAINED WITH AN OFF-LINE HPD SYSTEM. Bloch, M.; Schiff, M. (College de France, Paris); de la Vaissiere, C. (Paris Univ., Orsay (France). Institut du Radium).

Digitized flying-spot scanning of particle-track photographs is followed by precise measurements of the tracks using an HPD digitizer. A small (CDC 160A) computer is used to transfer the photographs to magnetic tape. During this on-line operation, the computer performs a very crude gating of the digitizings. The magnetic tapes can then be treated by an off-line CDC 3600, in order to generate an output acceptable to a geometry program. Flowsheets and sample outputs are shown. (T.F.H.)

38989 (CERN-65-11(p.219-27)) PRELIMINARY RESULTS ON HPD IONIZATION MEASUREMENTS AT CERN. Michejda, L. (European Organization for Nuclear Research, Geneva (Switzerland)).

The use of an HPD system for flying-spot analysis of ionization in bubble-chamber tracks is described. The analytical techniques involved are shown. (T.F.H.)

38990 (CERN-65-11(p.229-36)) HPD PROGRAMMING AT THE UNIVERSITY OF PENNSYLVANIA. Engman, J. D. (Pennsylvania Univ., Philadelphia).

Programming the IBM 7040 computer for flying-spot analysis of particle-track photographs using the HPD system is discussed. (T.F.H.)

38991 (CERN-65-11(p.237-58)) CURRENT STATUS OF THE DIGITAL AUTOMATIC SCANNING PROGRAMS. Marr, R. B. (Brookhaven National Lab., Upton, N. Y.).

Computer programs for analyzing particle-track data generated by flying-spot analyzers are discussed. The operations involved include track reconstruction, track editing, and vertex finding. (T.F.H.)

38992 (COO-1226-8) DEVELOPMENT OF A FAST NEUTRON DOSIMETRY SYSTEM. Chase, B. H.; Closser, W. H.; Speers, R. R.; Swartz, J. M.; Thurston, M. O. (Phylatron Corp., Columbus, Ohio). [1964]. Contract AT(11-1)-1226. 43p. Dep. (mn); $2.00(cy), 1(mn) CFSTI.

Experimental silicon p-i-n fast neutron dosimeters were prepared using a variety of processing procedures. Examination of the pre-irradiation characteristics of the devices indicate that the standard techniques with a few important changes still result in the best dosimeters with respect to high initial lifetime. It is now possible to make 80 mil base width devices with lifetimes as high as 100 μsec, while with the unmodified process, the lifetimes for these wide-based devices were always less than 40 μsec. Besides the modifications to the standard process, several other radically different processing techniques were tried. These include (a) plating of nickel doped with boron and nickel doped with phosphorus onto the silicon slices and then a subsequent double diffusion, (b) a variety of paint-on techniques, and (c) a double diffusion using a closed box technique. Some of these techniques have shown promise; however, at present the modified standard process has given the best results. Two types of prototype high sensitivity readout systems are being evaluated. Both readout systems are modified bridge circuits, but in each the balancing and reading methods are different. The circuits are duals of each other, one operating on the principle of a constant current through the dosimeter and the observation of a small current change, the other operating at a constant voltage with the observation of a resultant current change with irradiation. Due to the non-linear current-voltage characteristic of the diode, the relative change of current with irradiation is much greater than the relative change in voltage. Unfortunately, the gain in sensitivity attainable with constant voltage operation is accompanied by a de-

crease in thermal stability of the readout circuit. Due to this thermal stability problem, the constant current circuit is presently being used. A comparative dosimetry experiment was held at the DOSAR facility in Oak Ridge, Tennessee. The silicon p-i-n dosimeter compared very well with the other dosimetry used. (auth)

38993 (NP-15143) BUBBLE CHAMBER FOR WEAK RADIOACTIVITIES. Brautti, G.; Ceschia, M. (Trieste Univ. (Italy). Istituto di Fisica and Istituto Nazionale di Fisica Nucleare, Trieste (Italy)). [1959]. 11p. Dep. mn.

Two models of small bubble chambers, built to measure weak neutron fluxes, are described in detail. Such fluxes are measured by recording the average duration of metastable state to which the chamber's liquid is brought; this duration is an inverse ratio function of intensity. Some controlling circuits with interesting characteristics were built for these models. Points of maximum stability and sensitivity were determined, with different filling liquids. The outstanding observed characteristics were: (a) high sensitivity to neutrons from a few kev to several Mev, (b) insensitivity to thermal neutrons, and (c) insensitivity to gamma rays. (auth)

38994 (NP-15145) BUBBLE CHAMBER FOR WEAK RADIOACTIVITY. Final Research Report. Brautti, G.; Ceschia, M. (Trieste Univ. (Italy). Istituto di Fisica and Istituto Nazionale di Fisica Nucleare, Trieste (Italy)). [nd.]. 16p. Dep. mn.

A discussion is given of the wheel-mounted bubble chamber, capacity manometer circuit, electronic chronometer, timing circuit for automatic recycling, transistorized capacity manometer, transistorized thermoregulating circuit, transistorized timer circuit, and portable small bubble chamber. Experimental results are given for neutron and gamma sources used with ether, pentane, and isopentane in the bubble chamber. It is concluded that the chamber is sensitive to 24-kev but not to thermal neutrons, and that zones of the chamber sensitive to neutron fluxes are not sensitive to gamma rays. The operation of the chamber is described briefly. (D.L.C.)

38995 (NP-15259) RAZVITIE STSINTILLYATSIONNYKH I IONIZATSIONNYKH METODOV RADIOMETRII I DOZIMETRII. (Development of Scintillation and Ionization Methods of Radiometry and Dosimetry). Report No. 73. Arsaev, M. I.; Matveev, V. V.; Mysev, I. P.; Rudakova, G. M.; Samoilov, P. S.; Sulimova, N. E.; Uskov, V. S. (Gosudarstvennyi Komitet po Ispol'zovaniyu Atomnoi Energii SSSR). [1964]. 13p. Dep. mn.

Because of the variety of available scintillators, scintillation methods have widespread application. By simply changing the scintillator, the USD-1 type universal counter may be used for measuring the α activity of materials in the presence of a β and γ background, measuring the β activity of liquids, solids, and powdered materials in the presence of an α and γ background within a β energy range from 0.2 to 1.5 Mev, performing γ spectrometric studies, measuring low γ activities, and determining thermal and fast neutron fluxes up to 200 μR/sec. Work with labeled atoms requires the measurement of the absolute activity of low-energy β emitters; such measurements may be conveniently carried out with liquid scintillation counters, immersing the β emitter into the liquid, thereby achieving 4π geometry. The problems presented by this type of counters include the absence of an air-equivalent scintillator with a sufficiently high light yield and the difficulty of determining the bremsstrahlung. For fast neutron dosimetry ZnS(Ag) and H-containing organic materials are employed. Work is in progress for gaseous scintillation counters for the construction of high-sensitivity neutron detectors, to operate in a high γ background. (TTT)

38996 (PPAD-2137-548) OFF-LINE GLOBAL APPROACH TO PATTERN RECOGNITION FOR BUBBLE CHAMBER PICTURES. Bazin, M. J.; Benoit, J. W. (Princeton Univ., N. J. Plasma Physics Lab.). May 19, 1965. Contract AT(30-1)-2137. 12p. (CONF-650510-11). Dep. (mn); $1.00(cy), 1(mn) CFSTI.

From Purdue Conference on Instrumentation for High Energy Physics, Lafayette, Ind.

The macroscopic handling of data from bubble chamber photographs is discussed. Various methods are proposed for handling data in this manner. (M.O.W.)

38997 (UCRL-16149) NEUTRON SPECTRA FROM AN ORGANIC SCINTILLATOR (thesis). Young, Willis R. (Lawrence Radiation Lab., Univ. of California, Berkeley). June 1965. Contract W-7405-eng-48. 80p. Dep. mn; CFSTI, $3.00 cy, $0.75 mn.

The theoretical response of an organic scintillator to fast neutrons is developed in a general way. The general expressions are simplified by a simple model which allows a fast neutron as many as two n-p reactions before it leaves the system [double scattering model]. This results in an integral equation which expresses the proton recoil distribution as a function of incident neutron flux. A program code WILAG-3 is discussed which solves for the neutron flux from the double scattering model for a given proton recoil distribution. Neutron spectra derived from this model show significant improvement over spectra derived using a single scattering model. A program code WILCAL is discussed which locates the Compton edge when monoenergetic gammas illuminate an organic scintillator. This is used to calibrate the neutron spectra. The resolution of an organic scintillator for 14-Mev neutrons as a function of size is measured and compared for both the single and double scattering models. The neutron spectra of ^{239}Pu, Be, PoBe, ^{238}PuB, and PoMF as derived from both models are presented. (auth)

38998 MAGNETIC CHARACTERISTIC CURVE FOR A SPECIAL PERMANENT-MAGNET BETA-RAY SPECTROGRAPH SET OF TWO UNITS. Illes, F.; Berényi, D. (Inst. of Nuclear Research, Debrecen, Hungary). Acta Phys. Acad. Sci. Hung., 18: 265-7(1965).

The remanent magnetism in the air-gaps of a small conventional permanent-magnet spectrograph and a large semicircular permanent-magnet spectrograph was measured as a function of the magnetizing current after switching off the current in the coil surrounding the magnet prisms. The two spectrographs form one operative unit. (D.C.W.)

38999 THE WHOLE-BODY COUNTER OF THE RADIATION MONITORING CENTER OF THE LABOUR INSPECTORATE OF NORTH RHINE WESTPHALIA. Dreyhaupt, F. J. Arbeitsschutz, No. 3, 75-8(Mar. 1964).

The whole-body counter, which was finished in 1963, is equipped with a 29 cm sodium iodide (Tl) crystal scintillation counter which feeds pulses through a secondary photoelectron multiplier to a 512-channel pulse height analyzer. An oscillograph, x-y-recorder and automatic printout facilities are attached. Measurements are carried out in a standard chair. The subject wears a paper suit. Duration of measurement is 10 minutes. The scanning method can also be used. Shielding consists of 15 cm steel plates and 3 mm of lead at least 100 years old; the reduction factor in the energy range 0.1-2.0 Mev is 63. The height of the chamber is 213 cm, surface area about 4.2 m^2 plus the labyrinthine entrance of 1.5 m^2. (Occupa. Safety and Health Abstr., Vol. 3, No. 4, 1965)

39000 A MICROSCOPIC DIRECT-READING INSTRUMENT FOR SYSTEM OF COORDINATES. Rosseel, B. Atompraxis, 6: 323-5(June 1965). (In French)

In nuclear emulsions the length of a track of a particle was measured with the help of a microscope. For this microscope was supplied with an optical micrometer. The length of a track corresponded to the difference between the coordinates on the start and the end of the track. With the help of disks code transmitters were mechanically connected with the fine adjustment of the micrometer. The desired point was adjusted by a mechanically operated system. By the aid of a programmer and of a code converter the coordinate values are given to perforated tapes. In this way the necessary calculations with a computer were made possible. (auth)

39001 MULTI-CHANNEL NEUTRON MONITORING EQUIPMENT. Mahnau, H.; Marinz, W. (Herfurth GmbH, Hamburg). Atompraxis, 6: 327-9(June 1965). (In German)

A transistorized electronic circuit is described for a neutron monitoring equipment with tissue-equivalent proportional counters. Each channel consists of a probe with built-in amplifier and discriminator and of a ⅔ Esone-plug-in unit with logarithmic rate meter. (auth)

39002 MEASUREMENT OF SOFT β-EMITTING ISOTOPES BY MEANS OF LIQUID SCINTILLATORS. Fodorne, Csanyi Piroska. Atomtech. Tajekoztato, 8: 80-96(1965). (In Hungarian)

Absorption within the instrument and self absorption make the determination of soft β-emitting isotopes difficult. Depending on the energy of the emitted radiation, windowless G-M counters, instruments possessing 1 mg/cm^2 thick windows, ionization chambers, and liquid scintillators may be used for this purpose. Liquid scintillators are convenient to use because most labeled compounds are soluble in the scintillating liquid. Under favorable conditions, the generation of 1 photon requires about 10 ev; as a result of light absorption and scattering, about 10% of the photons are absorbed in the photocathode where their operational efficiency with respect to electrons is about 10 to 15%. The solvent chosen must permit a large light yield of the scintillator, it must be a good solvent of the radioactive isotope and should possess a reasonably low melting point. The emitted light usually lasts a few nanoseconds; its wave length is a characteristic property of the scintillating molecule. Design of liquid scintillation counters is similar to that of crystal scintillation counters. Usually, a 1000-fold amplification is achieved, using 1000 to 1300 v in the system. In order to improve the signal/noise ratio, 2 photoelectric electron amplifiers are used in coincidence; a single amplifier kept at −20°C was also used with good success. These instruments were considered to be especially well suited for measuring the activity of biological or medical specimens. (Review article, 19 references.) (TTT).

39003 AN AUTOMATIC GAMMA SCINTILLATION COUNTER. Kemplay, J. R. (Postgraduate Medical School, London). Brit. Commun. Electron, 12: 162-5 (Mar. 1965).

An automatic scintillation counter to be used with gamma emitting radioactive samples is described. The circuit logic is discussed and brief constructional details are given. The counter offers rapid sample changing and simple circuitry resulting from the use of an improved type of scintillation crystal assembly. This scintillation counter gives rapid sample changing combined with fast print out. The time taken between the completion of assay of one sample and commencement of assay of the next sample is eight seconds. A high degree of reliability, electronic and mechanical, was thus far achieved. This reliability is attributed to the rationalization of the circuitry and to the new technique in automatic sample changing. (J.F.P.)

39004 A TRANSISTOR RATEMETER WITH 2 μSEC RESOLUTION. Shepherd, B. Electron. Eng., 37: 437-41(July 1965).

A random pulse ratemeter having seven rate ranges from 10 p/s to 10 kp/s and six averaging time-constants from 0.25 sec to 50 sec is described. Each input pulse generates a stable width square pulse which, in turn, forces a fixed quantity of charge into a storage capacitor. The resultant voltage is amplified in a chopper amplifier enclosed in a Miller loop to give the required integrating time. Meter output indication and 1 ma and 100 mv recorder outputs with an accuracy of 2 percent are available. (auth)

39005 THE HARWELL 2000 SERIES LINEAR RATEMETER/INTEGRATOR. Wilkins, J. W. H.; Marsh, D. J. (Atomic Energy Research Establishment, Harwell, Berks, Eng.). Electron. Eng., 37: 456-9(July 1965). (AERE-R-4676).

Because of improved accuracy, digital techniques have superseded analog ones, over the last few years, in most rate and count measurements. Circuit improvements to the original analog system are described resulting in a simpler dual-purpose precision instrument, using low-voltage supplies. (auth)

39006 A PULSE HEIGHT MEASURING UNIT. Sach, C. I. (Australian Defence Scientific Service, [Victoria]). Electron. Eng., 37: 460-4(July 1965).

A unit which measures the peak value of a single negative polarity pulse is described. It was originally developed for the case of a pulse having a sharp negative front edge of magnitude between 1V and 5V followed by an exponential decay back to zero with a 2 sec time-constant. The value of the peak signal is displayed with an error of less than 5 per cent on a d.c. voltmeter providing the reading is taken within 10 sec of the event. The characteristics of the unit make it suitable for reading the peak value of single rectangular pulses with durations as short as 3 msec. (auth)

39007 MEASUREMENTS OF FAST NEUTRON SPECTRA BY THRESHOLD DETECTORS. Sekiguchi, Hiroyoshi; Tatsuo, Kikunari. Fuji Jiho, 36: 846-53(Oct. 1963). (In Japanese)

The energy spectra of the fast neutrons in the rotary specimen rack of the TRIGA-II Reactor and of the uranium converter of the Lid Tank shielding facility were measured with the following threshold detectors; In, Hg, Zn, Al, Fe, and Mg. To determine the induced radioactivities of these threshold detectors, gamma rays were measured with a scintillation counter. The effective threshold energy and effective cross section of these threshold detectors were calculated from the data on the excitation functions of each reaction and the fission neutron spectrum. The results of the experiments and the calculations are reported. (auth)

39008 THE GAMMA CAMERA—A NEW INSTRUMENT FOR RADIOISOTOPE TRACER MEASUREMENTS. Davis, R. G. (Ekco Electronics Ltd., Southend-on-Sea, Eng.). Instr. Pract., 19: 322-5(Apr. 1965).

The construction, operation, and medical uses of the Ekco γ camera are described and illustrated. A large thin NaI crystal is fitted with a multiple-hold collimator in front, usually of lead. The crystal is therefore illuminated only by parallel γ rays from the patient, and the distribution of scintillations in the crystal therefore corresponds to the distribution of the γ emitter in the patient. If this changes, the pattern of scintillations will immediately change too, since the whole of the region of interest is seen by the crystal at the same time. A matrix of nine photomultiplier tubes converts the scintillations to pulses which provide brilliance modulation and deflection signals for a storage cathode-ray tube. In this way a pattern of scintillations can be seen to build up on the screen. When an acceptable γ map has been built up it can be photographed (by a Polaroid camera, for example) and if desired the contrast of the picture can be adjusted to optimum for the display of hot or cold spots in the picture. The selected picture then can be superimposed on a photograph of the patient by simple double exposure, using a bracket on the side of the γ camera head to carry the Polaroid camera. Examples of pictures obtained in this way are shown. γ-Maps of comparable clinical value can be obtained, under similar conditions, in 30 min with a scanner in common use, and in 5 min with the γ camera. Spatial resolution is much the same but possibly better in the γ camera. A scaler and timer are usually provided to control the γ camera so that a given time is allowed for the production of a γ map, or conversely the time taken to produce a standard γ map is shown. In either case an indication of thyroid uptake can be provided, and this means that every patient can be scanned and an uptake measurement taken in less time than it now takes to measure thyroid uptake conventionally. The value of the γ camera in thyroid function measurements has been established, and some work has been done on brain tumors. Although these tumors take up little more labeled material than the surrounding tissue, the γ camera can often not only display them but also show the movement of the radioisotope in blood around the tumor. Only the γ camera can be used in this way for dynamic studies, and it thus has advantageous clinical applications. It is usually necessary in dynamic studies to use short-lived isotopes such as ^{99m}Tc, which give a very small dose of radiation to the patient even in

the large activities needed to produce dynamic γ maps with adequate detail. Various clinical and possible industrial applications of the camera are outlined. (BBB)

39009 COMPARATIVE STUDY OF THE EFFICIENCIES OF NaI(Tl), PLASTIC, AND LIQUID SCINTILLATORS FOR DETECTION OF THE γ OF THE ^{16}O ISOMER. Burdet, G.; Poizat, J. C. (Institut de Physique Nucleaire, Lyon). J. Phys. (Paris), 26: 153A-7A(Apr. 1965). (In French).

The linear absorption coefficients of various light scintillators were measured for 6.14 Mev γ rays from ^{16}O. The detection efficiencies of these scintillators were deduced according to their shape and dimensions and compared to those of NaI crystals of standard dimensions. (auth)

39010 FAST β-γ COINCIDENCE CIRCUIT FOR A SIEGBAHN-SLAETIS β SPECTROMETER. Andre, S. (Centre d'Etudes Nucleaires, Grenoble, France). J. Phys. (Paris), 26: 161A-6A(Apr. 1965). (In French).

A fast-slow β-γ coincidence circuit has been installed on a Siegbahn-Slätis β spectrometer, in order to measure β spectra leading to excited states in the final nucleus. The β detector (plastic scintillator NE 102) and γ detector (NaI(Tl) crystal) are coupled to 56 AVP photomultipliers. The resolving time at full efficiency is 13 ns. The stability for γ rays is satisfactory over a period of two days. (auth)

39011 NUCLEAR MAGNETIC RESONANCE EQUIPMENT FOR VERY LOW TEMPERATURE. Hecht, A. M. (Faculte des Sciences, Grenoble, France). J. Phys. (Paris), 26: 167A-8A(Apr. 1965). (In French).

The system studied permits the observation of nuclear magnetic resonance with the Varian spectrometer No. 4200 B, at 4°K and also between 20 and 273°K. The transmitting and detecting coils, wound on a teflon support, were placed inside a dewar. A heating coil around the sample provided the heat required to obtain the temperature above the surrounding cooling bath (liquid nitrogen, hydrogen or helium). The choice of the resonance mode, absorption or dispersion, was obtained with an electrical phase shifter operating at about 16 megacycles. (auth)

39012 A FLOW DETECTOR FOR α-PARTICLES AND FISSION FRAGMENTS OF NUCLEI. Kuzmiak, Mikulas (Inst. of Nuclear Research, Czechoslovak Academy of Sciences, Rez). Jaderna Energie, 11: 100-1(Mar. 1965). (In Czech).

A flow detector was developed to measure alpha activity or fission fragments in a flowing gas stream, which also acts as the ionizing gas. The chamber is constructed of Teflon; it has an electrode spacing of 1.5 cm and is operated at a potential of 1900 v, supplied from a battery. The amplifier used, also battery powered, has a vacuum tube, cathode-follower connected input stage, but, otherwise, it is fully transistorized. The counter chamber is surrounded by an electric heater and can be operated up to a temperature of 200°C. The collection time of the chamber is 0.88×10^{-3} sec, and the ratio of pulse amplitudes for fission fragments is 8.4. An example is shown of its use to measure the half life of a gaseous activity, in this case ^{220}Rn, evolved from a thorium solution. (TTT)

39013 CHANGERS FOR RADIOACTIVE SAMPLES FOR AUTOMATIC MEASUREMENT. Kubalek, Jiri. Jaderna Energie, 11: 103-4(Mar. 1965). (In Czech).

The general features of various automatic sample changers, such as the different types of changing mechanism, the difficulties introduced by the variation in dimensions of planchets, the different types of detectors used, and the different types of control mechanisms, are discussed. Salient features of a number of sample changers of German, French, Italian, and American manufacturers are compared with the characteristics of a sample changer made by Tesla. (TTT)

39014 THE INFLUENCE OF THE DISCRIMINATION AND DEAD TIMES ON THE PARAMETERS OF A COINCIDENCE SCINTILLATION DETECTOR OF LOW-ENERGY β RADIATION. Lakajecek, Milos. Jaderna Energie, 11: 147-9(Apr. 1965). (In Czech).

A mathematical derivation is given for equations relating the signal pulse rate, the noise pulse rate in each branch of the circuit, the resolving time, and the dead time of the circuit to the loss of signal count. Graphical plots of the resulting equations show the dependence of the maximum dead time which can be permitted at given noise levels for counting losses of 1 and 10%, respectively. As an example, it is cited that in counting tritium with a coincidence scintillation detector arrangement with a counting efficiency of 40 to 45% at -5 to -10°C the noise level is approximately 10^3 impulses per second. At ordinary temperatures, a noise level an order of magnitude higher is encountered. (TTT)

39015 ON MEASUREMENTS OF GAMMA DOSE EQUIVALENT AT THE BODY SURFACE BY MEANS OF CONDENSER IONIZATION CHAMBERS. Wetzel, L.; Rossbander, W. (Zentralinstitut fuer Kernforschung, Rossendorf, Ger.). Kernenergie, 8: 306-9(May 1965). (In German).

In the energy range from 60 kev to 2.06 Mev, five types of gamma condenser chambers have been irradiated "free in air" and at the surface of the breast region of a human-like paraffin phantom. Correction factors for representing the measuring values of the condenser chambers in units of the dose equivalent in muscle tissue and at the body surface are given. In the investigated range of energy, only the types DS 0.2 and KID-1 show variations of the correction factor less than ±20%. With the types DK 0.2, FDM 1, and FDM 2, the dose equivalent at the body surface is highly overestimated in the lower energy range. (auth)

39016 ON THE ABSORBED DOSE RATE DETERMINATION IN VINYLCHLORIDE. PART 1. CALCULATION AND EXPERIMENTAL DETERMINATION OF THE ENERGY EQUIVALENT OF THE ROENTGEN FOR VINYLCHLORIDE. Behrens, H.; Floreck, H. (Institut fuer Physik und Physikalische Chemie der Hochpolymeren, Leipzig). Kernenergie, 8: 312-18(May 1965). (In German).

The absorbed dose rate in vinylchloride was determined by measuring the radiation dose rate or the absorbed dose rate using a Fricke dosimeter irradiated with a 90- to 180-kev x rays. The energy equivalent of the roentgen for vinylchloride is given. Calculating it, the energy transfer coefficients were taken into account, as well as the attenuation of the x rays within the material under test in determining it from measurements using a Fricke dosimeter. The energy equivalents thus obtained as a function of spectral energy distribution of the x rays were compared to values obtained from measurements using a parallel-plate ionization chamber. The energy transfer coefficients used for the calculations are given. (auth)

39017 AUTOMATIC FOLLOWING OF TRACKS IN NUCLEAR EMULSIONS. Bernheim, A.; Doriot, G.; Fayolle, J. C.; Vedel, J. P.; Morand, M. (Universite, Paris). Nucl. Instr. Methods, 34: 345-6(June 1965). (In French).

By making the hypothesis that the track in a nuclear emulsion is almost horizontal, a control principle was determined and a device constructed to follow tracks automatically. A functional diagram and an electronic circuit for the system is given. Its operation is described. The technique described can be used in the horizontal or vertical plane. (J.S.R.)

39018 A WINDOWLESS HIGH-RESOLUTION LID-GERMANIUM DETECTOR. Armantrout, G. A.; Camp, D. C. (Univ. of California, Livermore). Phys. Letters, 17: 279-80(July 15, 1965). (UCRL-12333)

A description is given of a windowless lithium-drifted germanium diode, which is suitable for beta-ray spectroscopy as well as high-resolution gamma-ray spectroscopy. The initial evaluation of the detector resolution was made using a ^{57}Co and a ^{60}Co source. (L.B.S.)

39019 SPARK DETECTORS AND THEIR USES. Warczewski, Jerzy (Academy of Mining and Metallurgy, Krakow). Postepy Fiz., 16: 175-96(1965). (In Polish)

The state of the art of spark chamber design is reviewed, and the physical and electrical characteristics of a wide variety of spark chambers are outlined. These include nondirectional spark chambers and their use in telescope

counters, directional spark chambers as telescope counters, spark chambers that display the track of a charged particle, special spark chambers, and spark chambers with isotropic response. The track-producing spark chambers are reviewed at length, including the many-electrode type chamber of Fukui and Miyamoto, the two-electrode type, and chambers giving staircase-type tracks. (TTT)

39020 A MACHINE FOR AUTOMATIC MEASUREMENT, BY SCINTILLATION PROBING, OF LIQUID OR POWDERED RADIOACTIVE SAMPLES. LaFay, F. Presse Med., 72: 2390(Oct. 3, 1964). (In French)

Up to 50 radioactive samples can be placed in this automatic measuring device at the same time. The samples are then rotated, one at a time, in a glass tube for the counting. After the level of radiation is determined, the sample is replaced by another. The system of a circular, rotating magazine assures a perfect distribution of the measuring energy with a minimum of background noise. The high-tension energizer and preamplifier are encased in a metal cabinet forming the base of the machine. The complementary instruments have an extended range for measuring frequency and counting time. They can distinguish between integral and integral-differential characteristics. The measuring operations are carried out by an automatic cycle initiated by the electronic circuits. Push-buttons regulate the following procedures of the machine: consecutive counting of the samples, selection of the number of times each sample is tested, and stopping the machine after a certain number of samples have been measured. By push-buttons, the technician can interrupt the automatic cycle at any time. Combining this machine with other electronic equipment makes it possible to obtain a printed record of the sample's number, frequency, and the corresponding length of the calculating impulse. It is possible to include spectroscopic measurements in the series. (BBB)

39021 DESIGN OF A DEVICE FOR IMPROVING THE STABILITY AND PULSE COUNTING IN GEIGER COUNTER. Golub, V. S.; Velichko, V. A. Pribory i Tekhn. Eksperim., No. 2, 171(Mar.-Apr. 1965). (In Russian).

An instrument described previously for use in connection with Geiger counters was modified by including a new diode, a resistance, and a condenser in the circuit. Using a condenser with a capacity of 5 pF and a resistance of 5.6 kohm, the SBT-type counter was found to operate satisfactorily at temperatures down to −40°C. It is important that the condenser capacity should not exceed the permissible load capacity of the system. It is not necessary to include all the 3 items in the circuit; a choice can be made on the basis of operating requirements. (TTT)

39022 SIMPLE DATA DISPLAY SYSTEM FOR FAST SCANNING MASS SPECTROMETER. Marsden, D. G. H.; Forst, W.; Feng, K. K. (Universite Laval, Quebec). Rev. Sci. Instr., 36: 1109-11(Aug. 1965).

A simple display device is described that makes use of two independent time bases provided by some types of oscilloscopes. The device consists essentially of a diode gate driven from the oscilloscope by means of some rather simple associated circuitry. The ion beam signal is chopped, or sampled, peak after peak, smoothed by an RC filter, and displayed by means of a pen recorder, a recording galvanometer, or another oscilloscope. Most of the statistical fluctuation in peak height is thus eliminated. (auth)

39023 APPLICATION OF DIGITAL RECORDING TO SIMULTANEOUS COLLECTION IN MASS SPECTROMETRY. McCullough, H.; Krouse, H. R. (Univ. of Alberta, Edmonton). Rev. Sci. Instr., 36: 1132-4(Aug. 1965).

A commercial five-figure integrating voltmeter-ratiometer and digital printer were incorporated into the measuring circuit of a conventional simultaneous ion collection mass spectrometer. The ratio of two ion currents is printed to five figures. Increased precision and ease of measurement are among the advantages realized. (auth)

39024 4096 CHANNEL TIME ANALYZER WITH VARIABLE CHANNEL WIDTH. Rockwood, Curtis C. (Argonne National Lab., Ill.). Rev. Sci. Instr., 36: 1161-4(Aug. 1965).

A time analyzer for neutron time-of-flight studies is described. An accordion feature permits different channel widths in adjacent time regions. Eight independent selections of channel width for each of the 16 regions of 256 channels are provided, ranging by factors of 2 from 125 nsec to 16 μsec. A channel width multiplier increases all the widths by a factor of 8, 4, 2, or 1. Deadtime is 5 μsec per event stored. Channel capacity is 262,143 counts. Readout is punched paper tape, followed by verify in a tape reader. (auth)

39025 PULSE SHAPE DISCRIMINATION SYSTEM FOR ^{6}LiF (ZnS) SCINTILLATION COUNTERS. Legler, E.; Attwenger, W.; May, F.; Quittner, G. (Reaktorzentrum, Seibersdorf, Austria). Rev. Sci. Instr., 36: 1167-9(Aug. 1965). (SGAE-PH-16/1965).

A pulse-shape discrimination system for ^{6}LiF(ZnS) scintillators is described, and its electronic layout is discussed. Test results under typical operation conditions at the location of a neutron scattering experiment in a light water research reactor are given. They show that the system is able to suppress virtually all spurious (γ and tube noise) pulses down to a rather low discrimination level. By taking a low discrimination level, it is possible to exploit the potentially high efficiency of the scintillator to a much larger extent. In our particular case, the over-all counting efficiency could be doubled. (auth)

39026 LIQUID NEON–HYDROGEN BUBBLE CHAMBER. Prodell, A. G. (Brookhaven National Lab., Upton, N. Y.) Rev. Sci. Instr., 36: 1174-5(Aug. 1965). (BNL-8866).

Tracks were observed in various liquid neon-hydrogen mixtures in the 20-in. Brookhaven National Laboratory bubble chamber. A neon-hydrogen mixture was used whose radiation length is approximately equivalent to that of propane. Separation of some of the mixtures into two liquid phases was also observed. (auth)

39027 LITHIUM-DRIFTED POSITION SENSITIVE DETECTOR. Ludwig, E. J. (Rutgers, State Univ., New Brunswick, N. J.). Rev. Sci. Instr., 36: 1175-6(Aug. 1965).

An attempt was made to produce position-sensitive detectors with depletion depths of several millimeters by lithium drifting. The technique used involves evaporating a thin metallic layer onto the side opposite the lithium diffusion to provide a uniform resistive sheet. Detectors measuring 8 × 28 mm were tested with 5.5-Mev alpha particles and 4.2 Mev protons and exhibited energy spreads of 2−3.5% uncooled and 1−2% when cooled. The position linearity plot of the detectors indicated that the particle position could be determined to within 0.3 mm. (auth)

39028 DISCHARGE CHAMBER SENSITIVE TIME. Strelzoff, A.; Pondrom, L.; Kloeppel, P.; Fassnacht, S.; Limon, P. (Univ. of Wisconsin, Madison). Rev. Sci. Instr., 36: 1195-7(Aug. 1965).

Wide-gap discharge chambers were exposed to proton beams of 2×10^6/sec. It was found that the chamber could handle about 3 extra particles/μsec without obscuring the event of interest. The spatial response of the chamber would render it useful as a detector at high-energy energy accelerators in intense beams where simultaneous tracks at large opening angles must be observed. (auth)

39029 THERMOELECTRIC CONTROL APPARATUS FOR THE FABRICATION OF THICK LITHIUM-DRIFTED GERMANIUM DETECTORS. Palms, John M.; Greenwood, Arthur H. (Los Alamos Scientific Lab., N. Mex.). Rev. Sci. Instr., 36: 1209-13(Aug. 1965). (LA-DC-6521).

Lithium-drifted germanium radiation detectors were fabricated using thermoelectric cooler-heater modules to provide temperature stabilization during the drifting period. The thermoelectric modules provide rapid temperature control determined by the diode bias current. The control loop system is able to provide fast response because, contrary to a conventional oven heater and cold sink arrangement, one no longer has to balance a variable heat source with a constant heat sink. Power levels required for proper control were also substantially reduced.

The detector control unit incorporating a novel differential thermoelectric power circuit is described. The apparatus enables drifting to take place uniformly across the crystal. Depletion depths of 7 mm in crystals with an area up to 8 cm^2 were obtained. Linewidth of 5.4 kev for ^{54}Mn was achieved. The detailed technique of diode fabrication and typical detector characteristics are presented. (auth)

39030 IONIZATION CHAMBERS FILLED WITH DIELECTRIC LIQUIDS FOR DOSIMETRIC MEASUREMENTS. Ladu, M; Pelliccioni, M.; Piciotti, E.; Ramacciotti, D. (Universita, Camerino, Italy). Rev. Sci. Instr., 36: 1241-2(Aug. 1965).

A cylindrical plexiglas chamber with neoprene seals was constructed and tested first. To avoid alteration of the plexiglas by the dielectric and a high current flow even in the absence of a radiation source, a stainless steel chamber with teflon seals was then built. The characteristics of both chambers filled with n hexane were measured. (D.C.W.)

39031 LONG INTERVAL TIME-TO-PULSE-HEIGHT CONVERTER. Wasserman, R. (RCA Labs., Princeton, N. J.). Rev. Sci. Instr., 36: 1273-5(Aug. 1965).

A time-to-pulse-height converter which operates on time intervals of tens of microseconds to tens of milliseconds and handles contiguous time intervals is described. (D.C.W.)

39032 MOESSBAUER SPECTROMETER USING A PIEZOELECTRIC BAR IN RESONANT OSCILLATION. Gerson, Robert; Denno, William S. (Univ. of Missouri, Rolla). Rev. Sci. Instr., 36: 1344-6(Sept. 1965). (TID-21965).

A Mössbauer velocity spectrometer was constructed using a bar of piezoelectric ceramic (lead titanate zirconate) as the source of the Doppler-shift velocity. The bar was driven electrically at its longitudinal resonant frequency (22 kHz for a bar 7 cm long and 0.6×0.6 cm cross section), the resonant condition permitting the attainment of higher velocities than had previously been obtained with piezoelectric drives. The piezoelectric is driven with about 1 v of excitation to display the Mössbauer spectrum for iron. This type of spectrometer may be useful for special purposes, as when its small size or ruggedness is necessary. (auth)

39033 RESOLUTION OF SEMICONDUCTOR DETECTORS FOR FISSION FRAGMENTS. Haines, Eldon L.; Whitehead, A. Bruce (California Inst. of Tech., Pasadena). Rev. Sci. Instr., 36: 1385-6(Sept. 1965).

In a significant fraction of the low-energy collisions between particles of comparable mass, the transferred energy produces little or no ionization. If a fission fragment, in the latter portion of its range in a semiconductor detector, loses a fraction of its energy in nonionizing collisions, then the statistical uncertainty in the energy loss in such collisions contributes to the uncertainty in the amount of electric charge deposited in the detector. Because the collected charge is used as a measure of the fragment's energy, this effect degrades the energy resolution. Calculations for the variance of the energy lost in nonionizing atomic collisions were performed. (C.E.S.)

39034 COUNTING EFFICIENCY AND DIRECTIONAL EFFECTS OF SHIELDED LONG COUNTERS. Kobayashi, Hisanobu (Inst. of Physical and Chemical Research, Tokyo). Rika Gaku Kenkyusho Hokoku, 36: 1-4(1960). (In Japanese).

Experiments were performed to examine the counting efficiency and directional effects of shielded long counters, by using a Ra (100 mC)-Be neutron source. The counting efficiencies of the two types of counters, one with eight holes of one in. in dia on the paraffin surface and the other without holes were found to be 1.9% and 1.7%, respectively. (BBB)

39035 COSMIC RAY-NEUTRON MONITOR FOR ANTARCTIC OBSERVATIONS. Kodama, Masahiro; Fukushima, Shin (Inst. of Physical and Chemical Research, Tokyo). Rika Gaku Kenkyusho Hokoku, 36: 163-4(1960). (In Japanese).

A small, light-weight neutron monitor was prepared for observing cosmic-ray nucleonic components at the Syowa Base in the Antarctic. Its structure and characteristics are described and compared with the standard neutron monitor. (BBB)

39036 DISCHARGE MECHANISM OF Br-CONTAINING ARGON COUNTER. Akutsu, Juichi (Inst. of Physical and Chemical Research, Tokyo). Rika Gaku Kenkyusho Hokoku, 36: 640-5(1960). (In Japanese).

Some calculations were made referring to previous experiments on the counting characteristics of bromine counters, from which it was concluded that the photo-effect at the cathode does not play a part in the multiplication process of halogen quenched counters. (BBB)

39037 A SIMPLE AND INEXPENSIVE SAMPLE CHANGER FOR WINDOWLESS GAS-FLOW COUNTERS. Haasbroek, F. J.; Huynen, M. H. M. (Western Province Fruit Research Inst., Stellenbosh, Republic of South Africa). S. African J. Agr. Sci., 4: 263-5(June 1961).

For a radioisotope technique using weak β emitters, a windowless gas-flow counter was developed. Large numbers of samples were to be analyzed daily and a counter with low gas consumption and requiring short preflushing periods for the counting chamber was needed. These conditions were fulfilled by designing a new type of sample changer, in which the samples are preflushed by a turntable arrangement before being moved into the counting chamber. The sample changer consists of an upper and a lower Perspex disc (both 30 cm in dia and 2.5 cm thick). The two Perspex discs are mounted on two concentric axes, the upper disc remaining fixed while the lower disc can be rotated. The pressure between them can be varied by means of a heavy spring. The contact surfaces of the discs are machined to a width of 8 cm and extend 1 cm on both sides of the sample chambers. A gas seal is obtained by applying a thin layer of silicone grease between the contact surfaces. The efficacy of the gas seal was investigated by stopping the flow of gas while observing the counting rate. It was found that the counting rate remained constant for several hours after cutting off the supply of gas indicating that the rate at which the counter became contaminated with air was extremely low and that moderate flow rates are sufficient to ensure normal operation. (TCO)

39038 TRACKS OF CHARGED PARTICLES IN SOLIDS. Fleischer, R. L.; Price, P. B.; Walker, R. M. (General Electric Research Lab., Schenectady, N. Y.). Science, 149: 383-93(July 23, 1965).

Heavy charged particles create narrow damage trails in many solids. The display of such tracks by preferential chemical etching has provided useful tools in many areas of endeavor: solid-state track detectors for nuclear physics, neutron dosimeters for nuclear engineering, a new means of performing chemical microanalysis of certain elements, filters capable of separating different biological cells, a method of dating geological and anthropological materials, and a means of examining the history and space environment of extraterrestrial objects. (auth)

39039 ON THE EFFICIENCY OF γ ACTIVATION MEASUREMENTS USING WELL TYPE SCINTILLATION COUNTERS. Haberer, Klaus (Technische Hochschule, Karlsruhe, Ger.). Z. Anal. Chem., 210: 412-18(1965). (In German)

Results of investigations on the photopeak efficiency of well-type crystals were compared with values for crystals of different sizes given in literature. The efficiency was established to be primarily dependent on the thickness of the crystal layer surrounding the well. With this dependency peak efficiencies of any common-sized well-type crystals can be established. Evaluation of the total γ efficiency by simple checking of the peak-to-total ratio and by the dependence on the level of charge is described. (auth)

39040 DETECTION AND MEASUREMENT OF NUCLEAR RADIATIONS. Giorascu, F.; Oncescu, M. Bucharest, Academy of Rumanian Peoples Republic, 1964. 276p.

Methods of detection and measurement used in physics

and nuclear techniques are presented, and both the theoretical bases for detecting nuclear radiations and the aspects pertaining to the construction of radiation detectors and auxiliary installations are indicated. After mentioning the fundamental concepts concerning the interaction of nuclear radiations with the substance, which are necessary for analyzing the mechanism of formation of the information supplied by the radiation detector, various types of radiation detectors are examined. The properties of radiation detectors are comparatively discussed. Further, the auxiliary installations are described, function of the information supplied by the radiation detector. The role played by the statistical fluctuations in the measurement of radiations is discussed, considering their importance in the interpretation of data obtained with the aid of systems for detecting nuclear radiations. Finally, various methods of measurements, specific to the measured magnitude, i.e. activity, dose, neutron fluxes, are indicated. (Rumanian Sci. Abstr. Nat. Sci., Vo. 1, No. 8, 1964)

39041 NEW DETECTION METHODS. pp VII.1-25 of Photon Interactions in the Bev-Energy Range. Cambridge, Mass., The M.I.T. Press, 1965.

Descriptions are given of new detection methods for photon interactions, which include detection apparatus for gamma ray machines; a π^0 detection device for high-energy photoproduction experiments; development of sonic spark chambers at CERN; the interaction of monochromatic gamma rays with hydrogen; tagging of gamma rays at CEA; spark chamber automatic scanning system, SPASS, and precision encoding and pattern recognition. (L.B.S.)

39042 NITRATE HELIUM DOSIMETERS OF IONIZING RADIATION. Rudakov, N. P. (Bogomolets Inst. of Physiology, USSR). p.91-7 of Biologicheskoe Deistvie Neitronnogo Izlucheniya. Kiev, Naukova Dumka, 1965. (In Russian).

An analysis was made of nitrate-helium dosimeter performance in mixed gamma-neutron fields. The tests were made using dosimeters prepared from gelatin and agar jellies of ammonium, potassium, and sodium nitrates with additions of glucose and alkali. The amount of nitrate formed in the dosimeter was dose depended up to 1000 rad. The maximum nitrate yield was obtained in the dosimeter with the highest initial nitrate content (1 to 1.5M). The presence of glucose and alkali enhanced the nitrate ion accumulation rate. With identical initial nitrate concentrations, helium dosimeters exhibited higher nitrate yields than liquid nitrate dosimeters. (R.V.J.)

39043 THE USE OF PROPORTIONAL COUNTERS FOR NEUTRON DOSIMETRY. Pasechnik, V. M. p.98-103 of Biologicheskoe Deistvie Neitronnogo Izlucheniya. Kiev, Naukova Dumka, 1965. (In Russian).

Approaches to neutron dosimetry are described. The most expedient is employing the method of nuclear emission using the simplest type of neutron-nucleus interaction — elastic scattering. The dosimetry of neutrons of intermediate energies has a number of peculiarities. Their contribution to the general dose can be extremely significant. In practice the dose of intermediate neutrons is neglected because it is impossible to measure. The dose can be established if the spectrum of neutrons is known: the determination of a spectrum for intermediate neutrons solves the problem of quantitatively determining their contribution to the general dose. The basic problem in creating an intermediate neutron spectrometer has been the construction of a qualitative detector. Such a detector must be able to effectively register neutrons in the selected energy range and have a high resolving capacity. The ^{3}He (n,p)T reaction has extremely good detecting and spectrometric characteristics in that: the transverse cross section of neutron capture is large; the reaction cross section consistently depends on neutron energy; the low-level excited planes of reaction products are lacking; the energy range $q = E_{max}/E_{min} \sim 10$; and the optimal value of reaction energy is identical with neutron energy. Thus, the ^{3}He (n,p)T reaction is fully satisfactory for creating a qualitative detector spectrometer of neutrons in the 0–1-Mev range. A counter with a steel cylinder 50-mm diameter and 1.0-mm shell was constructed. The length of the cylinder was 280 mm with a volume of 400 cm^3. The diameter of the protective cylinder was 2.5 mm, and the length was 40 mm; the field cylinder diameter was 5 mm and its length 50 mm. The gas mixture was ^{3}He-270 mm Hg, Kr-1700 mm Hg, and CO_2-20 mm Hg. A solution for thermal neutrons of better than 15% could not be obtained due to helium impurity. Another proportional counter for recording fast neutron currents is illustrated, the sensitivity of which does not depend on neutron energy. The principal disadvantage of the so-called long counter is its sharp angular tendency. (ATD)

39044 GLASSES SENSITIVE TO X-RAYS OR GAMMA RAYS AND TO BOMBARDMENT BY ATOMIC PARTICLES AND THEIR APPLICATIONS. (to Compagnie de Saint-Gobain). British Patent 989,078. Apr. 14, 1965. Priority date Jan. 5, 1961, France.

A glass is described that is sensitive to irradiation by x rays or gamma rays or to bombardment by sub-atomic particles in which changes in structure produced by the irradiations can be destroyed by heat to cause the emission of light. The glass has a composition consisting of the molecular proportions of 0.5 to 10.0% GeO_2, 0.0 to 10.0% alkali metal oxide, 0.0 to 5.0% Al_2O_3 and/or B_2O_3, the balance being SiO_2. The glass is formed into suitable shapes, such as discs, after the starting materials have been melted in a high-frequency furnace at a temperature of 1700°C and annealed for 48 hr at a temperature of 600°C. After irradiation, the glass exhibits thermoluminescence when heated to a temperature of 300°C. The light emitted can be received by a photomultiplier, and the signal from the photomultiplier recorded to give a measure of the irradiation. An image can be recorded on the glass by subjecting it to irradiation through a mask that has varying transparency to the radiations and then heating the glass or exposing it to infrared radiations to develop the image. The glass is suitable for use for measuring radiation received by personnel and in place of photographic films for determining radiation strength. (B.L.M.)

39045 DEVICE FOR THE MEASUREMENT OF A SURFACE CONTAMINATION CAUSED BY ALPHA EMITTING SUBSTANCES. Weber, Karl Heinz; Galle, Reiner (to VEB Vakutronik). German Patent 1,192,331. May 6, 1965. Filed May 23, 1960.

A device for the measurement of surface contamination caused by alpha emitting substances facilitates the energy-independent measurement of the activity. The device consists of a proportional counter or a scintillation counter mounted on a cylindrical body provided with one or more cylindrical, axially directed channels, which rests on the surface to be measured. In order to obtain an energy independent measurement above a predetermined energy level the thickness of the cylindrical body and the diameter of the cylindrical channels were chosen in such a way that the maximum energy loss of a particle on its way from the surface diagonally across one of the channels to the detector was at most equal to the difference between the predetermined energy level and the threshold of the following discriminator. (Gmelin Inst.)

39046 LARGE-AREA COUNTER FOR EXCLUSIVE MEASUREMENT OF SOFT QUANTA RADIATION EMITTED BY A SAMPLE. Kiefer, H.; Fessler, H.; Maushart, R. (to Gesellschaft fuer Kernforschung mit Beschraenkter Haftung.). German Patent 1,193,617. May 26, 1965. Filed Sept. 19, 1961.

A large-area gridded proportional counter for measurement of soft x or gamma rays is described. It is a parallel-plate type and consists of a central counter volume separated by parallel grids from two outer shielding counter volumes arranged on opposite sides of the central counter volume. Both shielding counter volumes are switched in anticoincidence to the central counter volume. (Gmelin Inst.)

39047 NARROW BAND X-RAY DETECTOR. Brinkerhoff, Joris M. (to Laboratory for Electronics, Inc.).

U. S. Patent 3,176,130. Mar. 30, 1965. Filed June 9, 1961.

An apparatus for the measurement of a selected energy range of an incident beam of x rays includes a radiator element, an x-ray detector adapted to measure only radiation from the radiator element, and a filter plate interposed between the incident beam of x rays and the radiator element. The radiator element is formed of a material characterized by having its critical x-ray absorption edge at a first energy value equal to the lower limit of the selected energy range, and the filter element is formed of a material having its critical x-ray absorption edge at an energy value equal to the upper limit of the selected energy range. Preferably, the two materials should be selected so that their atomic numbers differ by only 1. The x-ray detector may be any of the conventional types such as a scintillation detector, proportional counter, or ion chamber. Radiation above the absorption edge of the filter plate will be substantially absorbed by this plate that will emit characteristic x rays. These x rays falling below the absorption edge of the radiator will pass through the radiator without significant interaction. X rays of energies below the absorption edge of the radiator incident upon the filter plate will pass through both the filter plate and the radiator, since both materials will have a high coefficient of transmission of x-rays of this energy. X rays with energies below the absorption edge of the filter plate but above that of the radiator will be readily transmitted by the filter and heavily absorbed in the radiator resulting in characteristic x rays being emitted by the radiator. (B.L.M.)

39048 READING APPARATUS FOR THERMOLUMINESCENT TYPE RADIATION DOSIMETERS. McCall, Richard C.; Barr, William H. (to Controls for Radiation, Inc.). U. S. Patent 3,176,133. Mar. 30, 1965. Filed Feb. 18, 1963.

A radiation dosimeter reader for energizing thermoluminescent materials and for sensing the resulting dosage indication includes a support element for the thermoluminescent material, a photon radiation sensor, and recording apparatus. The support element is preferably a stainless steel sheet on which the material is spread out over a relatively large area in a layer in the order of one crystal in thickness. The support element includes edge portions that engage electrical contacts when the support element is positioned in the field of view of the radiation sensor so that the electric current passes via the contacts through the support element to heat the element that in turn heats the layer of thermoluminescent material. The material is cycled through the desired temperature range, and the photomultiplier positioned within a magnetic shield inside of a substantially light tight casing detects the luminescence. The reading apparatus includes means by which the support element may be positioned in and removed from the light sensor field of view with no admission of external light so that the dark adapted characteristics of the photomultiplier tube are not impaired. (B.L.M.)

39049 INSTRUMENT FOR THE DETECTION OF INFRA-RED RADIATION. Weissenberg, Gustav (to Ernst Leitz GmbH). U. S. Patent 3,188,467. June 8, 1965. Priority date Dec. 11, 1958, Germany.

Apparatus for indicating infrared radiation consists essentially of a layer of a thermoluminescent substance and a source of radioactivity operatively associated with and exciting the thermoluminescent layer to a metastable condition in which luminous energy corresponding to the intensity distribution of the original infrared radiation is produced when the infrared radiation impinges upon the layer. In developing the apparatus as an image converter tube, a carrier permeable to visible light is arranged in a highly evacuated container having a window permeable to infrared radiation. The carrier has on the side opposite the window a layer of thermoluminescent and radioactive substances and on the other side a light-sensitive layer. Electron-optical means for focusing the electrons from the light-sensitive layer on a screen are arranged in a known manner at the back of the carrier. (A.G.W.)

39050 RADIOACTIVITY MEASUREMENT OF AIRBORNE PARTICULATE MATTER. Leuba, Richard J. (to Lab for Electronics, Inc.). U. S. Patent 3,189,742. June 15, 1965. Filed Nov. 22, 1961.

A fixed-filter monitor for measuring the radioactivity of particulate matter in a gaseous medium is designed for easy replacement of the filter. The monitor includes a housing having an opening in one end with a hinged end piece, which is locked in the closed position for operation of the monitor and which may be swung outward from the end of the housing for insertion and removal of the filter paper. The filter paper is mounted on a circular lip projecting inwardly from the center of the hinged end piece and is held in place by suction. A scintillation detector assembly is spaced apart from but close to the filter paper inside the housing. A pump provides suitable gas flow through the filter. (A.G.W.)

39051 RADIATION FALLOUT METER. Greer, Harold; Slocum, Richard William Jr. U. S. Patent 3,191,033. June 22, 1965. Filed May 11, 1962.

A radiation detector that can be operated by the average person and that has a long shelf life is intended to measure radioactive fallout caused by nuclear accidents or nuclear weapons. The meter includes a scintillating material enclosed in a light-tight housing. An eye piece secured to the housing permits viewing of the scintillating material. A light-absorbing means between the scintillating material and the eye piece is movable to vary the amount of light passing from the scintillating material to the eye piece. The viewer moves the light-absorbing means until substantially no light reaches his eye. A suitable scale indicates the radiation intensity corresponding to the adjustment of the light-absorbing material. (A.G.W.)

39052 FILM BADGE SYSTEM AND METHOD OF USING. Kocher, Leo F. (to U. S. Atomic Energy Commission). U. S. Patent 3,202,821. Aug. 24, 1965.

A dosimeter filter system comprises: a tantalum filter of sufficient thickness to block x rays, gamma rays having energies of less than about 35 kev, and beta radiation; an iron filter; a plastic filter; the iron and plastic filters being sufficiently thick to provide equal attenuation of hard beta radiation; and an open window; the iron filter, the plastic filter, and the open window all providing equal attenuation of photon energies in excess of about 50 kev. (AEC)

39053 TRANSISTORIZED REGULATED HIGH VOLTAGE SUPPLY. Glass, F. M. (to U. S. Atomic Energy Commission). U. S. Patent 3,202,902. Aug. 24, 1965.

A transistorized, highly regulated high-voltage supply is designed for portable radiation detectors such as a Geiger-Mueller tube or scintillation detector. The supply includes a battery, transistor blocking oscillator, step-up transformer, rectifier, and filter for providing the d-c output voltage. A gas tube is connected to the output terminal of the supply and in effective series relationship with the oscillator input. As the load on the supply is reduced, the supply voltage increases, causing the gas tube to pass a current which controls the bias on the oscillator to reduce the frequency of oscillation and thereby decrease the battery drain due to the oscillator. The frequency of oscillation of the oscillator is thus continuously adjusted by the feedback circuit to provide a continuous duty-cycle regulation of the oscillator. (AEC)

Radiation Effects

39054 (AD-607863) SOME ELECTRON RADIATION EFFECTS ON TRANSISTORS–A DATA RE-PRESENTATION TECHNIQUE (thesis). Brooks, Leon Preston Jr. (United States Naval Academy, Annapolis, Md. Science Labs.). May 5, 1964. 133p. (S-5) CFSTI, $4.00 cy, $1.00 mf.

The effects of a mono-energetic, constant-dose-rate electron beam on four transistor types are discussed. Measurements were taken in the grounded emitter configuration both under ambient conditions and while each specific device was under irradiation. The resulting data

are presented in a three-step reduction/re-presentation technique which utilizes the variation of gain degradation with ambient forward current gain of the device (BETA O) in a nuclear environment. The three steps are (1) the graphical or first approximation, (2) the computer analysis, and (3) the third step check (the use of pre-irradiated devices in breadboarded circuits). A discussion of the Composite Test System used to obtain the parameter profiles under irradiation is included, along with complete design procedure and calculations in the appendix. The validity of the accelerated testing concept in particular, and the whole present radiation effects program in general are investigated. An alternate type of radiation effects program is suggested. (auth)

39055 (GA-6266) RADIATION EFFECTS ON PRESSURE TRANSDUCER COMPONENTS. Final Report. Poll, R. A.; Jackson, D. F.; Cotter, L. D.; van Lint, V. A. J. (General Atomic, San Diego, Calif.). June 1965. Contract AF29(601)-6692. 106p. (AFWL-TR-65-49). CFSTI.

The performance of two types of pressure transducers and several cables in a radiation environment was evaluated by an experimental program. The transducers were (1) a quartz piezoelectric crystal assembly, and (2) several strain-gage transducers made by the Stanford Research Institute. The most important perturbations of these transducers by a short pulse of radiation are the emission and absorption of secondary electrons by parts of the device and the conductivity of insulating materials, including quartz, cable connectors, and cables. The experimentally measured results can be applied to evaluate the spurious signals and the perturbation of pressure-induced signals in a specified pulse radiation environment. The experimental program also included the evaluation of several zener diodes, Shockley diodes, and silicon controlled rectifiers. These devices are to be used in a pulsed power supply which will also be exposed to a pulsed radiation environment. The most important determinations for the SCRs and the Shockley diodes were the gamma levels required for complete turn-on and the neutron levels which would cause failure of these devices. The zener diodes were investigated to determine the transient effects due to gamma radiation and the permanent zener voltage changes due to neutron radiation. The mechanisms of these perturbations are presented to facilitate the designing of systems to minimize these same perturbations. (auth)

39056 (N64-29558) RIFT RADIATION EFFECTS PROGRAM: IRRADIATIONS NO. 5 AND 8 ELECTRICAL CABLES. (Lockheed Missiles and Space Co., Sunnyvale, Calif.). Apr. 15, 1964. Contracts NAS8-5600 and NAS8-9500. 70p. (NSP-64-25; NASA-CR-56779). CFSTI, $6.60 cy.

Presented are the results of measurements made during irradiation of coaxial cables RG 58C/U and RG 141/U; multiconductor cables MD-324, CDS-47831, PSC-C-39001, and RT 24(19)ST; and connector PT00P-14-5 S/PT06P-14-5 P. These cables were tested at 70°C under radiation dose rates of 10^4 to 2×10^6 r/hr and at total doses to 3×10^7 r. The conductance and currents found for the minimum and maximum dose rates are shown in a table. The empirical equations derived for slab geometry of dielectrics were not applicable to the majority of the data. (auth)

39057 (NP-15022(Vol.II)(Add.)) SNAP-8 RADIATION EFFECTS TEST PROGRAM. VOLUME II. ELECTRICAL INSULATION MATERIALS. Addendum to Report. (Lockheed-Georgia Co., Marietta). Jan. 1965. Contract [NAS 5-417], Subcontract No. OP367736. 9p. (ER-7591 (Add.)).

For Aerojet General Corp., Azusa, Calif.

An additional temperature test was performed on the X1-1 statorettes to better define their temperature insulation resistance characteristics. Insulation resistance measurements were made at ambient temperature and at periodic intervals as the temperature was increased to approximately 200°C, allowed to stabilize and decreased to ambient. Next, the irradiated statorette was dissected to observe the insulation around the inner conductors. The results are tabulated. The statorette capsules were leak checked at the completion of all tests. (M.O.W.)

39058 ON THE BEHAVIOUR OF SELENIUM PHOTOCELLS DURING AND AFTER IRRADIATION WITH Co^{60} GAMMA-RAYS. Storbeck, I. (Institut fuer Angewandte Physik der Reinststoffe, Dresden). Kernenergie, 8: 309-12(May 1965). (In German).

The behavior of selenium photocells was studied under different operating conditions before and after irradiation with ^{60}Co gamma rays. Up to exposures of 1×10^6 R, the current-voltage characteristics only show an insignificant shift to the side of smaller photocurrents. The dark current is nearly constant up to 1×10^6 R. The photocurrent decreases with increasing exposure. In darkened state, the photocurrent of selenium photocells amounts, during irradiation with 10^5 to 10^6 R/hr, to a few per cent of that produced by illumination with 10^2 to 10^4 lux. Therefore, selenium photocells may be considered to be nearly resistant to radiation up to exposures of 10^6 R, when the operating conditions are adequately chosen. Exposures of 10^8 R lead to deep variations of the photocurrent in comparison with that of the unirradiated state. (auth)

39059 IONIZING PARTICLE RADIATIONS EFFECTS AND SIMULATION CONSIDERATION. Duberg, J. E.; Hulten, W. C. Virginia Polytech. Inst., Eng. Ext. Ser. Circ., Pt. A, III.1-34([1964]).

Space radiation environment brought about the studies of radiation effects by means of space probes and earth satellite systems. The particular radiation environment encountered in space, which offers a great threat of damage to space vehicles including both manned and unmanned systems includes protons and electrons trapped in the earth's magnetosphere, and high-energy protons associated with solar flare events. Transient, permanent, surface, and chemical radiation effects are discussed. Studies were made on changes of electrical properties in semiconductors with proton irradiations, radiation effects on transistors and solar cells, radiation effects on semiconductor devices, effects of ionizing radiation on polymers, radioinduced changes in capacitor-type detectors, and effects of radiation on optical transmission properties of transparent materials. The NASA Space Radiation Effects Laboratory is described and its operation discussed. (F.J.H.)

ISOTOPE TECHNOLOGY

General

Refer also to abstract 39265.

39060 UTILIZATION OF RADIOISOTOPES. Otsuka, Iwao (Rikagaku Lab., Tokyo). Genshiryoku Kogyo, 11: No. 4, 33-6(Apr. 1965). (In Japanese)

The first radioisotopes used in Japan in 1943 were cyclotron produced. In the period following 1950, their use increased tremendously because of the greater availability. A tabulation is presented of the total curies of the more commonly used radioisotopes over the period 1950 to 1960. These include isotopes for tracer uses and radiation source uses. The various applications of radioisotopes in industrial fields are listed but are not described in detail. Applications in physical sciences, agriculture, medicine, and pharmacy are tabulated. A breakdown is made of the total amount of radioisotopes used by the sciences, industry, agriculture and biology, and medicine. A similar breakdown is made of the specific isotopes ^{3}H, ^{90}Sr, ^{131}I, and ^{60}Co. (TTT)

Industrial Applications

39061 (ADR-09-08a-63.1) RADIOISOTOPIC DETECTION OF MICROBIAL CONTAMINATION PRESENT IN JET FUEL. Becker, Dennis J.; Calvelli, Edward A. (Grumman Aircraft Engineering Corp., Bethpage, N. Y. Quality Control Dept.). June 1, 1963. 20p.

A radioisotopic method was developed for the rapid detection of microorganisms in jet fuel. Using this technique it is possible to reliably detect the presence of microorganisms within one hour after sampling, and semi-quantitatively determine the degree of contamination within two to three hours. This method is readily adaptable to field operation, since the amount of radioactive material required does not necessitate special handling or AEC licensing. (auth)

39062 (TID-21710(Rev.)) STUDY OF APPLICABILITY OF RADIATION PASTEURIZATION OF FRUITS IN THE SOUTH. (Southern Interstate Nuclear Board, Atlanta, Ga.). Sept. 15, 1964. Contract AT(38-1)-368. 110p. Dep. mn; CFSTI, $4.00 cy, $0.75 mn.

Results are reported from a study of the effects of radiation pasteurization on spoilage incurred in the marketing system for grapefruit, oranges, peaches, strawberries, and tomatoes. Data are included on the status of radiation pasteurization of fruits of specific interest in the Southern U. S. Eleven isotope facilities with adequate radiation sources located in the area are described and economic implications of their use for food irradiation are discussed. Data show that the value of grapefruit, oranges, and peaches saved was not enough to cover the cost of irradiation. The value of strawberries and tomatoes saved was more than the cost of irradiation. (C.H.)

39063 THE OCTOBER 9 TO 13 MEETING OF THE WORK GROUP FOR THE APPLICATION OF RADIOISOTOPES OF THE LIGHT INDUSTRY EXPERTS COMMITTEE OF COMECON. Kerese, Istvan Atomtech. Tajekoztato, 8: 55-8(1965). (In Hungarian)

Employed and experimental industrial operations and instruments using radioisotopes are reviewed. The most promising system was considered to be the measuring device giving the weight per unit surface of paper products in a continuous manner. The latest version employs an ionization chamber; simultaneous determination of humidity makes it possible to correct the values automatically. A β-absorption method was used to measure the unevenness of textile fibers. Determination of the level of various industrial liquids offers an important field for the application of radioisotopes. Sealed β sources containing T and various α emitters are employed in the textile industry to eliminate static electricity. Electron accelerators are used to sterilize catgut, surgical bandages, pharmaceutical preparations, and blood-collecting equipment. Tracer techniques are not widespread, but ^{35}S is used to determine the optimum amount of material carried by viscose fibers. (TTT)

39064 ATOMIC INDUSTRY NOTES. Takeuchi, Koichi; Kawakami, Koichi (Nippon Atomic Industry Group, Tokyo). Genshiryoku Kogyo, 11: No. 4, 73-8(Apr. 1965). (In Japanese)

The events leading to the formation of the five atomic industrial groups in Japan are described, along with subsequent progress made by these groups. The present status of these groups, the present atomic power picture, the projected power program up to 1975 and beyond, and the total finding of these groups are presented in tabular form. The growth in radioisotope utilization is outlined including a breakdown by industries using isotopes and specific industrial uses. (TTT)

39065 STRUCTURE OF THE PIGMENTS OF PRE-COOKED IRRADIATED MEATS. Tarladgis, Basil G.; Ehtashan-ud-Din, A. M. F. (Univ. of New South Wales, Sydney). Nature, 207: 489-91(July 31, 1965).

A study was made of the pigments responsible for color changes in cooked beef, lamb, pork, and veal after exposure to doses of from 1×10^5 to 5×10^6 rads γ radiation. The reflectance spectra of all samples were recorded using a recording spectrophotometer and the total pigment content of the various meats was extracted and measured for comparison with control samples. In general, the reflectance spectra of the various cooked meats were very similar and the intensity of all spectra increased with radiation dose. The spectra of the irradiated samples show that during irradiation the spin state of Fe of the porphyrins in the meat is altered while Fe is being reduced. The mechanism of color conversion of the cooked meats by ionizing radiation is outlined. It is concluded that the compound responsible for the color of irradiated cooked meats at radiation doses up to 5×10^5 rads is a mixture of high-spin ferric, high spin ferrous, and low-spin ferric porphyrin co-ordination compounds. At radiation doses above 5×10^5 rads, the mixture consists mostly of a low-spin ferrous and a low-spin ferric porphyrin. The contribution to the mixture of the low-spin ferrous form increases with the radiation dose. Cooked meats subjected to low radiation doses would be unstable from the lipid oxidation point of view, since most of the pigment would be in the high-spin form. Suitable autoxidants would prevent such oxidative changes. (C.H.)

39066 INDUSTRIAL PROSPECTS OF RADIATION CHEMISTRY. Davies, A. G. (Atomic Energy of Canada Ltd., Ottawa). Trans. Eng. Inst. Can., 7: E-2(Dec. 1964). (AECL-1939).

Radiation sources for the production of useful radioisotopes are surveyed and several examples discussed. A list summarizes the basic mechanisms of radiation chemistry and reactions of polymers are treated in some detail. Typical radiation yields and properties of products are given. Increased application of radioinduced processes in the textile, plastic, petroleum, and petrochemical industries is predicted. (F.S.A.)

39067 THE USE OF RADIOACTIVE ISOTOPES FOR CHECKING PRODUCTION PROCESSES. Verkhovskii, B. I. International Series of Monographs on Nuclear Energy. Division IV. Isotopes and Radiation. Volume 2. New York, The Macmillan Co., 1963. 82p. $3.75.

Translated by H. S. H. Massey from Primeneniye Radioaktivnykh Isotopov Dlya Kontrolya Proizvodstvennykh Protessov.

The use of radioactive isotopes for checking production processes is discussed under the following headings: radioactivity and radioactive radiations; recording radioactive radiations; and the use of radioactive radiations in instruments for checking technological processes. (F.J.H.)

39068 IRRADIATION DAMAGE IN LIPIDS AND ITS EFFECT ON FLAVOR. Merritt, Charles Jr.; Angelini, Pio (Army Natick Labs., Natick, Mass.). 41p. (CONF-650401-10). Gmelin, AED-CONF-65-041-31.

From American Chemical Society, Detroit.

Radiosterilization effects on lipids and flavor in meats are discussed. Analytical methods used to study the nature of irradiation damage are described. (P.C.H.)

Power Application

Refer also to abstract 38836.

39069 (BNWL-C-45) PROMETHIUM ISOTOPIC POWER DATA SHEETS. Van Tuyl, H. H. (comp.) (Battelle-Northwest, Richland, Wash. Pacific Northwest Lab.). Mar. 15, 1965. Contract AT(45-1)-1830. 8p. Dep. mn; CFSTI, $1.00 cy, $0.50 mn.

The knowledge and technology of Pm as a fuel for radioisotopic power sources are summarized. The data given cover the nuclear properties, purity, availability, compatibility with container materials, physical properties (of metal and oxide), and mechanical properties of Pm. (D.L.C.)

39070 (GEST-2046) RESEARCH AND DEVELOPMENT PROGRAM OF THERMIONIC CONVERSION OF HEAT TO ELECTRICITY. Technical Summary Report. (General Electric Co., Pleasanton, Calif. Special Purpose Nuclear Systems Operation). Dec. 31, 1964. Contract NObs-90496. 135p.

A continuation of a series of 1000-hr diffusion experiments of UO_2-Mo and UO_2-W fuel-emitter pairs in the temperature regime of 1600 to 1800°C for Mo and 1800 to 2200°C for W is reported. Identification of uranium diffusion and the limits of the uranium diffusion rates are investigated. An investigation of the diffusion rate of transport of oxygen through Mo or W in the temperature range of 1500 to 1800°C is presented. An insulator materials development program which includes the identification of the gaseous species and products which exist when high-purity alumina bodies and Nb and/or Nb-1% Zr are heated to temperatures of interest to elucidate possible gas-solid reactions in a thermionic converter is presented. A ceramic to metal seal development program includes: the development of cesium-resistant metallizing coatings for pure alumina ceramics, the development of Mo-alumina cermet structures for use as emitter-collector seal insulators, the evaluation and/or development of methods of bonding the metallic surface of insulators to structural metal members, and the long-time testing of materials and seals at high temperatures in both vacuum and cesium vapor environments. (M.O.W.)

39071 (MND-3169-68) NIMBUS DYNAMICS ANALYSIS FOR EJECTION MECHANISM. Burgio, R. G.; Miller, M. C. (Martin Co., Baltimore, Md. Nuclear Div.). June 1965. Contract AT(30-1)-2345. 62p. Dep. mn; CFSTI, $3.00 cy, $0.75 mn.

Ejection of the SNAP 19 generator from the NIMBUS-B satellite was studied theoretically using a modified 3 degree-of-freedom (pitch plane) trajectory computer program. Effects of initial altitude and satellite attitude were included. Nearly every case investigated showed that interference would exist between the generator and NIMBUS stabilization and control sub system immediately following ejection. Interference was reduced by approximately 50% when the following stabilization and control sub system protuberances were removed from the ejection path of the generator: sun shield horizon scanner, baffle-coarse yaw sensor, and albedo shield coarse yaw sensor. In the cases where there was no interference between the generator and NIMBUS, the generator was ejected well beyond the satellite. (auth)

39072 (NP-15187) RESEARCH AND DEVELOPMENT PROGRAM OF THERMIONIC CONVERSION OF HEAT TO ELECTRICITY. Third Quarter Report. (General Electric Co., Pleasanton, Calif. Special Purpose Nuclear Systems Operation). Mar. 29, 1965. Contract NObs-90496. 12p.

Three aspects of the program are reported; UO_2 refractory metal reaction kinetics, insulator materials development, and ceramic-to-metal seal development. Progress pertaining to these main areas is presented. (M.O.W.)

Separation and Production

See also CHEMISTRY — Separation Processes and Procedures.

Refer also to abstracts 38787 and 39762.

39073 AMERSHAM TODAY. Chem. Brit., 1: 287-8 (July 1965).

The development and operation of the Radiochemical Center at Amersham is described, and the radioisotope products it offers and the processes used in preparing them are discussed. About 2000 items based on 180 different radioisotopes are prepared. A cyclotron, specially designed for the purpose and now undergoing final tests, was installed to improve the supply of about 30 neutron-deficient isotopes that could not be made in a nuclear reactor. However, most elements are produced at the Isotope Production Unit at Harwell, and at Amersham the crude isotopes are chemically refined for use alone or in the synthesis of labeled compounds. In the field of labeled compounds much attention is still given to ^{14}C and ^{3}H, and 400 of the former and 200 of the latter compounds are now prepared. The synthesis of a ^{14}C-labeled organic compounds is usually begun using $^{14}Co_2$ via $Ba^{14}CO_3$, and tritiated water is the starting point for materials labeled with ^{3}H, which are generally produced by exchange reactions. The functions of the organic, inorganic, analytical, and natural radioelement departments are outlined. The natural radioelements department, for instance, is concerned with isotopes of the heavy elements, such as ^{241}Am, ^{227}Ac, and ^{228}Th. Various applications of isotopic compounds are discussed, as well as their distribution in the United Kingdom. About half of the two million £ yearly production of the Center is exported. (BBB)

39074 STUDIES ON ISOTOPE SEPARATION USING INORGANIC ION-EXCHANGER IN FUSED SALT. I. SEPARATION OF POTASSIUM ISOTOPES BY ZIRCONYL PHOSPHATE IN FUSED POTASSIUM NITRATE. Shinagawa, Mutsuaki; Oyoshi, Akira; Oyoshi, Emiko (Osaka Univ.). J. Nucl. Sci. Technol. (Tokyo), 2: 251-6(July 1965).

An attempt to separate K isotopes was made using ion exchange at 370°C. As the ion exchanger, zirconyl phosphate was used in fused KNO_3. The first step of the reaction was an irreversible hydrogen-potassium exchange reaction accompanied by NO_2 gas evolution, followed by an isotopic exchange reaction between ^{39}K and ^{41}K. ^{39}K was enriched in the zirconyl phosphate, with a simple process separation factor of 1.012 ± 0.003. The ion exchange capacity of zirconyl phosphate in fused salt was 8.7 ± 0.1 meq/g. (auth)

39075 AN ANALYSIS FOR THE ISOTOPE SEPARATION BY LIQUID-GAS CHEMICAL EXCHANGE. Ishida, Kenji; Mishima, Masao (Japan Atomic Energy Research Inst., Tokyo). J. Nucl. Sci. Technol. (Tokyo), 2: 270-2 (July 1965).

Isotope separation by chemical exchange between liquid and gas phases was analyzed by a method similar to Cohen's. Equations are given and their efficiency in explaining experimental results are discussed. (M.C.G.)

39076 ENRICHMENT OF INNER COMPONENTS OF POLYNARY ISOTOPE MIXTURES BY THERMAL DIFFUSION IN CLUSIUS-DICKEL COLUMNS WITH RESERVOIRS AT BOTH ENDS. Mueller, G.; Trommer, S.; Wilde, K. (Institut fuer Stabile Isotope, Leipzig). Kernenergie, 8: 297-306(May 1965). (In German).

The stationary distribution of the components of polynary isotope mixtures in the reservoirs at both ends of the column which together form a closed system is calculated. The problem of the mass balances may be reduced to the solution of a system of linear equations, if the contents of

the column are neglected with respect to the volumes of the reservoirs. The enrichment technique based on this distribution is suitable for the separation of inner components having small initial concentration. As compared with other continuous and batch processes of enrichment, the technique has at least shown to be equivalent to that based on stationary distribution of the isotopes in a closed column without reservoirs. This comparison has also shown that no method is suited for enriching all components of polynary isotope mixtures like this. In detail, three systems were studied: reactor-produced krypton containing ^{85}Kr, natural krypton, and natural argon. (auth)

39077 THE ISOTOPE SEPARATOR OF ROME UNIVERSITY. Ascoli, Sergio; Broch-Toniolo, Francesco; Cacace, Fulvio; Giacomello, Giordano (Universita, Rome and Centro Nazionale per la Chimica delle Radiazioni e dei Radioelementi (CNR), Rome). Ric. Sci. Rend., Sez. A, 8: 15-26(Jan.-Feb. 1965). (In Italian).

The electromagnetic isotope separator, recently put into operation in the radiochemical department of the Pharmaceutical Chemistry Institute of Rome University is described. The main features of the separator and its performance, as determined in a series of preliminary experiments, are illustrated. (auth)

MATHEMATICS AND COMPUTERS

Refer also to abstracts 38970, 39270, and 46112.

39078 (AEEW-M-507) THE SIMULTANEOUS USE OF SEVERAL PSEUDO-RANDOM BINARY SEQUENCES IN THE IDENTIFICATION OF LINEAR MULTIVARIABLE DYNAMIC SYSTEMS. Cummins, J. D. (Atomic Energy Establishment, Winfrith (England)). Feb. 1965. 13p. Dep.; BIS, $0.40; HMSO, 2s.

With several white noise sources the various transmission paths of a linear multivariable system may be determined simultaneously. The restrictions of pseudo-random two state sequences to effect simultaneous identification of several transmission paths and the consequential rejection of cross-coupled signals in linear multivariable systems are considered. The conditions for simultaneous identification are established by an example, which shows that the integration time required is large i.e. tends to infinity, as it does when white noise sources are used. (auth)

39079 (LA-DC-7160) APPLICATIONS OF A LANGUAGE FOR COMPUTING IN COMBINATORICS. Wells, Mark B. (Los Alamos Scientific Lab., Univ. of California, N. Mex.). [1964]. Contract W-7405-eng-36. 7p. (CONF-650505-5). Dep. mn; CFSTI, $1.00 cy, $0.50 mn.

From IFIP Congress 1965 Meeting, New York.

A language is reported for computing in combinatorics. This language is applied in finding the minimum number of (binary) comparisons necessary to rank in different weights. (M.O.W.)

39080 (LA-DC-7192) ANALYSIS OF INHERENT ERRORS IN MATRIX DECOMPOSITION USING UNNORMALIZED ARITHMETIC. Metropolis, N. (Los Alamos Scientific Lab., Univ. of California, N. Mex.). [1963]. Contract W-7405-eng-36. 6p. (CONF-650505-4). Dep. mn; CFSTI, $1.00 cy, $0.50 mn.

From IFIP Congress 1965 Meeting, New York.

An algorithm is described for the reduction of a square matrix triangular form; more specifically, a strategy is given for the selection of pivot elements for each stage of reduction by Gaussian elimination. (M.O.W.)

39081 (ORNL-TM-1176) DIAGNOSE, A ROUTINE TO DEBUG FORTRAN PROGRAMS. Thompson, J. A. (Oak Ridge National Lab., Tenn.). June 25, 1965. Contract W-7405-eng-26. 28p. Dep. mn; CFSTI, $2.00 cy, $0.50 mn.

A computer program, DIAGNOSE, to be used in debugging Fortran-63 programs, is available to users of the CDC-1604 at ORNL. DIAGNOSE will detect three common errors which occur during execution of programs: (1) erroneous subscripts, (2) use of variables which have not had values assigned to them, and (3) erroneous do-loop parameters. (auth)

39082 (TID-22032) CONVEX SETS AND THEIR APPLICATIONS. Argonne National Laboratory Applied Mathematics Division Summer Lectures, 1959. Fan, Ky (Notre Dame Univ., Ind.). Contract AT(11-1)-427. 162p. Dep. mn; CFSTI, $5.00 cy, $1.00 mn.

Properties of convex sets and their applications are considered. In order to make the exposition self-contained, a summary of definitions and results of General Topology and a brief introduction to topological linear spaces are given. The following three topics on convex sets are considered: separation properties, fixed point properties and extreme points. Each of these topics is illustrated with applications. (auth)

39083 CLUSTER-STAR INVERSION AND THE MOEBIUS FORMULA. Sherman, S. (Indiana Univ., Bloomington). J. Math. Phys. (N. Y.), 6: 1189-92(Aug. 1965).

The cluster-star equations are inverted by using the general Moebius inversion formula. Since Uhlenbeck and Ford have many instances of systems of equations to which general Moebius inversion can be applied, a general survey of Moebius inversion, some graph terminology, and the cluster-star inversion are presented. (auth)

39084 CLUSTER-STAR INVERSION BY MEANS OF GENERATING FUNCTIONALS. Stell, G. (New York Univ., New York). J. Math. Phys. (N. Y.), 6: 1193-1200 (Aug. 1965).

The cluster–star equations are inverted. These equations define a set of cluster functions U_m in terms of star functions V_n for $2 \leq n \leq m$. The inversion gives the V_n in terms of the U_m; $2 \leq m \leq n$. The cluster–star inversion yields the coefficients β_n that appear in the number-density expansion of the logarithm of the grand partition function Ξ of a statistical mechanical system in terms of the coefficients b_n that appear in its fugacity expansion, even when the system is in the presence of an external field. In the course of obtaining the inversion, an expression for the work necessary to bring a particle from infinity to a point r inside a classical system at equilibrium is obtained in terms of the V_m and the one-particle distribution function $\rho(r)$, and also in terms of the U_m and ρ. The expression in terms of the V_m and ρ was previously derived with restrictions on the form of the potential energy; the alternative expression in terms of the U_m seems to be new. Operators with essentially the same algebraic structure as the V_m appear in a recently considered asymptotic expansion of the distribution functions of a nonequilibrium system. The cluster–star inversion facilitates the determination of these operators in terms of the solution operators of the n-body Liouville equation, $n \geq 2$. (auth)

39085 ON PROJECTIVE REPRESENTATIONS OF FINITE GROUPS. Rudra, P. (Saha Inst. of Nuclear Physics, Calcutta). J. Math. Phys. (N. Y.), 6: 1273-7 (Aug. 1965).

The algebra of projective representation, belonging to a factor system, is presented. Exact expressions for the projection operators and Kronecker (inner) direct-product representation are obtained. Formulas for obtaining the characters of all the inequivalent irreducible projective representations and the Clebsch-Gordan coefficients are derived. (auth)

39086 SCALAR INVARIANTS OF A ROTATIONAL SYSTEM IN A LIE ALGEBRA. II. CASIMIR OPERATORS. Pease, M. C. (Stanford Research Inst., Menlo Park, Calif.). J. Math. Phys. (N. Y.), 6: 1334-40(Aug. 1965).

Matrix equations of the form $dW/dz = [S,W]$ are considered, where $S(z)$ is a matrix-valued function of z, embedded in a given semisimple Lie algebra, L. If the set X_i is a basis for L, W is expanded as w^iX_i. General conditions are obtained on an n-index form $p_{ijk\ldots}$ such that $p = (u^iv^jw^k \ldots p_{ijk\ldots})$ is a constant if u^i, v^j, w^k, etc., are solutions of the differential equation. It is shown that these forms are those that determine the vector invariants of the corresponding group. It is asked what transformations will map any solution of the differential equation onto another, regardless of the detailed behavior of $S(z)$. It is shown that the transformations that do this involve these same $p_{ijk\ldots}$. With this identification, procedures that can be used to calculate at least the two-index forms, p_{ij} can be obtained. The existence of two-index forms, other than the Killing metric g_{ij}, is shown to depend on the reducibility of the adjoint representation. Finally, it is shown that these same forms generate Casimir operators—i.e., operators that commute with all elements of the algebra, and hence with the group associated with it. The Casimir operator so obtained is given explicitly by $(p_{ijk\ldots}X^iX^jX^k \ldots)$, where the set, X^i, is the basis of the dual algebra. (auth)

39087 ANALYSIS OF EXPERIMENTAL DATA SATISFYING A DISTRIBUTION OF THE TYPE $x^m dx$. Roinishvili, N. N.; Mandritskaya, K. V. (Inst. of Physics, Academy of Sciences, Georgian SSR). Yadern. Fiz., 6: 1028-31(June 1965). (In Russian).

A method for analyzing distributions of the type $x^m dx$ is proposed. The essence of the method is the determination of the mean value of the ln of the measured quantities. This makes it possible to determine the non-displaced best es-

timation of the distribution exponent m and to formulate the strongest possible criterion for testing hypotheses of the type $x^m dx$. Several possible applications of the suggested method are given as examples. (auth)

39088 PLANNING OF EXPERIMENTS DISCRIMINATING BETWEEN POSSIBLE CURVES. Fedorov, V. V.; Klepikov, N. P. (Moscow State Univ.). Yadern. Fiz., 1: 1032-4(June 1965). (In Russian).

A method of planning experiments discriminating between two or several curves in the shortest possible time is suggested. (auth)

METALS, CERAMICS, AND OTHER MATERIALS

General

Refer also to abstracts 38543, 38546, 40112, 40113, 40177, 40196, 40197, and 40198.

39089 (AERE-M-1389) THE PREPARATION AND SOME PROPERTIES OF URANIUM CARBONITRIDES. Landsman, D. A.; Biddle, P.; Fox, A. C.; Harder, B. R.; Hyde, K. R.; Seddon, W. E. (Atomic Energy Research Establishment, Harwell (England)). Apr. 1964. 8p. Dep. mn.

Conditions used to prepare uranium carbonitrides in a fluidized bed are described and procedures for the analysis of the products outlined. Preliminary results on fission gas release after irradiation, and on sintering behavior were obtained. (auth)

39090 (ANL-7046(p.78-82)) NUCLEAR SAFETY. (Argonne National Lab., Ill.).

Summaries are given of work on fast reactor safety, TREAT operations, and reactions of fuels and cladding with liquid sodium. (J.R.D.)

39091 (BMI-1723(Del.)) PROGRESS RELATING TO CIVILIAN APPLICATIONS DURING APRIL 1965. Dayton, Russell W.; Paprocki, Stan J. (Battelle Memorial Inst., Columbus, Ohio). May 1, 1965. Contract W-7405-eng-92. 44p. Dep. mn; CFSTI, $1.00 cy, $0.50 mn.

Research and development summaries are given on reactor materials and components, reactor fuels, radioisotope and radiation applications, coated-particle fuels, and gas cooled reactors. (J.R.D.)

39092 (BNWL-SA-90) ELECTRON MICROSCOPE STUDIES OF SECOND PHASE PARTICLES IN DILUTE ALLOYS OF URANIUM. Mastel, B.; Bierlein, T. K.; Corey, C. L. (Battelle-Northwest, Richland, Wash. Pacific Northwest Lab.). Mar. 3, 1965. Contract AT (45-1)-1830. 11p. (CONF-650414-4). Dep.(mn); $1.00 (cy), 1(mn) CFSTI.

From 19th Metallographic Group Meeting, Oak Ridge, Tenn.

Transmission electron microscopy was successfully utilized to study particle size-density distributions in dilute alloys of uranium. The results of a quantitative metallographic procedure used for determining particle size-density distributions from transmission electron micrographs agree well with that derived from replica electron micrography. The increase in resolution inherent in transmission techniques permits inclusion of particles normally too small to be resolved by replica methods. (auth)

39093 (BNWL-SA-141) TUNGSTEN FIBER REINFORCED NICKEL COMPOSITES. Robinson, R. K.; Farnsworth, P. L. (Battelle-Northwest, Richland, Wash. Pacific Northwest Lab.). Mar. 15, 1965. Contract AT (45-1)-1830. 23p. (CONF-650419-2). Dep.(mn); $1.00 (cy), 1(mn) CFSTI.

From Meeting of Refractory Composites Working Group, Atlanta.

Composite plates containing ~10 vol % continuous, aligned W fibers in pure Ni matrices were prepared by pneumatic impaction. Good bonding and high densities were obtained, and the fibers were straight and randomly distributed in the composites. The yield strength and ultimate tensile strength were increased significantly. At 1050°C but not at room temperature, fractures in the W fibers propagate through the Ni. Small additions (~1 vol % of chopped W fibers) did not affect the strength of pneumatically impacted Ni. (D.L.C.)

39094 (CONF-117(p.11-19) THE PREPARATION AND PROPERTIES OF PARTICULATE OXIDE FUELS. Latta, R. E.; Browne, C. C. (General Electric Co., Cincinnati, Ohio. Nuclear Materials and Propulsion Operation).

Uranium dioxide is dimensionally unstable in oxidizing atmospheres at elevated temperatures, but it can be partially stabilized against oxidation by the addition of certain other oxides such as La_2O_3 or Y_2O_3. Solid solution powders of UO_2 with Y_2O_3 or with Y_2O_3 and ZrO_2 were prepared and spheroidized in a direct current plasma flame. Some fractional volatilization of UO_2 occurred during spheroidization, and starting compositions were adjusted to compensate for this fuel loss. X-ray examination of the fuel spheres indicated a single phase face-centered-cubic material. Potential applications of spherical oxide fuels are discussed. (auth)

39095 (CONF-117(p.81-97) THE PREPARATION AND PROCESSING OF FUEL FOR FISSIOCHEMICAL REACTORS. Pearson, R. L. (Aerojet-General Nucleonics, San Ramon, Calif.).

Preparation of a UO_2-liquid ammonia slurry for fissiochemical production of hydrazine is described. Because spherical or spheroid UO_2 particles of less than 3 microns are not commercially available, a ceramic grade UO_2 powder of 1 micron or less particle size was used. The powder was fired at 1300°C in hydrogen to strengthen the particles and slurried in liquid ammonia. This slurry caused no unacceptable erosion in out-of-pile tests. Irradiation of the slurry increased the range of particle size. Little change was observed in the shape of most solids although some crystals were observed. The slurry described will be tested in the MTR core; fission production distribution and rate of crystal growth will be determined. (auth)

39096 (CONF-117(p.103-26) PREPARATION AND PROPERTIES OF SPHERICAL PARTICULATE NUCLEAR FUELS FOR PLUTONIUM-FUELED REACTORS. Atkins, R. J.; Benson, E. M.; Caldwell, C. S.; Swain, R. S.; Zambernard, M. J. (Nuclear Materials and Equipment Corp., Apollo, Pa.).

Plutonium-based nuclear fuels in spherical particle form offer unique features in terms of fabrication, utilization, and spent fuel recovery. These features are discussed. The applications cover a broad range of reactor types such as thermal and epithermal converters, fast breeders and thermal burner reactors; therefore a wide spectrum of plutonium-based materials in varying compositions is of interest. Methods of preparation and spheroidization of plutonium and plutonium-uranium oxides are reported. Methods for the application of metallic coatings to the particles and the fabrication of suitable fuel by various consolidation techniques are also compared. Factors controlling compatibility of coatings and matrix materials with the substrate particles are discussed. (auth)

39097 (GEMP-346) EVALUATION OF THE ZIRCALOYS FOR USE IN THE 630A REACTOR. Betts, R. K. (General Electric Co., Cincinnati, Ohio. Nuclear Materials and Propulsion Operation). Feb. 26, 1965. Contract AT (40-1)-2847. 78p. Dep. mn; CFSTI, $3.00 cy, $0.75 mn.

Zircaloy-2 and -4 were evaluated through a literature survey to determine their suitability for use in the 630A Mark V-A and -B cores. On the basis of existing technology, they possess essentially equivalent, adequate mechanical properties and corrosion resistance for the conditions of interest. Either alloy appears suitable for the proposed application. There may be sufficient data already available to petition for ASME Boiler and Pressure Vessel Code approval of Zircaloy-2. Zircaloy-4, being the newer alloy, has not been used as widely nor evaluated as extensively. (auth)

39098 (INR-567/II/PS) THE USE OF DIRECTIONAL FREEZING OF THE MELT FOR BISMUTH LARGE SINGLE CRYSTALS PREPARATION. Bednarski, S. (Institute of Nuclear Research, Warsaw (Poland)). Dec. 1964. 10p. Dep.

Directional freezing of melted metal was used for the preparation of large single crystals of bismuth. The diameter of cylindrical crystals obtained by this technique is 75 mm and the length 180 mm; the average mosaic spread is about 10 minutes of arc. The described technique may be applicable to single crystal growth of some other materials which increase their volume during the solidification process. (auth)

39099 (MCW-1492, pp 7-11) ELECTROLYTIC PREPARATION OF URANIUM METAL FROM URANIUM DIOXIDE USING A FROZEN-CRUST CELL. Piper, R. D. (Mallinckrodt Chemical Works, Weldon Spring, Mo. Uranium Div.).

Use of a frozen crust of electrolyte on the walls of the cathode crucible permitted production of U metal from UO_2 at greater than 65% current efficiency in laboratory cells. Careful control of the composition of the CaF_2-LiF-UF_4 electrolyte, a low current density, and a steep temperature gradient are necessary to obtain satisfactory results. (auth)

39100 (SGAE-CH-16/1965) UNTERSUCHUNGEN UBER DIE ELEKTROLYTISCHE URANABSCHEIDUNG AUF METALLEN. (Study on Uranium Electrolytic Deposition on Metal). Pfeifer, V.; Bildstein, H. (Oesterreichische Studiengesellschaft fuer Atomenergie G.m.b.H., Seibersdorf. Institut fuer Chemie). 1965. 11p. Dep. (mn).

The use of ammonium fluoride as the electrolyte in the preparation of uranium films on steel, Al, and other metals was described for the first time. The investigation shows the dependence of the uranium deposition on the electrolyte concentration, the acidity, and the volume. The time expenditure depends on the ammonium fluoride concentration but can be strongly reduced by stirring with the anode. The deposition of the uranium is quantitative up to layer thicknesses of approximately 0.5 mg U/cm^2; therefore preparations can be prepared up to 1 mg U/cm^2 on a 6 cm^2 surface. (tr-auth)

39101 (TID-3315) NUCLEAR MATERIALS MANAGEMENT. An Annotated Bibliography of Selected Literature. Davis, Theodore, F. (Division of Technical Information Extension (AEC), Oak Ridge, Tenn.); Lovett, James E. (comps.) (Division of Nuclear Materials Management (AEC), Washington, D. C.). Aug. 1965. 156p. Dep. mn; CFSTI, $5.00 cy, $1.00 mn.

A total of 845 selected references to unclassified reports and published literature is presented covering all phases of activity in the field of nuclear materials management. An appendix detailing the scope of the field and Personal Author, Report Number and Availability, and Subject Indexes are included. (auth)

39102 (UCRL-13100) INVESTIGATION OF CHEMICAL VAPOR DEPOSITION OF BERYLLIUM FROM ORGANOBERYLLIUM COMPOUNDS. Final Report, June 1963-January 1964. Wood, J. M.; Chidester, J. B.; Dyble, E. (Ethyl Corp., Baton Rouge, La. Research and Development Dept.). Contract W-7405-eng-48. 21p. Dep. mn; CFSTI, $1.00 cy, $0.50 mn.

For Lawrence Radiation Lab., Univ. of California, [Berkeley].

The vapor deposition of beryllium metal by pyrolysis of vaporous di-t-butylberyllium was studied. The effects of the more critical plating parameters, such as temperature, pressure, and flow rate on the properties and purity of the deposit were determined. It was shown that a dense, continuous, adherent deposit can be produced from di-t-butylberyllium. Best results were obtained at a substrate temperature of 280-305° at pressures of 1 torr or less. At higher pressures, bubbles form in the deposit, while at temperatures above the preferred temperature the beryllium is deposited as a powder rather than as a coherent coating. Plating rates of 1 mil per hour and plating efficiencies of 35% per pass were achieved. The unreacted plating compound can be recovered with high efficiency and can be recycled. The coating is metallic gray in color, hard, and brittle, but not completely devoid of ductility. It is superficially smooth at thicknesses up to 1 mil, but nodules can be seen at thicknesses of 2-10 mils. The coating is highly oriented, with the z axis of the hexagonal crystal perpendicular to the substrate surface. Chemical analysis of deposits obtained under the preferred conditions indicate a minimum purity of 95 mole % beryllium metal, or 97 wt % beryllium. Principal impurities are beryllium carbide and hydride, and appear to be uniformly distributed throughout the deposit. The quality of the coating is equal to, if not better than, that produced by electrodeposition from organic media. (auth)

39103 INVESTIGATION OF THE OXYGEN ADSORPTION ON POLYCRYSTALLINE TUNGSTEN AND RHENIUM BY SURFACE IONIZATION OF COPPER AND SILVER. Weiershausen, Walter (Universitat, Marburg, Ger.). Ann. Physik (7), 15: 150-61(1965). (In German).

The adsorption of oxygen on W and Re was investigated using the ionization of Cu and Ag. It was found that through the adsorbed oxygen the work of emission from W is increased by a maxiumum of 1.85 ev and from Re by a maximum of 1.75 ev, probably in the formation of a monolayer. With a statistical model, an adsorption equation for the chemosorption of the oxygen was derived, which under certain neglects is transformed into the Langmuir adsorption equation. The oxygen adsorption can not be satisfactorily described with such an equation since the adsorption energy Q is not constant. Good agreement between experiment and theory was obtained with an approximation equation in which several Langmuir adsorption equations are superposed with different adsorption energies. Oxygen was adsorbed on poly-crystalline W with at least two discrete values of Q, which corresponds to two different adsorption stages of about 3.3 and 4.8 ev. In Re the adsorption energy assumes continuously all values up to 4 ev. From measurements of the input time of the adsorption equilibrium, it was concluded that the activation energy of the adsorption of oxygen on W is about 0.4 ev. (tr-auth)

39104 PRODUCTION OF NUCLEAR FUELS. PART 2. ENRICHED URANIUM. Ploeger, F.; Vietzke, H. (Nuklear-Chemie und -Metallurgie GmbH, Wolfgang, Ger.). Chem.-Ingr.-Tech., 37: 692-9(July 1965). (In German).

The uranium 235 isotope can be concentrated in the form of gaseous uranium hexafluoride either by the Calutron process, by the diffusion method with Al_2O_3 membranes, or by means of gas-centrifuges and separating nozzles. The hexafluoride is then converted either to uranium dioxide or the metal for use in nuclear reactors. (auth)

39105 THE NUCLEAR METALS: URANIUM. Mining Ann. Rev., 58-9(May 1965).

Production, exploration, reserves, and demands for uranium in 1964 are reviewed. There were no new discoveries of major U reserves during 1964. However, there were slight increases of reserves in Spain and India. It is expected that the production of U in the western world will decline from about 27,000 short tons U_3O_8 per year to about 14,000 tons annually by 1970. In the United States, production of U in 1964 amounted to 11,847 short tons, a fall of 2371 tons from the previous year. The decline was mainly due to the AEC delivery stretch-out program. In Canada, production of U_3O_8 during 1964 was estimated at 8093 short tons, of which 1801 tons U_3O_8 was delivered to the USAEC, 4292 tons to UKAEA, and 2000 tons were added to the Canadian Government stockpile. At the end of 1964 there were only three operating mines in Canada. In South Africa, production of U concentrates, as a by-product from gold operations, during 1964 was estimated at 4267 short tons. During the year three of the U mills were scheduled to close and eight mills were still in operation. Several producers in South Africa began research into the production of refined U of nuclear purity from ion exchange eluates, and a pilot plant was installed. In Australia 225 tons were produced and added to the stockpile. French output remained at about 2000 short tons U_3O_8, and reserves were reported to be sufficient to maintain this production rate for another 30 yr. Portugal continued to produce between 50 and 75 tons U_3O_8 per yr from the Urgeirica deposits, and Spanish production was about 75 tons. Present and estimated future demands for U are out-

lined. It was concluded, that the demand for U in the future is almost certain to rise very rapidly. (BBB)

39106 THE NUCLEAR METALS: CAESIUM AND RUBIDIUM. Mining Ann. Rev., 59-61(May 1965).

The production, applications, and demands for Cs and Rb are reviewed. Cs and Rb are extracted chiefly from pollucite, supplies of which come mainly from Bikita in Southern Rhodesia. However, reserves estimated at 300,000 tons of ore grading better than 20% Cs are being developed at Bernic Lake, Manitoba. Attention is being given to the recovery of pollucite from pegmatite ores from in the U. S. Cesium is regarded as the ideal fuel for ion engines. Cesium ion rockets eject a stream of charged particles to propel space vehicles at speeds as high as 100,000 mph. Their low fuel consumption makes possible space flights of up to 5 yr with greatly increased payload capability. The development of thermionic power conversion is also directing attention to Cs. Considerable research is being undertaken on magnetohydrodynamics, using a hot plasma gas seeded with Cs for making electricity by thermionic techniques. Cesium salts have minor applications in the production of vacuum tubes, photomultiplier tubes, and scintillation counters. Rubidium has possible uses in space exploration such as a heat-transfer fluid in such equipment as rockets and space ship generators. Rubidium compounds are employed in microchemical work and have certain medicinal uses. Some research and development is being done on their application in catalysis, photography, and electric batteries. Cesium (99+% purity) is quoted in the U. S. at $100 to $375 and Rb at $390 to $425. (BBB)

39107 THE NUCLEAR METALS: BERYLLIUM. Mining Ann. Rev., 61-2(May 1965).

Mining and exploration, extracting and smelting, production, and applications of Be are reviewed. Estimates for 1964 point to a world beryl production of 5000 short tons compared with 7400 tons in 1963. World reserves of ore were estimated to be about 6 million tons of high grade ore and another 4 million tons of low grade ore. This is equivalent to 800 million lb of metallic Be. The surveyed reserves of ore within the U. S. itself are at least 420,000 tons. A pilot plant to refine Be is to be established at Anaconda, Montana. The nature of the processes to be used is discussed. The ore is leached with H_2SO_4 and the leach liquor after suitable treatment is submitted to solvent extraction by di-2-ethylhexyl phosphoric acid (EHPA) followed by conversion of the Be-bearing EHPA to $Be(OH)_2$ and then calcination to BeO. About 82% recovery is claimed and the final BeO product is 98 to 99% pure. Production of Be-Cu alloys continued at a high level. A powdered Be-Cu alloy was developed for sintering to component shape. An experimental reactor is being built in the U. S. using a BeO moderator. As a moderator it is being contemplated for use in Germany in a high-temperature gas-cooled reactor to be coupled to a gas turbine for ship propulsion. (BBB)

39108 THE NUCLEAR METALS: ZIRCONIUM AND HAFNIUM. Lloyd-Jacob, David. Mining Ann. Rev., 62-3 (May 1965).

Production and uses of hafnium and zirconium are reviewed. The bulk of the free world's zircon is produced in Australia as a by-product of rutile production. In 1964 Australian production rose only slightly, from 183,900 long tons in 1963 to 185,400. The production in the U. S., the only other major producing country, was estimated at 54,000 long tons in 1963 and 50,000 in 1964. In fuel cladding, several types of reactors use Zircaloy-2, but its cost may prove a limiting factor. Zirconium is also a constituent of one type of fuel pellet used in starting up a new reactor. The cost and limited availability of zircon in the past year stimulated the use of substitutes and particularly of chromite sand in foundries. Certain grades of Zr metal are required to be Hf-free. Hafnium produced as a by-product of this operation was adequate to supply the demand for this metal. In the U. S. hafnium oxide is used in the control rods of nuclear reactors. Research program were carried out on Hf, particularly on the production of high-purity Hf metal and on the complete separation of Hf from Zr. Hafnium's properties as a neutron absorber may outweigh the cost and difficulty of separation and the attendant high price of $138 lb. (BBB)

39109 FUSION BY ELECTRON BOMBARDMENT AND ITS APPLICATION IN METALLURGY. Lehr, Pierre; Albert, Philippe (Centre d'Etudes de Chimie Metallurgique, Vitry-sur-Seine, France). Rev. Hautes Temp. Refractaires, 2: 31-46(Jan.-Mar. 1965). (In French)

The technology of an electron-bombardment furnace is outlined. It is shown that the process permits a significant and rapid purification of a metal by vacuum distillation of a great number of impurities either as elements or compounds. The physicochemical basis of this purification is considered. Experimental results are presented on the refining of iron and steel and the purification of the refractory metals of group IV, zirconium and hafnium. (auth)

39110 BORON STAINLESS STEEL FUEL ELEMENT CLADDING IN THE INDIAN POINT REACTOR. Johnson, C. R. (Babcock and Wilcox Co., Lynchburg, Va.). 58p. (CONF-654-92). Gmelin, AED-CONF-64-219-110.

From American Nuclear Society Meeting, San Francisco, Nov.-Dec. 1964.

A slightly boronated (250 ppm, 0.025 wt%) stainless steel was developed and used as a burnable poison fuel cladding. A series of alloys was melted and examined for boron homogeneity and fabricability. Tubes of consistently high quality were fabricated from alloys containing up to 750 ppm boron. The material is extremely hot-short and care must be exercised during forging and welding operations to prevent microfissures and possible gross cracks. Cold reductions were used to reduce the material to the final fuel cladding dimensions. Some boron was lost during intermediate and final heat treatments of the alloy as it was cold reduced. Vacuum and carefully dried argon atmospheres in the heat treating furnaces were found to minimize this depletion of boron; dry hydrogen was not satisfactory. Boron depletion became a significant factor only when the material approached the finish size where section thickness was minimal. A development program established a suitable welding technique and a weld joint design to overcome the inherent hot shortness of the material. Mechanical properties of all the experimental heats of boron steel were determined. Tensile properties of the boron-modified steels were independent of boron concentration (up to a boron content of 0.075%) and were essentially the same as those of unmodified type-304 stainless steel. The corrosion resistance of two experimental heats of boron stainless steel to borated high purity water at 600°F was determined. Results showed that the corrosion resistance of type-304 steel is not affected by additions of up to 0.05% boron. It was determined that irradiation had a slightly greater effect on the mechanical properties of the boron steel than on those of the unmodified steel. The ultimate tensile strength and the yield strength of the boron steels were increased in proportion to boron content. Total elongation of the tensile specimens was reduced by irradiation; boron concentration does not influence total elongation changes. Irradiation had no quantitative effect on the corrosion resistance of either the modified or unmodified type-304 stainless steel. There was no evidence of stress corrosion. (W.L.G.)

39111 FIELD-AIDED ELECTRON-BEAM ZONE REFINING OF TUNGSTEN. Hay, D. R.; Scala, E. (Cornell Univ., Ithaca, N. Y.). pp 550-66 of First International Conference on Electron and Ion Beam Science and Technology. New York, John Wiley and Sons, Inc., 1965.

The effect of field freezing on the efficiency of zone refining was studied in a commercially pure, unalloyed tungsten. The purity level of the zone-melted tungsten was examined as a function of the polarity and intensity of the applied field using the relative resistivity ratio as a measure of purity. It is shown that significant increases in zone-refining efficiency can be achieved through field freezing and that higher levels of purity are produced. The experimental results also demonstrate that both the zone re-

fining action and the purification by vacuum distillation play important roles in high melting-point systems. With field freezing superimposed, a higher rate of purification may be obtained than with conventional zone refining along with the potential for higher purities. (A.G.W.)

39112 EXPANDED PYROLYTIC GRAPHITE AND PROCESS FOR PRODUCING THE SAME. (to High Temperature Materials, Inc.). British Patent 991,581. May 12, 1965. Priority date Mar. 21, 1962, United States.

A process is reported for producing a pyrolytic graphite that has been expanded in the "c" direction in an amount of from 2 to 125 times the original dimension. The ratio of the number of crystallites in the graphite not having basal planes parallel to the deposition surface to the number of crystallites not having basal planes parallel to the deposition surface is from 100:1 to 1000:1. The graphite is subjected to a heat treatment at a temperature between 2500° and 3600°C for a time from 1 to 5 hours before being expanded. The process of expanding the graphite includes introducing between the layers of parallel carbon networks of the pyrolytic graphite an expanding agent, such as water or an organic or inorganic blowing agent. The expanding agent is then activated by heating and/or initiating a chemical reaction to generate an expanding gas in situ until the graphite has been expanded to the desired amount. (B.L.M.)

39113 BELL FURNACE FOR THE PREPARATION OF URANIUM METAL BY MAGNESIOTHERMIC REDUCTION. Delange, Maurice; Sauteron, Jean; Vertes, Paul (to Commissariat a l'Energie Atomique). British Patent 996,816. June 30, 1965. Priority date July 6, 1962, France.

A bell furnace for the production of uranium by the magnesiothermic reduction comprises a fixed supporting base constructed of refractory material, a crucible containing the reaction mixture mounted on a system designed to be adjusted for height, and a removable bell covering for the crucible. The cover rests on the crucible in a leak-tight manner. The bell is provided with heating elements and safety devices that prevent the start of the reaction until the bell is in position on the fixed base. The heating elements are made up of electric resistances mounted in the interior of the bell and divided into three groups that are located one above the other to provide three separate heating sources controlled by means of a set of electric cables and contactors grouped together on one of the external side walls of the bell. The adjustable system that predetermines the position of the crucible in the interior of the bell is composed of a movable support supported by jacks. A sand packing is provided in the base, and an annular portion of the bell penetrates into the packing to form the leak-tight joint between the fixed base and the removable bell. (B.L.M.)

39114 METHOD OF REINFORCING GRAPHITE ARTICLES BY DEPOSITING FUSED METALS. (to Nihon Genshiryoku Kenkyusho). British Patent 996,859. June 30, 1965. Priority date June 16, 1961, Japan.

A method of reinforcing a graphite article consists of depositing a fused metal or alloy in bold relief by electric arc along one or more lines extending around the article to adhere tightly to the surface of the article. The metal or alloy is deposited in such a manner as to leave the graphite exposed on either side of the lines or between the lines. The alloy consists substantially of Fe alloyed with 5 to 50% Ni, 0 to 40% Cr, 0 to 4% Mo, and <2% C. The wire or powder of the metal or alloy is attached or filled on the outer surface of the article and heated to a temperature of 1200 to 1600°C in an inert atmosphere. (B.L.M.)

Corrosion

Refer also to abstracts 39234 and 40195.

39115 (GEAP-4760) GENERAL CORROSION OF MATERIALS FOR NUCLEAR SUPERHEAT APPLICATIONS. Pearl, W. L.; Brush, E. G.; Gaul, G. G.; Wozadlo, G. P. (General Electric Co., San Jose, Calif. Vallecitos Atomic Lab). Mar. 1965. Contract AT(04-3)-189. 123p. Dep. mn; CFSTI $4.00 cy, $0.75 mn.

The general corrosion properties of several commercially available materials were investigated for application as fuel cladding in superheat reactor systems. The materials were corrosion tested under heat-transfer conditions at metal temperatures to 1410°F and isothermally at 1050 and 1150°F. The oxygen and hydrogen content of the steam was controlled to simulate those found in boiling water reactor systems. Each datum point obtained under heat-transfer conditions represented an integrated corrosion response over a temperature gradient along the length of the electrically heated test specimen. An analytical model was developed by which these data may be treated to yield corrosion behavior at a given, specific temperature. The model is used to extrapolate the corrosion behavior of Incoloy-800 as fuel cladding. For a three-year exposure at a metal temperature of 1300°F, Incoloy-800 was calculated to have a maximum corrosion of 0.0022 inch. The heat transfer corrosion data available for Incoloy-800, Incoloy-825, Inconel-600, Hastelloy-X and several Type-300 stainless steels are updated and summarized. Results are reported for a 10,000-hour study of several nickel and stainless steel alloys that were exposed isothermally to 1050 and 1150°F superheated steam. Hastelloy-X, Incoloy-825, Inconel-625, and Incoloy-800 had low initial and long-time linear corrosion rates and formed good protective and tenacious oxides up to 1150°F. Type-406 stainless steel had a high initial but low long-time linear corrosion rate and formed a protective and tenacious oxide up to 1150°F. Inconel-600 had adequate corrosion resistance to 1050°F but formed a nonprotective oxide film with a significant portion lost to the system at 1150°F. Type-304 stainless steel had a significant corrosion rate at 1050 and 1150°F but formed a relatively tenacious oxide at both temperatures that eventually reached a limiting thickness with subsequent spalling. (auth)

39116 (NP-15263) ULTRASONIC-INDUCED CAVITATION STUDIES IN LEAD–BISMUTH ALLOY AT ELEVATED TEMPERATURES. Technical Report No. 2. Garcia, R.; Hammitt, F. G. (Michigan Univ., Ann Arbor. Lab. for Fluid Flow and Heat Transport Phenomena). June 1965. 71p.

Cavitation studies were conducted in 70% lead–30% bismuth alloy at 500 and at 1500°F with a vibratory device utilizing a piezoelectric crystal transducer unit. Test specimens of various materials were attached to the ultrasonic transducer and vibrated at a frequency of ~18 kc/sec with a double amplitude of ~2 mils. The test materials were 304 stainless steel, 316 stainless steel, T-111 (Ta–8W–2Hf), T-222(A) (Ta–9.5W–2.5 Hf–.05C), Mo–½Ti, Nb–1Zr, and Nb–1Zr(A). The results obtained at 500°F indicate that the refractory alloys T-111 and T-222(A) are the most resistant to cavitation on the basis of mean depth of penetration (MDP). However, the Mo–½Ti, 316 stainless steel, and 304 stainless steel are all nearly as cavitation resistant. The Nb–1Zr and Nb–1Zr(A) were the least resistant to cavitation damage, being damaged quite severely. At 1500°F, both the T-111 and T-222(A) appear to be the most cavitation resistant. Very little damage was sustained by these materials in the tests conducted. Ranking behind the Ta alloys at 1500°F are the Mo–½Ti, Nb–1Zr, and 316 stainless steel. The Nb–1Zr(A) and the 304 stainless steel are the least cavitation resistant at this temperature. It was found for all the materials tested that the cavitation damage at 1500°F was greater than the damage at 500°F, based on the average MDP rate. A preliminary attempt was made to correlate the cavitation data obtained at 500 and 1500°F with the complete mechanical properties data that are available for the 7 specimens tested at the test temperatures. It was found that the rating of the materials based on a combination of the ultimate tensile strength, 0.2% yield strength, hardness, and strain energy agrees almost exactly with the ratings based on the cavitation data, whereas ranking according to hardness does so agree. None of the other properties taken singly are successful in this regard. A more precise correlation of the cavitation data with the mechanical properties data was achieved by utilizing the IBM 7090 computer and a least mean squares regression analysis (first-order inter-

action). When one assumes that the tensile strength (TS), yield strength (YS), strain energy (SE), and hardness (H) are the applicable mechanical properties, the predicting equation is of the form: Average MDP Rate = $K_1 + K_2 (SE)^{-2} + K_3 (SE)^{-3} + K_4 (SE)^{-1} + K_5 (H)^{-2}$, with a coefficient of determination of 0.99. When the % elongation (ELON) and the % reduction in area (RA) are introduced as additional correlating parameters, the predicting equation takes the form: Average MDP Rate = $K_1 + K_2 (RA)^{-3} + K_3 (SE)^{-2} + K_4 (YS)^{-3}$, with a coefficient of determination of 0.99, showing that the combination of strength and ductility to some extent replaces strain energy. (D.L.C.)

39117 (ORNL-P-1430) ALUMINUM AND TITANIUM CORROSION IN SALINE WATERS AT ELEVATED TEMPERATURES. Bohlmann, E. G.; Posey, F. A. (Oak Ridge National Lab., Tenn.). [1965]. Contract W-7405-eng-26. 47p. (CONF-651005-1). Dep. mn; CFSTI, $2.00 cy, $0.50 mn.

For Presentation at 1st International Symposium on Water Desalination, Washington, D. C.

Studies were conducted on the electrochemical corrosion of aluminum alloys 5454 and 6061 in 1 M NaCl at 150°C. Corrosion rates were followed with time by measurement of the polarization resistance of the specimens. The results show that the 5454 alloy is superior to the 6061 alloy under all conditions studied. Polarization curves of the alloys were measured under a variety of conditions in order to determine the nature of the difference in corrosion properties. The corrosion of nine titanium alloys in 1 and 2 M NaCl at 100 to 200°C was severe and very erratic. Only the Ti – 0.15 Pd alloy showed resistance to corrosion and it was not immune. (W.L.G.)

39118 (SC-DC-65-1520) DISPERSAL OF REACTOR CORE MATERIALS BY REENTRY PROCESSES. Quarterly Report. Beal, J. L.; Brown, W. R.; Pleuthner, R. L. (Cornell Aeronautical Lab., Inc., Buffalo, N. Y.). Apr. 1965. Contract AT(29-1)-789. 45p. Dep. mn; CFSTI, $2.00 cy, $0.50 mn.

For Sandia Corp., Albuquerque, N. Mex.

Zr rods were tested under simulated reentry conditions. Melting phenomena were observed and debris from rapidly ablating rods was collected. Temperature rise rates of the rods were determined by several methods and compared with rates calculated for different intensities of oxidation heating. Based on the tests, a method for computing the oxidation heating effect is suggested. (auth)

39119 THE KINETICS OF OXIDATION OF CARBON AND GRAPHITE BY OXYGEN AT 500 deg–600 deg. Gregg, S. J.; Tyson, R. F. S. (Univ. of Exeter, Eng.). Carbon, 3: 39-42(July 1965).

A linear Arrhenius plot was obtained for the oxidation of a sample of carbon in oxygen at 7.6 cm Hg pressure, using the Gulbransen microbalance and adopting a continuous technique. After an initial outgassing in situ at 1000°C, the sample was held in succession at each of a series of fixed temperatures in the range from 490 to 550°C till a constant rate of loss of weight (r) was obtained. The energy of activation E for the oxidation was calculated from the plot of log r against 1/T. The method was applied to carbons prepared by calcining the starting material (a mixture of ground petroleum coke and pitch, heated for four hr at 600°C) for a fixed time at a series of fixed temperatures between 1000 and 3000°C. The value of E, which varied according to the temperature of heat treatment, was 44 kcal $mole^{-1}$ for the most fully graphitized sample, viz that prepared at 3000°C. (auth)

39120 THE OXIDATION OF ORIENTED THIN LAYERS OF ZIRCONIUM. Denoux, Michel (C.N.R.S., Bellevue, France). Compt. Rend., 260: 5003-5(May 10, 1965). (In French).

Studies of the oxidation, in air and oxygen under reduced pressure, of oriented thin layers of zirconium made it possible to define the structural evolution of the oxide as a function of the temperature. The relations of epitaxie cubic oxide–metal and monoclinic oxide–cubic oxide were described. An interpretation of the results is presented based on the established crystallographic relations. (tr-auth)

39121 STUDY ON THE BEHAVIOR OF PUNCTURED FUEL ELEMENT FOR CALDER HALL TYPE REACTOR. 5. OXIDATION OF URANIUM BY PARTIALLY DECOMPOSED CARBON DIOXIDE. Taketani, Kiyoaki; Ikawa, Katsuichi (Japan Atomic Energy Research Inst., Tokyo). J. Nucl. Sci. Technol. (Tokyo), 2: 241-4(July 1965).

The oxidation rate of U rods by partially decomposed CO_2 was measured thermogravimetrically and compared with that by undecomposed CO_2, in an attempt to study the effect of ionizing radiation on the compatibility of U with CO_2. The decomposition was by silent discharge. Measurement was performed for cases of 0.29, 0.44, and 0.68% decomposed CO_2, at 500 and 600°C. It was found that the oxidation rate rises almost linearly with increasing percentage of decomposition of the CO_2. At 500°C the oxidation rate with 0.68% decomposed CO_2 was eighteen times higher than with undecomposed CO_2, and five times higher at 600°C. Such increase was related to O_2 content in the decomposed gas. (auth)

39122 ELECTROCHEMICAL CORROSION OF MOLYBDENUM IN MOLTEN CHLORIDE. Smirnov, M. V.; Ryzhik, O. A.; Savochkin, Y. P. (Ural Polytechnic Inst., USSR). Zashchita Metal., 1: 335-7(May-June 1965). (In Russian)

The stationary potentials of Mo relative to a chloride comparison electrode was measured in molten Po chloride at 790 to 920°C. On the basis of the experimental data the speed of corrosion of Mo in pure fused KCl was evaluated. The expression for the equilibrium constants of the interactions of metallic Mo with the salts of melts containing titanium tetrachloride was also obtained. (tr-auth)

39123 HIGH TEMPERATURE OXIDATION RESISTANT HAFNIUM–TANTALUM ALLOYS. Marnoch, K. (Marquardt Corp., Van Nuys, Calif.). 23p. (CONF-650203-9). Gmelin, AED-CONF-65-005-8.

From National American Inst. of Mechanical Engineers Meeting, Chicago.

A hafnium–tantalum alloy system was developed that has oxidation resistance at temperatures in excess of 4000°F. The exceptional oxidation resistance of the alloy is due to the parabolic growth of a stabilized hafnium oxide. The adherence of the oxide film is enhanced by the formation of tantalum-rich stringers normal to the oxide-metal interface. These characteristics provide an oxidation film that exhibits high density, impact resistance, and freedom from breakaway failure modes. In addition to being highly oxidation resistant, the alloy exhibits room temperature ductility and may be formed using techniques similar to those used for the refractory metals. The alloy may also be applied as a coating on refractory substrates by a variety of techniques, including plasma arc spraying, vapor deposition, and roll cladding. (auth)

Fabrication

Refer also to abstract 40125.

39124 (ANL-6995) THE MANUFACTURE OF GLASS-BONDED FUELS FOR DOPPLER COEFFICIENT MEASUREMENT. Ayer, J. E.; Hins, A. G.; White, D. E.; Carpenter, D. C.; Konicek, C. F. (Argonne National Lab., Ill.). Mar. 1965. Contract W-31-109-eng-38. 51p. Dep. mn; CFSTI, $2.00 cy, $0.50 mn.

A description is given of procedures used to manufacture and assemble glass-bonded, plutonium-containing fuels for Doppler coefficient measurement. Seventeen acceptable fuel rods containing $(U-Pu)O_2$ or PuO_2 pellets were made. The pellets, which were required to have low (about 70% theoretical) density, were held together by a silicate bond. The pellets were made by milling the oxide; compacting, granulating, and sintering the milled product; pressing pellets from "fired" granules treated with Na_2SiO_3; and sintering the pellets. The pellets were loaded into capsules, the capsules were decontaminated, welded closed, leak tested at

room temperature and at 1000°C, and radiographed. The acceptable fuel rods were shipped to the ANL Idaho Division for the determination of Doppler coefficient in ZPR-III. (auth)

39125 (BNWL-91) CERAMICS RESEARCH AND DEVELOPMENT QUARTERLY REPORT, JANUARY-MARCH 1965. (Battelle-Northwest, Richland, Wash. Pacific Northwest Lab.). Contract AT(45-1)-1830. 125p. Dep. mn; $4.00 cy, $1.00 mn.

Studies showed that PuO_2–62 wt% (80 Ni/20 Cr) cermets can be diffusion bonded to 80 Ni/20 Cr foil by pneumatic impaction at 1093°C and 17,000 atm. Calibration of the thermobalance system and associated apparatus was carried out, using CeO_2 and UO_2. Electron microscopic examination of replicas showed PuO_2 to be distributed throughout ballmilled and impacted UO_2–20 wt% PuO_2 fuel. A sample holder for hot stage reflection microscopy allows a full 30° specimen tilt. A device for measuring the thermionic work function of Pu compounds was assembled. Calibration runs are in progress on a differential thermal analysis (DTA) apparatus capable of operations to 1700°C. Measurements of the electrical conductivity of single crystal UO_2 were obtained to 1650°C. Comparisons of cathodic and chemical etching behavior on sintered and arc fused UO_2 reveal more rounded pits near grain boundaries in cathodically etched specimens and greater intraparticle detail and intergranular contrast in chemical etched specimens. Microspheres of PuO_2 are being fabricated as part of a program to determine the best size and shape of PuO_2 particles for use in cermets. An instrument was developed for determining pour and tap densities of impacted and crushed mixed oxide particles. Studies show that pneumatically impacted UO_2-PuO_2 is not materially degraded by controlling the O/U ratio of the feed material with U_3O_8 having a high off-gas content. A program is under way to determine the effects of pneumatic temperature, particle size, and particle shape on the density and mechanical properties of pneumatically impacted materials. About 3 kg of PuO_2 powder were purified, pneumatically impacted and characterized for use in basic studies. Post-irradiation examination of two capsules containing UN–20 wt% PuN is continuing. Increases in UO_2 melting point with low level irradiation (reported 4 yr ago) was not observed in sibling specimens remeasured after storage in air for 4 yr. A UO_2 fuel capsule was irradiated to test the hypothesis that once-molten UO_2 can solidify during continued irradiation because of improved thermal conductivity of the adjacent crystalline UO_2. Results indicate little change in the melt radius during 2 hr irradiation. UO_2–2% PuO pellets interspersed between natural UO_2 pellets were irradiated to obtain information of the amount and rate of PuO_2 dispersion into the natural UO_2. High and low density stainless steel–20 vol% PuO_2 cermets being irradiated in the MTR attained 1.6 to 3% burnup of the Pu. A thermocoupled short core PRTR fuel element was fabricated for irradiation. A vibrationally compacted UO_2–1 wt% PuO_2 PRTR fuel element failed after a burnup of 1.0×10^{20} fissions/cm^3 (3930 Mwd/tU). PRTR fuel loading includes seven UO_2–2.0% PuO_2 elements; the maximum burnup of ceramic fuel in PRTR as of March 31, 1965, is 2.28×10^{20} fissions/cm^3 (8059 Mwd/t). A UO_2–2 wt% PuO_2 PRTR fuel element containing salt cycle fuel was fabricated by remote handling techniques. General conclusions of initial tests to determine effects of process variables on Pu fuel elements are reported. EBWR fuel rod capsules were exposed to 4.8×10^{20} fissions/cm^3 (17,000 Mwd/t). Fifty-seven, full-size EBWR rods are under irradiation and of these, 21 have attained an exposure of 0.25×10^{20} fissions/cm^3 (860 Mwd/t). EBWR rods were fabricated for ANL with Al-Pu cores. Thirteen hundred EBWR fuel rods were repaired by welding new caps on suspect rods. Saxton fuel cladding testing was completed. Gas content of UO_2 was reduced by H_2 sintering to meet specifications for Saxton fuel. A PRTR fuel rod using Pu–15 wt% Zr alloy wire enrichment was fabricated. It was found that large (+60 mesh) PuO_2 particles formed by air burning Pu metal are suitable for incorporation in cermets. Pneumatic impaction was used to produce integrally clad and capped, stainless steel-UO_2 cermet pins with a cermet density >99% of theoretical. Stainless clad, stainless–20 wt% PuO_2 cermet fuel pins were fabricated. Metallographic observations and density measurements indicate low density stainless steel-UO_2 cermet billets produce extruded cermet pins comparable to pneumatically impacted high density cermet billets. (J.R.D.)

39126 (CONF-117(p.149-70)) PREPARATION AND EVALUATION OF CARBON-COATED FUEL PARTICLES. Browning, M. F.; Secrest, A. C.; Secrest, V. M.; Landrigan, R. B.; Blocher, J. M. Jr. (Battelle Memorial Inst., Columbus, Ohio).

The preparation, characterization, and performance of various types of pyrolytic carbon (PyC)-coated fuel particles are discussed. Most of the coatings studied have been deposited by pyrolysis of either methane or acetylene in a fluidized bed of the fuel particles at temperatures between 950 and 2000°C. However, the preparation of coatings by pyrolysis of other carbon compounds is also reported. Three types of coatings have been prepared: (1) monolithic–all PyC, (2) duplex–layers of porous and dense PyC, and (3) composite–layers of PyC and other materials. The out-of-pile characterization of these materials is presented along with a brief summary of their in-pile performance. All three types of coating have shown good out-of-pile integrity, but the duplex and composite coatings have given superior in-pile performance. The coating procedures are described, and process variables are correlated with deposition rate and coating properties. (auth)

39127 (NCSC–2981-9) A NUCLEAR FUEL CONSISTING OF VERY SMALL UNIFORMLY DISPERSED UC PARTICLES IN A URANIUM MATRIX. Final Report. Stoops, Robert F.; Haller, Mitchell W. (North Carolina State of the Univ. of North Carolina, Raleigh. Dept. of Engineering Research). Oct. 1964. Contract AT(40-1)-2981. 42p. (EURAEC–1412). Dep. mn; CFSTI, $2.00 cy, $0.50 mn.

Work Performed under United States–Euratom Joint Research and Development Program.

Procedures were developed for making cermets containing very small UC particles in a uranium matrix. Hot pressing mixtures of uranium hydride and carbon under carefully controlled conditions was by far the best forming method. Optimum results were obtained by hot pressing at temperatures between 1130 and 1200°C for three minutes or less with pressures of approximately 1000 psi. If longer times or higher temperatures were used, the UC particles became too large. If higher pressures were used, the liquid uranium was lost by extrusion between the punches and dies. Specimens were produced containing 30 to 55 vol % uranium and approximately 2×10^{11} particles/cc which is within the range thought necessary to inhibit swelling. However, the UC particles were not completely dispersed but were arrayed in a microscopic three dimensional network. This may reduce the effectiveness of the individual particles as fission gas nucleation sites, but this can best be determined by irradiation tests. Cursory evaluations indicate that the thermal conductivity, electric resistivity, oxidation resistance, and resistance to corrosion by boiling water of UC–uranium cermets are close to these properties of UC and uranium. A process was discovered by which refractory material powders can be formed into shapes with almost 100% of theoretical density by a modified hot pressing technique in which a low melting liquid phase surrounding the refractory material particles is removed by extrusion. This process has considerable potential for commercial application in the forming of materials such as UC and UN. (auth)

39128 (NMI–1267) FABRICATION OF SEAMLESS TUNGSTEN–25 w/o RHENIUM TUBING. Fundamental and Applied Research and Development in Metallurgy. Summary Technical Report, July 1, 1964–June 30, 1965. Isserow, S.; Friedman, G. I.; Jenkins, R. G.; Geary, A. L. (Nuclear Metals, Inc., West Concord, Mass.). July 15, 1965. Contract AT(30-1)-2784. 123p. Dep. mn; CFSTI $4.00 cy, $0.75 mn.

The development program was directed toward the

establishment of extrusion and drawing techniques for tungsten–25 wt % rhenium tubing in two sizes: 0.080-inch OD × 0.008-inch wall, and 0.250-inch OD × 0.020-inch wall. For each size, the primary extrusion is performed routinely. For the larger size, reliable techniques were developed and demonstrated for subjecting the extruded tubing to a series of moving-mandrel draws that iron the tubing to a reduction of about 30%. The successful application of moving-mandrel drawing and subsequent reeling for mandrel removal depends on the proper combination of mandrel material and working temperatures. In addition, the tubing must be properly conditioned by appropriate surface preparation and thermal treatment. For the smaller size, the proposed sequence is based on re-extrusion of the product of the primary extrusion. Although some apparently satisfactory tubing was obtained by re-extrusion, conditions for consistently obtaining sound tubing were not established. The billet for re-extrusion incorporates a removable core of calcium carbide within the inner molybdenum filler. This carbide core is removed chemically from the extruded tube by acid drilling. The re-extruded tubing (OD about 0.1-inch) can be drawn with or without the inner extrusion fillers. The continuing metallurgical evaluations include some routine checks at various stages of fabrication as well as tests intended to guide the selection of anneals introduced in fabrication sequences. (auth)

39129 (ORNL-TM-1116) COATED-PARTICLE FUELS DEVELOPMENT AT OAK RIDGE NATIONAL LABORATORY FOR PERIOD NOVEMBER 15, 1964 TO MAY 15, 1965. Harms, W. O.; Coobs, J. H. (comps.) (Oak Ridge National Lab., Tenn.). May 1965. Contract W-7405-eng-26. 102p. Dep. mn; CFSTI, $4.00 cy, $0.75 mn.

Development work on graphite-base fuels for gas-cooled reactors is summarized. Information is included on pyrolytic carbon coatings, testing of coated particles, properties and testing of pyrolytic carbon, coated graphite fuel particles, and irradiation testing. Research on processing of high-temperature gas-cooled reactor fuels is described. (J.R.D.)

39130 (RFP-507) A NUCLEAR MATERIALS MANAGEMENT CONTROL SYSTEM FOR URANIUM REACTOR FUEL ELEMENT FABRICATION (A HYPOTHETICAL CASE). Hazelton, L. D. (Rocky Flats Div., Dow Chemical Co., Golden, Calif.). [nd]. Contract AT(29-1)-1106. 59p. (CONF-650803-4). Dep.(mn); $3.00(cy), 2(mn) CFSTI.

From IAEA Symposium on Nuclear Materials Management, Vienna.

A method of collecting and disseminating a variety of data for effective Accountability, Production Control, and Process Control over materials and process operation found in a typical uranium fuel element fabricating facility is presented. The discussion and illustrations are focused on portions of the control system that are important in initiating a new system or when converting from electrical-accounting machine system to automatic data processing methods. Enough information is presented to provide guidelines to those interested in establishing a control system for the first time or in modernizing an already established system. (auth)

39131 JOINING TECHNIQUES FOR S.A.P.-CLAD NUCLEAR FUEL ELEMENTS. Hallam, R. C.; Burns, W. R. (Canadian General Electric Co., Ltd., Peterborough, Ont.). Can. Mining Met. Bull., 58: 332-7(Mar. 1965).

The proposed use of SAP materials, for nuclear fuel cladding presents a problem in the fabrication of fuel-element end closures. Conventional fusion welding processes cannot be used with SAP, since its gas content is easily liberated and, in addition, the aluminum oxide tends to coagulate thereby reducing the joint strength at elevated temperatures. A leak-tight, strong joint is mandatory with nuclear fuel, and the joining process must achieve a higher standard of consistency than that normally required in the commercial field. Two welding techniques were developed: pressure-diffusion bonding process and a resistance-welding process. Future fuels will have resistance-welded end closures, which will meet advanced design requirements and which will be economical. (auth)

39132 ON THE SINTERING BEHAVIOUR OF URANIUM. Hampe, E. (Zentralinstitut fuer Kernforschung, Rossendorf, Ger.). Kernenergie; 8: 291-7(May 1965). (In German).

The experimental results of uranium sintering studies obtained by various techniques of investigation in both the early and the late state of the sintering of loose powders and, for comparison, of compacts are described. By measuring the electric resistance and the linear shrinking, density measurements, and a modified bonding rupture test, the behavior of loose powders, made from uranium hydride, in vacuum sintering at 440 to 1100°C was investigated. Below 800°C, only bridge formation was observed. Mechanically solid bonding between the particles exists in the range above 600°C. The degree of bridge formation evidently is dependent on temperature of sintering only, but hardly on sintering time. Alpha–beta and beta–gamma transformations are disturbing to the sintering process. The compression of the samples only takes place in the range above 800°C. Obtaining densities of about 95% of uranium density is possible closely below the melting point. (auth)

39133 ON THE STUDY OF ELECTRIC ARC REDUCTION PROCESS FOR MAKING RAW METALLIC NIOBIUM. Kimoura, Kazo; Sasaki, Shistuo. Kinzoku Zairyo Gijutsu Kenkyusho Kenkyu Hokoku, 6: 112-18(1963). (In Japanese)

By means of an electric arc reduction process, raw metal containing 99% Nb was obtained from a mixture of Nb_2O_5 and NbC. Experimental results indicated that when the raw material mixing ratio Nb_2O_5/NbC = 35/65, the maximum niobium content of the reaction product was obtained. For a single melting, the applied pressure in the furnace was 1 atm, melting time 2 min, and current 250 amp. (F.J.H.)

39134 MANUFACTURE OF STAINLESS STEEL FUEL CANS FOR THE AGR. Cheadle, B. D. (H. M. Hobson Ltd., Wolverhampton, Eng.). Nucl. Eng., 10: 260-1(July 1965).

The manufacture of stainless steel fuel cans is discussed including testing and special problems. The dimensions and metallic composition of these fuel cans are given. The tangential form grinder for machining of the required form is explained and its performance described. The exhaustive tests are recounted in detail for inspection of the completed fuel can. Possible contamination by certain materials is also noted. (J.F.P.)

39135 PROCESSES FOR OBTAINING CONDUCTING AREAS ON THIN FILMS: APPLICATION IONIZATION CHAMBERS. Measday, D. F. (Harvard Univ., Cambridge, Mass.). Rev. Sci. Instr., 36: 1263-4(Aug. 1965).

To monitor a neutron beam produced by protons on a liquid deuterium target, it was decided to measure the number of protons striking the target in a position where the neutrons produced could travel down the collimator. An ionization chamber with plates of the same shape as the collimator was built. Plates were prepared by two methods. One involved the etching of aluminized Mylar; in the other method, the conducting plane was printed on Mylar by a silk-screen process using silver paint. (D.C.W.)

39136 MICROMACHINING BY SPUTTERING THROUGH A MASK OF CONTAMINATION LAID DOWN BY AN ELECTRON BEAM. Broers, A. N. (Cambridge Univ., Eng.). pp 191-204 of First International Conference on Electron and Ion Beam Science and Technology. New York, John Wiley and Sons, Inc., 1965.

Experiments on sputtering through a mask of contamination (hydrocarbon vapors polymerized by electron-beam impact) were carried out in the specimen chamber of a high-resolution scanning electron microscope. The probe of the microscope was used to lay down the contamination, and the microscope itself was used to follow the machining process. Photographs show results of studies on gold, copper, and tungsten. The technique was shown to be readily applicable to machining on a microscopic scale, though accuracy was limited by the fact that the contamination spreads to a diameter of about 500 Å before a layer is formed that is thick enough to protect the underlying surface from sputtering. A

particular advantage when conductors are being fabricated is that they can be made taller than they are wide. (A.G.W.)

39137 VARIABLE-GRADIENT, ELECTRON-BEAM HEATING METHODS FOR GROWING SINGLE CRYSTALS OF ZIRCONIUM. Wilson, J. C.; Picklesimer, M. L. (Oak Ridge National Lab., Tenn.). pp 502-20 of First International Conference on Electron and Ion Beam Science and Technology. New York, John Wiley and Sons, Inc., 1965.

Rather simple electron-beam heating methods were used to produce large single crystals of alpha Zr in the solid state by traversing a beta-phase zone along a specimen at rates of the order of 1 cm/hr. Temperature gradients of at least several hundred degrees C per cm are required in and adjacent to the zone. Crystals were produced in the form of bars, strips, and foils, and single crystals of Zircaloy-2 were produced by the same methods. Crystals of Zr were grown by floating zone melting of 4- to 13-mm diameter bars at the rate of 3 cm/hr. It was demonstrated that with electron-beam heating it is possible to produce continuously variable temperature patterns and temperature gradients with simple apparatus and at high power densities. (A.G.W.)

39138 SUBSTRUCTURE AND IMPURITIES IN NIOBIUM SINGLE CRYSTALS GROWN BY THE ELECTRON-BEAM, FLOATING-ZONE TECHNIQUE. Tedmon, C. S. Jr.; Rose, R. M. (Massachusetts Inst. of Tech., Cambridge). pp 521-40 of First International Conference on Electron and Ion Beam Science and Technology. New York, John Wiley and Sons, Inc., 1965.

A survey of the substructure, by etch-pit and electron microscopic techniques, and the resistivity ratios (300 and 4.2°K) of Nb crystals was made as a function of operating conditions during crystal growth, particularly the system pressure and the crystal growth rate. Very high dislocation densities, above 10^9 lines/cm^2 exist in crystals grown at rates of the order of 5 mm/min; in crystals grown at 0.2 mm/min the dislocation density is roughly two orders of magnitude lower. Resistivity ratio measurements, taken along the length of the crystals, revealed greater dependence of this property on interstitial contamination, as a function of operating pressure, than on substructure or possible zone-refining effects. Growth rates below 0.5 mm/min must be used to attain dislocation densities below 10^7 lines/cm^2. Higher resistivity ratios may be attained by growing crystals in higher vacua. (A.G.W.)

39139 ON THE DEFORMATION, RECRYSTALLIZATION, AND WELDING OF MOLYBDENUM SINGLE CRYSTALS. Rexer, E. (Inst. for Physics of Pure Materials, Dresden). pp 541-9 of First International Conference on Electron and Ion Beam Science and Technology. New York, John Wiley and Sons, Inc., 1965.

Molybdenum single crystals of predetermined orientations prepared by electron bombardment zone melting could be rolled at room temperature by more than 80%. Strain hardening illustrated by hardness values depends on orientation. Subsequent annealing of unpolished specimens caused recrystallization connected with strong embrittlement. With electrolytically polished specimens of some orientations, recrystallization and embrittlement can be made to occur at higher annealing temperatures or not at all. Crystals having the axis ⟨110⟩ and the rolling plane {100} showed lowest work hardening, and, after electrolytical polishing up to 2400°C, no recrystallization phenomena. For a series of orientations no reduction of ductility could be observed after electron-beam welding of rolled and polished single crystals except of crystals of the orientation ⟨110⟩ {110}. (auth)

39140 EXTRUSION OF ELECTROLYTIC GRADE CR BERYLLIUM. Lidman, W. G.; Moyer, K. H. (General Astrometals Corp., Yonkers, N. Y.). 18p. (CONF-729-24). Gmelin, AED-CONF-64-247-28.

From International Conference on Beryllium, Philadelphia, Oct. 1964.

Conclusions drawn from the studies are: Electrolytic high purity beryllium can be extruded to possess tensile properties that are better than present anticipated requirements. Rod extruded from powder was found to have superior properties than that extruded from fully dense hot pressed block. Increased reduction ratio appeared to improve the ultimate tensile strength without any significant bearing on ductility. Densities attained on extruded rod were relatively consistent and range from 1.850 to 1.855 g/cc. Densities appear to be slightly higher when fully dense block is used for starting material. (W.L.G.)

39141 EFFECT OF PROCESSING PARAMETERS ON SINTERING OF ThO_2. Neuman, Bruce H. (Nuclear Materials and Equipment Corp., Apollo, Penna.). 24p. (CONF-650513-8). Gmelin, AED-CONF-65-092-1.

From American Ceramic Society, Annual Meeting, Philadelphia.

The effect of presintering on the final density of sintered ThO_2 was investigated. Among the variables investigated were: rate of heating to 900°C presintering temperature, presintering temperatures of 400, 600, and 900°C, presintering atmosphere of dry and wet H_2 and CO_2, and green densities in the range of 50 to 70% theoretical density. The parameters studied are correlated with sintered density and grain size. (auth)

39142 FORMULATION OF PYROLYTIC GRAPHITE ARTICLES. (to General Electric Co.). British Patent 991,681. May 12, 1965. Priority date June 1, 1962, United States.

A method of forming an annealed article of pyrolytic graphite consists of depositing a body of pyrolytic graphite on a substrate at a temperature in the range of 2000 to 2500°C and then subjecting the body to a temperature of 3500°C. Annealed article produced by this method results in an article with superior crystalline perfection, preferred orientation, and less weakening structural defects. (B.L.M.)

39143 A PROCESS FOR THE PREPARATION OF A PROTECTIVE SURFACE LAYER ON ALUMINIUM OR ALUMINIUM ALLOYS. (to Institutt for Atomenergi). British Patent 991,817. May 12, 1965. Priority date Nov. 22, 1961, Norway.

A process is described for the preparation of a protective Ni and Al containing surface layer on Al or Al alloy. The body of Al or Al alloy is provided by chemical deposition with a coating composed of a P-containing Ni alloy. The coated body is then subjected to a fused salt bath consisting of either KNO_3-NaNO_2 or $NaNO_3-KNO_2$ in a weight ratio of 0.9 : 1.1 to 1.1 : 0.9 to extract the P from the Ni alloy and to effect alloying, by diffusion annealing, of the Al and Ni. The salt bath is maintained at a temperature between 450° and 600°C for a period of from 30 min to 100 hr. The Al alloy suitable for coating by this process consists of 8–15% Si, 0.5–2% Ni, 0.2–1% Fe, 0–1.5% Mg, 0–0.5% Ti, and 0–0.5% Zr. (B.L.M.)

39144 ALLOYS CONTAINING PYROLYTIC GRAPHITE. (to High Temperature Materials, Inc.). British Patent 992,047. May 12, 1965. Priority date Mar. 21, 1962, United States.

A process is described for the deposition of alloys composed of pyrolytic graphite and a metal, Al, Th, V, or U. The substrate to be coated is mounted in a furnace that is heated to a temperature range of 1500° to 1750°C after the pressure in the furnace has been reduced to at least 20mm Hg. A gaseous hydrocarbon, methane, natural gas, ethane, propane, or benzene is introduced into the furnace through an injector. A separate generating system is provided to produce a halide of the metal prior to injection of the metallic halide into the furnace. At the elevated temperature carbon and the metal are liberated from their respective compounds and deposited in the form of an alloy. After a coating of desired thickness is obtained, the gaseous reactants are shut off, and the temperature and pressure are allowed to return to normal. (B.L.M.)

39145 METHODS OF AND APPARATUS FOR PRODUCING ELECTRIC HEATER TUBES INCORPORATING RESISTORS. (to l'Equipement Thermique S. A.). British Patent 996,946. June 30, 1965. Priority date Jan. 2, 1963, France.

A method and apparatus are described for producing an electric heater tube having a resistor embedded in the metal. The filling metal is melted in a first container, and the heater tube is disposed vertically in a second container adapted to be heated. A pipe is provided at the bottom of the heater tube for supplying the molten metal that is pulled into the heater tube by means of a vacuum pump circuit attached to the top of the heater tube. A casing surrounding the tube for controlling the temperature of the metal in the tube is provided with means for producing a gradient along the casing so that the column of molten metal solidifies from the bottom upwards. (B.L.M.)

39146 PLUTONIUM ENRICHED URANIUM FUEL FOR NUCLEAR REACTORS. Michaud, Gaetan G. J.; Hart, Robt. G. (to Atomic Energy of Canada, Ltd.). Canadian Patent 696,525. Oct. 27, 1964.

The manufacturing process for a reactor fuel consisting of UO_2 enriched with 2 to 25% PuO_2 is described. The PuO_2 is in refractory form rather than in solid solution and this is an advantage for subsequent reprocessing with nitric acid. Sintering and compacting gave a product of 90% theoretical density. (F.S.A.)

39147 MALLEABLE TUBE-CLAD NUCLEAR REACTOR FUEL ELEMENT AND MANUFACTURING METHOD THEREFOR. Sparalis, C. W. (to General Electric Co.). Canadian Patent 702,595. Jan. 26, 1965.

UO_2 pellets were covered with stainless steel cladding in such a way that there was no gap between the pellets and the covering but there was a void at one end. In another method the pellets were surrounded with stainless steel foil before the cladding process. Greatly improved heat transfer was claimed. The special dies for forming the cladding tube and the swaging methods are described. (F.S.A.)

39148 FUEL ELEMENTS FOR NUCLEAR REACTORS. Bauer, Stefan George; Battle, Norman (to Rolls-Royce Ltd.). U. S. Patent 3,192,621. July 6, 1965. Priority date July 10, 1959, Great Britain.

A process is described for producing a reactor fuel element that is composed of cylindrical pellets of fissile material encased in a thin walled casing that is deformed into contact with some of the surfaces of the pellets. The thin walled tubular casing is of uniform internal diameter and has a wall thickness of 0.01 in. The substantially cylindrical pellets of fissile material have an external diameter less than that of the casing so as to be a slack fit in the casing and have a rebate at each end of the casing. The pellets are inserted in end to end abutment in the casing, closure plugs are inserted in the ends of the casing, and the casing is subjected to an external fluid pressure of 6000 psi to deform the casing into close contact with the external surface of the pellets and into annular channels so locating the pellets axially in the casing and providing for good heat transfer between the casing and the pellets. (B.L.M.)

Properties and Structure

Refer also to abstracts 38755, 38922, 39072, and 39118.

39149 (AD-425880) THE STRENGTH AND PLASTICITY OF ANISOTROPIC METALS. Final Report. Backofen, W. A.; Hosford, W. W. F. Jr. (Massachusetts Inst. of Tech., Cambridge. Metal Processing Lab.). Sept. 1963. Contract DA-19-020-ORD-5719. 55p. (WAL-TR-834.12/2-3). CFSTI, $5.60 cy.

Sheets of the magnesium alloys AZ31B, HK31A, and ZE10A in several different tempers were tested in tension and determinations were made of the ratio of width-to-thickness strains. Fracture appearance is explained on the basis of anisotropy in plastic flow, and implications for developing texture-hardening effects in these alloys are discussed. Titanium sheet of commercial purity (RC-70) and an alpha-titanium alloy ($2\frac{1}{2}$ Sn–5 Al) were tested in tension and plane-strain compression. Strain ratios of $R < 1$ in the RC-70 sheet were related to an unexpected texture with a strong concentration of (000) basal poles along the transverse direction. The low R values were responsible, in turn, for a texture softening in plane-strain compression. In the 5 Al: $2\frac{1}{2}$ Sn alloy, a strong (000) concentration near the sheet normal was responsible for higher R values and the observation of texture hardening in plane-strain compression. (CFSTI)

39150 (AECL-2250(Pt.1)) THE PROPERTIES OF COLD-WORKED ZIRCONIUM–2.5 WT PERCENT NIOBIUM FUEL SHEATHING. Steward, K. P. (Atomic Energy of Canada Ltd., Chalk River (Ontario)). Mar. 1965. 37p. Dep.; AECL, $1.00 cy.

The properties of two batches of cold-worked zirconium–2.5% niobium fuel sheathing for use in the WR-1 and CANDU Reactors were investigated by a number of short term tests. Axial tensile, ring tensile, and closed end burst test properties were determined at temperatures up to 500°C, and data were also accumulated on recovery, crystallographic texture, residual stress, and susceptibility to stress orientation. Both axial and ring tensile tests show similar trends to those observed in Zircaloy-2, strain-age hardening being evident between 250°C and 400°C, and minimum ductility at about 350°C. Burst strength above 400°C is less affected by temperature than axial or ring tensile strength, while minimum circumferential ductility occurs at about 450°C. Hardness tests indicate recovery at 450°C and 500°C, but not at 400°C; slight hardening is apparent after short times at 350°C. The recovery curves suggest two processes occurring simultaneously, namely, relaxation of cold work, and aging due to rejection of βNb from supersaturated solid solution. The usual duplex texture for tube-reduced zirconium alloy tubing is observed, and residual stresses are low. The hydride orientation numbers are batch 1 fn = 0.12 and batch 2 fn = 0.18, while the thresholds for stress-reorientation of hydrides are about 9000 psi and 10,000 psi for batches 1 and 2, respectively. (auth)

39151 (AFOSR-65-0981) NONDESTRUCTIVE EVALUATION OF METAL FATIGUE. Final Report. Kusenberger, Felix N.; Leonard, Byron E.; Barton, John R.; Donaldson, W. Lyle (Southwest Research Inst., San Antonio, Tex. Dept. of Electronics and Electrical Engineering). Mar. 1965. Contract AF 49(638)-1352. 98p.

The work accomplished and results obtained during the previous two years of program activity are briefly reviewed. A discussion of the factors which influenced the selection of focused ultrasonic Rayleigh wave techniques for use in the nondestructive evaluation of metal fatigue is included. Methods investigated for generating and focusing Rayleigh waves are presented. Transducer design considerations and fabrication methods employed are summarized and discussed. The selection of specimen materials and designs is presented, including engineering drawings of the steel and aluminum fatigue specimens. Experimental results obtained from small drilled holes in a number of specimen materials and geometries using surface wave techniques (plane wave) are shown including a number of Polaroid photographs of the reflection signal patterns. Results obtained from methods investigated for focusing Rayleigh waves are presented. Ultrasonic plane wave and magnetic inspection results on steel fatigue specimen No. 18 containing a tiny fatigue crack are given. Many inspection records and surface photographs are also shown. Reproductions of Polaroid photographs of ultrasonic signal patterns obtained while stress cycling an aluminum specimen are shown. Inspection records showing a large increase in signal amplitude corresponding with the development of fatigue damage in the form of a crack are included. X-ray diffraction measurements, using a 0.004-inch diameter collimator, were made in the vicinity of the tip of a small fatigue crack, and the results of these measurements are reported. (auth)

39152 (BMI-X-10132) FISSION-PRODUCT REACTIONS WITH AND RELEASE FROM FUEL-ELEMENT CLADDINGS. Quarterly Progress Report for April–June 1965. Sunderman, Duane N.; Morrison, David L.; Howes, James E. Jr.; Jablonowski, Edward J. (Bat-

telle Memorial Inst., Columbus, Ohio). July 1, 1965. Contract W-7405-eng-92. 14p. (EURAEC-1427). Dep. mn; CFSTI, $1.00 cy, $0.50 mn.

Work Performed Under United States–Euratom Joint Research and Development Program.

The diffusion of nongaseous fission products in Zircaloy-4 and Zr at 600 to 1000°C was investigated. Fission-product concentration tailing through specimens was observed at 800°C and below. Fission-product diffusion in stainless steel and Incoloy 800 was also studied. In-pile studies of fission-product diffusion in Fe–Ni–Cr, Fe–Ni, and Fe–Cr alloys were initiated. Data are included on compositions of Zircaloy-4 and stainless steel. Data are also included on fission-product diffusion in Zircaloy-4, Zr, stainless steel, Incoloy 800, and Fe–Cr alloy. (J.R.D.)

39153 (BNWL–33) THE BETA-ALPHA AND ALPHA-BETA TRANSFORMATIONS IN PLUTONIUM UNDER APPLIED STRESSES. Nelson, R. D.; Bierlein, T. K.; Bowman, F. E. (Battelle-Northwest, Richland, Wash. Pacific Northwest Lab.). Jan. 1965. Contract AT(45-1)-1830. 35p. Dep. mn; CFSTI, $2.00 cy, $0.50 mn.

Application of uniaxial compressive and tensile stresses markedly affects the total strain during the $\beta \rightarrow \alpha$ and $\alpha \rightarrow \beta$ transformations in plutonium. A number of conclusions can be drawn from the results: The total strain during $\beta \rightarrow \alpha$ transformation under compression is almost completely independent of the transformation rate. Applied compressive stresses above 9000 psi cause essentially all of the $\beta \rightarrow \alpha$ transformation strain to occur as a contraction parallel to the applied stress, i.e., $\Delta L/L_0 = \Delta V/V_0$. Applied tensile stresses of about 4000 psi cause all of the strain during the $\beta \rightarrow \alpha$ transformation to occur as a contraction perpendicular to the applied stress. No contraction is observed parallel to the applied tensile stress. Applied stresses during $\beta \rightarrow \alpha$ transformation produce a microstructural shape texture. The alpha grains are elongated in a direction parallel to the applied compressive stresses and perpendicular to the applied tensile stresses. The elongated grains are aligned in disks which are perpendicular to the direction of the compressive stress and parallel to the direction of the applied tensile stresses. Applied stresses during $\beta \rightarrow \alpha$ transformation produce a crystallographic texture. The (010) planes are aligned parallel to the applied tensile stresses and perpendicular to the applied compressive stresses. The anisotropic strains accompanying the $\alpha \rightarrow \beta$ transformation under uniaxial stress indicate that a texture also develops. The $\alpha \rightarrow \beta$ and $\beta \rightarrow \alpha$ transformations in textured plutonium result in anisotropic transformation strain in the absence of applied stress. Both applied uniaxial tensile stresses and uniaxial compressive stresses raise the temperature for the beginning of the $\beta \rightarrow \alpha$ transformation at a constant cooling rate and for stresses up to at least 7000 psi, the maximum stress studied. Applied tensile stresses above 2500 psi cause all of the $\alpha \rightarrow \beta$ transformation strain to occur as an expansion parallel to the applied stress, i.e., $\Delta L/L_0 > \Delta V/V_0$. Some phase transformation excess creep occurs during the transformations in specimens subjected to an external stress. Phase transformation excess creep is greater under tensile than under compressive stresses. Little or no $\beta \rightarrow \alpha$ transformation excess creep occurs under compressive stresses. The $\beta \rightarrow \alpha$ transformation fulfills many of the requirements for a martensitic type transformation. (auth)

39154 (BNWL-SA-54) IONIC DIFFUSION IN HIGH TEMPERATURE URANIUM DIOXIDE. Bates, J. L. (Battelle-Northwest, Richland, Wash. Pacific Northwest Lab.). July 1, 1965. Contract AT(45-1)-1830. 24p. (CONF-650704-7). Dep. mn; CFSTI, $1.00 cy, $0.50 mn.

From IAEA Symposium on Thermodynamics, Vienna.

A review is presented of recent high-temperature property measurements of UO_2 made both in- and out-of-reactor that pertain to atomic movement. The measurements of electrical conductivity, thermoelectric emf, solid state fission fragment migration, and U–O phase equilibria suggest that ionic diffusion in an electrical potential gradient is significant in the movement of fission products and oxygen in UO_2. (D.L.C.)

39155 (CALT-221-11) A STUDY OF CsCl TYPE INTERMEDIATE PHASES INVOLVING RARE EARTH ELEMENTS. Research and Development Report No. 36. Chao, C. C. (California Inst. of Tech., Pasadena. W. M. Keck Lab. of Engineering Materials). June 1965. Contract AT(04-3)-221. 87p. Dep. mn; CFSTI, $3.00 cy, $0.75 mn.

Results are presented of a systematic study of CsCl type phases in binary alloys of rare earth elements with other metals. Thirty-nine new phases of this type were found. The linear variation of the lattice parameter of CsCl phases with the trivalent ionic radius of the rare earth metal previously established for a limited number of alloys, was extended to seventy-nine phases. This linear relationship leads to some interesting qualitative arguments on the ionic size of the non-rare earth element in these phases. The electric resistivities of nineteen CsCl type phases of rare earths with copper, silver, and gold were measured between 4.2°K and about 250°K. With the exception of the yttrium–silver phase, all others exhibited an anomaly in the resistivity-temperature curve which is attributed to an antiferromagnetic transition. This conclusion is confirmed by previously published results of neutron diffraction experiments and magnetic susceptibility measurements. The electric resistivity results are interpreted on the basis of an indirect interaction between two rare-earth ions. These two ions can be both magnetic or non-magnetic, or mixed. (auth)

39156 (CEND-532) ADVANCED BONUS CORE DEVELOPMENT PROGRAM. Quarterly Progress Report No. 5, December 1964–February 1965. Gibbons, J. F.; Knapp, R. W.; Mordarski, W. J.; Anderson, L. E.; Grubelich, F. T. (Combustion Engineering, Inc., Windsor, Conn. Nuclear Div.). May 17, 1965. Contract AT(40-1)-3154. 235p. Dep.(mn); $6.00(cy), 4(mn) CFSTI.

Design of the thermal cycling fuel elements was completed and the detailed drawings were released for manufacture. The construction of the thermal cycling loop continues. An internal support for the autoclave and test elements was designed and the steam distribution manifold design was completed. Calculations were performed for various arrays of 15% enriched ABC solid multitube fuel elements to determine the maximum number of irradiation test assemblies which can be handled safely at any one time. Preliminary studies of fuel management were performed for the Advanced BONUS Core to determine the size, configuration, and zone description of the equilibrium core which will meet performance objectives and have minimum fuel cycle costs. Several configurations are discussed. A detailed summary of all the aging and corrosion data obtained to date under the ABC program is included. (M.O.W.)

39157 (CNLM-6337) STUDIES CONCERNING THE CHEMICAL STATE OF CARBON, NITROGEN AND OXYGEN IN ALKALI METALS. Kelly, K. J.; Hobart, E. W.; Bjork, R. G. (Pratt and Whitney Aircraft, Middletown, Conn. Connecticut Advanced Nuclear Engineering Lab.). Apr. 14, 1965. Contract AT(30-1)-2789. 12p. (CONF-650411-5). Dep.(mn); $1.00(cy), 1(mn) CFSTI.

From Joint NASA-AEC Liquid Metals Corrosion Meeting, Gatlinburg, Tenn.

The chemical states of carbon and nitrogen in lithium were demonstrated to be comparatively simple; namely the acetylide and nitride, respectively. There appear to be no complexes formed between these solutes and no influence by moderate concentrations of oxygen in lithium. Preliminary data indicate that the sodium–carbon system is more complex than its lithium counterpart. Methanides and acetylides apparently exist in significant quantities. Nitrogen and oxygen may form important complexes with carbon. Analytical chemistry methods for determination of carbon in lithium or sodium must include provisions for collection or oxidation of hydrocarbons evolved during hydrolysis. (auth)

39158 (GEAP-4751) MICROSTRUCTURAL EVALUATION OF SUPERHEAT CLADDING MATERIALS. Comprelli, F. A.; Lewis, J. E. (General Electric Co., San Jose, Calif. Atomic Power Equipment Dept.). Jan. 1965. Contract AT(04-3)-189. 61p. Dep. mn; CFSTI, $3.00 cy, $0.75 mn.

Data are presented which describe the thermal response characteristics of selected superheat alloys. The alloys include Incoloy-800, Incoloy-801, Incoloy-804, Incoloy-825, Type 310 stainless steel, Hastelloy-X, Hastelloy-F, Inconel-625, Inconel-718, and a G. E.-Modified Incoloy-800. Each alloy was evaluated by monitoring the room temperature hardness after exposure for various time intervals at 1200 or 1400°F. Light microscopy was used to monitor microstructural changes. Precipitate phases were identified by x-ray diffraction. Relative amounts of elements in each phase were determined by x-ray fluorescence. (auth)

39159 (LA-DC-6926) THE VAPOR PRESSURE OF PLUTONIUM. Mulford, Robert N. R. (Los Alamos Scientific Lab., Univ. of California, N. Mex.). [1965]. Contract W-7405-eng-36. 14p. (CONF-650704-3). Dep. mn; CFSTI, $1.00 cy, $0.50 mn.

From IAEA Symposium on Thermodynamics, Vienna.

The vapor pressure of liquid plutonium was determined over the temperature range 1100 to 1800°K by the Knudsen effusion method. The least squares equation which fits the data is $\log_{10} p(atm) = -17420/T(°K) + 4.913$. The standard deviation corresponds to about ±10% in the pressures calculated from this equation. The heat of vaporization computed from the temperature dependence of the experimental data is $\Delta H^{\circ}_{298} = 82.3$ kcal/g-atom. The heat computed by combining independent entropy and heat capacity data with the present measurements is $\Delta H^{\circ}_{298} = 82.1$ kcal/g-atom. Effects of oxygen upon the volatility of liquid plutonium were sought by comparing the vapor pressures observed with the liquid in contact with tantalum, tantalum carbide, magnesia, and plutonium sesquioxide. No differences were found. In addition, the vapor pressure was measured with different degrees of vacuum in the system. No effect was found here either, except that in very poor vacuums a surface film of oxide apparently formed and reduced the volatility by about a factor of 2. (auth)

39160 (LA-DC-6953) A MASS SPECTROMETRIC STUDY OF THE VAPOR PRESSURE OF $U_{(g)}$ AND $UC_{2(s)}$ OVER VARIOUS COMPOSITIONS IN THE URANIUM–CARBON SYSTEM. Storms, Edmund K. (Los Alamos Scientific Lab., Univ. of California, N. Mex.). [1965]. Contract W-7405-eng-36. 57p. (CONF-650704-10). Dep. mn; CFSTI, $3.00 cy, $0.50 mn.

From IAEA Symposium on Thermodynamics, Vienna.

The pressure of $U_{(g)}$ and $UC_{2(s)}$, and the resulting partial heats of vaporization of $U_{(g)}$ and $C_{(g)}$, were measured as a function of composition from UC + $U_{(l)}$ to UC_2 + C. An abrupt pressure change with composition was found near $UC_{1.0}$ and a much lesser change within the UC_2 region. The partial heat of vaporization of $U_{(g)}$ at ~2200°K shows a similar rapid change in value through $UC_{1.0}$ with a maximum near $UC_{1.2}$ at 167 ± 2 kcal/mole. Another maximum occurs in the UC_2 region at 147 ± 2 kcal/mole and $UC_{1.85}$. The heat of vaporization based on the UC_2 + C region is too low since the UC_2 phase changes composition with temperature. The measured pressures are consistent with congruent vaporization near $UC_{1.1}$. Evidence is presented supporting a value for the heat of vaporization of uranium near 126 kcal/mole. Using this value, the measured pressures in the U–C system show excellent agreement with the other thermodynamic measurements. A re-evaluation was made of the high temperature thermal functions of U, UC, and UC_2 with the result that significant changes must be made in the currently used values. Several areas of the phase diagram were determined both directly and from the pressure measurements and are compiled into a phase diagram of the system. (auth)

39161 (LA-DC-6956) DENSITIES OF SOME LOW MELTING PLUTONIUM ALLOYS. Perkins, Ralph H.; Geoffrion, Louis A.; Biery, John C. (Los Alamos Scientific Lab., Univ. of California, N. Mex.). [1964]. Contract W-7405-eng-36. 22p. (CONF-650704-8; SM-66/73). Dep. mn; CFSTI, $1.00 cy, $0.50 mn.

From IAEA Symposium on Thermodynamics, Vienna.

Densities of unstabilized and stabilized (1 wt % Ga) plutonium were measured over the temperature range 25–800°C. Gallium not only stabilizes the delta phase of plutonium in the solid state, but also influences its melting temperature and the density of the liquid metal. The Pu–2.5 wt % Fe and the Pu–2.5 wt % Fe–0.2 wt % Ga alloys were also studied with the volumeter. The unstabilized alloy melts at 411 ± 2°C with a 1.5% decrease in volume. Gallium addition suppresses phase transitions in the solid state and affects melting temperature and density of the molten alloy. Pu–Co–Ce alloys containing 3, 5, 6.2, and 8 g Pu/cc were studied with the volumeter. These alloys all melt in the range 425–442°C, and they become more dense on melting. The change in density on melting increases with increasing plutonium content from 1.3% for the 3 g Pu/cc alloy to 3% for the 8 g/cc material. The addition of manganese to 6.2 and 8 g/cc alloys significantly reduced this expansion on freezing. However, manganese additions of 5.5 wt % and higher adversely affected the melting temperatures of these fuels. (auth)

39162 (LA-DC-6957) SELF-DIFFUSION STUDIES OF GAMMA PLUTONIUM. Tate, Raymond E.; Edwards, Glen R. (Los Alamos Scientific Lab., Univ. of California, N. Mex.). [1964]. Contract W-7405-eng-36. 16p. (CONF-650704-4; SM-66/65). Dep. mn; CFSTI, $1.00 cy, $0.50 mn.

From IAEA Symposium on Thermodynamics, Vienna.

The diffusion behavior of face-centered orthorhombic gamma plutonium was studied using ^{238}Pu tracer in annealed couples. The results give $D = 2.1 \times 10^{-5} \exp(-16{,}700/RT)$ cm^2/sec. The low values of the frequency factor and activation energy are discussed briefly; autoradiographic experiments indicate that grain boundary diffusion is unlikely. (D.L.C.)

39163 (MLM-1244) REACTOR FUELS AND MATERIALS DEVELOPMENT—PLUTONIUM RESEARCH: 1964 ANNUAL REPORT. Wittenberg, L. J.; Grove, G. R. (Mound Lab., Miamisburg, Ohio). Dec. 31, 1964. Contract AT(33-1)-Gen-53. 56p. Dep. mn; CFSTI, $3.00 cy, $0.50 mn.

The phase equilibria study of the Pu–Ce–Ni system was completed. The portion of the ternary system containing 0 to 50 at. % Ni has two ternary eutectics at nearly the same temperature, 440 ± 3°C, and a wide range of low-melting compositions which are potential fuels for molten Pu reactors. All the compounds of the three limiting binary systems display primary phase fields in the ternary system with an extensive amount of solid solubility. No ternary compounds are formed. Pu and Ce form limited solid solutions with each other. The compound Ce_5Ni_2 forms a terminal solid solution of ternary composition. The existence of complete solid solubility between the compounds PuNi–CeNi, $PuNi_2$–$CeNi_2$, $PuNi_3$–$CeNi_3$, and $PuNi_5$–$CeNi_5$ is indicated. The phase equilibria investigation of the Pu–Ce–Fe system is nearly complete. A eutectic valley extends across the diagram at approximately 10 at. % Fe with temperatures ranging in this valley from 410 to 680°C. The compositions of interest as molten reactor fuels have a very limited range of Pu concentrations, i.e., 76 to 90 at. %, with liquidus temperatures at 435 to 410°C. All the compounds of the three limiting binary systems display primary phase fields in the ternary system. As a result of extensive solid solubility no ternary eutectics occur in the system. No ternary compounds are formed. Pu and Ce form limited solid solubility with each other. The primary phase field for the solid solution $CeFe_2$–$PuFe_2$ covers the major portion of the phase diagram. In the presence of Fe, a form of beta Ce (a low-temperature allotrope of Ce metal) rather than gamma Ce is stable at room temperature. An investigation of low-melting eutectic compositions is being conducted based on previous knowledge of four ternary systems (Pu–Ce–Cu, Pu–Ce–Co, Pu–Ce–Ni, and Pu–Ce–Fe). Preliminary results indicate that a rather broad low-melting region which contains an appreciable concentration of Pu surrounds a eutectic with a melting point as low as 375°C. Investigation of the phase equilibria in the Pu–Cd system revealed the presence of one congruently melting compound, $PuCd_2$, and three incongruently melting compounds, $PuCd_4$, $PuCd_6$ and $PuCd_{11}$. A wide liquid miscibility gap extends

from approximately 2 at. % Cd to the monotectic at 60 at. % Cd, with the monotectic reaction isotherm at 910°C. Individual additions of 0.1 at. % Fe, Co, or Ni to Pu caused transformations at 405 to 412°C which were readily detected by differential thermal analysis. Additions of 0.1 at. % Fe or Co to 96.55 at. % Pu–3.35 at. % Ga alloy caused additional transformations at 405°C and a lowering of the solidus and liquidus temperatures. The combined presence of 0.05 at. % Fe and 0.05 at. % Ni depressed the Pu–Fe eutectic temperature to 390°C for Pu and to 395°C for the Pu–Ga alloy. Single-crystal analysis of a Cu-rich Pu–Cu binary compound, which is isomorphous with the compound $CeCu_4$, indicated an orthorhombic unit cell with lattice parameters $a_0 = 10.06$ Å, $b_0 = 8.16$ Å, $c_0 = 5.14$ Å. Definitive single crystal analyses are in progress on the compounds $CeCu_4$ and $CeCu_5$. Two congruently melting compounds (PuPt and $PuPt_2$) and one incongruently melting compound Pu_2Pt are indicated in this system. All three compounds have melting points in excess of 1000°C. A eutectic is indicated at 10 at. % Pu, but a eutectic at high Pu concentrations was not obtained. Preliminary to the phase studies of the Pt group metals with Pu, the following Ce–Pt group compounds were identified from electron microprobe x-ray analysis data: Rh_2Ce, $Ir_{13}Ce_{15}$, Pd_2Ce, RhCe, Ir_2Ce_3, and Pd_3Ce_2. A study of high-purity, electrorefined Pu revealed that (1) a small thermal effect was observed at 110°C prior to the $\alpha \rightarrow \beta$ transformation at 125°C; (2) the $\delta \rightarrow \delta'$ transformation was completely separated from the $\delta' \rightarrow \epsilon$ transformation; (3) less than 1°C separated the start and the completion of the fusion reaction at 640°C. For the alloy Pu–1 wt % Ga, the energies required for the $\delta \rightarrow \epsilon$ and $\epsilon \rightarrow$ liquid phase transformations were 2.10 and 3.64 cal/g of alloy, respectively. Both of these values are appreciably larger than the energy required for the transformations in an ideal solid solution of the same concentrations of Pu and Ga. A plasma-produced B single crystal was found to be cubic with lattice parameter $a_0 = 23.71$ Å and space group Pn3n (O_h^2). The large unit cell, 8030 A^3, contains 1700 to 1800 atoms depending on the density; which will be determined. Continued development of the DTA technique, which has proven useful in the Pu alloy studies, has extended the working range of the equipment to 1500°C and made it possible to quantitatively determine energy exchange during a phase transformation in a sample. Measurements made with a new thermal diffusivity apparatus on annealed Armco Fe at 300 to 1000°C were in agreement with literature values. The thermal diffusivity of UC, measured under transient conditions, decreased rapidly from 0.104 cm^2/sec at 250°C to 0.050 cm^2/sec at 700°C and gradually increased to 0.055 cm^2/sec at 1000°C. The thermal diffusivity of $(U_{0.8}Pu_{0.2})C_{0.95}$ is apparently independent of temperature at 250 to 1000°C, with an average value of 0.039 cm^2/sec. The density of liquid Ce was determined up to 175°C above previous measurements (i.e., 1173°C). The results were in agreement with values extrapolated from the earlier work. The measured density of liquid Pu–1 wt % Ga alloy decreased from 16.160 g/cc at 682°C to 16.003 at 847°C. This alloy expanded during the transformation from the liquid to solid state. The densities of three ternary alloys which contain approximately 3, 5, and 8 g Pu/cc are 8.90, 9.98, and 11.70 g/cc, respectively, at 500°C. The viscosity-composition relationship in Pu–Ce alloys was investigated by measurement of the viscosities of nine compositions between 0 and 100 at. % Ce. For each of the nine alloys the viscosity decreased with temperature in a predictable manner. When viscosity was plotted as a function of composition, a maximum in viscosity occurred at 5 at. % Ce. As an adjunct to the viscosity measurements, the oscillating cup viscosimeter was used for a precise determination of the liquidus temperatures of alloys. The viscosities were measured for four alloys in the Pu–Ce–Co system whose compositions placed them in a low-melting valley in the equilibrium diagram. When viscosity values at the liquidus temperatures were plotted as a function of concentration, the values lay on a smooth curve which increased as Pu was substituted for Ce. The viscosity of Pu–1 wt % Ga alloy decreased from 8.75 centipoise at 672°C to 6.36 centipoise at 816°C. The liquidus temperature was determined to be 669 ± 2°C. The technique for the measurement of vapor pressure by differential thermal analysis (DTA) was extended to Zn. The vapor pressure of the molten metal was measured at 7 to 200 torr. The heats of mixing for liquid metals were successfully determined by a DTA method for 50–50 at. % compositions in the three systems: Cd–Bi, Bi–Pb, and Cd–Pb. New microsphere production techniques were employed which increased the rate of production and the density of PuO_2 microspheres. A technique was also developed for metallographic preparation of high-density PuO_2 microspheres. Use of this technique eliminated problems of breaking and pitting of the microspheres during the grinding and polishing stages of sample preparation. UO_2 microspheres as large as 250 microns in diameter were prepared in the induction-coupled plasma torch by use of an Ar–He gas mixture. U metal inclusions were detected in microspheres fused in the plasma torch; metallic inclusions were also found in the feed material. X-ray-diffraction investigation of microspheres composed of fused mixtures of PuO_2 and BeO revealed that no compounds or solid solubility exist in this system. Submicron particles of PuO_2 and UO_2 were obtained from the vapors which condensed when these materials were processed in the plasma torch. (auth)

39164 (N64–22193) ION EMITTER STUDIES. Final Report. Cho, A.; Shelton, H. (TRW Space Technology Labs., Thompson Ramo Wooldridge Inc., Redondo Beach, Calif.). May 11, 1964. Contract NAS3-2524. 88p. (NASA-CR-54045). CFSTI, $8.10 cy.

The effect of impurities on the cesium ion and neutral emission from hot porous tungsten are presented. These impurities include oxygen, carbon, calcium, silicon, boron, fluorine, and chlorine. The cesium neutral fraction and the critical temperature, when the clean or contaminated porous tungsten is emitting ions, are correlated with the work function and cesium binding energy inferred from the electron emission S-shaped curve. (auth)

39165 (NAA-SR-10462) PERMEATION OF HYDROGEN THROUGH METALS. Webb, R. W. (Atomics International, Canoga Park, Calif.). July 25, 1965. Contract AT(11-1)-Gen-8. 29p. Dep. mn; CFSTI, $2.00 cy, $0.50 mn.

The permeability of hydrogen through those metals being considered for use in SNAP reactor systems must be known in order to predict hydrogen mobility and migration in the NaK primary coolant system of the reactors. Of particular concern is the amount of hydrogen which will migrate into the mercury boiler loop. Data were gathered from the literature on the flux of hydrogen gas permeating various metals, and experiments were made with a hydrogen-sensitive mass spectrometer to collect additional data. The high-pressure data were fitted to the equation $\varphi = (CP^{\frac{1}{2}}/x) \exp [-(Q/RT)]$, which relates the flux to the hydrogen pressure, the metal thickness, and the activation energy for diffusion. Data on the low-pressure hydrogen permeation for Hastelloy N were not sufficient to justify a curve fitting. However, it was evident that Sievert's law ($\varphi = KP^{\frac{1}{2}}$) does not hold below 10 mm Hg, but that the permeation equation takes the form of: $\varphi = (CP/x) \exp [-(Q/RT)]$. (auth)

39166 (NAA-SR-Memo-11149) PROPERTIES OF CLADDING MATERIALS FOR SNAP HYDRIDE REACTORS. Burdi, G. F. (Atomics International, Canoga Park, Calif.). Mar. 22, 1965. Contract AT(11-1)-Gen-8. 23p. Dep. mn; CFSTI, $1.00 cy, $0.50 mn.

Data are presented on the physicochemical properties, mechanical properties, and irradiation properties of the following six alloys: Hastelloy N, Hastelloy X, Hastelloy R-235, Rene 41, TD Nickel, and TZM. (D.L.C.)

39167 (RFP–616) THE TOTAL HEMISPHERICAL EMITTANCE OF POLISHED AND OF OXIDIZED ALPHA PLUTONIUM. Preliminary Report. Karlsson, R. H. (Rocky Flats Div., Dow Chemical Co., Denver, Colo.).

July 7, 1965. Contract AT(29-1)-1106. 10p. Dep. mn; CFSTI, $1.00 cy, $0.50 mn.

The total hemispherical emittance of polished 99.66 wt % plutonium was determined to be 0.37 at 88.7 and 89.0°C. The emittance of a polished sample was measured after oxidation in a humid air atmosphere for 24, 66, and 168 hours. Emittances of 0.47, 0.54, and 0.70 were obtained. The apparatus was used to determine a total hemispherical emittance for candle soot of 0.96. Total errors were estimated to be less than ±3%. (auth)

39168 (TID-22015) THERMODYNAMIC AND OTHER ASPECTS OF METALLIC SYSTEMS. Annual Progress Report. Bever, M. B.; Robinson, P. M.; Titchener, A. L.; Li, Leach, J. S.; Chuang, K. C.; Gangulee, A.; Scattergood, R. O.; Waldman, J. (Massachusetts Inst. of Tech., Cambridge). June 1965. Contract AT(30-1)-1002. 12p. Dep. mn; CFSTI, $1.00 cy, $0.50 mn.

The deformation of $TlBi_2$ at 25°C, and the associated changes in its properties, were studied. The annealing behavior of deformed AgMg is being studied. The annealing kinetics of Au deformed at and below room temperature were determined. Heats of formation were measured at 273°K for InBi, In_2Bi, $TlBi_2$, CdTe, SnTe, PbTe, AuZn, and Ag-rich Ag–Mg alloys. Heats of solution of Sn and Pb at 623°K were calculated from measured heat effects on solution in liquid Bi in presence of Te; results for Cd are anomalous. (D.L.C.)

39169 (UCRL-16090) PRISMATIC LOOPS AND CLIMB KINETICS IN QUENCHED Al-1 PERCENT Mg ALLOY. Kannan, V. C. (Lawrence Radiation Lab., Univ. of California, Berkeley). May 1965. Contract W-7405-eng-48. 44p. Dep. mn; CFSTI, $2.00 cy, $0.50 mn.

Annealing of loops in quenched Al–1% Mg alloy was studied by hot-stage electron microscopy. The activation energy for loop climb was estimated to be 1.2 – 1.28 ev, which is in the same range as that found for pure aluminum. The absence of heterogeneous precipitation of vacancies and the bulk annealing results showed that the binding energy between magnesium atoms and vacancies, in the present alloy, is very small. It is concluded that (% supersaturated solute atoms/% vacancy) ratio primarily determines whether positive or negative climb can take place in a given alloy. The stacking fault energy was estimated by comparison of the shrinkage rates of perfect and imperfect loops as ~190 ergs/cm² at 207°C. (auth)

39170 (FTD-TT-64-1001) INVESTIGATION OF THE INTERNAL FRICTION OF POWDER–METALLURGICAL WC–Fe, WC–Ni AND WC–Fe–Ni ALLOYS. Chung, Ke Sun. Translated from Chosun Kwahakwon Tongbo, No. 1, 8-9(1962). 4p. CFSTI.

The internal friction of the Fe–WC, Ni–WC, and Fe–Ni–WC systems was studied as a function of composition and temperature to 800°C. Three internal friction peaks were found for the Fe–WC and Ni–WC systems and five for the Fe–Ni–WC system. In general, as the Fe and Ni contents increased, the amplitude of the internal friction peaks decreased. The kinetic energies were calculated and the physical mechanisms explained for the internal friction peaks in the Fe–Ni–WC system. (W.L.G.)

39171 (IS-Trans-17) ELECTROCAPILLARY CURVES OF LIQUID GALLIUM. Frumkin, A. N.; Polyanoskaya, N. S.; Gregorev, N. B. Translated by John C. Harvey (Ames Lab., Iowa State Univ. of Science and Tech.), from Doki. Akad. Nauk SSSR, 157: 1455-8(1964). 10p. Dep. mn; CFSTI, $1.00 cy, $0.50 mn; JCL, $1.10 fs, $0.80 mf.

A study was made of electrocapillary phenomena and adsorption of surface-active agents on clean Ga. The measurements were carried out in various solutions, and the effects of purity were evaluated. (D.L.C.)

39172 (ORNL-tr-633) COMPARATIVE X-RAY AND ELECTRON MICROSCOPY STUDIES OF THE SIZE OF GUINIER-PRESTON ZONES IN ALUMINUM-SILVER. Baur, R.; Gerold, V. Translated for Oak Ridge National Lab., Tenn., from Acta Met., 12: 1449-53(Dec. 1964). 11p. Dep. mn; JCL, $1.60 fs, $0.80 mf.

A comparative investigation on the size of spherical Guinier-Preston zones in an aluminum–silver alloy has shown that the x-ray and electron-microscopic average radii do not differ by more than 10%. The differences appear to be smaller for larger zone radii (45 Å) than for smaller radii (30 Å). (auth)

39173 (ORNL-tr-634) THE HEAT TONE IN THE STRAIN-HARDENING STATE OF ALUMINUM–ZINC ALLOYS. Gerold, Volkmar. Translated for Oak Ridge National Lab., Tenn., from Z. Metallk., 54: 257-62(1963). 19p. Dep. mn; JCL, $1.60 fs, $0.80 mf.

It is normally assumed that the amount of heat evolved during an isothermal precipitation is proportional to the amount of precipitate. However, this is no longer valid when precipitation and segregation processes are involved, in which a great number of very small particles are formed. It is shown with the example of an isothermal growth of the Guinier-Preston zones in an aluminum alloy containing 6.8 at. % Zn, in which the volume of zones remains constant and where only the number and size of the zones change, that the heat tone per unit of time can be explained completely by the change in the interfacial energy. The calculated heat tone agrees quite well with the measured values. (auth)

39174 (ORNL-tr-635) AGE-HARDENING OF ALUMINUM–SILVER ALLOYS. IX. X-RAY INVESTIGATIONS ON STRAIN HARDENING. Gerold, Volkmar. Translated for Oak Ridge National Lab., Tenn., from Z. Metallk., 46: 623-31(1955). 28p. Dep. mn; JCL, $2.60 fs, $1.04 mf.

X-ray studies at large and small angles were made in aged Al–Ag alloys containing 20 and 38% Ag. The results are interpreted in terms of segregation zones, and mechanisms are proposed for the strain-hardening and reformation processes. (D.L.C.)

39175 (ORNL-tr-638) APPLICATION OF ELECTRON-MICROSCOPIC FINE-RANGE DIFFRACTION FOR THE DETERMINATION OF THE ROLLING TEXTURE OF COPPER. Haessner, F.; Jakubowski, U.; Wilkens, M. Translated for Oak Ridge National Lab., Tenn., from Phys. Status Solidi, 7: 701-10(1964). 17p. Dep. mn; JCL, $1.60 fs, $0.80 mf.

The orientation of 95% cold-rolled copper relative to the rolling direction and sheet surface is determined by selected-area electron diffraction. The measurements were made on 600 spots distributed over a large area. The distribution of the poles found in this way agrees with the (111), (200), and (220) pole figures determined on the same sample by means of x rays. A discussion is given of the additional information which can be obtained from electron microscopy as compared with the x-ray method. (auth)

39176 THE TEMPERATURE VARIATION OF THE SCATTERING PROPERTIES OF CRYSTALS. Salter, L. S. (National Research Council, Ottawa). Advan. Phys., 14: 1-37(Jan. 1965).

It is shown how thermodynamic data (heat capacity, thermal expansion, etc.) may be used to estimate accurately certain scattering properties of crystals, assuming the validity of the quasi-harmonic approximation of lattice dynamics. In particular, Debye-Waller factors and incoherent neutron scattering cross sections can be readily correlated with thermodynamic data even through the form of the lattice frequency distribution of the crystal is not known. Thermodynamic data for vanadium, silicon, germanium, and copper were analyzed, and the results were used to illustrate the accurate estimation of the following entities: Debye-Waller factor, total incoherent neutron scattering cross section, differential incoherent neutron cross section in the weak-binding approximation and in the n-phonon approximation. The application of the method to Mössbauer effect phenomena is also discussed. Definite criteria are suggested for deciding the conditions under which the substitution of the Debye distribution for the actual frequency distribution of a crystal leads to acceptable estimates of one or more properties of the lattice vibrations. (auth)

39177 EUROPIUM AS AN ALKALINE EARTH METAL. Klemm, W.; Kook, H.; Muehlpfordt, W. (Universitaet,

Muenster, Ger.). Angew. Chem. Intern. Ed. Engl., 3: 704-5(Oct. 1964).

According to their atomic volumes, europium and ytterbium do not fit into the series of the rare-earth metals but resemble the alkaline-earth metals; their magnetic behavior also indicated that they contain the species M^{2+}, but not M^{3+}. The atomic volume of Eu lies between those of Ca and Sr, but closer to Ca; however, Eu does not crystallize in the face-centered cubic system as do Ca and Sr, but in the body-centered cubic system as does Ba. Extensive mixed crystal formation occurred in the system Ca/Eu. The lattices were face centered from 0 to about 55 at. % Eu, and body centered from about 60 to 100 at. % Eu. The miscibility gap for samples obtained by rapid cooling of the melt was only a few at. %. The variation of the lattice constants of the mixed crystals with a high Eu content roughly corresponded to that for bcc Ca (stable only at high temperatures), the volume of which does not differ appreciably from that of fcc Ca. The face-centered mixed crystals with a high Ca content behaved, as regards their lattice constants, as if the volume of Eu with a (hypothetical) face-centered crystal structure were a few percent more than the body-centered variety. Magnesium and Ca formed an Mg_2Ca phase, while in the system Mg/Sr, besides Mg_2Sr, the phase $Mg_{17}Sr_2$ and one or two phases in the range Mg_5Sr-Mg_4Sr also occurred. The existence of MgSr was controversial but it was possible to detect the following phases by x-ray methods in the system Mg/Eu: $Mg_{17}Eu_2$, one or two phases between Mg_5Eu and Mg_4Eu, Mg_2Eu, and MgEu (stable only below 500°C). In this behavior, therefore, Eu resembled Sr, and not Ca. The lattice constants of Mg_2Eu, which are given, are between those of Mg_2Ca and Mg_2Sr (closer to the latter). The values for $Mg_{17}Eu_2$ and $Mg_{17}Sr_2$ are particularly similar. However, the lattice constant of MgEu is not strictly compatible with the value for MgSr. Whereas $Mg_{17}Eu_2$ is practically volume additive, the formation of Mg_2Eu and MgEu is accompanied by a pronounced contraction; the electronegativities of Sr and Eu must therefore be somewhat different. Thus europium behaves toward magnesium as a typical alkaline earth metal, closely related to strontium. (BBB)

39178 THE OBSERVATION OF GAS ADSORPTION PHENOMENA BY REFLECTION HIGH-ENERGY ELECTRON DIFFRACTION. Sewell, P. B.; Cohen, M. (National Research Council, Ottawa). Appl. Phys. Letters, 7: 32-4(July 15, 1965).

The observations of monolayer adsorption phenomena on a nickel single-crystal surface, by grazing incidence reflection high-energy electron diffraction is reported. For the purpose of studying the growth of thin oxide films on metal surfaces by this method, a new demountable stainless steel, ultra-high-vacuum electron-diffraction apparatus was constructed. Using a collimated beam of 20-60 kv electrons, diffraction patterns from atomically smooth surfaces may be observed on a fluorescent screen while maintaining a base pressure below 2×10^{-10} torr. These diffraction patterns consist of a series of side lines, which are discussed. The structure develops during oxygen exposure of the nickel surface. The results agree with those of low-energy electron diffraction studies. It is hoped that new information can be obtained about surface reactions, in particular, the interface structure through several monolayers of adsorbed gas incorporated into a solid reaction product. (J.F.P.)

39179 A NEW STRUCTURE IN TANTALUM THIN FILMS. Read, Mildred H. (Bell Telephone Labs., Murray Hill, N. J.); Altman, Carl. Appl. Phys. Letters, 7: 51-2(Aug. 1, 1965).

X-ray diffraction patterns were obtained for β-tantalum. These show constant interplanar spacings and also a distinctive orientation relative to the substrate. Although the degree of orientation varies considerably from one which gives a pattern like a rotating single crystal with layers parallel to the surface of the substrate to one which shows the nearly complete rings of the random pattern, the center of the arcs have a constant position and subtend on the average an angle of 15°. The material has a fiber texture. The orientation is the same whether the film is sputtered on an amorphous, a polycrystalline, or a monocrystalline substrate, including metallic or nonmetallic materials. A wide-film x-ray camera, which can record reflections which lie at larger angles to the surface of the sample than the usual diffractometer detects, was used for more precise measurements of d values. (J.F.P.)

39180 REDUCTION OF THE ALKALI AND ALKALINE EARTH HALIDES IN HIGH-FREQUENCY DISCHARGES. I. HYDROGEN DISCHARGE. McTaggart, F. K. (Commonwealth Scientific and Industrial Research Organization, Melbourne). Australian J. Chem., 18: 937-48(July 1965).

The halides of the alkali and alkaline earth were reduced in a hydrogen discharge at 2450 Mc/s. The alkaline earth halides appear to react according to the overall equation $MCl_2 + H \rightarrow MCl + HCl$, and the monohalide subsequently disproportionates to an equimolar mixture of dihalide and metal. However, this reaction is not always in accord with thermodynamic predictions, which suggests that further elaboration of the reducing species is necessary. Halides of the alkali metals are reduced to metal, and the relative reaction rates range from 86 for lithium iodide to 1 for potassium bromide. Although for each metal, with the exception of potassium, the rate is least for the fluoride and greatest for the iodide as might be expected from the heats of formation, neither heat of formation nor bond energy appears to be the major factor involved in the rate of reduction, and an interesting relationship with the dimerization tendency of the halides is suggested. The role of halide sublimation rate and the distribution of energies in the active species are also discussed. (auth)

39181 REDUCTION OF THE ALKALI AND ALKALINE EARTH HALIDES IN HIGH-FREQUENCY DISCHARGES. II. THE ROLE OF ELECTRONS. McTaggart, F. K. (Commonwealth Scientific and Industrial Research Organization, Melbourne). Australian J. Chem., 18: 949-57 (July 1965).

The halides of Group I can be reduced to metals in low-pressure electrical discharges produced in hydrogen, helium, and nitrogen. Evidence is adduced to show that the active species are probably electrons, and that the energy conditions of the electrons are reflected in the effect of variation of gas pressure on the reduction rate. The effects of surface area and dimerization of the halides, the gas pressure, and power are also discussed, and the relationship between the reduction rate R and the power input P is shown to be $R = kP^{1.7}$, where k is a constant. (auth)

39182 CERIUM TETRAFLUORIDE. I. PREPARATION AND REACTIONS. Asker, W. J.; Wylie, A. W. (Commonwealth Scientific and Industrial Research Organization, Melbourne). Australian J. Chem., 18: 959-68 (July 1965).

Pure anhydrous cerium tetrafluoride is best prepared by fluorinating cerium dioxide at 350–500°C. A monohydrate can be obtained from aqueous solution in a variety of ways, but it cannot be dehydrated without decomposition. It loses water zeolitically in vacuum, showing relatively small changes in lattice parameters for loss of 70% of its water content. Thereafter the lattice collapses, forming well-crystallized cerium trifluoride and poorly crystallized anhydrous cerium tetrafluoride. The refractive indexes of anhydrous monoclinic cerium tetrafluoride were measured and its fluorine dissociation pressure at 500° shown to be less than 0.5 mm. At higher temperatures the tetrafluoride sublimes incongruenty, and at 835–841° it melts with extensive decomposition into a fluorine-poor liquid and a fluorine-rich vapor. Cerium tetrafluoride is easily reduced to the trifluoride by ammonia and by water vapor at low temperatures. At higher temperatures it is quantitatively converted by water vapor to cerium dioxide and hydrogen fluoride. When heated with cerium dioxide it is reduced to the trifluoride with liberation of oxygen. (auth)

39183 CERIUM TETRAFLUORIDE. II. THE SYSTEM CERIUM TETRAFLUORIDE–CERIUM TRIFLUORIDE. Asker, W. J.; Wylie, A. W. (Commonwealth Scientific

and Industrial Research Organization, Melbourne). Australian J. Chem., 18: 969-75(July 1965).

A tentative phase diagram is proposed that shows that the system CeF_4-CeF_3 is essentially eutectic in character. There is no solid solution in the terminal phases. The melting behavior of the tetrafluoride is complicated by its volatility and by its decomposition into a fluorine-rich vapor and a fluorine-poor liquid. Clarification of phase relationships requires that the system be regarded as portion of the system CeF_3-F_2. (auth)

39184 THE STRUCTURE OF PYROLYTIC CARBON DEPOSITED IN A FLUIDIZED BED. Bokros, J. C. (General Atomic Div., General Dynamics Corp., San Diego, Calif.). Carbon, 3: 17-29(July 1965). (GA-5163).

A variety of pyrolytic-carbon structures deposited in fluidized beds were categorized according to their structure. For a given coater configuration and flow rate, the structure of the deposits was found to vary systematically with bed temperature, gas composition, and bed surface area. The structures were divided into three groups according to their structure, i.e., laminar, isotropic, or granular. The structural data, together with kinetic measurements and published results on related processes, suggested that the low-temperature laminar structures were built up from large planar molecules that formed in the gas phase, then dehydrogenated, and, when deposited, aligned themselves parallel to each other and to the substrate. The isotropic low-density structures were formed at conditions where general gas-phase nucleation of droplets and soot occurred in the bed. The high-density granular structures form when there was orderly crystal growth over relatively large distances. (auth)

39185 X-RAY STUDIES OF GRAPHITE FORMED BY DECOMPOSING SILICON CARBIDE. Badami, D. V. (Morganite Research and Development Ltd., London). Carbon, 3: 53-7(July 1965).

The structural changes which occurred when single crystals of α-silicon carbide (6H) were heated in vacuo, were studied by using x-ray diffraction methods. The crystals were heated in an induction furnace for an hour to ~2280°C. This resulted in the formation of pseudomorphs, which retained the morphology of the original SiC crystals but had a complicated structure, which was made up of various stages in the development of a graphite lattice. A definite relation was found between the lattice of SiC and the structure of the resultant pseudomorph. The complex nature of the matrix is described and a possible mechanism of decomposition suggested. (auth)

39186 THE STRESS-STRAIN RELATIONSHIPS OF POLYCRYSTALLINE GRAPHITE UNDER COMPRESSION UP TO FRACTURE. Jenkins, G. M. (Berkeley Nuclear Lab., Gloucestershire, Eng.). Carbon, 3: 93-4(July 1965).

Relations to predict the strain response of graphite were compared. It was concluded that no predictions of stresses/strains to fracture can be made from the initial stress-strain relations. The main test of plastic flow was considered to be nonrecoverable permanent set. Permanent set was observed in graphite but it was wholly recoverable by suitable thermal cycling. It was concluded, that before slip is completed, before truly plastic flow occurs, the stress buildup is such that cracking occurs, first locally, and then in concert with others to form a major fracture. This was supported by the appearance of the major fractures both in compression and tension, which are typical of a brittle material even at 3% strain. Furthermore, even at this total strain of 3%, ~2% was recovered instantaneously on removing the load. (F.J.H.)

39187 TIME-DEPENDENT STRENGTHENING OF GRAPHITE IN TENSION AT 2500 deg C. Smith, Morton (Los Alamos Scientific Lab., N. Mex.). Carbon, 3: 96-7 (July 1965). (LA-DC-6873).

Experiments previously demonstrated an effect on the ultimate tensile strength of transverse specimens of molded graphite produced by extending them slowly in tension at 2500°C in advance of tensile testing at the same or at somewhat lower temperatures. It was concluded that the heating process would be strongly dependent on time under load, and experiments to study this time dependence were carried out. Results were consistent with the hypotheses that, even at 2500°C, permanent extension of graphite in tension was accomplished primarily by formation and opening of interlamellar cracks, and that, with time under load at elevated temperature, these cracks were repaired by stress-directed mass transport of carbon. (F.J.H.)

39188 LONGITUDINAL TENSILE PROPERTIES OF H4LM GRAPHITE EXTENDED TO -269 deg C. Eash, D. T. (Los Alamos Scientific Lab., N. Mex.). Carbon, 3: 97-8 (July 1965). (LA-DC-7053).

The tensile testing range for H4LM graphite was recently extended to -269°C. Three specimens each were tested in air at room temperature, in boiling liquid hydrogen (-253°C), and in boiling liquid helium (-269°C), employing a nominal engineering strain rate of 0.005 in./min. There was no significant change in the longitudinal tensile strength of graphite over the temperature range -269 to 500°C. The usual 0.1 to 0.2% of permanent elongation prior to fracture was observed for all of these specimens. (F.J.H.)

39189 A NEW STANNIDE OF VANADIUM V_2Sn_3. Jouault, Francoise; Lecocq, Pierre (Universite Paris). Compt. Rend., 260: 4777-9(May 3, 1965). (In French).

A new compound V_2Sn_3 with a $CuMg_2$ structure was obtained by diffusion of the pure constituents taken in the powdered form. The total reaction requires an anneal or 15 days at 600°C. The crystallographic properties and diffraction patterns are given. (J.S.R.)

39190 AMORPHOUS ZIRCONIA AND NON-STOICHIOMETRIC ZIRCONIA. Livage, Jacques; Mazieres, Charles (E.N.S.C.P., Paris). Compt. Rend., 260: 5047-8(May 10, 1965). (In French).

The heating under vacuum of amorphous zirconium oxide of large specific surface led to a sub-stoichiometric body, black in color. When this black zirconia was heated in air, it again became white and regained its weight. In evaluation of the non-stoichiometric compound, the result depended on the temperature, the length of treatment, and the quality of the vacuum. X-ray diagrams on the black zirconia did not differ from those obtained on the usual white phases. Coloration change was reversible. No color change could be detected with calcined zirconia. (J.S.R.)

39191 AMERICIUM. Ranschoff, M. J. A. Energie Nucl., 7: 246-7(June 1965). (In French).

A brief review is presented on the characteristics, uses, sources, production, and economics of americium and its isotopes. (P.C.H.)

39192 HEAT RESISTANCE PROPERTIES OF TITANIUM-NIOBIUM-CHROMIUM ALLOYS. Shakhova, K. I.; Budberg, P. B. Izv. Akad. Nauk SSSR, Metal., No. 2, 128-33(Mar.-Apr. 1965). (In Russian)

Studies of Ti-Nb-Cr alloy heat resistance after annealing at various temperatures showed that Cr is the best stabilizer of single phase β alloys. Binary and ternary phase alloys were strengthened by enrichment of the γ phase by niobium. The γ-phase alloys had the maximum absolute hardness and were not affected by temperatures up to 1000°C. (R.V.J.)

39193 THERMAL HARDNESS OF β ALLOYS OF Ti-Mo-Cr-Fe-Al SYSTEM. Ageev, N. V.; Glazunov, S. G.; Petrova, L. A.; Tarasenko, G. N.; Grankova, L. P. Izv. Akad. Nauk SSSR, Metal., No. 2, 141-6(Mar.-Apr. 1965). (In Russian)

Thermal resistance of annealed and forged Ti-Mo-Cr-Fe-Al alloys was measured at 20 to 1000°C and the hardness was tested at 20, 500, and 800°C under 1 kg pressure load for 1, 5, 15, and 30 min. The annealed alloys had higher hardness points than forged alloys. An analysis of the thermal hardness curves showed high thermal resistance of all Ti-Mo-Cr-Fe-Al alloys at 20 to 600°C. (R.V.J.)

39194 CONSTITUTION DIAGRAM AND PROPERTIES OF Nb–Mo–Si ALLOYS. Savitskii, E. M.; Baron, V. V.; Bychkova, M. I.; Bakuta, S. A.; Gladyshevskii, E. I. Izv. Akad. Nauk SSSR, Metal., No. 2, 159-66(Mar.-Apr. 1965). (In Russian)

Microscopic, thermal, and x-ray analysis of 117 Nb–Mo–Si systems revealed six polythermal cross sections ($NbSi_2$–$MoSi_2$, NbSi–MoSi, Nb_3Si_3–Mo_5Si_3, Nb_3Si–Mo_3Si, Nb–$MoSi_2$, (Nb, Mo)–Si). A diagram of phase equilibriums at 800°C was obtained. Ternary compounds of the system were not found. An analysis of the heat resistance and hardness curves showed that the maximum hardness was in a low modification of α–Nb_5Si_3 and maximum heat resistance was shown by $MoSi_2$ alloyed with small amount of Nb(0.5 wt %). (R.V.J.)

39195 ON LANTHANUM GERMANIDES. Lyutaya, M. D.; Goncharuk, A. B. (Inst. of Problems in Study of Materials, Academy of Sciences, USSR). Izv. Akad. Nauk SSSR, Neorgan. Materialy, 1: 326-9(1965). (In Russian).

Preparation of $LaGe_2$, LaGe, and La_5Ge_3 by melting metallic lanthanum (99.2% La) and germanium (99.9% Ge) in an arc furnace with tungsten electrodes in an argon atmosphere is described. The feasibility of producing various rare earth germanides was illustrated using lanthanum oxide transformed into lanthanum digermanate by thermogermanium treatment at 1500°C for an hour. It is shown that $LaGe_2$ is easily decomposed in water while LaGe and La_5Ge_3 are quite stable in water. (R.V.J.)

39196 SOLUBILITY OF CERTAIN TRANSITION METALS IN THE V_3Si COMPOUNDS AND THEIR INFLUENCE OF THE TRANSITION OF THE COMPOUNDS INTO A SUPERCONDUCTING STATE. Savitskii, E. M.; Baron, V. V.; Efimov, Yu. V.; Gladyshevskii, E. I. (Baikov Inst. of Metallurgy, USSR and Lvov State Univ.). Izv. Akad. Nauk SSSR, Neorgan. Materialy, 1: 354-61(1965). (In Russian).

Microstructure, microhardness, and x-ray analyses were made of transition metal (Ce, Cr, La, Mn, Mo, Nb, Pd, Re, Ti, and Zr) solubility in V_3Si and their influence on the temperature of transition of these elements into superconducting state. The binary compound V_3Si had a maximum critical transition temperature into the superconducting state. Replacement of vanadium atoms in the compound lattice by any transition metal reduced in the T_K point. (R.V.J.)

39197 EMISSION OF POTASSIUM IONS FROM MOLYBDENUM AT ELEVATED TEMPERATURES. Lichtman, David; Kirst, T. R. (Honeywell Research Center, Hopkins, Minn.). J. Appl. Phys., 36: 2123-4(July 1965).

Thermionic emission of K ions from a heated Mo ribbon was studied at 30 to 1100°C, using a mass spectrometer. Ion current maxima were observed at about 800°C and beginning at 1000°C and continuing throughout the range investigated. The type and nature of emission are similar to previous results for a W filament. Thus, the pulse type of thermionic ion emission is further verified and extended to Mo ribbon material. (M.J.T.)

39198 DYNAMIC ELASTIC PROPERTIES OF POLYCRYSTALLINE TUNGSTEN, 24°-1800°C. Lowrie, Robert; Gonas, A. M. (Union Carbide Research Inst., Tarrytown, N. Y.). J. Appl. Phys., 36: 2189-92(July 1965).

The velocities of ultrasonic shear and compressional waves in polycrystalline tungsten (99.4% dense) were measured by a pulse-echo technique from 24 to 1800°C. Adiabatic elastic constants were calculated from these velocities with accuracies of ±0.25% to ±0.65%, and corrections were applied to obtain equations for the elastic constants of fully dense tungsten as a function of temperature. (auth)

39199 MAGNETOSTRICTION OF NONFERROMAGNETIC METALS. Anderholm, N. C.; Peck, E. R. (Northwestern Univ., Evanston, Ill). J. Appl. Phys., 36: 2293-6 (July 1965).

Magnetostriction measurements, made with an interferometric dilatometer at room temperature, are reported for Bi, Sb, W, Nb, Mo, Ta, and V. The measurements were made using magnetic fields to 30 kG on high-purity single crystals. The results for Bi agree qualitatively with those of Kapitza and Shoenberg. Generally, the Sb results were smaller. The values obtained for the transition elements were the smallest of those measured, but quantitative information on their magnetostrictive properties was obtained. (auth)

39200 THERMAL EXPANSION OF A URANIUM MONOCARBIDE–ZIRCONIUM MONOCARBIDE SOLID SOLUTION. Kempter, Charles P.; Merryman, Roy G. (Los Alamos Scientific Lab., N. Mex.). J. Chem. Phys., 43: 1736-8 (Sept. 1, 1965). (LA-DC-7084).

The thermal expansion of a polycrystalline $(U_{0.30}, Zr_{0.70})C_{0.97}$ solid solution was determined between 25 and 982°C by means of a high-temperature x-ray diffraction technique. For the range 25 to 1000°C the average linear thermal-expansion coefficient was 7.78×10^{-6}/°C. The 25°C lattice parameter was 4.7822 Å, the calculated density 8.94 g/cm³, and the diamond pyramid hardness 1800 kg/mm². (auth)

39201 THERMAL EXPANSION OF TANTALUM MONOCARBIDE TO 3020 deg C. Kempter, C. P.; Nadler, M. R. (Los Alamos Scientific Lab., N. Mex.). J. Chem. Phys., 43: 1739-42(Sept. 1, 1965). (LA-DC-7090).

The dilatometric thermal expansion of a tantalum monocarbide rod was measured from 21 to 3020°C in a 20 psig argon atmosphere using a split-beam optical comparator. The linear thermal expansion from 20 to 3000°C was found to be 2.5%, which correspond to an average coefficient of linear thermal expansion of 8.4×10^{-6} per °C. No evidence of a high-temperature phase change was found. (auth)

39202 A REVIEW OF MECHANICAL TWINNING IN BODY-CENTRED CUBIC METALS AND ITS RELATION TO BRITTLE FRACTURE. Reid, C. N. (Univ. of Birmingham, Eng.). J. Less-Common Metals, 9: 105-22(Aug. 1965).

Mechanical twinning in body-centred cubic crystals was reviewed, with particular reference to the circumstances under which twins are associated with brittle cracks. Several features of the twinning process appeared to be conducive to crack formation, such as the difficulties of accommodation that arise at intersections and noncoherent boundaries, and the very rapid growth of twin lamellae. Cracks were observed at the intersections of twins with grain boundaries and other twins, and microcracks were seen within twinned regions. Also, the twin-matrix interface is sometimes a preferred path for crack propagation. However, it is only in single crystals stressed in tension along ⟨100⟩ directions that twins appeared to nucleate macroscopic fractures. In all other cases, the source of the main fracture was unknown, although it is clear that twins can create purely local cracks. (auth)

39203 SPECIFIC ELECTRICAL RESISTIVITY AND INTERSTITIALS IN TANTALUM CRYSTALS. van Torne, L. I. (Martin Co., Orlando, Fla.). J. Less-Common Metals, 9: 152-5(Aug. 1965).

The details of the calculation relating electric resistivity at 4.2°K to the interstitial level in a Ta crystal are given. The interstitial impurities are major scatterers at 4.2°K. The most probable interstitial impurities in Ta are carbon, nitrogen, and oxygen. The number of conduction electrons per unit volume in Ta was found to be $n = 4.96 \times 10^{22}$. The specific resistivity of a tantalum crystal after 3 electron beam zone passes was observed to be 1.41×10^{-22} stat Ω-cm. (F.J.H.)

39204 THE SOLUBILITY OF SODIUM IN SILICON. McCaldin, J. O.; Little, M. J.; Widmer, A. E. (North American Aviation Science Center, Thousand Oaks, Calif.). J. Phys. Chem. Solids, 26: 1119-23(July 1965).

Silicon crystals were exposed to the liquid solution of Na saturated with Si at 800°C for about one week. Penetration of Na into the crystals was measured by neutron activation analysis. Sodium concentrations of the order of 3×10^{17} cm^{-3} were found in a this ($\sim 50\ \mu$ thick) surface layer; in the interior of the specimens, the Na concentration was at

or below the detection limit of $\sim 10^{15}$ cm^{-3}. No n-type regions could be found in the Na-doped material by thermoelectric type testing, in striking contrast to the case of ion-injected Na, where donor concentrations of $\sim 10^{20}$ cm^{-3} are observed. It was concluded that the solubility of Na in Si at 800°C is of the order of 3×10^{17} cm^{-3}, but that under the nearly equilibrium conditions used less than one per cent of this is present as interstitial donors. (auth)

39205 THE GINZBURG-LANDAU PARAMETER OF TANTALUM. Buchanan, J.; Chang, G. K.; Serin, B. (Rutgers Univ., New Brunswick, N. J.). J. Phys. Chem. Solids, 26: 1183-4(July 1965).

The numerical value of the Ginzburg-Landau (G-L) parameter was determined for Ta by two methods. The slope of the upper critical field curve $(dH_{c2}/dT)T_c$ was divided by $\sqrt{(2)}$ $(dH_c/dT)T_c = 452$ G/°K, where H_c is the critical field of very pure Ta. This method assumes that the slope of the thermodynamic critical field curve at T_c is insensitive to impurities. Also, the value of $K(T) = H_{c2}/\sqrt{(2)}H_c$ was calculated assuming that the reduced thermodynamic critical curve $h(t) = H_c(T)/H_c(O)$ for the impure specimens is the same function of $t = T/T_c$ as for very pure specimens. The values so determined were found to be self-consistent. From these data, it was concluded that $K_p = 0.42 \pm 0.02$, which implies that Ta specimens will never have Type II superconducting properties. (P.C.H.)

39206 NEW ALLOYS FOR ATOMIC REACTOR MATERIALS. Mistuzuma, Yoshiseki. Kogyo Reametaru, No. 23, 33-41(1963). (In Japanese)

Different properties of atomic reactor fuel cladding materials are described. The cladding materials are used for reactors, such as aluminum alloy used for low-temperature-water research reactors, SAP parts used for CO_2-cooled power reactors, and zirconium or stainless steel used for light-water-cooled reactors. Niobium, vanadium, niobium alloys, and beryllium were studied. The relation between thermal neutron absorption of various fuel cladding materials and cladding thickness is shown. The corrosion resistance, high-temperature strength, and other properties of various alloys of aluminum, magnesium, zirconium, and niobium, which have low thermal neutron absorptions and can be used as cladding materials are also described. (F.J.H.)

39207 THE CRYSTAL STRUCTURE OF $ThGa_2$ AND $RuIn_3$. Holleck, H.; Nowotny, H.; Benesovsky, F. (Universitaet, Vienna). Monatsh. Chem., 95: 1386-90(1964). (In German).

$ThGa_2$ was prepared by heating mixtures of Th powder and finely divided Ga in sealed quartz ampoules at 850°C for 150 hours. This phase was discovered in samples containing 50%, 60%, and 66% Ga; the sample with 75 at. % Ga showed another phase in addition to $ThGa_2$, but it was not characterized further. Interpretation of the powder pattern for the 66% sample led to a tetragonal cell with the parameters $a = 4.23_7$ Å, $c = 14.67$ Å, and $c/a = 3.46_2$. This and the intensities indicated an α-$ThSi_2$ structure, which was supported by comparison of the intensities with those of $ThGe_2$. The adoption of the parameter $z = 0.415$ determined nearest neighbor distances as Ga-Ga, 2.42 and 2.50 Å, and Th-Ga, 3.21 and 3.24 Å. Mixtures of Ru and In were heated in the same way for 300 hours at 850°C. In the 75% In mixture a phase with the $CoGa_3$ structure was found, $RuIn_3$, with $a = 6.99_3$ Å, $c = 7.24_9$ Å, and $c/a = 1.03_5$. The x-ray density was 8.32 g/cm^3. A hexagonal closest packed, Ru-rich phase was observed with $a = 2.97_1$ Å, $c = 4.68_9$ Å, and $c/a = 1.57_8$. It was possibly Ru_3In with the DO_{19} type with statistical distribution; with ordering the a axis was doubled. This phase is not stable and decomposed on prolonged heating to Ru and $RuIn_3$. (BBB)

39208 THE H PHASES: Ti_2CdC, Ti_2GaC, Ti_2GaN, Ti_2InN, Zr_2InN, AND Nb_2GaC. Jeitschko, W.; Nowotny, H.; Benesovsky, F. (Universitaet, Vienna). Monatsh. Chem., 95: 178-9(1964). (In German).

Mixtures of the monocarbide and mononitride with transition metals were prepared in stoichiometric amounts and sealed in quartz ampoules. Powder patterns of the products indicated the presence of the Cr_2AlC-type (H phase) structure. Following are the temperature of preparation (°C), time of preparation (hours), lattice parameters a (Å), c (Å), and c/a, and the x-ray density (g/cm^3): Ti_2CdC, 750, 900, 3.099, 14.41, 4.653, 6.10; Ti_2GaC, 850 + 750, 800 + 200, 3.064, 13.305, 4.342, 5.45; Ti_2GaN, 850, 850, 3.004, 13.30, 4.428, 5.73; Ti_2InN, 850, 500, 3.074, 13.975, 4.547, 6.52; Zr_2InN, 850, 500, 3.277, 14.84, 4.526, 7.49; and Nb_2GaC, 750, 800, 3.131, 13.565, 4.332, 7.71. The ratio c/a decreased as the second metal moves from 2 b to 3 b to 4 b. All nitrides showed a greater c/a ratio than the analogous carbides, but had smaller unit cells. This was related to the more important defect structure in oxides relative to nitrides and in nitrides relative to carbides. The decrease in c/a ratio relative to close metal packing indicated that metalloid atoms are fitted in the double layers of the transition metals. (BBB)

39209 CRYSTAL CHEMICAL INVESTIGATIONS IN THE SYSTEMS (Ti, Nb, Ta, Mo, W)-(As, Sb). Boller, H.; Nowotny, H. (Universitaet, Vienna). Monatsh. Chem., 95: 1272-82(1964). (In German).

Starting materials were sealed in evacuated quartz ampoules and heated between 48 and 300 hr at 700 to 1100°C. X-ray powder patterns were obtained from the samples. In the system Mo-As, the compounds Mo_5As_4 and MoAs were found; the latter crystallizes in the B 31 type, with lattice constants $a = 5.98_8$, $b = 3.36_8$, and $c = 6.41_7$ Å. In the W-As system, a compound corresponding to the monoclinic Mo-As compound has $a = 7.99$, $b = 3.28$, and $c = 6.88$ Å, and $\beta = 99°12'$. No similar compounds in the Mo-Sb and W-Sb systems were noted. In the systems Nb-Sb and Ta-Sb, Nb_5Sb_4 and Ta_5Sb_4 were found. The lattice constants a (Å), c (Å), and c/a are given for Mo_5As_4, $(W,Ti)_5As_4$, Nb_5Sb_4, and Ta_5Sb_4 respectively as follows: 9.60, 3.278, 0.341, 9.572, 3.306, 0.345, 10.315, 3.572, 0.346; and 10.234, 3.543, 0.346. These compounds have the Ti_5Te_4 structure; they have a close packed structure with a high coordination number around the metal atom (12 to 14) and two As-As contacts, widely separated (3.3 to 3.5Å). (BBB)

39210 OBSERVATIONS OF THE MOESSBAUER EFFECT IN A MONOLAYER OF ^{119}Sn ON PLATINUM. Bowles, B. J.; Cranshaw, T. E. (Atomic Energy Research Establishment, Harwell, Berks, Eng.). Phys. Letters, 17: 258-9(July 15, 1965).

The Mössbauer effect of ^{119}Sn on platinum was studied in order to distinguish between the hypotheses of monolayer formation by adsorption in the electrical double layer and actual plating of a monolayer on to the platinum substrate. A Mössbauer resonance absorption line was observed and is shown together with results obtained from bulk metallic tin; and data derived from the spectra by a fitting program are given. The spectra showed that the monolayer of tin was not held in the double layer but that it was similar to metallic tin. (L.B.S.)

39211 LONG-RANGE INTERIONIC FORCES IN METALLIC LITHIUM. Meyer, A.; Nestor, C. W. Jr.; Young, W. H. (Oak Ridge National Lab., Tenn.). Phys. Letters, 18: 10-11(Aug. 1, 1965). (ORNL-P-1441).

A method for finding pseudo-atom phase shifts is outlined and is used to interpret the result of Johnson, who derived a long-range ion-ion potential for liquid lithium from neutron diffraction data. (D.C.W.)

39212 HYPERFINE FIELD OF ^{57}Fe IN Cu-Mn ALLOYS Johnson, C. E.; Cranshaw, T. E.; Ridout, M. S. (Atomic Energy Research Establishment, Harwell, Berks, Eng.). Phys. Letters, 18: 14-16(Aug. 1, 1965).

The Mössbauer spectra of ^{57}Fe in low concentrations in Cu-Mn alloys were measured in order to understand observations made on the hyperfine fields for Cu-Fe alloys using the Mössbauer effect. (D.C.W.)

39213 MEASUREMENT OF THE MAGNON DISPERSION RELATION OF IRON. Shirane, G. (Brookhaven National Lab., Upton, N. Y.); Nathans, R.; Steinsvoll, O.; Alperin, H. A.; Pickart, S. J. Phys. Rev. Letters, 15: 146-8(July 26, 1965).

The magnon dispersion curve for iron was investigated

using the diffraction method in conjunction with polarized neutrons. It was found that the dispersion curve deviates considerably from the quadratic law, $\hbar\omega = Dq^2$, even for relatively small wave vectors q, indicating a long-range magnetic interaction in this metal. (D.C.W.)

39214 THE METALLOGRAPHY OF HIGH-MELTING METALS. II. INTERMETALLIC COMPOUNDS. Benesovsky, Friedrich; Ihrenberger, Albin (Metallwerk Plansee AG., Reutte/Tirol, Austria). Prakt. Metallog., 2: 89-94 (June 1965). (In German)

The electrolytic lap polishing method is an excellent aid in the identification of phases in unknown binary and multiple systems of refractory transition metals and metalloids. As was shown by numerous examples, clear, easily interpreted micrographs are obtained in minimum time. (tr-auth)

39215 THE THERMAL CONDUCTIVITY OF STABILIZED ZIRCONIA AT HIGH TEMPERATURES. Nguyen Duc, X. (Institut Francais du Petrole, Rueil-Malmaison, France). Rev. Hautes Temp. Refractaires, 2: 55-63(Jan.-Mar. 1965). (In French)

The thermal conductivity of zirconia from different sources was investigated as a function of temperature up to about 1500°C. Samples in the form of blocks, thin layers, and powder were used. (D.C.W.)

39216 SOME RELATIONS BETWEEN THE STRUCTURE AND PHYSICAL AND MECHANICAL PROPERTIES OF THREE GRAPHITES. Smith, Edward A. (Schmiertechnik, 11: 158-63(May-June 1964). (In German)

The results of x ray diffraction and chemical decomposition studies are given for three commercial graphites, two artificial and one natural. The following properties of the graphites were studied: characteristic size of the powder particles, pulverization velocity in a ball mill, combustion velocity, coefficient of friction and sealing rate in lubrication, and electrical conductivity of coatings on glass. It was shown that the size of the graphite crystallites affect certain utilization properties. Some examples for the relation between these properties and various engineering applications are given. It is indicated that in certain applications it is necessary not only to specify the chemical purity but also the crystallite size. (tr-auth)

39217 EXPERIMENTAL DETERMINATION OF NIOBIUM ENTHALPY IN THE TEMPERATURE RANGE FROM 600 TO 2600 deg K. Kirrilin, V. A.; Sheindlin, A. E.; Chekhoskoi, V. Ya.; Zhukova, I. A. Teplofiz. Vysokikh Temp., 3: 395-400(May-June 1965). (In Russian).

Results of experiments for determining the enthalpy of niobium by the method of mixing in the temperature range 592 to 2587°K are presented, and an empirical equation for the calculation of enthalpy and true heat capacity in the temperature range 273.15 to 2740°K is given. Energies of formation of vacancies and concentrations of vacancies in niobium are determined on the basis of the measured values of enthalpy at high temperatures. (tr-auth)

39218 MEASUREMENT OF THE SPECIFIC HEAT OF Zr–Rh ALLOYS BETWEEN 0.9 AND 12°K. Dummer, Gerald (Technische Hochschule, Karlsruhe). Z. Physik, 186: 249-63(1963). (In German).

The specific heats of Zr–Rh alloys were measured between 0.9 and 12°K and at atomic percent Rh concentrations between 0 and 8. The transition temperatures (T_c), the electronic specific heats (γT), the electronic specific heats of superconducting state and the lattice specific heats $[\alpha(T/\Theta)^3]$ are calculated from the specific heat curves. The specimens with concentrations up to 3 at % Rh are inhomogeneous. No sharp superconducting transitions are observed. The structure of the specimens between 3 and 7 at % Rh is body centered cubic. In this phase Rh is dissolved nearly homogeneously. In this case the values of T_c, γ, and Θ are all rapidly varying and nearly linear functions of the atomic fractional Rh concentration. With the assumption that the measured γ-values are connected with the density of electronic states according to the relation of the free electron gas one gets a surprising strong dependence of the interaction parameter responsible for superconductivity as a function of the Rh concentration. This change of the interaction parameter is essentially smaller, if additional terms of the specific heat linear in T do not allow to determine the density of electronic states directly from γ. The superconducting state electronic specific heats obey the exponential law of the BCS theory. (auth)

39219 CORRELATION OF THERMODYNAMIC PROPERTIES AND ATOMIC TRANSPORT IN THE URANIUM DIOXIDE PHASE. Thorn, R. J.; Winslow, G. H. (Argonne National Lab., Ill.). Vienna, International Atomic Energy Agency, 1965, Preprint No. SM-66/82, 34p. (CONF-650704-28). ORINS.

From IAEA Symposium on Thermodynamics, Vienna.

The correlations of thermodynamic properties with atomic transport must be based upon a framework that is quantitative and circumspective. A model within this framework for the uranium dioxide phase is presented as a guide for studies relating basic (atomic) properties to the problems encountered in oxidation, sintering, phase separation, fission gas release, etc. The theoretical bases for the correlations are reviewed along with data pertinent to the correlations. A quantitative analysis was made of the thermodynamic and transport properties of the uranium dioxide phase. The theory by Rice et al. when combined with the thermodynamic theory of defects yielded for the self-diffusion coefficient, $D = \gamma a^2 \nu \theta_i (1 - \theta_i) e^{-U_\theta/RT} e^{-\sum U_j/RT}$, in which γ is a structural factor for a lattice with parameter a, ν is the mean vibrational frequency of the lattice, U_θ is the energy of the diffusing species vibrating in phase with its shell of nearest neighbours with an oscillating barrier expressed in terms of ΣU_j. All these quantities are related to the lattice dynamics and determine principally such macroscopic properties as specific heat and modulus of elasticity. The fraction θ_i of the interstitial sites occupied by ions is obtainable via the equation $\ln(\theta_i/1-\theta_i) - (E_i/RT) - (2\theta_i E_{ii}/RT) - \ln q_i = \ln(1-\theta_v/\theta_v) - (E_v/RT) + (2\theta_v E_{vv}/RT) - \ln q_v$, in which θ_v is the fraction of ion sites vacant, E_i(or E_v) is the energy required to produce an interstitial (or vacancy), E_{ii}(or E_{vv}) is the energy of interaction between interstitials (or vacancies) and q_i(or q_v) is the vibrational partition function for the defect. For the uranium dioxide phase the following values were obtained for the model: $E_i = 94.723$, $E_{ii} = 5.56$, $E_v = 132.887$, and $E_{vv} = 15.036$ (all in kcal/mol). These numbers correspond to $\theta_i = 0.00732$ and $\theta_v = 0.00216$ at 960°C for $UO_{2.003}$. The values of θ_i and θ_v vary with temperature and composition so as to predict measurements of the self-diffusion of oxygen obtained by Auskern and Belle. The correlation with the self-diffusion of oxygen in thoria (as a norm for ideally stoichiometric UO_2) is within experimental errors. In addition the self-diffusion of nitrogen in stoichiometric uranium dioxide appears to be interpretable on the basis of this same model. (auth)

39220 DIFFUSION, STRESS AND THE RATES OF PROCESSES LEADING TO DEFORMATION OF NUCLEAR FUEL ELEMENT CLADDING. Gittus, J. (United Kingdom Atomic Energy Authority, Springfields, Lancashire, Eng.). Vienna, International Atomic Energy Agency, 1965, Preprint No. SM-66/34, 17p. (CONF-650704-21). ORINS.

From IAEA Symposium on Thermodynamics, Vienna.

Stresses produced by the fuel, the coolant, and by temperature gradients can cause time-dependent distortion of the cladding on reactor fuel elements. A model, relating the rate of such deformations with the stress and the self-diffusion coefficient, was formulated. Based on dislocation theory and supported by electron microscopy, the model leads to an equation of the following form: $\dot{\epsilon} = \lambda D_\theta P_{\sigma,\theta}$ (1), where $\dot{\epsilon}$ is the uniform rate of deformation, D_θ is the self-diffusion coefficient of the prevailing temperature, $P_{\sigma,\theta} = (1/\sigma_s\sqrt{2\pi}) \int_{-\infty}^{\log 1\infty} \exp[-\frac{1}{2}(x - \log_{10}\sigma^m/\sigma_s)^2]\,dx$, $\lambda = 1/[1 - P\sigma,_\theta]$, σ is the applied stress, and σ_s and σ_m are materials constants. In the case of the cladding materials type 316 stainless steel and Magnox AL80, equation (1) fits the data over their full range (ten orders of magnitude) to within the

limits of experimental error. The model is in effect an extension to the solid state of Eyring's original process-rate theory of liquid viscosity, to which it reduces when λ is set at the interatomic spacing with $P\sigma_{,0}$ a function of exp [σ/kT]. It supports the view that metals and alloys comprise a continuum of normally distributed potential energy, which dislocations penetrate at a rate determined by the applied stress and circumvent at a rate determined by the rate of vacancy diffusion to jogs. (auth)

39221 DEFECT EQUILIBRIA OF PuO_{2-x}, 1100 deg C TO 1600 deg C. Atlas, L. M.; Schlehman, G. J. (Argonne National Lab., Ill.). Vienna, International Atomic Energy Agencyl 1965, Preprint No. SM-66/79, 18p. (CONF-650704-27). ORINS.

From IAEA Symposium on Thermodynamics, Vienna.

The variation of oxygen content and electrical resistivity (σ) with oxygen pressure ($p(O_2)$) was measured for PuO_{2-x} between 1100 and 1600°C. Procedures included equilibrating a ceramic specimen with H_2-H_2O-He mixtures, reoxidizing the specimen to $PuO_{2.00}$ in a fixed volume of O_2-He mixture, and determining the O_2 content of the oxidizing atmosphere with a katharometer. An alternative procedure consisted of equilibrating the specimen in a fixed volume of various H_2-H_2O-Ar mixtures and monitoring the concentrations of H_2 and H_2O. Experimental results are presented as plots of $\Delta G^{\circ}_{O_2}$ (the relative partial molar-free energy of oxygen) vs log x, $\Delta G^{\circ}_{O_2}$ vs temperature, log x vs log $p(O_2)$ and log σ vs log $p(O_2)$. The log-log plots of x and σ against $p(O_2)$ were linear over a wide composition range and at each temperature the composition line had a steeper slope than the conductivity line. A mass-action analysis of the data is presented, which relates the slope difference to a variation of the activity coefficient of trivalent plutonium ions with the concentration of defects. At 1100, 1200, and 1600°C, the defects were thought to be primarily quadruply dissociated interstitial plutonium atoms. A rise of temperature from 1200 to 1300°C appeared to produce an appreciable concentration of triply dissociated interstitials; an explanation is offered for this unusual retrograde pattern of dissociation. Oxygen activity data at 1200°C were used to determine an average energy of interaction between the interstitials and reduced plutonium ions (≈−10,400 to −10,900 cals/gram atom of Pu_i-Pu_i pairs). Evaluation of this energy permitted theoretical calculations of the temperature and composition at which homogeneous PuO_{2-x} should transform into separate phases. The calculated values are 675°C for $PuO_{1.75}$ as compared to experimental values of 650°C for $PuO_{1.83}$. (auth)

39222 NONSTOICHIOMETRY OF UO_2-CeO_2: THE SYSTEM $UO_2-CeO_2-CeO_{1.5}$ AT 900−1200 deg C. Hoch, M.; Furman, F. J. (Univ. of Cincinnati). Vienna, International Atomic Energy Agency, 1965, Preprint No. SM-66/3, 18p. (CONF-650704-12). ORINS.

From IAEA Symposium on Thermodynamics, Vienna.

The substoichiometric fluorite UO_2-CeO_2 phase, the behavior of the system $U_yCe_{1-y}O_{2-x}$, was investigated. Though UO_2 and CeO_2 are completely miscible, and in the $CeO_2-CeO_{1.5}$ system the fluorite phase extends to $CeO_{1.81}$, the $UO_2-CeO_2-CeO_{1.5}$ system is characterized by a large two-phase region, where two fluorite-type structures, one CeO_2-rich, the other UO_2-rich, coexist. Only in the UO_2-rich corner of the ternary system is a noticeable single-phase region present. This is in contrast to the $CeO_2-UO_{2.67}$ system where a large single-phase region exists. The oxygen activity as a function of composition x was measured in $U_yCe_{1-y}O_{2-x}$ (y = 0.85, 0.75 and 0.65) at 900°C using H_2/H_2O and metal/metal oxide equilibria. In all cases the oxygen activity increased extremely rapidly with decreasing x; the behavior of the system resembled that of dilute solutions of UO_{2+x} in ThO_2. Both systems can be explained by assuming defect complexes: a vacancy bound to two Ce^{3+}, an interstitial oxygen bound to two U^{5+}. (auth)

39223 IMPROVEMENTS RELATING TO ZIRCONIUM BASE ALLOYS. Winton, John; Murgatroyd, Robert (to United Kingdom Atomic Energy Authority). British Patent 997,761. July 7, 1965. Filed Mar. 27, 1963.

A method for strengthening a Zr base alloy containing 1 to 4 wt % Nb consists of introducing oxygen into the alloy to give an oxygen content in the range of 1000 to 2000 ppM by weight. The alloy is quenched in water from a temperature of not less than 875°C to effect conversion predominately to the beta phase and subsequently aged at a temperature in the range of 475 to 525°C for a period in excess of two hours. (B.L.M.)

39224 COLD WORKABLE COLUMBIUM BASE ALLOY. Schussler, Mortimer (Union Carbide Corp.). U. S. Patent 3,188,207. June 8, 1965. Filed Mar. 8, 1963.

A high strength Nb base alloy consists of about 10% W, 2.5% Zr, a maximum of 0.01% C, and a maximum of 0.04% in the aggregate of O_2, H_2, and N_2. The alloy can be cold rolled into thin sheets having an excellent combination of ductility, fabricability, weldability, and strength at temperatures of −325 to 3000°F. The alloy can be machined by conventional methods and can be cold rolled into foils as thin as 0.0005 in. (B.L.M.)

Radiation Effects

***See also* CHEMISTRY — Radiation Chemistry.**

Refer also to abstracts 38755, 38822, 39125, 39129, 39166, 40103, and 40195.

39225 (AFCRL-65-286) CALCULATED CROSS SECTIONS FOR ATOMIC DISPLACEMENTS PRODUCED BY ELECTRONS IN THE 1.0-3.0 Mev ENERGY RANGE. Physical Sciences Research Papers No. 99. Burke, Edward A.; Grossbard, Neil J.; Lowe, Lester F. (Air Force Cambridge Research Labs., L. G. Hanscom Field, Mass.). Mar. 18, 1965. 28p.

In deriving atomic displacement threshold energies from electron bombardment data it is necessary to employ numerical values of the electron scattering cross section calculated over a range of electron energies. For relativistic energies the Mott-Rutherford cross-section formula may be used. A computer program was developed to evaluate this formula for any value of atomic number and electron energy. The program is described and numerical values presented for atomic numbers 23, 29, 45, 46, 73, 74, 77, 78, and 79; electron energies between 1.0-3.0 Mev; and appropriate assumed threshold values. (auth)

39226 (AFCRL-65-305) RESEARCH INTO RADIATION DAMAGE EFFECTS IN SOLIDS. Final Report, April 1, 1962-March 31, 1965. Fleischer, R. L.; Price, P. B.; Walker, R. M. (Research Lab., General Electric Co., Schenectady, N. Y.). June 1965. Contract AF19 (628)-369. 32p.

The work has shown that almost all insulating solids, including natural minerals, glasses, and plastics record tracks of nuclear charged particles. After a description of the nature of tracks in solids and ways of seeing them, their uses in such diverse problems as measuring the age of geological and archeological specimens, studying the early history of the solar system recorded in meteorites, observing nuclear interactions, determining neutron fluxes, and separating biological cells of different sizes are discussed. (D.L.C.)

39227 (BMI-1729) IRRADIATION EVALUATION OF Al_2O_3-COATED UO_2 FUEL PARTICLES. Miller, Neil E.; Ritzman, Robert L.; Martin, Robert L.; Townley, Charles W. (Battelle Memorial Inst., Columbus, Ohio). June 16, 1965. Contract W-7405-eng-92. 22p. Dep. mn; CFSTI, $0.50 cy, $0.50 mn.

Effects of coating thickness, coating density, fuel-particle density, and fuel-particle diameter on behavior of Al_2O_3-coated UO_2 particles during irradiation at 100 to 1100°C were studied. Composite coatings of Al_2O_3 and BeO and/or pyrolytic carbon were also investigated. Where 40-μ Al_2O_3 coatings on dense UO_2 particles were found to fail in a few hours at 100°C, 60-μ composite coatings on dense UO_2, or 60-μ Al_2O_3 coatings on porous UO_2 particles showed no failure. At 815°C, 40-μ Al_2O_3 coatings on porous UO_2 particles showed no failure to high burnup, where similar

coatings on dense UO_2 began to show some failure after a burnup of 2 at. %. At 1100°C the 40-μ coatings on dense UO_2 particles operated without failure to a burnup of over 10 at. %. Failure of Al_2O_3 coatings on UO_2 particles is believed to be caused by irradiation-damage-induced swelling of both the UO_2 particle and the inner layer of the Al_2O_3 coating. At elevated temperatures, annealing of the damage prolonged the life of the coating. When particle swelling was reduced by using porous UO_2 and stronger coatings were produced by increasing their thicknesses, coating failure was eliminated. An optimum material of 60 μ of Al_2O_3 on 200-μ, porous UO_2 particles showed excellent performance at 100°C and withstood a burnup of over 10 at. % at 900°C. Diffusion of gaseous and solid fission products through Al_2O_3 coatings is sufficiently slow that release fractions can be maintained in the order of 10^{-6} or less when the coatings are intact. (auth)

39228 (BMI-1734) POSTIRRADIATION FISSION-PRODUCT RELEASE FROM COATED FUEL PARTICLES. Rosenberg, Harvey S.; Morrison, David L.; Townley, Charles W.; Sunderman, Duane N. (Battelle Memorial Inst., Columbus, Ohio). July 7, 1965. Contract W-7405-eng-92. 52p. Dep. mn; CFSTI, $1.25 cy, $0.50 mn.

For PyC-coated particles, the release of ^{140}Ba, ^{89}Sr, and ^{111}Ag was greater than 1000 ppm, the release of ^{132}Te, ^{131}I, ^{141}Ce, and ^{147}Nd was between 10 and 1000 ppm, and the release of ^{133}Xe, ^{103}Ru, and ^{95}Zr was less than 10 ppm for 6 hr of annealing at 1150°C. At a constant coating density the ^{140}Ba release was lowered by about two orders of magnitude as the thickness of the PyC coating was increased from 30 to 75 μ, and at a constant coating thickness the ^{140}Ba release was lowered by about one order of magnitude as the coating density was increased from 1.5 to 2.0 g per cm^3. The ^{140}Ba release was lowered by three orders of magnitude when a SiC barrier layer was present in the PyC coating. The time dependence of release is very complex and varies from one fission product to another. The release rate is increased by a factor of about six for each 150°C increase in temperature between 1000 and 1300°C. The mechanism of release is thought to involve diffusion and compound formation between the fission-product elements and the particle coating. The apparent diffusion coefficients in one type of PyC at 1150 C are 9×10^{-9} cm^2 per sec for ^{89}Sr, 6×10^{-10} cm^2 per sec for ^{140}Ba, 5×10^{-11} cm^2 per sec for ^{147}Nd, and 1.5×10^{-11} cm^2 per sec for ^{141}Ce. (auth)

39229 (BMI-X-10134) FISSION-FRAGMENT EFFECTS IN STRUCTURAL MATERIALS. Quarterly Progress Report for April–June 1965. Ritzman, Robert L.; Griesenauer, Neal M.; Jablonowski, Edward J. (Battelle Memorial Inst., Columbus. Ohio). July 1, 1965. Contract W-7405-eng-92. 10p. (EURAEC-1426). Dep. mn; CFSTI, $1.00 cy, $0.50 mn.

Work Performed Under United States–Euratom Joint Research and Development Program.

A research program is being conducted on mechanical-property changes produced in annealed AISI Type 304 stainless steel and annealed Zircaloy-2 by fission-fragment irradiations. Recoil impregnation of tube-burst and bend-test specimens of Zircaloy-2 and Type 304 stainless steel was completed. Stress-strain data calculated from bend tests of annealed Type 304 stainless steel indicated a nominal 0.2 per cent offset yield strength of 28,900 psi for non-irradiated material, 30,550 psi for material irradiated to a fast-neutron exposure of 9.2×10^{16} nvt, and 34,100 psi for material neutron irradiated and recoil impregnated to an exposure of 2.1×10^{14} fission fragments per cm^2. Bend testing of Zircaloy-2 and tube-burst tests of Zircaloy-2 and Type 304 stainless steel are in progress. Experiments involving fission-fragment-induced strain in Zircaloy-2 and Type 304 stainless steel have been completed. Volumetric expansion coefficients of both alloys have been calculated and compared for exposures of 7.1×10^{14} and 6.1×10^{15} fission fragments per cm^2. Strain effects were found to be more pronounced in Zircaloy-2 than in stainless steel. Electron metallographic analysis of the recoil-impregnated materials was initiated. No structural changes resulting from fission fragments or neutron damage were noted. (auth)

39230 (BNL-9332) A NEW SOURCE OF SMALL-ANGLE X-RAY SCATTERING. Perret, R. G.; Keating, D. T. (Brookhaven National Lab., Upton, N. Y.). June 29, 1965. Contract AT(30-2)-Gen-16. 18p. (CONF-650629-2). Dep. mn; CFSTI, $1.00 cy, $0.50 mn.

From Conference on Small-Angle X-Ray Scattering, Syracuse, N. Y.

A parasitic source of small-angle scattering in single crystals was observed. It is a multiple scattering effect involving the diffuse scattering from point imperfections and the Bragg scattering. Two cases can occur depending on the scattering sequence. The first case occurs when the direct beam is first diffusely scattered in such a direction as to be subsequently Bragg scattered to produce reflection conics. The second case occurs when the direct beam is first Bragg scattered and subsequently diffusely scattered about the direct beam to produce an apparent small-angle scattering. Similar effects should be observed in crystals with a diffuse scattering analogous to this. Thermal diffuse scattering is such a source, and the effect is observed in KCl and phenanthrene. A transmission Laue of phenathrene in which the thermal diffuse sources giving rise to the reflection conics are identified. Fricke and Gerold have reported strong evidence for similar observations in copper and aluminum. Other diffuse sources which could produce similar effects are found in heterogeneous alloys with clustering or in crystals with stacking disorders. This parasitic source of small-angle scattering was discussed using only geometrical and kinematical considerations for the scattering processes, neglecting absorption. (auth)

39231 (COO-1224-8) RADIATION EFFECTS ON THE PHYSICAL PROPERTIES OF POLYMETHYL—METHACRYLATE (thesis). Toosi, Mohammad Taghi Alizadeh (Illinois Inst. of Tech., Chicago). June 1965. Contract AT(11-1)-1224. 70p. Dep. mn; CFSTI, $3.00 cy, $0.75 mn.

An investigation was conducted on the radiation effects on the refractive index, dielectric constant, and density of polymethyl methacrylate. X rays and electrons were used, and an attempt was made to obtain equations for the effects. (D.L.C.)

39232 (FZK-227) EFFECTS OF NUCLEAR RADIATION AND VARIOUS ENVIRONMENTS ON A NUMBER OF SELECTED PLASTIC, GLASS-LAMINATE, AND CERAMOPLASTIC MATERIALS. Johnson, P. M.; Lewis, J. H.; Self, M. R. (General Dynamics/Fort Worth, Tex.). July 1965. Contract AF29(601)-6213. 90p. (AFWL-TR-65-40). CFSTI.

Eight plastic materials were irradiated under various environmental conditions and subsequently tested to determine changes in tensile properties, hardness, and specific gravity. Merlon polycarbonate was irradiated to six gamma dose levels in air at 75°F and two dose levels in a vacuum of approximately 3×10^{-7} torr. Plestar polycarbonate film was irradiated to six dose levels in air at 75°F. The acrylonitrile–butadiene–styrene (ABS) plastics Kralastic MV and SRA received six doses in air at 75°F, six doses in air at 240°F, and two doses in vacuum. Kralastic SR and a glass-reinforced diallyl phthalate were irradiated to three dose levels in air at 75°F and to two doses in vacuum. Supramica 500 ceramoplastic received three doses in air at 75° and 240°F. Maximum gamma dose in air and in vacuum was 2×10^{11} and 3.2×10^{10} ergs/gm (C), respectively. Irradiations were performed with the Ground Test Reactor at the Nuclear Aerospace Research Facility. All materials except the poly(n-vinyl carbazole), diallyl phthalate, and ceramoplastic were severely damaged at the highest doses. (auth)

39233 (GAMD-6321) THE RELEASE OF CONDENSABLE FISSION PRODUCTS FROM THE GAIL III-B FUEL ELEMENT. Zumwalt, L. R.; Busch, D. D. (General Atomic, San Diego, Calif. John Jay Hopkins Lab. for Pure and Applied Science). Apr. 19, 1965. Contract AT(04-3)-167. 16p. Dep. mn; CFSTI, $1.00 cy, $0.50 mn.

Estimates are given of the release of a number of condensable fission products from the GAIL III-B fuel element, based on fission-product deposits found in the General Atomic In-pile Loop at GETR. The releases are equal

to or less than these calculated using a noble gas model. The very low ^{140}Ba release is noted. (D.L.C.)

39234 (GEAP-4597) AEC FUEL CYCLE PROGRAM EXAMINATION OF UO_2 FUEL RODS OPERATED IN THE VBWR TO 10,000 MWD/TU. Williamson, H. E.; Baroch, C. J.; Hoffmann, J. P.; Ikeuye, D. T. (General Electric Co., San Jose, Calif. Atomic Power Equipment Dept.). Mar. 15, 1965. Contract AT(04-3)-189. 268p. Dep. mn; CFSTI, $6.00 cy, $1.50 mn.

Detailed examinations were performed on failed and non-failed Zircaloy-clad fuel rods that had been operated in the VBWR to calculated average exposures as high as 3×10^{20} fissions/cc (~10,000 Mwd/t). Cladding dimensional changes, cladding corrosion, irradiation-induced changes in cladding mechanical properties, fuel-cladding interactions, fuel microstructural changes, fission gas release, surface crud deposits, and the nature and extent of cladding defects were investigated. The results of these examinations are described. Evaluation of these data in conjunction with other data obtained in earlier examinations of Zircaloy-clad fuel rods and examination of stainless-steel-clad rods irradiated in VBWR is included in GEAP-4849. (auth)

39235 (NAA-SR-11309) THE EFFECT OF NEUTRON IRRADIATION ON THE LIQUID SODIUM DILATION OF GRAPHITE. Henry, D. L.; Miller, K. T.; Stearns, J. D. (Atomics International, Canoga Park, Calif.). June 30, 1965. Contract AT(11-1)-Gen-8. 27p. Dep. mn; CFSTI, $2.00 cy, $0.50 mn.

Unirradiated and irradiated graphite samples were exposed to sodium in the 600 to 1200°F temperature range. Expansion occurred in all samples; about 1% in the unirradiated graphite and from 2 to 5% in the irradiated graphite, depending upon the total neutron dosage. Some of this graphite had been irradiated up to 1.12×10^{21} nvt. Maximum expansion was found to occur in the direction normal to the extrusion axis of the graphite. Expansion in this direction exceeded that occurring in the direction parallel to the extrusion axis up to a factor of two. Lamellar compounds of sodium and graphite were not detected by x-ray diffraction but increases in c-spacing, up to 12%, were measured. The c-spacing change was attributed to random intercalation. The increase in c-spacing disappeared when the sodium-logged graphite was exposed to air, but the bulk expansion remained the same. Additions of potassium to the sodium, up to 0.1 wt % did not significantly affect the expansion of graphite in sodium. (auth)

39236 (WCAP-3269-36) FABRICATION AND IRRADIATION OF THIN-WALLED TYPE 304 STAINLESS STEEL CLAD FUEL RODS IN THE SAXTON REACTOR. McClintock, D. R. (Westinghouse Electric Corp., Pittsburgh, Pa. Atomic Power Div.). Jan. 1965. Contract AT(30-1)-3269. 53p. Dep. mn; CFSTI, $3.00 cy, $0.50 mn.

Ten thin-walled (9.7 mils) Type 304 stainless steel clad fuel rods were irradiated as part of the Saxton core to a maximum burnup of 8900 Mwd/Mt at a maximum heat flux of 410,000 Btu/hr/ft^2. The corresponding integrated fast flux exposure was 1.1×10^{21}nvt. Post-irradiation examinations revealed no evidence of failure or crack formation although the thin-walled clad was subjected to plastic deformation. (auth)

39237 THE ROLE OF CRYSTAL STRUCTURE IN DETERMINING THE MECHANICAL PROPERTIES OF GRAPHITE. Jenkins, G. M.; Williamson, G. K.; Barnett, J. T. (Berkeley Nuclear Labs., Gloucestershire, Eng.). Carbon, 3: 1-6(July 1965).

The mechanical hysteresis and compliance of polycrystalline graphite are shown to be very sensitive to crystal perfection as modified by graphitization, neutron irradiation, and post irradiation annealing. Electron microscope examination showed the effect of graphitization and irradiation damage on the dislocation structure and this was related to the effects observed on these particular mechanical properties. (auth)

39238 IRRADIATION-ACTUATED DEVICE FOR MEASURING THE TENSILE FRACTURE STRAIN OF GRAPHITE. Jackson, John L.; Hart, William E. (General Electric Co., Richland, Wash.). Carbon, 3: 94-6(July 1965). (HW-SA-3737)

The device is composed of four parts: sample, straining section, main body, and threaded end. The sample was inserted through the straining section and both were fitted into the main body. The threaded end was screwed until there was a slight tensile stress on the sample. Sixteen assemblies, eight high-strain-rate and eight low-strain-rate, were irradiated. Each functioned as predicted and produced strain in the tensile specimen. Six of the high-strain-rate assemblies strained the samples to failure at exposures ranging from 2 to 3×10^{20} n/cm^2. One assembly had a measured total strain of 0.3% at room temperature. This assembly was then heated in order to measure the strain at 550°C and slightly above. It failed at 0.4% strain at a temperature of 600°C. Another assembly with a measured total strain of 0.29% at room temperature was disassembled and the sample was found to have a permanent set of 0.23%. The system as designed had the limitation that stress on the sample changed continuously and therefore was not known at the fail point. (F.J.H.)

39239 MAGNETIC TAILING IN THE FERROMAGNETIC TRANSITION METALS IRRADIATED WITH ELECTRONS AT 22 deg K. Verdone, Janine; Peretto, Pierre; Moser, Pierre; Dautreppe, Daniel; Verdier, Jacques (Centre d'Etudes Nucleaires, Grenoble, France). Compt. Rend., 260: 5209-12(May 17, 1965). (In French).

Iron, nickel, and cobalt were studied by magnetic tailing after irradiation with electrons at 22°K. The results obtained made it possible to attribute the first stage of the resistivity anneal to the annihilation of near pairs, then to the annihilation without correlation of the interstices in the lacunas. A study of the influence, very complex, of the impurities (iron in nickel and nickel in iron) is presented. (tr-auth)

39240 EFFECT OF FAST NEUTRONS ON THE THERMOELECTRIC CAPACITY OF GERMANIUM MEASURED AT LOW TEMPERATURES. Van Dong, Nguyen (Centre d'Etudes Nucleaires, Saclay, France). Compt. Rend., 260: 5243-6(May 17, 1965). (In French).

The contribution of phonons on the thermoelectric power of Ge was studied between 16 and 100°K after irradiation by fast neutrons and after an isothermal anneal. The study shows the existence and the properties of the accumulation of the faults created by the bombardment. (tr-auth)

39241 OBSERVATIONS OF DISLOCATIONS IN COPPER USING BORRMANN TRANSMISSION TOPOGRAPHS. Young, F. W. Jr.; Sherrill, F. A.; Wittels, M. C. (Oak Ridge National Lab., Tenn.). J. Appl. Phys., 36: 2225-30(July 1965). (ORNL-P-760)

X-ray topographs were made of copper crystal plates $1 \times 1 \times Z$ cm, $Z \geq 0.1$, with (111) faces, using the Borrmann diffracted beams for AgK_α radiation. Dislocation lines were generally recorded as lines of less intensity on the x-ray plate. Both annealed and neutron irradiated crystals were investigated. In the latter the dislocations were pinned and were not moved by the small stresses accidentally imposed while making the topographs; dislocation arrangements in the bulk crystal were determined. The Burgers vectors were deduced from {111} topographs, employing the condition that for no contrast $g \cdot b = 0$. For edge dislocations, the additional condition $g \times n = 0$ was necessary for no contrast, and it was demonstrated that this type of contrast was more pronounced for dislocations grouped in a slip trace. It was found that dislocations could be seen all the way through crystals for $Z = 0.06$ cm. A semiquantitative correlation was established between etch pits formed at dislocation sites on the (111) surfaces and the dislocations revealed by the x-ray topography. It was possible to obtain complete sets of topographs on only a few annealed crystals; for these, an analysis of the dislocations produced by accidental microstrains was possible. (auth)

39242 EFFECTS OF IRRADIATION ON THERMALLY ACTIVATED FLOW IN IRON. Smidt, F. A. Jr. (Battelle-Northwest, Richland, Wash.). J. Appl. Phys., 36: 2317-18 (July 1965). (HW-SA-3752)

The interaction between dislocations and defects was studied by examining the influence of fast-neutron irradiation on the thermally activated flow stress of iron. Results are presented, showing the change in apparent activation volume and the change in activation energy with true strain at temperatures from 78 to 298°K, for samples of two purities—Ferrovac E and Battelle zone-refined iron. (M.J.T.)

39243 SOME PROPERTIES OF IRRADIATED LiF. Street, K. N.; Teghtsoonian, E. (Univ. of British Columbia, Vancouver). J. Appl. Phys., 36: 2319-20(July 1965).

Some observations are reported on the inhomogeneous annealing characteristics of gamma-irradiated LiF crystals and also on some aspects of the deformation behavior of radiation-hardened LiF. The measured M-band optical density is shown as a function of distance along the crystal, in cleaved and in cleaved and polished conditions after various annealing times. Results of pulse annealing experiments are also given. Observations of etch pit density are described. Reasons for the nonuniform annealing of color centers are discussed. Results of microhardness and tensile tests on both annealed and irradiated crystals are considered. (M.J.T.)

39244 EFFECT OF IONIZING RADIATION ON GLASSES: THE RELATION BETWEEN OPTICAL ABSORPTION AND THERMOLUMINESCENCE OF BORATE GLASSES. Spurny, Z.; Novotny, J. (Inst. of Nuclear Research, Czechoslovak Academy of Sciences, Prague). J. Phys. Chem. Solids, 26: 1107-10(July 1965).

The relation between coloration and thermoluminescence induced by x and gamma radiation in borate glasses is described. In a given range of temperatures and wavelength, only two types of traps were found. The energy necessary for decoloration and thermal destruction of luminescence traps was estimated and it was established that the color and thermoluminescence centers are the same. (auth)

39245 FISSION FRAGMENT DAMAGE IN SEMICONDUCTORS AND IONIC CRYSTALS. Izui, Kazuhiko (Japan Atomic Energy Research Inst., Tokyo). J. Phys. Soc. Japan, 20: 915-32(June 1965).

Electron microscopic observation is carried out on fission fragment-irradiated germanium, silicon and magnesium oxide which have different grain size and thickness. Tracks of fission fragments are observed in evaporated films of germanium with about 10-Å grain size and of magnesium oxide with about 50-Å grain size, while no track is observed in other materials. A number of small spots are found to appear in large crystal films of germanium and silicon after the irradiation. It is found by electron diffraction study that there are a number of small disturbed or recrystallized regions in highly irradiated large crystals of germanium and silicon. The mechanism of thermal spike is discussed in some detail on the basis of an estimate of the energy distribution of excited electrons and relaxation times for various collision processes of these electrons, and a new model which is applicable to non-metallic crystals is presented. Calculations of the temperature distribution in a spike region based on this model are found to give a good result consistent with the present experiment. (auth)

39246 STUDY OF RETICULAR DEFECTS IN ALUMINUM BY HARDENING AND BY IRRADIATION. Budin, C.; Lucasson, P. (Laboratoire de Chimie Physique, Orsay, France). Phys. Letters, 16: 229-30(June 1, 1965). (In French).

For the determination of the type of reticular defect mobile around 220°K in irradiated Al (stage III) and the type of chemical reaction predominating at this stage, two types of experiments were carried out. First, the restoration kinetics of a sample first tempered and then irradiated alternately were compared. The interaction of the faults produced by tempering with those produced by irradiation was then studied. The temperings from 350°C to the temperature of liquid N were done with a speed of the order of 6000°/sec. The irradiations were made at −170 ± 2°C. The results showed that stage III in Al can be attributed to the annihilation reaction of fixed lacunae by mobile interstices. The ratio of the resistivity of an interstice to that of a lacuna is near 4.5. (J.S.R.)

39247 ON THE ANELASTIC AFTER-EFFECT IN ELECTRON-IRRADIATED MOLYBDENUM. De Jong, M.; Wensink, B. L. (Universiteit, Amsterdam). Phys. Letters, 17: 200-2(July 15, 1965).

Thin molybdenum strips which were irradiated with 2.5 Mev electrons were bent elastically, and the anelastic after-effect was studied by measuring the time variation of the current necessary to keep the strip in the state of zero strain. The relaxation time and activation energy were calculated. The results show that the observed relaxations are caused by the reorientation of a defect produced during irradiation, and not by interstitially dissolved impurities. It is concluded that the after-effects are brought about by the reorientation of the single interstitial molybdenum atom. (L.B.S.)

39248 ON THE INTERPRETATION OF STAGE I RECOVERY AFTER ELECTRON IRRADIATION OF COPPER. Iseler, G. W.; Dawson, H. I.; Mehner, A. S.; Kauffman, J. W. (Northwestern Univ., Evanston, Ill.). Phys. Letters, 17: 212-13(July 15, 1965).

The isochronal recovery of the extra electric resistivity introduced into 99.999% copper by 2-Mev electrons were measured at temperature intervals of 0.75°K from 10 to 60°K. A typical curve of annealing peaks giving rates of electric resistivity recovery is shown, and conclusions concerning the structures in the various annealing states, labelled I_{A-E}, are discussed. It is concluded that the nature of the I_E stage cannot be explained by the simple second order process of the random migration of interstitials to vacancies only, which is in disagreement with the conclusions reached by Corbett et al. (L.B.S.)

39249 ULTRASONIC ATTENUATION IN COPPER. Kolouch, R. J.; McCarthy, K. A. (Tufts Univ., Medford, Mass.). Phys. Rev., 139: 700-1(Aug. 2, 1965).

The absolute electronic attenuation of longitudinal ultrasonic waves in a single crystal of pure copper at low temperatures was measured at three frequencies: 23.2, 29.8, and 47.8 Mc. The attenuation due to the dislocation-phonon interaction was completely suppressed by a ^{60}Co gamma irradiation. Comparison of the experimental results with the theory of Pippard suggests that the relaxation time for the ultrasonic attenuation is equal to that for the electrical resistivity, and that the fit of the experimental data requires that only the coefficient of Pippard's attenuation expression be adjusted. Such an adjustment can be explained by considering the true Fermi surface of copper, and the distortions the Fermi surface undergoes when the crystal is sustaining an ultrasonic wave. (auth)

39250 THEORY OF THE YIELD AND FANO FACTOR OF ELECTRON-HOLE PAIRS GENERATED IN SEMICONDUCTORS BY HIGH-ENERGY PARTICLES. Van Roosbroeck, W. (Bell Telephone Labs., Inc., Murray Hill, N. J.). Phys. Rev., 139: A1702-?(Aug. 30, 1965).

Yield of secondaries and ratio of variance to yield (Fano factor) are associated with a simple statistical model. This model applies almost independently of details of the physics, though introduction in it of refinements from band structure would be straightforward. The model is described in terminology of an equivalent problem which is formulated and called "crazy carpentry." Analytical and Monte Carlo results agree well. The statistics are largely determined at secondary energies of just a few ionization thresholds, above which yield increases linearly with energy, with an apparent threshold the same as the average final energy, or energy of a secondary when first it cannot ionize further. Limiting relative yield, equal to ionization threshold divided by average energy per electron-hole pair, and Fano factor are given in their dependence on losses to optical photons. The limiting case of given relative energy loss to very many phonons of very small energy generally provides close approximations, so that the results apply also whatever kinds of phonons are produced. Illustrative simple

cases are also treated, including the one-dimensional spacefilling problem known as the "parking problem." The theoretical yield is used to fit data of Vavilov on the enhanced quantum yield in silicon, and some physical implications are considered. (auth)

39251 THE RECOVERY OF NICKEL ABOVE ROOM TEMPERATURE. Mehrer, H.; Kronmueller, H.; Seeger, A. (Max-Planck-Institut fuer Metallforschung, Stuttgart and Technische Hochschule, Stuttgart). Phys. Status Solidi, 10: 725-38(Aug. 1, 1965). (In German).

The recovery of the coercive field strength and initial susceptibility of Ni single crystals above room temperature occurs in three stages. These can be interpreted as being due to the migration of interstitial atoms, of vacancies, and to self-diffusion. After neutron irradiation at 80°C a recovery stage is found in the temperature range 100 to 300°C. The activation energy of (0.5 ± 0.06) ev in the first part of this stage is interpreted as the difference between the migration and binding energy of divacancies. Comparison with a direct measurement of the migration energy of divacancies yields a divacancy binding energy of 0.3 ev. The last part of the stage is attributed to the migration of single vacancies (migration energy (1.46 ± 0.07) ev). The migration energy of interstitial atoms is determined from measurements of the recovery of the electrical resistivity after electron irradiation, giving (1.03 ± 0.04) ev in agreement with previous measurements. (auth)

39252 STUDY OF RADIATION DAMAGE BY USING FIELD EFFECT. Gereth, R. (IBM Watson Research Center, Yorktown Heights, N. Y.); Shockley, W. Proc. IEEE (Inst. Elec. Electron. Engrs.), 53: 748-9(July 1965).

The field is proposed as a sensitive tool to explore radiation induced defect centers. This technique allows combining two independent measurements within the same test sample. First, the bulk property of the center can be studied after neutron or electron irradiation. Second, the defect center can be included within the space charge region of a p-n junction by varying the reverse bias of said junction. This changes the carrier density within the vicinity of the center from the equilibrium condition to that of depletion. Thus, valuable information on the charge state of the radiation induced defect centers can be obtained when they are located within the space charge depletion region. (J.F.P.)

39253 INVESTIGATION OF AN IRRADIATED FR2-FUEL ELEMENT. Dienst, Wolfgang; Krautwedel, Ludwig (Kernforschungszentrum, Karlsruhe, Ger.). Z. Metallk., 56: 366-73(June 1965). (In German).

Samples were taken from a FR2-fuel rod which was irradiated with thermal neutron fluxes of 1.8 to 3.2 · 10^{13} n/cm^2 · s up to uranium burnup of 0.06 to 0.12 %. Microstructure, hardness, density and electrical conductivity were measured. Below 250° the uranium microstructure is completely destroyed by the irradiation, while the crystal structure is preserved. The microstructure is similar to that after heavy deformation. The hardness increases by 130 to 150 DPH. Density decreases by 0.3% per 0.1% uranium burnup, electric conductivity decreases by less than 1%. Cracks were not found. Above 250° partial recovery occurs which is complete above 450°C. Grain boundary defects or pores due to fission gas could not be found in the central area of the fuel rod, although the decrease of density and electrical conductivity points to a porosity of about 0.4%. The investigated changes of properties indicate that these fuel rods are suited for in-pile use, the critical areas being localized at the ring-plug connections of the three fuel rod parts, where overheating, and consequently crack formation precipitation of gases and possibly phase transformation were found. (auth)

39254 ON A METHOD FOR DETERMINATION OF THE DENSITY AND ENERGETIC POSITION OF RADIOINDUCED AGGLOMERATION CENTERS IN SILICON SINGLE CRYSTALS WITH THE HELP OF THE ELECTRIC BEHAVIOR OF MICROPLASMS. Ruge, Ingolf; Bernt, Helmut (Technische Hochschule, Munich). Z. Naturforsch., 20a: 549-52 (Apr. 1965). (In German).

At absorbed doses higher than approximately 10^6 R irradiation with ^{60}Co modifications in the electric behavior of microplasms (MP) were detected. The MP pulse did not occur statistically but in packets (delays). It was shown that from the delay frequency per pulse packet the energy position of the radioinduced agglomeration could be determined by means of the Shockley-Read theory. A relationship was derived by which the delay rate is a function of the density of the agglomerate, its energetic place, and some electrical parameters of the MP. This relation could be verified experimentally. (tr-auth)

39255 EFFECT OF ELECTRON BOMBARDMENT HEATING ON SURFACE OF TUNGSTEN. Doering, H. E.; Shahinian, P. (Naval Research Lab., Washington, D. C.). pp 481-501 of First International Conference on Electron and Ion Beam Science and Technology. New York, John Wiley and Sons, Inc., 1965.

The effects of a focused 10-kv electron beam on surfaces of tungsten were investigated. At temperatures between 1200 and 3400°C, the change in the surface was observed as it developed on both foils and polished sheet specimens. The damage appeared to be associated with the temperature to which the surface was subjected and with thermal cycling. Different types of damage were produced by stationary and oscillating beams. Stationary beams produced grain boundary grooving and surface pitting similar to that produced by thermal radiation heating. Damage produced by oscillating beams included ripples on grain surfaces, uneven grain boundary grooves, cracks, and tilted and dislodged grains; these effects are similar to those associated with thermal cycling. (A.G.W.)

39256 EXPERIMENTAL AND THEORETICAL INVESTIGATION OF RADIATION EFFECTS IN GLASSES. Schreurs, J.W.H.; Tucker, R. F. (Corning Glass Works, N. Y.). p.616-24 of Physics of Non-Crystalline Solids. Amsterdam, North-Holland Publishing Co. and New York, John Wiley and Sons, Inc., 1965.

The results of an absorption study of doped and undoped phosphate and silicate glasses are summarized. It was found that in both glasses the major visible absorption is due to trapped holes. Transitions due to trapped holes were also identified in the EPR spectra of both glasses. An explanation for the observations is proposed. (D.C.W.)

39257 METHOD OF IMPROVING PROPERTIES OF AN ALLOY BY RADIATION. Damask, Arthur C. (to U. S. Army). U. S. Patent 3,193,678. July 6, 1965. Filed Aug. 14, 1962.

A method is described for increasing the value of the order of an alloy that exhibits an ordered arrangement of atoms and in which the atomic diffusion occurs by a vacancy mechanism. The suitable alloy is one for which there is a theoretically producible equilibrium degree of order for any particular temperature, for which there is an atomic freezing-in temperature below which heat alone imparted to the alloy will not produce the equilibrium degree of order, and for which there is a vacancy freezing-in temperature below which no treatment will produce the equilibrium degree of order. The method includes holding the alloy above the vacancy freezing-in temperature while irradiating the zone with electromagnetic rays having an energy of at least 0.1 mev until the degree of order of the alloy approaches a predetermined percentage of the equilibrium degree of order at the holding temperature. (B.L.M.)

METEOROLOGY

See also GEOLOGY AND MINERALOGY — Site Survey and Selection.

Refer also to abstract 38813.

39258 (CONF-650534-1) THE ENERGY AND MOMENTUM BUDGET OF THE ATMOSPHERE ABOVE THE TROPOPAUSE. Newell, Reginald E. (Massachusetts Inst. of Tech., Cambridge. Dept. of Meteorology). 1965. Contract AT(30-1)-906. 43p. Dep.(mn); $2.00(cy), 1(mn) CFSTI.

From 6th International Space Science Symposium, Buenos Aires.

Momentum and heat transports computed from wind and temperature observations up to 30 km are used to construct momentum and energy budgets of the region. When radiation calculations are included the picture that emerges is of a large heat engine in each middle latitude troposphere feeding energy vertically to a refrigerator above and laterally to other refrigerators in the low latitudes of the tropics. A similar analysis applied to the 25–75 km region reveals another large heat engine below 55 km surmounted by a large pole-to-pole refrigerator. The possible interactions between the two circulation regimes are discussed with emphasis being placed on the transfer of energy from low layers to high layers. The arguments are qualitatively extended to the atmosphere above the mesopause and the momentum transport by tides is presented. Some aspects of the thermospheric structure are interpreted in terms of the concepts developed from studies of the lower atmosphere. (auth)

39259 (IDO–12041) AERODYNAMIC EFFECTS OF LARGE REACTOR COMPLEXES UPON ATMOSPHERIC TURBULENCE AND DIFFUSION. Islitzer, Norman F. (Weather Bureau, Idaho Falls, Idaho). May 1965. 34p. Dep. mn; CFSTI, $2.00 cy, $0.50 mn.

The additional turbulence immediately downwind of a large reactor complex due to aerodynamic effects from the buildings was measured. Wind stations consisting of a Beckman and Whitley 3-cup anemometer and a sensitive bivane were established at upwind and downwind locations around the MTR-ETR complex. It was found that the increase of the product of vertical and horizontal turbulence downwind of the structures over that measured on the upwind side could exceed a factor of 10 for individual 5-min periods and averaged out to a factor of 3.5 in strongly stable atmospheres. A counteracting measure is the reduction of wind speed downwind of the structures which is about 30 percent. Direct measurements of diffusion to 850 m downwind were made using a fluorescent tracer, uranine dye in solution, released just downwind of the main MTR reactor building. Several crosswind sampling lines were established as well as a line of four meteorological stations oriented along the center of the grid. There was a total of 13 releases, 11 in moderately unstable atmospheres and 2 during inversion hours, for 30-min periods. The crosswind spread of the particles and the centerline dosages were measured and compared to those experienced over a flat plain from previous experiments. It was found that the building effects reduced concentrations of the tracer by about a factor of 5 at 100 m downwind and a factor of 2 at 850 m downwind on the average during lapse conditions. Occasional ten-fold reductions in concentration were measured near the buildings. It appears that during unstable conditions the additional building turbulence is not very significant beyond about 800 m. The results of the inversion tests were inconclusive because it was difficult to maintain a wind that would carry the effluent in a well-defined plume over the sampling grid during such conditions. One test indicated that the reduction of concentration from building turbulence could be as high as a factor of 50. (auth)

39260 (LA–3328) BIBLIOGRAPHY OF ATMOSPHERIC OZONE TO 40 Km: ITS CONCENTRATION, DISTRIBUTION, METHODS OF DETECTION, AND RELATIONSHIP WITH OTHER METEOROLOGICAL PHENOMENA. Jackson, Betty S. (Los Alamos Scientific Lab., Univ. of California, N. Mex.). Apr. 6, 1965. Contract W-7405-eng-36. 34p. Dep. mn; CFSTI, $2.00 cy, $0.50 mn.

The literature search includes journals, books, and reports from 1960 through March 1965. Two references are given for older publications. (M.O.W.)

PHYSICS

General

Refer also to abstract 40231.

39261 (AROD-3979:2) SOME ASPECTS OF CORRELATION IN MANY-PARTICLE SYSTEMS. Final Report. Miller, Allen (Syracuse Univ., N. Y.). May 1965. Contract DA-31-124-ARO (D)-93. 27p.

An expansion is given for the ground-state energy of a system of interacting Bose particles, using Rayleigh-Schrödinger perturbation theory with the scattering part of the interaction as the perturbation. The result in second order reproduces the energy shift found by various authors. The energy spectrum of the zero-order Hamiltonian contains a gap of magnitude $\rho_0 V_0$ where V_k is the Fourier transform of the two-particle interaction. This gap removes the third-order divergence resulting when the entire interaction is used as the perturbation. The structure factor, computed to first order, is in qualitative agreement with experiment for large momentum values. For non-zero temperature, expressions are obtained for the depletion of the zero-momentum mode and the specific heat, using the zero-order Hamiltonian. The specific heat exhibits a discontinuity at the critical point. Quantitative estimates for the magnitude of the specific heat at the critical point yield results which are in fair agreement with empirical values for liquid helium. (auth)

39262 (BNL-8990) ON THE PROPAGATION OF FREE SOUNDWAVES IN RAREFIED GASDYNAMICS. Sirovich, Lawrence (Brown Univ., Providence, R. I. Div. of Applied Mathematics); Thurber, James K. (Adelphi Univ., Garden City, N. Y. Graduate School of Mathematics). [1964]. Contract AT(30-2)-Gen-16. 43p. (CONF-640704-1). Dep.(mn); $2.00(cy), 1(mn) CFSTI.

From 4th International Symposium on Rarefied Gasdynamics, Toronto.

A theory of sound propagation, employing general kinetic models, in an unbounded medium is presented. Numerical results for rigid sphere and Maxwell gas models are obtained. These are compared with already existing theories. (auth)

39263 (CONF-796) PROCEEDINGS OF THE THIRD ANNUAL EASTERN UNITED STATES THEORETICAL PHYSICS CONFERENCE, UNIVERSITY OF MARYLAND, COLLEGE PARK, MARYLAND, OCTOBER 30-31, 1964. (Maryland Univ., College Park. Dept. of Physics and Astronomy). 350p.

Twenty-five papers are included; separate abstracts have been prepared for 18. Four of the papers were previously abstracted in NSA, 19: 3112, 3113, 4974, and 12567. The 3 papers not abstracted separately are concerned with problems of the solid state, and with the canonical formalism for the quantum many-body problem. (T.F.H.)

For abstracts of individual papers see: 39264, 39452, 39453, 39454, 39455, 39456, 39457, 39458, 39459, 39625, 39626, 39627, 39628, 39629, 39630, 39684, 40073, and 40074.

39264 (CONF-796(Paper 14)) STIMULATED PHOTON-PHOTON SCATTERING. Gatland, I. R. (Georgia Inst. of Tech., Atlanta); Gold, L. (Martin Co., Baltimore, Md. Research Inst. for Advanced Studies); Moffat, J. W. (Toronto Univ. (Ontario)).

The feasibility of the use of crossed-beam experiments (using laser beams) for measuring the photon-photon interaction is discussed. It is concluded that available lasers should give about 0.35 counts/sec in the experimental configurations envisioned. (T.F.H.)

39265 (IA-1021) RESEARCH LABORATORIES SEMI-ANNUAL REPORT, JULY-DECEMBER 1964. (Israel Atomic Energy Commission, Yavne. Soreq Nuclear Research Center). 174p. Dep. mn.

Research on fission processes, gamma resonant scattering and Mössbauer effect is summarized along with work on properties of semiconducting and insulating diamonds. Electron spin resonance spectra of SrO and CaO single crystals were investigated. Infrared absorption spectra and neutron inelastic scattering by H_2-bonded ferroelectrics, alkali hydroxides, and alkaline earth hydroxides were also studied. Fast reactor physics studies were conducted on Doppler and Na void effects, neutron cross sections, and perturbation. Research is reported on molten salt chemistry, chemistry of actinides and rare earths, and solution chemistry. Studies on radiosensitization of enzymes by Cu ions are reported along with studies of short-lived nuclides, neutron-emitting systems, and high-energy chemical interactions. (J.R.D.)

39266 (JINR-P-2195) SPONTANNYE PEREKHODY PRI PROKHOZHDENII SVETA CHEREZ ANIZOTROPNYE SREDY. (Spontaneous Transitions by Light Propagation Through Anisotropic Media). Baryshevskii, V. G.; Lyuboshits, V. L.; Podgoretskii, M. I. (Joint Inst. for Nuclear Research, Dubna (USSR). Lab. of High Energy and Joint Inst. for Nuclear Research, Dubna (USSR). Lab. of Theoretical Physics). 1965. 4p. Dep. mn.

The spontaneous emission of electromagnetic waves by light propagation through the anisotropic medium was treated. Estimates were obtained for the probability of the spontaneous change of light polarization. (auth)

39267 (NP-15157) MAGNETOHYDRODYNAMIC IONIZING SHOCK WAVES IN A CONDUCTING MEDIUM. Green, B.; May, R. M. (Sydney Univ. (Australia). School of Physics). Feb. 1965. 35p. (TR-17) Dep. mn.

Numerical calculations for the flow parameters (velocity, density, pressure, etc.) in a magnetohydrodynamic shock wave propagating in a conducting medium are presented. The effect of ionization in the shock front is included. The results are presented graphically for a complete range of the initial magnetic field strength and direction, and several arbitrary values of the ionization energy of the downstream fluid. (auth)

39268 (ORNL-P-1395) FINITE AMPLITUDE WAVES IN LIQUIDS AND SOLIDS. Breazeale, M. A. (Tennessee Univ., Knoxville and Oak Ridge National Lab., Tenn.). [1963]. Contract W-7405-eng-26. 4p. (CONF-650910-1). Dep. mn; CFSTI, $1.00 cy, $0.50 mn.

From International Congress on Acoustics, Liege.

The distortion of an initially sinusoidal ultrasonic wave recently observed in solids can be described in a way analogous to that previously used for liquids, except for certain complications associated with crystalline properties. The non-linearity parameters can be introduced in a relatively simple way if the terms in the nonlinear differential equation are grouped properly. This results in a formalism which allows one to discuss nonlinear effects in liquids and solids analogously and to point out parameters which differ significantly and thus characterize the two media. Measurements were made by different techniques, using results found in one medium to suggest lines of investigation in the other. (M.O.W.)

39269 (SU-SEL-64-133) QUARTERLY RESEARCH REVIEW NO. 11, OCTOBER 1 THROUGH DECEMBER 31, 1964. (Stanford Univ., Calif. Stanford Electronics Labs.). Contract AT(04-3)-326. 171p. Dep.(mn); $5.00(cy), 3(mn) CFSTI.

Research and development at the laboratories for electron devices, solid-state electronics, systems theory and radioscience are reported. Information is included on microwaves, plasma, transistors, information theory, linear systems, control systems, and ionospheric irregularities. (J.R.D.)

39270 (TID-21894) QUARTERLY PROGRESS REPORT NO. 77. Zimmermann, H. J.; Harvey, G. G.

(Massachusetts Inst. of Tech., Cambridge. Research Lab. of Electronics). Apr. 15, 1965. Contract AT(30-1)-1842. 436p. Dep.(mn); $7.36(cy), 7(mn) CFSTI.

Research progress is reported on molecular beams, microwave spectroscopy, radio astronomy, optical and infrared spectroscopy, properties of solids, geophysics, gravitation, magnetic resonance, acoustics, plasma, communication theory, information processing and transmission, mechanical translation, biophysics, neurophysiology, neurology, and network syntheses. (J.R.D.)

39271 (UCRL-12204) PHYSICS DEPARTMENT PROGRESS REPORT, JULY–SEPTEMBER 1964. Lorenz, A. (ed.) (Lawrence Radiation Lab., Univ. of California, Livermore). Contract W-7405-eng-48. 70p. Dep(mn); $3.00(cy), 2(mn) CFSTI.

Abstracts are prepared for the four sections on nuclear and atomic physics, thermodynamic properties of matter, fluid and hydrodynamics, and radiation physics. (M.O.W.)

For abstracts of individual sections see: 38813, 39272, 39273, and 39788.

39272 (UCRL-12204, pp 27-48) THERMODYNAMIC PROPERTIES OF MATTER. (Lawrence Radiation Lab., Univ. of California, Livermore).

A brief discussion of each of the following is included: quantum corrections in the Thomas-Fermi model, approximate Thomas-Fermi potential, phase transitions of repulsive lattice gas models, pair distribution function of a classical electron gas, calculation of virial coefficients for squares and cubes with attractive forces, hard-sphere bulk viscosity, numerical solution to the Schroedinger equation with the complete screened Coulomb potential, calculation of helium energies, properties of materials, shock-induced phase transitions using a quartz gage, equation of state measurements, the dynamic equation of state of rocks, absorption spectroscopy of compressed samples II, and the inclined mirror equation of state measurements. (M.O.W.)

39273 (UCRL-12204, pp 60-5) RADIATION PHYSICS. (Lawrence Radiation Lab., Univ. of California, Livermore).

A brief discussion of each of the following is included: stimulated Brillouin scattering, laser ion source, Vaidya's radiating Schwarzschild metric, and generation of Einstein's field equations by computer. (M.O.W.)

39274 (JPRS-30799) THE USE OF SHOCK WAVES IN HIGH-PRESSURE PHYSICS. Al'tshuler, L. V. Translated from Usp. Fiz. Nauk, 85: 197-258(Feb. 1965). 95p. (TT-65-31343). CFSTI, $3.00 cy.

A literary survey of applications of shock waves in high-pressure physics is presented. A study of the results obtained since the end of the second World War is presented. A review of the dynamic methods used to study explosives and the equations of state of super-dense gases, metals, and ionic and valent crystals is presented. Consideration is also given to questions involving phase transformations in shock waves, the application to geophysics of the results obtained, and problems concerning the dynamic strength of metals and conductivity induced by shock. (M.O.W.)

39275 CALCULATION OF THE TRAJECTORY OF AN ELECTRON MOVING BETWEEN COAXIAL TUBES IN THE PRESENCE OF A HOLLOW ELECTRON BEAM. Szilagyi, M. Acta Phys. Acad. Sci. Hung., 18: 333(1965).

The trajectory of an electron starting off the internal boundary of an axially symmetrical hollow dense electron beam moving between two coaxial long conductive cylinders is determined. The influence of different parameters of the system on the electron motion is investigated. Formulas are given for the determination of the maximum beam pervasion and system length. (auth)

39276 A THERMAL BOUNDARY-LAYER PROBLEM IN MAGNETOHYDRODYNAMICS. Fillo, John (Syracuse Univ., N. Y.). AIAA (Am. Inst. Aeron. Astronaut.) J., 3: 1339-40(July 1965).

The thermal boundary-layer equations for steady plane aligned-fields flow are derived and examined. The thermal boundary-layer equations are derived for fluids subject to large magnetic Reynolds numbers, small magnetic Prandtl numbers, and Prandtl numbers of order one. Also, only constant-property fluids and incompressible flow are considered. In order to discuss the thermal boundary layer, account must be taken of the fact that the flow regime is split into three regions. Thus the following model is proposed: an undisturbed region where the temperature is infinity; a magnetoinviscid-thermal layer where thermal conduction is negligible, and only convection and joule heating contribute to the transport of thermal energy; and a viscous-thermal layer where thermal conduction, convection, viscous, and joule heating are important. (J.F.P.)

39277 AN MHD BOUNDARY-LAYER COMPATIBILITY CONDITION. Hugelman, Rodney D. (Wright-Patterson Air Force Base, Ohio); Haworth, Donald R. AIAA (Am. Inst. Aeron. Astronaut.) J., 3: 1367-9(July 1965).

It is shown by a magnetohydrodynamic example that the conditions for satisfying the boundary layer equations are insufficient in this case, if these equations are only satisfied on the average over the boundary-layer thicknesses. It is shown that an additional compatibility condition is necessary. The other force affecting the velocity profile besides the pressure gradient is the ponderomotive force. (J.F.P.)

39278 LAMINAR MHD CHANNEL ENTRANCE FLOWS. Tan, C. W. (Grumman Aircraft Engineering Corp., Bethpage, N. Y.). AIAA (Am. Inst. Aeron. Astronaut.) J., 3: 1369-71(July 1965).

Closed-form analytic solutions are obtained with the appropriate Hartmann-like velocity distributions (Hartmann, J. and Lazariun, F., "Hg-Dynamics II," Kgl. Danske Videnskab. Selskab, Mat-Fys, Medd., 15: 7(1937)). The Hartmann channel is considered. Laminar, two-dimensional, steady, incompressible, low magnetic Reynolds-number flow is assumed, with magnetic and electric fields mutually normal to the flow direction. Hall effects are assumed to be small and thus are neglected. All of the electric, mechanical, and thermal properties of the moving fluid or of the stationary walls will be assumed constant. Variation of the free-stream velocity in the flow direction is allowed. (J.F.P.)

39279 RELATIVISTIC MAGNETOHYDRODYNAMICS. Pham Mau Quan. Ann. Inst. Henri Poincare, 2: 151-65 (1965). (In French).

The relativistic equations of magnetohydrodynamics assume a simple form which lends itself to some fruitful interpretations in classical terms of space and time. Their compatibility was studied by means of an analysis of the Cauchy problem. The characteristic varieties render an account of the hydrodynamic waves and the Alfven waves. A local study was made concerning the propagation of these waves; the classical results were almost obtained with some relativistic corrections. Finally, the magnetohydrodynamic shocks are studied as corresponding to the singular measures supported by some hypersurfaces. A local interpretation is given. (tr-auth)

39280 THE STRUCTURE OF A SHOCK FRONT IN ATOMIC HYDROGEN. II. THE REGION OF INTERNAL RELAXATION. Skalafuris, Angelo J. (Smithsonian Astrophysical Observatory, Cambridge, Mass.). Astrophys. J., 142: 351-68(July 1, 1965).

The region of internal relaxation behind a shock front is examined by use of kinetic theory. Spatial variations of temperature, density, and ionized fraction are determined, and the relaxation region is shown to be essentially adiabatic. Ionizational cooling of the electron gas, relative to heavier particles, increases the shock thickness at higher shock speeds as much as two orders of magnitude. The region of internal relaxation is shown to be optically thin to Lyman and Balmer radiation. (auth)

39281 EXPERIMENTAL STUDY, NEAR THE RESONANCE, OF THE FORCED OSCILLATIONS OF A HEAVY,

VISCOUS, ELECTROCONDUCTIVE LIQUID IN THE PRESENCE OF A MAGNETIC FIELD. Crausse, Etienne; Dorlhac, Francois; Poirier, Yves (Centre d'Enseignement Superier Scientifique, Avignon, France). Compt. Rend., 260: 5192-4(May 17, 1965). (In French).

An experimental study was made near the resonance of the sinusoidal forced oscillations of a heavy, viscous, electroconductive liquid. They evolved in a rectangular guide and were exposed to the action of a transverse magnetic field. (tr-auth)

39282 APPARENT VARIATIONS OF THE ELECTRON TEMPERATURE IN A FLAME. Debiesse, Jean; Klein, Siegfried; Kraus, Pierre (Institut National des Sciences et Techniques Nucleaires, Saclay, France). Compt. Rend., 260: 5213-16(May 17, 1965). (In French).

The determination of the electron temperature of a flame using a double probe leads to results that seem to put in doubt the range of validity the theories accepted up to the present. They no longer seem valid either when the temperature of the double probe is below 100°C or when an electronegative gas is injected on one of the probes. (tr-auth)

39283 ION DISTRIBUTION IN THE DRIFT REGION OF TUBULAR ELECTRON BEAMS. Hartnagel, Hans (Univ. of Sheffield, Eng.). Intern. J. Electron. 18(1): 431-48 (May 1965).

For pressures of 10^{-7} to 10^{-4} torr, ions are formed by electron-molecule collisions. In the drift region of a tubular electron beam, ions are focused on the center of the beam by the space charge force of the beam electrons. The ion density is calculated analytically and numerically. Slow electrons are trapped in the potential well created by the ions. The origin of these slow electrons is investigated. Experimental results which give the density of slow electrons are presented; they verify the presented theory to a certain degree. (auth)

39284 SEPARATION OF THE INTERACTION POTENTIAL INTO TWO PARTS IN TREATING MANY-BODY SYSTEMS. I. GENERAL THEORY AND APPLICATIONS TO SIMPLE FLUIDS WITH SHORT-RANGE AND LONG-RANGE FORCES. Lebowitz, J. L.; Stell, G.; Baer, S. (Yeshiva Univ., New York). J. Math. Phys. (N. Y.), 6: 1282-98(Aug. 1965).

Systematic methods are developed for investigating the correlation functions and thermodynamic properties of a classical system of particles interacting via a pair potential $v(r) = q(r) + w(r)$. The method is then applied to the case in which $w(r)$ is a Kac potential $w(r,\gamma) = \gamma^{\nu}\varphi(\gamma r)$ (ν the dimensionality of the space) whose range γ^{-1} is very long compared to the range of $q(r)$. The work is related closely to the work of Kac, Uhlenbeck, and Hemmer. The main new feature of the method is the separation of the correlations, e.g., the two-particle Ursell function $F(r)$, into a short-range part $F^{S}(r,\gamma)$ and a long-range part $F^{L}(y,\gamma)$, $y \equiv \gamma r$; r the distance between the particles. The two parts of F are defined in terms of their representation by graphs with density (or fugacity) vertices and K- and Φ-bonds, $K(r) = e^{-\beta\Phi(r)} - 1$, $\Phi = -\beta w$. A resummation of these graphs then yields a simple graphical representation for the long-range part of the correlation functions in terms of graphs with Φ-bonds and hypervertices made up of the short-range part of the correlations. This representation is then used to make separate expansions of $F^{S}(r,\gamma)$ and $F^{L}(y,\gamma)$ and through them of the thermodynamic parameters in powers of γ. Explicit calculations of the Helmholtz free energy are carried out to a higher order in γ than done previously by Hemmer, and it is shown how to carry out the calculation, in principle, to any order. (auth)

39285 CHARGE STATE OF ULTRA-FINE AEROSOLS IN WEAKLY IONIZED MEDIA. APPLICATION TO LARGE ATMOSPHERIC IONS. Bricard, J.; Girod, P.; Pradel, J. J. Phys. (Paris), 26: 141A-7A (Apr. 1965). (In French)

The fixation of small ions of air on monodispersed aerosols of a radius between 5×10^{-7} and 10^{-5} cm has been studied by means of calculation as a function of the intensity of ionization Q (i.e., the number of pairs of ions formed per cm^3 of air and per second). The different values of the diffusion coefficients of small positive and negative ions have been taken into account. It is shown that, under conditions which are specified, an excess of negative particles and of positive ions can appear, whereas the medium in general remains uncharged. The ratios N'/N'' n'/n'' of the concentrations of particles and of the small negative and positive ions are calculated as well as the proportion of neutral particles. It is shown that these ratios depend on the quantity Q/N^2: where N designates the total number of the particles present in the aerosol and their dimensions. The results have been applied to the formation of large radioactive ions and the ionic balance of the large ions, which are the condensation nuclei of the atmosphere in an artificially ionized medium. (auth)

39286 STUDY OF AN ELECTRIC DISCHARGE IN HYDROGEN AND DEUTERIUM. Bobin, J. L.; Durand, Y.; Loichot, R.; Veyrie, P. J. Phys. (Paris), 26: 180-8(Apr. 1965). (In French)

The discharge of a capacitor bank between electrodes in deuterium or hydrogen under 50 mm of pressure creates a spark channel. Its behavior has been recorded as a function of time. During the first quarter period, its radial expansion is a linear function of time. By means of optical methods, the electron density along the discharge axis could be determined. Hence, a discharge channel structure is derived. (auth)

39287 EFFECTS OF X-RAY POLARIZATION ON PENDELLOESUNG FRINGES. Hattori, Hiroyuki; Kuriyama, Hideo; Kato, Norio (University, Nagoya, Japan). J. Phys. Soc. Japan, 20: 1047-50(June 1965).

A theory of Pendellösung fringes due to the incident beam of an unpolarized spherical wave is presented. The agreement with the observations pertaining to the fading of the fringes is very well. The observed fringe distance Λ is given by $(1/\Lambda = \frac{1}{2}(1 + \cos 2\theta_B)\, 1/\Lambda_\perp)$, where θ_B the Bragg angle and $\Lambda_\perp$ is the fringe distance for a plane-polarized spherical wave, the electric vector of which is perpendicular to the plane of reflection. The positions of maxima and minima of the fringes are interchanged before and after the fading position. These results give the theoretical and experimental bases for a new method of determining crystal structure factors. (J. Phys. Soc. Japan 20: 988(1965)).

39288 ANOMALOUS PEAKS IN THE MASS SPECTRA OF H_2 AND D_2 OBTAINED WITH A SINGLE-FOCUSING MASS SPECTROMETER. Hartman, Thomas E. (Texas Instruments Inc., Dallas). J. Vacuum Sci. Technol., 2: 213-14(July-Aug. 1965).

The mass spectra of 99.9% pure hydrogen and deuterium were obtained in the pressure range 10^{-5} to 10^{-8} torr. Anomalous mass peaks were observed corresponding to M/e values which are nonintegral. The hydrogen 2.53 mass peak is discussed. This peak has a width and shape similar to normal mass peaks and has a corresponding anomalous mass peak in deuterium at 5.06, apparently arising from the same cause. Several explanations for these peaks are considered but found to be not responsible. Although the origin remains unexplained, evidence suggests that the cause exists in the analyzer or detector rather than in the source section of the instrument. (J.F.P.)

39289 A NOVEL APPROACH TO THE THEORY OF SHOT NOISE. Srinivasan, S. K. (Indian Inst. of Tech., Madras). Nuovo Cimento (10), 38: 979-92(July 16, 1965).

The theory of shot effect is examined on the basis of an inhomogeneous Poisson process. The "Poisson" parameter $\lambda(t)$ characterizing the stochastic process is generalized in such a manner that λ itself becomes a random variable depending on the number and the position of events on the time axis. It is found that the number density of arrivals of electrons in the theory of shot effect has exactly the same behaviour as the process under consideration. Such a process is strongly non-Markovian and the calculation of moments and correlation functions of the output turns out to be difficult. However it is shown that a knowledge of the moments

of and the correlation of events on the t-axis is sufficient to determine these functions. The conjecture of Rowland regarding the behaviour of the mean square of the cumulative response for shot effect is proved and in addition an explicit expression for the power spectrum of the response is derived. Other physical phenomena which can be explained on the basis of the stochastic model are cited. (auth)

39290 ANTINORMALIZATION PROPERTIES OF THE CORRELATION FUNCTIONS. Liboff, Richard L. (Cornell Univ., Ithaca, N. Y.). Phys. Fluids, 8: 1236-9(July 1965).

An antinormalization condition is derived for the s-particle correlation function C_s, according to which $\int C_s\, dk = 0$, $1 \le k \le s \le N$. The differential of phase for the kth particle is written dk. There are N particles in the whole system. When added to two previously known asymptotic conditions on the s-particle distribution about vanishing and infinite interparticle distance, respectively, this constraint forms three independent properties of the s-particle correlation. For the special case of the two-body (equilibrium) correlation $C_2(r)$, it is proved that a sufficient condition in order that C_2 have two zeros on the open r axis ($0 < r < \infty$) is that C_2 be negative in an interval about the point at infinity. Application to the Debye correlation is discussed, and it is concluded that this function has at least two zeros in the nonlinear domain about the origin. (auth)

39291 GASEOUS DIFFUSION IN A TEMPERATURE GRADIENT. Mason, E. A.; Weissman, Stanley (Univ. of Maryland, College Park). Phys. Fluids, 8: 1240-3(July 1965).

The theory of diffusion in a temperature gradient was tested by comparing the results of gas mixing experiments and gas unmixing experiments, the unmixing being caused by thermal diffusion. Both types of measurements were carried out in the same apparatuses with the same temperature distributions, so that corrections cancel on taking ratios. Measurements are reported on $H_2-{}^{37}Ar$, $H_2-{}^{85}Kr$, $D_2-{}^{85}Kr$, T_2-N_2, T_2-Kr, and T_2-CO_2 over a maximum temperature range of about 195 to 435°K. The theory is confirmed within experimental uncertainty, provided that account is taken of the variation of the thermal diffusion ratio during the course of the diffusion. The ratio of the experimental results to their theoretical predictions is 0.991 ± 0.023. It is therefore possible to make reliable measurements of diffusion coefficients in the presence of temperature gradients. (auth)

39292 INERTIAL-RANGE SPECTRUM OF HYDROMAGNETIC TURBULENCE. Kraichnan, Robert H. Phys. Fluids, 8: 1385-7(July 1965).

It is suggested that Kolmogorov's concept of independence of widely separated wavenumbers in the inertial range of turbulence be modified for the hydromagnetic case. When the magnetic energy in the sub-inertial wavenumbers exceeds the total energy in the inertial range, the predicted asymptotic inertial-range energy spectrum is proportional to $k^{-\frac{3}{2}}$ instead of $k^{-\frac{5}{3}}$ and displays exact equipartition between magnetic and kinetic energy. Generalized Lagrangian functions for hydromagnetic flow are introduced to provide a suitable basis for quantitative turbulence approximations. The proposed formalism permits following the fate of given Alfvén wavefronts as well as that of given fluid particles. (C.E.S.)

39293 LONGITUDINAL WAVES IN A WEAKLY IONIZED GAS. Ingard, Uno; Gentle, Kenneth W. (Massachusetts Inst. of Tech., Cambridge). Phys. Fluids, 8: 1396-7 (July 1965).

Sound propagation in a weakly ionized gas is considered. In an experiment (K. W. Gentle and U. Ingard, Appl. Phys. Letters, 5: 105(1964)) in which the neutral-gas temperature in the plasma column of a glow discharge was determined from measurements of the speed of a sound pulse transmitted through the column it was assumed that the relation between the sound speed and the neutral-gas temperature was the same as in an un-ionized gas. The validity of this assumption is considered. (C.E.S.)

39294 HARMONIC GENERATION IN A MICROWAVE DISCHARGE. Murphy, Brian (Yale Univ., New Haven). Phys. Fluids, 8: 1534-40(Aug. 1965).

The first two harmonics generated in a microwave discharge in which a weak d-c field is present are calculated. The mechanism by which harmonics are generated is assumed to be a modulation of the electron collision frequency by the microwave field. The second harmonic is strongest at a pressure for which the collision frequency is well below the frequency of the perturbing microwave field. The third harmonic is strongest when the collision frequency is approximately equal to the frequency of the microwave field. These results are found to be in reasonable agreement with the observations of Uenohara. (auth)

39295 MOESSBAUER EFFECT IN Cs^{133}. Perlow, G. J.; Boyle, A. J. F.; Marshall, J. H.; Ruby, S. L. (Argonne National Lab., Ill.). Phys. Letters, 17: 219-20 (July 15, 1965).

The Mössbauer effect of the 81-kev gamma ray from the first excited state of ^{133}Cs following the decay of ^{133}Ba was observed in experiments using a $BaCl_2 \cdot 2H_2O$ and $BaAl_4$ sources and CsCl and Cs_2CO_3 absorbers. The spectra are shown and the results are summarized. (L.B.S.)

39296 THE MAGNETIC CONTRIBUTION TO THE HEAT CAPACITY OF NEODYMIUM AT LOW TEMPERATURES. Janovec, V.; Morrison, J. A. (National Research Council, Ottawa). Phys. Letters, 17: 226-7(July 15, 1965).

It is shown that the formula for the magnetic contribution to the total heat capacity of the rare earth metal in the simple spin wave theory gives a better description than complex expressions that contain an energy gap parameter in the spin wave spectrum arising from magnetic anisotropy. The heat capacities were calculated for neodymium and are compared with measured values. (L.B.S.)

39297 THE STRUCTURE OF THE ENERGY SPECTRA OF IONS SCATTERED FROM SINGLE CRYSTALS. Mashkova, E. S.; Molchanov, V. A.; Parilis, E. S.; Turaev, N. Yu. (Moscow State Univ.). Phys. Letters, 18: 7-8(Aug. 1, 1965).

The results are presented of investigations of the structure of the energy distribution in ion scattering from single crystals. The (100) and (114) planes of Cu were bombarded with 30-kev Ar^+ ions. The results were compared with theoretical predictions. (D.C.W.)

39298 VALIDITY OF TOWNSEND'S IONIZATION FUNCTION IN NONUNIFORM ELECTRIC FIELDS. Golden, D. E.; Fisher, L. H. (Lockheed Missiles and Space Co., Palo Alto, Calif.). Phys. Rev., 139: A1452-5(Aug. 30, 1965).

A number of authors have concluded that experimental values of prebreakdown ionization-gas-current multiplications in nonuniform electric fields are not correctly predicted by generalizing Townsend's ionization function for uniform fields to nonuniform fields. It is shown that the reported failures are mainly due to the use of incorrect values of the first Townsend ionization coefficient. (auth)

39299 BEHAVIOR OF ^3He IN THE CRITICAL REGION. Sherman, Robert H. (Los Alamos Scientific Lab., N. Mex.). Phys. Rev. Letters, 15: 141-2(July 26, 1965).

The results of some recent pressure-volume-temperature measurements on ^3He in the critical region are presented. Significant departures were found in the shape of the coexistence curve, compressibility, and degree of the critical isotherm from the behavior expected for classical systems such as Xe and CO_2. (D.C.W.)

39300 MEGAGAUSS FIELDS GENERATED IN EXPLOSIVE-DRIVEN FLUX COMPRESSION DEVICES. Herlach, F.; Knoepfel, H. (EURATOM-C.N.E.N., Frascati, Italy). Rev. Sci. Instr., 36: 1088-95(Aug. 1965).

Chemical explosives are used to compress magnetic flux trapped within a metallic liner system. In this way, final magnetic fields from 0.5 in a volume of 40 cm^3 to 3.7 Mgauss in 1.5 cm^3 were produced and carefully measured. The conversion efficiency of explosive into electromagnetic

energy was as high as 10% in the most favorable cases. The different compression experiments, including B_z and B_ϕ configurations in various geometrical arrangements, are described in detail; and their results are analyzed and discussed. (auth)

39301 STEADY MAGNETOHYDRODYNAMIC FLOW OF AN INCOMPRESSIBLE VISCOUS FLUID INVOLVING AN IGNORABLE CO-ORDINATE. Jeffrey, Alan (Rolls-Royce Ltd., Derby, Eng.). Z. Angew. Math. Phys., 16: 386-95 (May 25, 1965).

A situation is discussed in which the flow equations simplify to a convenient standard form which, although not equivalent to a classical hydrodynamical problem, is never the less of use in studying the flow of real conducting fluids through ducts. Specifically it is shown how, by use of a particular form of magnetic vector potential and a change of variables, steady incompressible magnetohydrodynamic viscous flow problems involving an ignorable coordinate may be reduced to the solution of Poisson's equation and two independent linear second order partial differential equations. (J.F.P.)

39302 QUASI-ONE-DIMENSIONAL MAGNETOHYDRODYNAMIC FLOW WITH HEAT ADDITION. [Part] III. Gundersen, Roy M. (Univ. of Wisconsin-Milwaukee, Milwaukee). Z. Angew. Math. Phys., 16: 413-18(May 25, 1965).

A method is presented for studying quasi-one-dimensional magnetohydrodynamic flows subjected to arbitrary orientation of the magnetic field with small heat addition. Slow, fast, and intermediate wave speeds are discussed. The fast and slow speeds may be treated simultaneously, and solutions may be obtained with an unspecified wave speed; the intermediate wave must be considered separately. The solutions obtained include the previously obtained solutions as special limiting cases. It is convenient to use the pressure as a dependent variable, so that a system of governing equations is obtained in which only derivatives of the entropy along a particle path appear. (J.F.P.)

39303 IRREVERSIBILITY IN THE SCOPE OF THE LIOUVILLE EQUATION. Pfirsch, D.; Priess, S. (Max-Planck-Institut fuer Physik und Astrophysik, Munich). Z. Naturforsch., 20a: 756-69(June 1965). (In German).

The Liouville equation is solved directly for a homogeneous monatomic gas with weak interaction up to the second order of the interaction parameter within the framework of the multi-time method. The solution allows a simultaneous discussion of the H function, which is obtained with the N-particle function or with the single particle function or master equation resulting from integration of the N-particle function. The results lead to an explanation for the irreversibility in the scope of the Liouville equation as a phase mixing between the individual systems of the ensemble virtually described by a Liouville function, or to the explanation by means of Prigogine's cascade mechanism. (tr-auth)

39304 ON SOME PROBLEMS IN UNSTABLE QUANTUM MECHANICAL SYSTEMS. Kerler, Werner; Petzold, Joachim (Universitaet, Marburg, Ger.). Z. Physik, 186: 168-89(1965). (In German).

If an exponential decay law is measured (which clearly need not be found in every case) it can not be concluded that the line shape must be lorentzian. To show that the possible energy spectra may differ from a Lorentz shape by a measurable amount, an example of such a spectrum is constructed, leading to an exponential decay law in an even better approximation than a lorentzian spectrum. Various facts about decaying systems are discussed in connection with scattering theory. It is shown that ordinary Moessbauer experiments are not suited for line shape measurements, and modified experiments are proposed. (auth)

39305 X-RADIATION FROM A FLASH X-RAY DISCHARGE COLUMN. Haendel, S. K.; Sundstroem, I. (Uppsala Univ.). Z. Physik, 186: 271-6(1965).

An experimental system for studying radiation phenomena from a flash x-ray discharge column is described. Studies of the discharge current as well as the x-radiation from the interelectrode space indicate that a pinch effect acts on the discharge column; x radiation is emitted from different parts along the column; and the development degree of the pinch determines the column x-ray intensity. (auth)

39306 ENGINEERING MAGNETOHYDRODYNAMICS. Sutton, George W.; Sherman, Arthur. McGraw-Hill Series in Mechanical Engineering. New York, McGraw-Hill Book Company, 1965. 564p. $19.75.

The properties and behavior of ionized gases in electric and magnetic fields are treated first following essentially the microscopic viewpoint. The macroscopic motion of electrically conducting compressible fluids is then considered, and applications to propulsion and power generation are described. (D.C.W.)

39307 FIRST INTERNATIONAL CONFERENCE ON ELECTRON AND ION BEAM SCIENCE AND TECHNOLOGY. Bakish, Robert (ed.). The Electrochemical Society Series. New York, John Wiley and Sons, Inc., 1965. 957p. $24.50. (CONF-407).

Forty-six papers and one abstract of a paper are included; separate abstracts have been prepared for fourteen. Eight papers were previously abstracted for NSA; see abstracts 18: 4210, 32123, 34502, 39421, 40083 and 19: 6289, 7657, and 9058. Papers not abstracted discuss ion propulsion and use of electron beams in microelectronics, recording and information storage, materials processing, materials joining, and microanalysis. (A.G.W.)

For abstracts of individual papers see: 38838, 38949, 38950, 39111, 39136, 39137, 39138, 39139, 39255, 39308, 39328, 39416, 39417, and 39441.

39308 VERIFICATION AND USE OF HERRMANN'S OPTICAL THEORY OF THERMAL VELOCITY EFFECTS IN ELECTRON BEAMS IN THE LOW-PERVEANCE REGIME. Amboss, K. (Hughes Research Labs., Malibu, Calif.). pp 86-107 of First International Conference on Electron and Ion Beam Science and Technology. New York, John Wiley and Sons, Inc., 1965.

Various aspects of Herrmann's theory are reviewed, and conclusions from the theory are presented. An experimental verification of the theory was carried out on a beam of perveance 0.015×10^{-6}. Good agreement between theory and experiment was obtained. Imperfections in the electron gun caused significant discrepancies between theory and experiment. The structure of the beam faded slowly with distance, an effect which the theory does not predict, but the fading was sufficiently slow that the theory can be applied to the problem of optimizing the transmission of thermal beams through long drift tubes. (A.G.W.)

39309 COLLISION PHENOMENA IN IONIZED GASES. McDaniel, Earl W. Wiley Series in Plasma Physics. New York, John Wiley and Sons, Inc., 1964.

A survey on collision processes is presented stressing noncollective processes. Atomic collisions and transport phenomena interpreted in terms of such impacts are considered. Both theory and experimental techniques are covered. (D.C.W.)

39310 ELECTROMAGNETIC THEORY AND GEOMETRICAL OPTICS. Kline, Morris; Kay, Irvin W. Pure and Applied Mathematics. A Series of Texts and Monographs. Volume XII. New York, Interscience Publishers, 1965. 538p. $15.00.

The electromagnetic approach to geometrical optics is given for both isotropic and for anisotropic media. Wave fronts and rays in both media are also discussed. Asymptotic series solution and asymptotic expansions of time-harmonic fields and a complex integral representation of these fields are given. The electromagnetic integrals of diffraction optics and asymptotic evaluation of the diffraction integrals are discussed with emphasis on the diffraction integral for unpolarized light. Included are some applications of the asymptotic series. (J.F.P.)

39311 ANALYSIS AND COMPUTATION OF ELECTRIC AND MAGNETIC FIELD PROBLEMS. Binns, K. J.; Law-

renson, P. J. A Pergamon Press Book. New York, The Macmillan Company, 1963. 343p. $12.50.

A comprehensive treatment of both analytical and numerical methods for the derivation of two-dimensional solutions for stationary and quasi-stationary electric and magnetic fields is presented. The basic theory of electric and magnetic fields, direct and image methods of solution, transformation methods, and finite-difference methods are covered. (D.C.W.)

39312 POLYENERGETIC PARTICLE DEFLECTING SYSTEM. Belbeach, Roger L. (to U. S. Atomic Energy Commission). U. S. Patent 3,202,817. Aug. 24, 1965.

A method and apparatus are described for achromatically deflecting a beam of particles having various particle energies to preserve the properties of beam parallelism and diameter and to provide equal path lengths for all particles in the beam to preserve longitudinal bunching. The beam is passed through an array including various combinations of bending and quadrupole magnets of a construction and positioning determined by precise mathematical relations to provide the desired results. (AEC)

Accelerators

Refer also to abstracts 38658 and 39752.

39313 (COO-921-16) THE UNIVERSITY OF MICHIGAN 83-INCH CYCLOTRON. Final Report. Parkinson, W. C.; Tickle, R. S. (Michigan Univ., Ann Arbor. Coll. of Literature, Science, and the Arts). May 1965. Contract AT(11-1)-921. 21p. Dep.(mn); $1.00(cy), 1(mn) CFSTI.

The construction, the manpower employed, the cost breakdown by major categories, and the operational experience of the Michigan 83-inch spiral-ridge cyclotron are summarized. (M.O.W.)

39314 (JINR-P-2131) ELEKTROSTATICHESKOE POLE RAVNOMERNO ZARYAZHENNYKH OB'EMOV TSILINDRICHESKOI KONFIGURATSII. (An Electrostatic Field of Uniformly Charged Volumes of a Cylindrical Configuration). Danilov, V. I.; Puzynin, I. V. (Joint Inst. for Nuclear Research, Dubna (USSR). Lab. of Nuclear Problems). 1965. 38p. Dep. mn.

The electrostatic field of uniformly charged cylindrical configuration was calculated. The general case of these configurations is a part of a cylindrical ring with a central angle of $2\phi_0$. The potential and the components of the field were determined with the aid of a specially constructed function U_0 satisfying the Laplace equation. Some particular cases of the general solution were considered — the electrostatic field of a cylindrical ring, of a sector, of a cylinder with finite dimensions. Their limiting cases at semi-infinite and infinitely large height were considered. The results of the work may be used to estimate the effect of the spatial charge of a bunch of accelerated particles on the stability of their motion. They may also help to calculate the maximal intensity attainable in different accelerators. (auth)

39315 (JINR-P-2177) RASPREDELENIE POLYA PRONIKAYUSHCHEGO IZLUCHENIYA V PREDELAKH SANITARNO-ZASHCHITNOI ZONY SINKHROFAZOTRONA NA 10 Gev. (A Distribution of the Penetrating Radiation Field Over the Protective Zone of the 10 Gev Synchrophasotron). Lebedev, V. N.; Zolin, L. S.; Salatskaya, M. I. (Joint Inst. for Nuclear Research, Dubna (USSR). Lab. of High Energy). 1965. 15p. Dep. mn.

The results are presented on an investigation of neutron component of the radiation field around (up to 500 m) the 10 Bev synchrophasotron of the Joint Institute for Nuclear Research. It was found that from 60 to 90% of the total dose (depending on the distance) is due to fast neutrons with a mean energy of the order of 0.7–3 Mev. The neutron flux having an energy of more than 20 Mev is likely to be of importance only at short distances from the synchrophasotron. The problems of reducing the radiation levels outside the accelerator building are also considered. (auth)

39316 (JINR-P-2199) ISSLEDOVANIE DVIZHENIYA IONOV V TSENTRAL'NOI OBLASTI TSIKLOTRONA S PROSTRANSTVENNOI VARIATSIEI NAPRYAZHENNOSTI MAGNITNOGO POLYA. (Investigation of the Ion Motion in the Central Region of the Fixed Field Alternating-Gradient Cyclotron). Glazov, A. A.; Kropin, A. A.; Novikov, D. L.; Onishchenko, L. M. (Joint Inst. for Nuclear Research, Dubna (USSR). Lab. of Nuclear Problems). 1965. 19p. Dep. mn.

The results are given of theoretical calculation and experimental investigation of the ion motion in the central region of the relativistic cyclotron model. It was confirmed that the theoretical estimates for choosing the geometry of the central region of the accelerator are correct. (auth)

39317 (NRL-6248) CALCULATIONS ON UNIFORM-FIELD BENDING MAGNETS. Shapiro, P.; Podgor, S.; Theus, R. B. (Naval Research Lab., Washington, D. C.). Jan. 14, 1965. 36p.

The focal properties of some uniform-field bending magnets were calculated. Tables and graphs of the image and magnification for deflection angles of 20, 22-½, 35, 40, and 45 degrees, as a function of the object distance and the angle the particle beam makes with the entrance and exit faces of the magnet are given. These numerical results are useful when designing ion-optical systems for particle accelerators. (auth)

39318 (UCRL-14194) BEAM TRAJECTORIES UNDER THE INFLUENCE OF SELF-FIELDS AND EXTERNAL FOCUSSING ELEMENTS. Beal, J. W. (Lawrence Radiation Lab., Univ. of California, Livermore). May 21, 1965. Contract W-7405-eng-48. 18p. Dep. mn; CFSTI, $1.00 cy, $0.50 mn.

The general, relativistic equations for the trajectory of a charged particle in an electromagnetic field of axial symmetry are derived from the principle of least action. Self-field effects are included. Under the proper assumptions the general results are shown to reduce to the well-known paraxial ray equation including self-field terms. A computer program is described which numerically integrates the differential equation to obtain the trajectory under the influence of the self-fields as well as the external fields. The results demonstrate the effectiveness of the focusing elements as a function of particle energy, beam current, and initial beam slope and radius. The results presented are for electron beams; the conversion to ion beams is obvious. (auth)

39319 PERIODIC ELECTROSTATIC FOCUSING OF SHEET ELECTRON BEAMS. Szilagyi, M. Acta Phys. Acad. Sci. Hung., 18: 335-50(1965). (In Russian).

An investigation of the periodic electrostatic focusing of sheet electron streams is given. The focusing system has a plane of symmetry, which coincides with the medium plane of the beam. The beam thickness may be comparable with the period of the system. The following optimal focusing conditions are determined: the value of the focusing potential, the approximate electron trajectories, the beam perveance, and the required current density distribution in the beam cross section. The paraxial approximation is considered as a special case. In this case, the focusing conditions for sheet beams are compared with those for the cylindrical ones. Finally, the electrode shapes for the considered type of electric field are determined, and the beam perveance as a function of geometric parameters is given. It is found that the maximum value of the perveance is achieved out of the paraxial region. (auth)

39320 HELICITY AND TRANSVERSE MOMENTUM OF THE EXTREME RELATIVISTIC FERMION IN A CIRCULAR ACCELERATOR. Costa de Beauregard, O. (Inst. Henri Poincare, Paris). Ann. Inst. Henri Poincare, 2: 131-50 (1965). (In French).

The Dirac-Weyl equations of the extreme relativistic electron are solved explicitly in two cases of cylindrical

symmetry (with a magnetic directing field parallel to the axis, z): Ψ wave z independent, zero outside two values of the polar radius r; and Ψ wave with a Gaussian distribution along z. It is shown in the first case that, although the k_z component of the momentum is zero, the j_z component of the Dirac current is generally non-zero, its value depending on that of curl σ (σ, spin density); and, in the second case, that, even if the k_z Gaussian distribution is centered on the value $k_z = 0$, the mean value Ż of the z Gaussian distribution generally runs (with the c velocity) along helices of axis z. These are two different descriptions of the translational inertial spin effect previously defined; the relation between the preceding results and the conclusions of the general theory is explained. The principal difficulties in an experimental search for the effect are briefly discussed. (auth)

39321 POSITRON FOCUSING IN AN ACCELERATING FIELD. Hong, G. W. (Univ. of California, Livermore). J. Appl. Phys., 36: 2306-8(July 1965).

The equation of motion of positrons (or electrons) in an accelerating field and a focusing magnetic field is analyzed with relativistic effects included. An iterative procedure is used to solve the resulting nonlinear differential equation. An example is included to illustrate this technique; it is found that the assumptions involved are consistent with the numerical calculations. The feasibility of the proposed focusing scheme can be determined from the results obtained by this method of analysis. (auth)

39322 RELATIVISTIC ISOCHRON-CYCLOTRON AT KARLSRUHE. Naturw. Rundschau, 18: 166(Apr. 1965). (In German).

At the beginning of work in Karlsruhe no information about the energy region to be used (50-Mev deuterons; inner current 100 μA; extracted current, 10 μA) was available. Difficulties were encountered since previously the isochron principle had not been applied to relativistic cyclotrons; a construction principle which gave a particularly secure solution to the magnetic field problem was used. The separation between the pole pieces was made as small as possible. This was achieved by development of a new type of high frequency accelerator system, which passes into the field depressions so that no additional space between the poles is needed. Improved particle optics and electrostatic optics permitted improved current quality, particularly in extracted current. A new method of measuring the phase of the ion cloud relative to the high frequency phase allows fine installation of the magnetic field. A new septum construction decreases the quantity of current lost in the septum, thus contributing to the quality of the extracted current. (BBB)

39323 HELIUM TREATMENT OF VAC-ION PUMPS TO REMOVE DEPOSITED ARGON. Dean, Norman (Stanford Univ., Calif.). Rev. Sci. Instr., 36: 1266-7 (Aug. 1965).

It was found that argon was being released from the pumping surfaces of the Vac-Ion pumps of the vacuum system of the electron storage rings at the Hansen High-Energy Physics Laboratory. The argon was removed by discharges in helium inside the pumps with subsequent evacuation by a turbo-molecular pump. (D.C.W.)

39324 EXTERNAL BEAM EXTRACTION RATE CONTROL FOR THE COSMOTRON ACCELERATOR. Cottingham, J. G.; Kovarik, V. J.; Pellegrin, J. L. (Brookhaven National Lab., Upton, N. Y.). Rev. Sci. Instr., 36: 1339-40(Sept. 1965). (BNL-8974).

The delivery rate of the external proton beam from the Cosmotron is made more uniform by a feedback system acting on the internal orbit center. This improves the experimental statistics and makes more efficient use of available beams. (auth)

39325 STORAGE RINGS FOR PARTICLE PHYSICS. Pentz, Michael J. (CERN, Geneva). Sci. J., 1: 43-8 (July 1965).

The merits and problems of storage rings are discussed. The utility of storage rings in comparison with more powerful accelerators is considered, together with research on storage rings. CERN activities in this field are stressed. (D.C.W.)

39326 THE 25-Mev LINEAR ACCELERATOR. THE MOST POWERFUL IN JAPAN. Hatano, Hisakazu; Okada, Tsutomu (Tokyo Shibaura Electric Co., Ltd.). Toshiba Rev., Intern. Ed., No. 21, 45-9(1965).

The design and performance of the Japanese 25-Mev linear accelerator are described. It is intended for use as an x-ray source for studing methods of measuring large radiation doses. The electron energy can range from 4 Mev at its minimum to 25 Mev at it maximum; the pulse width as well as the pulse recurrent frequency is variable over a wide range. The performance of the system as a whole is stabilized by a motor-generator with automatic voltage regulation. A description is given of accelerating tubes and their accessories, the electron gun, the microwave oscillation and amplification, and the klystrons. Various uses for this accelerator are listed. (J.F.P.)

39327 NEW ELECTRON ACCELERATORS. pp IX.1-4 of Photon Interactions in the Bev-Energy Range. Cambridge, Mass., The M.I.T. Press, 1965.

Brief summaries are presented of the status of the Frascati 1.5-Bev storage ring, Orsay linear accelerator, DESY strong-focusing electron synchrotron, Lund electron synchrotron, University of Glasgow 4-Bev strong-focusing electron synchrotron, Tokyo University 0.75-Bev accelerator, Stanford linear accelerator, and the Cornell synchrotron. (L.B.S.)

39328 EXPERIMENTAL INVESTIGATION OF THE STRUCTURE OF HIGH-POWER-DENSITY ELECTRON BEAMS. Bas, E. B.; Cremosnik, G. (Eidgenoessische Technische Hochschule, Zurich). pp 108-32 of First International Conference on Electron and Ion Beam Science and Technology. New York, John Wiley and Sons, Inc., 1965.

An experimental arrangement is described for measuring the current density distribution in high-power electron beams, the space angle distribution of the beam current, and the crossover position on the system axis. Examples of applications of the method are shown. The influence of the residual gas pressure on the angular distribution of the beam current is discussed briefly. (A.G.W.)

39329 DYNAMICS OF STELLAR SYSTEMS. Ogorodnikov, K. F. A Pergamon Press Book. Translated by J. B. Sykes from Dinamika Zvezdnykh Sistem. New York, The Macmillan Company, 1965. 368p. $15.00.

The general principles on which stellar dynamics is based are presented, and the derivation from these principles of the modern concepts of motions in stellar systems is considered. The relation between stellar dynamics and the other branches of the exact natural sciences, particularly hydrodynamics and statistical physics, is explained. (D.C.W.)

39330 ACCELERATOR BEAM ENERGY MONITOR. Gibney, Gerard G.; Indeck, Bernard (to Ethicon, Inc.). U. S. Patent 3,179,804. Apr. 20, 1965. Filed Jan. 15, 1962.

A continuous energy indicator is provided that enables the determination of the electron beam energy of a linear accelerator at all times. The apparatus includes an insulated and shielded metal plate one corner of which is positioned in the edge of the scanned electron beam. As the scanned beam narrows with increasing electron energy, the plate area that the beam impinges on decreases faster than the density of the electrons per cm^2 increases. Means are included for amplifying, rectifying, and measuring the primary current produced in the plate by the absorbed electrons. (B.L.M.)

Astrophysics and Cosmology

Refer also to abstract 39683.

39331 (NEIC-RR-11) NUCLEAR ASTROPHYSICS—A BIBLIOGRAPHICAL SURVEY. PART IV. Kuchowicz, B. (Nuclear Energy Information Center, Warsaw (Poland)). 1965. 52p. Dep.

Several indexes are listed concerning nuclear astrophysics. They are: author, language, report, conferences, meetings, and various other indexes. (M.O.W.)

39332 OBSERVATIONAL RESULT ON X-RAYS. Fisher, Philip C.; Clark, Dwight B.; Meyerott, Arthur J.; Smith, Kermit L. (Lockheed Missiles and Space Co., Palo Alto, Calif.). Ann. Astrophys., 27: 809-12(Nov.-Dec. 1964).

The results of a rocket experiment (Aerobee 4.70 Flight) performed on March 20, 1963, in an attempt to locate and obtain spectral information about stellar sources of soft x rays in the 0.2- to 20-kev (60- to 0.6-Å) range are reported. The x rays were detected by several well-collimated (5×10^2) gas-filled proportional counters protected by anticoincidence plastic-scintillator-photomultiplier shields. A celestial sphere isophote plot derived from all counts recorded by the Aerobee 4.70 detectors is shown. The rocket's 0.5- to 3.5-kev and 2- to 20-kev counters alternately observed the upward (night) sky and the downward (earth-obscured) sky. Each detected event was assigned to an elemental area of the celestial sphere. The rocket's motion was such that individual elemental areas were scanned from 2 to 9 times by each of the detectors. Observed events were segregated into two broad and overlapping energy intervals, 0.5 to 8 kev and 4 to 20 kev. A noticeably high count rate in a given sphere region was compared to the background count rate predicted for that particular region to assess the statistical significance (number of standard deviations, σ, above background) of the high count rate. With the exception of what appeared to be horizon related sources, only a single region was as much as 2.5 σ above the predicted background. The count rate was noticeably high on five of the seven successive passes over this region and the actual counts in the 0.5- to 8-kev interval totaled 25 as compared to a predicted background of 14 (the relatively stronger Scorpius source was below the rocket horizon so could not have been observed; nor was the Crab Nebula source observed). Because of their low statistical significance, the data alone are insufficient to establish the real existence of any of the high count regions. (TCO)

39333 SPECTRAL AND PHOTOMETRIC MEASUREMENTS OF SOLAR X-RAY EMISSION BELOW 60 A. Blake, R. L.; Chubb, T. A.; Friedman, H.; Unzicker, A. E. (Naval Research Lab., Washington, D. C.). Astrophys. J., 142: 1-12(July 1, 1965).

On July 25, 1963, spectral measurements of solar x-ray emission were made with a Bragg x-ray crystal spectrometer carried in an Aerobee Rocket. Line emissions from O_{VII}, O_{VIII}, N_{VII}, and Fe_{XVII} were recorded between 13 and 25 Å. The O_{VII} line emission came mainly from the solar disk as a whole; the Fe_{XVII} emissions came from a localized active region near the center of the Sun. Studies of the distribution and sizes of x-ray emitting areas on the solar disk have been carried out using slit scans of the sun. Sources of 8–15-Å x-rays are geometrically smaller than 44–60-Å sources. Some 8–15-Å sources have dimensions of the order of 1′. On April 4, 1963, essentially all the radiation observed in the 8–15-Å band originated in active regions; about half the 44–60-Å emission was localized in the same regions, the remainder being distributed over the disk. (auth)

39334 STRUCTURE AND EVOLUTION OF MEDIUM-MASS STARS. II. THE EXTENT OF THE CONVECTIVE CORE IN MIDDLE MAIN-SEQUENCE STARS. Pearce, W. P.; Bahng, J. (Northwestern Univ., Evanston, Ill.). Astrophys. J., 142: 164-9(July 1, 1965).

Five series of homogeneous main-sequence models were constructed, with the objective of finding the mass at which the convective core vanishes. The range of masses considered is $2.0 \geq M/M_\odot \geq 0.90$, and five different chemical compositions were employed, with $0.6 \leq X \leq 0.8$, and $0.01 \leq Z \leq 0.02$. The detailed structure and extent of convective regions in the envelope have not been considered. The mass at which the disappearance of the convective core takes place was found to range from 1.360 to 0.915 $M_\odot$, depending principally on the hydrogen abundance. (auth)

39335 STRUCTURE AND EVOLUTION OF MEDIUM-MASS STARS. III. EFFECT OF RADIATION PRESSURE ON STELLAR MODELS. Auman, J. R.; Bahng, J. (Northwestern Univ., [Evanston, Ill.]). Astrophys. J., 142: 170-3 (July 1, 1965).

A study was made of the effect of including radiation pressure in the calculation of interior models for main-sequence stars in the mass range from 2 to 5 $M_\odot$. The inclusion of radiation pressure reduces the total luminosity slightly, but the radius remains practically unchanged. The largest effect is found in the size of the convective core; it is increased substantially when the radiation pressure is taken into account. Although the resulting changes on the structure of main-sequence stars are quite small, the reduced luminosity and increased convective core will appreciably lengthen the time scale of subsequent evolution of these stars. (auth)

39336 THE DEPTH OF THE CONVECTIVE ENVELOPE ON THE LOWER MAIN SEQUENCE AND THE DEPLETION OF LITHIUM. Weymann, Ray; Sears, R. L. (California Inst. of Tech., Pasadena). Astrophys. J., 142: 174-81(July 1, 1965).

Herbig's observations strongly indicate that extensive lithium depletion must occur after stars of about solar type reach the main sequence. Solar models constructed using opacity tables which include bound-bound effects have envelopes which reach down to about $T = 2 \times 10^6$. Nevertheless, these models are not deep enough, by a small, but significant, amount, to deplete ^7Li. Similar conclusions follow from a study of homogeneous models from 1.2 $M_\odot$ to 0.55 $M_\odot$. A suggestion that extensive mass loss could be responsible for the Li depletion is examined but is found to require a rate of mass loss about 3 orders of magnitude higher than is now believed to occur for the Sun. "Convective-overshoot" effects are roughly estimated, and it is concluded that penetration to depths of about $3 \times 10^{6.6}$°K is energetically possible only for convective elements starting at the very top of the convective envelope where $\log P \lesssim 7$. We estimate the probability that such elements actually do reach to depths of $T = 3 \times 10^6$ by using the mixing length analogously to the mean free path in kinetic theory. Taking the mean free path at every point comparable to the size of the element at every point, and taking the initial element size to be comparable to the initial local pressure scale height, we find the probability of penetration to be completely negligible, and on this basis would conclude that convective overshooting does not enhance the lithium-depletion rate. However, a firm physical justification for a calculation of this type does not exist. It is felt that a theory of convective overshoot must be developed along the lines initiated by Böhm — but with careful treatment of the topmost layers—before the question of enhanced lithium depletion by convective overshoot can be finally settled. (auth)

39337 MASS LOSS AND THE FORMATION OF WHITE-DWARF STARS. Auer, L. H.; Woolf, N. J. (Princeton Univ., N. J.). Astrophys. J., 142: 182-8(July 1, 1965).

The presence of white dwarfs in the Hyades and a suspected one in the Pleiades indicate that stars with masses greater than 2.5 $M_\odot$, and possibly 7 $M_\odot$, can become white dwarfs. Calculations show that the excess mass cannot be lost merely through rotational shedding if the star always rotates like a solid body. Consideration of wide pairs containing a white dwarf indicates that mass is probably lost on a time scale greater than 10^4 years. Nuclear fuel must

be the major source of energy for mass ejection, although in the case of too massive stars it will be insufficient to eject enough mass to permit a stable white-dwarf configuration. It is noted that the minimum masses for helium and carbon burning are comparable with the observed mean mass of white dwarfs, indicating that mass loss continues until nuclear burning ceases. (auth)

39338 RADIOACTIVITY IN SUPERNOVA REMNANTS. Clayton, D. D.; Craddock, W. L. (Rice Univ., Houston, Tex.). Astrophys. J., 142: 189-200(July 1, 1965).

A calculation is made of the implications of the idea developed by Burbidge et al. that the nearly exponential decrease after the first 100 days of the light curves of Type I supernovae is due to nuclear energy released by the spontaneous fission of ^{254}Cl. Uncertainty of the correctness of the Cf-hypothesis qualifies any interpretation of supernovae light-curves, the location and mechanism of heavy-element nucleosynthesis by rapid neutron captures, and the present-day energy balance in supernova remnants. It is that, if the Cf-hypothesis is correct, the Crab Nebula presently has a radioactive energy input of 1.2×10^{38} ergs/sec, of which amount 92 per cent is in the form of kinetic energy of heavy ions (5–6-Mev alpha-particles and 60–140-Mev fission fragments). That much energy would be significantly related to observed properties of the nebula. An experimental test of the Cf-hypothesis may be made by searching for gamma-ray lines associated with transbismuth radioactivity. The anticipated line spectrum is complex. The strongest line flux is $9.7 \times 10^{-5} cm^{-2} sec^{-1}$ from the Crab for the 390-kev line of ^{249}Cf. Good angular and energy resolution will be required to resolve the lines from the sky background. (auth)

39339 THERMODYNAMIC QUANTITIES FOR A GAS OF TRANSVERSE PLASMONS. Inman, Cullen L. (New York Univ., New York). Astrophys. J., 142: 201-7(July 1, 1965).

The coupling of the radiation field to a dense electron gas changes the thermodynamic properties of a photon gas in a way that may substantially affect astrophysical applications. Number density, pressure, energy density, specific heat, and entropy density are calculated for such a gas composed of tranverse plasmons (equivalently, for massive bosons at zero chemical potential). New expansions for these functions are given. (auth)

39340 THE SIZE OF A SOLAR H II REGION. Williams, Robert E. (Univ of Wisconsin, [Madison]). Astrophys. J., 142: 314-20(July 1, 1965).

Using rocket observations of the far-ultraviolet solar spectrum, the degree of ionization of the interstellar gas surrounding the sun is calculated under certain simplifying assumptions for various densities and electron temperatures of the gas. In addition, the effect of the frequency dependence of the hydrogen absorption coefficient in determining the size of the transition zone of H II region is investigated. (auth)

39341 PROFILES OF LYMAN-ALPHA SCATTERED BY FREE ELECTRONS IN THE SOLAR CORONA. Hughes, Cara Joy (Harvard Coll. Observatory, Cambridge, Mass.). Astrophys. J., 142: 321-5(July 1, 1965).

The profile of Lα radiation Doppler scattered by free electrons in the solar corona was examined, both as a function of the coronal temperature and of the geometric properties of scattering along a line of sight off the solar limb. The significance of the profile width at half-intensity as a measure of coronal temperature is then discussed. (auth)

39342 AN EMPIRICAL DETERMINATION OF THE DEPTH VARIATION IN THE SOLAR PHOTOSPHERE OF THE TOTAL PHOTON FLUX. Waddell III, J. Astrophys. J., 142: 326-34(July 1, 1965).

The total photon-number flux is calculated as a function of depth in the solar photosphere. It is demonstrated that the total photon-number flux decreases inward to the star. It is also shown that the same effective temperature characterizing the energy flux also characterizes the emergent photon number flux. It is further indicated that, in the upper photospheric regions of the solar atmosphere, the total photon-number flux is characterized by a zero or near-zero divergence. (auth)

39343 STANDING MODE OF COMPRESSIONAL-BODY GRAVITY WAVE IN THE SOLAR CHROMOSPHERE. Uchida, Yutaka (Princeton Univ., N. J.). Astrophys. J., 142: 335-50(July 1, 1965).

Propagation features of the low-frequency hydrodynamic waves under the influence of gravity are investigated in relation to the observed solar chromospheric oscillation. It is shown that, in addition to the vertical acoustic mode investigated by Bahng and Schwarzschild, the compressional gravity-wave mode can yield a standing wave in the low chromosphere for a frequency and a horizontal wavelength near the observed values. The equations reduce to the form $d^2\phi/dz^2 + f(\omega, k_x; z)\,\phi = 0$, where ϕ is the Fourier coefficient in time and the horizontal distance of $\rho_0^{\frac{1}{2}} \times$ (vertical displacement). The behavior of $f(\omega, k_x; z)$ for some given temperature profiles is investigated for various ω and k_x, and it is shown that the temperature minimum in the low chromosphere behaves like a "potential well" in quantum mechanics (if we remember that our reduced equation has the same form as the one-dimensional Schrödinger equation) for the compressional gravity-wave mode with ω and k_x around the observed values. The analysis of this eigenvalue problem indicates that the fundamental resonance value of $2\pi/\omega$ is near the observed period of 5 minutes, if we take k_x corresponding to the observed lateral scale of the oscillation cell. The eigensolution corresponding to these parameters seems to explain fairly well the observed properties of the oscillation. (auth)

39344 A MULTIPLE-BOUNCE THEORY FOR THE EXPANSION AND RETARDATION OF A COLD-PLASMA EXPLOSION BUBBLE. Kruskal, M. D.; Bernstein, I. B., Kulsrud, R. M. (Princeton Univ., N. J.). Astrophys. J., 142: 369-82(July 1, 1965). (MATT–271).

The free expansion and beginning of retardation of a mainly spherical bubble of cold plasma is analyzed by considering the multiple collisions of its elements with the interface separating it from the external ambient medium. This medium is not analyzed but is merely treated as exerting a known pressure on the bubble. The thickness of the layer of material that has already collided is computed, and an appropriate and simple "snowplow approximation" is obtained by treating this layer as thin, which for most purposes is legitimate. In dimensionless units chosen to make both the plasma mass and its initial radial velocity unity and the external pressure $(4\pi)^{-1}$, the behavior of the bubble radius for small t is given by $R(t) = t - at^{\frac{5}{2}} + \ldots$, where a = 0.2225 for the multiple-bounce treatment and is 6 per cent larger for the snowplow approximation. The thickness of the layer is $\frac{1}{4}$ of the "lag" ($at^{\frac{5}{2}}$) of the bubble behind free expansion. (auth)

39345 SOLAR ABUNDANCES OF GALLIUM, SILVER, AND INDIUM. King, R. B.; Lawrence, G. M.; Link, J. K. (California Inst. of Tech., Pasadena; Princeton Univ., N. J.; and Univ. of California, Berkeley). Astrophys. J., 142: 386-7(July 1, 1965).

The absolute oscillator strengths of thirty-eight lines in the spectra of ten elements were measured using the atomic beam technique. For silver, gallium and indium, the lines measured in the atomic beam were the same lines used previously in a comprehensive study of elements in the solar atmosphere. A simple revision of the previously derived solar abundances can be made since the oscillator strengths of these lines enter directly into the abundance determinations. The f-values of identified lines of the above three elements are compared with previous results. (J.F.P.)

39346 LITHIUM IN THE SOLAR-DISK SPECTRUM. Lynds, C. R. (Kitt Peak National Observatory, Tucson, Ariz.). Astrophys. J., 142: 396-9(July 1, 1965).

Spectroscopic observations were made of the solar disk spectrum in the region of the lithium lines at λ 6707 Å. The very high signal-to-noise ratio achieved shows that, for features having central absorptions of less than 1 per cent, there is a serious problem of interpretation in this, and probably most, regions of the solar spectrum, because of the large numbers of weak features probably present at such low levels of absorption. Agreement between observed and calculated intensity distributions is poor. There is fairly clear evidence for at least two interloping features of unknown origin in the observed distribution at λ 6707 Å and at λ 6708 Å. The total equivalent width for the lithium components used in the synthesis is 1.6 mÅ. This value is considered to be an upper limit. (J.F.P.)

39347 OBSERVATIONS OF EXTREMELY COOL STARS. Neugebauer, G.; Martz, D. E.; Leighton, R. B. (California Inst. of Tech., Pasadena). Astrophys. J., 142: 399-401(July 1, 1965).

As part of a program of infrared astronomy, a survey of the sky in two infrared spectral ranges, 0.68 to 0.92 μ and 2.01 to 2.41 μ is being carried out. The purpose is to obtain an unbiased census of objects that emit in the 2.0 to 2.5 μ atmospheric window. A number of strikingly red stars are already found. Since most of these superred stars occur in the Milky Way, interstellar reddening may be of some consequence, but in a few cases the stars seem to be intrinsically extremely red. The survey instrument consists of a 62 inch, f/1 aluminized plastic mirror capable of 2 inch resolution. Characteristics of the ten extremely red objects found are described. (J.F.P.)

39348 THE SPECTRA OF TWO EXTREMELY RED OBJECTS. Muench, Guido; Scargle, Jeffrey D. (Carnegie Institution of Washington, D. C. and California Inst. of Tech., Pasadena). Astrophys. J., 142: 401-2(July 1, 1965).

A photographic spectrum of the extremely red object in Taurus was obtained. The spectrum exhibits the characteristics of a very advanced spectral type, the most prominent features being the VO band systems around λλ 7400 and 7900 Å. The band heads of TiO appear less pronounced than in the M6 giant standard HD 196610 and through the region λλ 6700-8900 Å also show a steeper density gradient than the M6 standard. The lack of standards for later types does not allow the assignment of a precise spectral type, but from the definitions of the classification system previously established, it is determined that the spectral type is not earlier than M8, and is probably not a main-sequence object. Measurements of the energy flux in the Taurus object and also in the Cygnus object were also made. These fluxes are given. (J.F.P.)

39349 PHOTOMETRIC RESULTS OF A SPECIAL SURVEY FOR INTERLOPERS. Sandage, Allan; Vernon, Philippe (Carnegie Institution of Washington, D. C. and California Inst. of Tech., Pasadena). Astrophys. J., 142: 412-14(July 1, 1965).

Since photoelectric photometry of ultraviolet objects called interlopers showed each to have the highly peculiar colors characteristic of quasi-stellar radio sources but to be radio quiet, a special survey was made to find similar objects in large numbers for study of their group properties. Thirty-one interlopers with strong ultraviolet excess were found. The survey should be reasonably complete for objects brighter than $B \simeq 19^m$ which meet this color restriction. Photoelectric photometry of twenty-one of the objects provided the initial clue to the existence of radio-quiet, blue quasi-stellar galaxies whose optical properties are similar to those of the interlopers. With the identification of most of these objects as intrinsically bright stellar-appearing galaxies, previous catalogs provide a large finding list to determine whether the quasi-stellar galaxies are weak radio emitters. It is expected that such study will shed light on the evolutionary process of radio decay after the intense quasi-stellar source radio phase. (J.F.P.)

39350 COSMIC BLACK-BODY RADIATION. Dicke, R. H.; Peebles, R. J. E.; Roll, P. G.; Wilkinson, D. T. (Princeton Univ., N. J.). Astrophys. J., 142: 414-19 (July 1, 1965).

The temperature of the universe is considered in earliest times. Thus the discussion is not limited to closed oscillating models. If the universe is filled with blackbody radiation, it is noted that as the universe expands the cosmological redshift would serve to adiabatically cool the radiation, while preserving the thermal character. The radiation temperature would vary inversely as the expansion parameter of the universe. Measurements of background radiation imply a temperature in excess of 10^{10} °K during the highly contracted phase of the universe. It is concluded that the universe is closed and oscillating from present data and simplifying assumptions. (J.F.P.)

39351 $^{34}S/^{32}S$ RATIOS FOR THE DIFFERENT FORMS OF SULPHUR IN THE ORGUEIL METEORITE AND THEIR MODE OF FORMATION. Monster, Jan; Anders, Edward; Thode, H. G. (McMaster Univ., Hamilton, Ont.). Geochim. Cosmochim. Acta, 29: 773-9(July 1965).

The ($^{34}S/^{32}S$) ratios for the three main sulfur-containing compounds of the Orgueil meteorite, elemental sulfur, troilite sulfur, and sulfate sulfur, were determined. It was found that sulfate sulfur was slightly depleted in ^{34}S with respect to elemental sulfur, whereas troilite sulfur was slightly enriched in this isotope. However, a tentative material balance taking into account the various forms of sulfur gave a value of $\delta^{34}S$ very close to zero for total sulfur in the Orgueil meteorite. Minor fluctuations in the isotopic composition seemed to exist in both elemental sulfur and sulfate sulfur from one fragment to another. It is shown that the distribution of the sulfur isotopes found for the Orgueil meteorite sulfur compounds would be compatible with the assumption that a uni-directional, low-temperature reaction between elemental sulfur and liquid water led to the formation of both troilite sulfur and sulfate or their precursors. (auth)

39352 MOLECULAR EQUILIBRIA AND CONDENSATION IN A SOLAR NEBULA AND COOL STELLAR ATMOSPHERES. Lord III, Harry C. (Univ. of California, San Diego, La Jolla). Icarus, 4: 279-88(July 1965).

A theoretical study is made of the molecular equilibria present in a gas cloud with cosmic elemental abundances, temperatures of 2000 or 1700°K, and total pressures of approximately 1 atm and 5×10^{-4} atm, with special consideration of the formation of a condensed phase. From some 150 species considered, Al_2O_3, W, ZrO_2, and $MgAl_2O_4$ are found to be condensed at 2000°K at a total pressure of 1 atm. Decreasing the temperature or increasing the pressure condenses more species, which in general are of complex structure. It is shown that in the atmospheres of cool stars polyatomic molecules and possibly condensed species play an important role. The calculated equilibria should be useful for spectral studies, and the order and type of condensates should prove helpful in the future in cosmochemical problems. (auth)

39353 THE NEW ASTRONOMIES. Goldberg, Leo. Intern. Sci. Technol., No. 44: 18-27(Aug. 1965).

The influence of space vehicles and new techniques of astronomy are discussed. The data from astronomical studies beyond the obscuring effects of the atmosphere has verified some theories and proposed others. Progress in the ultraviolet and in the infrared astronomy is noted. X-ray sources and neutron stars are discussed. The influence of plasma physics is also discussed and other newly discovered phenomena as well. A summary is given of some of the astronomical research completed and in prospect. (J.F.P.)

39354 EFFECT OF ROTATION ON THE STABILITY OF VERY MASSIVE STARS. Roxburgh, Ian W. (High Altitude Observatory, Boulder, Colo.). Nature, 207: 363-4 (July 24, 1965).

The approximate method of Fowler is used to examine the effect of rotation on the stability of massive objects, with mass of order 10^6 to 10^8 $M_\odot$. Formulas for the total stellar energy and the lower limit of the radius for stellar stability are obtained, for nonrotating and rotating sys-

tems, taking into consideration the dominance of radiation pressure and general relativistic effects. It is found that none of the nonrotating massive objects with $M \geq 10^6\ M_\odot$ achieves an equilibrium configuration where H burning at the center balances the energy loss by radiation. For rotating objects, the instability boundary is decreased to $M \simeq 10^7\ M_\odot$. Equations for the time needed to contract to the instability radius are obtained for both conditions. Effects of nonuniform rotation are considered briefly. (M.J.T.)

39355 COOLING OF NEUTRON STARS. Tsuruta, Sachiko (Smithsonian Astrophysical Observatory, Cambridge, Mass.); Cameron, A. G. W. Nature, 207: 364-6 (July 24, 1965).

A summary is given of cooling calculations for neutrons stars, using star models based on composite equations of state with nuclear forces included. Two potentials for interactions between neutrons, suggested by Levinger and Simmons, were used, which span a range of possible behavior of the nuclear forces at high densities. The equation of state was cut off with one of two possible pressure saturation conditions prescribed by general relativity. The gravitational and proper masses determined as a function of central density for the two composite equations of state, using numerical integration of the general relativistic equations of hydrostatic equilibrium are shown. Representative cooling curves for neutron star models were calculated for three models with different mass-density relations, fitting hot atmospheres composed of iron and magnesium to the models, and taking into account three neutrino cooling rates (pair emission from the plasma process, the URCA process, and the bremsstrahlung process) and photon surface emission. Cooling curves as a function of age are shown for the iron atmosphere. (M.J.T.)

39356 GLOBULAR CLUSTERS AS REMNANTS OF QUASARS. Wyller, Arne A. (Univ. of Oslo, Blindern). Nature, 207: 394-5(July 24, 1965).

A model for the formation of globular clusters, drawing on concepts of the gravitational-collapse and the spherical-galaxy-formation theories, is outlined qualitatively; some consequences of this model for the explanation of quasar characteristics are discussed. Proto globular clusters are identified with the supermassive objects of Hoyle and Fowler, with similar evolution up to the onset of nuclear burning; the central core of the star then collapses, transferring energy to the outer envelope. The quasar energy sources are the nuclear burning of H into He and the gravitational energy from the final implosion of the core. The young (10^9 years old) and the halo globular clusters in the galaxy are discussed in terms of this model, considering age, light-emission variations, and element abundances. (M.J.T.)

39357 A SEARCH FOR LOW-ENERGY GAMMA-RAYS FROM THE QUASAR 3C286. Adams, D. J.; Hillier, R. R.; Janes, A. F. (Univ. of Bristol, Eng.). Nature, 207: 396(July 24, 1965).

Observations made on the quasar 3C286, using a balloon-carried scintillation telescope at 100,000 ft, are reported. The combined energy spectrum recorded from the direction of 3C286, with background subtracted, is shown. The resulting upper limits on gamma fluxes from the quasar, due to electron-positron annihilation, neutron capture in H, and interaction of high-energy electrons with optical photons through the inverse Compton effect, are given. (M.J.T.)

39358 LACK OF HOMOLOGY IN THE OSCILLATIONS OF NEUTRON STARS. Tsuruta, Sachiko (Smithsonian Institution Astrophysical Observatory, Cambridge, Mass.). Nature, 207: 470-2(July 31, 1965).

It is postulated that the presence of dense stellar matter in the form of a neutron star may be responsible for some of the celestial x ray sources. Results are presented from recent calculations that show how various possible forms of the nuclear potential are related to the general stability of high-density objects. Models for stable stars in hydrostatic equilibrium were constructed by solving the general relativistic equations of hydrostatic equilibrium. The results of the calculations indicated that homologous vibration of these neutron star models do not accurately represent the fundamental mode, and more complicated trial functions must be used to test for instability of such models. (C.H.)

39359 COLLAPSIBLE STARS. Kilmister, C. W. (London Univ.). New Scientist, 27: 76-8(July 8, 1965).

Relativity theory and gravitational theory are briefly reviewed; and a brief history is given on their development. The behavior and observation of collapsing bodies is discussed. Observation by neutrino emission is suggested for massive, invisible objects formed by gravitational collapse. The energy of the very bright quasars is unaccounted for. (J.F.P.)

39360 SINGULARITIES IN HOMOGENEOUS WORLD MODELS. Hawkins, S.; Ellis, G. F. R. (Cambridge Univ., Eng.). Phys. Letters, 17: 246-7(July 15, 1965).

A general relativistic model of the universe is considered, in which it is implied that a spacelike hypersurface of transitivity exists, defined uniquely by a group of motions. It is shown that the conditions specified for the character of the space-time imply that there is a physical singularity in the universe. (L.B.S.)

39361 NEUTRINO ASTROPHYSICS. Jatczak, Jerzy. Postepy Astron., 13: 63-84(Apr.-June 1965). (In Polish)

The processes of cosmic neutrino and antineutrino production: nuclear reactions in stars, URCA-process, universal Fermi interaction between electrons and neutrinos, and interactions of cosmic rays with nuclei are considered. At high values of the stellar density and temperature, neutrino energy losses may be larger than the amount of energy which is carried off as a result of photon radiation. Energy emission from stars by neutrino pairs may be of interest for studying stars in their last stage of evolution. It is possible that the energy density of neutrinos and antineutrinos in the universe is comparable to or higher than the nucleon energy density. (auth)

39362 EXPLODING GALAXIES. Sandage, Allan R. (Mount Palomar Observatory, Calif.). Sci. Am., 211: 38-47(Nov. 1964).

Evidence, largely from radioastronomy, indicating that cosmic rays originate in galactic explosions is reviewed. The mechanism by which electromagnetic radiation in the radio region of the spectrum is generated by radio galaxies is considered. In the most likely model, radio waves are generated by the interaction of relativistic electrons and a magnetic field. As an electron gyrates around a line of force in a magnetic field, it accelerates and consequently emits energy in the form of synchrotron radiation. The exploding-galaxy hypothesis as a working model for interpreting data is discussed, and some findings made on M 82 are related. Preliminary measurements indicate that the synchrotron radiation process is sufficiently energetic to account for the ionization of the hydrogen gas in the filaments and hence for the characteristic Hα emission lines. Thermonuclear reactions, which convert H to He, are comparatively inefficient, producing only 6×10^{18} erg for every g converted. Even if the conversion of mass to radio energy were 100% efficient, 10 billion solar masses of H would be required to produce 10^{62} ergs of radio energy. This figure, however, corresponds to the entire mass of a medium-sized galaxy. Thus, conventional energy sources are not adequate to explain the phenomenon, and some totally new energy principle may have to be devised. A possible new mechanism is provided by a model, in which, when any scattered mass condenses, gravitational potential energy is released. This can be a very efficient process, since the potential energy varies directly with the square of the mass and inversely with the final radius. (TCO)

39363 RADIO ASTRONOMICAL AND SATELLITE STUDIES OF THE ATMOSPHERE. Aarons, Jules (Air Force Cambridge Research Lab., Bedford, Mass.). Trans. N. Y. Acad. Sci., 27: 215-26(Dec. 1964).

The influence of atmospheric and ionospheric absorp-

tion on solar and cosmic radiation is discussed. The simplest absorption is illustrated by the Sudden Cosmic Noise Absorption (SCNA). Many flares will emit x rays. The ionization of the D layer of the ionosphere, from 60 to 90 km, will result in absorption of the hot cosmic noise background. In the example used, shortly after the commencement of a flare, radio emission at 3800 Mc/sec increased considerably (closely paralleling the optical emission). A little later at 10 and at 30 Mc/sec there was a decrease in signal, i.e., the start of the sudden cosmic noise absorption. In the case illustrated, after the flare disappeared, the absorption vanished. Another type of absorption observed on the same type of equipment, the riometer, is an effect of the aurora. Auroral absorption is produced by high energy electrons (20-40 kev) whereas lower energy electrons of a few electron volts produce the optical auroral effect. The mechanism involved is that particles from the outer radiation belt rain down or precipitate on the ionosphere at certain latitudes, i.e., in the auroral zones. While there is correlation between optical auroras and auroral absorption, there isn't complete one-to-one correspondence. The greatest precipitation of electrons above 40 kev takes place after magnetic midnight. Solar flares of great intensity and specific radiation characteristics emit the high energy protons which arrive within one half an hour to several hours after the flare emission. Satellite experiments have shown that there were three times as many electrons above the 400-km height as below it. During magnetic storms the high latitude electronic content decreases (while other techniques showed that the equatorial electron content increased or resulted in a bulge of electrons relative to normal values). A satellite transmitting on a frequency from 20 to 200 Mc/sec provides a means for making an instantaneous picture of the irregularity structure of the ionosphere as well as the total electron content. Other aspects of scintillations, which have been studied with both radioastronomy and with transmissions from satellites, are discussed. (TCO)

39364 NEAR-EARTH AND INTER-PLANETARY PLASMA. Gringauz, K. I. Vestn. Akad. Nauk SSSR, No. 5, 60-6(May 1965). (In Russian).

Recent measurements of charged particle flux obtained on space probes at various distances from the earth have confirmed the main features of the solar wind theory proposed by Parker in 1958. Data from Soviet moon probes show that the concentration of positive ions N_i varies from 10^2 to 10^3 particles cm^{-3} at heights of 10,000 to 20,000 km. Thermal ions could not be detected above 22,000 to 24,000 km. Soviet moon probes showed charged particle fluxes of 1 to 3×10^8 cm^{-2} sec^{-1} at a distance of 100,000 km from the earth. A flux as high as 10^9 cm^{-2} sec^{-1} was observed on a Venus probe during a strong magnetic storm recorded on earth. Data from the American rocket Explorer 10 (maximum distance of ~200,000 km from the earth) showed that the proton energy was 400 to 500 km/sec in good agreement with the theoretical value calculated by Parker. Continuous observations by Mariner-2 probe to Venus showed the variations in the velocity of the solar wind. The field strength in interplanetary space is 1 to 3×10^{-5} oersteds. New data from Explorer-18 indicates that the interplanetary magnetic field has a spiral structure. Valuable data have been obtained on the thickness of the ionosphere of the earth. (TTT).

Atomic Physics

Refer also to abstracts 38937, 39788, and 39879.

39365 (COO-720-047) EXCHANGE EFFECTS IN SCATTERING OF SLOW ELECTRONS BY ATOMS. Chinh, Le Dinh (Case Inst. of Tech., Cleveland, Ohio. Nuclear Physics Lab.). [1963]. Contract AT(11-1)-720. 61p. Dep.(mn); $3.00(cy), 2(mn) CFSTI

The identity of incident and atomic electrons in the scattering of electrons by atoms requires that the wave function of the system be antisymmetrized. This antisymmetrized wave function gives rise to extra terms in the potential energy of the system: the exchange potential. A general equation is written which takes into account the exchange effects in scattering of electrons by an atom. The cross section for scattering of an electron by an atom can be found using this equation once the orbitals of the atomic electrons are known. This equation is applied to lithium and solved numerically. (M.O.W.)

39366 (JINR-P-2185) ATOMNYI ZAKHVAT OTRITSATEL'NYKH MYUONOV V KHIMICHESKIKH SOEDINENIYAKH. (Atomic Capture of Negative Muons in Chemical Compounds). Zinov, V. G.; Konin, A. D.; Mukhin, A. I. (Joint Inst. for Nuclear Research, Dubna (USSR). Lab. of Nuclear Problems). 1965. 19p. Dep. mn.

The atomic capture of negative muons in binary compounds is studied. The ratio of probabilities of the muon atomic capture in oxides changes periodically with the growth of the charge in accordance with the Mendeleev Chart. It also depends on the type of a compound. The ratio of probabilities of the atomic capture in compounds of metals with halogens and metal alloys is described satisfactorily by a linear dependence. (auth)

39367 (LA-DC-6548) COUPLING CONSIDERATIONS IN TWO-ELECTRON SPECTRA. Cowan, Robert D. (Los Alamos Scientific Lab., Univ. of California, N. Mex.); Andrew, Kenneth L. (Purdue Univ., Lafayette, Ind. Dept. of Physics). [1964]. Contract W-7405-eng-36. 64p. Dep.(mn); $3.00(cy), 2(mn) CFSTI.

The energy level structure, relative line strengths, and Landé g-factors of two-electron configurations are discussed for four important types of pure coupling LS, LK, jK(jl), and jj. Transitions from one type of coupling to another are discussed in detail, using the configuration pf as an example. The appropriateness of LS- and jj-coupling notation in two-electron spectra is quite limited for atoms of medium atomic weight, where nearly all excited configurations show a strong tendency toward pair (LK to jK) coupling. For other atoms, pair coupling occurs mainly for high values of orbital angular momentum of the excited electron; the coupling may be near LK for small values of the principal quantum number of this electron, and it approaches pure jK as this quantum number increases. It is emphasized that LK or jK notation would best be used only when the coupling conditions approximate LK or jK coupling, respectively; either notation can serve to unambiguously identify levels throughout the range of intermediate pair couplings, but will not correctly designate the nature of the quantum states because of reversals of the L and j compositions of certain states as the coupling conditions change from pure LK to pure jK. (auth)

39368 (NP-15089) ETUDE DES EFFETS QUADRUPOLAIRES SUR LES NIVEAUX D'ENERGIE DANS UN ATOME DE MANGANESE μ-MESIQUE (these). (Study of the Quadrupolar Effects on the Energy Levels in a μ-Mesic Manganese Atom (thesis)). Berthier, Louis (Lyon Univ. (France)). June 1965. 36p. Dep.(mn).

The energy levels of the μ-mesic atom caused by the monopolar potential are calculated for the case of a manganese atom that has captured a negative μ meson. It is shown that the existence of a quadrupolar potential causes a modification of these calculated energy levels. This perturbation is a method that can be used to define the size of the quadrupole moment of the nucleus. (J.S.R.)

39369 (NP-15140) THEORY OF ATOMIC BEAM OPTICAL DOUBLE RESONANCE SPECTROSCOPY. Special Technical Report. Serber, R. (Columbia Univ., New York. Columbia Radiation Lab.). Apr. 15, 1965. Contract DA28-043 AMC-00099(E). 34p. (CU-4-65-AMC-00099(E)Phy.).

The theory of the atomic beam optical double resonance spectroscopy first introduced by I. I. Rabi is developed. An expression for the transition probability is derived which includes terms that may lead to line shifts and distortions. The approximations made in obtaining this result are given, and means for attaining a more precise line-shape formula are indicated. (auth)

39370 (ORNL-P-1336) CHANNELING EFFECTS ON THE ENERGY LOSS OF HIGH ENERGY (20-80 Mev) ^{79}Br AND ^{127}I IONS IN GOLD. Datz, S.; Noggle, T. S.; Moak, C. D. (Oak Ridge National Lab., Tenn.). [1965]. Contract W-7405-eng-26. 25p. (CONF-650627-1). Dep. mn; CFSTI, $1.00 cy, $0.50 mn.

From Conference on Electromagnetic Isotope Separators and Related Ion Accelerators, and their Applications to Physics, Aarhus, Denmark.

Multicomponent beams of Br and I ions with energies up to 80 Mev were used to study the effect of crystallographic orientation on energy losses in thin gold single crystals. The spectra obtained from various setups are included. (M.O.W.)

39371 (TID-22044) CROSS-OVER SIGNALS IN ATOMIC HYDROGEN (thesis). Himmell, Lewis Craig (Michigan Univ., Ann Arbor). 1965. Contract AT(11-1)-1112. 222p. Dep.(mn); $6.00(cy), 4(mn) CFSTI

The angular distribution function for resonant fluorescent scattering of Lyman alpha photons on atomic hydrogen when there are degeneracies in the excited states is examined. The calculations included all effects in the hamiltonian that were larger than 0.1 Mc/sec. The theory was then applied to atomic hydrogen assuming an infinitely massive proton. The Dirac equation, with some radiative corrections added phenomenologically, was used to determine the energy levels of the system. The level crossings were obtained by means of an external axially symmetric magnetic field. Finally, the general theory of resonance fluorescence in hydrogen is considered. (M.O.W.)

39372 EXTRAORDINARY ORBITALS IN THE UNITED ATOM MODEL. Tamassy-Lentei, I. (Kossuth Lajos Univ., Debrecen, Hungary). Acta Phys. Acad. Sci. Hung., 18: 359-65(1965).

For a representation of the one-electron orbitals in the united atom model, one can use, in addition to the usual hydrogen-like orbitals, also extraordinary functions, continuous in the electron coordinates but having only piecewise continuous derivatives. Computations are made for H_2^+ with a linear combination of middle point centered on ordinary $\psi_{1\sigma}$, $\psi_{1\sigma'}$, ψ_{2p_z} and extraordinary $|\psi_{2p_z}|$ orbitals. The results obtained for the energy show a considerable improvement on introducing the extraordinary orbital $|\psi_{2p_z}|$. (auth)

39373 POSITION OF LANTHANUM IN THE PERIODIC TABLE. Hamilton, David C. (Univ. of Calif., Los Angeles). Am. J. Phys., 33: 637-40(Aug. 1965).

In a widely used version of the periodic table, lanthanum is classed in the same column with scandium and yttrium. However, in a number of respects lutetium resembles scandium and yttrium more closely than lanthanum does. Hence the periodic table should be modified so that scandium, yttrium, and lutetium are in the same column. (auth)

39374 ON THE ENERGY DISTRIBUTION OF THE PARTICLES EMITTED BY THE CATHODE DISINTEGRATION. Benninghoven, A. (Universitat, Cologne). Ann. Physik (7), 15: 113-43(1965). (In German)

The secondary ion spectra and energy distributions of a series of secondary ions emitted in the decomposition of aluminum, duraluminum, and magnesium targets by Hg ions (200 to 2000 ev) were measured with a single-focusing, 60° mass spectrometer. The secondary ion spectrum shows, in addition to ions from the target metal, ions from impurities of the target and from the residual gas. A semiqualitative explanation of the differences in the energy distributions of the secondary ions is given using energy transfer functions. (D.C.W.)

39375 ENERGY DEPENDENCE OF THE MEAN ENERGY PER ION PAIR AT LOW ELECTRON ENERGIES. Booz, J.; Ebert, H. G. (Universitaet Gottingen, Ger.). Biophysik, 2: 226-32(1965). (In German)

From the magnitudes of mean energy expenditure in the production of an electron by collision ionization in a microwave field, measured for various gases in a hollow resonator, the mean energy per ion pair in ionization by slow electrons (about 50 to 200 ev) could be calculated approximately. The results show that the mean energies per ion pair in air, nitrogen, hydrogen, and argon are constant within the measurement accuracy for electron energies from 200 ev to 3 Mev. Under about 100 ev, the mean energies per ion pair in hydrogen and argon increase very rapidly with decreasing electron energy. In air and nitrogen this increase begins at about 200 ev. (tr-auth)

39376 ON THE MEASUREMENT OF PHOTOELECTRIC CROSS-SECTION OF GAMMA-RAYS. Oberoi, R. S.; Mohan, Radhe; Sood, B. S. (Punjab Univ., Patiala, India). Current Sci. (India), 34: 372(June 20, 1965).

Measurements were made on the photoelectric cross section of 662 kev gamma rays for K-electrons in lead by measuring the intensity of K radiation following the interaction. This method though indirect is relatively simple and has wide applicability. The fluorescent yield at 662 kev for lead being 0.965, the measured photoelectric cross section was found equal to 12.4 ± 0.9 barns/atom. (P.C.H.)

39377 ABSOLUTE PHOTOELECTRIC CROSS-SECTIONS OF 145 kev GAMMA RAYS IN TANTALUM AND PLATINUM. Parthasaradhi, K.; Lakshminarayana, V.; Jnanananda, Swami (Andhra Univ., Waltair, India). Indian J. Pure Appl. Phys., 3: 223-4(1965).

Absolute photoelectric cross sections of 145 kev gamma rays in tantalum and platinum have been determined experimentally using a well-type plastic crystal scintillation spectrometer, and found to be 421 ± 42 and 519 ± 52 barns per atom respectively. The results are in agreement with the theoretical values computed from the expressions of Heitler-Stobbe and Nagel as well as with the interpolated values from the NBS Circular 583. (auth)

39378 NUCLEAR SPIN RELAXATION IN GASES AND LIQUIDS. IV. INTERPRETATION OF EXPERIMENTS IN GASES. Bloom, M. (Harvard Univ., Cambridge, Mass.); Oppenheim, I.; Lipsicas, M.; Wade, C. G.; Yarnell, C. F. J. Chem. Phys., 43: 1036-47(Aug. 1, 1965).

The theory of nuclear spin relaxation in gases and liquids developed by Bloom and Oppenheim was used to interpret measurements of spin lattice relaxation times for various gaseous systems over wide ranges of temperature and density. The systems discussed include: molecular H_2 with different ortho and para concentrations; mixtures of H_2 with He, Ne, Ar, N_2, CO_2, O_2, CO, NO, and N_2O; and normal D_2. The analysis led to a determination of the form of the anisotropic intermolecular potentials providing that the form of the isotropic part of the intermolecular potentials was known. Values of quadrupole moments for H_2, O_2, N_2, CO, NO, N_2O, CO_2, and D_2 were obtained, which were in good agreement with previous values. Thus, nuclear spin relaxation was concluded to be a valuable tool for obtaining anisotropic intermolecular potentials. (auth)

39379 CORRECTIONS TO THE INCOHERENT SCATTERING FACTORS FOR ELECTRONS AND X RAYS. Bonham, R. A. (Tokyo Univ. and Indiana Univ., Bloomington). J. Chem. Phys., 43: 1460-4(Sept. 1, 1965).

The usual use of the closure relation in the derivation of the incoherent scattering factor for electrons and x rays involved approximations and introduced errors in the final result. Corrections through third order for these errors are given. The correction terms were found to be of a simple form and can be quite important not only in the limit of low energy for the incident electron or x-ray beam but also for atoms of large atomic number. The magnitudes of the corrections for Ne and Ge are given for 40-kv electrons. In the x-ray case corrections are given for Ge for Cu Kα x radiation. (auth)

39380 DIPOLE MATRIX ELEMENTS FOR HELIUM IN THE FIRST-ORDER SHIELDING APPROXIMATION. Sando, Kenneth M.; Epstein, Saul T. (Univ. of Wisconsin, Madison). J. Chem. Phys., 43: 1620-1(Sept. 1, 1965).

The first-order shielding approximation was used to calculate dipole matrix elements for the 2^1S–2^1P and 1^1S–2^1P transitions in two-electron atoms. (auth)

39381 MANY-ELECTRON-THEORY AB INITIO CALCULATION FOR THE Be ATOM. Geller, Murray (Jet Propulsion Lab., Pasadena, Calif.); Taylor, Howard S.; Levine, Howard B. J. Chem. Phys., 43: 1727-36(Sept. 1, 1965).

The details and results of an ab initio calculation of the energy of the Be atom using the Sinanoğlu many-electron theory are presented. Comparisons were made with earlier calculations on the Be atom by this technique and by other techniques. The pitfalls and shortcomings of the many-electron theory on extension to larger systems are discussed. (auth)

39382 ATOMIC TERMS FOR EQUIVALENT ELECTRONS. Karayianis, N. (Harry Diamond Labs., Washington, D. C.). J. Math. Phys. (N. Y.), 6: 1204-9(Aug. 1965).

The problem of determining the number of times, b(lNLS), a given term occurs in an atomic configuration of the form $(nl)^N$ is considered by the methods of group theory. The b are shown to be related to the classical problem of partitioning numbers. Several expressions relating b to other, simpler partitions are obtained, which result in a recursion relation for the b. A table for b(4NLS) is included to complement existing tables for the range $1 \leq l \leq 3$. (auth)

39383 THEORETICAL STUDIES OF LANTHANIDE AND ACTINIDE SPECTRA. Wybourne, B. G. (Argonne National Lab., Ill.). J. Opt. Soc. Am., 55: 928-35(Aug. 1965).

The role and feasibility of theoretical calculations in the interpretation of the energy levels of the rare earths and their associated electronic properties is explored. It is shown that the density of states places a fundamental limitation on establishing a unique correlation between the experimental and theoretical energy levels in rare earths. For most rare-earth electron configurations containing five or more electrons (or holes) outside closed shells, the density of states is sufficiently high as to preclude the possibility of a unique correlation except for those levels built upon the lowest energy states of the f^N core. The levels of the f^N(N = 5 to 9) configurations follow the Wigner statistical distribution quite closely, with the result that most of the electronic properties that distinguish the character of one level from another are smeared out. It is suggested that whenever the density of states is high, the energy levels and their associated properties will be statistically distributed. (auth)

39384 SPARK SPECTRUM OF BERKELIUM. Gutmacher, Ralph G.; Hulet, E. Kenneth; Lougheed, Ronald (Univ. of Calif., Livermore). J. Opt. Soc. Am., 55: 1029-30(Aug. 1965). (UCRL-12274).

Berkelium emission lines are recorded and the persistent lines determined for possible analytical applications. Berkelium, in the tetravalent state, was separated from all radioactive species except ^{141}Ce to ^{144}Ce by extraction chromatography. Cerium was separated by elution; and other impurities were removed. The wavelength region was covered from 2500 to 4500 Å. Two aliquants of the berkelium fraction were excited in a high-voltage spark, and their spectra photographed. The results showed several of the berkelium lines have wide hyperfine structure. It is hoped that a study of the resolved flag pattern, which could show up to eight components while the nuclear spin was stated to be $\frac{1}{2}$, can be made soon. Also a spectroscopic means for the determination of berkelium may be useful since its radioactive assay is difficult. (J.F.P.)

39385 ANALYSIS OF THE SPECTRUM OF TRIPLY IONIZED PRASEODYMIUM (Pr IV). Sugar, Jack (National Bureau of Standards, Washington, D. C.). J. Opt. Soc. Am., 55: 1058-61(Sept. 1965).

The spectrum of Pr^{3+} produced by a sliding spark discharge was photographed in the wavelength range of 800 to 3100 Å with a 35-ft Eagle vacuum spectrograph. An analysis of the resulting line list led to the discovery of all the levels of the $4f^2$(except the $^1S_0$), 4f5d, 4f6s, and 4f6p configurations. The interaction parameters for each configuration were derived from a least-squares fit of the energy formulas to the observed levels. (auth)

39386 NATURAL WIDTH OF SPECTRAL LINES AND IRREVERSIBILITY. Mizushima, M.; Robert, D.; Galatry, L. (Faculte des Sciences, Rennes, France). J. Phys. (Paris), 26: 194-8(Apr. 1965). (In French)

A theory of the natural line shape derived from the study of the time evolution of the density operator for an atom and field oscillators is proposed. The finite width is a direct consequence of the presence of a propagator in the evolution equations; the matrix elements of this propagator were computed up to the second order. The influence of the field intensity was taken into account to this approximation and gives a modification of the shift of the line only. The formalism used makes obvious the strong relation between the natural line width and the irreversible character of the evolution. (auth)

39387 ON THE WEIZSÄCKER CORRECTION TO THE THOMAS-FERMI THEORY OF THE ATOM. Yonei, Katsumi; Tomishima, Yasuo (Okayama Univ., Japan). J. Phys. Soc. Japan, 20: 1051-7(June 1965).

In order to investigate the validity of the Weizsäcker correction to the Thomas-Fermi theory of the atom, the problem in which the Weizsäcker correction is multiplied by a constant weighting factor λ is solved for the atom neglecting the interactions between electrons completely, in view of the fact that the Weizsäcker term is essentially the correction to the statistical expression of the kinetic energy of electrons. The energy values thus obtained are compared with the exact quantum mechanical values, and it is shown that the Weizsäcker term is too large in its original form and a weighting factor $\lambda \approx \frac{1}{5}$ (in contrast to the Kirzhnits' conclusion $\lambda \approx \frac{1}{9}$) is necessary to give a substantial improvement over the Thomas-Fermi solution. (auth)

39388 AN EXPERIMENTAL DETERMINATION OF THE PHOTO-IONIZATION CROSS-SECTION OF ATOMIC HYDROGEN. Beynon, J. D. E. (Radio and Space Research Station, Ditton Park, Bucks.). Nature, 207: 405 (July 24, 1965).

The radiation intensity emitted from an absorption cell illuminated by light at 850.6 Å was measured for the evacuated cell, the cell filled with molecular hydrogen, and the cell filled with partially dissociated hydrogen. The mean value of the photoionization cross section of atomic hydrogen, at 850.6 Å, calculated from these measurements, is $(5.15 \pm 0.18) \times 10^{-18} cm^2$. (M.J.T.)

39389 THE INFLUENCE OF ELECTRONIC SCREENING ON HIGH-ENERGY BREMSSTRAHLUNG AND PAIR PRODUCTION. Soerenssen, A. (Norges Tekniske Hogskole, Trondheim). Nuovo Cimento (10), 38: 745-70 (July 16, 1965).

The differential cross sections for bremsstrahlung and for pair production, the cross sections integrated over angles for bremsstrahlung and pair production, and the cross section integrated over angles and energies for pair production are obtained as single integrals over the atomic form factor. It is shown that the shell structure of the atom does not give corresponding wiggles in the bremsstrahlung spectrum. It is shown that the shape of the bremsstrahlung spectrum is only slightly dependent on the angle of emission. The total cross section for pair production for 12 elements ranging from Li to U and for 41 energies ranging from 10 Mev to 100 Bev are computed numerically with the use of Hartree-Fock-Slater atomic form factors. These are compared with cross sections computed from Thomas-Fermi-Molière form factors. For 1 Bev the error in the Thomas-Fermi-Molière cross section is 2.2% in the case of Li, 0.51% in the case of U. These errors are of the same order of magnitude as the radiative correction, viz. of the order of 1%. The computed Hartree-Fock-Slater cross sections agree fairly well with experiments. Radiative corrections have not been taken into account. (auth)

39390 OSCILLATING REAL VECTORS IN COULOMB-BOUND ELECTRON FIELDS. Perkins, G. A. Nuovo Cimento (10), 38: 1006-20(July 16, 1965).

This study is based on relativity and Maxwell's and Dirac's equations, without any amendments or added hypothesis. Dirac's electron equations are used in a tensor form mathematically identical with Whittaker's but showing more clearly their relation to certain real oscillating vectors, suggested by Kramers. Those vectors are evaluated for various Coulomb-bound states, and in each state the spin, about the preferred axis, corresponds to a rotation of the vectors in physical space. The orbital angular momentum is represented by phase gradients, which vanish in the S states. Corresponding to the concept that neither the spin, nor the orbital, angular momentum is a constant of the motion, it is found that the vectors do not rotate precisely in a plane normal to the preferred axis, and their magnitudes are somewhat dependent on time. In many states the vector pattern is precisely fixed, in a rotating co-ordinate system. Two of the oscillating vectors are analogous to electric and magnetic polarizations, but if they are polarizations they would apparently emit radiation even in the hydrogen atom ground state. However, the vector analogous to magnetic current density almost vanishes, and the possibility is suggested that the known "virtual" radiative effect causes it to vanish completely. It is shown that if the magnetic current vanishes everywhere, curl A vanishes in free space so no radiation can be emitted. (auth)

39391 ON THE BROWNIAN-MOTION MODEL FOR THE EIGENVALUES OF A RANDOM MATRIX. Rosenzweig, N. (Weizmann Inst. of Science, Rehovoth, Israel). Nuovo Cimento (10), 38: 1047-53(July 16, 1965).

The fundamental solution for the Brownian motion of the eigenvalues of a random matrix in Dyson's (J. Math. Phys., 3: 1191(1962)) model is represented as an integral with respect to the measure on the orthogonal group in N dimensions. The solution is discussed for some special cases only. In two dimensions the distribution of the spacing between the eigenvalues is calculated as a function of the time and is found to depend only upon the initial value of the spacing. (auth)

39392 PRODUCTION OF A PARTIALLY POLARIZED ELECTRON BEAM WITH POLARIZATION DEGREE OF P = 17% ± 2% AT 10^{-8} A RADIATION INTENSITY THROUGH ELASTIC SCATTERING OF 300 ev ELECTRONS ON A Hg-ATOM BEAM. Steidl, H.; Reichert, E.; Deichsel, H. (Universitat, Mainz). Phys. Letters, 17: 31-2(June 15, 1965). (In German).

The dependence of the polarization degree on the scattering angle was investigated in the Mott scattering of slow electrons on Hg in the electron energy range between 300 and 700 ev. The dependence of the measured scattering current on the scattering angle after single elastic electron scattering on Hg atomic beams, and the polarization degree after single elastic electron scattering were determined at 300, 400, 500, and 700 ev. The results show that the maximum polarization occurred at the minimum intensity of the scattering current. For 300-ev electrons at the maximum angular distribution at 95°, a polarization degree of P = 17 ± 2% is present. (J.S.R.)

39393 ON THE NARROW RESONANCE IN THE SCATTERING OF ELECTRONS BY ATOMIC HYDROGEN. Kleinpoppen, H.; Raible, V. (Universitaet, Tubingen, Ger.). Phys. Letters, 18: 24-5(Aug. 1, 1965).

A hydrogen atomic beam was modulated and crossed by a low-energy electron beam. The intensity of scattered electrons was measured as a function of electron energy. A resonance centered around 9.73 ± 0.12 ev was observed at scattering angles of 70, 90, and 94°. (D.C.W.)

39394 PULSED OPERATION OF THE NEUTRAL XENON LASER. Clark, P. O. (Hughes Research Labs., Malibu, Calif.). Phys. Letters, 17: 190-2(July 15, 1965).

Pulsed laser action in neutral xenon was observed on several 5d-6p transitions. The results show that the pulsed laser oscillations fall into two distinct groups: those whose output was enhanced by short, high-current pulses and those whose intensity was a maximum for long, low-current pulses. The current and time dependence of two representative lines is illustrated. In addition to illustrating the pronounced effect of pulse amplitude and pulse length on the various transitions, the measurements also indicated that those transitions which favor short, high current pulses have much higher gain in the pulsed mode of operation than in the cw mode. (L.B.S.)

39395 KEV CHANNELING AND THERMOCHEMICAL PROPERTIES OF INTERSTITIAL IMPURITIES. McCaldin, J. O.; Brinkman, J. A. (North American Aviation Science Center, Thousand Oaks, Calif.). Phys. Letters, 17: 221-2 (July 15, 1965).

It is pointed out that the interatomic potential between a normally interstitial impurity and its host crystal is usually weak enough to give small energy losses for projectile ions of a few kev penetrating the channeling directions in crystals. The possibility offered by interstitial systems of a quantitative comparison between the potentials inferred from channeling experiments and the potentials known from thermochemical data is discussed. Examples for comparing channeling and interstitial diffusion are given for He in the host crystals Si and Ge. (L.B.S.)

39396 STATISTICAL EQUIVALENT OF THE BOLTZMANN EQUATION. Biswas, A. C. (Tata Inst. of Fundamental Research, Bombay). Phys. Letters, 17: 244-5 (July 15, 1965).

It is shown that the streaming terms in the full Boltzmann equation is the effect of the first order transitions in the μ-space as described by the Smoluchowski model of fluctuation of concentrations with a restriction on the possible transitions, thus it is shown that the Boltzmann equation has an equivalent statistical equation. (L.B.S.)

39397 MOMENTUM-TRANSFER CROSS SECTIONS FOR SLOW ELECTRONS IN KRYPTON AND XENON. Braglia, G. L. (Universita, Parma, Italy). Phys. Letters, 17: 260-1(July 15, 1965).

Momentum-transfer cross sections for elastic collisions of electrons on krypton and xenon were obtained from experimental and derived total cross sections, and are compared with those obtained from drift velocity and characteristic energy data. The results are tabulated. (L.B.S.)

39398 FORMATION OF EXCITED HYDROGEN ATOMS BY CHARGE EXCHANGE IN HYDROGEN-LIKE TARGETS. Hiskes, J. R. (Univ. of California, Livermore). Phys. Letters, 17: 263-4(July 15, 1965). (UCRL-14234)

A survey was made of the population distribution of the excited levels of hydrogen formed by protons incident on hydrogen-like targets. Capture cross sections were calculated for all levels of hydrogen through n = 15, for 10- to 140-kev protons incident on H(1S), H(2S), H(7S), and H(6p) neutralizers, and for values of the effective neutralizer charge, Z = 10, 1.5, 2.0, and 3.0. The results are discussed. (L.B.S.)

39399 ROTATIONAL STRUCTURE IN THE ENERGY LOSS SPECTRUM OF H_2. Boersch, H.; Geiger, J.; Topschowsky, M. (Technische Universitaet, Berlin). Phys. Letters, 17: 266-7(July 15, 1965).

The energy loss spectrum of a mixture of ortho and para molecular hydrogen was investigated using 30-kev electrons with an optimal energy resolution of 0.012 ev. Lyman bands were observed up to $v^1 = 19$, and the rotational structure of the vibrational bands were resolved. The spectrum of para hydrogen was also investigated. Theoretical curves were obtained using optical selection rules, and were found to be in satisfactory agreement with the experimental energy loss spectra. (L.B.S.)

39400 RUBIDIUM SPIN RELAXATION IN THE RARE GASES UNDER ULTRACLEAN CONDITIONS. Franz, F. A. (Univ. of Illinois, Urbana). Phys. Rev., 139: 603-11(Aug. 2, 1965).

The spin relaxation of optically pumped rubidium vapor

induced by rubidium–rare-gas atomic collisions was investigated in an ultraclean environment. The experiment was performed under conditions such that the partial pressure of nonrare-gas impurities was less than 1×10^{-8} torr, and that the time between Rb-Rb spin exchange collisions was short compared to the spin relaxation time. The cross sections (in cm^2) for disorientation of rubidium were found to be: He, 3.3×10^{-25}; Ne, 3.3×10^{-24}; Ar, 1.1×10^{-22}; Kr, 7.3×10^{-21}; Xe, 1.3×10^{-19}. The fact that these cross sections are considerably smaller than previously reported values is attributed primarily to the low degree of impurity contamination. When compared with already existing values for cesium and sodium, the disorientation cross sections of these three alkali metals are seen to have a remarkably similar dependence on buffer-gas atomic number. The new experimental values are also compared with recent theoretical calculations. (auth)

39401 ATOMIC OSCILLATIONS IN THE STATISTICAL APPROXIMATION. Brandt, Werner (New York Univ., New York); Lundqvist, Stig. Phys. Rev., 139: 612-17 (Aug. 2, 1965).

The dipolar spectral distribution function, or the photoabsorption cross section, of atoms is derived in the statistical approximation starting from general dynamic equations describing the density fluctuations induced in the atom by an external field. A local form of the theory is used to find that coherence between the motion in different parts of the atom causes a modification of the spectral function. The modification can be put in the form of a dispersion denominator, and, if this denominator becomes small in certain frequency ranges, the absorption is enhanced by what can be identified as collective resonances of the atom as a whole. (auth)

39402 INDEX OF REFRACTION AND SUM RULES FOR HELIUM. Migneron, R.; Levinger, J. S. (Cornell Univ., Ithaca, N. Y.). Phys. Rev., 139: 646-8(Aug. 2, 1965).

Recent measurements by Lowry and by Lukirskii of the atomic photoeffect for helium can be combined with calculations for discrete transitions and for the high-energy photoeffect to give the oscillator density for the entire range. Dispersion theory is used to calculate the index of refraction n. Satisfactory agreement is found with experiments in the visible and in the near ultraviolet, and the value of n from 2700 to 600 Å is predicted. The predicted values agree satisfactorily with values calculated by Chen and Dalgarno. These oscillator densities are used to calculate the sum rules S(0), S(1), and S(2), which weight with the zeroth, first, and second powers of the photon energy, respectively. Each result agrees with values based on ground-state wave functions to 5% accuracy. It is concluded that in general the oscillator density is known to about 5% accuracy. (auth)

39403 NUCLEAR-SPIN-LATTICE RELAXATION OF V^{51} AND Tc^{99} IN V–Tc ALLOYS. Van Ostenburg, D. O.; Spokas, J. J.; Lam, D. J. (Argonne National Lab., Ill.). Phys. Rev., 139: 713-16(Aug. 2, 1965).

The spin-lattice relaxation time, T_1, associated with the ^{51}V and ^{99}Tc nuclei in the V–Tc binary alloy system was measured over a range of compositions at room, liquid-nitrogen, and liquid-helium temperatures. The quantity T_1T (T = absolute temperature) is strongly composition-dependent, but only slightly temperature-dependent, indicating that the predominant relaxation path is via conduction electrons. Of the possible terms contributing to conduction-electron relaxation, that due to the orbital motion of the d-band electrons is believed predominant. (auth)

39404 ELECTRON EJECTION FROM SINGLE CRYSTALS DUE TO 1- TO 10-kev NOBLE-GAS ION BOMBARDMENT. Carlston, C. E.; Magnuson, G. D.; Mahadevan, P. (General Dynamics/Convair, San Diego, Calif.). Phys. Rev., 139: 729-36(Aug. 2, 1965).

The secondary-electron ejection coefficient γ was measured for the (110), (100), and (111) planes of Cu, Al, Ag, Ni, and Mo bombarded by the singly charged noble-gas ions Ne^+, Ar^+, Kr^+, and Xe^+ in the energy range from 1 to 10 kev. Surfaces were kept clean to within a fraction of a monolayer contamination by the sputtering action of the incident ion beams. The ratios $\gamma_{hkl}/\gamma_{h'k'l'}$ are quite constant, which would tend to indicate a theoretical model based on simple geometrical considerations of the opacity of the single-crystal planes. However, the fact that the ratios are relatively insensitive to the ion-bombardment energy indicates that a model based upon the transparency of the target is not sufficient to explain the phenomenon. The dependence of γ on the bombarding-ion mass is also explored. (auth)

39405 KINETIC EMISSION OF ELECTRONS FROM MONOCRYSTALLINE TARGETS. Harrison, D. E. Jr. (Naval Postgraduate School, Monterey, Calif.); Carlston, C. E.; Magnuson, G. D. Phys. Rev., 139: 737-45(Aug. 2, 1965).

A single-collision theory of the emission of electrons from a metal surface subjected to high-energy ion bombardment is developed, which gives reasonable agreement with the data of Carlston, Magnuson, Mahadevan, and Harrison, in the 1 to 10-kev energy range. The model is based upon a Thomas-Fermi-Firsov energy-transfer calculation modified to include an explicit dependence upon lattice orientation. Orientation effects appear naturally, and orientation-dependent cross sections are not required, but the distribution of possible impact parameters for a particular crystal orientation of central importance. The theory is used to determine semiempirical interaction potentials between the moving particle and a lattice atom. These potentials are more like Abrahamson's atom-atom potentials than the Gibson potentials used in radiation-damage studies. (auth)

39406 SPECTRAL ANALYSIS OF PHOTOEMISSIVE YIELDS IN Si, Ge, GaAs, GaSb, InAs, AND InSb. Cohen, M. L.; Phillips, J. C. (Bell Telephone Labs., Murray Hill, N. J.). Phys. Rev., 139: 912-20(Aug. 2, 1965).

The data of Allen and Gobeli on photoemissive yields from partially cesiated surfaces of several semiconductors with photon energies between 2 and 6 ev are analyzed in detail. The results are shown to be consistent with direct transitions in energy-band models obtained from semiempirical pseudopotentials based on interband optical edges. The correlation with reflectivity structure is good, and several new transitions are resolved which were not apparent in previous optical studies. (auth)

39407 ELECTRON CAPTURE INTO EXCITED HELIUM LEVELS BY FAST He^+ IMPACT ON He, N_2, AND O_2. Head, Charles E.; Hughes, R. H. (Univ. of Arkansas, Fayetteville). Phys. Rev., 139: A1392-7(Aug. 30, 1965).

Collision cross sections were measured for electron capture into the $3\,^3S$, $3\,^1P$, $3\,^3P$, $3\,^1D$, $3\,^3D$, $4\,^1S$, $4\,^3S$, $4\,^1D$, $4\,^3D$, and $5\,^1D$ levels of helium by He^+ impact on He, for electron capture into the $3\,^1D$, $3\,^3D$, $4\,^1D$, and $4\,^3D$ levels of helium by He^+ impact on N_2, and for electron capture into the $3\,^3D$ level of helium by He^+ impact on O_2. These cross sections were obtained in an impact energy range of 20 to 120 kev. (auth)

39408 USE OF APPROXIMATE FUNCTIONS IN EVALUATING THE BORN MATRIX ELEMENT FOR H_2^+. Peek, James M. (Sandia Lab., Albuquerque, N. Mex.). Phys. Rev., 139: A1429-31(Aug. 30, 1965).

The Born matrix element for the $1s\sigma_g$-$2p\sigma_u$ transition in H_2^+, at an internuclear separation R of $2.0a_0$, is calculated using the linear-combination-of-atomic-orbitals (LCAO) and screened LCAO functions for H_2^+. A comparison with the results found using the eigenfunctions and one other approximation is given. The R dependence of the error for these approximations is also investigated. The behavior of the Born matrix element for large momentum transfer is shown to be accurately predicted by these approximate functions for intermediate and large R. The small-momentum-transfer behavior is less accurately predicted. The usefulness of these approximate functions for extremes in the momentum transfer is correlated with their local behavior in space. The calculation of the total cross section for scattering of an electron and of a hydrogen atom with

these approximate functions is discussed and compared with the results for the eigenfunctions. (auth)

39409 ELECTRON EMISSION FROM TUNGSTEN UNDER PROTON BOMBARDMENT. Ewing, Ronald I. (Sandia Lab., Albuquerque, N. Mex.). Phys. Rev., 139: A1840-3(Sept. 13, 1965).

The yield of electrons from clean polycrystalline tungsten under bombardment by protons at normal incidence was measured as a function of proton energy in the range 50 to 225 kev. The maximum value of the yield is 1.65 ± 0.03 electrons per proton at a proton energy of 125 kev. The tungsten surface was cleaned by flash heating a tungsten ribbon to 2400°K in a vacuum chamber in which the total pressure was about 2×10^{-10} torr. The yield was measured with the surface at room temperature, about two minutes after the surface was cleaned, while the time for a monolayer of residual gases to form on the surface was greater than two hours. (auth)

39410 L_2-L_3N COSTER-KRONIG TRANSITION PROBABILITIES AND L-SUBSHELL FLUORESCENCE YIELDS OF Hg AND Ta. Rao, P. Venugopala; Crasemann, Bernd (Univ. of Oregon, Eugene). Phys. Rev., 139: A1926-9 (Sept. 13, 1965). (RLO-1921-1).

The probability for the radiationless transfer of L_2 vacancies to the L_3 subshells of Hg and Ta was measured directly, by observing the spectra of L x rays from ^{204}T and ^{181}W in coincidence with K_{α_2} x rays. The L_α component of the coincident spectrum provides a measure of the L_2-L_3N Coster-Kronig transition probability, L_2-L_2M transitions being energetically impossible in this region. The following values are found: for Hg, $f_{L_2L_3} = 0.08 \pm 0.02$; for Ta, $f_{L_2L_3} = 0.20 \pm 0.04$. The x-ray coincidence experiments show that the average number of x-ray quanta emitted after creation of a primary vacancy in the L_2 subshell is $\nu_{L_2} = 0.42 \pm 0.02$ for Hg and $\nu_{L_2} = 0.31 \pm 0.01$ for Ta. Subshell fluorescence yields are found to be $\omega_{L_2} = 0.39 \pm 0.03$ and $\omega_{L_3} = 0.40 \pm 0.02$ for Hg; $\omega_{L_2} = 0.25 \pm 0.02$ and $\omega_{L_3} = 0.27 \pm 0.01$ for Ta. (auth)

39411 THEORETICAL FITTING OF THE ARGON K ABSORPTION SPECTRUM ON A ONE-ELECTRON MODEL. Watanabe, Takeshi (Cornell Univ., Ithaca, N. Y.). Phys. Rev., 139: A1747-51(Sept. 13, 1965).

The one-electron model was used to analyze the argon K absorption spectrum near the K edge. It was assumed that the absorption spectrum consists of (1) two Lorentzians due to 1s → 4p and 1s → 5p resonant transitions, (2) a modified arctangent to account for the 1s → np ($n \geq 6$) and the 1s → continuum transitions, and (3) a constant background due to the L, M ionizations. The transmission spectrum containing adjustable parameters was constructed on the one-electron model and was then smeared by the experimental window function. The values of these parameters were selected to minimize the χ^2 value between the observed transmission curve and the smeared-model transmission curve. The criterion showed that the present model fits the observed curve. Pertinent parameters were interpreted in terms of oscillator strengths and the K-state width. The oscillator strengths (0.00217 and 0.00066) of the 1s → 4p and 1s → 5p transitions show fair agreement with the theoretical values (0.00166 and 0.00053). The K-state width parameter is 0.68 ev, which compares well with the value obtained by several different spectral methods as well as the value obtained from the K fluorescence yield. (auth)

39412 OBSERVATION OF THE ISOTOPE SHIFT OF $K_{\alpha 1}$ X RAYS OF URANIUM. Brockmeier, R. T. (California Inst. of Tech., Pasadena); Boehm, F.; Hatch, E. N. Phys. Rev. Letters, 15: 132-5(July 26, 1965).

The isotope shift of the $K_{\alpha 1}$ x rays of ^{233}U and ^{238}U was determined experimentally. The result appears to be in good agreement with a prediction based on a model of a uniformly charged, incompressible spherical nucleus of radius $R = R_0A^{\frac{1}{3}}$. A more detailed analysis taking into account the effects of even-odd staggering, nuclear deformation, and finite compressibility of the nucleus was attempted. (D.C.W.)

39413 ROTATIONAL STRUCTURE AT THRESHOLD IN THE H_2^+ ELECTRON-IMPACT IONIZATION SPECTRUM. McGowan, J. William; Fineman, M. A. (General Atomic Div., General Dynamics Corp., San Diego, Calif.). Phys. Rev. Letters, 15: 179-81(Aug. 2, 1965).

As part of a study of electron collisions with atomic and molecular hydrogen, structure in the H_2 ionization spectrum was identified. This structure is associated with the rotational states of the hydrogen molecule and ion involved in the electron-impact ionization of hydrogen. The beam of electrons used had an energy width at half-height of about 0.05 ev. The results show that a number of ionization channels are available; that is, direct rotational and vibrational excitation of the ion in competition with autoionization. (J.F.P.)

39414 ROTATIONAL TEMPERATURES OF H_2 DETERMINED WITH 15 kev ELECTRONS. Reich, H. J.; Schmoranzer, H. (Technische Universitaet, Berlin). Z. Physik, 186: 305-9(1965). (In German)

Rotational temperatures were determined from the intensities of the vacuum ultraviolet $H_2(2p^1\,\Pi_u \rightarrow 1s^1\,\Sigma_g^+)$ emission lines, excited by 15 kev electron impact. Their experimental values for the unperturbed $2p^1\,\Pi_g$ rotational levels verify theoretical predictions, and show that the fast electron impact populates $2p^1\,\Pi_g$ out of the ground state by $\Delta J = 0$, analogous to the valid optical selection rule. (auth)

39415 ADVANCES IN ATOMIC AND MOLECULAR PHYSICS. VOLUME 1. Bates, D. R.; Estermann, Immanuel. New York, Academic Press, 1965. 413p. $13.50.

Survey articles are included on the molecular orbital theory of the spin properties of conjugated molecules, electron affinities of atoms and molecules, atomic rearrangement collisions, production of rotational and vibrational transitions in encounters between molecules, the study of intermolecular potentials with molecular beams at thermal energies, and high-energy and high-intensity molecular beams. (D.C.W.)

39416 A REVIEW OF THE (MACROSCOPIC) LAWS FOR THE ELECTRON PENETRATION THROUGH MATTER. Schumacher, B. W. (Ontario Research Foundation, Toronto). pp 5-70 of First International Conference on Electron and Ion Beam Science and Technology. New York, John Wiley and Sons, Inc., 1965.

Observations that can be made, laws that can be stated, and certain functions and numerical coefficients that can be used in studying electron penetration through matter are reviewed under the following headings: scattering, energy dissipation, particle dissipation, absorption of β rays from radioactive isotope sources, graphical representation of attenuation and range data, and backscattering. The review is limited to electrons in the energy range 1 kev to 10 Mev. Results of various investigators taken from the literature are included as illustrations. Further measurements needed in some areas are suggested. (89 references) (A.G.W.)

39417 MECHANISM OF HIGH-POWER-DENSITY ELECTRON-BEAM PENETRATION IN METAL. Schwartz, Helmut (Rensselaer Polytechnic Inst. of Connecticut, East Windsor Hill). pp 158-86 of First International Conference on Electron and Ion Beam Science and Technology. New York, John Wiley and Sons, Inc., 1965.

Experimental and theoretical investigations of the deep penetration of high-power-density electron beams showed that the effect can be explained in a purely classical way. Electrons are stopped in the material and transfer their kinetic energy to heat by increasing the amplitude of the vibrational energy of the lattice electrons, which in turn transmit this energy to the whole lattice. The heat brings the material along the path of the electron beam to melting and successively to evaporation. Extensive electron probe x-ray microanalysis and radioactive tracing techniques showed that the electron-beam affected material went through a complete mixing all along the electron-beam zone. High-speed cinematographs indicated that during most of the time the surface is closed by a liquid metal

film that ruptures at certain instances for a very short period. Determinations of the surface temperature and the temperature at the bottom of the hole showed a difference of about 2500°C between them. (A.G.W.)

39418 NUCLEAR MAGNETIC RESONANCE OF ^{61}Ni IN NICKEL METAL. Cowan, D. L.; Anderson, L. W. (Univ. of Wisconsin, Madison). 17p. (CONF-641004-13). Gmelin, AED-CONF-64-220-37.

From American Physical Society, Chicago.

The zero-applied-field nuclear magnetic resonance of ^{61}Ni in high purity, well annealed Ni metal was investigated at room temperature. The technique of rotary saturation was used to obtain a value for the domain wall enhancement factor $\eta = 1700$. Fast passage and saturation effects were observed and interpreted according to theories developed by Portis for inhomogeneously broadened spin systems. This analysis led to a value for the longitudinal relaxation time $T_1 = 0.16$ msec, and to an observed nuclear dispersion to absorption ratio in the power absorbed of $\beta = 0.5$ at low r-f levels. Fast passage effects were used to obtain a tracing of the distribution of nuclear magnetic fields in the sample. (auth)

Cosmic Radiation

See also Elementary Particles and Radiations. Nuclear Properties and Reactions.

39419 (ATN-63(9219)-1) DEVELOPMENT OF EXPERIMENTAL TECHNIQUES FOR MEASURING THE DISTRIBUTION OF HYDROGEN AND HELIUM ISOTOPES IN SPACE. General Research. Blake, J. B.; Gram, P. A. M. (Aerospace Corp., El Segundo, Calif.). Apr. 12, 1963. 18p.

High- and low-energy counter telescopes are being developed for measuring protons, deuterons, tritons, ^3He nuclei, and ^4He nuclei in space. (D.L.C.)

39420 (NP-15117) ELECTRONS, HYDROGEN AND HELIUM NUCLEI OBSERVED IN THE PRIMARY COSMIC RADIATION DURING 1963. Freier, P. S.; Waddington, C. J. (Cosmic Ray Group, Univ. of Minnesota, Minneapolis). May 1965. Contract Nonr-710(60). 41p. (CR-74)

Singly and doubly charged particles in the cosmic radiation were observed during a balloon flight made over Fort Churchill on the 28th July 1963. These particles were detected in nuclear emulsions mounted in a mechanical device which imposed unique temporal resolution between those entering during the balloon ascent and those entering while the balloon floated at ceiling altitude. The integral intensity at the top of the atmosphere of protons having $E > 74$ Mev was determined to be 2440 ± 160 protons/m^2 ster.sec. while that of helium nuclei having $E > 62$ Mev per nucleon was 272 ± 13 nuclei/m^2 ster.sec. The differential energy spectra of the protons and helium nuclei were studied over the energy ranges of 74 Mev $\leq E \leq 4$ Bev and 62 Mev per nucleon $\leq E \leq 1.67$ Bev per nucleon respectively. Because of the unprecedented energy range covered in the proton study, it was possible to compare these particles over a far greater spread of overlapping rigidities than has hitherto been possible. Small numbers of electrons were also observed with results which are in reasonable agreement with those previously reported by other workers. The problem of correcting for secondary electrons appears unresolved, but if ignored, a total intensity of 63 ± 26 electrons/m^2 ster.sec. with 130 $\leq E \leq 5$ Bev was observed under 2 g/cm^2 of air. (auth)

39421 (NP-15154) TIME VARIATIONS IN COSMIC RAYS AND RADIOSONDE MEASUREMENTS. Final Technical Report. Escobar, Ismael — Vidaurre, Rafael (ed.) (Universidad Mayor de San Andres, La Paz (Bolivia). Laboratorio de Fisica Cosmica de Chacaltaya). Aug. 1964. Contract AF-AFOSR 63-319. 149p.

Analysis on data registered at Chacaltaya was performed, comparing results in some special cases with data from other stations. This analysis involves calculation of harmonic parameters and correlations of cosmic ray events with solar activity in the range of Forbush decreases and diurnal variations. (auth)

39422 (TID-21895) A STUDY OF THE DETECTION OF SUPER SHOWERS BY ATMOSPHERIC SCINTILLATION. Progress Report. Greisen, K. (Cornell Univ., Ithaca, N. Y.). [1965]. Contract AT(30-1)-3038. 12p. Dep.(mn); $1.00(cy), 1(mn) CFSTI

Progress toward developing a new method of detecting cosmic ray showers based on atmospheric fluorescence, so as to extend knowledge of the highest energy cosmic rays, is reported. Problems concerning the observing stations and equipment are reported. (M.O.W.)

39423 ENERGY FLOW OF EXTENSIVE AIR SHOWERS. Tanahashi, Goro (Univ. of Tokyo). J. Phys. Soc. Japan, 20: 883-906(June 1965).

Two sets of detectors of nuclear active particles were operated in extensive air shower arrays at sea level. The results obtained from these detectors agreed with each other, so that the energy spectrum of nuclear active particles in extensive air showers was determined with reasonable accuracy in the size range of 3×10^4 to 5×10^6 particles. At sea level the average energy of the most energetic nuclear active particles and the energy flow carried by nuclear active particles ($E > 10$ Bev) are nearly proportional to the shower size, and they are $1.2 \pm 0.4 \times 10^{12}$ ev and $5.3 \pm 2.0 \times 10^{12}$ ev, respectively, for a shower of the size (determined from the scintillators) of 10^5 particles. These results and the energy carried by the electron-photon component were compared with values calculated on the basis of some conventional models of the nuclear interaction. The inelasticity and the mean free path of the nuclear interaction were thus found to be 0.65 ± 0.15 and 80 ± 10 gcm^{-2}, respectively, in the energy range of 10^{14} to 10^{15} ev. (auth)

39424 THE DENSITY SPECTRUM OF AIR SHOWERS AT SEA LEVEL AND MOUNTAIN ALTITUDES. McCaughan, J. B. T. (Univ. of Sydney); McCusker, C. B. A.; Seet, S. H.; Wand, R. H.; O'Donnell, B.; Prescott, J. D.; Wilson, B. G. Nuovo Cimento (10), 38: 697-706(July 16, 1965).

The cosmic-ray differential density spectrum in the range 3 to 10,000 p/m^2 was obtained, using Wilson cloud chambers, at sea level and at 2285 m a.s.l. In neither case can the whole spectrum be fitted by a single power law. Using a three-parameter fit the sea-level spectrum is best approximated by two power laws of exponents -2.491 ± 0.036 and -3.42 ± 0.32, respectively, joining at 560 ± 180 particles per square meter. At 2285 m a.s.l. the three best parameters are -2.432 ± 0.015, $-4.8^{+1.0}_{-0.5}$ and 6000^{+1000}_{-800} particles per square meter. The change with altitude supports the hypothesis that the change in exponent is due to a steepening of the primary cosmic-ray energy spectrum. (auth)

39425 ORIGIN OF COSMIC X RAYS. Hoyle, F. (Cambridge Univ., Eng., and California Inst. of Tech., Pasadena). Phys. Rev. Letters, 15: 131-2(July 26, 1965).

The inverse Compton effect is discussed in relation to synchrotron emission as the source of cosmic x radiation. Numerical estimates are included. (D.C.W.)

39426 VARIATION OF COSMIC-RAY INTENSITY OBSERVED ON DECEMBER 23, 1957. Murakami, Kazuaki; Kudo, Shoko (Inst. of Physical and Chemical Research, Tokyo). Rika Gaku Kenkyusho Hokoku, 36: 5-11(1960). (In Japanese).

An abnormal diurnal variation was found in Japan on December 23, 1957, with reference to the world-wide data obtained during the International Geophysical Year. The maximum intensity of this diurnal variation appeared at about 3 o'clock local time, while usually the intensity shows a minimum at this time. No disturbances in the geomagnetic field could be detected on that occasion, in spite of the fact that the usual diurnal variation is related to the geomagnetic field. Some attempts to explain the un-

expected diurnal variation are presented and examined. (BBB)

39427 THE HELIUM NUCLEI OF THE PRIMARY COSMIC RADIATION AS STUDIED OVER A SOLAR CYCLE OF ACTIVITY, INTERPRETED IN TERMS OF ELECTRIC FIELD MODULATION. Freier, P. S.; Waddington, C. J. (Univ. of Minnesota, Minneapolis). Space Sci. Rev., 4: 313-72(May 1965).

Since no really satisfactory theory exists to describe the modulation processes of the cosmic radiation, and the experimental data are not yet in a definitive form, an attempt is made to collect all the existing data on one particular charge component of the primary cosmic radiation, that is the helium nuclei, and to study it in terms of the light it throws on these modulation processes. Thus the measurements of the intensities of helium nuclei, the time variations of these intensities, and the modulation of the cosmic radiation are discussed. A comparison is made of the experimental data with the electric field modulation model. A discussion of the electric field model with its success and failures is also given. (J.F.P.)

39428 ANGULAR DISTRIBUTION OF NUCLEAR INTERACTIONS OF HIGH ENERGY COSMIC RAY PARTICLES WITH PARAFFIN. Kuang, Hao-hwai; Li, Ru-bai; Tan, Yue-hen; Liu, Yung-yuih. Wu Li Hsueh Pao, 21: 976-82 (May 1965). (In Chinese).

A cloud chamber experiment is described, in which the angular distribution of secondary particles produced in nuclear interaction by high energy cosmic ray particles with paraffin is studied. Sixty-four $n_s \geq 4$ events with average primary energy of 70 Bev were analyzed. The result shows that, in this energy region, the angular distribution in cms is not isotropic but possesses maxima in the 0 and 180° directions; furthermore, there is already an appreciable fraction (≥ 20%) of the events with angular distribution exhibiting the features given by the fireball model. (auth)

39429 NUCLEAR-ACTIVE HIGH-ENERGY PARTICLES AND THE ACCOMPANYING COSMIC-RAY EXTENSIVE AIR SHOWERS. Murzina, E. A.; Nikol'skii, S. I.; Tukish, E. I.; Yakovlev, V. I. (Lebedev Inst. of Physics, Moscow). Yadern. Fiz., 1: 1079-92(June 1965). (In Russian)

Experimental results are given on the energy spectrum of nuclear-active particles in the region of 3×10^{12} to 10^{14} ev at a height of 3860 m above sea level and on extensive air showers accompanying these particles. The energy spectrum can not be described by a power function with a single exponent in the whole region considered. The mean free paths for absorption and nucleon interaction in the atmosphere are determined. For particle energies higher than 10^{13} ev, they are equal to 120 g/cm^2 and 83 g/cm^2, respectively. An analysis of the distribution of extensive air showers, accompanying nuclear-active particles with energies $\geq 3 \times 10^{12}$ ev with respect to the total number of particles indicates that the character of the elementary interaction changes for nucleons with energies higher than 10^{13} ev. (auth)

Direct Energy Conversion

Refer also to abstracts 38836 and 40238.

39430 (AD-426092) THERMOELECTRIC POWER MODULES. Quarterly Progress Report No. 3, July 15-October 15, 1963. Van Heyst, Hans P. (Radio Corp. of America, Harrison, N. J. Direct Energy Conversion Dept.). Oct. 31, 1963. Contract DA36-039-AMC-00110(E). 21p. CFSTI, $2.60 cy.

Si-Ge thermoelectric power module tests were conducted under continuous operation and thermal cycling conditions. The modules were tested with leaded gasoline, propane gas, and a mixture of manufactured and natural gas heat sources. Modules were also evaluated under mechanical shock of approximately 35 g, and under vibration conditions of 8 g. Two thermoelectric power modules completed 4200 hours, and two other modules completed 2500 hours of continuous unattended operation with no deterioration in electrical power output. One module completed 1950 hours of operation on-time and 195 cycles on a thermal cycling test with a gasoline fired heat source. (auth)

39431 (AD-608554) A STUDY PROGRAM ON CESIUM VAPOR FILLED THERMIONIC CONVERTERS HAVING HIGH VACUUM WORK FUNCTION EMITTER MATERIALS. Yearly Summary Report, November 1, 1963-October 31, 1964. Kennedy, A. J. (Martin Co., Baltimore, Md. Nuclear Div.). Contract Nonr-3639(00). 81p. (MND-3177) CFSTI, $3.00 cy, $0.75 mf.

Ruthenium, a material having relatively low neutron absorption cross section, was investigated both as an emitter and collector in a thermionic converter. Both hot pressed and plasma sprayed ruthenium emitters were found to behave like high vacuum work function materials (i.e., display high output current densities at relatively low cesium pressures). Significant differences were noted, however, in the performance of the two ruthenium emitters prepared by the different processes. The performance of the ruthenium emitters is compared to that of iridium and rhenium emitters. Generally, the ruthenium data show a higher output power density, particularly at relatively wide (10 to 30 mil) interelectrode gaps. The ruthenium plasma sprayed collector assumes its minimum values at a temperature which is lower than that for a molybdenum collector by approximately 100°K. The value of collector work function at optimum is indicated to be approximately equal for ruthenium and molybdenum. (auth)

39432 (JUL-256-TP) ANGEWANDTE MAGNETOHYDRODYNAMIK. HEFT 2. BEITRAG ZUR THEORIE DER LINEAREN MHD-INDUKTIONSGENERATOREN. (Applied Magnetohydrodynamics. 2. Report on the Theory of Linear MHD-Induction Generators). Claassen, H. A. (Kernforschungsanlage, Juelich (West Germany). Institut fuer Technische Physik). Feb. 1965. 31p. Dep.(mn).

The theory of the linear MHD moving field induction generators is considered. The basic equation system for the generator is derived. The equations for the linear MHD induction generator are given. The electrodynamic equation system is solved for the case $\mu = 0$. The impedance of the linear MHD induction generator is derived, and the performance of the Lorentz force and Joule loss are determined. The results are discussed. (J.S.R.)

39433 (LA-DC-6898) SPECTROGRAPHIC INVESTIGATION OF THE IGNITED MODE OF THERMIONIC CONVERTER OPERATION. Reichelt, Walter H. (Los Alamos Scientific Lab., Univ. of California, N. Mex.). [1965]. Contract W-7405-eng-36. 11p. (CONF-650908-2). Dep. mn; CFSTI, $1.00 cy, $0.50 mn.

From International Conference on Thermionic Electrical Power Generation, London.

Electron temperature and ion density profiles across the interelectrode gap of a thermionic diode were determined spectrographically. The diode was operating in the ignited mode and profiles were determined for a number of points on the I-V curves in both the power and nonpower quadrants. Tungsten emitter temperatures were 1705, 1800, and 1910°K and the cesium reservoir temperatures were 548, 573, and 598°K. The current densities ranged from 2 to 10 amps/cm^2 for the cell spacing of 1 mm. The electron temperature and density values generally decreased toward the collector from a maximum near the emitter of 3200°K and 2 to 5×10^{14} ions/cm^3, respectively. (auth)

39434 (N64-26371) THERMIONIC AND THERMOELECTRIC ENERGY CONVERSION. Literature Search No. 575. (Jet Propulsion Lab., Calif. Inst. of Tech., Pasadena). Mar. 9, 1964. 251p. (NASA-CR-58125). CFSTI, $16.50 cy.

The following are included in this document: (1) general—annotated bibliographies; general article reviews and books; conferences; theory and apparatus and measurement techniques; (2) materials—thermoelectric and thermionic properties; (3) power generation—thermoelectric and thermionic converters; and miscellaneous thermal

energy conversion devices; and (4) thermoelectric cooling. (auth)

39435 (JPRS-31048) A STUDY OF THE PROPERTIES OF A THERMIONIC DIODE PLACED IN AN AUTONOMOUS DISCHARGE PLASMA. Morgulis, N. D.; Korchevoy, Yu. P. Translated from At. Energ., 18: 447-51(May 1965). 12p. (TT-65-31546). CFSTI, $1.00 cy.

Physical properties of the thermionic diode are studied when it is placed in an autonomous discharge plasma in cesium and mercury pairs. It is shown that it is possible to obtain increased emf and diode output voltage by this means, the governing factor being the temperature of the plasma electrons. A measurement is made of the distribution of the parameters of the mercury plasma in the interelectrode space of a similar diode. (M.O.W.)

39436 HIGH PRESSURE CAESIUM THERMIONIC CONVERTER WITH TUNGSTEN CATHODE. Orlinov, V.; Stefanov, B.; Zarkova, L.; Konstantinov, E. Compt. Rend. Acad. Bulgare Sci., 18: 15-18(1965).

The experimental results are presented which were obtained with a new construction of a thermionic converter having a tungsten wire cathode and a cylindrical nickel anode. The V-A characteristics and the dependence of the converter under investigation operating in a diffusional state of the plasma created by the surface ionization of cesium on the hot cathode, are depicted. Various other properties are also investigated and described. (J.F.P.)

39437 A THEORETICAL STUDY OF MHD POWER GENERATION. III. THE LIFT OF ELECTRON TEMPERATURE. Michiyoshi, Itaru; Numano, Masahiro (Kyoto Univ.). J. Nucl, Sci. Technol. (Tokyo), 2: 203-11(June 1965).

Lift of the electron temperature in the electromagnetic field is discussed. In view of the small ionization degree in the working gas of MHD power generation, the collision of charged particles with each other is assumed to be negligible. Under this assumption the differential equations to determine the collective behavior of electrons in the electromagnetic field were derived from the Boltzmann equation, and have served to yield some theoretical information on the lift of electron temperature. The electron temperature reaches a new steady value in about 10μsec after the application of an electromagnetic field, and the temperature increase is proportional to the reduced mass of main and seed gas particles if the seeding rate is properly chosen to obtain maximum electrical conductivity of the working gas. Futhermore, the electron temperature increase is of the order of 100°C in typical MHD power generators operated on He + Cs gas. This means that the ionization degree of the seed material, and consequently, the electrical conductivity, are expected to increase by about 30% compared with those corresponding to the gas temperature, when considering practical ranges of operating temperature. (auth)

39438 NONEQUILIBRIUM CHARACTERISTICS OF THE WORKING PLASMAS FOR MAGNETOPLASMADYNAMIC (MPD) GENERATORS. Hiramoto, Tatsumi (Japan Atomic Energy Research Inst., Tokyo). J. Phys. Soc. Japan, 20: 1061-72(June 1965).

The possible nonequilibrium ionization in an MPD generator is theoretically described. A generalized Saha equation is derived and found to be different from that based on the electron temperature, when the electron temperature is slightly higher than the gas temperature. The effective elastic collision loss factor is larger than 2, due to the de-excitational radiation at lower electron temperatures or due to the recombinational radiation at higher temperatures. The theory reasonably explains the current-electric field characteristic and other nonequilibrium characteristics experimentally obtained. The value of the peak in the electric field appearing in the above characteristics is determined; this peak does not appear in the atmospheric helium seeded with cesium, at gas temperatures $\geq$1500°K or at initial electron densities $\geq 10^{16} m^3$. It is shown why the nonequilibrium ionization is not produced when the generators are operated at low gas temperatures. (auth)

39439 PROBLEMS OF ENERGY CONVERSION BY ION CONVECTION. Knoernschild, Eugen (DVL-Institut fuer Energiewandlung und Elektrische Antriebe, Stuttgart). Raumfahrtforschung, 9: 7-16(Jan.-Mar. 1965). (In German)

Energy generators aboard of space vehicles should guarantee reliable operation for months or years. This goal seems to be easier to realize with systems without moving parts (by thermionic or magnetohydrodynamic generators). Far less known are systems using ion convection for energy conversion (in principle, the inversion of ion propulsion). While in this case ions are accelerated in an electric field by consumption of electric energy in the case of an ion converter the working medium is expanded and accelerated within a nozzle. The working medium then is ionized and forced to run against the self-induced electric field. The reduction of the kinetic energy of the working fluid is converted into electric energy. The operational characteristics of such an ion convection converter are shown and possible applications are discussed. Published proposals and test results are examined. An optimization of the ion convection converter shows that this method can compete in certain areas with the known direct conversion methods. (auth)

39440 MULTI-COMPONENT, STATIONARY NON-EQUILIBRIUM FLOW IN A MPD ENERGY CONVERTER. Mayser, B.; Eichert, K.; Siegert, H. J. (Technische Hochschule, Stuttgart). Z. Naturforsch., 20a: 813-23 (June 1965). (In German).

A system of equations is given for the calculation of a one-dimensional plasma flow in a perpendicular magnetic field in order to study the kinetic processes in a magnetoplasmadynamic (MPD) energy converter. The ionization and recombination processes occurring in the plasma are described by the equations in which no equilibrium is assumed. The equations are limited to a forward- and backward-motion reaction, but can be easily extended to include several reactions. The flow behavior for various working gases and injection substances are discussed. (tr-auth)

39441 FUNDAMENTALS OF THERMIONIC ENERGY CONVERSION. Nottingham, W. B. (Massachusetts Inst. of Tech., Cambridge). pp 71-85 of First International Conference on Electron and Ion Beam Science and Technology. New York, John Wiley and Sons, Inc., 1965.

Problems relating to microscopic phenomena involved in thermionic energy conversion are reviewed, and the approach that forms the basis of extensive research programs now underway in this area is indicated. The interrelation between component parts of a thermionic energy converter, thermionic emission in the presence of Cs, desirable collector properties, and analysis of voltage-current curves are discussed. It is concluded that further research is needed to establish the fundamental properties of the materials useful in thermionic energy conversion. (A.G.W.)

39442 M.H.D. GENERATORS FOR SPACE POWER. Kerrebrock, Jack L. (Massachusetts Inst. of Tech., Cambridge). 24p. (CONF-650416-2). ORINS

From 4th Symposium on Advanced Propulsion Concepts, Palo Alto, Calif.

A restatement of the potential of magnetohydrodynamic generators is made in the light of present knowledge, a summary is made of the critical problems, and areas are indicated which require investigation in the future. The discussion concerns systems with solid fuel reactors, nonequilibrium ionization, nonequilibrium generator behavior, a comparison of magnetohydronamic generators and turbines, and systems with gaseous reactors. It is noted that there is still much uncertainty about the behavior of magnetohydrodynamic generators in space although the behavior of nonequilibrium plasmas is rather well understood. The real potential of magnetohydrodynamic generators for space power generation lies in their coupling with high temperature reactors, having gaseous or liquid cores. (J.F.P.)

39443 THERMIONIC ENERGY CONVERTER. (to Standard Telephones and Cables Ltd.). British Patent 997,432. July 7, 1965. Priority date Nov. 4, 1960, United States.

A thermionic energy converter is described for converting solar energy to electrical energy that is more efficient than known converters. The converter includes a plurality of coaxial pairs of electrodes in the form of hollow conical frustrums. The electrodes are arranged in a tandem relation with respect to each other to place an edge of one electrode of each pair in contact with the edge of an adjacent pair so that the electrodes additively combine the energy conversion of each of the pairs of electrodes. (B.L.M.)

39444 HIGH VACUUM THERMIONIC CONVERTER. Beggs, James E. (to General Electric Co.). U. S. Patent 3,176,164. Mar. 30, 1965. Filed Nov. 3, 1958.

A thermionic converter includes an electron emissive cathode and an electron collecting anode closely spaced to the cathode to minimize the space charge effect in the interelectrode region. The spacing between the electrodes is maintained by a number of pillars extending from a point beneath the surface of the anode electrode and into contact with the cathode electrode. Support means for the pillars includes a cathode contact member in conductive contact with the cathode and insulator means disposed between the anode and the supporting means. The construction minimizes the radiative and conductive heat transfer to the anode. (B.L.M.)

39445 SERIES CONNECTION AND SPACING TECHNIQUES FOR THERMIONIC CONVERTERS. Lawrence, Jackson (to General Electric Co.). U. S. Patent 3,176,165. Mar. 30, 1965. Filed Nov. 15, 1960.

An apparatus for converting heat energy, e.g. from a nuclear reactor, to electrical energy has a generally cylindrical structure and includes a plurality of thermionic converter units connected in series. Each unit includes a generally cylindrical cathode with a surrounding hollow cylindrical collector electrode in closely spaced relation to the exterior surface of the cathode. Junction means join the thermionic units mechanically together in end to end relation and include electrically conducting means extending from the central portion of one end of the cathode of one unit to the adjacent end of the collector electrode of a second unit. The electric connections have limited cross section to minimize the heat transfer from the cathode to collector electrode, and heat shield means is interposed between the cathode electrodes of adjacent units and the mechanical junction between adjacent units. Each converter unit includes a gaseous medium in the interelectrode space, and a passageway between adjacent units for the medium is provided through the junction means. (B.L.M.)

39446 THERMIONIC GENERATOR. Guenther, Karl-Georg; Haenlein, Walter (to Siemens-Schuckertwerke AG). U. S. Patent 3,176,166. Mar. 30, 1965. Priority date July 27, 1961, Germany.

A thermionic energy converter includes a low pressure vessel having a cathode and an anode insulated and spaced from each other. The cathode forming combustion chamber means has an outwardly flaring outlet that opens into the vessel. Conduit means are provided for introducing directly into the combustion chamber means a mixture of a fluid driving and heating medium and an ionizable metal addition finely distributed in the driving and heating medium. The mixture is heated by the medium within the cathode for driving the mixture toward the anode, the metal addition is ionized when contacting the outlet of the cathode, and the ions are electrically discharged when contacting the anode. Two electrical terminals connect the anode and cathode to provide electric energy. A conduit means including a source of combustion gases communicates with the combustion chamber means and is arranged so that the combustion gases are burned in the chamber means to convey heat directly to the mixture in the cathode. A feed-back conduit means leads from the anode to the conduit means for returning a portion of the mixture. (B.L.M.)

39447 MHD INDUCTION DEVICE. Neitzel, Robert E. (to General Electric Co.). U. S. Patent 3,176,169. Mar. 30, 1965. Filed June 29, 1960.

A MHD induction device for generating alternating power includes means for defining the flow path of a conductive fluid and flow control means disposed in the radial portion of the flow path impart a radially inward direction to the fluid as it moves through the path defining means. An axially rotating magnetic field is impressed on the radial portion of the flow path and interacts with the rotating gas to produce a circulating current in the gas. The circulating current interacts with the magnetic means and induces an alternating electromotive force. (B.L.M.)

39448 MAGNETOHYDRODYNAMIC TRANSFORMER. Stuetzer, Otmar M. (to Litton Systems, Inc.). U. S. Patent 3,179,824. Apr. 20, 1965. Filed Apr. 17, 1962.

A MHD transformer includes means for defining a flow path for the conductive fluid, a MHD pump in the flow path for pumping the conductive fluid, and a MHD generator in the flow path downstream of the pump for developing an electric potential as the fluid flows through the generator. By varying various parameters in the design of pump and generator, the transformer may be adapted for use as either a voltage transformer or current transformer, i.e. a voltage or current step-up transformer. Since the resistance of the conductive fluid is extremely low, the transformer has an extremely low impedance. (B.L.M.)

39449 MAGNETOHYDRODYNAMIC EQUIPMENT FOR PRODUCING A. C. POWER. Rosa, Richard J. (to Avco Corp.). U. S. Patent 3,179,873. Apr. 20, 1965. Filed Apr. 29, 1960.

Electric power generating equipment is described that includes a MHD generator and associated switching equipment adapted to produce a-c electric power. The generator includes pairs of discrete electrodes with which current flow can be alternately established by means of switches. Conventional circuit elements are included in circuit with the switches for developing the a-c output. The inherent rectifying characteristic of the generator is used to prevent reverse flow of current through the generator at the time of switch opening. This prevents electrical erosion of switch contacts and serious energy losses. (B.L.M.)

Elementary Particles and Radiations

Refer also to abstracts 39661 and 39912.

39450 (BNL–9232) A SCATTERING EXPERIMENT USING DIGITIZED DISCHARGE PLANES. Bleser, E.; Anderson, E.; Collins, G. B. (and others) (Brookhaven National Lab., Upton, N. Y.). May 28, 1965. Contract AT(30-2)-Gen-16. 11p. (CONF–650510-12). Dep. (mn); $1.00(cy), 1(mn) CFSTI.

From Purdue Conference on Instrumentation for High Energy Physics, Lafayette, Ind.

Preliminary experience at the Brookhaven AGS of an experiment using wire chambers with a magnetic-core readout connected on-line to a PDP-6 computer is reported. The experiment is designed to measure momentum spectra for inelastic proton-proton scattering over a wide range of angles and incident energies. The system layout and properties are described, including the rate at which data can be taken and the overall efficiency. Sample results are shown. (M.J.T.)

39451 (CALT–68–43) DISTRIBUTION OF LEPTON PAIRS FROM VECTOR MESON DECAYS. Internal Report No. 15. Beder, Douglas S. (California Inst. of Tech., Pasadena). June 1965. Contract AT(11-1)-68. 26p. Dep. mn; CFSTI, $2.00 cy, $0.50 mn.

Expressions are derived for the differential cross section for lepton pair production resulting from decay of a vector meson. The vector meson is assumed to originate in a reaction of the type pseudoscalar meson + baryon →

vector meson + baryon. The particular reactions considered are $\pi^- + p \rightarrow \rho^0 + n$ or $\rightarrow \omega^0 + n$. The pure peripheral model is used to discuss the lepton differential cross section, assuming that either PS or V exchange dominates the production amplitude and employing Feynman diagrams. The angular distribution of the decay leptons is obtained in terms of the V production density matrix and the $V \rightarrow e^+e^-$ amplitudes. The predictions for the angular distribution based on experimental analysis of ρ and ω production are discussed. Current ideas about decay widths into lepton pairs of the known V mesons are briefly reviewed. (M.J.T.)

39452 (CONF-796(Paper 13)) THE MASSES OF ELEMENTARY PARTICLES FROM THE GEOMETRY OF SPACE-TIME. Sachs, Mendel (Boston Univ., Mass.). 16p.

A formulation of unified field theory is presented in which the perturbing effects of measuring devices upon the measured phenomena are taken into account. The derivation of the masses of the elementary particles from the results of this theory is discussed. (T.F.H.)

39453 (CONF-796(Paper 15)) QUANTUM MECHANICAL THREE-BODY PROBLEM FOR ATTRACTIVE POTENTIALS. Eyges, Leonard (Air Force Cambridge Research Labs., Laurence G. Hanscom Field, Bedford, Mass.). 32p.

The quantum mechanical problem of finding the ground-state energy and eigenfunction for three identical particles bound by attractive inter-particle potentials is considered. It is advantageous to write the wave function in a special functional form, for which was derived an integral equation which is equivalent to the Schrödinger equation. A new method for solving this equation, by expanding it into a set of "effective" two-body functions, is presented; these functions are the eigenfunctions of a two-body problem with a potential of the same shape as the interparticle potential in the three-body problem, but of enhanced strength. The integral equation then becomes a set of coupled equations for certain functions $f_l(\varkappa)$, the "coefficients" in this expansion. By choosing the effective two-body strength properly, one can optimize the convergence of this expansion so that a good approximation is obtained by retaining only the lowest ($l = 0$) term. The resultant single integral equation for $f_0(\varkappa)$ can then be solved by an approximate method. As a test and check, the one-dimensional three-body problem is treated with δ-function interactions, and the results are compared with the exact ones. The first approximation in this method yields an eigenvalue and eigenfunction accurate to a few percent. The method is also applied to the three-dimensional problem with exponential interparticle potentials, and the results are compared with variational calculations. (auth)

39454 (CONF-796(Paper 18)) DEPARTURES FROM THE EIGHTFOLD WAY. Coleman S. ([Los Alamos Scientific Lab., Univ. of California, N. Mex.]). 19p.

The medium-strong interaction is studied. Relations between medium-strong and electromagnetic interactions are investigated. A model for these two types of interactions, based on universal octet dominance, is described. Weak interactions are also studied. (T.F.H.)

39455 (CONF-796(Paper 19)) ON THE PROBLEM OF COMBINING INTERNAL- AND SPACE-TIME SYMMETRIES. Nilsson, Jan (Virginia Univ., Charlottesville). 25p.

The problem of coupling between the internal and space-time properties of elementary particles is considered under conditions that are general enough to yield a non-trivial coupling and non-trivial mass relation between multiplets. Under these conditions, however, non-unitary representations of the Poincaré group must be used. The non-unitarity is related to the instability of the particles, and the mass splittings in a multiplet are related to the instability of the members. (T.F.H.)

39456 (CONF-796(Paper 21)) SU(6) AND NON-LEPTONIC HYPERON DECAY. Rosen, S. P. (Purdue Univ., Lafayette, Ind.). 5p.

The unitary and intrinsic spins of elementary particles are combined to form an $SU(3) \times SU(2)$ subgroup of SU(6). In this model, nonleptonic hyperon decay can be represented using the (35) representation, which contains a $J = 0$ octet to account for s-wave decay and a $J = 1$ octet to account for p-wave decay. The results of the use of the (35) representation are studied. (T.F.H.)

39457 (CONF-796(Paper 23)) WEAK INTERACTIONS. Feinberg, G. (Columbia Univ., New York). 12p.

Several hypotheses are proposed to explain the experimentally observed CP-nonconserving decay $K^0 \rightarrow$ (2 charged pions). (T.F.H.)

39458 (CONF-796(Paper 24)) EXTRAPOLATION OF NUCLEON ELECTROMAGNETIC FORM FACTORS. Wang, C. P.; Levinger, J. S. (Cornell Univ., Ithaca, N. Y.). 16p.

A conformal transformation is used to facilitate extrapolation of the isovector magnetic nucleon form factor, to find the spectral function of this form factor. A peak is found around 620 Mev, or somewhat below the energy of the isovector ρ resonance. The electric form factor is analyzed for elastic electron-deuteron scattering, in terms of the difference between the measured value and the calculated value based on assumptions concerning the deuteron wave function, and also the isoscalar electric nucleon form factor G_{ES}. By extrapolation of this difference, G_{ES} is found in the time-like region $t_A < t < 9\mu^2$, where t_A is the anomalous threshold and μ is the pion mass. These values of G_{ES} are statistically consistent with values for space-like momentum transfer: in particular, consistency is found with values based on scattering of thermal neutrons. G_{ES} is extrapolated, using values for space-like and also time-like momentum transfer, and a spectral function is found with a peak near 700 Mev, and indications of a dip around 1150 Mev. The peak and dip could be ascribed to the ω and ϕ isoscalar resonances, respectively. (auth)

39459 (CONF-796(Paper 28)) SU_6 IN RELATIVISTIC PARTICLE MECHANICS. Schroer, B. (Pittsburgh Univ., Pa.). 6p.

An analysis is carried out of relativistic mechanics in SU(6) field theory. A method is found for obtaining spin independence in the particle representations. Nonlocal characteristics, macrocausality, and other concepts are discussed within the framework of this analysis. (T.F.H.)

39460 (CONF-650410-3) LOW ENERGY HYPERON-PROTON SCATTERING INTERACTIONS. Technical Report No. 469. Burnstein, R. A. (Maryland Univ., College Park. Dept. of Physics and Astronomy). June 1965. Contract AT(40-1)-2504. 30p. Dep.(mn); $2.00(cy), 1(mn) CFSTI. From American Physical Society, Washington, D. C.

Low energy hyperon-proton interactions which are discussed are: (Λ,p) elastic scattering, (Σ^-,p) absorption, and Σ^+ and Σ^- elastic scattering. The SU_3 symmetry scheme is used in this discussion. A detailed investigation is presented. (M.O.W.)

39461 (COO-1195-35) PHOTOPRODUCTION OF POSITIVE PIONS NEAR THRESHOLD IN HYDROGEN (thesis). Simpson, James D. (Illinois Univ., Urbana. Dept. of Physics). June 1964. Contract AT(11-1)-1195. 55p. Dep. mn; CFSTI, $3.00 cy, $0.50 mn.

An experiment was done to improve available measurements of π^+ photoproduction cross sections very near threshold. A 14" hydrogen bubble chamber was used in an x-ray beam with $E_{max} = 230$ Mev. Meson tracks could be observed from their origins in the photon beam. Only those events were used in which the π^+ stopped and decayed in the visible region of the chamber. To suppress electron background, the x-ray beam from the betatron was hardened before it passed through the bubble chamber. Each x-ray pulse contained a total energy of about 10^6 Mev. A special high pressure ion chamber was used to monitor the beam flux. The uncertainty in the calibration of the monitor is about 2.4%. From 435,000 sets of photographs, about 9100 usable photoproduction events were found. The scan-

ning efficiency appears to be greater than 99%. The 90° center-of-momentum matrix-element-squared is found to agree well with an evaluation of the theoretical prediction of Chew, Goldberger, Low, and Nambu. The threshold value for the a_0 coefficient is found to be 21.1 ± 0.8 μb/str. In conjunction with the theoretically predicted value for the minus-to-plus ratio and by using a theorem by Kroll and Ruderman, a value of 0.0788 ± 0.0030 is obtained for the renormalized pion-nucleon coupling constant. (auth)

39462 (CU-1932-239) ANTIPROTON ANNIHILATION IN HYDROGEN AT REST. [PART] I. REACTION $\bar{p} + p \rightarrow K + \bar{K} + \pi$. Barash, N.; Franzini, P.; Kirsch, L.; Miller, D.; Steinberger, J.; Tan, T. H.; Plano, R.; Yaeger, P. (Nevis Labs., Columbia Univ., Irvington-on-Hudson, N. Y.). May 1965. Contract AT(30-1)-1932. 30p. (CU-239; NEVIS-133; R-501). Dep.(mn); $2.00(cy), 1(mn) CFSTI.

In a study of 735,000 antiproton annihilations at rest in the hydrogen bubble chamber, 182 examples of the reaction $K_1K_1\pi^0$ and 851 examples of the reactions $K_1K^+\pi^-$ were recorded. The distributions in the internal variables of these reactions are presented. A substantial fraction of the latter reaction proceeds through an intermediate K* state; $\bar{p} + p \rightarrow K + K^*$. The theory of the interference effects in this reaction is presented and compared with the experimental result. It is concluded that the KK* annihilation proceeds dominantly from the ^3S, I = 1 state of the $\bar{N}N$ system. The fraction of $\bar{p}p$ annihilations into KK* is given as $f_{KK^*} = (2.1 \pm 0.3) \times 10^{-3}$. (auth)

39463 (IC/65/62) THE DIFFICULTIES OF THE N/D APPROACH IN BOOTSTRAPS. Isaev, P. S. (International Centre for Theoretical Physics, Trieste (Italy)). June 1965. 8p. Dep. mn.

Brief critical remarks are made on the two methods for solving bootstrap equations. The two methods under consideration are; (1) the cut-off parameter, and (2) the Regge asymptotic behavior of the amplitudes. (M.O.W.)

39464 (ISS-64/49) RELAZIONE SULL'ATTIVITA DELLA SCOTTOSEZIONE SANITA DELL'INFN NEL 1963–64. (Progress Report of the Sanita Subsection of the INFN During the Period 1963–64). (Istituto Superiore di Sanita, Rome (Italy). Laboratori di Fisica). Dec. 28, 1964. 28p. Dep. mn.

The activities of the Sanità Subsection of the INFN during 1963–64 are reported. Research work in the fields of strong, weak and electromagnetic interaction is described. News is given of the beginning of the theoretical group work and of the Computing Center activities. Finally the recent achievements of the technical research are described. (auth)

39465 (JINR-E-2125) ASYMPTOTICS OF THE FEYNMAN GRAPHS. III. SPINOR GRAPHS. Efremov, A. V. (Joint Inst. for Nuclear Research, Dubna (USSR). Lab. of Theoretical Physics). 1965. 23p. Dep. mn.

A recipe is proposed for extracting off the asymptotics of any planar and some nonplanar Feynman graphs with spinor lines from their topological structure. (auth)

39466 (JINR-E-2173) THE PROBLEM OF MASS FORMULAS IN THE ISL(6) THEORY. Shuran'I, P. (Joint Inst. for Nuclear Research, Dubna (USSR). Lab. of Theoretical Physics). 1965. 6p. Dep. mn.

It is shown that the so-called intrinsically broken ISL(6) theory of elementary particles cannot lead to any nontrivial mass formula. (auth)

39467 (JINR-E-2194) ON THE STRUCTURE OF VECTOR AND AXIAL CURRENTS IN BROKEN $\tilde{U}(12)$ SYMMETRY. Winternitz (Vinternitts), P.; Makarov, A. A.; Nguyen van Hieu; Tkachev, L. G.; Uglirzh, M. (Joint Inst. for Nuclear Research, Dubna (USSR). Lab. of Theoretical Physics). 1965. 7p. Dep.mn.

It is shown that the baryon vector and axial current formfactors in the intrinsically broken $\tilde{U}(12)$ symmetry theory can be expressed through three independent functions. Possible experimental verifications of the obtained relations are discussed. (auth)

39468 (JINR-P-2123) NEODNORODNAYA GRUPPA SL(6) S RASSHIRENNOI PODGRUPPOI TRANSLYATSII. (Inhomogeneous Group SL(6) With an Extended Subgroup of Translations). Kadyshevskii, V. G.; Todorov, I. T. (Joint Inst. for Nuclear Research, Dubna (USSR). Lab. of Theoretical Physics). 1965. 23p. Dep. mn.

The invariants of the inhomogeneous group SL(6) are looked for and the simplest equations invariant with respect to the type of the group are discussed. It is shown that the theory becomes still more effective if the subgroup of translations is extended so that the momentum would belong to the representation D (20,20). (auth)

39469 (JINR-P-2170) FAZOVYI ANALIZ NUKLON-NUKLONNOZO RASSEYANIYA PRI ENERGII 400 Mev. (The Phase-Shift Analysis of Nucleon-Nucleon Scattering at 400 Mev). Kazarinov, Yu. M.; Kiselev, V. S.; Simonov, Yu. N. (Joint Inst. for Nuclear Research, Dubna (USSR). Lab. of Nuclear Problems). 1965. 14p. Dep. mn.

The phase shift analysis on nucleon-nucleon scattering was performed at an energy close to 400 Mev. Five solutions fitting satisfactorily the experimental data were found. It is likely that out of these solutions only one agrees, within the experimental error, with the set obtained by interpolating the solutions found earlier at 300 and 630 Mev. (auth)

39470 (JINR-P-2171) O $\gamma 3\pi$ I $\rho\pi\gamma$ VZAIMODEISTVIYAKH. (On $\gamma 3\pi$ and $\rho\pi\gamma$ Interactions). Meshcheryakov, V. A.; Solov'ev, L. D.; Tkebuchava, F. G. (Joint Inst. for Nuclear Research, Dubna (USSR). Lab. of Theoretical Physics). 1965. 23p. Dep. mn.

It is shown that the data on $\rho\pi\gamma$-interaction and on $\gamma 3\pi$-interaction near the threshold are in agreement with the dynamical picture of $\gamma 3\pi$-interaction following from the dispersion relations when the high energy contribution is taken into account. The available data on $\rho\pi\gamma$-interaction are considered and special emphasis is laid upon the normalization of the interaction constants used in literature. The connection of $\rho\pi\gamma$ interaction with similar interactions of other vector and pseudoscalar mesons is treated in the framework of SU(3) and SU(6) symmetries. (auth)

39471 (JINR-P-2175) GRUPPA SU_{12} KAK OB'EDINENIE SIMPLEKTICHESKOI I SPINOVOI SIMMETRII. (Group SU_{12} as a Generalization of the Symplectic and Spin Symmetries). Struminskii, B. V.; Todorov, I. T.; Fakirov, D. G. (Joint Inst. for Nuclear Research, Dubna (USSR). Lab. of Theoretical Physics). 1965. 6p. Dep. mn.

It is suggested to unite the symplectic group of internal symmetries Sp_6 with the spin group SU_2 under the unitary group SU_{12}. The formulas which are well-known from the SU_6-symmetry were obtained for the magnetic moments and masses of the baryons. Some new relations were also found for the amplitudes of the radiative decays of vector mesons. (auth)

39472 (JINR-P-2178) ISSLEDOVANIE VZAIMODEISTVII π^--MEZONOV S IMPUL'SOM 9 Gev/c S YADRAMI KSENONA, SOPROVOZHDAEMYKH ROZHDENIEM LAMBDA-I K^0-CHASTITS. (An Investigation of 9 Gev/c Negative Pion Interactions With Xenon Nuclei Accompanied by Lambda and K^0 Production). Bogdanovich, E.; Dobrovol'skii, T.; Ivanovskaya, I. A.; Mal'tsev, V. M.; Penchev, G. I.; Filipkovskii, A. (Joint Inst. for Nuclear Research, Dubna (USSR). Lab. of High Energy). 1965. 20p. Dep. mn.

The cross sections for Λ and K^0 production on the xenon nuclei by 9 Bev/c negative pions were obtained to be $\sigma_\Lambda = (139 \pm 11)$ mb and $\sigma_{K^0} = (168 \pm 17)$ mb. The momentum and angular distributions of Λ and K^0 particles were also found. These results are compared with similar data obtained on the hydrogen nuclei and with the calculations by the Monte-Carlo method. On this basis, a conclusion is drawn about the cascade character of the particle interaction with the nucleus. (auth)

39473 (JINR-P-2186) O SOSTAVNOI MODELI BARIONOV NA OSNOVE URAVNENIYA DLYA TREKH CHASTITS. (On Composite Model of Baryons on the Basis of Three-

Body Equation). Bogolyubov, P. N. (Joint Inst. for Nuclear Research, Dubna (USSR). Lab. of Theoretical Physics). 1965. 37p. Dep. mn.

The three-body equation was treated in the following cases: (1) when the electromagnetic field is absent; and (2) when a weak electromagnetic field is present. (auth)

39474 (JINR-P-2190) ISSLEDOVANIE LEPTONNYKH RASLADOV K_2^0-MEZONOV. (An Investigation of the Leptonic Decays of K_2^0 Mesons). Anikina, M.; Vardenga, G.; Zhuravleva, M. (and others) (Joint Inst. for Nuclear Research, Dubna (USSR). Lab. of Nuclear Problems and Joint Inst. for Nuclear Research, Dubna (USSR). Lab. of High Energy). 1965. 10p. Dep. mn.

On the basis of an analysis of 816 leptonic K_2^0 decays it is shown that for the constant form factor the vector interaction is responsible for the leptonic decays. Under the assumption of $(\mu - e)$-universality the ratio of the $K_{\mu 3}$ decay probability to that of the K_{e3} decay was obtained to be $R = 0.76^{+0.10}_{-0.08}$. The ratio of the form factors was found to be $\xi = (f_-/f_+) = +0.8^{+0.6}_{-0.4}$. (auth)

39475 (LAL-27) PRODUCTION DE POSITRONS A L'ACCELERATEUR D'ORSAY. DETERMINATION DE LA SECTION EFFICACE A 0° SUR CIBLES EPAISSES. (Production of Positrons at the Orsay Accelerator. Determination of Cross Section at 0° on Thick Targets). Aggson, T. L.; Burnod, L. (Laboratoire de l'Accelerateur Lineaire, Univ. de Paris, Orsay (France)). Oct. 1962. 20p. Dep.(mn)

The production of positrons from a beam of electrons was measured as a function of the energy of the incident particle, thickness of the Pb target, and energy distribution of the positrons emitted. The energy of the incident electrons varied from 55 to 220 Mev. The curves obtained show a slow displacement toward higher energies of the energy corresponding to the maximum for positron production for increasing incident-electron energy. The good linearity of the optimum positron production as a function of the energy of the incident electrons argues in favor of obtaining positrons at the highest possible electron energy. (J.S.R.)

39476 (NP-15197) VOZMOZHNOE NESKOKHRANENIE CP-CHETNOSTI I PRIRODA PRAVILA $\Delta T = \frac{1}{2}$. (Possible Non-Conservation of CP-Parity and the Nature of the Law $\Delta T = \frac{1}{2}$). Report No. 343. Zal'dovich, B. Ya.; Okun, P. B. (Gosudarstvennyi Komitet po Ispol'zovaniyu Atomnoi Energii SSSR, Moscow. Institut Teoreticheskoi i Eksperimental'noi Fiziki). 1965. 7p. Dep. mn.

The Wolfenstein's model is discussed in which the $K_2^0 \to 2\pi$ decay is due to the difference in phases of the primary nonleptonic interaction and of the nonleptonic interaction that appears in the second order of perturbation theory due to the virtual leptons exchange. It is shown that in order to get observable scale of CP-violation it is necessary in this model to abandon the nonleptonic interaction lagrangian in the form of the product of charged currents. This suggests that the primary nonleptonic lagrangian satisfies the strict $\Delta T = \frac{1}{2}$ rule. (auth)

39477 (NP-15202) REALIZATSIYA TREKHMERNOI UNITARNOI GRUPPY SFERICHESKIMI FUNKTSIYAMI. (Realization of a Three-Dimensional Unitary Group by Means of Spherical Functions). Report No. 311. Magomedov, M. R.; Sudakov, V. V. (Gosudarstvennyi Komitet po Ispol'zovaniyu Atomnoi Energii SSSR, Moscow. Institut Teoreticheskoi i Eksperimental'noi Fiziki). 1964. 30p.

Using the useful parametrization of three-dimension unitary U_3-group the representation of this group in the form of "spherical functions" is realized. Supermultiplets are classified in the form of square diagrams on a plane (-S, 2T). Infinitesimal operators in the form of a linear differential operator are introduced and their matrix elements for arbitrary representation are calculated. (auth)

39478 (NP-15210) NEKOTORYE VOPROSY TEORII VZAIMODEISTVIYA ELEMENTARNYKH CHASTITS PRI BOL'SHIKH ENERGIYAKH (DISSERTATSIYA). (Some Problems of the Theory of Interaction of High-Energy Elementary Particles (thesis)). Rekalo, M. P. (Akademiya Nauk Ukrainskoi SSR, Kharkov. Fiziko-Tekhnicheskii Institut). 1964. 100p. Dep. mn.

The asymptotic behavior of the amplitudes of processes involving strongly interacting particles at high energies is considered on the basis of the hypothesis on Regge poles. Studies are made on polarization phenomena in π-N scattering and fermion Regge poles, γ-N scattering, $\gamma + N \to N + \pi$ interactions, the asymptotic relation between large-angle differential scattering cross sections, and isotopic relations for pion photoproduction reactions. Production of kaons and kaon resonances in electron and photon reactions on nucleons is considered. Annihilation of antibaryons at high energies is studied, including transformation of a baryon-antibaryon pair into a meson and photon ($\bar{Y} + N \to K + \gamma$, $\bar{N} + N \to \pi + \gamma$) and into a meson and virtual photon ($\bar{Y} + N \to K + e^+ + e^-$, $\bar{N} + N \to \pi + e^+ + e^-$) and two-photon annihilation of antinucleons. Matrix-element structure and the isotopic relations are discussed for inelastic high-energy processes. Questions of the theory of electromagnetic interactions of pions and nucleons are considered, with discussions of sign determination of the $\pi^0 \to 2\gamma$ decay amplitude and the threshold anomaly in pion photoproduction on nucleons. 83 references. (M.J.T.)

39479 (NP-15216) DANNYE O PP-REZONANSE S Q = 148 Mev. (Data on pp-Reactions With Q = 148 Mev). Report No. 273. Verebrusov, V. S.; Veselovskii, G. S.; Grashin, A. F.; Demidov, V. S.; Kuznetsov, E. V.; Kuznetsov, E. P.; Ponosov, A. K.; Protasov, V. P.; Sergeev, F. M.; Shalamov, Ya. Ya. (Gosudarstvennyi Komitet po Ispol'zovaniyu Atomnoi Energii SSSR, Moscow. Institut Teoreticheskoi i Eksperimental'noi Fiziki). 1964. 8p. Dep. mn.

The data were obtained, suggesting some evidence for the existence of pp-resonance with exciting energy Q = 148 ± 3 Mev and width $\Gamma \lesssim 5$ Mev as well as pd-resonance with exciting energy Q' = 143 ± 3 Mev and $\Gamma \lesssim 5$ Mev. The existence of a new πN-resonance with mass M = 938 + 150 Mev could explain the effect observed. (auth)

39480 (NP-15247) O RASPADE $f^0 \to \pi^0 + \pi^0$. (Concerning the Decay $f^0 \to \pi^0 + \pi^0$). Report No. 266. Barmin, V. V.; Dolgolenko, A. G.; Elenskii, Ya. S.; Erofeev, I. A.; Krestnikov, Yu. S.; Meshkovskii, A. G.; Tikhomirov, G. D.; Trebukhovskii, Yu. V.; Shebanov, V. A. (Gosudarstvennyi Komitet po Ispol'zovaniyu Atomnoi Energii SSSR, Moscow. Institut Teoreticheskoi i Eksperimental'noi Fiziki). 1964. 13p. Dep. mn.

The reaction $\pi^- + p \to n + 4\gamma$ was investigated in propane–xenon bubble chamber at π^--meson momentum of 2.8 Bev/c. The kinematic analysis of angular distribution showed that nearly 30% of the cross section can be explained by $\pi^- + p \to n + f^0(f^0 \to \pi^0 + \pi^0)$ reaction. This fact proves exactly, that the f^0 meson has even spin. The decay rate $R = [w(f^0 \to \pi^+ + \pi^-)/w(f^0 \to \pi^0 + \pi^0)] = 3.2 \pm 1.5$ was estimated. (auth)

39481 (NP-15248) SLABYE VZAIMODEISTVIYA NA VSTRECHNYKH ELEKTRONNYKH PUCHKAKH. (Weak Interactions of Colliding Electron Beams). Report No. 246. Isffe, B. L.; Okun, L. B.; Rudik, A. P. (Gosudarstvennyi Komitet po Ispol'zovaniyu Atomnoi Energii SSSR, Moscow. Institut Teoreticheskoi i Eksperimental'noi Fiziki). 1964. 30p. Dep. mn.

Possible experiments are discussed for the investigation of weak interaction on the electron-electron and electron-positron colliding beams at the energies of the order of 100-1000 Bev when the weak interaction becomes strong. The main results are given and refer to the processes which occur in the second order of perturbation theory on weak interaction and are described by graphs. (auth)

39482 (NP-15252) UGLOVAYA KORRELYATSIYA MEZHDY π-MEZONOM I LEPTONOMI I OPREDELENIE FORM-FAKTOROV V $K_{\mu 3}$-RASPADE. (Angular Correlation Between π-Mesons and Leptons and Determination of Form Factors in $K_{\mu 3}$-Decay). Report No. 281. Tsukermai, I. S. (Gosudarstvennyi Komitet po Ispol'zovaniyu Atomnoi Energii SSSR, Moscow. Institut Teoreticheskoi i Eksperimental'noi Fiziki). 1964. 9p. Dep. mn.

The form of the angular correlation curves between pion

and leptons directions in $K_{\mu 3}$ decay is shown to be sensitive to the choice of one of two possible values of the form factor ratio. (auth)

39483 (SGAE-PH-20/1965) STUDIE UBER DAS VERHALTEN VON GAMMASTRAHLUNG IN LUFT. (Study of the Behavior of Gamma Radiation in Air). Tisljar, Maria (Oesterreichische Studiengesellschaft fuer Atomenergie G.m.b.H., Seibersdorf. Physik-Institut). 1965. 10p. Dep.(mn).

For air shielding purposes it is necessary to know how far the effect of a strong γ source, as for instance after nuclear explosions, can extend. Two limiting cases were examined. In one the dose output for a monoenergetic point source was calculated for a great distance. The second limiting case was the calculation of the dose output of the center of an air space field simultaneously with a specific activity. The results showed that for a point γ source with the energy 550 kev in a finite homogenous air space, the growth factor at a distance of 1.4 km is 155. For the second limiting case, a factor of 1.7 was calculated for the effect of the scattering. (J.S.R.)

39484 (TID-22038) TIME REVERSAL INVARIANCE IN $\Sigma^0 \rightarrow \Lambda^0 + e^+ + e^-$. Technical Report No. 476. Glasser, R. G.; Burnstein, R. A.; Day, T. B. (and others) (Maryland Univ., College Park. Dept. of Physics and Astronomy). July 1965. Contract AT(40-1)-2504. 6p. Dep. (mn); $1.00(cy), 1(mn) CFSTI.

The Dalitz decay of the Σ hyperon was investigated for time reversal invariance. The polarization of Λ is considered in the investigation. (M.O.W.)

39485 (UCRL-8030(Pt.1)(Mar. '65, ed.)) DATA ON PARTICLES AND RESONANT STATES. Rosenfeld, Arthur H.; Barbaro-Galtieri, Angela; Barkas, Walter H.; Bastien, Pierre L.; Kirz, Janos; Roos, Matts (Lawrence Radiation Lab., Univ. of California, Berkeley). Mar. 1965. Contract W-7405-eng-48. 37p. Dep. mn; CFSTI, $2.00 cy, $0.50 mn.

The data are summarized in three tables. Table 5 covers all the stable particles: leptons, mesons, and baryons, i.e., those states which are immune to decay via the strong interaction. There are two tables of data on the unstable particles, one on meson resonances and one on baryon resonances. These tables include basic information on stable mesons and baryons. Each table is of slightly different form; thus Table 5 includes mass differences and magnetic moments, whereas the baryon table includes information on what pion and K-meson beams will form certain resonances. (M.O.W.)

39486 (UCRL-12359) WIGNER'S ANALYSIS OF THE UNITARY REPRESENTATIONS OF THE POINCARE GROUP. Halpern, Francis R.; Branscomb, Elbert (Lawrence Radiation Lab., Univ. of California, Livermore). Feb. 1965. Contract W-7405-eng-48. 61p. Dep. mn; CFSTI, $3.00 cy, $0.75 mn.

An exposition of Wigner's analysis of the irreducible unitary representations of the inhomogeneous Lorentz group is presented including the calculation of several useful matrices and the detailed consideration of the structure of the various little groups and their representations. The theory of induced representations and little groups is briefly discussed in an appendix because it is the basis for Wigner's analysis and is of general applicability. (auth)

39487 (UCRL-14193) SCATTERING PHASE SHIFT EQUATIONS AND RESONANCE EQUATIONS. Roper, L. David (Lawrence Radiation Lab., Univ. of California, Livermore). May 21, 1965. Contract W-7405-eng-48. 39p. Dep. mn; CFSTI, $2.00 cy, $0.50 mn.

Equations that relate the phase shifts and partial-wave amplitudes for elastic scattering are presented. The effect of inelasticity on elastic scattering is included. Also, resonance equations are given, and many curves show the behavior of a resonance as a function of the various resonance parameters for the case of π-p scattering. In particular, the unusual behavior of highly absorptive resonances is emphasized. (auth)

39488 (UCRL-16058) ENERGY SPECTRA OF THE $K^+_{\pi 3}$ DECAY MODES (thesis). Greiner, Douglas E. (Lawrence Radiation Lab., Univ. of California, Berkeley). May 15, 1965. Contract W-7405-eng-48. 48p. Dep.(mn); $2.00(cy), 1(mn) CFSTI.

Emulsion measurements of the energy spectra of τ'^+ and τ^+ decay are presented. The τ'^+ energy spectrum was measured between 0 and 20 Mev kinetic energy. The energies were determined by range measurements. There were a total of 376 τ'^+ events in this region. If the Q value is known a τ^+ decay is kinematically overdetermined by knowledge of the directions of the momenta of the secondaries. The energies of the 3065 τ^+ events in this sample were determined by this method. It is shown that the density in a Dalitz plot with no charge information is sensitive to nonlinear terms in the square of the matrix element. The τ'^+ decay data were combined with an earlier bubble chamber measurement of the spectrum which covered the region 10 Mev to the maximum allowed energy. The data from both decays were fitted with a power series parameterization of the matrix element and the Brown and Singer resonance theory. The 0–10 Mev portion of the τ'^+ spectrum was found to deviate markedly from the linear behavior observed above 10 Mev. Thus the low-energy portion of the τ'^+ spectrum is quite sensitive to the resonance hypothesis parameters. The analysis of the τ decay utilized all information available in the sample by using a maximum likelihood method along with a chi-square analysis to test goodness-of-fit. (auth)

39489 THE MUON DECAY IN THE RENORMALIZABLE VECTOR BOSON THEORY. Nyiri, J.; Sebestyen, A. (Central Research Inst. of Physics, Hungarian Academy of Sciences, Budapest). Acta Phys. Acad. Sci. Hung., 18: 351-7 (1965).

The mechanism of the muon decay is investigated on the basis of a renormalizable vector boson (RVB) theory. It is found that the RVB and Fermi theories lead essentially to the same results. (auth)

39490 ELECTROMAGNETIC PROPERTIES OF ELEMENTARY PARTICLES IN THE B_7-SYMMETRY MODEL. Kapustsik, Edvard (Joint Inst. for Nuclear Research, Dubna, USSR). Acta Phys. Polon., 27: 737-48(1965). (In Russian)

The electromagnetic properties of elementary particles in the B_7-symmetry model are investigated. The results obtained do not contradict the experimental data. (tr-auth)

39491 ON THE POSSIBILITY OF UNITING THE LORENTZ GROUP WITH THE UNITARY SYMMETRY GROUP. Kapustsik, E.; Obryk, E. (Joint Inst. for Nuclear Research, Dubna, USSR). Acta Phys. Polon., 27: 749-52(1965).

One of the possible methods for the unification of the nonhomogeneous Lorentz group with the SU(3) group into a single 18-parameter Lie group is examined. It is found that all the commutators of the generators of the Lorentz group with the generators of the SU(3) group are equal to zero, assuming the commutativity of the generators corresponding to the operators of total isotopic spin I, its third component I_z, total spin S_p, its third component S_z, and the 4-momentum p_μ. (tr-auth)

39492 RELATIVISTIC THEORY OF ANGULAR CORRELATIONS IN SUCCESSIVE TWO-BODY DECAYS OF UNSTABLE PARTICLES. Henry, Claude; de Rafael, Eduardo (Institut des Hautes Etudes Scientifiques, Buressur-Yvette, France). Ann. Inst. Henri Poincare, 2: 87-104(1965).

Relations for the study of angular correlations in successive two-body decay processes are derived from general relativistic invariance principles. The description of arbitrary spin states in discussed in terms of the density matrix formalism. Multipole expansion techniques derived from the basic transformation laws of physical states and operators are used. (auth)

39493 GROUP OF INVARIANCE OF A RELATIVISTIC SUPERMULTIPLET THEORY. Michel, Louis (Institut des Hautes Etudes Scientifiques, Bures-sur-Yvette, France); Sakita, Bunji. Ann. Inst. Henri Poincare, 2: 167-70(1965).

The problem of defining the invariance group for a relativistic supermultiplet theory is considered. (D.C.W.)

39494 INTERNAL GROUPS AND THE HEISENBERG THEORY OF ELEMENTARY PARTICLES. Geheniau, J. (Universite, Brussels). Ann. Inst. Henri Poincare, Sect. A, 1: 21-30(1964). (In French).

The consequence of the introduction of the equations of the Heisenberg theory of elementary particles into the model of the 8-fold way and the space-time rotator model are considered on the basis of some examples. (J.S.R.)

39495 ON A NONLOCAL THEORY. Wataghin, G. Ann. Inst. Henri Poincare, Sect. A, 1: 47-53(1964). (In French).

A nonlocal theory in which cut-off operators are introduced into the interaction Hamiltonians and into the S matrix is presented. The covariants of this nonlocal theory with respect to the Lorentz group is verified rigorously. The nonlocal theory is proposed to eliminate divergencies and to permit an approximate calculation of collision cross sections, masses, and coupling constants beginning with a new universal constant, the fundamental length $l = (2M_p)^{-1}$ (where M_p is a constant of the order of the proton mass). (J.S.R.)

39496 GENERALIZED BOGOLIUBOV TRANSFORMATION FOR BOSONS. Andriambololona, Raoelina (Faculte des Sciences, Marseille). Compt. Rend., 260: 5205-7 (May 17, 1965). (In French).

The generalized Bogoliubov transformation was studied under the optics of unitary transformations. The Bogoliubov translation, rotation, and inhomogeneous transformation were introduced. (tr-auth)

39497 POLARIZED PROTON TARGETS FOR EXPERIMENTS WITH HIGH-ENERGY PARTICLES. Bilenkii, S. M.; Lapidus, L. I.; Ryndin, R. M. Fortschr. Physik, 13: 1-70 (1965). (In German)

The possible applications of polarized proton targets in high-energy physics are discussed as an introduction to the study of polarization phenomena. The areas discussed are asymmetry relations in the case of a polarization perpendicular to the reaction plane, symmetry limitations and principles for the form of the reaction amplitude, density matrix, asymmetry relations in the case of a randomly oriented polarization, possible methods for the determination of the parities of strange particles in experiments with polarized targets, nucleon-nucleon scattering, meson-meson scattering, photoproduction of π and K mesons, and scattering of gamma quanta and electrons on nucleons. 85 references. (J.S.R.)

39498 PHOTOPRODUCTION OF MESONS(π). Stichel, P. (Universitaet, Hamburg and Deutsches Elektronensyschrotron (DESY), Hamburg). Fortschr. Physik, 13: 73-136(1965). (In German).

The kinematics of photoproduction and invariances were treated. The swelling behavior of the multipole and the Kroll-Ruderman theorem were discussed. The relation between the first resonance in π-N scattering and photoproduction was considered within the framework of the K-matrix formalism. The method for the production of linear polarized photons was described. An isobaric model used for a description of the photoproduction in the region of the second and third resonance is considered only as a semiphenomenological theory. A phenomenological description is given of the second resonance in π-N scattering and photoproduction. The inelastic three-particle channel $2\pi + N$ was approximated through an effective two-particle channel $N^* + \pi$. The third resonance in photoproduction is also discussed. 78 references. (J.S.R.)

39499 ANOTHER ATTEMPT TO DETERMINE THE n-n SCATTERING LENGTH. Rendic, D.; Cerineo, M.; Slaus, I.; Tomas, P. (Inst. Ruder Boskovic, Zagreb). Glasnik Mat.-Fiz. Astron., Ser. II, 19: 275-83(1964).

A correction for the neutron-neutron system is calculated. The electron-nucleon scattering with the only-one-photon exchange is described by a matrix element. Other attempts to calculate the $^1S_0$ neutron-neutron scattering length are also discussed. Because of experimental difficulties a system containing at least three particles must be investigated. (J.F.P.)

39500 TRANSFORMATION FROM A LINEAR MOMENTUM TO AN ANGULAR MOMENTUM BASIS FOR RELATIVISTIC PARTICLES OF NONZERO MASS AND ANY SPIN. Moses, H. E. (MIT Lincoln Lab., Lexington, Mass.). J. Math. Phys. (N. Y.), 6: 1244-54(Aug. 1965).

The infinitesimal generators of the inhomogeneous Lorentz group are given in a basis in which the components of the linear-momentum operators are diagonal and in another basis in which the square of the angular momentum is diagonal for all unitary irreducible ray representations of the group. It was shown previously how the two bases are related for representations corresponding to zero mass and any finite spin. It is pointed out how the two bases are related for representations corresponding to nonzero mass and any spin. Thus relativistic plane waves can be expanded into relativistic spherical waves and vice-versa for particles of any spin and any mass. The relation between the linear- and angular-momentum bases could be used to integrate the infinitesimal generators in the angular-momentum basis and thereby obtain closed expressions which show how the angular momentum of particles of nonzero mass and any spin transform under changes of frame of reference. (auth)

39501 FOKKER ACTION PRINCIPLE FOR PARTICLES WITH CHARGE, SPIN, AND MAGNETIC MOMENT. Schild, A.; Schlosser, J. A. (Univ. of Texas, Austin and Univ. of Chicago). J. Math. Phys. (N. Y.), 6: 1299-1306(Aug. 1965).

A Fokker action principle is obtained for a system of particles with charge, spin, and magnetic moment, interacting through time-symmetric electromagnetic fields. Conservation laws are derived for the energy and the linear and angular momentum of the system. A limiting process is performed, which involves a renormalization of mass, in order that the magnitude of the spin of each particle remain constant. (auth)

39502 BORN RECIPROCITY PRINCIPLE AND UNITARY SYMMETRY. Shin, Ernest E. H. (Massachusetts Inst. of Tech., Cambridge). J. Math. Phys. (N. Y.), 6: 1307-8(Aug. 1965).

In view of the past attempts by Born et al. to explain elementary particles using the Born reciprocity principle as a postulate and of the recent success of unitary symmetry schemes, it is sought to establish a contact between the reciprocity principle and unitary symmetry in connection with the problem of elementary particles. (auth)

39503 GEOMETRIC THEORY OF NEUTRINOS. Penney, R. (Ford Motor Co., Dearborn, Mich.). J. Math. Phys. (N. Y.), 6: 1309-14(Aug. 1965).

It is shown that the conditions $R^{\mu}_{\mu} = 0$, $R_{00} \geq 0$, $R^{\beta}_{\alpha}R^{\lambda}_{\beta} = \frac{1}{4}R_{\rho\tau}R^{\rho\tau}\delta^{\lambda}_{\alpha}$, $R_{\alpha\beta|\sigma} = (R_{\rho\tau}R^{\rho\tau})_{|\sigma}R_{\alpha\beta}$, in the limit that the scalar $R_{\alpha\beta}R^{\alpha\beta}$ vanishes, reproduce the physics of neutrinos. That is, these conditions ensure the existence of a two-component spinor which obeys the Weyl equation and represents a field of completely polarized neutrinos. (auth)

39504 GENERAL OPERATOR POTENTIAL FOR THE TWO-NUCLEON SYSTEM. Tharrats, J.; Cerceau, O.; Rojo, O. (Universidad Central, Caracas). J. Math. Phys. (N. Y.), 6: 1315-20(Aug. 1965).

The interaction between two nucleons is assumed to be described by a general hermitian operator having certain symmetry and invariance properties. It is shown that the usual phenomenological potentials employed in dealing with the two-nucleon system, i.e., nonlocal, velocity-dependent, and hard-core, are related by means of unitary transformations of the interaction operator. In addition it is shown that another such transformation of the total hamiltonian

operator leads to the effective mass formalism. Some numerical results on phase shifts are compared with most accepted values. (auth)

39505 IMPROVED METHOD FOR QUANTUM MECHANICAL THREE-BODY PROBLEMS. I. ATTRACTIVE POTENTIALS. Eyges, Leonard (Air Force Cambridge Research Labs., Bedford, Mass.). J. Math. Phys. (N. Y.), 6: 1320-8(Aug. 1965).

The quantum-mechanical ground-state problem for three identical particles bound by attractive interparticle potentials is discussed. For this problem it was previously shown that it is advantageous to write the wavefunction in a special functional form, for which an integral equation which is equivalent to the Schroedinger equation was derived. A new method for solving this equation is presented. The method involves an expansion in a set of effective two-body functions; these are the eigenfunctions of a two-body problem with a potential of the same shape as the interparticle potential in the three-body problem, but of enhanced strength. The integral equation then becomes a set of coupled equations for certain functions $f_l(\kappa)$, the coefficients in this expansion. By choosing the effective two-body strength properly, the convergence of this expansion can be optimized so that a good approximation is got by retaining only the lowest ($l = 0$) term. The resultant single integral equation for $f_0(\kappa)$ can then be solved by an approximate method. As a test and check, the one-dimensional three-body problem with δ-function interactions is treated, and the results are compared with the known exact one. It is found that the first approximation in the method, which is almost trivial to apply, yields an eigenvalue and eigenfunction accurate to a few percent. The method is also applied to the three-dimensional problem with exponential interparticle potentials, and a comparison of the results with the best numerical calculations is given. (auth)

39506 CONCERNING SPACE-TIME, SYMMETRY GROUPS, AND CHARGE CONSERVATION. Sudarshan, E. C. G. (Syracuse Univ., New York). J. Math. Phys. (N. Y.), 6: 1329-31(Aug. 1965). (NYO-3399-02).

Under the restriction to a symmetry group whose generators can be linearly expressed in terms of the generators of the Lorentz group and of an internal symmetry group, it is shown that charge conservation implies that the symmetry group is a direct product of the Lorentz group and the internal symmetry group. Only local structure of the groups and their unitary representations are considered. (auth)

39507 SYMMETRY OF STRONG INTERACTIONS. Itzykson, C.; Jacob, M. (Stanford Linear Accelerator Center, Calif.). J. Phys. (Paris), 26: 199-216(Apr. 1965). (In French).

Recent developments are reviewed in strong interaction symmetries. A simple approach starting from very well known facts such as charge independence and isotopic spin is emphasized. Unitary symmetry after a short introduction to the language of lie algebras is presented. The experimental data, on masses, multiplets, and scattering cross sections are confronted with the theory. Certain hypothesis concerning the structure of electromagnetic and weak currents of strongly interacting particles is briefly indicated. Finally some generalizations to higher groups and in particular the SU_6 symmetry are mentioned. General methods are sketched to study the properties of the groups involved. (auth)

39508 PRODUCTION OF NUCLEON ISOBARS IN HIGH ENERGY NUCLEON-NUCLEON COLLISIONS. Chang, L.; Koba, Z. (Univ. of Copenhagen). Nucl. Phys., 71: 673-94(Sept. 1965).

Assuming predominance of elastic and quasi-elastic isobar production processes in high energy nucleon-nucleon collisions, $N + N \rightarrow N + N$, $N + N^*$, $N^* + N^*$, and using experimental information on the elastic scattering as the input, differential cross sections of the isobar production are worked out on the basis of unitarity and time reversal invariance together with certain simplifying kinematical assumptions. The isobars will be, on the average, more collimated than the elastically scattered nucleons; their angular distribution will possibly show a very sharp peak followed by a rather flat tail. (auth)

39509 STUDY OF POSITRONIUM IN WATER AND ICE FROM 22 TO −144°C BY ANNIHILATION QUANTA MEASUREMENTS. Colombino, P.; Fiscella, B.; Trossi, L. Nuovo Cimento (10), 38: 707-23(July 16, 1965).

Measurements on water and ice at several temperatures down to −144°C were performed using the standard setup of the linear detectors of positron annihilation radiation. The nature of the narrow component that changes with temperature or state is studied. The shape of such a component is evaluated by simplified theoretical calculations. Positronium formation and its decay modes are discussed quantitatively. (auth)

39510 A STUDY OF THE Σ^- CAPTURE PROCESS IN HYDROGEN. Carrara, R.; Cresti, M.; Grigoletto, A.; Limentani, S.; Peruzzo, L.; Santangelo, R.; Willmann, R. B. (Universita, Padua and Istituto Nazionale di Fisica Nucleare, Padua). Nuovo Cimento (10), 38: 724-7(July 16, 1965).

A sample of Σ^-'s captured in hydrogen was analyzed. The ratio of the rate for Σ^0 production to the total capture rate was determined for Σ^- capture at rest. (auth)

39511 BARYON NUMBER 2, UNITARY SINGLET AS A TEST OF ONE-PARTICLE-EXCHANGE DYNAMICAL MODELS. Diu, B. (CERN, Geneva); Rubinstein, H. R. Nuovo Cimento (10), 38: 831-43(July 16, 1965).

B_8-B_8 scattering is studied making use of the fact that the forces contain the same $\bar{B}BP$ hamiltonian as the P_8-B_8 problem. This circumstance is exploited to find consistency conditions in low partial waves using experimental data. Results are consistent only if a new particle exists with quantum numbers $B = 2$, $T = Y = J = 0$, and F/D ratio in $\bar{B}BP$ coupling $\simeq 1/3$. It is argued that if this state does not exist the dynamical calculations, based on one-particle exchange and lowest-lying threshold dominance, would have to be reconsidered. Besides this, such a particle would have interesting properties, in particular if its mass lies below $2m_A$, as could very well be the case: a possibility would then be open to study the weak decays of Σ^0. (auth)

39512 METHOD OF INTEGRATION OF THE ENERGY VARIABLES IN THE GRAPHS OF THE THEORY OF PERTURBATIONS. Gaudin, M. (Centre d'Etudes Nucleaires, Saclay, France). Nuovo Cimento (10), 38: 844-71(July 16, 1965). (In French).

Using an algebraic identity, the product of propagators associated with the lines of a given graph of the perturbation theory, is decomposed into partial fractions. This allows a systematic summation over the energy variables of a diagram in statistical mechanics. The result is a sum of terms each corresponding to one of the "trees" into which the graph can be decomposed. (auth)

39513 CAN MASSLESS DIRAC PARTICLES HAVE ELECTRIC CHARGE? Pradhan, T. (Saha Inst. of Nuclear Physics, Calcutta). Nuovo Cimento (10), 38: 883-8 (July 16, 1965).

By a nonperturbative method which makes use of masslessness (absence of massive particles) and invariance under Lorentz transformations, γ_5 gauge, charge-gauge and charge conjugation transformations, it is shown that a massless Dirac particle cannot acquire charge through minimal interaction, no matter how strongly it is coupled to the electromagnetic field. (auth)

39514 COVARIANT POLARIZATION THEORY OF SPIN-ONE PARTICLES. Sankaranarayanan, A. (Ames Lab., Ames, Iowa). Nuovo Cimento (10), 38: 889-906 (July 16, 1965). (IS-1077).

A covariant theory of polarization effects in the scattering of spin-one particles by spinless targets is developed. The most generally written covariant S-matrix and density matrices $\rho(p)$ and $\rho'(p')$ before and after the scattering, respectively, are split into two parts so as not to mix up the energy states by using the hole-theory condition of STAPP.

Finally, by substituting the results thus obtained in the scattering equation $\rho'(p') = S\rho(p)\bar{S}$, the polarization effects are studied and the corrections to the nonrelativistic theory obtained. A brief discussion of some calculational aids for the spin-one formalism used in this paper is also included because of its pertinence to some nuclear reaction problems. (auth)

39515 FINAL-STATE INTERACTIONS IN K_{e4}^+ DECAY. Iliopoulos, J. (Universite de Paris, Orsay, France). Nuovo Cimento (10), 38: 907-24(July 16, 1965).

A model is presented which permits the determination of the meson(π)-meson(π) scattering length in the L = 0, I = 0 state to start from the experimental results on the meson-(K_{e4}^+) decay. Definite relations are established between the decay form factors and the $K\bar{K} \rightarrow 2\pi$ partial wave amplitudes. The crossed channel is approximated by the exchange of a K* resonance. A theory of two parameters is obtained for the $\pi - \pi$ scattering length and the value of the form factor $q^2 \approx 5m_\pi^2$. These parameters can be determined by the experimental spectra of two mesons(π) and from the different asymmetries in the angular distribution of the disintegration products. (J.F.P.)

39516 NONOBSERVABILITY OF PSEUDOSCALAR CHARGE DENSITY. von Baeyer, H. C. (McGill Univ., Montreal). Nuovo Cimento (10), 38: 925-31(July 16, 1965).

It is shown that the pseudoscalar charge density of spin-½ particles induced by parity-violating interactions is not physically observable. Its effect on the spin direction of an electron in a longitudinal electric field is explicitly calculated and found to be null. This result contradicts recent calculations of Hiida. (auth)

39517 BARYON-RESONANCE PRODUCTION BY NEUTRINOS. Berman, S. M. (Stanford Linear Accelerator Center, Calif.); Veltman, M. Nuovo Cimento (10), 38: 993-1005(July 16, 1965).

The production of the $\frac{3}{2}^-, \frac{3}{2}$ resonance by neutrinos incident on nucleons is considered in the framework of the Rarita-Schwinger formalism for spin-$\frac{3}{2}$ particles. With the help of the conserved vector theory, and the Goldberger-Treiman relation, the value of certain coefficients is estimated. Wherever information is lacking, the static theory is used. The interaction determined in this way is then used to obtain total cross-sections. The result is that the total cross-section on complex nuclei as function of neutrino energy behaves similarly to, but is in absolute value larger than, the elastic process cross-section. Properties of the spin-$\frac{3}{2}$ density matrix under the combined assumptions of time-reversal invariance and Born approximation are derived and the general expression for the angular distribution of the decay pion in the f^* rest frame is given. (auth)

39518 VECTOR MESONS AND COMPLEX ANGULAR MOMENTUM. Martinis, M.; Ahmed, K. (Imperial Coll. of Science and Tech., London). Nuovo Cimento (10), 38: 1021-39(July 16, 1965).

The analytic behavior in the complex angular momentum plane, of the amplitude for a vector meson coupled to a scalar "nucleon" through a conserved current is examined. The graph with the exchange of two vector mesons is considered. This graph is iterated in the vector meson channel (called s channel). The partial wave projection of the lowest order graph (4th order) has a simple pole at l = 1, which is obtained after an analytical continuation from higher l. When the singular part of the graph at l = 1 is taken as the kernel of the Bethe-Salpeter equation it is found that for $s \neq 6\mu^2$ its solution has two simple moving poles in the neighbourhood of l = 1 in the l-plane. However, the Regge trajectory has two branches which intersect each other at the branch point $s = 6\mu^2$. (auth)

39519 DOUBLE PRODUCTION OF CHARGED PIONS IN HYDROGEN BY PHOTONS OF ENERGY BETWEEN 600 AND 850 Mev. Beneventano, M.; Finzi, R.; Paoluzi, L.; Sebastiani, F.; Severi, M.; Villa, F. (Universita, Rome and Istituto Nazionale di Fisica Nucleare, Rome). Nuovo Cimento (10), 38: 1054-60(July 16, 1965).

The reaction $\gamma + p \rightarrow (p\pi^+) + \pi^-$ was studied for the π^- production cross section, where $(p\pi^+)$ is the well-known first resonant state of the nucleon. It was supposed that if an excited state of the nucleon is formed, it may subsequently decay into a lower excited state instead of decaying directly into a nucleon and a meson(π). For this purpose the differential cross section for the meson(π) was measured in this reaction at different photon energies, keeping the equivalent mass of the system $p\pi^+$ constant. The angle of emission of the meson(π^-) corresponded to a center of mass angle of about 60°. The data show an increase in the cross section at a photon energy of about 630 Mev. There was no other such similar increase. It was concluded that a coherent interpretation of the experimental results is provided by the assumption that a resonant state of isospin ½ is formed, which decays preferably into the isobar P_{33} and a negative meson(π). No evidence was found for the resonant state D_{13}. (J.F.P.)

39520 SOME PROPERTIES OF THE OVERLAP FUNCTION. Kowalski, K. L. (Case Inst. of Tech., Cleveland). Nuovo Cimento (10), 38: 1073-6(July 16, 1965).

In view of the critical role of the overlap function in determining the elastic scattering at high energies an attempt was made to investigate those properties of this function which are independent of any particular model and which must themselves be predicted by any model. It is evident from the relation between the overlap function and the absorptive part of the scattering amplitude that their properties are quite similar. Attention is called to this fact and to some of its direct consequences. (J.F.P.)

39521 WEAK-STRONG COUPLING COMPLEMENTARITY IN RENORMALIZED PERTURBATION THEORY. Frank, W. M. (Weizmann Inst. of Science, Rehovoth, Israel). Nuovo Cimento (10), 38: 1077-81(July 16, 1965).

An exactly solvable model is presented in which only the boson propagator is regularized and the renormalized perturbation series diverges but can be expanded with infinite radius of convergence about the point at infinity. In this model, a theory where only the boson propagator is regularized, the renormalized perturbation series is found to be a divergent, asymptotic expansion which has a series expansion in negative powers of z with an infinite radius of convergence. This feature of an infinite radius of convergence about the point at infinity is a likely characteristic only of the generous regularization of the boson propagator. The same result is expected to apply for all sufficiently regularized boson propagators. These results show that when weak coupling fails, strong coupling becomes applicable, suggesting the search for nonperturbative approaches which are perturbative in the strong coupling. Indications suggest that the highest symmetries are possessed by the interaction terms and are broken by the free hamiltonian. (J.F.P.)

39522 A TREATMENT OF THE RANDOM PHASE APPROXIMATION FOR ABSORPTIVE CORRECTIONS. Fairlie, D. B. (Univ. of Durham, Eng.). Nuovo Cimento (10), 38: 1086-7(July 16, 1965).

An alternative derivation of a recent result on the absorptive corrections to the peripheral model is given. This result is derived by means of standard results on the distribution of eigenvalues of random matrices, using slightly different statistical assumptions on the distribution of elements. (J.F.P.)

39523 GENERALIZED CONSERVATION LAWS FOR FREE FIELDS WITH MASS. O'Connell, R. F.; Tompkins, D. R. (Louisiana State Univ., Baton Rouge, La.). Nuovo Cimento (10), 38: 1088-91(July 16, 1965).

The method of obtaining generalized conservation laws for massless free fields is extended to the case of free fields with mass. Also the conservation laws for free fields with mass are derived without the use of lagrangians or Noether's theorem. (J.F.P.)

39524 D/F RATIOS AND BARYON MAGNETIC MOMENTS IN THE SV_{12} SCHEME. Roman, P.; Aghassi, J. J. (Boston Univ.). Nuovo Cimento (10), 38: 1092-5(July 16, 1965).

Some dynamical predictions for the baryon-meson vertices are calculated. The results show that while this scheme yields an excellent classification of states and a most accurate mass formula, it probably is not accurate for grasping intricate features of dynamics at high energy. Further interesting relations can be obtained by noting the baryon supermultiplet decomposition. (J.F.P.)

39525 VARIATIONAL PRINCIPLES FOR QUASI-STATIONARY STATES. Rudakov, V. S. (Leningrad State Univ.). Phys. Letters, 17: 261-2(July 15, 1965).

The radial Schrödinger equation is considered, which leads to an eigenvalue problem for the complex energy k^2. Variational principles are formulated for the complex k^2 on the unphysical sheet of the complex energy surface. The perturbation formula for the energy of quasi-stationary states is derived. (L.B.S.)

39526 SEARCH FOR RADIATIONLESS ANNIHILATION OF POSITRONS. Shimizu, S.; Mukoyama, T.; Nakayama, Y. (Kyoto Univ.). Phys. Letters, 17: 295-6(July 15, 1965).

An experiment was performed in search for the radiationless annihilation of 300-kev positrons in a lead foil target, using a lithium-drifted silicon junction detector for the ejected bound electrons and a 400-channel pulse-height analyzer. A peak was observed in the electron spectra which is interpreted as the radiationless annihilation of positrons with a K- and/or L-shell electron. The cross section was found to be $(3.0 \pm 0.9) \times 10^{-26}$ cm^2, as a sum of those for KK, KL, KM, and LL pairs of bound electrons. The ratio of the number of radiationless annihilations to that of the two-quantum annihilation was found to be $1 : 6.8 \times 10^4$. (L.B.S.)

39527 PROTON-ANTIPROTON ANNIHILATION INTO TWO MESONS. Alles, W. (CERN, Geneva); Borchi, E.; Martucci, G.; Gatto, R. Phys. Letters, 17: 328-9(July 15, 1965).

An analysis is made of proton-antiproton annihilation at rest into two O^-, 1^- mesons within the framework of SU_6 symmetry. Production amplitudes are given for annihilations from the ^1S $\bar{p}p$ and ^3S $\bar{p}p$ states. (L.B.S.)

39528 THE $\eta \to \pi^+\pi^0\pi^-$ DECAY WITH C-VIOLATION. Nauenberg, M. (Stanford Univ., Calif.). Phys. Letters, 17: 329-31(July 15, 1965).

Calculations are presented of the effect of C violation on the η decay scheme. It is assumed that in addition to a $\Delta I = 1\eta \to 3\pi$ transition due to virtual electromagnetic interactions, there exists a $\Delta I = 0$ transition induced by the interaction H which violates C. Some details of a model for $\eta = 3\pi$ decay are given. (L.B.S.)

39529 CONSEQUENCES OF SU_6 FOR TOTAL BARYON-BARYON AND BARYON-ANTIBARYON CROSS-SECTIONS. Buccella, F. (Universita, Florence); Martucci, G.; Gatto, R. Phys. Letters, 17: 333-4(July 15, 1965).

Relations are derived among the total cross sections for baryon-proton scattering and for antibaryon-proton scattering, using the optical theorem in connection with SU_6 arguments. The relations are verified to hold in the $\tilde{U}(12)$ relativistic extension of SU_6. (L.B.S.)

39530 INVESTIGATION OF THE COULOMB-NUCLEAR INTERFERENCE IN ELASTIC K^-p SCATTERING AT LOW ENERGIES. Schlosser, K.; Buschbeck-Czapp, B.; Hromadnik, H.; Otter, G. (Universitaet, Vienna). Phys. Letters, 17: 334-6(July 15, 1965).

An analysis was made of the angular distributions of elastic K^-p interactions at low energies. The absolute value R and the phase angle α of the nuclear part of the elastic scattering were determined by a maximum likelihood fit to the c.m. distributions for the intervals 100 to 200 Mev/c and 200 to 360 Mev/c, from which the Coulomb nuclear interference was determined. The results are compared with theoretical values calculated from the scattering lengths solutions. (L.B.S.)

39531 ON THE DECAY OF THE X AND ϕ MESONS. Badier, J. (Ecole Polytechnique, Paris); Demoulin, M.; Goldberg, J. (and others). Phys. Letters, 17: 337-40 (July 15, 1965).

The decay modes of the X meson into $\eta\pi\pi$, $\pi^+\pi^-\gamma$ and of the φ meson into K^+K^-, $K^0_1K^0_2$, $\pi^+\pi^-\pi^0$ were observed in an analysis of the $K^- + p \to \Lambda + X$ and $K^- + p \to \Lambda + \varphi$ interactions at 3 Bev. Relative probabilities for the observed decay modes are presented. (L.B.S.)

39532 BARYON-BARYON SCATTERING AND SU(6). Cline, D.; Olsson, M. (Univ. of Wisconsin, Madison). Phys. Letters, 17: 340-2(July 15, 1965). (COO-881-52)

The predictions of SU_6 are compared with experimental data for low energy NN, Ap, and Σ^+p scattering. The known Ap parameters which define the singlet and triplet S-wave Ap scattering amplitudes are used to predict the S-wave Σ^+p elastic cross section. A large discrepancy was found between the SU(6) predictions and the experimental Σ^+p cross section. (L.B.S.)

39533 GROUP SU(12) AS A GENERALIZATION OF THE SYMPLECTIC AND SPIN SYMMETRIES. Fakirov, D. G.; Struminskii, B. V.; Todorov, I. T. (Joint Inst. for Nuclear Research, Dubna, USSR). Phys. Letters, 17: 342-4(July 15, 1965).

It is shown that if the group of the third rank Sp(6) is taken as the internal symmetry group after uniting it with the spin group according to the scheme leading from $SU(3) \otimes SU(2)$ to SU(6), all the basic results of the SU(6) scheme may be obtained. A 143-parametric unitary group SU(12) appears in place of SU(6) for this case. (L.B.S.)

39534 EXPERIMENTAL RESULTS ON THE ANNIHILATION $\bar{p}p \to \bar{K}K\pi$ AT REST; NON-K^*-RESONATING EVENTS. Armenteros, R. (CERN, Geneva); Edwards, D. N.; Jacobsen, T. (and others). Phys. Letters, 17: 344-7(July 15, 1965).

The properties of the events outside of the K^* bands on a symmetrized Dalitz plot for $\bar{p}p \to K^0, K^\pm\pi^\mp$ are presented. Two enhancements for which both k's have an energy less than 760 Mev were observed at 1025 and 1250 Mev in the $\bar{K}K$ effective mass spectra, with widths of approximately 40 and 50 Mev, respectively. A broad enhancement was also observed at 1285 Mev ($\Gamma = 120$ Mev) in the $K^0_1K^0_1\pi^0$ mode. The possible quantum number assignments are discussed. An upper limit of 0.04 was assigned for the branching ratio of $K^0K^\pm/\rho^0\pi^\pm$. (L.B.S.)

39535 EVIDENCE FOR A NON-STRANGE MESON OF MASS 1290 Mev. D'Andlau, Ch. (College de France, Paris); Astier, A.; Della Negra, M. (and others). Phys. Letters, 17: 347-52(July 15, 1965).

An analysis was made of $\bar{p}p$ annihilations with 1.2 Bev/c $\bar{p}$ in a hydrogen bubble chamber, and evidence was obtained for the existence of a non-strange meson with a mass of 1290 Mev, as width of ~25 Mev, and decaying into the $K\bar{K}\pi$ final state. The neutral $K\bar{K}\pi$ enhancement was observed in different $\bar{p}p$ annihilation channels, which was identified as the D meson. It is suggested that the D^0 is produced mainly by a two-body production mechanism, and decays via strong interactions. The quantum numbers $I^G = 0^+$ or 1^+, and $J^P = 1^+$ or 2^-, with 0^- not completely excluded, were assigned. (L.B.S.)

39536 VANISHING OF THE E2 PART OF THE $N^*_{33} \to N + \gamma$ AMPLITUDE IN THE NON-RELATIVISTIC QUARK MODEL OF ELEMENTARY PARTICLES. Becchi, C.; Morpurgo, G. (Universita, Genoa and Instituto Nazionale di Fisica Nucleare, Genoa). Phys. Letters, 17: 352-4 (July 15, 1965).

A test of the non-relativistic quark model of elementary particles is proposed in which it is shown that the E2 amplitude of the $N^*_{33} \to N + \gamma$ process vanishes for two independent reasons: both the wave functions for a particle of the baryonic octet and of the baryonic decuplet have $L = 0$, and the spin functions are orthogonal. Remarks are given on the meaning of the non-relativistic calculation in the framework of a relativistic theory; the ratio E2/M1 expected without the operation of the selection rule; and evidence of the consistency of data on photopion production

near the 33 resonance with the predictions of the model. (L.B.S.)

39537 EVIDENCE FOR A NEW $\pi^+\pi^-$ RESONANCE AT 1.67 Gev. Goldberg, M. (CERN, Geneva); Judd, F.; Vegni, G. (and others). Phys. Letters, 17: 354-7(July 15, 1965).

Investigations were made of the $\pi^+d \rightarrow \bar{p}p\pi^+\pi^-$ reaction at 6.0 Bev/c and the $\pi^-p \rightarrow n\pi^+\pi^-$ reaction at 8.0 Bev/c. The experimental analysis and results are presented for each. Two common features were observed in both experiments in the $\pi^+\pi^-$ system at approximately 1.65 Bev: a peak in the mass spectrum and a discontinuity in the variation of the forward backward asymmetry. It is concluded that the observed peak is a resonance peripherally produced, with mass and full width estimates of 1.67 ± 0.03 Bev and 0.18 ± 0.04 Bev, respectively. (L.B.S.)

39538 CIRCULAR POLARIZATION OF γ QUANTA IN ABSORPTION OF NEUTRONS BY PROTONS AND ISOTOPIC STRUCTURE OF WEAK INTERACTIONS. Danilov, G. S. (Ioffe Inst. of Physics, Leningrad). Phys. Letters, 18: 40-1(Aug. 1, 1965).

It is shown that the circular polarization of the gamma quantum in the interaction $n + p \rightarrow d + \gamma$ is determined by only the isoscalar part of weak interactions and that the asymmetry of the gamma quanta is due only to its isovector part. (D.C.W.)

39539 MEASUREMENT OF THE ELECTRON ASYMMETRY IN THE LEPTONIC DECAY OF POLARIZED Λ^0. Barlow, J. (CERN, Geneva); Blair, I. M.; Conforto, G.; Ferrero, M. I.; Rubbia, C.; Sens, J. C.; Duke, P. J.; Mann, A. K. Phys. Letters, 18: 64-8(Aug. 1, 1965).

The asymmetry, with respect to the spin direction of the hyperon (Λ^0), in the angular distribution of electrons from the leptonic decay of polarized hyperons (Λ^0) was measured. The ratio of the axial and polar vector coupling constants in V-A theory was estimated from the asymmetry parameter obtained. (D.C.W.)

39540 THE PARITY OF THE $Y_1^*(1660)$. Leveque, A. (Laboratoire de Physique Corpusculaire a Haute Energies, CEN, Saclay, France); Ville, M.; Negus, P. J. (and others). Phys. Letters, 18: 69-72(Aug. 1, 1965).

The results are presented of an attempt to determine the parity of the $Y_1^*(1660)$ through an analysis of the interaction $K^- + p \rightarrow Y_1^{*+}(1660) + \pi^-$, followed by $Y_1^{*+}(1660) \rightarrow \Sigma^- + 2\pi^+$. The results indicate that the $Y_1^*(1660)$ has positive parity. (D.C.W.)

39541 DEUTERON ELECTRODISINTEGRATION AND NEUTRON FORM FACTORS. Gourdin, M.; Le Bellac, M.; Renard, F. M.; Tran Thanh Van, J. (Laboratoire de Physique Theorique et Hautes Energies, Orsay, France). Phys. Letters, 18: 73-6(Aug. 1, 1965).

A fully relativistic and gauge-invariant theory for obtaining neutron form factors from data on deuteron-electron interactions is outlined. The results of analyses of quasi-elastic peak experiments and coincidence experiments are included. This covariant theory appears to be rather well adapted to the electrodisintegration process in the range of momentum transfer $0 \leq q^2 \leq 20$ fm^{-2}. (D.C.W.)

39542 OBSERVATION OF CORRELATIONS BETWEEN VECTOR-MESON AND BARYON-RESONANCE DECAYS. Goldhaber, G.; Brown, J. L.; Butterworth, I.; Goldhaber, S.; Hirata, A. A.; Kadyk, J. A.; Shen, B. C.; Trilling, G. H. (Univ. of California, Berkeley). Phys. Letters, 18: 76-80(Aug. 1, 1965). (UCRL-16201)

Experimental data on the interactions $\pi^+ + p \rightarrow 2\pi^+ + \pi^- + p$, $K^+ + p \rightarrow K^+ + \pi^- + \pi^+ + p$, and $K^+ + d \rightarrow K^+ + \pi^- + \pi^+ + p(n)$ at 3.65, 1.96, and 2.30 Bev/c, respectively, are presented showing the existence of decay correlations between the K^{*0} vector-meson resonances and the $\frac{3}{2}$, $\frac{3}{2}$ baryon resonance (1238). (D.C.W.)

39543 S-MATRIX DERIVATION AND EXTENSION OF E. GERJUOY'S MOMENTUM TRANSFER THEOREM. Corinaldesi, E. (Boston Univ.). Phys. Letters, 18: 81 (Aug. 1, 1965).

The bases of Gerjuoy's momentum transfer theorem for potential scattering are summarized, and it is shown that the theorem also holds for non-hermitian potentials. A theorem for the momentum transfer of all field quanta of a single species that are involved in a set of interactions is obtained. (D.C.W.)

39544 CABIBBO ANGLES AND JOHNSON-TREIMAN RELATION. Gourdin, M. (Laboratoire de Physique Theorique et Hautes Energies, Orsay, France). Phys. Letters, 18: 82-3(Aug. 1, 1965).

Formulas for the axial vector coupling constants associated with hypercharge-conserving and -violating transitions are derived involving integrals in which the total cross sections for $\pi^\pm$–p and K^0–p, $\bar{K}^0$–p scattering appear. The two integrals are connected by a Johnson-Treiman relation. Under the assumption of the equality of the two integrals, the equality of the two Cabibbo angles for the weak vector and the weak axial vector currents is obtained, showing that the renormalization of the axial vector coupling constants is independent of hypercharge. (D.C.W.)

39545 APPLICATIONS OF THE OPTICAL MODEL TO KP INTERACTIONS. Marshall, L. (Univ. of Colorado, Boulder); Oliphant, T. Phys. Letters, 18: 83-5(Aug. 1, 1965).

Some data on K^--p elastic scattering at 1.26 and 2.00 Bev/c were analyzed using optical model codes. (D.C.W.)

39546 THREE-QUANTUM ANNIHILATION OF POSITRONS IN METALS AND INSULATORS. Bertolaccini, M.; Bussolati, C.; Zappa, L. (Istituto di Fisica del Politecnico, Milan). Phys. Rev., 139: 696-9(Aug. 2, 1965).

The three-quantum decay of positrons annihilating in some metals and in some insulators was investigated by using a triple coincidence method. Relative measurements were made by comparing the three-quantum yield in each substance with that of aluminum. Small differences between the three-quantum yields of various metals were found: in Pb, where this effect appears to be the largest, the relative yield is $P/P_0 = 1.16 \pm 0.03$. At present any simple attempt to explain this result is unsuccessful. From the relative three-quantum rates measured in insulators, and on the basis of a simple model, the following information was obtained: the contribution to three-quantum production in insulators due to the positronium atom arises only from the orthostate decaying with a partial lifetime τ_3 equal to that in free space ($\tau_3 = 1.39 \times 10^{-7}$ sec). No evidence was found of three-quantum production arising from interaction of the positronium with matter. The remaining three-quantum annihilations occur with the same yield characteristic of positrons in AL ($P_f/P_0 = 1.00 \pm 0.05$). From the same measurements in insulators, the yield in Al is $P_0 = (2.64 \pm 0.08)10^{-3}$, in good agreement with the value predicted by Ore and Powell (2.70×10^{-3}). (auth)

39547 NONEXISTENCE OF THE TETRANEUTRON. Tang, Y. C.; Bayman, F. F. (Univ. of Minnesota, Minneapolis). Phys. Rev. Letters, 15: 165-8(July 26, 1965).

A variational calculation was made on the energy of the n^4 system. The results indicate that there is neither a bound state nor a resonant state of the n^4 system. (D.C.W.)

39548 FURTHER EVIDENCE FOR A POSSIBLE I = $\frac{5}{2}$ N^* RESONANCE AT 1580 Mev. Alexander, G.; Benary, O.; Reuter, B.; Shapiro, A.; Simopoulou, E.; Yekutieli, G. (The Weizmann Inst. of Science, Rehovoth, Israel). Phys. Rev. Letters, 15: 207-10(Aug. 2, 1965).

A search was made in p-p collisions at 5.5 Bev/c at different final-state channels for possible formation of an I = $\frac{5}{2}$ N^* resonance. The work was carried out with 30,000 pictures taken with a hydrogen bubble chamber exposed to a secondary beam of protons at 5.52 Bev/c. The data were analyzed in terms of resonance production as a function of their momentum transfer. The angular distribution of the final-state nucleons and nucleon-meson (π) systems showed a marked forward backward peaking. An enhancement was found at 1.58 Bev, and was attributed to the formation of an $N_{\frac{5}{2}}^*$ resonance. (J.F.P.)

39549 HIGH-ENERGY PHOTOPRODUCTION OF NEUTRAL RHO MESONS. Lanzerotti, L. J.; Blumenthal, R. B.; Ehn, D. C.; Faissler, W. L.; Joseph, P. M.; Pipkin, F. M.; Randolph, J. K.; Russell, J. J.; Stairs, D. G.; Tenenbaum, J. (Harvard Univ., Cambridge, Mass.). Phys. Rev. Letters, 15: 210-13(Aug. 2, 1965).

Measurements were made of the photoproduction of charged pion pairs in a mass range from 0.300 to 1.5 Bev using a 5.5 Bev bremsstrahlung beam. Copious production of the mesons (ρ) was observed in the forward direction. The dependence of the meson (ρ) photoproduction cross section on gamma-ray energy, production angle, and atomic number of the target nucleus indicates that a diffraction-like mechanism is dominant. Spectrometer arms were used to detect meson (π) pairs with a total mass acceptance of 21%. The mesons (ρ) were shown to be transversely polarized. The data indicated that the photoproduction is dominated by the diffraction mechanism. (J.F.P.)

39550 NUCLEON-NUCLEON TOTAL CROSS SECTIONS BETWEEN 1 AND 8 Gev/c. George, R. F. (Cavendish Lab., Cambridge, Eng.); Riley, K. F.; Tapper, R. J.; Bugg, D. V.; Salter, D. C.; Stafford, G. H. Phys. Rev. Letters, 15: 214-16(Aug. 2, 1965).

Measurements were made of the two total cross sections σ(p-p) and σ(p-d) over the laboratory momentum range 1.1 to 7.8 Bev/c by the attenuation technique. These cross sections were measured with an average statistical accuracy of ±0.1%, and systematic errors were of the same order. Results showed that the cross sections are in general slowly varying functions of cm energy; but there is evidence for a small, broad structure centered on an energy of 2.75 Bev in σ(p-p). A proton beam was obtained by diffraction scattering and directed through each of three identical target vessels, one containing liquid hydrogen, one containing liquid deuterium, and the third an evacuated dummy. (J.F.P.)

39551 ANALYSIS OF $\pi\rho$ ENHANCEMENTS IN $\pi^- + d$ INTERACTIONS AT 3.2 Bev/c. Seidlitz, Leo; Dahl, Orin I.; Miller, Donald H. (Univ. of California, Berkeley). Phys. Rev. Letters, 15: 217-21(Aug. 2, 1965).

The properties of the $\pi^-\rho^-$ and $\pi^-\rho^0$ systems are compared under similar kinematic conditions. It is concluded that the enhancements observed in the A_1 region, one of the two peaks of a previously discovered enhancement, cannot result from the decay of an I = 2 state. Data in the A_2 region are consistent with the decay of an I = 1 state produced through exchange of an I = 1 system. Interpretation of the A_1 enhancement as a kinematic effect is discussed. For a comparison of production and decay properties of the A_1 and A_2 systems in a variety of final states, π^-d interactions at 3.2 Bev/c were analyzed. The possibility remains that the A_1 peak in π^+p experiments consists of a narrow resonance superimposed upon background enhancements. Observation of such a peak is difficult because of decreased production on deuteron targets or because of poorer resolution. (J.F.P.)

39552 SEARCH FOR C-NONCONSERVING DECAYS $\phi \to \rho + \gamma$ AND $\omega + \gamma$. Lindsey, James S.; Smith, Gerald A. (Univ. of California, Berkeley). Phys. Rev. Letters, 15: 221-24(Aug. 2, 1965).

Experiments were performed for observation of the meson (ϕ) decay. Approximately 70% of the 740,000 pictures taken of the 72 in. hydrogen bubble chamber exposed to an incident meson (K^-) beam at momenta of 2.1 to 2.7 Bev/c at the bevatron were analyzed. The reactions $K^- + p \to \Lambda^0 + \phi^0$; $\phi^0 \to K^+ + K^-$, $\phi \to K_1^0 + K_2^0$, and $K^- + p \to \Lambda^0 + \pi^+ + \pi^-$ + (all neutrals) were considered. The enhancement previously identified as the $\pi^+\pi^-\gamma$ decay mode of the η (959) was observed, but no enhancement is observed at or near the known location of the meson (ϕ). Branching ratios were also found for the meson (ϕ) decay $\phi \to \rho + \gamma$ and $\phi \to \omega + \gamma$. (J.F.P.)

39553 SPIN OF THE $Y_1^*(1405)$. Engler, A. (Carnegie Inst. of Tech., Pittsburgh); Fisk, H. E.; Kraemer, R. W.; Meltzer, C. M.; Westgard, J. B.; Bacon, T. C.; Hill, D. G.; Hopkins, H. W. K.; Robinson, D. K.; Salant, E. O. Phys. Rev. Letters, 15: 224-28(Aug. 2, 1965).

A study was made of three-body final states, hyperon + K + π, in meson (π)-nucleon collisions at an incident meson (π) momentum of 1.68 Bev/c. The purpose of this investigation was to obtain information on the spin of the Y_0^* (1405) resonance by observing angular correlations in its decay. The results, by use of a moments analysis, are consistent with spin $\frac{1}{2}$, but the statistics at present are too poor for a parity determination. The decay of the Y_1^* (1385) resonance was also examined; and it was found that spin $\frac{1}{2}$ is ruled out, spin $\frac{3}{2}$ is acceptable, and spin $\frac{5}{2}$ is not required by these data. There is no direct evidence for interference in any of the three-body final states giving rise to the Y_1^*. The data were obtained from approximately 2×10^5 π^-p and 1.2×10^5 π^+d pictures. The incident beam momentum corresponds to a cm energy 50 Mev below the threshold for the reaction K^* (890) + Σ. (J.F.P.)

39554 THE ACTUAL MASS OF POTENTIAL ENERGY. [PART] II. Brillouin, L. (Columbia Univ., New York). Proc. Natl. Acad. Sci. U. S., 53: 1280-4(June 1965).

The actual mass of potential energy is considered for mechanical systems of particles when dimensions and velocities remain small. Relativity theory is used to define potential energy, and the motion of a particle under a constant force, such as in an accelerator, is discussed. The critical value of potential energy of a particle-antiparticle collision corresponding to annihilation is derived. The critical energy is large enough to make up for the mass of two particles of mass M_0 each. (C.E.S.)

39555 ON THE COVARIANT EXTENSION OF SU(6). Charap, J. M.; Matthews, P. T. (Imperial Coll., London). Proc. Roy. Soc. (London), Ser. A, 286: 300-12(July 20, 1965).

The covariant generalizations of SU(6) invariant interactions were considered within the framework of U(6) ⊗ U(6). This group, in general, appeared to lead to parity doubling for the mesons, but not the baryons. However, the parity doubling interpretation implied indefinite metric, which could be avoided by using the Bargmann-Wigner equations to eliminate the offending terms. These equations relate sets of terms, which would together make multiplets of $\tilde{U}(12)$, and the multiplets correspond physically to those of SU(6). Five different Yukawa interactions were derived, invariant with respect to U(6) ⊗ U(6), all of which had the SU(6) static limit. The linear combination of these was found which is invariant for $\tilde{U}(12)$. (auth)

39556 THE $\underline{572}^+$ MULTIPLET IN $\tilde{SU}(12)$. Delbourgo, R.; Rashid, M. A. (International Centre for Theoretical Physics, Trieste, Italy). Proc. Roy. Soc. (London), Ser. A, 286: 412-14(July 20, 1965). (IC/65/14)

The $\tilde{SU}(12)$ invariant form factors for the vertex function of the $\underline{364}^+ - \underline{143}^- - \underline{572}^+$ multiplets are presented in detail. A characteristic combination of (3D + 5F) contrasts with the (3D + 2F), which appears in the analogous form factors of the $\underline{364}^+ - \underline{364}^+ - \underline{143}^-$ vertex function. (auth)

39557 ON THE HIGH ENERGY QUASI-ELASTIC PROTON-PROTON SCATTERING. Takada, Yoshio; Bando, Masako (Kyoto Univ.). Progr. Theoret. Phys. (Kyoto), 33: 657-65(Apr. 1965).

Quasi-elastic p-p scattering processes are investigated. The calculations are carried out by using the modified peripheral model. The final state interactions are qualitatively understood in the light of the classical arguments. (auth)

39558 V-θ BOUND STATE IN THE LEE MODEL. Muta, Taizo (Tokyo Univ.). Progr. Theoret. Phys. (Kyoto), 33: 666-75(Apr. 1965).

The complete solution to the problem of the V-θ bound state B in the N-θ-θ sector of the Lee model is given by the use of the technique devised by Amado. The wave function of the bound state B has a left-hand cut arising from the virtual process $B \to N + \theta + \theta$ as well as a pole corresponding to its mass. The eigenvalue equation for

the mass of B is equivalent to the equation which determines the dynamical pole of the V-θ scattering amplitude if we eliminate zeros from it. There exists no V-θ bound state when the coupling constant is fairly weak ($Z_V \sim 1$) or it attains the critical value ($Z_V = 0$). Also discussed is the case that the V particle is unstable, where the V-θ system (or equivalently N-θ-θ system) is unstable, too. (auth)

39559 BOOTSTRAP MECHANISM AND SYMMETRIES OF STRONG INTERACTIONS. Yamada, Masao (Tokyo Univ.). Progr. Theoret. Phys. (Kyoto), 33: 676-91(Apr. 1965).

Kinds of symmetries consistent with the bootstrap mechanism in the baryon-pseudoscalar meson scattering problem are discussed. There, the one-baryon exchange approximation is used. The masses of baryons and their coupling constants are calculated numerically. The global the cosmic and the G_2 symmetries are allowable, but the SU(3) symmetry is excluded. (auth)

39560 CURRENT-CURRENT INTERACTION AND NONLEPTONIC DECAYS OF HYPERONS. RELATION BETWEEN INTERMEDIATE MESON AND B-MATTER. Fujii, Kanji; Ito, Yukio; Iwata, Kenzo; Terazawa, Osamu (Hokkaido Univ., Sapporo). Progr. Theoret. Phys. (Kyoto): 33: 692-704(Apr. 1965).

Under the assumption that the charged vector mesons W as intermediaries of weak interactions exist, the following problems are considered: Is it possible to understand in a unified way the universality of weak coupling constants, the charged current-current picture of weak interactions and the $|\Delta I| = \frac{1}{2}$ enhancement of nonleptonic decays? How can we understand the distinctive character of W? A possible answer to the problems seems to be obtained if one considers the problems by standing on a "genetical" viewpoint of elementary particles (such as the Nagoya model). In order to answer to these problems from this viewpoint, a model of the W meson is proposed on the basis of the quartet model, and on the same basis the semi-weak two-body interactions are introduced, which are expected to play a main role (i.e. to lead the $|\Delta I| = \frac{1}{2}$ enhancement) in nonleptonic interactions. In this model, W^+ mesons are assumed to be composed of strongly correlated $\bar{B}_0$ and B_+. Thus, the peculiarity of W mesons will be understood in intimate connection with that of B matters. The weak interaction is generated from some kind of primordial charge-exchange process between a lepton and B matter. In the $\Delta S = 0$ nonleptonic transitions, amplitudes with $\Delta I = 0$ are much larger than amplitudes with $|\Delta I| = 1$. Even number of W mesons expected to interact strongly; therefore, multiple lepton production should occur in super high energies. An investigation of whether the picture is made similar to that of the proposed model is applicable to other models of elementary particles is made in order to see whether the quartet model is more preferable than the quark model and Bacry-Nuyts-Van Hove model. Even if the latter models are modified along the spirit of Nagoya model, the essential picture of the present model is not applicable to the quark model, and in Bacry-Nuyts-Van Hove model one fails to obtain the $|\Delta I| = \frac{1}{2}$ enhancement. (auth)

39561 ON THE BEHAVIOR OF COMPOSITE PARTICLES. Okabayashi, Takao; Yamada, Masao (Tokyo Univ.). Progr. Theoret. Phys. (Kyoto), 33: 705-25(Apr. 1965).

A method to define the Green function of a composite particle and its vertex function for the effective coupling with its constituent particles is proposed, and applied to Zachariasen's soluble model. The eigenvalue equation introduces a cutoff mass, and suppresses the high energy behavior of various quantities. The results are compared with the dispersion-theoretical approach, and the position in bound state problems occupied by the S-matrix theory is discussed from the standpoint of Green's function. The dispersion-theoretical calculation of the propagator of bound state seems to be meaningless, but the results are as follows: For the model the Z factor of the bound state vanishes only in the sense ∞^{-1}, if the cutoff mentioned above is not taken into account, and such a property is not essential to bound state problems. Further, the self-energy of the state is infinite. The problem of elementarity also is discussed from a formal point of view. (auth)

39562 A POSSIBLE ASSIGNMENT OF LEPTON QUANTUM NUMBERS AND EMPIRICAL LEPTON MASS FORMULA. Katsumori, Hiroshi (Institut Henri Poincare, Paris). Progr. Theoret. Phys. (Kyoto), 33: 755-6 (Apr. 1965).

A possible assignment of lepton quantum numbers is proposed from which an empirical lepton mass formula may be conjectured. The formula is derived. It is noted that whatever the mass splitting interaction may be, this interaction must violate the charge independence. (J.F.P.)

39563 ELECTROMAGNETIC PROPERTIES OF RESONANT STATES. Katsumori, Hiroshi (Kyoto Univ.). Progr. Theoret. Phys. (Kyoto), 33: 757-8(Apr. 1965).

Since the unified electromagnetic form factors supposed to be a generalization of the Nishijima and Gell-Mann formula lead to the same relation on the electromagnetic mass shifts of baryons as in the unitary symmetry scheme, a similar argument is applied to higher spin resonant states. The result is compared with those of the unitary symmetry scheme. (J.F.P.)

39564 SPECULATIONS ON THE MESON-DEUTERON INTERACTION. Minami, Shigeo (Osaka City Univ.). Progr. Theoret. Phys. (Kyoto), 33: 759-60(Apr. 1965).

Since there is a discrepancy between the SU_6 prediction and a phase shift analysis of p-p scattering at 660 Mev, which shows a small D_2 phase shift, in the two-baryon system with Y = 2, it is suggested that the D_{12} should not be regarded as a resonance in the p-p system, but as a resonance in the π-d system. The $\bar{K}$-d, η-d, and K-d interactions are also discussed. (J.F.P.)

39565 HIGHER SYMMETRY SCHEME OF HADRONS Sp(3). Shima, Kazuhisa; Tanabe, Kosai (Tokyo Univ.). Progr. Theoret. Phys. (Kyoto), 33: 760-2(Apr. 1965).

An outline is given of a higher symmetry scheme of hadrons built on the unitary symplectic group of rank three, Sp(3). In this scheme fourteen baryons and fourteen ps mesons are considered, and a third quantum number called superstrangeness is introduced. The subsequent development of the Sp(3)-symmetric theory is described. (J.F.P.)

39566 SU(3) SYMMETRY AND RELATION BETWEEN BARYONS AND LEPTONS. [PART] II. Tanaka, Sho (Univ. of Helsinki and NORDITA, Copenhagen). Progr. Theoret. Phys. (Kyoto), 33: 762-4(Apr. 1965).

The three unitary triplet leptons in a previously proposed baryon-boson model are investigated to discover whether they might be new, thus far unknown leptons. The assumption is made that the basic triplets are different entities from the actual leptons, with considerably heavier mass and extremely short lifetimes. Moderately strong interaction is introduced in addition to the unitary invariant strong interactions in order to explain the rapid decay of the heavier triplet, the large mass difference between meson (μ) and electron, and the breakdown of the SU(3) symmetry in a unified way. The moderately strong interaction is mainly considered; and the qualitative consequences following from it are discussed. (J.F.P.)

39567 NOTE ON THE PRODUCTION OF WEAK BOSON. Hiroshige, Noboru; Matsuda, Masanori (Hiroshima Univ.). Progr. Theoret. Phys. (Kyoto), 33: 764-6 (Apr. 1965).

The possibility of detecting the weak bosons W, having neither baryon nor lepton number, is investigated in some detail. The total cross section for the reaction $\nu_e + e^- \rightarrow W^- + \gamma$ is calculated taking the current of the weak boson field which interacts with the electromagnetic field and neglecting the contribution from the magnetic moment of W^- to this current. The expected number of events in this mode is larger than that of another decay mode because of infrared divergence making the cross section comparable

to that of the other resonance process near the threshold. Also the energy region of the neutrino is wider in the calculated process. (J.F.P.)

39568 REMARKS ON A MODEL OF HADRONS BASED ON THE GROUP Sp(6). Toyoda, Akira; Umemura, Isao (Nagoya Univ., Japan). Progr. Theoret. Phys. (Kyoto), 33: 766-7(Apr. 1965).

Remarks on one of the models of hadrons based on the group Sp(6) are made. The fundamental representation of the group is six dimensional and contains two SU(3) triplets. The physical particles are assumed to be composed of the basic particles. This scheme of hadrons has an attractive feature of predicting the $\omega-\phi$ mixing, but there are too many unwanted particles especially for the assignment of baryons and their resonances. (J.F.P.)

39569 ON THE TRANSVERSE MOMENTUM DISTRIBUTION OF HIGH ENERGY $p + p \rightarrow \pi^+ + d$ REACTION. Hama, Mitsuru; Shimoida, Hiroo (Osaka Univ.). Progr. Theoret. Phys. (Kyoto), 33: 768-9(Apr. 1965).

Since the only possible mechanism which interprets the sharp forward peak of the $p + p \rightarrow \pi^+ + d$ interaction may be a peripheral one where one proton is scattered backward by a meson(π) in the cloud of the other proton to form a deuteron with that neutron, the sharp backward peak of π-N elastic scattering is used for this scattering of a proton with a cloud meson(π) of the other proton. It is seen that the π-N backward scattering seems to explain the experiments at least qualitatively. (J.F.P.)

39570 MODIFICATION OF HAMADA-JOHNSTON POTENTIAL. Hamada, Tetsuo; Nakamura, Yosiaki; Tamagaki, Ryozo (Ibaraki Univ., Mito, Japan and Hokkaido Univ., Sapporo). Progr. Theoret. Phys. (Kyoto), 33: 769-70 (Apr. 1965).

Since the Hamada-Johnston potential (Nucl. Phys., 34: 382(1962), leads to a triplet odd two-nucleon bound state, no such state being known, this potential is modified. It is shown that this modified potential does not destroy the fit to available two-nucleon data considered in the original potential. This is accomplished by calculating the triplet odd scattering phase shifts at several energies below 320 Mev using the modified potential. It is found that the fit is not altered in any significant way; thus it is consistent with available two-nucleon data. (J.F.P.)

39571 SYMMETRY SU(9). Miyazawa, Hironari; Sugawara, Hirotaka (Tokyo Univ.). Progr. Theoret. Phys. (Kyoto), 33: 771-2(Apr. 1965).

The symmetry group for strongly interacting particles is generalized and extended to include both baryons and mesons in a supermultiplet. Although there is a difference in statistics and the use of anticommutators and commutators seems dissimilar such that they can in no way be regarded as like particles, nevertheless, both kinds of particles obey Boltzman statistics in a low-density limit. This shows that fermions and bosons do behave similarly in some limiting case. A system of identical particles is considered in a case where the spin-spin interaction is very large compared with the spin-orbit coupling. The LS coupling scheme works in this case, considering only spin variables where both symmetric and antisymmetric states are allowed. (J.F.P.)

39572 PRODUCTION OF N_{11} RESONANCE AND PROPERTIES OF THE NEUTRAL VECTOR MESONS. Ebata, Takeshi (Tokyo Univ.). Progr. Theoret. Phys. (Kyoto), 33: 773-4(Apr. 1965).

Since neutral vector mesons (ω and ϕ) are usually thought to be coupled to some conserved current and are frequently discussed in connection with conservation of hypercharge and baryon number, the suggestion is made that the study of the $I = \frac{1}{2}$, $J = \frac{1}{2}$ πN resonance may be suitable for an experimental check of these properties of the neutral vector mesons. Experimental evidence shows that the vertex of this resonance is predominantly coupled to neutral vector mesons (ω and/or ϕ). This is valid because one-particle exchange is already verified. From the analysis of meson(π) decay distribution of this excited resonance the coupling form of neutral vector meson is inferred. (J.F.P.)

39573 ON THE UNIFICATION OF HADRONIC AND LEPTONIC WEAK INTERACTIONS. Hori, Shoichi; Chiba, Shin; Tati, Takao; Wakasa, Akira (Kanazawa Univ., Japan). Progr. Theoret. Phys. (Kyoto), 33: 776-7(Apr. 1965).

The $\Delta I = \frac{1}{2}$ was experimentally proven valid for hadronic decays. But also the Cabibbo interaction (N. Cabibbo, Phys. Rev. Letters 10: 531(1963)) seems to explain leptonic and semi-leptonic interactions quite well. A proposal to unify these interactions is made. For this purpose a form of the weak hamiltonian is used. It is found that the strangeness-changing hadronic interaction transforms as $K_0 + \bar{K}_0$ and satisfies $\Delta I = \frac{1}{2}$ rule. The interaction is also considered when mediated by intermediate vector bosons. (J.F.P.)

39574 SOME ASPECTS OF FINAL-STATE INTERACTION STUDIES AT HIGH ENERGIES. Selove, W. (Univ. of Pennsylvania, Philadelphia). Rev. Mod. Phys., 37: 460-72(July 1965).

A review is presented of some aspects and applications of the energy-plot method and the momentum-transfer analysis used in the study of resonant states in high-energy physics with attention given to the connection with, and the possible applicability to, problems in low-energy physics. A detailed discussion is presented on the $\pi + N \rightarrow \pi + \pi + N$ interaction and on meson (ρ) production, using the one-pion exchange (OPE) analysis. Examples of other final-state interactions are also considered. (L.B.S.)

39575 PROBLEMS IN THE ANALYSES OF FINAL-STATE RESONANCES. Adair, Robert K. (Yale Univ., New Haven and Brookhaven National Lab., Upton, N. Y.). Rev. Mod. Phys., 37: 473-84(July 1965).

The parallel between the view on strong interactions and elementary particles and Wigner's view on nuclear forces and light nuclei is shown in a brief review on elementary particle theory. Detailed considerations are given to the Lorentz-invariant phase space, the meaning of phase space and the character of the distortions which are anticipated as a consequence of effects other than specific interactions between the particles which make up the final state. Kinematic effects and dynamic distortion of final-state resonances are discussed. (L.B.S.)

39576 PERIPHERAL PRODUCTION AND DECAY CORRELATIONS OF RESONANCES. Jackson, J. D. (Univ. of Illinois, Urbana). Rev. Mod. Phys., 37: 484-500(July 1965).

Quasi-two-body channels in multiparticle final states are considered. The peripheral nature of the production process and the one-meson-exchange model, decay correlations, absorptive effects as a source of collimation, and the peripheral model with absorption are treated. Examples of $\pi N(\pi)\rho N$, $\pi^+ p(\pi)\rho N^{*}$, $K^+ p(\pi$ and $V)K^{*+}p$, and KN (π and V) K*N interactions are discussed, and calculations of the differential cross sections based on one-pion exchange and the mixture of pion and vector exchange are presented. It is concluded that the peripheral model including absorptive effects gives a remarkably good description of many quasi-two-body reactions involving the production of one or two unstable resonances in the range of a few Bev. (L.B.S.)

39577 SOME WORK ON THE THEORETICAL INTERPRETATION OF THE REACTION $D + P \rightarrow P + P + N$. Kim, Y. E.; Kane, J. V. (Bell Telephone Labs., Inc., Murray Hill, N. J.). Rev. Mod. Phys., 37: 519-22(July 1965).

Calculations based on the Frank-Gammel zero-range theory were made of the inelastic scattering differential cross sections of the $d + p \rightarrow p + p + n$ reaction for a number of values of the scattering parameters, and the results were compared with experimental data. The measured and calculated cross sections are shown. (L.B.S.)

39578 PROTON DISINTEGRATION OF THE DEUTERON — A TEST OF THE CHEW-LOW EXTRAPOLA-

TION METHOD. Carlson, Richard F. (Univ. of Minnesota, Minneapolis). Rev. Mod. Phys., 37: 531-2(July 1965).

The $p + d \rightarrow p + p + n$ reaction was studied in an experiment performed to test the Chew-Low extrapolation method. The measurements were carried out using a 40-Mev proton beam focused on a CD_2 target. The ratio of the measured cross section to the theoretical cross section was plotted as a function of the spectator energy E_p; the results supports the validity of the Chew-Low theory. (L.B.S.)

39579 INELASTIC PROTON-DEUTERON SCATTERING AT 135 Mev. Esten, M. J.; Griffith, T. C.; Lush, G. J.; Metheringham, A. J. (London Univ.). Rev. Mod. Phys., 37: 533-6(July 1965).

A general survey is made of inelastic p-d interactions at 135 Mev using a counter-controlled high-pressure Wilson cloud chamber with proton beams from the Harwell synchrotron. Differential cross sections were studied for charged particles, high-energy neutrons, and spectator protons. The results are shown and discussed. (L.B.S.)

39580 A FORM OF BOLTZMANN'S TRANSPORT EQUATION FOR RELATIVISTIC PARTICLES. Lozupone, Vito (Universita, Rome). Ric. Sci. Rend., Sez. A, 7: 683-94(Dec. 1964). (In Italian).

By means of the equations of the theory of relativity for the dynamics of a particle, a form of Boltzmann's transport equation was obtained. It is expressed by means of the distribution function of the momentum with absence of collisions assumed. The invariance of the equation for a Lorentz transformation is also shown. (auth)

39581 ON THE EQUIVALENCE OF TWO DISTRIBUTION FUNCTIONS. Lozupone, Vito (Universita, Rome). Ric. Sci. Rend., Sez. A, 7: 695-708(Dec. 1964). (In Italian)

On considering distribution functions suitable to describe the dynamic behavior of a system of punctiform particles a general relation between the function f, the numerical density in the space of the phases, and the function N, the angular-energetic flux density of the particles, was obtained. Using this relation and a relativistic form of Boltzmann's equation expressed in terms of f, a form of the equation in terms of the N function was obtained. By means of this form of the equation, and in confirmation of the results, the Liouville theorem was derived. (auth)

39582 CONTRIBUTION TO THE RELATIVISTIC STUDY OF THE POLARIZATION OF THE ELECTRON. Gabos, Z.; Simon, Eva. Studia Univ. Babes-Bolyai, Ser. Math.-Phys., 10: 115-29(1965). (In Rumanian).

For the study of the polarization of the free electron, the Dirac bispinors are generally used as base functions. The advantages offered by the use (as base functions) of the Darwin bispinors were studied, and it is shown, in the framework of the Darwin representation, that the magnitudes characterizing the longitudinal and transverse polarization are obtained directly. As an example, the β decay of non-oriented neutrons is studied. (tr-auth)

39583 THE FINE STRUCTURE OF THE EFFECTIVE MASS SPECTRUM. Stan, I.; Weissmann, A. Studia Univ. Babes-Bolyai, Ser. Math.-Phys., 10: 141-5(1965). (In Rumanian).

The fine structure of the effective mass was calculated as a function of the principal quantum number of the plasmon field. If the equation of the effective mass is established for the case of electron-electron interaction with long radius of action, beginning with the rule of collective summation f and using a parabolic periodic potential, the displacement of the ground level (interaction with vacuum), the division of the effective mass spectrum as a function of interaction, and the variation of the absolute value of the effective mass with temperature are obtained. The results obtained are compared with those that V. P. Smirnov found for the one-dimensional case. (tr-auth)

39584 MASS FORMULAS IN SCHWINGER'S MODEL. Malyuta, Y. M. (Inst. of Physics, Academy of Sciences, Ukrainian SSR). Ukr. Fiz. Zh., 10: 229-32(Feb. 1965). (In Ukrainian).

Schwinger's model (Phys. Rev. 135: B816(1964)) revealed that meson, baryons, and isobars may be constructed from two triplets, one of which ($\psi_1\psi_2\psi_3$) has a baryon number equal to unity, while the other ($V_1V_2V_3$) possesses a baryon number equal to 2. On the basis of this model, mass formulas were developed for baryons, mesons, and isobars, resulting in better agreement with experimental data. The meson and baryon nonets were examined with respect to their contributions to the mass operator; and from them and the isobar decuplet, the final mass formulas were derived. (TTT)

39585 THE NEUTRON-DEUTERON DOUBLET SCATTERING LENGTH AND THE THREE-NUCLEON BOUND STATE WITH TENSOR FORCES. Sitenko, A. G.; Kharchenko, V. F. (Inst. of Physics, Academy of Sciences, Ukranian SSR). Yadern. Fiz., 1: 994-1001(June 1965).

The motion of three nucleons is considered, the interaction between which is described by the Yamaguchi potential, taking tensor forces into account. The three-nucleon bound-state problem and the scattering of a zero-energy neutron on a deuteron are reduced to the solution of a system of one-dimensional integral equations. The double neutron-deuteron scattering length, binding energy, and three-nucleon bound-state wave function are determined from a numerical solution of the integral equations. (auth)

39586 INVESTIGATION OF THE ENERGY SPECTRA AND ANGULAR CORRELATIONS OF PARTICLES IN $K_2^0 \rightarrow \pi^\pm + e^\mp + \nu$ DECAY. Kotlyarevskii, D. M.; Mestvirishvili, A. N.; Nyagu, D.; Okonov, E. O.; Petrov, N. I.; Rusakov, V. A.; Chkhaidze, L. V.; Wu, Tsung-fan (Joint Inst. for Nuclear Research, Dubna, USSR and Inst. of Physics, Academy of Sciences, Georgian SSR). Yadern. Fiz., 1: 1035-44(June 1965). (In Russian)

The spectra and angular correlations of particles in the $K_2^0 \rightarrow \pi^\pm + e^\mp + \nu$ decay were investigated, using a Wilson chamber in a magnetic field. It was determined from the statistics of 360 K_{e3}-decays that, in agreement with the universal (V-A) weak interaction theory, the vector variant gives a good description of the experimental data. The g_v form factor depends weakly on the meson (π) energy. The scalar and tensor variants can not be taken as the only variants responsible for the interaction. The possible contribution of these variants to the decay interactions is not more than 10 to 15%. The charge ratio in K_{e3} decay is also given. (auth)

39587 POLARIZATION EFFECTS IN NEUTRINO-ELECTRON SCATTERING, TAKING INTO ACCOUNT RADIATION CORRECTIONS. Perelomov, A. M. (Inst. of Theoretical and Experimental Physics, Moscow). Yadern. Fiz., 1: 1045-9(June 1965). (In Russian)

Radiation corrections of the order α to the scattering of neutrinos on polarized electrons and corrections to the recoil electron polarization are calculated in the Feynman-Gell-Mann weak interaction scheme without an intermediary meson (W). If the differential cross section for the scattering of neutrinos on polarized electrons or the recoil electron polarization is measured with sufficient accuracy, information can be obtained on the neutrino electromagnetic form factor. (auth)

39588 STRANGE CURRENT VECTOR CONSTANTS IN THE SECOND APPROXIMATION WITH RESPECT TO THE MODERATELY STRONG INTERACTION. Zakharov, V. I.; Kobzarev, I. Yu. (Inst. of Theoretical and Experimental Physics, Moscow). Yadern. Fiz., 1: 1050-2(June 1965). (In Russian)

It is shown that the vector constants for hyperon beta decay are renormalized in the second approximation with respect to the SU_3-symmetry-breaking interaction L_{MS}. A relation between the constants valid in the second approximation with respect to L_{MS} is obtained. (auth)

39589 K_{l4} DECAY AND SU(3) SYMMETRY. Zakharov, V. I. (Inst. of Theoretical and Experimental Physics, Moscow). Yadern. Fiz., 1: 1053-5(June 1965). (In Russian)

A relation between vector interaction constants in K_{l4} and

$\eta \rightarrow \pi^+\pi^-\gamma$ decays is found in the limit of complete SU(3) symmetry. The relation obtained and available experimental data make it possible to estimate the vector interaction contribution to observable effects in K_{e4} decay. The estimation leads to a considerable right-left asymmetry in the positron emission. (auth)

39590 ON A POSSIBILITY OF DETERMINING NUCLEON FORM FACTORS FOR TIME-LIKE MOMENTUM TRANSFERS. Rekalo, M. P. (Inst. of Physics and Tech., Academy of Sciences, Ukrainian SSR). Yadern. Fiz., 1: 1066-70(June 1965). (In Russian).

A method of determining electromagnetic nucleon form factors for time-like momentum transfers from the study of the $\pi^- + p \rightarrow n + e^+ + e^-$ process is discussed. This process is very suitable for a study of form factors in the region $0 \leq -k^2 \leq 4M^2$, which is unphysical for (e^+e^-) or $(\bar{p}p)$ colliding beam experiments. (auth)

39591 INVESTIGATION OF FOUR-PRONG STARS IN π^-p INTERACTIONS AT 3.5 GeV/c PRIMARY MOMENTA. Ainutdinov, M. S.; Vasil'eva, N. V.; Zombkovskii, S. M.; Selector, Ya. M.; Shulyachenko, V. N. Yadern. Fiz., 1: 1071-8(June 1965). (In Russian)

Four-prong stars produced by mesons (π^-) with a momentum of 3.5 Bev/c in liquid hydrogen were investigated. A liquid hydrogen bubble chamber with a diameter of 25 cm in a 14 kgauss magnetic field was installed on the meson (π) beam of the ITEP synchrophasotron. The momentum of the mesons (π^-) in the primary beam, determined by weighing the meson (π^-) trajectory by the "floating wire with current" method, proved to be equal to 3.5 ± 0.13 Bev/c. Some ~80000 stereophotographs were obtained with the average load ~15 mesons (π^-) to expand the chamber. The photographs were scanned twice. Events occuring in the considered volume with meson (π) tracks longer than 3 cm were measured on the ITEP automatic measuring device. The spatial distribution was reproduced, and the kinematical analysis was performed on an electronic computer according to a special program. (auth)

39592 KN SCATTERING AT LOW ENERGIES. Lyul'ka, V. A.; Startsev, A. A. (All-Union Research Inst. of Nuclear Geophysics and Geochemistry). Yadern. Fiz., 1: 1093-1100(June 1965). (In Russian)

A model for K-N scattering at low energies is considered, in which the long-range forces are determined by the exchange of ω and ρ mesons, and the short-range forces are described phenomenologically with the help of two parameters uniquely connected with the scattering lengths. It is shown, that if $g_{\omega KK}g_{\omega NN}/4\pi = -9 \pm 1$ and $g_{\rho KK}g_{\rho NN}/4\pi = 2.5 \pm 0.5$, the model is in good agreement with the experimental values of the s- and $p_{\frac{1}{2}}$-wave phases in both isotopic states. Various problems in which the results of this investigation can be applied are briefly discussed. (auth)

39593 ON AN APPLICABILITY OF THE ISOBAR MODEL FOR THE Λ HYPERON PRODUCTION IN π^--p INTERACTIONS. Visknevskii, V. F.; Tu, Yuan-Tsai; Moroz, V. I.; Nikitin, A. V.; Troyan, Yu. A.; Chiung, Chiang Shao; Chang, Wan-Yu; Shakhbazyan, B. A.; Yang, Wu-Kuang (Joint Inst. for Nuclear Research, Dubna, USSR). Yadern. Fiz., 1: 1101-5(June 1965). (In Russian)

The experimental data on the production of hyperons (Λ) by mesons (π^-) with momenta of 10 and 16 Bev/c on protons were analyzed by a previously described method which is based on the assumption that hyperons (Λ) are generated in two-body reactions of the type $\pi^- + p \rightarrow A + B$, where A may be either a hyperon (Λ) or one of the well-known isobars which yields by decay a hyperon (Λ). The results of this analysis are in satisfactory agreement with the experiment. (auth)

39594 THE STRUCTURE OF G_2 MULTIPLETS. Mandel'tsveig, V. B. (Inst. of Theoretical and Experimental Physics, Moscow). Yadern. Fiz., 1: 1106-12(June 1965). (In Russian)

The irreducible representations of the algebra G_2 are reduced to the representations of the subalgebras D_2 and A_2 by a method suggested in a previous paper. The results of the calculations are shown on diagrams. (auth)

39595 CROSSING SYMMETRY AND SPIRAL AMPLITUDE THEORY. Surkov, E. L. Yadern. Fiz., 1: 1113-20(June 1965). (In Russian)

It is shown that the geometrical crossing-transformation method, suggested by Smorodinsky, gives the correct results. Crossing transformations for the Compton effect, π-N scattering, and N-N scattering are considered as illustrations. (auth)

39596 A MODEL OF THE THREE-PARTICLE UNITARITY CONDITION FOR COMPLEX MOMENTA. Azimov, Ya. I.; Gribov, V. N.; Danilov, G. S.; Dyatlov, I. T. (Ioffe Inst. of Physics and Tech., Leningrad). Yadern. Fiz., 1: 1121-6(June 1965). (In Russian)

A continuation of three-particle amplitudes to complex momenta is constructed on the basis of the non-relativistic Skornyakov–Ter-Martirosyan equation describing the contact pair-interaction of three identical particles. The exact three-particle unitarity condition is written for such a model. For arbitrary J, this condition contains additional terms in which the integration is performed with respect to unphysical values of the pair energies. (auth)

39597 MEASUREMENTS OF THE CROSS-SECTIONS FOR THE PHOTOPRODUCTION OF POSITIVE PIONS ON HYDROGEN IN THE REGION OF THE FIRST RESONANCE. Freytag, D.; Schwille, W. J.; Wedemeyer, R. J. Z. Physik, 186: 1-22(1965).

The differential cross sections for meson(π^+) photoproduction on protons at 200 to 430 Mev were determined for several angles from 20 to 160° in the laboratory system. The total cross sections were also determined. The results were compared with other experimental values and with theoretical predictions. (D.C.W.)

39598 RELATIVISTIC POTENTIAL SCATTERING. Mueller, Harald J. W. Z. Physik, 186: 79-84(1965).

Relativistic potential scattering by a superposition of Yukawa potentials is considered. In particular, high-energy asymptotic expansions are obtained for the wave functions and the Regge trajectories. Finally, the behavior of the Regge poles is discussed. (auth)

39599 POLARIZATION OF 0.5, 1, AND 2 Mev ELECTRON PRODUCED CERENKOV-RADIATION. Aiginger, Hannes (Atominstitut der Oesterreichische Hochschule, Wien, Ger.). Z. Physik, 186: 277-87(1965). (In German).

The theory of Cherenkov radiation predicts a virtually complete linear polarization of the emitted radiation. In disagreement with this result, measurements have always given a large amount of unpolarized light. With an improved geometry that avoids the influence of light quanta resulting from scattered electrons, it was possible to show that the Cherenkov radiation is almost completely linearly polarized. The contribution of scintillation quanta to the remaining unpolarized light was estimated. (auth)

39600 BOUND STATES IN MANY CHANNEL AND SINGLE CHANNEL CALCULATIONS. Hertel, Peter (Universitet, Heidelberg). Z. Physik, 186: 288-98(1965).

A distinction is made between bound states which can be calculated by a many-channel method and those which can already be obtained parameter free by an inelastic single-channel calculation. Two many-channel models are investigated, and it is shown that in some cases an inelastic single-channel calculation needs additional parameters which are furnished by the many-channel treatment only. The results may have some bearing on the problem whether the nucleon is a bound state. (auth)

39601 POSSIBLE CONSEQUENCES OF THE $K_2^0 \rightarrow \pi^+ + \pi^-$ DECAY (CP VIOLATION AND OTHER INTERPRETATIONS). Cabibbo, N. (CERN, Geneva). pp 256-92 of Symmetries in Elementary Particle Physics. New York, Academic Press, 1965.

A review is given of the main decay modes of neutral K mesons. Some problems connected with previous ex-

periment on the decay of the long-lived component of a K^0 beam into $\pi^+ + \pi^-$, possible theoretical interpretations, and their experimental consequences are discussed. (L.B.S.)

39602 SYMMETRIES IN ELEMENTARY PARTICLE PHYSICS. 1964 International School of Physics Ettore Majorana, a CERN-MPI-NATO Advanced Study Institute. Zichichi, A. (ed.). New York, Academic Press, 1965. 440p. $7.95 (Paperbound); $12.00 (Clothbound).

Nineteen lectures are presented. Separate abstracts were prepared for thirteen; one abstract was prepared for six. (L.B.S.)

For abstracts of individual lectures see: 39601, 39603, 39604, 39605, 39606, 39607, 39608, 39609, 39610, 39611, 39612, 39613, 39614, and 39615.

39603 SYMMETRY PRINCIPLES IN PARTICLE PHYSICS. Kabir, P. (CERN, Geneva). pp 11-48 of Symmetries in Elementary Particle Physics. New York, Academic Press, 1965.

A general introduction to the role played by considerations of invariance in quantum theory is presented, and the extent to which they determine the laws of physics is discussed. Consideration is given to superselection rules, generators of continuous transformations, inhomogeneous euclidean group, Lorentz transformations, inhomogeneous Lorentz group, and the relation to usual spin description. The implications of invariance under discrete symmetry operations, T, C, and P, and the TCP theorem are discussed. The Yang-Mills field is also discussed. (L.B.S.)

39604 ELEMENTS OF SU_3. Berman, S. M. (Stanford Linear Accelerator Center, Calif.). pp 49-110 of Symmetries in Elementary Particle Physics. New York, Academic Press, 1965.

Lectures are presented on the general idea of SU_3 and properties of SU_3 representations, multiplet structure, tensors, mass differences in multiplets, electromagnetism and currents in SU_3, decay widths and cross-section relations. No knowledge of group theory is assumed, and certain general results about semi-simple Lie groups are demonstrated only in the context of SU_3. (L.B.S.)

39605 CONSEQUENCES OF SU_3 SYMMETRY IN WEAK INTERACTIONS. Feynman, R. P. (California Inst. of Tech., Pasadena). pp 111-74 of Symmetries in Elementary Particle Physics. New York, Academic Press, 1965.

Lectures are presented on the relation of SU_3 and the weak interactions, which include general features of weak interactions, strangeness changing weak decays, principles of SU_3 symmetry, meson and baryon couplings, generalization of the Goldberger-Treiman relation, and the $\Delta I = \frac{1}{2}$ rule for strangeness changing non-leptonic decays. (L.B.S.)

39606 VECTOR AND AXIAL CURRENTS UNDER FIRST ORDER SYMMETRY BREAKING. Gatto, R. (Universita, Florence). pp 175-91 of Symmetries in Elementary Particle Physics. New York, Academic Press, 1965.

The weak and electromagnetic currents are discussed in the eightfold way with first order symmetry breaking. It is shown that to the first order in the symmetry-breaking interaction all the vector coupling constants are not renormalized, assuming that the vector currents and the electromagnetic current belong to the same unitary octet, and that the breaking of unitary symmetry is due to a term behaving like the eighth component of an octet. (L.B.S.)

39607 FRACTIONALLY CHARGED PARTICLES AND SU_6. Zweig, G. (California Inst. of Tech., Pasadena). pp 192-34 of Symmetries in Elementary Particle Physics. New York, Academic Press, 1965.

It is assumed that the strongly interacting particles are composites of a few fundamental units. The Sakata model is considered in which the strongly interacting particles can be constructed for the three baryon units p_0, n_0, and Λ_0, with charges $\frac{2}{3}$, $-\frac{1}{3}$, and $-\frac{1}{3}$, respectively. The ace model is treated in which the group of unitary unimodular (SU_3) transformations and their effects on the aces or combination of aces are considered. Representations in SU_6 symmetry are also considered. (L.B.S.)

39608 SU_4. Tarjanne, P. (Univ. of Helsinki). pp 235-43 of Symmetries in Elementary Particle Physics. New York, Academic Press, 1965.

The properties of SU_4 are investigated in order to explain the multitude of mass spectrum fine structure of known and suggested boson resonances. The representations of SU_4 and their particle assignments are presented. The problem of non-degeneracy of the particles belonging to the same multiplet is considered. Cabibbo's theory of weak interactions is generalized by requiring that the weak currents transform like components of the adjoint (15-dimensional) representation of SU_4. (L.B.S.)

39609 SOME PROPERTIES OF THE SU_n REPRESENTATION. Biedenharn, L. C. (CERN, Geneva). pp 244-55 of Symmetries in Elementary Particle Physics. New York, Academic Press, 1965.

The methods of Weyl, Schwinger, and Gelfand are discussed descriptively to illustrate the common structure of the SU_n representations in terms of diagrams. The idea of triality for SU_3 is discussed from this point of view as an example. (auth)

39610 METHODS FOR ASSIGNING SPIN AND PARITY TO BARYON RESONANCES. Ashkin, J. (Carnegie Inst. of Tech., Pittsburgh). pp 293-310 of Symmetries in Elementary Particle Physics. New York, Academic Press, 1965.

The method of Byers and Fenster for determining the spin and parity of baryon resonances is discussed. An idealized form of the two-body decay, $Y^* \rightarrow Y + \text{meson}$, is considered. The decay from a statistical mixture of spin states and density matrices for Y^* and Y, intensity distribution, angular distribution of the polarization of Y, Lorentz frames in which to measure the decay of Y^* and Y, and restrictions on the tensor polarizations of the Y^* are discussed. (L.B.S.)

39611 GENERAL REVIEW OF NEUTRINO PHYSICS. Bernardini, G. (Universita, Rome). pp 311-40 of Symmetries in Elementary Particle Physics. New York, Academic Press, 1965.

Experiments on interactions of high-energy neutrinos are reviewed. Results of bubble and spark chamber experiments on elastic and inelastic events, the production of lepton pairs, and the intermediate vector boson W are discussed. (L.B.S.)

39612 FUTURE EXPERIMENTS IN NEUTRINO PHYSICS. Block, M. M. (Northwestern Univ., Evanston, Ill.). pp 341-59 of Symmetries in Elementary Particle Physics. New York, Academic Press, 1965.

The future experiments planned by the CERN neutrino bubble chamber group are briefly summarized, and possible new spark chamber experiments using deuterium targets are described. (L.B.S.)

39613 MEASUREMENT OF THE ANGULAR CORRELATION OF ELECTRONS RELATIVE TO Λ SPIN IN Λ^0-β DECAY. Conforto, G. (CERN, Geneva). pp 360-6 of Symmetries in Elementary Particle Physics. New York, Academic Press, 1965.

The angular correlation of the decay electron relative to the spin direction of polarized Λ^0 particles was measured in order to determine the form of the interaction which is responsible for the Λ-β decay. The Λ^0's beryllium targets according to the reaction $\pi^+ + n \rightarrow K^+ + \Lambda^0$ at an incident pion momentum of 1.0 Bev/c, and an analysis was made of the $\Lambda \rightarrow p + e + \nu$ and $\Lambda \rightarrow p + \pi^-$ events. The results are discussed, and the experimental arrangement is shown. (L.B.S.)

39614 MOMENTUM SPECTRUM OF POSITRONS FROM MUON DECAY. Sherwood, B. A. (Univ. of Chicago). pp 367-9 of Symmetries in Elementary Particle Physics. New York, Academic Press, 1965.

An experiment is in progress to study the decay of the muon $\mu \rightarrow e\nu\bar{\nu}$, using digitized spark chambers to transmit the spatial coordinates of the electron directly to a MANIAC III computer. The aim of the experiment is to measure the parameter ρ (a ratio of coupling constants predicted to be $\frac{3}{4}$ for V-A) to an accuracy of approximately 0.1% and to measure the electron decay asymmetry parameter as a function of momentum. Preliminary analysis of the data yielded $\rho = 0.746 \pm 0.01$. (L.B.S.)

39615 PRESENT STATUS OF STRONG ELECTROMAGNETIC AND WEAK INTERACTIONS. Feynman, R. P. (California Inst. of Tech., Pasadena). pp 400-18 of Symmetries in Elementary Particle Physics. New York, Academic Press, 1965.

A general summary is given of the present status in the areas of fundamental physics: gravitation, electromagnetism, weak interactions, and strong interactions. The conservation laws are reviewed, in which the validity of the principles of special relativity and the superposition of quantum mechanical amplitudes is assumed. The questions pertaining to theories in electrodynamics, strong interactions, and symmetry are examined in more detail, and some fundamental problems are mentioned. The question of dynamics is also discussed. (L.B.S.)

39616 PROCEEDINGS OF THE CONFERENCE ON PHOTON INTERACTIONS IN THE BEV-ENERGY RANGE, JANUARY 26–30, 1963. M.I.T. Report 2. Feld, Bernard T. (ed.). Cambridge, Mass., The M.I.T. Press, 1965. 162p. $5.00.

Fifty-six papers are presented in nine topic sections; separate abstracts were prepared for each section. (L.B.S.)

For abstracts of individual sections see: 39041, 39327, 39617, 39618, 39619, 39620, 39621, 39622, and 39623.

39617 QUANTUM ELECTRODYNAMICS AND ELECTROMAGNETIC FORM FACTORS. pp I.1-10 of Photon Interactions in the Bev-Energy Range. Cambridge, Mass., The M.I.T. Press, 1965.

Remarks and brief discussions are presented on quantum electrodynamics and electromagnetic form factors, which include the relation between theory and experiment, a renormalized theory of spin one electrodynamics, the connection between gauge invariance and mass, the determination of the nucleon form factors by means of the Rosenbluth formula, and the interpretation of nucleon form factors. (L.B.S.)

39618 REGGE POLES I. pp II.1-16 of Photon Interactions in the Bev-Energy Range. Cambridge, Mass., The M.I.T. Press, 1965.

The possible types of behavior of scattering amplitudes are tabulated as a function of complex angular momentum J with corresponding implications for high energy behavior in the crossed channel. Theoretical experiments for examining the type of behavior that may be found in a correct, relativistically invariant theory of elementary particle process containing unitarity, analyticity, crossing symmetry, etc., are given. Two problems are considered: Reggeization of processes like Compton scattering and photoproduction where the photon is external; and analysis of the internal particles. The question of whether some conventional field theories might not exhibit Regge behavior is considered. The results of some recent investigations concerning elementary vector mesons and the high-energy limit of scattering amplitude are discussed. Helicity amplitudes and complex angular momentum in V-A interaction and under γ_5-invariance are also discussed. The possibility of investigation Regge behavior in a renormalizable field theory form the Lie equations of the renormalization group is considered. (L.B.S.)

39619 REGGE POLES II. pp III.1-7 of Photon Interactions in the Bev-Energy Range. Cambridge, Mass., The M.I.T. Press, 1965.

The results are presented of an experiment in which the elastic differential cross sections for p-p and π^--p scattering were measured at 7 to 20 Bev/c. Differential scattering curves are shown, and the data were found to be inconsistent with simple Regge pole theory. Experimental data on elastic electron-proton scattering are presented and compared with predictions of the Rosenbluth formula which assumes that the photon is a spin 1 fundamental particle and that only one photon is exchanged. (L.B.S.)

39620 PHOTOPRODUCTION, EXPERIMENTAL. pp IV.1-21 of Photon Interactions in the Bev-Energy Range. Cambridge, Mass., The M.I.T. Press, 1965.

Photoproduction experiments were performed and results are reported on: cross sections and angular distributions for the $\gamma_v + p \rightarrow \pi^+ + n$, and $\gamma + p \rightarrow \pi^0 + p$ interactions; cross sections σ_η for $\gamma + p \rightarrow \eta + p$ and branching ratio of $\eta \rightarrow \gamma + \gamma$ decay mode relative to other neutral decay modes; K^+ production cross sections and Λ_0 polarization in the $\gamma + p \rightarrow K^+ + \Lambda^0$ and $\gamma + p \rightarrow K^+ + \Sigma^0$ interactions; decay rate determination by Coulomb production for $A \rightarrow B + \gamma$ processes; and neutral pion photoproduction and Primakoff effect experiments. (L.B.S.)

39621 PHOTOPRODUCTION, THEORY. pp V.1-14 of Photon Interactions in the Bev-Energy Range. Cambridge, Mass., The M.I.T. Press, 1965.

The photoproduction of vector mesons, heavy intermediate bosons $W^{\pm}$, photoproduction of pions and pion-nucleon scattering, and electropion production are discussed. (L.B.S.)

39622 NEW EXPERIMENTAL APPROACHES. pp VI.1-20 of Photon Interactions in the Bev-Energy Range. Cambridge, Mass., The M.I.T. Press, 1965.

Various experimental arrangements of the diamond crystal radiator for coherent bremsstrahlung are discussed. Diagrams are presented of polarizations and intensities in the bremsstrahlung spectra for 6 Bev electrons. A method is proposed for measuring the linear polarization of photons in the many-Bev region. A calculation of monochromatic bremsstrahlung from thin crystals is reported. A scheme for producing polarized photon beams, and sources of polarized electrons are discussed. Experiments on the Frascati storage ring and the Stanford colliding beam experiment are also briefly discussed. (L.B.S.)

39623 EXPERIMENTS IN PROGRESS AT CEA. pp VIII.1-19 of Photon Interactions in the Bev-Energy Range. Cambridge, Mass., The M.I.T. Press, 1965.

Experiments on electromagnetic pair production, electron scattering, and photoproduction of mesons are reported. A description is given of a 40 in. liquid hydrogen bubble chamber used in photoproduction experiments with the M.I.T. synchrotron. Other experiments are briefly mentioned. (L.B.S.)

Field Theory and Quantum Mechanics

Refer also to abstracts 39554 and 39618.

39624 (AROD-223:60) THE COMPLEX SPACE-TIME MODEL. I. COMPLEX SPACE-TIME AND CLASSICAL FIELD THEORY. II. THE QUANTIZED COMPLEX SPACE-TIME AND QUANTUM THEORY OF FREE FIELDS. III. COMPLEX SPACE-TIME AND GEOMETRIZATION OF ELECTROMAGNETISM. Das, A. (Carnegie Inst. of Tech., Pittsburgh, Pa. Dept. of Mathematics). Apr. 1965. 60p.

Classical fields are discussed in complex space-time with a view of subsequent generalization to quantum field theory in quantized space-time. A covariant quantization of complex space-time is proposed. The general theory of quantized free fields is developed in the background of quantized space-time. It is shown that if one demands the covariance under general circular transformations, the electromagnetic potentials can be geometrized as the affine connections necessary for such covariance. (M.O.W.)

39625 (CONF-796(Paper 12)) GRAVITATION AND QUANTUM MECHANICS OF MACROSCOPIC OBJECTS. Karolyhazy, Frederick (North Carolina Univ., Chapel Hill). 19p.

Macroscopic inconsistencies of the space-time manifold appear in the theory of measurement in quantum mechanics and in the reconciliation of quantum mechanics with general relativity. The concept of "smearing" of space-time is introduced, in order to make consistent the relation between macroscopic bodies and macroscopic space-time. (T.F.H.)

39626 (CONF-796(Paper 22)) REPRESENTATION OF DISCRETE SYMMETRY OPERATORS. Mariwalla, K. H. (South Carolina Univ., Columbia and Georgia Univ., Athens). 32p.

Representations of discrete symmetry operators connected with space, time and generalized charge are considered. The following cases are discussed: non-relativistic quantum mechanics; quantum theory of free fields (Klein Gordon and Dirac fields) in terms of field operators rather than positive and negative frequency parts; and direct algebraic relations between the "generators" and the appropriate observables (this algebra is found to be isomorphic to the Lie algebra of generators of rotation in an n-dimensional Euclidean space). (auth)

39627 (CONF-796(Paper 26)) ON THE EXISTENCE OF SOLUTIONS TO THE FIELD EQUATIONS. Taylor, J. G. (Rutgers—The State Univ. of New Jersey, New Brunswick). 9p.

The field equations arising from local Lagrangians for quantized fields are considered, for the case in which the interactions are finite polynomials in the fields. The path to be followed in order to prove existence and uniqueness of solutions of these field equations is outlined. (T.F.H.)

39628 (CONF-796(Paper 29)) AXIOMATIC FIELD THEORY. Wightman, A. S. (Princeton Univ., N. J.). 13p.

It is noted that explicit solubility of a two-dimensional field theory depends on several necessary conditions: that the equivalence or Borchers class of a free field in two dimensions contains a particular set of polynomials; that there exists no zero-mass scalar field in two dimensional space-time; that there exists a free zero-mass two-component "spinor" field in two-dimensional space-time; and that the divergence of a vector field in two-dimensional space-time is equal to the curl of a suitably defined dual vector. These results and others in axiomatic field theory are summarized. (T.F.H.)

39629 (CONF-796(Paper 30)) ON THE PROOF OF THE LSZ ASYMPTOTIC CONDITION. Hepp, Klaus (Institute for Advanced Study, Princeton, N. J.). 10p.

The asymptotic condition in relativistic quantum field theory describes the connection of the dynamical quantities (the interacting fields) with the asymptotic states and fields necessary for the computation of physical observables. The LSZ asymptotic conditions, which are postulated in a general framework without the introduction of equations of motion, are proved for a neutral scalar field, and the extension of the results to more general cases is discussed. (T.F.H.)

39630 (CONF-796(Paper 31)) FOLDY-WOUTHUYSEN TRANSFORMATION IN COVARIANT SPINOR FORMULATION. Jehle, Herbert; Parke, William C. (George Washington Univ., Washington, D. C.). 6p.

The Foldy-Wouthuysen transformation, which splits the four-component Dirac equation for the free particle into a pair of two-component equations, is related to a pair of Lorentz transformations. The characteristics of the transformation are studied in a covariant spinor formalism that shows the Lorentz covariance of the Dirac equation and that clarifies the relation between the two-component and four-component spinors. (T.F.H.)

39631 (IS–1111) THE RANDOM PHASE APPROXIMATION IN THE MANY BOSON PROBLEM. Etters, R. D. (Ames Lab., Iowa State Univ. of Science and Tech.). [1964]. Contract AT(11-1)-72. 16p. (CONF-758-26). Dep. mn; $1.00 cy, $0.50 mn; Gmelin, AED-CONF-65-003-64.

From American Physical Society Meeting, New York, Jan. 1965.

The equation of motion method is used to determine the excitation spectrum of a many-boson system. It is found that the equation of motion for the operator $\mu_k^+ = \Sigma_p \alpha(p,k) A_{p+k}^+ A_p$, when linearized by the RPA, yields an approximate excitation spectrum of the same form as found by Bogoliubov. $\alpha(p,k)$ is a c-number coefficient. However, the result requires no a priori assumption concerning the population of a single, low-lying, momentum state. In general, the excitation operator μ_k^+ is shown to be of the form used by Feynman and Cohen in their work on He(II), while at low momenta it reduces to the density fluctuation operator. Furthermore, in the weak coupling limit, μ_k^+ is identical to that of Bogoliubov. A relation between the excitation spectrum derived by Feynman and that found here is established. The liquid structure factor is then calculated and is shown to yield the standard result at low momenta. The f-sum rule is also derived. (auth)

39632 THE CLASSICAL MOTION OF PARTICLES IN ARBITRARY TENSOR FIELDS. Ionescu Pallas, N. J. Acad. Rep. Populare Romine, Studii Cercetari Fiz., 15: 133-40(1964).

The vector field of electromagnetic interaction was studied from an experimental point of view. Other types of fields corresponding to other representations of the Lorentz group are only proposed for the purpose of describing mesonic and gravitational phenomena. These fields were constructed on a basis of pure analogy, the model being represented by the equations of electrodynamics. Some physicists attempted to reconsider the problem of gravity in the Minkovski space, in order to avoid mathematical difficulties arising from the curvature of space. The impossibility of the existence of a linear theory in the Minkovski space is demonstrated. The Lorentz invariant linear approximation of the gravity theory does not give a correct value for the advance of the perihelion of planets. Likewise, the linear theory of Birkhoff and Vallarta does not result from a principle of stationary actions and, therefore, cannot be considered within the framework of physical theories. The non-linear theories are not dealt with, as they are less important due to the arbitrariness prevailing in the choice of non-linearities as well as to the great difficulties arising from the quantization of the corresponding fields. (Rumanian Sci. Abstr., Nat. Sci., Vol. I, No. 7, 1964).

39633 NOTES ON THE QUANTUM-MECHANICAL DISCUSSION OF THE GIBBS PARADOX. Fay, Gy. (Polytechnical Univ., Budapest). Acta Phys. Acad. Sci. Hung., 18: 273-83(1965).

Starting from the deductive development of quantum theory as worked out by Neumann and making use of the quantum-theoretical propositional calculus, it is shown that the quantum theoretical entropy of any physical property increases if the property is replaced by a logically weaker one. (auth)

39634 ISOMAGNETIC INTERACTIONS OF YANG-MILLS FIELD. Tybor, Vatslav (Univ. of Lodz, Poland). Acta Phys. Polon., 27: 693-8(1965). (In Russian)

The minimum interaction of spinor and vector fields with fixed spin is examined in the nonrelativistic limit. A generalization of the Pauli-type interaction is found, and it is shown that the isotopic gyromagnetic ratio is a vector in isospace. (tr-auth)

39635 MAGNETIC-MOMENT-TYPE INTERACTIONS OF FIELDS WITH SPIN 1. Tybor, Vatslav (Univ. of Lodz, Poland). Acta Phys. Polon., 27: 699-711(1965). (In Russian)

The interactions of scalar, spinor, and vector fields with fixed spin are studied, taking into account the dimensionless coupling constants and the constants of dimensionality of length. The generalized group of isotopic representations is obtained. Examples are given for the case when the in-

clusion of the constants of dimensionality of length does not disturb the isotopic properties of the theory with dimensionless coupling constants. (tr-auth)

39636 ASYMPTOTIC PROPERTIES OF THE ELECTROMAGNETIC AND GRAVITATIONAL FIELDS. Kozarzewski, B. (Higher Pedagogical School, Katowice, Poland. Acta Phys. Polon., 27: 775-81(1965).

The Newman-Penrose method is used to investigate the asymptotic properties of the electromagnetic and gravitational fields. A generalization of the Goldberg-Sachs theorem is proved. (auth)

39637 NEW APPROACH TO SPECIAL RELATIVITY. Weinstock, Robert (Oberlin Coll., Ohio). Am. J. Phys., 33: 640-5(Aug. 1965).

A development of the theory of special relativity is based on a principle of relativity for inertial frames as applied to mechanical phenomena only. The Lorentz-transformation equations and the familiar mass-variation formula are deduced from the observation that mass does vary with speed; but in these the speed of light c is everywhere replaced by a universal speed k—namely, the speed at which the mass of any particle must become infinite—which arises as a consequence of the assumptions. The experimental result that the free-space speed of light with respect to the earth is equal to k then implies the same free-space speed of light with respect to every inertial frame—the usual starting point of the theory. (auth)

39638 EQUATIONS OF THE LEE MODEL IN THE $V\theta \rightleftharpoons N\theta\theta$ SECTOR. Houard, Jean-Claude (College de France, Paris). Ann. Inst. Henri Poincare, 2: 105-30(1965). (In French).

A linear integral equation associated with the $V\theta \rightleftharpoons N\theta\theta$ sector of the Lee model is solved. The eigenstates of this sector are then derived as well as the scattering amplitudes for some particles outside their mass shell. (tr-auth)

39639 DIRAC FIELD, NEUTRINO FIELD, AND C, P, T TRANSFORMATIONS ON A SPACE-TIME CURVE. Lichnerowicz, Andre (College de France, Paris). Ann. Inst. Henri Poincare, Sect. A, 1: 233-90(1964). (In French).

A theory of neutrinos on a space-time curve is developed, and within the framework thus created a theory of the C, P, T transformations is worked out. Spinors on a space-time curve provided with two orientations are first considered. The concept of structured space of spinor reference marks plays the principal role, and the spinors considered are always 4-component spinors. Real Dirac matrices were adopted systematically. The general theory of the Dirac field is then considered, and it is shown how the classical theory of the flat case is extended without difficulty to any space-time curve. It is then easy to develop the theory of the neutrino field considered as a Dirac field without a mass term. After decomposition of the corresponding ψ spinor into positive and negative spinors, it is possible to deduce from the theory the rigorous anticommutators of the fields ψ_+ and ψ_- and to study the principal properties observable. The C, P, or T invariances of the different physical field theories are studied within the framework adopted. This framework and the corresponding formulism make almost trivial the study of invariances. (J.S.R.)

39640 THE COEXISTENCE OF PHOTONS AND WAVES IN THE ELECTROMAGNETIC RADIATIONS AND THE THEORY OF THE DOUBLE SOLUTION. de Broglie, Louis. Energie Nucl., 7: 135-40(May 1965). (In French).

An explanation is given of the usefulness of the wave concept of radiation in its electromagnetic state in spite of the existence of photons by the double solution theory in interpretation of wave mechanics. A summary of the theory of the double solution is given. Emphasis is placed on photon waves being classical electromagnetic waves of very weak amplitude, hertzian waves, lasers, stationary states, and states preceding atomic transition. The theory of the double solution which represents photons as very small regions of very high wave amplitude attached to a very weak electromagnetic wave may be the only solution to the difficult problem of photons in the structure of waves. This associated wave of the photon is believed to explain their coherence. (J.F.P.)

39641 WAVE MECHANICAL THREE-PARTICLE MODEL. Bebie, Hans (Universitaet, Bern). Helv. Phys. Acta, 38: 255-61(May 15, 1965). (In German).

Wave functions of three-particle systems were constructed from known two-particle wave functions. Less weight was given to the familiar form of the interaction than to the exact expressions for the wave functions. Three nonrelativistic particles of spin 0 are considered in their center of gravity system. Bound states between the second and third particles were analyzed, but in the consideration of the products of wave matrices no bound states occur. (tr-auth)

39642 NUMERICAL SPECTROSCOPY. Rotenberg, Manuel (Univ. of California, San Diego, La Jolla). J. Chem. Phys., 43: 1657-61(Sept. 1, 1965).

A numerical procedure for solving the time-dependent Schrödinger equation is given. It was found that by observing the power spectrum generated by the time-dependent solution, the set of eigenvalues of the corresponding stationary problem can be determined directly. The procedure involved solving the time-dependent Schrödinger equation, Fourier analyzing the solution, and finally averaging the squared modules of the solution over space. Formulas to accomplish these tasks efficiently are given. (auth)

39643 DECOMPOSITION OF THE LORENTZ TRANSFORMATION MATRIX INTO SKEW-SYMMETRIC TENSORS. Bazanski, Stanislaw L. (Lehigh Univ., Bethlehem, Penna.). J. Math. Phys. (N. Y.), 6: 1201-3(Aug. 1965).

Any matrix describing a finite proper orthochronous Lorentz transformation of the null tetrad in Minkowski space may be written as a polynomial of the second order in skew-symmetric tensors. From a geometrical point of view these tensors describe two-dimensional planes which are mapped by the Lorentz transformation into themselves. (auth)

39644 TRACE FORMALISM OF QUANTUM MECHANICAL EXPECTATION VALUES. Langerholc, John (Univ. of Pittsburgh). J. Math. Phys. (N. Y.), 6: 1210-18(Aug. 1965).

The trace of a positive bounded operator in a Hilbert space is defined and shown to be independent of the basis used in the definition. The trace of the product WA is defined for bounded A and positive bounded W with unit trace and is also shown to be basis-invariant. An integral representation is derived and used to define Tr(WA) for unbounded A. Linearity, isotony, and continuity with respect to uniform covergence are proved for Tr(WA) as a function of (bounded) A. Several formulas used in statistical mechanics are derived, and it is proved that if A and B are commuting positive operators, then $Tr(W(A + B)) = Tr(WA) + Tr(WB)$. A counter example is given which shows that the commonly used definition of Tr(WA) in terms of an orthonormal basis is not invariant under permutation of the basis vectors even in the case of a very simple unbounded operator A. An expectation-value function M which associates the expectation value M(A) to the operator A is assumed given and subject to certain restrictions. For bounded operators, these include positivity, normalization, additivity, and a condition which may be considered as a requirement of regularity for the probability function induced by M. Modifications of these requirements are imposed for unbounded operators, and von Neumann's statistical formula is proved: there is a unique bounded positive operator W with unit trace for which $M(A) = Tr(WA)$. The requirements placed on M are weaker than those of von Neumann, and are in fact satisfied by Tr(WA) as a function of A. (auth)

39645 CAN THE POSITION VARIABLE BE A CANONICAL COORDINATE IN A RELATIVISTIC MANY-PARTICLE THEORY? Kerner, Edward H. (Univ. of Delaware, Newark). J. Math. Phys. (N. Y.), 6: 1218-27(Aug. 1965).

The time-symmetrical interaction of charges (Wheeler–Feynman electrodynamics) is shown in principle to yield second-order Newtonian-type equations of motion under the restriction that the motions be analytic extensions of free-particle motions. The means of explicitly generating the electrodynamic equations of motion describing invariant world-lines are given. These physically relevant equations do not fit into Dirac's (1949) formulation of hamiltonian relativistic particle dynamics, where either world-line invariance is given up, or only trivially straight world lines can be described (zero-interaction theorem of Currie, Jordan, Sudarshan, 1963). The misfit is due to the requirement in Dirac's scheme that position x be canonical. Under the Lie–Königs theorem, however, hamiltonian statements of dynamics with invariant world lines remain possible when suitable Q(x,x) are introduced instead of x as canonical position variables. A group of necessary conditions on the structure of any dynamics that permits x to be canonical are worked out to indicate how stringent is this permission in general. (auth)

39646 QUANTUM ELECTRODYNAMICS WITH VANISHING BARE FERMION MASS. Bose, S. K.; Biswas, S. N. (Univ. of Delhi). J. Math. Phys. (N. Y.), 6: 1227-30(Aug. 1965).

Quantum electrodynamics is studied in the approximation suggested by Johnson, Baker, and Willey. The approximate Dyson equation of this model is transformed into a second-order, nonlinear differential equation by the application of a method due to Green. The solutions of this equation are then studied under various simplifying assumptions. (auth)

39647 HOMOGENEOUS SOLUTIONS OF THE EINSTEIN–MAXWELL EQUATIONS. Ozsvath, Istan (Southwest Center for Advanced Studies, Dallas). J. Math. Phys. (N. Y.), 6: 1255-65(Aug. 1965).

The solutions of the Einstein–Maxwell equations are investigated under the assumption that the metric of the space–time and the electromagnetic field are invariant under the transformations of a four-parametric, simply transitive group. In the case of null electromagnetic fields there are two different possibilities; If $\Lambda = 0$, all the solutions are Robinson waves; if $\Lambda \neq 0$, there exists only one solution. There exist no other solutions for null electromagnetic fields. In the case of nonnull electromagnetic fields two solutions are found. One metric is known to have been given by Robinson; a new solution of type I is presented. (auth)

39648 ALL HOMOGENEOUS SOLUTIONS OF EINSTEIN'S FIELD EQUATIONS WITH INCOHERENT MATTER AND ELECTROMAGNETIC RADIATION. Ozsvath, Istvan (Southwest Center for Advanced Studies, Dallas). J. Math. Phys. (N. Y.), 6: 1265-8(Aug. 1965).

The theorem is proved that the Einstein field equations with dust and electromagnetic null field have only two homogeneous solutions. (auth)

39649 PARTICLELIKE SOLUTIONS TO NONLINEAR SCALAR WAVE THEORIES. Rosen, Gerald (Southwest Research Inst., San Antonio). J. Math. Phys. (N. Y.), 6: 1269-72(Aug. 1965).

According to a recent theorem proved by Derrick, no absolutely stable time-independent particle-like solution of finite energy is obtainable from a large class of Lorentz-covariant scalar wave theories. A solvable nonlinear scalar wave theory, is studied, and a rigorous metastable particle-like solution of finite energy, a quasistatic solution having a rate of dissolution which is free to be arbitrarily small relative to the associated particle rest mass, is derived. Derrick's theorem notwithstanding, the specific example presented suggests that particle-like quasistatic solutions to a nonlinear scalar wave theory may still be of some relevance to meson field physics, where no absolutely stable but instead metastable elementary particles are present. (auth)

39650 STUDIES IN PERTURBATION THEORY. IX. CONNECTION BETWEEN VARIOUS APPROACHES IN THE RECENT DEVELOPMENT — EVALUATION OF UPPER BOUNDS TO ENERGY EIGENVALUES IN SCHROEDINGER'S PERTURBATION THEORY. Loewdin, Per-Olov (Univ. of Florida, Gainesville and Uppsala Univ., Sweden). J. Math. Phys. (N. Y.), 6: 1341-53(Aug. 1965).

The treatment of Schroedinger's perturbation theory based on the use of a series of inhomogeneous differential equations of iterative character is briefly surveyed. As an illustration, the method is used to derive the general expression for the expectation value of the hamiltonian to any order which provides an upper bound for the ground-state energy. It is indicated how the well-known theory for inhomogeneous equations may be utilized also in this special case. The solution of the Schroedinger equation by means of the partitioning technique and the concept of reduced resolvents is then treated. It is shown that the expressions obtained are most conveniently interpreted in terms of inhomogeneous differential equations. A study of the connection with the first approach reveals that the two methods are essentially equivalent, but also that the use of reduced resolvents and inverse operators may give an alternative insight into the mathematical structure of perturbation theory, particularly with respect to the bracketing theorem and the use of power series expansions with a remainder. It is emphasized that the combined use of the two methods provides a simpler and more powerful tool than any one of them taken separately. (auth)

39651 PSEUDOPOTENTIALS FOR A HARD SPHERE GAS. Bocchieri, P.; Campagnoli, G. (Universita di Pavia, Italy) and I.N.F.N. Gruppo di Pavia). Nucl. Phys., 71: 426-32(1965).

An explicit form for the N-hard-sphere pseudopotential is given. A detailed discussion is made in the case of N = 3 but the arguments given can be easily extended to the general case. For N = 2 one finds in a simple and explicit way the results of Luban. (auth)

39652 THE LENGTH SCALE IN QUANTUM ELECTRODYNAMICS WITHOUT A BARE MASS. Maris, Th. A, J.; Herscovitz, V. E.; Jacob, G. (Universidade do Rio Grande do Sul, Porto Alegre, Brazil). Nuovo Cimento (10), 38: 783-95(July 16, 1965).

A definite length scale in quantum electrodynamics without a bare mass can only be induced by a coupling with another system. This problem is studied in a model consisting of one charged "neutrino" field and charged strongly interacting particle fields. A criterion is derived which is similar to the principle of extremalization of the energy in mechanics. The approximation used allows only the conclusion that the ratio between the lepton mass and the strongly interacting particle masses is not of zeroth order in the renormalized electromagnetic coupling constant. (auth)

39653 THE STRUCTURE COEFFICIENTS OF PROPER SELF-ENERGY PARTS FOR SIMPLE MODELS OF QUANTUM FIELD THEORY. Soffer, J.; Visconti, A. (Faculte de Sciences, Marseille). Nuovo Cimento (10), 38: 817-30 (July 16, 1965).

Precise meaning is given to the formal calculations of H. Lehman, K. Symansik, and W. Zimmerman (Nuovo Cimento, 1: 1425(1955)), using formal series. The divergent part of a N-point propagator is expressed by means of the structure coefficients. The two-point propagator is considered; starting from Dyson's equation the proper self-energy part of a self-interacting field is studied. This analysis leads to unrenormalizability criteria. Finally the case of a generalized Lee model is examined which completely explains the calculations. (J.F.P.)

39654 SIGNIFICANCE OF THE AHARONOV-BOHM EFFECT. Liebowitz, B. Nuovo Cimento (10), 38: 932-50(July 16, 1965).

It is shown that in an Aharonov-Bohm experiment: Due to superposition of the electron's magnetic field and the solenoid's interior magnetic field there exists an interaction energy U_m whose gradient represents a force on the electron which has not hitherto been recognized or provided for in the classical formalism. This force is non-

Lorentzian, it does do work, and explains the A.B. phase shift classically. The long-standing action-reaction difficulty involved in the application of the Biot-Savart law to unclosed circuits is eliminated by this new force in this context. The same force ($-\text{grad } U_m$) is implicitly contained in the Schrödinger equation of the A.B. effect. Thus there is no need to modify the concept of force or vector potential as proposed by Aharonov and Bohm. In the Appendix, detailed calculations are outlined showing that currents generated in the solenoid by a passing electron are negligible. (auth)

39655 NONLINEAR QUANTUM FIELD THEORIES AT SMALL DISTANCES. Mitter, H. (Massachusetts Inst. of Tech., Cambridge and Max-Planck-Institut fuer Physik und Astrophysik, Munich). Nuovo Cimento (10), 38: 1040-6(July 16, 1965). (MIT-2098-129).

For scalar, real, nonlinear field theories the compatibility of asymptotic scale invariance at small distances with the field equations and causality is shown for n-point functions involving only one coordinate difference (generalized propagators). No approximation method is necessary, if a certain symmetry property of these functions is assumed. For nonrenormalizable theories the quantization (which is then noncanonical) is not entirely fixed by the field equations and causality. "Tamm-Dancoff"-like approximations are briefly criticized. (auth)

39656 ON THE ENERGY OF THE GRAVITATIONAL FIELD. Horsky, J. (Brno Univ.). Phys. Letters, 17: 268-9(July 15, 1965).

It is shown that the formulation of conservation laws in general relativity proposed by Fock leads to a negative energy of the static gravitational field. (L.B.S.)

39657 DEGENERATE BOSE SYSTEM. V. LINEAR RESPONSE FUNCTION. Mohling, Franz (Univ. of Colorado, Boulder). Phys. Rev., 139: 664-81(Aug. 2, 1965).

A microscopic theory of the linear response function is developed for the degenerate Bose system. Considerable simplification of the calculational prescription is achieved by the use of a tensor notation applied to the two-dimensional space spanned by $i\tau$ and $\beta - i\tau$, where τ is a time variable and $\beta = (\kappa T)^{-1}$. The sharp lines observed experimentally for liquid helium II are shown to occur as δ-function singularities in the theory. Part of the broadening of these lines is also calculated. It is shown that (the inelastic part of) the structure factor $S(q)$ may become large as $q \to 0$ for nonzero temperatures, a property which is due to the divergence of the momentum distribution $\langle n(p) \rangle$ as p^{-2} when $p \to 0$ and $T \neq 0$. Present experiments are consistent with this possibility. The calculations performed suggest that the double-quasiparticle model presented previously most likely results in a single experimental excitation spectrum, as observed for liquid helium II. (auth)

39658 NEW METHOD FOR CALCULATING THE ONE-PARTICLE GREEN'S FUNCTION WITH APPLICATION TO THE ELECTRON-GAS PROBLEM. Hedin, Lars (Argonne National Lab., Ill.). Phys. Rev., 139: 796-823(Aug. 2, 1965).

A set of successively more accurate self-consistent equations for the one-electron Green's function is derived. They correspond to an expansion in a screened potential rather than the bare Coulomb potential. The first equation is adequate for many purposes. Each equation follows from the demand that a corresponding expression for the total energy be stationary with respect to variations in the Green's function. The main information to be obtained, besides the total energy, is one-particle-like excitation spectra, i.e., spectra characterized by the quantum numbers of a single particle. This includes the low-excitation spectra in metals as well as configurations in atoms, molecules, and solids with one electron outside or one electron missing from a closed-shell structure. In the latter cases an approximate description is obtained by a modified Hartree-Fock equation involving a Coulomb hole and a static screened potential in the exchange term. As an example, spectra of some atoms are discussed. To investigate the convergence of successive approximations for the Green's function, extensive calculations are made for the electron gas at a range of metallic densities. The results are expressed in terms of quasiparticle energies $E(k)$ and quasiparticle interactions $f(k,k')$. The very first approximation gives a good value for the magnitude of $E(k)$. To estimate the derivative of $E(k)$ both the first- and the second-order terms are needed. The derivative, and thus the specific heat, is found to differ from the free-particle value by only a few percent. The correction to the specific heat keeps the same sign down to the lowest alkali-metal densities, and is smaller than those obtained recently by Silverstein and by Rice. The results for the paramagnetic susceptibility are unreliable in the alkali-metal-density region owing to poor convergence of the expansion for f. Aside from the proof of a modified Luttinger-Ward-Klein variational principle and a related self-consistency idea, the emphasis is on the development of a numerically manageable approximation scheme. (auth)

39659 ON THE HOYLE-NARLIKAR THEORY OF GRAVITATION. Hawking, S. W. (Department of Applied Mathematics and Theoretical Physics, Cambridge, Eng.). Proc. Roy. Soc. (London), Ser. A, 286: 313-19(July 20, 1965).

It is shown that the direct-particle action principle from which Hoyle & Narlikar derived their theory of gravitation not only yields the Einstein field equations in the "smooth-fluid" approximation, but also implies that the "m"-field be given by the sum of half the retarded field and half the advanced field calculated from the world lines of the particles. This is in effect a boundary condition for the Einstein equations, and it appears that it is incompatible with an expanding universe since the advanced field would be infinite. A possible way of overcoming this difficulty would be to allow the existence of negative mass. (auth)

39660 MOLECULAR ORBITALS IN MOMENTUM SPACE. Shibuya, Tai-ichi; Wulfman, C. E. (Univ. of the Pacific, Stockton, Calif.). Proc. Roy. Soc. (London), Ser. A, 286: 376-85(July 20, 1965).

The troublesome problem of developing cusps in ordinary molecular wavefunctions can be avoided by working with momentum-space wavefunctions for these have no cusps. The need for continuum wavefunctions can be eliminated if a hydrogenic basis set in Fock's projective momentum space is used. This basis set is the set of R_4 spherical harmonics and as a consequence algebraic expressions for all the integrals required in the solution of the momentum space Schrödinger equation may be obtained solely by the ordinary angular momentum calculus. A number of these integrals and a number of R_4 transformation coefficients were tabulated. The method was then applied to several simple united-atom and l.c.a.o. wavefunctions for H_2^+. Ground state energies and corrected wavefunctions were obtained. It was found in this numerical work that the method is most appropriate at internuclear distances somewhat less than the equilibrium distance. In Fock's representation both l.c.a.o. and united-atom approximations became exact as the internuclear distance approached zero. The united-atom expansion can be viewed as an eigenvalue equation for the root-mean-square momentum, $p_0 = \sqrt{(-2E)}$. In the molecule, the matrix operator corresponding to p_0 is related to the operator for the united-atom by a sum of unitary transformations, one for each nucleus in the molecule. (auth)

39661 QUANTUM LAWS IN CONNECTION WITH STOCHASTIC PROCESSES. Aron, J. C. (Universite, Algiers). Progr. Theoret. Phys. (Kyoto), 33: 726-54 (Apr. 1965).

It is shown that, with suitable conventions, Schrödinger's equation can be deduced from the laws of stochastic diffusion; uncertainty relations, concrete meaning of mass-energy equivalence, minimal constants of time and length and vanishing of negative energy also appear resulting from the basic conventions. An extension to mechanics with spin is worked out, and a model of Dirac's fluid is elaborated. Stochastic assumptions also lead to

the energy states and quantum numbers of the hydrogen atom. Suggestions are made on the physical interpretation of the model, on its relation to the wave-particle dualism, and on the meaning of quantized states. (auth)

39662 ON THE NEW THEORY OF GRAVITATION OF HOYLE AND NARLIKAR. Kimura, Toshiei (Hiroshima Univ.). Progr. Theoret. Phys. (Kyoto), 33: 774-6(Apr. 1965).

A new theory of gravitation was developed starting from the consideration that the mass is a direct particle field and arises from all other particles in the universe. An examination is made as to whether this field-theoretical version is possible. The same result is achieved by starting from the Lagrangian density as that of the original new theory. It is concluded that in order to treat this theory in terms of field theory proper c- and q-number theories must be used by using expectation values suitably. (J.F.P.)

39663 AN EXACT STATIONARY SOLUTION OF EINSTEIN'S EQUATIONS. Bonnor, W. B.; Swaminarayan, N. S. (London Univ. and Univ. of Manchester, Eng.). Z. Physik, 186: 222-6(1965).

An exact stationary solution of Einstein's empty-space field equations is given. It represents two massless sources possessing angular momentum, and held in position by stresses. The solution conforms with Mach's principle in the following sense: the spinning sources cause a rotation of the local inertial frame relative to test particles at infinity. (auth)

39664 RADIATION AND NOISE IN QUANTUM ELECTRONICS. Louisell, William H. McGraw-Hill Physical and Quantum Electronics Series. New York, McGraw-Hill Book Company, 1964. 416p. $14.50.

A nonrelativistic treatment of quantum field theory and statistics is presented. The Dirac formulation of quantum mechanics is given first, after which a quantized one-dimensional harmonic oscillator according to Dirac is studied. The Pauli spin operators are introduced to describe certain particles nonrelativistically. Mathematical techniques for handling creation, annihilation, and spin operators are then developed. The fundamental concepts of Dirac's theory of the quantization of the radiation field are then presented, and the interaction of radiation with matter is treated. The density operator is also considered. Linear amplifiers of the parametric and maser variety are then treated as examples of the principles presented, together with an attenuator. (D.C.W.)

Geophysics

39665 CLIMATIC CHANGE IN COSMIC PERSPECTIVE. Oepik, E. J. (Univ. of Maryland, College Park and Armagh Observatory, Ireland). Icarus, 4: 289-307(July 1965).

Three groups of paleoclimatic problems are discussed. They are the theoretical long-term progressive change going on since the origin of the solar system, the recurrent periods of deterioration of global climate (glacial epochs or major ice ages), and climatic fluctuations during one ice age (glacials and interglacials) of the quarternary. Topics considered are the long-term variation, variation of solar mass and gravitational constant, the astronomical chronology of the quarternary, climatic heat balance, glaciation and insulation, and the causes of the ice ages. (J.F.P.)

39666 ON THE FORMATION OF THE F_1 AND F_2 LAYERS. Aggarwal, S. (National Physical Lab., New Delhi). Indian J. Pure Appl. Phys., 3: 200-4(1965).

The problem of bifurcation of the F layer produced by a single ionization process and a height-dependent loss coefficient was re-examined. A model of recombination coefficient gradually varying with height given by A. P. Mitra [J. geophys. Res., 64: 733(1959)] together with a Chapman-like production function gives results more in conformity with the observed values of the parameters (particularly near the magnetic equator) than those obtained previously by J. A. Ratcliffe [J. atmos. terr. Phys., 8: 260(1956)] with an idealized step-function model of recombination coefficient. It is also found that the F_1 peak would appear only when the height of the peak of electron production is quite low, being around 150 km. during midday. (auth)

39667 DISTURBED CONDITION OF LOWER IONOSPHERE AT GEOMAGNETIC EQUATOR DURING MAGNETIC STORMS. Deshpande, S. D. (Government Polytechnic, Khamgaon, India). Indian J. Pure Appl. Phys., 3: 214-17(1965).

Data reported by the Equatorial Indian Station, Kodaikanal (geomagnetic lat., 0°44′ N), on geomagnetic storms and selected sudden ionospheric disturbances were analysed with a view to obtaining information on the changes in the lower ionosphere associated with magnetic storms at low latitudes. It was found that the D region of the ionosphere, responsible for the communication fadeouts is affected by the storms to a significant extent only for a short duration round about the hours of change of phases of the magnetic storm. The storm-time variation of fE_s at low latitudes also shows appreciably high values of E_s penetration frequency at about the same hours. (auth)

39668 THE INFLUENCE OF HORIZONTAL AIR MOTIONS ON F2-REGION IONIZATION. Varnasavang, V. (London Univ.); Hargreaves, Sylvia; Kendall, P. C. J. Atmospheric Terrest. Phys., 27: 707-21(June 1965).

The effect of large-scale neutral air motions in the F2 layer is studied theoretically for special models by numerical methods (with production and loss of electrons) and by approximate methods (when production and loss are absent). The results show that generally neutral air transport towards the equator enhances the electron density at the peak, in agreement with theoretical results obtained at moderate latitudes. The work is also of interest in connection with the theories of ion drag and of electrodynamic lifting of the F2 layer. (auth)

39669 VARIATIONS IN CRITICAL FREQUENCY OF THE F2-LAYER OF THE IONOSPHERE ASSOCIATED WITH GEOMAGNETIC STORMS AT EQUATORIAL STATIONS. Kotadia, K. M. (Gujarat Univ., Ahmedabad, India). J. Atmospheric Terrest. Phys., 27: 723-33(June 1965).

A few instances of SC type geomagnetic storms are studied to find changes in f_0F2 at three longitudinally displaced equatorial stations for different local seasons and commencement times of the storms. It is shown that the progressive phases and magnitude of the changes in f_0F2 at a place depend more on the SC time and severity of the storm rather than on the season. f_0F2 data of Kodaikanal (I = 3.5°N) are then studied for 59 SC type geomagnetic storms classified into four groups according to times of commencement. SD and Dst variations of f_0F2 are computed employing the method earlier used by Kotadia and Ramanathan (1962) for a low latitude station like Ahmedabad (I = 34°N). The SD variation shows values of f_0F2 above normal for most of the day until about 2300 hours with a pronounced peak near sunrise. The Dst variation shows increased values of f_0F2, the increase being larger on the second 24-hour interval of the storm, and decreased values during the first few hours after the commencement. Variations in the horizontal intensity of the earth's magnetic field for the same storms as used for f_0F2 analysis are also included. The results are then discussed to give a possible explanation. (auth)

39670 MEASUREMENTS OF THE ELECTRON CONTENT OF THE IONOSPHERE DURING SOME MAGNETICALLY DISTURBED PERIODS IN WINTER. Taylor, G. N. (Univ. of Manchester, Eng.). J. Atmospheric Terrest. Phys., 27: 735-43(June 1965).

The ways in which the ionospheric total-electron content and equivalent-slab thickness are likely to be affected by magnetic disturbances are discussed. Data from lunar radar observations are presented which show that magnetic activity produces a significant decrease of the integrated electron-production rate just after dawn, and that certain levels of activity are associated with increased equivalent

slab thicknesses during the night. No evidence of any significant change in the integrated loss rate at night is found. Some unusual long period oscillatory variations of the electron content have been observed during the main phase of a disturbance. (auth)

39671 SOME AURORA AUSTRALIS LOWER BORDER HEIGHTS, 1961. Aitken, W. M. (Arctic Inst. of North America, Washington, D. C.). J. Atmospheric Terrest. Phys., 27: 745-9(June 1965).

A number of pairs of photographs of auroral forms taken simultaneously at Amundsen-Scott and Ellsworth Stations, Antarctica in 1961 were analyzed to determine lower border heights. These first figures from observation within the zone of maximum occurrence substantially agree with observations from points distant from the zone. Most penetrations were to altitudes of 95 to 110 km. One display appears to have penetrated below 90 km. Apparent speeds in excess of 100 m/sec were noted for north-south motion. The long baseline and uncontrolled processing variables detract from the accuracy of the figures, but this first data remains of interest to investigators in this area of ionospheric phenomena. (auth)

39672 OBSERVATIONS ON THE ASSOCIATION OF AURORAL LUMINOSITY WITH AURORAL X-RAYS AND COSMIC NOISE ABSORPTION. Rosenberg, T. J. (Univ. of California, Berkeley). J. Atmospheric Terrest. Phys., 27: 751-9(June 1965).

Simultaneous observations of auroral luminosity and bremsstrahlung x rays from the same balloon payload are reported. Comparison of the balloon measurements with riometer records has shown the same variety of associations that appear in other studies of auroral phenomena. Because the photometer and scintillation counter geometries are fixed relative to each other and view equivalent regions of the sky at the production layer, it has been possible to investigate behavioral differences in the low and high energy portions of the precipitated electron spectrum with more certainty than when comparing balloon and ground-based observations. Certain aspects of the present observations suggest that temporal variations in these two energy ranges are rather independent, on occasion. These observations support the suggestion that two mechanisms having characteristically different energy spectra control the acceleration and/or precipitation of energetic electrons. Correlations of auroral luminosity with x rays then depend upon the degree of coupling between the mechanisms. (auth)

39673 SEASONAL DEPENDENCE OF SC-FIELD IN MIDDLE AND LOW LATITUDES. Maeda, Rikio; Fukushima, Naoshi; Nagata, Takesi (Tokyo Univ.). J. Geomagnet. Geoelec., 16: 239-46(1964).

An analysis of world-wide geomagnetic field-change for eight SC's during IGY indicates that the uniform northward external magnetic field for SC in middle and low latitudes shows a systematic seasonal dependence, namely, the uniform external magnetic field inclines towards the sunlit side in the summer hemisphere, and towards the night side in winter. This systematic seasonal dependence of the SC-field may be explained as due to the geometrical relation between the incident direction of the solar wind and the geomagnetic dipole axis. (auth)

39674 LOW LATITUDE WHISTLER ECHOES AND AN ESTIMATE OF ELECTRON DENSITY IN THE OUTER IONOSPHERE. Ondoh, Tadanori; Nemoto, Chyoshiro (Radio Research Labs., Ibaraki, Japan). J. Geomagnet. Geoelec., 16: 267-71(1964).

The observation of low-latitude whistler echoes is reported; and an estimate of electron density in the outer ionosphere from whistler dispersions is made. Whistler activity in low-lying latitude is usually small during the daytime because of an increase of D-layer absorption. But on January 14-16, 1964, whistlers were received all day. Thus the estimation of diurnal variation of electron density in the outer ionosphere can be made. This diurnal electron density variation is found to be on an average between 500 km and 1540 km in height. (J.F.P.)

39675 SOLAR FLARE EFFECT ON THE IONOSPHERIC F2-REGION. Sakurai, Kunitomo (Kyoto Univ.). J. Geomagnet. Geoelec., 16: 273-6(1964).

A survey is given of ionospheric F2 layer-phenomena observations associated with solar flares. These solar flares are shown to be associated with solar cosmic rays and solar type IV outbursts. This suggests that a sudden increase in the ionizing radiation of the F2 layer may clearly be associated with energetic particle phenomena. Although the formation of the F2 layer is mainly contributed by solar radiation, it has been shown that solar flares which produce sudden ionization increases of the F2 layer are always associated with solar cosmic ray events. Analysis of spectroscopic measurements suggests that the increases in the F2 layer associated with solar flares are attributed to the enhancement of the line emission from He II and He I atoms. (J.F.P.)

39676 SOME IONOSPHERIC EFFECTS OF THE SOLAR WIND. Piddington, J. H. (Commonwealth Scientific and Industrial Research Organization, Sydney). J. Inst. Telecommun. Engrs., 10: 285-91(Aug. 1964).

During geomagnetic storms the ionosphere is disturbed (ionospheric storms). However, the cause of geomagnetic storms (the solar wind) is always present to some degree and appears to be responsible for some ionospheric anomalies and irregularities. The mechanism by which the solar wind affects the ionosphere is by electrodynamic and hydromagnetic drift caused by pressure and by friction of the wind on the cavity. This causes widespread magnetospheric drift motions some of them into and out of the ionosphere. Other magnetospheric motions are caused by the quiet-day dynamo field Sq and by the Earth's rotation. The magnetosphere itself is a large reservoir of ionization (much greater than the ionosphere), and the various motions cause increases and decreases of F-region electron density, thus accounting for many disturbances and anomalies. (auth)

39677 MEASUREMENTS OF THE TOTAL ELECTRON CONTENT AND THE EQUIVALENT SLAB THICKNESS OF THE MIDLATITUDE IONOSPHERE. Bhonsle, R. V.; da Rosa, Aldo V.; Garriott, O. K. (Stanford Univ., Calif.). J. Res. Natl. Bur. Std., 69D: 929-37(July 1965).

The total electron content N_T and the equivalent slab thickness τ of the midlatitude ionosphere are determined from differential Doppler measurements on the radio transmissions from the Transit 4A satellite and the ionosonde data near Washington, D. C., and Ottawa. The trends of diurnal, seasonal, and sunspot cycle variations of N_T and τ at midday are described. It is found that in 1962 both N_T and τ were considerably decreased in magnitude as compared to the corresponding values near the peak of the sunspot cycle. The inferred mean electron-ion temperature is found to be generally in excess of the neutral gas temperature. The ratio T_e/T_g in the daytime is estimated to be 1.8 in summer and about 1.1 to 1.2 in winter, which may reflect corresponding changes in the ratio Q/N_e^2, where Q is the heat input to the electrons and N_e is the electron density. The relationship between τ and K_p appears to be rather ambiguous in contrast with the positive correlation between the neutral gas temperature and K_p. (auth)

39678 A COMPARISON OF RADAR AURORAL REFLECTION DATA WITH ACOUSTIC WAVE THEORY. Leadabrand, Ray L. (Stanford Research Inst., Menlo Park, Calif.). J. Res. Natl. Bur. Std., 69D: 959-64(July 1965).

A comparison is made between 400 and 800 MHz radar auroral reflection data and the concept that the irregularities in electron density responsible for the auroral echoes are plasma waves generated by instabilities in the ionospheric current system. The waves so generated would have their wave fronts parallel to the earth's magnetic field lines and would travel at the acoustic velocity of the medium. The comparison indicates that, although many of the key features of the plasma acoustic-wave concept can be found in the radar auroral data, the spectral characteristics of the auroral echoes are much too complicated to be simply understood in their present form. (auth)

39679 THE EXPLORER XVII SATELLITE. Spencer, N. W. (Goddard Space Flight Center, Greenbelt, Md.). Planetary Space Sci., 13: 593-8(July 1965).

Explorer XVII, the first Aeronomy satellite, employed for instrument housing, a vacuum-tight stainless steel sphere, whose construction reflected the most useful and established ultra-high vacuum techniques. The sensors carried included ionization gages, magnetic mass spectrometers and electrostatic probes, each mounted in and projecting through the stainless steel shell. Accessory equipment to provide the necessary supporting functions for the experiments included a PCM telemetry system, a command and control system, and a silver-zinc battery power supply which provided for fifty hours of satellite operation over a period of 100 days commencing 3, April, 1963. The quantity of data obtained greatly surpasses all previous rocket data, and provides new information about the atmosphere for altitudes and geographical locations not previously explored. (auth)

39680 DETAILED BEHAVIOUR OF THE MIDLATITUDE IONOSPHERE FROM THE EXPLORER XVII SATELLITE. Brace, L. H. (Goddard Space Flight Center, Greenbelt, Md.); Spencer, N. W.; Dalgarno, A. Planetary Space Sci., 13: 647-66(July 1965).

Cylindrical electrostatic probe experiments, similar to those employed in rocket flights, were included with the neutral particle mass spectrometer and total density gage experiments in the Explorer XVII satellite. Probe results are reported in more detail and their significance discussed in the context of the heat balance in the ionosphere. The ion and electron density measurements are discussed. These experimental results are also discussed with the various effects on the data. Graphs and a table of data are included. (J.F.P.)

39681 THE SI^+-SI^- PAIR AND INTERPLANETARY FORWARD-REVERSE SHOCK ENSEMBLES. Sonett, C. P.; Colburn, D. S. (Ames Research Center, Moffett Field, Calif.). Planetary Space Sci., 13: 675-92(July 1965).

On the basis of arguments given by Gold regarding the source of the storm's sudden commencement, it follows that the sudden impulse is due to the arrival at the magnetosphere of an interplanetary shock wave. From the general inadmissibility of rarefaction shocks together with the fast decrease in the horizontal component of the Earth's field associated with the SI^-, it is argued that the source of this disturbance is a shock wave pointing backward to the Sun and being simultaneously convected outward by the flow of the solar wind. Since the SI^- often follows an SI^+ by several hours, the two shocks are taken to be part of a complex structure in which the two waves are separated by a contact discontinuity, the whole being convected outward by the solar wind. Such shock structures are known to occur in the laboratory under suitable starting conditions and also take place as an aftermath of nuclear explosions. The conditions leading to this situation follow from the over-expansion in an expanding blast wave; they can also result from interaction of an advancing blast wave with a density discontinuity in the solar wind or even from a gradual increase in the velocity of the piston gas pushing out from a solar disturbance. Likely conditions leading to the shock pair are explored, and a procedure is given for examining graphically the change in gas states responsible for the phenomena. For that case where the SI^- occurs without being preceded by a positive impulse (SI^+), it is argued that the generation of the pair took place by the expansion of the flow of fresh gas from the Sun and the forward wave dissipated prior to the time of the observation in accord with theoretical requirements on expanding shocked flow. (auth)

39682 THE PROPERTIES OF THE IONOSPHERE WHICH AFFECT H.F. TRANSMISSION. East, F. R. (Marconi Co., Ltd., Chelmsford, Eng.). Point Point Telecommun., 9: 5-22(Feb. 1965).

The nature of the ionosphere is reviewed in relation to its influence on h-f radio waves. The three main layers of significance, D, E, and F, extend upwards into the ionosphere from an elevation of about 60 km. During the day the F layer separates into the F_1 and F_2 layers. F_2 is the most highly ionized layer, and therefore the most reflective, being subject to the effects of cosmic rays and meteors in addition to corpuscular emissions and uv radiation from the sun. Evidence of the presence of trapped corpuscular emissions is given by the fact that F_2 ionization is more concentrated in regions about 20° from the magnetic poles, and closely follows the nonuniform distribution of the earth's magnetic field. The layers below the F_2 are affected by uv rays of increasing penetrative power, but, because of their high gaseous density, have a greater natural tendency to deionize. The main characteristics of each of the other layers are outlined. Energy from h-f waves is lost to the ionized layers because the energy interchanged between the waves and the ions and free electrons is given up whenever the latter combine or collide with neutral atoms. Most absorption occurs in the D layer, which lies closest to the earth, considerably less absorption in the E layer, and very little in the layers above. Auroral zones, centered near the magnetic poles, introduce additional absorption in radio paths traversing them. Apart from the normal daily variations in ionospheric absorption, it is subject also to sudden increases (sudden ionospheric disturbances), which seriously affect communications. These occur most frequently during periods of maximum sunspot activity, being caused by solar flares which enhance the intensity of uv radiation for periods lasting from a few minutes to several hours. Within 36 hr of a solar flare, a geomagnetic storm may also develop. This again causes abnormal absorption and at the same time reduces the density of the F_2 layer, thus lowering its critical frequency. Recovery takes place in a matter of days, rather than hours, and the effect on communications is more serious. Magnetic storms are much less frequent than solar flares. Also discussed are progress in predicting solar disturbances, maximum and minimum usable radio frequencies, various types of fading, and multiple path delays. (BBB)

39683 ON ELECTROMAGNETIC EFFECTS IN THE NEIGHBOURHOOD OF A SATELLITE OR A VEHICLE MOVING IN THE IONOSPHERE OR INTERPLANETARY SPACE. Al'pert, Ja. L. (Academy of Sciences of the USSR, Moscow). Space Sci. Rev., 4: 373-415(May 1965).

The effects arising in the neighborhood of a body moving in the ionosphere or interplanetary space, and the character of their variations when the body moves off from the earth are discussed. The results of theoretical calculations are considered. Various disturbances are estimated: concentration and particle flux disturbances, the body potential, scattering of radio waves, the electric field, excitation of plasma waves, erosion of the body surface, etc. Some experimental data characterizing the considered effects are used. (auth)

Low Temperature Physics

Refer also to abstract 38779.

39684 (CONF-796(Paper 4)) LOW-TEMPERATURE EXPANSION OF THE SPONTANEOUS MAGNETIZATION OF A HEISENBERG FERROMAGNET. Morita, Tohru; Tanaka, Tomoyasu (Catholic Univ. of America, Washington, D. C.). 7p.

The magnetization of a low-temperature Fermi quasiparticle gas is formulated, using the Heisenberg hamiltonian and an effective-energy distribution function for the quasi-particles. (T.F.H.)

39685 (LA-DC-7086) THE COEXISTENCE CURVE OF He^3. Sherman, Robert H. (Los Alamos Scientific Lab., Univ. of California, N. Mex.). [1964] Contract W-7405-eng-36. 7p. (CONF-650428-1). Dep. mn; CFSTI, $1.00 cy, $0.50 mn.

From Conference on Phenomena in the Neighborhood of the Critical Point, Washington, D. C.

Results are reported on some recent P-V-T measurements on ^3He in the critical region. A significant departure was found in the shape of the coexistence curve from the behavior expected for classical systems such as Xe and CO_2. (M.O.W.)

39686 (LA-DC-7164) CHILLDOWN AND STORAGE LOSSES OF LARGE LIQUID HYDROGEN STORAGE DEWARS. Liebenberg, D. H.; Stokes, R. L.; Edeskuty, F. J. (Los Alamos Scientific Lab., Univ. of California, N. Mex.). [1965]. Contract W-7405-eng-36. 14p. (CONF-650802-3). Dep. mn; CFSTI, $1.00 cy, $0.50 mn.

From Cryogenic Engineering Conference, Houston, Tex.

The time history of the boiloff gas quantity was measured and compared with the total measured liquid input for a 55,000 gallon LH_2 storage dewar. These measurements showed that this vacuum perlite insulated dewar chills more quickly and requires less liquid hydrogen for chilldown than is generally calculated from theory. The measured steady state heat flux is less by a factor of 2 than conservative calculations would predict. (auth)

39687 A SUPERCONDUCTIVE MODEL WITH TWO KINETIC ENERGIES. Nemeth, J. (Roland Eoetvoes Univ., Budapest and Inst. of Nuclear Research, Debrecen, Hungary). Acta Phys. Acad. Sci. Hung., 18: 221-31(1965)

A model in which the kinetic energy has two possible values is studied. Energies are calculated in the second-order approximation using both an exact wave function and the BCS wave function. The correction to the BCS method is considered. The energy is also determined using the quasi-spin formalism. (D.C.W.)

39688 CRITICAL SUPERCURRENTS IN NIOBIUM CARBONITRIDES. Pessall, N.; Jones, C. K.; Johansen, H. A.; Hulm, J. K. Appl. Phys. Letters, 7: 38-9(July 15, 1965).

Independent experimental observations on the superconducting properties of niobium carbonitrides which indicate that the starting materials and different preparation procedures for the compounds are the predominant factors in determining the critical current characteristics are reported. In particular the upper critical field and critical current properties of such compounds is investigated. Critical currents were obtained using the four-probe method by observing an abrupt appearance of resistance while increasing the current at constant values for field and at 4.2°K. The possibility is noted of plasma-spraying compounds onto a suitable substrate suggests applications of these materials in high-field superconducting magnets. (J.F.P.)

39689 ORDER-DISORDER EFFECT ON SUPERCONDUCTIVITY: THE Mo-Ir SYSTEM. Sadagopan, V.; Pollard, E. R.; Giessen, B. C.; Gatos, H. C. (Massachusetts Inst. of Tech., Cambridge). Appl. Phys. Letters, 7: 73 (Aug. 1, 1965).

A striking difference was observed in the ordered and disordered states of the intermediate phase of the molybdenum-iridium alloy. The disordered phase exhibited a superconducting transition temperature of about 1.85°K, whereas the ordered phase exhibited a transition temperature of 8.8°K. The disorder intermediate phase is hexagonal closed packed and exhibits a broad homogeneity range. The present Molr phase represents the first instance where order-disorder is found to have a pronounced effect on superconductivity. Since this type of order-disorder transformation can readily be controlled and since it is likely that various degrees of order can be achieved it is hoped that the study of the energy band structure of such phases might provide an experimental handle to the understanding of superconductivity. (J.F.P.)

39690 APPLICATIONS OF SUPERCONDUCTIVITY. PART I. SOFT SUPERCONDUCTORS. Thomas, E. J. (Manchester Univ., Eng.). Brit. Commun. Electron., 12: 156-61(Mar. 1965).

The general properties of superconductors are described; and some of the uses to which they have already been put are indicated. The applications depending on each property are described. Previously the cost of maintaining materials near absolute zero was prohibitively expensive. But now with a reduction in the cost of refrigeration, the superconducting properties of various metals can be put to use. Some of the uses described are the superconducting galvanometer, the high Q r-f cavity, lossless coaxial cables, thermometers, bolometers, modulators, choppers, amplifiers, oscillators, computer elements, current switches. Other applications are described, some of these using the Meissner effect also. (J.F.P.)

39691 DETERMINATION OF SUPERCONDUCTING TRANSITION REGION BY SUPERFLUID PHASE TRANSITION. Garbuny, Max; Gottlieb, Milton (Westinghouse Electric Corp., Pittsburgh). J. Appl. Phys., 36: 2167-8 (July 1965).

A phenomenon is reported consisting of the appearance of a vapor film in He II over superconducting lead film regions driven normal by a critical current. Potential probe measurements verify that the area under the vapor film coincides with the extent of the normal domain within the superconducting environment. Length of the bubble increases linearly with voltage drop across the sample, while the current changes only a few percent for voltage changes of 10:1 or more. This behavior is interpreted by a critical heat flux density which dominates the electrical properties once the vapor film is established. Quantitative relations of this kind are not observed if either He I or normal metals are substituted under otherwise equal conditions. (auth)

39692 CURRENT DISTRIBUTION IN A THIN-FILM SUPERCONDUCTING STRIP TRANSMISSION LINE. Sass, A. R.; Skurnick, I. D. (Lewis Research Center, Cleveland). J. Appl. Phys., 36: 2260-7(July 1965).

In the long-wavelength limit, the current distribution in a thin-film superconducting strip transmission line can be described by an inhomogeneous Fredholm equation of the second kind. By considering a fluxoid conservation derivation of this equation, physical insight into the structure of the kernel follows naturally. An approximate analytic solution to the integral equation is derived for a specified range of geometrical parameters commonly encountered in practice. The solution is obtained by making use of the Liouville-Neumann method of successive iterations and approximating the resulting series by a series involving powers of a defined coupling factor. It is shown that the critical current of the thin-film superconducting strip transmission line, based on the calculations and a critical-current-density hypothesis, is underestimated by less than 10%. (auth)

39693 CRYOSORPTION PUMPING OF HYDROGEN AND HELIUM AT 20 deg K. Stern, S. A.; Mullhaupt, J. T.; Hemstreet, R. A.; DiPaolo, F. S. (Union Carbide Corp., Tonawanda, N. Y.). J. Vacuum Sci. Technol., 2: 165-77(July-Aug. 1965).

The feasibility of pumping hydrogen and helium gas in large vacuum chambers by adsorption at low temperatures was investigated. The adsorptive capacity of seven selected adsorbents for hydrogen and helium was determined under equilibrium conditions at temperatures between 20 and 40°K and at pressures from 3×10^{-8} to 1×10^{-3} Torr. The adsorptive capacity for hydrogen on coconut charcoal and on several types of molecular sieves at 20°K was found to be very large. Above 30°K, adsorptive capacities were found to be too low to be of practical interest. Cryosorption pumping under constant hydrogen gas leak was demonstrated for three of the adsorbents studied: molecular sieves 5A and 13X, and coconut charcoal. However, only the adsorbent surface directly exposed to the gas flow was found to be effective. The capacity and pumping efficiency of this surface were strongly dependent on the temperature. As a result, the adsorbent must be well shielded from radiation, and good thermal contact between the adsorbent bed and the refrigerant must be assured. It is concluded that cryosorption is a promising technique for pumping hydrogen in large space simulation chambers, but cryosorption pumping of helium at 20°K does not appear practical. (auth)

39694 GUIDED MOTION OF VORTICES AND ANISOTROPIC RESISTIVITY IN TYPE-II SUPERCONDUCTORS. Niessen, A. K.; van Suchtelen, J.; Staas, F. A.; Druyvesteyn, W. F. Philips Res. Rept., 20: 226-34(June 1965).

In Hall specimens made of superconducting materials, transverse voltages, which did not change sign on reversal of the magnetic-field direction, were found. These voltages were associated with an anisotropic structure of the material. Two different phenomena were found: one for the magnetic field perpendicular to the surface in the H_{c1}-H_{c2} region (which can be explained by a model of guided vortex motion), and another in the H_{c2}-H_{c3} region for parallel field, which is discussed in terms of surface superconductivity. The model may be refined in order to account for a reversible "Hall" component of the transverse voltage. (auth)

39695 ALTERNATING-CURRENT LOSSES IN Nb/Zr SUPERCONDUCTIVE COILS. Grenier, C.; Elschner, B. Philips Res. Rept., 20: 235-52(June 1965).

In the range of frequencies studied, between 20 and 600 c/s, it is suggested that power loss by alternating current in superconductive coils is due to hysteresis. Agreement with the model proposed by H. London in terms of field penetration in the superconductive material was well achieved when field variation of the critical-current density was taken into account. A field- and temperature-dependent variation of the self-inductance of the coil also coincided with this penetration effect. (auth)

39696 SUPERFLUID FLOW IN A VENTURI TUBE. Meservey, R. (Massachusetts Inst. of Tech., Cambridge). Phys. Fluids, 8: 1209-12(July 1965).

It is shown from Bernouilli's equation that a Venturi tube or Pitot tube as ordinarily used will have practically no level difference with irrotational fluids. A quantitative solution is given in the case of a Venturi tube of various dimensions. The observed level difference with water follows simply from the rotational acceleration term of the Navier–Stokes equation. This result for irrotational fluids is discussed with respect to experiments using liquid helium and superconductors. (auth)

39697 EFFECT OF A CYLINDRICAL BOUNDARY ON THE ADDED MASS OF TWO CYLINDERS IN LIQUID HELIUM. Hussey, R. G.; Reynolds, J. M. (Louisiana State Univ., Baton Rouge). Phys. Fluids, 8: 1213-17 (July 1965).

An expression is derived for the added mass of two equal circular cylinders (radius a) moving normal to the line of centers in an ideal fluid enclosed by a fixed cylindrical boundary (radius b). The two moving cylinders, with centers 2c apart, have velocities equal in magnitude but opposite in direction. Except for extreme cases, the added mass per unit length of each cylinder is given by $M = \pi a^2 \rho [1 - (1/2\gamma^2) + (8\beta^4\gamma^2)/(\beta^4 - \gamma^4)^2]$, where ρ is the fluid density, $\beta = b/a$, and $\gamma = c/a$. This expression is compared with the results of a torsion pendulum experiment in liquid helium II. For $\gamma = 4.9$ and $8.6 < \beta < 11$, the predicted change in moment of inertia is in good agreement with that observed in liquid helium between 2.15 and 1.3°K. The observed damping is independent of boundary radius. (auth)

39698 RESISTANCE OF TYPE II SUPERCONDUCTORS IN THE MIXED STATE. Casimir, H. B. G. (Philips' Gloeilampenfabrieken, Eindhoven, Netherlands). Phys. Letters, 17: 177-8(July 15, 1965).

The assumption that resistance and Hall effect in type II superconductors in the mixed state are due to induction by a moving flux pattern is considered. A squirrel cage model is presented for investigating the nature of the driving force and the damping mechanism that control the motion of flux. (L.B.S.)

39699 PROXIMITY EFFECTS UNDER MAGNETIC FIELDS. I. EXPERIMENTS. Burger, J. P.; Deutscher, G.; Guyon, E.; Martinet, A. (Universite de Paris, Orsay, France). Phys. Letters, 17: 180-1(July 15, 1965).

Tunneling and flux penetration measurements on superimposed normal (Zn) and superconducting (InBi) films in a parallel magnetic field H are reported. It was found that proximity effects on the normal side are reduced when H reaches the breakdown field H_b. The transition is found to be very large at low temperatures. (L.B.S.)

39700 PROXIMITY EFFECTS UNDER MAGNETIC FIELDS. II. INTERPRETATION OF BREAKDOWN. De Gennes, P. G.; Hurault, J. P. (Universite de Paris, Orsay, France). Phys. Letters, 17: 181-2(July 15, 1965).

It was previously observed that the tunneling density of states and the flux permeability of a normal metal layer N deposited on a superconducting surface substrate S show an abrupt change at a certain (weak) field H_b. An interpretation is given of the breakdown field H_b; and it is shown that this behavior is expected at not too high temperatures. (L.B.S.)

39701 SUPERCONDUCTIVITY OF GERMANIUM AND SILICON UNDER HIGH PRESSURE. Buckel, W.; Wittig, J. (Technische Hochschule, Karlsruhe, Ger.). Phys. Letters, 17: 187-8(July 15, 1965). (In German)

A study was made of the superconductivity of pulverized Ge and Si samples under pressures of 120 to 130 kbar. It was observed that the resistance of the Si sample continually dropped nearly 10^7 with increasing pressure. Similar results were observed for Si. The samples showed a metal-like resistance decrease with decreasing temperature, whereas the residual resistance ratio R(300°K)/R(10°K) was found to be between 18 and 27 for Ge, and only between 2 and 27 for Si. It was therefore assumed that the Si sample was incompletely transformed to the metallic phase. The superconducting transition curves are shown. (L.B.S.)

39702 THE RADIAL VELOCITY OF MAGNETIC FIELD PENETRATION IN TYPE II SUPERCONDUCTORS. Flippen, R. B. (E. I. du Pont de Nemours and Co., Wilmington, Del.). Phys. Letters, 17: 193-4(July 15, 1965).

Measurements are reported of the radial velocity of magnetic field penetration in Nb and Nb-25%Zr in pulsed magnetic fields having rise times of 10^8 to 10^9 Oe/sec. The experimental arrangement is described. It was found that the velocity of field penetration ranges from 3100 to 4700 cm/sec for Nb at 4.2°K. Measurements on Nb-Zr yielded rates of 10,000 to 15,000 cm/sec. (L.B.S.)

39703 REVERSIBLE MAGNETOCALORIC EFFECT IN SUPERCONDUCTING NIOBIUM. Ohtsuka, T. (Tokyo Univ.). Phys. Letters, 17: 194-6(July 15, 1965).

Measurements were made on the magnetocaloric effect in the mixed state of a pure niobium single crystal, using a conventional adiabatic calorimetry apparatus. It is shown that under favorable sample conditions, the magnetocaloric effect, which was completely reversible throughout the mixed state, provides a simple and unambiguous method for determining the upper critical field and also specific heat jumps. (L.B.S.)

39704 ON THE MOVEMENT OF FLUX LINES IN A TYPE II SUPERCONDUCTOR. Lorch, H. O. (English Electric Co. Ltd., Stafford, Eng.). Phys. Letters, 17: 196-7(July 15, 1965).

It is suggested that Abrikosov fluxoids do not move bodily sideways continuously under Lorentz forces, and that the concepts of flux pinning, flux creep, flux flow and flux jumping, are, in this respect, unsound. Arguments are presented in support of these suggestions. (L.B.S.)

39705 MAGNETIC FIELD DEPENDENCE OF KNIGHT SHIFT IN SUPERCONDUCTORS. Bennemann, K. H. (Cambridge Univ., Eng.). Phys. Letters, 17: 197-9 (July 15, 1965).

Equations are derived for the Knight shift in superconductors, which show the effect of the magnetic field and the Pauli paramagnetism. Calculations were made of the ratio of the Knight shift in the superconducting and corresponding normal states as a function of temperature, and the resulting curves are shown. (L.B.S.)

39706 MAGNETIC FIELD DEPENDENCE OF THE SURFACE RESISTANCE OF SUPERCONDUCTING TANTALUM AT 35 Gc/s. Kao, Yi-han (State Univ. of New York, Stony Brook); Budnick, J. I. Phys. Letters, 17: 218-19 (July 15, 1965).

An experiment was performed using a vacuum purified foil of superconducting tantalum placed at the bottom of a TE_{104} mode rectangular cavity which was terminated one arm of a microwave cavity. The magnetic field was in the plane of the sample and perpendicular to the microwave electric field. The variation of the surface resistance in the magnetic field was observed by measuring the change in Q on the resonant cavity. Typical recorder tracings of the field dependence of surface resistance show a negative magnetic field dependence in addition to some peculiar behavior which is presumed to be due to complicated surface phenomena. (L.B.S.)

39707 ORIGIN OF RESISTANCE IN TYPE-II SUPERCONDUCTORS. Romer, R. H. (Centre de Recherches sur les Tres Basses Temperatures, Grenoble, France). Phys. Letters, 17: 223-4(July 15, 1965).

The hypothesis that transverse flux line motion leads to longitudinal voltages by an inductive mechanism is examined. (L.B.S.)

39708 SUPERCONDUCTIVITY IN TUNGSTEN FILMS. Kammerer, O. F.; Strongin, M. (Brookhaven National Lab., Upton, N. Y.). Phys. Letters, 17: 224-5(July 15, 1965).

Superconducting transition temperatures were found up to 4.1°K in tungsten films. X-ray line broadening measurements were made in an attempt to separate out the effects of strain and particle size. No definite conclusion was possible as to their relative contributions to the line broadening. An investigation of the effect of oxygen on the T_c is in progress. (L.B.S.)

39709 MEASUREMENT OF NOISE IN THE RESISTIVE STATE OF TYPE II SUPERCONDUCTORS. Van Ooijen, D. J.; Van Gurp, G. J. (Philips' Gloeilampenfabrieken, Eindhoven, Netherlands). Phys. Letters, 17: 230-1(July 15, 1965).

Measurements were made on the frequency spectra of noise on current carrying vanadium foils at 4.2°K in a transverse magnetic field. The results support the model of flux entities crossing the superconductor. (L.B.S.)

39710 HALL EFFECT IN TYPE II SUPERCONDUCTORS. Staas, F. A.; Niessen, A. K.; Druyvesteyn, W. F. (Philips' Gloeilampenfabrieken, Eindhoven, Netherlands). Phys. Letters, 17: 231-3(July 15, 1965).

An experiment which was previously performed on deformed samples was repeated on cold-rolled NbTa(thickness 20μ) after the specimen was either etched or carefully annealed, and the Hall voltages were determined by reversing both magnetic field and current. The Hall voltages were found to be smooth and continuous functions of H. The Hall angle was plotted versus H at T = 1.3°K, from which it is seen that although the different treatments may give rise to some variation of H_{c2} the form of the curves is the same. Calculations for the motion of flux lines in the mixed state, giving rise to longitudinal and transverse voltages, are discussed. (L.B.S.)

39711 TEMPERATURE DEPENDENCE OF A GENERALIZED GINZBURG-LANDAU COEFFICIENT FOR WEAK AND STRONG COUPLING SUPERCONDUCTORS. Paskin, A. (Brookhaven National Lab., Upton, N. Y.). Phys. Letters, 17: 235-7(July 15, 1965).

It is shown that the generalized form of the two-fluid model, which was found to match the temperature dependence of the critical field for strong and weak coupling superconductors, can also be incorporated into a formulation that explains the observed temperature dependence of κ, where κ is the entire coefficient in the linearized equations which corresponds to the Ginzburg-Landau parameter κ_{GL}. (L.B.S.)

39712 THE ELECTRODYNAMICS OF FLUX PENETRATION IN SUPERCONDUCTORS. Goodman, B. B. (Centre de Recherches sur les tres basses Temperatures, Grenoble, France). Phys. Letters, 18: 8-9(Aug. 1, 1965).

Flux penetration and fluxoid motion in superconductors are studied starting from the Ginzberg-Landau equation for the local current density. (D.C.W.)

39713 ABSORPTION OF TRANSVERSE MICROWAVE PHONONS BY Al-Pb SUPERCONDUCTING DIODES. Abeles, B.; Goldstein, Y. (RCA Labs., Princeton, N. J.). Phys. Letters, 18: 11-13(Aug. 1, 1965).

The interaction of transverse phonons with the tunnel diode was investigated. Measurements of the temperature and bias dependence of the excess current induced by the phonons show that the excess current has two components. One is proportional to d^2I/dV^2 as in the case of longitudinal phonons, and the other component suggests that the temperature of the tunnel diode increases appreciably due to strong absorption of transverse microwave phonons. (D.C.W.)

39714 INDEPENDENCE OF THE DENSITY OF ROTATING LIQUID HELIUM ON THE ANGULAR VELOCITY. Andronikashvili, E. L.; Tsakadze, J. S. (Inst. of Physics, Academy of Sciences of the Georgian SSR, Tbilisi, USSR). Phys. Letters, 18: 26-7(Aug. 1, 1965).

The dependence of the density of helium II on its angular velocity was investigated. It was found that the density of helium II increased with the angular velocity. The effect of a temperature increase on the velocity dependence of the density was also studied. The results indicate that there exists some specific mechanism of helium II packing which is not associated with the presence of centrifugal pressure, but is apparently connected with the existence of quantized vortices of the Onsager-Feynman type. (D.C.W.)

39715 MOESSBAUER EFFECT STUDY OF PHASE TRANSITION IN ICE. Dezsi, I.; Keszthelyi, L.; Molnar, B.; Pocs, L. (Central Research Inst. for Physics, Budapest). Phys. Letters, 18: 28-9(Aug. 1, 1965).

The temperature dependence of the Mössbauer effect for iron salts in ice was observed. The results were explained in terms of a phase transition in ice. (D.C.W.)

39716 SPECIFIC HEAT OF THE MIXED STATE IN SUPERCONDUCTING ALLOYS. Maki, Kazumi (Univ. of Chicago). Phys. Rev., 139: 702-5(Aug. 2, 1965).

A previous theory of superconducting alloys in magnetic fields is used to make a detailed study of the specific heat of the mixed state in superconducting alloys. The jump of the specific heat at the transition from the mixed state to the normal state is explicitly calculated for various values of κ, the Ginzburg-Landau parameter. In fields just above the lower critical field H_{c1}, it is found that the specific heat at lower temperature is expressed in terms of H_{c1} as $C_m = -(1/4\pi)T(d^2H_{c1}/dT^2)B + (dH_{c1}/dT)(\partial B/\partial T)$, where $B = (\pi/e)n$ (n being the number of flux lines per unit area), and the first term, coming from the free energy associated with a flux line, is proportional to T. (auth)

39717 EFFECTS OF GAP ANISOTROPY IN SUPERCONDUCTORS CONTAINING PARAMAGNETIC IMPURITIES. Fulde, Peter (Univ. of California, Berkeley). Phys. Rev., 139: 726-8(Aug. 2, 1965).

The effect of the gap anisotropy on the transition temperature of a superconductor containing paramagnetic impurities is calculated by an extension of the theory of Markowitz and Kadanoff. Deviations from the linear decrease of transition temperature with impurity concentration as predicted by Abrikosov and Gorkov will depend on the relative magnitudes of the spin-flip and the no-spin-flip parts of the impurity scattering potential. It is shown that such a deviation should be observable and provide a test of the Abrikosov-Gorkov theory. (auth)

39718 INFLUENCE OF A MAGNETIC FIELD ON TUNNELING FROM A TYPE-II ALLOY SUPERCONDUCTOR. Tomasch, W. J. (Atomics International, Canoga Park, Calif.). Phys. Rev., 139: 746-57(Aug. 2, 1965).

Planar tunnel diodes were utilized to study the influence of longitudinal and transverse magnetic fields ($H_{||}$ and $H_{\perp}$, respectively) on electron tunneling phenomena involving type-II superconducting alloys (1.1–4.2°K). Each diode consisted of a very thick Pb–Tl alloy film separated from a much thinner Al film by an extremely thin natural aluminum oxide layer. Zero-field current-voltage (I-V) diode characteristics observed with the Al superconducting demonstrated the existence of a sharply defined alloy energy gap which is essentially independent of alloy composition. With the Al superconducting, very high diode impedances were observed in longitudinal fields for voltages exceeding half the zero-field Al energy gap, suggesting that very nearly all of the alloy surface retains a nonzero energy gap to at least twice the bulk thermodynamic critical field H_c. Furthermore, a form of sharp I-V structure persisted to values of $H_{||}$ satisfying $H_{c1} < H_{||} < 2H_c$, where H_{c1} is the Abrikosov lower critical field. This structure was interpreted tentatively in terms of a field-induced distribution of alloy energy gaps $2\epsilon_i$ satisfying $\epsilon_m \leq \epsilon_i \leq \epsilon_M$, where ϵ_m is the distribution minimum, probably corresponding to the value at the surface, and ϵ_M is the distribution maximum, which approximately equals the zero-field half energy gap. In transverse fields, evidence of superconductivity in the alloy ceases at $H_t = H_1$, which correlates well numerically with bulk values of the Abrikosov upper critical field H_{c_2}. In longitudinal fields, however, evidence of superconductivity was observed to persist to H_l, where H_l/H_t ranges between 1.7 and 1.9 depending on alloy composition. The results indicate that in longitudinal fields superconductivity persists beyond H_{c2} within a few coherence lengths of the surface, and extends over a major fraction of the surface. Furthermore, the numerical value of H_l/H_t is in reasonable accord with the sheath critical field ratio predicted by Saint-James and de Gennes for longitudinal fields. For transverse fields, they predict that the sheath will not appear above H_{c2}, consistent with present observations. The measurements are believed to be typical of bulk specimens for which flux entry is delayed to fields substantially greater than H_{c1} because of surface smoothness. (auth)

39719 MAGNETIC-FIELD DEPENDENCE OF THE KNIGHT SHIFT IN SUPERCONDUCTORS. Fulde, Peter (Univ. of California, Berkeley); Maki, Kazumi. Phys. Rev., 139: 788-93(Aug. 2, 1965).

Spin-orbit interaction is assumed to cause the Knight shift in superconductors at zero temperature. The magnetic-field dependence of the shift caused by the depairing effect of the field is calculated. Numerical results for the spin susceptibility as a function of the field are presented. (auth)

39720 NUCLEAR SPIN-LATTICE RELAXATION AND KNIGHT SHIFT IN TUNGSTEN METAL. Narath, A.; Fromhold, A. T. Jr. (Sandia Lab., Albuquerque, N. Mex.). Phys. Rev., 139: 794-5(Aug. 2, 1965).

The nuclear spin-lattice relaxation time T_1 and Knight shift K of ^{183}W were measured in tungsten metal in the temperature range 1.1–4.0°K. The experimental measurements give $T_1T = 37 \pm 2$ sec °K. A comparison of this value with the electronic specific-heat coefficient of tungsten indicates that the dominant relaxation mechanism arises from the contact interaction. The Knight shift K = 1.06%, on the other hand, results almost entirely from the orbital paramagnetism of the d band. The results show that approximately 80% of the conduction-electron susceptibility of tungsten is of orbital origin. (auth)

39721 MAGNETIC PROPERTIES OF INTRINSIC LONDON SUPERCONDUCTORS. Maki, Kazumi (Univ. of Chicago); Tsuzuki, Toshio. Phys. Rev., 139: 868-77 (Aug. 2, 1965).

A theory of intrinsic London superconductors in the vicinity of the transition point where the transition from the mixed state to the normal state takes place is presented. The equations for local superconductors for impurity-free metal, deduced previously by Gor'kov, are explicitly solved by using the variational function of Abrikosov. Use is made of the results due to Gor'kov concerning the upper critical field of pure superconductors. It is shown that the mixed state in the immediate subcritical region is expressed in terms of κ_1 and κ_2, which coincide at the critical temperature with κ, the Ginzburg-Landau parameter. The upper critical field is expressed in terms of κ_1, while the slope of the magnetization curve is given in term of κ_2. The explicit calculation of κ_1 and κ_2 shows that κ_2 increases more rapidly than κ_1 as temperature decreases, and diverges at low temperature. (auth)

39722 MULTIPLE SCATTERING AND MANY-BODY THEORY: FREE ENERGY OF ELECTRONS IN HELIUM. Coopersmith, M. (Univ. of Chicago and Case Inst., Cleveland). Phys. Rev., 139: A1359-73(Aug. 30, 1965).

An electron in helium vapor at 4°K is characterized by its s-wave scattering length off helium atoms. This scattering length is small compared with the average interparticle spacing in the helium vapor. A particle interacting via hard-core repulsion with an ideal gas was taken as a model. This establishes a connection with the hard-sphere Bose problem of more general interest. The model described above is simpler because it has only Boltzmann statistics and because the electron is very light compared with the helium atoms. For this model, the interaction free energy of the electron was calculated assuming that it is in statistical equilibrium with the helium gas. In the s-wave approximation, it is shown that this interaction free energy is rigorously $2\pi\rho\alpha(\hbar^2/m)$ due to single scattering, all higher order multiple-scattering effects being zero. Here, ρ is the average density of helium atoms, α is the scattering length, and m is the electron mass. Since the p-wave approximation contributes a term of order $\rho\alpha^3$, it is evident that the term $2\pi\rho\alpha(\hbar^2/m)$ is good to higher densities than might previously have been supposed. This provides partial justification for the "bubble" model of the electron mobility since the term $2\pi\rho\alpha(\hbar/m)$ is certainly good up to densities at which the free energy of the "bubble" configuration becomes smaller. (auth)

39723 QUANTIZED VORTEX RINGS IN SUPERFLUID HELIUM, A PHENOMENOLOGICAL THEORY. Huang, Kerson; Olinto, A. Cesar (Massachusetts Inst. of Tech., Cambridge). Phys. Rev., 139: A1441-51(Aug. 30, 1965). (MIT–2098-139).

Rayfield and Reif (RR) and Careri, Cunsolo, and Mazzoldi (CCM) have done some experiments involving ion complexes moving through liquid helium in a constant uniform electric field. The results of RR give direct and compelling evidence that the ion complexes become attached to quantized vortex rings, the existence of which was conjectured by Feynman and Onsager. Their experiments, however, do not yield details concerning the interactions between ion complex and vortex ring. The results of CCM, on the other hand, exhibit a wealth of gross and fine structures, but they do not seem to be immediately understandable in simple terms. An attempt is made to explain all the results of RR and CCM in terms of a phenomenological theory of quantized vortex rings. Guided by experiments, it is hypothesized that an ion complex can create a vortex ring only if its velocity v and effective radius R satisfy the condition $6\pi vR = nh/m$, (n = 1, 2, 3, ...), where h is Planck's constant and m the helium mass. The number 6π is semiempirical. An experiment is suggested to test this hypothesis directly. After creation, the interaction of the vortex ring and the ion complex is described phenomenologically, with all parameters determined directly by experiments. This leads to a definite model that describes in detail the history of an ion complex in liquid helium. The determination of parameters makes extensive use of experimental data, but only one number from CCM. The model then reproduces quantitatively all the data of CCM. (auth)

39724 CRITICAL CURRENTS IN SUPERCONDUCTING FILMS OF INDIUM. Chaudhari, R. D.; Brown, J. B. (Univ. of British Columbia, Vancouver). Phys. Rev., 139: A1482-8(Aug. 30, 1965).

Critical currents in the region near the transition temperature T_c were measured for thin indium films, of thick-

ness 585 to 3600 Å, deposited on sapphire cylinders. The coherence length obtained from the normal resistivities is compared with previous values and the increase of T_c with decreasing film thickness is determined. Measurements are reported on a 585-Å-thick film which combine the use of a compensated geometry avoiding the difficulties associated with specimen edges, and current pulses with a rise time of 7 nsec in which the transition is not obscured by specimen heating. Two regions are observed; for $(T_c - T) \leq 0.11°K$ the critical currents vary with the 1.5 power of the temperature difference, in accord with the Ginzburg-Landau theory, while for $0.11°K \leq (T_c - T) \leq 0.30°K$ the temperature dependence becomes nearly linear. The approach to this behavior depends on (a) shortening the measuring-pulse rise time, and, particularly, (b) reducing the fraction of normal resistance restored. Paradoxically, because of (b), even d-c currents lead to similar results. (auth)

39725 SUPERCONDUCTIVITY OF Nb_3Ge. Matthias, B. T.; Geballe, T. H.; Willens, R. H.; Corenzwit, E.; Hull, G. W. Jr. (Bell Telephone Labs., Inc., Murray Hill, N. J.). Phys. Rev., 139: A1501-3(Aug. 30, 1965).

Evidence is presented to show that the maximum transition temperature of compounds with the β-W type structure (A15) occurs at the stoichiometric composition A_3B, when B is a nontransition element. The niobium–germanium A15-type compound, which normally forms with excess Nb, has a transition temperature of 6.9°K. It was found that Nb_3Ge compounds prepared by rapid-quench techniques, in the presence of excess germanium, have transition temperatures as high as 17°K. This large increase in transition temperature is attributed to a closer approach to the stoichiometric 3:1 composition. (auth)

39726 SUPERCONDUCTING PENETRATION DEPTH OF NIOBIUM. Maxfield, B. W.; McLean, W. L. (Rutgers State Univ., New Brunswick, N. J.). Phys. Rev., 139: A1515-22(Aug. 30, 1965).

The variation with temperature of the penetration depth of weak magnetic fields into niobium was measured. The variation was more rapid than expected from the BCS theory of superconductivity, in contrast to the situation in previously measured superconductors where it was less rapid. Just as in the previous cases, the results can be understood in terms of a variation of the energy gap different from that predicted by the BCS theory. A comparison with the energy gap deduced by Dobbs and Perz from their ultrasonic-attenuation measurements is given. The penetration depth at absolute zero, $\lambda(0)$, is estimated from the present results to be 470 ± 50 Å, while the London penetration depth $\lambda_L(0)$ is 390 ± 50 Å. (auth)

39727 SPIN-ORBIT COUPLING AND THE KNIGHT SHIFT IN NONTRANSITION-METAL SUPERCONDUCTORS. Appel, Joachim (General Atomic Div., General Dynamics Corp., San Diego, Calif.). Phys. Rev., 139: A1536-? (Aug. 30, 1965).

The Knight shift K_s of nontransition-metal superconductors is discussed in terms of three contributions, namely: (a) The Van Vleck part of the contact shift attributed to the spin-orbit coupling force of the periodic potential which, in the presence of an external magnetic field, causes virtual high-energy rearrangement of conduction electrons near and inside the Fermi surface; (b) that part of the contact shift which is attributed to low-energy rearrangements of conduction electrons and affected by spin-reversing scattering; and (c) the diamagnetic orbital shift. For the calculation of (a), Wannier's theory of a Bloch electron in a magnetic field is generalized to the original Pauli Hamiltonian $\mathcal{H}_0$, describing the relativistic dynamical behavior of a conduction electron in the effective periodic potential of the lattice. This leads to an effective Hamiltonian which couples only Bloch-type spinors of the same band index, but of the same and of different spin indices. With the help of the eigenfunctions of $\mathcal{H}_0$, the hyperfine contact interaction is treated by perturbation theory. To arrive at simple expressions for the corresponding Knight shift and nuclear spin-relaxation time, valid for arbitrary strength of spin-orbit coupling, the energy-band function in the absence of the field is approximated by a parabola. Formulas for (b) and (c) are taken from the literature. The relative importance of the three contributions to K_s is discussed for Al, Sn, and Hg, where the Knight shift has been observed in the normal and in the superconducting states. If one assumes that spin-reversing scattering is caused merely by spin-orbit interactions at atomic imperfections such as displaced surface atoms of small particles, and not by paramagnetic impurities, one finds that in Al neither of the two spin-orbit coupling effects is sufficiently strong to account for more than ~2% of the residual shift $K_s(0)$. For the experimental Sn sample, (a) and (b) have the ratio 1:3 and, together with the orbital shift, can account for ⅔ of the observed $K_s(0)$. For Hg, (a) and (b) are of comparable magnitude at T = 0 and together account for more than ½ of the observed shift $K_s(0)$. (auth)

39728 NUCLEAR MAGNETIC RESONANCE IN LIQUID He^3. Beal, B. T.; Hatton, J. (Oxford Univ., Eng.). Phys. Rev., 139: A1751-62(Sept. 13, 1965).

The nuclear magnetic susceptibility χ of liquid ^3He was studied as a function of temperature (0.07 to 4.2°K) and pressure (0.7 to 27.5 atm). It was found that Curie's law holds above 2°K, where the experimental results showed an rms deviation of less than 1.5%. At 1.1°K the liquid is (5 ± 1.5%) degenerate; no pressure dependence of χ could be detected above 1.2°K. As the temperature is reduced below 1.1°K, the product χT falls monotonically and χ tends toward the constant zero-temperature limiting value; χ increases with increasing pressure in this temperature range and values of T_F^{**}, the magnetic degeneracy temperature, as a function of pressure are given. The low-temperature results are considered in the light of the Fermi-liquid theory of Landau and its extension to finite temperatures. A plot of reduced susceptibility versus reduced temperature, of the type suggested by Goldstein, indicates that data at all pressures and temperatures may be described closely (within 3%) by a single function. Comparison of this work is made with published results from other laboratories. The spin-lattice relaxation time was also investigated over the same pressure and temperature ranges, and lower limits for $(T_1)_{bulk}$ at low temperatures have been deduced. An analysis of the type suggested by Low and Rorschach was applied for this purpose. The results are the first reported in the Fermi-liquid region, and at higher temperatures they are compared with data published elsewhere. Low-temperature thermometry was facilitated by measurement of the nuclear susceptibility of ^{19}F in the calcium fluoride crystal immersed in the liquid ^3He. (auth)

39729 SOLID-SUPERFLUID TRANSITION IN He^4 AT ABSOLUTE ZERO. Gersch, H. A.; Tanner, J. M. (Georgia Inst. of Tech., Atlanta). Phys. Rev., 139: A1769-82 (Sept. 13, 1965).

A solid-superfluid phase transition applicable to ^4He at the absolute zero of temperature is described, utilizing a cell model. Below the critical density which marks the onset of the superfluid, the system has these properties: The energy for adding a particle to the system without creating excitations becomes equal to that for removing a particle; the excitation spectrum changes from quadratic to linear in momentum for low-momentum excitations; and the zero-momentum state exhibits macroscopic occupation. The maximum occupation of the zero-momentum level is estimated to be about 6%. An estimate of the effective repulsive energy between a pair of ^4He atoms confined within a specific volume yields about 16°K. The excitation spectra obtained from averaging on a simple cubic, a body-centered cubic, and a face-centered cubic system are compared with the experimental curve from neutron inelastic-scattering measurements on liquid helium. (auth)

39730 MEASUREMENTS OF A THERMAL-CONDUCTIVITY LENGTH DEPENDENCE IN HELIUM II. Madden, H. H.; Bohm, H. V.; Cowan, M. D.; Alcaraz, E. C. (Wayne State Univ., Detroit). Phys. Rev., 139: A1783-92(Sept. 13, 1965).

Helium II heat-flow measurements were made in bundles

of hollow glass fibers (<10 μ in diameter) over the temperature range 1.5 to 2.1°K. A linear heat-current-temperature-difference relation was observed using channels 3, 6, and 9 cm in length. The experimental thermal conductivity varies approximately as ^{11}T and decreases with increasing length of the channels; the latter result is apparently not accounted for by the theory of London and Zilsel. This length dependence is shown to be explainable in terms of a nonlinear temperature distribution along the channels. The consequence of this "length effect" on experimental determinations of normal fluid viscosity by heat-flow methods is briefly discussed. (auth)

39731 EFFECTIVE INTERATOMIC POTENTIALS FOR LIQUID HELIUM ABOVE AND BELOW THE λ POINT. Khan, Ashfaq A.; Broyles, A. A. (Univ. of Florida, Gainesville). Phys. Rev., 139: A1805-6(Sept. 13, 1965).

Effective interatomic pair potentials for liquid helium at 1.06 and 2.29°K were computed with the following properties. If the Slater sum is approximated by a Boltzmann factor with these pair potentials, the neutron-diffraction intensities obtained by Henshaw agree with the computed intensities. The effective potential above the λ point (2.29°K) shows a very shallow well displaced toward larger atomic separations. The effective potential below the λ point (1.06°K) shows no well at all but appears as a purely repulsive potential with a very long-ranged tail. (auth)

39732 CALCULATION OF THE THERMAL CONDUCTIVITY OF PURE SUPERCONDUCTING LEAD. Ambegaokar, Vinay; Woo, James (Cornell Univ., Ithaca, N. Y.). Phys. Rev., 139: A1818-23(Sept. 13, 1965).

A calculation of the thermal conductivity of normal and superconducting lead was performed. A semiempirical model for the density of phonon states and the electron-phonon coupling constants is used. The calculation is based on the strong-coupling theory. It is found that the quasiparticle limit of this theory is valid for the calculation. The results are in fair agreement with experiment. A physical explanation for the anomalously large drop in the thermal conductivity of superconducting lead is suggested. (auth)

39733 TRANSMISSION OF MAGNETIC PULSES THROUGH TYPE-II SUPERCONDUCTING PLATES. Meissner, Hans (Stevens Inst. of Tech., Hoboken, N. J.). Phys. Rev., 139: A1920-6(Sept. 13, 1965).

The penetration of perpendicular magnetic pulses of 1.6 μsec duration through a type-II superconducting plate was observed in a perpendicular magnetic field. The plate was a single crystal of Pb with 8% In and had a thickness of 1.65 mm. For large enough pulses the shape of the transmitted pulse agrees closely with that expected from the diffusion equation $\partial^2 H/\partial x^2 = \mu_0 \sigma \partial H/\partial t$. The time delay of the transmitted pulse as well as the height of the transmitted pulse can be used to find the value of an effective resistivity ρ. For large pulses the data obtained by the two methods agree with each other and are all somewhat below a line given by $\rho/\rho_n = (H - H_{c1})/(H_{c2} - H_{c1})$. Near H_{c1} pinning effects are observed: A change ΔH of the superimposed field which aids the pulsed field causes anomalously large pulse penetration. The pulses remain unchanged if ΔH is opposed to the pulsed field. The delay time is not affected by a small change of the superimposed field, indicating that the effective resistivity does not change, but that the change of the superimposed field increases the pressure against the pinning centers and aids the pulse penetration. (auth)

39734 NEW PHENOMENON IN SEMIMETALS AND SEMICONDUCTORS. Esaki, L.; Stiles, P. J. (International Business Machines Corp., Yorktown Heights, N. Y.). Phys. Rev. Letters, 15: 152-4(July 26, 1965).

An unusual effect was observed at low temperatures when a current flowed through and extremely small ohmic contact between a normal metal and a single crystal of Bi, Sb, or semiconducting Bi–Sb alloys. As the current increased to a value I_c, the resistance of the sample switched from a low resistance R_L at low currents to a high resistance R_H. The effect had no polarity with respect to bias voltage. Under certain conditions, when the current is decreased from a value $> I_c$, the transition from R_H to R_L occurs at a current $I_c' < I_c$, causing a hysteresis. A tentative explanation is proposed according to which the region of the single crystal in ohmic contact with the metal becomes superconducting. (D.C.W.)

39735 DEPENDENCE OF SUPERCONDUCTING ENERGY GAP ON TRANSPORT CURRENT BY THE METHOD OF ELECTRON TUNNELING. Levine, James L. (Columbia Univ., New York). Phys. Rev. Letters, 15: 154-6 (July 26, 1965).

The variation of the superconducting energy gap with transport current was studied by electron tunneling. Thin films and a compensated geometry were used to minimize diamagnetic effects. The measurements were made near the transition temperature of the films; the results are in qualitative agreement with the predictions of the Ginzburg-Landau equations. (D.C.W.)

39736 SUPERCONDUCTIVITY OF SELENIUM UNDER VERY HIGH PRESSURE. Wittig, J. (Technische Hochschule, Karlsruhe, Ger.). Phys. Rev. Letters, 15: 159 (July 26, 1965).

The superconducting transition was observed in selenium under a pressure of about 130 kbar. The transition temperature was considered in relation to the dependence of the transition temperature of group-VI B elements upon atomic mass. (D.C.W.)

39737 GAPLESS SURFACE EXCITATIONS IN LIQUID HELIUM. Brewer, D. F.; Symonds, A. J.; Thomson, A. L. (Univ. of Sussex, Eng.). Phys. Rev. Letters, 15: 182-84 (Aug. 2, 1965).

Verification is made of measurements showing that for a given film thickness the onset temperature for superflow was well below that of the specific-heat maximum by as much as 0.4°K although in the bulk the two temperatures coincide. It is also verified that in very fine channels of diameter approximately 70 Å the two temperatures were the same. The experiments were performed by measuring the specific heat of helium contained within the pores of Vycor glass in the approximate temperature range 0.5 to 2.5°K. (J.F.P.)

39738 CHANGE IN THE CRYSTAL STRUCTURE OF SOLID NORMAL HYDROGEN NEAR 1.5°K. Clouter, M.; Gush, H. P. (Univ. of Toronto). Phys. Rev. Letters, 15: 200-203(Aug. 2, 1965).

An effect in the infrared absorption spectrum of solid normal hydrogen was observed which provides evidence that the crystal structure of hydrogen changes in the neighborhood of 1.5°K. The change in spectrum occurs at the same temperature as the λ anomaly in the specific heat. The absorption spectra were obtained using a monochromator equipped with an optical cryostat. It is thought that the observed phase transition arises because of an ordering of the orthomolecules which have a quadrupolar moment. (J.F.P.)

39739 MAGNETIC FIELD DEPENDENCE OF KNIGHT SHIFT DUE TO SPIN-ORBIT COUPLING IN SUPERCONDUCTORS. Bennemann, K. H. (Cambridge Univ., Eng.). Phys. Status Solidi, 10: K123-6(Aug. 1, 1965).

The theory by A. A. Abridosov and L. P. Gorkov (Soviet Physics, 15: 752(1962)) is extended using the Green's functions given by K. Maki (Progr. Theor. Phys., 32: 29(1964)). (J.F.P.)

39740 HIGH FIELD SUPERCONDUCTING ALLOYS FOR PULSE TRANSMISSION. Cummings, A. J. (Edgerton, Germeshausen and Grier, Inc., Las Vegas, Nev.). Rev. Sci. Instr., 36: 1275(Aug. 1965).

The response of a 274-m length of coaxial cable fabricated from a Nb–Zr center conductor and a braided Nb outer conductor to subnanosecond pulses was investigated. The risetime of the superconducting cable and normal lead-in cables was measured to be 0.65 nsec; the risetime of the superconducting cable was calculated to be ap-

proximately 0.61 nsec. Cables of pure Nb were found to be operable at nsec pulse amplitudes in excess of 12 kv. (D.C.W.)

39741 27.6 cm INTERNAL DIAMETER SUPERCONDUCTING MAGNET. Stekly, Z. J. J. (Avco-Everett Research Lab., Everett, Mass.); Lucas, E. J.; de Winter, T. A.; Laverick, C. Rev. Sci. Instr., 36: 1291-6(Sept. 1965).

The design construction and testing of a 27.6 cm bore superconducting magnet are described. The magnet was operated at 32,800 G at an average current of 10 amp and a stored energy level of 300,000 J during a 9 day test. (auth)

39742 MAGNETIC FIELD REDUCTION IN AN EXPANDABLE SUPERCONDUCTING ENCLOSURE. Brown, R. E.; Hubbard, W. M. (Naval Ordnance Lab., Silver Spring, Md.). Rev. Sci. Instr., 36: 1378-9(Sept. 1965).

Results obtained with a device for achieving the reduction of the trapped magnetic field intensity are reported. The device is essentially a flexible-walled superconducting enclosure of variable cross sectional area. (C.E.S.)

39743 TUNGSTEN–PLATINUM ALLOY FOR HEATER WIRE IN CALORIMETRY BELOW 0.1 deg K. Ho, James C.; Phillips, Norman E. (Univ. of California, Berkeley). Rev. Sci. Instr., 36: 1382(Sept. 1965).

A 9% W–91% Pt alloy that is suitable for measurements below about 0.1°K on samples that have small heat capacities is discussed. The heat capacity of the alloy in the temperature range between 0.07 and 1.2°K is illustrated. (C.E.S.)

39744 ON SPECIFIC CONVECTION CURRENTS IN SUPERFLUID SOLUTIONS OF He^3-He^4. Ptukha, T. P. (Inst. of Physics, Kiev). Ukr. Fiz. Zh., 10: 225-6(Feb. 1965). (In Ukrainian).

In experiments involving the study of the superfluidity of $^3He-^4He$ solutions at extremely low temperatures, the presence of convection currents may cause serious errors. Therefore, the potential causes of such currents, except natural convection, were examined in solutions containing $\epsilon = 10^{-2}$ of ^3He at the temperature range from 0.5 to 2.15°K. The results indicated that the temperature gradient may produce a slight oxidation of the container, causing additional convective currents or heat exchange between the liquid and the walls. This is of special importance for experiments involving heat fluxes. As long as no heat is liberated, the heat exchange between the container and the superfluid mixture must be prevented by eliminating causes susceptible to produce a temperature or concentration gradient. (TTT)

39745 SUPERCONDUCTIVITY OF LANTHANUM FILMS. Artemenko, I. A.; Voitovich, I. D. Ukr. Fiz. Zh., 10: 239-40(Feb. 1965). (In Ukrainian).

Vapor-deposited thin lanthanum layers on glass at 10^{-5} mm of Hg pressure were studied in liquid He, in order to determine their superconductivity in the range from 4.2 to 2.5°K. The thickness of the layers was 4000 Å, and their length and width were 10 and 1 mm, respectively. The specific resistance of the layers was measured in the critical temperature range from 3.50 to 3.56°K, after precooling the specimens with liquid N, in order to detect the transition from the normal to the superconducting stage; a current of 60 μamp was used for the test. The specific resistivity of La films was found to be high because the critical current at which there is sudden transition of the film is much lower than in the case of Sn and In films. The data indicate that this critical current is a linear function of the temperature. (TTT)

39746 THE TRANSITION TEMPERATURE OF VARIOUS SUPERCONDUCTING METALS UNDER THE INFLUENCE OF VERY THIN OXIDE LAYERS. Ruehl, W. (Physikalisch-Technische Bundesanstalt, Brunswick). Z. Physik, 186: 190-202(1965). (In German)

The superconducting transition of thin films of Al, In, Tl, Pb, Sn, and Ga^+ was investigated by resistance measurements before and after low temperature oxidation of the surface. The films are condensed onto a crystalline quartz plate to a thickness of about 100 Å or less at a temperature of mostly 105°K. The oxidation process may be understood by the tunneling of electrons from the metal to some acceptor levels of the oxygen molecules at the outside of the oxide layer. Thus, a strong electric field arises which, on the one hand, facilitates the motion of metal ions outwards to form oxide molecules and, on the other hand, is suspected to affect the transition temperature. The experimental results show a shift of the transition to higher temperatures with the metals, Al, In, and Tl, and, with the metals Sn, Pb, and Ga^+, to lower temperatures. These results agree qualitatively very well with previous direct measurements of the influence of surface charges on the superconducting transition of Sn and In. The T_c shift depends clearly upon the film thickness and amounts to about 0.3 to 0.4°K for the thinnest films used. Some experiments are undertaken in order to prove the existence of the electric field. Removing the residual oxygen molecules on top of the oxide layer destroys the acceptor levels and causes a reduction of the transition temperature to the value observed with the oxygen free film. As expected, the thickness of the oxide layer is not important for the magnitude of the T_c shift. (auth)

39747 SUPERCONDUCTIVITY AND PARTICLE SIZE IN HETEROGENEOUS COPPER-LEAD ALLOYS. Raub, Ch. J.; Raub, E. (Univ. of California, San Diego, La Jolla). Z. Physik, 186: 310-18(1965). (In German).

It was shown that small lead particles of a size of 1 μm and smaller distributed in a copper matrix can cause this heterogeneous alloy to exhibit complete superconductivity. According to the size of the lead particles and their distribution the transition temperatures vary between 0.3 and 7°K. (auth)

39748 THE SUPERCONDUCTING TRANSITION WIDTH IN PURE LEAD. Neighbor, J. E.; Cochran, J. F.; Shiffman, C. A. (Massachusetts Inst. of Tech., Cambridge). 9p. (CONF-651-89). Gmelin, AED-CONF-64-140-113.

From 9th International Conference on Low Temperature Physics, Columbus, Ohio, Aug.-Sept. 1964.

The transition width of the transition from the superconducting to the normal state was measured in very pure lead. Results of measurements of the temperature variation of the specific heat at the critical temperature and of the variation of the magnetic susceptibility indicate a transition width of 3×10^{-4}°K or less. (W.L.G.)

39749 MAGNETIZATION OF CURRENT CARRYING COLD WORKED NbZr SUPERCONDUCTING WIRES. Bergeron, C. J. Jr.; Williams, M. W.; Haubold, A. D. (Louisiana State Univ., New Orleans). 12p. (CONF-758-32). Gmelin, AED-CONF-65-003-73.

From American Physical Society Meeting, New York, Jan. 1965.

The paramagnetic effect predicted by the force-free current model was observed, but the quantitative agreement with theory was not good. The force-free calculation does not allow for the observed asymmetry, rather the same paramagnetic flux at I_c is predicted for I parallel to H_{ext} and for I antiparallel to H_{ext}. Results indicate that for small externally imposed transport currents the current is constrained to flow in a helical path whose pitch is determined by the magnitude of the longitudinal external magnetic field, but whose sense appears to be fixed, independent of the direction of the external field. (W.L.G.)

39750 VANADIUM–TITANIUM COMPOSITION IN A SUPERCONDUCTIVE DEVICE. Matthias, Bernd T. (to Bell Telephone Labs., Inc.). U. S. Patent 3,188,530. June 8, 1965. Filed Apr. 24, 1961.

Alloys of the V–Ti system, in the compositional range 10-90 at. % V and 90-10 at. % Ti, are capable of withstanding fields of the order of 88 kG and greater while in the superconducting state and may be worked into wire configurations by conventional metallurgical techniques. A superconducting device includes the alloy, means for maintaining the alloy at a temperature at least as low as its

critical temperature, and means for producing a field of at least 30 kG about at least a portion of the alloy. (A.G.W.)

Neutron Physics

See also REACTOR TECHNOLOGY — Criticality Studies.

39751 (AE-185) A NEW METHOD FOR PREDICTING THE PENETRATION AND SLOWING-DOWN OF NEUTRONS IN REACTOR SHIELDS. Hjaerne, L.; Leimdoerfer, M; (Aktiebolaget Atomenergi, Stockholm (Sweden)). May 1965. 25p.

A new approach is presented in the formulation of removal-diffusion theory. The "removal cross-section" is redefined and the slowing-down between the multigroup diffusion equations is treated with a complete energy transfer matrix rather than in an age theory approximation. The method, based on the new approach, contains an adjustable parameter. Examples of neutron spectra and thermal flux penetrations are given in a number of differing shield configurations and the results compare favorably with experiments and moments-method calculations. (auth)

39752 (AECL-2177) THE AECL SYMPOSIUM ON THE GENERATION OF INTENSE NEUTRON FLUXES, CHALK RIVER, ONTARIO, 22-23 APRIL 1965. (Atomic Energy of Canada Ltd., Chalk River (Ontario)). 76p. (CONF-650433) Dep.; AECL, $2.00 cy.

Separate abstracts were prepared for the 10 included papers. (M.O.W.)

For abstracts of individual papers see: 39753, 39754, 39755, 39756, 39757, 39758, 39759, 39760, 39761, and 39762.

39753 (AECL-2177, Introduction) [INTRODUCTION AND NOTES ON INTENSE NEUTRON GENERATOR]. Lewis, W. B. (Atomic Energy of Canada Ltd., Chalk River (Ontario). Chalk River Nuclear Labs.). 8p.

The cost estimation for building and maintaining an Intense Neutron Generator (ING) is discussed. Various applications are discussed, and a brief outline for the study to be presented of the ING is included. (M.O.W.)

39754 (AECL-2177, Paper 1) THE OVERALL PROJECT. Bartholomew, G. A. (Atomic Energy of Canada Ltd., Chalk River (Ontario). Chalk River Nuclear Labs.). 8p.

The arguments which lead to the selection of the method for neutron production are presented. Diagrams show the thermal neutron assembly, the proton accelerator coupling with the neutron facility, and the system with beam splitting arrangements. The overall plan of the project is discussed. (M.O.W.)

39755 (AECL-2177, Paper 2) THE 65-mA 1-Gev PROTON ACCELERATOR. Tunnicliffe, P. R. (Atomic Energy of Canada Ltd., Chalk River (Ontario). Chalk River Nuclear Labs.). 7p.

The separated-orbit cyclotron proton accelerator is proposed for use with the Intense Neutron Generator. The requirements of the accelerator are described and the cost estimation for building and maintaining operation is discussed. (M.O.W.)

39756 (AECL-2177, Paper 3) THE INTENSE-NEUTRON-GENERATOR TARGET. Fraser, J. S. (Atomic Energy of Canada Ltd., Chalk River (Ontario). Chalk River Nuclear Labs.). 8p.

Lead and bismuth are considered for use as proton beam targets in the Intense Neutron Generator. The physics requirements of the target are studied employing Monte Carlo calculations for thick targets. Problems encountered in the design of the target are discussed. (M.O.W.)

39757 (AECL-2177, Paper 4) THE ING RESEARCH FACILITIES. Milton, J. C. D. (Atomic Energy of Canada Ltd., Chalk River (Ontario). Chalk River Nuclear Labs.). 8p.

Some of the facilities that the Intense Neutron Generator could provide and a brief indication of what might be done with them are described. These facilities are presented in three groups; thermal and near-thermal neutrons, proton and secondary particle beams, and the storage ring. (M.O.W.)

39758 (AECL-2177, Paper 5) NUCLEAR POWER IMPLICATIONS OF ING. Millar, C. H. (Atomic Energy of Canada Ltd., Chalk River (Ontario). Chalk River Nuclear Labs.). 7p.

The potential sources of nuclear energy and AECL's past role in the high-energy nuclear physics field are briefly reviewed. These potential power applications of high-energy accelerators are considered; the state of knowledge of high-energy reactions between charged particles and heavy nuclei, the prospective value of high-energy accelerators to nuclear power development, and the value of the Intense Neutron Generator in furthering such developments. (M.O.W.)

39759 (AECL-2177, Paper 6) RADIO-FREQUENCY SYSTEM FOR THE INTENSE NEUTRON GENERATOR (ING). Ward, A. G. (Atomic Energy of Canada Ltd., Chalk River (Ontario). Chalk River Nuclear Labs.). 7p.

Requirements for a r-f system for use with the Intense Neutron Generator are given. The transit-time devices such as triodes, tetrodes, klystrons, and amplitrons are discussed. A block diagram shows a system which may be used. (M.O.W.)

39760 (AECL-2177, Paper 7) SOME ENGINEERING PROBLEMS WITH AN INTENSE NEUTRON GENERATOR. Wolfe, W. A. (Atomic Energy of Canada Ltd., Chalk River (Ontario). Chalk River Nuclear Labs.). 7p.

Protons accelerated to 1 Bev by controlled electric fields and steered by precise magnetic fields, strike a flowing liquid lead–bismuth eutectic target, causing a nuclear cascade, and thus produce a flux of 10^{16} n/cm^2. The engineering required for this and to maintain a vacuum of 10^{-6} torr for the proton beam is discussed. Engineering aspects of the liquid-metal target, beam focusing, beam transport, beam deflection, r-f cavities, magnet design, and vacuum systems are discussed. (M.O.W.)

39761 (AECL-2177, Paper 8) SHIELDING AND ACTIVATION. Ewan, G. T. (Atomic Energy of Canada Ltd., Chalk River (Ontario). Chalk River Nuclear Labs.). 7p.

Activation and shielding problems associated with the final stage of the proton accelerator for the Intense Neutron Generator and with the neutron target area, are discussed. Activation data of aluminum, carbon, copper, and iron are presented. (M.O.W.)

39762 (AECL-2177, Paper 9) POSSIBLE NUCLIDE PRODUCTION IN THE INTENSE NEUTRON GENERATOR. Rowat, D. L. (Atomic Energy of Canada Ltd., Ottawa (Ontario). Commercial Products Div.). 7p.

The possibilities of commercial nuclide production in the Intense Neutron Generator are discussed. The possibility of producing heavy elements is considered. The estimated annual yields for beryllium-7, cobalt-57, cobalt-58, and barium-133 are given. (M.O.W.)

39763 (EUR-2413.e) ON THE INTERPRETATION OF THE EXPONENTIAL EXPERIMENT IN NATURAL URANIUM. Dierckx, R.; Kistner, G.; Misenta, R. (European Atomic Energy Community, Ispra (Italy)). Joint Nuclear Research Center. 1965. 24p.

A summary of the results of two exponential experiments in natural uranium is given. The experiments were performed at Los Alamos and Saclay. The experiments are analyzed and a systematic difference of the relaxation lengths, measured with detectors sensitive to high and low energy neutrons, is found. This systematic difference disappears upon application of corrections that are functions of the energy of the detected neutrons. These energy-dependent corrections increase the asymptotic diffusion length by about 1% for both experiments, compared with the asymptotic diffusion length obtained by energy-independent corrections. (auth)

39764 (GA-6087(Rev.)) NEUTRON CROSS SECTIONS FOR U^{238}. Joanou, G. D.; Stevens, C. A. (General Atomic, San Diego, Calif. John Jay Hopkins Lab. for Pure and Applied Science). Apr. 16, 1965. Contract SNPC-27. 22p. (NASA-CR-54290(Rev.)).

Compiled and evaluated data were incorporated into the GAM-II slowing down program and into the GATHER-II thermalization program. Tables are given of ^{238}U resonance parameters, comparisons of calculated values and values from Hellstrand's empirical formulas for the resonance integrals of U metal and UO_2, and ^{238}U neutron cross sections from 0.001 to 2.380 ev and from 0.01 to 15.0 Mev. (M.J.T.)

39765 (INR-611/IX-A/R) THE INITIAL VALUE PROBLEM FOR A SLAB WITH ANISOTROPIC SCATTERING. Mika, Janusz (Institute of Nuclear Research, Warsaw (Poland)). Apr. 1965. 27p. (CONF-650504-43). Dep.

From IAEA Symposium on Pulsed Neutron Methods, Karlsruhe, Ger.

The spectral properties of the Boltzmann operator describing the transport of monoenergetic neutrons with anisotropic scattering in a slab are considered. The Hille–Yosida theorem is applied to obtain the semigroup of operators solving the initial value problem. (auth)

39766 (ORNL-TM-1171) A NEW METHOD FOR THE EVALUATION OF NEUTRON EMISSION, KERMA, KERMA EQUIVALENT, DOSE EQUIVALENT AND THE SPECTRUM BELOW 1 Mev FOR (α,n) SOURCES, USING BONNER SPHERES. Mehta, S. K. (Oak Ridge National Lab., Tenn.). July 1965. Contract W-7405-eng-26. 154p. Dep.(mn); $5.00(cy), 3(mn) CFSTI.

Thesis presented to Univ. of Tennessee, Knoxville.

Neutron emission (F), kerma (K), kerma equivalent (Keq), dose equivalent (DE), the ratios K/F, Keq/F, and DE/F, and an upper bound to the neutron spectrum below 1 Mev were obtained for Am–Be, Pu–Be, Po–Be, and Am–B neutron sources by using modified Bonner sphere neutron spectrometer. The spectrometer consisted of 0- to 12-in.-diam. Bonner spheres and 0- to 3-in.-diam. spheres modified by the addition of boron and cadmium covers. The results were computed by the OPTIMO linear programming code which synthesizes optimal combinations of the response of the various spheres. The known smoothness of the neutron spectra from the source is utilized, and an upper bound to the spectra above 5.5 Mev is taken from other measurements, since the response of the Bonner spheres does not have enough variation above 5.5 Mev. The response of the modified spheres to monoenergetic neutrons was calculated by assuming exponential absorption below 1 kev and by S_n transport calculations above 1 kev. The errors given refer to the 68 per cent confidence intervals and include all known sources of error. (auth)

39767 (ORNL-TM-1192) SOURCE, A NEUTRON DISTRIBUTION ROUTINE FOR THE 05R MONTE CARLO CODE. Mihalczo, J. T.; Morrison, G. W.; Irving, D. (Oak Ridge National Lab., Tenn.). July 8, 1965. Contract W-7405-eng-26. 14p. Dep. mn; CFSTI, $1.00 cy, $0.50 mn.

SOURCE is a FORTRAN 63 program for determining the energy, speed, and initial spatial distribution of neutrons arising from fission. The energy distribution within the batch of neutrons is obtained by sampling a Maxwellian fission spectrum which depends upon the energy of the neutrons producing fission. The program locates the neutrons at a point or distributes them spatially, either uniformly or according to a cosine function. Two isotopes producing fission neutrons having a slightly different energy distribution can be treated in the program by an approximation (using an average temperature) giving the correct first moment of the resulting overall energy distribution. (auth)

39768 (RPI-328-21) ASYMPTOTIC AND STEADY STATE SPECTRUM MEASUREMENTS IN A MULTIPLYING MEDIUM. Cerbone, R. J.; Gaerttner, E. R.; Slovacek, R. E. (Rensselaer Polytechnic Inst., Troy, N. Y. Dept. of Nuclear Engineering and Science). [1964]. Contract AT(30-3)-328 7p. Dep. mn; CFSTI, $1.00 cy, $0.50 mn.

The asymptotic technique and the steady state technique were used to measure the slow neutron spectrum in a homogeneous multiplying medium. For both types of measurement, the neutron beam was obtained from the center as well as the surface of the medium. The ability of calculational methods to determine the slow neutron spectrum in a pulsed subcritical system is examined. (M.O.W.)

39769 (SC-DC-65-1544) ENERGY TRANSFER BY NEUTRONS TO CERTAIN MATERIALS. Buckalew, W. H. (Sandia Corp., Albuquerque, N. Mex.). [June 1965]. Contract AT(29-1)-789. 8p. (CONF-650707-2). Dep. (mn); $1.00(cy), 1(mn) CFSTI.

From IEEE Annual Conference on Nuclear and Space Radiation Effects, Ann Arbor, Mich.

The energy absorbed in hydrogen, carbon, nitrogen, oxygen, aluminum, silicon, germanium, tantalum, and bismuth from interactions with neutrons in the energy range of 0 to 14 Mev is calculated. In these calculations the results were normalized to one neutron per square centimeter incident per gram of target material, thus making it a simpler matter to calculate the energy absorbed in compounds containing these elements. (M.O.W.)

39770 A NEW NEUTRON GENERATOR TUBE. de La Barre, F. Electron. Ind. (Paris), No. 72, 112-16(1964). (In French)

A neutron generator that is simple, easy to control, and portable was developed. Its principle is indicated by describing the tube and examining some of its industrial application. (J.S.R.)

39771 ON THE MONOENERGETIC NEUTRON TRANSPORT PROBLEM FOR HOMOGENEOUS PLANE SLABS. Collatz, S. (Zentralinstitut fuer Kernforschung, Rossendorf, Ger.). Kernenergie, 8: 283-91(May 1965). (In German).

The monoenergetic neutron transport problem for a homogeneous plane slab is solved in an improved way by expansion in the eigenfunctions of the transport equation. The extrapolation distance for a thick slab was calculated in some approximations using two simple methods of calculation (use of slide rule is sufficient). Finally, the infinite two-zone problem is studied. (auth)

39772 NEUTRON SOURCES AND NEUTRON FIELDS. Michaelis, W. (Kernforschungszentrum, Karlsruhe, Ger.). Kerntechnik, 7: 256-61(June 1965). (In German)

After a brief survey on the various types of nuclear reactions for neutron production, energetic considerations are made, and the properties of the most important neutron sources are discussed. Radioactive sources, neutron production with artificially accelerated particles as well as by nuclear reactors are considered. The general formalism for the description of neutron fields is given. The special case of the slowing down spectrum is treated in more detail. Deviations from the 1/E dependence of this spectrum are discussed. (auth)

39773 DISCRETE RELAXATION TIMES IN NEUTRON THERMALIZATION. Kuscer, Ivan; Corngold, Noel (Brookhaven National Lab., Upton, N. Y.). Phys. Rev., 139: 981-90(Aug. 2, 1965). (BNL-8920).

On the basis of the Van Hove theory, an analysis is given of those properties of the neutron-scattering law which influence the decay constants (the reciprocal relaxation times) in neutron thermalization. It is shown how the known differences in the long-time behavior of the correlation functions for a gas, a liquid, and a solid are reflected in the different behavior of the differential cross sections at low energies. This behavior ultimately determines the general character of the spectrum of decay constants for a uniform neutron distribution in an infinite medium. For a gaseous moderator, either there is an infinite set of discrete decay constants, strongly accumulating towards the lower limit $\lambda^* = \min[v\Sigma(v)]$ of the continuous spectrum, or else the spectrum below λ^* is empty altogether. On the other hand, for a solid, the set of discrete decay constants is always finite, or possibly empty. The liquid appears to allow, in principle, all three possibilities, but normally the spectrum is expected to resemble that of a solid. In any

case, the existence of the lowest decay constant λ_0 (and hence the existence of an infinite set for a gas) is trivial whenever absorption is absent or of the 1/v kind. Only an absorption rate $v\Sigma_a(v)$ which strongly increased in the small-v region could cause the complete disappearance of the discrete spectrum. In this event any initial neutron distribution slowly evolves towards a singular distribution containing a $\delta(v)$ term, or some weaker singularity, and the decay rate approaches λ^*. (auth)

Nuclear Properties and Reactions

Refer also to abstracts 38744, 38786, 39403, 40112, and 40115.

39774 (AEET-209) FISSION PRODUCTS DATA AND ITS APPLICATION IN STUDYING FALLOUT FROM NUCLEAR WEAPON TESTS. Rangarajan, C.; Mishra, U. C.; Lalit, B. Y.; Gopalakrishnan, Sarada; Sadasivan, S. (comps.) (Atomic Energy Establishment, Trombay (India)). 1965. 27p. Dep. mn.

Relevant data on the fission products released in nuclear weapon tests are tabulated. The respective tables give: half life and beta and gamma energies; yields for thermal, fission spectrum, and 14-Mev neutrons on ^{233}U, ^{235}U, ^{238}U, ^{232}Th, and ^{239}Pu; and production ratios from bomb debris data. (D.L.C.)

39775 (AEEW-M-513) NEUTRON CROSS-SECTIONS OF Be9 IN THE ENERGY RANGE 1 Mev TO 15 Mev. Doherty, G. (Atomic Energy Establishment, Winfrith (England)). Mar. 1965. 13p. Dep.; BIS, $0.40; HMSO, 2s.

Self consistent neutron cross sections for the energy range 1 to 15 Mev are tabulated. The cross section for the (n,2n) reaction in the important energy region 2–4 Mev is still not well determined but the shape was adjusted to give agreement with a recent integral measurement. The angular distribution of elastically scattered neutrons, and the energy distribution of neutrons from the (n,2n) reaction are not reviewed. (auth)

39776 (AEEW-M-517) MLBW—A MULTI-LEVEL BREIT-WIGNER COMPUTER PROGRAMME. Gregson, K.; James, M. F.; Norton, D. S. (Atomic Energy Establishment, Winfrith (England)). Mar. 1965. 19p. Dep.; BIS, $0.40; HMSO, 2s. 0d.

MLBW is a Fortran computer program that calculates unbroadened neutron cross-sections for a non-fissile natural element from resonance parameters, using the multilevel Breit-Wigner approximation. Resonances can be considered that are excited by neutrons with orbital angular momentum quantum numbers 1 ranging from 0 to 5. (auth)

39777 (AEEW-M-518) TEMPO—A GENERAL DOPPLER BROADENING PROGRAMME FOR NEUTRON CROSS-SECTIONS. Gregson, K.; James, M. F. (Atomic Energy Establishment, Winfrith (England)). Feb. 1965. 13p. Dep.; BIS, $0.40; HMSO, 2s. 0d.

TEMPO is a Fortran computer program which uses numerical quadrature to calculate Doppler broadened cross sections from tabulated values of the unbroadened cross sections. (auth)

39778 (BNL-9355) ACTIVITY REPORT ON BROOKHAVEN WORK ON THE COMPILATION, STORAGE AND EVALUATION OF NUCLEAR CROSS SECTION DATA. Chernick, Jack (Brookhaven National Lab., Upton, N. Y.). [May 1965]. Contract AT(30-2)Gen-16. 19p. (CONF-650524-3). Dep. mn; CFSTI, $1.00 cy, $0.50 mn.

From European Nuclear Energy Agency and Atomic Energy Commission Seminar, Upton, N. Y.

The history of neutron data evaluation at Brookhaven is presented. Bibliographies of Sigma Center publications and technical reports, AEC publications, reactor cross section evaluation publications (technical reports), and journal articles are included. (M.O.W.)

39779 (IEA-86) TOTAL NEUTRON CROSS SECTIONS OF PRASEODYMIUM, YTTERBIUM, LUTETIUM AND ERBIUM. Amaral, L. Q.; Abreu, M.; Bianchini, F. G.; Mattos, M. C. (Instituto de Energia Atomica, Sao Paulo (Brazil)). 1963. 28p. (CONF-631104-3) Dep. mn.

From Meeting on the Utilization of Research Reactors, Sao Paulo, Brazil.

The total neutron cross section of oxides of the rare earths praseodymium, ytterbium, lutetium and erbium was measured by transmission within the neutron energy range 0.0005 to 1 electron volt, and very special attention was given to obtain values at the thermal energy 0.025 ev. The oxide samples were at a high degree of purification. A nuclear resonance presented in the considered energy range in ^{176}Lu was studied; the parameters found agree with the published values. The theoretical expected behavior of the cross section at low energy enables one to determine the partial cross sections at thermal energy, however not too accurately. (auth)

39780 (INR-596/PL) A STUDY OF THE ENERGY SPECTRUM OF ALPHA PARTICLES FROM THE $Tb^{159}(n,\alpha)Eu^{156}$ REACTIONS WITH 14.2 Mev NEUTRONS. Jaskola, M.; Osakiewicz, W.; Turkiewicz, J.; Wilhelmi, Z. (Institute of Nuclear Research, Warsaw (Poland)). Jan. 1965. 12p. Dep.

The energy spectrum of α-particles from $^{159}Tb(n,\alpha)^{156}Eu$ reaction at 14.2 Mev was studied using semiconductor detector techniques. The characteristic feature of the observed energy spectrum is the existence of four separate maxima in the energy region 15–21 Mev. The positions of these maxima are explained assuming that there exists a large contribution of the knock-out process in the mechanism of the investigated reaction. (auth)

39781 (JAERI-1073) LOW-ENERGY GAMMA-RAY SPECTRA FOLLOWING RESONANCE NEUTRON CAPTURES. MEASUREMENT BY AN NaI SCINTILLATION SPECTROMETER. Kawarasaki, Yuki (Japan Atomic Energy Research Inst., Tokyo). Oct. 1964. 44p. Dep. mn.

The energies and relative intensities of the prominent peaks of the gamma spectra in their low energy portions, following the neutron captures at the resonances of neutron energy less than 20 ev were measured with a single NaI(Tl) crystal scintillation spectrometer. The JAERI 20-Mev Linac was used as the pulsed neutron source and the time-of-flight method to select the neutron energies of resonances. The elements investigated were Ag, Cd, In, Sb, Sm, Eu, Dy, Er, Tm, Hf, Ta, Pt, and Au. (auth)

39782 (JINR-P-2191) O TOCHNOSTI RASCHETA CHASTOTY KOLLEKTIVNYKH KOLEBANII YADER V RAMKAKH METODA U,V-PREOBRAZOVANIYA. (On Accuracy of Calculations of Collective Oscillation Frequency by u-v Transformation Method). Bang, E. M.; Dzholos, R. V.; Markov, A. S.; Mikhailov, I. N. (Joint Inst. for Nuclear Research, Dubna (USSR). Lab. of Theoretical Physics). 1965. 14p. Dep. mn.

The frequencies of octupole oscillations of rare-earth nuclei are calculated on the basis of the method which allows to take into account the conservation of the number of particles more accurately than by the method of approximate secondary quantization. The calculations show that the modification of the theory leads to a more smooth dependence of the collective oscillation frequency on A and Z. The results vary more essentially when describing nuclei at the beginning of the rare-earth group. (auth)

39783 (ORNL-P-1345) ON RADIATIVE TRANSITION IN ^{207}Pb AND ^{208}Pb FOLLOWING RESONANCE NEUTRON CAPTURE ON ^{206}Pb AND ^{207}Pb. Biggerstaff, J. A.; Bird, J. R.; Gibbons, J. H.; Good, W. M.; Macklin, R. L. (Oak Ridge National Lab., Tenn.). [1964]. Contract W-7405-eng-26. 3p. (CONF-650706-6). Dep.(mn); $1.00(cy), 1(mn) CFSTI

From International Conference on the Study of Nuclear Structure with Neutrons, Antwerp.

Neutron transmission measurements of ^{206}Pb and ^{207}Pb

were made. This permitted the study of radiative transitions in ^{207}Pb and ^{208}Pb. Results of this study are presented. (M.O.W.)

39784 (ORNL-P-1352) STRONG p-WAVE NEUTRON RESONANCES IN ^{120}Sn, ^{116}Sn AND ^{124}Sn. Harvey, J. A.; Fuketa, Toyojiro (Oak Ridge National Lab., Tenn.). [1963]. Contract W-7405-eng-26. 4p. (CONF-650706-8) Dep.(mn); $1.00(cy), 1(mn) CFSTI

From International Conference on the Study of Nuclear Structure with Neutrons, Antwerp.

Neutron transmission measurements were made on 10 cm thick metal samples of ^{120}Sn and ^{116}Sn. Measurements were also made on a 2.5 cm thick sample of ^{124}Sn. The resonances were analyzed with the area and shape analysis programs which include Doppler and resolution broadening. Resonance results are presented. (M.O.W.)

39785 (ORNL-P-1356) INTERMEDIATE STATES AS OBSERVED BY DIFFERENTIAL SCATTERING OF NEUTRONS BY DOUBLY CLOSED SHELL NUCLEI. Johnson, C. H.; Fowler, J. L. (Oak Ridge National Lab., Tenn.). [1964]. Contract W-7405-eng-26. 5p. (CONF-650706-3). Dep.(mn); $1.00(cy), 1(mn) CFSTI.

From International Conference on the Study of Nuclear Structure with Neutrons, Antwerp.

The differential cross section and phase shift analyses for neutrons scattered from ^{16}O and ^{208}Pb are included. Results were corrected for the effects of spurious neutron backgrounds, self-attenuation and multiple scattering in the sample, finite angular resolution, and the energy dependence of the detector efficiency. (M.O.W.)

39786 (ORNL-P-1419) INFORMATION ON CONVERSION COEFFICIENTS FROM COULOMB EXCITATION AND LIFE-TIME MEASUREMENTS. Stelson, P. H. (Oak Ridge National Lab., Tenn.). [1965]. Contract W-7405-eng-26. 22p. (CONF-650525-5). Dep. mn; CFSTI, $1.00 cy, $0.50 mn.

From International Conference on the Internal Conversion Process, Nashville, Tenn.

A review of all the available information on total E2 conversion coefficients for even-even 2+ → 0 transitions for rare-earth and very heavy nuclei is presented. Tables of conversion coefficient data, both experimental and theoretical, are presented. (M.O.W.)

39787 (SGAE-PH-19/1965) MESSUNG VON PAARER-ZEUGUNGSQUERSCHNITTEN FUR 6.13 Mev GAMMA-STRAHLUNG. (Measurement of Pair Production Cross Sections for 6.13 Mev Gamma Rays). Bak, Hae-Ill; Weinzierl, Peter (Oesterreichische Studiengesellschaft fuer Atomenergie G.m.b.H., Seibersdorf. Physik-Institut). 1965. 10p.

The pair production cross section for Cu, Ni, and Ag were measured for the 6.13-Mev gamma radiation of ^{16}N. Through a combination of transmission measurements with a relativity measurement of the pair production events for the selected elements, the pair production cross section could be determined without use of the theoretical values for the Compton cross section. The results agree within the limits of error of 3 to 7% with the Bethe-Heitler theory. (tr-auth)

39788 (UCRL-12204, pp 1-27) NUCLEAR AND ATOMIC PHYSICS. (Lawrence Radiation Lab., Univ. of California, Livermore).

A brief discussion of each of the following is included; nuclear structure, correction to the potential in Born approximation arising from direct channel strips, reciprocal bootstrap mechanism, least-squares analysis and significance tests for a set of functions of discrete abscissas, pion-proton phase-shift analyses, possible electromagnetically induced muonium-antimuonium conversion, K_1^0 regeneration by magnetic field and apparent CP violation, the Lehmann, Symanzik, and Zimmerman formalism in the Lee model, reaction threshold tabulations, epithermal fission cross sections of americium-241, the angular distribution, and polarization of neutrons from the ^{9}Be(p,n$_0$)^{9}B and ^{11}B(p,n$_0$)^{11}C reactions, beta decay asymmetry and nuclear magnetic moment of argon-35, magnetic studies at the Livermore pool type reactor, M-shell fluorescence yields of bismuth, lead, gold, and osmium, copper L_{III} shell x ray production by 25 to 100 kev protons, effect of thin carbonaceous films on 500 kev helium ion sputtering of copper, energy distribution of gamma rays in the atmosphere, and the polarization of neutrons from the ^{12}C(p,n$_0$) ^{13}N and ^{15}N(p,n$_0$)^{15}O reactions. (M.O.W.)

39789 NEW ALPHA-DECAY BARRIER PENETRABILITIES WITH IGO POTENTIAL: EVEN- AND ODD-MASS NUCLEI. Kohlmann, L.; Voeroes, T. (Central Research Inst. for Physics, Budapest). Acta Phys. Acad. Sci. Hung., 18: 284-94(1965).

The IGO potential is used for the calculation of barrier penetrabilities for ground- and excited-state transitions of even-mass nuclei and for transitions of odd-mass nuclei, measured after 1959. The barrier penetration factors were calculated by numerical integration in the WKB approximation, taking into account centrifugal barrier effects for even-even nuclei, but ignoring noncentral interactions. Using the calculated penetration factors and the experimental alpha half lives, the reduced level widths were calculated in each case. Hindrance factors for odd-mass alpha-particle emitters are also given. (auth)

39790 INVESTIGATION OF $Mo^{92}(n,2n)Mo^{91,91m}$ REACTION. Bacso, J. (Inst. of Nuclear Research, Hungarian Academy of Sciences, Debrecen, Hungary); Csikai, J.; Pazsit, A. Acta Phys. Acad. Sci. Hung., 18: 295-8(1965).

The occurrence of ^{92}Mo(n,2n)^{91m}Mo reaction was demonstrated at 14.8-Mev neutron energy, and the isomeric cross-section ratio $\sigma_g/\sigma_m = 10.6$ was determined. For the reactions ^{92}Mo(n,2n)^{91g,91m}Mo, the cross-section values $\sigma_g = 159$ mb, and $\sigma_m = 15$ mb were found. (auth)

39791 CALCULATION OF NUCLEAR QUADRUPOLE MOMENTS. Tisza, M. (Univ. for Technical Sciences, Budapest). Acta Phys. Acad. Sci. Hung., 18: 321-4(1965).

The quadrupole moments of some nuclei are determined, starting from Skyrme's semiempirical energy formula for a nucleon gas and minimizing the energy by means of a three-parameter variational expression for the nucleon density. The quadrupole moments are calculated from the obtained densities, and the results are compared with the empirical data. (auth)

39792 ON THE MAGNETIC PROPERTIES OF THE ^{153}Eu NUCLEUS. Bochnacki, Z.; Ogaza, S. (Inst. of Nuclear Phys., Krakow). Acta Phys. Polon., 27: 649-53 (1965).

Experimental data on the magnetic properties of the ^{153}Eu nucleus are analyzed in terms of the effective spin g-factor. The first-order Coriolis coupling corrections to the magnetic moments of ^{153}Eu are calculated, and the corrected expressions are used to evaluate the effective spin g-factor. The spin polarization is then estimated using a simple spin-spin long-range nucleon-nucleon force, and it is shown that the spin polarization explains the observed change of g from its free-nucleon value. (D.C.W.)

39793 A SIMPLIFIED PROCEDURE FOR SHELL MODEL CALCULATIONS OF ALPHA DECAY RATES OF EVEN-EVEN DEFORMED NUCLEI. Sandulescu, A.; Stancu, F. (Inst. for Atomic Physics, Bucharest). Acta Phys. Polon., 27: 655-69(1965).

A simplified expression of the overlap integral which occurs in the alpha decay theory was obtained using a harmonic oscillator wave function for the intrinsic alpha-particle wave function, the frequency of which being equal to the frequency of the shell model. By means of this simplified expression, by projecting out from the superfluid model wave function with 24 proton and 24 neutron Nilsson levels, an internal alpha-particle wave function was calculated first. The reduced intensity b_2 for some transuranium elements was then calculated using the modified Fröman's matrix method for treating the propagation

through the anisotropic barrier. The theoretical results describe well the variation with the mass number of the experimental reduced relative intensity b_2, but the values obtained by us are larger than the experimental ones and also than the Mang and Rasmussen results previously obtained, using a superfluid model wave function with 10 proton and 10 neutron Nilsson levels. (auth)

39794 STRESS-INDUCED VARIATIONS IN THE SPECTRAL DISTRIBUTION OF γ-RADIATION FROM Cs^{137} TRANSMITTED BY GRAPHITED CARBON. Bujok, J. (Central Mining Institute, Katowice, Poland); Sujak, B. Acta Phys. Polon., 27: 671-80(1965).

Variations in the spectral energy distribution of ^{137}Cs gamma radiation transmitted by graphitized carbon were investigated in their dependence on vertical load in order to clarify observed variations in the intensity of gamma radiation scattered on carbon due to stresses. (D.C.W.)

39795 ADVANCED MÖSSBAUER-EFFECT EXPERIMENTS. Haskins, J. R. (Gettysburg Coll., Penna.). Am. J. Phys., 33: 646-56(Aug. 1965).

Various possible student experiments with the Mössbauer effect beyond the basic resonance experiments are discussed. The information was collected on visits to various research and teaching laboratories in which Mössbauer experimentation is carried on. (auth)

39796 STUDY OF THE NUCLEAR LEVELS OF BISMUTH-212 (ThC) EXCITED IN THE α DECAY OF ASTATINE-216. Briand, Jean-Pierre; Chevallier, Pierre (Universite, Paris). Compt. Rend., 260: 5251-4(May 17, 1965). (In French).

The α fine structure of the nuclear levels of ^{212}Bi, excited during the α decay of ^{216}At, was studied by observation. Eight new rays of the α fine structure were detected. The ^{212}Bi levels thus obtained were compared with those already known from the study of the transition $^{212}Pb(ThB) \xrightarrow{\beta^-}$ ThC. (tr-auth)

39797 CROSS SECTIONS FOR SOME (n,2n) REACTIONS. Vuletin, J.; Cindro, N. (Faculty of Electrical Engineering, Split, Yugoslavia). Glasnik Mat.-Fiz. Astron., Ser. II, 19: 269-73(1964).

The total cross sections for $^{14}N(n,2n)^{13}N$ and $^{19}F(n,2n)^{18}F$ reactions were measured by the activation method and the results compared to the predictions of the compound nucleus theory. The discrepancies between theory and experiment are explained in terms of the failure of the suppositions of the simple statistical theory. (auth)

39798 STUDY OF (n,p) AND (n,d) REACTIONS ON ^{10}B AT 14.4 Mev. Valkovic, V.; Tomas, P.; Slaus, I.; Cerineo, M. (Inst. Ruder Boskovic, Zagreb). Glasnik Mat.-Fiz. Astron., Ser. II, 19: 285-300(1964).

Proton, deuteron, and triton spectra were obtained from 14.4 Mev neutrons incident on a boron-10 target. The proton and deuteron differential cross sections were obtained. Study of $^{10}B(n,p)^{10}Be$ reactions showed that processes leading to low excited states of ^{10}Be are predominantly direct interactions. It is also seen that either the effective neutron-proton interaction is spin-independent or the interaction in the singlet state of the spin-dependent interaction is weaker than in the triplet one. Deuteron spectra from the $^{10}B(n,d)^{9}Be$ revealed only two peaks corresponding to the ground state and 2.43 Mev state of ^{9}Be. Limits could only be placed on groups related to other states. Analysis of the angular distribution showed the configuration of the ground state of boron-10. (J.F.P.)

39799 VARIATIONAL TREATMENT OF THE HeH^+ ION AND THE β-DECAY IN HT. Wolniewicz, L. (Univ. of Chicago). J. Chem. Phys., 43: 1087-91(Aug. 15, 1965).

The nonrelativistic energies of the HeH^+ ion were computed by the variational method for the ground state and for the first excited $^1\Sigma^+$ state. The wave function employed was a 64-term generalized James–Coolidge expansion. The computed binding energy of the ground state amounts to $D_e = 16448.3\ cm^{-1}$ at the equilibrium separation $R_e = 1.46324$ au. The excited state was found to be repulsive. The HeH^+ wavefunctions were used to compare quantitatively the theory of β decay in molecules with experiment. It is shown that for the HT molecule, the theory predicted the dissociation in at least 17.8% of the events while the corresponding experimental number was 6.8% ± 1.9%. (auth)

39800 YIELDS OF ^{85}Kr IN THERMAL NEUTRON FISSION OF ^{235}U AND ^{239}Pu. Katcoff, S.; Rubinson, W. (Brookhaven National Lab., Upton, N. Y.). J. Inorg. Nucl. Chem., 27: 1447-50(July 1965). (BNL-8555).

By absolute radiochemical measurements the yields of 10.76-yr ^{85}Kr in thermal neutron fission of ^{235}U and ^{239}Pu were determined: (0.273 ± 0.004)% and (0.099 ± 0.004)%, respectively. The indicated errors are standard deviations per determination. Detailed investigation of possible sources of error in the fission counting, separation procedure, and ^{85}Kr gas counting led to overall error estimates of ±3% in the yield from ^{235}U and of ±5% in the yield from ^{239}Pu. (auth)

39801 THE DECAY OF ^{189}W. Kauranen, P.; Ihochi, H. (Univ. of Arkansas, Fayetteville). J. Inorg. Nucl. Chem., 27: 1451-56(July 1965).

^{189}W was produced through the reaction $^{192}Os(n,\alpha)^{189}W$ and its half life was determined to be 11.5 ± 0.3 min. Gamma rays with an energy of 130, 178, 258, and 417 kev as well as others with lower intensity were observed. Some coincidence measurements are reported. An endpoint energy of 2.5 ± 0.2 Mev for the β spectrum of ^{189}W was obtained. (auth)

39802 HELIUM ION-INDUCED FISSION OF ^{194}Pt, ^{195}Pt AND ^{196}Pt AT 41 AND 34 Mev. Neuzil, E. F.; Phelps, M. E.; Ross, F. (Western Washington State Coll., Bellingham). J. Inorg. Nucl. Chem., 27: 1463-70(July 1965).

A study was made of the 41- and 34-Mev helium ion-induced fission of enriched platinum isotopes ^{194}Pt, ^{195}Pt, and ^{196}Pt. The fission fragment mass distribution curves were all gaussian in shape but the even-even species ^{194}Pt and ^{196}Pt produced curves, which were wider than the even-odd species ^{195}Pt. In addition as the bombarding energy was lowered to 34 Mev, the width at half maximum, $W_{\frac{1}{2}}$, of even-even species curves decreased from about 22 ± 1 (at 41 Mev) mass units wide at the half maximum to 17 ± 1 (at 34 Mev) mass units, whereas the width for ^{195}Pt remained rather constant with a value of $W_{\frac{1}{2}}$ of 17 ± 1 mass units. It also appeared that the value of the cross section (σ_f) for fission decreased much more rapidly with decreasing energy for ^{195}Pt than for ^{194}Pt and ^{196}Pt. At 41 Mev the values of σ_f for ^{194}Pt, ^{195}Pt, and ^{196}Pt were 22.1, 79.6, and 24.7 μbarns, respectively. At 34 Mev the values were 9.1, 2.16, and 8.2 μbarns, respectively. (auth)

39803 THE SHORT-LIVED ^{127}Sn ISOMER. Kauranen, P. (Univ. of Helsinki). J. Inorg. Nucl. Chem., 27: 1713-15(July 1965).

Because of the proximity of the low-lying $h_{11/2}$ and $d_{\frac{3}{2}}$ (or $S_{\frac{1}{2}}$) neutron states, nuclear isomerism was predicted and observed in most odd-A tin isotopes. ^{127}Sn was produced through the (n,α) reaction from ^{130}Te, and the decay of the short-lived ^{127}Sn was directly observed after rapid chemical separation of the tin fraction. It was concluded that the observed activity of approximately 4 min was the short-lived ^{127}Sn isomer, and that the decay of ^{127}Sn isomer was connected with the emission of the 495-kev γ ray. A value of 4.1 ± 0.3 min is given, as a weighted mean, for the half life. The similarity between the two decay structures suggested that the 4.1-min ^{127}Sn was the low spin isomer. (F.J.H.)

39804 INELASTIC SCATTERING OF 6.35-Mev DEUTERONS. LIMIT OF EXCITATION OF THE 3.56-Mev LEVEL (T = 1). Johnson, G.; Langevin-Joliot, H.; Roussel, P. (Laboratoire Joliot-Curie de Physique Nucleaire, Orsay, France). J. Phys. (Paris), 26: 161-6(Apr. 1965). (In French).

An investigation of the $^6Li(d,d')^6Li^*$ (3.56 Mev) reaction, $E_d = 6.35$ Mev, which is forbidden by the isotopic spin selection rule is described. The experiment is based

on geometric discrimination through the use of semiconductor detectors for the recoil nucleus and the scattered particle. A probable upper limit is given of the ratio of the differential cross section of the T = 1 forbidden reaction to that of the $^{6}Li(d,d')^{6}Li^{*}$ (2.18 Mev) T = 0 allowed reaction of <3.5 (±3) 10^{-4} and <2 (±1.5) 10^{-4} 50 and 60° respectively. Sequential reactions such as $^{12}C(d,n)^{13}N^{*}(p + {}^{12}C)$ were observed. (auth)

39805 THEORY OF NUCLEAR REACTIONS. IX. FEW-LEVEL APPROXIMATIONS. Mahaux, C. (Univ. of Liege). Nucl. Phys., 71: 241-66(1965).

Practical few-level approximations are introduced in the frame of a general theory of nuclear reactions. The one-level approximation without background is applied to the analysis of the excitation curve of the reaction $^{9}Be(\gamma,n)$. The connection existing in a particular case between the partial widths of the theory and those appearing in the R-matrix treatment is shown. The one-level approximation with constant background gives a good description of the cross sections of the reactions $^{12}C(p,\gamma)^{13}N$ and $^{13}C(p,\gamma)^{14}N$. The two-level approximation without background is used in the case of the reactions $^{15}N(p,\alpha_0)^{12}C$ and $^{15}N(p,\gamma_0)^{16}O$. Extrapolation of the results to stellar energies is discussed. (auth)

39806 EVEN PARITY STATES IN O^{16}. Eisenberg, J. M.; Spicer, B. M.; Rose, M. E. (Univ. of Virginia, Charlottesville). Nucl. Phys., 71: 273-98(1965).

Even parity states in ^{16}O are studied using the shell model in the jj coupling scheme with a zero-range, spin-dependent residual interaction. This necessitates consideration of both one particle-one hole excitations through two oscillator shells and two particle-two hole excitations. The unperturbed energy spectrum is taken from data of the single particle levels in ^{15}O and ^{17}O. Energy eigenvalues and eigenfunctions have been obtained for spin and isospin values $J^{\pi}(T) = 0^{+}(0, 1, 2)$, $1^{+}(0, 1)$, $2^{+}(0, 2)$, $3^{+}(0)$, $4^{+}(0, 1)$. Transition matrix elements for photo- and electro-excitation are computed. An extensive comparison of these results with experimental data on energy levels below 20 Mev has been carried out. Reasonable agreement is obtained for those levels with well-established spin and isospin assignments. In addition, some support is provided for tentative assignments drawn from nuclear reaction data. Comparison above 20 Mev, where there is a high density of predicted even parity levels, is made difficult by the dearth of experimental data. In contrast to the rather satisfactory results for energy values, electron scattering form factors as well as the pair emission rate from the lowest 0^{+} level are generally much smaller than the observed values, although form factor shapes appear to agree with the limited available data. (auth)

39807 THE ALPHA HALF-LIFE OF BERKELIUM-247; A NEW LONG-LIVED ISOMER OF BERKELIUM-248. Milsted, J.; Friedman, A. M.; Stevens, C. M. (Argonne National Lab., Ill.). Nucl. Phys., 71: 299-304(1965).

A ^{247}Bk sample was prepared by intensive helium-ion bombardment of a curium sample containing ^{246}Cm. The alpha half life was determined by a mass-spectrometric isotopic dilution method, using ^{249}Bk as the diluent. The value obtained was 1380 ± 250 yr, considerably shorter than previous estimates. The isotopic analyses disclosed a species of mass 248 in constant abundance in three samples analyzed over a period of about 10 months. This was ascribed to an isomer of ^{248}Bk with a half-life greater than 9 yr. No growth of ^{248}Cf was detected, and a lower limit for the β^{-} half-life can be set at about 10^{4} yr. No alpha activity attributable to the new isomer has been detected; the alpha half-life is probably greater than 300 yr. (auth)

39808 NUCLEAR PHOTOEFFECT ON THREE-PARTICLE NUCLEI. Fetisov, V. N.; Gorbunov, A. N.; Varfolomeev, A. T. (Academy of Sciences, Moscow). Nucl. Phys., 71: 305-42(1965).

The yields and effective cross sections of the $^{3}He(\gamma,p)D$ and $^{3}He(\gamma,n)2p$ reactions are measured in the γ-quantum energy interval from the threshold to 170 Mev. The yields of the (γ,p) and (γ,n) reactions prove to be the same within the statistical errors, and the integral cross sections σ_0 and σ_{-1} equal to 26.5 ± 1.3 Mev · mb and 1.34 ± 0.05 mb (the γ,p reaction) and 43.6 ± 2.7 Mev · mb and 1.42 ± 0.07 mg (the (γ,n) reaction). The rms charge distribution radius of ^{3}He calculated from the experimental value of σ_{-1} under the assumption of the complete symmetry of the spatial part of the ground state wave function of ^{3}He equals $\langle R_c^2 \rangle^{1/2} = 1.81 \pm 0.06$ fm. The angular distributions and energy spectra of the products of the reactions are also given. Experimental data are compared with theoretical predictions. (auth)

39809 SEARCH FOR A SECOND STATE IN Ne^{20} NEAR 4.97 Mev. Meyer-Schuetzmeister, L.; Segel, R. E. (Argonne National Lab., Ill.). Nucl. Phys., 71: 343-7 (1965).

We have searched for a state in ^{20}Ne which would form a doublet with the known 2^{-} state at 4.97 Mev. Such a state is desired so that the observed stellar neon may be produced in the helium-burning stage of stellar evolution. Alpha spectra from the $^{23}Na(p,\alpha)^{20}Ne$ reaction were analyzed by a broad-range magnetic spectrograph but failed to show any evidence that the 4.97 Mev state is a doublet. The data place limitations on the relative energy and intensity of a second state near 4.97 Mev. Qualitatively, the spectra would be difficult to reconcile with a doublet separation greater than 15 kev. It is concluded that it is very improbable that the 4.97 Mev state is a doublet; alternative modes of producing neon in ordinary states are mentioned. (auth)

39810 MAGNETIC MOMENTS OF SOME EXCITED STATES OF Sn AND Pb ISOTOPES. Lombard: R. J. (Laboratoire de Physique Theorique, Orsay). Nucl. Phys., 71: 348-52(1965).

The gyromagnetic factor of the first 4^{+} state of the Pb isotopes and the first 5^{-} state of the Sn isotopes have been calculated in the quasi-particle model, and compared with experiment. (auth)

39811 MEASUREMENTS OF d,pγ DIRECTIONAL CORRELATIONS IN ^{20}F. Newsome, Ross W. Jr. (Univ. of Michigan). Nucl. Phys., 71: 353-72(1965).

The reaction $^{19}F(d,p\gamma)^{20}F$ was used to measure the directional correlations of the proton groups in coincidence with subsequent gamma radiations produced in de-excitation of the 2.05, 1.31, 1.06, 0.99 and 0.65 Mev levels of ^{20}F. The effective deuteron energy was 0.448 Mev. For the 2.05 Mev level, the 1-2 correlation between the protons and the 1.40 Mev gamma transition to the first excited state was measured simultaneously with the 1-3 correlation between the same proton energy group and the 0.65 Mev gamma transition, with the intermediate 1.40 Mev gamma radiation unobserved. These correlations were measured in two configurations: one with the protons being detected at an average angle of 170° with the beam passing through a center hole in an annular-shaped detector, and the other with a disc-shaped detector at 135° and the gamma detector moving in the plane of the reaction. A plane-wave analysis of these data gave essentially identical correlation coefficients for these two configurations. Directional correlations were also measured in the 170° configuration between the proton energy groups and the subsequent ground-state gamma transitions from the 1.31, 1.06, 0.99, and 0.65 Mev levels. A plane-wave analysis of these data is compared with a distorted-wave analysis of related data from a previous experiment. A thorough computational comparison between all of these data and the predicted correlations, based on a plane-wave analysis using postulated spin values which are consistent with the proton angular distribution data, did not yield a unique spin value for any of these levels. It was possible in some cases, however, to put rather stringent conditions on the ratios of the angular-momentum matrix elements associated with the incoming and outgoing radiations which are compatible with the postulated spins. (auth)

39812 CALCULATION OF SPURIOUS STATES DUE TO CENTER-OF-MASS MOTION. Giraud, B. (Centre d'Etudes Nucleaires de Saclay, France). Nucl. Phys., 71: 373-81(1965). (In French)

A complete orthonormal set of the spurious states due to center-of-mass motion has been calculated, for some nuclei of mass number 14, 15, 16, 17, 18, 38, 39, 40, 41, 42, in the case of jj coupling configurations corresponding to one major shell excitation. Tables of these states are given for ^{15}O and ^{17}O. For ^{16}O and ^{40}Ca, the spurious states corresponding to two major shell excitations of jj configurations have also been calculated, and tables of these states are given for ^{16}O in the case $J = 0^+$, $T = 0$. (auth)

39813 THE HALF-LIFE OF ^{16}N. Gray, Peter R.; Zander, Arlen R. (Phillips Petroleum Co., Bartlesville, Okla.). Nucl. Phys., 71: 382-4(1965).

The radioactive half life of ^{16}N was measured by gamma scintillation spectroscopy. The weighted average of twelve individual determinations is 7.16 ± 0.04 sec. (auth)

39814 EFFECT OF SHORT-RANGE REPULSION IN NUCLEAR MATTER [PART] II. Wong, Chun Wa (Univ. of Copenhagen). Nucl. Phys., 71: 385-401(1965).

The effects of using soft-core potentials in nuclear matter are investigated by the Moszkowski-Scott separation method using free-particle energies in intermediate states. Changes in the binding energy per particle are estimated relative to the Yale potential, which has a binding energy of only 8 Mev/A. In the $^1S_0$ state the binding energy increases by 0.6 to 0.9 Mev if the hard core is replaced by the soft core in such a way that the resulting potentials have essentially the same phase shifts, and by another 2 to 2.5 Mev if the potential is made to fit the Livermore phase shifts. An additional 1 Mev may appear because the soft-core potential needs a weaker quadratic spin-orbit term, at least in the singlet-even states. The situation in the other states is discussed briefly and problems connected with the fit to the $^3S_1$ phase shifts and the strength of the tensor force are pointed out. (auth)

39815 THE FREE REACTION MATRIX AS A RESIDUAL INTERACTION IN FINITE NUCLEI. Kahana, S.; Tomusiak, E. (McGill Univ., Montreal, Quebec). Nucl. Phys., 71: 402-16(1965).

The individual particle spectra of ^{18}O and ^{42}Ca are calculated using as a residual interaction the reason matrix of two isolated nucleons. The reaction matrix is determined by the demand that it correctly predict the tangents of the phase shifts in the isobaric triplet states of the two-nucleon system. A reasonable fit to the spectra is obtained if the residual short-range repulsion (above 100 Mev) in the two-nucleon $^1S_0$ state is ignored. (auth)

39816 THE RADIATIVE CAPTURE CROSS SECTION OF IODINE AT 24 kev AND THERMAL ENERGY. Robertson, J. C. (The National Physical Lab., Teddington, Middx., Eng.). Nucl. Phys., 71: 417-25(1965).

The $^{127}I(n,\gamma)^{128}I$ reaction has been studied at 24 kev and at thermal energy. A CsI crystal was used both as the target and detector. A calibrated Sb–Be photoneutron source was used at 24 kev, and the reactor Gleep at Harwell was used as the thermal neutron source. Values of σ of 6.17 ± 0.2 barn and 832 ± 26 mb were obtained at thermal energy and 24 kev respectively. (auth)

39817 ANGULAR DISTRIBUTIONS FROM THE $^{11}B(d,n_0)^{12}C$ AND $^{11}B(d,n_1)^{12*}C$ REACTIONS FOR DEUTERON ENERGIES FROM 1.5 TO 4.7 Mev. Class, C. M.; Price, J. E.; Risser, J. R. (Rice Univ., Houston, Texas). Nucl. Phys., 71: 433-40(1965). (TID-21732)

The angular distributions of resolved n_0 and n_1 neutron groups from $^{11}B + d$ were measured at bombarding energies of 1.51 ± 0.05, 1.96 ± 0.05, 2.36 ± 0.04, 2.77 ± 0.04, 3.07 ± 0.04, 3.47 ± 0.04, 3.77 ± 0.04, 4.11 ± 0.04, and 4.68 ± 0.03 Mev. They were obtained using a neutron spectrometer of low resolving power consisting of a polyethylene radiator with gas proportional dE dx and scintillation E counters operating in coincidence to detect the recoil protons from the radiator. The shapes of the angular distributions do not allow an unambiguous specification of the reaction mechanism, which could involve both compound nucleus formation and direct interaction. (auth)

39818 SPINS OF Gd^{153}, Dy^{159} AND Pm^{148}. Ali, Dolores (Univ. of California, Berkeley). Nucl. Phys., 71: 441-8 (1965). (UCRL-11837).

Ground-state nuclear spins of 236-d ^{153}Gd, 134-d ^{159}Dy, and 5.3-d ^{148}Pm have been measured by the atomic-beam magnetic-resonance method. They are found to be $I(^{153}Gd) = 3/2$, $I(^{159}Dy) = 3/2$, and $I(^{148}Pm) = 1$. The spins of ^{153}Gd and ^{159}Dy are found to be consistent with collective-model state assignments for the odd neutrons, $3/2^+$ [651] and $3/2^-$ [521] respectively. The spin of ^{148}Pm is found to be consistent with shell-model state assignments $g_{7/2}$ for the odd proton and $(f_{7/2})^{-3}$ for the odd neutrons. (auth)

39819 LEVELS OF ^{56}Ni FROM THE REACTION $^{58}Ni(p,t)^{56}Ni$ AT 28 Mev. Hott, Charles G.; Kondo, M.; Rickey, M. E. (Univ. of Colorado, Boulder). Nucl. Phys., 71: 449-58(1965).

Tritons were observed from the (p,t) reaction on ^{58}Ni leading to the ground state of ^{56}Ni with a Q of −13.987 ± 0.018 Mev, and to excited states of ^{56}Ni at excitations (±0.05 Mev) of 2.71, 3.94, 5.35 and 6.62 Mev. The ground state results from L = 0 pickup by comparison with other angular distributions for known $0^+ \rightarrow 0^+$ (p,t) reactions. Angular distributions for the stronger excited state transitions have been measured. (auth)

39820 THE CAPTURE OF PROTONS BY Be^7. Tombrello, T. A. (California Inst. of Tech., Pasadena). Nucl. Phys., 71: 459-64(1965).

The capture of low-energy protons by ^7Be is calculated using a single-particle model for the ground state of ^8B. All the model parameters are determined from the experimental data for the reactions $^7Li(n,n)^7Li$ and $^7Li(n,\gamma)^8Li$. The calculated results for $^7Be(p,\gamma)^8B$ are in agreement with the experimental data, and permit an extrapolation to energies corresponding to stellar temperatures. (auth)

39821 ON THE FORMAL THEORY OF ELASTIC SCATTERING. Dolinszky, T. (Central Research Inst. for Phys., Budapest). Nucl. Phys., 71: 465-78(1965).

The formalism of the theory of scattering is combined with the Sturm-Liouville expansion theorem to develop a dispersion formula, including a potential scattering term, for the transition matrix element. The calculation of the scattered wave by means of the Green operator eliminates any heuristic postulate as to the nature of the asymptotic behavior. Owing to the non-linear energy dependence of the energy denominators, a single term of the transition matrix element represents contributions from an infinite number of poles. The singularities of the transition matrix are obtained as roots of the transcendental equations which specify the homogeneous boundary conditions within the Sturm-Liouville expansion. The dispersion formula is approximated, in the vicinity of an isolated pole, by a one-level term of the Breit-Wigner type. (auth)

39822 THE $\Omega_p = \Omega_n = 1/2$ EXCITATIONS IN THE ODD NUCLEUS ^{171}Tm. Hansen, P. G.; Nielsen, H. L.; Williams, E. T.; Wilsky, K. (Research Establishment Risoe, Roskilde, Denmark). Nucl. Phys., 71: 481-96(Sept. 1965).

The decay of 50 h ^{171}Er was investigated by electron and gamma-ray spectrometry and coincidence techniques. Excited levels, characterized by the quantum numbers (K,I^π), were established at the following energies in kev: 61(2,3⁻), 407(1,1⁻), 446(1,2⁻), 475(0,0⁻), 535(0,1⁻) and 610(1,1⁺). The levels can be interpreted in terms of the Nilsson orbitals expected in this region. Thus the four states from 407 to 535 kev are taken to belong to the configuration p $1/2^+[411] \pm n\ 1/2^-[521]$, which gives rise to bands with K = 0 and K = 1. These two bands have an anomalous structure, partly because of the even-odd splitting in the K = 0 band, partly because of the Coriolis coupling between the two bands. By an analysis of the beta-transition probabilities in the decay of ^{171}Er and of ^{170}Tm it is shown that the Coriolis coupling vanishes in the odd-spin states in agreement with expectations. However, an analysis based on the level

spacings in ^{170}Tm and ^{172}Tm indicates that the appreciable rotational perturbations of the even-spin states deviate from the theoretical value. (auth)

39823 NEUTRON INDUCED NUCLEAR REACTION IN Br AND Rb IN THE ENERGY RANGE OF 13 TO 17 Mev. Koenig, V. (Universitaet, Hamburg). Nucl. Phys., 71: 497-510(Sept. 1965). (In German).

Studies of the reactions Br(n,α), Rb(n,α), and Rb(n,p) for neutron energies of 13 to 17 Mev are presented. An experimental set up is used in which the target also acts as a detector. The reactions occur in CsBr(Tl) and RbI(Tl) scintillation crystals, both of which allow discrimination of different kinds of particles by pulse-shape discrimination. For all the reactions, cross sections are evaluated, and for the Br(n,α) reaction the energy spectra are measured. The experimental data of the (n,α) reactions are compared with the prediction of the statistical theory of nuclear reactions. By analysis of the energy spectra the fraction of α-particles which are produced in an evaporation process is calculated. This fraction matches the theoretically computed cross-section very well. The comparison of these cross sections with similar measurements in the range of 14 to 15 Mev neutron energy gives evidence that the intense increase of the (n,α) cross sections for nuclei with an N value close to the magic neutron number N = 50 does not occur; such an increase has been assumed up to now. (auth)

39824 INFLUENCE OF SOLID STATE EFFECTS ON β-γ DIRECTIONAL CORRELATION IN ^{166}Ho. Martin, B.; Schmidlin, P.; Daniel, H. (Max-Planck-Institut fuer Kernphysik, Heidelberg). Nucl. Phys., 71: 523-8(Sept. 1965).

The β-γ directional correlation of ^{166}Ho was measured in metal, oxide, and chloride sources, in order to study the influence of solid state effects on the correlation. In metal sources an energy-independent attenuation factor G_2 = 0.356 ± 0.005 was found. The oxide and chloride sources showed attenuation factors which varied with the β energy. Between 0.5 and 1.8 Mev G_2 was found to increase from 0.16 to 0.25 (oxide), and from 0.25 to 0.37 (chloride evaporated in vacuo). (auth)

39825 NEUTRONS FROM PROTONS ON ISOTOPES OF TIN. Wood, R. M.; Borchers, R. R.; Barschall, H. H. (Univ. of Wisconsin, Madison). Nucl. Phys., 71: 529-45 (Sept. 1965). (COO-7-354).

Neutron spectra resulting from the bombardment of eight isotopes of tin with protons of energies between 7 and 14 Mev were obtained at a laboratory angle of 60°. At 10 and 14 Mev angular distributions were measured. The statistical model of nuclear reactions was used to deduce the dependence of the level densities in the residual nuclei on excitation energy, but contrary to the predictions of the model, the deduced level densities showed an apparent dependence on bombarding energy. The effect of the pairing energy on the neutron spectra from targets containing even and odd numbers of neutrons is discussed. (auth)

39826 THE EXCITED STATES OF ^{52}Cr. Knye, Geoffrey; Willmott, J. C. (Univ. of Liverpool). Nucl. Phys., 71: 561-85(Sept. 1965).

Triple angular correlations of γ rays de-exciting states populated by the inelastic scattering of protons from ^{52}Cr were measured. These measurements have enabled spin assignments to be made to the following excited states: 2.370 (4^+), 2.648 (0), 2.965 (2^+), 3.161 (2) and 3.80 (2 or 3). The multipole mixing ratios E2/M1 were also determined for the γ rays involved in these correlations giving 0.936 (E2), 1.214 (E2), 1.531 (6.25 ± 1.5), 1.727 (0.175 ± 0.065) and 2.35 (−0.20 ± 0.075 if the 3.80 Mev state has spin 2 or −2 ± 0.5 if it has spin 3). The results of these measurements and previous ones were compared with semi-empirical jj coupling shell model calculations based on the work of de-Shalit. Good agreement is obtained but this does not imply that the nucleus is accurately described by jj coupling wave functions, since the method allows the inclusion of other configurations which could give rise to collective effects. (auth)

39827 ENERGY LEVELS OF ^{31}S AND ^{19}Ne. Wesolowski, J. J.; Anderson, J. D.; Hansen, L. F.; Wong, C.; McClure, J. W. (Univ. of California, Livermore). Nucl. Phys., 71: 586-92(Sept. 1965). (UCRL-12358).

Recently Colli et al., using the ^{32}S(n,d)^{31}P reaction, reported the existence of a 450-kev level in ^{31}P. However, the investigation of other reactions has shown no evidence for such a level. Using the Livermore neutron time-of-flight facility and the (p,n) reaction on ^{31}P, for the analog of this proposed level in the mirror nucleus ^{31}S. Neutron spectra were obtained for angles between 30 and 120° and for proton energies from 7.5 to 13.0 Mev. Although the correspondence between the observed levels in ^{31}S and those reported for ^{31}P was excellent up to the maximum excitation energy studied, viz., 3.7 Mev, no evidence for a level at 450 kev excitation was obtained. The reaction ^{19}F(p,n)^{19}Ne also was studied up to an excitation energy of 3.0 Mev in ^{19}Ne. Besides confirming the results obtained by Freeman and West, a previously unreported level at 2.8 Mev was observed. (auth)

39828 LEVELS OF ^{36}Ar EXCITED IN THE ^{35}Cl(p,γ)^{36}Ar REACTION. Erne, F. C.; Endt, P. M. (Rijksuniversiteit Utrecht, Nederland). Nucl. Phys., 71: 593-605(Sept. 1965).

With protons in the energy range E_p = 0.4-3.1 Mev, sixty-five resonances were found in the reaction ^{35}Cl(p,γ)^{36}Ar. About forty of these resonances were not reported earlier. The resonance energies and the resonance strengths are given. The gamma spectra at the resonances were investigated with scintillation spectrometers. From single and coincidence spectra the gamma branchings of most of the resonances and of thirteen lower ^{36}Ar levels were obtained. At some of the investigated resonances, gamma rays were observed from proton emission to the first and second excited state of ^{35}Cl. (auth)

39829 CLUSTER STRIPPING PROCESSES. Abul-Magd, A. Y.; El-Nadi, M.; Vysotsky, G. L. (Atomic Energy Establishment, Cairo). Nucl. Phys., 71: 606-24 (Sept. 1965).

The distorted wave theory of stripping reactions is generalized to include those reactions with cluster transfer. General expressions are derived for the angular distributions, polarization, and angular correlations in these reactions. (auth)

39830 RADIATIVE CAPTURE OF DEUTERONS IN ^{16}O. Owens, R. O.; Winter, R. G. (Nuclear Physics Lab., Oxford). Nucl. Phys., 71: 625-33(Sept. 1965).

The cross section for the radiative capture of deuterons in ^{16}O was determined for center-of-mass energies 0.4-3.5 Mev from measurements of the ^{18}F activity produced when deuterium gas was bombarded by an oxygen ion beam. The cross section rises from 0.1 μb at 0.4 Mev to 25 μb at 3.5 Mev and shows some resonance structure. The results can be interpreted satisfactorily in terms of compound nucleus formation. The estimated radiative width of the compound state is approximately 2 ev over the excitation range studied (8.1-11.1 Mev). (auth)

39831 MOMENTS OF INERTIA OF ASYMMETRIC NUCLEI. Banerjee, P.; Sengupta, S. (Presidency College, Calcutta). Nucl. Phys., 71: 634-40(Sept. 1965).

It is known that the nuclear moments of inertia, calculated on the basis of the hydrodynamical model, yield values which are too small in comparison with the experimental values. An expression for the moment of inertia of an asymmetric nucleus is derived in the framework of the cranking model and taking into account the residual interactions between nucleons. The results is a generalization of the Moszkowski formula, where the residual interaction parameter p is dependent on the axis of rotation. With suitable values of the parameters this model can reproduce the experimental moments of inertia obtained from the energy level data. Calculations show that the general trend of variation of the reduced width for electric quadrupole transitions with the energy ratio of the two 2^+ states is also given satisfactorily in this model. (auth)

39832 THE REACTION $Be^9(He^3,n)C^{11}$ FROM 1.3 TO 5.4 Mev. Din, G. U.; Weil, J. L. (Rice Univ., Houston). Nucl. Phys., 71: 641-61(Sept. 1965). (TID-21508).

Excitation functions of $^9Be(^3He,n_0)^{11}C$ and $^9Be(^3He,n_1)^{11*}C$ at $\theta_{lab} = 0$, 90, and 160° were measured in the energy range of 1.30 to 4.90 Mev ^3He bombarding energy. The excitation functions for the two groups are similar in shape and show only very broad structure. Angular distributions were measured for both neutron groups at 1.59, 1.77, 1.97, 2.19, 2.48, 2.80, 3.11, 3.46, 3.81, 4.12, 4.52, 4.90, and 5.35 Mev ^3He bombarding energies. Analysis of the angular distributions in terms of Legendre polynomials, together with other evidence, indicates that a level is formed in the ^{12}C compound nucleus with a width of several hundred kilovolts at an excitation energy of 27.8 Mev. These angular distributions show strong changes in shape with increasing energy. For the ground state group, the angular distribution changes from near symmetry about 90° to strong peaking at 0° as the energy increases. The first excited state group changes from a weak to a strong backward peak, then to forward and backward peaking and, finally, to dominant forward peaking as the energy increases. An interpretation in terms of double stripping is given for the higher energy ground state angular distributions. (auth)

39833 THE g FACTORS OF THE EXCITED STATES IN ^{192}Os, ^{192}Pt, AND ^{194}Pt. Keszthelyi, L.; Berkes, I.; Dezsi, I.; Pocs, L. (Central Research Inst. for Physics, Budapest). Nucl. Phys., 71: 662-72(Sept. 1965).

The g factors of the 316-kev 2^+ state in ^{192}Pt, the 329-kev 2^+ and the 622-kev 2^+ states in ^{194}Pt were investigated by measuring the rotation of the angular correlation patterns in the internal field at the nucleus in Fe-Ir alloy. The results are 0.24 ± 0.05, 0.21 ± 0.03 and 0.131 ± 0.03, respectively. For the 206-kev 2^+ state in ^{192}Os the value of $\omega\tau$ is found to be 0.235 ± 0.034. The internal field is, however, not known in Os and a reliable value of the g factor cannot be derived. The values of the g factors cannot be derived. The values of the g factors in Pt do not agree with the predictions of the phenomenological theory of vibration. (auth)

39834 THE HYPERFRAGMENT $^7He_\Lambda$. Law, J. (Battersea Coll. of Tech., London). Nuovo Cimento (10), 38: 807-16(July 16, 1965).

A factor contributing to the apparent binding-energy difference between $^7He_\Lambda$ and $^7Be_\Lambda$ is the possibility of the existence of an isomeric state for $^7He_\Lambda$. A shell-model calculation was performed for the E2 decay rate from this conjectured state and the results suggest a lower limit of 10^{-9} for the lifetime. Comparison with estimates of the Λ decay lifetime for $^7He^*_\Lambda$ adds weight to the existence of the isomeric state. (auth)

39835 INVESTIGATION OF $^{23}Na(d,\alpha)^{21}Ne$ REACTION. El-Behay, A. Z.; Comsan, M. N. H.; Farouk, M. A.; Jhingan, M. L.; Zaloubovsky, I. I. (Atomic Energy Establishment, Cairo). Nuovo Cimento (10), 38: 1082-5(July 16, 1965).

Information is obtained about the differential cross sections and the mechanism of the $^{23}Na(d,\alpha)^{21}Ne$ reaction at low deuteron energies. The absolute cross sections of this reaction were obtained with respect to the spectrum of elastic alpha peaks. Excitation functions and angular distributions are measured only for the first four groups of the α particles. Curves of these excitations indicate a number of irregularities in differential cross sections. Some of them are related to several groups of levels in the compound nucleus magnesium-25. Angular distributions measured in the back hemisphere have a shape more typical of the compound process. From these data the differential cross sections were investigated in terms of the $(2I + 1)$ rule. The intensity of these groups divided by this factor approaches unity best with certain values of the ground and first excited states of neon-21. (J.F.P.)

39836 PRESSURE WAVE GENERATION IN A FISSIONING GAS. II. EFFECTS OF DISSOCIATION AND MULTIPHASE COMPOSITION. Smith, H. P. Jr.; Evans, R. D.; Busch, C W.; Oppenheim, A. K. (Univ. of California, Berkeley). Phys. Fluids, 8: 1421-4(Aug. 1965).

The analysis of pressure pulses which are generated in a fissioning gas by neutron irradiation is extended to the case of a dissociating medium including a condensed phase. After a satisfactory check of the process induced in boron trifluoride that was treated previously, the analysis is applied to borazine for which the former method would be quite inadequate since now the effects of dissociation, involving the formation of free liquid boron, become predominant in controlling the thermodynamic behavior of the substance. (auth)

39837 POLARIZATION IN INELASTIC SCATTERING OF 150 Mev PROTONS ON THE FIRST LEVELS OF C^{12}. Tatischeff, B.; Geoffrion, B.; Le Guyader, J.; Marty, N.; Roland, C.; Willis, A. (Faculte des Sciences, Orsay, France). Phys. Letters, 16: 282-4(June 1, 1965). (In French).

The polarizations of protons inelastically scattered at 152 Mev to the 4.43-, 7.66-, and 9.64-Mev levels of ^{12}C were measured as a function of angle. The experimental results were, in general, compared to theoretical curves calculated with the Gammel-Thaler potential for nucleon-nucleon scattering. The theoretical curve for the 2^+, T = 0, 4.4-Mev level was calculated for the case of a pure L-S coupling. (D.C.W.)

39838 CHARACTERISTICS OF ALPHA DECAY OF LIGHT POLONIUM ISOTOPES. Brun, C.; Le Beyec, Y.; Lefort, M. (Laboratoire Joliot-Curie, Orsay, France). Phys. Letters, 16: 286-8(June 1, 1965). (In French).

In the course of a study of the excitation functions of the reactions (p,xn) induced on bismuth by protons at 80 to 155 Mev, each isotope of polonium was characterized according to the threshold and the maximum of the excitation function, and the alpha emissions of the isotopes with mass numbers 197, 198, 199, 200, and 201 were identified. The half-lives, branching ratios, and alpha energies for ^{197}Po, ^{198}Po, ^{199}Po, ^{200}Po, ^{201}Po, and ^{202}Po are tabulated. (D.C.W.)

39839 SEPARATION OF FINAL STATES IN THE REACTION (p,t) AT 155 Mev. STUDY OF $^{12}C(p,t)^{10}C$. Bachelier, D.; Bernas, M.; Brissaud, I.; Radvanyi, P.; Roy, M. (Faculte des Sciences, Orsay, France). Phys. Letters, 16: 304-6(June 1, 1965). (In French).

The triton groups corresponding to the different final states of the ^{10}C residual nucleus in the reaction $^{12}C(p,t)^{10}C$ at 155 Mev were separated by magnetic analysis. The triton spectra obtained show that four states of ^{10}C are excited with a comparable intensity: the ground state (0^+) and the levels at 3.4 ± 0.1 Mev (2^+), 5.6 ± 0.1 Mev, and 10.2 ± 0.2 Mev. A very slightly excited level appears near 7.2 ± 0.2 Mev. It is concluded that the assignment of $J = 0^+$ and $J = 2^+$ to the ground state and to the 3.4-Mev level of ^{10}C, respectively, agrees with theoretical predictions. The assignment of $J = 0^+$ to the 5.6-Mev level appears probable; the 10.2-Mev level has perhaps the characteristics 2^+. The excitation in ^{10}C of four states with a comparable intensity indicated for these states a description by a mixture of configurations that can be limited essentially to the 1 p shell or better by a deformed nucleus model. (J.S.R.)

39840 NUCLEAR RESONANCE SPIN-ECHO STUDY OF Eu^{153} IN EuO. Uriano, G. A.; Streever, R. L. (National Bureau of Standards, Washington, D. C.). Phys. Letters, 17: 205-6(July 15, 1965).

The nuclear magnetic resonance of ^{153}Eu was studied in 97% pure EuO powder in zero applied magnetic field using a spin-echo technique. The resonance line shape was determined at 4.2 and 20.3°K by plotting the spin-echo amplitude as a function of frequency across the inhomogeneously broadened line. Relaxation time measurements were also made, and are tabulated along with the center of gravity and nuclear hyperfine field of the lines observed at 138.0 and 132.7 Mc/s at 4.2 and 20.3°K, respectively. A search was also made for the ^{153}Eu resonance in europium metal powder. A weak resonance line was observed at approximately 123 Mc/s. (L.B.S.)

39841 EVIDENCE FOR ISOMERIC STATES OF ^{199}Po AND ^{201}Po. Tielsch, E. (Max-Planck-Institut fuer Kernphysik, Heidelberg and CERN, Geneva). Phys. Letters, 17: 273-4(July 15, 1965).

Polonium isotopes were produced by bombardment of bismuth targets with 220 Mev protons, and the alpha spectra were measured over several half-lives of the Po isotopes using a surface barrier solid state counter. The α-decay energies and half-lives of ^{199}Po–^{201}Po obtained from the spectra are tabulated. The decay curves for ^{201}Po and ^{199}Po show two distinct α-lines for each, which are identified as the decays of isomeric states. (L.B.S.)

39842 THE EFFECT OF CHEMICAL STATE ON THE DECAY CONSTANT OF A NUCLEAR ISOMER ^{235m}U. Shimizu, S.; Mazaki, H. (Kyoto Univ.). Phys. Letters, 17: 275-6(July 15, 1965).

An experiment was performed to study the effect of the chemical state on the decay constant of ^{235m}U. Details are given of the source preparation, the measuring system, and the experimental method. A least squares analysis applied to the observed results for metallic uranium (U) and uranium atoms embedded in a carbon base (UC) yielded $[\lambda(U) - \lambda(UC)]/\lambda(U) = (3.2 \pm 0.05) \times 10^{-3}$. (L.B.S.)

39843 NUCLEAR g-FACTOR OF THE 3.2 Mev 5$^-$ STATE IN THE DOUBLE-CLOSED SHELL NUCLEUS ^{208}Pb. Johansson, K.; Gustafsson, S.; Svensson, A. G.; Waeppling, R. (Uppsala Univ.). Phys. Letters, 17: 277-8(July 15, 1965).

The magnetic moment of the 3.2-Mev 5$^-$ state in ^{208}Pb was measured by perturbing the 511–583 kev γ-γ angular correlations in a magnetic field of 51,000 gauss. Coincident spectra were recorded at 90, 135, 180, and 270° with a 400 channel analyzer. Assuming the g-factor of the 2.6 Mev 3$^-$ state to be zero, the results obtained for the 3.2 Mev state are $g = -0.013$ and $\mu = -0.07$. Calculations assuming pure j-j coupling and a spherical scheme yielded $\mu_{5^-} = -0.26$ nm. (L.B.S.)

39844 EXCITATION OF 2$^+$, 5$^-$ AND 3$^-$ STATES OF ^{90}Zr BY INELASTIC ALPHA-PARTICLE SCATTERING. Ogata, H.; Tomita, S.; Inoue, M.; Okuma, Y.; Kumabe, I. (Kyoto Univ.). Phys. Letters, 17: 280-2(July 15, 1965).

A beam of 34.4-Mev alpha particles were used to bombard an enriched thin target of ^{90}Zr. Cross sections were measured for the elastic and inelastic scattering leading to the 5$^-$ state and for the inelastic scattering leading to the 2$^+$ and 3$^-$ state of ^{90}Zr, and were analyzed using an INS DWBA-1 code. Deformabilities of the multipole components of the deformation are tabulated together with the ratios of the reduced transition probabilities to the single particle estimate. The results indicate that the 2$^+$ and the 5$^-$ states have a weak collective character and that the 3$^-$ state at 2.74 Mev is a collective state arising from the octupole vibration. (L.B.S.)

39845 ON SOME NEGATIVE PARITY STATES IN ^{148}Sm. Bhatt, K. H. (Physical Research Lab., Ahmedabad, India). Phys. Letters, 17: 282-3(July 15, 1965).

It is suggested that the negative parity states 1$^-$, 5$^-$, 3$^-$, and 4$^-$ previously observed in ^{148}Sm might be due to the simultaneous excitation of a quadrupole and octupole-phonon, and that such double excitation would give rise to five states. A calculation, which shows also the location of the missing 2$^-$ state, was made of the energy splittings of the negative parity states, and was found to be in satisfactory agreement with the experimental spectrum. Selection rules for the gamma transitions from these states are given. (L.B.S.)

39846 ON THE VIOLATION OF GALLAGHER AND MOSZKOWSKI'S COUPLING RULES IN ^{166}Ho. Struble, G. L.; Rasmussen, J. O. (Univ. of California, Livermore). Phys. Letters, 17: 283-6(July 15, 1965). (UCRL-16102).

Recent attempts to justify theoretically the validity of the empirical coupling rules for deformed odd-odd nuclei are considered, which state that the lower energy band of the two possible rotational bands formed from a given proton-neutron configuration will be the one which maximizes the parallel coupling of the intrinsic spins of the odd neutron and proton. The effects of the neutron-photon residual interaction are considered in a shell model calculation, and a comparison of the experimentally observed single-particle excitations and their theoretically predicted energies are shown for intrinsic states in ^{166}Ho. It is shown that the violation of Gallagher and Moszkowski's rule occurs when the configuration interaction is taken into account. (L.B.S.)

39847 A POSSIBLE DOORWAY STATE IN ^{209}Pb AND ^{208}Pb. Farrell, J. A.; Kyker, G. C. Jr.; Bilpuch, E. G.; Newson, H. W. (Duke Univ., Durham, N. C.). Phys. Letters, 17: 286-90(July 15, 1965).

The total neutron cross sections of the principal isotopes of lead are examined from a single particle viewpoint in search for a sub-giant resonance near the energy of the 2p 1h state. Experimental evidence was found that a 2p 1h state, which is seen as a single resonance in ^{208}Pb corresponding to a $\frac{1}{2}^+$ level in ^{209}Pb, acts as a sub-giant resonance in the cross sections of ^{206}Pb and ^{207}Pb. (L.B.S.)

39848 ON THE ANOMALOUS STABILITY OF THE $\frac{5}{2}^-$ LEVEL IN ^{13}C. Balashov, V. V. (Moscow State Univ.); Pal, D.; Fetisov, V. N. Phys. Letters, 17: 290-2(July 15, 1965).

The anomalous stability of the $\frac{5}{2}^-$ level in ^{13}C in the 6 Mev region, which is excited by the ^{14}N(p,2p)^{13}C quasi elastic scattering reaction, was examined. The neutron width of the $\frac{5}{2}^-$ level is calculated within the framework of the Bethe-Feshbach method and the R-matrix theory. The examination shows that an estimate of the degree of purity of anomalous long-lived states may be obtained within the framework of the ordinary diagonalization procedure using wave functions of the infinite oscillator well even at very high excitation energies of mixed states. (L.B.S.)

39849 RELAXATION EFFECTS IN ANGULAR CORRELATIONS. Dillenburg, D.; Maris, Th. A. J. (Universidade do Rio Grande do Sul, Porto Alegre, Brazil). Phys. Letters, 17: 293-4(July 15, 1965).

The spin relaxation in angular correlations caused by a statistical interaction of the decaying system in an isotropic environment is investigated. For the case of x-gamma angular correlations, it is shown that a much weaker assumption than the perturbative one guarantees that the characteristic angular distributions are Legendre polynomials; that it is sufficient to assume that the influence of the environment can be simulated by applying on each individual nucleus a sequence of external time-dependent potentials which have a duration of the order of the correlation time. (L.B.S.)

39850 THE ^{40}Sc-^{40}Ca MASS DIFFERENCE AND THE ^{40}Sc GROUND STATE SPIN. Rickey, M. E.; Kunz, P. D.; Kraushaar, J. J.; Anderson, W. G. (Univ. of Colorado, Boulder). Phys. Letters, 17: 296-8(July 15, 1965).

The ^{40}Ca–^{40}Sc mass difference was determined to be 14.47 ± 0.06 Mev from a measurement of the Q-value for the ^{40}Ca(^{3}He,t)^{40}Sc ground state transition, using a 37.5-Mev ^{3}He beam focused on a natural calcium target. The results of beta decay studies using sources of ^{40}Sc from the ^{40}Ca(p,n) reaction at 25 Mev, together with the mass difference results, show that the main positron branch proceeds to the 5$^-$, 4.48 Mev state in ^{40}Ca with a calculated end-point on 8.97 ± 0.06 Mev, which is compared with the value of 9.10 ± 0.09 from the positron end-point measurement. The positron branch to the 5$^-$ state in ^{40}Ca is used to establish the ground state of ^{40}Sc as 4$^-$, the 7.65 Mev state in ^{40}Ca is assigned as a 4$^-$, T = 1 state. The predictions of the intermediate coupling shell model for the half-life of ^{40}Sc were found to be in good agreement with the experimental results. (L.B.S.)

39851 MEASUREMENT OF $d_{\frac{3}{2}}$ CORE EXCITATION IN ^{45}Ca FROM BETA DECAY. Cohen, S.; Lawson, R. D. (Argonne National Lab., Ill.). Phys. Letters, 17: 299-301 (July 15, 1965).

It is pointed out that the beta decay of ^{45}Ca to the 12-kev hole state in ^{45}Sc can occur only if there is a finite probability that the ground state of ^{45}Ca has a part that corresponds to two $d_{\frac{3}{2}}$ proton holes coupled to the low-lying states of ^{47}Ti. A recent measurement of the log f_1t for the beta transition is used to deduce the magnitude of the specific type of core excitation that can contribute to the decay. The form of the hole-state wave function and the ^{45}Ca ground state eigenfunction is described using the generating procedure. A comparison is made of the experimental and theoretical values of log f_1t, which is found to be in good agreement. (L.B.S.)

39852 ^{207}Tl STATES EXCITED IN THE (t,α) REACTION ON ^{208}Pb. Hinds, S. (Atomic Weapons Research Establishment, Aldermaston, Eng.); Middleton, R.; Bjerregaard, J. H.; Hansen, O.; Nathan, O. Phys. Letters, 17: 302-5(July 15, 1965).

A study was made of the one-proton hole states of ^{207}Tl from the ^{208}Pb(t,α)^{207}Tl reaction at incident energies of 12.0 and 13.5 Mev. Energy spectra and angular distributions are shown of alpha particles leading to the ground state, first three excited states below 1.7 Mev, and to the 3.48 Mev state. The results indicate a direct pickup mechanism. A comparison is made of the experimental scheme with the proposed assignments and the theoretical level scheme predicted by the shell model. Other preliminary distorted wave calculations are found to be in essential agreement with the pickup interpretation and the hole-state assignments. (L.B.S.)

39853 VARIATION IN YIELD OF THE ISOTOPIC SPIN FORBIDDEN REACTION ^{12}C(^{6}Li,α_1)^{14}N. Carlson, R. R.; Heikkinen, D. W. (Univ. of Iowa, Iowa City). Phys. Letters, 17: 305-7(July 15, 1965).

Measurements were made of the cross sections for the ^{12}C(^{6}Li,α_1)^{14}N reaction at 4.0 to 5.5 Mev, which corresponds to an excitation of 15.9 to 16.9 Mev in the ^{18}F compound nucleus. Total cross sections were also obtained for the ^{12}C(^{6}Li,p_0)^{17}O, ^{12}C(^{6}Li,d_0)^{16}O, ^{12}C(^{6}Li,α_0)^{14}N, and the ^{12}C(^{6}Li,α_2)^{14}N for functions of bombarding energy for comparison with the spin forbidden transition. A decrease in α_1 yield was observed for increasing bombarding energy, which is taken as evidence for an increase in the effective isotopic spin purity of the compound nucleus at higher excitation energies. The cross sections for the other groups continue to increase and are attributed to the Coulomb barrier. (L.B.S.)

39854 RESONANCE PEAK IN PERTURBED GAMMA–GAMMA ANGULAR CORRELATION. Leisi, H. J. (Franklin Inst., Swarthmore, Penna.). Phys. Letters, 17: 308-10 (July 15, 1965).

The observation of a resonance peak in the gamma-gamma correlation measurement of the 172–203 kev cascade in ^{127}I, in a weak magnetic field, is reported. The resonance peak is approximated by a Lorentzian shape curve, symmetrical around zero field, and a least-squares fit yields a half width at half maximum of 195 ± 41 gauss. A theoretical expression is obtained for the correlation function, and the lifetime of the 203 kev state, calculated from the measured width ΔH, was found to be $\tau \approx 3 \times 10^{-10}$ s. The absolute value of the anisotropy at zero field was also measured, and from comparison with the measured depth of the resonance, it is concluded that the data are not incompatible with strictly time-independent interaction. (L.B.S.)

39855 ISOSPIN SELECTION RULES FOR ELECTRON SCATTERING. Bishop, G. R. (Glasgow Univ.). Phys. Letters, 17: 310-11(July 15, 1965).

It is asserted that selection rules for electron scattering analogous to those for radiative transitions can be formulated, with the advantage that they may apply to all electric multipoles as well as all magnetic multipoles. An example is presented of an analysis for the relative isospin of the levels in ^{12}C from data on electro-excitation of the 16.1 Mev, 2^+ level on ^{12}C. (L.B.S.)

39856 ISOSPIN SELECTION RULES AND THE 5.10 Mev LEVEL OF ^{14}N. Bishop, G. R. (Glasgow Univ.). Phys. Letters, 17: 311-13(July 15, 1965).

Properties of the 5.10 Mev level in ^{14}N and its decay to the ground state are investigated from results of recent measurements. Reduced transition probabilities are derived, which correspond to the E1 and M2 transitions which compete with the E3 transition. Preliminary calculations are made which show that the states can be taken as pure isospin singlets, and that the selection rules are relaxed only by the normally neglected current contributions to the transition matrix elements. (L.B.S.)

39857 ENERGY GAP IN NUCLEAR MATTER IN THE CASE OF SOFT CORE POTENTIALS. Boschan, P. (Joint Inst. for Nuclear Research, Dubna, USSR). Phys. Letters, 17: 313-15(July 15, 1965).

Energy gap equations are solved by iteration using the Bressel potential, the Volkov potential, and the Volkov effective potential. The curves are presented for the energy gaps as functions of density and effective mass. (L.B.S.)

39858 THE DISAPPEARANCE OF NUCLEAR PAIRING CORRELATIONS AS INFLUENCED BY ROTATION. Grin, Yu. T.; Larkin, A. I. (Kurchatov Inst., Moscow). Phys. Letters, 17: 315-17(July 15, 1965).

The effect of nuclear rotation in deformed nuclei on the pairing correlation of nucleons is investigated. An expression is obtained for the critical moment I_c at which the nucleon pairing correlation becomes zero, and the moment of inertia of the nucleus J approaches a rigid-body value. Estimates were obtained for the regions on the rare earths and the heavy elements. A plot is shown of the dependence of J on I. (L.B.S.)

39859 THE ft VALUES FOR ^{42}Sc, ^{46}V AND ^{50}Mn AND THE CONSERVED VECTOR CURRENT HYPOTHESIS. Freeman, J. M. (Atomic Energy Research Establishment, Harwell, Berks, Eng.); Murray, G.; Burcham, W. E. Phys. Letters, 17: 317-20(July 15, 1965).

Measurements previously made of the ft values of Fermi transitions are extended to include the $0^+ \rightarrow 0^+$, T = 1 decays ^{42}Sc(β^+)^{42}Ca, ^{46}V(β^+)^{46}Ti, and ^{50}Mn(β^+)^{50}Cr. The thresholds of the reactions ^{42}Ca(p,n)^{42}Sc, ^{46}Ti(p,n)^{46}V, and ^{50}Cr(p,n)^{50}Mn were measured by an activation technique, and the corresponding β^+ end-points were deduced by calculating the Q-values and allowing for the mass difference between the neutron and hydrogen atom. Calculations were made of ft values using the Fermi-function tables of Dzhelopov and Zyrianova, and also including modified screening corrections and radiative corrections. The results confirm the 2.2% discrepancy between the vector coupling constant G_v and the coupling constant in μ-meson decay G_μ, which is explained by the proposal of Cabibbo that the vector current includes components not only for transitions in which strangeness is conserved, but also for weak decays in which $\Delta S = 1$. (L.B.S.)

39860 ELASTIC ELECTRON SCATTERING FROM LEAD ISOTOPES AND POSSIBLE DISPERSION EFFECTS. Peterson, G. A.; Ziegler, J. F.; Clark, R. B. (Yale Univ., New Haven). Phys. Letters, 17: 320-2(July 15, 1965).

The elastic scattering of electrons from ^{207}Pb and ^{208}Pb was studied in search for evidence of dispersion effects which might appear in the difference of ratios of the cross sections for the two isotopes. Precise absolute values of the cross sections could not be determined, thus it was impossible to identify the individual cross section changes as evidenced in the ratio changes. (L.B.S.)

39861 A THREE-PARTICLE ISOMERIC STATE IN ^{109}In. Alexander, K. F.; Brinckmann, H. F.; Heiser, C.; Lang, G.; Neubert, W.; Rotter, H. (Zentralinstitut fuer Kernforschung, Rossendorf, Ger. and Joint Inst. for Nuclear Research, Dubna, USSR). Phys. Letters, 17: 322-3(July 15, 1965).

Experiments were performed to locate the three-particle isomeric state in ^{109}In and to determine its decay mode. The ^{109m_2}In activity was found by bombarding a Rh target

with ^{12}C ions at 40 to 80 Mev. The energies and intensities of the observed γ-lines are given. A coincidence experiment was also performed to determine the excitation energy of the isomeric state, using the $^{107}Ag(\alpha,2n)^{109}In$ reaction. The characteristics of the 204 ms state are discussed and the probable decay scheme is presented. (L.B.S.)

39862 NEW VALUES OF NEUTRON SEPARATION ENERGIES. Jackson, H. E.; Namenson, A. I.; Thomas, G. E. (Argonne National Lab., Ill.). Phys. Letters, 17: 324-5(July 15, 1965).

Data for neutron separation energies are reported, which were obtained by accurate measurements of the energies of primary ground state transitions or the sum of cascade transitions to the ground state from the capture state, for ^{10}Be, ^{13}C, ^{15}N, ^{25}Mg, ^{26}Mg, ^{27}Mg, ^{28}Al, and ^{57}Fe. (L.B.S.)

39863 RECOILLESS γ EMISSION IN ^{156}Gd AND ^{158}Gd FOLLOWING NEUTRON CAPTURE REACTIONS. Fink, J.; Kienle, P. (Technische Hochschule, Munich and Technische Hochschule, Darmstadt, Ger.). Phys. Letters, 17: 326-7(July 15, 1965).

The Moessbauer effect of the 89.0 kev γ ray of ^{156}Gd and the 79.5 kev γ ray of ^{158}Gd following the capture of slow neutrons in ^{155}Gd and ^{157}Gd was studied. Mirror experiments were performed in which the target and absorber substances were interchanged, and the transmission spectra are shown as a function of the Doppler shift. The effect of the recoils on the change in the fraction of recoilless γ rays and also the hyperfine splitting, due to ion displacements, is investigated. The results are discussed. (L.B.S.)

39864 ON THE SLOW NEUTRON, GAMMA-FISSION REACTION. Lynn, J. E. (Atomic Energy Research Establishment, Harwell, Berks, Eng.). Phys. Letters, 18: 31-4(Aug. 1, 1965).

The width of the (γ-f) process was investigated theoretically. It was concluded that a much more realistic estimate of the width is obtained by calculating the primary gamma spectrum using Lang's parameters in Newton's level density model and the giant resonance form for the matrix element behavior. Numerical estimates for ^{239}Pu, ^{241}Pu, ^{233}U, and ^{235}U were obtained. (D.C.W.)

39865 ALPHA-GAMMA CORRELATION STUDY OF THE $^{56}Fe(\alpha,\alpha'\gamma_{0.84})^{56}Fe$ REACTION. Eidson, W. W.; Cramer, J. G. Jr.; Eckley, G. P. (Indiana Univ., Bloomington). Phys. Letters, 18: 34-6(Aug. 1, 1965).

Measurements of angular correlations in the $^{56}Fe(\alpha,\alpha'\gamma)^{56}Fe$ reaction at 22.2 Mev were made at thirty scattering angles from 30 to 110°. The results were compared with DWBA predictions and with predictions of the adiabatic theory. An explanation for the behavior of the correlation symmetry axis is proposed. (D.C.W.)

39866 PRECISION MEASUREMENTS OF SOME GAMMA-TRANSITION ENERGIES IN THE 800 kev REGION USING A Ge(Li) DETECTOR. Parsignault D. (California Inst. of Tech., Pasadena). Phys. Letters, 18: 36-8(Aug. 1, 1965).

The energy of gamma lines in the decay of ^{54}Mn and ^{46}Sc were measured using lithium-drifted germanium detectors. The energy of the gamma transition following the decay of ^{54}Mn to ^{54}Cr was measured, together with the energies of the two gamma transitions following the decay of ^{46}Sc to ^{46}Ti. For calibration purposes, the energy of a gamma line in ^{160}Dy was also measured. (D.C.W.)

39867 NUCLEAR MAGNETIC RESONANCE OF POLARIZED ^{17}F FORMED THROUGH THE $^{16}O(d,n)^{17}F$ REACTION. Sugimoto, K.; Mizobuchi, A.; Nakai, K.; Matuda, K. (Osaka Univ.). Phys. Letters, 18: 38-9 (Aug. 1, 1965).

The nuclear magnetic moment of ^{17}F was determined from an NMR experiment performed by measuring the anisotropy of beta particles emitted by the ^{17}F. (D.C.W.)

39868 FORM FACTORS OF ^3H AND ^4He WITH REPULSIVE-CORE POTENTIALS. Tang, Y. C. (Univ. of Minnesota, Minneapolis); Herndon, R. C. Phys. Letters, 18: 42-5(Aug. 1, 1965).

A calculation of the body form factors of ^3H and ^4He is outlined in which nucleon-nucleon potentials containing hard cores with radii of 0.45 or 0.50 fm were used. It is concluded that, with such potentials, it is possible to fit quite well the experimental values of the binding energies of ^3H and ^4He, the Coulomb energy of ^3He, and the body form factors of ^3H, ^3He, and ^4He. (D.C.W.)

39869 ON THE MECHANISM OF THE REACTION $^{11}B(^{16}O, ^{15}N)^{12}C$ AT 30 Mev. Bock, R.; Grosse-Schulte, M.; Van Oertzen, W.; Ruedel, R. (Max Planck Institut fuer Kernphysik, Heidelberg). Phys. Letters, 18: 45-6 (Aug. 1, 1965).

The results of an experimental investigation of the $^{11}B(^{16}O,^{15}N)^{12}C$ reaction at 30 Mev are presented. Preferred population of the ground state and the third excited state of ^{15}N was observed, providing strong evidence for a pickup mechanism. Further evidence for a direct mechanism of these two transitions was obtained from the angular distributions for population of different ^{15}N levels with ^{12}C in the ground state. (D.C.W.)

39870 MAGNETIC MOMENTS OF SINGLE PARTICLE STATES IN ^{207}Pb AND ^{209}Bi. Blomqvist, J. (NORDITA, Copenhagen); Freed, N.; Zetterstroem, H. O. Phys. Letters, 18: 47-50(Aug. 1, 1965).

The results are presented of calculations of the magnetic dipole moments for the ground state and the first excited state of ^{207}Pb and for the ground state of ^{209}Bi. The different contributions to the magnetic dipole moments were determined. (D.C.W.)

39871 ON THE RELATION BETWEEN t-MATRICES IN FREE SCATTERING, NUCLEAR MATTER AND FINITE NUCLEI. Kallio, A. (Univ. of Minnesota, Minneapolis). Phys. Letters, 18: 51-4(Aug. 1, 1965). (COO-1371-14)

A simplified version of the Scott-Moszkowski separation method was recently used in shell model calculations in which the nuclear reaction matrix was approximated by the long-range part of the potential $v_1(d,r_{12})$ and in which the separation distance was kept constant. It is shown that this method is accurate enough if the average relative momentum is properly chosen. Furthermore, the close connection with free scattering, established by Scott and Moszkowski, is shown to be true for finite nuclei as well. (D.C.W.)

39872 EFFECTIVE TENSOR INTERACTION IN NUCLEI. Kuo, T. T. S.; Brown, G. E. (Princeton Univ., N. J.). Phys. Letters, 18: 54-8(Aug. 1, 1965).

The treatment of tensor interactions is studied with specific consideration of the Hamada-Johnson interaction. It is shown that the $^3S_1$-state tensor contribution can be accurately approximated by the closure relation with an effective energy denominator. (D.C.W.)

39873 CONFIGURATION MIXING IN THE CONTINUUM AND NUCLEAR REACTIONS. [PART] II. Gillet, V.; Bloch, C. (Centre d'Etudes Nucleaires de Saclay, Gif-sur-Yvette, France). Phys. Letters, 18: 58-61(Aug. 1, 1965).

The qualitative behavior of the total cross section for gamma absorption is discussed in the framework of a previously presented theory of nuclear reactions (Phys. Letters, 16: 62(1965)). The effects of configuration mixing are considered. (D.C.W.)

39874 THE GROUND STATE OF ^{40}Ca AND THE REACTIONS $^{40}Ca(^3He,\alpha)^{39}Ca$, $^{42}Ca(^3He,\alpha)^{41}Ca$ AND $^{40}Ca(^3He,d)^{41}Sc$. Bock, R.; Duhm, H. H.; Stock, R. (Max Planck Institut fuer Kernphysik, Heidelberg). Phys. Letters, 18: 61-3(Aug. 1, 1965).

The ground-state configuration of ^{40}Ca and the excitation structures of ^{41}Ca and ^{41}Sc were investigated by observing the reactions $^{40}Ca(He\text{-}3,\alpha)^{39}Ca$, $^{42}Ca(He\text{-}3,\alpha)^{41}Ca$, and $^{40}Ca(He\text{-}3,d)^{41}Sc$ at 18.05 Mev. The angular distributions were compared with DWBA predictions; and spectroscopic factors, excitation energies, and l values were determined. (D.C.W.)

39875 REACTIONS INVOLVING SIMPLE ISOBARIC ANALOGUE RESONANCES. Robson, D.; Fox, J. D.; Richard, P.; Moore, C. F. (Florida State Univ., Tallahassee). Phys. Letters, 18: 86-8(Aug. 1, 1965).

The theory of isobaric analog resonances is applied to a specific class of resonances, and an experimental verification of the theory is summarized. (D.C.W.)

39876 MOESSBAUER LINE BROADENING IN POWDERED CRYSTALS. Peshkin, Murray (Argonne National Lab., Ill.). Phys. Rev., 139: 717-22(Aug. 2, 1965).

The line broadening of recoilless radiation is an important tool for studying isomer shifts and nuclear magnetic-dipole and electric-quadrupole interactions with crystalline fields. When the line shape is not well resolved, it is not always possible to obtain the desired information from experimental velocity spectra. It is pointed out that the use of moment theorems can sometimes give access to quantitative information which would not otherwise be available. The results given apply only to powdered samples, and then only in the absence of any anisotropy of the recoilless radiation or absorption being analyzed. (auth)

39877 MOESSBAUER CROSS SECTION OF Fe^{57} IN IRON. Hanna, S. S.; Preston, R. S. (Argonne National Lab., Ill.). Phys. Rev., 139: 722-5(Aug. 2, 1965).

The Mössbauer cross section for ^{57}Fe nuclei in metallic iron was measured by determining the Mössbauer absorption as a function of absorber thickness. The method used is independent of the recoilless fraction and the line width of the source. The effects of instrumental resolution and background radiation in the detector are also minimized. The measured cross section is in agreement with the value calculated from measured nuclear quantities and the Debye temperature of iron. (auth)

39878 ELECTRON-NUCLEAR DOUBLE RESONANCE OF Fe^{57} IN MgO. Locher, P. R.; Geschwind, S. (Bell Telephone Labs., Murray Hill, N. J.). Phys. Rev., 139: 991-4(Aug. 2, 1965).

The accuracy of the value of the nuclear magnetic moment of ^{57}Fe was increased by a factor of 10 by an electron-nuclear double resonance measurement in the Fe^{3+} state in MgO, where the paramagnetic shielding correction is less than 1 part in 10^3. The value found is $\mu I(Fe^{57}) = +0.09024 \pm 0.00007$ nm. Ludwig and Woodbury's earlier determination, $+0.0903 \pm 0.0007$ nm, is in excellent agreement with this result, although approximately ten times less accurate. An additional term in the hyperfine interaction of the type S^3I was observed. The hyperfine field at the ^{57}Fe nucleus is shown to differ by less than ½% from the value found by Robert for Fe^{3+} in octahedral coordination in yttrium iron garnet (YIG). Thus, whatever zero-point spin deviation may be present in YIG is apparently less than anticipated theoretically. (auth)

39879 IMPORTANCE OF NUCLEAR-SPIN EFFECTS IN EXTRACTING ALKALI SPIN-EXCHANGE CROSS SECTIONS FROM ZEEMAN OPTICAL-PUMPING SIGNALS. Gibbs, Hyatt (Univ. of California, Berkeley). Phys. Rev., 139: A1374-91(Aug. 30, 1965). (UCRL-11814).

The importance of the nuclear spins in the analysis of alkali spin-exchange experiments employing optical pumping by circularly polarized light and performed in low magnetic fields is demonstrated. Since the exchange interaction is an electronic process, the spin-exchange cross section is expected to be essentially independent of the nuclear spins. However, the hyperfine coupling is sufficient to make the expressions for the signals depend upon the nuclear spins. Failure to include the nuclear-spin effects in the analysis can lead to errors as large as several hundred percent in the deduced cross sections. The signal for general nuclear spin is found for the Franzen-type transient experiment and for the Dehmelt-type steady-state experiment in the limit of low light intensity. The results are quite sensitive to the process assumed for the relaxation of the ground-state populations. The solutions are given for a general process in which randomly oriented disorientation fields interact with the spins of the alkali atom only through the electron spin. The steady-state-signal expression includes the effects of self spin exchange and partial disorientation in the excited state. Only the diagonal elements of the density matrix are included. (auth)

39880 NUCLEAR SPIN-LATTICE RELAXATION IN THE PRESENCE OF MAGNETIC-FIELD GRADIENTS. Schearer, L. D.; Walters, G. K. (Rice Univ., Houston, Tex.). Phys. Rev., 139: A1398-1402(Aug. 30, 1965).

Brownian motion of a spin in the presence of a magnetic-field gradient can significantly influence the spin-lattice relaxation time. A theory is developed to describe this effect, and experiments on gaseous ^3He which confirm the theory in detail are reported. Practical situations where this mechanism can dominate, such as in the construction and use of polarized ^3He targets in nuclear-scattering experiments, are discussed. In a homogeneous magnetic field, relaxation times of approximately 7 hr at low pressures permit one to establish an upper limit of $7 \times 10^{-18}e$ cm for the electric-dipole moment of the ^3He nucleus. (auth)

39881 STUDIES IN X-RAY PRODUCTION BY PROTON BOMBARDMENT OF C, Mg, Al, Nd, Sm, Gd, Tb, Dy, AND Ho. Khan, J. M.; Potter, D. L.; Worley, R. D. (Univ. of California, Livermore). Phys. Rev., 139: A1735-46(Sept. 13, 1965). (UCRL-14107).

Thick-target yields, x-ray production, and ionization cross sections are presented for nine elements bombarded with protons of 15- to 1900-kev energy. The measurements are made by observing the x-ray emission (proportional-counter detection) when protons are stopped in thick samples of the target material. The x rays are produced in K, L, and M shells: C(K), Mg(K), and Al(K) in the intervals 15–110 kev and 500–1900 kev; Nd(L), Sm(L), Gd(L), Tb(L), Dy(L), and Ho(L) in the interval 500–1700 kev; Nd(M), Sm(M), Gd(M), Tb(M), Dy(M), and Ho(M) in the intervals 25–100 kev and 500–1700 kev. Where available, previous results are included to complete the presentation for these elements. A study of carbon-contamination buildup is included. (auth)

39882 ENERGY LOSS AND RESULTANT CHARGE OF RECOIL PARTICLES FROM ALPHA DISINTEGRATIONS IN SURFACE DEPOSITS OF ^{210}Po AND ^{241}Am. Cano, Gilbert L.; Dressel, Ralph W. (New Mexico State Univ., University Park). Phys. Rev., 139: A1883-92(Sept. 13, 1965).

Recoil particles from the $^{210}Po(\alpha)^{206}Pb$ and $^{241}Am(\alpha)^{237}Np$ disintegrations in surface deposits on platinum planchets were studied experimentally using both a low-resolution magnetic spectrometer, employing an electron multiplier detector, and a hemispherical ionization chamber. The average energy of the ^{206}Pb recoil ions emitted from thin deposits of ^{210}Po showed an exponential degradation with time after preparation, starting with the nascent energy of 103 kev and decreasing to ⅔ of this value in five days. Approximately 90% of the ^{206}Pb recoil atoms are emitted singly ionized and 10% are doubly ionized. The ^{237}Np recoils from thicker deposits of ^{241}Am apparently were mostly neutral but a small number were emitted with six units of charge and with an average kinetic energy of only 65 ± 15 kev compared with their nascent energy of 92.4 kev. Ejected recoils are accompanied by large numbers of secondary particles having energies less than 40 ev. With thin source deposits there are about five positively charged ions and three detected neutral secondary particles emitted per disintegration; but with thicker deposits these numbers rise to 15 positive ions and 10 neutrals, respectively. Negative ions may also be present but were excluded from observation by the experimental conditions. The average energy loss for the ^{206}Pb recoil particle in passing through argon gas was determined to be 121 ± 6 ev/ion-pair. The extrapolated range for a nascent energy ^{206}Pb recoil particle in argon at STP is 78 ± 2 μ. This value agrees with the range reported by Jessi and Sadauskis and lies within 2% of the value calculated from an energy-loss theory originally developed by Bohr. (auth)

39883 RANGE-MOMENTUM RELATION FOR HEAVY RECOIL IONS IN EMULSION. Henke, R. P.; Benton, E. V. (Naval Radiological Defense Lab., San Francisco). Phys. Rev., 139: A2017-21(Sept. 13, 1965).

The range-momentum relation for Ag and Br ions ($\beta < 0.04$) in Ilford K.5 nuclear emulsion is given. The measurements were made using the elastic collisions of ^{40}Ar, ^{20}Ne, and ^{12}C with nuclei of the emulsion. Mass separation between the Ag and Br (heavy) and the C, N, and O (light) recoil groups was achieved by the method of least squares applied to the kinematics and by the grouping of the events on a range-momentum plot. The empirical range-momentum relation is found to be $R = (1.99 \pm 0.13) \times 10^{-3}p + (2.76 \pm 0.69) \times 10^{-7}p^3$, where R is the residual range in microns, and p is the momentum in Mev/c. The range-momentum relation was used to improve the generalized range-energy expression given by Heckman et al., at low velocities. (auth)

39884 CHARGE SPECTRUM OF RECOILING ^{216}Po IN THE α DECAY OF ^{220}Rn. Szucs, S.; Delfosse, J. M. (Universite, Louvain, Belg.). Phys. Rev. Letters, 15: 163-5(July 26, 1965).

The charge distribution of recoiling ^{216}Po in the alpha decay of ^{220}Rn was investigated experimentally. (D.C.W.)

39885 IMPORTANCE OF THE IMAGINARY TERM IN DISTORTED-WAVE BORN-APPROXIMATION CALCULATIONS OF ^{3}He INELASTIC SCATTERING. Flynn, E. R. (Los Alamos Scientific Lab., N. Mex.); Bassel, R. H. Phys. Rev. Letters, 15: 168-70(July 26, 1965).

The scattering of 22-Mev ^{3}He ions from thin foils of ^{56}Fe, ^{58}Fe, and ^{58}Ni was studied. The elastic-scattering data were fitted by the optical model, and the parameters obtained were used in DWBA calculations for inelastic scattering. The results show that the imaginary part of the optical potential contributes almost all of the scattering cross section. (D.C.W.)

39886 CONTINUUM RESONANCES IN ^{4}He(p,p')^{4}He. Williams, Lawrence E. (Univ. of Minnesota, Minneapolis). Phys. Rev. Letters, 15: 170-2(July 26, 1965).

Two and possibly three resonances were observed in the inelastic-proton continuum resulting from bombardment of a ^{4}He gas target with 40-Mev protons. The excitation energies and full widths at half maximum of the two definite resonances were determined. (D.C.W.)

39887 2J + 1 DEPENDENCE OF TOTAL CROSS SECTIONS IN LITHIUM + BORON REACTIONS. Carlson, R. R.; McGrath, R. L. (Univ. of Iowa, Iowa City). Phys. Rev. Letters, 15: 173-5(July 26, 1965).

The total cross sections for ^{6}Li and ^{7}Li reactions with ^{10}B and ^{11}B were investigated experimentally. The results support the prediction of the statistical compound-nucleus theory that the total cross section for production of a residual nucleus with spin J is porportional to 2J + 1. Specifically, the results indicate that the reactions proceed to low-lying states primarily by a statistical compound-nucleus mechanism when the lithium nuclei have an energy equal to the Coulomb barrier. (D.C.W.)

39888 ELECTROMAGNETIC RADII OF H^3 AND He^3. Dalitz, R. H.; Thacker, T. W. (Clarendon Lab., Oxford). Phys. Rev. Letters, 15: 204-207(Aug. 2, 1965).

The form factors for the ^{3}H and ^{3}He charge structure and magnetic-moment structure were recently determined from elastic electron scattering experiments. The results showed that the rms radii and form factors for the ^{3}H and ^{3}He charge distributions are substantially different. A simple origin for an asymmetry between the three nucleons in these systems is pointed out, namely that the unlike nucleon in ^{3}H has a binding energy greater than that for the like nucleons in ^{3}He. The effects of this binding-energy asymmetry of the rms radii of ^{3}H and ^{3}He are explained by a simple model. It is shown that this asymmetry is capable of accounting for the effects observed. (J.F.P.)

39889 CROSS-SECTION MEASUREMENTS MADE WITH NEUTRONS FROM A NUCLEAR DETONATION. Hemmendinger, A. Phys. Today, 18: 17-23(Aug. 1965). (LA-DC-7122).

Time-of-flight experiments, conventionally dependent on neutrons from an accelerator, have long been used in the slow grinding out of cross-section data. The vastly larger supply of neutrons from an underground nuclear explosion was employed in a scaled-up time-of-flight experiment. The results of that experiment, which are regarded as preliminary, were reported to the American Physical Society in April, during the 1965 spring meeting in Washington, D. C., and the following article is based on the invited paper presented by Dr. Hemmendinger at that time. More precise results are expected from an experiment carried out on June 11, 1965, data from which are still being processed. The author is a group leader at the Los Alamos Scientific Laboratory in New Mexico. (auth)

39890 ON THE NUCLEAR CORRELATIONS IN DEUTERON PICKUP AND STRIPPING REACTIONS. Cheon, Il-Tong (Kyoto Univ.). Progr. Theoret. Phys. (Kyoto), 33: 638-47(Apr. 1965).

Discussions given are about the effects of correlations on the deuteron pickup and stripping reactions. The correlations may be expected to affect more strongly the deuteron pickup or stripping reactions than (p,p') reactions. (auth)

39891 PION RESCATTERING CORRECTION TO THE DECAY RATE OF HYPER-TRITON. Yazaki, Koichi (Tokyo Univ.). Progr. Theoret. Phys. (Kyoto), 33: 648-56 (Apr. 1965).

The meson(π) decay rate of the hyper triton is calculated, including meson(π) rescattering effect. It is shown, that this effect is as important as the effect of the Pauli principle previously discussed. The agreement with the observed decay rate is satisfactory. (auth)

39892 ON FISSION-TECHNETIUM I. von Baeckmann, A.; Feuerstein, H. (Kernforschungszentrum, Karlsruhe, Ger.). Radiochim. Acta, 4: 111-12(June 1965). (In German).

A combined extraction method for rapid separation of technetium isotopes from molybdenum isotopes was carried out so that the half lives of these isotopes could be determined. Half lives of 62 sec for ^{103}Mo and 42 sec for ^{105}Mo were found. Values for the half lives of ^{103}Tc and ^{105}Tc were 50 sec and 7.8 min, respectively. The half life of ^{106}Tc was 37 ± 4 sec and 29 ± 3 sec for ^{107}Tc. (M.C.G.)

39893 CONFERENCE ON CORRELATIONS OF PARTICLES EMITTED IN NUCLEAR REACTIONS, GATLINBURG, TENNESSEE, 15-17 OCTOBER 1964. Rev. Mod. Phys., 37: 327-536(July 1965). (CONF-641005)

Forty papers are presented; separate abstracts were prepared for 38. Two papers were previously abstracted for NSA; see 19: 14309 and 14505. (L.B.S.)

For abstracts of individual papers see: 39574, 39575, 39576, 39577, 39578, 39579, 39894, 39895, 39896, 39897, 39898, 39899, 39900, 39901, 39902, 39903, 39904, 39905, 39906, 39907, 39908, 39909, 39910, 39911, 39912, 39913, 39914, 39915, 39916, 39917, 39918, 39919, 39920, 39921, 39922, 39923, 39924, and 39925.

39894 A SURVEY OF SIMPLE MECHANISMS OF THREE-PARTICLE REACTIONS. Zupancic, C. (Bell Telephone Labs., Inc., Murray Hill, N. J. and Brookhaven National Lab., Upton, N. Y.). Rev. Mod. Phys., 37: 330-5 (July 1965). (BNL-8511).

A discussion is presented on the treatment of nuclear reactions with three outgoing particles. The sequential processes, where the reaction proceeds via a long-lived intermediate two-body system, and the quasifree of peripheral process, where one of the incoming particles interacts only with one constituent of the other incoming particle, are investigated. More complicated processes are considered; amplitudes in quantum mechanics for simultaneously occurring processes and properly taking into account the principle of indistinguishability of identical particles; the transition between the two limiting cases of sequential and peripheral processes, under conditions

when three-body effects are not important; and the presence of three strongly interacting particles in the final state. (L.B.S.)

39895 SEQUENTIAL DECAY THEORY FOR THE $B^{11}(p,3\alpha)$ REACTION. Swan, P. (Rice Univ., Houston, Tex.). Rev. Mod. Phys., 37: 336-46(July 1965).

A survey is made of the two classes of experimental evidence for sequential decay—measurements of total yield distributions of particles and energy distributions of the first-emitted particles, and measurement of the triple correlation distribution for the first and second-emitted particles—and of the various treatments of final state interactions. The reaction kinematics for three final particles, reaction amplitude for $^{11}B(p,\alpha)2\alpha$ triple correlations, symmetrization of the wave function, and fractional parentage coefficients and polarization of ^{12}C are discussed. Details of amplitude components for $^{11}B(p,\alpha)2\alpha$ and complex amplitude phase factors are discussed in the appendices. (L.B.S.)

39896 ANGULAR MOMENTA AND PAULI PRINCIPLE IN NUCLEAR REACTIONS $\alpha + A \rightarrow C^* \rightarrow b_1 + b_2 + b_3$. Kramer, Peter (Universitaet, Marburg, Ger.). Rev. Mod. Phys., 37: 346-9(July 1965).

It is noted that, due to the Pauli principle, the asymptotic wave function for short range forces should be replaced by a sum over all nucleon permutations in the breakup of a compound nucleus into k clusters, and that the function must be classified according to the group S_k on cluster permutations. It is shown that the function which contains the correlations in energy and angle of the clusters emitted can be characterized by the relative angular momenta in addition to the generalized angular momentum. The distribution of relative angular momentum and the classification of states according to S_3 are derived from appropriate subgroups of R_6, and the eigenfunctions which are closely related to the classification in terms of S_3 and the irreducible representations of S_3 are tabulated. The results are applied to the three-body breakup $^{11}B + p \rightarrow {}^{12}C(16.11\ \text{Mev}, 2^+) \rightarrow 3\alpha$, and the calculated and experimental Dalitz plots are shown. (L.B.S.)

39897 APPARENT, BUT ENERGY-DEPENDENT PSEUDO-RESONANCES DUE TO RESCATTERING IN SEQUENTIAL PROCESSES. Kacser, Claude (Univ. of Maryland, College Park); Aitchison, I. J. R. Rev. Mod. Phys., 37: 350-4(July 1965).

The kinematic conditions for the final-state interactions of the $^3He + {}^6Li \rightarrow \alpha + \alpha + p$ reaction are discussed, with particular emphasis on the matrix element dependence on higher rescattering effects. Calculations were performed and the graphs are shown for the spectrum versus beam energy for producing α pairs at fixed relative energies. It is argued that rescattering always occurs in three-body final-state interactions, and the effects can be distinguished from new resonances by their dependence on incident beam energy. (L.B.S.)

39898 THE $Be^9(He^3,\alpha\alpha\alpha)$ REACTION. Moazed, C.; Etter, J. E.; Holmgren, H. D.; Waggoner, M. A. (Univ. of Maryland, College Park). Rev. Mod. Phys., 37: 354-7 (July 1965).

A study was made of the two dimensional energy spectra for the $^9Be(^3He,\alpha)2\ ^4He$ reaction at 3.0 Mev at $\theta_A = +60$ and $\theta_B = -100°$, where θ_A and θ_B are the angles of two of the alpha particles. It is considered that the reaction proceeds through the 0^+ state of ^8Be, with the emission of the initial alpha particle at the angle θ_A. Information concerning the various states of ^8Be and the α-α scattering resonances are obtained from construction of the kinematic curve on the spectrum. The lack of yield in various regions of the spectrum indicates that at bombarding energies in the region of 3 Mev the phase-space distribution of the final state produced by the $^9Be(^3He,\alpha\alpha\alpha)$ reaction is strongly modulated by the two-body interactions among the various components of the final state. (L.B.S.)

39899 THE $B^{10}(He^3,p\alpha\alpha\alpha)$ REACTION PROCESS. Waggoner, M. A.; Etter, J. E.; Holmgren, H. D.; Moazed, C. (Univ. of Maryland, College Park). Rev. Mod. Phys., 37: 358-61(July 1965).

The sequential processes that are energetically possible for the $^{10}B(^3He,p\alpha\alpha\alpha)$ reactions are presented. The various states of the intermediate systems are studied from kinematic curves on the two-dimensional energy spectrum of the coincident proton and alpha particle from the reaction at 2.45 Mev. A number of states of ^{12}C and the 2.34, 2.81 and 11.62 Mev states of ^9Be were observed. It is concluded that the reaction proceeds to the four-body final state primarily through sequential two-body decays or by processes in which two-body interactions among the components of the final state strongly modulate the phase-space distribution. (L.B.S.)

39900 THE $Li^6(He^3,p\alpha\alpha)$ REACTION. Young, F. C.; Jayaraman, K. S.; Etter, J. E.; Holmgren, H. D.; Waggoner, M. A. (Univ. of Maryland, College Park). Rev. Mod. Phys., 37: 362-4(July 1965).

The kinematic calculations for the $^6Li(^3He,p\alpha\alpha)$ reaction proceeding through the various intermediate states to the three-body final state were carried out for 2.7 Mev incident ^3He. The α-α kinematic curve in the experimentally observed two-dimensional energy spectrum at $\theta_A = +60$ and $\theta_B = -100$ showed peaks in the yield corresponding to the $^3/_2^-$ ground state of ^5Li and the 16.62 to 16.92 Mev states (unresolved) of ^8Be. The $^1/_2^+$ first excited state of ^5Li was observed in the α-α kinematic curve for the spectrum at $\theta_A = +60$ and $\theta_B = -70$. It is concluded that at low bombarding energies the final state two-body interactions between the three final-state particles strongly modulate the phase-space distribution of states. (L.B.S.)

39901 DISINTEGRATION IN FLIGHT OF DEUTERONS UNDER THE INFLUENCE OF NUCLEAR FIELDS. Udo, F. (Institut voor Kernphysisch Onderzoek, Amsterdam). Rev. Mod. Phys., 37: 365-9(July 1965).

The results of an investigation are reported concerning the neutron-proton correlation generated by disintegration in flight of deuterons scattered by Au and Cu. Three experiments were performed at 26- and 23-Mev deuteron energy. Measurement of the spectra and the angular distribution of the protons produced in the disintegration process; and measurements of the angular and energy correlation between the outgoing neutrons and protons. (L.B.S.)

39902 STUDY OF THE $Ca^{40}(\alpha,2\alpha)$ REACTIONS. Bauer, R. W. (Massachusetts Inst. of Tech., Cambridge); Heymann, G.; Kossler, W.; Wall, N. S.; Gruhn, C. R. Rev. Mod. Phys., 37: 369-71(July 1965). (MIT-2098-81).

Angular and energy correlations of the alpha particles produced by the $^{40}Ca(\alpha,2\alpha)^{36}Ar$ were measured for incident alpha energies of 28.7 and 30.5 Mev, using a two-dimensional pulse-height analyzer for an angular range of 20 to 135° with solid-state detectors confined to the reaction plane. The experimental results are discussed with reference to both direct and sequential reaction mechanisms. (L.B.S.)

39903 PROTON-γ COMPETITION IN THE $Cu^{63}(p,2p)$ Ni^{62} REACTION AT 10.5 Mev. Parkinson, E. E.; Bodansky, D. (Univ. of Washington, Seattle). Rev. Mod. Phys., 37: 372-4(July 1965).

An attempt was made to clarify the role of gamma competition in the compound nucleus process by a measurement of the relative proton and gamma emission widths. The cross section for populating levels in which the gamma-proton competition is significant was determined from $^{63}Cu(p,p')$ measurements, and the proton yield from these levels was then determined from $^{63}Cu(p,2p)$ measurements. The results were considered in the light of the statistical theory of compound nuclear reactions. For the level of ^{63}Cu at 2.08 Mev above the proton separation energy the ratios $(\Gamma p/\Gamma\gamma)_J$ were formed to be approximately 2.5, 0.5, 0.07, 0.0065, and 0.0004 for states of spin $^1/_2$, $^3/_2$, $^5/_2$, $^7/_2$, and $^9/_2$, respectively. (L.B.S.)

39904 INFORMATION ON NUCLEAR STRUCTURE FROM (p,2p) AND OTHER KNOCK-OUT REACTIONS. Riou, M. (Laboratoire Joliot-Curie de Physique Nucleaire, Orsay, France). Rev. Mod. Phys., 37: 375-87 (July 1965).

General remarks are made on (p,2p) reactions which were carried out with co-planar, symmetric, and nonsymmetric kinematic geometry, and comparison is made with other reactions. The experimental parameters used by different groups in previous experiments are tabulated, and the progress performed in energy and angular resolution is indicated. The values of binding energies observed in (p,2p) summed-energy spectra are summarized and are also tabulated along with the l-assignment deduced from angular correlation or energy-sharing distributions, the shell-model state assignment, and the proton separation energies deduced from mass differences, corresponding to the ground state of the residual nucleus. Proton momentum distribution parameters are discussed and are tabulated for 1S and 1p states of ^{4}He to ^{12}C. Other knock-out reactions are discussed, such as the (p,pd) and (p,pα). The (π^{+},2p) and (π^{-},pn) reactions are also briefly discussed. (L.B.S.)

39905 INFORMATION OBTAINABLE FROM (p,2p) REACTIONS. McCarthy, I. E. (Univ. of California, Davis). Rev. Mod. Phys., 37: 388-92(July 1965).

A discussion is presented on the theoretical interpretation of the (p,2p) reaction as the direct knockout of a proton from a nucleus by a single-particle interaction with an incident proton. The analysis is carried out in the distorted-wave Born approximation, and the derivation of the distorted-wave matrix element is outlined. Calculations were made of the angular correlation for 155 Mev incident protons or ^{12}C, and the results are compared with experiment. (L.B.S.)

39906 PROBLEMS IN THE ANALYSIS OF QUASIFREE SCATTERING. Jackson, Daphne F. (Univ. of Washington, Seattle and Battersea Coll. of Tech., London). Rev. Mod. Phys., 37: 393-5(July 1965).

The problems involved in an accurate analysis of the (p,pd) reaction are discussed. The interaction of the incident proton with the nucleus is separated into a direct interaction with the deuteron cluster and an optical potential. The matrix element constructed for two forms for the direct interaction with plane and distorted waves. The feasibility of calculating the direct term is discussed, and application is made to the ^{6}Li(p,pd) reaction. It is concluded that owing to distortion and exchange effects, the (p,pd) reaction on light nuclei is now complex, both in interpretation and computation, than has previously been supposed. (L.B.S.)

39907 A SIMPLE ANALYSIS OF THE Li^{6}(p,pd)He^{4} REACTION. Devins, D. W.; Scott, Bruce L.; Forster, H. H. (Univ. of Southern California, Los Angeles). Rev. Mod. Phys., 37: 396-8(July 1965).

A analysis is made of the ^{6}Li(p,pd)^{4}He reaction at 155 and 30.5 Mev. Calculations were made of the angular correlations using Gaussian, exponential, and Yukawa probability distribution functions, and the results are presented. (L.B.S.)

39908 QUASI-ELASTIC p-α SCATTERING IN C^{12}. Yuasa, Toshiko; Hourani, Eid (Universite, Paris). Rev. Mod. Phys., 37: 399-401(July 1965).

A kinematic analysis was made of the experimental results from a bubble chamber investigation of the ^{12}C(p,pα)^{8}Be, which demonstrated the existence of direct quasi-elastic scattering of protons ($\bar{E}_0$ = 85 Mev) by nuclear alpha particles. The angular distributions of the scattered protons, of the emitted α particles, and of the proton-alpha correlations are shown; and an estimate is given of the total cross section leaving the residual nucleus in the ground on first excited state. (L.B.S.)

39909 STRUCTURE OF He^{3} AND H^{3} FROM HIGH-ENERGY ELECTRON SCATTERING. Griffy, T. A. (Stanford Univ., Calif.); Oakes, R. J. Rev. Mod. Phys., 37: 402-5(July 1965).

The cross sections for the knockout of a proton by an inelastically scattered electron in ^{3}He and ^{3}H were computed in two approximations: the nonrelativistic approximation in which the three-body nucleus is described by a wave function; and the nucleon-pole approximation. The results are compared and discussed. (L.B.S.)

39910 DISTORTED-WAVE BORN APPROXIMATION FOR STRIPPING TO VIRTUAL LEVELS. Huby, R.; Mines, J. R. (Univ. of Liverpool). Rev. Mod. Phys., 37: 406-8 (July 1965).

The distorted-wave Born approximation is adapted to the case of stripping reactions leading to three-body final states by the two-stage process A + d $\rightarrow$ p + B* $\rightarrow$ p + n + A. A procedure for evaluating the stripping amplitude is found and a numerical application is mentioned. (L.B.S.)

39911 SEQUENTIAL DECAY OF ^{12}C INTO THREE α PARTICLES. Phillips, G. C. (Rice Univ., Houston, Tex.). Rev. Mod. Phys., 37: 409-17(July 1965).

An investigation was made of the ^{11}B(p,3α) reaction at 2 to 5.64 Mev to develop experimental and theoretical techniques for treating nuclear reactions that lead to three-particle final states. The simultaneous and sequential breakup mechanisms were examined. The two-parameter and three-parameter pulse-height spectra are shown and discussed. It is concluded that the ^{11}B(p,3α) reaction proceeds through a sequential mechanism involving the ground state and first excited state of ^{8}Be. Other conclusions are made on the order of emission of the alpha particles, interference effects, and the angular variables in the three-particle final states. (L.B.S.)

39912 ANGULAR DISTRIBUTIONS IN THREE-α AND THREE-NUCLEON SYSTEMS. Duck, Ian (Rice Univ., Houston, Tex.). Rev. Mod. Phys., 37: 418-29(July 1965).

Calculations of the angular distributions of three α particles following breakup of selected states in ^{12}C are described. The theories used to describe the final-state interaction are presented, and are followed by a discussion of the calculations as applied to the experimental results of Bronson. It is concluded that the sequential model provides a detailed understanding of the three-alpha breakup of ^{12}C. A description is also given of angular distribution calculations in inelastic proton-deuteron scattering, and the results are compared with experimental results. Calculations were also made for the (n,d) inelastic scattering to examine the sensitivity of the (p,n,n) angular distributions to changes in the (n,n) scattering lengths. (L.B.S.)

39913 THE ^{3}He(^{3}He,2p)^{4}He REACTION. Aldridge III, J. P.; Wildenthal, B. H.; Youngblood, D. H. (Rice Univ., Houston, Tex.). Rev. Mod. Phys., 37: 430-3(July 1965).

The ^{3}He(^{3}He,2p)^{4}He reaction was studied at 4.9 Mev by measuring the energy spectra of all pairs of reaction products detected in coincidence. The proton-proton and the proton-alpha energy correlation were recorded by an on-line, two-dimensional computer-analyzer system, and the spectra were projected as functions of the energy of the detected proton in order to examine the variation of intensity along the three-body locus. Calculations were performed to determine the relative contributions for transitions through various intermediate states, which show peaks at the proper positions for decay through the ^{5}Li ground state. (L.B.S.)

39914 p-^{4}He FINAL-STATE INTERACTION IN ^{3}He (^{3}He,2p)^{4}He. Bacher, A. D.; Tombrello, T. A. (California Inst. of Tech., Pasadena). Rev. Mod. Phys., 37: 433-6 (July 1965).

The ^{3}He(^{3}He,2p)^{4}He reaction was investigated at 3 to 18 Mev in order to obtain information about the reaction mechanism over a wide range of bombarding energies, and to develop a consistent method for determining the total reaction cross section that can be extended to lower bombarding energies. Typical proton spectra at 9.94 and 15.56 Mev are shown in addition to p-α and p-p coinci-

dence spectra at 9.91 Mev. It is noted that, while there is sufficient energy available in the intermediate state for additional final-state interactions to occur, the reaction maintains a particular sequential mechanism over a broad energy range; and that the major portion of the observed high-energy proton spectrum can be reconstructed on the basis of a sequential decay through the ^{5}Li state. (L.B.S.)

39915 SEQUENTIAL EMISSION IN THE REACTION ^{7}Li(d,n)2 α. Jones, C. M.; Bair, J. K.; Johnson, C. H.; Willard, H. B.; Reeves III, M. (Oak Ridge National Lab., Tenn.). Rev. Mod. Phys., 37: 437-41(July 1965). (ORNL-P-886).

The ^{7}Li(d,n)2α reaction was studied at 1.8 to 7.0 Mev by observing the two emitted alpha particles in coincidence. The geometrical arrangement of the experiment is described. A circular projection transformation was made of the three-dimensional correlation functions, and the results are shown for bombarding energies of 2.0, 4.0, and 7.0 Mev. Sharp peaks were observed whose positions are consistent with the assumption of sequential decay via known levels of the possible intermediate nuclei ^{5}He and ^{7}Be. (L.B.S.)

39916 PARTICLE-PARTICLE ANGULAR CORRELATION FOR THE ^{9}Be(^{3}He,α)^{8}Be $\rightarrow \alpha\alpha$ REACTION. Moazed, C.; Etter, J. E.; Holmgren, H. D.; Waggoner, M. A. (Univ. of Maryland, College Park). Rev. Mod. Phys., 37: 441-3 (July 1965).

Particle-particle angular correlations for the ^{9}Be(^{3}He,α)-^{8}Be(16.92) $\rightarrow 2\alpha$ were measured as a function of the angle of the breakup of the ^{8}Be(16.92) state for the initial alpha particle emitted at 20°, 40°, 60°, 90° and 140°, in order to determine the spin of this state and to obtain information concerning the nature of the initial reaction mechanism. The graphs of the angular correlation function least-square fitted to the observed angular correlations are shown, and the amplitudes and phase angles are tabulated. A spin of 2^+ was assigned to the ^{8}Be(16.92) state. It is concluded that more detailed calculations including distortion effects and possibly interferences between various modes are needed in order to determine the nature of the initial interaction. (L.B.S.)

39917 SPECTROSCOPIC STUDIES WITH THE ^{10}B(^{3}He,p$\alpha\alpha\alpha$) REACTION. Etter, J. E.; Waggoner, M. A.; Moazed, C.; Holmgren, H. D.; Han, C. (Univ. of Maryland, College Park). Rev. Mod. Phys., 37: 444-7 (July 1965).

The concept of state or resonance in the interaction of final-state components is used in a description of the intermediate systems involved in the decay of the ^{10}Be + ^{3}He system to the p$\alpha\alpha\alpha$ final state. The results of spectroscopic studies yielded evidence of excited states of ^{7}Li, ^{9}Be, ^{9}B, and ^{12}C, through which the reaction can proceed by the sequential process. Information relevant to the J^π assignments to states of ^{9}B and ^{12}C are tabulated and discussed. (L.B.S.)

39918 DIRECT THREE-BODY DECAY ^{12}C $\rightarrow 3\alpha$ IN THE REACTION ^{11}B(p,α)2α AT THE 163-kev RESONANCE. Dehnhard, D. (Universitaet, Marburg, Ger.). Rev. Mod. Phys., 37: 450-2(July 1965).

It was previously shown that in the plane perpendicular to the proton beam the α-particle spectrum and the α-α coincidence spectra reveal a strong anomaly at the 163-kev resonance of the ^{11}B(p,α) reaction. A detailed study was made of the reaction, in particular to examine the dependence of the anomaly on the incident proton spectra. The results are discussed. (L.B.S.)

39919 MECHANISM OF THE REACTION ^{11}B(p,α)2α BELOW AND IN THE VICINITY OF THE 675-kev RESONANCE. Kamke, D.; Krug, J.; Richter, F.-W. (Universitaets Bochum und Marburg, Ger.). Rev. Mod. Phys., 37: 453-4(July 1965).

Single α-spectrum and α-α coincidence spectra from the ^{11}B(p,α)2α reaction at 250 and 675 kev were studied. A block diagram is shown of the experimental and electronics arrangement. It is concluded that from the resonances at 675 and 1388 kev the decay is via ^{8}Be, from the .163 kev resonance a sequential decay takes place only via ^{8}Be ground state, the remaining disintegrations of the ^{12}C state being a three-particle decay. (L.B.S.)

39920 THE 2 ^{6}Li $\rightarrow 3\alpha$ REACTION. Norbeck, E.; Mancusi, M. D.; Carlson, R. F. (Univ. of Iowa, Iowa City). Rev. Mod. Phys., 37: 455-7(July 1965).

The use of a two-counter four-parameter analyzer for detailed angular correlation studies of the 2 ^{6}Li $\rightarrow 3\alpha$ reaction is briefly discussed. A part of the coincidence spectra obtained is shown, and the results are discussed. (L.B.S.)

39921 A STUDY OF THE ^{7}Li + d $\rightarrow 2\alpha$ + n REACTION AT LOW ENERGY. Bilwes, R.; Bourotte, B. (Centre de Recherches Nucleaires, Strasbourg). Rev. Mod. Phys., 37: 458-9(July 1965).

Kinematic considerations are given to the various processes of the ^{7}Li + d $\rightarrow 2\alpha$ + n reaction. It is concluded that the reaction essentially goes through the two-step process involving ^{8}Be and ^{5}He levels as far as their excitation is energetically possible and, with a weak probability, through direct three-body breakups. (L.B.S.)

39922 COMPARISON OF EXCITED STATE OF ^{4}He FROM TWO DIFFERENT REACTIONS. Meyerhof, W. E. (Stanford Univ., Calif.). Rev. Mod. Phys., 37: 512-15 (July 1965).

A comparison is made of the results of an analysis of the D + T reaction by Werntz in which evidence was found for a 20.3 Mev excited state in ^{4}He, and the results of an analysis of the D + ^{3}He reaction by Donovan et al., in which an additional state was suggested at 21.2 Mev in ^{4}He. It is shown that the state near 20 Mev is very likely to be identical with the 0^+ s-wave resonance found by Werntz. It is also shown that the feature in the proton spectra interpreted as a ^{4}He state near 21.2 Mev can be explained as a p-wave final state interaction in the p + T system. (L.B.S.)

39923 THEORY OF THE THREE-NUCLEON SYSTEM. Aaron, R. (Northeastern Univ., Boston and Univ. of California, Livermore); Amando, R. D.; Yam, Y. Y. Rev. Mod. Phys., 37: 516-18(July 1965).

A calculation is presented of the binding energy, the low-energy scattering parameters, and angular distributions for the three-nucleon system, which extends the exact three-body theory to include spin-dependent two-body forces. A summary of theoretical and experimental results for the neutron-deuteron system is presented. (L.B.S.)

39924 ENERGY-ANGULAR CORRELATIONS AND SEQUENTIAL DECAY IN THE ^{2}H(p,2p)n AND ^{1}H(d,2p)n REACTIONS. Simpson, W. D.; Bronson, J. D.; Jackson, W. R.; Phillips, G. C. (Rice Univ., Houston, Tex.). Rev. Mod. Phys., 37: 523-8(July 1965).

An investigation was made of the energy and angular distributions from the reactions ^{2}H(p,2p)n and ^{1}H(d,2p)n by detecting the two breakup protons in coincidence for a number of different laboratory angles and bombarding energies. Three-dimensional isometric projections of coincident counts are shown for the reactions at 9.0 and 10.5 Mev incident energies. Evidence of the virtual singlet deuteron is presented, along with evidence indicating sequential breakup in the ^{1}H(d,2p)n reaction via an intermediate state in the (p + p) system corresponding to the di-proton. (L.B.S.)

39925 D(p,2p)n REACTION AT 31 Mev. Bunch, S. M.; Kim, C. C.; Forster, H. H. (Univ. of Southern California, Los Angeles). Rev. Mod. Phys., 37: 528-30(July 1965).

An experiment is described in which the angular distributions of the protons emitted in the D(p,2p)n reaction at 31 Mev were measured. Diagrams are presented of the electronics using coincidence-anticoincidence logic, and of the electronics using two-dimensional analysis. The differential cross sections were calculated for three low-energy cutoff points, using the impulse approximation in the spectator model, and the results are compared with the experimental distributions. (L.B.S.)

39926 INVESTIGATIONS OF THE GROUND STATE OF THE THREE-NUCLEON SYSTEM BY ONE-DIMENSIONAL EQUATION. Shcherbin, Yu. P. Vestn. Leningr. Univ., No. 4, Ser. Fiz. i Khim., No. 1, 142-5(1965). (In Russian).

In order to determine the binding energy of three-nucleon systems, the function Ψ of the three-nucleon system was developed on the basis of eigenfunctions of one-dimensional equations; this method was extended for other classes of potentials. The properties of a completely symmetrical function Ψ_0 were studied for the case of three-nucleon collisions, with the intention of analyzing the results for various classes of potentials, rather than optimizing the variational data. The calculation of the binding energy in the asymptotic region for two-nucleon collisions yielded better results using the function $\Psi_0(\xi)$ than by means of the function $\Psi = \pi_{i=1}^{3} f(x_i)$. If the bound-state function is more compact, it follows better the latter equation, and the asymptotic behavior plays a smaller role in the range of the two-nucleon collisions. The validity and the effectiveness of the one-dimensional equations were confirmed for several classes of potentials on the basis of numerical examples. The method was found useful in cases in which the potentials have a complex and singular structure at short distances, as specifically, in nucleon-nucleon interactions. (TTT)

39927 THE INFLUENCES OF PAIRING FORCE ON THE PROPERTIES OF ACTINIDE NUCLEI. Wu, Tsung-shyh; Tseng, Chin-yen. (Peking Univ.). Wu Li Hsueh Pao, 21: 915-50(May 1965). (In Chinese).

By making use of the method for treating the pairing force, which conserves the number of particles, the influences of pairing force on the various properties of actinide nuclei were analyzed, including the intrinsic spectra of odd-A nuclei and even-even nuclei, β-decays and α-decays, etc. The general formula expressing the influences of pairing force on the various types of α-decay, are given. First, Nilsson's parameters, which, after the pairing force being taken into account, can account for the observed intrinsic spectra of odd-A nuclei, are determined. It is found that they may be chosen as follows: $\kappa \sim 0.050$, $\eta \sim 4.4-5.4(\delta \sim \kappa\eta \sim 0.22-0.27)$ $\mu \sim 0.70(N = 5)$, $\mu \sim 0.62-0.66(N = 6)$, for protons, $\mu \sim 0.43-0.45(N = 6)$, $\mu \sim 0.41-0.43(N = 7)$, for neutrons. Subsequently, with such realistic single-particle spectra, the intrinsic spectra and β-decays of neighboring even-even nuclei (^{228}Th, ^{230}Th, ^{232}U, ^{234}U, ^{244}Cm) are analyzed in detail. Some observed levels ($E \gtrsim 1$ Mev) may be explained as the pair-broken states or the pair-excitation states. According to calculation, there exist still many levels in the energy region, $E \sim 1-2$ Mev, but they have not been observed yet. In the β-decay experiments, the majority of these levels can not be detected easily, but some of them, easily. The systematically occurring vibrational bands in the spectra of even-even nuclei could not be considered as the pair-broken states or the pair-excitation states. They are γ-vibrational states, $K\pi = 2^+$, $E \sim 0.8-1.0$ Mev; β-vibrational states, $K\pi = 0^+$, $E \sim 0.7-0.9$ Mev; octupole b-vibrational states, $K\pi = 0^-$, $E \sim 0.5-0.7$ Mev. The influences of pairing force on the α-decay probabilities are treated both with the BCS method and with the present method. The results, especially for the favored α-dacay, are quite different in the two methods. For example, when about 10 levels are involved, the retardation factors for the favored α-decay of even-even nuclei are: $R = R_Z R_N \approx 200$ (BCS wave function), $R = R_Z R_N \approx 70$ (exact solution). Compared with the exact solution, the occupation probability of the ν-th levels, $\nu_{p\nu}^2$, in the BCS method converges too slowly. In the BCS wave function, the portion, in which the number of particles is equal to the average number of particles, is about one third. After the influence of pairing force is taken into account, the nuclear radius constant derived from the α decay is about $r_0 \sim 1.35$ fm. The favored α-decay of odd-A nuclei and the unfavored α-decay are also discussed. The so-called F-factors are calculated and compared with experiments. (auth)

39928 THE γ SPECTRUM OF Eu^{152*} WITH THE HALF LIFE 9,2 HOURS. Dzhelepov, B. S.; Zhukovskii, N. N.; Maloyan, A. G. Yadern. Fiz., 1: 941-7(June 1965). (In Russian).

The relative intensities of 13 gamma lines from ^{152*}Eu were determined using magnetic spectrometers. Four new ^{152*}Eu gamma lines which must be added to the decay scheme are found. A new excitation level with the energy 1680 kev, is introduced in ^{152}Sm. A deviation from the Alaga rules is noted, when the 1511-kev (1^-) level is de-excited to the 2^+ or 0^+ rotation levels of the ground state. (auth)

39929 Gd^{159m} AND Sb^{117m} ISOMERS. Gritsyna, V. T.; Klyucharev, A. P.; Remaev, V. V. Yadern. Fiz., 948-50 (June 1965). (In Russian).

An isomer with a half life of 0.46 msec, produced in the irradiation of a ^{160}Gd target by protons is investigated. It is found that the $E\gamma = 170$-kev isomer transition belongs to the ^{159}Gd nucleus. The (p,xn) reaction on tin, producing the nucleus ^{117m}Sb was studied, so as to confirm the previously detected isomer ^{117m}Sb with a half life of 0.164 msec. The isomer ^{117m}Sb was not found in reactions. (auth)

39930 ON THE DECAY OF Ho^{161}. Abdurazakov, A. A.; Gromov, K. Ya.; Kuznetsov, V. V.; Huo, Ma; Muziol, G.; Molnar, F.; Molnar, A.; Muktasimov, F.; Han, Ch'u Jun (Joint Inst. for Nuclear Research, Dubna, USSR and Tashkent Polytechnic Inst.). Yadern. Fiz., 1: 951-7(June 1965). (In Russian).

The spectra of gamma rays and conversion electrons in the decay of ^{161}Ho were studied. New transitions of ^{161}Ho were found, with energies 210.8, 234.5, 239.7, 339.7, 416.0, and 760 kev. The relative intensities of the gamma rays and conversion electrons were measured. The half life of ^{161}Ho was determined to be 2.48 ± 0.05 hr. The multipolarity of a number of gamma transitions was determined. The decay scheme of ^{161}Ho was analyzed on the basis of the data obtained. (auth)

39931 3-HOUR ACTIVITY OF LUTETIUM. Avotina, M. P.; Grigorev, E. P.; Dzhelepov, B. S.; Zolotavin, A. V. (Leningrad State Univ.). Yadern. Fiz., 1: 958-60(June 1965). (In Russian).

The presence of the isomer ^{176m}Lu among the products of the deep splitting of tantalum by 660-Mev protons was confirmed. The L_{II}-, L_{III}-, M_{II}-, M_{III}- and N-line intensities of the 88.37 ± 0.03-kev transition in ^{176}Hf were measured. (auth)

39932 ABSORPTION OF γ QUANTA AND STOPPED π MESONS BY NUCLEI WITH TWO-NUCLEON EMISSION AND THE STRUCTURE OF LIGHT NUCLEI. Kopaleishvili, T. I. (Tbilissi State Univ., USSR). Yadern. Fiz., 1: 961-70(June 1965). (In Russian).

The absorption of high-energy ($E > 100$ Mev) gamma quanta and stopped mesons (π) by nuclei, accompanied by the emission of two nucleons, is investigated theoretically using the independent pair model. Expressions are obtained for the distribution of nucleons emitted in (π^-, nn) and (π^-, np) processes on ^{16}O and ^{12}C nuclei, with respect to their relative energy and also for the (γ,np) total cross section on the same nuclei as a function of the gamma quantum energy. The obtained quantities are used to investigate the role of the interaction between the emitted final-state nucleons and the correlated nucleon pair in the nucleus for these processes. Other light nuclei structure problems are also considered. The theoretical results are compared with existing experimental data. (auth)

39933 EXCITATION SPECTRA OF Tl^{208} AND Bi^{208} NUCLEI. Birbrair, B. L.; Guman, V. N. (Ioffe Inst. of Physics and Tech., Leningrad). Yadern. Fiz., 1: 971-5 (June 1965).

The energy levels of ^{208}Tl and ^{208}Bi nuclei are considered as neutron-proton hole and proton-neutron hole type excited states of ^{208}Pb. The calculated binding energies and excitation spectra of these nuclei are in fair agreement with the experiments. The values of the f' and g' constants of the zero harmonic Γ^{ω} are specified. (auth)

39934 PHOTONUCLEAR REACTIONS WITH α-PARTICLE EMISSION AND FOUR-PARTICLE CORRELATIONS IN LIGHT NUCLEI. Dzhibuti, R. I.; Mamasakhlisov, V. I.; Macharadze, T. S. (Inst. of Physics, Academy of Sciences, Georgian SSR). Yadern. Fiz., 1: 976-83(June 1965). (In Russian).

The (γ,α) reactions on light nuclei are considered, using the shell model with four-particle correlations. The influence of the Coulomb and nuclear interaction of reaction products on the total cross section and angular distribution of α particles for E2 + M1-transitions is investigated. The results are compared with the experimental data. (auth)

39935 A METHOD FOR CALCULATING CROSS SECTIONS IN THE OPTICAL MODEL. Babikov, V. V. (Joint Inst. for Nuclear Research, Dubna, USSR). Yadern. Fiz., 1: 984-6(June 1965). (In Russian).

A method is proposed for calculating cross sections in the optical model of nuclear reactions. It is very convenient in practical calculations. (auth)

39936 ON THE APPLICABILITY OF THE EVAPORATION THEORY TO THE EMISSION OF MULTICHARGED PARTICLES BY HEAVY NUCLEI. Lepekhin, F. G.; Makarov, M. M.; Tkach, L. N. (Ioffe Inst. of Physics and Tech., Leningrad). Yadern. Fiz., 1: 987-93(June 1965). (In Russian).

The angular distributions, energy spectra, and relative probabilities for the emission of multicharge particles from heavy nuclei were calculated on a computer, according to the evaporation theory. A comparison of the results with experimental data shows that these quantities can not be completely described by the evaporation theory. The region in which the evaporation theory can be applied is estimated, and the parameters are found, giving the best agreement between theory and experiment, for particles in this region. (auth)

39937 CIRCULAR POLARIZATION OF γ QUANTA ACCOMPANYING THE REACTION $B^{10}(d,p)B^{11}$. Szentpetery, I.; Eroe, J.; Fodor, I.; Zimanyi, J. (Central Inst. for Studies in Physics, Budapest). Yadern. Fiz., 1: 1002-4(June 1965). (In Russian).

The circular polarization of the 4.46-Mev γ-rays, which were in coincidence with protons emitted in various directions with respect to the deuteron beam, was measured in the $^{10}B(d,p\gamma)^{11}B$ reaction, at 0.40 Mev. Theoretical calculations were performed on the basis of DWBA. (auth)

39938 THE ENERGY DISTRIBUTION OF PHOTOPROTONS FROM Si^{28}. Goryachev, B. I.; Ishkanov, B. S.; Kapitonov, I. M.; Yurev, B. A.; Shevchenko, V. G. (Moscow State Univ.). Yadern. Fiz., 1: 1005-8(June 1965). (In Russian).

The energy distributions of photoprotons from the reaction $^{28}Si(\gamma,p)^{27}Al$ induced by gamma-bremsstrahlung with the maximal energy $E_{\gamma\ max}$ = 23, 25 and 27 Mev were measured using a semiconducting detector. Photoproton groups with the energies $E_p \sim 6.0$, 6.9, 7.8 and 9.3 Mev show up in the energy distributions. The energy levels of the ^{28}Si nucleus are obtained, assuming that the ^{27}Al nucleus stays in the ground state. The obtained scheme of excitation levels is in good agreement with data obtained from (γ,p), (γ,n) and (p,γ) reactions. The results are compared with calculations according to the particle-hole model. (auth)

39939 INTERACTIONS OF 14.1-Mev NEUTRONS WITH TRITIUM. Velyukhov, G. E.; Prokof'ev, A. N. (Ioffe Inst. of Physics and Tech., Leningrad). Yadern. Fiz., 1: 1009-13(June 1965). (In Russian).

The experimental spectrum of charged particles from the reactions T(n,n); T(n,2n)d; T(n,3n)p for the angles 0, 10 and 20° in the laboratory system is described. The lines belonging to the elastic neutron-tritium scattering and the 7.8-Mev ($\theta = 0°$) deuteron group corresponding to the final-state interaction of two neutrons from the reaction T(n,2n)d show up clearly in the spectrum. Arguments are given confirming such an interpretation of this particle group, and the corresponding differential cross section for $\theta = 0°$ is estimated. (auth)

39940 INVESTIGATION OF ANGULAR AND ENERGETIC CORRELATIONS IN THE Ni(d,np)Ni REACTION BY THE NEUTRON-PROTON COINCIDENCE METHOD. Nemets, O. F.; Sokolov, M. V.; Struzhko, B. G. Yadern. Fiz., 1: 1014-18(June 1965). (In Russian).

The coincidences of neutrons and protons from the disintegration of 13.6-Mev deuterons on Ni nuclei were investigated for 0_p = 20, 30 and 40°. The angular correlations have two maxima. The maximum at $0_n = 0°$ can be due to a stripping reaction, followed by the emission of a second nucleon from the compound nucleus. (auth)

39941 THE REACTION (He^3,α) ON Be^9, N^{14} AND O^{16}. Artemov, K. P.; Goldberg, V. Z.; Islamov, B. I.; Rudakov, V. P.; Serikov, I. N. Yadern. Fiz., 1: 1019-24(June 1965). (In Russian).

The reaction (He-3,α) on the nuclei ^9Be, ^{14}N and ^{16}O was investigated at several energies in the region 17 to 36 Mev. The angular distributions of alpha particles were obtained, corresponding to the formation of the residual nucleus ^8Be in the state O and 2.9 Mev, ^{13}N in the states: 0; 2.37; 3.51 + 3.56; 6.91 + 7.18 and 11.4 Mev and ^{15}O in the states 0; 5.17 + 5.24 and 6.16 Mev. The angular distributions are typical for direct nuclear reactions. The reaction $^9Be(He\text{-}3,\alpha)^8Be$ (ground state) is compared with the theory, considering this reaction as the pick-up of a weakly bound neutron from ^9Be. The position of the first three minima in the experimental angular distribution curves and the dependence of their position on the ^3He ion energy are in agreement with the theoretical predictions. The excitation cross section for higher levels of the residual nuclei ^8Be, ^{13}N and ^{15}O are large in comparison with the cross sections for the creation of these nuclei in the ground state. The cross section for the emission of alpha particles from the reaction (He-3,α) into the forward hemisphere, summed over all investigated levels of ^{13}N is of the same order of magnitude as the corresponding cross section for the four investigated levels of ^{15}O. (auth)

39942 COULOMB EXCITATION OF THE FIRST LEVELS OF Zr^{90} AND Zr^{96}. Gangrskii, Yu. P.; Lemberg, I. Kh. (Ioffe Inst. of Physics and Tech., Leningrad). Yadern. Fiz., 1: 1025-7(June 1965). (In Russian).

The Coulomb excitation of the first levels of ^{90}Zr and ^{96}Zr was investigated using the coincidences between the inelastic scattering of ions and gamma quanta emitted in the de-excitation of excited states. ^{14}N ions with an energy of 44 Mev were used as bombarding particles. The measured reduced transition probabilities for the first levels in ^{90}Zr and ^{96}Zr are respectively equal to 0.42 ± 0.015 $e^2 \times 10^{-48}$ cm^4 (3.5 times higher than the single-particle estimation) and 0.005 ± 0.022 $e^2 \times 10^{-48}$ cm^4 (4.5 times higher than the single-particle estimation). The previously unknown value of the first level energy in ^{96}Zr was found to be 0.75 ± 0.05 Mev. The experimental level energies and reduced probabilities are compared with calculations based on a simple quantitative model, taking pairing and quadrupole-quadrupole interactions between outer nucleons into account. The agreement with experimental data is better when the one-particle neutron state spectrum, taken from (d,p) reactions on zirconium isotopes, is used in the calculations than when the Nilsson scheme is used. (auth)

39943 A COVARIANT METHOD FOR CALCULATING CROSS SECTIONS AND ITS APPLICATION TO SOME REACTIONS INDUCED BY NEUTRINOS. Zheleznykh, I. M. (Lebedev Inst. of Physics, Moscow). Yadern. Fiz., 1: 1056-65(June 1965). (In Russian).

Some consequencies of a covariant method for calculating cross sections (the improved Weizsäcker-Williams method) are discussed. A system of equations is given to determine the coefficients $a(q^2, kq)$, $b(q^2, kq)$ figuring in the covariant method, and the contribution of the so-called longitudinal part of the cross section is considered. The cross section of the reaction $\nu_e + Z \rightarrow e^- + W^+ + Z'$ is calculated analytically. Terms of the type $g^2 E_\nu q_{max}$ are taken into account in asymptotic formulas for the cross section of lepton pair production in inelastic high-energy neutrino scattering in the field of a nucleus $\nu + Z \rightarrow \nu' + l^- + l^+ + Z'$. The cross section of the corresponding photo-

processes $\nu + \gamma \rightarrow \nu' + l^- + l^+$ is calculated with the same accuracy. (auth)

39944 DETERMINATION OF THE SPIN OF THE 2426 kev LEVEL IN Kr^{82}. Koch, J.; Muennich, F.; Schaare, W.; Fischer, K.; Fricke, K. (Technische Hochschule, Brunswick). Z. Naturforsch., 20a: 845-6(June 1965).

A spin of 3^+ was determined for the 2426 kev level in ^{82}Kr by measuring the angular correlation of the 1648 kev-777 kev $\gamma\gamma$ cascade from the decay of ^{82}Br. The dipole-quadrupole mixing ratio of the 1648 kev γ-ray was found to be -0.15 ± 0.02, which indicates that the transition is nearly pure dipole with a quadrupole admixture of $2.1 \pm 0.5\%$. (L.B.S.)

39945 MEASUREMENT OF THE CIRCULAR POLARIZATION OF THE 498-kev γ QUANTA OF ^{103}Rh. Kneissl, U.; Schneider, H. (Universitaet, Giessen, Ger.). Z. Naturforsch., 20a: 846-9(June 1965). (In German).

Measurements were made of the circular polarization of the 498-kev γ quanta of ^{103}Rh, from which the spin of the 538-kev level can be determined if the mixing ratio of the 498-kev γ-ray is known and lies outside the boundary $0.4 < \delta < 2.6$. Under the assumption of a strong pure E2 transition with a M1 admixture less than 13%, which is supported by the measurement of the K/L ratio, a spin of $5/2^+$ follows for the 538-kev level. The results using lower v/c values for the polarization indicate that the 650-kev level has a spin of $7/2^+$. (L.B.S.)

39946 A STUDY OF THE RADIATION FROM Am^{241}. Michaelis, W. Z. Physik, 186: 42-62(1965).

The radiation from the alpha decay of ^{241}Am was investigated by studying the fine structure of the alpha spectrum and by performing alpha-gamma and gamma-gamma coincidence measurements. For the daughter nucleus, ^{237}Np, a level scheme is proposed which comprises 21 excited states and 39 gamma transitions. Evidence was found for the existence of previously unknown gamma rays at (80), 82, 88, (90), 100, 150 (two transitions), 170, (~210), 295, (300), 360, 420, 460 and 690 kev, as well as for the probable occurrence of a new fine structure alpha group at 4754 kev corresponding to a level at 804 kev. For the alpha groups and for most of the gamma rays absolute intensities are given. For some transitions, the K-conversion coefficients and multipolarities were determined. The results are discussed within the framework of the unified model. The level density agrees well with the predictions of the superfluid model and is approximately twice the density yielded from Nilsson's theory. (auth)

39947 THE K-CONVERSION COEFFICIENT OF THE 321 kev E1 TRANSITION IN Hf^{177}. Bashandy, E.; El-Sayad, M. G. Mousa; El-Aassar, M. Riad (Atomic Energy Establishment, Cairo). Z. Physik, 186: 108-13(1965).

The K-conversion coefficient of the 321-kev E1 transition in ^{177}Hf was measured by means of an iron free double focusing beta-ray spectrometer, using the internal-external conversion method. The result obtained for $\alpha_K(321) = 0.162 \pm 0.016$ is in disagreement with the theoretical values for pure E1 transition ($\alpha_K = 0.0154$) calculated by Sliv and Band. The large anomaly observed in the K-conversion process of the inhibited E1 transition is compatible with a large M2 admixture or, more probably, with the presence of penetration matrix elements. (auth)

39948 CORIOLIS COUPLING IN THE QUANTUM MECHANICAL N-BODY PROBLEM. Weiguny, A. (Universitaet Freiburg i. Br.). Z. Physik, 186: 227-39(1965). (In German)

In describing a system of N particles (nucleons) in the body-fixed coordinate system of instantaneous principal axes of inertia, in the rotation-vibration part of the Hamiltonian there occur the hydrodynamical moments of inertia. It is, however, not possible to use them as effective moments of inertia as long as the Coriolis term in the Hamiltonian does not vanish. In order to obtain a quantitative picture of the Coriolis coupling influence upon the moments of inertia, it is shown by means of a unitary transformation how the Coriolis coupling can be eliminated in the limiting case of a rigid body and how by such a procedure the hydrodynamical moments of inertia are transformed into the rather different moments of the rigid body. (auth)

39949 ON THE APPLICABILITY OF A SEPARABLE POTENTIAL IN NUCLEAR PHYSICS. Mueller, D.; Werner, E. (Universitaet, Heidelberg). Z. Physik, 186: 299-304(1965). (In German).

It is shown that a separable potential represents an interaction acting only in a one-dimensional subspace of Hilbert-space. Thus the particular role played by the collective state in the schematic model is a consequence of the simplifications made in replacing realistic forces by a separable potential. (auth)

39950 POLARIZATION OF NEUTRONS FROM (D,n) REACTIONS ON CARBON. Garber, Donald Ivan. Thesis, Cleveland, Case Inst. of Tech., 1964. 43p.

The polarization of neutrons from the $^{12}C(D,n)^{13}N$ ground state reaction and the $^{13}C(D,n)^{14*}N$ reaction leading to the 5.69-, 5.10-, and 4.91-Mev excited states in ^{14}N were measured at a deuteron energy of 2.8 Mev. The $^{12}C(n,n)$ scattering served as the analyzer, and the various neutron groups were resolved by using the time-of-flight technique. The $^{13}C(D,n)$ reactions proceeding to the 5.69 and 4.91 levels in ^{14}N are $l_p = 0$ stripping reactions and their polarizations are small at forward angles as expected. The other two reactions studied are both $l_p = 1$ stripping reactions and both polarizations exceed 33%. Therefore, the need for spin orbit forces in the optical model potential is indicated. (Dissertation Abstr.)

39951 GRUNDBEGRIFFE DER KERNPHYSIK. 2. VERBESSERTE AUFLAGE. (Concepts of Nuclear Physics. 2. Revised Edition). Braunbek, Werner. Thiemig-Taschenbucher, Band 23. Munich, Verlag Karl Thiemig KG, 1964. 123p.

The concepts of nuclear physics are presented in a brief form for the layman. The concepts and phenomena that are of significance in nuclear energy production, reactor technology, and work with radioisotopes are emphasized. (J.S.R.)

Plasma Physics and Thermonuclear Processes

39952 (AFCRL-65-348) MEASUREMENT OF THE STARK WIDTHS AND SHIFTS OF NITROGEN ION LINES (thesis). Scientific Report No. 4. Day, Richard A. (Maryland Univ., College Park. Dept. of Physics and Astronomy). May 1965. Contract AF19(628)-269. 84p.

A hot plasma composed of helium and ionized nitrogen was created by reflecting the shock wave produced in an electromagnetic T-tube. The plasma temperature was measured by monitoring three nitrogen ion lines, whose intensity is a steep function of temperature. The profiles of various lines emitted in the plasma were obtained by scanning a monochromator from shot to shot. The half width of HeI 3889Å was compared to empirically corrected calculations to obtain the electron density. The half widths of the nitrogen ion lines were measured from the impact broadened profiles; the shifts were obtained by comparing these profiles with unshifted lines from a pulsed capillary discharge. The results indicate agreement between experiment and a recent Stark broadening theory within 20% except for lines originating from the 4f level where Debye screening effects are important. No evidence was found for plasma polarization shift. (auth)

39953 (CLM-R-40) MICROWAVE EMISSION FROM THE ZETA PLASMA. Wort, D. J. H. (Culham Lab., United Kingdom Atomic Energy Authority, Abingdon (England)). Feb. 1965. 31p. Dep.; BIS, $0.90; HMSO, 4s. 6d.

Simultaneous measurements of the thermal microwave noise emitted by the ZETA plasma at 2 and 4 mm wave-

lengths were used, with simplifying assumptions, to deduce the plasma density and electron temperature as a function of time throughout the ZETA current pulse. Before peak current the plasma is turbulent, and parameters describing the turbulence are deduced. After peak current the plasma is quasi-uniform, although there is a steady loss of plasma. This loss appears to be arrested during a quiescent period, and at this time a partial cessation of turbulence leads to a change of density profile and improved containment. At low initial pressures the microwave results provide qualitative confirmation of spectroscopic measurements of pump-out and injection. A tentative model of the turbulence mechanism within the plasma is proposed, and it is found that the turbulent heat transfer is sufficiently great for the plasma to be roughly isothermal. It is concluded that this new microwave technique can afford valuable information about the behavior of the plasma. (auth)

39954 (COO-1233-20) THERMONUCLEAR PLASMA STUDIES. Quarterly Status Report No. 9. (Wisconsin Univ., Madison. Physics Dept.). Apr. 30, 1965. Contract AT(11-1)-1233. 17p. Dep.(mn); $1.00(cy), 1(mn) CFSTI.

Energy and purity analyses of the plasma from a conical inductive plasma gun; energy analyses of ions from a Marshall-type gun injecting into a linear quadrupole; and analyses of the motion of plasma within a toroidal octupole are reported. This last analysis is carried out by taking simultaneous measurements at several points spaced around the octupole. The results are concerned with the filling process taking place in the first 50 μsec, when 100- to 200-v ions are flowing around in a plasma cloud. After distribution, plasma remains for the duration of the magnetic field (about 2.5 msec). (T.F.H.)

39955 (IAE-663) IMPUL'SNYE PLAZMENNYE INZHEKTORY. VZAIMODEISTVIE PLASMENNYKH SGUSTKOV S MAGNITIYMI POLYAMI. (Pulsed Plasma Injectors. The Interaction of Plasma Bunches With Magnetic Fields). Komel'kov, V. S.; Safronov, B. S. (Institut Atomnoi Energii, Gosudarstvennyi Komitet po Ispol'zovaniyu Atomnoi Energii SSSR, Moscow). 1964. 62p. Dep. mn.

Research on plasma injectors and the interaction between plasmoids and magnetic fields is described. Present research on plasma injectors is devoted primarily to the micromechanisms which determine the main processes and the properties of the plasmoids. Pulsed plasma injectors are still the only sources of high-density plasma, but they generate plasmoids containing many impurities. Various methods of ridding the plasma of the impurities are discussed, and it is concluded that elimination of neutral and slow particles from the plasmoids is feasible. Maximum purity can be attained by controlling the initial gas distribution in the working volume. The most efficient of the cylindrical coaxial injectors are those producing gushing pinches (end-type injectors). The nature of the frontal plasmoids, which move with velocities exceeding the velocity of the current layer, still remains unclear, and the experimental data indicate that the snowplow model used to describe acceleration in injectors is not applicable. (ATD)

39956 (LA-DC-7043) THE FAST PLASMA FROM A COAXIAL GUN. Marshall, John; Henins, Ivars (Los Alamos Scientific Lab., Univ. of California, N. Mex.). [1964]. Contract W-7405-eng-36. 26p. (CONF-650911-9). Dep. mn; CFSTI, $2.00 cy, $0.50 mn.

From 2nd Conference on Plasma Physics and Controlled Nuclear Fusion Research, Abingdon, Berks., Eng.

An investigation of the phenomena accompanying the acceleration of the fast plasma from a coaxial gun was made using a variety of techniques including particle analysis, electric probing, space current probing by Rogowsky loops, diamagnetism as measured by external pickup loops, high-speed photography both directly of the discharge between the gun electrodes and indirectly by the light of the secondary plasma produced when the fast plasma strikes a target. The gun is normally operated with an axial bias magnetic field between the electrodes. The fast plasma injected into a guide field contains $\sim 5 \times 10^{17}$ deuterons with a wide spread of energy peaking around 8 kev. It is generated over a period of slightly more than 1 μsec, beginning 2 μsec after first breakdown. When the gun is fired into a field free region, the production of the fast plasma appears to be consistent with a model based on the expansion of a fully ionized magnetized moving plasma into vacuum. Such a model would predict that a large fraction of the magnetic and streaming kinetic energy of the moving plasma between the gun electrodes would appear as kinetic energy of the front part of the plasma. The acceleration of the plasma is a gradual one over a distance of 50 cm or so beyond the gun muzzle. When the gun is fired into a 16-kG axial guide field the acceleration process is localized to a region within a few cm of the gun muzzle, the ions and electrons enter the guide field by separate processes and by different paths. The detailed acceleration mechanism is still not understood. (auth)

39957 (MATT-320) THE RELATIONSHIP BETWEEN RESISTIVE INSTABILITIES AND MICROINSTABILITIES IN INHOMOGENEOUS PLASMAS. Stringer, T. E. (Princeton Univ., N. J. Plasma Physics Lab.). May 1965. Contract AT(30-1)-1238. 32p. Dep. mn; CFSTI, $2.00 cy, $0.50 mn.

Previous work on microinstabilities in a collision-free inhomogeneous plasma ($\nu_e, \nu_i \ll \omega$), and on resistive instabilities in a collisional plasma where ν_e is assumed much greater than ω are considered. These different results should all correspond to the two limiting cases of a more general theory in which the ratio ν_e/ω is arbitrary. The general theory presented is believed to describe these cases. Resonant particle effects were not included, but the equations are in a form where this can readily be added. (M.O.W.)

39958 (MATT-327) MEASUREMENT OF ION CONCENTRATIONS AND ELECTRON TEMPERATURE IN A BARIUM PLASMA. Johnson, L. C.; Hinnov, E.; Rynn, N. (Princeton Univ., N. J. Plasma Physics Lab.). May 1965. Contract AT(30-1)-1238. 30p. Dep. mn; CFSTI, $2.00 cy, $0.50 mn.

Determination of spatial distribution of barium ion densities and electron temperatures in a fully ionized barium plasma is described. The ion densities are deduced from measurement of resonance fluorescence of the barium ion excited by an external light source. The space resolution is provided by the volume of the overlap of the exciting beam and the field of view of the measuring monochromator. The exciting beam is modulated, and the detector includes a phase-sensitive lock-in amplifier. The electron temperature is deduced from the rate of electronic excitation and the measured plasma brightness without the externally induced fluorescence. It is only obtained as an average along the line of sight of the monochromator. Comparison of the measurements of the two resonance lines allows the conclusion that the effective threshold Gaunt factor for excitation of the 6^2P states of Ba^+ is approximately 0.34. In addition, the oscillator strengths of the 5^2D-6^2P transitions of Ba^+ were determined and found to be about twice as large as those calculated by the Coulomb approximation. (auth)

39959 (N64-22435) A COVARIANT THEORY OF RELATIVISTIC BROWNIAN MOTION. I. LOCAL EQUILIBRIUM. Hakim, Remi (Paris Univ., Orsay. Laboratoire de Physique Theorique et Hautes Energies). May 1964. 51p.

Some relativistic methods in statistical mechanics and their applications to the construction of a covariant theory of Brownian movement are discussed. Times that are long compared with the relaxation time β^{-1} are given exclusively. As a consequence of this covariant theory, relativistic Wiener integrals are derived. (auth)

39960 (N64-33202) SPECTROSCOPIC INVESTIGATIONS OF PLASMA PROPERTIES. Quarterly Summary Report No. 1, May 11–August 10, 1964. (Allison Div., General Motors Corp., Indianapolis, Ind.). Sept. 9, 1964.

Contract NASw-922. 29p. (NASA-CR-58969; EDR-3969). CFSTI, $2.00 cy, $0.50 mn.

A new spectroscopic method was conceived that allows temperature or pressure measurement in low-temperature plasmas. The fundamental theory, upon which the method is based, was developed. For the case of seeded plasmas, the method could be modified to further increase the exactness. To test this spectroscopic technique, a plasma source permitting adjustment of electron density and temperature was designed and constructed. Preliminary experiments showed that the source performs satisfactorily. (auth)

39961 (NP-15112) PRE-IONIZATION AND SHOCK WAVE IONIZATION IN A CROSSED-FIELD PLASMA SOURCE Brand, G. F.; Chung, S. K.; Robinson, L. C. (Sydney Univ. (Australia). School of Physics). Apr. 1965. 18p. (ER-14) Dep. mn.

An experimental investigation into the development of ionization in a crossed-field plasma source is described. The observations, based mainly on microwave interferometry and reflection techniques, show two stages of ionization. For the first, or pre-ionization stage, measured values of the electron density under various preparation conditions are presented, and estimated values of collision frequency are used for the calculation of the conductivity of the pre-ionized gas. Observations are made of the second stage of ionization, wherein a supersonic ionization front propagates through the pre-ionized gas raising it to a highly ionized state. (auth)

39962 (NP-15167) SPACE CHARGE AND CURRENTS IN THE CONTINUOUS ROTATING PLASMA ACCELERATOR. Rijnhuizen Report 65-23. Minardi, E. (Stichting voor Fundamenteel Onderzoek der Materie, Jutphaas (Netherlands). Instituut voor Plasma-Fysica). Mar. 1965. 14p. Dep. mn.

A device was previously proposed for obtaining a regime of continuous injection of plasma by means of a configuration of crossed static electric and magnetic fields. The previous results are extended by studying carefully the effect on a possible space-charge on the plasma motion and the distribution of current in the plasma. The space-charge formation could prevent the plasma acceleration, unless a current parallel to the magnetic field is allowed to flow in order to remove the space-charge and to maintain the electric field exactly perpendicular to the magnetic field (no deacceleration along the magnetic lines of force). This parallel current is calculated and the schematic general picture of the current distribution in the plasma is given. This picture implies that the plasma must be electrically connected with the D.C. generator. The results obtained are discussed in view of their application for thermonuclear purposes. (auth)

39963 (NP-15198) ISSLEDOVANIE PLAZMENNOGO SGUSTKA, DVIZHUSHCHEGOSYA V TOROIDAL'NOM MAGNITNOM POLE. (Study of a Plasma Bunch in Motion in a Toroidal Magnetic Field). Il'enko, B. P.; Lats'ko, E. M.; Zykov, V. G.; Tolok, V. T. (Akademiya Nauk Ukrainskoi SSR, Kharkov. Fiziko-Tekhnicheskii Institut). 1964. 16p. Dep. mn.

The polarization of a plasma cluster moving in a toroidal magnetic field was investigated. It was noted that the vector of the polarization electric field is the sum of three components V_z, V_R, and V_r. The interaction of the electric fields in colliding clusters in a toroidal magnetic field was also studied. (tr-auth)

39964 (NP-15201) PRODOL'NYE KOLEBANIYA V MNOGOSKOROSTNOM PLAZMENNOM PUCHKE. (Longitudinal Oscillations in a Multi-Velocity Plasma Beam). Repalov, N. S.; Khizhnyak, N. A. (Akademiya Nauk Ukrainskoi SSR, Kharkov. Fiziko-Tekhnicheskii Institut). 1964. 8p. Dep. mn.

The effect of thermal velocity spreading of particles on the modulating properties of a klystron buncher is studied. It is shown that the presence of thermal diffusion of particles leads in the expression for the current density to a multiplication factor whose form coincides with that of the coherence multiplier for interactions of spatially broadened clusters. Thus it may be confirmed that the thermal velocity scattering of particles leads to an incoherent interaction of particles in velocity space. (tr-auth)

39965 (NP-15203) OPREDELENIE PROSTRANSTVENNOGO RASPREDELENIYA PLOTNOSTI PLAZMY PO REFRAKTSII MIKROVOLN. (Determination of Spatial Distribution of Plasma Density by Microwave Refraction). Dushin, L. A.; Kononenko, V. I.; Skibenko, A. I. (Akademiya Nauk Ukrainskoi SSR, Kharkov. Fiziko-Tekhnicheskii Institut). 1964. 17p. Dep. mn.

It is shown that the value of the density at any point of the plasma cross section can be found from the variation of the position of the point of exit of the beam from the plasma with the angle of incidence at fixed frequency. Experiments are described on the investigation of the spatial distribution of plasma density by refraction of a microwave beam incident on the plasma cylinder in the plane normal to the cylinder axis and in the plane transversing this axis. The results of the studies by both methods are in good agreement with each other and with theoretical calculations. (tr-auth)

39966 (ORNL-P-1245) THE PRODUCTION OF 10^{-9} TORR WITHIN A LARGE PLASMA CONTAINER (DCX-1). Wells, E. R. (Oak Ridge National Lab., Tenn.) [1964]. Contract W-7405-eng-26. 31p. (CONF-650512-2) Dep. (mn); $2.00(cy), 1(mn) CFSTI.

From Symposium on Engineering Problems of Controlled Thermonuclear Research, Livermore, Calif.

Changes in the High Energy Injection Device DCX-1, now capable of operating pressures of 10^{-9} torr with an injected beam of more than 10 Mamp, are reported. Diagrams of the primary equipment changes are included. (M.O.W.)

39967 (ORNL-P-1337) SEVERE MICROINSTABILITY-DRIVEN LOSSES IN AN ENERGETIC PLASMA. Dunlap, J. L.; Postma, H.; Haste, G. R.; Reber, L. H. (Oak Ridge National Lab., Tenn.). [1965]. Contract W-7405-eng-26. 16p. (CONF-650911-8). Dep. mn; CFSTI, $1.00 cy, $0.50 mn.

From 2nd Conference on Plasma Physics and Controlled Nuclear Fusion Research, Abingdon, Berks, Eng.

The established plasma is severely limited by microinstability-driven losses of fast protons. There are indications of stabilizing effects associated with disordered proton orbits. Three techniques for increasing this disorder were explored. Only one, increasing the precessional motion by changing the injection trajectory, was beneficial. This technique raises the density threshold for instability by large factors (40 to 300), but relaxes the density limitation by only a factor of 2. (auth)

39968 (ORNL-P-1338) ANOMALOUS PLASMA DIFFUSION IN MAGNETIC WELLS. Fowler, T. K.; Guest, G. E. (Oak Ridge National Lab., Tenn.). [1965]. Contract W-7405-eng-26. 23p. (CONF-650911-4). Dep. mn; CFSTI, $1.00 cy, $0.50 mn.

From 2nd Conference on Plasma Physics and Controlled Nuclear Fusion Research, Abingdon, Berks., England.

Aside from possible short wavelength modes causing anomalous diffusion which is discussed, criteria for preventing universal instabilities in magnetic wells and average wells were obtained. Stabilization is easiest when $T_e \ll T_i$. For all magnetic geometries (with solid conductors) the preferred operating range is about the same, $T_i \sim 300$ kev $\sim 10\ T_e$. Operation at lower temperatures (in torii) must rely on other means of stabilizing universal modes. (auth)

39969 (ORNL-P-1373) PLASMA HEATING BY MEANS OF BEAM PLASMA INTERACTION AT OAK RIDGE NATIONAL LABORATORY. Alexeff, I.; Neidigh, R. V.; Jones, W. D.; Peed, W. F.; Stirling, W. L. (Oak Ridge National Lab., Tenn.). [1964]. Contract W-7405-eng-26. 40p. (CONF-650911-3). Dep. mn; CFSTI, $2.00 cy, $0.50 mn.

From 2nd Conference on Plasma Physics and Controlled Nuclear Fusion Research, Abingdon, Berks., England.

The development of the beam-plasma work is briefly discussed. The most important points of each experiment are pointed out. These early experiments include the Neidigh pressure-gradient arc, and the initial hot-electron experiments performed in a small mirror machine. Further hot-electron work in which electrons are heated and trapped by an electron beam directed along magnetic lines of force but off axis in a large mirror machine. Reported are the burnout experiments, in which a small volume of plasma is kept at a high degree of ionization in the presence of a surrounding neutral-gas source, by means of very high steady-state rates of applied power. (M.O.W.)

39970 (ORNL-P-1374) ENERGETIC NEUTRAL INJECTION INTO AN ELECTRON-CYCLOTRON PLASMA. Ard, W. B.; Dandl, R. A.; England, A. C.; Haas, G. M.; Lazar, N. H. (Oak Ridge National Lab., Tenn.). [1965]. Contract W-7405-eng-26. 29p. (CONF-650911-2). Dep. mn; CFSTI, $2.00 cy, $0.50 mn.

From 2nd Conference on Plasma Physics and Controlled Nuclear Fusion Research, Abingdon, Berks., England.

A beam of 20 kev hydrogen atoms was directed through an electron-cyclotron plasma (ECP) contained in a magnetic mirror. The observed density is more than a factor of ten greater than that obtainable from neutral gas trapping under comparable conditions. The measured currents of charge-exchanged 20-kev protons and the decay of these currents are in experimental agreement with the calculated neutral density inside the ECP. The experiments were performed with a large volume (50 liters) ECP in order to ascertain the effectiveness of plasma shielding against thermal neutral gas. The extension of this work to higher densities of hot ions by the employment of much denser ECP and the effect of such critical parameters as thermal neutral reflux and energetic beam current are discussed. The density, power, and stability bounds on mm wavelength ECP's currently under investigation are also described. (auth)

39971 (ORNL-P-1438) OPERATING AND REPAIR EXPERIENCES ON DCX-2 COILS. DeCamp, S. M. (Oak Ridge National Lab., Tenn.). [nd]. Contract W-7405-eng-26. 10p. (CONF-650512-4). Dep.(mn); $1.00(cy), 1(mn) CFSTI.

From Symposium on Engineering Problems of Controlled Thermonuclear Research, Livermore, Calif.

The description of the DCX-2 coils is presented. Some operating and repair experiences that were previously encountered are presented. Photographs of the DCX-2 injection device are included. (M.O.W.)

39972 (SU-IPR-17) STUDIES OF PLASMA OSCILLATIONS. Quarterly Status Report No. 22, March 1, 1965-May 31, 1965. Crawford, F. W. (Stanford Univ., Calif. Inst. for Plasma Research). June 1965. Contract AT(04-3)-326. 32p. Dep. mn; CFSTI, $2.00 cy, $0.50 mn.

Research on ion wave propagation and positive column instabilities, electron beam probing of plasmas, beam-plasma interactions, and positive column resonances and propagation is reported. (M.O.W.)

39973 (UCRL-14131) THEORETICAL STUDIES OF ELECTRON INJECTION AND E-LAYER BUILD-UP IN ASTRON. Killeen, John; Neil, V. Kelvin; Heckrotte, Warren (Lawrence Radiation Lab., Univ. of California, Livermore). June 7, 1965. Contract W-7405-eng-48. 25p. (CONF-650911-7). Dep. (mn); $1.00(cy), 1(mn) CFSTI.

From 2nd Conference on Plasma Physics and Controlled Nuclear Fusion Research, Abingdon, Berks, Eng.

Two aspects of the creation of the E-layer are considered. (1) A theoretical investigation is made of the injection system by means of which the relativistic electrons are to be trapped in the magnetic mirror field, and (2) the electrons are introduced continuously at the physical ends of the E-layer region. Their subsequent motion and the buildup of the layer are then governed by the appropriate self-consistent equations. (M.O.W.)

39974 ON THE ORIGIN OF ROTATION IN MAGNETICALLY CONFINED PLASMAS. Haines, M. G. (Imperial Coll., London). Advan. Phys., 14: 167-211(Apr. 1965).

The mechanisms that can lead to rotation of plasma in an electrodeless discharge (commonly called a theta pinch) and in a mirror machine are surveyed. Eight proposed mechanisms are examined, of which two are found to be incorrect in some way. Another mechanism, in which the reaction is purely electromagnetic, applies only to the tenuous plasma of a mirror machine. The remaining five theories apply to the highly compressed plasma of a theta pinch. These all rely fundamentally on the large difference in mass between an ion and an electron, i.e., either on Hall currents or the correction for finite ion Larmor radius in the stress tensor. The mechanisms which incorporate the Hall effect cause an equal and opposite mechanical reaction either on the wall, or on external conductors, or on the plasma at each end of the discharge axis. The mechanisms which use the collisionless stress tensor predict either radial division into oppositely rotating plasma or a transfer of angular momentum to the walls by collisions during the initial stage of physical contact. This last theory is new and arose as a result of a critical examination of an earlier theory. Experimental evidence for rotation has been confined mainly to high speed photographic techniques, and methods of obtaining a more definite measurement of the rotation and its origin are suggested. A distinction is made between the angular motions associated with the center of mass, the guiding centers and the diamagnetic current, and also considers the stability of a rotating plasma including the Hall effect and the collisionless stress tensor. (auth)

39975 STEADINESS OF A PLASMAJET. Pfender, Emil (Univ. of Minnesota, Minneapolis); Cremers, Clifford J. AIAA (Am. Inst. Aeron. Astronaut.) J., 3: 1345-6 (July 1965).

The restriking of an arc with superimposed axial flow and the effects produced are studied in an open geometry, which permits unobstructed viewing of the entire arc column. This restriking leads to a saw-toothed shape of the voltage fluctuations because the breakdown time is very small compared to the time required for the anode arc terminus to travel downstream to the nozzle exit. For the experimental arrangement, a rod shaped thoriated tungsten cathode was positioned with its axis parallel to the surface of a plane water-cooled anode, and a gas flow (argon) was introduced parallel to the axis of the cathode. From a number of high-speed movies taken simultaneously with voltage fluctuations, the characteristic behavior of the fluctuating mode of the arc could be established. (J.R.D.)

39976 ON THE PROBLEM OF THERMAL EQUILIBRIUM IN LOW-CURRENT ARCS. I. CONSIDERATION OF EXISTING COMPREHENSION. Krysmanski, K. H. (Universitat, Greifswald, Ger.). Ann. Physik (7), 15: 162-78 (1965). (In German).

The state of an arc plasma can be described relatively simply when thermal equilibrium is present. For high-current arcs no uncertainty exists on these conditions; for lower current intensity it can be calculated generally with a sufficiently adequate approximation. The works of Ornstein and Brinkman, Mannkopff, and Witte, as well as others, are cited as proofs. A critical evaluation shows, however, that these proofs are unsatisfactory. This discussion is devoted, in addition to indications on the difficulties and many still unconsidered systematic error sources, to various temperature measurement methods. (tr-auth)

39977 ON THE PROBLEMS OF THERMAL EQUILIBRIUM IN LOW-CURRENT ARCS. II. EXPERIMENTAL INVESTIGATIONS AND RESULTS. Krysmanski, K. H. (Universitat, Greifswald, Ger.). Ann. Physik (7), 15: 207-24(1965). (In German).

Spectroscopic investigations on carbon and iron arcs lead to results that can be explained as deviations from thermal equilibrium. Measurements of the radial pattern of the excitation temperature of different components show differences that do not rest on measurement errors. Special perturbations were observed in the wall areas. Arcs in hydrogen atmospheres and in the low-pressure region show sharp deviations from a Boltzmann distribution with respect to the term occupation. (tr-auth)

39978 GAS LASER MEASUREMENTS OF THE ELECTRON DENSITY OF A PLASMA PRODUCED BY A VERY FAST THETA-PINCH PREHEATER. Warnock, A. C. C.; Deuchars, W. M.; Irving, J.; Kidd, D. E. (Univ. of Strathclyde, Glasgow). Appl. Phys. Letters, 7: 29-30(July 15, 1965).

Electron-density measurements in a plasma produced by a combination of radio-frequency (21 Mc) and very fast (0.5 Mc) 250-J theta-pinch discharges were made using a gas laser interferometer. Variation of the electron density of the plasma produces a phase change in the 3.39 μ radiation. This gives rise to modulation of the visible radiation from the laser cavity. All measurements were made in hydrogen gas in the pressure range 20-70 mtorr at different radial distances from the axis of the quartz discharge tube. The values of the electron density were calculated on the basis of the plane mirror theory. These experiments indicate that the increased sensitivity expected in the gas laser interferometer from the use of a concave external mirror cannot be realized for operation with coupled radiations due to the inherently low Q-value of such a system. (J.F.P.)

39979 TIME-DEPENDENT ELECTRON DENSITY MEASUREMENTS IN A FAST THETA-PINCH DISCHARGE. Deuchars, W. M.; Kidd, D. E.; Irving, J.; Warnock, A. C. C. (Univ. of Strathclyde, Glasgow). Appl. Phys. Letters, 7: 30-2(July 15, 1965).

An interferometric technique was developed for the study of electron density in the plasma produced in the first half-cycle of a fast preheated theta pinch. The basic geometry of the interferometer is that of a conventional Michelson interferometer in which the light source is a He-Ne laser operated at 6328 A. Two lenses reduce the laser beam divergence to a small angle of approximately 0.5 mrad and the lengths of the arms are adjusted so the angle is less than the angular width of the central spot of the interference pattern. The intensity of the emergent beam from the interferometer is almost uniform across its cross section and will vary between a maximum and minimum depending on the difference on the optical path lengths of the two arms. Measurements were made using hydrogen in the initial pressure range 5-25 mtorr. It was shown that this interferometric technique is well-suited to the determination of electron density variations in high-density, rapidly varying plasmas and in the plasmas produced in the theta-pinch discharges. (J.F.P.)

39980 MICROWAVE STUDY OF THERMALLY IONIZED PLASMAS. Iannuzzi, M.; Enriques, L. (EURATOM-C.N.E.N., Frascati, Italy). Appl. Phys. Letters, 7: 47-8 (July 15, 1965).

The results of an experiment are reported which was carried out to examine the possibility of studying the properties of alkali plasmas produced in an incandescent container by using microwave diagnostics. This is an interesting problem due to the recent and increasing importance of alkali plasmas produced by thermal ionization in the study of ionic waves, azimuthal drift instability, etc. Highly ionized alkali plasmas were produced in a hot cylindrical tantalum cavity which can be heated to 2500°K. Only two modes can be excited over the whole range of temperatures studied; these were identified. When cesium vapor is introduced into the cavity, changes in the Q and shifts in the resonant frequency are observed. For the same pressure of cesium vapor outside the cavity, plasma densities as a function of the cavity temperature were obtained both from the electric characteristic and by measuring the shifts of the resonant frequency. (J.F.P.)

39981 CORRELATION OF COHERENT OSCILLATIONS AND HALL CURRENTS IN THE LINEAR HALL ACCELERATOR. Burlock, Joseph; Brooks, David R. (Langley Research Center, Hampton, Va.). Appl. Phys. Letters, 7: 49-51(Aug. 1, 1965).

Detailed investigation of the instabilities previously observed indicates a close relation between the Hall currents observed in the linear Hall accelerator and the phase velocity of the dominant oscillation. Observation of the plasma in the accelerator with electrostatic probes showed the presence of a coherent oscillation with an azimuthal wavelength equal to the circumferential distance and rotating in the same direction as the particle drift. This phase velocity was found to vary with pressure but retained its general characteristics over a wide range of parameters. The resemblance is shown between the Hall current behavior and the dispersion relation in some limiting cases. Measurements with directional probes revealed collection of azimuthal and radial ion fluxes with spectra identical with the observed potential perturbations, suggesting that these perturbations are important in non-classical diffusion and conduction. (J.F.P.)

39982 HIGH-FREQUENCY CONTAINMENT OF PLASMA. Teichmann, Jiri (Inst for Physics, Czechoslovak Academy of Sciences, Prague). Beitr. Plasmaphysik, 5: 13-57(1965). (In German)

The possibilities for the utilization of h-f fields for the spatial limitation of plasmas, for the sealing of magnetic traps with static fields, and for the stabilization of the plasma-vacuum boundary were investigated on the basis of the elementary single-particle theory, the MHD theory, and the kinetic theory of the effect of fields varying periodically with time. Experiments were described which verify the theoretical conclusion or do not correspond to them. 110 references. (tr-auth)

39983 INVESTIGATION OF A STATIONARY ARGON DISCHARGE AT HIGH CURRENT DENSITIES. Hayess, Erhard; Rademacher, Karl (Physikalisch-Technisches Institut, Berlin). Beitr. Plasmaphysik, 5: 59-74(1965). (In German)

At current densities between 13.8 and 40.6 amp/cm^2, a discharge in argon at a pressure of 0.58 torr was investigated in the stationary state. The electron temperature and the carrier concentration could be determined with a special probe measurement method. The pattern of both magnitudes as a function of the current density and tube radius indicated a strong influence of the electron pressure on the discharge. However, it was shown that the effect of the gas temperature was preponderant. In the radial potential distribution, the effect of the self-magnetic field could be detected. The electron mobility is in good agreement with the theoretically calculated values. Investigations of the operating voltage, of the discharge current, and the irradiation show no instability of the discharge and no oscillations. At high current densities, ion lines of argon with relatively high excitation voltage and considerable intensity were produced. (tr-auth)

39984 ON THE PRESENT STATE OF INVESTIGATIONS OF SHOCK FRONTS IN NEUTRAL GASES AND IN PLASMA. PART I. THE HYDRODYNAMIC THEORY OF SHOCK FRONTS IN NEUTRAL GASES. Morgenroth, H. (Physikalisch-Technisches Institut, Berlin). Beitr. Plasmaphysik, 5: 75-94(1965). (In German)

A review of the methods used for the treatment of the structure of plain shock wave fronts in neutral gas and in plasma is given. The hydrodynamic theory of plain shock fronts in neutral gas, including the third approximation in the sense of the Chapman-Enskog method, is described. (tr-auth)

39985 DEGREE OF BLACKNESS AND THERMAL RADIATION OF HOMOGENEOUS, MAGNETIC FIELD-FREE PLASMA IN THE RADIOFREQUENCY REGION NEAR THE PLASMA FREQUENCY. Mollwo, L. (Heinrich-Hertz-Institut, Berlin). Beitr. Plasmaphysik, 5: 123-33(1965). (In German)

The results of Salzberg and Barlow were analyzed for the case of a corona condensation. It was shown that an adjustment of the usual inset is necessary for the blackening degree of a medium. (J.S.R.)

39986 THE TEMPERATURE PROFILE OF A FADING LOW-CURRENT ARC IN AIR. Kloss, H. G.; Rademacher, K. (Physikalisch-Technisches Institut, Berlin). Beitr. Plasmaphysik, 5: 135-42(1965). (In German)

The temperature of a fading plasma of a 6-mm-long, 8.5-amp carbon arc in air was measured by two different

methods. Time-resolved temperature profiles were obtained by blackening comparison with the stationary arc. This showed a good agreement with the values for the axis temperature measured by the shock wave method. During the first millisecond after the startup of the arc, a cooling velocity of 1.2°/μsec was obtained for the arc axis. (tr-auth)

39987 MEASUREMENT OF THE TEMPERATURE AND ELECTRON DENSITY IN A SUPERSONIC PLASMA BEAM AT LOW PRESSURES. Boldt, Werner (Physikalisch-Technisches Institut, Berlin). Beitr. Plasmaphysik, 5: 143-54(1965). (In German)

Measurements on an argon plasma beam at low pressure (7 torr) were reported. The argon plasma beam was produced from the plasma beam generator, described previously, with an ultrasonic velocity into a glass receptacle. From the absolute intensities of the electron continuum and atomic lines, the radial distribution of the temperature and the electron density of the plasma beam at the output from the Laval nozzle was determined and was compared with the values obtained from the gas dynamics formulas. The assumption of the local thermal equilibrium and of ideal gases with varying specific heats is at the basis of the evaluation of the measurement results. The justification for this method is also supplemented by the consistency of the results obtained. (tr-auth)

39988 ION WAVES AND ION-CURRENT WAVES. Schuetz, Ulrich (Institut fur Magnetohydrodynamik, Jena, Ger.). Beitr. Plasmaphysik, 5: 155-60(1965). (In German)

By a series of different experiments, an attempt was made to detect ion waves in a magnetic field-free plasma. The measured velocities of the wave propagation was much too large to be justified by the propagation of ion waves. The observations can be explained by a form of wave propagation not previously described—the ion-current wave. The ion-current wave arises through superposition of ion current of equal frequency and different velocity as it is formed in a thin plasma by modulated production of charged carriers in the plasma volume, recombination of the charged carrier at the material vessel walls, and collision-free motion of ions. Ion waves can be expected in plasmas which are significantly free of macroscopic electrical fields; for example, in the center of very expanded plasmas or in plasmas with magnetic walls. (tr-auth)

39989 EFFECT OF SURROUNDING GAS PRESSURE ON THE PHYSICAL STATE OF ARC DISCHARGE PLASMA. Grechikhin, L. I.; Tyunina, E. S. (Inst. of Physics, Belorussian SSR). High Temp. (USSR)(English Transl.), 2: 622-7(Sept.-Oct. 1964).

Translated from Teplofiz. Vysokikh Temp., 2: 689-95(Sept.-Oct. 1964).

Various methods of measuring charged-particle concentration from the broadening of the spectral lines of the sodium atom under direct current arc conditions are considered. An explanation is given for the discrepancy between measurements of charged-particle concentration made with respect to different lines. It is shown that, as the surrounding gas pressure in the direct current arc plasma increases, the following changes take place: the source becomes more homogeneous, its dimensions decrease, and the temperature and concentration of the charged particles rise. (auth)

39990 BEHAVIOUR OF THE FIRST BALMER LINES IN A HIGH DENSITY PLASMA. Vujnovic, V. (Univ. of Zagreb). Intern. J. Electron., 18(1): 411-18(May 1965).

Observation of Balmer line profiles revealed their relative constriction and growing asymmetry with increasing ion density, measured in the range of 2×10^{16} to 3×10^{17} ion/cm^3. The fit of these profiles with the existing theoretical profiles gives smaller densities by the use of higher series members and smaller densities by the use of a red wing as compared with that of a violet wing. The phenomenon is believed to be caused by a combined action of the transition from the impact to the quasi-static line broadening effect of electrons and of the dissolution (preionization) of discrete energy levels. The change in the line broadening mechanism due to the electrons makes the line narrower than in the case in which there would be no such change, because the quasi-static broadening does not rise so steeply with density as the impact broadening. The dissolution effect on the other hand, is accompanied by a decrease in line intensity and in asymmetry, the red wing being narrower than the violet one. The dissolution estimated by the use of the available data is in accordance with the experimental evaluation. (auth)

39991 COMPRESSION OF A CYLINDRICAL PLASMA BY A MAGNETIC FIELD. Anderson, N. (Univ. of York, Eng.). Intern. J. Electron., 18(1): 473-6(May 1965).

The heating of a cylindrical plasma by an oscillating external magnetic field is investigated. It is found that if the frequency of the external field is considerably less than the collision frequency of the ions the method of heating is not satisfactory. (auth)

39992 PLASMA—THE FOURTH STATE. Gottlieb, Melvin B. Intern. Sci. Technol., No. 44: 44-50(Aug. 1965).

The properties and behavior of plasma are described. The conditions for the creation of a plasma and their composition are discussed. The behavior of a plasma in a magnetic field, its properties as a motor or generator are also explained. Microwaves in a plasma are also discussed. It is pointed out that in dynamic problems such as instabilities, growth and decay of waves, and flow problems it is necessary to assume that the velocities, currents, and time-dependent parts of the magnetic and electric fields are small quantities in order to solve the equations. (J.F.P.)

39993 HIGH-FREQUENCY LASER INTERFEROMETRY IN PLASMA DIAGNOSTICS. Gerardo, J. B.; Verdeyen, J. T.; Gusinow, M. A. (Univ. of Illinois, Urbana). J. Appl. Phys., 36: 2146-51(July 1965).

The time response of the laser interferometer is studied, and the parameters that are instrumental in limiting its time response are discussed. It is shown that by judicious selection of parameters the laser interferometer is capable of detecting resonances in excess of 50 per microsecond, which is close to the theoretical limit of the resonant structure used. The applicability of the interferometer to measurement of very rapidly changing plasma electron densities is demonstrated. (auth)

39994 INTERACTION OF MICROWAVES WITH AN INHOMOGENEOUS AND ANISOTROPIC PLASMA COLUMN. Yeh, C.; Rusch, W. V. T. (Univ. of Southern California, Los Angeles). J. Appl. Phys., 36: 2302-6(July 1965).

The problem of the interaction of microwaves with a radially inhomogeneous plasma column confined by an impressed axial static magnetic field is treated analytically. Extensive numerical results for the backscattering cross sections are presented for various interesting ranges of the parameters involved. It is found that the homogeneous model for interpretation of experimental data can sometimes lead to ambiguous results. This ambiguity arises because of the interdependence of the average plasma frequency, the gyrofrequency, and the inhomogeneity of the plasma density distribution. Further measurements are suggested to distinguish these effects. (auth)

39995 HYDROMAGNETIC RADIATION DUE TO THE MIRRORING DIAMAGNETIC PARTICLES. Tamao, Tsutomu (Tohoku Univ., Sendai). J. Geomagnet. Geoelec., 16: 247-65(1964).

Hydromagnetic radiations generated by the motion of energetic charged particles in a uniform cold plasma are investigated. A hydromagnetic Cherenkov radiation emitted by diamagnetic particles moving coherently along the uniform field lines is first discussed and its differential energy spectrum is obtained. Next, hydromagnetic disturbances of the isotropic mode due to the mirroring motion of diamagnetic particles are quantitatively studied. Frequency and intensity variations with time for the emitted

signals are given in several numerical illustrations. It is shown that the frequency of arrived signals with an appreciable intensity decreases with increasing of time. This falling-tone character is ascribed to the Doppler effect of the moving source with the decreasing velocity, when it is approaching toward the observing point. (auth)

39996 END STABILIZATION EFFECT IN THE SLOW THETA PINCH. Miyamoto, Tetsu; Hamada, Shigeo; Ohnishi, Haruyuki (Nihon Univ., Japan). J. Phys. Soc. Japan, 20: 1088(June 1965).

The behavior of a helium plasma column in a theta pinch device with and without mirrors was studied. The results indicate that the stabilizing effect lies on both end parts of the plasma column (outside the mirrors). (D.C.W.)

39997 IMPROVED MICROWAVE REFLECTION MEASUREMENT OF PLASMAS PRODUCED BY SHOCK WAVES. Takeda, Susumu; Funahashi, Akimasa (Nagoya Univ., Japan). J. Phys. Soc. Japan, 20: 1090(June 1965).

The electron density and collision frequency in a plasma produced behind shock waves reflected at the end of a shock tube that terminates in a waveguide were measured using a microwave reflection probe at the tube end of the electromagnetically driven shock tube. The electron temperature was calculated from its dependence on the electron density and the electron-ion collision frequency. (D.C.W.)

39998 CURRENT DENSITY DISTRIBUTIONS IN A COAXIAL PLASMA GUN. Be, Sucki; Enokubo, Fumiaki; Mikoshiba, Shigeo; Nakano, Yoshiel (Tokyo Inst. of Tech.). J. Phys. Soc. Japan, 20: 1091(June 1965).

The magnetic flux density between the electrodes of a coaxial plasma gun were measured using a magnetic probe. The axial and radial current density distributions at 7 μsec after firing were calculated from the results. It was found that the currents become vortices and go out of the gun. (D.C.W.)

39999 NONTHERMAL PROPERTIES OF A POST-SHOCK PLASMA. Michel, F. C. (Rice Univ., Houston, Tex.). Phys. Fluids, 8: 1283-7(July 1965).

It is sometimes argued that either the electrons or ions get the majority of the thermal energy in a shock transition. The permissible ratio of electron to ion temperature in a postshock collisionless plasma is examined for a thermalized, preshock plasma. For weak shocks it is shown, from basic entropy considerations, that T_e must equal T_i. It is argued that unless some special dissipation mechanism that applies only to strong shocks is postulated, the result $T_e = T_i$ may be generalized to the case of strong shocks. (auth)

40000 KELVIN-HELMHOLTZ INSTABILITY IN AN ANISOTROPIC PLASMA. Talwar, S. P. (Goddard Space Flight Center, Greenbelt, Md.). Phys. Fluids, 8: 1295-9(July 1965).

The instability arising due to a tangential discontinuity of velocity in an unbounded, anisotropic plasma subject to a uniform magnetic field is investigated using the Chew, Goldberger, and Low approximation. Formal conditions for monotonic instability and the growing-wave instability are written. It is found that monotonic instability is possible, for a range of relative speeds, only if the plasma is characterized by the condition $2p_{||} > p_{\perp}$. For $2p_{||} < p_{\perp}$ the configuration is, however, overstable for relative speeds less than a certain critical value. The bearing of the results on the stability of the magnetospheric boundary and the coronal streamers is discussed, and it is suggested that a possible fine structure in the solar wind may satisfy the requirement for instability and thus produce irregularities of plasma properties and the magnetic field in the medium. (auth)

40001 FINITE LARMOR RADIUS EQUATIONS WITH NONUNIFORM ELECTRIC FIELDS AND VELOCITIES. Rosenbluth, Marshall N.; Simon, Albert (General Atomic Div., General Dynamics Corp., San Diego, Calif.). Phys. Fluids, 8: 1300-22(July 1965).

A low-β collisionless plasma cylinder confined in a uniform magnetic field is considered. The well-known flute instabilities occur due to plasma rotation or radial gravity which simulates field line curvature. The effects of finite Larmor radius and nonuniform rotation are included deriving a proper set of hydromagnetic equations and variational principles for determining stability. In most cases these are merely sufficient but in a variety of cases may be both necessary and sufficient for stability. (auth)

40002 "UNIVERSAL" OVERSTABILITY OF A RESISTIVE INHOMOGENEOUS PLASMA. Chen, Francis F. (Princeton Univ., N. J.). Phys. Fluids, 8: 1323-33(July 1965). (MATT-311).

An inhomogeneous plasma with finite resistivity in a straight or curved magnetic field is subject to instabilities of electrostatic drift waves with small but finite $k_{||}$. The influence of these instabilities of various factors such as finite β, resistive and viscous damping, and finite Larmor radius is investigated; and explicit, experimentally useful expressions for the frequency and growth rate are given. (auth)

40003 EQUILIBRIUM OF A TOROIDAL PLASMA WITH FINITE RESISTIVITY AND INERTIA. Knorr, Georg (Princeton Univ., N. J.). Phys. Fluids, 8: 1334-8(July 1965).

A theoretical study of the equilibrium of a dilute plasma in toroidal geometry with rotational transform was carried out, taking into account finite resistivity and finite inertia. If an additional nonvanishing density gradient drift of the plasma perpendicular to the magnetic field is assumed, the plasma drifts out of the toroid. The characteristic time of this process is found to be a factor of 2 r/R (where R and r are the major and minor radii of the toroid, respectively) smaller than the time which is associated with the mere diffusion from a toroid. (auth)

40004 LOW-FREQUENCY INSTABILITY OF PARTIALLY IONIZED PLASMA. Morse, David L. (Massachusetts Inst. of Tech., Cambridge). Phys. Fluids, 8: 1339-46(July 1965).

The stability of a partially ionized plasma in a magnetic field is investigated. The electron and ion flow equations and continuity equations are used to describe low-frequency, macroscopic variations of plasma density and space potential. The solutions to the linearized forms of these equations consist of a set of eigenfunctions of perturbed density eigenfunction. It is found that rotating flutelike density perturbations may grow when a steady radial electric field is present, either parallel or antiparallel to the unperturbed density gradient. The growth rate is proportional to a corrected electric field, which includes the time-invariant gradients of both density and space potential. The stabilizing effects of diffusion, parallel and perpendicular to the magnetic field, are considered. (auth)

40005 INFLUENCE OF SMALL TRANSVERSE FIELDS AND IMPURITIES ON θ-PINCH STABILITY AND CONFINEMENT. Hintz, Eduard (Univ. of Maryland, College Park); Kolb, Alan C. Phys. Fluids, 8: 1347-55(July 1965).

The stability and confinement of θ-pinch plasmas in the relatively slow Pharos discharge, where the duration of the current pulse is ~20–30 μsec, was investigated. The heating rates (~100 ev/μsec early in the discharge) are modest because of the relatively low voltage on the coil (~15 kv). Care was taken to reduce field nonuniformities in the coil-collector assembly so that the compressed plasma would not drift toward the wall. It is shown that small transverse fields (<1% of the maximum B_z) cause rotational instability: in particular, a pulsed Ioffe-hexapole field induces rotational instability if the field is present in the plasma before the start of the main compression. The time constant for the growth of the instability depends on the electron temperature and can be altered with 0.1% added impurity. The plasma is lost out the ends in 10–15 μsec without an initial bias field. The confinement time can be extended to ~30 μsec with a reverse bias field. In the latter case the plasma contracts axially to a length of 60–80 cm with a 1.8-m coil; this central plasma column is connected to the

ends by a narrow thread of plasma with a radius of a few millimeters. Axial studies show that instabilities, when they occur, grow faster at points away from the midplane. The origin of the rotation is discussed in terms of a model in which axial Hall currents, due to transverse fields, lead to a torque. (auth)

40006 MOTION OF A TEST PARTICLE IN A PLASMA. Perkins, Francis (Cornell Univ., Ithaca, N. Y.). Phys. Fluids, 8: 1361-7(July 1965).

The motion of a charged test particle in a completely ionized gas without a magnetic field is investigated. The possible trajectories of this test particle are described by a distribution function that spreads out in phase space as time increases. A convergent kinetic equation which accounts for long-range collective effects and short-range collisions in a consistent manner is derived to describe the time evolution of the distribution function. Expressions for the energy loss rate and dynamical friction are calculated from appropriate moments of the kinetic equation, and they show how the Coulomb logarithm, $\ln \Lambda$, varies with the velocity of the test particle. The errors introduced by the use of a convergent kinetic equation are estimated, and these indicate that the kinetic equation method gives the test particle's diffusion in phase space only on coarse grained time and spatial scales. For the case of a fast electron, the time scale must be larger than the electron plasma period and the spatial scale larger than e^2/KT. (auth)

40007 OBSERVATIONS ON A FULLY IONIZED BARIUM PLASMA. Rynn, N.; Hinnov, E.; Johnson, L. C. (Princeton Univ., N. J.). Phys. Fluids, 8: 1368-74(July 1965). (MATT-316)

A series of spectroscopic measurements in a fully ionized barium plasma column is described and discussed. The plasma was generated in the Q-1 device in a manner similar to that used to make alkali-metal plasmas. The observations show that the density contours and the temperature profiles in the body of the plasma were strongly influenced by conditions at the end plates. The results also indicate that the losses at the ends of the column dominated over the losses in the body of the plasma. Evidence is presented for the existence of internal circulating currents along the confining magnetic field lines in the absence of externally applied potentials. A verification of the Thompson effect in a current-carrying, fully ionized plasma is also presented. (auth)

40008 ALMOST LONGITUDINAL INSTABILITIES IN A PLASMA-BEAM SYSTEM. Wright, Harvel; Wiginton, C. L.; Neufeld, Jacob (Oak Ridge National Lab., Tenn.). Phys. Fluids, 8: 1375-84(July 1965). (ORNL-P-417)

A plasma-beam system immersed in a magnetic field B_0 is investigated under the assumption that the plasma is stationary, cold, uniform, and extended and that the beam of charged particles is uniform in density and moving in a direction parallel to that of B_0. Instabilities which are almost longitudinal are investigated with respect to conditions of occurrence, strength and type of instabilities, and dependence on the angle between the direction of B_0 and the direction of the excited waves. Two logically distinct types of waves which occur are defined and investigated. An almost longitudinal Cherenkov wave has a phase velocity equal to the projection of the beam velocity in the direction of the wave. An almost longitudinal cyclotron wave has a frequency equal to the Doppler-shifted gyrofrequency of the particles in the beam. Typical examples are analyzed numerically and presented graphically. Certain simple analytical expressions which apply to the significant regions of instability are derived and tabulated. (auth)

40009 FLOW OF PLASMA AROUND A MAGNETIC DIPOLE. Bostick, W. H.; Byfield, H.; Casale, P.; DiMarco, J. (Stevens Inst. of Tech., Hoboken, N. J.). Phys. Fluids, 8: 1397-9(July 1965).

A sequence of image converter photographs taken by the light of a copper plasma flowing past a dipole field produced by a loop coil is shown. From these pictures, the equatorial plasma stand off distance R_1 may be measured and compared with the value determined by assuming complete field exclusion at R_1 (whence the field strength should be theoretically $B_1 = 2M/R_1^3$), and specular reflection of the plasma particles at this point ($2mnv^2 = B_1^2/8\pi$). For the case of copper ions of average speed $v = 2 \times 10^6$ cm/sec and ion density $n = 10^{14}/cm^3$, $M = 8.2 \times 10^5$ abamp-turns cm^2, the computed value of R_1 is 4.5 cm, and the measured value is 5–6 cm. Magnetic signals dB/dt and electric field and plasma flow density measurements are also illustrated. (C.E.S.)

40010 MOTION OF θ-PINCH PLASMA IN ASYMMETRIC FIELDS. Goldman, L. M.; Hurwitz, H. Jr. (General Electric Research Labs., Schnectady, N. Y.). Phys. Fluids, 8: 1399-1400(July 1965).

The motion of θ-pinch plasma in asymmetric fields was investigated to establish experimental limits to such motion for a small aspect ratio (~2:1) device. The coil in the θ-pinch device was distorted to give a radius of curvature of 200 cm to the axial magnetic field lines. It was found that with reversed trapped fields the plasma drifted with approximately the expected velocity; however, in the absence of reversed trapped field, no drift was observed. This absence of drift was observed for zero trapped field and for positive initial fields up to 4000 G. Varying the initial pressure from 10 to 40 mtorr had no effect on the drift. (C.E.S.)

40011 THIRD HARMONIC OF CURRENT DENSITY IN A PLASMA. Sodha, Mahendra Singh; Kaw, Predhiman Krishan (Indian Inst. of Tech., New Delhi). Phys. Fluids, 8: 1402-4(July 1965).

A distribution function that includes the coefficient of v_z^2 in its expansion was used for the solution of the Boltzmann equation to obtain an expression for the third harmonic component of current density. An interesting conclusion is that this component does not vanish when the electron collision frequency is independent of the electron velocity. (C.E.S.)

40012 STIMULATED INCOHERENT SCATTERING OF LIGHT FROM PLASMAS. Goldman, M. V. (Harvard Univ., Cambridge, Mass. and Hughes Research Labs., Malibu, Calif.); Du Bois, D. F. Phys. Fluids, 8: 1404-5 (July 1965).

The optimum conditions for observing stimulated incoherent scattering of light from plasma are outlined. Equations are presented for the total and differential cross sections. (C.E.S.)

40013 SYNCHROTRON RADIATION FROM A SELF-CONSISTENT PLASMA. Lichtenberg, A. J.; Tuma, D. (Univ. of California, Berkeley). Phys. Fluids, 8: 1405-7 (July 1965).

An attempt is made to calculate the effect of the decreasing number of high energy electrons with time on the synchrotron radiation spectrum from a hot plasma in a magnetic field. (C.E.S.)

40014 "BOHM DIFFUSION" IN THE Q-1 DEVICE. D'Angelo, N. (Princeton Univ., N. J.). Phys. Fluids, 8: 1407-8(July 1965).

Experiments in the Q-1 cesium device have shown that if a voltage is applied between the end plates the plasma density decreases continuously with increasing voltage while the e-folding length of the radial density profile becomes increasingly larger. This has been taken as an indication of a transition from classical to enhanced (or Bohm) diffusion, the latter setting is when a sufficiently large current is carried by the plasma column. A mechanism that might account for the observed flattening of the radial density profiles is discussed. (C.E.S.)

40015 FORM OF THE ELECTRON DISTRIBUTION FUNCTION IN A TIME-VARYING PLASMA. Papa, Robert J. (Cambridge Research Labs., Bedford, Mass.). Phys. Fluids, 8: 1408-10(July 1965).

Three conditions are explicitly stated in terms of the electron temperature relaxation time, the electron density

relaxation time, the Maxwellianization time, and the effective diffusion time. These three conditions ensure that the isotropic part of the electron distribution function will remain Maxwellian even though the electron temperature and electron density are functions of time and gradients exist within the electron gas. (C.E.S.)

40016 FLAME PLASMA SEEDED WITH SULFUR HEXAFLUORIDE. Hoffman, J.; Westbrook, E. A. (Mitre Corp., Bedford, Mass.). Phys. Fluids, 8: 1410-11(July 1965).

An experiment consisting of microwave probe measurements of electron concentration in an alkali-seeded flame as sulfur hexafluoride was added is described. An open flame was generated with acetylene, oxygen, and nitrogen in 1.35:1:1.25 volume ratio. Alkali salts were added by atomization of an aqueous solution into the O_2-N_2 stream. Values of the electron concentration, collision frequency, and electron reduction are given for various amounts of sulfur hexafluoride added. (C.E.S.)

40017 COOPERATIVE EFFECTS IN A TENUOUS ENERGETIC PLASMA CONTAINED BY A MAGNETIC MIRROR FIELD. Damm, C. C.; Foote, J. H.; Futch, A. H. Jr.; Gardner, A. L.; Gordon, F. J.; Hunt, A. L.; Post, R. F. (Univ. of California, Livermore). Phys. Fluids, 8: 1472-88(Aug. 1965). (UCRL-12034).

The formation and characteristics of a steady-state hydrogen plasma contained in a magnetic mirror field are described. The mean ion energy is 20 kev. The plasma is formed by ionizing and trapping a portion of a beam of energetic hydrogen atoms passing through the confining field. The methods of measurement used to determine the plasma properties are described. Measurements of the radial and azimuthal trapped-ion distributions, the average ion and electron densities, and the plasma potential are compared with the predictions of simple theory, neglecting cooperative plasma effects. The observed deviations from these simple predictions show that the plasma properties are dominated by cooperative phenomena. The plasma density is found to be limited to a low value ($\sim 4 \times 10^7$ ions/cm^3) by a flute or drift instability. This instability is characterized by a low frequency rotation of the plasma at a frequency typically close to the ∇B precession frequency of a 20-kev proton in the nonuniform mirror field. The plasma density at the unstable limit is observed to be related to the value of plasma potential. This relationship can be understood quantitatively by an extension of an earlier theoretical treatment of the drift instability to the case of unequal ion and electron densities. The flute oscillation frequency is also derived from this theory. Oscillations at the ion gyrofrequency are observed, marking the presence of an electrostatic resonance type of instability. Coupling of these modes with the flute oscillations is described, but detailed identification of the electrostatic resonance modes cannot yet be made. (auth)

40018 UNIVERSAL INSTABILITY IN COMPLEX FIELD GEOMETRIES. Krall, Nicholas A.; Rosenbluth, Marshall N. (General Atomic Div., General Dynamics Corp., San Diego, Calif.). Phys. Fluids, 8: 1488-1503 (Aug. 1965).

An inhomogeneous collisionless plasma in a magnetic field B is unstable to an electrostatic oscillation propagating nearly perpendicular to B but with a large phase velocity parallel to B. The stability of this mode is studied in a more complicated plasma equilibrium, including magnetic shear, finite plasma length, currents parallel to B, temperature gradients, and gravity-simulated magnetic cusp or mirror curvature. It is found that many of these equilibria are stable to this mode, which has been misnamed a "universal instability." (auth)

40019 HIGH-FREQUENCY VELOCITY SPACE INSTABILITIES. Gruber, S.; Klein, M. W.; Auer, P. L. (Sperry Rand Research Center, Sudbury, Mass.). Phys. Fluids, 8: 1504-9(Aug. 1965).

The electrostatic dispersion relation is examined for high-frequency instabilities in a collisionless, infinite, magneto-active plasma with electrons having non-Maxwellian velocity distributions. Growing waves are found, and the complex frequency solutions are calculated. The variation of wave growth with electron density, angle of propagation, and frequency is calculated for several distributions of electron velocity. Calculations of the spectrum when the electrons have an axial velocity spread are included. (auth)

40020 SUSTAINED PLASMA OSCILLATIONS NEAR THE CREST OF A MOVING STRIATION. Swartz, G. A.; Napoli, L. S. (RCA Labs., Princeton, N. J.). Phys. Fluids, 8: 1517-20(Aug. 1965).

Plasma oscillations in the frequency range of 2 to 4 Gc were observed with a radially directed probe in a tubular plasma column. The plasma oscillations, which are generated by application of a pulsed electric field at the plasma cathode or anode in an argon hot-cathode arc, are sustained for as long as 50 μsec after the pulsed field is removed. The oscillations occur near the crests of a moving striation. The plasma oscillations are associated with the striation and are most intense near the plasma anode. The frequency detected by the probe increases with increasing plasma density but is not related to the 300-G magnetic field which is applied parallel to the plasma column. The oscillations may be the result of the two-stream interaction of the plasma electrons with a group of high energy electrons associated with the striation. (auth)

40021 EFFECT OF COLLISIONS ON ION CYCLOTRON WAVES. Sachs, David L. (Univ. of California, Los Angeles). Phys. Fluids, 8: 1520-30(Aug. 1965). (UCRL-11407(Rev.1)).

The behavior of a transverse electromagnetic wave propagating in the direction of a uniform magnetic field in an unbounded fully ionized plasma is examined. Linearized kinetic equations with collision terms of the Krook-Bhatnager-Gross type extended by Liboff to include interspecies collisional effects are used in the solution of an inhomogeneous wave equation. The region of ion cyclotron resonance is closely investigated, and the transition of the dispersion relation from the low-temperature collision-dominated regime to the high-temperature regime is observed. It is found that moments of the kinetic equations are adequate in the collision-dominated regime, but the kinetic equation for the ions must be used at higher temperatures. At these higher temperatures a complete solution of the problem requires numerical work near the source plane. Far from the source, explicit solutions for the fields can be written. (auth)

40022 STABILITY OF FINITE AMPLITUDE ION CYCLOTRON WAVES IN PLASMA. Jukes, J. D. (Culham Lab., Abingdon, Berks, Eng.). Phys. Fluids, 8: 1531-3 (Aug. 1965).

A circularly polarized, shear Alfvén wave of finite amplitude is shown to become rapidly unstable as its frequency ω_1 approaches ion cyclotron resonance Ω. A particular mode of decay is into two perturbations consisting of a shear Alfvén wave of slightly lower frequency and an acoustic wave of much lower frequency. The decay rate is proportional to $S^{\frac{1}{2}}/(1-\omega_1/\Omega)$ where S is the power flux. (auth)

40023 HIGHLY IONIZED DENSE PLASMA IN A CESIUM PENNING ARC. Swartz, G. A.; Napoli, L. S. (RCA Labs., Princeton, N. J.). Phys. Fluids, 8: 1550-8 (Aug. 1965).

A stable cesium plasma with a density of 10^{15} ions/cm^3 and 50% ionization was produced by a Penning arc. A hot, high work function, anode is shown to be a significant factor in the achievement of this very dense highly ionized plasma. Plasma instabilities, which are normally present in the Penning arc, were found to be rotating in the $j \times B$ direction. These instabilities are damped when the arc pressure is 0.5 torr and the arc boundary is irregular. Radial and axial plasma density variations were measured. The radial density gradient decreased when the plasma became stable. The axial plasma density variation indicates

that the prime source of plasma electrons is the hot cathode. (auth)

40024 CONNECTION BETWEEN CORRELATIONS AND FLUCTUATIONS IN A PLASMA. Feix, Marc R. (Langley Research Center, Hampton, Va.); Von Hagenow, Karl. Phys. Fluids, 8: 1565-7(Aug. 1965).

A generalization of the Hagfors method outside equilibrium is considered. A meaningful relation is obtained between the two particle correlation functions and space time fluctuations. A one species electron plasma with a neutralizing smeared motionless background is treated. (C.E.S.)

40025 GAPS IN THE SPECTRUM OF ELECTROSTATIC PLASMA WAVES. Dreicer, H. (Los Alamos Scientific Lab., N. Mex. and CNEN, Frascati, Italy). Phys. Fluids, 8: 1568-70(Aug. 1965). (LA-DC-6915).

The magnitude of gaps in the spectrum of purely electrostatic plasma oscillations propagating strictly perpendicular to a uniform static magnetic field is considered. The approximate dispersion equation for these electrostatic waves propagating through a uniform infinite plasma characterized by a Maxwellian electron velocity distribution and a rigid smeared-out positive-ion background is treated. A set of numerical solutions to this equation is provided, and the circumstances under which this equation exhibits spectral gaps are examined. (C.E.S.)

40026 DENSITY MODULATIONS IN RADIO FREQUENCY PLASMAS. Schlueter, H.; Durham, J.; Ransom, C. J. (Univ. of Texas, Austin). Phys. Fluids, 8: 1571-2(Aug. 1965).

Electrodeless hydrogen and helium ring discharges in a static axial magnetic field exhibit striation-like helical structures. Stratifications appear perpendicular to the r-f electric field. In attempts at explaining discharge stratifications it is important whether the region of increased light emission coincides with regions of increased or decreased electron density. An experiment is reported on striation-like structures of hydrogen r-f discharges in which the brighter plasma arms are regions of decreased electron density but increased temperature. (C.E.S.)

40027 A WARM MAGNETOPLASMA MICROINSTABILITY. Crawford, F. W.; Tataronis, J. A. (Stanford Univ., Calif.). Phys. Letters, 17: 240-1(July 15, 1965).

Dispersion characteristics are computed of perpendicularly-propagating cyclotron harmonic wave modes in a plasma having a delta-function transverse electron velocity distribution. The computed curves indicate that in a warm infinite plasma immersed in a magnetic field, an infinite series of perpendicularly-propagating modes can exist; in finite plasmas growing waves can be expected either due to the presence of boundaries or structures supporting slow waves, or to direct mode coupling and absolute instability at sufficiently large values of (ω_p^2/ω_c^2). (L.B.S.)

40028 PLASMA ACOUSTIC WAVES ON AN INHOMOGENEOUS COLUMN. Crawford, F. W.; Tataronis, J. A. (Stanford Univ., Calif.). Phys. Letters, 17: 247-9(July 15, 1965).

Dispersion curves for propagation along a warm nonuniform plasma are computed for the case of infinite planar geometry and a Gaussian electron density profile to show that the Tonk-Dattner resonances, whose origin has been shown to be due to radial propagation of plasma acoustic waves, can be interpreted as the long-wavelength cutoffs of a series of modes of propagation along the column. The curves are shown for both symmetric and asymmetric potential symmetries. (L.B.S.)

40029 RESONANCES IN THE LIGHT SCATTERED FROM A PLASMA. Weinstock, J. (National Bureau of Standards, Washington, D. C.). Phys. Letters, 18: 21-2 (Aug. 1, 1965).

The effects of transverse motion of a plasma on the spectrum of light scattered from the plasma are investigated. Specifically, the manner in which the transverse motion modifies the scattering resonances is considered. (D.C.W.)

40030 ON TWO STREAM INSTABILITY OF RADIAL INHOMOGENEOUS ELECTRON BEAMS. Kopecky, V.; Vaclavik, J. (Czechoslovak Academy of Sciences, Prague). Phys. Letters, 18: 29-30(Aug. 1, 1965).

The system of two interpenetrating monoenergetic homogeneous electron beams in the presence of an immovable ion background is unstable for potential perturbations with wave numbers k satisfying the condition $(ku)^2 < 2\omega_0^2$, where u is the beam velocity and ω_0 is the Langmuir electron frequency. The effect of radial beam inhomogeneity on this instability is investigated. The results show that the radial inhomogeneity partially stabilizes the system. (D.C.W.)

40031 EXPERIMENTS ON MAGNETICALLY PRODUCED AND CONFINED ELECTRON CLOUDS. Janes, G. S. (Avco-Everett Research Lab., Everett, Mass.). Phys. Rev. Letters, 15: 135-8(July 26, 1965).

Experimental evidence is presented indicating that a stable dense cloud of electrons with an associated negative electrostatic potential well can be produced inductively in cylindrical geometries. The electron cloud is produced by injecting electrons near the outer cylindrical wall while an axial magnetic field is rising. The equilibrium configuration, some empirical evidence regarding stability limits on the electron density, and the experimental verification of the inductive-charging concept are discussed. (D.C.W.)

40032 PRODUCTION OF Bev POTENTIAL WELLS. Janes, G. S.; Levy, R. H.; Petschek, H. E. (Avco-Everett Research Lab., Everett, Mass.). Phys. Rev. Letters, 15: 138-40(July 26, 1965).

The production of large electrostatic potential wells by a cloud of electrons suspended in a magnetic, according to the concept of the preceding article, is discussed, including possible applications of this concept. (D.C.W.)

40033 COMBINATION SCATTERING OF MICROWAVES FROM SPACE-CHARGE WAVES IN A LABORATORY MAGNETOPLASMA. Chen, Y. G.; Leheny, R. F.; Marshall, Thomas C. (Columbia Univ., New York). Phys. Rev. Letters, 15: 184-187(Aug. 2, 1965).

The observation of combination scattering of microwaves from plasma waves propagating through a magnetoplasma formed in a Q machine is reported. The measurements were made with a radiometer which detects the microwave signal backscattered by the plasma when a low-power microwave beam is directed through the plasma parallel to the confining magnetic field. The study is restricted to electron effects, while the ions are considered stationary. The frequency spectrum of scattered radiation, resulting from an electromagnetic wave interacting with the collective motion of charges in a plasma, depends on the fluctuating plasma dielectric constant which itself is determined by these charge motions. (J.F.P.)

40034 ON TRANSIENT WAVE PROPAGATION IN A PLASMA. Case, Carl T. (AF Cambridge Research Labs., Bedford, Mass.). Proc. IEEE (Inst. Elec. Electron. Engrs.), 53: 730-1(July 1965).

A group of curves is presented for the initial buildup of a step sinusoidal carrier propagating in an unbounded, lossless, isotropic plasma. Curves are also presented for the reflection of a sine wave step carrier from a semi-infinite plasma medium. (J.F.P.)

40035 FURTHER COMMENTS ON "THE TRANSIENT PHENOMENA IN AN ISOTROPIC PLASMA WITHOUT COLLISION LOSS." Knop, C. M. (NESCO, Pasadena, Calif.). Proc. IEEE (Inst. Elec. Electron. Engrs.), 53: 751-2(July 1965).

The transient behavior of a carrier of short time duration reflected from a semi-infinite collisionless plasma of a certain plasma frequency was previously determined. Further work is now reported leading to an exact expression in terms of a convergent series of Bessel functions

for the reflected response due to the incident step-function carrier. A computation of this response using this expression is given for the corresponding case considered previously. (J.F.P.)

40036 AMPLIFICATION OF MICROWAVES BY THE INTERACTION OF AN ELECTRON BEAM WITH A CESIUM PLASMA. Katoh, H.; Ayaki, K.; Ozawa, M.; Asami, Y. (Nippon Electric Co., Tokyo). Proc. IEEE (Inst. Elec. Electron. Engrs.), 53: 754(July 1965).

The amplification of microwaves is described. This phenomenon is caused by the interaction of an electron beam with a cesium plasma generated by surface ionization on a heated tungsten wire. The frequency characteristics were investigated in the plasma amplifier while its density was measured by the couple-probe method. It was observed that the plasma frequencies calculated from the plasma densities were nearly equal to those corresponding to the peaks of gain in the frequency characteristics. It appeared that the maximum gain is attained when the plasma frequency is nearly equal to that of the input microwave. (J.F.P.)

40037 RESEARCH ON PLASMAS PRODUCED IN BLOWN ARCS. Sy, Alassane Abdoul (CNRS, Paris). Rev. Hautes Temp. Refractaires, 2: 65-93(Jan.-Mar. 1965). (In French)

The effect of various parameters on the electrical characteristics of an arc was studied, as well as the dynamics of the plasma (Ar or Ar-H) jet. A duoplasmatron device was used. It was found that the only electrical parameter which determines the optical and thermal properties of the plasma is the electrical power furnished to the arc. The existence of two regimes (laminar and turbulent) of plasma flow was established. An investigation of the optical and thermal properties of the plasma showed that the equation of state of perfect gases is applicable to this type of plasma. An experimental law of variation of the enthalpy of the plasma with the power and the argon flow rate was obtained. It was concluded that thermodynamic equilibrium among the various types of particles was achieved. (D.C.W.)

40038 ULTRAFAST HIGH VOLTAGE PROBE. Leavitt, G. E.; Shipman, J. D. Jr.; Vitkovitsky, I. M. (Naval Research Lab., Washington, D. C.). Rev. Sci. Instr., 36: 1371-2(Sept. 1965).

High-voltage probes that operate in a range of 50 to 600 kv are described. The high frequency response of the probe is about 500 Mc. The probes consist of a capacitive voltage division to a level at which single non-inductive film resistors can be used. One such resistor in series with the transmission line, terminated by a matched recording oscilloscope input impedance, serves both as an additional voltage divider and as part of an RC network with a time constant chosen to be much longer than the pulses to be measured. (C.E.S.)

40039 OPTICAL INVESTIGATION OF TEMPERATURE DISTRIBUTION AND ELECTRON CONCENTRATION IN ARGON PLASMA. Gol'farb, V. M.; Dresvin, S. V. (Leningrad Pedagogical Inst.). Teplofiz. Vysokikh Temp., 3: 333-9(May-June 1965). (In Russian)

Temperature and electron concentration and their distribution in a high-frequency induction discharge plasma in argon at atmospheric pressure were determined using optical devices. In a large part of the plasma cluster, the temperature reached about 9500°K and the electron concentration about 1×10^{16} cm^{-3}, at power injected into the plasma of 2 to 3 kv and 26 Mc. (tr-auth)

40040 STATE OF GAS BEHIND STRONG SHOCK WAVE. Biberman, L. M.; Yakubov, I. T. (Moscow Inst. of Power Engineering). Teplofiz. Vysokikh Temp., 3: 340-53(May-June 1965). (In Russian).

A system of kinetic and gasdynamic equations, determining the state of a gas behind strong shock waves, is described. A method of solution is proposed, taking into account the presence of all excited states of real atoms. Relaxation in air is studied for shock-wave velocities ≥10 km/sec. The basic processes are explained, and the relaxation times are calculated. (tr-auth)

40041 INVESTIGATION OF NEON PLASMA COMPLEX CONDUCTIVITY USING A Q-METER. Aleksandrov, A. F.; Yatsenko, L. M. (Moscow State Univ.). Teplofiz. Vysokikh Temp., 3: 354-9(May-June 1965). (In Russian).

Results are presented of measurements of the active and reactive components of the conductivity of a plane capacitor, containing between the plates plasma of the positive column of a gas discharge in the frequency range 0.5 to 25 Mc at discharge current strengths of 5 to 100 mamp and at various gas pressures. A comparison of the experimental results with results of a theoretical calculation of capacitor conductivity, taking into account thermal motion of the charged particles, is given. Satisfactory agreement is obtained. (tr-auth)

40042 DIELECTRIC PERMEABILITY OF ISOTHERMAL PLASMA. Shister, A. R. Teplofiz. Vysokikh Temp., 3: 360-9(May-June 1965). (In Russian).

An expression for the complex dielectric permeability tensor of a plasma, valid in the region of frequencies lower, as well as higher, than the frequency of Langmuir electron oscillations, is obtained, starting from the kinetic equation taking into account the effect of a magnetic field on the collisions of particles. (tr-auth)

40043 SPECTROSCOPIC STUDIES OF ARGON JET FLOWING FROM PLASMATRON NOZZLE. Moskvin, Yu. V.; Chesnokova, N. N. Teplofiz. Vysokikh Temp., 3: 370-5(May-June 1965). (In Russian).

Results are presented of an experimental investigation of the temperature of argon during emission from a plasmatron nozzle at a wide range of specific powers. A weak dependence of temperature on specific power and the presence of temperature inhomogeneity in the cross section of the jet were established. A conclusion on the existence of local thermal equilibrium was drawn on the basis of the data obtained. The possibility of using the continuous emission spectrum of argon in the region of constant intensity for temperature measurements and also the accuracy of these measurements are evaluated. (tr-auth)

40044 LAMINAR MAGNETOGASDYNAMIC BOUNDARY LAYER ON THE CONDUCTING SURFACE OF CROSSED ELECTRIC AND MAGNETIC FIELDS. Genkin, A. L. Teplofiz. Vysokikh Temp., 3: 401-8(May-June 1965). (In Russian)

A method for calculating the laminar magnetogasdynamic boundary layer at a conducting surface is given. A solution of the non-self-similar problem is obtained for the case of constant nuclear temperature of the flow. The solutions can be used for determining the effect of the boundary layer on the flow in crossed electric and magnetic fields and for calculating the coefficients of friction and heat transfer. (tr-auth)

40045 SOME PROBLEMS IN PHYSICS OF HIGH-TEMPERATURE PLASMA. Artsimovich, L. A. Vestn. Akad. Nauk SSSR, No. 5, 39-45(May 1965). (In Russian)

In reviewing the requirements of a thermonuclear plasma, it is pointed out that the plasma should be completely ionized with electron and ion temperatures of 10^8 to 10^9 degrees. At present theory is leading experiment. Theory indicates that quasineutrality must be maintained, that is, there should be a mutual compensation of the ion and electron space charges. It is noted that collisions can be ignored at thermonuclear temperatures (the effective cross section for coulombic interaction decreases to 10^{-23} cm^2 at 10^9 degrees). The electrical conductivity of a high-temperature plasma increases rapidly with temperature, and exceeds the electrical conductivity of a typical metal by a factor of several hundred at 10^9 degrees. A magnetic trap using the pinch effect or magnetic mirrors is used to confine the hot plasma. The instability problem is foremost in plasma physics. Theory shows that if the strength of an applied longitudinal magnetic field is sufficiently great, conditions are ripe for overcoming the most dangerous, large-scale instabilities peculiar to a conducting plasma. Small-scale instabilities must be also avoided. Plasma loops (toroidal) with electron and ion temperatures

of a few million degrees have been attained at a particle concentration of $10^{13}/cm^3$. The lifetime of the plasma particles is a few milliseconds. Various methods of heating the plasma have been proposed (external injection, turbulent heating of a plasma, etc), but at present attention is focused on creating conditions to attain a stable confinement of the hot plasma in the trap. By creating a magnetic field which increases on all sides, plasma confinement in a limited space has been proved at a particle concentration of $10^{10}/cm^3$. The density must be raised to 10^{13}-10^{14} particles/cm^3 in order to consider the problem as solved. Many new kinds of instabilities are being discovered each month. It is pointed out that fast particles with a non-Maxwellian distribution are continuously generated in an unstable plasma. It will be difficult to produce a plasma without these fast particles. (TTT)

40046 STABLE PLASMA PRODUCTION IN TRAPS WITH MAGNETIC MIRRORS. Ioffe, M. S. Vestn. Akad. Nauk SSSR, No. 5, 46-52(May 1965). (In Russian)

Chute instabilities in the usual mirror traps are caused by the presence of a magnetic field which decreases in a radial direction. The resulting drift in the crossed E and H fields is directed outward, and plasma is ejected transverse to the magnetic field in the form of a "tongue". Plasma chute instabilities can be overcome by changing the configuration of the magnetic field in such a way that the magnetic field strength increases not only in a longitudinal direction, but also in a radial direction. The radial fall in the main magnetic field can be overcome, and the magnetic field can be made to increase in a radial direction by using a supplementary system of stabilizing coils. Such a combined field was created in the PR-5 unit which had a maximum field strength $H_{||}$ (longitudinal) of 5000 oersteds in the center of the trap and a strength H_m = 6500 oersteds in the stoppers (mirrors). The distance between stoppers was 120 cm. The maximum field created by the stabilizing coil was $H_\perp$ = 4500 oersteds. The ratio $\alpha_\perp = [1 + (H_\perp/H_{||})^2]^{0.5}$ was 1.4 at the maximum value of $H_{||}$. A minimum pressure of 1×10^{-6} mm Hg std could be attained in the trap. If $\alpha_\perp > 1.1$, the plasma confinement time τ shows a sharp increase from 0.05 to 3.5 milliseconds. The fast ions are lost by a charge transfer mechanism. (TTT)

40047 TURBULENT HEATING OF PLASMA. Zavoiskii, E. K. Vestn. Akad. Nauk SSSR, No. 5, 53-9(May 1965). (In Russian)

In addition to heating a cold plasma by injecting an electron beam into the magnetic trap, it is also possible to heat the electrons and ions of a plasma by exciting collective motions in the plasma by means of a strong electromagnetic field. With a plasma concentration < 10^{13} cm^{-3} and at least 50% ionization of the cold plasma, experiments with high-frequency shock fields propagated transverse to a constant magnetic field showed that up to 30% of the energy in the strong electromagnetic wave is transferred to the plasma over a path length of half a wavelength. The radius r of the plasma loop should satisfy the condition: $r > U_A/4\nu$. Here U_A is the Alfven velocity of the wave, and ν is the wave frequency. Also we have $\xi H_\sim^2/8\pi = nk(T_e + T_i)$. Here $\xi = 0.3$; $H_\sim$ is the strength of the high-frequency magnetic field; T_e and T_i are the electron and ion temperatures after passage of the wave, and k is the Boltzmann constant. The maximum electron energy is at 500 ev, and the maximum ion energy is at 175 ev for n = 10^{12} cm^{-3}, $H_\sim$ = 500 oersteds, and H = 350 oersteds. The frequency ν is 1.2×10^7 cycles/sec. The ions in the plasma may be heated directly or as a result of an ion beam instability. The ion temperature at maximum compression is estimated at 3 kev at a plasma density of n = 5×10^{12} cm^{-3}. Ion charge transfer must be weak at high plasma electron temperatures, because high-energy ions were retained in the magnetic trap for a period of about 2 milliseconds. (TTT)

40048 NOZZLE FLOW OF A FULLY IONIZED PLASMA BASED ON TWO FLUID THEORY. Pai, S. I.; Tsao, C. K. (Univ. of Maryland, College Park). Z. Angew. Math. Phys., 16: 360-9(May 25, 1965).

The one-dimensional steady channel flow of a fully ionized plasma is studied by the two-fluid theory, and the results are compared with those of classical single-fluid theory. Only the strict one-dimensional flow is considered in which all quantities are functions of the longitudinal coordinate and strictly independent of the transverse coordinate; Maxwell's equations must be obeyed. The analysis of ordinary gasdynamics is followed by considering the flow in a nozzle of given shape under various flow rates and applied electromagnetic fields. Thus the similarity and deviations between the results of single-fluid theory and two-fluid theory can be clearly observed. (J.F.P.)

40049 STRUCTURE OF AXISYMMETRIC FORCE-FREE MAGNETIC FIELDS IN A DISSIPATIVE PLASMA. Middendorf, Heinz Dieter (Jever, Ger.). Z. Angew. Math. Phys., 16: 370-85(May 25, 1965).

A more refined theoretical model is given for the pinch mechanism by which a current in an ionized gas may become constricted. An energy equation is added to the force-free field condition equation for axisymmetric geometry. In order to overcome some of the difficulties inherent in the nonlinear nature of the problem Alfven's analysis is also reformulated in a more tractable way. It is shown that closed-form solutions of an almost exact character can be obtained. (J.F.P.)

40050 LIGHT MIXING AND THE GENERATION OF THE SECOND HARMONIC IN A PLASMA IN AN EXTERNAL MAGNETIC FIELD. Kegel, Wilhelm H. (Institut fuer Plasmaphysik, Garching, Ger.). Z. Naturforsch., 20a: 793-800(June 1965).

The theory of light scattering in a plasma is extended by including an external electric field (e.g. the field of a laser beam) in calculating the density fluctuations. It is shown that in the presence of a time constant homogeneous magnetic field there arise density fluctuations with the frequency and the wave number of the external electric field. Expansions of the general expressions are obtained for the case that the frequency is large compared to the electron gyrofrequency. The special case that the external electric field is a transverse wave is discussed in detail. The light of a second beam may be scattered by these forced density fluctuations. The scattered light has the sum and the difference frequency of the two light beams, i.e. light mixing occurs. In the framework of this theory the effect occurs only if the two beams are parallel. If the scattering of the same beam that forces the density fluctuations is considered, the scattered light is the second harmonic. (auth)

40051 SUPPLEMENTARY RANKINE-HUGONIOT CALCULATIONS FOR THERMAL PLASMAS. Artmann, J. (Institut fuer Plasmaphysik, Stuttgart). Z. Naturforsch., 20a: 857-8(June 1965). (In German).

Calculations are presented of the parameters behind a strong shock front in thermal plasmas, which takes into account the ionization potential decrease derived from the Debye-Huckel theory along with previous calculations. Diagrams are presented for the relative density and temperature as functions of the shock front velocity for hydrogen at 0.1, 1.0 and 10.0 torr and for helium and argon at 1.0, 10, and 100 torr. (L.B.S.)

40052 EFFECT OF ION-NEUTRAL COLLISIONS ON PLASMA ROTATION. Drawin, H. W.; Fumelli, M.; Voslamber, D. (EURATOM-CEA, Fontenay-aux-Roses, France). Z. Naturforsch., 20a: 859-60(June 1965).

By calculating the Boltzmann collision integral for collisions between ions and neutral particles, two different formulas were derived for the rotation velocity v_θ of a cylindrical plasma column driven by $I_r B_z$ forces. For $v_\theta < v_{th}$ the rotation velocity is proportional to $I_r B_z$, whereas for $v_\theta > v_{th}$ a dependency $v_\theta \sim (I_r B_z)^{1/2}$ is obtained. v_{th} denotes the mean thermal velocity of the ions. (auth)

40053 CHARGE DENSITY OF EXCITED HYDROGEN LEVELS IN STATIONARY PLASMA WITH CONSIDERATION OF THE DIFFUSION OF NEUTRAL PARTICLES. Drawin, H. W. (Euratom-C.E.A. Fontenay-aux-Roses, France). Z. Physik, 186: 99-107(1965). (In German)

When strong diffusion of neutral particles from outer zones of the plasma into the inner region of a plasma column takes place, the population densities of the excited atoms deviate from those obtained without a diffusion current of neutral particles. By solving the corresponding rate equations, the population densities of the hydrogen levels in a nonthermal, optically thin plasma with a superposed diffusion current of hydrogen atoms are calculated. Numerical values are given for electron temperatures T_e = 5, 10, and 30 ev, and for electron densities varying from $n_e = 10^8$ to 10^{14} cm^{-3}. (auth)

40054 REVIEWS OF PLASMA PHYSICS. VOLUME 1. Leontovich, M. A. (Ed.). Authorized Translation from the Russian by Herbert Lashinskii. New York, Consultants Bureau, 1965. 335p. $12.50.

Four papers on certain general problems in the description of a plasma are presented. A separate abstract is prepared for each paper. (A.G.W.)

For abstracts of individual papers see: 40055, 40056, 40057, and 40058.

40055 MOTION OF CHARGED PARTICLES IN ELECTROMAGNETIC FIELDS IN THE DRIFT APPROXIMATION. Sivukhim, D. V. p.1-104 of Reviews of Plasma Physics. Vol. 1. New York, Consultants Bureau, 1965.

The basic features of the motion of a particle in a constant uniform magnetic field are reviewed. The idea of a guiding center of the particle is introduced, and it is shown that to a first approximation the smoothed velocity of the particle equals the smoothed velocity of the guiding center. A new derivation of the equations of drift theory is given, which is simpler mathematically than previous derivations and is suitable for both relativistic and nonrelativistic velocities. Extension of drift theory to the case of strong transverse electric fields is considered. (A.G.W.)

40056 PARTICLE INTERACTIONS IN A FULLY IONIZED PLASMA. Trubnikov, B. A. p.105-204 of Reviews of Plasma Physics. Vol. 1. New York, Consultants Bureau, 1965.

The kinetic effects that derive from particle interactions in a fully ionized homogeneous gas are considered. The emphasis is on maximum simplicity and clarity of development. The approach is based on a relatively novel and systematic use of special potential functions and electrostatic analogies. The motion of test particles in a plasma is considered in detail in Part I, and a nonrigorous derivation of the kinetic equation is given in Part II. Part III is concerned with the analysis of certain kinetic effects in a plasma. (auth)

40057 TRANSPORT PROCESSES IN A PLASMA. Braginskii, S. I. p.205-311 of Reviews of Plasma Physics. Vol. 1. New York, Consultants Bureau, 1965.

Transport coefficients are listed for a fully ionized plasma consisting of electrons and a single ion species. The coefficients are given qualitative physical interpretations, evaluated in order-of-magnitude terms, and computed numerically from the kinetic equation. Certain paradoxes, which arise in the use of the transport equations to describe a plasma in a strong magnetic field and which are the source of various errors and ambiguities in the literature, are considered. The application of the transport equations for particles of different species in analyses that assume a plasma model based on a single complex gas is described for fully and partially ionized plasmas. (44 references) (A.G.W.)

40058 THERMODYNAMICS OF A PLASMA. Vedenov, A. A. p.312-26 of Reviews of Plasma Physics. Vol. 1. New York, Consultants Bureau, 1965.

Computation of the thermodynamic functions for a system of interacting particles in thermal equilibrium is considered for two cases: the classical Coulomb system and the quantum Coulomb system. Problems are included as illustrations. A formula for the degree of ionization of a partially ionized plasma is given. (A.G.W.)

40059 ON IONIZING SHOCK WAVE PLASMA DIAGNOSTICS. Miller, B.; Marshall, T.; Gross, R. A. (Columbia Univ., New York). 23p. (CONF-650416-6). ORINS

From 4th Symposium on Advanced Propulsion Concepts, Palo Alto, Calif.

The problem of measuring with a probe the magnetic field in a plasma, which is moving with respect to the probe, is examined. It is shown that the usual integration with respect to time is, in general, not proper. The correct expression for the case of a plasma and its associated fields produced by a strong shock wave in an electromagnetically driven shock tube is derived. The fundamental relations for the technique of measuring electron density by the use of coherent light is also explained. Both these techniques are relevant to measurements of dense, hot, transient plasmas, such as those generated by strong ionizing shock waves. (J.F.P.)

40060 FUSION RESEARCH APPARATUS. Kerst, Donald W.; Ohkawa, Tihiro (to General Dynamics Corp.). U. S. Patent 3,194,739. July 13, 1965. Filed Aug. 20, 1962.

An apparatus having cusped geometry for confining plasma comprises an elongated, generally tubular jacket of conductive material that is internally fluted to provide a number of generally longitudinally extending arcuate grooves and ridges. An elongated conductive member is disposed in each groove in spaced relation to the wall of the groove. The portion of the member adjacent to the groove is generally arcuate in shape. A current passed through the conductive member and the jacket establishes a first magnetic field in an area adjacent to the ridges and a second in an area defined by the wall of each groove and the adjacent arcuate portion of the conducting member. The square root of the strength of the first magnetic field to that of the second field is less than the ratio of half the spacing between the arcuate portion and the groove wall to the radius of the groove wall. (B.L.M.)

Shielding

Refer also to abstracts 39761, 40156, and 40246.

40061 (BNWL-SA-79) NEUTRON ATTENUATION MECHANISMS IN CONCRETES. Greenborg, J. (Battelle-Northwest, Richland, Wash. Pacific Northwest Lab.). [June 3, 1965]. Contract AT(45-1)-1830. 47p. (CONF-650602-38). Dep. (mn); $2.00(cy), 1(mn) CFSTI.

From American Nuclear Society 11th Annual Meeting, Gatlinburg, Tenn.

A brief description is given of the neutron. This is followed by a discussion of the physics of interaction of a neutron with a nucleus and then extending this subject into the effect of neutron interaction with many nuclei in a small volume (as is found in common solids and liquids). Material mixing is discussed last with emphasis on estimation of neutron attenuation efficiency in relation to concrete composition. (M.O.W.)

40062 (N64-29366) COMPUTER CODES FOR THE EVALUATION OF SPACE RADIATION HAZARDS. VOL. 4. SPACE RADIATION DOSES FROM ELECTRON BREMSSTRAHLUNG RADIATION. Moshofsky, Raymond P. (Boeing Co., Seattle, Wash. Aero-Space Div.). [1964]. 48p. (NASA-CR-58295; D2-90418-4). CFSTI, $4.60 cy.

This IBM 7090 FORTRAN program calculates the bremsstrahlung radiation dose received through several slabs of shield material; only electron-produced bremsstrahlung are considered. Required inputs to this program are the incident electron spectrum; photon attenuation coefficients; buildup coefficients; shield materials and thicknesses, and solid angles; and flux-to-dose conversion factors. The calculated dose is called the electron bremsstrahlung radiation dose and is computed in an equation. The program may also be used to estimate the bremsstrahlung radiation dose received by men or equipment inside a vehicle situated in a region of electron radiation. To perform these calculations, the program requires a resolution of all material in the vehicle into an equivalent polyhedral shell. (auth)

40063 (NP-15125) RADIATION PROTECTION FOR MANNED ORBITING SPACE STATIONS. Jordan, T. M.; Koprowski, E. F.; Langley, R. W. (Douglas Aircraft Co., Inc., Santa Monica, Calif. Missile and Space Systems Div.). Sept. 1964. 87p.

Results of a detailed parametric investigation of radiation shielding requirements for first generation manned orbiting space stations are presented. The radiation sources considered were: trapped protons, trapped electrons (natural and artificial) and associated bremsstrahlung, and solar flare protons. Basic shielding data is presented for the above radiation sources for spherical shield configurations. This data is included because of its general applicability to a variety of shield configurations. These results are presented for circular orbits of 100, 200, 400, and 600 nautical mile altitudes and 28.7, 45, 60, and 90 degree inclinations. In addition, data are presented for extrapolation of the presented data to other altitudes. Two specific space stations were studied. The shielding analysis was based on the actual vehicle geometry, including onboard equipment and supplies, and included self shielding effects of a typical crew member represented by two elliptical cylinders. Typical results are presented for the dose received by various critical organs for several of the circular orbits mentioned above. (auth)

40064 (NP-15132) CHARGE, A SPACE RADIATION SHIELDING CODE. Lilley, J. R. (Douglas Aircraft Co., Santa Monica, Calif. Missile and Space Systems Div.). Apr. 1965. 111p. (SM-46335)

CHARGE, a FORTRAN program for the analysis of primary proton and electron passage through plane or spherical shields containing up to 100 regions, is described. The attendant generation and transmission of electron-induced x-rays (bremsstrahlung) and proton-induced secondary protons and neutrons are described. Proton and electron analyses use a modification of the range-energy relation applied to as many as one hundred energy groups, while the bremsstrahlung transmission calculation assumes an exponential attenuation corrected by semi-empirical dose buildup factors applied individually to a similar number of gamma ray energies. Availability of several bremsstrahlung source options permit comparison of most commonly used approximations. Energy dependent removal cross sections are used to calculate secondary neutron transmission. The ambient charged particle differential spectra may be specified as varying either as a power of energy or as an exponential of energy over each of several specified energy ranges, in tabulated or functional form. The analysis used is described and results are compared to other calculations and to experiments. (auth)

40065 (NP-15152) AN ABSOLUTE MEASUREMENT OF THERMAL NEUTRON ALBEDO FOR SEVERAL MATERIALS. Doty, Duane Robert (Naval Civil Engineering Lab., Port Hueneme, Calif.). May 1965. 35p. (R-377). CFSTI, $2.00 cy.

Albedo is a concept which has proved useful in the calculation of the penetration of nuclear weapons radiation through a shelter entranceway. The application of the albedo approach to describe the behavior of neutrons impinging upon various materials is presented. Values of thermal neutron albedo for lead, iron, paraffin, aluminum, carbon, and high-density concrete were measured. The results are in reasonable agreement with theoretical calculations. Verification of the angular dependence of neutron scattering was attempted, but with only partial success. Albedo as a function of thickness of the scattering material was measured for paraffin, carbon, and aluminum. The results essentially conform with theory. The possibility of using a simple empirical formula for albedo calculations of thermal-neutron streaming through shelter ducts is apparent. (auth)

40066 (NP-15155) A USER'S MANUAL FOR SALOMON, AN IBM-7090 CODE FOR GAMMA TRANSPORT CALCULATIONS. Engstroem, G. (Forsvarets Forskningsanstalt, Stockholm (Sweden)). Nov. 1964. 19p. Dep. mn.

SALOMON is a FORTRAN program that utilizes the Monte Carlo technique to treat gamma transport problems in multislab one-dimensional plane geometry. The preparation of input data and other information of essence to the user are described. (auth)

40067 STATISTICAL DISTRIBUTION OF X-RAY INTENSITIES IN THE PRESENCE OF PSEUDOSYMMETRY IN THE STRUCTURE: PART I. SPACE GROUP P1. Srinivasan, R. (Univ. of Madras). Indian J. Pure Appl. Phys., 3: 187-90(1965).

The probability distribution of x-ray intensity was considered in a structure containing pseudosymmetry, arising from the presence of centrosymmetry in a part of the unit (the asymmetric unit), the remaining portion of which has a non-centrosymmetric configuration. Using the Fourier transform approach an expression is derived for the general case in which finite numbers of such centric and acentric groups in any given proportion are distributed randomly in a non-centrosymmetric unit cell. It is found that even if there are only two centric groups in the structure, the distribution of intensity is fairly close to the ideal non-centrosymmetric one and when there is only one centric and one acentric group in the structure, the distribution depends on the relative proportion of these. Graphs are given which enable one to assess the degree of centrosymmetry in such a case. (auth)

40068 AN APPROXIMATE CALCULATION METHOD OF FLUX FOR SPHERICAL AND CYLINDRICAL SOURCES WITH A SLAB SHIELD. Ono, Hironori; Tsuruo, Akira; (Japan Atomic Energy Research Inst., Tokyo). J. Nucl. Sci. Technol. (Tokyo), 2: 229-35(June 1965).

An approximate calculation method for unscattered flux from spherical and cylindrical sources with a slab shield is presented. The method is based on modifying the source geometry to a form convenient for calculation: The sphere is approximated by a conical fragment of spherical shell, and the cylinder by a columnar fragment of cylindrical shell. The procedure for manual calculation is relatively simple, and the difference between results of approximate and exact calculations is less than +5% for large sources ($\mu_s R_0 \gtrsim 4$), and ±15% for small sources ($\mu_s R_0 \approx 0.25$). Graphs of the functions for approximate calculation are presented. The method has several advantages over Rockwell's method. (auth)

40069 EFFECTIVE ATOMIC NUMBERS OF HETEROGENEOUS MATERIALS. Murty, R. C. (Univ. of Western Ontario). Nature, 207: 398-9(July 24, 1965).

The validity of various expressions for the effective atomic number, Z_{eff}, of heterogeneous materials is examined. The equations $Z_{eff} = (\Sigma p_i Z_i^4/\Sigma p_i Z_i)^{1/3}$, $(\Sigma p_i Z_i^{3.1})^{1/3.1}$, $\Sigma(p_i Z_i/A_i)/\Sigma(p_i A_i)$, and $\Sigma p_i Z_i$, where p_i is the fraction by weight of the whole mixture occupied by the element with atomic number Z_i and atomic weight A_i, are evaluated for brass, bronze, carbon steel, monel metal, concrete, perspex, and NaI. The third expression is suggested for an approximation to a single effective atomic number. The effects of the different gamma absorption processes — photoelectric effect, Compton effect, and pair production — on effective atomic number are discussed. (M.J.T.)

40070 ELECTRON-PHOTON CASCADES IN LEAD. MONTE-CARLO CALCULATION FOR PRIMARY ELECTRON ENERGIES BETWEEN 100 AND 1000 Mev. Nagel, Hans-Hellmut (Universitaet, Bonn). Z. Physik, 186: 319-46(1965). (In German).

A Monte-Carlo program was used for the calculation of electron-photon cascade showers in lead. Bremsstrahlung, electron-electron scattering, multiple scattering, ionization loss, pair creation, Compton effect, and photoelectric effect are taken into account, with empirically corrected values for the cross sections of these processes. Electrons are followed down to $E_e = 1.5$ Mev and photons to $E_\gamma = 0.25$ Mev. (auth)

40071 THE PROPAGATION OF GAMMA QUANTA IN MATTER. Leipunskii, O. I.; Novozhilov, B. V.; Sakharov, V. N. Translated by Prasenjit Basu from Rasprostraneniye

Gamma-Kvantov v Veshchestve. International Series of Monographs on Nuclear Energy. Division X: Reactor Design Physics. Volume 6. New York, Pergamon Press, 1965. 232p. $15.00.

The theory of the absorption and propagation of gamma radiation, including the effects of multiple scattering, is presented. Data on the attenuation and the angular and spectral distribution of gamma radiation are included. (D.C.W.)

40072 SPACE RADIATION SHIELDING. Goedeke, A. Donald (Douglas Aircraft Co., Inc., Santa Monica, Calif.). pp 324-49 of Space Exploration. New York, McGraw-Hill Book Co., 1964.

A survey is presented on the present knowledge of the nature and properties of space radiation. The relation between biological dose restrictions and dosages expected in space are analyzed. The problems of shielding are discussed in the light of vehicle advancements, missions, radiation-warning techniques, and the most recent data on radiation and high-energy nuclear reactions. Active and passive shielding would include the use of electromagnetic and electrostatic fields, although present techniques are not adequate. Passive shielding utilizing aluminum, beryllium, and magnesium to absorb radiation would be effective. (Aerospace Med., 36 (Jan. 1965))

Solid State Physics

See *also* CHEMISTRY — Inorganic and Physical Chemistry
METALS, CERAMICS, AND OTHER MATERIALS — Properties and Structure

Refer also to abstract 38585.

40073 (CONF-796(Paper 1)) THE STRONGLY COUPLED ELECTRON-PHONON SYSTEM IN NORMAL AND SUPERCONDUCTING METALS. Schrieffer, J. R. (Pennsylvania Univ., Philadelphia). 7p.

A theoretical interpretation of the strongly coupled electron-phonon system in metals is attempted, and the relation between this theory and that developed for weak couplings is investigated. The strong-coupling theory is concluded to be adequate for strong couplings and p-band metals below the melting point; for other substances, the results are not as satisfactory. (T.F.H.)

40074 (CONF-796(Paper 3)) SUMMARY: THEORIES OF MAGNETISM IN METALS. Anderson, P. W. (Bell Telephone Labs., Inc., Murray Hill, N. J.). 4p.

Theoretical developments in the field of magnetism in metals are surveyed. 19 references. (T.F.H.)

40075 (IEA-84) MAGNETIC SCATTERING OF NEUTRONS IN FERROMAGNETIC SAMPLES CONTAINING ABSORBED HYDROGEN. Suarez, Achilles A.; Mafra, Olga Y.; Herdade, Silvio B. (Instituto de Energia Atomica, Sao Paulo (Brazil)). Dec. 1964. 21p. (CONF-631104-2). Dep. mn.

From Meeting on the Utilization of Research Reactors, Sao Paulo, Brazil.

Experiments were carried out at the IEA swimming pool reactor to verify an anomaly, reported by N. Mitrofanov, in the magnetic scattering of neutrons by hydrogenated ferromagnetic samples. No remarkable anomaly was observed, however, with epi-thermal neutrons in iron containing absorbed hydrogen and with thermal neutrons in a nickel–palladium alloy charged with hydrogen. (auth)

40076 (IS–1172) RELATIVISTIC EFFECTS IN CRYSTALS. Loucks, T. L. (Ames Lab., Iowa State Univ. of Science and Tech.). June 14, 1965. Contract W-7405-eng-42. 13p. (CONF-650542–1). Dep. mn; CFSTI, $1.00 cy, $0.50 mn.

From Midwest Theoretical Conference, Columbus, Ohio.

The relativistic effects on the Fermi surfaces of metals are studied. An investigation for finding Bloch functions which satisfy the Dirac hamiltonian $H = \overline{\alpha} \cdot \overline{p} + \beta + V$ where V is the crystal potential and has the periodicity of the lattice is presented. (M.O.W.)

40077 (IS-T–18) ANTIFERROMAGNETISM IN DILUTE CHROMIUM ALLOYS (thesis). Trego, Alan LaMar (Ames Lab., Iowa State Univ. of Science and Tech.). May 1965. Contract W-7405-eng-82. 120p. Dep. mn; CFSTI, $4.00 cy, $0.75 mn.

The electrical resistivity and thermoelectric power of single crystals of dilute alloys of vanadium, manganese, and rhenium in chromium were studied as a function of temperature between 4.2 and 450°K. Pronounced anomalies were observed in the transport properties just below the Néel temperature and these are interpreted in terms of the magnitude and position of the magnetic superzone energy gaps and the change in magnetic disorder scattering. The electrical resistivity of a single crystal of pure chromium cooled through the Néel temperature in magnetic fields up to 55 kilogauss either parallel or perpendicular to the [100] current direction was studied from 270 to 320°K. The resulting changes in the magnitude of the anomaly are interpreted in terms of the induced anisotropy in the amplitudes of the magnetization waves. The antiferromagnetism of the alloys was studied at 95 and 300°K by neutron diffraction. The addition of vanadium causes the diffraction peaks to decrease in intensity and move away from (100), while manganese and rhenium cause them to increase and approach (100) so that, above a certain concentration, the oscillatory magnetization becomes commensurate with the lattice. (auth)

40078 (NP-15111) SURFACE STUDIES USING THE MOESSBAUER EFFECT. Burton, J. W.; Frauenfelder, H.; Godwin, R. P. (Illinois Univ., Urbana. Dept. of Physics). [1964]. Contract AF49(638)-1048. 28p.

The Mössbauer effect, because of its sensitivity to strength and angular distribution of binding, to magnetic and electric fields, and to the density of s electrons at the nucleus, can be used as a tool to study surfaces. Some of the basic aspects of the theory of this technique are given. The experimental approach is reviewed, and results are discussed. (M.O.W.)

40079 (NP–15114) DYNAMICAL PROPERTIES OF A ONE-DIMENSIONAL CRYSTAL WITH FREE ENDS. Clem, John R.; Godwin, Robert P. (Illinois Univ., Urbana. Dept. of Physics). [1964]. 36p.

Analytical results are provided for the mean square displacement and velocity of the particles of a simple one-dimensional lattice with free ends in the T = 0°K and high temperature limits. The results for the mean square displacement are used to show that the effective Debye temperature (as it would be measured by the Moessbauer effect or diffraction experiments) for a central atom is twice that of an end atom. It is also shown that in this model the effective Debye temperature which would be found in "bulk" Moessbauer or diffraction measurements is slightly greater than that derived from specific heat measurements. (auth)

40080 (NP–15182) BATTELLE INDEXING CHARTS FOR DIFFRACTION PATTERNS OF TETRAGONAL, HEXAGONAL AND ORTHORHOMBIC CRYSTALS. Bell, J. C.; Austin, A. E. (Battelle Memorial Inst., Columbus, Ohio). [nd.]. 33p.

Charts for indexing powder diffraction patterns were constructed using Harrington's modification of the Hull-Davy charts. The charts for the tetragonal and orthorhombic systems cover b/a from 0.99 to 0.70 and c/a from 0.2 to 5.0, while these for the hexagonal system cover c/a from 0.2 to 5.0. (D.L.C.)

40081 (SC-DC-65-1500) RESULTS OF AUGMENTED PLANE WAVE CALCULATIONS OF THE BAND STRUCTURE OF CERIUM METAL. Waber, J. T. (Los Alamos Scientific Lab., Univ. of California, N. Mex.); Switendick,

A. C. (Sandia Corp., Albuquerque, N. Mex.). [June 1965]. Contract AT(29-1)-789. 14p. (CONF-650804-5). Dep. (mn); $1.00(cy), 1(mn) CFSTI.

From 5th Rare Earth Research Conference, Ames, Iowa.

Ten sets of electronic band structure calculations were performed for cerium metal by using the augmented plane wave method for five configurations of the type $6s^2 5d^x 4f^{2-x}$ and the lattice constants appropriate to the FCC gamma and FCC alpha phases. It is shown that the location of the f band is strongly dependent on the atomic configuration assumed by starting the calculation. The relation of these results to previous atomic calculations is discussed. It is believed that the bands should not be occupied to a common energy level according to a simple Fermi-Dirac distribution, but rather that the 4 electrons outside the xenon core should be arranged in the f as well as in the s and d bands so as to be reasonably consistent with the configuration assumed. As a consequence the f-band location is dependent on the degree to which it is occupied. The two-electron calculations by Waber, Liberman, and Cromer of the total energy for a cerium atom confined to a Wigner-Seitz sphere lend further support to this assignment hypothesis. (auth)

40082 PRINCIPAL MAGNETIC SUSCEPTIBILITIES OF $Dy_2(SO_4)_3 \cdot 8H_2O$ SINGLE CRYSTAL AND THE NATURE OF ITS CRYSTALLINE ELECTRIC FIELD. Chachra, S. P.; Neogy, D. (Burdwan Univ., India). Indian J. Pure Appl. Phys., 3: 191-4(1965).

The principal magnetic susceptibilities of a $Dy_2(SO_4)_3 \cdot 8H_2O$ single crystal were measured in the temperature range 300-80°K. The variation observed in the magnetic anisotropy of the crystal with temperature is explained on the assumption of a single tetragonal field existing in the neighborhood of the Dy^{3+} ion. It was concluded that it is not possible to obtain g values by paramagnetic resonance for temperatures above that of liquid helium. (auth)

40083 INELASTIC SCATTERING OF FAST ELECTRONS BY CRYSTALS. I. INTERBAND EXCITATIONS. Whelan, M. J. (Case Inst. of Tech., Cleveland). J. Appl. Phys., 36: 2099-2103(July 1965).

The inelastic scattering of fast electrons due to interband electron transitions in crystals of Li, Be, Ne, Al, and Cu is examined making use of single atom matrix elements given by Freeman. Values of the Fourier coefficients V_g and V_g^i of the real and imaginary part of the potential are computed for 100-kv electrons. It is concluded that while interband transitions may account for an appreciable part of the average absorption due to V_o^i, V_g^i is too small to account for the anomalous absorption effect observed in crystals. The result is in agreement with Yoshioka's conclusion based on the Fermi-Thomas model. (auth)

40084 INELASTIC SCATTERING OF FAST ELECTRONS BY CRYSTALS. II. PHONON SCATTERING. Whelan, M. J. (Case Inst. of Tech., Cleveland). J. Appl. Phys., 36: 2103-10(July 1965).

The inelastic scattering of fast electrons due to phonon excitation is examined using a simple Einstein model. The method of analytic approximation to the atomic electron scattering factor given by Smith and Burge enables analytic expressions for the Fourier coefficients of the imaginary potential due to phonon scattering to be obtained. The Fourier coefficients are computed for several elements and reflections, and the temperature dependence is examined. It is concluded that phonon scattering could account for the localization of the complex potential at the atomic positions as required to explain anomalous absorption effects, in agreement with previous results of Yoshioka and Kainuma. (auth)

40085 RECOMBINATION IN GAMMA-IRRADIATED SILICON. Glaenzer, Richard H.; Wolf, Clarence J. (McDonnell Aircraft Corp., St. Louis). J. Appl. Phys., 36: 2197-2201(July 1965).

The lifetimes of excess carriers in phosphorus-doped, float-zoned silicon were measured before and after irradiation by cobalt-60 gamma rays. Recombination in the samples prior to irradiation was dominated by a donor-like recombination center located 0.13 ev above the valence band. After irradiation, two recombination centers were found in the samples: one located at $E_c - 0.17$ ev and the other at $E_c - 0.40$ ev. The center at $E_c - 0.17$ ev can be identified with the oxygen-vacancy defect (Si-A center), but no positive identification of the $E_c - 0.40$ ev center can be made. By assuming that the $E_c - 0.40$ ev center is the phosphorus-vacancy complex, the hole capture cross section of the center was estimated as 9×10^{-14} cm^2. (auth)

40086 CALCULATION OF ACTIVATION ENERGIES FOR INTERSTITIAL DIFFUSION BY A SIMPLE ELASTIC MODEL. McNeil, M. B. (Univ. of Missouri, Rolla). J. Appl. Phys., 36: 2328-9(July 1965).

The model of Ferro for computation of activation energies for interstitial diffusion in bcc materials, which assumes the interstitial atoms occupy the octahedral positions in the lattice and behave as rigid spheres, is briefly described. Ferro's equation for the activation energy is used to recompute activation energies of H, N, O, C, and B in Cr, Fe, Mo, Nb, Ta, and W, using better values for parameters which depend on the deformation coefficients. Comparison with results from experimental determinations of activation energies shows that there is, at best, a qualitative correlation with the values derived using Ferro's model. (M.J.T.)

40087 THEORY OF RADIATION FROM A WAVE PACKET. Bierman, Arthur (City Coll., New York). J. Chem. Phys., 43: 1662-75(Sept. 1, 1965). (TID-21731).

The theory of radiation from a time-dependent state (wave packet) was developed, using Heitler's method. It was first applied to a two-component wave packet, and general expressions for the radiation rate and the spectral distribution were derived. They were evaluated to lowest order in the perturbing hamiltonian, and a number of special cases were considered. The theory was then generalized to an N-component wave packet, and formulas for the radiation rate and spectral distribution were derived. The latter is briefly discussed within the context of an approximation method. The general conclusions were: the radiation rate from a wave packet has a periodic component; energy nonconserving transitions appear; and interference terms tend to distort the Breit-Wigner shape of the spectral distribution. (auth)

40088 RADIATION FROM AN EXCITON WAVE PACKET. Bierman, Arthur (City Coll., New York). J. Chem. Phys., 43: 1675-9(Sept. 1, 1965). (TID-21730).

Properties of radiative transitions from exciton states in a linear chain and in a ring (periodic boundary conditions) were examined. The two models exhibited a persistent difference in the radiation rate even for stationary state transitions. Exciton wave packets are shown to radiate weakly if they originate at the end of the linear chain, strongly if they originate near the middle of the chain. The latter radiation showed also a strong periodic component. The radiation rate of a wave packet from a ring turns out to be the same as the rate from an isolated monomer and had no periodic components. For both the ring and the chain the wave packet was much more stable against decay than a stationary state. Radiation from a wave packet showed little deviation from the Breit-Wigner shape. (auth)

40089 ON IRREDUCIBLE REPRESENTATIONS OF SPACE GROUPS. Rudra, P. (Saha Inst. of Nuclear Physics, Calcutta). J. Math. Phys. (N. Y.), 6: 1278-82 (Aug. 1965).

A logical extension is made of Seitz-Koster's method of space-group representations to the points on the surface of the Brillouin zone, using protective representations. This method is applied in the case of the space group D_4^4. (auth)

40090 FLUORESCENCE CONVERSION EFFICIENCY OF NEODYMIUM GLASS. DeShazer, L. G.; Komai, L. G. (Hughes Aircraft Co., Culver City, Calif.). J. Opt. Soc. Am. 55: 940-44(Aug. 1965).

The relative effectiveness of the major absorption bands

in producing fluorescence of the neodymium ion in glass was investigated. The chief result was that the conversion efficiency, the number of fluorescence photons per absorbed photon, was nearly independent of the absorption band pumped. For 5% Nd in barium crown glass, the conversion efficiency was 0.43 for the total fluorescence, and 0.26 for the 1.06-μ fluorescence. (auth)

40091 NEUTRON DIFFRACTION STUDY OF ANTIFERROMAGNETISM IN UO_2. Willis, B. T. M.; Taylor, R. I. (Atomic Energy Research Establishment, Harwell, Berks, Eng.). Phys. Letters, 17: 188-90(July 15, 1965).

Antiferromagnetic ordering in single crystals of UO_2 was studied by the neutron diffraction method. The integrated intensities of sixteen hkk magnetic reflections and eighteen hkk nuclear reflections were measured, and the intensity data were interpreted satisfactorily assuming a magnetic structure consisting of ferromagnetic (200) planes of uranium atoms, with antiferromagnetic coupling of the magnetic moments in adjacent (200) planes. Curves showing the intensity variation with temperature of magnetic reflection 100, and the magnetic form factor for uranium atoms in UO_2 are presented and discussed. (L.B.S.)

40092 ON THE DETECTION OF SECOND SOUND IN CRYSTALS BY LIGHT SCATTERING. Griffin, A. (Univ. of California, San Diego, La Jolla). Phys. Letters, 17: 208-10(July 15, 1965).

It is suggested that Rayleigh scattering of light may be useful as a probe for collective temperature waves in pure anharmonic crystals. A formal dispersion relation for second sound (in normal systems) is reported, which involves a frequency dependent thermal conductivity coefficient. (L.B.S.)

40093 INELASTIC SCATTERING OF NEUTRONS BY AN ANHARMONIC CRYSTAL AT LOW TEMPERATURES. Maris, H. J. (Case Inst. of Tech., Cleveland). Phys. Letters, 17: 228-30(July 15, 1965).

It is pointed out that at T = 0°K some of the vibrational modes in a perfect dielectric crystal have indefinitely long phonon lifetimes and that there should therefore be some peaks in the neutron scattering cross section which are extremely narrow at low temperatures. An expression for the width $2\Gamma(qj)$ of the neutron peaks is given, and the results of a calculation for the slow transverse modes for which $\Gamma(qj) = 0$ at T = 0°K are shown. (L.B.S.)

40094 EFFECT OF PRESSURE ON THE MAGNETIC PROPERTIES AND CRYSTAL STRUCTURE OF Gd, Tb, Dy, AND Ho. McWhan, D. B.; Stevens, A. L. (Bell Telephone Labs., Murray Hill, N. J.). Phys. Rev., 139: 682-9 (Aug. 2, 1965).

X-ray diffraction powder patterns taken at high pressure suggest by analogy to Gd that Tb, Dy, and Ho have first-order transitions from a hcp to a Sm-type structure at high pressure. The c/a ratio of the hcp phases increases with pressure toward the ideal value. The change of the Curie or Néel temperature with pressure of Gd, Tb, Dy, and Ho was measured up to 85 kbar by an a-c method in which the sample forms the core of a transformer. The first-order transitions are observed in changes in the magnetic properties. The initial susceptibility shows two new peaks in isobaric temperature cycles made above the transitions. The difference between the ordering temperature of the low- and high-pressure phases near the transition are -37, -21, -12, and -9°K for Gd, Tb, Dy, and Ho, respectively. The change in the Curie point of Gd(I) is -1.72 ± 0.7°K/kbar. The changes in Néel temperature are: Gd(II) -1.46 ± 0.11, Tb(I) -1.07 ± 0.03, Tb(II) -0.83 ± 0.08, Dy(I) -0.66 ± 0.04, Dy(II) -0.67 ± 0.07, Ho(I) -0.48 ± 0.01°K/kbar. The results are compared with other measurements on rare-earth metals. (auth)

40095 SOLID-LIQUID AND SOLID-SOLID TRANSFORMATIONS IN RARE-EARTH METALS AT HIGH PRESSURES. Jayaraman, A. (Bell Telephone Labs., Murray Hill, N. J.). Phys. Rev., 139: 690-6(Aug. 2, 1965).

The fusion behavior and solid-solid transformations in the rare-earth metals were investigated at pressures in the range 6-65 kbar. The phase diagrams are presented for La, Pr, Nd, Sm, Gd, and Tb. The initial melting slopes of Dy to Lu were obtained. Since most of the rare-earth (R.E.) metals melt from a bcc structure, they offer a series for comparison. When the initial melting slope is plotted against atomic number, they fall into groups according to their valency; the typically divalent metals Eu and Yb in one, and the typically trivalent metals La, Gd, and Lu in another. Samarium and the metals from Tb to Tm have melting slopes which are intermediate between those of the typically divalent and trivalent metals. It is suggested that these metals assume a partial divalent character in the liquid state and possibly also in the bcc phase. This suggestion derives support from the fact that the gaseous neutral atoms of the R.E. elements, with the exception of La, Gd, and Lu, have no 5d electron and are therefore divalent. Cerium exhibits a unique fusion behavior, and its negative melting slope is attributed to the tetravalency (4f → 5d electron promotion) of the atoms in the liquid. For the very small melting slope of Pr, it is suggested that the atoms in the liquid have partial tetravalent character due to 4f → 5d electron promotion. Comparisons with alkali metals are made, and it is deduced that the R.E. metals are quite compressible at high temperatures. Pressure induced transformations in the rare-earth metals are in the sequence hcp → Sm-type → double hcp → fcc. A plausible mechanism based on the variation of c/a ratio with pressure is discussed for hcp → Sm-type transformation. (auth)

40096 FINITE LINEWIDTHS AND "FORBIDDEN" THREE-PHONON INTERACTIONS. Leggett, A. J.; Haar, D. Ter (Clarendon Lab., Oxford). Phys. Rev., 139: 779-88(Aug. 2, 1965).

Thermodynamic perturbation theory is used to study the effect of the finite energy spread of phonon excitations upon the possibility of three-phonon interactions which could not otherwise conserve energy. It is shown that a proper treatment of this effect is equivalent to a consideration of higher order processes in which the interacting phonons occur in virtual intermediate states, but that such processes can not in general be adequately taken into account simply by assigning a lifetime to one or more of the interacting phonons. It is also shown that the higher order terms of conventional perturbation theory should be modified, whether or not the three-phonon process is energetically allowed; if it is, these modified terms should be substituted for the three-phonon contribution rather than added to it. A qualitative discussion is given of applications to liquid helium II and to dielectric solids. (auth)

40097 MEAN-SQUARE DISPLACEMENT MEASUREMENTS OF Fe^{57} IN Zn. Kuendig, Walter; Ando, Ken; Boemmel, Hans (Univ. of California, Los Angeles). Phys. Rev., 139: 889-91(Aug. 2, 1965).

The Mössbauer effect of ^{57}Fe in polycrystalline Zn was measured as a function of temperature. It was found that the quadrupole splitting between 120 and 373°K decreases from 0.50 ± 0.01 to 0.46 ± 0.01 mm/sec. The chemical shift with respect to an Fe absorber at room temperature is -0.525 ± 0.010 mm/sec. From intensity measurements of the two quadrupole lines, the mean-square displacement $\langle x^2 \rangle$ can be evaluated. At room temperature $\langle x^2 \rangle$ parallel to the c axis was found to be $\langle x^2 \rangle_{||} = 0.0231 \pm 0.0016$ Å^2, and the anisotropy of the mean-square displacement $\epsilon = \langle x^2 \rangle_{\perp} / \langle x^2 \rangle_{||}$ was found to be $\epsilon = 0.33 \pm 0.05$. The results are compared with lattice-dynamical calculations. (auth)

40098 COLOR CENTERS IN CsBr SINGLE CRYSTALS IRRADIATED AT LIQUID-HELIUM TEMPERATURE. Van de Wiele, F.; Jacobs, G. (Laboratorium voor Kristallografie en Studie van Vaste Stoffen, Gent, Belg.). Phys. Rev., 139: 924-8(Aug. 2, 1965).

The principal absorption bands induced by irradiation at liquid-helium temperature with x rays in CsBr crystals are the complex F band and two overlapping V bands at 435 and 497 mμ. In view of the dichroic properties of these V bands, the most obvious model seems to be a Br_2^- molecular ion lying in the ⟨100⟩ directions. The two observed

absorption bands would be due to two transitions in the same center. Regarding the bleaching properties, the F center can not be the only color center responsible for the structure of the complex absorption band. Hypotheses are proposed about the interactions between the V and F centers. (auth)

40099 ANGULAR DISTRIBUTION AND THICKNESS DEPENDENCE OF TRANSITION RADIATION FROM THIN ALUMINUM FOILS. Herickhoff, R. J.; Hanson, W. F.; Arakawa, E. T.; Birkhoff, R. D. (Oak Ridge National Lab., Tenn.). Phys. Rev., 139: A1455-8(Aug. 30, 1965). (ORNL-P-1225).

The angular distribution of photons emitted from Al foils 320 Å in thickness bombarded with 80-kev electrons, and the dependence of the peak intensity on foil thickness, were determined experimentally in the wavelength region from 650 to 1100 Å. The absolute efficiency of the optical spectrometer was determined in the visible-wavelength region from a standard lamp and extrapolated into the vacuum ultraviolet-wavelength region using the measured grating efficiency and quantum efficiency of sodium salicylate. Experimental photon intensities were found to be approximately one half of the theoretical photon intensities. The intensity at the peak wavelength had a maximum of 22 and 157° from the foil normal, with zero intensity at 0, 180, and 90°. The angles for which the theoretical curves exhibit maximum intensity are 15 and 168°. The wavelength for which the experimental curves exhibit maximum intensity was found to decrease as the angle of observation increased from 0 to 40° or decreased from 180 to 140°. The plasma wavelength and energy, 835 Å and 14.9 ev, respectively, were obtained by extrapolating to 0°. The intensity at the wavelength of maximum emission was found to decrease rapidly as the foil thickness was increased from 180 to 435 Å and then to remain fairly constant out to 700 Å. (auth)

40100 PERTURBATION-THEORETICAL APPROACH TO MAGNETO-OPTICAL PHENOMENA IN THE SPECTRAL REGION OF ZERO ABSORPTION. Nedoluha, Alfred (Naval Ordnance Lab., Corona, Calif.). Phys. Rev., 139: A1489-1501(Aug. 30, 1965).

The effect of a weak magnetic field on a many-electron system in an isolated ground state is calculated by a perturbation-theoretical method. The calculation is based on the property of internal localization of both the one-particle density matrix and a certain two-particle Green's function of the system, and is performed in the independent-particle approximation. After splitting off phase factors, recurrence relations for the expansion of the density matrix and Green's function in powers of the magnetic field strength H are derived. From the density matrix one obtains the energy of the system and from the Green's function the magneto-optical coefficients. In an approximation linear in H the gyration vector is given explicitly; the contributions to polarizability tensor and energy vanish in this approximation. The gyration vector obtained is in agreement with the results derived for small systems, accessible to nondegenerate one-particle perturbation theory, and for ideal crystals, treated by Roth in a modified Bloch representation. (auth)

40101 NONLINEAR AND LINEAR SHIELDING OF RARE-EARTH CRYSTAL-FIELD INTERACTIONS. Freeman, A. J. (Massachusetts Inst. of Tech., Cambridge); Watson, R. E. Phys. Rev., 139: A1606-15 (Aug. 30, 1965).

It was shown previously that significant nonlinear shielding of the rare-earth electrostatic crystalline-field interactions may occur, and hence that the standard parameterization scheme used to determine the crystal-field parameters, $V_L^M = A_L^M\langle r^L\rangle$, was questionable. These nonlinear effects arise from the same distortions of the closed shells in rare-earth ions which produce the (larger) linear shielding of the crystal field V_c. Both nonlinear and linear shielding effects were investigated for the rare-earth ions Ce^{3+}, and Tb^{3+} through Yb^{3+} inclusive. The method of single substituted configurations is employed and is shown to avoid the difficulties associated with the traditional single-determinant perturbation-theory approach previously used exclusively by various authors. Results based on both methods are given and compared; significant differences in linear-shielding predictions are found to be introduced by the inexact traditional approach. Calculations for the nonlinear 5p → 4f effects were performed, and results displayed, as a function of the strength of V_c (based on the point-charge model). The relevance of these effects to experiment is examined qualitatively. (auth)

40102 FERMI SURFACE IN TUNGSTEN. Mattheiss, L. F. (Bell Telephone Labs., Murray Hill, N. J.). Phys. Rev., 139: A1893-1904(Sept. 13, 1965).

The results of nonrelativistic, augmented-plane-wave energy-band calculations were used to calculate the Fermi surface in body-centered cubic tungsten, neglecting spin-orbit coupling. The resulting Fermi surface is very similar to one proposed earlier by Lomer for group-VI transition metals and agrees qualitatively with the available experimental results. Spin-orbit coupling is found to have little effect on the basic Fermi-surface topology in tungsten and its consequences can be understood qualitatively in terms of a simplified tight-binding calculation. Within the energy range of the tungsten 5d bands, the electronic density of states contains four distinct peaks, three of which lie below the tungsten Fermi energy. Assuming a rigid-band model, the energy-band results were used to predict the Fermi surface in the group-V transition metals. (auth)

40103 PREFERENTIAL THERMAL REORIENTATION OF V_K CENTERS IN POTASSIUM IODIDE. Keller, F. J.; Murray, R. B. (Oak Ridge National Lab., Tenn.). Phys. Rev. Letters, 15: 198-200(Aug. 2, 1965). (ORNL-P-1282).

The thermal activation energy for reorientation of V_k centers in KI was measured. It was found that reorientation occurs almost entirely through steps in which the V_k axis changes by 60°, and that the probability of reorienting through 90° is negligibly small. Crystals of KI containing ~0.1 mole% TlI or KNO_3 as an electron-trapping impurity were irradiated at 78°K with either 1.7 Mev electrons or x rays from a 40 kev source. In all cases it was found that a plot of anisotropy versus time was accurately described by a single exponential. (J.F.P.)

40104 NEUTRON DIFFRACTION STUDY OF FERROMAGNETIC U_3P_4. Ciszewski, R.; Murasik, A.; Troc, R. (Inst. of Nuclear Research, Swierk, Poland). Phys. Status Solidi, 10: K85-8(Aug. 1, 1965).

Since U_3P_4 was reported to exhibit a transition to the ferromagnetic state at 138°K, a neutron diffraction study was made of this crystal. The synthesis of U_3P_4 was carried out as previously by direct reaction of calculated amounts of nuclear pure uranium powder and redistilled red phosphorus. The mixture was fired in evacuated and sealed quartz tubes at 400°C for one day and subsequently at 1000°C for two days. X-ray examination showed no foreign lines. The neutron diffraction pattern obtained at liquid nitrogen temperature is presented and shows an increase of the peaks especially in the low-angle region arising from the magnetic contribution. The integrated intensities due to magnetic scattering were calculated using the values of the magnetic form factor. The magnetic moment was found to be 1.5 ± 0.1 BM at 80°K. (J.F.P.)

40105 ON THE X-RAY COLORATION OF THERMALLY BLEACHED γ-IRRADIATED SODIUM CHLORIDE AND EVIDENCE FOR PERTURBED F-BAND. Sastry, P. V.; McCarthy, K. A. (Tufts Univ., Medford, Mass.). Phys. Status Solidi, 10: 585-94(Aug. 1, 1965).

Gamma-irradiated sodium chloride crystals (irradiated into the second stage), on partial thermal bleaching at moderate temperatures (160-200°C) show the evolution of an absorption band, which has the characteristic properties of a colloid band. Further thermal bleaching leaves the crystals colorless. When such partially or completely thermally bleached crystals are x-irradiated at room temperature, they show enhanced colorability and give evidence for the presence of perturbed F centers. A significant difference between the effects of soft and hard x radiation is

observed. The results are discussed in the light of the mechanism of color center production by radiation. (auth)

40106 DAMPING OF THE ELECTRON SPECTRUM AND QUANTUM THEORY OF GALVANOMAGNETIC PHENOMENA. Askerov, B. M.; Gashimzade, F. M. (Inst. of Physics, Baku, USSR). Phys. Status Solidi, 10: 621-30 (Aug. 1, 1965).

The components of the conductivity tensor in the presence of a magnetic field are calculated, the quantization of the electron orbits being taken into account. The interaction between the electrons and lattice imperfections is included in the one-particle Green's function of the electron, and the response of the latter on the external perturbation is studied. A linear approximation is used for the external field. The interactions of the electrons with the impurities (infinitely localized, ionized) and phonons (acoustical, optical) are based on the Born approximation. (auth)

40107 OPTICAL ABSORPTION OF Cu-CENTERS IN ALKALI HALIDES. Kraetzig, E.; Timusk, T.; Martienssen, W. (Universitaet, Frankfurt am Main). Phys. Status Solidi, 10: 709-23(Aug. 1, 1965).

It is shown from optical absorption measurements that under x irradiation at low temperatures Cu^{+} ions in Cu-doped KCl, KBr, and KI crystals trap electrons and holes. During this process Cu^{0} and Cu^{++} centers are formed, which may be compared with Ag^{0} and Ag^{++} centers in alkali halides. In the case of the Cu^{++} centers the symmetry of the surrounding halogen ions is lowered by a Jahn-Teller distortion. This distortion, however, is different from that of the Ag^{++} centers studied by Delbecq, Hayes, O'Brien, and Yuster. (auth)

40108 SCATTERING MATRIX AND SURFACE MODES. [PART] II. Fukushima, Masahisa (Hokkaido Univ., Sapporo). Progr. Theoret. Phys. (Kyoto), 33: 624-37(Apr. 1965).

The surface vibrations of the 2D lattice with nearest neighbor interactions are investigated by the scattering matrix method. The following cases are treated: One impurity is adsorbed or absorbed on a surface of the lattice; one of the surfaces is composed exclusively of impurity atoms. In the former cases we get the conclusion that the localized modes can appear more easily when an impurity atom is adsorbed at the center of the surface than when it is adsorbed at the corner. In the latter, it is concluded that, if only the force constants between surface atoms and sub-surface ones differ from that between inner atoms, the whole localized modes appear simultaneously at a certain critical value of the force constant, while if a surface is composed of isotopic impurities, localized modes gradually appear, beginning from the top of the unperturbed frequency band. Finally the spectral density of the impurity band is calculated for the isotopic case. (auth)

40109 THE RESONANT SCATTERING OF LATTICE WAVES BY AN EXTENDED PLANE DEFECT. Kobori, Itaru (Doshisha Univ., Kyoto). Sci. Eng. Rev. Doshisha Univ., 5: 166-8(Feb. 1965).

An investigation of the scattering of lattice waves by an extended isotopic plane defect showed that resonance occurs at frequencies which lie in the interval of the frequency band of the pure lattice, the resonance corresponding to the appearance of localized modes. In an extended isotopic plane defect, resonant scattering of lattice waves occurred in the case of a point defect represented by a heavier isotope. The scattering potential, which is characteristic of the extended defect, is a matrix of infinite rank. Then the frequency spectrum of the defect modes becomes a band that overlaps the unperturbed frequency spectrum, and resonance occurs for the waves of corresponding energy. Green's function was used to formulate the problem. The resonance has a close relation to the appearance of the localized modes as in the cases of the bound state which appears in the scattering of electrons by impurities. To determine the localization of the defect modes Green's function was calculated. It gave the amplitude of the oscillation associated with the defect modes, and showed that the modes associated with the plane defect damp exponentially. The results indicated that the modes associated with the extended defect are localized and those modes appear in the range of the frequency interval of the pure lattice. (TCO)

40110 PHYSICS OF NON-CRYSTALLINE SOLIDS. Proceedings of the International Conference, Delft, July, 1964. Prins, J.A. (Ed.). Amsterdam, North-Holland Publishing Company and New York, John Wiley and Sons, Inc., 1965. 683p. (CONF-640708). $27.50.

Papers (54) are included on structure, devitrification, neutron diffraction, heat conduction, ESR, NMR, magnetism, ultrasonics, relaxation, fracture, coordination, and optical and electric properties. A separate abstract was prepared for one paper on radiation effects in glasses. (D.C.W.)

For an abstract of the individual paper see: 39256.

REACTOR TECHNOLOGY

General

Refer also to abstract 39259.

40111 (ANL-7046) REACTOR DEVELOPMENT PROGRAM PROGRESS REPORT. (Argonne National Lab., Ill.). May 1965. Contract W-31-109-eng-38. 94p. Dep. (mn); $3.00(cy), 2(mn) CFSTI.

Progress is summarized in sections on liquid-metal cooled reactors, general reactor technology, advanced systems research and development, and nuclear safety. Separate abstracts were prepared for each section. (J.R.D.)

For abstracts of individual sections see: 39090, 40112, 40177, and 40257.

40112 (ANL-7046(p.36-66)) GENERAL REACTOR TECHNOLOGY. (Argonne National Lab., Ill.).

Summaries are given of work on experimental reactor and nuclear physics, theoretical reactor physics, high-temperature materials, reactor fuels and materials, engineering development, chemical separations, sodium coolant chemistry, and plutonium recycle reactors. (J.R.D.)

40113 (ANL–7071) REACTOR DEVELOPMENT PROGRAM. Progress Report, June 1965. (Argonne National Lab., Ill.). July 30, 1965. Contract W-31-109-eng-38. 75p. Dep. mn; CFSTI, $3.00 cy, $0.75 mn.

Progress is reported in sections on EBR-III, FARET, fast reactor development, fast reactor fuel development, fuel processing, reactor and nuclear physics, high-temperature materials, heat transfer, chemical separations, Pu recycle reactors, Argonne Advanced Research Reactor, energy conversion systems, reactor kinetics, and TREAT. (J.R.D.)

40114 (BNWL–104) MINIMIZED FUEL CYCLE COST FOR A SIMULATED PRESSURIZED WATER REACTOR. PART I. Deonigi, D. E.; Horton, P. A.; McConiga, A. F. (Battelle-Northwest, Richland, Wash. Pacific Northwest Lab.). Apr. 1965. Contract AT(45-1)-1830. 89p. Dep. mn; CFSTI, $3.00 cy, $0.75 mn.

Data are presented which assume that the reactor type being considered was constructed and that the lattice spacing, or fuel-to-moderator ratio will remain fixed. Under these conditions, the minimum fuel costs were calculated over a series of changing economic conditions which include the variation of cost parameters. (M.O.W.)

40115 (CONF–650602-33) CROSS SECTIONS FOR REACTOR DESIGN. Francis, N. C. (Knolls Atomic Power Lab., Schenectady, N. Y.). June 1965. Contract W-31-109-eng-52. 11p. Dep. mn; CFSTI, $1.00 cy, $0.50 mn.

From American Nuclear Society 11th Annual Meeting, Gatlinburg, Tenn.

The need for cross section libraries is pointed out. Diagrams show; the scattering of 0.56 Mev neutrons from thorium-232 using a non-spherical optical model, and the calculated and experimental neutron total cross section for carbon-12 from 2.8 to 5 Mev. (M.O.W.)

40116 (TID–8200(12th Rev.)) NUCLEAR REACTORS BUILT, BEING BUILT, OR PLANNED IN THE UNITED STATES AS OF JUNE 30, 1965. (Office of the Assistant General Manager for Reactors (AEC), Washington, D. C.). 25p. Dep. mn; CFSTI, $1.00 cy, $0.50 mn.

A compilation of information is presented concerning facilities built, being built or planned in the United States on June 30, 1965, which are capable of sustaining nuclear chain reactions. Classified projects and facilities are not included. (J.R.D.)

40117 (ZFK-RN-17) INTERNATIONALES SYMPOSIUM. WASSERPROBLEME AN KERNREAKTOREN 25-27, 4 1962 IN ROSSENDORF. (International Symposium on Water Problems in Nuclear Reactors, Rossendorf, Germany, April 25–27, 1962). (Zentralinstitut fur Kernphysik, Rossendorf bei Dresden (East Germany)). Mar. 1963. 208p. (CONF-620402). Dep.(mn).

From International Symposium on Water Problems in Nuclear Reactors, Rossendorf, Ger.

Fourteen papers are included; separate abstracts have been prepared for 13. Seven are in German and 7 in Russian. One of the papers was abstracted previously in NSA, 19: 19419. (T.F.H.)

For abstracts of individual papers see: 38697, 38698, 38759, 38760, 40127, 40128, 40129, 40130, 40260, 40261, 40262, 40263, and 40264.

40118 (WAPD-T–1782) STRUCTURAL ANALYSIS OF A REACTOR SUBASSEMBLY UNDER THERMAL, HYDRAULIC, AND FUEL EXPANSION LOADS. Friedrich, Carl M. (Bettis Atomic Power Lab., Pittsburgh, Pa.). May 1965. Contract AT(11-1)-Gen-14. 20p. (CONF-650602–35). Dep. mn; CFSTI, $1.00 cy, $0.50 mn.

From American Nuclear Society 11th Annual Meeting, Gatlinburg, Tenn.

A structural analysis is presented for a reactor subassembly of rectangular flat plates subjected to temperature, pressure, coolant flow, and fuel growth. Elastic, plastic, and creep material properties are used to determine the resulting transient stresses and deformations. The effect of plate deflections on channel thickness is used to modify the hydraulic forces which are combined with axial and transverse buckling loads. (auth)

40119 IMPROVEMENTS IN APPARATUS FOR AND A METHOD OF HANDLING MATTER CONTAINING RADIOACTIVE PARTICLES FILTERED FROM A FLUID. (to Babcock and Wilcox Ltd.). British Patent 991,714. May 12, 1965. Priority date May 31, 1961, Germany.

A method of handling matter containing radioactive particles filtered from a fluid circuit, either liquid or gaseous, is described. The method is particularly applicable to the removal of radioactive particles trapped on a filter in a cooling system for a gas cooled reactor, radioactive corrosion products occurring in reactors and associated piping, or graphite particles arising from the core of a graphite moderated reactor. The method consists of immobilizing the matter by solidifying the liquid which, when solidified, serves to hold the particles in position and then removing the matter together with the solidified liquid from the fluid circuit while the matter is so immobilized. If the fluid is water, simply freezing the water will immobilize the matter and radioactive particles; however, if the fluid is CO_2, liquid CO_2 must be added, evaporated, and solidified to immobilize the matter. The apparatus for the removal of matter containing radioactive particles from a water coolant includes a removable filter upon which the particles lodge and cooling means adapted to reduce the ambient temperature at the filter to freeze the water to immobilize the particles on the filter and to enable the filter to be removed with the particles. In a gas circuit, the apparatus includes a filter in a filter chamber, a removable collecting vessel arranged to receive the matter from the filter, supply means for the liquid CO_2, valves for closing the inlet and outlet of the filter chamber, and means for withdrawing the gas from the filter chamber to govern the pressure within the chamber to effect evaporation and solidification of the liquid CO_2. (B.L.M.)

Auxiliaries and Components

Refer also to abstract 38911.

40120 (GAMD–5434) GENERAL ATOMIC IN-PILE LOOP FISSION PRODUCT TRAPPING SYSTEM: REGEN-

ERATIVE H_2O–CO_2 TRAP AND LIQUID NITROGEN COOLED NO. 2 CHARCOAL TRAP ASSEMBLY. INFORMATION DATA PACKAGE AND DESIGN ANALYSIS. Kiefer, R. J.; Winkler, E. O. (General Atomic, San Diego, Calif. John Jay Hopkins Lab. for Pure and Applied Science). July 6, 1964. Contract AT(04-3)-167. 55p. Dep. mn; CFSTI, $3.00 cy, $0.50 mn.

The previous Fission Product Trapping System required a continuous, inefficiently high flow of liquid N_2 coolant to the H_2O-CO_2 and No. 3 Charcoal Traps, and the No. 3 Trap had a rapid heat-up rate when the flow was interrupted, resulting in a release of the absorbed fission products. The integral regenerative H_2O-CO_2 Trap and No. 2 Charcoal Trap (Liquid N_2 cooled) was designed to avoid the above difficulties. The system design, operation, hazards evaluation, and performance and stress analysis are discussed. (D.L.C.)

40121 (GEAP-4574) SURVEY OF PIPING FAILURES FOR THE REACTOR PRIMARY COOLANT PIPE RUPTURE STUDY. Gibbons, W. S.; Hackney, B. D. (comps.) (General Electric Co., San Jose, Calif. Atomic Power Equipment Dept.). May 1964. Contract AT(04-3)-189. 244p. Dep. mn; CFSTI, $5.00 cy, $1.25 mn.

An industrial piping failure survey covering 701 contacts in electric utilities, petroleum refineries, chemical processing, marine applications, architect-engineers, component manufacturers, piping fabricators and erectors, insurance companies, and others was conducted as part of the Reactor Primary Coolant Rupture Study. The total of 315 replies received, when combined with published failure cases, provided 399 failure case histories of interest to the study. The term, "failure" was defined as any defective condition encountered during startup, testing, and/or service that required repair or replacement corrective action. (auth)

40122 (GEAP-4862) REACTOR CONTROL SYSTEMS BASED ON COUNTING AND CAMPBELLING TECHNIQUES. Wide-Range Instrumentation Development Program. Seventh Quarterly Progress Report, February–April 1965. Boyd, L. R.; DuBridge, R. A.; Green, W. K.; Pielage, H. W.; Stanley, L. (General Electric Co., San Jose, Calif. Atomic Power Equipment Dept.). May 1965. Contract AT(04-3)-189. 72p. Dep. mn; CFSTI $3.00 cy, $0.75 mn.

The analytical predictions and the results of a nuclear instrumentation development program are reported. The program was concerned with development of full-range reactor control systems incorporating either in-core or out-of-core ion chambers. Electronic systems were developed utilizing counting techniques for source and lower intermediate range neutron fluxes, and mean-square voltage (Campbell) techniques for intermediate and power range fluxes. (J.R.D.)

40123 (IAE-787) VODOOCHISTKA I VODOPODGOTOVKA NA YADERNYKH REAKTORAKH. (Water Purification and Water Preparation at Nuclear Reactors). Chernorotov, E. S.; Potekhin, N. V.; Novikov, P. D. (Institut Atomnoi Energii, Gosudarstvennyi Komitet po Ispol'zovaniyu Atomnoi Energii SSSR, Moscow). 1964. 14p. Dep. mn.

A method for increasing the efficiency of operation of mixed layers of ion resins during purification of the water of the primary coolant loops of research or power reactors, at the expense of using prefilters or cation-resin layers in hydrogenous form, is considered. Operating experience of such systems in the research reactor RPT and for purification of the water of the primary loop in the Lenin atomic-icebreaker reactors is presented. (tr-auth)

40124 (IAE-789) K VOPROSY O STANDARTIZATSII KONTROLYA NAD CHISTOTOI VODY V KONTURAKH YADERNYKH REAKTOROV. (On the Question of Standardizing the Monitoring of Water Purity in Nuclear Reactor Loops). Alekseev, B. A. (Institut Atomnoi Energii, Gosudarstvennyi Komitet po Ispol'zovaniyu Atomnoi Energii SSSR, Moscow). 1964. 46p. Dep. mn.

Basic questions of standardization of points of sampling, periodicity of analyses, and methods involved for water of the primary coolant loop of water-cooled and -moderated research reactors and of power systems with water under pressure and with evaporation and filtration water-purification apparatus are considered. (tr-auth)

40125 (NAA-SR-9821) CALANDRIA CORE WELD JOINT DEVELOPMENT. Roberts, J. G. (Atomics International, Canoga Park, Calif.). June 30, 1965. Contract AT(11-1)-Gen-8. 51p. Dep. mn; CFSTI, $1.25 cy, $0.50 mn.

With the advent of the large SGR suspended reactor with a calandria core containing a lattice work of process channels, it has become necessary to study and design methods for the installation, maintenance, or replacement of the process channels. Thus, with regard to welded joints and machine parting characteristics, a development program was initiated to determine joint configuration and replacement processes. The design and initial test of cutting and welding equipment developed to remotely cut and reweld the bottom process tube joint are discussed. (auth)

40126 (NAA-SR-11327) LARGE SGR CONTROL ROD DEVELOPMENT. Dermer, M. D. (Atomics International, Canoga Park, Calif.). July 25, 1965. Contract AT-11-1-GEN-8. 39p. Dep. mn; CFSTI, $2.00 cy, $0.50 mn.

A development program was initiated to design, fabricate and test an absorber column with a 10 to 12 year lifetime, for use in the proposed Large Sodium Graphite Reactor (LSGR). The combined shim-safety control rod planned for the LSGR will be a variation of the Hallam Reactor control rod design with the major innovation to be the absorber column. Dysprosium oxide in an annulus formed by an integral tube of Hastelloy-X and a center graphite filler log was chosen as the primary poison material. Full scale elevated temperature testing at reactor profile temperatures gradients simulated approximately 5 years of column lifetime with no adverse effects observed. A prototypical absorber column of this design was incorporated in the SRE-PEP control rod to gain long term irradiation and operational data to aid in the development of a full scale prototype combined shim-safety control rod for the LSGR. (auth)

40127 (ZFK-RN-17(p.9-23)) PROBLEMATIK DER pH-MESSUNG IM REAKTORBETRIEB. (Problematics of the pH Measurement in Reactor Operation). Hirsch, W. (Institut Atomnoi Energii, Gosudarstvennyi Komitet po Ispol'zovaniyu Atomnoi Energii SSSR, Moscow).

The problems of pH measurements in reactor operation are explained. The technological conditions of measurement in research reactors of the WWR-S type are introduced. (J.S.R.)

40128 (ZFK-RN-17(p.75-94)) METODIKA IZMERENIYA OBMENNOI EMKOSTI I KINETICHESKIKH KHARAKTERISTIK IONITOV. (A Method for Measuring Exchange Capacitance and Kinetic Characteristics of Ionites). Alekseev, B. A.; Il'ina, D. S.; Chernorotov, E. S. (Institut Atomnoi Energii, Gosudarstvennyi Komitet po Ispol'zovaniyu Atomnoi Energii SSSR, Moscow).

The exchange capacitance of ion-exchange resins used for water purification in research and power reactors is measured by potentiometric titration of cation or anion exchange resins by alkali or acid solutions, and analyzing the time dependence of the titration. (R.V.J.)

40129 (ZFK-RN-17(p.114-26)) DIE AUSWIRKUNGEN DER STRAHLENBESTANDIGKEIT VON KUNSTHARZIONENAUSTAUSCHERN AUF DEREN ANWENDUNG IN RADIOAKTIVEN KREISLAUFEN. (The Effects of the Radiostability of Synthetic Resin Exchangers on Their Application in Radioactive Circuits). Boehm, R. (VEB Farbenfabrik, Wolfen (East Germany)).

The radiostability of synthetic resins based on styrene and phenol is discussed with respect to specific exchangers in water purification. Other factors determining their use in conventional water purification installations are considered. (J.S.R.)

40130 (ZFK-RN-17(p.165-78)) DIE VERWENDUNG NATURLICHER KATIONENAUSTAUSCHER FUR DIE REINIGUNG RADIOAKTIVER ABWASSER. (The Application of Natural Cation Exchangers for the Purification of Radioactive Wastes). Winkler, R.; Sachse, G. (VEB Atomkraftwerk, Rheinsberg (East Germany)).

A bibliographic review is given of the applicability of natural cation exchangers for the purification of radioactive water. Mineral ion exchangers, fixation of radioactive cations on the exchangers, the addition of clay in precipitation methods, natural organic exchangers, organo-mineral exchangers, and the use of natural ion exchangers in the purification of reactor water are considered. (J.S.R.)

40131 (ORNL-tr-585) PRESSURE TANKS FOR NUCLEAR REACTORS. Tricket, Kenneth A.; Rogers, James T. Jr. Translated for Oak Ridge National Lab., Tenn., from French Patent 1,345,789. Nov. 4, 1963. 16p. Dep. mn; JCL, $1.60 fs, $0.80 mf.

A pressurized tank with internal insulation and external cooling is designed for gas-cooled reactors. The tank is designed to reduce the wall temperature to ≤343°C, and to improve the thermodynamic yield of the closed-loop reactor system. (D.L.C.)

40132 (ORNL-tr-590) NUCLEAR REACTOR. Fotesque, Peter; Nichol, David. Translated for Oak Ridge National Lab., Tenn., from Japanese Patent. Dec. 13, 1960. 20p. Dep. mn; JCL, $1.60 fs, $0.80 mf.

A new control rod driving system of a nuclear reactor is reported. A detailed description of the driving system is presented. The functions of the system are discussed in detail. (M.O.W.)

40133 CIRCUITS FOR THE DETECTION AND LOCALIZATION OF BURST FUEL ELEMENTS IN A NUCLEAR REACTOR COOLED WITH ORGANIC FLUIDS. (PART II). Cesari, F. (CNEN, Rome). Ing. Nucl., 6: 37-59(Jan.-Feb, 1965). (In Italian)

Some criteria on the ordinary and extraordinary operation of the system and a brief analysis of the most probable incidents are reported. (tr-auth)

40134 CONCRETE PRESSURE VESSELS FOR NUCLEAR REACTORS. Warner, P. C. Nucl. Eng., 10: 249-52(July 1965).

The general design philosophy of concrete pressure vessels is discussed. Comments on their structural and thermal problems are noted. Only cylindrical vessels are referred to with their axis vertical. The design philosophy is to calculate stresses at successive operating states using well-established analytical methods and to associate the results with limiting stress levels for those conditions. These methods have limitations and must be backed up by calculation and experimental work. A fully authenticated design results which is inherently safe and has substantial margins of strength. A general description is given; and also discussed are structural analysis, ultimate load, thermal design, and safety characteristics. (J.F.P.)

40135 COMPONENTS. Power Reactor Technol., 7: No. 3, 269-75(Summer 1964).

The design and operating characteristics of the primary coolant pumps for the Lithium Cooled Reactor Experiment are shown. The design of an in-pile liquid-Na flow controller is outlined. A control rod actuator using primary reactor-coolant water is described. The design of a pressure-balanced control rod having a fueled follower, originally designed for EOCR, is described. The design of a prototype control rod drive for Pathfinder is noted. (T.F.H.)

40136 IMPROVEMENTS IN NUCLEAR REACTORS. to Societe Anglo-Belge Vullain S.A.). British Patent 992,030. May 12, 1965. Priority date Mar. 9, 1961, Belgium.

A cover for a nuclear reactor is characterized in that the cover has extensions penetrating into the reactor vessel. These extensions increase the mechanical resistance of the cover and at the same time constitute thermal shields. (B.L.M.)

40137 A BOILING-WATER NUCLEAR REACTOR INSTALLATION. (to Licentia Patent-Verwaltungs- GmbH). British Patent 992,033. May 12, 1965. Priority date Mar. 14, 1961, Germany.

An emergency system for a boiling-water reactor includes an emergency condenser and an emergency steam collecting vessel connected through valves to the pipe that carries the steam delivered by the reactor. The emergency steam collecting vessel is dimensioned so that it can receive the quantity of steam that is generated in the reactor in the interval of time between the cut-off of the turbine and the bringing into operation of the emergency condenser. The collecting vessel is partially filled with water with air above the water level, and the steam is introduced into the body of water through nozzles. (B.L.M.)

40138 NUCLEAR FUEL ELEMENT. Kealy, Wellesley Ashe; Smart, Richard; McGonigal, Gerard (to United Kingdom Atomic Energy Authority). British Patent 996,512. June 30, 1965. Filed Aug. 30, 1962.

A nuclear fuel element is equipped with a temperature measuring device composed of an acoustic resonator. The resonator includes a gas-filled resonant tube, a first and second electroacoustic transducer, a first tube leading from the first transducer to the resonant tube, and a second tube leading from the resonant tube to the second transducer. The first and second tubes are of smaller internal diameter than the gas-filled resonant tube that is apertured to admit ambient gas. Each transducer includes a diaphragm, a drive coil, a gas-tight partition between the diaphragm and the drive coil, and a magnetic core that is linked with the drive coil and penetrates the partition. In order to detect the temperature of a fuel element equipped with this resonator, electrical leads from the transducers are led from the fuel elements out of the reactor or may be led to breakable contacts on the element that are arranged to cooperate with similar contacts on adjacent fuel elements or on the reactor structure. In either case, the electrical leads enable temperature-indicating electrical signals to be carried between the resonator on the fuel element and electrical apparatus including an oscillator outside the reactor. (B.L.M.)

40139 NUCLEAR REACTOR. Sidebotham, Ernest William; Ashcroft, David John; Prince, Michael John (to United Kingdom Atomic Energy Authority). British Patent 996,784. June 30, 1965. Filed July 18, 1963.

A fluid-driven mechanical pump is driven by the primary reactor coolant and is particularly applicable to integral type reactors in which the primary coolant circulating pump must be located within the reactor vessel. The reactor includes a core housed within the reactor vessel and conduits penetrating the vessel for energization of the pump by operating fluid. The pump is mechanically linked to the fluid-driven motor housed in the vessel and immersed in the primary coolant. The pump operating fluid is delivered through conduits by a master circulator located outside the reactor vessel. The circulator also serves to circulate secondary coolant through the vessel in heat exchange relationship with the primary coolant. (B.L.M.)

40140 ELECTROMAGNETIC SYSTEM FOR THE MOVEMENT OF A CONTROL ELEMENT IN AN ATOMIC REACTOR. Schreiber, Franz (to Siemens-Schuckertwerke AG). German Patent 1,190,117. Apr. 1, 1965. Filed Aug. 5, 1961.

An apparatus for moving a control rod in steps is described. It consists of an extension to the rod moving in a tubular element and mover coils disposed longitudinally along the said extension. In the intervals between movings of the rod the mover coils were energized with a holding current, which was lower than the current necessary for moving the rod so that the mover coils also served as gripper coils. (Gmelin Inst.)

40141 PRESSURIZED GAS HEATER FOR STEAM GENERATING HEAT EXCHANGER ESPECIALLY FOR UTILIZATION OF THE WASTE HEAT OF A NUCLEAR

REACTOR COOLING SYSTEM. Huet, Andre. German Patent 1,188,085. Mar. 4, 1965. Priority date Jan. 2, 1959, France.

The heat exchanger consists of a vertically arranged double-walled vessel surrounding the heat exchanging tubes and means for recirculating the cooled gas from the outlet of the heat exchanger to the gas inlet of the heat exchanger via the space between the two walls of the vessel. The recirculation of the gas is achieved by the arrangement of nozzles at the gas inlet, which communicate with the space between the walls of the heat exchanger and are directed to the hot gas stream entering the heat exchanger through a diffusor. (Gmelin Inst.)

40142 SHOCK-ABSORBING DEVICE FOR MOVING BODIES IN NUCLEAR REACTORS. Jeffery, Derek Boyd (to The General Electric Co. Ltd.). German Patent 1,194,074. June 3, 1965. Priority date Nov. 3, 1959, Great Britain.

The arresting device for falling bodies in nuclear reactors consists of an impacting member, a vertically resilient means coupling the impacting member and the falling body, shear pins that fail when the load in the vertically resilient means exceeds a predetermined amount to allow the body to continue its fall free of the impacting member, and energy dissipating means for finally arresting the body. The energy dissipating means consist of a hollow tube helically wound about a piston element, which is compressed by the continued fall of the body. (Gmelin Inst.)

40143 NUCLEAR REACTOR CONTROL DEVICE. Costes, Didier; Lebey, Jacques (to Commissariat a l'Energie Atomique). U. S. Patent 3,192,123. June 29, 1965. Priority date July 27, 1962, France.

A control device for rapid-shut down of a nuclear reactor includes a vertical channel in the reactor core subjected to a pressure equal to the pressure in the fuel channels. A reservoir located at a level above the level of the channel is adapted to receive the neutron-absorbing material in divided form. Valve means including a closure means and seat are provided between the reservoir and the channel. The difference between the pressure in the channel and the adjustable pressure in the reservoir serves to hold the closure member on the seat, and upon a predetermined drop of the pressure in the vertical channel the valve opens and the substance drops into the channel. Provisions are made for returning the material to the reservoir after it has dropped into the channel. This material return system can comprise a vertical tube that dips as far as the base of the channel and that is connected at its top end to a chamber disposed above the reservoir. The chamber is connected to the reservoir by way of a lock having two valves, one between the chamber and lock and the second between the lock and reservoir. Means are provided for operating these two valves at the appropriate times and for producing the appropriate negative pressure in the chamber at all times. (B.L.M.)

40144 NUCLEAR REACTOR FUELING APPARATUS. Long, Everett; Greaves, Thomas Cyril; Knight, William John (to The English Electric Co., Ltd.). U. S. Patent 3,194,741. July 13, 1965. Priority date Jan. 31, 1961, Great Britain.

A fuelling apparatus for a reactor provides access to a group of fuel elements through an access hole in the biological shield. The portion of the charging apparatus inside the pressure vessel includes a rotatable charge chute in the access duct, an extension tube having one free end and being pivoted at its other end on the charge chute within the pressure vessel, and an assembly of fixed fuel elements guide tubes over the core. The lower end of each guide tube is aligned with a fuel channel of the group, and the upper ends of the guide tubes define a continuous spiral and are positioned on a number of pitch circles that constitute a part of the continuous spiral. By appropriate rotational movement of the charge chute and/or appropriate angular movement of the movable guide member access may be obtained through the appropriate fixed guide tube to any particular fuel channel within the group. (B.L.M.)

40145 FUEL LOADING AND UNLOADING ARRANGEMENT FOR NUCLEAR REACTORS. Aubert, Michel; Fortin, Guillaume; Gugenberger, Rene; Martin, Roger; Rouge, Pierre (to Commissariat à l'Énergie Atomique). U. S. Patent 3,194,742. July 13, 1965. Priority date Aug. 3, 1962, France.

A fuel handling machine is provided for use with a graphite moderated gas cooled reactor having a moderator core formed by parallel spaced fuel channels, a pressure vessel and a biological shield surrounding the core, a servicing chamber inside the pressure vessel and biological shield, a lock between the servicing chamber and the atmosphere, and means for transferring fuel elements between the chamber and the channels. An intermediate fuel storage means is provided inside the pressure vessel and the biological shield. An arm is rotatable in the servicing chamber about its vertical axis, and the fuel element handling machine is movable along the arm. Means are provided for positioning the arm with the servicing machine in servicing relationship to the fuel element channel for the insertion or withdrawl of a fuel element, positioning the arm with the machine in servicing relation to the fuel element storage means, and for movement of the machine between arm and lock for conveying fuel elements between the machine and lock. (B.L.M.)

40146 NUCLEAR REACTOR CORE ARRANGEMENT. Deddens, James C.; Kopchinski, Norbert L. Jr.; Meyers, Gilbert Wayne; Barringer, Howard S. (to The Babcock and Wilcox Co.). U. S. Patent 3,194,743. July 13, 1965. Filed Mar. 9, 1959.

A reactor core arranged for an extended lifetime operation is made up of a number of uniform groups of fuel element assemblies having a square cross section and having a movable control rod through the central channel of the assembly. The groups are positioned to provide peripheral flow channels between adjacent fuel element assemblies of adjoining groups. Fixed control rods are located in some of the peripheral flow channels and flow control filler rods are located in the other peripheral channels. The fixed control rods may be replaced with flow control filler rods during the lifetime of the core when the reactivity has been reduced to obviate the need for at least some of the fixed control rods. The core is also divided into a number of symmetrical, longitudinally uniform fuel concentration zones that include a centrally arranged inner zone and at least one annular shaped concentrically located outer zone with the fissionable to fertile material weight percent ratio being lowest in the inner zone and increasing outwardly to the periphery of the core. Flux depressor plates located in the flow channels about the outer portion of the core reduce the flux or power peaking of the core. (B.L.M.)

Criticality Studies

See also PHYSICS — Criticality Studies.

Refer also to abstract 38825.

40147 (AEEW-M-448) ENOCH (A ONE-DIMENSIONAL SPACE DEPENDENT BURN-UP PROGRAMME). Wilkinson, M. C. (Atomic Energy Establishment, Winfrith (England)). July 1965. 34p. Dep.; BIS, $0.90; HMSO, 4s 6d.

The ENOCH code is designed for radial burnup studies in cylindrical reactors. It uses a four-group model of the neutron physics and a library of point burnup data computed with METHUSELAH or some similar code. Provision is made for representing charge, discharge, or shuffling of the annular zones according to a preset fuel management scheme. (auth)

40148 (BNWL-111) KINETICS I. A NEUTRON KINETICS CODE IN FORTRAN IV. Little, Winston W. Jr. (Battelle-Northwest, Richland, Wash. Pacific Northwest Lab.). July 1965. Contract AT(45-1)-1830. 25p. Dep. mn; CFSTI, $1.00 cy, $0.50 mn.

A numerical solution to the lumped parameter kinetics

equation is described. The method presented is particularly well-suited for the analysis of prompt critical excursions. In order to make the code useful for practical problems, a simple heat transfer model is attached to the kinetics equations. A FORTRAN IV source deck listing, input information, and a sample problem are given in the appendices. (auth)

40149 (BNWL-SA-61) A SYSTEM OF CHAINED COMPUTER CODES FOR REACTOR FUEL CYCLE ANALYSIS. Eschbach, E. A.; Deonigi, D. E.; Merrill, E. T.; Neef, W. I. (Battelle-Northwest, Richland, Wash. Pacific Northwest Lab.). May 1965. Contract AT(45-1)-1830. 38p. (CONF-650501-14). Dep. (mn); $2.00(cy), 1(mn) CFSTI.

From the Application of Computing Methods to Reactor Problems, Argonne, Ill.

A brief discussion of several computer codes and their function in reactor fuel analysis is presented. These codes consider economics and many variations in fuel performance. (M.O.W.)

40150 (CEA-R-2565) UTILISATION DU REACTEUR RAPSODIE POUR LA MESURE DU COEFFICIENT DOPPLER DES PILES RAPIDES DE PUISSANCE. (Utilization of the Rapsodie Reactor For the Measurement of the Doppler Effect). Zaleski, C. P.; Abdon, R.; Ladet, J.; Puig, L P.; Stevens, L. (Commissariat à l'Énergie Atomique, Cadarache (France). Centre Études Nucléaires). June 1964. 33p. (EUR-2233.f).

It is shown that a special loading of a 400-liter core in the reactor "Rapsodie" could simulate the same neutronic conditions as those encountered in fast power reactors. Various methods designed to measure the Doppler effect in this core are described and compared. In particular, a computation of the errors involved is set. This computation leads to the conclusion that such an experiment could give a valid estimation of the Doppler coefficient of large fast reactors. The neutronic computations set for this study are described. (auth)

40151 (EIR-79) THE THEORY OF THE MODIFIED PULSED SOURCE TECHNIQUE. Gozani, Tsahi (Eidgenoessisches Institut fuer Reaktorforschung, Wurenlingen (Switzerland)). Apr. 1965. 39p. Dep.(mn)

The theory of the modified pulsed source technique is analyzed. This technique is characterized by the simultaneous experimental determination of reactivity and generation time. Both quantities are given in units of dollars and therefore are not subject to theoretical arbitrariness. The various theoretical definitions of reactivity, e.g. static, dynamic or kinetic, only change the dollar units. The approximations involved in the analytical expressions of prompt and delayed neutron populations are examined and their accuracy is demonstrated. The cases of delta and rectangular pulsed sources are analyzed in detail. The effect of finite pulse width is taken into account. Effects due to the approach-to-equilibrium of delayed neutrons are considered and experimental as well as theoretical methods for correcting them are proposed. These methods are important in that they render results independent of possible changes in source intensity. In the discussion of the effect of spatial harmonics on the modified pulsed source technique it is shown that the two methods of Gozani and of Garelis and Russell depend inversely on the harmonics content. This is helpful in bracketing the correct values of reactivity and generation time. A glossary of practical formulas is given at the end of the work. (auth)

40152 (GA-6462) A SURVEY OF SEVERAL METHODS FOR COMPUTING CELL CROSS SECTIONS. Fenech, H.; Goodjohn, A.; Pomraning, G. C. (General Atomic, San Diego, Calif. John Jay Hopkins Lab. for Pure and Applied Science). June 16, 1965. Contract AT(04-3)-187. 52p. Dep. mn; CFSTI, $3.00 cy, $0.50 mn.

Several approximate calculational methods are developed for solving for the space-energy flux distribution in a cell. These methods are applied to the problem of computing the self-shielding effect through the ^{240}Pu resonance. It is concluded that none of the methods is accurate enough to predict this self-shielding. Hence at the present time it seems that the only method available which gives the desired accuracy is the S-N method (GAPLSN code). (auth)

40153 (IA-1001) PHILCO 2000 CODE FOR THE CALCULATION OF RESONANCE ESCAPE PROBABILITY IN HETEROGENEOUS REACTORS BY THE MONTE CARLO METHOD. Rothenstein, W.; Tabak, D. (Israel Atomic Energy Commission, Yavne. Soreq Nuclear Research Center). Feb. 1965. 64p. Dep. mn.

A Monte Carlo code for the calculation of the resonance escape probability in heterogeneous thermal reactors is described. It is an adaptation of the New York University IBM 704 code for the Philco 2000 computer, but it differs from the IBM code in the calculation of the resonance line shape functions and in the treatment of the cross sections in the statistical region, where the resonances are unresolved. The code was used to estimate the effective p-wave resonance integral and the effect of the presence of void channels in reactor lattices on the resonance capture. (auth)

40154 (LA-3229,pp 344-61) CAVITY REACTOR. Jarvis, George A. (Los Alamos Scientific Lab., Univ. of California, N. Mex.).

A series of measurements on the D_2O reflected cavity reactor mockup are reported. The measurements presented include the following: fuel distribution studies, structural materials, nozzle mockups, reflector heating, composite reflector, and plutonium vs uranium as fuel. (M.O.W.)

40155 (LA-3229, pp 362-76) CRITICALITY. Mills, C. B. (Los Alamos Scientific Lab., Univ. of California, N. Mex.).

The effects of simple and complex geometries on critical concentration are computed for ^{235}U. The effects of different geometries on criticality are then pointed out for the conceptually simplest situation, that of a single large rocket power plant. Since criticality is closely connected with rocket reactor design, an investigation of design ideas is presented. (M.O.W.)

40156 (NP-15161) A NEW METHOD FOR PREDICTING THE PENETRATION AND SLOWING-DOWN OF NEUTRONS IN REACTOR SHIELDS. Hjaerne, L.; Leimdoerfer, M. (Forsvarets Forskningsanstalt, Stockholm (Sweden)). Jan. 1965. 25p. Dep. mn.

A new approach is presented in the formulation of removal-diffusion theory. The "removal cross-section" is redefined and the slowing-down between the multi-group diffusion equations is treated with a complete energy transfer matrix rather than in an age theory approximation. The method, based on the new approach, contains one adjustable parameter which seems to be universally constant. Examples of neutron spectra and thermal flux penetrations are given in a number of differing shield configurations and the results compare favorably with experiments and Moments Method calculations. (auth)

40157 (ORNL-TM-1175) THE DETERMINATION OF NEUTRON FLUX IN NUCLEAR REACTORS BY THE UNCOLLIDED-FLUX ESTIMATOR APPLIED TO MONTE CARLO COLLISIONS. Webster, J. Wallace (Oak Ridge National Lab., Tenn.). [1965]. Contract W-7405-eng-26. 38p. Dep. mn; CFSTI, $2.00 cy, $0.50 mn.

An investigation was made of the uncollided-flux estimator, applied to Monte Carlo collisions, as a means of determining the neutron flux at specified spatial points of a reactor. The uncollided-flux estimator is essentially an evaluation of the flux as given by the Boltzmann equation in integral form. The mathematical formulation and FORTRAN programs are presented. The method is applied to two sample-reactor problems: (1) the Godiva assembly, and (2) an 8-unit interacting array of highly enriched uranium-metal cylinders. The scalar flux in Godiva, calculated using the collisions from 15,000 neutrons, is found to be in excellent agreement with the flux calculated by the Carlson S_n method. In the second problem, using the collisions from about 10,000 neutrons, the distorting effect on the flux distribution of the nearby interacting cylinder

shows up clearly; but more neutrons would be necessary for satisfactory accuracy. (auth)

40158 (UNC-5123) SODIUM VOID COEFFICIENT OF REACTIVITY. A REVIEW AND STUDY OF ANALYTICAL WORK. Monroe, C. W. (United Nuclear Corp., White Plains, N. Y. Development Div.). May 1965. Contract AT(30-1)-2832. 126p. Dep. mn; CFSTI, $4.00 cy, $1.00 mn.

It is disclosed that the most widely accepted method for determining sodium reactivity effects employs a standard synthesis technique using diffusion theory in one-dimensional cylinder-and-slab geometries. The majority of multigroup diffusion theory codes used employ an option whereby group-and-region-dependent bucklings may be specified as input quantities, facilitating a relatively accurate iterative procedure. Effective group cross sections are derived from many sources of data; the high energy groups usually employ the cross sections of Yiftah, Okrent, and Moldauer. Whenever possible, the most recent energy-dependent data for cross sections, $\nu(E)$, and the capture-to-fission ratios of fissile isotopes were used. A refined treatment of elastic scattering resonances (the ELMOE code) has established the necessity of using composition-dependent cross sections. Computations using several cross section sets indicate trends in the sodium void effect for a variety of conditions. Conclusions from these results are presented. (auth)

40159 (WAPD-T-1774) CRITICAL DIMENSIONS OF WATER REFLECTED SYSTEMS CONTAINING $^{235}U-H_2O-Zr$. Rutledge, G. P.; Dobbe, F. A.; Price, C. H. (Bettis Atomic Power Lab., Pittsburgh, Pa.). June 1965. (Contract AT(11-1)-Gen-14. 12p. (CONF-650602-36). Dep. mn; CFSTI, $1.00 cy, $0.50 mn.

From American Nuclear Society 11th Annual Meeting, Gatlinburg, Tenn.

An analytical approach was utilized to determine critical dimension of the water reflected homogeneous $Zr-H_2O-^{235}U$ system for application in fuel handling criticality control work. The k_{eff} of this system as a function of composition and buckling was previously presented. This was extended by calculating the associated extrapolation distance. In addition, all the parameters needed to calculate critical dimensions from the geometric buckling equation are placed in convenient graphical form. (M.O.W.)

40160 (WAPD-TM-479) CHIC-KIN—A FORTRAN PROGRAM FOR INTERMEDIATE AND FAST TRANSIENTS IN A WATER MODERATED REACTOR. Redfield, J. A. (Bettis Atomic Power Lab., Pittsburgh, Pa.). Jan. 1965. Contract AT-11-1-Gen-14. 109p. Dep. mn; CFSTI, $4.00 cy, $1.00 mn.

A FORTRAN program is described which treats fast and intermediate reactivity transients in a water-cooled heterogeneous nuclear reactor. The program calculates the power, temperatures, and internal pressure surges when control rod motion, inlet temperature, inlet flow, and system pressure are known functions of time. The validity of this analysis tool is indicated by comparisons with SPERT I experimental transients. (auth)

40161 (ZfK-TPh-11) VIELGRUPPENPARAMETERSATZE ZUR BERECHNUNG SCHNELLER REAKTOREN. (Many-Group Parameter Sets for Calculation of Fast Reactors). Falkenberg, Dietrich (Deutsche Akademie der Wissenschaften zu Berlin (East Germany) and Zentralinstitut fuer Kernphysik, Rossendorf bei Dresden (East Germany)). July 1964. 74p. Dep.(mn).

A series of methodical problems connected with the calculation of group parameters from the fundamental nuclear physics data was explained. The calculation method of the group constants from the basic data and not the state of knowledge of the nuclear data itself was the central point. The form of the material parameter in the basic equations for neutron diffusion, calculation instructions for the group constants from the energy-dependent nuclear physics data, the group widths and average to the mean relations used in the ABAJAN sets, and the calculation of mean group values for the microscopic effective cross sections of each individual element were considered. (J.S.R.)

40162 ON THE CHARACTERISTIC ENERGY OF A PULSED SUBCRITICAL ASSEMBLY. Mueller, K.-H. (CCR EURATOM, Ispra, Italy). Phys. Letters, 16: 274-5(June 1, 1965). (In French).

A Monte Carlo calculation was made of a neutron flux distribution in a subcritical sphere with a monoenergetic isotropic point source in the center. Initial primary neutron energies from 10^{-5} to 10 Mev were considered. The characteristic time pattern of the neutron flux showed that the buckling observed with $E_0 = 0.5$ Mev degenerated into a minimum-maximum pattern with decreasing energy. The most suitable input energy for the arrangement used was 0.005 Mev. The space distribution of the neutron flux at various times shows the fluctuation during the passage through the minimum-maximum region. For $t < 2 \times 10^{-6}$ sec, the space-time of the energy distribution of the neutrons has stabilized. In a GODIVA sphere, the Monte Carlo calculation gave a characteristic energy of 8 Mev. The minimum of the leakage curve was between 0.5 to 1.5×10^{-7} sec, and the subsequent maximum was between 2 and 3×10^{-7} sec. (J.S.R.)

40163 PHYSICS. Power Reactor Technol., 7: No. 3, 206-22(Summer 1964).

Critical and exponential experiments are reported in boiling-water, water-moderated, heavy-water-moderated, graphite-moderated, zirconium-hydride-moderated, fast, and spectral-shift (water–heavy water) assemblies. Kinetics of heavy-water lattices are investigated. The resonance integrals of $^{238}UO_2$, Th, and ThO_2 are evaluated. Burnup effects on the poisoning characteristics of Ag, In, Cd, Lu, Sm, Tm, B, Er, Gd, Yb, Li, Hf, Ho, Eu, and Dy are measured and compared. The shield design for ML-1 is shown. The cross section for $^{16}O(n,p)$ at 12 to 17 Mev is measured. 38 references. (T.F.H.)

40164 CONFERENCE ON NOISE ANALYSIS IN NUCLEAR SYSTEMS. Valerino, M. F. Power Reactor Technol., 7: No. 3, 248-64(Summer 1964).

Methods for analyzing reactor noise, including the use of auto- and cross-correlation functions, power spectral density methods, transfer function methods, and noise sources, are reviewed. Noise measurements in zero-power and power (Halden, Saxton, Vallecitos Boiling Reactor, and N.S. Savannah) reactors are reported. (T.F.H.)

Design and Feasibility

40165 (GA-6303) FINITE ELEMENT ANALYSIS OF AXISYMMETRIC COMPOSITE STRUCTURES. Rashid, Y. R. (General Atomic, San Diego, Calif. John Jay Hopkins Lab. for Pure and Applied Science). June 4, 1965. Contract AT(04-3)-167. 81p. Dep. mn; CFSTI, $3.00 cy, $0.75 mn.

The analysis of axisymmetric composite structures by the finite-element method with particular emphasis on the analysis of a prestressed concrete reactor (PCRS) is dealt with. Displacements and stresses in nonhomogeneous elastic structures are obtained by the method presented for any combination of the following loading conditions: body forces, surface loads, thermal loads, locked-in residual stresses, and prestressing loads. In a PCRS, the conventional steel reinforcement, the prestressing cables, and the steel liner are considered as structural components that contribute to the load-carrying capacity of the over-all structure. Field equations of n-dimensional (n = 1, 2, 3) finite-element idealization of a solid are symbolically presented. They are then specialized to triangular axisymmetric ring elements, axisymmetric shell elements represented as truncated cones, and one-dimensional tension-compression members. Detailed derivations of stiffness and load matrices for these types of elements are given. Solutions of equilibrium equations and boundary conditions are discussed in detail. Example analyses of a prestressed concrete reactor structure are presented. (auth)

40166 IMPROVEMENTS IN NUCLEAR REACTORS. (to Babcock and Wilcox, Ltd.). British Patent 992,021. May 12, 1965. Priority date Nov. 8, 1960, Germany.

A reactor design is proposed in which the fuel magazine wall forms an external part of the pressure compartment, and the magazine wall is constructed of thin, metallic sheeting made flexible by means of flutes or corrugations so that the sheet may be pressed inwardly against the spacing means by a fluid pressure differential between the compartment and the magazine while the reactor is in operation. The magazine contains the bundles of fuel elements made up of upright rows of co-axially aligned fuel pins having end portions of reduced diameter that serve to accommodate peripheral parts of upright annular rollers acting as spacers between adjacent fuel pins. The magazine wall serves to pack the spacing means between and around the fuel elements; while each wall is formed with outwardly projecting flutes that serve to space neighboring magazines from one another. The spacing means within a magazine are arranged in horizontal layers that extend across each magazine, and each layer includes individually removable spacers located between adjacent fuel elements. Each fuel bundle is arranged to be cooled by flow of fluid coolant through the magazine, and each pressure compartment is arranged in a pressure vessel and is pressurized with fluid coolant fed through a conduit to an opening in the pressure wall. The compartment is connected through the conduit to a relatively high pressure point in the fluid coolant circuit. (B.L.M.)

40167 NUCLEAR REACTOR. Frisch, Erling (to Westinghouse Electric Corp.). U. S. Patent 3,194,740. July 13, 1965. Filed Jan. 30, 1961.

A pressurized water reactor adapted to be operated either for testing or for power production is described. The core is submerged under a head of circulating coolant, and means are associated with the core for separating the cooling and moderating portions of the circulating fluid(s). The fuel element design and supporting means for the elements permit easy removal or insertion of the elements to facilitate assembly of the core and to minimize shutdown time required to replace, interchange, or recycle the fuel elements. The peak power output or fluxile density of the core can be changed readily by varying the number or arrangement of fuel elements within the core or by adding or subtracting fuel from the individual elements. A number of testing facilities are provided by which samples of various structural, cooling, and moderating materials may be tested under different conditions of temperature, pressure, and fluxile density. (B.L.M.)

Fuels

40168 (CONF-117) PREPARATION AND PROCESSING OF PARTICULATE NUCLEAR FUELS. Proceedings of a Symposium [Held at] New York, September, 9, 1963. Blocher, John M. Jr., (ed.) (Battelle Memorial Inst., Columbus, Ohio). Contract [W-7405-eng-92]. 202p. Dep. mn; CFSTI, $2.00 cy, $1.25 mn.

Twelve papers are presented on particulate fuels whose particle size, shape, distribution, or coating is a significant design factor in their end use. Requirements, fabrication, coating, and reprocessing are covered in the papers. Separate abstracts were prepared for five of the papers; for the other seven papers, see NSA 17: 25693; 18: 3875, 6785, 26008, 22520, and 33687; and 19: 20528. (D.L.C.)

For abstracts of individual papers see: 39094, 39095, 39096, 39126, and 40169.

40169 (CONF-117(p.67-79)) FUEL REQUIREMENTS FOR FISSIOCHEMICAL PRODUCTION. Pearson, R. L.; Cusack, J. H.; Deutsch, D. E. (Aerojet-General Nucleonics, San Ramon, Calif.).

Fuel systems for a fissiochemical reactor were evaluated. The efficiency at which fission fragments deposit their energy depends largely upon fuel geometry and composition. Three types of fuel can be used to generate fission fragments: homogeneous solutions or mixtures, fixed fuels, and heterogeneous mixtures. It was concluded that a slurry of spherical particles of fully enriched UO_2, less than 3 microns in diameter, suspended in liquid ammonia is best suited for fissiochemical production of hydrazine. The slurry should be stable, insoluble, nonabrasive and noncorrosive, should form uniform dispersions and loosely packed sediment, should not promote catalytic decomposition of the product, and should have minimum susceptibility to irradiation damage. (auth)

40170 (HW-71813) MINIMIZER—A COMPUTER CODE FOR DETERMINING MINIMUM FUEL COST. Eschbach, E. A.; Deonigi, D. E.; McConiga, A. F. (General Electric Co., Richland, Wash. Hanford Atomic Products Operation). Dec. 1964. Contract AT(45-1)-1350. 83p. Dep. mn; CFSTI, $3.00 cy, $0.75 mn.

The MINIMIZER code is an IBM-7090 computer code used in conjunction with other Hanford Laboratories computer codes to estimate the most probable minimum fuel cost from a set of fuel cost data. The determination of a minimum fuel cost is important to selection of overall optimum reactor operating conditions. In addition, deriving the operating point from the minimum fuel cost point provides a consistent basis for evaluating process and economic changes within a given fuel cycle and for comparing fuel cycles using different fuel materials. The MINIMIZER code is described and its accuracy with various sets of data is demonstrated. Machine printouts of the computer program and of a complete example case are presented. (auth)

40171 (KAPL-M-6475) KER-4—THE THERMAL ANALYSIS OF CYLINDRICAL FUEL RODS. Anderson, W. Kermit; Mueller, Gerhard O. (Knolls Atomic Power Lab., Schenectady, N. Y.). June 1, 1965. Contract W-31-109-eng-52. 23p. Dep. mn; CFSTI, $1.00 cy, $0.50 mn.

The KER-4 computer program is used when performing parameter studies on cylindrical and tubular reactor fuel elements. Given a set of input conditions such as porosity, thermal conductivity, heat generation, physical dimensions, and boundary temperatures, the KER-4 program will calculate the temperature distribution in the fuel element. The background information leading to the development of the computer program, a description of the analytical work, a discussion of the program, an input description and sample problem, and a discussion of input quantities are given. (auth)

40172 FUEL ELEMENTS. Power Reactor Technol., 7: No. 3, 237-47(Summer 1964).

Fabrication processes for stainless-steel-clad stainless steel–UO_2 cermet fuel tubes, UO_2 fuel rods, an "annular multitube" UO_2 fuel element, a SAP fuel cladding configuration, cladding tubing, and end closures for fuel elements are reviewed. Economic aspects of the fabrication of UO_2 pellet and compressed powder fuels are analyzed. (T.F.H.)

40173 IMPROVEMENTS IN OR RELATING TO NUCLEAR REACTOR FUEL ELEMENTS. Dodd, Cyril Lano (to United Kingdom Atomic Energy Authority). British Patent 997,629. July 7, 1965. Filed July 11, 1963.

A reactor fuel element of the type in which the sheathed fuel body is supported in a graphite sleeve is provided with means for connecting the fuel body and the sleeve, with an overload coupling, and with means associated with the sheathed body for engagement by fuel element handling equipment. If the fuel element becomes jammed in the fuel channel, the provision for engagement by handling equipment provides means by which the sheathed fuel body may be disconnected from the sleeve by exerting sufficient withdrawal force on the fuel body to break the overload coupling. This coupling includes a shear pin in engagement with an end fitting of the sheathed body and in engagement with a bridge piece spanning the graphite sleeve which serves to support the element in the sleeve. The sheath of the fuel body is provided with coarse-pitched helical fins and longitudinal flow splitters of greater height than

the fins. The outer portion of the flow splitters are engaged in longitudinal slots on the internal surface of the graphite sleeve. (B.L.M.)

40174 LOCATING MEANS FOR POSITIONING NUCLEAR FUEL COMPONENTS. Hackett, Herman Joseph (to United Kingdom Atomic Energy Authority). U. S. Patent 3,194,746. July 13, 1965. Priority date Feb. 20, 1962, Great Britain.

A spacer member is provided between the oblique faced adjacent ends of fuel elements for positioning the elements one above the other in a longitudinally extending channel formed in the moderating material. The spacers have peripheral projections that extend between the fuel component and the wall of the channel serving to locate the components with respect to the wall. The disposition of the projections on the spacer is such that the radial component due to the axially downward force set up at the oblique end faces is transmitted to the channel wall positioning the element with respect to the wall. However, the components can undergo dimensional changes in radial planes substantially without restraint. (B.L.M.)

Power and Power-Breeder Reactors

Refer also to abstract 39134.

40175 (ACNP-63592) LARGE FAST REACTOR DESIGN STUDY. Monthly Report, August 1963. (Allis-Chalmers Mfg. Co., Washington, D. C. Nuclear Power Dept.). Contract AT(11-1)-1316. 8p. Dep.(mn); $1.00 (cy), 1(mn) CFSTI.

The safety and kinetics of a large, fast, Na-cooled, oxide-fueled 1000-Mw(e) reactor are analyzed. The design of the fuel assemblies and the primary system components is discussed. (T.F.H.)

40176 (AGN-TM-407) ARMY GAS-COOLED REACTOR SYSTEMS PROGRAM. AGN-GAM, AN IBM 7090 CODE TO CALCULATE SPECTRA AND MULTIGROUP CONSTANTS. Wilcox, T. P.; Perkins, S. T. (Aerojet-General Nucleonics, San Ramon, Calif.). Apr. 1965. Contract AT(10-1)-880. 151p. Dep. mn; CFSTI, $3.00 cy, $1.00 mn.

The AGN-GAM (IBM 7090) code is discussed together with the subroutines for writing and revising the library tapes. The code solves either the P-1 or B-1 equations for 75 quarter lethargy energy groups from 10 Mev to 0.07 ev to determine the slowing down fluxes and currents in a reactor core. Provision is also made to solve P-1 equations to determine these quantities in a reflector region. Broad group constants, weighted by the flux (or current) quantities, are then derived for use in diffusion, isotropic transport or anisotropic transport calculations. The method of Adler, Hinman and Nordheim is used to calculate resonance absorption and fission cross sections. Self-shielding factors can be included in the computations. The output cross section data can be punched directly into IBM cards for use in any of several nuclear codes. (auth)

40177 (ANL-7046(p.1-35)) LIQUID-METAL-COOLED REACTORS. (Argonne National Lab., Ill.).

Research and development are reported on EBR-II, FARET, ZPR-6, ZPR-9, ZPPR, fast reactor fuels, and fast reactor fuel reprocessing. (J.R.D.)

40178 (BNL-9279) FUEL MANAGEMENT IN THE SETTLED-BED FAST REACTOR. Green, L.; Levine, M. M.; Winsche, W. E.; Epel, L. G.; Chernick, J. (Brookhaven National Lab., Upton, N. Y.). [June 1965]. Contract AT(30-2)-Gen-16. 8p. (CONF-650602-29). Dep.(mn); $1.00(cy), 1(mn) CFSTI.

From American Nuclear Society 11th Annual Meeting, Gatlinburg, Tenn.

Fuel management schemes of beds with ordered packing are discussed. The countercurrent principle of reactor refueling, which achieves a steady state distribution of isotopes by moving the fuel through the reactor at a constant rate, is discussed. (M.O.W.)

40179 (CVNA-236) MONTHLY OPERATING REPORT, MAY 1965. (Carolinas Virginia Nuclear Power Associates, Inc., Parr, S. C.). Contract AT(30-1)-2289. 32p. Dep. mn; CFSTI, $2.00 cy, $0.50 mn.

The CVTR continued to operate at essentially the full licensed power level of 44.3 Mw during the month, and a record of more than 100 million pounds of steam were delivered to the turbine-generator at the Parr Steam Plant. The reactor availability for the month was 100%. Advantage was taken of a shutdown for operator testing to perform maintenance work in the vapor container. The AEC Advisory Committee on Reactor Safeguards held a formal hearing to consider the CVNPA application to increase the licensed power of the CVTR to the design level of 65 Mw. Aspects of plant operation and maintenance were reviewed along with future plans. (J.R.D.)

40180 (DL-56) TOMORROW'S FISSION REACTOR AND ITS MATERIALS DEMANDS. Lewis, W. B. (Atomic Energy of Canada Ltd., Chalk River (Ontario)). Feb. 1964. Reprinted Apr. 1965. 20p. (AECL-2236; CONF-640207-1). Dep.; AECL, $0.50 cy.

From American Society for Testing Materials Conference, Philadelphia.

Good neutron economy, high thermal efficiency and long life will be demanded for economic operation of nuclear power reactors. The neutron economic penalty for stainless steel within the reactor amounts typically to $300/yr per kilogram and for zirconium to $15/yr per kilogram. High thermal efficiency demands high temperatures that set limits on life. Basic problems are set by the permeability of all solids at high temperatures to their own and to foreign atoms. Fortunately, radiation damage tends to anneal out at high temperatures because of this atomic mobility. Unfortunately, interaction between the heat transport fluid and its confining boundaries, coupled with the economic penalty of allowing any release of radioactive fission products, sets problems still unsolved and for which even basic scientific understanding remains to be developed. Tests of corrosion, stress-rupture, creep, delayed failure and fatigue under operating conditions measure the degree of success in achieving long term stability but give only meager hints of the internal processes we seek to control. Nevertheless, by applying ignorance factors to act as "safety" factors, large reactors of economic promise can already be engineered. Further research and testing hold great promise of scientific satisfaction and economic reward. (auth)

40181 (EUR-2429.i) CENTRALE ELETTRONUCLEARE DI LATINA RELAZIONE ANNUALE 1964. (Latina Nuclear Power Plant Annual Report, 1964). (Ente Nazionale per l'Energia Elettrica, Rome (Italy)). May 1965. 60p. Dep.(mn).

The objectives of the first year of commercial operation of the Latina Nuclear Power Plant are briefly summarized. The experience gained is discussed. Detailed reports are given on the results of plant use, operational experience, and core behavior. The chemical plant and health physics are also considered. (J.S.R.)

40182 (GA-5537) A STUDY OF A GAS-COOLED FAST BREEDER REACTOR. INITIAL STUDY: CORE DESIGN ANALYSIS AND SYSTEM DEVELOPMENT PROGRAM. Final Summary Report. (General Atomic, San Diego, Calif. John Jay Hopkins Lab. for Pure and Applied Science). Aug. 15, 1964. Contract AT(04-3)-167. 272p. Dep. mn; CFSTI, $6.00 cy, $1.50 mn.

The prospects of gas cooling for fast breeder reactors intended for the large-scale economic production of electric power are examined. The effects of major variables in the design and performance of gas-cooled cores are examined. A reference plant with selected engineering considerations is discussed. Details of the nuclear-analysis work are presented. Additional information is given

concerning fuel-cycle economics, metallurgical design of the fuel element, and the overall development program. (M.O.W.)

40183 (GA-5924) 40-MW(E) PROTOTYPE HIGH-TEMPERATURE GAS-COOLED REACTOR POSTCONSTRUCTION RESEARCH AND DEVELOPMENT PROGRAM. Summary Progress Report for the Period Ending, October 1964. (General Atomic, San Diego, Calif. John Jay Hopkins Lab. for Pure and Applied Science). Dec. 15, 1964. Contract AT(04-3)-314. 16p. Dep.(mn); $1.00(cy), 1(mn) CFSTI

The detailed description of the initial phases of the zero-power program is presented. Poisoned dummy elements are designed to duplicate approximately the neutron absorption cross section of a fuel element. Through the use of the poison, this initial critical core will approximate the nuclear characteristics of the actual end-of-life condition of the core, when all the rods have been withdrawn. A series of detailed measurements of control rod worths, power distributions, and reactivity worths is started during this initial stage. (M.O.W.)

40184 (GA-6406) 40-MW(E) PROTOTYPE HIGH-TEMPERATURE GAS-COOLED REACTOR POSTCONSTRUCTION RESEARCH AND DEVELOPMENT PROGRAM. Quarterly Progress Report for the Period Ending April 30, 1965. General Atomic, San Diego, Calif. John Jay Hopkins Lab. for Pure and Applied Science). May 31, 1965. AT-(04-3)-314. 25p. Dep. mn; CFSTI, $1.00 cy, $0.50 mn.

Those analyses that were performed on the zero-power phase of reactor operation are presented. The reactor core with dummy graphite elements was accessible, and results of neutron measurements made within the core are given. These results are part of those reported for test procedure AO-1. An up-to-date revision of test procedures to be performed during the zero-power phase of measurements is also included. (M.O.W.)

40185 (JAERI-1075) ON BURN-UP CHARACTERISTICS OF PRESSURE TUBE TYPE D_2O MODERATED POWER REACTORS. Yasukawa, Sigeru (Japan Atomic Energy Research Inst., Tokyo). Oct. 1964. 39p. (In Japanese).

The fuel burn-up characteristics for pressure-tube-type D_2O-moderated power reactors are analyzed by one-dimensional burnup code in which both in-out and out-in refueling can be treated. The selected power reactors are those designed by industrial groups in Japan in 1963, when the work connected with the selection of coolant type was started for pressure-tube-type D_2O-moderated power reactors. The main contents are the following: comparison of the characteristics of point burnup and one dimensional burnup; effect of reflector thickness on fuel burnup; burnup characteristic under one batch for the 5 designed reactors; burnup characteristic under refueling for the 5 designed reactors; and poisoning effect, etc. A burnup characteristic for bidirectional refueling is not studied. (auth)

40186 (JAERI-1076) DEVELOPMENT OF A CORE DYNAMICS MODEL FOR THE JPDR, AND ANALYSIS OF THE RESULTS OF THE TEST OF THE CORE DYNAMICS. (Japan Atomic Energy Research Inst., Tokyo). Dec. 1964. 65p. (In Japanese).

A core dynamics model was proposed for the JPDR (natural circulation, single cycle, boiling water reactor plant). On the basis of analytical models of so-called distributed parameters, and the experimental data obtained during the JPDR initial power-up test, it was decided to develop the JPDR dynamics model of lumped parameters rather than of distributed parameters and to make the model as accurate as possible. To establish the model, three equations of mass, energy, and momentum balances were used, with numerical constants measured during JPDR power operation. The adequacy of the developed model was checked, and the model was compared with other models by computation of such transient and dynamic operations as experienced with the JPDR. The effect, on the frequency characteristics, of variations of the model parameters from the normal was investigated; and the model was compared with the other models also employed in the analysis of the JPDR. (auth)

40187 (NAA-SR-Memo-7753) FABRICATION RECORD OF OMRE TEST ELEMENTS 9-2 AND 10-1. Hayes, H. G. (Atomics International, Canoga Park, Calif.). Sept. 28, 1962. Contract AT(11-1)-Gen-8. 41p. Dep. mn; CFSTI, $2.00 cy, $0.50 mn.

Data and information related to the fabrication, assembly and instrumentation of OMRE 4th Core Test Elements 9-2 and 10-1 are reported. Each test element contained 18 finned, Al clad fuel plates, assembled into bundles 6 plates high by 3 plates long. Both assemblies were housed in type 347 stainless steel fuel boxes. The test elements were instrumented to measure fuel cladding surface and coolant exit temperatures. Changes in fuel element design specifications used previously on OMRE Test Elements 9-1 and 11-1 include: increased fuel cladding fin heights; increased dimple heights; upsetting fuel plate cladding outer rails on each of the 3 top and 3 bottom plates in the fuel bundle; redesigning of the fuel plate locking pins; and changes in the number of thermocouples used for cladding and coolant temperature measurement. (auth)

40188 (NYO-3420-2) HYDROGEN EVOLUTION WITHIN CONTAINMENT IN PM-TYPE PLANTS. Final Report. (Nuclear Utility Services, Inc., Washington, D. C.). June 18, 1965. Contract AT(30-1)-3420. 88p. Dep. mn; CFSTI, $3.00 cy, $0.75 mn.

The history of hydrogen evolution in PM-type plants is briefly reviewed. The PM-3A spent core test program is presented along with the hypothesis on the elimination of hydrogen evolution. The proposed hydrogen evolution test program is outlined. (M.O.W.)

40189 (ORNL-TM-733(Rev.)) MSRE DESIGN AND OPERATIONS REPORT. PART VI. OPERATING SAFETY LIMITS FOR THE MOLTEN-SALT REACTOR EXPERIMENT. Beall, S. E.; Guymon, R. H. (Oak Ridge National Lab., Tenn.). Aug. 3, 1965. Contract W-7405-eng-26. 4p. Dep. mn; CFSTI, $1.00 cy, $0.50 mn.

Limits are set for various parameters related to the Molten-Salt Reactor Experiment. In some cases the limits report the level at which the reactor will be shut down by automatic monitoring devices. The containment, fuel system, coolant system, control rods, nuclear control and safety instrumentation, personnel radiation monitoring, personnel and procedures, and experimental limits are considered. (M.O.W.)

40190 (ORNL-TM-784) COST STUDY OF A LARGE SODIUM COOLED FAST BREEDER REACTOR FOR A SEA WATER DESALINATION PLANT. Gall, W. R. (Oak Ridge National Lab., Tenn.). Mar. 1964. Contract W-7405-eng-26. 56p. Dep. mn; CFSTI, $3.00 cy, $0.75 mn.

A very rough preliminary design study and cost estimate are presented for a 25,000 Mwt plutonium fueled fast breeder reactor for use in a desalination plant. Designed for operation with sodium temperatures below 800°F, the primary system can be constructed of carbon or low alloy steels. The reactor vessel is 44 ft inside diameter, and with a coolant temperature rise of 260°F, four pumps circulate 2,400,000 gpm of sodium through four 6250 Mw once-through steam generators. Saturated steam at 600 psia drives eight 540 Mw(e) turbine-generator units, exhausting at 25 psia to the evaporator plant. (auth)

40191 (RL-SA-42) APPLICATION OF NPR TECHNOLOGY TO THE NATIONAL NUCLEAR PROGRAM. Kosmata, H. R. (General Electric Co., Richland, Wash. Hanford Atomic Products Operation). June 1965. Contract AT(45-1)-1350. 18p. (CONF-650602-39). Dep. mn; CFSTI, $1.00 cy, $0.50 mn.

From American Nuclear Society 11th Annual Meeting, Gatlinburg, Tenn.

The Hanford N Reactor is discussed and the project status is given. Described are items of interest to the national nuclear program, such as; Zircaloy tubes, carbon steel primary loop piping, Zircaloy clad metallic ura-

nium fuel, large process equipment, large energy systems, and the modular design concept. (M.O.W.)

40192 (TID-22003) ARDENNES NUCLEAR POWER PLANT QUARTERLY REPORT NO. 11, JANUARY 1-MARCH 31, 1965. I. DESIGN STUDIES. II. PREFABRICATED COMPONENTS. III. ON-SITE WORK. (Societe d'Energie Nucleaire Franco-Belge des Ardennes, Chooz-Lez-Givet (France)). May 6, 1965. 28p. Dep. mn; CFSTI, $2.00 cy, $0.50 mn.

Original in French

Design studies were conducted on buildings, ventilation stacks, and fuel element storage. Results of safety studies are reported. Control room switch panels and automatic units were designed. On-site work is described on civil engineering, reactor assembly, and other associated tasks. Pictorial evidence of progress is included. (J.R.D.)

40193 (TRG-Report-921) STUDIES OF RANDOM FLUCTUATIONS OF D.F.R. POWER. Menzies, D. C.; Backhouse, A. M. (Reactor Group, United Kingdom Atomic Energy Authority, Dounreay (Scotland)). Jan. 15, 1965. 19p.

A large number of recordings of fluctuations in DFR flux have been made since the reactor commenced full-power operation. These recordings have been analyzed, and the auto-correlation function of the flux signals measured. Two features appear in all correlation functions: a damped oscillation with a frequency proportional to coolant flow-rate, and a damping time-constant, identified with the fuel time-constant, of about 0.4 sec; a long exponential decay with an apparent time-constant of about 50 sec and an amplitude which has remained constant, within expected statistical variations, over the period covering all measurements. The measured time-constant is studied in relation to the reactor impulse function. (auth)

40194 (WASH-1055) ESTIMATED GROWTH OF CIVILIAN NUCLEAR POWER. (Division of Operations Analysis and Forecasting (AEC), Washington, D. C.). Mar. 1965. 20p. Dep.; GPO, $0.20 cy.

Projections of the megawatts of installed capacity of civilian nuclear power are made through 1970 and then for the period 1970-1980. A forecast of 60,000 to 90,000 Mw(e) by the end of 1980 in the U. S. and the same range in the rest of the Free World is made for installed nuclear capacity utilizing enriched uranium. Fuel assumptions and requirements are considered. (D.L.C.)

40195 (WCAP-3269-5) LARGE CLOSED-CYCLE WATER REACTOR RESEARCH AND DEVELOPMENT PROGRAM. Progress Report, July 1-September 30, 1964. (Westinghouse Electric Corp., Pittsburgh, Pa. Atomic Power Div.). Contract AT(30-1)-3269. 147p. Dep. mn; CFSTI, $4.00 cy, $1.00 mn.

Progress is reported in sections on reactor physics development, reactor core development, chemical shim development, plant development, reactor hazards analyses, and critical experiments. (J.R.D.)

40196 (WCAP-3269-6) LARGE CLOSED-CYCLE WATER REACTOR RESEARCH AND DEVELOPMENT PROGRAM. Progress Report, October 1-December 31, 1964. (Westinghouse Electric Corp., Pittsburgh, Pa. Atomic Power Div.). Contract AT(30-1)-3269. 127p. Dep. mn; CFSTI, $4.00 cy, $0.75 mn.

Progress is reported in sections on reactor physics development, reactor core development, chemical shim development, plant development, reactor hazards analysis, and critical experiments. (J.R.D.)

40197 (WCAP-3718) LARGE CLOSED-CYCLE WATER REACTOR RESEARCH AND DEVELOPMENT PROGRAM. Progress Report, July 1-September 30, 1962. (Westinghouse Electric Corp., Pittsburgh, Pa. Atomic Power Div.). Contract AT(30-1)-3269. 93p. Dep. mn; CFSTI, $3.00 cy, $0.75 mn.

Progress is summarized in sections on reactor physics development, reactor core development, chemical shim development, plant development, reactor hazards analysis, and critical experiments. (J.R.D.)

40198 (WCAP-3721) LARGE CLOSED-CYCLE WATER REACTOR RESEARCH AND DEVELOPMENT PROGRAM. Progress Report, October 1-December 31, 1962. (Westinghouse Electric Corp., Pittsburgh, Pa. Atomic Power Div.). Contract AT(30-1)-3269. 62p. Dep. mn; CFSTI, $3.00 cy, $0.75 mn.

Progress is reported in sections on reactor physics development, chemical shim development, plant development, and reactor hazard analysis. (J.R.D.)

40199 PRELIMINARY OPERATIONAL EXPERIENCES WITH THE HINKLEY POINT NUCLEAR POWER PLANT. Eastwood, D. C. (English Electric Co. Ltd., Whetstone, Eng.). At. Strom, 10: 87-91(Oct. 1964). (In German)

The engineering and technical developments that made possible the design and construction of the Hinkley point reactor was summarized. Engineering and nuclear data for the reactor are tabulated. The factors that made possible a higher coolant gas pressure are discussed. The problems that had to be solved before and during construction are indicated. (J.S.R.)

40200 EVOLUTION OF POWER AND COMPETITIVE NUCLEAR SYSTEMS. Barbato, M.; Dalla Volta, F. (Comitato Nazionale Energia Nucleare, Rome). Atomo, Petrol. Elettricita, No. 6, 255-68(1963). (In Italian)

The role that nuclear energy can play in the evolution of the energy system is discussed with particular respect to the present Italian situation. The present Italian energy situation, its evaluation within the framework of the European community, the role of nuclear energy and the present transition phase, the cost competitiveness, and electronuclear prospects, future availability of uranium and its effect on the energy cost are the factors considered. (J.S.R.)

40201 THREE YEARS OF OPERATING EXPERIENCE WITH THE KAHL NUCLEAR POWER STATION. Meyer, F. (Versuchsatomkraftwerk Kahl GmbH, Kahl am Main, Ger.). Atomwirtschaft, 10: 282-6(June 1965). (In German).

Operation of the experimental nuclear power station at Kahl met and exceeded expectations. The fuel elements showed no detectable defects, nor was any damage experienced on the control rods and their drives. The availability of the plant was comparatively good, and downtime resulted essentially because of defects in, or malfunctioning of, conventional plant components. By far the majority of the scrams released proved to be unnecessary. They were caused, chiefly, by inductive influences on the linear amplifiers. Following several modifications to the handling facilities, the manipulation of irradiated fuel elements was found to be relatively simple. The activity concentrations released via the waste water and waste air at the stack were well below permissible limits. It was postulated that the results obtained from operation of the Kahl experimental nuclear power station may have provided certain prerequisites for further relaxations, particularly with regard to the extent and frequency of tests. A brief description is included of the main instances of malperformance. (auth)

40202 THE WYLFA POWER PLANT. Atoomenergie Haar Toepassingen, 7: 70-2(Apr. 1965). (In Dutch)

The characteristics of the Wylfa power plant are briefly described with emphasis on the spherical pressure vessel and the simplification of the control chamber. (J.S.R.)

40203 USE OF DIGITAL COMPUTERS IN FRENCH CONVENTIONAL AND NUCLEAR POWER STATIONS. Jonon, P. Automatisme, 10: 14-25(Jan. 1965). (In French)

Development in plant and control methods is reviewed for the periods 1947-55 and 1955-62. The contribution of digital computers to economic monitoring, optimization, control reliability, and reduction of costs and heat rate is briefly considered. EDF stations equipped with computers, the types used, and their capabilities are listed and discussed. (auth)

40204 PRODUCTION OF NUCLEAR ENERGY. Pretsch, Joachim (Kernforschung und Kerntechnik im

Bundesministerium fuer Wissenschaftliche Forschung, Bad Godesberg, Ger.). Brennstoff-Waerme-Kraft, 17: 167-9 (Apr. 1965). (In German).

The German nuclear energy program (both short-term and long-range) is reviewed on the basis of a bibliographic survey of the publications appearing in 1964. 74 references. (J.S.R.)

40205 THE S.G.H.W. REACTOR AT WINFRITH HEATH. Comit. Nazl. Energia Nucl., Notiziario, 11: No. 5, 37-41 (May 1965). (In Italian)

The design, principal parameters, and state of construction of the steam-generating heavy-water-moderated reactor being built at Winfrith Heath are summarized. (J.S.R.)

40206 CONTROL AT TRAWSFYNYDD. Control, 9: 159-62(Mar. 1965).

The nuclear power station at Trawsfynydd was the fifth ordered in Britain for the commercial production of electricity. The design is similar to that of other first-generation stations so far built or under construction in Britain. It has two reactors fuelled with natural uranium canned in magnox (a magnesium alloy) and cooled by high-pressure carbon dioxide. Large heat exchangers (six on each reactor) raise steam at high and low pressures to drive four 145-Mw turbogenerators to give a nominal electrical output of 500 Mw. Both reactors have achieved criticality, and one reactor was operated at 580 Mw (t). (Atomdokumentation, 7: No.7, May 1965)

40207 THE FUTURE OF NUCLEAR POWER IN NEW YORK CITY. Waring, M. L. (Consolidated Edison Co., New York). EEI (Edison Elec. Inst.) Bull., 33: 85-91(Mar. 1965).

Various problems encountered in the siting of nuclear power installations in heavily populated areas are discussed. One potential threat to atomic power plant development is the liability insurance rate required. It is suggested that the evidence concerning nuclear power plant safety is overwhelmingly favorable, there being no case in which a power reactor endangered public health or safety. The feasibility and advantages of having nuclear power plants sited in large cities are discussed. Vulnerability to interference with the continuous flow of fuel (such as by strikes) and the expense of fuel storage are practically eliminated. A few truck-loads of atomic fuel, brought in about once a year, will fill the requirements of a million-kw reactor. And the entire load for a million-kw reactor can be stored in a space of 25 by 40 ft. Most important is the advantage atomic power holds over fossil fuels as concerns air pollution control. Nuclear power plants in the city will provide economic steam electric power, and virtually eliminate dependence on a long and a complex fossil fuel supply system. They will make possible the economic local storage of large quantities of fuel, and eliminate the need for costly transmission that would be required for plants located outside the city. They will provide steam for heating, air conditioning, and processing of the city's buildings and industries, as well as electricity. It is concluded that nuclear power plants can be built and operated safely in New York City, and that the superiority of these plants makes it imperative that they be used to supply much of the future thermal-electric requirements. (BBB)

40208 ELECTRICAL SECTION OF THE REACTOR AT THE FIRST ATOMIC POWER STATION. Morozov, I. V. Elektr. St., 36: 45-9(Apr. 1965).

Details are given of the operation of the electrical section of the reactor at the first atomic power station (USSR), and recommendations are made on the basis of operational experience. The layout of the reactor electrical circuit is described, and an account is given of the "safety circuit," together with its independent switchboard, on which depends the reliable operation of the plant. A description is provided of a method of pumping the emergency coolant using the main circulating unit which can be operated from the station battery. (auth)

40209 SPECIAL CHARACTERISTICS OF THE NUCLEAR POWER STATION IN THE ARDENNES. Erkes, P.; Grau, P. Energie Nucl., 7: 189-203(June 1965). (In French).

The design of the Ardennes nuclear power station sets it apart from the other stations in the same category (enriched uranium and pressurized water) in that it has a certain number of technical, thermal, and nuclear improvements. The technical improvements concern the fuel assembly (especially the type of stainless steel used for the sheathing, and the relationship between the steel and uranium dioxide volumes), the design and function of the control of reactivity by chemical poisoning, and the transfer of the irradiated fuel. The thermal and nuclear improvements are related to the production of energy in the core, the extraction of energy and its transfer to a secondary circuit, and the core loading cycle: multiregional loading with cycled fuel. Finally, some details are given about the construction of the power station, and in particular the building of the emplacements for the reactor and the auxiliary equipment. The construction progress as well as the economic perspectives are also discussed. (auth)

40210 HOW DOES THE DRAGON PROJECT STAND. Caprioglio, Pietro; De Bacci, Mario. Euratom Bull., 3: No. 3, 20-3(Sept. 1964).

The design and development of the Dragon high temperature, gas-cooled reactor project is described. The objectives, cost, and special problems of the project are discussed. The fuel cycle is also discussed; enriched uranium carbide mixed with thorium carbide is used as a fuel. An advantage of thorium is that its final product is uranium-233, a valuable fissile material, better than any other for thermal reactors. It is noted that thus far the most spectacular achievement is the completion of the experimental reactor, which has just gone critical. (J.F.P.)

40211 HEAVY WATER REACTOR NUCLEAR POWER PLANT WITH A 275-MW(e) PHWP AND A 260-MW(e) BLWP UNITS. Holt, J. O. (Canadian General Electric Co. Ltd., Peterborough, Ont.); Olsen, J. L.; Williams, N. L.; Colomb, A.; Graf, P. Neue Tech., 7: 126-40(June 1965). (In German).

A 535-Mw(e) power plant consisting of a 275-Mw(e) heavy water moderated and cooled pressure-tube reactor and a 260-Mw(e) heavy water moderated, boiling light water cooled reactor is described. (D.C.W.)

40212 DESIGN AND CONSTRUCTION OF THE OLDBURY PRESSURE VESSELS. Brown, A. Houghton (The Nuclear Power Group, Knutsford, Eng.). Nucl. Eng., 10: 254-5(July 1965).

The Oldbury Reactor is a graphite-moderated gas-cooled reactor. It is the eighth of a series built using natural uranium. The vessel was built to withstand a pressure of three times the gas pressure. The design is discussed, and the dimensions are given. The vessel penetrations and the stressing of the cables are explained. The testing program is also discussed. (J.F.P.)

40213 THE DOUNREAY FAST REACTOR. SUSTAINED FULL POWER OPERATION. Phillips, J. L. (Dounreay Experimental Reactor Establishment, Eng.). Nucl. Eng., 10: 264-7(July 1965).

The final achievement of a satisfactory state of purity of the metal coolant in the Dounreay Fast Reactor and the development of the satisfactory metallic driver fuel element are described. The testing and sampling procedures are discussed. The performance of the Mark 3 fuel elements are discussed including their design and performance at low temperatures, in the transformation range, and at high temperatures. The use of the reactor as a demonstration power reactor and as an irradiation tool is also described. (J.F.P.)

40214 A COMPUTER MODEL FOR STUDYING SGHWR SAFETY. Booth, D. L. (English Electric Co., Whetstone, Eng.). Nucl. Eng., 10: 268-71(July 1965).

A mathematical model of the prototype Steam Generating Heavy Water Reactor which was developed for analyzing the performance of the plant under severe fault conditions. This reactor concept is a heavy water moderated pressure

tube system with boiling light water coolant. The model is used to survey the behavior of an uncontrolled SGHWR under severe fault conditions as well as to demonstrate the effectiveness of remedial action. For this work an analog rather than a digital computer is used. The model is explained with treatment of the two-phase coolant, the coolant enthalpy in the channel, two phase pressure drops, variations in coolant flow around the circuit, the coolant circuit, and the steam drum. The operation of the computer is also explained. (J.F.P.)

40215 POWER REACTOR TECHNOLOGY. Volume 7, Number 3. Zinn, Walter H.; Dietrich, J. R. (General Nuclear Engineering Corp., Dunedin, Fla.). Summer 1964. $0.70(GPO) (domestic), $0.90(GPO) (foreign). (One of the Technical Progress Reviews prepared quarterly for the Division of Technical Information, USAEC). 130p.

Ten sections are included; separate abstracts have been prepared for all. (T.F.H.)

For abstracts of individual sections see: 38814, 40135, 40163, 40164, 40172, 40216, 40217, 40218, 40220, and 40267.

40216 RESOURCES AND FUEL CYCLES. Power Reactor Technol., 7: No. 3, 201-5(Summer 1964).

The economics of various fuel cycling methods for power reactors are reviewed. The fuel cycle schemes used in SENN and CANDU are cited as examples. (T.F.H.)

40217 DESIGN AND CONSTRUCTION PRACTICE: PATHFINDER AND BONUS. Mitchell, III Walter. Power Reactor Technol., 7: No. 3, 276-312(Summer 1964).

Design and construction practices followed in Pathfinder and BONUS are compared and contrasted, as regards general features, boiler and superheater fuels, control elements, pressure vessels, core structures, control and instrumentation, recirculation systems, turbine-generator systems, condensate systems, feedwater systems, plant arrangement and containment, and purification and radioactive waste disposal. (T.F.H.)

40218 SPECIFIC REACTOR TYPES. Power Reactor Technol., 7: No. 3, 322-7(Summer 1964).

The nucleonic and mechanical characteristics of a Zircaloy core structure for the N.S. Savannah reactor are analyzed. Design parameters for the Whiteshell Reactor No. 1 (WS-1) reactor are presented. The evaluation of Zr alloys and SAP for use in organic-cooled reactors is discussed. (T.F.H.)

Production Reactors

40219 (RL-SA-21) APPLICATIONS OF NPR TECHNOLOGY TO THE NATIONAL NUCLEAR PROGRAM. Kosmata, H. R. (General Electric Co., Richland, Wash. Hanford Atomic Products Operation). Feb. 2, 1965. Contract AT(45-1)-1350. 2p. (CONF-650602-3). Dep. mn; CFSTI, $1.00 cy, $0.50 mn.

From American Nuclear Society 11th Annual Meeting, Gatlinburg, Tenn.

The fitting of the N reactor in the total national nuclear program is discussed. Possible power ratings and applications of the N reactor to desalination are discussed. (M.O.W.)

40220 CONTAINMENT, RADIATION CONTROL, AND SITING. Power Reactor Technol., 7: No. 3, 265-8(Summer 1964).

An outline is given of the design and operation of the vented containment system used in NPR. (T.F.H.)

Propulsion and Space

See also ENGINEERING — Space Propulsion.

Refer also to abstracts 38836 and 39442.

40221 (LA-3229) PROCEEDINGS OF AN ADVANCED NUCLEAR PROPULSION SYMPOSIUM. Cooper, Ralph S. (comp.) (Los Alamos Scientific Lab., Univ. of California, N. Mex.). Jan. 1965. Contract W-7405-eng-36. 371p. (CONF-640410). Dep.(mn); $7.00(cy), 6(mn) CFSTI.

Separate abstracts are prepared for the 20 included papers. (M.O.W.)

For abstracts of individual papers see: 40154, 40155, 40222, 40223, 40224, 40225, 40226, 40227, 40228, 40229, 40230, 40231, 40232, 40233, 40234, 40235, 40236, 40237, 40238, and 40239.

40222 (LA-3229, pp 10-47) SPACE TRANSPORTATION. Hunter II, M. W. (Bellcomm, Inc., Washington, D. C.).

A general report covering the basic ground rules for space transportation is presented. Such things as planetary transportation and the type of rockets most suitable are discussed. Many aspects of the overall program are discussed. (M.O.W.)

40223 (LA-3229, pp 48-62) BNL FLUIDIZED BED STUDIES. Hatch, L. P. (Brookhaven National Lab., Upton, N. Y.)

Experimental studies were carried out on the overall performance and mechanical aspects of rotating fluidized beds. These studies and results from them are presented. (M.O.W.)

40224 (LA-3229, pp 63-82) FLASH X-RAY ANALYSIS OF FLUIDIZED BEDS. Romero, Jacob B. (Boeing Co., Seattle, Wash.).

The flash x ray machine was used to study the internal structure of fluidized beds and to make basic measurements on their properties. The most important results obtained indicate that the fluidized bed consists of distinct dilute and dense phases, with the latter maintaining constant properties — particularly density. The flow through the dilute phase is in the form of gas bubbles, whose sizes and frequencies increase with flowrate and whose velocities follow closely the theory of Davies and Taylor. The constancy of dense phase bed density with flowrate provides good evidence on the validity of the Two-Phase Theory of Fluidization. Observations of bubble sizes, shapes, and velocities strongly suggest a liquidlike nature for the fluidized bed. (M.O.W.)

40225 (LA-3229, pp 83-5) FLUIDIZED BEDS. Juveland, A. C.; Deinken, H. P.; Dougherty, J. E. (Los Alamos Scientific Lab., Univ. of California, N. Mex.).

Experimental work is reported on aspects of fluidized beds. Heat transfer, evaporation losses at high temperature, and mechanical properties are the main topics reported. References are given for supplementary information. (M.O.W.)

40226 (LA-3229, pp 86-8) FLUIDIZED BEDS. Cooper, Ralph (Los Alamos Scientific Lab., Univ. of California, N. Mex.).

A number of aspects of the fluidized bed concept are examined. Previous literature is used for obtaining calculations on criticality, heat transfer, and fuel loss. (M.O.W.)

40227 (LA-3229, pp 90-110) THE LIQUID-CORE NUCLEAR ROCKET. Grey, Jerry (Princeton Univ., N. J.).

A multiple arrangement of fuel elements is examined. The introduction of a low-temperature, highly efficient hydrogenous moderator in the cooler portions of the reactor is considered. These two considerations were effective in reducing the critical mass by several orders of magnitude, reducing the dimensions of the system by almost an order of magnitude, and increasing the thrust-weight-ratio by several orders of magnitude. A detailed description of the two considerations is presented. Experimental work describes bubble flow and heat transfer in configurations resembling those of the liquid-core nuclear rocket fuel element. (M.O.W.)

40228 (LA-3229, pp 111-15) EXPERIMENTAL WORK IN RELATION TO THE GLOW-PLUG CONCEPT. McKee, J. W. (General Electric Co., Santa Barbara, Calif.).

A central problem in the application of gaseous fission reactors to space propulsion is to reduce the amount of fissionable material which leaves the system with the propellant. A glow-plug propulsion system is designed to be used as a partition. Experimental work to determine the possible performance of the glow-plug propulsion system is discussed. (M.O.W.)

40229 (LA-3229, pp 116-36) THE TRANSPARENT PARTITION GASEOUS CORE REACTOR CONCEPT. Knapp, D. E. (Douglas Aircraft Co., Inc., Santa Monica, Calif.).

Properties of transparent materials, which could possibly be used for the partition, are considered. The thermal conductivities, thermal stress characteristics, optical absorption, and the chemical stability of BeO, sapphire, and fused quartz are considered. (M.O.W.)

40230 (LA-3229, pp 137-47) WORK ON NUCLEAR LIGHT BULB AT UAC RESEARCH LABORATORIES. McLafferty, George H. (United Aircraft Corp., East Hartford, Conn. Research Labs.).

The main problem in a nuclear light bulb which is different from other gaseous nuclear rocket concepts is the problem of annealing the radiation-induced coloration in the transparent wall material. Investigations with fused silica as the wall material are reported. It is believed that the absorption of light energy in a transparent wall might be on the order of a quarter to a half percent of the energy radiated through the wall. Measurements of the amount of absorption of light energy in several commercial samples of fused silica are included. (M.O.W.)

40231 (LA-3229, pp 149-76) HIGH-TEMPERATURE GAS INTERACTIONS. Grey, Jerry (Princeton Univ., N. J.).

Some experimental techniques for study of extremely high-temperature gas interactions involving the extremely high heat transfer rates and other environmental problems normally encountered in gaseous-core reactor concepts are presented. A method for obtaining total radiation measurements of argon, nitrogen, and helium gases is briefly discussed. A technique to determine the mixing characteristics of a partly ionized gas with a cool coaxial flow is discussed. (M.O.W.)

40232 (LA-3229, pp 177-9) COAXIAL FLOW GASEOUS NUCLEAR REACTOR CONCEPT. Rom, Frank E. (National Aeronautics and Space Administration, Cleveland, Ohio. Lewis Research Center).

A brief description of the coaxial flow gaseous nuclear reactor concept is given. In this concept separate coaxial streams of uranium (or plutonium) and hydrogen are introduced into a reflector moderated cavity. The hydrogen flows coaxially and concentric with the uranium core. The uranium flows at a lower velocity than the hydrogen to maintain an acceptable ratio of uranium-to-hydrogen mass flow ratio. The resulting mixture of hydrogen and uranium is exhausted through a nozzle to produce thrust. (M.O.W.)

40233 (LA-3229, pp 180-207) COAXIAL FLOW RESEARCH STUDIES. Ragsdale, Robert G. (National Aeronautics and Space Administration, Cleveland, Ohio. Lewis Research Center).

Fluid mechanics, heat transfer, and nucleonics of coaxial flow are discussed. Under fluid mechanics, an analysis of a coaxial flow system is discussed. The experimental program on heat transfer is described. It is primarily aimed at radiation heat transfer to a transparent gas made opaque by the addition of small solid particles. Previous work on nucleonics is reviewed. (M.O.W.)

40234 (LA-3229, pp 208-21) COAXIAL FLOW RADIATION HEAT TRANSFER ANALYSIS. Kascak, Albert F. (National Aeronautics and Space Administration, Cleveland, Ohio. Lewis Research Center).

An analysis of the radiant heat transfer in coaxial flow is presented. A physical model is set up for the heat transfer analysis. Assumptions for this model are described, and the results from these assumptions are presented. (M.O.W.)

40235 (LA-3229, pp 222-36) GAS CORE REACTORS. Stumpf, Henry J. (California Inst. of Tech., Pasadena).

The two major problems confronting the gaseous vortex scheme are containment of the fuel and heat deposition in the tube walls. These two problem areas and their effect upon the system are discussed. (M.O.W.)

40236 (LA-3229, pp 237-50) SEPARATION MEASUREMENTS IN BINARY SPECIES GASEOUS VORTEX FLOWS AND FLOW VISUALIZATION STUDIES IN A WATER VORTEX. Pivirotto, T. J.; Roschke, E. J. (Jet Propulsion Lab., Calif. Inst. of Tech., Pasadena).

A gaseous-core nuclear reactor propulsion concept is reviewed briefly, and the major fluid dynamics problems associated with this concept are discussed. Some results of the experimental binary separation and flow visualization studies are presented. Analytical studies of various types were made. Experiments were held at room temperature, and no tests were conducted on flows in which there were reactions or heat transfer. (M.O.W.)

40237 (LA-3229, pp 251-85) VORTICES AND VORTEX MATRICES. Rosenzweig, Martin L.; Lewellen, Steve (Aerospace Corp., El Segundo, Calif.).

The fluid dynamics of vortex flows are considered. Most of the work is with a single fluid. The problems of pressure diffusion and those of fission fragment heating are considered. Theoretical work concerning the end-wall boundary layer growth in these vortex tubes and the interaction with the primary vortex flow is presented. A diagram of a vortex matrix is presented and discussed. (M.O.W.)

40238 (LA-3229, pp 286-312) NUCLEAR PROPULSION SCHEMES USING MAGNETOHYDRODYNAMIC CONVERSION TECHNIQUES. Rosa, Richard J.; Brogan, Thomas R. (Avco-Everett Research Lab., Everett, Mass.).

A brief description of an MHD generator is presented. Possible schemes for using the MHD generator coupled with nuclear reactors are discussed. The brief history of the MHD generator development is reviewed. (M.O.W.)

40239 (LA-3229, pp 315-43) CRITICALITY OF GAS CORE REACTORS. Holl, R. J. (Douglas Aircraft Co., Inc., Santa Monica, Calif.).

Some of the nuclear calculations concerning the criticality of gas core reactors are described. Methods for calculation are described and were used to survey fuel materials, reflector materials, core dimensions, and reflector thicknesses. (M.O.W.)

40240 (LA-3263) PULSED NEUTRON ANALYSIS IN THE LOS ALAMOS COUPLED REACTOR EXPERIMENT. Chezem, Curtis G.; Helmick, Herbert H. (Los Alamos Scientific Lab., Univ. of California, N. Mex.). Mar. 16, 1965. Contract W-7405-eng-36. 17p. Dep. mn; CFSTI, $1.00 cy, $0.50 mn.

A general kinetic model is derived to describe the time behavior of the neutron populations, $G_i(t)$, in each core of a lumped-parameter m-core array where Core No. 1 is pulsed. For a two-core array, the model yields: $G_1(t) = \Sigma_{i=1}^{4} A_i e^{R_i t}$ and $G_2(t) = \Sigma_{i=1}^{4} B_i e^{R_i t}$, where the A_i and B_i are functions of the neutronic properties, coupling parameters and reactivity settings of the system, R_1 and R_2 are Rossi-α-like parameters "split" by the coupling effect, and R_3 and R_4 are "split" terms involving an interaction time lag. To test the kinetic model, one of the cores of a two-core array of Kiwi-B4 reactors was repetitively pulsed by a 14-Mev neutron pulse generator and the $G_i(t)$ were observed. Agreement between the experimental and theoretical impulse responses is quite good. The usefulness of the interaction time lag concept is questioned. (auth)

40241 (LA-DC-6845) MEASUREMENT OF THE POWER-TO-CORE TEMPERATURE TRANSFER FUNCTION OF KIWI-B-4E. Balcomb, J. Douglas (Los Alamos Scientific Lab., Univ. of California, N. Mex.). [1964]. Contract W-7405-eng-36. 15p. (CONF-650610-19). Dep. mn; CFSTI, $1.00 cy, $0.50 mn.

From American Institute of Aeronautics and Astronau-

tics, Propulsion Joint Specialists Conference, Colorado Springs.

During the full power hold of the restart of the Kiwi-B-4E reactor, a noise signal was fed into the temperature control system in order to cause reactor power perturbations. The purpose was to obtain a measurement of the dynamic response of core temperature to changes in power over a range of frequencies. The resulting power perturbations were 67 Mw peak-to-peak and 10.6 Mw rms and the observed temperature perturbations were 2.9 to 5.7°R rms depending on the sensor location. The results were analyzed utilizing the crosscorrelation method and agree fairly well with the mathematical models which were used for stability analysis and controller design. The range of frequencies covered in the experiment is from 0.025 to 0.7 cps. The experiment shows that good quality data can be obtained from one or more minutes of steady-state reactor operation without interference to the control systems, the operators, or the reactor performance. (auth)

40242 (LA-DC-7118) ADVANCED NUCLEAR PROPULSION CONCEPTS. Cooper, Ralph S. (Los Alamos Scientific Lab., Univ. of California, N. Mex.). [1965]. Contract W-7405-eng-36. 38p. (CONF-650711-2). Dep. mn; CFSTI, $2.00 cy, $0.50 mn.

From AIAA 2nd Annual Meeting and Technical Demonstration, San Francisco.

This survey of high thrust nuclear propulsion beyond solid core reactors shows many concepts in the research phase but very few ready for engineering development. Fluidized particle beds offer a modest increase in I_{sp} to about 1100 seconds and the possibilities of high power density and ease of reuse. Liquid core reactors may give up to 1500 seconds, depending upon the fuel vaporization in flowing hydrogen, but are limited to modest thrust by the flow rate of bubbles. Gas core reactors could go to 2500 seconds if the interrelated problems of fluid flow, heat transfer and nuclear criticality could be solved. Heat transfer is usually by radiation which leads to high fuel temperatures (≥20,000°K), and to high pressures (≥200 atm), making any nuclear experiments very difficult. The various concepts differ by the flow patterns designed to reduce the fuel loss rate to acceptable proportions, and include coaxial and vortex flows, and the use of magnetohydrodynamic effects. The closed pulse system requires large thrust chamber mass and several thousand pulses of very low yield. The open pulse system (Orion) seems technically feasible at 2500 seconds but needs a nuclear ablation test for confirmation and its eventual use is clouded by political considerations. (auth)

40243 (LA-DC-7169) PROJECT ROVER CRYOGENIC EVALUATION LABORATORY. Stokes, R. W. (Los Alamos Scientific Lab., Univ. of California, N. Mex.). [nd]. Contract W-7405-eng-36. 28p. (CONF-650802-2). Dep. mn; CFSTI, $2.00 cy, $0.50 mn.

From Cryogenic Engineering Conference, Houston, Tex.

Project Rover is a program to develop a nuclear rocket engine for space applications. The Cryogenic Evaluation Laboratory supports this program by testing cryogenic components related to the program test effort and by supplying data pertinent to cryogenic test facility operations. A complete description of the laboratory is presented and is supported by facility photographs. A description of the liquid hydrogen test program is included which presents the results of the laboratory activities. They include flowrate element calibration, frequency and step response measurements, cryogenic valve tests, line chilldown studies, dynamic dewar pressurization studies, dynamic LH_2 consumption studies, and cryogenic flange chilldown studies. (auth)

40244 (LA-DC-7170) LIQUID HYDROGEN IN NUCLEAR ROCKET TESTING. Edeskuty, Frederick J. (Los Alamos Scientific Lab., Univ. of California, N. Mex.). [1965]. Contract W-7405-eng-36. 32p. (CONF-650611-3). Dep. mn; CFSTI, $2.00 cy, 10.50 mn.

From Symposium on Heat Flow below 100°K and its Technological Applications, Grenoble, France.

The testing of liquid hydrogen for use as a propellant for rockets is reported. Some of the operational and design problems of the cryogenic systems at the Nuclear Rocket Development Station are discussed. The most prominent problems discussed are: stress analysis in liquid hydrogen transfer lines, turbine energy source, perlite compaction, dewar cooldown, and safety. (M.O.W.)

40245 (N64-23519) RIFT NRDS OPERATIONS PLAN. Report 504. (Lockheed Missiles and Space Co., Sunnyvale, Calif.). Apr. 1964. Contracts NAS 8-5600 and NAS 8-9500. 143p. (NASA-CR-56561; NSP-64-24). CFSTI, $11.00 cy.

The plans for carrying out the RIFT Stage Captive Test Program at the Nuclear Rocket Development Station in Nevada are described. The following are discussed: (1) objectives of the program, governing policies, directives, and assumptions; (2) the Nuclear Rocket Development Station; (3) facilities test equipment, and test articles; (4) organization; and (5) concept and sequence of operations. (CFSTI)

40246 (N64-29787) INTRODUCTION TO NUCLEAR PROPULSION. Lectures 5 and 6. SHIELD PHYSICS. Moteff, John (General Electric Co., Cincinnati, Ohio. Nuclear Materials and Propulsion Operation). [1963]. Contract NAS8-5215. 34p. (NASA-CR-52958; GEMP-190d). CFSTI, $6.60 cy.

A summary of basic radiation physics is presented. Descriptions are given of gamma-ray cross sections, neutron cross sections, relaxation length, radiation units, and radiation dosimetry and conversion. Under shielding calculation methods, descriptions are presented of: narrow beam attenuation, broad beam attenuation with buildup, inverse square law, radiation from shielded distributed source with self-absorption heat generation in shields, and scattering of radiation. (M.O.W.)

40247 (N64-29788) INTRODUCTION TO NUCLEAR PROPULSION. Lectures 7 and 8. REACTOR SYSTEM DESIGN. Motsinger, Russell E. (General Electric Co., Cincinnati, Ohio. Nuclear Materials and Propulsion Operation). [1963]. Contract NAS8-5215. 40p. (NASA-CR-52957; GEMP-190e). CFSTI, $7.60 cy.

The main topics under discussion are; the general philosophy of reactor design in the initial design sequence, nuclear characteristics and control effects, afterheat and aftercooling, mechanical design considerations, and assessment of uncertainty factors in the initial design sequence. (M.O.W.)

40248 (NUS-180) NURSE-1—A NUCLEAR ROCKET SAFETY EVALUATION CODE FOR THE CONTROL DATA 3600. Couchman, M. L.; DeAgazio, A. W.; Kim, Y. S. (Nuclear Utility Services, Inc., Washington, D. C.). Dec. 1964. 282p. Dep. mn; CFSTI, $6.00 cy, $1.50 mn.

The NURSE-1 Code may be used to evaluate the radiation hazards resulting from rapid releases of fission products from nuclear rocket engines. The original work on NURSE-1 was done in FORTRAN II on an IBM 7090 with 32K memory. However, owing to a change in computer assignment, NURSE-1, as released, is programmed in FORTRAN 3600 for use on a CONTROL DATA 3600. NURSE-1 requires 64K memory. Six tapes are used in addition to those required by the SCOPE Monitor System. Generation of a library tape containing nuclear and atmospheric diffusion data necessary for the operation of the code, and the library data are described. The program is used to determine several different doses at positions down- and cross-wind from excursions for releases occurring in the lower atmosphere. The code has several options which permit selection of the kinds of doses to be calculated. The models and parameters employed are believed to represent the best information available. It is anticipated that the models and parameters may change as the nuclear rocket program matures, and the NURSE-1 code is designed for ready replacement of models or parameters as better information becomes available. (auth)

40249 (TID-22014) HEAT TRANSFER AND HYDRAULIC STUDIES FOR SNAP-4 FUEL ELEMENT GEOMETRIES.

Topical Report No. 4. Biderman, R.; Matzner, B. (Columbia Univ., New York. Engineering Research Labs.). Sept. 16, 1964. Contract AT(30-3)-187. 22p. Dep. mn; CFSTI, $1.00 cy, $0.50 mn.

The operation of a 12-Rod Test Section 5 is described. Test Sections 1 and 2 were uniformly heated. In Test Sections 3 and 4 the heat flux on the two central rods was 2.6 and 1.5 times greater than the heat flux on each of the ten outer rods. In these four experiments it was observed that the two central rods exhibited considerably higher burnout heat fluxes than the outer rods which faced the unheated walls of the housing tube. In Test Section 5 the minimum spacing between the outer rods and shroud walls was increased from 0.022″ to 0.032″ in order to improve the burnout performance of the outer rods. Nineteen burnout points (Runs 91-109) were taken with Assembly A of Test Section 5 before a shut down was forced due to test section leaks. After repairs were made 10 burnout points (Runs 110-119) were then obtained with Assembly B before an unintentional physical burnout ended the running period. The results from Assembly B gave higher values of pressure drop and burnout heat flux than for Assembly A, which indicated a more concentric orientation of rod bundle "B" with respect to the housing tube. The burnout performance of all the runs from Assembly B and most of the runs from Assembly A was better than those obtained previously using Test Sections 1 and 2 which had a closer outer rod to housing tube minimum spacing. (auth)

40250 THE STEAM GENERATOR OF THE NERO PROJECT AND THE SCALE MODEL STUDIES. Heshuijsen, W. F. Atoomenergie Haar Toepassingen, 7: 61-70(Apr. 1965). (In Dutch)

In the NERO design of a marine reactor, two vertical steam generators are projected. Tests were carried out with various types of primary steam separators and secondary steam dryers on a scale model in a similar installation. After a description of the heat transfer calculations, the superheating and the scale model, the testing program was discussed. (tr-auth)

40251 DEVELOPMENT OF THE PWR FOR SHIP PROPULSION. Taylor, A. J. (Babcock and Wilcox Ltd., London). Nucl. Eng., 10: 258-9(July 1965).

Study of ship operational conditions, nuclear fuel costs, and the capital cost of nuclear units must all be considered in the prospective development of the pressurized water reactor for ship propulsion. Commercial ship operators in the United States are considering re-equipping their fleet with nuclear vessels. The economics of annual tonnage, nuclear fuel, and plant capital are discussed. The seacore design for the reactor is also discussed. A need for a prototype ship powered by a nuclear reactor is suggested which could demonstrate the ability of an advanced reactor plant to meet the operating needs of marine service. (J.F.P.)

40252 THE CONTROL OF NUCLEAR ROCKET ENGINES IN THE LOW POWER–NO FLOW REGION. Hohmann, Garold L. (Westinghouse Electric Corp., Pittsburgh); Strait, Bobby G. New York, American Inst. of Aeronautics and Astronautics, 1965, Preprint AIAA Paper No. 65-597, 12p. $1.00. (CONF-650610-12). ORINS.

From American Inst. of Aeronautics and Astronautics, Propulsion Joint Specialists Conference, Colorado Springs.

Flight missions using nuclear reactor propulsion will require completely automatic control systems. These systems must include a method of repeatably changing the reactor from a subcritical shutdown condition to a power level which will allow operation by the high power control system. An automatic startup technique developed for the NERVA nuclear engine increases engine power by programming the control rods out, increasing reactivity, in an open loop manner. The open loop program is derived from system variables and takes the form of an exponential movement of the control rods to a position near delayed critical and a slow linear ramp movement of the rods from this position outward until the high power control system is switched in returning the control rods to their delayed critical position. In this manner, only one range of nuclear detectors covering three or four decades of power is required for full power operation. The total startup time through six to ten decades of power can be safely achieved in several seconds or adjusted to take several minutes. This technique was first successfully tested on a "KIWI" reactor in May, 1964. (auth)

40253 GROUND TEST RADIATION EXPERIENCE AT THE KIWI B-4 TESTS. Malenfant, Richard E.; Graves, Glen A. (Los Alamos Scientific Lab., N. Mex.). New York, American Inst. of Aeronautics and Astronautics, 1965, Preprint AIAA Paper No. 65-593, 14p. $1.00. (CONF-650610-11). ORINS.

From American Inst. of Aeronautics and Astronautics, Propulsion Joint Specialists Conference, Colorado Springs.

An extensive series of radiation level measurements from the Kiwi B-4 tests at NRDS have provided the detailed information on the radiation environments from ground operation of propulsion reactors which is necessary for the prediction and evaluation of future problems. The complexity of test site areas almost precludes obtaining this information by calculation alone, particularly post-shutdown, the condition of greatest practical interest. The components (direct beam, air scatter, and activation) of the total dose rates post-shutdown were separated and identified by comparing measurements taken before and after reactor removal from the test area. These values were well-confirmed through cross-check measurements on reactors free of activation fields. The isolated reactors exhibited lower dose fields than expected. No evidence of local fission product contamination was found. Area activation was relatively high—at some post-shutdown times and distances, activation and reactor dose rates were comparable—but the activation decayed fairly rapidly with effective half-life groupings near 2½ hours, 15 hours, and 30 days. Reactor shields will be needed to control activation and permit sustained area occupation after tests of large energy release—e.g., 10^7 megawatt-sec—but with them, operations like dewar refilling can proceed steadily after about three days. (auth)

40254 PROGRESS IN THE DEVELOPMENT OF REFRACTORY METALS FOR USE IN NUCLEAR ROCKET NOZZLES. Gibson, David C.; Fox, H. M.; Walter, Robert J.; Kennedy, James J. (Rocketdyne, Canoga Park, Calif.). New York, American Inst. of Aeronautics and Astronautics, 1965, Preprint AIAA Paper No. 65-602, 63p. $1.00. (CONF-650610-16). ORINS

From American Inst. of Aeronautics and Astronautics, Propulsion Joint Specialists Conference, Colorado Springs.

A program directed toward the development of refractory materials for use in nuclear rocket nozzles is reviewed. It is proposed that the use of refractory metals in applications where heat fluxes are high can result in extended capability or improved cycle life. The properties of refractory metals which permit this are described along with strains experienced by refractory and conventional materials in representative applications. The progress in the fabrication of basic nozzle tubing is discussed. Materials used here are Ta-10W and Mo-50Re. Developments in the application of coatings to refractory metals to protect against hydrogen embrittlement are reviewed. Results with a 1-mil coating of tin-aluminum are illustrated and discussed. Finally, an experimental method for evaluating nozzle-tube materials at simulated operating conditions is presented. The device allows a single-nozzle tube to be subjected to simulated operating conditions. The strain in the material resulting from the temperature difference between the crown and the back side of the tube is simulated, and the temperatures are achieved by electrical resistance heating the crown of the tube. The device is described and illustrated. (auth)

40255 IMPROVEMENTS IN MARINE PROPULSION UTILISING ENERGY FROM NUCLEAR FISSION. Pedrick,

Arthur Paul. British Patent 997,738. July 7, 1965. Filed Mar. 20, 1963.

A propulsion system is described for a ship, surface or submerged, having within its hull a nuclear reactor. Heat from the reactor evaporates water derived from that in which the vessel is buoyant or immersed, and the steam produced by such evaporation is restricted against free expansion so that it acquires kinetic energy in the form of an exhaust jet. The reactive thrust from the jet operates to propel the vessel. A plurality of such propulsion units are mounted on either side of the main machinery spaces or on either side of the rudder near the stern of the ship, and the evaporation takes place in these externally mounted units. In a submarine, the evaporation takes place in an annular space extending around the main pressure shell. The propulsion system can also be incorporated into the space in ships previously occupied by a steam boiler with steam turbine system to convert the ship to one powered by a nuclear reactor. (B.L.M.)

Research and Test Reactors

Refer also to abstracts 39253 and 39265.

40256 (AERE-M-1590) ATTEMPTS TO DETERMINE THE FAST-NEUTRON SPECTRUM IN A THERMAL REACTOR BY MEANS OF Li^6 AND He^3 SEMICONDUCTOR SPECTROMETERS. Silk, M. G. (Atomic Energy Research Establishment, Harwell (England)). May 1965. 24p. Dep.; BIS, $0.70; HMSO, 3s. 6d.

Helium-3 and lithium-6 semiconductor neutron spectrometers were used to determine the fast-neutron spectrum in GLEEP, a thermal reactor with a graphite moderator. A fast electronic circuit of resolving time 100 nsec was used to eliminate pile-up effects as far as possible, and by combining the results obtained from both spectrometers the neutron spectrum was determined over an energy range from 0.8 to 6.4 Mev. The experimental spectra are shown to be in agreement with theoretical spectra derived by Monte-Carlo calculations. The results suggest that silicon-neutron reactions are relatively unimportant in this case. A small peak observed in the lithium-6 spectra may confirm that there is a discontinuity in the cross-section for the $^6Li(n,\alpha)^3H$ reaction in the neutron-energy region between 2 to 2.5 Mev. (auth)

40257 (ANL-7046(p.67-77)) ADVANCED SYSTEMS RESEARCH AND DEVELOPMENT. (Argonne National Lab., Ill.).

Development of the Argonne Advanced Research Reactor is described. (J.R.D.)

40258 (BNL-9237) HFBR CONTAINMENT TEST, APRIL 9, 10, 1965. Tichler, P. R. (Brookhaven National Lab., Upton, N. Y.). June 1965. Contract AT(30-2)-Gen-16. 32p. Dep. mn; CFSTI, $2.00 cy, $0.50 mn.

Safety considerations require that the leak rate from the HFBR containment building should not exceed 5% of the building volume per day at a 2 psi overpressure. The results of a test to measure the HFBR leak rate are presented. The test consisted of pressurizing the containment building with a blower to some initial pressure and observing the pressure decay with time. The measured average leak rate, using the reference volume method was 3.7 ± 0.3%/day. This average leak rate, which was obtained during a period in which the over-pressure varied from 2.01 to 1.36 psi, can be prorated to a leak rate at 2 psi overpressure by making the conservative assumption that the leak rate is directly proportional to the overpressure. On this basis a leak rate of 4.4 ± 0.4%/day is obtained. (auth)

40259 (ORNL-TM-1181) OAK RIDGE RESEARCH REACTOR QUARTERLY REPORT, JANUARY, FEBRUARY, AND MARCH OF 1965. Casto, W. R.; Tabor, W. H.; Hurt III, S. S. (Oak Ridge National Lab., Tenn.). May 25, 1965. Contract W-7405-eng-26. 37p. Dep. mn; CFSTI, $2.00 cy, $0.50 mn.

ORR operating time was reduced from 90.6 to 78.9% during this quarter, because there were two major shutdowns and an emergency shutdown of 3½ days for repair of two reactor water pump motors. Two newly designed ^{16}N channels were completed and connected to the slow scram system. These instruments will act as a safeguard for detecting ruptured fuel elements and will also indicate reactor power. Extraneous metal resulting from scoring became deposited between the shim-rod piston and the drive tube and caused binding between these parts on the No. 5 drive unit. The coupling between the drive motor and the gear box on No. 6 drive unit was repaired. New stainless steel canisters containing charcoal for I_2 adsorption were installed in the pressurizable off-gas system. An analysis of charcoal that had been in use as an I_2 adsorber for 14 months was made. The sample showed slight degradation as compared with new charcoal. Tests determining the feasibility of using fuel elements containing 240 grams of ^{235}U were started. A series of temperature measurements on depleted fuel elements in the shipping carrier was made. The highest temperature recorded (150°F) is safe. (auth)

40260 (ZFK-RN-17(p.68-74)) BEMERKUNGEN ZUR WASSERBOSCHAFFENHEIT DER PRIMARKREISLAUFE DER FORSCHUNGSREAKTOREN DER SOZIALISTISCHEN LANDER. (Remarks on the Quality of the Primary Circuit Water in Research Reactors of the Socialist Countries). Westphal, D. (Zentralinstitut fur Kernphysik, Rossendorf bei Dresden (East Germany)). Dep.(mn).

The specifications given for the water in research reactors of the socialist countries are evaluated, and the experiences gained in water purification with ion exchangers are indicated. The water parameters of the reactors are tabulated. (J.S.R.)

40261 (ZFK-RN-17(p.179-98)) UBERBLICK UBER DIE IM JAHRE 1961 AM ROSSENDORFER FORSCHUNGSREAKTOR DURCHGEFUHRTEN ARBEITEN. (Review of the Work Carried Out in the Year 1961 at the Rossendorf Research Reactor). Westphal, D.; Findeisen, A. (Zentralinstitut fur Kernphysik, Rossendorf bei Dresden (East Germany)). Dep.(mn).

Testing of a lithium exchanger, improvement of the methods of chemical analysis with continuous monitoring of impurities in the water of the primary circuit, and gas analytical measurements for the determination of the H_2 concentration in the out-gas are determined. (J.S.R.)

40262 (ZFK-RN-17(p.25-31)) KONDUKTOMETR NEPRERYVNOGO DEISTVIYA DLYA IZMERENIYA UDEL'NOGO SOPROTIVLENIYA VODY V ZAMKNUTYKH KONTURAKH. (Conductometer for Continuous Measurements of Specific Water Resistance in Closed Loops). Loginov, V. A. (Akademiya Nauk SSSR, Moscow. Institut Atomnoi Energii).

The quantity of dissolved salts in the coolant water is usually estimated from the resistivity of the water, measured using a conductometer. The requirements of geometry, measuring range, temperature compensation, measurement accuracy, and continuous measuring for the conductometer for the RPT reactor are listed. The conductometer primary pickup element and the temperature compensation circuit are described. The variation of the combined resistance of the conductometer pickup with temperature and with water resistivity is shown. (M.J.T.)

40263 (ZFK-RN-17(p.32-43)) ERFAHRUNGEN MIT DER KONTINUIERLICHEN MESSUNG DES pH-WERTES UND DER LEITFAHIGKEIT DES DESTILLIERTEN WASSERS IM PRIMARKREISLAUF DES TSCHECHOSLOWAKISCHEN FORSCHUNGSREAKTORS WWR-S IN REZ. (Experiences With the Continuous Measurement of the pH Value and the Conductivity of the Distilled Water in the Primary Circuit of the Czechoslovakian Research Reactor WWR-S in Rez). Vozenilek, Fr. (Ustav Jaderneho Vyzkumu, Ceskoslovenska Akademie Ved, Rez).

The method and circuits for the continuous measurement of the pH and conductivity of the distilled water are briefly

described. The advantages and disadvantages of the installation of the measurement devices over the active zone of the reactor are discussed. The effect of the purification filter on the pH was indicated. (J.S.R.)

40264 (ZFK-RN-17(p.54-67)) BERICHT UBER DIE WASSERSEITIGEN ERFAHRUNGEN AM UNGARISCHEN FORSCHUNGSREAKTOR. (Report on the Water-Side Experiences on the Hungarian Research Reactor). Nagy, O. (Magyar Tudomanyos Akademia, Budapest).

The cleansing procedures used for the container and tubes are briefly described, and the composition of the water in the primary circuit is given. The mixing bed for the purification in the primary circuit and the purification procedure is described. Corrosion phenomena and activity of the secondary circuit are indicated. (J.S.R.)

40265 THE APPLICATION OF THE P.E.R.T. METHOD TO THE ESSOR PROJECT. Tiberghien, P. Y. (C.C.R. Ispra, Italy); Rouviere, J. Energie Nucl., 7: 204-13(June 1965). (In French)

The PERT method (Program Evaluation and Review Technique) allows the establishment of a work schedule, to control it and to eventually modify it during utilization. The principles of this technic are discussed and its application (for the design and installation phases) to the building of the Essor reactor, a test reactor of the Orgel system, which uses heavy water as a moderator and an organic liquid for cooling is reported. (auth)

40266 THE NRE PROJECT—A NEW CRITICAL FACILITY AT THE EIR FOR ZERO REACTIVITY EXPERIMENTS. Lutz, H. R.; Meier, R. W. (Eidgenoessisches Institut fuer Reaktorforschung, Wurenlingen, Switzerland). Neue Tech., 7: 111-25(June 1965). (In German).

As an addition to the existing facilities for physical studies of D_2O-moderated reactor lattices at the EIR, a project for a critical facility of the zero-reactivity type was developed. The reasons for the choice of this concept are given. The status of the design study as of April 1965 is described in detail, and an explanation of the principle of zero-reactivity experiments is given. The theory for evaluating these experiments and calculations for determining nuclear characteristics are presented. (auth)

40267 OPERATING EXPERIENCE. Power Reactor Technol., 7: No. 3, 313-21(Summer 1964).

Operating experience and performance of the Indian Point Power Reactor, the Plutonium Recycle Test Reactor, the Savannah River Components Test Reactor, and the Experimental Boiling Water Reactor are reviewed. (T.F.H.)

WASTE DISPOSAL AND PROCESSING

See also BIOLOGY AND MEDICINE — Ecology.
CHEMISTRY — Radiochemistry.
CHEMISTRY — Separation Processes and Procedures.
HEALTH AND SAFETY.

Refer also to abstract 38329.

40268 (BNWL-63) A SEQUENCE FOR PREDICTING WASTE TRANSPORT BY GROUND WATER. Nelson, R. W. (Battelle-Northwest, Richland, Wash. Pacific Northwest Lab.). Apr. 15, 1965. Contract AT(45-1)-1830. 12p. Dep. mn; CFSTI, $1.00 cy, $0.50 mn.

Tabular field data and fitting functions submitted to a digital computer give the ground water potential equations for heterogenous soils. Added to special boundary conditions, this potential equation is the key for computing the permeability distribution. The second computer program has four sequential operations. The first two provide permeability distribution and the last two give water travel time and flux distribution which enables water waste transport calculations. The nonlinear boundary value problem interrelates all pertinent variables, and when solved, gives the new ground water potential for flow system changes. The nonlinear equations are then solved digitally by a piecewise method for computations of predicted distribution of ground water potentials. The present computer program has a limit on problem size (8000 equations), but an enlarged program is being developed. Travel paths and times of flow and subsequently, the water arrival distribution are determined from the water potential function. An arrival curve is then used to plot the concentration of wastes entering streams. (auth)

40269 (IDO-22047-USGS) HYDROLOGY OF SUBSURFACE WASTE DISPOSAL — NATIONAL REACTOR TESTING STATION, IDAHO. Annual Progress Report, 1964. Morris, D. A.; Barraclough, J. T.; Chase, G. H.; Teasdale, W. E.; Jensen, R. G. (Geological Survey, Idaho Falls, Idaho). May 1965. 304p. Dep. mn; CFSTI, $7.00 cy, $1.50 mn.

Research was conducted on the hydrologic aspects of the disposal of low-level aqueous waste to the NRTS environment. Geologic and geohydrologic data were analyzed, and some new data are reported. Studies were made of the TRA waste-disposal pond area. The effects of the Alaskan earthquake on the water levels are described. (D.L.C.)

40270 (JUL-249-RW) PACKAGING DISASSEMBLED FUEL ELEMENTS AND RADIOACTIVE WASTE IN THE HOT CELLS AT THE KERNFORSCHUNGSANLAGE JUELICH. Retz, A.; Schmiddem, P.-J.; Stephan, W.; Rau, J. (Kernforschungsanlage, Juelich (West Germany). Institut fuer Reaktorwerkstoffe). Apr. 1965. 22p. Dep. mn.

Depending on type of material, activity level, and fire and health hazard, several methods of waste and fuel packaging are used in the Hot Cells at Kernforschungsanlage Jülich. Low level wastes such as plastics, rags, and small tools are remotely welded into plastic bags of 0.2–0.4 mm thickness. Wastes of higher activity level are packed into disposable cans. Tests for the tightness of the containers are described. For highly active fuel wastes which must be most securely packaged and stored, three methods were tested: remote argon-arc welding of stainless-steel and aluminum cans, electromagnetic closing of aluminum cans, and cold-pressure welding of aluminum cans. By comparison of leak-tightness, resistance to mechanical damage, and costs, the method of cold-pressure welding was chosen. (auth)

40271 (RAI-350) THE REMOVAL OF METALLIC IONS BY FOAMING AGENTS AND SUSPENSIONS: LABORATORY AND ENGINEERING STUDIES. Annual Report, July 1, 1963–June 30, 1964. Weinstock, Jacques J. (Radiation Applications Inc., Long Island City, N. Y.). Mar. 23, 1965. Contract W-7405-eng-26, Subcontract 2024. 41p. Dep. mn; CFSTI $2.00 cy, $0.50 mn.
For Oak Ridge National Lab., Tenn.

A research program was conducted on the application of foam separation to the decontamination of the low-activity waste (LAW) stream at ORNL. The continued study of the combined foam separation and phosphate-iron coagulation process established the following optimum concentrations of reactants: Armeen Z (flotation agent), None; UCAR C-149 (coagulation agent), 3 mg/l; WSR-35 (coagulation agent), 5 mg/l; Na_3PO_4, 60-70 mg/l; $FeSO_4$ (freshly prepared), 64 mg/l; DBS in feed, ~133 mg/l; and DBS to bottom of column, ~17 mg/l. All these concentrations are given in terms of milligrams per liter of LAW. The study also established the fact that a relatively long mixing time (at least 15-20 minutes) is necessary to make the process effective. The screening of biodegradable surfactants included experimental determinations of solubilities, critical micelle concentrations, foamabilities, and single-stage equilibrium distribution factors for strontium. The two materials which gave the best performance in these tests were Alipal LO 436 and Nacconol 40 FX. These materials were then further tested in a 2-inch-diameter, multistage, foam-separation column, and both gave decontamination factors at least equal to the best previously obtained with DBS (Siponate DS-10). The examination of pressure drops in foam-carrying tubes produced data that can be correlated in terms of a friction factor as a function of Reynolds Number. This correlation is similar to that used with pipes carrying more conventional fluids. (D.L.C.)

40272 PROBLEMS IN DISPOSAL OF RADIOACTIVE LIQUID WASTES IN SALT. Kubota, Hisashi (Oak Ridge National Lab., Tenn.). Chem. Eng. Progr., Symp. Ser., 60: No. 53, 68-73(1964).

The disposal of radioactive liquid wastes in salt, and its problems are discussed. Laboratory studies on the cold chemistry of the system, the role of radiation, alteration of cavity geometry, and results of field experiments using simulated waste solution in salt models and in 3000-gal. cavities are considered. (F.J.H.)

40273 THE CENTER AT THE HAGUE. Duboz, M. Energie Nucl., 7: 228-45(June 1965). (In French)

The Center at The Hague which is being built by the C. E. A. in the north-west part of the Cotentin Peninsula, is to be used for the treatment of irradiated fuels coming from nuclear power stations belonging to the Électricité de France. Descriptions are given of the site, arrangement of the buildings, and processes that will be used in the irradiated fuel treatment plant for the following operations: mechanical de-canning, chemical peeling, dissolving, extractions for the elimination of fission products, separation of uranium from plutonium, and treatment of plutonium (purification, preparation of the metal using oxalate, fluoride, and extraction by calciothermal method). Special attention is given to the treatment of radioactive effluents, the design of active buildings, and to the controls: process and health. (auth)

40274 PROBLEMS RELATING TO THE TREATMENT OF RADIOACTIVE EFFLUENTS. Dejonghe, P. J. Belge Radiol., 48: 249-67(1965). (In French).

The insolubilization of concentrates in hot asphalt was studied. As a result a system, which has already been

carried out on a large scale, was set-up. Also a study of radioelement dispersion into the soil was made. It is thus possible to foresee exactly the movement pattern of a radioactive contamination in the soil; this allows to establish the measures to be taken in case of accidental release of radioactivity and also to calculate the receptive capacity of a given environment. When treating high level radioactive liquid waste, a selective separation of the most toxical radioelements by means of synthetic mineral ion-exchangers is aimed at. Finally, all problems of treatment or storage were studied particularly with regard to the cost of the proceeding. (P.C.H.)

40275 TEMPERATURE DISTRIBUTION IN GAMMA-ACTIVE SPHERES. Sundaram, V. K.; Gopinath, D. V.; Ganguly, A. K. (Atomic Energy Establishment, Trombay, India). Nucl. Struct. Eng., 2: 151-8(July 1965).

One of the ultimate methods proposed for high-level radioactive waste disposal is to contain the activity in ceramic bodies and bury them underground or in deep sea. The limit of the activity that can be incorporated in such bodies is decided by the temperature rise in the body due to the absorption of nuclear radiation. The temperature distribution in a solid sphere containing long-lived gamma emitters and buried in a medium having the same thermal properties is discussed. Analytical expressions are given for heat source distribution and for calculations of temperature distribution in and out of a solid sphere containing gamma activity. Numerical values obtained with energies in the range of 0.5 to 3 Mev and in spheres of radii 10, 20, and 30 cm are presented. The results were compared with those of the beta case. (auth)

40276 RADIOACTIVITY REMOVAL BY WATER AND WASTE TREATMENT PROCESSES. Public Works, 96: 104-7(May 1965).

Removal from water of low-level radioactivity, such as that entering sewage from hospitals and other installations using radioisotopes, is considered. The treatments for removal of radionuclides described include specific chemical precipitation, sand filtration, lime and soda softening, ion exchange, as well as several nonconventional processes. Iodine, widely used by hospitals, can be removed by the addition of small amounts of copper sulfate, activated carbon, or silver nitrate. Coagulation is unsatisfactory for removal of ^{90}Sr. With an excess of cesium, strontium, or iodine, removal efficiency of coagulation is low; with an excess of trivalent ions of phosphorous, zirconium, and niobium, efficiency is high. Combined coagulation, settling, and filtration gives high removals (up to 99% of the initial activity) of ^{32}P. Lime alone is effective in removing zirconium and niobium. Lime and soda treatment provides >90% reduction in the common radioisotopes of barium, lanthanum, strontium, cadmium, scandium, and yttrium. Treatment plants using zeolite, green sand, or cation and anion exchangers can remove small concentrations of radionuclides readily (over 94% of tungsten, yttrium, scandium, strontium, barium, lanthanum, cesium, barium, cadmium, zirconium, niobium, and iodine). Of the conventional processes of water treatment, ion exchange was found to offer the most promise. Of the nonconventional processes, phosphate coagulation and slurrying with metallic dusts showed decontamination factors as high as 1000. In general, water treatment processes can provide decontamination factors as high as 10, or slightly higher with modified methods. Of the biological processes of waste treatment, sand filter treatment showed the highest decontamination with factors as high as 100 reported. Since radionuclides remain in sludge after digestion, the use of sludge from radioactively contaminated sewage, for fertilizer creates a problem, especially for radionuclides of long half life. Factors to be considered include the radiation dose from surface contact with the contaminated fertilizer and the transfer of radionuclides from the soil to above-ground portions of the plant. Strontium, which is taken up readily from soil by plants, is not concentrated in sludges. (BBB)

40277 SAFE DISPOSAL OF RADIOACTIVE WASTE IN WATER AND ATMOSPHERE. Davids, J. A. G. (Water-Bodem-Lucht, 54: No. 4, 74-84(1964).

ICRP recommendations on disposal of radioactive waste in water and the atmosphere are discussed. Some practical problems are considered: the disposal of ^{41}Ar in the atmosphere, the disposal in the Thames by the center at Harwell, the disposal in the Columbia river at Hanford, the disposal of liquid waste in the sea, and the disposal of low-level waste water at Petten. (J.V.E.)

GENERAL AND MISCELLANEOUS

40278 (AD-425879) THE APPLICATION OF PULSE SEQUENTIAL CIRCUITRY TO CONTROL DEVICES. Marcus, Ira R. (Harry Diamond Labs., Washington, D. C.). Nov. 20, 1963. 21p. (TR-1185). CFSTI, $1.60 cy.

The application of pulse sequential circuitry theory to the design of an all solid-state electronic control circuit is described. In pulse sequential circuits, an output program occurs only upon receiving a unique input sequence. A prototype model was built and its performance was satisfactory. It demonstrated the ease with which pulse sequential circuitry theory can be applied to the solution of pulse sequential problems. (auth)

40279 (BDX-613-72) A SENSITIVE, HIGH-SPEED, DC VOLTAGE COMPARATOR (thesis). Piper, Robert G. (Bendix Corp., Kansas City, Mo.). [June 1965]. Contract AT(29-1)-613. 108p. Dep. mn; CFSTI, $4.00 cy, $0.75 mn.

Submitted to Kansas Univ., Lawrence.

Factors important in the design and application of a sensitive, high-speed, d-c voltage comparator are examined. A specific transistor comparator design, suitable for use in many practical applications, is presented and considered in terms of these design factors. A detailed investigation of this design is made to determine what static and dynamic performance can be provided by the design, what factors limit various phases of the overall performance, and how these factors are interrelated. An experimental comparator was constructed to verify some of the assumptions. The comparator circuit can not be optimized simultaneously for the best sensitivity, accuracy, and dynamic response because of conflicting design requirements. The compromise in the experimental comparator circuit provided a static sensitivity of 0.385 Mv. The application of a 20 Mv input signal caused the output to change states in approximately 10 nsec. Under certain conditions a maximum error of about 4.3 Mv can occur. (auth)

40280 (BDX-613-73) SOLDERABILITY TESTING. Harding, William B. (Bendix Corp., Kansas City, Mo.). [July 1965]. Contract AT(29-1)-613. 40p. (CONF-650702-2). Dep. mn; CFSTI, $2.00 cy, $0.50 mn.

From American Electroplater's Convention, New York.

The theory underlying solderability (wetting and penetration) is presented. Spread tests, dip tests, and penetration tests of solderability are reviewed and their limitations discussed. (D.L.C.)

40281 (BNWL-113-5) PLUTONIUM ABSTRACTS. Volume 5, Number 5. (Battelle-Northwest, Richland, Wash. Pacific Northwest Lab.). June 30, 1965. Contract AT(45-1)-1830. 40p. Dep. mn; CFSTI, $2.00 cy, $0.50 mn.

A total of 83 annotated references is presented on new developments in plutonium technology. The references are arranged under the following headings: biology & medicine, chemistry, health & safety, metallurgy, miscellaneous, physics, and reactor technology. (D.L.C.)

40282 (BNWL-SA-171) COMPUTER APPLICATIONS IN SIMULATION. Thieme, G. G. (Battelle-Northwest, Richland, Wash. Pacific Northwest Lab.). Apr. 26, 1965. Contract AT(45-1)-1830. 18p. Dep.(mn); $1.00(cy), 1(mn) CFSTI

An analog simulation of the dual purpose Hanford N-reactor was prepared. Studies were performed to determine the dynamic characteristics of the plant and to determine the effects of possible plant, operator, and control system malfunctions. Various operational procedures and proposed design changes were also studied. An analog model of a biological system was made for the purpose of defining the distribution of radioisotopes in the body of man or animals for various types of radioisotopes and for various animals. The application of analog simulation to river routing is discussed. Applications to wind turbulence data are also discussed. An analog simulation of the PRTR kinetic equations was made using five groups of delayed neutrons, temperature feedback of reactivity, and provisions for simulating the reactor inputs associated with various conceivable accidents. (M.O.W.)

40283 (COO-1198-237) FERROUS MARTENSITES. Wayman, C. M. (Illinois Univ., Urbana. Dept. of Mining, Metallurgy, and Petroleum Engineering and Illinois Univ., Urbana. Materials Research Lab.). Jan. 1965. Contract AT(11-1)-1198. 38p. (CONF-650537-1). Dep. mn; CFSTI, $2.00 cy, $0.50 mn.

From Conference on the Physical Metallurgy of Bainite and Martensite, Scarborough, Eng.

The morphology and fine structure (internal dislocations and twins) of martensite in iron-base alloys were studied. The relations between the fine structure and theories on the crystallography and strength of martensite are considered. The two-stage growth of martensite plates in certain cases is pointed out, and attention is called to the formation of surface martensite and needle-like martensite in some alloys. (auth)

40284 (LA-DC-6993) ON ELECTRICAL CONDUCTIVITY IN DETONATION PRODUCTS. Hayes, Bernard (Los Alamos Scientific Lab., Univ. of California, N. Mex.). [1964]. Contract W-7405-eng-36. 6p. (CONF-651003-2). Dep. mn; CFSTI, $1.00 cy, $0.50 mn.

For Presentation at 4th Symposium on Detonation, Silver Spring, Md.

A discussion is presented of electronic techniques appropriate to high-resolution electrical conductivity measurements in the detonation products of condensed explosives. Evidence is given which shows that if the detonation products contain free carbon, that carbon is the main conductor of electricity. The usefulness of the measurement technique to explore reaction-zone structure is demonstrated. (auth)

40285 (MLM-1284) DETERMINATION OF TERTIARY BUTYL PERBENZOATE IN MOLDING POWDERS. Hartzel, L. W. (Mound Lab., Miamisburg, Ohio). [July 1, 1965]. Contract AT(33-1)-Gen-53. 4p. Dep. mn; CFSTI, $1.00 cy, $0.50 mn.

Sully's method for the iodimetric determination of organic peroxides was adapted for tertiary butyl perbenzoate in thermosetting diallyl phthalate molding powder. Results are reported for unfilled and filled formulations. (D.L.C.)

40286 (NAA-SR-11200) AEC UNCLASSIFIED PROGRAMS. Quarterly Technical Progress Report, January-March 1965. (Atomics International, Canoga Park, Calif.). Apr. 15, 1965. Contract AT(11-1)-Gen-8. 266p. Dep. (mn); $6.00(cy), 5(mn) CFSTI.

Work on the SRE power expansion program is about 87% complete. Phase-out of the large SGR was initiated to enable redirection of effort to fast breeder reactor design and development. A reference coupled fast reactor was chosen for study. Calculation methods for parametric surveys, and improved cross-sections were developed. A program to study the effects of O_2 depletion on burning rates and I_2 release of Na fires was initiated. Research was conducted on two-phase Na boiling, transient heating of carbide fuels, and evaluation of SRE components. Progress on preoperational testing of the Sodium Component Test Installation is summarized. Development of processes for producing SAP-clad UO_2 fuel elements for the PNPF is reported. The design of Core II prototype elements for Core I was completed, and specifications for Core II UO_2 pellets were issued. In the Hallam fuel element evaluation program U-Mo and UC elements were operated to burnups of 2050 to 2700 Mwd/t. It was demonstrated that Zr process tubes can be reused. Work on advanced develop-

ment was devoted to multicycle reprocessing, measurement of Doppler coefficients, radiation effects on fuels, BeO reactor materials, neutron age measurements, neutron diffusion, neutron cross sections, reactor coolant fission product retention, neutron flux monitors, reactor accident atmospheric effects, fission damage in fuels, synthesis and structure of metal hydrides, high-temperature chemistry of metal salts, organic compound radiolysis, electron structure of metals, and radiation effects on crystalline solids. (J.R.D.)

40287 (NP-15188) SURVEY OF ACTIVITIES, 1964. (Institutt for Atomenergi, Halden (Norway). OECD Halden Reaktor Prosjekt). 27p. Dep. mn.

A survey of activities was made on the following: reactor development, nuclear ship project, OECD Halden reactor project, metallurgy, chemistry, reactor physics and dynamics, the Kjeller computer installation, neutron physics, isotope production, health physics, technical information, the Netherlands'-Norwegian reactor school, and international cooperation. The staff at IFA is discussed and an abstract of accounts is given. (M.O.W.)

40288 (NVO-98-5) TASK IV INTERIM PROGRESS REPORT. Metzler, Allan R. (National Marine Consultants, Anaheim, Calif.). Apr. 26, 1965. Contract AT (26-1)-98. 60p. Dep. mn; CFSTI, $3.00 cy, $0.75 mn.

Calibration, simulation tests, and evaluation of deep ocean measuring systems and prototype sensors are described. Laboratory tests are described and data obtained by wave sensors are included. Field test results for deep ocean measuring systems and wave sensors are also included. (J.R.D.)

40289 (PNE-406) A REPORT OF AN ARCHAEOLOGICAL SURVEY AT OGOTORUK CREEK, ALASKA. Hadleigh-West, Frederic (Alaska Univ., College. Dept. of Anthropology). Nov. 1959. Contract AT(04-3)-310. 54p. Dep. (mn); $3.00(cy), 1(mn) CFSTI.

An archaeological survey in the vicinity of the mouth of Ogotoruk Creek on the northwest coast of Alaska, near Cape Thompson, was conducted during the summer of 1959. All evidence found in the course of the survey indicates a light recent occupation of the area. Some of this was seasonal and transient in nature. The earliest evidence of occupation was believed to be about the mid-19th century. A list is included of artifacts found at each site during excavation. (C.H.)

40290 (PNE-407) ARCHAEOLOGICAL SURVEY AND EXCAVATIONS AT OGOTORUK CREEK, NORTHWESTERN ALASKA. Project Chariot—Final Report. Hadleigh-West, Frederick (Alaska Univ., College. Dept. of Anthropology and Geography). Dec. 1961. Contract AT(04-3)-310. 90p. Dep. (mn); $3.00(cy), 2(mn) CFSTI.

An archaeological survey of the vicinity of the mouth of Ogotoruk Creek on the northwest coast of Alaska near Cape Thompson, was conducted during the summers of 1959 and 1960. Results showed that Ogotoruk was not the site of a large Eskimo population, nor did it reveal any depth in time. Descriptions and drawings of artifacts from 4 sites are included. (C.H.)

40291 (SC-R-65-923) A GENERIC CLASSIFICATION FOR TEACHING MACHINES. Simmons, G. J. (Sandia Corp., Albuquerque, N. Mex.). June 1965. Contract AT(29-1)-789. 15p. (CONF-650548-1). Dep. mn; CFSTI, $1.00 cy, $0.50 mn.

From National Society for Programmed Instruction, 3rd Annual Convention, Philadelphia.

A classification is developed for teaching machines based on the nature of the interaction between the student and the programmed instructional material. This approach makes it possible to functionally classify devices of widely different complexities without being misled by the sophisticated device design (or lack of it). Four basic machine types are identified and discussed: (1) linear, (2) recyclical, (3) remedial-cyclical (branching), and (4) adaptive. (auth)

40292 (SC-TM-202-56-51) BASE AND SURFACE PRESSURE VARIATION WITH MACH NUMBER ON A RIGHT CIRCULAR CONE. Iversen, James D. (Sandia Corp., Albuquerque, N. Mex.). Sept. 12, 1956. Contract AT(29-1)-789. 16p. Dep. mn; CFSTI, $1.00 cy, $0.50 mn.

Wind-tunnel test results and theoretical and empirical methods are used to determine the surface and base static pressure on a 30° included-angle right circular cone and the variation of that pressure with Mach number and location on the cone. The results are used to determine a combination of pressure port locations which gives a ratio of measured pressure to ambient pressure that does not vary with Mach number. A combination of base pressure and surface pressure that gives this constant ratio within desired limits is suggested. (auth)

40293 (SCL-DC-65-86) GRAPHICAL LATHE PART PROGRAMMING SYSTEM. Final Report. (IIT Research Inst., Chicago, Ill.). July 1965. Contract AT(29-1)-789. 68p. Dep. mn; CFSTI, $3.00 cy, $0.75 mn.

For Sandia Corp., Livermore, Calif.

A proposed system (GLPPS) is described for the application of on-line graphical communication techniques to the area of N/C part programming. The system utilizes a light-pen/CRT input/output station, together with a general purpose digital computer. GLPPS is a system specifically directed at the problem of generating part programs for N/C lathes and is designed to interface with the APT Automatically Programmed Tools system. A discussion is given of some of the general relations between graphical communications techniques and languages, time-shared on-line access to a large-scale digital computer, and the problems of design and fabrication of lathe parts. Two descriptions are given of GLPPS: one from the viewpoint of the system designer and one from the viewpoint of the on-line user. An appendix describes an approach to the implementation of one of the essential features of GLPPS, the lathe simulator. (auth)

40294 (TID-3730) BIBLIOGRAPHIES OF ATOMIC ENERGY LITERATURE. Issued or in Progress During the Period, June-July 1965. (Division of Technical Information Extension (AEC), Oak Ridge, Tenn.). 15p. Free(DTI Extension).

A total of 84 bibliographies are listed. Subject, author, and report number indexes are included. (D.L.C.)

40295 (TID-4025(Rev.1)(Pt.1)(Suppl.4)) TRANSLATION TITLE LIST AND CROSS REFERENCE GUIDE. Stratton, Frances E. (ed.) (Division of Technical Information Extension (AEC), Oak Ridge, Tenn.). Mar. 1965. 336p. Dep. mn; CFSTI, $7.00 cy, $1.50 mn.

A list is presented of the unclassified translations received by the Division of Technical Information Extension during the period Jan. 1, 1964 through Dec. 31, 1964. Original source and author indexes are included. (D.L.C.)

40296 (TID-21856) AN ORDERED TRIPLET CODE FOR MESSENGER RNA WITH NO TWO TRIPLETS CODING FOR THE SAME AMINO ACID. Osgood, Edwin E. (Oregon Univ., Portland. Div. of Experimental Medicine). [1964]. Contract AT(45-1)-581. 14p. Dep. (mn); $1.00(cy), 1(mn) CFSTI.

An ordered triplet code for messenger RNA is presented that uses 32, or exactly half of the possible triplet codes. This code was found to account for all nitrous acid induced mutants and abnormal hemoglobin data by a single substitution. No two amino acids are coded by the same nucleotide sequence and it is postulated that it provided the correct sequence for each triplet. All 64 possible triplet codes are tabulated in a form convenient for showing at a glance the permissible single step interchanges. Other suggested codes may be checked against the possible amino acid exchanges for in vivo fit. The rationale for the assignment of the codes and correlation with results of statistical data are discussed. Illustrative data from hemoglobin studies and spontaneous and nitrous acid induced mutants of tobacco mosaic virus are included. (25 references.) (C.H.)

40297 (UCRL-7753) HIGH-SPEED MICROWAVE PHASE SHIFTERS USING VARACTOR DIODES. Gardner, A. L.; Hawke, Ronald S. (Lawrence Radiation Lab., Univ. of California, Livermore). July 24, 1964. Contract W-7405-eng-48. 15p. Dep.(mn); $1.00(cy), 1(mn) CFSTI.

A reflection-type microwave phase shifter is described which is similar to the units developed by Hardin et al., and employs the voltage-variable capacitance of varactor diodes as the adjustable element. The "pill-type" diodes tune their associated circuit through a resonance to produce phase shifts of over 90 degrees. With proper adjustment of the coupling (a simple procedure) the output amplitude is made essentially constant. The use of two diodes in r-f series bucking configuration permits higher-power operation, although the unit is essentially a low-power device. (auth)

40298 (UCRL-14141) SECTORIAL PARALLEL PLATE TRANSMISSION LINE. Kelly, Robert E. (Lawrence Radiation Lab., Univ. of California, Livermore). Sept. 1964. Contract W-7405-eng-48. 30p Dep. mn; CFSTI, $2.00 cy, $0.50 mn.

Differential equations for voltage and current are derived for a nonuniform transmission line and are used to solve the problem of a sectorial shaped line composed of two parallel plates separated by a dielectric of constant thickness. The complex power is calculated and used to gain information regarding energy propagation for various conditions. The characteristic impedance is found to be complex in general and dependent upon distance along the line, therefore serving as a continuous impedance transformer which would be quite useful for pulses. These results, using the transmission line equations for voltage and current, are shown to be consistent with the electric and magnetic fields derived from Maxwell's equations. The problem of a uniform rectangular parallel plate transmission line is also analyzed. (auth)

40299 (LA-tr-65-12) VISCOSIMETRIC STUDIES OF THE KINETICS OF THE THERMAL DENATURATION OF DNA AFTER ATTACHMENT OF PROTAMINE AS COMPARED TO NATIVE NUCLEOPROTAMINE. Zimmermann, E. Translated by Lawrence R. Gurley and Gretchen R. Riese (Los Alamos Scientific Lab., N. Mex.), from Biochem. Z., 341: 129-38(1965). 13p. Dep. mn; JCL, $1.60 fs, $0.80 mf.

The function of DNA as genetic determinant of protein biosynthesis and bacterial transformation is connected to its tertiary structure. In the chromosomal apparatus of the somatic cell nucleus the DNA forms natural complexes with the basic proteins, histones, or protamines. Its presence represents a regulation mechanism of protein biosynthesis, since chromosomal sections occupied by polyamines are metabolically inactive. The capacity for complex formation is not restricted only to basic proteins as the adequate binding partner, but is also possible, for example, with cytoplasmic proteins, ribonucleic acids, purine and pyrimidine bases, and a series of organic dyes. As a result of changed hydrophobe mutual effect, the stability of the molecule is affected distinctly as a function of the binding partner. Such effects can be verified in the thermally induced denaturation of intact DNA and can be applied for the characterization and differentiation of the complex partner. Data are presented from a viscosimetric study of the modification of the kinetics of the denaturation process of DNA after attachment of protamine as compared to native DNA protamine complex. Nucleoprotamine from herring spermatozoa and protamine hydrochloride were used for the study. The experimental results on the thermal transformation of the DNA will find application in the formation of DNA-RNA hydrides for the purification of identical messenger RNA. (auth)

40300 A REVIEW OF THE BRITISH NUCLEAR INDUSTRY IN 1965. Bray, P. J. (Fairey Engineering Ltd., Heston, Eng.). Neue Tech., 7: 141-4(June 1965).

The activities, development, direction, and organization of the British nuclear industry are summarized. (D.C.W.)

40301 YADERNOE ORUZHIE I ZASHCHITA OT NEGO. (Nuclear Weaponry and Protection Against It). Vlasov, I. Moscow, Izdatel'stvo Dosaaf, 1963. 48p.

General characteristics of nuclear weapons are reviewed, including the characteristics of a nuclear explosion and the means of using nuclear weapons. Destructive effects of nuclear weapons are described, with discussions of the shock wave, light radiation, penetrating radiation, environmental radioactive contamination, and characteristics of the explosion site. Principles of organization of protection against nuclear weapons and individual and collective means of protection are discussed. The basic responsibility and regulation of conduct of the population in conditions of nuclear attack are considered. (M.J.T.)

40302 PROCEEDINGS OF FRANCE-JAPAN CONFERENCE ON NUCLEAR TECHNOLOGY, TOKYO, NOV. 12-14, 1962. [Tokyo, Japan Atomic Industrial Forum, Inc.]. 258p. (CONF-621102).

Proceedings of the France-Japan Conference on Nuclear Technology are presented. The papers presented were previously abstracted for NSA and appeared as 17: 12380, 12526, 12527, 12641, 12642, 12705, 12740, 13715, 13716, 13717, 13718, 13720, 13721, 13722, 13793, 13795, 13797, 13798, 13799, 13800, and 24868. (M.C.G.)

CORPORATE AUTHOR INDEX

This index contains entries for this period for all report literature and, in addition, for certain published literature items for which it is felt that a corporate approach is especially desirable, e.g., symposia, conference proceedings, and meetings.

Each entry under a corporate author is a shortened version of the title of the publication, followed by the *NSA* volume and abstract number. Report numbers are given in parentheses.

The phrase "Progress report" is abbreviated as "Prog. rpt.," permitting a more rapid and complete alphabetical arrangement of the titles without changing the location of the progress report titles in relation to the other titles.

A

ACF INDUSTRIES, INC., ALBUQUERQUE, N. MEX.
Electron microprobe data quantification, 19: 38536 (ACF-6)
Evaluation of nitrogen in 304 ELC stainless steel using the platinum flux technique, 19: 38537 (ACF-7)

ADELPHI UNIV., GARDEN CITY, N. Y. GRADUATE SCHOOL OF MATHEMATICS.
On the propagation of free soundwaves in rarefied gasdynamics, 19: 39262 (BNL-8990)

AEROJET-GENERAL CORP., AZUSA, CALIF.
SNAP-8 radiation effects test program. II., 19: 39057 (NP-15022)

AEROJET-GENERAL NUCLEONICS, SAN RAMON, CALIF.
AGN-GAM—an IBM 7090 code to calculate Army GCR spectra and multigroup constants, 19: 40176 (AGN-TM-407)
Fuel requirements for fissiochemical production, 19: 40169 (CONF-117(p.67-79))
Preparation and processing of fuel for fissiochemical reactors, 19: 39095 (CONF-117(p.81-97))

AEROSPACE CORP., EL SEGUNDO, CALIF.
Development of experimental techniques for measuring the distribution of H and He isotopes in space, 19: 39419 (ATN-63(9219)-1)
Vortices and vortex matrices, 19: 40237 (LA-3229, pp 251-85)

AEROSPACE TECHNOLOGY DIV., LIBRARY OF CONGRESS, WASHINGTON, D. C.
Space physiology, Vol. 3, 19: 38358 (AD-612660)

AIR FORCE CAMBRIDGE RESEARCH LABS., L. G. HANSCOM FIELD, MASS.
Calculated cross sections for atomic displacements produced by electrons in the 1.0 to 3.0-Mev energy range, 19: 39225 (AFCRL-65-286)
Quantum mechanical three-body problem for attractive potentials, 19: 39453 (CONF-796(Paper 15))

AKADEMIYA NAUK SSSR, MOSCOW. INSTITUT ATOMNOI ENERGII.
Continuous measurements of specific water resistance in closed circuits, 19: 40262 (ZFK-RN-17(p.25-31))

AKADEMIYA NAUK UKRAINSKOI SSR, KHARKOV. FIZIKO-TEKHNICHESKII INSTITUT.
Determination of spatial distribution of plasma density, 19: 39965 (NP-15203)
Longitudinal oscillations in a multi-velocity plasma beam, 19: 39964 (NP-15201)
Study of a plasma bunch in motion in a toroidal magnetic field, 19: 39963 (NP-15198)
Theory of interaction of high-energy elementary particles, 19: 39478 (NP-15210)

AKTIEBOLAGET ATOMENERGI, STOCKHOLM (SWEDEN).
Penetration and slowing-down of neutrons in reactor shields, 19: 39751 (AE-185)

ALASKA UNIV., COLLEGE. DEPT. OF ANTHROPOLOGY.
Archeological survey at Ogotoruk Creek, 19: 40289 (PNE-406)

ALASKA UNIV., COLLEGE. DEPT. OF ANTHROPOLOGY AND GEOGRAPHY.
Archeological survey and excavations at Ogotoruk Creek, 12/61, 19: 40290 (PNE-407)

ALLIS-CHALMERS MFG. CO., BETHESDA, MD. ATOMIC ENERGY DIV.
Prog. rpt. on steam separation technology, 4–6/65, 19: 38801 (ACNP-65004)

ALLIS-CHALMERS MFG. CO., WASHINGTON, D. C. NUCLEAR POWER DEPT.
Prog. rpt. on large fast reactor design, 8/63, 19: 40175 (ACNP-63592)

ALLISON DIV., GENERAL MOTORS CORP., INDIANAPOLIS, IND.
Prog. rpt. on plasma properties, 5/11–8/10/64, 19: 39960 (N64-33202)

AMES LAB., IOWA STATE UNIV. OF SCIENCE AND TECH.
Antiferromagnetism in dilute chromium alloys (thesis), 19: 40077 (IS-T-18)
Random phase approximation in the many-boson problem, 19: 39631 (IS-1111)
Relativistic effects in crystals, 19: 40076 (IS-1172)

ARGONNE NATIONAL LAB., ILL.
Advanced systems research and development, 19: 40257 (ANL-7046 (p.67-77))
Automatic analysis of photographic data in biology, 19: 38910 (CERN-65-11(p.43-56))
Convex sets and their applications, 19: 39082 (TID-22032)
General reactor technology, 19: 40112 (ANL-7046(p.36-66))
Investigation of fused-salt processes for preparation of uranium sulfides, 19: 38574 (ANL-7008)
Liquid-metal-cooled reactors, 19: 40177 (ANL-7046(p.1-35))
List processing in automatic analysis of spark chamber data, 19: 38973 (CERN-65-11(p.15-23))
Manufacture of glass-bonded fuels for Doppler coefficient measurement, 19: 39124 (ANL-6995)
Nuclear safety, 19: 39090 (ANL-7046(p.78-82))
Prog. rpt. on reactor development, 5/65, 19: 40111 (ANL-7046)
Program for calibrating flying-spot cathode ray tube for CHLOE, 19: 38975 (CERN-65-11(p.35-41))
Reactor development program, 19: 40113 (ANL-7071)
Theoretical estimates of pile-up distortion, 19: 38969 (ANL-6949)

ARMY ENGINEER NUCLEAR CRATERING GROUP, LIVERMORE, CALIF.
Crater studies, Project DUGOUT, 19: 38789 (PNE-601F)

ARMY ENGINEER WATERWAYS EXPERIMENT STATION, VICKSBURG, MISS.
Stem design and shotcrete, grout, and concrete support, 19: 38788 (PNE-501F)

ATLANTIC RESEARCH CORP., ALEXANDRIA, VA.
Prog. rpt. on boiling heat transfer, 1–3/65, 19: 38807 (NYO-2404-70)

ATOMIC ENERGY ESTABLISHMENT, TROMBAY (INDIA).
Counter for fast neutron dosimetry, 19: 38968 (AEET/HP/D-1)
Fission products data and its application in studying fallout from nuclear weapon tests, 19: 39774 (AEET-209)

ATOMIC ENERGY ESTABLISHMENT, TROMBAY (INDIA). HEALTH PHYSICS DIV.
Maximum permissible concentrations of fission product mixtures in air and water for occupational exposures, 19: 38872 (AEET/HP/TH-15)

ATOMIC ENERGY ESTABLISHMENT, WINFRITH (ENGLAND).
ENOCH (a one-dimensional space-dependent burn-up program), 19: 40147 (AEEW-M-448)
MLBW—a multi-level Breit-Wigner computer program, 19: 39776

(AEEW-M-517)
Neutron cross sections of Be-9 in energy range 1 to 15 Mev, 19: 39775 (AEEW-M-513)
TEMPO—a general Doppler broadening program for neutron cross sections, 19: 39777 (AEEW-M-518)
The simultaneous use of several pseudo-random binary sequences in the identification of linear multivariable dynamic systems, 19: 39078 (AEEW-M-507)

ATOMIC ENERGY OF CANADA LTD., CHALK RIVER (ONTARIO).
Conference on generation of intense neutron fluxes, Chalk River, 4/65, 19: 39752 (AECL-2177)
Intense Neutron Generator target, 19: 39756 (AECL-2177, Paper 3)
Intense Neutron Generator research facilities, 19: 39757 (AECL-2177, Paper 4)
Introduction and notes on the Intense Neutron Generator, 19: 39753 (AECL-2177, Introduction)
Nuclear power implications of the Intense Neutron Generator, 19: 39758 (AECL-2177, Paper 5)
Overall Project—Intense Neutron Generator, 19: 39754 (AECL-2177, Paper 1)
Possible nuclide production in the Intense Neutron Generator, 19: 39762 (AECL-2177, Paper 9)
Properties of cold-worked Zr–Nb fuel sheathing, 19: 39150 (AECL-2250(Pt. I))
Radio-frequency system for the Intense Neutron Generator, 19: 39759 (AECL-2177, Paper 6)
Shielding and activation of the Intense Neutron Generator, 19: 39761 (AECL-2177, Paper 8)
Some engineering problems with an Intense Neutron Generator, 19: 39760 (AECL-2177, Paper 7)
The 65-mA 1-Bev proton accelerator, 19: 39755 (AECL-2177, Paper 2)
Tomorrow's fission reactor and its materials demands, 19: 40180 (DL-56)

ATOMIC ENERGY OF CANADA LTD., CHALK RIVER (ONTARIO). CHALK RIVER NUCLEAR LABS.
Intense Neutron Generator target, 19: 39756 (AECL-2177, Paper 3)
Intense Neutron Generator research facilities, 19: 39757 (AECL-2177, Paper 4)
Introduction and notes on the Intense Neutron Generator, 19: 39753 (AECL-2177, Introduction)
Nuclear power implications of the Intense Neutron Generator, 19: 39758 (AECL-2177, Paper 5)
Overall Project—Intense Neutron Generator, 19: 39754 (AECL-2177, Paper 1)
Radio-frequency system for the Intense Neutron Generator, 19: 39759 (AECL-2177, Paper 6)
Shielding and activation of the Intense Neutron Generator, 19: 39761 (AECL-2177, Paper 8)
Some engineering problems with an Intense Neutron Generator, 19: 39760 (AECL-2177, Paper 7)
The 65-mA 1-Bev proton accelerator, 19: 39755 (AECL-2177, Paper 2)

ATOMIC ENERGY OF CANADA, LTD., OTTAWA (ONTARIO). COMMERCIAL PRODUCTS DIV.
Possible nuclide production in the Intense Neutron Generator, 19: 39762 (AECL-2177, Paper 9)

ATOMIC ENERGY RESEARCH ESTABLISHMENT, HARWELL (ENGLAND).
Attempts to determine fast-neutron spectrum in thermal reactor, 19: 40256 (AERE-M-1590)
The preparation and some properties of U carbonitrides, 19: 39089 (AERE-M-1389)

ATOMIC POWER DEVELOPMENT ASSOCIATES, INC., DETROIT, MICH.
Determination of oxygen in sodium metal, 19: 38539 (APDA-168)

ATOMICS INTERNATIONAL, CANOGA PARK, CALIF.
Calandria core weld joint development, 19: 40125 (NAA-SR-9821)
Effect of neutron irradiation on the liquid Na dilation of graphite, 19: 39235 (NAA-SR-11309)
Electrolysis of U carbide in fused salt using molten metal cathodes, 19: 38754 (NAA-SR-10737)
Fabrication record of OMRE test elements, 19: 40187 (NAA-SR-Memo-7753)
Kinetics of reaction of UC with water, 19: 38581 (NAA-SR-11401)
Large SGR control rod development, 19: 40126 (NAA-SR-11327)
Permeation of hydrogen through metals, 19: 39165 (NAA-SR-10462)
Prog. rpt. on AEC unclassified programs, 1–3/65, 19: 40286 (NAA-SR-11200)
Properties of cladding materials for SNAP hydride reactors, 19: 39166 (NAA-SR-Memo-11149)

AVCO-EVERETT RESEARCH LAB., EVERETT, MASS.
Nuclear propulsion schemes using MHD conversion techniques, 19: 40238 (LA-3229, pp 286-312)

B

BABCOCK AND WILCOX CO., BARBERTON, OHIO. BOILER DIV.
Prog. rpt. on Na-heated steam generator, 4/65, 19: 38803 (BAW-1280-20)

BATTELLE MEMORIAL INST., COLUMBUS, OHIO.
Conference on particulate nuclear fuels, New York, 9/63, 19: 40168 (CONF-117)
Fuel requirements for fissiochemical production, 19: 40169 (CONF-117(p.67-79))
Indexing charts for diffraction patterns of tetragonal, hexagonal and orthorhombic crystals, 19: 40080 (NP-15182)
Irradiation evaluation of Al_2O_3-coated UO_2 fuel particles, 19: 39227 (BMI-1729)
Postirradiation fission-product release from coated fuel particles, 19: 39228 (BMI-1734)
Preparation and evaluation of carbon-coated fuel particles, 19: 39126 (CONF-117(p.149-70))
Preparation and properties of particulate oxide fuels, 19: 39094 (CONF-117(p.11-19))
Preparation and processing of fuel for fissiochemical reactors, 19: 39095 (CONF-117(p.81-97))
Preparation and properties of spherical particulate nuclear fuels for Pu-fueled reactors, 19: 39096 (CONF-117(p. 103-26))
Prog. rpt. on civilian applications, 4/65, 19: 39091 (BMI-1723(Del.))
Prog. rpt. on fission-fragment effects in structural materials, 4–6/65, 19: 39229 (BMI-X-10134)

BATTELLE MEMORIAL INST., GENEVA (SWITZERLAND).
Prog. rpt. on fission-product reactions with and release from fuel-element claddings, 4–6/65, 19: 39152 (BMI-X-10132)

BATTELLE-NORTHWEST, RICHLAND, WASH. PACIFIC NORTHWEST LAB.
A sequence for predicting waste transport by ground water, 19: 40268 (BNWL-63)
Beta-α and α-β transformations in Pu under applied stresses, 19: 39153 (BNWL-63)
Computer applications in simulation, 19: 40282 (BNWL-SA-171)
Electron microscope studies of second phase particles in dilute alloys of U, 19: 39092 (BNWL-SA-90)
Evaluation of exposure from multiple environmental sources in the environs of the Hanford plants, 19: 38874 (BNWL-SA-53)
Extension of stratigraphic units of south-central Washington. II., 19: 38844 (BNWL-SA-140)
Extension of stratigraphic units of south-central Washington. I., 19: 38843 (BNWL-SA-135)
High-volume nondestructive test applications at Hanford, 19: 38823 (BNWL-SA-97)
Ionic diffusion in high-temperature UO_2, 19: 39154 (BNWL-SA-54)
KINETICS I—neutron kinetics code in FORTRAN IV, 19: 40148 (BNWL-111)
Minimized fuel cycle cost for simulated pressurized water reactor. I., 19: 40114 (BNWL-104)
Neutron attenuation mechanisms in concretes, 19: 40061 (BNWL-SA-79)
Non-equilibrium tissue distributions of uranium and thorium following inhalation of uranium ore by rats, 19: 38333 (BNWL-SA-226)
Plutonium Abstracts, Vol. 5, No. 5, 19: 40281 (BNWL-113-5)
Plutonium particle-induced neoplasia of the canine lung. I., 19: 38359 (BNWL-SA-230)
Prog. rpt. on ceramics development, 1–3/65, 19: 39125 (BNWL-91)
Prog. rpt. on development of D_2O-moderated reactors, 12/64, 19: 38805 (BNWL-C-3)
Promethium isotopic power data sheets, 19: 39069 (BNWL-C-45)
Small specimens, suitable for irradiation damage studies on reactor structural materials, 19: 38822 (BNWL-SA-2)
System of chained computer codes for reactor fuel cycle analysis, 19: 40149 (BNWL-SA-61)
Tungsten fiber reinforced nickel composites, 19: 39093 (BNWL-SA-141)

BELL TELEPHONE LABS., MURRAY HILL, N. J.
Theories of magnetism in metals, 19: 40074 (CONF-796(Paper 3))

BELLCOMM, INC., WASHINGTON, D. C.
Space transportation, 19: 40222 (LA-3229, pp 10-47)

BENDIX CORP., KANSAS CITY, MO.
Sensitive, high-speed, d-c voltage comparator (thesis), 19: 40279 (BDX-613-72)
Solderability testing, 19: 40280 (BDX-613-73)

BETTIS ATOMIC POWER LAB., PITTSBURGH, PA.
CHIC-KIN—FORTRAN program for intermediate and fast transients, 19: 40160 (WAPD-TM-479)
Critical dimensions of water reflected systems containing ^{235}U–H_2O–Zr, 19: 40159 (WAPD-T-1774)
Structural analysis of a reactor subassembly under thermal, hydraulic, and fuel expansion loads, 19: 40118 (WAPD-T-1782)

BIRMINGHAM-SOUTHERN COLL., ALA. DEPT. OF BIOLOGY.
Comparison of x-ray- and uv-induced abberations in pollen tube chromosomes of Tradescantia, 19: 38360 (TID-21695)
BOEING CO., SEATTLE, WASH.
Flash x-ray analysis of fluidized beds, 19: 40224 (LA-3229, pp 63-82)
BOEING CO., SEATTLE, WASH. AERO-SPACE DIV.
Computer codes for evaluation of space radiation hazards. IV., 19: 40062 (N64-29366)
BOSTON UNIV., MASS.
Masses of elementary particles from geometry of space-time, 19: 39452 (CONF-796(Paper 13))
BRIGHAM YOUNG UNIV., PROVO, UTAH.
Small vertebrates in U areas of upper Colorado River Basin, 19: 38330 (TID-22078)
BROOKHAVEN NATIONAL LAB., UPTON, N. Y.
Activity report on Brookhaven work on the compilation, storage and evaluation of nuclear cross section data, 19: 39778 (BNL-9355)
BNL fluidized bed studies, 19: 40223 (LA-3229, pp 48-62)
Fuel management in the settled bed fast reactor, 19: 40178 (BNL-9279)
Getting results from an HPD system, 19: 38970 (BNL-9236)
HFBR containment test, 19: 40258 (BNL-9237)
New source of small-angle x-ray scattering, 19: 39230 (BNL-9332)
Numerical continuation backwards in time for solutions of heat equation, 19: 38804 (BNL-8185)
Role of oxygen in solid-state polymerization. I., 19: 38694 (BNL-9200)
Scattering experiment using digitized discharge planes, 19: 39450 (BNL-9232)
Solid-state electromotive force techniques. The free energy of formation of $NiCl_2$, $CoCl_2$, and several double salts of KCl, 19: 38575 (BNL-9343)
Status of digital automatic scanning programs, 19: 38991 (CERN-65-11 (p. 237-58))
Status of HPD programs at BNL, 19: 38980 (CERN-65-11(p.97-113))
^{3}H thymidine (^{3}HTdR) incorporated into DNA; dosimetric and radiobiological considerations, 19: 38873 (BNL-9331)
BROWN UNIV., PROVIDENCE, R. I. DIV. OF APPLIED MATHEMATICS.
On the propagation of free soundwaves in rarefied gasdynamics, 19: 39262 (BNL-8990)
BUNDESGESUNDHEITSAMT, BERLIN (WEST GERMANY). INSTITUT FUER WASSER-, BODEN- UND LUFTHYGIENE.
Alloying with Na diuranate for coloring artificial teeth, 19: 38473 (NP-14923)
Calcium as prophylactic against uptake of Sr-90, 19: 38335 (NP-14926)
Strontium-90 balance for the year 1961/62, 19: 38876 (NP-14927)

C

CALIFORNIA INST. OF TECH., PASADENA.
Distribution of lepton pairs from vector meson decays, 19: 39451 (CALT-68-43)
Gas core reactors, 19: 40235 (LA-3229, pp 222-36)
CALIFORNIA INST. OF TECH., PASADENA. W. M. KECK LAB. OF ENGINEERING MATERIALS.
A study of CsCl type intermediate phases involving rare earth elements, 19: 39155 (CALT-221-11)
CALIFORNIA UNIV., LOS ANGELES. LAB OF NUCLEAR MEDICINE AND RADIATION BIOLOGY.
Effect of chelates on the movement of fission products through soil columns, 19: 38329 (TID-20471)
CARNEGIE INST. OF TECH., PITTSBURGH, PA. DEPT. OF MATHEMATICS.
Complex space-time model. I, II, and III, 19: 39624 (AROD-223:60)
CAROLINAS VIRGINIA NUCLEAR POWER ASSOCIATES, INC., PARR, S. C.
Monthly operating report, May 1965, 19: 40179 (CVNA-236)
CASE INST. OF TECH., CLEVELAND, OHIO. NUCLEAR PHYSICS LAB.
Exchange effects in scattering of slow electrons by atoms, 19: 39365 (COO-720-047)
CATHOLIC UNIV. OF AMERICA, WASHINGTON, D. C.
Low-temperature expansion of spontaneous magnetization of Heisenberg ferromagnet, 19: 39684 (CONF-796(Paper 4))
COLLEGE DE FRANCE, PARIS.
Control of HPD by small computer, 19: 38987 (CERN-65-11(p.207-18))
Results obtained with off-line HPD system, 19: 38988 (CERN-65-11 (p.183-206))
COLUMBIA UNIV., NEW YORK.
Integral FILTER technique for HPD, 19: 38985 (CERN-65-11(p.153-72))
Weak interactions, 19: 39457 (CONF-796(Paper 23))
COLUMBIA UNIV., NEW YORK. COLUMBIA RADIATION LAB.
Theory of atomic beam optical double resonance spectroscopy, 19: 39369 (NP-15140)
COLUMBIA UNIV., NEW YORK. ENGINEERING RESEARCH LABS.
Heat transfer and hydraulic studies for SNAP-4 fuel element geometries, 19: 40249 (TID-22014)
COMBUSTION ENGINEERING, INC., WINDSOR, CONN. NUCLEAR DIV.
Prog. rpt. on BONUS core development, 12/64–2/65, 19: 39156 (CEND-532)
COMISION NACIONAL DE ENERGIA ATOMICA, BUENOS AIRES (ARGENTINA).
Preparation of potassium ferrocyanide labeled with ^{59}Fe, 19: 38743 (NP-15262)
COMMISSARIAT A L'ENERGIE ATOMIQUE, CADARACHE (FRANCE). CENTRE D'ETUDES NUCLEAIRES.
Utilization of Rapsodie reactor for measurement of Doppler effect, 19: 40150 (CEA-R-2565)
COMMISSARIAT A L'ENERGIE ATOMIQUE, GRENOBLE (FRANCE). CENTRE D'ETUDES NUCLEAIRES.
Determination of free U in UC–U and UC–U–C alloys, 19: 38540 (CEA-Note-397)
CORNELL AERONAUTICAL LAB., INC., BUFFALO, N. Y.
Prog. rpt. on re-entry dispersal of reactor core materials, 1–3/65, 19: 39118 (SC-DC-65-1520)
CORNELL UNIV., ITHACA, N. Y.
Detection of super showers by atmospheric scintillation, 19: 39422 (TID-21895)
Extrapolation of nucleon electromagnetic form factors, 19: 39458 (CONF-796(Paper 24))
COSMIC RAY GROUP, UNIV. OF MINNESOTA, MINNEAPOLIS.
Electrons, H and He nuclei in primary cosmic radiation, 1963, 19: 39420 (NP-15117)
CULHAM LAB., UNITED KINGDOM ATOMIC ENERGY AUTHORITY, ABINGDON (ENGLAND).
Microwave emission from the Zeta plasma, 19: 39953 (CLM-R-40)

D

DEPARTMENT OF DEFENSE, WASHINGTON, D. C.
Electrical power generation systems for space applications, 19: 38836 (NASA-SP-79)
DEUTSCHE AKADEMIE DER WISSENSCHAFTEN ZU BERLIN (EAST GERMANY).
Many-group parameter sets for calculation of fast reactors, 19: 40161 (ZfK-TPh-11)
DIVISION OF NUCLEAR MATERIALS MANAGEMENT (AEC), WASHINGTON, D. C.
Nuclear materials management. An annotated bibliography of selected literature, 19: 39101 (TID-3315)
DIVISION OF OPERATIONS ANALYSIS AND FORECASTING (AEC), WASHINGTON, D. C.
Estimated growth of civilian nuclear power, 19: 40194 (WASH-1055)
DIVISION OF RAW MATERIALS (AEC), WASHINGTON, D. C.
Geology of Cuzco-Anta-Urubamba Area, Peru, 19: 38845 (RME-4584)
DIVISION OF TECHNICAL INFORMATION EXTENSION, (AEC), OAK RIDGE, TENN.
Bibliographies of atomic energy literature, 19: 40294 (TID-3730)
Nuclear materials management. An annotated bibliography of selected literature, 19: 39101 (TID-3315)
Translation title list, 19: 40295 (TID-4025(Rev.1)(Pt.1)(Suppl.4))
DOUGLAS AIRCRAFT CO., INC., LONG BEACH, CALIF.
The transparent partition gaseous core reactor concept, 19: 40229 (LA-3229, pp 116-36)
DOUGLAS AIRCRAFT CO., INC., SANTA MONICA, CALIF.
Criticality of gas core reactors, 19: 40239 (LA-3229, pp 315-43)
DOUGLAS AIRCRAFT CO., INC., SANTA MONICA, CALIF. MISSILE AND SPACE SYSTEMS DIV.
CHARGE—space radiation shielding code, 19: 40064 (NP-15132)
Radiation protection for manned orbiting space stations, 19: 40063 (NP-15125)
DYNATECH CORP., CAMBRIDGE, MASS.
Boiling flow regimes and critical heat flux, 19: 38809 (NYO-3304-3)

E

EIDGENOESSISCHES INSTITUT FUER REAKTORFORSCHUNG, WUERENLINGEN (SWITZERLAND).
Theory of modified pulsed source technique, 19: 40151 (EIR-79)
ELECTRO-OPTICAL SYSTEMS, INC., PASADENA, CALIF.
Prog. rpt. on iron rocket system, 7–9/65, 19: 38834 (N64-29495)
ENTE NAZIONALE PER L'ENERGIA ELETTRICA, ROME (ITALY).
Prog. rpt. on Latina nuclear power plant, annual, 1964, 19: 40181 (EUR-2429.i)
ETHYL CORP., BATON ROUGE, LA. RESEARCH AND DEVELOPMENT

DEPT.
Prog. rpt. on chemical vapor deposition of Be from organoberyllium compounds, final, 6/63–1/64, 19: 39102 (UCRL-13100)
EUROPEAN ATOMIC ENERGY COMMUNITY.
Exponential experiment in natural U, 19: 39763 (EUR-2413.e)
Prog. rpt. on Latina nuclear power plant, annual, 1964, 19: 40181 (EUR-2429.i)
The fluorescence of *p*-hydroxydiphenyl in aqueous solution, 19: 38687 (EUR-2423.e)
EUROPEAN ATOMIC ENERGY COMMUNITY, ISPRA (ITALY). JOINT NUCLEAR RESEARCH CENTER.
Exponential experiment in natural U, 19: 39763 (EUR-2413.e)
The fluorescence of *p*-hydroxydiphenyl in aqueous solution, 19: 38687 (EUR-2423.e)
EUROPEAN ORGANIZATION FOR NUCLEAR RESEARCH, GENEVA (SWITZERLAND).
Automatic analysis of photographic data in biology, 19: 38910 (CERN-65-11(p.43-56))
Automatic analysis of spark chamber pictures using the CERN HPD, 19: 38974 (CERN-65-11(p.25-33))
CERN picture number finding routine, 19: 38979 (CERN-65-11(p.91-5))
CERN version of FILTER, 19: 38981 (CERN-65-11(p.115-21))
Conference on programming for flying-spot devices, Bologna, 10/64, 19: 38971 (CERN-65-11)
Control of HPD by small computer, 19: 38987 (CERN-65-11(p.207-18))
Experience with CERN HAZE program, 19: 38982 (CERN-65-11(p.123-37))
Experience with SPASS system, 19: 38972 (CERN-65-11(p.7-13))
FORTRAN diagnostic routine used with CERN HAZE, 19: 38984 (CERN-65-11(p.145-52))
Getting results from an HPD system, 19: 38970 (BNL-9236)
HPD programing at Rutherford Lab., 19: 38986 (CERN-65-11(p.173-81))
HPD programing at Univ. of Pennsylvania, 19: 38990 (CERN-65-11 (p.229-36))
Integral FILTER technique for HPD, 19: 38985 (CERN-65-11(p.153-72))
List processing in automatic analysis of spark chamber data, 19: 38973 (CERN-65-11(p.15-23))
Post FILTER routine of CERN HAZE, 19: 38983 (CERN-65-11(p.139-43))
Precision encoding and pattern recognition system, 19: 38978 (CERN-65-11(p.81-90))
Program developments in CERN-FSD spark system, 19: 38977 (CERN-65-11(p.71-9))
Program for calibrating flying-spot cathode ray tube for CHLOE, 19: 38975 (CERN-65-11(p.35-41))
Results obtained with off-line HPD system, 19: 38988 (CERN-65-11 (p.183-206))
Results of HPD ionization measurements, 19: 38989 (CERN-65-11 (p.219-27))
Spark chamber photograph analysis using LUCIOLE, 19: 38976 (CERN-65-11(p.57-69))
Status of digital automatic scanning programs, 19: 38991 (CERN-65-11 (p.237-58))
Status of HPD programs at BNL, 19: 38980 (CERN-65-11(p.97-113))

F

FEDERAL RADIATION COUNCIL, WASHINGTON, D. C.
Protective action guides for Sr-89, Sr-90 and Cs-137, 19: 38877 (NP-15183)
FORSVARETS FORSKNINGSANSTALT, STOCKHOLM (SWEDEN).
A user's manual for salomon, an IBM-7090 code for gamma transport calculations, 19: 40066 (NP-15155)
Penetration and slowing-down of neutrons in reactor shields, 19: 40156 (NP-15161)

G

GENERAL ATOMIC, SAN DIEGO, CALIF.
Radiation effects on pressure transducer components, 19: 39055 (GA-6266)
GENERAL ATOMIC, SAN DIEGO, CALIF. JOHN JAY HOPKINS LAB. FOR PURE AND APPLIED SCIENCE.
A survey of several methods for computing cell cross sections, 19: 40152 (GA-6462)
Finite element analysis of axisymmetric composite structures, 19: 40165 (GA-6303)
Gas-cooled fast breeder reactor core design analysis and system development, 19: 40182 (GA-5537)
Neutron cross sections for ^{236}U, 19: 39764 (GA-6087(Rev.))
Prog. rpt. on HTGCR post-construction R and D program, 10/64, 19: 40183 (GA-5924)
Prog. rpt. on HTGCR post-construction R and D program, 2–4/65, 19: 40184 (GA-6406)
Regenerative H_2O–CO_2 trap and liquid N cooled No. 2 charcoal trap assembly, 19: 40120 (GAMD-5434)
The release of condensable fission products from the GAIL III-B fuel element, 19: 39233 (GAMD-6321)
GENERAL DYNAMICS/FORT WORTH, TEX.
Effects of nuclear radiation and various environments on a number of selected plastic, glass-laminate, and ceramoplastic materials, 19: 39232 (FZK-227)
GENERAL ELECTRIC CO., CINCINNATI, OHIO. NUCLEAR MATERIALS AND PROPULSION OPERATION.
Evaluation of zirconloys for use in 630A reactor, 19: 39097 (GEMP-346)
Nuclear propulsion. Shield physics, 19: 40246 (N64-29787)
Nuclear propulsion. Reactor system design, 19: 40247 (N64-29788)
Preparation and properties of particulate oxide fuels, 19: 39094 (CONF-117(p. 11-19))
GENERAL ELECTRIC CO., CINCINNATI, OHIO. SPACE POWER AND PROPULSION SECTION.
Prog. rpt. on electromagnetic alkali metal pump, 12/27/63–3/27/64, 19: 38781 (N64-25903)
GENERAL ELECTRIC CO., PLEASANTON, CALIF. SPECIAL PURPOSE NUCLEAR SYSTEMS OPERATION.
Prog. rpt. on thermionic conversion, semiannual, 7–12/64, 19: 39070 (GEST-2046)
Prog. rpt. on thermionic conversion, 7–9/64, 19: 39072 (NP-15187)
GENERAL ELECTRIC CO., RICHLAND, WASH. HANFORD ATOMIC PRODUCTS OPERATION.
Application of NPR technology to the national nuclear program, 19: 40191 (RL-SA-42)
Applications of NPR technology to the national nuclear program, 19: 40219 (RL-SA-21)
MINIMIZER—a computer code for determining minimum fuel cost, 19: 40170 (HW-71813)
Pressure-drop characteristics of two eccentrically positioned orifices in series. I., 19: 38810 (RL-SA-31)
The distribution of Am^{3+} between xylene–DBBP solutions and nitrate solutions, 19: 38750 (HW-81166)
Use of U(IV) as Pu reductant in Purex Process, 19: 38751 (HW-82163)
GENERAL ELECTRIC CO., SAN JOSE, CALIF. ATOMIC POWER EQUIPMENT DEPT.
Examination of Zy-clad UO_2 fuel rods, 19: 39234 (GEAP-4597)
Maximum two-phase vessel blowdown from pipes, 19: 38802 (APED-4827)
Microstructural evaluation of superheat cladding materials, 19: 39158 (GEAP-4751)
Piping failures for reactor coolant pipe rupture study, 19: 40121 (GEAP-4574)
Prog. rpt. on reactor control systems, 2–4/65, 19: 40122 (GEAP-4862)
Prog. rpt. on transition boiling heat transfer, 4–6/65, 19: 38806 (GEAP-4908)
Program recommendations—reactor pipe rupture study, 19: 38824 (GEAP-4474)
GENERAL ELECTRIC CO., SAN JOSE, CALIF. VALLECITOS ATOMIC LAB.
Corrosion of materials for nuclear superheat applications, 19: 39115 (GEAP-4760)
GENERAL ELECTRIC CO., SANTA BARBARA, CALIF.
Experimental work in relation to the glow-plug concept, 19: 40228 (LA-3229, pp 111-15)
GENERAL NUCLEAR ENGINEERING CORP., DUNEDIN, FLA.
Power Reactor Technology, Vol. 7, No. 3, 1964, 19: 40215
GEOLOGICAL SURVEY, IDAHO FALLS, IDAHO.
Hydrology of subsurface waste disposal, National Reactor Testing Station, Idaho, 19: 40269 (IDO-22047-USGS)
GEOLOGICAL SURVEY, MENLO PARK, CALIF.
Potential applications of nuclear explosives in development and of H_2O resources, 19: 38791 (TEI-857)
GEORGE WASHINGTON UNIV., WASHINGTON, D. C.
Foldy-Wouthuysen transformation in covariant spinor formulation, 19: 39630 (CONF-796(Paper 31))
GEORGIA INST. OF TECH., ATLANTA.
Stimulated photon-photon scattering, 19: 39264 (CONF-796(Paper 14))
GEORGIA UNIV., ATHENS.
Representation of discrete symmetry operators, 19: 39626 (CONF-796(Paper 22))
GEOSCIENCE LTD., SOLANA BEACH, CALIF.
Prog. rpt. on heat transfer for nuclear auxiliary power systems, 3–5/65, 19: 38811 (SAN-409-24)
GOSUDARSTVENNYI KOMITET PO ISPOL'ZOVANIYU ATOMNOI ENERGII SSSR.

Development of scintillation and ionization methods of radiometry and dosimetry. Report No. 73, 19: 38995 (NP-15259)

GOSUDARSTVENNYI KOMITET PO ISPOL'ZOVANIYU ATOMNOI ENERGII SSSR, MOSCOW. INSTITUT TEORETICHESKOI I EKSPERIMENTAL'NOI FIZIKI.

Angular correlation between π mesons and leptons and determination of form factors in K decay, 19: 39482 (NP-15252)

Data on p,p reactions with Q = 148 Mev, 19: 39479 (NP-15216)

Decay $\Gamma^0 \rightarrow \pi^0 + \pi^0$, 19: 39480 (NP-15247)

Non-conservation of CP parity and nature of law $\Delta T = \frac{1}{2}$, 19: 39476 (NP-15197)

Realization of a three-dimensional unitary group by means of spherical functions, 19: 39477 (NP-15202)

Weak interactions of colliding electron beams, 19: 39481 (NP-15248)

GRUMMAN AIRCRAFT ENGINEERING CORP., BETHPAGE, N. Y.

Determination of organic residue from solvents by radioisotopic method, 19: 38538 (ADR-08-13-63.1)

GRUMMAN AIRCRAFT ENGINEERING CORP., BETHPAGE, N. Y. QUALITY CONTROL DEPT.

Radioisotopic detection of microbial contamination present in jet fuel, 19: 39061 (ADR-09-08a-63.1)

H

HARRY DIAMOND LABS., WASHINGTON, D. C.

The application of pulse sequential circuitry to control devices, 19: 40278 (AD-425879)

HEALTH AND SAFETY LAB., NEW YORK OPERATIONS OFFICE (AEC), N. Y.

Control of liquid hydrogen hazards at experimental facilities, 19: 38875 (HASL-160)

HONEYWELL, INC., MINNEAPOLIS, MINN. AERONAUTICAL DIV.

Modulator materials study, 19: 38914 (SC-DC-65-1332)

I

IIT RESEARCH INST., CHICAGO, ILL.

Graphical lathe part programming system, 19: 40293 (SCL-DC-65-86)

ILLINOIS INST. OF TECH., CHICAGO.

Radiation effects on the physical properties of polymethyl-methacrylate, 19: 39231 (COO-1224-8)

ILLINOIS UNIV., URBANA. DEPT. OF MINING, METALLURGY, AND PETROLEUM ENGINEERING.

Ferrous martensites, 19: 40283 (COO-1198-237)

ILLINOIS UNIV., URBANA. DEPT. OF PHYSICS.

Dynamical properties of one-dimensional crystal with free ends, 19: 40079 (NP-15114)

Photoproduction of positive pions near threshold in hydrogen (thesis), 19: 39461 (COO-1195-35)

Surface studies using Moessbauer effect, 19: 40078 (NP-15111)

ILLINOIS UNIV., URBANA. MATERIALS RESEARCH LAB.

Ferrous martensites, 19: 40283 (COO-1198-237)

IMPERIAL COLL. OF SCIENCE AND TECH., LONDON (ENGLAND).

HPD programing at Rutherford Lab., 19: 38986 (CERN-65-11(p.173-81))

INSTITUT ATOMNOI ENERGII, GOSUDARSTVENNYI KOMITET PO ISPOL'ZOVANIYU ATOMNOI ENERGII SSSR, MOSCOW.

Measuring exchange capacitance and kinetic characteristics of ionites, 19: 40128 (ZFK-RN-17(p.75-94))

Problematics of pH measurement in reactor operation, 19: 40127 (ZFK-RN-17(p.9-23))

Pulsed plasma injectors, 19: 39955 (IAE-663)

Radiative stability of ion-exchange resins, 19: 38697 (ZFK-RN-17 (p.139-64))

Standardizing monitoring of H_2O purity in reactor loops, 19: 40124 (IAE-789)

Water purification and treatment for reactors. II., 19: 38759 (ZFK-RN-17(p.95-117)

Water purification and preparation at reactors, 19: 40123 (IAE-787)

INSTITUTE FOR ADVANCED STUDY, PRINCETON, N. J.

Proof of LSZ asymptotic condition, 19: 39629 (CONF-796(Paper 30))

INSTITUTE OF NUCLEAR RESEARCH, WARSAW (POLAND).

Energy spectrum of α particles from the $^{159}Tb(n,\alpha)^{156}Eu$ reaction with 14.2-Mev neutrons, 19: 39780 (INR-596/PL)

Initial value problem for a slab with anisotropic scattering, 19: 39765 (INR-611/IX-A/R)

Ion-exchange filter for EWA reactor, 19: 38760 (ZFK-RN-17(p.127-38))

Use of directional freezing of melt for Bi large single crystals preparation, 19: 39098 (INR-567/II/PS)

INSTITUTO DE ENERGIA ATOMICA, SAO PAULO (BRAZIL).

Magnetic scattering of neutrons in ferromagnetic samples, 19: 40075 (IEA-84)

Total neutron cross sections of Pr, Yb, Lu, and Er, 19: 39779 (IEA-86)

INSTITUTT FOR ATOMENERGI, HALDEN (NORWAY). OECD HALDEN REAKTOR PROSJEKT.

Survey of activities, 1964, 19: 40287 (NP-15188)

INSTITUTUL DE FIZICA ATOMICA, ACADEMIA R. P. R., BUCHAREST (ROMANIA).

Decomposition of H_2O in reactor, 19: 38698 (ZFK-RN-17(p.199-207))

INTERNATIONAL CENTRE FOR THEORETICAL PHYSICS, TRIESTE (ITALY).

Difficulties of N/D approach in bootstraps, 19: 39463 (IC/65/62)

IOWA STATE UNIV. OF SCIENCE AND TECH., AMES. COLL. OF VETERINARY MEDICINE.

Effects of subcutaneous implantation of rare-earth metals, 19: 38334 (COO-1170-1)

IOWA STATE UNIV. OF SCIENCE AND TECHNOLOGY, AMES. INST. FOR ATOMIC RESEARCH.

Effects of subcutaneous implantation of rare-earth metals, 19: 38334 (COO-1170-1)

ISRAEL ATOMIC ENERGY COMMISSION, YAVNE. SOREQ NUCLEAR RESEARCH CENTER.

Code for calculation of resonance escape probability in heterogeneous reactors, 19: 40153 (IA-1001)

Prog. rpt., semiannual, 7-12/64, 19: 39265 (IA-1021)

Study of interaction between lanthanide and nitrate ions, 19: 38578 (IA-1014)

ISTITUTO NAZIONALE DI FISICA NUCLEARE, TRIESTE (ITALY).

Bubble chamber for weak radioactivities, 19: 38993 (NP-15143)

Bubble chamber for weak radioactivity, 19: 38994 (NP-15145)

ISTITUTO SUPERIORE DI SANITA', ROME (ITALY). LABORATORI DI FISICA.

Prog. rpt., 1963-64, 19: 39464 (ISS-64/49)

J

JAPAN ATOMIC ENERGY RESEARCH INST., TOKYO.

Burn-up characteristics of pressure-tube-type D_2O-moderated power reactors, 19: 40185 (JAERI-1075)

Core dynamics model for JPDR, 19: 40186 (JAERI-1076)

Low-energy γ-ray spectra following resonance neutron captures. Measurement by an NaI scintillation spectrometer, 19: 39781 (JAERI-1073)

JET PROPULSION LAB., CALIF. INST. OF TECH., PASADENA.

Separation measurements in binary species gaseous vortex flows and flow visualization studies in a water vortex, 19: 40236 (LA-3229, pp 237-50)

Thermionic and thermoelectric energy conversion, 19: 39434 (N64-26371)

JOINT INST. FOR NUCLEAR RESEARCH, DUBNA (USSR). LAB OF HIGH ENERGY.

An investigation of the leptonic decays of $K^0_{\mu 3}$ mesons, 19: 39474 (JINR-P-2190)

Distribution of penetrating radiation field over protective zone of 10-Bev synchrophasotron, 21: 39315 (JINR-P-2177)

Interactions of 9-Bev π^- mesons with Xe nuclei, 19: 39472 (JINR-P-2178)

Spontaneous transitions by light propagation through anisotropic media, 19: 39266 (JINR-P-2195)

JOINT INST. FOR NUCLEAR RESEARCH, DUBNA (USSR). LAB OF NUCLEAR PROBLEMS.

An investigation of the leptonic decays of $K^0_{\mu 3}$ mesons, 19: 39474 (JINR-P-2190)

Atomic capture of μ^- in chemical compounds, 19: 39366 (JINR-P-2185)

Electrostatic field of uniformly charged volumes of a cylindrical configuration, 19: 39314 (JINR-P-2131)

Investigation of the ion motion in the central region of the fixed-field alternating-gradient cyclotron, 19: 39316 (JINR-P-2199)

Phase-shift analysis of nucleon-nucleon scattering at 400 Mev, 19: 39469 (JINR-P-2170)

JOINT INST. FOR NUCLEAR RESEARCH, DUBNA (USSR). LAB OF NUCLEAR REACTIONS.

Spontaneous transitions by light propagation through anisotropic media, 19: 39266 (JINR-P-2195)

JOINT INST. FOR NUCLEAR RESEARCH, DUBNA (USSR). LAB OF THEORETICAL PHYSICS.

Accuracy of calculations of collective oscillation frequency by u-v transformation method, 19: 39782 (JINR-P-2191)

Asymptotics of the Feynman graphs. III., 19: 39465 (JINR-E-2125)

Composite model of baryons on basis of three-body equation, 19: 39473 (JINR-P-2186)

Group SU_{12} as generalization of symplectic and spin symmetries,

19: 39471 (JINR-P-2175)
Inhomogeneous group SL(6) with an extended subgroup of translations, 19: 39468 (JINR-P-2123)
On $\gamma \rightarrow 3\pi$ and $\rho \rightarrow \pi\gamma$ interactions, 19: 39470 (JINR-P-2171)
On the structure of vector and axial currents in broken U(12) symmetry, 19: 39467 (JINR-E-2194)
The problem of mass formulas in the ISL(6) theory, 19: 39466 (JINR-E-2173)

K

KANSAS UNIV., LAWRENCE.
Sensitive, high-speed, d-c voltage comparator (thesis), 19: 40279 (BDX-613-72)
KERNFORSCHUNGSANLAGE, JUELICH (WEST GERMANY). INSTITUT FUER PHYSIKALISCHE CHEMIE.
Self-diffusion in liquid ammonia, 19: 38579 (JUL-238-PC)
KERNFORSCHUNGSANLAGE, JUELICH (WEST GERMANY). INSTITUT FUER REAKTORWERKSTOFFE.
Disassembly and sampling of graphite ball fuel elements, 19: 38792 (JUL-250-RW)
Disassembly of test irradiations and fuel elements in small cast iron, α–γ-cells and their subsequent handling, 19: 38795 (JUL-253-RW)
Handling high-level α–γ boxes, 19: 38793 (JUL-251-RW)
Improving economy with use of standardized, movable, in-cell boxes, and decontamination of their equipment, 19: 38794 (JUL-252-RW)
Packaging disassembled fuel elements and radioactive waste in hot cells, 19: 40270 (JUL-249-RW)
KERNFORSCHUNGSANLAGE, JUELICH (WEST GERMANY). INSTITUT FUER TECHNISCHE PHYSIK.
Theory of linear MHD-induction generators. II., 19: 39432 (JUL-256-TP)
KERNFORSCHUNGSZENTRUM, KARLSRUHE (WEST GERMANY). INSTITUT FUER RADIOCHEMIE.
Radiochemical synthesis of ^{14}C-labeled trichloromethylcycloalkane, 19: 38695 (KFK-317)
KNOLLS ATOMIC POWER LAB., SCHENECTADY, N. Y.
Cross sections for reactor design, 19: 40115 (CONF-650602-33)
KER-4—the thermal analysis of cylindrical fuel rods, 19: 40171 (KAPL-M-6475)

L

LABORATOIRE DE L'ACCELERATEUR LINEAIRE, UNIV. DE PARIS, ORSAY (FRANCE).
Production of positrons and determination of cross sections, 19: 39475 (LAL-27)
LAWRENCE RADIATION LAB., UNIV. OF CALIFORNIA, BERKELEY.
Axial dispersion in liquid flow through packed beds, 19: 38812 (UCRL-11951)
Data on particles and resonant states, 19: 39485 (UCRL-8030 (Pt.1)(Mar.'65, ed.))
Energy spectra of Kr_{83} decay modes, 19: 39488 (UCRL-16058)
Kinetics of chlorination of UCl_4 by Cl_2, 19: 38587 (UCRL-11986)
Neutron spectra from an organic scintillator, 19: 38997 (UCRL-16149)
Precision encoding and pattern recognition system, 19: 38978 (CERN-65-11(p. 81-90))
Prog. rpt. on chemical vapor deposition of Be from organoberyllium compounds, final, 6/63–1/64, 19: 39102 (UCRL-13100)
Reaction distribution in a porous anode, 19: 38591 (UCRL-16113)
Studies of atomic hydrogen at low pressures, 19: 38590 (UCRL-16050)
Thermodynamic stabilities of Nb and Ta oxides, 19: 38586 (UCRL-11957)
Ultracentrifuge photoelectric scanner, multiple cell, 19: 38921 (UCRL-11623)
Vapor pressure and heat of sublimation of CeF_3, 19: 38592 (UCRL-16150)
LAWRENCE RADIATION LAB., UNIV. OF CALIFORNIA, LIVERMORE.
Beam trajectories under the influence of self-fields and external focusing elements, 19: 39318 (UCRL-14194)
Chemical bonding and the sulfur K-x-ray spectrum, 19: 38588 (UCRL-12496)
Electron injection and E-layer build-up in Astron, 19: 39973 (UCRL-14131)
Fluid and hydrodynamics, 19: 38813 (UCRL-12204, pp 48-59)
High-speed microwave phase shifters using varactor diodes, 19: 40297 (UCRL-7753)
Isotope program of Project Gnome, 19: 38787 (PNE-102F)
Low-density, low-pressure solid explosive, 19: 38589 (UCRL-14186)
Nuclear and atomic physics, 19: 39788 (UCRL-12204, pp 1-27)
Prismatic loops and climb kinetics in quenched Al–Mg alloy, 19: 39169 (UCRL-16090)
Prog. rpt. on physics, 7–9/64, 19: 39271 (UCRL-12204)

Proposed standard for titration of aqueous solutions of boron, 19: 38561 (UCRL-14166-T)
Radiation physics, 19: 39273 (UCRL-12204, pp 60-5)
Scattering phase shift equations and resonance equations, 19: 39487 (UCRL-14193)
Sectorial parallel plate transmission line, 19: 40298 (UCRL-14141)
Thermodynamic properties of matter, 19: 39272 (UCRL-12204, pp 27-48)
Wigner's analysis of the unitary representations of the Poincare group, 19: 39486 (UCRL-12359)
LOCKHEED AIRCRAFT CORP., SUNNYVALE, CALIF.
RIFT NRDS operations plan, 19: 40245 (N64-23519)
LOCKHEED–GEORGIA CO., MARIETTA.
SNAP-8 radiation effects test program. II., 19: 39057 (NP-15022)
LOCKHEED MISSILES AND SPACE CO., SUNNYVALE, CALIF.
RIFT radiation effects program, 19: 39056 (N64-29558)
LOS ALAMOS SCIENTIFIC LAB., UNIV. OF CALIFORNIA, N. MEX.
Advanced nuclear propulsion concepts, 19: 40242 (LA-DC-7118)
Analysis of inherent errors in matrix decomposition using unnormalized arithmetic, 19: 39080 (LA-DC-7192)
Application of miniature intrinsic thermocouples for reactor transient diagnostics, 19: 38911 (LA-DC-7004)
Applications of a language for computing in combinatorics, 19: 39079 (LA-DC-7160)
Augmented plane wave calculations of band structure of Ce metal, 19: 40081 (SC-DC-65-1500)
Behavior of perlite in compression, 19: 38779 (LA-DC-7158)
Bibliography of atmospheric ozone to 40 Km: its concentration, distribution, methods of detection, and relationship with other meteorological phenomena, 19: 39260 (LA-3328)
BNL fluidized bed studies, 19: 40223 (LA-3229, pp 48-62)
Cavity reactor, 19: 40154 (LA-3229, pp 344-61)
dewars, 19: 39686 (LA-DC-7164)
Chilldown and storage losses of large liquid hydrogen storage
Coaxial flow gaseous nuclear reactor concept, 19: 40232 (LA-3229, pp 177-9)
Coaxial flow radiation heat transfer analysis, 19: 40234 (LA-3229, pp 208-21)
Coaxial flow research studies, 19: 40233 (LA-3229, pp 180-207)
Coexistence curve of ^3He, 19: 39685 (LA-DC-7086)
Coupling considerations in two-electron spectra, 19: 39367 (LA-DC-6548)
Criticality, 19: 40155 (LA-3229, pp 362-76)
Criticality of gas core reactors, 19: 40239 (LA-3229, pp 315-43)
Densities of some low-melting Pu alloys, 19: 39161 (LA-DC-6956)
Departures from eightfold way, 19: 39454 (CONF-796(Paper 18))
Determination of Pu in spent reactor fuels, Pu metal, alloys and compounds, 19: 38542 (LA-DC-6938)
Experimental work in relation to the glow-plug concept, 19: 40228 (LA-3229, pp 111-15)
Fast plasma from a coaxial gun, 19: 39956 (LA-DC-7043)
Flash x-ray analysis of fluidized beds, 19: 40224 (LA-3229, pp 63-82)
Fluidized beds, 19: 40225 (LA-3229, pp 83-5)
Fluidized beds, 19: 40226 (LA-3229, pp 86-8)
Gas core reactors, 19: 40235 (LA-3229, pp 222-36)
High-temperature gas interactions, 19: 40231 (LA-3229, pp 149-76)
Kinetic studies on extraction of Eu by Li amalgam and comparison to removal by electrolysis, 19: 38753 (LA-DC-7013)
Liquid-core nuclear rocket, 19: 40227 (LA-3229, pp 90-110)
Liquid hydrogen in nuclear rocket testing, 19: 40244 (LA-DC-7170)
Measurement of power-to-core temperature transfer function of Kiwi-B-4E, 19: 40241 (LA-DC-6845)
Nuclear propulsion schemes using MHD conversion techniques, 19: 40238 (LA-3229, pp 286-312)
On electrical conductivity in detonation products, 19: 40284 (LA-DC-6993)
Practical application of thermodynamics to Pu process reactions at high temperature, 19: 38752 (LA-DC-6947)
Proceedings of an advanced nuclear propulsion symposium, 19: 40221 (LA-3229)
Production of heavy nuclides by multiple neutron capture in nuclear explosions, 19: 38786 (LA-DC-7111)
Project Rover cryogenic evaluation laboratory, 19: 40243 (LA-DC-7169)
Pulsed neutron analysis in the Los Alamos Coupled Reactor Experiment, 19: 40240 (LA-3263)
Self-diffusion studies of gamma Pu, 19: 39162 (LA-DC-6957)
Separation measurements in binary species gaseous vortex flows in flow visualization studies in a water vortex, 19: 40236 (LA-3229, pp 237-50)
Solubility of selected elements in liquid Pu. IV., 19: 38580 (LA-3385)
Space transportation, 19: 40222 (LA-3229, pp 10-47)
Spectrographic investigation of the ignited mode of thermionic converter

operation, 19: 39433 (LA-DC-6898)
Status report on theory and experiments on heat pipes at Los Alamos, 19: 38780 (LA-DC-7206)
The response of pressure transmission lines, 19: 38912 (LA-DC-7025)
The transparent partition gaseous core reactor concept, 19: 40229 (LA-3229, pp 116-36)
The vapor pressure of plutonium, 19: 39159 (LA-DC-6926)
Vapor pressure of $U_{(c)}$ and $UC_{2(s)}$ in U–C system, 19: 39160 (LA-DC-6953)
Versatile high-temperature thermal analysis apparatus, 19: 38913 (LA-DC-7071)
Vortices and vortex matrices, 19: 40237 (LA-3229, pp 251-85)
Work on nuclear light bulb at UAC research laboratories, 19: 40230 (LA-3229, pp 137-47)

LYON UNIV. (FRANCE).
Quadrupolar effects on energy levels in a μ-mesic manganese atom, 19: 39368 (NP-15089)

M

MAGYAR TUDOMANYOS AKADEMIA, BUDAPEST.
Water-side experiences on Hungarian research reactor, 19: 40264 (ZFK-RN-17(p.54-67))

MALLINCKRODT CHEMICAL WORKS, WELDON SPRING, MO. URANIUM DIV.
Electrolytic preparation of U metal from UO_2 using a frozen-crust cell, 19: 39099 (MCW-1492, pp 7-11)
Prog. rpt. on process development, 1–3/65, 19: 38543 (MCW-1492)
Spectrochemical method for determination of U in electrolyte, 19: 38544 (MCW-1492, pp 13-19)
Spectrochemical method for determination of impurity elements in Th compounds, 19: 38545 (MCW-1492, pp 23-8)

MARTIN CO., BALTIMORE, MD. NUCLEAR DIV.
Nimbus dynamics analysis for ejection mechanism, 19: 39071 (MND-3169-68)
Prog. rpt. on Cs-vapor filled thermionic converters, annual, 11/63–10/64, 19: 39431 (AD-608554)

MARTIN CO., BALTIMORE, MD. RESEARCH INST. FOR ADVANCED STUDIES.
Stimulated photon-photon scattering, 19: 39264 (CONF-796(Paper 14))

MARYLAND UNIV., COLLEGE PARK. DEPT. OF PHYSICS AND ASTRONOMY.
Axiomatic field theory, 19: 39628 (CONF-796(Paper 29))
Conference on theoretical physics, 3rd annual Eastern U. S., Univ. of Maryland, 10/64, 19: 39263 (CONF-796)
Departures from eightfold way, 19: 39454 (CONF-796(Paper 18))
Existence of solutions to field equations, 19: 39627 (CONF-796 (Paper 26))
Extrapolation of nucleon electromagnetic form factors, 19: 39458 (CONF-796(Paper 24))
Foldy-Wouthuysen transformation in covariant spinor formulation, 19: 39630 (CONF-796(Paper 31))
Gravitation and quantum mechanics of macroscopic objects, 19: 39625 (CONF-796(Paper 12))
Low-energy hyperon-proton scattering interactions, 19: 39460 (CONF-650410-3)
Low-temperature expansion of spontaneous magnetization of Heisenberg ferromagnet, 19: 39684 (CONF-796(Paper 4))
Masses of elementary particles from geometry of space-time, 19: 39452 (CONF-796(Paper 13))
Measurement of Stark widths and shifts of nitrogen ion lines (thesis), 19: 39952 (AFCRL-65-348)
Problem of combining internal- and space-time symmetries, 19: 39455 (CONF-796(Paper 19))
Proof of LSZ asymptotic condition, 19: 39629 (CONF-796(Paper 30))
Quantum mechanical three-body problem for attractive potentials, 19: 39453 (CONF-796(Paper 15))
Representation of discrete symmetry operators, 19: 39626 (CONF-796(Paper 22))
Stimulated photon-photon scattering, 19: 39264 (CONF-796(Paper 14))
Strongly coupled electron-phon system in normal and superconducting metals, 19: 40073 (CONF-796(Paper 1))
SU(6) and nonleptonic hyperon decay, 19: 39456 (CONF-796(Paper 21))
SU_6 in relativistic particle mechanics, 19: 39459 (CONF-796 (Paper 28))
Theories of magnetism in metals, 19: 40074 (CONF-796(Paper 3))
Time reversal invariance in $\Sigma^0 \to \Lambda^0 + e^+ + e^-$, 19: 39484 (TID-22038)
Weak interactions, 19: 39457 (CONF-796(Paper 23))

MASSACHUSETTS INST. OF TECH., CAMBRIDGE.
Experience with SPASS system, 19: 38972 (CERN-65-11(p.7-13))
Precision encoding and pattern recognition system, 19: 38978 (CERN-65-11(p. 81-90))
Prog. rpt. on metallic systems, annual, 1964, 19: 39168 (TID-22015)

MASSACHUSETTS INST. OF TECH., CAMBRIDGE. DEPT. OF CHEMICAL ENGINEERING.
Gamma-radiation effects on growth of KCl crystals, 19: 38696 (MIT-2909-4)

MASSACHUSETTS INST. OF TECH., CAMBRIDGE. DEPT. OF METEOROLOGY.
The energy and momentum budget of the atmosphere above the tropopause, 19: 39258 (CONF-650534-1)

MASSACHUSETTS INST. OF TECH., CAMBRIDGE. DEPT. OF NUCLEAR ENGINEERING.
Gamma-radiation effects on growth of KCl crystals, 19: 38696 (MIT-2909-4)

MASSACHUSETTS INST. OF TECH., CAMBRIDGE. METALS PROCESSING LAB.
Strength and plasticity of anisotropic metals. Final report, 19: 39149 (AD-425880)

MASSACHUSETTS INST. OF TECH., CAMBRIDGE. RESEARCH LAB. OF ELECTRONICS.
Prog. rpt. on electronics, 4/15/65, 19: 39270 (TID-21894)

MAX-PLANCK-INSTITUT FUR PHYSIK UND ASTROPHYSIK, MUNICH (WEST GERMANY).
Post FILTER routine of CERN HAZE, 19: 38983 (CERN-65-11(p. 139-43))

MEDICAL RESEARCH COUNCIL, LONDON (ENGLAND).
Assay of Sr-90 in human bone in the United Kingdom, 19: 38863

MICHIGAN UNIV., ANN ARBOR.
Cross-over signals in atomic hydrogen (thesis), 19: 39371 (TID-22044)

MICHIGAN UNIV., ANN ARBOR. COLL. OF LITERATURE, SCIENCE AND THE ARTS.
University of Michigan 83-inch cyclotron, 19: 39313 (COO-921-16)

MICHIGAN UNIV., ANN ARBOR. LAB. FOR FLUID FLOW AND HEAT TRANSPORT PHENOMENA.
Ultrasonic-induced cavitation studies in lead–bismuth alloys at elevated temperatures, 19: 39116 (NP-15263)

MOUND LAB., MIAMISBURG, OHIO.
Determination of tertiary butyl perbenzoate in molding powders, 19: 40285 (MLM-1284)
Prog. rpt. on reactor fuels and materials, annual, 1964, 19: 39163 (MLM-1244)

N

NATIONAL AERONAUTICS AND SPACE ADMINISTRATION, CLEVELAND, OHIO. LEWIS RESEARCH CENTER.
Coaxial flow gaseous nuclear reactor concept, 19: 40232 (LA-3229, pp 177-9)
Coaxial flow radiation heat transfer analysis, 19: 40234 (LA-3229, pp 208-21)
Coaxial flow research studies, 19: 40233 (LA-3229, pp 180-207)

NATIONAL AERONAUTICS AND SPACE ADMINISTRATION, WASHINGTON, D. C.
Electrical power generation systems for space applications, 19: 38836 (NASA-SP-79)

NATIONAL INST. FOR RESEARCH IN NUCLEAR SCIENCE, CHILTON (ENGLAND). RUTHERFORD HIGH ENERGY LAB.
HPD programming at Rutherford Lab., 19: 38986 (CERN-65-11(p. 173-81))

NATIONAL MARINE CONSULTANTS, ANAHEIM, CALIF.
Task IV interim progress report, 19: 40288 (NVO-98-5)

NAVAL CIVIL ENGINEERING LAB., PORT HUENEME, CALIF.
Measurement of thermal neutron albedo for materials, 19: 40065 (NP-15152)

NAVAL RADIOLOGICAL DEFENSE LAB., SAN FRANCISCO, CALIF.
Influence of AET on hypoxia on recovery from radiation injury in mice, 19: 38450 (USNRDL-TR-651)

NAVAL RESEARCH LAB., WASHINGTON, D. C.
Calculations on uniform-field bending magnets, 19: 39317 (NRL-6248)

NEVIS LABS., COLUMBIA UNIV., IRVINGTON-ON-HUDSON, N. Y.
Antiproton annihilation in H at rest. I., 19: 39462 (CU-1932-239)

NORTH CAROLINA STATE OF THE UNIV. OF NORTH CAROLINA, RALEIGH. DEPT. OF ENGINEERING RESEARCH.
Nuclear fuel consisting of very small uniformly dispersed UC particles in a uranium matrix, 19: 39127 (NCSC-2981-9)

NORTH CAROLINA UNIV., CHAPEL HILL.
Gravitation and quantum mechanics of macroscopic objects, 19: 39625 (CONF-796(Paper 12))

NORTHWESTERN UNIV., CHICAGO, ILL. DEPT. OF PATHOLOGY.
Incorporation of thymidine into DNA of organs of mice, 19: 38336 (TID-21106)

NOTRE DAME UNIV., IND.

Convex sets and their applications, 19: 39082 (TID-22032)
NUCLEAR ENERGY INFORMATION CENTER, WARSAW (POLAND).
Bibliography on nuclear astrophysics. IV., 19: 39331 (NEIC-RR-11)
NUCLEAR MATERIALS AND EQUIPMENT CORP., APOLLO, PA.
Preparation and properties of spherical particulate nuclear fuels for Pu-fueled reactors, 19: 39096 (CONF-117(p. 103-26))
NUCLEAR METALS, INC., WEST CONCORD, MASS.
Prog. rpt. on W–Re tube fabrication, 7/64–6/65, 19: 39128 (NMI-1267)
NUCLEAR UTILITY SERVICES, INC., WASHINGTON, D. C.
Hydrogen evolution with-in containment in PM-type plants, 19: 40188 (NYO-3420-2)
NURSE-1—a nuclear rocket safety evaluation code for the control data 3600, 19: 40248 (NUS-180)

O

OAK RIDGE GASEOUS DIFFUSION PLANT, TENN.
Mass spectrometric analysis of BF_3, 19: 38541 (K-L-6057)
OAK RIDGE NATIONAL LAB., TENN.
Aluminum and titanium corrosion in saline waters at elevated temperatures, 19: 39117 (ORNL-P-1430)
An evaluation of a fast complementary, hybrid bistable multivibrator, 19: 38920 (TID-22019)
Anomalous plasma diffusion in magnetic wells, 19: 39968 (ORNL-P-1338)
Beta-type absorbed dose from non-beta-emitting radionuclides, 19: 38878 (ORNL-P-1405)
Channeling effects on the energy loss of high-energy (20-80 Mev) ^{79}Br and ^{127}I ions in gold, 19: 39370 (ORNL-P-1336)
Chemistry and thermodynamics of MSRE fluoride solutions, 19: 38582 (ORNL-P-1428)
Cost study of large Na-cooled fast breeder for desalination, 19: 40190 (ORNL-TM-784)
Determination of neutron flux in nuclear reactors, 19: 40157 (ORNL-TM-1175)
DIAGNOSE, a routine to debug FORTRAN programs, 19: 39081 (ORNL-TM-1176)
Energetic neutral injection into an electron-cyclotron plasma, 19: 39970 (ORNL-P-1374)
Evaluation of neutron emission, kerma, kerma equivalent, dose equivalent and spectrum, 19: 39766 (ORNL-TM-1171)
Finite amplitude waves in liquid and solids, 19: 39268 (ORNL-P-1395)
Information on conversion coefficients from Coulomb excitation and life-time measurements, 19: 39786 (ORNL-P-1419)
Intermediate states as observed by differential scattering of neutrons by doubly closed shell nuclei, 19: 39785 (ORNL-P-1356)
Mechanized durability tests of six-foot Punkah-pump, 19: 38832 (ORNL-TM-1155)
Motion of particles in fluidized beds and implications for the preparation of coated nuclear fuel particles, 19: 38782 (ORNL-TM-1170)
MSRE design and operations report- VI., 19: 40189 (ORNL-TM-733(Rev.))
On radiative transition in ^{207}Pb and ^{206}Pb following resonance neutron capture on ^{206}Pb and ^{207}Pb, 19: 39783 (ORNL-P-1345)
Operating and repair experiences on DCX-2 coils, 19: 39971 (ORNL-P-1438)
Plasma heating by means of beam plasma interaction, 19: 39969 (ORNL-P-1373)
Production of 10^{-9} torr within a large plasma container (DCX-1), 19: 39966 (ORNL-P-1245)
Prog. rpt. on coated-particle fuels, 11/64–5/65, 19: 39129 (ORNL-TM-1116)
Prog. rpt. on ORR operations 1–3/65, 19: 40259 (ORNL-TM-1181)
Prog. rpt. on Th fuel cycle development, 10–12/63, 19: 38755 (ORNL-3611)
Severe microinstability-driven losses in an energetic plasma, 19: 39967 (ORNL-P-1337)
SOURCE, a neutron distribution routine for the 05R Monte Carlo code, 19: 39767 (ORNL-TM-1192)
Strong p-wave neutron resonances in ^{120}Sn, ^{118}Sn, and ^{124}Sn, 19: 39784 (ORNL-P-1352)
OESTERREICHISCHE STUDIENGESELLSCHAFT FUER ATOMENERGIE G.M.B.H., SEIBERSDORF. INSTITUT FUER CHEMIE.
Isolation of carrier-free Sr-90 and Ba-140 from irradiated U, 19: 38757 (SGAE-CH-17/1965)
Uranium electrolytic deposition on metals, 19: 39100 (SGAE-CH-16/1965)
OESTERREICHISCHE STUDIENGESELLSCHAFT FUER ATOMENERGIE G.M.B.H., SEIBERSDORF. PHYSIK-INSTITUT.
Behavior of γ radiation in air, 19: 39483 (SGAE-PH-20/1965)
Nondestructive testing of fuel elements, 19: 38825 (NP-15176)
Pair production cross sections for 6.13 Mev γ rays, 19: 39787 (SGAE-PH-19/1965)
OFFICE OF THE ASSISTANT GENERAL MANAGER FOR REACTORS (AEC), WASHINGTON, D. C.
Nuclear reactors built, being built, or planned in the United States as of June 30, 1965, 19: 40116 (TID-8200(12th Rev.))
OREGON UNIV., PORTLAND. DIV. OF EXPERIMENTAL MEDICINE.
Ordered triplet code for messenger RNA, 19: 40296 (TID-21856)

P

PARIS UNIV., ORSAY (FRANCE). INSTITUT DU RADIUM.
Results obtained with off-line HPD system, 19: 38988 (CERN-65-11 (p. 183-206))
PARIS UNIV., ORSAY (FRANCE). LABORATOIRE DE PHYSIQUE THEORIQUE ET HAUTES ENERGIES.
Covariant theory of relativistic Brownian motion. I., 19: 39959 (N64-22435)
PENNSYLVANIA UNIV., PHILADELPHIA.
HPD programing at Univ. of Pennsylvania, 19: 38990 (CERN-65-11 (p.229-36))
Strongly coupled electron-phon system in normal and superconducting metals, 19: 40073 (CONF-796(Paper 1))
PHYLATRON CORP., COLUMBUS, OHIO.
Development of fast neutron dosimetry system, 19: 38992 (COO-1226-8)
PITTSBURGH UNIV., PA.
SU_6 in relativistic particle mechanics, 19: 39459 (CONF-796 (Paper 28))
PRATT AND WHITNEY AIRCRAFT, MIDDLETOWN, CONN. CONNECTICUT ADVANCED NUCLEAR ENGINEERING LAB.
Chemical state of C, H, and O in alkali metals, 19: 39157 (CNLM-6337)
PRINCETON UNIV., N. J.
Axiomatic field theory, 19: 39628 (CONF-796(Paper 29))
High-temperature gas interactions, 19: 40231 (LA-3229, pp 149-76)
Liquid-core nuclear rocket, 19: 40227 (LA-3229, pp 90-110)
PRINCETON UNIV., N. J. GUGGENHEIM LABS. FOR THE AEROSPACE PROPULSION SCIENCES.
Prog. rpt. on combustion of metals, 7–12/64, 19: 38583 (SC-DC-65-1401)
PRINCETON UNIV., N. J. PLASMA PHYSICS LAB.
Measurement of ion concentrations and electron temperature in Ba plasma, 19: 39958 (MATT-327)
Off-line global approach to pattern recognition for bubble chamber pictures, 19: 38996 (PPAD-2137-548)
Relationship between resistive instabilities and microinstabilities in inhomogeneous plasmas, 19: 39957 (MATT-320)
PUBLIC HEALTH SERVICE, WASHINGTON, D. C. DIV. OF RADIOLOGICAL HEALTH.
Radioactive decay correction factors, 19: 38744 (PHS-999-RH-12)
PURDUE UNIV., LAFAYETTE, IND.
SU(6) and nonleptonic hyperon decay, 19: 39456 (CONF-796(Paper 21))
PURDUE UNIV., LAFAYETTE, IND. DEPT. OF PHYSICS.
Coupling considerations in two-electron spectra, 19: 39367 (LA-DC-6548)

R

RADIATION APPLICATIONS INC., LONG ISLAND CITY, N. Y.
Prog. rpt. on removal of metallic ions by foaming agents and suspensions, annual, 7/63–6/64, 19: 40271 (RAI-350)
RADIO CORP. OF AMERICA, HARRISON, N. J. DIRECT ENERGY CONVERSION DEPT.
Prog. rpt. on thermoelectric modules, 7/15–10/15/63, 19: 39430 (AD-426092)
REACTOR GROUP, UNITED KINGDOM ATOMIC ENERGY AUTHORITY, DOUNREAY (SCOTLAND).
Random fluctuations of DFR power, 19: 40193 (TRG-Report-921)
RENSSELAER POLYTECHNIC INST., TROY, N. Y. DEPT. OF NUCLEAR ENGINEERING AND SCIENCE.
Asymptotic and steady state spectrum measurements in a multiplying medium, 19: 39768 (RPI-328-21)
RESEARCH LAB., GENERAL ELECTRIC CO., SCHENECTADY, N. Y.
Prog. rpt. on radiation damage in solids, final, 4/62–3/65, 19: 39225 (AFCRL-65-305)
ROCKY FLATS DIV., DOW CHEMICAL CO., DENVER, COLO.
Electric discharge as trap for diffusion-pump vacuum systems, 19: 38877 (RFP-572)
Preliminary studies on reactions of burning Pu in various solvents, 19: 38879 (RFP-566)
Prog. rpt. on technical services, 12/64–2/65, 19: 38546 (RFP-552)
Total hemispherical emittance of polished and of oxidized alpha Pu. Preliminary Report, 19: 39167 (RFP-616)

Volumetric calibration of process vessels using digital computer techniques, 19: 38756 (RFP-488)
ROCKY FLATS DIV., DOW CHEMICAL CO., GOLDEN, COLO.
Handling and measurement of plutonium shipments, 19: 38535 (RFP-508)
Nuclear materials management control system for U reactor fuel element fabrication, 19: 39130 (RFP-507)
RUTGERS–THE STATE UNIV. OF NEW JERSEY, NEW BRUNSWICK.
Existence of solutions to field equations, 19: 39627 (CONF-796 (Paper 26))
RUTGERS–THE STATE UNIV. OF NEW JERSEY, NEW BRUNSWICK. SCHOOL OF CHEMISTRY.
Intermolecular bonding effects in Sn^{119m} Moessbauer spectroscopy, 19: 38577 (CONF-650425-6)
Moessbauer parameters for metal-organic (Fe,Sn) compounds, 19: 38576 (CONF-650425-2)

S

SANDIA CORP., ALBUQUERQUE, N. MEX.
ACCEL: Automated circuit card etching layout, 19: 38915 (SC-DC-65-1419)
Application of electron microscopy in dimensional metrology, 19: 38916 (SC-DC-65-1589)
Augmented plane wave calculations of band structure of Ce metal, 19: 40081 (SC-DC-65-1500)
Base and surface pressure variation with Mach number on a right circular cone, 19: 40292 (SC-TM-202-56-51)
Close-in air blast from row charge in basalt, 19: 38790 (PNE-608F)
Electronic integrators for instrumentation applications, 19: 38918 (SC-R-65-904, pp 49-58)
Energy transfer by neutrons to certain materials, 19: 39769 (SC-DC-65-1544)
Extended range velocity gage for measurements in high shock environments, 19: 38917 (SC-R-65-904, pp 23-48))
Four papers concerning recent work on ground motion measurements, 19: 38864 (SC-R-65-904)
Generic classification for teaching machines, 19: 40291 (SC-R-65-923)
Ground motion measurements, 19: 38865 (SC-R-65-904, pp 3-22)
Instrumenting nuclear explosions, 19: 38919 (SC-R-65-904, pp 59-74)
Modulator materials study, 19: 38914 (SC-DC-65-1332)
Prog. rpt. on combustion of metals, 7–12/64, 19: 38583 (SC-DC-65-1480)
Prog. rpt. on re-entry dispersal of reactor core materials, 1–3/65, 19: 39118 (SC-DC-65-1520)
Reaction between U(IV) and various valence states of Np, 19: 38584 (SC-RR-65-219)
Structure and electrical properties of vacuum-deposited CdS thin films, 19: 38585 (SC-TM-64-1677)
SANDIA CORP., LIVERMORE, CALIF.
Graphical lathe part programming system, 19: 40293 (SCL-DC-65-86)
SOCIETE D'ENERGIE NUCLEAIRE FRANCO-BELGE DES ARDENNES, CHOOZ-LEZ-GIVET (FRANCE).
Prog. rpt. on Ardennes nuclear power plant, 1–3/65, 19: 40192 (TID-22003)
SOUTH CAROLINA UNIV., COLUMBIA.
Representation of discrete symmetry operators, 19: 39626 (CONF-796(Paper 22))
SOUTHERN INTERSTATE NUCLEAR BOARD, ATLANTA, GA.
Study of applicability of radiation pasteurization of fruits in the South, 19: 39062 (TID-21710(Rev.))
SOUTHWEST RESEARCH INST., SAN ANTONIO, TEX.
Nondestructive assay of nuclear fuels, 19: 38547 (TID-21475)
SOUTHWEST RESEARCH INST., SAN ANTONIO, TEX. DEPT. OF ELECTRONICS AND ELECTRICAL ENGINEERING.
Nondestructive evaluation of metal fatigue, 19: 39151 (AFOSR-65-0981)
STANFORD UNIV., CALIF. INST. FOR PLASMA RESEARCH.
Prog. rpt. on plasma oscillations, 3–5/65, 19: 39972 (SU-IPR-17)
STANFORD UNIV., CALIF. STANFORD ELECTRONICS LABS.
Prog. rpt., 10–12/64, 19: 39269 (SU-SEL-64-133)
STICHTING VOOR FUNDAMENTEEL ONDERZOEK DER MATERIE, JUTPHAAS (NETHERLANDS). INSTITUUT VOOR PLASMA-FYSICA.
Space charge and currents in continuous rotating plasma accelerator, 19: 39962 (NP-15167)
SYDNEY UNIV. (AUSTRALIA). SCHOOL OF PHYSICS.
Magnetohydrodynamic ionizing shock waves in a conducting medium, 19: 39267 (NP-15157)
Pre-ionization and shock wave ionization in crossed-field plasma source, 19: 39961 (NP-15112)
SYRACUSE UNIV., N. Y.
Prog. rpt. on correlation in many-particle systems, final, 2/63–1/65, 19: 39261 (AROD-3979:2)

T

TENNESSEE UNIV., KNOXVILLE.
Evaluation of neutron emission, kerma, kerma equivalent, dose equivalent and spectrum, 19: 39766 (ORNL-TM-1171)
Finite amplitude waves in liquids and solids, 19: 39268 (ORNL-P-1395)
TENNESSEE UNIV., KNOXVILLE. DEPT. OF ELECTRICAL ENGINEERING.
An evaluation of a fast complementary, hybrid bistable multivibrator, 19: 38920 (TID-22019)
TEXAS TECHNOLOGICAL COLL., LUBBOCK.
The effects on rat behavior of developmental aberrations induced by irradiation *in utero*, 19: 38361 (TID-21951)
THAYER SCHOOL OF ENGINEERING, DARTMOUTH COLL., HANOVER, N. H.
Rise velocity of cylindrical bubbles in inclined tubes, 19: 38808 (NYO-3114-8)
TORONTO UNIV. (ONTARIO).
Stimulated photon-photon scattering, 19: 39264 (CONF-796(Paper 14))
TRIESTE UNIV. (ITALY). ISTITUTO DI FISICA.
Bubble chamber for weak radioactivities, 19: 38993 (NP-15143)
Bubble chamber for weak radioactivity, 19: 38994 (NP-15145)
TRW SPACE TECHNOLOGY LABS., THOMPSON RAMO WOOLDRIDGE INC., REDONDO BEACH, CALIF.
Ion emitter studies, 19: 39164 (N64-22193)

U

UNION CARBIDE CORP., OAK RIDGE, TENN. Y-12 PLANT.
Nuclear materials management in a recovery facility for unirradiated enriched uranium, 19: 38758 (Y-KA-7)
The preparation of radioactive phosphorus-32 sources on metal plates, 19: 38745 (Y-1484)
UNITED AIRCRAFT CORP., EAST HARTFORD, CONN. RESEARCH LABS.
Work on nuclear light bulb at UAC research laboratories, 19: 40230 (LA-3229, pp 137-47)
UNITED NUCLEAR CORP., WHITE PLAINS, N. Y. DEVELOPMENT DIV.
Sodium void coefficient of reactivity. A review and study of analytical work, 19: 40158 (UNC-5123)
UNITED STATES–EURATOM JOINT RESEARCH AND DEVELOPMENT PROGRAM.
Nuclear fuel consisting of very small uniformly dispersed UC particles in a uranium matrix, 19: 39127 (NCSC-2981-9)
Prog. rpt. on fission-fragment effects in structural materials, 4–6/65, 19: 39229 (BMI-X-10134)
Prog. rpt. on fission-product reactions with and release from fuel-element claddings, 4–6/65, 19: 39152 (BMI-X-10132)
Prog. rpt. on steam separation technology, 4–6/65, 19: 38801 (ACNP-65004)
Prog. rpt. on transition boiling heat transfer, 4–6/65, 19: 38806 (GEAP-4908)
UNITED STATES NAVAL ACADEMY, ANNAPOLIS, MD.
Radiation effects on transistors, 19: 39054 (AD-607863)
UNIVERSIDAD MAYOR DE "SAN ANDRES," LA PAZ (BOLIVIA). LABORATORIO DE FISICA COSMICA DE CHACALTAYA.
Time variations in cosmic rays and radiosonde measurements, 19: 39421 (NP-15154)
USTAV JADERNEHO VYZKUMU, CESKOSLOVENSKA AKADEMIE VED, REZ.
Measurement of pH value and conductivity of distilled water in primary circuit of reactor WWR-S in Rez, 19: 40263 (ZFK-RN-17(p.32-43))

V

VEB ATOMKRAFTWERK, RHEINSBERG (EAST GERMANY).
Natural cation exchangers for purification of radioactive wastes, 19: 40130 (ZFK-RN-17(p.165-78))
VEB FARBENFABRIK, WOLFEN (EAST GERMANY).
Effects of radiostability of synthetic resin exchangers on application in radioactive circuits, 19: 40129 (ZFK-RN-17(p.114-26))
VIRGINIA UNIV., CHARLOTTESVILLE.
Problem of combining internal- and space-time symmetries, 19: 39455 (CONF-796(Paper 19))

W

WASHINGTON UNIV., SEATTLE.

Pressure-drop characteristics of two eccentrically positioned orifices in series. I., 19: 38810 (RL-SA-31)

WEATHER BUREAU, IDAHO FALLS, IDAHO.

Aerodynamic effects of large reactor complexes upon atmospheric turbulence and diffusion, 19: 39259 (IDO-12041)

WESTINGHOUSE ELECTRIC CORP., LIMA, OHIO. AEROSPACE ELECTRICAL DIV.

Converters (d-c to d-c) for nuclear-thermionic energy sources, 19: 38835 (N65-27619)

WESTINGHOUSE ELECTRIC CORP., PITTSBURGH, PA. ATOMIC POWER DIV.

Fabrication and irradiation of thin-walled type 304 stainless steel clad fuel rods in the Saxton Reactor, 19: 39236 (WCAP-3269-36)

Prog. rpt. on large closed-cycle water reactor, 7–9/64, 19: 40195 (WCAP-3269-5)

Prog. rpt. on large closed-cycle water reactor, 10–12/64, 19: 40196 (WCAP-3269-6)

Prog. rpt. on large closed-cycle water reactor, 7–9/62, 19: 40197 (WCAP-8718)

Prog. rpt. on large closed-cycle water reactor, 10–12/62, 19: 40198 (WCAP-3721)

WISCONSIN UNIV., MADISON. DEPT. OF PHYSICS.

Prog. rpt. on thermonuclear plasma studies, 2–4/65, 19: 39954 (COO-1233-20)

Y

YALE UNIV., NEW HAVEN, CONN.

Precision encoding and pattern recognition system, 19: 38978 (CERN-65-11(p.81-90))

Z

ZENTRALINSTITUT FUER KERNPHYSIK, ROSSENDORF BEI DRESDEN (EAST GERMANY).

Conference on water problems in reactors, Rossendorf, Germany, 4/62, 19: 40117 (ZFK-RN-17)

Continuous measurements of specific water resistance in closed circuits, 19: 40262 (ZFK-RN-17(p.25-31))

Decomposition of H_2O in reactor, 19: 38698 (ZFK-RN-17(p.199-207))

Effects of radiostability of synthetic resin exchangers on application in radioactive circuits, 19: 40129 (ZFK-RN-17(p.114-26))

Ion-exchange filter for EWA reactor, 19: 38760 (ZFK-RN-17(p. 127-38))

Many-group parameter sets for calculation of fast reactors, 19: 40161 (ZfK-TPh-11)

Measurement of pH value and conductivity of distilled water in primary circuit of reactor WWR-S in Rez, 19: 40263 (ZFK-RN-17(p.32-43))

Measuring exchange capacitance and kinetic characteristics of ionites, 19: 40128 (ZFK-RN-17(p.75-94))

Natural cation exchangers for purification of radioactive wastes, 19: 40130 (ZFK-RN-17(p.165-78))

Problematics of pH measurement in reactor operation, 19: 40127 (ZFK-RN-17(p.9-23))

Quality of primary circuit water in research reactors, 19: 40260 (ZFK-RN-17(p.68-74))

Radiative stability of ion-exchange resins, 19: 38697 (ZFK-RN-17 (p. 139-64))

Review of work at Rossendorf research reactor, 1961, 19: 40261 (ZFK-RN-17(p.179-98))

Water purification and treatment for reactors. II., 19: 38759 (ZFK-RN-17(p. 95-117))

Water-side experiences on Hungarian research reactor, 19: 40264 (ZFK-RN-17(p.54-67))

PERSONAL AUTHOR INDEX

Each entry after an author's name is a shortened version of the title of the report or article, followed by the *NSA* volume and abstract number. Report numbers are given in parentheses.

The phrase "Progress report" is abbreviated as "Prog. rpt.," permitting a more rapid and complete alphabetical arrangement of the titles without changing the location of the progress report titles in relation to the other titles.

Because of problems involving the mechanical preparation of this index, all accent marks are omitted. The following changes in spelling have been introduced to reduce some of the confusion which might result from omitting the accents:

ä	becomes	ae
ö		oe
ø		oe
ü		ue (except in transliterated Chinese names)

A

AARON, R., Theory of the three-nucleon system, 19: 39923

AARONS, Jules, Radio astronomical and satellite studies of the atmosphere, 19: 39363

ABDON, R., Utilization of Rapsodie reactor for measurement of Doppler effect, 19: 40150 (CEA-R-2565)

ABDURAZAKOV, A. A., Decay of ^{161}Ho, 19: 39930

ABELES, B., Absorption of transverse microwave phonons by Al–Pb superconducting diodes, 19: 39713

ABRAHAMER, I., Study of interaction between lanthanide and nitrate ions, 19: 38578 (IA-1014)

ABRAMS, K., Status of HPD programs at BNL, 19: 38980 (CERN-65-11 (p.97-113))

ABREU, M., Total neutron cross sections of Pr, Yb, Lu, and Er, 19: 39779 (IEA-86)

ABUL-MAGD, A. Y., Cluster stripping processes, 19: 39829

ADAIR, Robert K., Problems in the analyses of final-state resonances, 19: 39575

ADAMS, D. J., A search for low-energy γ rays from the quasar 3C286, 19: 39357

ADAMS, Gail D., Neutron measurements relating to patients treated with x-rays from 70-Mev synchrotron, 19: 38517

ADAMS, R. O., Electric discharge as trap for diffusion-pump vacuum systems, 19: 38839 (RFP-572)

ADAMS, Robert M., Clinically useful calculations of the dose distribution from multiple radiation sources, 19: 38526

ADLER, George, Role of oxygen in solid-state polymerization. I., 19: 38694 (BNL-9200)

AGAR, James Darrel, Pressure-drop characteristics of two eccentrically positioned orifices in series. I., 19: 38810 (RL-SA-31)

AGEEV, N. V., Thermal hardness of β alloys of Ti–Mo–Cr–Fe–Al system, 19: 39193

AGGARWAL, S., Formation of the F_1 and F_2 layers, 19: 39666

AGGSON, T. L., Production of positrons and determination of cross sections, 19: 39475 (LAL-27)

AGNASSI, J. J., D/F ratios and baryon magnetic moments in the SV_{12} scheme, 19: 39524

AGOPIAN, K., Effect of Rn inhalation on chronic diseases of nose and paranasal cavities, 19: 38528

AHMED, K., Vector mesons and complex angular momentum, 19: 39518

AIGINGER, Hannes, Polarization of 0.5-, 1-, and 2-Mev electron produced Cherenkov radiation, 19: 39599

AINSWORTH, E. J., Influence of AET and hypoxia on recovery from radiation injury in mice, 19: 38450 (USNRDL-TR-851)

AINUTDINOV, M., Four-prong stars in π^-p interactions at 3.5 Bev, 19: 39591

AITCHISON, I. J. R., Apparent, but energy-dependent pseudo-resonances due to rescattering in sequential processes, 19: 39897

AITKEN, W. M., Some aurora australis lower border heights, 1961, 19: 39671

AKAISHI, Jun, Fallout radioactivity in diet and excreta. The levels at Tokai District, Japan in 1962 to 1963, 19: 38894

AKHTAR, Sayeed, Removal of ^{3}H from ^{3}He by adsorption on charcoal, 19: 38773

AKUTSU, Juichi, Discharge mechanism of Bi-containing argon counter, 19: 39036

ALBAUGH, F. W., Prog. rpt. on development of D_2O-moderated reactors, 12/64, 19: 38805 (BNWL-C-3)

ALBERT, Philippe, Fusion by electron bombardment and its application in metallurgy, 19: 39109

ALBERTI, G., Ion exchange in fused salts. I., 19: 38771

ALCARAZ, E. C., Measurements of a thermal-conductivity length dependence in helium II, 19: 39730

ALCOCK, C. B., Study of cation diffusion in UO_2 using α spectrometry, 19: 38681

ALDRIDGE III, J. P., Reaction ^{3}He(^{3}He,2p)^{4}He, 19: 39913

ALEKSANDROV, A. F., Investigation of neon plasma complex conductivity using a Q-meter, 19: 40041

ALEKSEEV, B. A., Measuring exchange capacitance and kinetic characteristics of ionites, 19: 40128 (ZFK-BN-17(p.75-94))

ALEKSEEV, B. A., Radiation stability of ion-exchange resins, 19: 38697 (ZFK-RN-17(p.139-64))

ALEKSEEV, B. A., Standardizing monitoring of H_2O purity in reactor loops, 19: 40124 (IAE-789)

ALEKSEEV, B. A., Water purification and treatment for reactors. II., 19: 38759 (ZFK-RN-17(p.95-117))

ALEXANDER G., Possible $N^*_{1/2}$ resonance at 1580 Mev, 19: 39548

ALEXANDER, K. F., Three-particle isomeric state in ^{109}In, 19: 39861

ALEXEFF, I., Plasma heating by means of beam plasma interaction, 19: 39969 (ORNL-P-1373)

ALHA, A., Strontium-90 content of human bones in Finland, 1960-1962, 19: 38850

ALI, Dolores, Spins of ^{153}Gd, ^{159}Dy, and ^{149}Pm, 19: 39818

ALKIRE, Richard Collis, Reaction distribution in a porous anode (thesis), 19: 38591 (UCRL-16113)

ALLEN, J. D., Electron microprobe data quantification, 19: 38536 (ACF-6)

ALLES, W., Proton-antiproton annihilation into two mesons, 19: 39527

ALLULLI, S., Ion exchange in fused salts. I., 19: 38771

ALPERIN, H. A., Measurement of the Magnon dispersion relation of iron, 19: 39213

AL'PERT, Ja. L., Electromagnetic effects in the neighborhood of a satellite or a vehicle moving in the ionosphere or interplanetary space, 19: 39683

ALSTON, M. H., Precision encoding and pattern recognition system, 19: 38978 (CERN-65-11(p.81-90))

ALTMAN, Carl, New structure in Ta thin films, 19: 39179

AL'TSHULER, L. V., The use of shock waves in high-pressure physics, 19: 39274 (JPRS-30799)

ALVAREZ, M. R., Radiation-induced increase in H^3-valine incorporation by the chromosomes of Vicia faba, 19: 38417

AMADO, R. D., Theory of the three-nucleon system, 19: 39923

AMARAL, L. Q., Total neutron cross sections of Pr, Yb, Lu, and Er, 19: 39779 (IEA-86)
AMBERGAOKAR, Vinay, Calculation of the thermal conductivity of pure superconducting lead, 19: 39732
AMBOSS, K., Use of Herrmann's optical theory of thermal velocity effects in electron beams, 19: 39308
AMIS, E. S., Reaction between U(IV) and various valence states of Np, 19: 38584 (SC-RR-65-219)
AMMON, J., On contamination in ^{131}I solutions (distribution after intravenous injections in rats), 19: 38351
AMMON, Johannes H., Heat exchanger, 19: 38821
ANDERHOLM, N. C., Magnetostriction of nonferromagnetic metals, 19: 39199
ANDERS, Edward, Ratios ($^{34}S/^{32}S$) for different forms of S in Orgueil meteorite and their mode of formation, 19: 39351
ANDERSON, E., Scattering experiment using digitized discharge planes, 19: 39450 (BNL-9232)
ANDERSON, Herbert L., Thickness measurement using alpha particles, 19: 38965
ANDERSON, J. D., Energy levels of ^{31}S and ^{19}Ne, 19: 39827
ANDERSON, L. E., Prog. rpt. on BONUS core development, 12/64–2/65, 19: 39156 (CEND-532)
ANDERSON, L. W., Nuclear magnetic resonance of ^{61}Ni in nickel metal, 19: 39418
ANDERSON, N., Compression of a cylindrical plasma by a magnetic field, 19: 39991
ANDERSON, P. W., Theories of magnetism in metals, 19: 40074 (CONF-796(Paper 3))
ANDERSON, W. G., Mass difference ^{40}Sc–^{40}Ca and the ^{40}Sc ground state spin, 19: 39850
ANDERSON, W. Kermit, KER-4—the thermal analysis of cylindrical fuel rods, 19: 40171 (KAPL-M-6475)
ANDO, Ken, Mean-square displacement measurements of ^{57}Fe in Zn, 19: 40097
ANDRADA, J. A., The effect of triiodothyroacetic acid on ^{131}I incorporation by the thyroid, 19: 38348
ANDRE, S., Fast β–γ coincidence circuit for a Siegbahn-Slatis β spectrometer, 19: 39010
ANDREW, Kenneth L., Coupling considerations in two-electron spectra, 19: 39367
ANDRIAMBOLOLONA, Roselino, Generalized Bogoliubov transformation for bosons, 19: 39496
ANDRONIKASHVILI, E. L., Independence of the density of rotating liquid helium on the angular velocity, 19: 39714
ANGELINI, Pio, Irradiation damage in lipids and its effect on flavor, 19: 39068
ANGELINO, G. C., Characteristics and design of a co-current distillation column, 19: 38766
ANIKINA, M., An investigation of the leptonic decays of K_l^0 mesons, 19: 39474 (JINR-P-2190)
ANSELIN, Francois, Process and apparatus for the preparation of U and Pu nitrides, 19: 38685
ANZALONE, G., Thyroid function in patients with advanced cancer of the portio. Effects of radium therapy, 19: 38492
AOYAMA, Takashi, Effect of halogenated pyrimidines on radiosensitivity of mouse strain L cells and their radioresistant variant, 19: 38459
APPEL, Joachim, Spin-orbit coupling and the Knight shift in nontransition-metal superconductors, 19: 39727
ARAKAWA, E. T., Angular distribution and thickness dependence of transition radiation from thin aluminum foils, 19: 40099
ARAKELYANTS, M. I., Rock age of the Vindhyan system (India) according to glauconites, 19: 38853
ARALOVA, G. A., Radiation effects on sulfhydryl (SH) group of albumen blood structures, 19: 38427
ARCHIBALD, Paul B., Low-density, low-pressure solid explosive, 19: 38589 (UCRL-14186)
ARD, W. B., Energetic neutral injection into an electron-cyclotron plasma, 19: 39970 (ORNL-P-1374)
ARMANTROUT, G. A., A windowless high-resolution lidgermanium detector, 19: 39018
ARMENTEROS, R., Annihilation $\bar{p}p \to \bar{K}K\pi$, 19: 39534
ARNDT, Richard Harold, Device for the irradiation of an object with charged particle beams, 19: 38831
ARON, J. C., Quantum laws in connection with stochastic processes, 19: 39661
ARSAEV, M. I., Development of scintillation and ionization methods of radiometry and dosimetry, 19: 38995 (NP-15259)
ARTEMENKO, I. A., Superconductivity of La films, 19: 39745
ARTEMOV, K. P., Reaction ($^3He,\alpha$) on ^9Be, ^{14}N and ^{16}O, 19: 39941
ARTMANN, J., Supplementary Rankine-Hugoniot calculations for thermal plasmas, 19: 40051
ARTSIMOVICH, L. A., Some problems in physics of high-temperature plasma, 19: 40045
ASAMI, Y., Amplification of microwaves by the interaction of an electron beam with Cs plasma, 19: 40036
ASCOLI, Sergio, Isotope separator of Rome University, 19: 39077
ASHCROFT, David John, Nuclear reactor, 19: 40139
ASHCROFT, David John, Shielded containers for nuclear fuel elements, 19: 38908
ASHER, Harry, Radiation medicine, 19: 38470
ASHKIN, J., Methods for assigning spin and parity to baryon resonances, 19: 39610
ASKER, W. J., Cerium tetrafluoride. I. Preparation and reactions, 19: 39182
ASKER, W. J., Cerium tetrafluoride. II. System CeF_4–CeF_3, 19: 39183
ASKEROV, B. M., Damping of electron spectrum and quantum theory of galvanomagnetic phenomena, 19: 40106
ASLANOV, G. A., Arsenate-iodometric determination of Y, 19: 38551
ASPREY, L. B., Alkali fluoride complexes of Pa(IV), 19: 38625
ASTIER, A., Evidence for non-strange meson of mass 1290 Mev, 19: 39535
ATKINS, R. J., Preparation and properties of spherical particulate nuclear fuels for Pu-fueled reactors, 19: 39096 (CONF-117(p.103-26))
ATLAS, L. M., Defect equilibria of PuO_{2-x}, 1100 to 1600°C, 19: 39221
ATTWENGER, W., Pulse shape discrimination system for $^6LiF(ZnS)$ scintillation counters, 19: 39025
ATWATER, H. A., Irradiation of additive-containing polymethylmethacrylate, 19: 38706
AUBECQ, Maurice, Installation for purification of Ar for glove boxes, 19: 38769
AUBERT, Michel, Fuel loading and unloading arrangement for nuclear reactors, 19: 40145
AUER, L. H., Mass loss and formation of white-dwarf stars, 19: 39337
AUER, P. L., High-frequency velocity space instabilities, 19: 40019
AUMAN, J. R., Structure and evolution of medium-mass stars. III., 19: 39335
AUSTIN, A. E., Indexing charts for diffraction patterns of tetragonal hexagonal and orthorhombic crystals, 19: 40080 (NP-15182)
AUZINS, Peteris V., Trapped-hole center containing F in MgO, 19: 38729
AVARGUES, M., Biological effects of ionizing radiation, 19: 38421
AVILINA, V. N., Complex formation of Th with 8-hydroxyquinaldoxime and caproic acid, 19: 38567
AVOTINA, M. P., 3-hour activity of lutetium, 19: 39931
AYAKI, K., Amplification of microwaves by the interaction of an electron beam with Cs plasma, 19: 40036
AYER, J. E., Manufacture of glass-bonded fuels for Doppler coefficient measurement, 19: 39124 (ANL-6995)
AZIMOV, Ya. I., Model of three-particle unitarity condition for complex momenta, 19: 39596

B

BABIKOV, V. V., A method for calculating cross sections in the optical model, 19: 39935
BABULEVICH, E. N., Water purification and treatment for reactors. II., 19: 38759 (ZFK-RN-17(p.95-117))
BACCHETTI, Silvio, Influence of post-radiational incubation conditions on x-ray survival of diploid yeast, 19: 38422
BACHELIER, D., Separation of final states in reaction (p,t), 19: 39839
BACHER, A. D., Final-state p-^{4}He interaction in ^{3}He(^{3}He,2p)^{4}He, 19: 39914
BACKHOUSE, A. M., Random fluctuations of DFR power, 19: 40193 (TRG-Report-921)
BACKOFEN, W. A., Strength and plasticity of anisotropic metals, 19: 39149 (AD-425880)
BACON, T. C., Spin of the $Y_0^*(1405)$, 19: 39553
BACSO, J., Investigation of $^{92}Mo(n,2n)^{91,91m}Mo$ reaction, 19: 39790
BADAMI, D. V., X-ray studies of graphite formed by decomposing SiC, 19: 39185
BADIER, J., Decay of the x and ϕ mesons, 19: 39531
BAER, S., Separation of interaction potential into two parts in treating many-body systems. I., 19: 39284
BAES, C. F. Jr., Chemistry and thermodynamics of MSRE fluoride solutions, 19: 38582 (ORNL-P-1428)
BAHNG, J., Structure and evolution of medium-mass stars. II., 19: 39334
BAHNG, J., Structure and evolution of medium-mass stars. III., 19: 39335
BAILEY, Donald W., Potentiating effect of neonatal thymectomy on x-ray-induced intercapillary glomerulosclerosis, 19: 38409
BAILEY, P. T., Influence of radiation on ovarian maturation and histolysis of pupal fat body in Diptera, 19: 38406
BAILEY, Paul C., Comparison of x-ray- and uv-induced aberrations in pollen tube chromosomes of Tradescantia, 19: 38360 (TID-21695)
BAIR, J. K., Sequential emission in the reaction $^7Li(d,n)2\alpha$, 19: 39915
BAIR, W. J., Plutonium particle-induced neoplasia of the canine lung. I.,

19: 38359 (BNWL-SA-230)
BAK, Hoe-Ill, Pair production cross sections for 6.13 Mev γ rays, 19: 39787 (SGAE-PH-19/1965)
BAKACSNE POLGAR, E., Radioactive contamination of atmospheric precipitation of Budapest with special regard to radioactive strontium, 19: 38852
BAKER, J. M., E.P.R. and ENDOR of Tb^{4+} in thoria, 19: 38655
BAKER, R. G., Use of radioiodinated fatty acid for photoscans of the heart, 19: 38490
BAKER, Sol R., Radiation therapy of cancer, 19: 38487
BAKISH, Robert, Conference on electron and ion beam science and technology, Toronto, 5/64, 19: 39307
BAKUTA, S. A., Constitution diagram and properties of Nb–Mo–Si alloys, 19: 39194
BALAKAEVA, T. A., Scandium oxalate-carbonate compounds, 19: 38672
BALASHOV, V. V., Anomalous stability of the ⅝⁻ level in ^{13}C, 19: 39848
BALCOMB, J. Douglas, Measurement of power-to-core temperature transfer function of Kiwi-B-4E, 19: 40241 (LA-DC-6845)
BALDWIN, W. F., Visible mutation frequencies in Dahlbominus oogonia produced by acute x rays and chronic γ radiation, 19: 38392
BALKASHEVA, L. U., Effect of fast neutrons on culture and morphological characteristics of Bacillus mesentericus, 19: 38449
BALLAM, Joseph, Magnetic momentum analyzing slit with current conducting stripe secured to the magnetic poles, 19: 38967
BANDO, Masako, High-energy quasi-elastic proton-proton scattering, 19: 39557
BANERJEE, P., Moments of inertia of asymmetric nuclei, 19: 39831
BANG, E. M., Accuracy of calculations of collective oscillation frequency by s-v transformation method, 19: 39782 (JINR-P-2191)
BARASH, N., Antiproton annihilation in H at rest. I., 19: 39462 (CU-1392-239)
BARBARO-GALTIERI, Angela, Data on particles and resonant states, 19: 39485 (UCRL-8030(Pt.I)(Mar.'65, ed.))
BARBATO, M., Evolution of power and competative nuclear systems, 19: 40200
BARCATTA, F. A., Prog. rpt. on ion rocket system, 7–9/65, 19: 38834 (N64-29495)
BARKAS, Walter H., Data on particles and resonant states, 19: 39485 (UCRL-8030(Pt.I)(Mar.'65, ed.))
BARLOW, J., Electron asymmetry in leptonic decay of polarized Λ^0, 19: 39539
BARMIN, V. V., Decay $f^0 \to \pi^0 + \pi^0$, 19: 39480 (NP-15247)
BARNARD, D. J., The use of Cr-51 in the determination of red cell volumes in experimental animals, 19: 38346
BARNETT, J. T., Role of crystal structure in determining mechanical properties of graphite, 19: 39237
BARNETT, T. O., An evaluation of a fast complementary, hybrid bistable multivibrator, 19: 38920 (TID-22019)
BAROCH, C. J., Examination of Zy-clad UO_2 fuel rods, 19: 39234 (GEAP-4597)
BARON, V. V., Constitution diagram and properties of Nb–Mo–Si alloys, 19: 39194
BARON, V. V., Solubility of certain transition metals in the V_3Si compounds and their influence of the transition of the compounds into a superconducting state, 19: 39196
BARR, William H., Reading apparatus for thermoluminescent-type radiation dosimeters, 19: 39048
BARRACLOUGH, J. T., Hydrology of subsurface waste disposal, national reactor testing station, Idaho. Annual Progress Report, 1964, 19: 40269 (IDO-22047-USGS)
BARRINGER, Howard S., Nuclear reactor core arrangement, 19: 40146
BARRINGER, R. E., The preparation of radioactive phosphorous-32 sources on metal plates, 19: 38745 (Y-1484)
BARRIOS, Arthur A., High-frequency skywave communication system performance in nuclear environment, 19: 38783
BARRITT, B. H., Retarded embryo sac development in irradiated clones of apples, 19: 38411
BARSCHALL, H. H., Neutrons from protons on isotopes of tin, 19: 39825
BARTHOLOMEW, G. A., Overall project–Intense Neutron Generator, 19: 39754 (AECL-2177, Paper 1)
BARTON, John R., Nondestructive evaluation of metal fatigue, 19: 39151 (AFOSR-65-0981)
BARYSHEVSKII, V. G., Spontaneous transitions by light propagation through anisotropic media, 19: 39266 (JINR-P-2195)
BAS, E. B., Experimental investigation of the structure of high-power density electron beams, 19: 39328
BASDEKAS, Demetrios L., Nondestructive assay of nuclear fuels, 19: 38547 (TID-21475)
BASERGA, Renato, Incorporation of thymidine into DNA of organs of mice, 19: 38336 (TID-21106)
BASHANDY, E., K-conversion coefficient of the 321-kev E1 transition in ^{177}Hf, 19: 39947
BASSEL, R. H., Distorted-wave Born-approximation calculations of ^3He inelastic scattering, 19: 39885
BASTIEN, P., Precision encoding and pattern recognition system, 19: 38978 (CERN-65-11(p.81-90))
BASTIEN, Pierre L., Data on particles and resonant states, 19: 39485 (UCRL-8030(Pt.I)(Mar.'65, ed.))
BASU, Prasenjit, Propagation of γ quanta in matter, 19: 40071
BATES, D. R., Advances in atomic and molecular physics. I., 19: 39415
BATES, J. L., Ionic diffusion in high-temperature UO_2, 19: 39154 (BNWL-SA-54)
BATES, Roger G., Dissociation constant of acetic acid in D_2O from 5 to 50°C, 19: 38645
BATTLE, Norman, Fuel elements for nuclear reactors, 19: 39148
BAUDIN, G., Determination of free U in UC–U and UC–U–C alloys, 19: 38540 (CEA-Note-397)
BAUER, R. W., Reaction $^{40}Ca(\alpha,2\alpha)^{36}Ar$, 19: 39902
BAUER, Stefan George, Fuel elements for nuclear reactors, 19: 39148
BAUR, R., Comparative x-ray and electron microscopy studies Guinier-Preston zones in aluminum–silver, 19: 39172 (ORNL-tr-633)
BAXENDALE, J. H., Pulse radiolysis of aqueous solutions of some inorganic compounds, 19: 38728
BAXTER, J., The use of Cr-51 in the determination of red cell volumes in experimental animals, 19: 38346
BAYMAN, B. F., Nonexistence of the tetraneutron, 19: 39547
BAZANSKI, Stanislaw L., Decomposition of the Lorentz transformation matrix into skew-symmetric tensors, 19: 39643
BAZIN, M. J., Off-line global approach to pattern recognition for bubble chamber pictures, 19: 38996 (PPAD-2137-548)
BE, Sucki, Current density distributions in a coaxial plasma gun, 19: 39998
BEAK, Peter, The deuteration of some N-methyl-4-pyridones, 19: 38689
BEAL, B. T., Nuclear magnetic resonance in liquid ^3He, 19: 39728
BEAL, J. L., Prog. rpt. on re-entry dispersal of reactor core materials, 1–3/65, 19: 39118 (SC-DC-65-1520)
BEAL, J. W., Beam trajectories under the influence of self-fields and external focusing elements, 19: 39318 (UCRL-14194)
BEALL, S. E., MSRE design and operations report. VI., 19: 40189 (ORNL-TM-733(Rev.))
BEANLANDS, D. S., Use of radioiodinated fatty acid for photoscans of the heart, 19: 38490
BEASLEY, T. M., Non-equilibrium tissue distributions of uranium and thorium following inhalation of uranium ore by rats, 19: 38333 (BNWL-SA-226)
BEBEMEL, I., Decomposition of H_2O in reactor, 19: 38698 (ZFK-RN-17(p.199-207))
BEBIE, Hans, Wave mechanical three-particle model, 19: 39641
BECCHI, C., Vanishing of E2 part of $N^*_{33} \to N + \gamma$ amplitude, 19: 39536
BECKER, Dennis J., Radioisotopic detection of microbial contamination present in jet fuel, 19: 39061 (ADR-09-08a-63.1)
BECKER, W., ESONE—A nuclear electronics system, 19: 38924
BEDER, Douglas S., Distribution of lepton pairs from vector meson decays. Internal Report No. 15, 19: 39451 (CALT-68-43)
BEDNARSKI, S., Use of directional freezing of melt for Bi large single crystals preparation, 19: 39098 (INR-567/II/PS)
BEGGS, James E., High-vacuum thermionic converter, 19: 39444
BEHRENS, H., Absorbed dose rate determination in vinylchloride. I., 19: 39016
BELBEACH, Roger L., Polyenergetic particle deflecting system, 19: 39312
BELL, Alan, Heat exchangers, 19: 38820
BELL, Alan, Improvements in water tube steam generators, 19: 38815
BELL, Alan, Improvements in water tube steam generators, 19: 38816
BELL, Alan, Improvements in water tube steam generators, 19: 38817
BELL, George I., Production of heavy nuclides by multiple neutron capture in nuclear explosions, 19: 38786 (LA-DC-7111)
BELL, J. C., Indexing charts for diffraction patterns of tetragonal hexagonal and orthorhombic crystals, 19: 40080 (NP-15182)
BELL, R. P., Kinetic hydrogen isotope effects in ionization of ketonic substances, 19: 38692
BELOKONSKI, I., Auto-immunization and auto-allergization in guinea pigs infected with tuberculosis with preliminary x-ray treatment, 19: 38375
BELOTTE, J., Study of deep postradiotherapeutic digestive stenoses, 19: 38522
BELUGIN, Yu. F., Complexing of 2-hydroxyethylimisodiacetic acid with rare earth elements, 19: 38671
BENARY, O., Possible $N^*_{\gamma_3}$ resonance at 1580 Mev, 19: 39548
BENESOVSKY, F., Crystal structure of $TbGe_2$ and $RuIn_3$, 19: 39207
BENESOVSKY, F., The H phases: Ti_2CdC, Ti_2GaC, Ti_2GaN, Ti_2InN, Zr_2InN, and Nb_2GaC, 19: 39208
BENESOVSKY, Friedrich, Metallography of high-melting metals. II., 19: 39214
BENEVENTANO, M., Double production of charged pions in hydrogen by

photons of energy between 600 and 850 Mev, 19: 39519
BENNEMANN, K. H., Magnetic field dependence of Knight shift in superconductors, 19: 39705
BENNEMANN, K. H., Magnetic field dependence of Knight shift due to spin-orbit coupling in superconductors, 19: 39739
BENNINGHOVEN, A., Energy distribution of particles emitted by cathode disintegration, 19: 39374
BENOIT, J. W., Off-line global approach to pattern recognition for bubble chamber pictures, 19: 38996 (PPAD-2137-548)
BENSON, E. M., Preparation and properties of spherical particulate nuclear fuels for Pu-fueled reactors, 19: 39096 (CONF-117(p.103-26))
BENTON, E. G., Range-momentum relation for heavy recoil ions in emulsion, 19: 39883
BERANGER, Gerard, Relation between modifications observed in zirconia during electrotransport tests and during oxidation of Zr, 19: 38604
BERENYI, D., Magnetic characteristic curve for a special permanent-magnet β-spectrograph set of two units, 19: 38998
BERGERON, C. J. Jr., Magnetization of current carrying cold worked NbZr superconducting wires, 19: 39749
BERGLES, A. E., Boiling flow regimes and critical heat flux, 19: 38809 (NYO-3304-3)
BERGUSHEVSKI, Z., Ion-exchange filter for EWA reactor, 19: 38760 (ZFK-RN-17(p. 127-38))
BERKES, I., The g factors of excited states in ^{192}Os, ^{192}Pt, and ^{194}Pt, 19: 39833
BERMAN, S. M., Baryon-resonance production by neutrinos, 19: 39517
BERMAN, S. M., Elements of SU_3, 19: 39604
BERMUDEZ POLONIO, J., Determination of Nb, Ta, and U in niobio-tantalates by x-ray-fluorescence spectrometry, 19: 38549
BERNARD, Y., Contribution to study of radioprotective properties of 2-mercaptobenzothiazole, 19: 38466
BERNARDINI, G., General review of neutrino physics, 19: 39611
BERNAS, M., Separation of final states in reaction (p,t), 19: 39839
BERNHEIM, A., Automatic following of tracks in nuclear emulsions, 19: 39017
BERNIER, J. P., Gamma-encephalography with ^{203}Hg-neohydrin, 19: 38510
BERNSTEIN, I. B., Multiple-bounce theory for expansion and retardation of cold-plasma explosion bubble, 19: 39344
BERNT, Helmut, Density and energetic position of radioinduced agglomeration centers in Si crystals, 19: 39254
BERTHIER, Louis, Quadrupolar effects on energy levels in μ-mesic manganese atom, 19: 39368 (NP-15089)
BERTINA, L. E., Complexing of 2-hydroxyethyliminodiacetic acid with rare earth elements, 19: 38671
BERTOLACCINI, M., Three-quantum annihilation of positrons in metals and insulators, 19: 39546
BERUL, S. I., Reaction of $NaPO_3$ with Ce, Nd, and Sm oxides, 19: 38668
BESSON, J., Determination of free U in UC–U and UC–U–C alloys, 19: 38540 (CEA-Note-397)
BESSON, Jean, Hydrolysis mechanism at high temperature of UC, 19: 38606
BETTS, R. K., Evaluation of Zircaloys for use in 630A reactor, 19: 39097 (GEMP-346)
BEVER, M. B., Prog. rpt. on metallic systems, annual, 1964, 19: 39168 (TID-22015)
BEYNON, J. D. E., Experimental determination of photoionization cross section of atomic hydrogen, 19: 39388
BEZDEK, M., Oxidative extraction separation of Ru from solutions of its compounds, 19: 38763
BHATT, K. H., Negative parity states in ^{148}Sm, 19: 39845
BHATTACHARJEE, S. B., Reactivation of radiation-killed E. coli with ribonuclease, 19: 38465
BHAUMIK, M. L., Time-resolved spectroscopy of europium chelates, 19: 38634
BHIDE, V. G., Moessbauer effect in ferroelectric $BaTiO_3$, 19: 38651
BHONSLE, R. V., Measurements of total electron content and equivalent slab thickness of mid-latitude ionosphere, 19: 39677
BIANCHINI, F. G., Total neutron cross sections of Pr, Yb, Lu, and Er, 19: 39779 (IEA-86)
BIBERMAN, L. M., State of gas behind strong shock wave, 19: 40040
BIDDLE, P., The preparation and some properties of U carbonitrides, 19: 39089 (AERE-M-1389)
BIDERMAN, R., Heat transfer and hydraulic studies for SNAP-4 fuel element geometries, 19: 40249 (TID-22014)
BIEDENHARN, L. C., Some properties of the SU_n representation, 19: 39609
BIERLEIN, T. K., Beta-α and α-β transformations in Pu under applied stresses, 19: 39153 (BNWL-33)
BIERLEIN, T. K., Electron microscope studies of second phase particles in dilute alloys of U, 19: 39092 (BNWL-SA-90)
BIERMAN, Arthur, Radiation from an exciton wave packet, 19: 40088
BIERMAN, Arthur, Theory of radiation from a wave packet, 19: 40087
BIERY, John C., Densities of some low-melting Pu alloys, 19: 39161 (LA-DC-6956)
BIGGERSTAFF, J. A., On radiative transition in ^{207}Pb and ^{206}Pb following resonance neutron capture on ^{206}Pb and ^{207}Pb, 19: 39783 (ORNL-P-1345)
BILDSTEIN, H., Uranium electrolytic deposition on metals, 19: 39100 (SGAE-CH-16/1965)
BILENKII, S. M., Polarized proton targets for experiments with high-energy particles, 19: 39497
BILPUCH, E. G., Possible doorway state in ^{209}Pb and ^{208}Pb, 19: 39847
BILWES, R., Reaction $^7Li + d \rightarrow 2\alpha + n$ at low energy, 19: 39921
BINNS, K. J., Analysis and computation of electric and magnetic field problems, 19: 39311
BIRBRAIR, B. L., Excitation spectra of ^{208}Tl and ^{208}Bi nuclei, 19: 39933
BIRD, J. R., On radiative transition in ^{207}Pb and ^{206}Pb following resonance neutron capture on ^{206}Pb and ^{207}Pb, 19: 39783 (ORNL-P-1345)
BIRKETT, J. D., Diffusion in deuterio-normal hydrocarbon mixtures, 19: 38646
BIRKHOFF, R. D., Angular distribution and thickness dependence of transition radiation from thin aluminum foils, 19: 40099
BISHOP, G. R., Isospin selection rules for electron scattering, 19: 39855
BISHOP, G. R., Isospin selection rules and the 5.10-Mev level of ^{14}N, 19: 39856
BISWAS, A. C., Statistical equivalent of the Boltzmann equation, 19: 39396
BISWAS, S. N., Quantum electrodynamics with vanishing bare fermion mass, 19: 39646
BJERREGAARD, J. H., Thallium-207 states excited in the (t,α) reaction on ^{208}Pb, 19: 39852
BJORK, R. G., Chemical state of C, N, and O in alkali metals, 19: 39157 (CNLM-6337)
BLACKALL, P. M., Automatic analysis of spark chamber pictures using the CERN HPD, 19: 38974 (CERN-65-11(p.25-33))
BLACKALL, P. M., Program developments in CERN-FSD spark system, 19: 38977 (CERN-65-11(p.71-9))
BLAIR, I. M., Electron asymmetry in leptonic decay of polarized Λ^0, 19: 39539
BLAKE, J. B., Development of experimental techniques for measuring the distribution of H and He isotopes in space, 19: 39419 (ATN-63(9219)-1)
BLAKE, R. L., Spectral and photometric measurements of solar x-ray emission below 60 A, 19: 39333
BLANQUET, M. P., Radioisotopes and their medical applications, 19: 38505
BLESER, E., Scattering experiment using digitized discharge planes, 19: 39450 (BNL-9232)
BLOCH, C., Configuration mixing in the continuum and nuclear reactions, 19: 39873
BLOCH, F. W., Radiation chemistry of cyclic fluorocarbons, 19: 38709
BLOCH, M., Results obtained with off-line HPD system, 19: 38988 (CERN-65-11(p.183-206))
BLOCHER, J. M. Jr., Preparation and evaluation of carbon-coated fuel particles, 19: 39126 (CONF-117(p.149-70))
BLOCHER, John M. Jr., Conference on particulate nuclear fuels, New York, 9/63, 19: 40168 (CONF-117)
BLOCK, M. M., Future experiments in neutrino physics, 19: 39612
BLOMQVIST, J., Magnetic moments of single particle states in ^{207}Pb and ^{209}Bi, 19: 39870
BLONDEAU, Emile, Atmospheric fallout collector, 19: 38906
BLOOM, M., Nuclear spin relaxation in gases and liquids. IV., 19: 39378
BLUM, P., Determination of free U in UC–U and UC–U–C alloys, 19: 38540 (CEA-Note-397)
BLUMENTHAL, R. B., High-energy photoproduction of ρ^0 mesons, 19: 39549
BOBIN, J. L., Electric discharge in hydrogen and deuterium, 19: 39286
BOCCHIERI, P., Pseudopotentials for a hard sphere gas, 19: 39651
BOCHNACKI, Z., Magnetic properties of the ^{153}Eu nucleus, 19: 39792
BOCK, R., Mechanism of the reaction $^{11}B(^{16}O,^{15}N)^{12}C$ at 30 Mev, 19: 39869
BOCK, R., The ground state of ^{49}Ca and the reactions $^{40}Ca(^3He,\alpha)^{39}Ca$, $^{42}Ca(^3He,\alpha)^{41}Ca$ and $^{40}Ca(^3He,d)^{41}Sc$, 19: 39874
BODANSKY, D., Proton-γ competition in the $^{63}Cu(p,2p)^{62}Ni$ reaction at 10.5 Mev, 19: 39903
BODI, Lewis J., X-ray luminescence sample compartment with automatic shutter, 19: 38936
BOEHM, F., Isotope shift of $K_{\alpha 1}$ x rays of uranium, 19: 39412
BOEHM, R., Effects of radiostability of synthetic resin exchangers on application in radioactive circuits, 19: 40129 (ZFK-RN-17(p.114-26))
BOEKER, Elisabeth H., Radiation safety, 19: 38482
BOEMI, P., Thyroid function in patients with advanced cancer of the penis. Effects of radium therapy, 19: 38492
BOEMMEL, Hans, Mean-square displacement measurements of ^{57}Fe in Zn,

19: 40097
BOENZI, D., Tuff for removal of Cs^+ from solutions. I., 19: 38768
BOERSCH, H., Rotational structure in energy loss spectrum of H_2, 19: 39399
BOGDANOVICH, E., Interactions of 9-Bev π^- mesons with Xe nuclei, 19: 39472 (JINR-P-2178)
BOGOLYUBOV, P. N., Composite model of baryons on basis of three-body equation, 19: 39473 (JINR-P-2186)
BOHLMANN, E. G., Aluminum and titanium corrosion in saline waters at elevated temperatures, 19: 39117 (ORNL-P-1430)
BOHM, H. V., Measurements of a thermal-conductivity length dependence in helium II, 19: 39730
BOKOVA, G. B., Chromatographic method of determining U and Pu in air, 19: 38554
BOKROS, J. C., Structure of pyrolytic carbon deposited in a fluidized bed, 19: 39184
BOLDT, Werner, Measurement of temperature and electron density in supersonic plasma beam, 19: 39987
BOLLER, H., Crystal chemical investigations in systems (Ti, Nb, Ta, Mo, W)–(As, Sb), 19: 39209
BOLTZ, D. F., Determination of oxygen in sodium metal, 19: 38539 (APDA-168)
BOND, V. P., H^3thymidine (H^3TdR) incorporated into DNA; dosimetric and radiobiological considerations, 19: 38873 (BNL-9331)
BONDAR, I. A., Synthesis of divalent rare earth silicates, 19: 38621
BONHAM, James, The deuteration of some N-methyl-4-pyridones, 19: 38689
BONHAM, R. A., Corrections to incoherent scattering factors for electrons and x rays, 19: 39379
BONNOR, W. B., Exact stationary solution of Einstein's equations, 19: 39663
BOOTH, D. L., Computer model for studying SGHWR safety, 19: 40214
BOOZ, J., Energy dependence of mean energy per ion pair at low electron energies, 19: 39375
BORCHERS, R. R., Neutrons from protons on isotopes of tin, 19: 39825
BORCHI, E., Proton-antiproton annihilation into two mesons, 19: 39527
BORN, W., Radiation sensitivity of Malherbe's calcifying epithelioma, 19: 38494
BOSCHAN, P., Energy gap in nuclear matter in the case of soft-core potentials, 19: 39857
BOSE, S. K., Quantum electrodynamics with vanishing bare fermion mass, 19: 39646
BOSTICK, W. H., Flow of plasma around magnetic dipole, 19: 40009
BOTSARIS, Gregory D., Gamma-radiation effects on growth of KCl crystals, 19: 38696 (MIT-2909-4)
BOUCEK, J., Cerebral circulography with radioisotopes, 19: 38489
BOUROTTE, B., Reaction $^7Li + d \rightarrow 2\alpha + n$ at low energy, 19: 39921
BOWERSOX, D. F., Solubility of selected elements in liquid Pu. IV., 19: 38580 (LA-3303)
BOWLES, B. J., Moessbauer effect in monolayer of ^{119}Sn on Pt, 19: 39210
BOWMAN, D. H., Convenient cadmium-metal standard for checking neutron, soil moisture probes, 19: 38869
BOWMAN, F. E., Beta-α and α-β transformations in Pu under applied stresses, 19: 39153 (BNWL-33)
BOYD, L. R., Prog. rpt. on reactor control systems, 2–4/65, 19: 40122 (GEAP-4862)
BOYLE, A. J. F., Moessbauer effect in Cs-133, 19: 39295
BRACE, L. H., Behavior of the mid-latitude ionosphere from Explorer XVII, 19: 39680
BRAGINSKII, S. I., Transport processes in a plasma, 19: 40057
BRAGLIA, G. L., Momentum-transfer cross sections for slow electrons in Kr and Xe, 19: 39397
BRAMLEY, Richard, NMR studies of uranyl citrate in D_2O at low pD, 19: 38623
BRANCA, G., Tuff for removal of Cs^+ from solutions. I., 19: 38768
BRAND, G. F., Pre-ionization and shock wave ionization in crossed-field plasma source, 19: 39961 (NP-15112)
BRANDT, Werner, Atomic oscillations in the statistical approximation, 19: 39401
BRANSCOMB, Elbert, Wigner's analysis of the unitary representations of the Poincare group, 19: 39486 (UCRL-12359)
BRAUNBEK, Werner, Concepts of nuclear physics. II. Revised edition, 19: 39951
BRAUN CANTILO, J. A., The effect of triiodothyroacetic acid on ^{131}I incorporation by the thyroid, 19: 38348
BRAUTTI, G., Bubble chamber for weak radioactivities, 19: 38993 (NP-15143)
BRAUTTI, G., Bubble chamber for weak radioactivity. Final research report, 19: 38994 (NP-15145)
BRAY, P. J., Review of the British nuclear industry in 1965, 19: 40300
BRDICKA, R., Preparation of ^{35}S-labeled cystine, 19: 38747
BREAZEALE, M. A., Finite amplitude waves in liquids and solids, 19: 39268 (ORNL-P-1395)
BREBANT, Charles, Dimensional inspection bench for parts having cylindrical bodies, 19: 38830
BREGAZZI, M., Observations on reaction of polymer carbons with CO_2, 19: 38599
BREGER, A. Kh., Data on rate of air exchange in premises with powerful γ installations, 19: 38883
BREWER, D. F., Gapless surface excitations in liquid helium, 19: 39737
BRIAND, Jean-Pierre, Study of the nuclear levels of Bi-212 excited in the α decay of At-216, 19: 39796
BRICARD, J., Charge state of ultra-fine aerosols in weakly ionized media, 19: 39285
BRIGLIA, Donald D., Electron collision cross section plotter, 19: 38943
BRIGLIA, Donald D., Total cross sections for ionization and attachment in gases by electron impact. II., 19: 38631
BRIGOLI, B., Characteristics and design of a co-current distillation column, 19: 38766
BRILLOUIN, L., Actual mass of potential energy. II., 19: 39554
BRINCKMANN, H. F., Three-particle isomeric state in ^{109}In, 19: 39861
BRINKERHOFF, Joris M., Narrow-band x-ray detector, 19: 39047
BRINKLEY, B. R., Evidence of lysogeny in derivatives of Escherichia coli, 19: 38381
BRINKMAN, J. A., Kev channeling and thermochemical properties of interstitial impurities, 19: 39395
BRINKMANN, G., Improving economy with use of standardized, movable, in-cell boxes, and decontamination of their equipment, 19: 38794 (JUL-252-RW)
BRISSAUD, I., Separation of final states in reaction (p,t), 19: 39839
BRITO DA CUNHA, A., Lethals and their suppressors in experimental populations of Drosophila willistoni, 19: 38391
BROCH-TONIOLO, Francesco, Isotope separator of Rome University, 19: 39077
BROCKMEIER, R. T., Isotope shift of $K_{\alpha 1}$ x rays of uranium, 19: 39412
BROERS, A. N., Micromachining by sputtering through a mask of contamination laid down by an electron beam, 19: 39136
BROGAN, Thomas R., Nuclear propulsion schemes using conversion techniques, 19: 40238 (LA-3229, pp 286-312)
BRONSON, J. D., Energy-angular correlations and sequential decay in the $^2H(p,2n)a$ and $^1H(d,2p)a$ reactions, 19: 39924
BROOKS, David R., Correlation of coherent oscillations and Hall currents in the linear Hall accelerator, 19: 39981
BROOKS, Leon Preston Jr., Radiation effects on transistors, 19: 39054 (AD-607863)
BROWN, A. Houghton, Design and construction of Oldbury pressure vessels, 19: 40212
BROWN, D. J., Extension of stratigraphic units of south-central Washington. I., 19: 38843 (BNWL-SA-135)
BROWN, D. J., Extension of stratigraphic units of south-central Washington. II., 19: 38844 (BNWL-SA-140)
BROWN, Donald W., Purification of radioactive Na o-iodohippurate, 19: 38507
BROWN, G. E., Effective tensor interaction in nuclei, 19: 39872
BROWN, J. B., Critical currents in superconducting films of indium, 19: 39724
BROWN, J. L., Observation of correlations between vector-meson and baryon-resonance decays, 19: 39542
BROWN, L. L., Nitrogen isotope effects in decomposition of diazonium salts, 19: 38690
BROWN, R. E., Extension of stratigraphic units of south-central Washington. I., 19: 38843 (BNWL-SA-135)
BROWN, R. E., Extension of stratigraphic units of south-central Washington. II., 19: 38844 (BNWL-SA-140)
BROWN, R. E., Magnetic field reduction in an expandable superconducting enclosure, 19: 39742
BROWN, W. R., Prog. rpt. on re-entry dispersal of reactor core materials, 1–3/65, 19: 39118 (SC-DC-65-1520)
BROWNE, C. C., Preparation and properties of particulate oxide fuels, 19: 39094 (CONF-117(p.11-19))
BROWNING, M. F., Preparation and evaluation of carbon-coated fuel particles, 19: 39126 (CONF-117(p.149-70))
BROYLES, A. A., Effective interatomic potentials for liquid helium above and below the λ point, 19: 39731
BROYLES, Leland E., Apparatus for wipe testing radioactive sources, 19: 38909
BRUCE, W. R., Convenient ^{137}Cs unit for irradiating cell suspensions and small laboratory animals, 19: 38415
BRUN, C., Alpha decay of light Po isotopes, 19: 39838
BRUSH, E. G., Corrosion of materials for nuclear superheat applications, 19: 39115 (GEAP-4760)
BRUTOVSKY, M., Extraction of nitrosoruthenium(III) complexes from a

nitrate medium with 30% TBP. Effect of complexing reagents and acid deficiency, 19: 38764
BUBEN, N. Ya., Kinetics of destruction of free radicals by ionizing radiation, 19: 38719
BUCCELLA, F., Consequences of SU_6 for total baryon-baryon and baryon-antibaryon cross-sections, 19: 39529
BUCHANAN, J., Ginzburg-Landau parameter of Ta, 19: 39205
BUCKALEW, W. H., Energy transfer by neutrons to certain materials, 19: 39769 (SC-DC-65-1544)
BUCKEL, W., Superconductivity of germanium and silicon under high pressure, 19: 39701
BUDBERG, P. B., Heat-resistance properties of Ti–Nb–Cr alloys, 19: 39192
BUDIN, C., Study of reticular defects in Al, 19: 39246
BUDNICK, J. I., Magnetic field dependence of the surface resistance of superconducting tantalum at 35 Gc/s, 19: 39706
BUECHLER, A., Vaporization in LiF–BeF_2 system, 19: 38679
BUGG, D. V., Nucleon-nucleon total cross sections between 1 and 8 Bev/c, 19: 39550
BUJOK, J., Stress-induced variations in the spectral distribution of γ-radiation from ^{137}Cs transmitted by graphited carbon, 19: 39794
BUNCH, S. M., Reaction D(p, 2p)n at 31 Mev, 19: 39925
BURCHAM, W. E., ft Values for ^{42}Sc, ^{46}V, and ^{56}Mn and conserved vector current hypothesis, 19: 39859
BURD, D., Integral FILTER technique for HPD, 19: 38985 (CERN-65-11 (p.153-72))
BURDET, G., Comparative study of the efficiencies of NaI(Tl), plastic, and liquid scintillators for detection of the γ of the ^{18}O isomer, 19: 39009
BURDI, G. F., Properties of cladding materials for SNAP hydride reactors, 19: 39166 (NAA-SR-Memo-11149)
BURGER, J. P., Proximity effects under magnetic fields, I., 19: 39699
BURGIO, R. G., Nimbus dynamics analysis for ejection mechanism, 19: 39071 (MND-3169-68)
BURKE, Edward A., Calculated cross sections for atomic displacements produced by electrons in the 1.0 to 3.0-Mev energy range, 19: 39225 (AFCRL-65-286)
BURLOCK, Joseph, Correlation of coherent oscillations and Hall currents in the linear Hall accelerator, 19: 39981
BURNAZYAN, A. I., Radiation medicine, 19: 38470
BURNOD, L., Production of positrons and determination of cross sections, 19: 39475 (LAL-27)
BURNS, W. R., Joining techniques for SAP-clad nuclear fuel elements, 19: 39131
BURNSTEIN, R. A., Low-energy hyperon-proton scattering interactions. Technical Report No. 469, 19: 39460 (CONF-650410-3)
BURNSTEIN, R. A., Time reversal invariance in $\Sigma^0 \rightarrow \Lambda^0 + e^+ + e^-$, 19: 39484 (TID-22038)
BURREN, J. W., HPD programming at Rutherford Lab., 19: 38986 (CERN-65-11(p.173-81))
BURTON, J. W., Surface studies using Moessbauer effect, 19: 40078 (NP-15111)
BURTON, W. M., Monochromatic photography in the extreme ultraviolet, 19: 38928
BURYKINA, A. L., Investigation of contact interactions of metal borides with graphite at high temperatures in vacuum, 19: 38654
BUSCH, C. W., Pressure wave generation in a fissioning gas. II., 19: 39836
BUSCH, D. D., The release of condensable fission products from the GAIL III-B fuel element, 19: 39233 (GAMD-6321)
BUSCHBECK-CZAPP, B., Investigation of the coulomb-nuclear interference in elastic K^-p scattering at low energies, 19: 39530
BUSO, Roberto, Chronic thiouracil feeding and accumulation of ^{131}I in some organs of C_3H mice, 19: 38350
BUSSOLATI, C., Three-quantum annihilation of positrons in metals and insulators, 19: 39546
BUTLER, J., Program for calibrating flying-spot cathode ray tube for CHLOE, 19: 38975 (CERN-65-11(p.35-41))
BUTLER, J. W., Automatic analysis of photographic data in biology, 19: 38910 (CERN-65-11(p.43-56))
BUTLER, Margaret K., Automatic analysis of photographic data in biology, 19: 38910 (CERN-65-11(p.43-56))
BUTTERWORTH, I., Observation of correlations between vector-meson and baryon-resonance decays, 19: 39542
BYCHKOVA, M. I., Constitution diagram and properties of Nb–Mo–Si alloys, 19: 39194
BYFIELD, H., Flow of plasma around magnetic dipole, 19: 40009
BYKOVETS, N. P., Application of scintillation granules for measuring β radiation from radioactive isotopes, 19: 38737
BYRNE, J. T., Handling and measurement of plutonium shipments, 19: 38535 (RFP-508)

C

CABIBBO, N., Possible consequences of $K^0_1 \rightarrow \pi^+ + \pi^-$ decay, 19: 39601
CACACE, Fulvio, Isotope separator of Rome University, 19: 39077
CADDOCK, B. D., Determination of Na in heavy fuel oils by neutron-activation analysis, 19: 38550
CALDWELL, C. S., Preparation and properties of spherical particulate nuclear fuels for Pu-fueled reactors, 19: 39096 (CONF-117(p.103-26))
CALVELLI, Edward A., Radioisotopic detection of microbial contamination present in jet fuel, 19: 39061 (ADR-09-08a-63.1)
CAMAHORT, Jose Luis, Kinetics of chlorination of UCl_6 by Cl_2 (thesis), 19: 38587 (UCRL-11986)
CAMERON, A. G. W., Cooling of neutron stars, 19: 39355
CAMP, D. C., A windowless high-resolution lidgermanium detector, 19: 39018
CAMPAGNOLI, G., Pseudopotentials for a hard sphere gas, 19: 39651
CAMPO, Cesar Gomez, Radiobotany and its application, 19: 38327
CANNON, J. R., Numerical continuation backwards in time for solutions of heat equation, 19: 38804 (BNL-8185)
CANO, Gilbert L., Energy loss and resultant charge of recoil particles from α disintegrations in surface deposits of ^{210}Po and ^{241}Am, 19: 39682
CANTOR, Robert E., Tumor scanning with Cs-131, 19: 38508
CAPALNA, S., Protective effect against x-ray lesions of glycine on some enzyme systems, 19: 38467
CAPPELLI, B., First radiobiological and pharmacodynamic studies on radioprotective effect of morphine, 19: 38453
CAPRIOGLIO, Pietro, How does the Dragon Project stand, 19: 40210
CARACH, J., Results of radioactivity measurements of dust and rainfall in western Slovakia in 1961-1963, 19: 38881
CARLSON, R. R., Reaction $2\ ^6Li \rightarrow 3\alpha$, 19: 39920
CARLSON, R. R., Variation in yield of the isotopic spin forbidden reaction $^{12}C(^6Li,\alpha_1)^{14}N$, 19: 39853
CARLSON, R. R., $2J + 1$ dependence of total cross sections in lithium + boron reactions, 19: 39887
CARLSON, Richard F., Proton disintegration of the deuteron—test of the Chew-Low extrapolation method, 19: 39578
CARLSTON, C. E., Electron ejection from single crystals due to 1- to 10-kev noble-gas ion bombardment, 19: 39404
CARLSTON, C. E., Kinetic emission of electrons from monocrystalline targets, 19: 39405
CARPENTER, D. C., Manufacture of glass-bonded fuels for Doppler coefficient measurement, 19: 39124 (ANL-6995)
CARPENTER, J. A., Motion of particles in fluidized beds and implications for the preparation of coated nuclear fuel particles, 19: 38782 (ORNL-TM-1170)
CARRARA, R., Study of Σ^- capture process in hydrogen, 19: 39510
CARRO, Amigo S., Lesions from atomic and thermonuclear arms, 19: 38478
CARRUTHERS, Robert, Energy transfer circuits particularly for the transfer from an inductive store to an inductive load, 19: 38960
CARTER, Melvin W., Environmental behavior of nuclear debris, 19: 38857
CASALE, P., Flow of plasma around magnetic dipole, 19: 40009
CASAS, Carmen B., Chronic thiouracil feeding and accumulation of ^{131}I in some organs of C_3H mice, 19: 38350
CASE, Carl T., Transient wave propagation in a plasma, 19: 40034
CASIMIR, H. B. G., Resistance of type II superconductors in the mixed state, 19: 39698
CASTO, W. R., Prog. rpt. on ORR operations 1–3/65, 19: 40259 (ORNL-TM-1181)
CATER, David E., Vaporization, thermodynamics, and dissociation energy of LaS, 19: 38644
CERBONE, R. J., Asymptotic and steady state spectrum measurements in a multiplying medium, 19: 39768 (RPI-328-21)
CERCEAU, O., General operator potential for the two-nucleon system, 19: 39504
CERINEO, M., Another attempt to determine the n-n scattering length, 19: 39499
CERINEO, M., Study of (n,p) and (n,d) reactions on ^{10}B at 14.4 Mev, 19: 39798
CEROVAC, H., Assessment of average occupational exposure to ionizing radiation, 19: 38474
CERRAI, E., Determination of rare earths in SAP material. II., 19: 38553
CESARI, F., Circuits for detection and localization of burst fuel elements. II., 19: 40133
CESCHIA, M., Bubble chamber for weak radioactivities, 19: 38993 (NP-15143)
CESCHIA, M., Bubble chamber for weak radioactivity. Final research report, 19: 38994 (NP-15145)
CHACHRA, S. P., Principal magnetic susceptibilities of $Dy_2(SO_4)_3 \cdot 8H_2O$ single crystal, 19: 40082
CHADWICK, J. R., E.P.R. and ENDOR of Th^{4+} in thoria, 19: 38655
CHAIKOFF, I. L., Induction of neoplasms in rat thyroid glands by x irradia-

tion of a single lobe, 19: 38367
CHANG, G. K., Ginzburg-Landau parameter of Ta, 19: 39205
CHANG, L., Production of nucleon isobars in high-energy nucleon-nucleon collisions, 19: 39508
CHANG, Man-wei, Action of secondary electrons in systems of radiation chemistry, 19: 38703
CHANG, Wen-Yu, Applicability of isobar model for Λ hyperon production in π^-p interactions, 19: 39593
CHAO, C. C., A study of CaCl type intermediate phases involving rare earth elements, 19: 39155 (CALT-221-11)
CHARAP, J. M., Covariant extension of SU(6), 19: 39555
CHARKES, N. David, Tumor scanning with Cs-131, 19: 38508
CHARYULU, K. K. N., Regional oxygenation and therapeutic response to irradiation, 19: 38374
CHASE, B. H., Development of fast neutron dosimetry system, 19: 38992 (COO-1226-8)
CHASE, G. H., Hydrology of subsurface waste disposal, national reactor testing station, Idaho. Annual Progress Report, 1964, 19: 40269 (IDO-22047-USGS)
CHAUDHARI, R. D., Critical currents in superconducting films of indium, 19: 39724
CHEADLE, B. D., Manufacture of stainless steel fuel cans for the AGR, 19: 39134
CHEBOTAREV, E. E., RBE of fast neutrons, 19: 38438
CHEBOTAREV, E. E., The effect of neutron radiation on some physical and and chemical properties of the blood, 19: 38440
CHEKHOSKOI, V. Ya., Niobium enthalpy between 600 and 2600°K, 19: 39217
CHEN, Francis F., "Universal" overstability of a resistive, inhomogeneous plasma, 19: 40002
CHEN, Ru-yong, Isotopic effects in liquid hydrogen, 19: 38639
CHEN, Y. G., Combination scattering of microwaves from space-charge waves in a laboratory magnetoplasma, 19: 40033
CHEON, Il-Tong, Nuclear correlations in deuteron pickup and stripping reactions, 19: 39890
CHERKAS, Paul, Retractable mount for radiation thickness gauge, 19: 38959
CHERNICK, J., Fuel management in the settled-bed fast reactor, 19: 40178 (BNL-9279)
CHERNICK, Jack, Activity report on Brookhaven work on the compilation, storage and evaluation of nuclear cross section data, 19: 39778 (BNL-9355)
CHERNOROTOV, E. S., Measuring exchange capacitance and kinetic characteristics of ionites, 19: 40128 (ZFK-RN-17(p.75-94))
CHERNOROTOV, E. S., Water purification and treatment for reactors. II., 19: 38759 (ZFK-RN-17(p. 95-117))
CHERNOROTOV, E. S., Water purification and preparation at reactors, 19: 40123 (IAE-787)
CHERNYAVSKII, A. F., Multichannel time-delay analyzer, 19: 38932
CHESNOKOVA, N. N., Spectroscopic studies of argon jet flowing from plasmatron nozzle, 19: 40043
CHEVALLIER, Pierre, Study of the nuclear levels of Bi-212 excited in the α decay of At-216, 19: 39796
CHEZEM, Curtis G., Pulsed neutron analysis in the Los Alamos Coupled Reactor Experiment, 19: 40240 (LA-3263)
CHIBA, Shin, On the unification of hadronic and leptonic weak interactions, 19: 39573
CHIDESTER, J. B., Prog. rpt. on chemical vapor deposition of Be from organoberyllium compounds, final, 6/63–1/64, 19: 39102 (UCRL-13100)
CHINH, Le Dinh, Exchange effects in scattering of slow electrons by atoms, 19: 39365 (COO-720-047)
CHIUNG, Chiang Shao, Applicability of isobar model for Λ hyperon production in π^-p interactions, 19: 39593
CHIZARI, E., Protective effect against x-ray lesions of glycine on some enzyme systems, 19: 38467
CHKHAIDZE, L. V., Investigation of the energy spectra and angular correlations of particles in $K^0_2 \to \pi^+ + e^- + \nu$ decay, 19: 39586
CHO, A., Ion emitter studies, 19: 39164 (N64-22193)
CHU, Ernest H. Y., Effects of uv radiation on mammalian cells. I., 19: 38395
CHU, Ey-Lung, Magnetic momentum analyzing slit with current conducting strips secured to the magnetic poles, 19: 38967
CHUANG, K. C., Prog. rpt. on metallic systems, annual, 1964, 19: 39168 (TID-22015)
CHUBB, T. A., Spectral and photometric measurements of solar x-ray emission below 60 A, 19: 39333
CHUNG, Ke Sun, Internal friction of powder-metallurgical WC–Fe, WC–Ni and WC–Fe–Ni alloys, 19: 39170 (FTD-TT-64-1001)
CHUNG, S. K., Pre-ionization and shock wave ionization in crossed-field plasma source, 19: 39961 (NP-15112)
CHUPRININ, F. I., Determination of specific conductance of refractory materials in vacuum, 19: 38922 (AAEC/Trans-18)
CHUTNA, Jitka, Polyvalent tolerance in newborn and sublethally irradiated adult mice, 19: 38376
CHWOJNIK, A., Comparative study of radionephrography and excretion urography, 19: 38520
CINDRO, N., Cross sections for some (n,2n) reactions, 19: 39797
CISZEWSKI, R., Neutron diffraction study of ferromagnetic U_3P_4, 19: 40104
CITTADINI, G., First radiobiological and pharmacodynamic studies on radioprotective effect of morphine, 19: 38453
CLAASSEN, H. A., Theory of linear MHD-induction generators. II., 19: 39432 (JUL-256-TP)
CLACK, Peter J., Coin identification apparatus utilizing radiation bombardment, 19: 38956
CLAPP, Paul, Regional oxygenation and therapeutic response to irradiation, 19: 38374
CLARK, D. D., List processing in automatic analysis of spark chamber data, 19: 38973 (CERN-65-11(p.15-23))
CLARK, Dwight B., Observational result on x rays, 19: 39332
CLARK, G. Wayne, Single-crystal growth of ThO_2 from Li ditungstate solvent, 19: 38628
CLARK, P. O., Pulsed operation of the neutral xenon laser, 19: 39394
CLARK, R. B., Elastic electron scattering from lead isotopes and possible dispersion effects, 19: 39860
CLARK, W. J., Plutonium particle-induced neoplasia of the canine lung. I., 19: 38359 (BNWL-SA-230)
CLASS, C. M., Angular distributions from the $^{11}B(d,n_0)^{12}C$ and $^{11}B(d,n)^{12*}C$ reactions for deuteron energies from 1.5 to 4.7 Mev, 19: 39817
CLAWSON, L., Boiling flow regimes and critical heat flux, 19: 38809 (NYO-3304-3)
CLAYTON, D. D., Radioactivity in supernova remnants, 19: 39338
CLEGG, M. D., Electron microscopy of cells irradiated with microbeam of α particles, 19: 38386
CLEGG, M. D., Technique for microbeam irradiation of single cells in tissue culture, 19: 38385
CLEM, John R., Dynamical properties of one-dimensional crystal with free ends, 19: 40079 (NP-15114)
CLEVELAND, Richard J., Prolongation of renal homograft function by local graft radiation, 19: 38425
CLINE, D., Baryon-baryon scattering and SU(6), 19: 39532
CLOSSER, W. H., Development of fast neutron dosimetry system, 19: 38992 (COO-1226-8)
CLOUTER, M., Change in the crystal structure of solid normal hydrogen near 1.5°K, 19: 39738
COCHRAN, J. F., Superconducting transition width in pure lead, 19: 39748
COCKRILL, J., Status of HPD programs at BNL, 19: 38980 (CERN-65-11 (p.97-113))
COHAN, Morton D., Activation analysis applications of an on-line digital computer, 19: 38568
COHEN, M., Observation of gas adsorption phenomena by high-energy electron diffraction, 19: 39178
COHEN, M. L., Spectral analysis of photoemission yields in Si, Ge, GaAs, GaSb, InAs, and InSb, 19: 39406
COHEN, S., Measurement of $d_{3/2}$ core excitation in ^{48}Ca from β decay, 19: 39851
COLBURN, D. S., Si^+–Si^- pair and interplanetary forward-reverse shock ensembles, 19: 39681
COLBY, L. J. Jr., Kinetics of reaction of UC with water, 19: 38581 (NAA-SR-11401)
COLEMAN, S., Departures from eightfold way, 19: 39454 (CONF-796 (Paper 18))
COLLATZ, S., On the monoenergetic neutron transport problem for homogeneous plane slabs, 19: 39771
COLLINS, G. B., Scattering experiment using digitized discharge planes, 19: 39450 (BNL-9232)
COLLINS, Vincent P., Clinically useful calculations of the dose distribution from multiple radiation sources, 19: 38526
COLMAN, D. M., Proposed standard for titration of aqueous solutions of boron. A preliminary report, 19: 38548 (UCRL-14166-T)
COLOMB, A., HWR power plant with 275-MW(e) PHWP and a 260-MW(e) BLWP units, 19: 40211
COLOMBINO, P., Positronium in water and ice from 22° to −144°C by annihilation quanta measurements, 19: 39509
COMBRISSON-LE BOLLOC'H, A., Use of radioisotopes for medical diagnosis, 19: 38493
COMPRELLI, F. A., Microstructural evaluation of superheat cladding materials, 19: 39158 (GEAP-4751)
COMSAN, M. N. H., Investigation of $^{23}Na(d,\alpha)^{21}Ne$ reaction, 19: 39835
CONFORTO, G., Angular correlation of electrons relative to Λ spin in Λ^0 beta decay, 19: 39613
CONFORTO, G., Electron asymmetry in leptonic decay of polarized Λ^0,

19: 39539
CONNELLY, D. J., Prog. rpt. on heat transfer for nuclear auxiliary power systems, 3–5/65, 19: 38811 (SAN-409-24)
CONNOLLY, P., Status of HPD programs at BNL, 19: 38980 (CERN-65-11 (p.97-113))
CONSTANT, R., Determination of specific activity of I-131 without carrier isotope, 19: 38609
CONTE, A., Ion exchange in fused salts. I., 19: 38771
COOBS, J. H., Prog. rpt. on coated-particle fuels, 11/64–5/65, 19: 39129 (ORNL-TM-1116)
COOPER, Ralph, Fluidized beds, 19: 40226 (LA-3229, pp 86-8)
COOPER, Ralph S., Advanced nuclear propulsion concepts, 19: 40242 (LA-DC-7118)
COOPER, Ralph S., Proceedings of an advanced nuclear propulsion symposium, 19: 40221 (LA-3229)
COOPERSMITH, M., Multiple scattering and many-body theory: free energy of electrons in helium, 19: 39722
COPP, Douglas Harold, Extraction ratio and bone clearance of ^{89}Sr as a measure of effective bone blood flow, 19: 38340
CORDFUNKE, E. H. P., Thermodynamic properties of U(VI) compounds, 19: 38676
CORENZWIT, E., Superconductivity of Nb_3Ge, 19: 39725
COREY, C. L., Electron microscope studies of second phase particles in dilute alloys of U, 19: 39092 (BNWL-SA-90)
CORINALDESI, E., S-matrix derivation and extension of E. Gerjuoy's momentum transfer theorem, 19: 39543
CORNGOLD, Noel, Discrete relaxation times in neutron thermalization, 19: 39773
COSGROVE, James F., X-ray luminescence sample compartment with automatic shutter, 19: 38936
COSTA DE BEAUREGARD, O., Helicity and transverse momentum of extreme relativistic fermion in a circular accelerator, 19: 39320
COSTES, Didier, Nuclear reactor control device, 19: 40143
COSTINER, Emma, Radioactivity in thyroid and plasma of rats marked with ^{131}I and treated with vitamin B_{12}, 19: 38337
COTTER, L. D., Radiation effects on pressure transducer components. Final report, 19: 39055 (GA-6266)
COTTER, T. P., Status report on theory and experiments on heat pipes at Los Alamos, 19: 38780 (LA-DC-7206)
COTTINGHAM, J. G., External beam extraction rate for the Cosmotron, 19: 39324
COTZIAS, G. C., Nomogram for estimation of microcuries and millimicrograms from counts per minute, 19: 38749
COUCHMAN, M. L., NURSE-1—a nuclear rocket safety evaluation code for the control data 3600, 19: 40248 (NUS-180)
COWAN, D. L., Nuclear magnetic resonance of ^{61}Ni in nickel metal, 19: 39418
COWAN, M. D., Measurements of a thermal-conductivity length dependence in helium II, 19: 39730
COWAN, Robert D., Coupling considerations in two-electron spectra, 19: 39367 (LA-DC-6548)
CRADDOCK, W. L., Radioactivity in supernova remnants, 19: 39338
CRAMER, J. G. Jr., Alpha-gamma correlation study of the $^{56}Fe(\alpha,\gamma^x\gamma_{0.84})^{60}Fe$ reaction, 19: 39865
CRANSHAW, T. E., Hyperfine field of ^{57}Fe in Cu–Mn alloys, 19: 39212
CRANSHAW, T. E., Moessbauer effect in monolayer of ^{119}Sn on Pt, 19: 39210
CRAPO, L. M., Study of collision narrowing by comparison of molecular-beam and gas-phase nuclear resonance spectra, 19: 38629
CRASEMANN, Bernd, L_3–L_3N Coster-Kronig transition probabilities and L-subshell fluorescence yields of Hg and Ta, 19: 39410
CRAUSSE, Etienne, Study of forced oscillations of a heavy, viscous, electroconductive liquid in presence of magnetic field, 19: 39281
CRAWFORD, F. W., Plasma acoustic waves on inhomogeneous column, 19: 40028
CRAWFORD, F. W., Prog. rpt. on plasma oscillations, 3–5/65, 19: 39972 (SU-IPR-17)
CRAWFORD, F. W., Warm magnetoplasma microinstability, 19: 40027
CREMERS, Clifford J., Steadiness of a plasmajet, 19: 39975
CREMOSNIK, G., Experimental investigation of the structure of high-power density electron beams, 19: 39328
CRENNELL, D., Status of HPD programs at BNL, 19: 38980 (CERN-65-11 (p.97-113))
CRESTI, M., Study of Σ^- capture process in hydrogen, 19: 39510
CRINER, G., Numerical data for ^{131}I uptake measurements in rabbits, 19: 38341
CROOKS, J. E., Kinetic hydrogen isotope effects in ionization of ketonic substances, 19: 38692
CROSS, A. M., Immunologic role of thymus in radiation chimeras, 19: 38451
CRUCIANI, V., Renal excretion of colloidal Au^{198}. An experimental morphological study, 19: 38342

CSIKAI, J., Investigation of $^{92}Mo(n,2n)^{91,91m}Mo$ reaction, 19: 39790
CSUPKA, S., Results of radioactivity measurements of dust and rainfall in western Slovakia in 1961-1963, 19: 38881
CUMMINGS, A. J., High field superconducting alloys for pulse transmission, 19: 39740
CUMMINS, J. D., The simultaneous use of several pseudo-random binary sequences in the identification of linear multivariable dynamic systems, 19: 39078 (AEEW-M-507)
CUNNINGHAM, J. R., Convenient ^{137}Cs unit for irradiating cell suspension and small laboratory animals, 19: 38415
CURRY, Kenneth J., Evaluation of nitrogen in 304 ELC stainless steel using the platinum flux technique, 19: 38537 (ACF-7)
CUSACK, J. H., Fuel requirements for fissiochemical production, 19: 40169 (CONF-117(p.67-79))

D

DAHL, Orin I., Analysis of np enhancements in $\pi^- + d$ interactions at 3.2 Bev/c, 19: 39551
DALGARNO, A., Behavior of the mid-latitude ionosphere from Explorer XVII, 19: 39680
DALITZ, R. H., Electromagnetic radii of ^{3}H and ^{3}He, 19: 39888
DALLA VOLTA, F., Evolution of power and competative nuclear systems, 19: 40200
DALRYMPLE, Glenn V., Effect of irradiation on ferrokinetics of cross-circulated dogs, 19: 38382
DALTON, C., Dental lesions in rat induced by radiomimetic agents, 19: 38325
DAMASK, Arthur C., Method of improving properties of an alloy by radiation, 19: 39257
DAMM, C. C., Cooperative effects in tenuous energetic plasma contained by magnetic mirror field, 19: 40017
DANDL, R. A., Energetic neutral injection into an electron-cyclotron plasma, 19: 39970 (ORNL-P-1374)
D'ANDLAU, Ch., Evidence for non-strange meson of mass 1290 Mev, 19: 39535
D'ANGELO, N., "Bohm diffusion" in the Q-1 device, 19: 40014
DANIEL, H., Influence of solid-state effects on β-γ directional correlation in ^{166}Ho, 19: 39824
DANILOV, G. S., Circular polarization of γ quanta in absorption of neutrons by protons, 19: 39538
DANILOV, G. S., Model of three-particle unitarity condition for complex momenta, 19: 39596
DANILOV, V. I., Electrostatic field of uniformly charged volumes of a cylindrical configuration, 19: 39314 (JINR-P-2131)
DA ROSE, Aldo V., Measurements of total electron content and equivalent slab thickness of mid-latitude ionosphere, 19: 39677
DAS, A., Complex space-time model. I., II., and III., 19: 39624 (AROD-223:60)
DATZ, S., Channeling effects on the energy loss of high-energy (20-80 Mev) ^{79}Br and ^{127}I ions in gold, 19: 39370 (ORNL-P-1336)
DAUB, Guido H., Liquid scintillators. XIII., 19: 38691
DAUTREPPE, Daniel, Magnetic tailing in ferromagnetic transition metals irradiated with electrons at 22°K, 19: 39239
DAVIDS, J. A. G., Safe disposal of radioactive waste in water and atmosphere, 19: 40277
DAVIES, A. G., Industrial prospects of radiation chemistry, 19: 39066
DAVIES, Sherwood, Guides, standards and regulations from State Health Department point of view, 19: 38887
DAVIS, A. G., Industrial prospects of radiation chemistry, 19: 39066
DAVIS, Elwin N., Conference on applied spectroscopy, Vol. 4, Chicago, 6/64, 19: 38572
DAVIS, R. G., The gamma camera—a new instrument for radioisotope tracer measurements, 19: 39008
DAVIS, Theodore F., Nuclear materials management, 19: 39101 (TID-3315)
DAVISON, Fred C., Effects of subcutaneous implantation of rare-earth metals, 19: 38334 (COO-1170-1)
DAWSON, H. I., Interpretation of stage I recovery after electron irradiation of Cu, 19: 39248
DAY, Richard A., Measurement of Stark widths and shifts of nitrogen ion lines (thesis), 19: 39952 (AFCRL-65-348)
DAY, T. B., Time reversal invariance in $\Sigma^0 \to \Lambda^0 + e^+ + e^-$, 19: 39484 (TID-22038)
DAYTON, Russell W., Prog. rpt. on civilian applications, 4/65, 19: 39091 (BMI-1723(Del.))
DE AGAZIO, A., NURSE-1—a nuclear rocket safety evaluation code for the control data 3600, 19: 40248 (NUS-180)
DEAN, Herman, Helium treatment of vac-ion pumps to remove deposited argon, 19: 39323
DE BACCI, Mario, How does the Dragon Project stand, 19: 40210
DEBIESSE, Jean, Apparent variations of the electron temperature in a flame,

18: 39282
DE BROGIE, Louis, Coexistence of photons and waves in electromagnetic radiations, 19: 39640
DE BRUIN, H. J., Determination of specific conductance of refractory materials in vacuum, 19: 38922 (AAEC/Trans-18)
DE CAMP, S. M., Operating and repair experiences on DCX-2 coils, 19: 39971 (ORNL-P-1438)
DEDDENS, James C., Nuclear reactor core arrangement, 19: 40146
DE GENNES, P. G., Proximity effects under magnetic fields. II., 19: 39700
DEHNHARD, D., Direct three-body decay $^{12}C \rightarrow 3\alpha$, 19: 39918
DEICHSEL, H., Production of partially polarized electron beam, 19: 39392
DEINKEN, H. P., Fluidized beds, 19: 40225 (LA-3229, pp ω3-5)
DE JONG, M., Anelastic after-effect in electron-irradiated Mo, 19: 39247
DEJONGHE, P., Problems relating to treatment of radioactive effluents, 19: 40274
DE LA BARRE, F., Neutron generator tube, 19: 39770
DELANGE, Maurice, Bell furnace for the preparation of uranium metal by magnesiothermic reduction, 19: 39113
DE LA VAISSIERE, C., Results obtained with off-line HPD system, 19: 38988 (CERN-65-11(p.183-206))
DELBOURGO, R., The 572• multiplet in SU(12), 19: 39556
DELFOSSE, J. M., Charge spectrum of recoiling ^{210}Po in the α decay of ^{220}Rn, 19: 39884
DELLA NEGRA, M., Evidence for non-strange meson of mass 1290 Mev, 19: 39535
DELTHIL, S., Postradiotherapy cranial sarcoma after treatment of retinoblastoma, 19: 38486
DEMIDOV, V. S., Data on p,p reactions with Q = 148 Mev, 19: 39479 (NP-15216)
DEMIN, N. N., Biological effects [of radiation], 19: 38432
DEMOULIN, M., Decay of the x and ϕ mesons, 19: 39531
DENNO, William S., Mössbauer spectrometer using a piezoelectric bar in resonant oscillation, 19: 39032
DENOUX, Michel, Oxidation of oriented thin layers of Zr, 19: 39120
DEONIGI, D. E., MINIMIZER--a computer code for determining minimum fuel cost, 19: 40170 (HW-71813)
DEONIGI, D. E., Minimized fuel cycle cost for simulated pressurized water reactor. I., 19: 40114 (BNWL-104)
DEONIGI, D. E., System of chained computer codes for reactor fuel cycle analysis, 19: 40149 (BNWL-SA-61)
DE RAFAEL, Eduardo, Relativistic theory of angular correlations in successive two-body decays of unstable particles, 19: 39492
DEREVYAKIN, V. A., Radiation effects on the disintegration rate of aluminate solutions, 19: 38738
DERMER, M. D., Large SGR control rod development, 19: 40126 (NAA-SR-11327)
DESAI, B. M., Complex formation between uranyl ions and β-resorcylic acid, 19: 38607
DESAI, M. H., Complex formation between uranyl ions and β-resorcylic acid, 19: 38607
DE SHAZER, L. G., Fluorescence conversion efficiency of neodymium glass, 19: 40090
DESHPANDE, S. D., Disturbed condition of lower ionosphere at geomagnetic equator during magnetic storms, 19: 39667
DE SOUZA, H. L., Lethals and their suppressors in experimental populations of Drosophila willistoni, 19: 38391
DESPOTOVIC, Lj, Assessment of average occupational exposure to ionizing radiation, 19: 38474
DETERDING, J. H., Determination of Na in heavy fuel oils by neutron-activation analysis, 19: 38550
DE TOLEDO, J. S., Lethals and their suppressors in experimental populations of Drosophila willistoni, 19: 38391
DEUCHARS, W. M., Gas laser measurements of electron density of a plasma, 19: 39978
DEUCHARS, W. M., Time-dependent electron density measurements in a fast theta-pinch discharge, 19: 39979
DEUTSCH, D. E., Fuel requirements for fissiochemical production, 19: 40169 (CONF-117(p.67-79))
DEUTSCH, M., Experience with SPASS system, 19: 38972 (CERN-65-11 (p.7-13))
DEUTSCHER, G., Proximity effects under magnetic fields. I., 19: 39699
DEVERALL, J., Status report on theory and experiments on heat pipes at Los Alamos, 19: 38780 (LA-DC-7206)
DEVINS, D. W., Analysis of the $^6Li(p,pd)^4He$ reaction, 19: 39907
DE V. SMIT, W. G., Effect of bulk density and of hydrogen in forms other free water on calibration curve of the neutron moisture meter, 19: 38948
DE WINTER, T. A., 27.6 cm internal diameter superconducting magnet, 19: 39741
DEZSI, I., Moessbauer effect study of phase transition in ice, 19: 39715
DEZSI, I., The g factors of excited states in ^{192}Os, ^{192}Pt, and ^{194}Pt, 19: 39833
DICKE, R. H., Cosmic black-body radiation, 19: 39350
DIENST, Wolfgang, Investigation of an irradiated FR2-fuel element, 19: 39253
DIERCKX, R., Exponential experiment in natural U, 19: 39763 (EUR-2413.e)
DIETRICH, J. R., Power Reactor Technology, Vol. 7, No. 3, 1964, 19: 40215
DIETRICH, W. C., The preparation of radioactive phosphorous-32 sources on metal plates, 19: 38745 (Y-1484)
DIKE, R. S., Quick closing light shutter, 19: 38942
DILLENBURG, D., Relaxation effects in angular correlations, 19: 39849
DI MARCO, J., Flow of plasma around magnetic dipole, 19: 40009
DIN, G. U., Reaction $^9Be(^3He,n)^{11}C$ from 1.3 to 5.4 Mev, 19: 39832
DI PAOLO, F. S., Cryosorption pumping of hydrogen and helium at 20°K, 19: 39693
DIU, B., Baryon number 2, unitary singlet as a test of one-particle-exchange dynamical models, 19: 39511
DMITRIEV, M. T., Effect of ionizing radiation on the air content of industrial premises, 19: 38884
DOBBE, F. A., Critical dimensions of water reflected systems containing $^{235}U-H_2O-Zr$, 19: 40159 (WAPD-T-1774)
DOBROVOL'SKII, T., Interactions of 9-Bev π^- mesons with Xe nuclei, 19: 39472 (JINR-P-2178)
DOBYRIN, S. Ya., Mass-spectrometric study of evaporation of LaB_6 evaporation, 19: 38673
DODD, Cyril Leon, Improvements in or relating to nuclear reactor fuel elements, 19: 40173
DOE, Bruce R., Isotopic composition of uranium in zircon, 19: 38849
DOERING, H. E., Effect of electron bombardment heating on surface of tungsten, 19: 39255
DOHER, L. W., Volumetric calibration of process vessels using digital computer techniques, 19: 38756 (RFP-488)
DOHERTY, G., Neutron cross sections of Be-9 in energy range 1 to 15 Mev, 19: 39775 (AEEW-M-513)
DOLGOLENKO, A. G., Decay $f^0 \rightarrow \pi^0 + \pi^0$, 19: 39480 (NP-15247)
DOLINSZKY, T., Formal theory of elastic scattering, 19: 39821
DOLL, R., Epidemiological observations on susceptibility to cancer in man with special reference to age, 19: 38364
DOLLFUS, M. A., Postradiotherapy cranial sarcoma after treatment of retinoblastoma, 19: 38486
DONALDSON, W. Lyle, Nondestructive evaluation of metal fatigue, 19: 39151 (AFOSR-65-0981)
DORFMUELLER, Th., Self-diffusion in liquid ammonia, 19: 38579 (JUL-238-PC)
DORIHAC, Francois, Study of forced oscillations of a heavy, viscous, electroconductive liquid in presence of magnetic field, 19: 39281
DORIOT, G., Automatic following of tracks in nuclear emulsions, 19: 39017
DOTY, Duane Robert, Measurement of thermal neutron albedo for materials, 19: 40065 (NP-15152)
DOUGHERTY, J. E., Fluidized beds, 19: 40225 (LA-3229, pp 83-4)
DOUGLAS, D. A. Jr., Prog. rpt. on Th fuel cycle development, 10--12/63, 19: 38755 (ORNL-3611)
DOURY, Andre, Atmospheric fallout collector, 19: 38906
DOYLE, E. F., Boiling flow regimes and critical heat flux, 19: 38809 (NYO-3304-3)
DRAGONI, G., Biological effects of radioactive phosphorus. An electrophoretic study of whole and denatured serum, 19: 38368
DRAWIN, H. W., Charge density of excited hydrogen levels in stationary plasma with consideration of the diffusion of neutral particles, 19: 40053
DRAWIN, H. W., Effect of ion-neutral collisions on plasma rotation, 19: 40052
DREICER, H., Gaps in spectrum of electrostatic plasma waves, 19: 40025
DRESSEL, Ralph W., Energy loss and resultant charge of recoil particles from α disintegrations in surface deposits of ^{210}Po and ^{241}Am, 19: 39882
DRESVIN, S. V., Optical investigation of temperature distribution and electron concentration in argon plasma, 19: 40039
DREYHAUPT, F. J., Whole-body counter, 19: 38999
DROESSMAR, F., Promethium prepared in pure form, 19: 38772
DRURY, J. S., Nitrogen isotope effects in decomposition of diazonium salts, 19: 38690
DRUYVESTEYN, W. F., Guided motion of vortices and anisotropic resistivity in type-II superconductors, 19: 39694
DRUYVESTEYN, W. F., Hall effect in type II superconductors, 19: 39710
DRYAGINA, I. V., Effects of ionizing radiation on gladiolas, 19: 38430
DUBERG, J. E., Ionizing particle radiations effects and simulation consideration, 19: 39059
DUBEY, S. N., Stability of Be chelates of catecholdisulphonic and chromotropic acids in aqueous solutions, 19: 38641
DU BOIS, D. F., Stimulated incoherent scattering of light from plasmas, 19: 40012

DUBOZ, M., The center at the Hague, 19: 40273
DU BRIDGE, R. A., Prog. rpt. on reactor control systems, 2–4/65, 19: 40122 (GEAP-4862)
DUCK, Ian, Angular distributions in 3α and 3N systems, 19: 39912
DUHM, H. H., The ground state of ^{40}Ca and the reactions ^{40}Ca(^{3}He,α)^{39}Ca, ^{42}Ca(^{3}He,α)^{41}Ca and ^{40}Ca(^{3}He,d)^{41}Sc, 19: 39874
DUKE, P. J., Electron asymmetry in leptonic decay of polarized Λ^0, 19: 39539
DUKOR, P., Immunologic role of thymus in radiation chimeras, 19: 38451
DUMANOVIC, J., Growth inhibition in cereal seedlings induced by γ irradiation at different oxygen tensions, 19: 38418
DUMMER, Gerald, Specific heat of Zr–Rh alloys between 0.9 and 12°K, 19: 39218
DUNAEVA, K. M., Reaction of various U oxides with sulfuric acid, 19: 38657
DUNLAP, J. L., Severe microinstability-driven losses in an energetic plasma, 19: 39967 (ORNL-P-1337)
DURAND, Y., Electric discharge in hydrogen and deuterium, 19: 39286
DURHAM, J., Density modulations in r-f plasmas, 19: 40026
DUSHIN, L. A., Determination of spatial distribution of plasma density, 19: 39965 (NP-15203)
DVORINA, L. A., Lanthanum silicides and their crystal structure, 19: 38613
DWYER, James J., Prolongation of renal homograft function by local graft radiation, 19: 38425
DYATLOV, I. T., Model of three-particle unitarity condition for complex moments, 19: 39596
DYATLOV, N. M., Complexing of 2-hydroxyethyliminodiacetic acid with rare earth elements, 19: 38671
DYBLE, E., Prog. rpt. on chemical vapor deposition of Be from organoberyllium compounds, final, 6/63–1/64, 19: 39102 (UCRL-13100)
DZHABISHVILI, N. A., Investigation of yttrium chloride reactions with potassium phosphates, 19: 38620
DZHABISHVILI, N. A., Yttrium phosphates, 19: 38619
DZHELEPOV, B. S., The γ spectrum of ^{152}Eu with the half life 9.2 hours, 19: 39928
DZHELEPOV, B. S., 3-hour activity of lutetium, 19: 39931
DZHIBUTI, R. I., Photonuclear reactions with α-particle emission and four-particle correlations in light nuclei, 19: 39934
DZHOLOS, R. V., Accuracy of calculations of collective oscillation frequency by u-v transformation method, 19: 39782 (JINR-P-2191)

E

EASH, D. T., Longitudinal tensile properties of H4LM graphite extended to –269°C, 19: 39188
EAST, F. R., Properties of the ionosphere which affect h-f transmission, 19: 39682
EASTWOOD, D. C., Preliminary operational experiences with the Hinkley Point, 19: 40199
EATON, G. W., Retarded embryo sac development i.. irradiated clones of apples, 19: 38411
EBATA, Takeshi, Production of N_{11} resonance and properties of the neutral vector mesons, 19: 39572
EBERT, H. G., Energy dependence of mean energy per ion pair at low electron energies, 19: 39375
ECKLEY, G. P., Alpha-gamma correlation study of the ^{56}Fe($\alpha,\alpha'\gamma_{0.84}$)^{56}Fe reaction, 19: 39865
EDESKUTY, F. J., Chilldown and storage losses of large liquid hydrogen storage dewars, 19: 39686 (LA-DC-7164)
EDESKUTY, Frederich J., Liquid hydrogen in nuclear rocket testing, 19: 40244 (LA-DC-7170)
EDWARDS, D. N., Annihilation $\bar{p}p \to \bar{K}K\pi$, 19: 39534
EDWARDS, Glen R., Self-diffusion studies of gamma Pu, 19: 39162 (LA-DC-6957)
EDWARDS, R. K., Thermodynamics of yttrium–hydrogen system, 19: 38642
EFENDIEV, G. Kh., Reactions of $A_2^{III}B_3^{VI}$ La and Ga selenides, 19: 38598
EFIMOV, Yu. V., Solubility of certain transition mtals in the V_3Si compounds and their influence of the transition of the compounds into a superconducting state, 19: 39196
EFREMOV, A. V., Asymptotics of the Feynman graphs. III., 19: 39465 (JINR-E-2124)
EGAN, J. J., Solid-state electromotive force techniques. The free energy of formation of $NiCl_2$, $CoCl_2$, and several double salts of KCl, 19: 38575 (BNL-9343)
EGER, Magda, Effects of γ rays on RNA and protein content of amoeba, 19: 38371
EHN, D. C., High-energy photoproduction of ρ^0 mesons, 19: 39549
EHRENBERG, L. Growth inhibition in cereal seedlings induced by γ irradiation at different oxygen tensions, 19: 38418
EHTASHAM-UD-DIN, A. M. F., Structure of the pigments of precooked irradiated meats, 19: 39065
EICH, Glen B., Isotopic methods for the determination of blood volume, 19: 38525
EICHERT, K., Multi-component, stationary nonequilibrium flow in a MPD energy converter, 19: 39440
EICK, H. A., Preparation and thermodynamics of EuC_2, 19: 38680
EICK, Harry A., Vaporization, thermodynamics, and dissociation energy of LaS, 19: 38644
EIDSON, W. W., Alpha-gamma correlation study of the ^{56}Fe($\alpha,\alpha'\gamma_{0.84}$)^{56}Fe reaction, 19: 39865
EINSTEIN, P. A., Some observation on the formation of tracks in thin, supported metal films produced by an electron beam, 19: 38950
EISENBERG, J. M., Even parity states in ^{16}O, 19: 39806
EL-AASSAR, M. Riad, K-conversion coefficient of the 321-kev E1 transition in ^{177}Hf, 19: 39947
EL-BEHAY, A. Z., Investigation of ^{23}Na(d,α)^{21}Ne reaction, 19: 39835
ELDREDGE, Arnold L., Hydrogen–oxygen vertical brazing furnace, 19: 38938
ELENSKII, Yu. S., Decay $f^0 \to \pi^0 + \pi^0$, 19: 39480 (NP-15247)
ELIEZER, I., Study of interaction between lanthanide and nitrate ions, 19: 38578 (IA-1014)
ELISEEV, A. A., Lanthanum selenides, 19: 38614
ELLI, Raffaella, Influence of post-radiational incubation conditions on x-ray survival of diploid yeast, 19: 38422
ELLIS, G. F. R., Singularities in homogeneous world models, 19: 39360
EL-NADI, M., Cluster stripping processes, 19: 39829
EL-SAYAD, M. G. Mouse, K-conversion coefficient of the 321-kev E1 transition in ^{177}Hf, 19: 39947
ELSCHNER, B., Alternating-current losses in Nb/Zr superconductive coils, 19: 39695
ENDT, P. M., Levels of ^{36}Ar excited in the ^{35}Cl(p,γ)^{36}Ar reaction, 19: 39828
ENGLAND, A. C., Energetic neutral injection into an electron-cyclotron plasma, 19: 39970 (ORNL-P-1374)
ENGLANDER-GOLDEN, Paula, Total cross sections for ionization and attachment in gases by electron impact. I., 19: 38630
ENGLER, A., Spin of the $Y_0^*(1405)$, 19: 39553
ENGMAN, J. D., HPD programming at Univ. of Pennsylvania, 19: 38990 (CERN-65-11(p.229-36))
ENGSTROEM, G., A user's manual for salomon, an IBM-7090 code for gamma transport calculations, 19: 40066 (NP-15155)
ENOKUBO, Fumiaki, Current density distributions in a coaxial plasma gun, 19: 39998
ENRIQUES, L., Microwave study of thermally ionized plasmas, 19: 39980
ENZICKER, A. E., Spectral and photometric measurements of solar x-ray emission below 60 A, 19: 39333
EPEL, L. G., Fuel management in the settled-bed fast reactor, 19: 40178 (BNL-9279)
EPPERSON, D., Numerical data for ^{131}I uptake measurements in rabbits, 19: 38341
EPSTEIN, Saul T., Dipole matrix elements for He in first-order shielding approximation, 19: 39380
ERFURTH, H., Disassembly and sampling of graphite ball fuel elements, 19: 38792 (JUL-250-RW)
ERICKSON, G. F., Status report on theory and experiments on heat pipes at Los Alamos, 19: 38780 (LA-DC-7206)
ERKES, P., Special characteristics of nuclear power station in the Ardennes, 19: 40209
ERNE, F. C., Levels of ^{36}Ar excited in the ^{35}Cl(p,γ)^{36}Ar reaction, 19: 39828
EROE, J., Circular polarization of γ quanta accompanying reaction ^{10}B(d,p)^{11}B, 19: 39937
EROFEEV, I. A., Decay $f^0 \to \pi^0 + \pi^0$, 19: 39480 (NP-15247)
ESAKI, L., New phenomenon in semimetals and semiconductors, 19: 39734
ESCHBACH, E. A., MINIMIZER–a computer code for determining minimum fuel cost, 19: 40170 (HW-71813)
ESCHBACH, E. A., System of chained computer codes for reactor fuel cycle analysis, 19: 40149 (BNWL-SA-61)
ESCOBAR, Ismael, Time variations in cosmic rays and radiosonde measurements. Final technical report, 19: 39421 (NP-15154)
ESSINGTON, E. H., Effect of chelates on the movement of fission products through soil columns, 19: 38329 (TID-20471)
ESTEN, M. J., Inelastic proton-deuteron scattering at 135 Mev, 19: 39579
ESTERMANN, Immanuel, Advances in atomic and molecular physics. I., 19: 39415
ESTILL, W. B., Application of electron microscopy in dimensional metrology, 19: 38916 (SC-DC-65-1589)
ESTRIN, I. M., Morphological changes in some organs of white rats due to neutron irradiation, 19: 38444
ETTER, J. E., Angular correlations for ^{9}Be(^{3}He,α)^{8}Be → 2α reaction, 19: 39916

ETTER, J. E., Reaction $^{9}Be + {}^{3}He \rightarrow 3\alpha$, 19: 39898
ETTER, J. E., Reaction $^{10}B + {}^{3}He \rightarrow p + 3\alpha$, 19: 39899
ETTER, J. E., Reaction $^{6}Li + {}^{3}He \rightarrow p + 2\alpha$, 19: 39900
ETTER, J. E., Spectroscopic studies with the $^{10}B(^{3}He,p2\alpha)$ reaction, 19: 39917
ETTERS, R. D., Random phase approximation in the many-boson problem, 19: 39631 (IS-1111)
EVANS, J. R., Use of radioiodinated fatty acid for photoscans of the heart, 19: 38490
EVANS, R. D., Pressure wave generation in a fissioning gas. II., 19: 39836
EVTUSHOK, T. M., Investigation of contact interactions of metal borides with graphite at high temperatures in vacuum, 19: 38654
EWAN, G. T., Shielding and activation of the Intense Neutron Generator, 19: 39761 (AECL-2177, Paper 8)
EWING, Ronald I., Electron emission from W under proton bombardment, 19: 39409
EYGES, Leonard, Improved method for quantum mechanical three-body problems. I., 19: 39505
EYGES, Leonard, Quantum mechanical three-body problem for attractive potentials, 19: 39453 (CONF-796(Paper 15))

F

FACETTI, J. F., Neutron-induced reactions in aromatic phosphorus compounds, 19: 38700
FAHMY, Myrtle, J., Genetic properties of exogenous deoxyribonucleic acid at various levels of degradation in Drosophila melanogaster, 19: 38408
FAHMY, O. G., Genetic properties of exogenous deoxyribonucleic acid at various levels of degradation in Drosophila melanogaster, 19: 38408
FAIRLIE, D. B., A treatment of the random phase approximation for absorptive corrections, 19: 39522
FAISSLER, W. L., High-energy photoproduction of ρ^{0} mesons, 19: 39549
FAKIROV, D. G., Group SU_{12} as generalization of symplectic and spin symmetries, 19: 39471 (JINR-P-2175)
FAKIROV, D. G., Group SU(12) as a generalization of the symplectic and spin symmetries, 19: 39533
FALCHETTI, Roberto, Influence of post-radiational incubation conditions on x-ray survival of diploid yeast, 19: 38422
FALK, Charles D., Isotopic exchange of hydridoplatinum(II) complex with D_2O, 19: 38627
FALKENBERG, Dietrich, Many-group parameter sets for calculation of fast reactors, 19: 40161 (ZfK-TPh-11)
FALTER, Kenneth H., Radioactive decay correction factors, 19: 38744 (PHS-999-RH-12)
FAN, Ky., Convex sets and their applications, 19: 39082 (TID-22032)
FANALE, F. P., Helium–uranium ratios for Pleistocene and Tertiary fossil ammonites, 19: 38868
FARNSWORTH, P. L., Tungsten fiber reinforced nickel composites, 19: 39093 (BNWL-SA-141)
FAROUK, M. A., Investigation of $^{23}Na(d,\alpha)^{21}Ne$ reaction, 19: 39835
FARRELL, J. A., Possible doorway state in ^{209}Pb and ^{208}Pb, 19: 39847
FASSNACHT, S., Discharge chamber sensitive time, 19: 39028
FAUGERAS, Pierre, Plant for liquid-liquid extraction by the counter-current flow process, 19: 38777
FAY, Gy., Quantum-mechanical discussion of Gibbs paradox, 19: 39633
FEDEROV, V. V., Planning of experiments discriminating between possible curves, 19: 39088
FEDOROV, I. A., Scandium oxalate-carbonate compounds, 19: 38672
FEDOROVA, N., Radiation-induced solid-state polymerization. I., 19: 38699
FEIGENBUTZ, L. V., Prog. rpt. on heat transfer for nuclear auxiliary power systems, 3–5/65, 19: 38811 (SAN-409-24)
FEINBERG, G., Weak interactions, 19: 39457 (CONF-796(Paper 23))
FEINENDEGEN, H, H^{3}thymidine ($H^{3}TdR$) incorporated into DNA; dosimetric and radiobiological considerations, 19: 38873 (BNL-9331)
FEIX, Marc R., Connection between correlations and fluctuations in plasma, 19: 40024
FELD, Bernard T., Conference on photon interactions in Bev-energy range, Laboratory of Nuclear Science, M.I.T., 1/63, 19: 39616
FELDMAN, Isaac, NMR studies of uranyl citrate in D_2O at low pD, 19: 38623
FENECH, H., A survey of several methods for computing cell cross sections, 19: 40152 (GA-6462)
FENG, K. K., Simple data display system for fast-scanning mass spectrometer, 19: 39022
FERRARI PARABITA, G., Mandibular radionecrosis, 19: 38527
FERRERO, M. I., Electron asymmetry in leptonic decay of polarized Λ^{0}, 19: 39539
FESSLER, H., Large-area counter for exclusive measurement of soft quanta radiation emitted by a sample, 19: 39046
FETISOV, V. N., Anomalous stability of the $\frac{1}{2}^{-}$ level in ^{13}C, 19: 39848
FETISOV, V. N., Nuclear photoeffect on three-particle nuclei, 19: 39808
FEUERSTEIN, H., Fission technetium. I., 19: 39892
FEYNMAN, R. P., Consequences of SU_3 symmetry in weak interactions, 19: 39605
FEYNMAN, R. P., Present status of strong electromagnetic and weak interactions, 19: 39615
FIELD, Frank H., Mass spectrometer, 19: 38958
FIELDEN, E. M., Pulse radiolysis of aqueous solutions of some inorganic compounds, 19: 38728
FIETZ, W. A., Stable current regulator for superconducting solenoids, 19: 38945
FILATOV, V. F., Reactive changes in organs of rabbits with radiation sickness, 19: 38431
FILIPKOVSKII, A., Interactions of 9-Bev π^{-} mesons with Xe nuclei, 19: 39472 (JINR-P-2178)
FILLO, John, Thermal boundary-layer problem in magnetohydrodynamics, 19: 39276
FINCH, C. B., Single-crystal growth of ThO_2 from Li ditungstate solvent, 19: 38628
FINDEISEN, A., Review of work at Rossendorf research reactor, 1961, 19: 40261 (ZFK-RN-17(p.179-98))
FINEMAN, M. A., Rotational structure at threshold in the H_2 electron-impact ionization spectrum, 19: 39413
FINK, J., Recoilless γ emission in ^{156}Gd and ^{158}Gd following neutron capture reactions, 19: 39863
FINZI, R., Double production of charged pions in hydrogen by photons of energy between 600 and 850 Mev, 19: 39519
FIOCCHI, R., Separation efficiency in diffusion of nonisotopic gaseous mixtures, 19: 38767
FIRSOV, E. I., Multichannel time-delay analyzer, 19: 38932
FISCELLA, B., Positronium in water and ice from 22° to −144°C by annihilation quanta measurements, 19: 39509
FISCHER, K., Determination of spin of 2426-kev level in ^{82}Kr, 19: 39944
FISHER, D. A., Numerical data for ^{131}I uptake measurements in rabbits, 19: 38341
FISHER, L. H., Validity of Townsend's ionization function in nonuniform electric fields, 19: 39298
FISHER, Philip C., Observational result on x rays, 19: 39332
FISK, C. J., ACCEL: automated circuit card etching layout, 19: 38915 (SC-DC-65-1419)
FISK, H. E., Spin of the $Y_1^{*}(1405)$, 19: 39553
FLEISCHER, R. L., Prog. rpt. on radiation damage in solids, final, 4/62–3/65, 19: 39226 (AFCRL-65-305)
FLEISCHER, R. L., Tracks of charged particles in solids, 19: 39038
FLIPOT, A. Jean, Installation for purification of Ar for glove boxes, 19: 38769
FLIPPEN, R. B., The radial velocity of magnetic field penetration in type II superconductors, 19: 39702
FLORECK, H., Absorbed dose rate determination in vinylchloride. I., 19: 39016
FLUENDY, M. A. D., Magnetic velocity selector for hydrogen atom beams using an unfolding technique, 19: 38929
FLYNN, E. R., Distorted-wave Born-approximation calculations of ^{3}He inelastic scattering, 19: 39885
FLYNN, G. W., Study of collision narrowing by comparison of molecular-beam and gas-phase nuclear resonance spectra, 19: 38629
FODOR, I., Circular polarization of γ quanta accompanying reaction $^{10}B(d,p)^{11}B$, 19: 39937
FODORNE, Csanyi Piroska, Measurement of soft β-emitting isotopes by means of liquid scintillators, 19: 39002
FOJTIK, A., Preparation of ^{35}S-labeled cystine, 19: 38747
FOLSOM, Theodor R., Zinc-65 and other fallout nuclides in marine organisms of California coast, 19: 38895
FOMICHEVA, V. I., Chromatographic method of determining U and Pu in air, 19: 38554
FOOTE, J. H., Cooperative effects in tenuous energetic plasma contained by magnetic mirror field, 19: 40017
FORST, W., Simple data display system for fast-scanning mass spectrometer, 19: 39022
FORSTER, H. H., Analysis of the $^{6}Li(p,pd)^{4}He$ reaction, 19: 39907
FORSTER, H. H., Reaction D(p,2p)n at 31 Mev, 19: 39225
FORTIN, Guillaume, Fuel loading and unloading arrangement for nuclear reactors, 19: 40145
FOSTER, Leigh Curtis, X-ray tube with adjustable electron beam cross section, 19: 38964
FOSTER, R. F., Evaluation of exposure from multiple environmental sources in the environs of the Hanford plants, 19: 38874 (BNWL-SA-53)
FOTESQUE, Peter, Nuclear reactor, 19: 40132 (ORNL-tr-590)
FOWELL, P., High-temperature isothermal calorimeter, 19: 38675
FOWLER, Eliot Patrick, Design of d-c amplifiers, 19: 38961
FOWLER, J. L., Intermediate states as observed by differential scattering

of neutrons by doubly closed shell nuclei, 19: 39785 (ORNL-P-1356)
FOWLER, T. K., Anomalous plasma diffusion in magnetic wells, 19: 39968 (ORNL-P-1338)
FOX, A. C., The preparation and some properties of U carbonitrides, 19: 39089 (AERE-M-1389)
FOX, H. M., Progress in the development of refractory metals for use in nuclear rocket nozzles, 19: 40254
FOX, J. D., Reactions involving simple isobaric analog resonances, 19: 39875
FRAMPTON, C. W., Evidence of lysogeny in derivatives of Escherichia coli, 19: 38381
FRANCHET-SASSOLAS, G., Fixation curve of ^{131}I in thyroid in subjects treated with iodinated contrast media, 19: 38354
FRANCIS, N. C., Cross sections for reactor design, 19: 40115 (CONF-650602-33)
FRANCOIS, Henri, Atmospheric fallout collector, 19: 38906
FRANK, W. M., Weak-strong coupling complementarity in renormalized perturbation theory, 19: 39521
FRANZ, F. A., Rubidium spin relaxation in the rare gases under ultra-clean conditions, 19: 39400
FRANZINI, P., Antiproton annihilation in H at rest. I., 19: 39462 (CU-1932-239)
FRASER, J. S., Intense Neutron Generator target, 19: 39756 (AECL-2177, Paper 3)
FRAUENFELDER, H., Surface studies using Moessbauer effect, 19: 40078 (NP-15111)
FREED, N., Magnetic moments of single particle states in ^{207}Pb and ^{209}Bi, 19: 39870
FREEMAN, A. J., Nonlinear and linear shielding of rare-earth crystal-field interactions, 19: 40101
FREEMAN, J. M., ft Values for ^{42}Sc, ^{46}V, and ^{56}Mn and conserved vector current hypothesis, 19: 39859
FREIER, P. S., Electrons, H and He nuclei in primary cosmic radiation, 1963, 19: 39420 (NP-15117)
FREIER, P. S., Helium nuclei of primary cosmic radiation as studied over solar cycle of activity, 19: 39427
FREY, K., Genetic variability in quantitative characters induced by thermal neutron treatment of diploid, tetraploid, and hexaploid oat seeds, 19: 38419
FREYTAG, D., Measurements of cross sections for photoproduction of π^0 on H in region of first resonance, 19: 39597
FRICKE, K., Determination of spin of 2426-kev level in ^{82}Kr, 19: 39944
FRIEDMAN, A. M., Alpha half life of berkelium-247; a new long-lived isomer of berkelium-248, 19: 39807
FRIEDMAN, G. I., Prog. rpt. on W–Re tube fabrication, 7/64–6/65, 19: 39128 (NMI-1267)
FRIEDMAN, H., Special and photometric measurements of solar x-ray emission below 60 A, 19: 39333
FRIEDMAN, Harold L., Calculation of Hall effect in ionic solutions, 19: 38643
FRIEDRICH, Carl M., Structural analysis of a reactor subassembly under thermal, hydraulic, and fuel expansion loads, 19: 40118 (WAPD-T-1782)
FRISCH, Erling, Nuclear reactor, 19: 40167
FROELEN, H., Genetic effects of supra-lethal x-ray treatment of male mice, 19: 38393
FROMHOLD, A. T. Jr., Nuclear spin-lattice relaxation and Knight shift in tungsten metal, 19: 39720
FRUMKIN, A. N., Electrocapillary curves of liquid gallium, 19: 39171 (IS-Trans-17)
FUJII, Kenji, Current-current interaction and nonleptonic decays of hyperons, 19: 39560
FUJIMORI, Eiji, Ultraviolet light-induced change in collagen macromolecules, 19: 38701
FUJITA, Minoru, Fallout radioactivity in diet and excreta. The levels at Tokai district, Japan in 1962 to 1963, 19: 38894
FUKETA, Toyojiro, Strong p-wave neutron resonances in ^{120}Sn, ^{118}Sn, and ^{124}Sn, 19: 39784 (ORNL-P-1352)
FUKUDA, Hiroshi, Fallout radioactivity in diet and excreta. The levels at Tokai District, Japan in 1962 to 1963, 19: 38894
FUKUSHIMA, Masahisa, Scattering matrix and surface modes. II., 19: 40108
FUKUSHIMA, Noboshi, Seasonal dependence of SC-field in middle and low latitudes, 19: 39673
FUKUSHIMA, Shin, Cosmic-ray-neutron monitor for antarctic observations, 19: 39035
FULDE, Peter, Effects of gap anisotropy in superconductors containing paramagnetic impurities, 19: 39717
FULDE, Peter, Magnetic-field dependence of Knight shift in superconductors, 19: 39719
FUMELLI, M., Effect of ion-neutral collisions on plasma rotation, 19: 40052
FUNAHASHI, Akimasa, Improved microwave reflection measurement of plasmas produced by shock waves, 19: 39997
FURMAN, F. J., Nonstoichiometry of UO_2–CeO_2: the system UO_2–CeO_2–$CeO_{1.5}$ at 900 to 1200°C, 19: 39222
FUTCH, A. H., Jr., Cooperative effects in tenuous energetic plasma contained by magnetic mirror field, 19: 40017

G

GABELMAN, John W., Geology of Cuzco-Anta-Urubamba Area, Peru, 19: 38845 (RME-4584)
GABLER, F., On the combination of the phase contrast process with fluorescence microscopy, 19: 38923 (UCRL-Trans-1228)
GABOS, Z., Relativistic study of polarization of the electron, 19: 39582
GAERTTNER, E. R., Asymptotic and steady state spectrum measurements in a multiplying medium, 19: 39768 (RPI-328-21)
GALATRY, L., Natural width of spectral lines and irreversibility, 19: 39386
GALIMOV, E. M., Age effect in isotopic composition of carbon of stalactite annulations of the Crimea highlands, 19: 38854
GALL, W. R., Cost study of large Na-cooled fast breeder for desalination, 19: 40190 (ORNL-TM-784)
GALLAGHER, P. K., Fluorescence of Eu(III) in D_2O–H_2O mixtures, 19: 38636
GALLE, Reiner, Device for measurement of surface contamination caused by α-emitting substances, 19: 39045
GANGRSKII, Yu. P., Coulomb excitation of first levels of ^{90}Zr and ^{96}Zr, 19: 39942
GANGULEE, A., Prog. rpt. on metallic systems, annual, 1964, 19: 39168 (TID-39168)
GANGULY, A. K., Temperature distribution in γ-active spheres, 19: 40275
GARBER, Donald Ivan, Polarization of neutrons from (d,n) reactions on carbon, 19: 39950
GARBUNY, Max, Determination of superconducting transition region by superfluid phase transition, 19: 39691
GARCIA, R., Ultrasonic-induced cavitation studies in lead–bismuth alloy at elevated temperatures, 19: 39116 (NP-15263)
GARCIA DEL RIO, H., Comparative study of radionephrography and excretion urography, 19: 38520
GARDER, L., Integral FILTER technique for HPD, 19: 38985 (CERN-65-11 (p.153-72))
GARDNER, A. L., Cooperative effects in tenuous energetic plasma contained by magnetic mirror field, 19: 40017
GARDNER, A. L., High-speed microwave phase shifters using varactor diodes, 19: 40297 (UCRL-7753)
GARDNER, J. W., HPD programming at Rutherford Lab., 19: 38986 (CERN-65-11(p.173-81))
GARNETT, J. L., Catalytic deuterium exchange reactions with organics. XII., 19: 38596
GARNETT, J. L., Catalytic deuterium exchange reactions with organics. XIII., 19: 38597
GARRIOTT, O. K., Measurements of total electron content and equivalent slab thickness of mid-latitude ionosphere, 19: 39677
GARSHINA, L. S., Phase composition of CaF_2–YF_3, SrF_2–YF_2, and BaF_2–YF_3, 19: 38615
GARTON, G., E.P.R. and ENDOR of Tb^{4+} in thoria, 19: 38655
GARY, Robert, Dissociation constant of acetic acid in D_2O from 5 to 50°C, 19: 38645
GARY-BOBO, J., Study of deep postradiotherapeutic digestive stenoses, 19: 38522
GASHIMZADE, F. M., Damping of electron spectrum and quantum theory of galvanomagnetic phenomena, 19: 40106
GATLAND, I. R., Stimulated photon-photon scattering, 19: 39264 (CONF-796(Paper 14))
GATOS, H. C., Order-disorder effect on superconductivity: The Mo–Ir system, 19: 39689
GATTO, R., Consequences of SU_6 for total baryon-baryon and baryon-antibaryon cross-sections, 19: 39529
GATTO, R., Proton-antiproton annihilation into two mesons, 19: 39527
GATTO, R., Vector and axial currents under first-order symmetry breaking, 19: 39606
GAUDIN, M., Method of integration of the energy variables in the graphs of the theory of perturbations, 19: 39512
GAUL, G. G., Corrosion of materials for nuclear superheat applications, 19: 39115 (GEAP-4760)
GEARY, A. L., Prog. rpt. on W–Re tube fabrication, 7/64–6/65, 19: 39128 (NMI-1267)
GEBALLE, T. H., Superconductivity of Nb_3Ge, 19: 39725
GEBELT, R. E., Preparation and thermodynamics of EuC_2, 19: 38680
GEHENIAU, J., Internal groups and Heisenberg theory of elementary particles, 19: 39494
GEIGER, J., Rotational structure in energy loss spectrum of H_2, 19: 39399
GEIST, D., Electron paramagnetic resonance of Eu^{2+} in CdF_2, 19: 38664
GEL'FMAN, A. Ye., Application of scintillation granules for measuring β

radiation from radioactive isotopes, 19: 38737
GELLER, Murray, Many-electron calculation for the Be atom, 19: 39381
GEL'MAN, A. D., Behavior of Pu(V) nitrate solutions, 19: 38731
GEL'MAN, A. D., Preparation and properties of Pu(V) nitrate solutions, 19: 38656
GENKIN, A. L., Laminar magnetogasdynamic boundary layer on the conducting surface of crossed electric and magnetic fields, 19: 40044
GENTLE, Kenneth W., Longitudinal waves in a weakly ionized gas, 19: 39293
GEOFFRION, B., Scattering of protons on C-12, 19: 39837
GEOFFRION, Louis A., Densities of some low-melting Pu alloys, 19: 39161 (LA-DC-6956)
GEORGACOPULO, P., Strengthening of ionizing action of ^{198}Au induced by H_2O_2, 19: 38389
GEORGE, D. W., On the release of metallic impurities from graphite at temperatures above 1750 deg C, 19: 38762
GEORGE, R. F., Nucleon-nucleon total cross sections between 1 and 8 Bev/c, 19: 39550
GEORGI, P., Observations concerning the unstable behavior of ^{14}C-phenylethylamine carbamate in liquid scintillation mixtures, 19: 38746
GERARDO, J. B., High-frequency laser interferometry in plasma diagnostics, 19: 39993
GERBAULET, K., The fluorescence of p-hydroxydiphenyl in aqueous solution, 19: 38687 (EUR-2423.e)
GERECKE, G. E., Converters (d-c to d-c) for nuclear-thermionic energy sources, 19: 38835 (N65-27619)
GERETH, R., Study of radiation damage by using field effect, 19: 39252
GEROK, Wolfgang, Severe radioinduced hemolysis in hereditary deficiency of reduced glutathione in blood cells, 19: 38509
GEROLD, V., Comparative x-ray and electron microscopy studies Guinier-Preston zones in aluminum–silver, 19: 39172 (ORNL-tr-633)
GEROLD, Volkmar, Age-hardening of Al–Ag alloys, 19: 39174 (ORNL-tr-635)
GEROLD, Volkmar, Heat tone in the strain-hardening state of Al–Zn alloys, 19: 39173 (ORNL-tr-634)
GERRARD, Martha, New reaction for producing strontium, 19: 38593 (ORNL-tr-674)
GERSCH, H. A., Solid-superfluid transition in ^4He at absolute zero, 19: 39729
GERSDORF, R., Design of high field magnet coils for long pulses, 19: 38935
GERSHON-COHEN, J., Tumor scanning with Cs-131, 19: 38508
GERSON, Robert, Mössbauer spectrometer using a piezoelectric bar in resonant oscillation, 19: 39032
GESCHWIND, S., Electron-nuclear double resonance of ^{57}Fe in MgO, 19: 39878
GESZTESSY, Akos, Measurement of radiation in traumatologic intervention, 19: 38477
GEZENTSVEI, Z. A., Functional condition of G-I tract before and after I-131 treatment, 19: 38529
GIACOMELLO, Giordano, Isotope separator of Rome University, 19: 39077
GIBBONS, J. F., Prog. rpt. on BONUS core development, 12/64–2/65, 19: 39156 (CEND-532)
GIBBONS, J. H., On radiative transition in ^{207}Pb and ^{206}Pb following resonance neutron capture on ^{206}Pb and ^{207}Pb, 19: 39783 (ORNL-P-1345)
GIBBONS, W. S., Piping failures for reactor coolant pipe rupture study, 19: 40121 (GEAP-4574)
GIBBS, Hyatt, Importance of nuclear-spin effects in extracting alkali spin-exchange cross sections from Zeeman optical-pumping signals, 19: 39879
GIBBS, Priscilla, Clinically useful calculations of the dose distribution from multiple radiation sources, 19: 38526
GIBNEY, Gerard G., Accelerator beam energy monitor, 19: 39330
GIBSON, David C., Progress in the development of refractory metals for use in nuclear rocket nozzles, 19: 40254
GIESSEN, B. C., Order-disorder effect on superconductivity: The Mo–Ir system, 19: 39689
GILLET, V., Configuration mixing in the continuum and nuclear reactions. II., 19: 39873
GIOFFRE, L., Renal excretion of colloidal Au^{198}. An experimental morphological study, 19: 38342
GIORASCU, F., Detection and measurement of nuclear radiations, 19: 39040
GIRAUD, B., Calculation of spurious states due to center-of-mass motion, 19: 39812
GIROD, P., Charge state of ultra-fine aerosols in weakly ionized media, 19: 39285
GITTUS, J., Diffusion, stress and the rates of processes leading to deformation of nuclear fuel element cladding, 19: 39220
GLADYSHEVSKII, E. I., Constitution diagram and properties of Nb–Mo–Si alloys, 19: 39194
GLADYSHEVSKII, E. I., Lanthanum silicides and their crystal structure, 19: 38613
GLADYSHEVSKII, E. I., Solubility of certain transition metals in the V_3Si compounds and their influence of the transition of the compounds into a superconducting state, 19: 39196
GLAENZER, Richard H., Recombination in γ-irradiated Si, 19: 40085
GLAESER, H. J., Electron paramagnetic resonance of Eu^{2+} in CdF_2, 19: 38664
GLASS, F. M., Transistorized regulated high-voltage supply, 19: 39053
GLASSER, R. G., Time reversal invariance in $\Sigma^0 \rightarrow \Lambda^0 + e^+ + e^-$, 19: 39484 (TID-22038)
GLAVATI, O. L., Production of stereospecific polymers by the γ-irradiation of inclusion compounds, 19: 38725
GLAZOV, A. A., Investigation of the ion motion in the central region of the fixed-field alternating-gradient cyclotron, 19: 39316 (JINR-P-2199)
GLAZUNOV, I. S., Signs, symposiums and treatment of radiation sickness, 19: 38471
GLAZUNOV, S. G., Thermal hardness of β alloys of Ti–Mo–Cr–Fe–Al system, 19: 39193
GLINSKII, K. K., Research on the system $LiF–ZrF_4$, 19: 38610
GLOWER, D. D., Hysteresis studies of reactor-irradiated single-crystal Ba titanate, 19: 38705
GODDARD, John F., Kinetic studies on extraction of Eu by Li analgam and comparison to removal by electrolysis, 19: 38753 (LA-DC-7013)
GODWIN, R. P., Surface studies using Moessbauer effect, 19: 40078 (NP-15111)
GODWIN, Robert P., Dynamical properties of one-dimensional crystal with free ends, 19: 40079
GOEDEKE, A. Donald, Space radiation shielding, 19: 40072
GOFMAN, J. W., Chemical bonding and the sulfur K-x-ray spectrum, 19: 38588 (UCRL-12496)
GOLD, L., Stimulated photon-photon scattering, 19: 39264 (CONF-796 (Paper 14))
GOLD, Raymond, Theoretical estimates of pile-up distortion, 19: 38969 (ANL-6949)
GOLDBERG, J., Decay of the x and ϕ mesons, 19: 39531
GOLDBERG, Leo, The new astronomies, 19: 39353
GOLDBERG, M., Evidence for new $\pi^+\pi^-$ resonance at 1.67 Bev, 19: 39537
GOLDBERG, P., Boiling flow regimes and critical heat flux, 19: 38809 (NYO-3304-3)
GOLDBERG, V. Z., Reaction $(^3He,\alpha)$ on ^9Be, ^{14}N and ^{16}O, 19: 39941
GOLDEN, D. E., Validity of Townsend's ionization function in nonuniform electric fields, 19: 39298
GOLDHABER, G., Observation of correlations between vector-meson and baryon-resonance decays, 19: 39542
GOLDHABER, S., Observation of correlations between vector-meson and baryon-resonance decays, 19: 39542
GOLDIN, A. S., Analytical radiochemistry in health physics, 19: 38889
GOLDIN, A. S., Strontium-90 measurements in milk, 19: 38556
GOLDMAN, L. M., Motion of θ-pinch plasma in asymmetric fields, 19: 40010
GOLDMAN, M. V., Stimulated incoherent scattering of light from plasmas, 19: 40012
GOLDSTEIN, Y., Absorption of transverse microwave phonons by Al–Pb superconducting diodes, 19: 39713
GOL'FARB, V. M., Optical investigation of temperature distribution and electron concentration in argon plasma, 19: 40039
GOLUB, Morton A., Radiation-induced cis-trans isomerization of polybutadiene. IV., 19: 38711
GOLUB, V. S., Device for improving stability and pulse counting in Geiger counter, 19: 39021
GONAS, A. M., Dynamic elastic properties of polycrystalline W from 24 to 1800°C, 19: 39198
GONCHARENKO, S. V., Effect of fast neutrons on culture and morphological characteristics of Bacillus mesentericus, 19: 38449
GONCHARUK, A. B., Lanthanum germanides, 19: 39195
GONZALEZ, C., Genetic variability in quantitative characters induced by thermal neutron treatment of diploid, tetraploid, and hexaploid oat seeds, 19: 38419
GOOD, W. M., On radiative transition in ^{207}Pb and ^{206}Pb following resonance neutron capture on ^{206}Pb and ^{207}Pb, 19: 39783 (ORNL-P-1345)
GOODJOHN, A., A survey of several methods for computing cell cross sections, 19: 40152 (GA-6462)
GOODMAN, B. B., Electrodynamics of flux penetration in superconductors, 19: 39712
GOPALAKRISHNAN, Sarada, Fission products data and its application in studying fallout from nuclear weapon tests, 19: 39774 (AEET-209)
GOPINATH, D. V., Temperature distribution in γ-active spheres, 19: 40275
GORBUNOV, A. N., Nuclear photoeffect on three-particle nuclei, 19: 39808
GORDON, F. J., Cooperative effects in tenuous energetic plasma contained

by magnetic mirror field, 19: 40017
GORIZONTOV, P. D., Pathology of radiation sickness, 19: 38433
GORNAYA, M. S., Activity of α toxin of Cl. perfringens type A radiation mutants, 19: 38446
GORNAYA, M. S., Radiation effects on antigenic and immunogenic properties of perfringens bacteria toxins. I., 19: 38447
GORODETSKII, A. A., RBE of fast neutrons, 19: 38438
GORODETSKOGO, A. A., Biological effects of neutron radiation, 19: 38437
GORYACHEV, B. I., The energy distribution of photoprotons from ^{28}Si, 19: 39938
GOTTA, H., Comparative study of radionephrography and excretion urography, 19: 38520
GOTTLIEB, H., High-temperature isothermal calorimeter, 19: 38675
GOTTLIEB, Melvin B., Plasma—the fourth state, 19: 39992
GOTTLIEB, Milton, Determination of superconducting transition region by superfluid phase transition, 19: 39691
GOURDIN, M., Cabibbo angles and Johnson-Treiman relation, 19: 39544
GOURDIN, M., Deuteron electrodisintegration and neutron form factors, 19: 39541
GOZANI, Tsahi, Theory of modified pulsed source technique, 19: 40151 (EIR-79)
GRABER, B., Fixation curve of ^{131}I in thyroid in subjects treated with iodinated contrast media, 19: 38354
GRAF, P., HWR power plant with 275-MW(e) PHWP and a 260-MW(e) BLWP units, 19: 40211
GRAFFMAN, Sten, Fixation of carbon-11 in cells of proton-irradiated blood, 19: 38722
GRAHAM, Donald P., Improvement of the activity of platinum hydrogenation catalysts by high-energy irradiation, 19: 38742
GRAM, P. A. M., Development of experimental techniques for measuring the distribution of H and He isotopes in space, 19: 39419 (ATM-63(9219)-1)
GRANKOVA, L. P., Thermal hardness of β alloys of Ti–Mo–Cr–Fe–Al system, 19: 39193
GRANT, John, Improvements in or relating to conveyor systems for package irradiation plants, 19: 38797
GRASHIN, A. F., Data on p,p reactions with Q = 148 Mev, 19: 39479 (NP-15216)
GRAU, P., Special characteristics of nuclear power station in the Ardennes, 19: 40209
GRAVES, Glen A., Ground test radiation experience at the Kiwi B-4 tests, 19: 40253
GRAY, Peter R., Half life of ^{16}N, 19: 39813
GREAVES, Thomas Cyril, Nuclear reactor fuelling apparatus, 19: 40144
GRECHIKHIN, L. I., Effect of surrounding gas pressure on physical state of arc discharge plasma, 19: 39989
GREEN, B., Magnetohydrodynamic ionizing shock waves in a conducting medium, 19: 39267 (NP-15157)
GREEN, Brian Noel, Mass spectrometer ion collector with a secondary particle collecting electrode extending over the collector, 19: 38962
GREEN, J. H., Kinetic energy of fragment ions using r-f mass spectrometer, 19: 38927
GREEN, J. H., Performance of Bennett r-f mass spectrometer, 19: 38926
GREEN, John W., Effects of subcutaneous implantation of rare-earth metals, 19: 38334 (COO-1170-1)
GREEN, L., Fuel management in the settled-bed fast reactor, 19: 40178 (BNL-9279)
GREEN, W. K., Prog. rpt. on reactor control systems, 2–4/65, 19: 40122 (GEAP-4862)
GREENBORG, J., Neutron attenuation mechanisms in concretes, 19: 40061 (BNWL-SA-79)
GREENE, N. D., Prog. rpt. on heat transfer for nuclear auxiliary power systems, 3–5/65, 19: 38811 (SAN-409-24)
GREENHALGH, E., Observations on reaction of polymer carbons with CO_2, 19: 38599
GREENWOOD, Arthur H., Thermoelectric control apparatus for the fabrication of thick lithium-drifted germanium detectors, 19: 39029
GREER, Harold, Radiation fallout meter, 19: 39051
GREGG, S. J., Kinetics of oxidation of carbon and graphite by oxygen at 500 to 600°C, 19: 39119
GREGOREV, N. B., Electrocapillary curves of liquid gallium, 19: 39171 (IS-Trans-17)
GREGSON, K., MLBW—a multi-level Breit-Wigner computer program, 19: 39776 (AEEW-M-517)
GREGSON, K., TEMPO—a general Doppler broadening program for neutron cross sections, 19: 39777 (AEEW-M-518)
GREINER, Douglas E., Energy spectra of Ky_{83} decay modes, 19: 39488 (UCRL-16058)
GREISEN, K., Detection of super showers by atmospheric scintillation, 19: 39422 (TID-21895)
GRENIER, C., Alternating-current losses in Nb/Zr superconductive coils, 19: 39695
GREY, Jerry, High-temperature gas interactions, 19: 40231 (LA-3229, pp 149-76)
GREY, Jerry, Liquid-core nuclear rocket, 19: 40227 (LA-3229, pp 90-110)
GRIBOV, V. N., Model of three-particle unitarity condition for complex momenta, 19: 39596
GRIESENAUER, Noel M., Prog. rpt. on fission-fragment effects in structural materials, 4–6/65, 19: 39229 (BMI-X-10134)
GRIFFIN, A., On the detection of second sound in crystals by light scattering, 19: 40092
GRIFFITH, T. C., Inelastic proton-deuteron scattering at 135 Mev, 19: 39579
GRIFFY, T. A., Structure of ^3He and ^3H from high-energy electron scattering, 19: 39909
GRIGAR'YAN, M. S., Pathological effects of radiation injuries, 19: 38426
GRIGOLETTO, A., Study of Σ^- capture process in hydrogen, 19: 39510
GRIGOREV, E. P., 3-hour activity of lutetium, 19: 39931
GRIGOR'YAN, M. S., Radiation effects on sulfhydryl (SH) group of albumen blood structures, 19: 38427
GRIN, Yu. T., Disappearance of nuclear pairing correlations as influenced by rotation, 19: 39858
GRINENKO, V. A., Age effect in isotopic composition of carbon of stalactite annulations of the Crimea highlands, 19: 38854
GRINGAUZ, K. I., Near-earth and inter-planetary plasma, 19: 39364
GRITSYNA, V. T., Isomers ^{159m}Gd and ^{117m}Sb, 19: 39929
GROMOV, K. Ye., Decay of ^{161}Ho, 19: 39930
GROSS, R. A., Ionizing shock wave plasma diagnostics, 19: 40059
GROSSBARD, Neil J., Calculated cross sections for atomic displacements produced by electrons in the 1.0 to 3.0-Mev energy range, 19: 39225 (AFCRL-65-286)
GROSSE-SCHULTE, M., Mechanism of the reaction $^{11}B(^{16}O,^{18}N)^{12}C$ at 30 Mev, 19: 39869
GROVE, G. R., Prog. rpt. on reactor fuels and materials, annual, 1964, 19: 39163 (MLM-1244)
GROVER, G. M., Status report on theory and experiments on heat pipes at Los Alamos, 19: 38780 (LA-DC-7206)
GRUBELICH, F. T., Prog. rpt. on BONUS core development, 12/64–2/65, 19: 39156 (CEND-532)
GRUBER, John B., Optical-absorption intensities of rare-earth ions in crystals, 19: 38652
GRUBER, S., High-frequency velocity space instabilities, 19: 40019
GRUHN, C. R., Reaction $^{40}Ca(\alpha,2\alpha)^{36}Ar$, 19: 39902
GUENTHER, Horst, Urological injuries after treatment of carcinoma of uterine neck, 19: 38532
GUENTHER, Karl-Georg, Thermionic generator, 19: 39446
GUEST, G. E., Anomalous plasma diffusion in magnetic wells, 19: 39968 (ORNL-P-1338)
GUGENBERGER, Rene, Fuel loading and unloading arrangement for nuclear reactors, 19: 40145
GUILLAUMONT, Robert, Study of Pa(V) and Pa(IV), 19: 38602
GUIMARD, Jacqueline, Differential action of x and uv rays on Macrobiotes areolatus, 19: 38373
GUINET, P., Fixation curve of ^{131}I in thyroid in subjects treated with iodinated contrast media, 19: 38354
GUMAN, V. N., Excitation spectra of ^{208}Tl and ^{208}Bi nuclei, 19: 39933
GUNDERSEN, Roy M., Quasi-one-dimensional MHD flow with heat addition. III., 19: 39302
GUNTON, R. W., Use of radioiodinated fatty acid for photoscans of the heart, 19: 38490
GUREWITSCH, Anatole M., Method and system for electron irradiation of materials, 19: 38954
GURLEY, Lawrence R., Viscosimetric studies of kinetics of thermal denaturation of DNA, 19: 40299 (LA-tr-65-12)
GUSAROV, I. I., Organization and equipment of a radon laboratory, 19: 38498
GUSH, H. P., Change in the crystal structure of solid normal hydrogen near 1.5°K, 19: 39738
GUSINOW, M. A., High-frequency laser interferometry in plasma diagnostics, 19: 39993
GUSSENHOVEN, M. S., Adhesion of polished quartz crystals under ultra-high vacuum, 19: 38840
GUSTAFSSON, S., Nuclear g factor of the 3.2-Mev 5⁻ state in the double-closed shell nucleus ^{208}Pb, 19: 39843
GUTMACHER, Ralph G., Spark spectrum of berkelium, 19: 39384
GUTTMAN, Paul H., Potentiating effect of neonatal thymectomy on x-ray-induced intercapillary glomerulosclerosis, 19: 38409
GUYMON, R. H., MSRE design and operations report. VI., 19: 40189 (ORNL-TM-733(Rev.))
GUYON, E., Proximity effects under magnetic fields. I., 19: 39699

H

HAAR, D. Ter, Finite linewidths and "forbidden" three-phonon interactions, 19: 40096

HAAS, G. M., Energetic neutral injection into an electron-cyclotron plasma, 19: 39970 (ORNL-P-1374)

HAASBROEK, F. J., A simple and inexpensive sample changer for windowless gas-flow counters, 19: 39037

HABERER, Klaus, On the efficiency of γ activation measurements using well-type scintillation counters, 19: 39039

HACKETT, Herman Joseph, Locating means for positioning nuclear fuel components, 19: 40174

HACKNEY, B. D., Piping failures for reactor coolant pipe rupture study, 19: 40121 (GEAP-4574)

HADFIELD, Timothy J., Turntable-type drier for granular material, 19: 38800

HADLEIGH-WEST, Frederick, Archeological survey at Ogotoruk Creek, 19: 40289 (PNE-406)

HADLEIGH-WEST, Frederick, Archeological survey and excavations at Ogotoruk Creek, 12/61, 19: 40290 (PNE-407)

HAENDEL, S. K., X radiation from a flash x-ray discharge column, 19: 39305

HAENLEIN, Walter, Thermionic generator, 19: 39446

HAESSNER, F., Application of electron-microscopic fine-range diffraction for the determination of the rolling texture of Cu, 19: 39175 (ORNL-tr-638)

HAGSTRUM, H. D., Focused slow ion beam for study of electron ejection from solids, 19: 38937

HAHN, Paul B., Strontium-90 measurements in milk, 19: 38556

HAINES, Eldon L., Resolution of semiconductor detectors for fission fragments, 19: 39033

HAINES, M. G., Origin of rotation in magnetically confined plasmas, 19: 39974

HAINSKI, Z., Determination of rare earths in SAP material. II., 19: 38553

HAKIM, Remi, Covariant theory of relativistic Brownian motion. I., 19: 39959 (N64-22435)

HALLAM, R. C., Joining techniques for SAP-clad nuclear fuel elements, 19: 39131

HALLER, Mitchell W., Nuclear fuel consisting of very small uniformly dispersed UC particles in a uranium matrix, 19: 39127 (NCSC-2981-9)

HALMANN, M., Isotope effects on vibrational transition probabilities. III., 19: 38632

HALPERN, Francis R., Wigner's analysis of the unitary representations of the Poincare group, 19: 39486 (UCRL-12359)

HALPERN, Jack, Isotopic exchange of hydridoplatinum(II) complex with D_2O, 19: 38627

HAMA, Mitsuru, Transverse momentum distribution of the high-energy $p + p \rightarrow \pi^+ + d$ reaction, 19: 39569

HAMADA, Shigeo, End stabilization effect in slow theta pinch, 19: 39996

HAMADA, Tetsuo, Modification of Hamada-Johnston potential, 19: 39570

HAMAGUCHI, Hiroshi, Anion-exchange behavior of Sc, rare earths, Th and U in magnesium nitrate solution, 19: 38770

HAMILTON, David C., Position of La in the periodic table, 19: 39373

HAMMITT, F. G., Ultrasonic-induced cavitation studies in lead–bismuth alloy at elevated temperatures, 19: 39116 (NP-15263)

HAMPE, E., Sintering behavior of uranium, 19: 39132

HAN, C., Spectroscopic studies with the $^{10}B(^3He,p2\alpha)$ reaction, 19: 39917

HAN, Ch'u Jun, Decay of ^{161}Ho, 19: 39930

HANERFELD, H., Post FILTER routine of CERN HAZE, 19: 38983 (CERN-65-11(p.139-43))

HANNA, S. S., Moessbauer cross section of ^{57}Fe in iron, 19: 39877

HANRAHAN, Robert J., Radiation chemistry of cyclopentane, 19: 38712

HANSEL, James G., Prog. rpt. on combustion of metals, 7–12/64, 19: 38583 (SC-DC-65-1480)

HANSEN, Carl Woodrow, Coin identification apparatus utilizing radiation bombardment, 19: 38956

HANSEN, G. J., Electronic integrators for instrumentation applications, 19: 38918 (SC-R-65-904, pp 49-58))

HANSEN, G. J., Four papers concerning recent work on ground motion measurements, 19: 38864 (SC-R-65-904)

HANSEN, L. F., Energy levels of ^{31}S and ^{19}Ne, 19: 39827

HANSEN, O., Thallium-207 states excited in the (t,α) reaction on ^{208}Pb, 19: 39852

HANSEN, P. G., The $\Omega_p = \Omega_n = \frac{1}{2}$ excitations in the odd nucleus ^{173}Tm, 19: 39822

HANSON, W. F., Angular distribution and thickness dependence of transition radiation from thin aluminum foils, 19: 40099

HARDER, B. R., The preparation and some properties of U carbonitrides, 19: 39089 (AERE-M-1389)

HARDING, WILLIAM B., Solderability testing, 19: 40280 (BDX-613-73)

HARDY, Gy., Radiation-induced solid-state polymerization. I., 19: 38699

HARGREAVES, Sylvia, Influence of horizontal air motions on F2-region ionization, 19: 39668

HARMS, W. O., Prog. rpt. on coated-particle fuels, 11/64–5/65, 19: 39129 (ORNL-TM-1116)

HARRIS, C. Craig, Beta-type absorbed dose from non-beta-emitting radionuclides, 19: 38878 (ORNL-P-1405)

HARRISON, D. E. Jr., Kinetic emission of electrons from monocrystalline targets, 19: 39405

HART, Robt. G., Plutionium enriched U fuel, 19: 39146

HART, William E., Irradiation-actuated device for measuring the tensile fracture strain of graphite, 19: 39238

HARTMAN, Thomas E., Anomalous peaks in mass spectra of H_2 and D_2 obtained with single-focusing mass spectrometer, 19: 39288

HARTNAGEL, Hans, Ion distribution in drift region of tubular electron beams, 19: 39283

HARTZEL, L. W., Determination of tertiary butyl perbenzoate in molding powders, 19: 40285 (MLM-1284)

HARVEY, G. G., Prog. rpt. on electronics, 4/15/65, 19: 39270 (TID-21894)

HARVEY, J. A., Strong p-wave neutron resonances in ^{126}Sn, ^{118}Sn, and ^{124}Sn, 19: 39784 (ORNL-P-1352)

HARVEY, John C., Electrocapillary curves of liquid gallium, 19: 39171 (IS-Trans-17)

HASKINS, J. R., Advanced Moessbauer-effect experiments, 19: 39795

HASTE, G. R., Severe microinstability-driven losses in an energetic plasma, 19: 39967 (ORNL-P-1337)

HATANO, Hisakazu, 25-Mev linear accelerator in Japan, 19: 39326

HATCH, E. N., Isotope shift of $K_{\alpha 1}$ x rays of uranium, 19: 39412

HATCH, L. P., BNL fluidized bed studies, 19: 40223 (LA-3229, pp 48-62)

HATTON, J., Nuclear magnetic resonance in liquid ^3He, 19: 39728

HATTORI, Hiroyuki, Effects of x-ray polarization on Pendelloesung fringes, 19: 39287

HAUBOLD, A. D., Magnetization of current carrying cold worked NbZr superconducting wires, 19: 39749

HAVLOVIC, Vratislav, Apparatus for the collection of samples of aerosols on membrane filters, 19: 38896

HAVLOVIC, Vratislav, External γ exposure to man from fission products dispersed in the atmosphere, 19: 38891

HAWKE, Ronald S., High-speed microwave phase shifters using varactor diodes, 19: 40297 (UCRL-7753)

HAWKING, S. W., Hoyle-Narlikar theory of gravitation, 19: 39659

HAWKINS, R. J., Study of cation diffusion in UO_2 using α spectrometry, 19: 38681

HAWKINS, S., Singularities in homogeneous world models, 19: 39360

HAY, D. R., Field-aided electron-beam zone refining of tungsten, 19: 39111

HAYE, C., Postradiotherapy cranial sarcoma after treatment of retinoblastoma, 19: 38486

HAYES, Bernard, On electrical conductivity detonation products, 19: 40284 (LA-DC-6993)

HAYES, F. Newton, Liquid scintillators. XIII., 19: 38691

HAYES, H. G., Fabrication record of OMRE test elements, 19: 40187 (NAA-SR-Memo-7753)

HAYESS, Erhard, Stationary Ar discharge of high current densities, 19: 39983

HAYON, E., Radiolysis of D_2O in pD range 0 to 14, 19: 38710

HAZARD, J. Beach, Autoradiography of the thyroid, 19: 38533

HAZELTON, L. D., Nuclear materials management control system for U reactor fuel element fabrication, 19: 39130 (RFP-507)

HEAD, A. E., Spark chamber photograph analysis using LUCIOLE, 19: 38976 (CERN-65-11(p.57-69))

HEAD, Charles E., Electron capture into excited helium levels by fast He^+, impact on He, N_2, and O_2, 19: 39407

HEAD, D., Nitrous oxide as a scavenger in the radiolysis of water, 19: 38720

HEBBORN, P., Dental lesions in rat induced by radiomimetic agents, 19: 38325

HECHT, A. M., Nuclear magnetic resonance equipment for very low temperature, 19: 39011

HECKROTTE, Warren, Electron injection and E-layer build-up in Astron, 19: 39973 (UCRL-14131)

HEDDLE, John A., Lack of interaction of x-ray- and neutron-induced chromosome breaks in barley, 19: 38399

HEDIN, Lars, New method for calculating the one-particle Green's function with application to the electron-gas problem, 19: 39658

HEIKKINEN, D. W., Variation in yield of the isotopic spin forbidden reaction $^{12}C(^6Li,\alpha_1)^{14}N$, 19: 39853

HEISER, C., Three-particle isomeric state in ^{109}In, 19: 39861

HELMICK, Herbert H., Pulsed neutron analysis in the Los Alamos Coupled Reactor Experiment, 19: 40240 (LA-3263)

HEMMENDINGER, A., Cross-section measurements made with neutrons from a nuclear detonation, 19: 39889

HEMSTREET, R. A., Cryosorption pumping of hydrogen and helium at 20°K, 19: 39693

HENDERSON, Douglas, Isotopic effects in liquid hydrogen, 19: 38639

HENINS, Ivars, Fast plasma from a coaxial gun, 19: 39956 (LA-DC-7043)
HENKE, R. P., Range-momentum relation for heavy recoil ions in emulsion, 19: 39883
HENRY, Claude, Relativistic theory of angular correlations in successive two-body decays of unstable particles, 19: 39492
HENRY, D. L., Effect of neutron irradiation on the liquid Na dilation of graphite, 19: 39235 (NAA-SR-11309)
HEON, M., Gamma-encephalography with ^{203}Hg-neohydrin, 19: 38510
HEPP, Klaus, Proof of LSZ asymptotic condition, 19: 39629 (CONF-796(Paper 30))
HERBER, R. H., Intermolecular bonding effects in ^{119m}Sn Moessbauer spectroscopy, 19: 38577 (CONF-650425-3)
HERBER, R. H., Moessbauer parameters for metal-organic (Fe,Sn) compounds, 19: 38576 (CONF-650425-2)
HERCIK, F., Sensitization of capacity of Escherichia coli B for phage T3 to x-rays by iodoacetamide, 19: 38455
HERDADE, Silvio B., Magnetic scattering of neutrons in ferromagnetic samples, 19: 40075 (IEA-84)
HERICKHOFF, R. J., Angular distribution and thickness dependence of transition radiation from thin aluminum foils, 19: 40099
HERLACH, F., Megagauss fields generated in explosive-driven flux compression devices, 19: 39300
HERNADI, F., Effect of chemical radioprotective substances on damage to DNA of intestinal wall by nitrogen mustard and degranol, 19: 38460
HERNDON, R. C., Form factors of ^{3}H and ^{4}He with repulsive-core potentials, 19: 39868
HERREN, M., Handling high-level α-γ boxes, 19: 38793 (JUL-251-RW)
HERSCOVITZ, V. E., Length scale in quantum electrodynamics without a bare mass, 19: 39652
HERTEL, Peter, Bound states in many- and single-channel calculations, 19: 39600
HERZOG, F., On the combination of the phase contrast process with fluorescence microscopy, 19: 38923 (UCRL-Trans-1228)
HESHUIJSEN, W. F., Steam generator of the NERO Project and the scale model studies, 19: 40250
HESTER, D. L., Hysteresis studies of reactor-irradiated single-crystal Ba titanate, 19: 38705
HEYMANN, G., Reaction ^{40}Ca(α,2α)^{36}Ar, 19: 39902
HIKAWA, Ikuko, Anion-exchange behavior of Sc, rare earths, Th and U in magnesium nitrate solution, 19: 38770
HILL, D. G., Spin of the Y_0^*(1405), 19: 39553
HILLIER, R. R., A search for low-energy γ rays from the quasar 3C286, 19: 39357
HILLS, A. W. D., Study of cation diffusion in UO_2 using α spectrometry, 19: 38681
HILTON, R. M., Effect of Y^{+3} on the reduction of Sm^{+3} in CaF_2, 19: 38595
HIMES, George E., Absorbed radiation dose and excretion of cesium-131 in humans, 19: 38503
HIMES, George E., Cesium-131 uptake and distribution in human heart, 19: 38502
HIMMELL, Lewis Craig, Cross-over signals in atomic hydrogen (thesis), 19: 39371 (TID-22044)
HINDS, S., Thallium-207 states excited in the (t,α) reaction on ^{208}Pb, 19: 39852
HINNOV, E., Measurement of ion concentrations and electron temperature in Ba plasma, 19: 39958 (MATT-327)
HINNOV, E., Observations on a fully ionized barium plasma, 19: 40007
HINRICHS, H. Richard, Incorporation of thymidine into DNA of organs of mice, 19: 38336 (TID-21106)
HINS, A. G., Manufacture of glass-bonded fuels for Doppler coefficient measurement, 19: 39124 (ANL-6995)
HINTZ, Eduard, Influence of small transverse fields and impurities on θ-pinch stability and confinement, 19: 40005
HIRAMOTO, Tatsumi, Nonequilibrium characteristics of the working plasmas for MPD generators, 19: 39438
HIRATA, A. A., Observation of correlations between vector-meson and baryon-resonance decays, 19: 39542
HIROSHIGE, Noboru, Production of weak bosons, 19: 39567
HIROTA, Kozo, Catalytic isotopic isomerization of deuterated toluene-d_1 on platinum black, 19: 38693
HIRSCH, W., Problematics of pH measurement in reactor operation, 19: 40127 (ZFK-RN-17(p.9-23))
HISKES, J. R., Formation of excited hydrogen atoms by charge exchange in hydrogen-like targets, 19: 39398
HJAERNE, L., Penetration and slowing-down of neutrons in reactor shields, 19: 40156 (NP-15161)
HJAERNE, L., Penetration and slowing-down of neutrons in reactor shields, 19: 39751 (AE-185)
HO, James C., Tungsten–platinum alloy for heater wire in calorimetry below 0.1°K, 19: 39743

HOAGLAND, R. G., Small specimens, suitable for irradiation damage studies on reactor structural materials, 19: 38822 (BNWL-SA-2)
HOBART, E. W., Chemical state of C, N, and O in alkali metals, 19: 39157 (CNLM-6337)
HOCH, M., Nonstoichiometry of UO_2–CeO_2: the system UO_2–CeO_2–$CeO_{1.5}$ at 900 to 1200°C, 19: 39222
HOECK, Helmuth, Secretion of γ radioactivity in milk in relation to contamination of feeds in spring 1962, 19: 38858
HOEFT, J., Microwave rotation spectra of GeS, 19: 38663
HOFFMAN, J., Flame plasma seeded with SF_6, 19: 40016
HOFFMANN, J. P., Examination of Zy-clad UO_2 fuel rods, 19: 39234 (GEAP-4597)
HOHMANN, Gerold L., Control of nuclear rocket engines in low power-no flow region, 19: 40252
HOLDEN, H., Tumors of the bladder. III., Radiotherapy, 19: 38504
HOLL, R. J., Criticality of gas core reactors, 19: 40239 (LA-3229, pp 315-43)
HOLLECK, H., Crystal structure of $ThGa_2$ and $RuIn_3$, 19: 39207
HOLMGREN, H. D., Angular correlations for ^{9}Be(^{3}He,α)^{8}Be → 2α reaction, 19: 39916
HOLMGREN, H. D., Reaction ^{9}Be + ^{3}He → 3α, 19: 39898
HOLMGREN, H. D., Reaction ^{10}B + ^{3}He → p + 3α, 19: 39899
HOLMGREN, H. D., Reaction ^{6}Li + ^{3}He → p + 2α, 19: 39900
HOLMGREN, H. D., Spectroscopic studies with the ^{10}B(^{3}He,p2α) reaction, 19: 39917
HOLT, J. Garrett, Intercomparison by mailed dosimeters of high-energy electron beams, 19: 38723
HOLT, J. O., HWR power plant with 275-MW(e) PHWP and a 260-MW(e) BLWP units, 19: 40211
HOLTORFF, J., Late bladder changes caused by radiotherapy of uterine carcinoma, 19: 38531
HOLZMANNOVA, Alice, Sensitization of capacity of Escherichia coli B for phage T3 to x-rays by iodoacetamide, 19: 38455
HONG, G. W., Positron focusing in an accelerating field, 19: 39321
HOPE, C. S., Computer optimization of 4-Mev treatment planning, 19: 38511
HOPKINS, H. W. K., Spin of the Y_0^*(1405), 19: 39553
HORI, Shoichi, On the unification of hadronic and leptonic weak interactions, 19: 39573
HORIKAWA, Masaketsu, Effect of halogenated pyrimidines on radiosensitivity of mouse strain L cells and their radioresistant variant, 19: 38459
HORSKY, J., Energy of the gravitational field, 19: 39656
HORTON, J. C., Mass spectrometric analysis of BF_3, 19: 38541 (K-L-6057)
HORTON, P. A., Minimized fuel cycle cost for simulated pressurized water reactor. I., 19: 40114 (BNWL-104)
HORVAT, Durdo, Effects of γ rays on RNA and protein content of amoeba, 19: 38371
HOSCHOIAN, J. C., The effect of triiodothyroacetic acid on ^{131}I incorporation by the thyroid, 19: 38348
HOSFORD, W. F. Jr., Strength and plasticity of anisotropic metals, 19: 39149 (AD-425880)
HOTT, Charles G., Levels of ^{58}Ni from the reaction ^{58}Ni(p,t)^{56}Ni at 28 Mev, 19: 39819
HOUARD, Jean-Claude, Equations of the Lee model in the V$\theta \neq N\theta\theta$ sector, 19: 39638
HOUGH, P., Status of HPD programs at BNL, 19: 38980 (CERN-65-11 (p.97-113))
HOUGH, P. V. C., Getting results from an HPD system, 19: 38970 (BNL-9236)
HOURANI, Eid, Quasi-elastic (p,α) scattering in C^{12}, 19: 39908
HOUSEAUX, Oscar, Improvements in or relating to thermal exchange, 19: 38818
HOWARD, A. J., Concentration dependence of thermal-diffusion factor for ^{3}He–^{4}He and H_2–D_2, 19: 38633
HOWES, James E. Jr., Prog. rpt. on fission-product reactions with and release from fuel-element claddings, 4–6/65, 19: 39152 (BMI-X-10132)
HOWIE, J. M., Experience with CERN HAZE program, 19: 38982 (CERN-65-11(p.123-37))
HOYLE, F., Origin of cosmic x rays, 19: 39425
HROMADNIK, H., Investigation of the coulomb-nuclear interference in elastic K^-p scattering at low energies, 19: 39530
HUANG, Kerson, Quantized vortex rings in superfluid helium: a phenomenological theory, 19: 39723
HUBBARD, W. M., Magnetic field reduction in an expandable superconducting enclosure, 19: 39742
HUBY, R., Distorted-wave Born approximation for stripping to virtual levels, 19: 39910
HUDGINS, Philip T., Clinically useful calculations of the dose distribution from multiple radiation sources, 19: 38526
HUET, Andre, Pressurized gas heater for steam generating heat exchanger, 19: 40141

HUGELMAN, Rodney D., MHD boundary-layer compatibility condition, 19: 39277
HUGHES, B. Mason, Radiation chemistry of cyclopentane, 19: 38712
HUGHES, Cora Joy, Profiles of Lyman-α scattered by free electrons in the solar corona, 19: 39341
HUGHES, R. H., Electron capture into excited helium levels by fast He^+, N_2, and O_2, 19: 39407
HULET, E. Kenneth, Spark spectrum of berkelium, 19: 39384
HULL, G. W. Jr., Superconductivity of Nb_3Ge, 19: 39725
HULM, J. K., Critical supercurrents in niobium carbonitrides, 19: 39688
HULSTON, J. R., Variations in ^{33}S, ^{34}S, and ^{36}S contents of meteorites and their relation to chemical and nuclear effects, 19: 38847
HULTEN, W. C., Ionizing particle radiations effects and simulation consideration, 19: 39059
HUME, David M., Prolongation of renal homograft function by local graft radiation, 19: 38425
HUNT, A. L., Cooperative effects in tenuous energetic plasma contained by magnetic mirror field, 19: 40017
HUNTER II, M. W., Space transportation, 19: 40222 (LA-3229, pp 10-47)
HUO, Ma, Decay of ^{161}Ho, 19: 39930
HURAULT, J. P., Proximity effects under magnetic fields. II., 19: 39700
HURRELL, J. P., E.P.R. and ENDOR of Th^{4+} in thoria, 19: 38655
HURST, G. S., Penetration of radiation from nuclear weapons: applicability to Hiroshima and Nagasaki survey, 19: 38892
HURT III, S. S., Prog. rpt. on ORR operations 1–3/65, 19: 40259 (ORNL-TM-1181)
HURWITZ, H., Jr., Motion of θ-pinch plasma in asymmetric fields, 19: 40010
HUSSEY, R. G., Effect of a cylindrical boundary on the added mass of two cylinders in liquid helium, 19: 39697
HUYNEN, M. H. M., A simple and inexpensive sample changer for windowless gas-flow counters, 19: 39037
HYDE, James S., ENDOR of free radicals in solution, 19: 38638
HYDE, K. R., The preparation and some properties of U carbonitrides, 19: 39089 (AERE-M-1389)

I

IANNUZZI, M., Microwave study of thermally ionized plasmas, 19: 39980
ICHIKAWA, Yoshiko, Fallout radioactivity in diet and excreta. The levels at Tokai District, Japan in 1962 to 1963, 19: 38894
INOCHI, H., The decay of ^{180}W, 19: 39801
INRENBERGER, Albin, Metallography of high-melting metals. II., 19: 39214
IKAWA, Katsuichi, Oxidation of U by partially decomposed CO_2, 19: 39121
IKEUYE, D. T., Examination of Zy-clad UO_2 fuel rods, 19: 39234 (GEAP-4597)
IL'ENKO, B. P., Study of a plasma bunch in motion in a toroidal magnetic field, 19: 39963 (NP-15198)
IL'INA, D. S., Measuring exchange capacitance and kinetic characteristics of ionites, 19: 40128 (ZFK-RN-17(p.75-94))
ILIOPOULOS, J., Final-state interactions in $K^+_{\ell 4}$ decay, 19: 39515
ILLES, F., Magnetic characteristic curve for a special permanent-magnet β-spectrograph set of two units, 19: 38998
INDECK, Bernard, Accelerator beam energy monitor, 19: 39330
INGARD, Uno, Longitudinal waves in a weakly ionized gas, 19: 39293
INMAN, Cullen L., Thermodynamic quantities for gas of transverse plasmons, 19: 39339
INOUE, M., Excitation of 2^+, 5^-, and 3^- states of ^{90}Zr by inelastic α-particle scattering, 19: 39844
INUKAI, Kan, Radiation-induced addition reaction of alcohols to 1,2-dichlorotetrafluorocyclobutene and 1,2-dichlorohexafluorocyclopentene, 19: 38708
IOFFE, M. S., Stable plasma production in traps with magnetic mirrors, 19: 40046
IONESCU PALLAS, N. J., The classical motion of particles in arbitrary tensor fields, 19: 39632
IOZEFOVICH, F. D., Complexing of 2-hydroxyethyliminodiacetic acid with rare earth elements, 19: 38671
IPPOLITIVA, E. A., Reaction of various U oxides with sulfuric acid, 19: 38657
IPPOLITOV, E. G., Phase composition of CaF_2–YF_3, SrF_2–YF_3, and BaF_2–YF_3, 19: 38615
IRVING, D., SOURCE, a neutron distribution routine for the 05R Monte Carlo code, 19: 39767 (ORNL-TM-1192)
IRVING, J., Gas laser measurements of electron density of a plasma, 19: 39978
IRVING, J., Time-dependent electron density measurements in a fast theta-pinch discharge, 19: 39979
IRWIN, J. C., High-temperature pulsed light source, 19: 38939
ISAEV, P. S., Difficulties of N/D approach in bootstraps, 19: 39463 (IC/65/62)
ISELER, G. W., Interpretation of stage I recovery after electron irradiation of Cu, 19: 39248
ISETT, D. D., ACCEL: automated circuit card etching layout, 19: 38915 (SC-DC-65-1419)
ISFFE, B. L., Weak interactions of colliding electron beams, 19: 39481 (NP-15248)
ISHIDA, Kenji, Isotope separation by liquid-gas chemical exchange, 19: 39075
ISHIKAWA, Sumio, Chemical reaction by ionizing radiation. IV., 19: 38732
ISHKANOV, B. S., The energy distribution of photoprotons from ^{28}Si, 19: 39938
ISLAMOV, B. I., Reaction $(^3He,\alpha)$ on ^9Be, ^{14}N and ^{16}O, 19: 39941
ISLITZER, Norman F., Aerodynamic effects of large reactor complexes upon atmospheric turbulence and diffusion, 19: 39259 (IDO-12041)
ISONO, Toshiaki, Behavior of organic liquid phase in TBP–kerosene extraction, 19: 38563
ISONO, Toshiaki, Use of Mg–Al alloy for reduction of UO_2Cl_2 and of $FeCl_3$ in aqueous solutions, 19: 38662
ISSEROW, S., Prog. rpt. on W–Re tube fabrication, 7/64–6/65, 19: 39128 (NMI-1267)
ISUPOVA, E. N., Synthesis and properties of La borates, 19: 38611
ITO, Yukio, Current-current interaction and nonleptonic decays of hyperons, 19: 39560
ITZYKSON, C., Symmetry of strong interactions, 19: 39507
IVANOV, L. I., Quantitative analysis of complex γ spectra of radioactive metals and alloys, 19: 38566
IVANOVSKAYA, I. A., Interactions of 9-Bev π^- mesons with Xe nuclei, 19: 39472 (JINR-P-2178)
IVERSEN, James D., Base and surface pressure variation with Mach number on a right circular cone, 19: 40292 (SC-TM-202-56-51)
IVERSON, M. L., Electrolysis of U carbide in fused salt using molten metal cathodes, 19: 38754 (NAA-SR-10737)
IWAMOTO, Junko, Fallout radioactivity in diet and excreta. The levels at Tokai District, Japan in 1962 to 1963, 19: 38894
IWASAKI, Tomiko, Sensitivity of Artemia eggs to γ radiation. I., 19: 38383
IWASAKI, Tomiko, Sensitivity of Artemia eggs to γ radiation. II., 19: 38384
IWASE, Eiichi, Behavior of organic liquid phase in TBP–kerosene extraction, 19: 38563
IWASE, Eiichi, Preparation of uranous salt by intermediate formation of uranyl sulfide, 19: 38659
IWASE, Eiichi, Reaction between U oxides and CCl_4, 19: 38661
IWASE, Eiichi, Use of Mg–Al alloy for reduction of UO_2Cl_2 and of $FeCl_3$ in aqueous solutions, 19: 38662
IWASHIMA, I., Rapid radiochemical determination of ^{131}I in liquid milk, 19: 38560
IWATA, KENZO, Current-current interaction and nonleptonic decays of hyperons, 19: 39560
IZUI, Kazuhiko, Fission fragment damage in semiconductors and ionic crystals, 19: 39245

J

JABLONOWSKI, Edward J., Prog. rpt. on fission-product reactions with and release from fuel-element claddings, 4–6/65, 19: 39152 (BMI-X-10132)
JABLONOWSKI, Edward J., Prog. rpt. on fission-fragment effects in structural materials, 4–6/65, 19: 39229 (BMI-X-10134)
JACKSON, Betty S., Bibliography of atmospheric ozone to 40 Km: its concentration, distribution, methods of detection, and relationship with other meteorological phenomena, 19: 39260 (LA-3328)
JACKSON, D. F., Radiation effects on pressure transducer components. Final report, 19: 39055 (GA-6266)
JACKSON, Daphne F., Problems in analysis of quasi-free scattering, 19: 39906
JACKSON, H. E., New values of neutron separation energies, 19: 39862
JACKSON, J. D., Peripheral production and decay correlations of resonances, 19: 39576
JACKSON, John L., Irradiation-actuated device for measuring the tensile fracture strain of graphite, 19: 39238
JACKSON, W. R., Energy-angular correlations and sequential decay in the $^2H(p,2p)n$ and $^1H(d,2p)n$ reactions, 19: 39924
JACOB, G., Length scale in quantum electrodynamics without a bare mass, 19: 39652
JACOB, M., Symmetry of strong interactions, 19: 39507
JACOBS, G., Color centers in CsBr single crystals irradiated at liquid-helium temperature, 19: 40098
JACOBSEN, T., Annihilation $\bar{p}p \to \bar{K}Kn$, 19: 39534
JAKUBOWSKI, U., Application of electron-microscopic fine-range diffraction for the determination of the rolling texture of Cu, 19: 39175 (ORNL-tr-638)
JAMES, M. F., MLBW—a multi-level Breit-Wigner computer program, 19: 39776 (AEEW-M-517)

JAMES, M. F., TEMPO—a general Doppler broadening program for neutron cross sections, 19: 39777 (AEEW-M-518)
JANES, A. F., A search for low-energy γ rays from the quasar 3C286, 19: 39357
JANES, G. S., Experiments on magnetically produced and confined electron clouds, 19: 40031
JANES, G. S., Production of Bev potential wells, 19: 40032
JANOVEC, V., Magnetic contribution to heat capacity of Nd at low temperatures, 19: 39296
JAROSCH, K., Exposure of population of upper Austria to radiation and its relationship to morbidity statistics, 19: 38495
JARVIS, George A., Cavity reactor, 19: 40154 (LA-3229, pp 344-61)
JASELSKIS, Bruno, Preparation and properties of monoalkali xenates, 19: 38624
JASKOLA, M., Energy spectrum of α particles from the $^{159}Tb(n,\alpha)^{156}Eu$ reaction with 14.2-Mev neutrons, 19: 39780 (INR-596/PL)
JASHY, George R., Nuclear materials management in a recovery facility for unirradiated enriched uranium, 19: 38758 (Y-KA-7)
JATCZAK, Jerzy, Neutrino astrophysics, 19: 39361
JAYARAMAN, A., Solid-liquid and solid-solid transformations in rare-earth metals at high pressures, 19: 40095
JAYARAMAN, K. S., Reaction $^6Li + {}^3He \rightarrow p + 2\alpha$, 19: 39900
JEFFERY, Derek Boyd, Shock-absorbing device for moving bodies in nuclear reactors, 19: 40142
JEFFREY, Alan, Steady MHD flow of incompressible viscous fluid, 19: 39301
JEHLE, Herbert, Foldy-Wouthuysen transformation in covariant spinor formulation, 19: 39630 (CONF-796(Paper 31))
JEITSCHKO, W., The H phases: Ti_2CdC, Ti_2GaC, Ti_2GaN, Ti_2InN, Zr_2InN, and Nb_2GaC, 19: 39208
JENEY, A., Effect of chemical radioprotective substances on damage to DNA of intestinal wall by nitrogen mustard and degranol, 19: 38460
JENKINS, G. M., Role of crystal structure in determining mechanical properties of graphite, 19: 39237
JENKINS, G. M., The stress-strain relationships of polycrystalline graphite under compression up to fracture, 19: 39186
JENKINS, Mansell John, Improvements in C articles, 19: 38684
JENKINS, R. G., Prog. rpt. on W–Re tube fabrication, 7/64–6/65, 19: 39128 (NMI-1267)
JENSEN, R. G., Hydrology of subsurface waste disposal, national reactor testing station, Idaho. Annual Progress Report, 1964, 19: 40269 (IDO-22047-USGS)
JESSEE, R. D., Converters (d-c to d-c) for nuclear-thermionic energy sources, 19: 38835 (N65-27619)
JHINGAN, M. L., Investigation of $^{23}Na(d,\alpha)^{21}Ne$ reaction, 19: 39835
JIMENEZ, Roberto J., Serialograph with spaced carriers for movable X-ray film cassettes, 19: 38955
JNANANANDA, Swami, Absolute photoelectric cross sections of 145-kev γ rays in Ta and Pt, 19: 39377
JOANOU, G. D., Neutron cross sections for ^{238}U, 19: 39764 (GA-6087(Rev.))
JOHANSEN, H. A., Critical supercurrents in niobium carbonitrides, 19: 39688
JOHANSSON, K., Nuclear g factor of the 3.2-Mev 5^- state in the double-closed shell nucleus ^{208}Pb, 19: 39843
JOHNSON, C. E., Hyperfine field of ^{57}Fe in Cu–Mn alloys, 19: 39212
JOHNSON, C. H., Intermediate states as observed by differential scattering of neutrons by doubly closed shell nuclei, 19: 39785 (ORNL-P-1356)
JOHNSON, C. H., Sequential emission in the reaction $^7Li(d,n)2\alpha$, 19: 39915
JOHNSON, C. R., Boron–stainless steel fuel element cladding in Indian Point, 19: 39110
JOHNSON, Ernest W., Vaporization, thermodynamics, and dissociation energy of LaS, 19: 38644
JOHNSON, G., Inelastic scattering of 6.35-Mev deuterons. Limit of excitation of the 3.56-Mev level (T = 1), 19: 39804
JOHNSON, L. C., Measurement of ion concentrations and electron temperature in Ba plasma, 19: 39958 (MATT-327)
JOHNSON, L. C., Observations on a fully ionized barium plasma, 19: 40007
JOHNSON, P. M., Effects on nuclear radiation and various environments on a number of selected plastic, glass-laminate, and ceramo-plastic materials, 19: 39232 (FZK-227)
JOHNSTON, F. J., Radiolysis of monodisperse colloidal sulfur, 19: 38714
JONES, C. K., Critical supercurrents in niobium carbonitrides, 19: 39688
JONES, C. M., Sequential emission in the reaction $^7Li(d,n)2\alpha$, 19: 39915
JONES, W. D., Plasma heating by means of beam plasma interaction, 19: 39969 (ORNL-P-1373)
JONES, Wallace A., Skin changes induced by uv-irradiated linolenic acid extract, 19: 38366
JONON, P., Use of digital computers in French conventional and nuclear power stations, 19: 40203
JORDAN, T. M., Radiation protection for manned orbiting space stations, 19: 40063 (NP-15125)
JORDAN O., Victor, Geology of Cuzco-Anta-Urubamba Area, Peru, 19: 38845 (RME-4584)
JOSEPH, P. M., High-energy photoproduction of ρ^0 mesons, 19: 39549
JOUAULT, Francoise, New stannide of vanadium V_2Sn_3, 19: 39189
JUCKER, C., Mandibular radionecrosis, 19: 38527
JUDD, F., Evidence for new $\pi^+\pi^-$ resonance at 1.67 Bev, 19: 39537
JUKES, J. D., Stability of finite amplitude ion cyclotron waves in plasma, 19: 40022
JULLIEN, P., Early leukemias appearing in young and young adult AkR mice exposed to x rays, 19: 38372
JUNG, Bo, Fixation of carbon-11 in cells of proton-irradiated blood, 19: 38722
JUVELAND, A. C., Fluidized beds, 19: 40225 (LA-3229, pp 83-5)

K

KABIR, P., Symmetry principles in particle physics, 19: 39603
KABLER, M. N., Luminescence from ionized F-aggregate centers in alkali halide crystals, 19: 38648
KACSER, Claude, Apparent, but energy-dependent pseudo-resonances due to rescattering in sequential processes, 19: 39897
KADYK, J. A., Observation of correlations between vector-meson and baryon-resonance decays, 19: 39542
KADYSHEVSKII, V. G., Inhomogeneous group SL(6) with an extended subgroup of translations, 19: 39468 (JINR-P-2123)
KAHANA, S., The free reaction matrix as a residual interaction in finite nuclei, 19: 39815
KAHN, B., Analytical radiochemistry in health physics, 19: 38889
KAKUSHKINA, M. L., Toxic lipids in animals suffering from radiation injuries, 19: 38429
KALITIUK, Ryszard, γ-γ logging of soft radiations, 19: 38867
KALLIO, A., Relation between s-matrices in free scattering, nuclear matter, and finite nuclei, 19: 39871
KALMYKOVA, I. S., Complexing in Sc–diantipyrilmethane–iodide system, 19: 38670
KALMYKOVA, N. N., Complexing of 2-hydroxyethyliminodiacetic acid with rare earth elements, 19: 38671
KALYAZIN, E. P., Reactions of some hydrocarbons with CO_2 under influence of radiation, 19: 38727
KAMKE, D., Reaction $^{11}B(p,\alpha)2\alpha$ below 675 kev, 19: 39919
KAMMERER, O. F., Superconductivity in tungsten films, 19: 39708
KANE, J. V., Theoretical interpretation of reaction $d + p \rightarrow p + p + n$, 19: 39577
KANNAN, V. C., Prismatic loops and climb kinetics in quenched Al–Mg alloy, 19: 39169 (UCRL-16090)
KAO, Yi-hsu, Magnetic field dependence of the surface resistance of superconducting tantalum at 35 Gc/s, 19: 39706
KAPITONOV, I. M., The energy distribution of photoprotons from ^{28}Si, 19: 39938
KAPUSTSIK, E., Possibility of uniting the Lorentz group with the unitary symmetry group, 19: 39491
KAPUSTSIK, Edvard, Electromagnetic properties of elementary particles in the B_2-symmetry model, 19: 39490
KARAEV, Z. Sh., Reactions of $A^{III}_2B^{VI}_3$ La and Ga selenides, 19: 38598
KARAYIANIS, N., Atomic terms for equivalent electrons, 19: 39382
KARLSSON, R. H., Total hemispherical emittance of polished and of oxidized alpha Pu, 19: 39167 (RFP-616)
KAROLYHAZY, Frederick, Gravitation and quantum mechanics of macroscopic objects, 19: 39625 (CONF-796(Paper 12))
KARRER, K., Effect of x irradiations of weak and moderate intensity on tumors of mice, 19: 38387
KASCAK, Albert F., Coaxial flow radiation heat transfer analysis, 19: 40234 (LA-3229, pp 208-21)
KATCOFF, S., Yields of ^{85}Kr in thermal neutron fission of ^{235}U and ^{239}Pu, 19: 39800
KATO, Norio, Effects of x-ray polarization on Pendelloesung fringes, 19: 39287
KATOH, H., Amplification of microwaves by the interaction of an electron beam with Cs plasma, 19: 40036
KATSUMORI, Hiroshi, Electromagnetic properties of resonant states, 19: 39563
KATSUMORI, Hiroshi, Possible assignment of lepton quantum numbers and empirical lepton mass formula, 19: 39562
KAUFFMAN, H. Myron Jr., Prolongation of renal homograft function by local graft radiation, 19: 38425
KAUFFMAN, J. W., Interpretation of stage I recovery after electron irradiation of Cu, 19: 39248
KAURANEN, P., The decay of ^{189}W, 19: 39801
KAURANEN, P., The short-lived ^{127}Sn isomer, 19: 39803
KAW, Predhiman Krishan, Third harmonic of current density in a plasma,

19: 40011
KAWAKAMI, Koichi, Atomic industry notes, 19: 39064
KAWARASAKI, Yuki, Low-energy γ-ray spectra following resonance neutron captures. Measurement by an NaI scintillation spectrometer, 19: 39781 (JAERI-1073)
KAY, Irvin W., Electromagnetic theory and geometrical optics, 19: 39310
KAYE, Geoffrey, Excited states of ^{52}Cr, 19: 39826
KAZAKOV, G. A., Rock age of the Vindhyan system (India) according to glauconites, 19: 38853
KAZARINOV, Yu. M., Phase-shift analysis of nucleon-nucleon scattering at 400 Mev, 19: 39469 (JINR-P-2170)
KEALY, Wellesley Asho, Nuclear fuel element, 19: 40138
KEARNY, Cresson H., Mechanized durability tests of six-foot Punkah-pump, 19: 38832 (ORNL-TM-1155)
KEATING, D. T., New source of small-angle x-ray scattering, 19: 39230 (BNL-9332)
KEDDY, E. S., Status report on theory and experiments on heat pipes at Los Alamos, 19: 38780 (LA-DC-7206)
KEENE, J. P., Pulse radiolysis of aqueous solutions of some inorganic compounds, 19: 38728
KEGEL, Wolhelm H., Light mixing and geseration of second harmonic in plasma in an external magnetic field, 19: 40050
KELLER, F. J., Preferential thermal reorientation of V_K centers in KI, 19: 40103
KELLER, G., Problems of radiation protection associated with gynecological application of brachycurie therapy, 19: 38514
KELLER, Hans Ludwig, Dose distribution and dose determination in pendulum irradiation (200 kv at 17 Mev), 19: 38534
KELLY, K. J., Chemical state of C, N, and O in alkali metals, 19: 39157 (CNLM-6337)
KELLY, Robert E., Sectorial parallel plate transmission line, 19: 40298 (UCRL-14141)
KEMBER, N. F., In vivo cell survival system based on recovery of rat growth cartilage from radiation injury, 19: 38407
KEMME, J. E., Status report on theory and experiments on heat pipes at Los Alamos, 19: 38780 (LA-DC-7206)
KEMP, E. L., Quick closing light shutter, 19: 38942
KEMPLAY, J. R., Automatic γ scintillation counter, 19: 39003
KEMPTER, C. P., Thermal expansion of TaC to 3020°C, 19: 39201
KEMPTER, Charles P., Thermal expansion of UC–ZrC solid solution, 19: 39200
KENDALL, K., Influence of AET and hypoxia on recovery from radiation injury in mice, 19: 38450 (USNRDL-TR-851)
KENDALL, P. C., Influence of horizontal air motions on F2-region ionization, 19: 39668
KENNEDY, A. J., Prog. rpt. on Cs-vapor filled thermionic converters, annual, 11/63–10/64, 19: 39431 (AD-608554)
KENNEDY, James J., Progress in the development of refractory metals for use in nuclear rocket nozzles, 19: 40254
KERESE, Istvan, Meeting of work group for application of radioisotopes, 19: 39063
KERLER, Werner, Problems in unstable quantum mechanical systems, 19: 39304
KERMOSHCHUK, J. O., Determination of oxygen in sodium metal, 19: 38539 (APDA-168)
KERNER, Edward H., Can the position variable be a canonical coordinate in a relativistic many-particle theory?, 19: 39645
KERREBROCK, Jack L., MHD generators for space power, 19: 39442
KERST, Donald W., Fusion research apparatus, 19: 40060
KESZTHELYI, L., Moessbauer effect study of phase transition in ice, 19: 39715
KESZTHELYI, L., The g factors of excited states in ^{192}Os, ^{192}Pt, and ^{194}Pt, 19: 39833
KHAN, Ashfaq A., Effective interatomic potentials for liquid helium above and below the λ point, 19: 39731
KHAN, J. M., Studies in x-ray production by proton bombardment of C, Mg, Al, Nd, Sm, Gd, Tb, Dy, and Ho, 19: 39881
KHARCHENKO, V. F., Neutron-deuteron doublet scattering length and three-nucleon bound state with tensor forces, 19: 39585
KHIZHNYAK, N. A., Longitudinal oscillations in a multi-velocity plasma beam, 19: 39964
KHOVOSTOV, Kh. Kh., Methods for surveying air contamination by radioactive aerosols, 19: 38903
KIDD, D. E., Gas laser measurements of electron density of a plasma, 19: 39978
KIDD, D. E., Time-dependent electron density measurements in a fast theta-pinch discharge, 19: 39979
KIEFER, H., Large-area counter for exclusive measurement of soft quanta radiation emitted by a sample, 19: 39046
KIEFER, R. J., Regenerative H_2O–CO_2 trap and liquid N cooled No. 2 charcoal trap assembly, 19: 40120 (GAMD-5434)
KIENLE, P., Recoilless γ emission in ^{156}Gd and ^{158}Gd following neutron capture reactions, 19: 39863
KILLEEN, John, Electron injection and E-layer build-up in Astron, 19: 39973 (UCRL-14131)
KILMISTER, C. W., Collapsible stars, 19: 39359
KIM, C. C., Reaction D(p,2p)n at 31 Mev, 19: 39925
KIM, Y. E., Theoretical interpretation of reaction d + p → p + p + n, 19: 39577
KIM, Y. S., NURSE-1—a nuclear rocket safety evaluation code for the control data 3600, 19: 40248 (NUS-180)
KIMOURA, Kazo, Electric arc reduction process for making raw metallic Nb, 19: 39133
KIMURA, Toshiei, New theory of gravitation of Hoyle and Narlikar, 19: 39662
KING, C. Judson, Axial dispersion in liquid flow through packed beds, 19: 38812 (UCRL-11951)
KING, K. M., Convenient cadmium-metal standard for checking neutron, soil moisture probes, 19: 38869
KING, R. B., Solar abundances of gallium, silver, and indium, 19: 39345
KINK, R. A., The concentration dependence of Kl-Tl photoluminescence and radioluminescence yield, 19: 38735
KIOTAN, I., Decomposition of H_2O in reactor, 19: 38698 (ZFK-RN-17 (p.199-207))
KIRICHINSKII, B. R., Irradiation of animals with fast neutrons and measurements of tissue doses in a nuclear reactor, 19: 38439
KIRICHINSKII, B. R., RBE of fast neutrons, 19: 38438
KIRICHINSKII, B. R., The effect of neutron radiation on some physical and chemical properties of the blood, 19: 38440
KIRRILIN, V. A., Niobium enthalpy between 600 and 2600°K, 19: 39217
KIRSCH, L., Antiproton annihilation in H at rest. I., 19: 39462 (CU-1932-239)
KIRST, T. R., Emission of potassium ions from molybdenum at elevated temperatures, 19: 39197
KIRTON, J., Paramagnetic resonance of Ho(III) ions in Ca tungstate, 19: 38650
KIRZ, Janos, Data on particles and resonant states, 19: 39485 (UCRL-8030(Pt.I)(Mar.'65, ed.))
KISELEV, V. S., Phase-shift analysis of nucleon-nucleon scattering at 400 Mev, 19: 39469 (JINR-P-2170)
KISTNER, G., Exponential experiment in natural U, 19: 39763 (EUR-2413.e)
KLAN, V., Cerebral circulography with radioisotopes, 19: 38489
KLEE, A., Cerebral blood flow determined by saturation and desaturation with Kr-85, 19: 38491
KLEIBEL, F., Indications and effects of additional antibiotic treatment in radiotherapy, 19: 38512
KLEIN, M. W., High-frequency velocity space instabilities, 19: 40019
KLEIN, Siegfried, Apparent variations of the electron temperature in a flame, 19: 39282
KLEINPOPPEN, H., Narrow resonance in scattering of electrons by atomic hydrogen, 19: 39393
KLEMM, W., Europium as an alkaline earth metal, 19: 39177
KLEMPARSKAYA, N. N., Infection and immunity in irradiated animals, 19: 38434
KLEPFER, H. H., Program recommendations—reactor pipe rupture study, 19: 38824 (GEAP-4474)
KLEPIKOV, N. P., Planning of experiments discriminating between possible curves, 19: 39088
KLEPPA, O. J., Thermodynamics of fused salts and fused salt mixtures, 19: 38683
KLINE, Morris, Electromagnetic theory and geometrical optics, 19: 39310
KLOEPPEL, P., Discharge chamber sensitive time, 19: 39028
KLOSS, H. G., Temperature profile of fading low-current arc, 19: 39986
KLUCHERT, W., Individual protection against radioactivity in times of war, 19: 38475
KLYUCHAREV, A. P., Isomers ^{159m}Gd and ^{117m}Sb, 19: 39929
KNAPP, D. E., The transparent partition gaseous core reactor concept, 19: 40229 (LA-3229, pp 116-36)
KNAPP, R. W., Prog. rpt. on BONUS core development, 12/64–2/65, 19: 39156 (CEND-532)
KNEISSEL, U., Measurement of the circular polarization of the 498-kev γ quanta of ^{103}Rh, 19: 39945
KNIGHT, William John, Nuclear reactor fuelling apparatus, 19: 40144
KNOCH, W., Extraction process in nuclear technology, 19: 38761 (CEA-tr-A-1809)
KNOEPFEL, H., Megagauss fields generated in explosive-driven flux compression devices, 19: 39300
KNOERNSCHILD, Eugen, Problems of energy conversion by ion convection, 19: 39439
KNOP, C. M., Further comments on "the transient phenomena in an isotropic plasma without collision loss," 19: 40035

KNORR, Georg, Equilibrium of toroidal plasma with finite resistivity and inertia, 19: 40003

KNOWLTON, James Albert Jr., Device for the irradiation of an object with charged particle beams, 19: 38831

KNOX, George, Epidemiology of childhood leukaemia in Northumberland and Durham, 19: 38326

KNYAZEVA, E. M., Zirconium reactions with complexing agents, 19: 38667

KOBA, Z., Production of nucleon isobars in high-energy nucleon-nucleon collisions, 19: 39508

KOBAYASHI, Hisanobu, Counting efficiency and directional effects of shielded long counters, 19: 39034

KOBAYASHI, Ichiro, Reaction between U oxides and CCl_4, 19: 38661

KOBAYASHI, Ichiro, Thermal decomposition and air-oxidation of some U compounds, 19: 38660

KOBAYASHI, Ichiro, Use of Mg–Al alloy for reduction of UO_2Cl_2 and of $FeCl_3$ in aqueous solutions, 19: 38662

KOBORI, Itaru, The resonant scattering of lattice waves by an extended plane defect, 19: 40109

KOBZAREV, I. Yu., Strange-current vector constants in second approximation with respect to moderately strong interaction, 19: 39588

KOCH, J., Determination of spin of 2426-kev level in ^{82}Kr, 19: 39944

KOCHER, Leo F., Film badge system and method of using, 19: 39052

KOCK, H., Europium as an alkaline earth metal, 19: 39177

KODAMA, Masahiro, Cosmic-ray-neutron monitor for antarctic observations, 19: 39035

KOENIG, V., Neutron-induced nuclear reaction in Br and Rb in the energy range of 13 to 17 Mev, 19: 39823

KOHLMANN, L., New α-decay barrier penetrabilities with IGO potential, 19: 39789

KOHN, Harold W., Gamma-radiation-induced exchange of D with silica surfaces, 19: 38626

KOKUBE, Toshiro, Zirconium compounds and their uses, 19: 38647

KOLBANOVSKII, Yu. A., Hydrogen adsorption on Al_2O_3 during irradiation, 19: 38717

KOLOMINA, S. M., Influence of ionizing radiation on antitumoral effects of Krutnin antibiotic, 19: 38428

KOLOUCH, R. J., Ultrasonic attenuation in copper, 19: 39249

KOMAI, L. G., Fluorescence conversion efficiency of neodymium glass, 19: 40090

KOMAREK, E. E., Structure and electrical properties of vacuum-deposited CdS thin films, 19: 38585 (SC-TM-64-1677)

KOMEL'KOV, V. S., Pulsed plasma injectors, 19: 39955 (IAE-663)

KONDO, M., Levels of ^{58}Ni from the reaction $^{58}Ni(p,t)^{56}Ni$ at 28 Mev, 19: 39819

KONDO, Teruo, Effect of halogenated pyrimidines on radiosensitivity of mouse strain L cells and their radioresistant variant, 19: 38459

KONICEK, C. F., Manufacture of glass-bonded fuels for Doppler coefficient measurement, 19: 39124 (ANL-6995)

KONIN, A. D., Atomic capture of μ^- in chemical compounds, 19: 39366 (JINR-P-2185)

KONONENKO, V. I., Determination of spatial distribution of plasma density, 19: 39965 (NP-15203)

KONSTANTINOV, E., High pressure Cs thermionic converter with W cathode, 19: 39436

KOPALEISHVILI, T. I., Absorption of γ quanta and stopped π^- mesons by nuclei with two-nucleon emission and the structure of light nuclei, 19: 39932

KOPCHINSKI, Norbert L. Jr., Nuclear reactor core arrangement, 19: 40146

KOPECKY, V., Two-stream instability of radial inhomogeneous electron beams, 19: 40030

KOPROWSKI, E. F., Radiation protection for manned orbiting space stations, 19: 40063 (NP-15125)

KORCHEVOY, Yu. P., A study of the properties of a thermionic diode placed in an autonomous discharge plasma, 19: 39435 (JPRS-31048)

KORENEV, Yu. M., Research on the system $LiF–ZrF_4$, 19: 38610

KORNILOVA, E. E., Lanthanum germanates, 19: 38612

KOROLEVA, L. N., Synthesis of divalent rare earth silicates, 19: 38621

KORYUKOV, V. N., Radiation effects on the disintegration rate of aluminate solutions, 19: 38738

KOSMATA, H. R., Application of NPR technology to the national nuclear program, 19: 40191 (RL-SA-42)

KOSMATA, H. R., Applications of NPR technology to the national nuclear program, 19: 40219 (RL-SA-21)

KOSSLER, W., Reaction $^{40}Ca(\alpha,2\alpha)^{36}Ar$, 19: 39902

KOSTYRKO, A., Ion-exchange filter for EWA reactor, 19: 38760 (ZFK-RN-17(p. 127-38))

KOTADIA, K. M., Variations in critical frequency of the F2-layer of the ionosphere associated with geomagnetic storms at equatorial stations, 19: 39669

KOTLYAREVSKII, D. M., Investigation of the energy spectra and angular correlations of particles in $K^+_{\pi 2}\to\pi^+ + e^+ + \nu$ decay, 19: 39586

KOULUMIES, Marja, Effect of x irradiation of laryngeal cancer on function of thyroid, 19: 38484

KOULUMIES, Rolf, Effect of x irradiation of laryngeal cancer on function of thyroid, 19: 38484

KOVACS, G., Radiation-induced solid-state polymerization. I., 19: 38699

KOVACS, P., Effect of chemical radioprotective substances on damage to DNA of intestinal wall by nitrogen mustard and degranol, 19: 38460

KOVALENKO, S. I., Determination of specific conductance of refractory materials in vacuum, 19: 38922 (AAEC/Trans-18)

KOVALSKI, V. V., Biogenic migration of U in the lake Issyk-Kul, 19: 38855

KOVARIK, V. J., External beam extraction rate for the Cosmotron, 19: 39324

KOVBA, L. M., Reaction of various U oxides with sulfuric acid, 19: 38657

KOWALSKI, K. L., Some properties of the overlap function, 19: 39520

KOYANAGI, Taku, Determination of Sr in bone with ion exchange separation-flame photometric method, 19: 38345

KOZARZEWSKI, B., Asymptotic properties of electromagnetic and gravitational fields, 19: 39636

KRAEMER, R. W., Spin of the $Y_1^*(1405)$, 19: 39553

KRAETZIG, E., Optical absorption of Cu centers in alkali halides, 19: 40107

KRAICHNAN, Robert H., Inertial-range spectrum of hydromagnetic turbulence, 19: 39292

KRALL, Nicholas A., Universal instability in complex field geometries, 19: 40018

KRAMER, Peter, Angular momenta and Pauli principle in nuclear reactions $a + A \to C^* \to b_1 + b_2 + b_3$, 19: 39896

KRAUS, Pierre, Apparent variations of the electron temperature in a flame, 19: 39282

KRAUSE, Marguerite O., Incorporation of ^{14}C-labeled precursors into the DNA, RNA, and proteins of L-cell nuclei, 19: 38339

KRAUSHAAR, J. J., Mass difference $^{40}Sc–^{40}Ca$ and the ^{40}Sc ground state spin, 19: 39850

KRAUTWEDEL, Ludwig, Investigation of an irradiated FR2-fuel element, 19: 39253

KRAYEVSKII, N. A., Pathological anatomy of radiation damage, 19: 38436

KREMENSKAYA, I. N., Complex formation of Th with 8-hydroxyquinaldozine and caproic acid, 19: 38567

KRESTNIKOV, Yu. S., Decay $f^0 \to \pi^0 + \pi^0$, 19: 39480 (NP-15247)

KRISCHER, W., CERN version of FILTER, 19: 38981 (CERN-65-11(p.115-21))

KRISHNAMURTHI, T. N., Maximum permissible concentrations of fission product mixtures in air and water for occupational exposures, 19: 38872 (AEET/HP/TH-15)

KRONMUELLER, H., Recovery of Ni above room temperature, 19: 39251

KROPIN, A. A., Investigation of the ion motion in the central region of the fixed-field alternating-gradient cyclotron, 19: 39316 (JINR-P-2199)

KROUSE, H. R., Application of digital recording to simultaneous collection in mass spectrometry, 19: 39023

KRUG, J., Reaction $^{11}B(p,\alpha)2\alpha$ below 675 kev, 19: 39919

KRUGER, P. Gerald, Superconducting pseudo-Helmholtz coil, 19: 38933

KRUPKE, William F., Optical-absorption intensities of rare-earth ions in crystals, 19: 38652

KRUSE, F. H., Alkali fluoride complexes of Pa(IV), 19: 38625

KRUSKAL, M. D., Multiple-bounce theory for expansion and retardation of cold-plasma explosion bubble, 19: 39344

KRYLOV, E. I., Orthoniobates of yttrium sub-group elements, 19: 38617

KRYSMANSKI, K. H., Thermal equilibrium in low-current arcs. I., 19: 39976

KRYSMANSKI, K. H., Thermal equilibrium in low-current arcs. II., 19: 39977

KU, Teh-Lung, An evaluation of the $^{234}U/^{238}U$ method as a tool for dating pelagic sediments, 19: 38866

KUANG, Hao-hwei, Angular distribution of interactions of high-energy cosmic-ray particles with paraffin, 19: 39428

KUBALEK, Jiri, Changers for radioactive samples for automatic measurement, 19: 39013

KUBOTA, Hisashi, Problems in disposal of radioactive liquid wastes in salt, 19: 40272

KUCHOWICZ, B., Bibliography on nuclear astrophysics. IV., 19: 39331 (NEIC-RR-11)

KUDO, Shoko, Variation of cosmic-ray intensity observed on December 23, 1957, 19: 39426

KUENDIG, Walter, Mean-square displacement measurements of ^{57}Fe in Zn, 19: 40097

KUHN, E., Problems of radiation protection associated with gynecological application of brachycurie therapy, 19: 38514

KUHNS, James G., Skin changes induced by uv-irradiated linolenic acid extract, 19: 38366

KULAKOWSKI, A., Surgical management of postradiation ulcerations and

scars of the skin, 19: 38513
KULIKOVA, A. A., Lanthanum silicides and their crystal structure, 19: 38613
KULSRUD, R. M., Multi-bounce theory for expansion and retardation of cold-plasma explosion bubble, 19: 39344
KUMABE, I., Excitation of 2^+, 5^-, and 3^- states of ^{90}Zr by inelastic α-particle scattering, 19: 39844
KUMAGAI, Y., Radiation effects on fate of reticulocytes in peripheral blood in rats. I., 19: 38414
KUMAR, Sushil, Photodynamic action and post-irradiation modifying effects of methylene blue and acridine orange in barley and Vicia faba, 19: 38462
KUNDEL, Harold L., Effect of irradiation on ferrokinetics of cross-circulated dogs, 19: 38382
KUNZ, P. D., Mass difference ^{40}Sc–^{40}Ca and the ^{40}Sc ground state spin, 19: 39850
KUO, T. T. S., Effective tensor interaction in nuclei, 19: 39872
KURBATOVA, L. I., Functional condition of G-I tract before and after I-131 treatment, 19: 38529
KURCZNE CSIKY, I., Radioactive contamination of atmospheric precipitation of Budapest with special regard to radioactive strontium, 19: 38852
KURIYAMA, Hideo, Effects of x-ray polarization on Pendelloesung fringes, 19: 39287
KURODA, Rokuro, Anion-exchange behavior of Sc, rare earths, Th and U in magnesium nitrate solution, 19: 38770
KURSHAKOV, N. A., Signs, symposium and treatment of radiation sickness, 19: 38471
KUSCER, Ivan, Discrete relaxation times in neutron thermalization, 19: 39773
KUSENBERGER, Felix N., Nondestructive evaluation of metal fatigue, 19: 39151 (AFOSR-65-0981)
KUZMIAK, Mikulas, Flow detector for α-particles and fission fragments of nuclei, 19: 39012
KUZ'MICHEVA, E. U., Reaction of various U oxides with sulfuric acid, 19: 38657
KUZNETSOV, E. P., Data on p,p reactions with Q = 148 Mev, 19: 39579 (NP-15216)
KUZNETSOV, E. V., Data on p,p reactions with Q = 148 Mev, 19: 39479 (NP-15216)
KUZNETSOV, S. I., Radiation effects on the disintegration rate of aluminate solutions, 19: 38738
KUZNETSOV, V. V., Decay of ^{161}Ho, 19: 39930
KUZNETSOVA, G. P., Heavy lanthanide formates, 19: 38669
KVICALA, V., Cerebral circulography with radioisotopes, 19: 38489
KYKER, G. C. Jr., Possible doorway state in ^{209}Pb and ^{208}Pb, 19: 39847

L

LACHER, J. R., High-temperature isothermal calorimeter, 19: 38675
LACOMBE, Paul, Relation between modifications observed in zirconia during electrotransport tests and during oxidation of Zr, 19: 38604
LADET, J., Utilization of rapsodie reactor for measurement of Doppler effect, 19: 40150 (CEA-R-2565)
LADNER, H.-A., Influencing radiation effects in man and animals, 19: 38461
LADU, M., Ionization chambers filled with dielectric liquids for dosimetric measurements, 19: 39030
LADYGIN, B. Ya., Gamma-radiolysis of methanol, 19: 38716
LA FAY, F., A machine for automatic measurement, by scintillation probing, of liquid or powdered radioactive samples, 19: 39020
LAIHO, K., Strontium-90 content of human bones in Finland, 1960-1962, 19: 38850
LAKAJECEK, Milos, The influence of the discrimination and dead times on the parameters of a coincidence scintillation detector of low-energy β radiation, 19: 39014
LAKSHMINARAYANA, V., Absolute photoelectric cross sections of 145-kev γ rays in Ta and Pt, 19: 39377
LALIT, B. Y., Fission products data and its application in studying fallout from nuclear weapon tests, 19: 39774 (AEET-209)
LAM, D. J., Nuclear-spin-lattice relaxation of ^{51}V and ^{99}Tc in V–Tc alloys, 19: 39403
LAMERS, Kenneth W., Ultracentrifuge photoelectric scanner, multiple cell, 19: 38921 (UCRL-11623)
LAMERTON, Leonard F., Cell cycle of mouse embryonic tissue under continuous γ irradiation, 19: 38405
LANDRIGAN, R. B., Preparation and evaluation of carbon-coated fuel particles, 19: 39126 (CONF-117(p.149-70))
LANDSMAN, D. A., The preparation and some properties of U carbonitrides, 19: 39089 (AERE-M-1389)
LANG, G., Three-particle isomeric state in ^{109}In, 19: 39861
LANG, K., Effects of liposoluble vitamins on Sr-90 metabolism of growing rats. I., 19: 38347
LANGENDORFF, H., Principles and possibilities of biological-chemical radioprotection from action of external radiation, 19: 38452
LANGERHOLC, John, Trace formalism for quantum mechanical expectation values, 19: 39644
LANGEVIN-JOLIOT, H., Inelastic scattering of 6.35-Mev deuterons. Limit of excitation of the 3.56-Mev level (T = 1), 19: 39804
LANGLEY, R. W., Radiation protection for manned orbiting space stations, 19: 40063 (NP-15125)
LANZEROTTI, L. J., High-energy photoproduction of ρ^0 mesons, 19: 39549
LAPIDUS, L. I., Polarized proton targets for experiments with high-energy particles, 19: 39497
LARKIN, A. I., Disappearance of nuclear pairing correlations as influenced by rotation, 19: 39858
LARSSON, Boerje, Fixation of carbon-11 in cells of proton-irradiated blood, 19: 38722
LASHINSKII, Herbert, Reviews of plasma physics, 19: 40054
LASSEN, N. A., Cerebral blood flow determined by saturation and desaturation with Kr-85, 19: 38491
LATORRE, C. O., Determination of Nb, Ta, and U in niobiotantalates by x-ray-fluorescence spectrometry, 19: 38549
LATS'KO, E. M., Study of a plasma bunch in motion in a toroidal magnetic field, 19: 39963 (NP-15198)
LATTA, R. E., Preparation and properties of particulate oxide fuels, 19: 39094 (CONF-117(p.11-19))
LAUGHLIN, John S., Intercomparison by mailed dosimeters of high-energy electron beams, 19: 38723
LAULICHT, I., Isotope effects on vibrational transition probabilities. III., 19: 38632
LAURENSON, L., Techniques for measuring organic content of vacuum atmospheres, 19: 38564
LAVERICK, C., 27.6 cm internal diameter superconducting magnet, 19: 39741
LAVROVA, O. Yu., Complexing of 2-hydroxyethyliminodiacetic acid with rare earth elements, 19: 38671
LAW, J., The hyperfragment $^7He_\Lambda$, 19: 39834
LAWRENCE, Arthur, Improvements in water tube steam generators, 19: 38815
LAWRENCE, Arthur, Improvements in water tube steam generators, 19: 38816
LAWRENCE, Arthur, Improvements in water tube steam generators, 19: 38817
LAWRENCE, G. M., Solar abundances of gallium, silver, and indium, 19: 39345
LAWRENCE, Jackson, Series connection and spacing techniques for thermionic converters, 19: 39445
LAWRENCE, Walter, Jr., Regional oxygenation and therapeutic response to irradiation, 19: 38374
LAWRENSON, P. J., Analysis and computation of electric and magnetic field problems, 19: 39311
LAWSON, A. W., Ferromagnetic and paramagnetic resonance in EuS, 19: 38649
LAWSON, R. D., Measurement of $d_{3/2}$ core excitation in ^{45}Ca from β decay, 19: 39851
LAWTON, Elliott J., Method and system for electron irradiation of materials, 19: 38954
LAZAR, N. H., Energetic neutral injection into an electron-cyclotron plasma, 19: 39970 (ORNL-P-1374)
LAZAREV, A. N., Infared spectra and structure of silicates with divalent rare earth cations, 19: 38622
LEACH, J. S. Ll., Prog. rpt. on metallic systems, annual, 1964, 19: 39168 (TID-22015)
LEADABRAND, Ray L., Comparison of radar auroral reflection data with acoustic wave theory, 19: 39678
LEARY, J. A., Practical application of thermodynamics to Pu process reactions at high temperature, 19: 38752 (LA-DC-6947)
LEARY, J. A., Solubility of selected elements in liquid Pu. IV., 19: 38580 (LA-3303)
LEAVITT, G. E., Ultrafast high-voltage probe, 19: 40038
LEBEDEV, V. N., Distribution of penetrating radiation field over protective zone of 10-Bev synchrophasotron, 19: 39315 (JINR-P-2177)
LEBEDINSKII, A. V., Biological effects [of radiation], 19: 38432
LEBEDINSKII, A. V., Radiation medicine, 19: 38470
LE BEL, Etienne, Radioisotope indicators in hematology, 19: 38356
LE BELLAC, M., Deuteron electrodisintegration and neutron form factors, 19: 39541
LEBEY, Jacques, Nuclear reactor control device, 19: 40143
LE BEYEC, Y., Alpha decay of light Po isotopes, 19: 39838
LEBLOND, Ph., Control of HPD by small computer, 19: 38987 (CERN-65-11(p.207-18))
LEBOWITZ, J. L., Separation of interaction potential into two parts in

treating many-body systems. I., 19: 39284

LEE, H. M., Prolongation of renal homograft function by local graft radiation, 19: 38425

LEE, Thomas L., Vaporization, thermodynamics, and dissociation energy of LaS, 19: 38644

LEFEVRE, George, Jr., Factors modifying mutation frequency patterns detected after irradiation of Drosophila melanogaster males, 19: 38390

LE FOLL, Jean, Improvements in or relating to thermal exchange, 19: 38818

LEFORT, M., Alpha decay of light Po isotopes, 19: 39838

LEFREVRE, Jean, Reprocessing HNO_3 solution containing compounds after extraction of U and Pu irradiated alloys, 19: 38778

LEGGETT, A. J., Finite linewidths and "forbidden" three-phonon interactions, 19: 40096

LEGLER, E., Pulse shape discrimination system for ^{6}LiF (ZnS) scintillation counters, 19: 39025

LE GUYADER, J., Scattering of protons on C-12, 19: 39837

LEHENY, R. F., Combination scattering of microwaves from space-charge waves in a laboratory magnetoplasma, 19: 40033

LEHR, Pierre, Fusion by electron bombardment and its application in metallurgy, 19: 39109

LEIGHTON, R. B., Observations of extremely cool stars, 19: 39347

LEIMDOERFER, M., Penetration and slowing-down of neutrons in reactor shields, 19: 39751 (AE-185)

LEIMDOERIER, M., Penetration and slowing-down of neutrons in reactor shields, 19: 40156 (NP-15161)

LEIPUNSKII, O. I., Use of neutron multipliers and generators in neutron activation analysis, 19: 38565

LEIPUNSKII, O. I., Propagation of γ quanta in matter, 19: 40071

LEISI, H. J., Resonance peak in perturbed γ-γ angular correlation, 19: 39854

LEMBERG, I. Kh., Coulomb excitation of first levels of ^{90}Zr and ^{96}Zr, 19: 39942

LENGYEL, S., Simultaneous measurement of ion diffusion coefficients and ion mobility by use of isotopes, 19: 38665

LENZE, Eberhard, Improvements in light projectors, 19: 38951

LEONARD, Byron E., Nondestructive evaluation of metal fatigue, 19: 39151 (AFOSR-65-0981)

LEONTOVICH, M. A., Reviews of plasma physics, 19: 40054

LEPEKHIN, F. G., Applicability of evaporation theory to emission of multicharged particles by heavy nuclei, 19: 39936

LEPENDINA, O. L., Influence of the structure of hydrocarbons on formation of radicals in low-temperature γ-radiolysis in solid phase, 19: 38724

LEUCHARS, E., Immunologic role of thymus in radiation chimeras, 19: 38451

LEUSCHKE, Guenter, Report on the research on the mechanism of flame propagation in dust clouds, 19: 38827

LEVCHUK, Yu. N., Irradiation of animals with fast neutrons and measurements of tissue doses in a nuclear reactor, 19: 38439

LEVEQUE, A., Parity of the $Y_1^*(1660)$, 19: 39540

LEVET, Jean-Claude, New oxybromide of U(V), 19: 38603

LEVINE, Howard B., Many-electron-theory calculation for the Be atom, 19: 39381

LEVINE, James L., Dependence of superconducting energy gap on transport current by the method of electron tunneling, 19: 39735

LEVINE, M. M., Fuel management in the settled-bed fast reactor, 19: 40178 (BNL-9279)

LEVINGER, J. S., Extrapolation of nucleon electromagnetic form factors, 19: 39458 (CONF-796(Paper 24))

LEVINGER, J. S., Index of refraction and sum rules for helium, 19: 39402

LEVRAT, R., Fixation curve of ^{131}I in thyroid in subjects treated with iodinated contrast media, 19: 38354

LEVY, R. H., Production of Bev potential wells, 19: 40032

LEWELLEN, Steve, Vortices and vortex matrices, 19: 40237 (LA-3229, pp 251-85)

LEWIS, J. E., Microstructural evaluation of superheat cladding materials, 19: 39158 (GEAP-4751)

LEWIS, J. H., Effects of nuclear radiation and various environments on a number of selected plastic, glass-laminate, and ceramo-plastic materials, 19: 39232 (FZK-227)

LEWIS, W. B., Introduction and notes on the Intense Neutron Generator, 19: 39753 (AECL-2177, Introduction)

LEWIS, W. B., Tomorrow's fission reactor and its materials demands, 19: 40180 (DL-56)

LI, Jin-zhao, Studies on effect of ionizing radiation upon mitochondrial structure and function. I., 19: 38424

LI, Ru-hoi, Angular distribution of interactions of high-energy cosmic-ray particles with paraffin, 19: 39428

LI, Shen-guang, Studies on effect of ionizing radiation upon mitochondrial structure and function. I., 19: 38424

LIBOFF, Richard L., Antinormalization properties of correlation functions, 19: 39290

LICHNEROWICZ, Andre, Dirac field, neutrino field, and C.P.T transformations on a space-time curve, 19: 39639

LICHTENBERG, A. J., Synchrotron radiation from self-consistent plasma, 19: 40013

LICHTMAN, David, Emission of potassium ions from molybdenum at elevated temperatures, 19: 39197

LIDIARD, A. B., Mass transfer along a temperature gradient, 19: 38678

LIDMAN, W. G., Extrusion of electrolytic-grade CR Be, 19: 39140

LIEBENBERG, D. H., Chilldown and storage losses of large liquid hydrogen storage dewars, 19: 39686 (LA-DC-7164)

LIEBOWITZ, B., Significance of the Aharonov-Bohm effect, 19: 39654

LIID'YA, G. G., The concentration dependence of KI-Tl photoluminescence and radioluminescence yield, 19: 38735

LILEEV, I. S., Lanthanum germanates, 19: 38612

LILEEV, I. S., Synthesis and properties of La borates, 19: 38611

LILLEY, J. R., CHARGE—space radiation shielding code, 19: 40064 (NP-15132)

LIM, Mahn Jick, Vapor pressure and heat of sublimation of CeF_3, 19: 38592 (UCRL-16150)

LIMENTANI, S., Study of Σ^- capture process in hydrogen, 19: 39510

LIMON, P., Discharge chamber sensitive time, 19: 39028

LIN, Zhi-huan, Studies on effect of ionizing radiation upon mitochondrial structure and function. I., 19: 38424

LINDNER, R., Extraction process in nuclear technology, 19: 38761 (CEA-tr-A-1809)

LINDSAY, S., Induction of neoplasms in rat thyroid glands by x irradiation of a single lobe, 19: 38367

LINDSEY, James S., Search for C-nonconserving decays $\phi \to \rho + \gamma$ and $\omega + \gamma$, 19: 39552

LINDSFORS, R., Strontium-90 content of human bones in Finland, 1960-1962, 19: 38850

LINK, J. K., Solar abundances of gallium, silver, and indium, 19: 39345

LIPSICAS, M., Nuclear spin relaxation in gases and liquids. IV., 19: 39378

LITTLE, M. J., The solubility of sodium in silicon, 19: 39204

LITTLE, Winston W. Jr., Kinetics I—neutron kinetics code in FORTRAN IV, 19: 40148 (BNWL-111)

LITTON, James Jr., Energetic electron beams and cold cathode boundary conditions, 19: 38949

LIU, Yung-yuih, Angular distribution of interactions of high-energy cosmic-ray particles with paraffin, 19: 39428

LIVAGE, Jacques, Amorphous zirconia and non-stoichiometric zirconia, 19: 39190

LLOYD-JACOB, David, The nuclear metals: zirconium and hafnium, 19: 39108

LOBER, M., Observations concerning the unstable behavior of ^{14}C-phenylethylamine carbamate in liquid scintillation mixtures, 19: 38746

LOCHER, P. R., Electron-nuclear double resonance of ^{57}Fe in MgO, 19: 39878

LOCKER, A., Effect of cysteamine and AET on oxygen consumption and body temperature of mice, 19: 38469

LOCOCQ, Pierre, New stannide of vanadium V_2Sn_3, 19: 39189

LOEWDIN, Per-Olov, Studies in perturbation theory. IX., 19: 39650

LOEWENSTEIN, N., An injection probe for rapid placement of radioisotopes in soil, 19: 38870

LOGINOV, V. A., Continuous measurements of specific water resistance in closed circuits, 19: 40262 (ZFK-RN-17(p.25-31))

LOICHOT, R., Electric discharge in hydrogen and deuterium, 19: 39286

LOMBARD, R. J., Magnetic moments of some excited states of Sn and Pb isotopes, 19: 39810

LONG, Everett, Nuclear reactor fuelling apparatus, 19: 40144

LOPEZ ZUMEL, M. C., Contribution to study of radioprotective properties of 2-mercaptobenzothiazole, 19: 38466

LORCH, H. O., Movement of flux lines in type II superconductor, 19: 39704

LORD III, Harry C., Molecular equilibria and condensation in solar nebula and cool stellar atmospheres, 19: 39352

LORENZ, A., Prog. rpt. on physics, 7–9/64, 19: 39271 (UCRL-12204)

LOSCHER, J., Comparison of fallout β activity in precipitation and total β activity in milk in Greifswald District during 1963, 19: 38862

LOUCKS, T. L., Relativistic effects in crystals, 19: 40076 (IS-1172)

LOUGHEED, Ronald, Spark spectrum of berkelium, 19: 39384

LOUISELL, William H., Radiation and noise in quantum electronics, 19: 39664

LOVETT, James E., Nuclear materials management, 19: 39101 (TID-3315)

LOWE, Lester F., Calculated cross sections for atomic displacements produced by electrons in the 1.0 to 3.0-Mev energy range, 19: 39225 (AFCRL-65-286)

LOWRIE, Robert, Dynamic elastic properties of polycrystalline W from 24 to 1800°C, 19: 39198

LOZUPONE, Vito, A form of Boltzmann's transport equation for relativistic particles, 19: 39580
LOZUPONE, Vito, Equivalence of two distribution functions, 19: 39581
LUCAS, E. J., 27.6 cm internal diameter superconducting magnet, 19: 39741
LUCASSON, P., Study of reticular defects in Al, 19: 39246
LUDWIG, E. J., Lithium-drifted position-sensitive detector, 19: 39027
LUEBA, Richard J., Radioactivity measurement of airborne particulate matter, 19: 39050
LUENING, K. G., Genetic effects of supra-lethal x-ray treatment of male mice, 19: 38393
LUK'YANOV, V. F., Zirconium reactions with complexing agents, 19: 38667
LULICHEV, A. N., Determination of specific conductance of refractory materials in vacuum, 19: 38922 (AAEC/Trans-18)
LUNDBERG, Max, Concentration of some elements in enamel of (impacted) human teeth, 19: 38562
LUQUE, Albert, Thermoelectric properties of boron carbide at high temperatures, 19: 38605
LUSH, G. J., Inelastic proton-deuteron scattering at 135 Mev, 19: 39579
LUTZ, H. R., NRE Project—a new critical facility at the EIR for zero reactivity experiments, 19: 40266
LUVISETTO, M. L., FORTRAN diagnostic routine used with CERN HAZE, 19: 38984 (CERN-65-11(p.145-52))
LYNDS, C. R., Lithium in the solar-disk spectrum, 19: 39346
LYNN, J. E., On the slow neutron, gamma-fission reaction, 19: 39864
LYONS, P. A., Diffusion in deuterio-normal hydrocarbon mixtures, 19: 38646
LYUBOSHITS, V. L., Spontaneous transitions by light propagation through anisotropic media, 19: 39266 (JINR-P-2195)
LYUL'KA, V. A., KN scattering at low energies, 19: 39592
LYUTAYA, M. D., Lanthanum germanides, 19: 39195

M

MA, Te Hsiu, Far-red-induced mitotic delay and the apparent increase of x-ray induced chromatid aberrations in Tradescantia microspores, 19: 38416
MAAROOS, A. A., The concentration dependence of KI-Tl photoluminescence and radioluminescence yield, 19: 38735
MAC DONALD, C. G., Nickel-catalysed hydrogen exchange of alkylaromatic hydrocarbons and toluic acid derivatives with deuterium oxide, 19: 38688
MACFARLANE, J. J., α-Dehydro dimer—a major product in irradiated methyl laurate, 19: 38721
MACHARADZE, T. S., Photonuclear reactions with α-particle emission and four-particle correlations in light nuclei, 19: 39934
MAC KENZIE, D. R., Radiation chemistry of cyclic fluorocarbons, 19: 38709
MACKLIN, R. L., On radiative transition in ^{207}Pb and ^{206}Pb following resonance neutron capture on ^{206}Pb and ^{207}Pb, 19: 39783 (ORNL-P-1345)
MADDEN, H. H., Measurements of a thermal-conductivity length dependence in helium II, 19: 39730
MAEDA, Rikio, Seasonal dependence of SC-field in middle and low latitudes, 19: 39673
MAENNICH, Oscar, Method of carrying out chemical-metallurgical processes with use of the heat, which is produced in a nuclear reactor, 19: 38686
MAFRA, Olga Y., Magnetic scattering of neutrons in ferromagnetic samples, 19: 40075 (IEA-84)
MAGALHAES, L. E., Lethals and their suppressors in experimental populations of Drosophila willistoni, 19: 38391
MAGARIBUCHI, S., Studies of radiation injury to the kidney, using radioisotope renograms, 19: 38379
MAGNUSON, G. D., Electron ejection from single crystals due to 1- to 10-kev noble-gas ion bombardment, 19: 39404
MAGNUSON, G. D., Kinetic emission of electrons from monocrystalline targets, 19: 39405
MAGOMEDOV, M. R., Realization of a three-dimensional unitary group by means of spherical functions, 19: 39477 (NP-15202)
MAHADEVAN, P., Electron ejection from single crystals due to 1- to 10-kev noble-gas ion bombardment, 19: 39404
MAHAUX, C., Theory of nuclear reactions. IX. Few-level approximations, 19: 39805
MAHNAU, H., Multi-channel neutron monitoring equipment, 19: 39001
MAKAROV, A. A., On the structure of vector and axial currents in broken U(12) symmetry, 19: 39467 (JINR-E-2194)
MAKAROV, M. M., Applicability of evaporation theory to emission of multicharged particles by heavy nuclei, 19: 39936
MAKEI, T., Serum protein in atomic bomb survivors. II., 19: 38377
MAKI, Kazumi, Magnetic properties of intrinsic London superconductors, 19: 39721
MAKI, Kazumi, Specific heat of mixed state in superconducting alloys, 19: 39716
MAKROV, V. I., Reactions of some hydrocarbons with CO_2 under influence of radiation, 19: 38727
MALENFANT, Richard E., Ground test radiation experience at the Kiwi B-4 tests, 19: 40253
MALLARD, John R., Medical radioisotope scanning, 19: 38516
MALLETT, B. L., The partition of trace amounts of xenon between human blood and brain tissues at 37 deg C, 19: 38353
MALOYAN, A. G., The γ spectrum of ^{152}Eu with half life 9.2 hours, 19: 39928
MAL'TSEV, V. M., Interactions of 9-Bev π^- mesons with Xe nuclei, 19: 39472 (JINR-P-2178)
MALYUTA, Y. M., Mass formulas in Schwinger's model, 19: 39584
MAMASAKHLISOV, V. I., Photonuclear reactions with α-particle emission and four-particle correlations in light nuclei, 19: 39934
MANCUSI, M. D., Reaction 2 ^{6}Li → 3α, 19: 39920
MANDEL'TSVEIG, V. B., Structure of G_2 multiplets, 19: 39594
MANDRITSKAYA, K. V., Analysis of experimental data satisfying distribution of type $x^m dx$, 19: 39087
MANN, A. K., Electron asymmetry in leptonic decay of polarized Λ^0, 19: 39539
MARAIS, P. G., Effect of bulk density and of hydrogen in forms other than free water on calibration curve of the neutron moisture meter, 19: 38948
MARCENKO, Elena, Restoration of irradiated algae after period of darkness, 19: 38410
MARCUS, Ingo, Radiolysis of binary paraffin-olefin solutions. II., 19: 38707
MARCUS, Ira R., The application of pulse sequential circuitry to control devices, 19: 40278 (AD-425879)
MARCUS, Y., Study of interaction between lanthanide and nitrate ions, 19: 38578 (IA-1014)
MARIA, Monique, Differential action of x and uv rays on Macrobiotes areolatus, 19: 38373
MARINZ, W., Multi-channel neutron monitoring equipment, 19: 39001
MARIS, H. J., Inelastic scattering of neutrons by an anharmonic crystal at low temperatures, 19: 40093
MARIS, Th. A. J., Length scale in quantum electrodynamics without a bare mass, 19: 39652
MARIS, Th. A. J., Relaxation effects in angular correlations, 19: 39849
MARIWALLA, K. H., Representation of discrete symmetry operators, 19: 39626 (CONF-796(Paper 22))
MARKELS, Michael Jr., Prog. rpt. on boiling heat transfer, 1–3/65, 19: 38807 (NYO-2404-70)
MARKIN, T. L., Thermodynamic data for Pu oxides, 19: 38682
MARKOV, A. S., Accuracy of calculations of collective oscillation frequency by u-v transformation method, 19: 39782 (JINR-P-2191)
MARNOCH, K., High-temperature oxidation-resistant Hf–Ta alloys, 19: 39123
MARQUES, Roberto O., Preparation of potassium ferrocyanide labeled with ^{59}Fe. Report No. 145, 19: 38743 (NP-15262)
MARR, R. B., Status of digital automatic scanning programs, 19: 38991 (CERN-65-11(p.237-58))
MARSDEN, D. G. H., Simple data display system for fast-scanning mass spectrometer, 19: 39022
MARSH, D. J., Harwell 2000 series linear rateneter/integrator, 19: 39005
MARSHALL, J. H., Moessbauer effect in Cs-133, 19: 39295
MARSHALL, John, Fast plasma from a coaxial gun, 19: 39956 (LA-DC-7043)
MARSHALL, L., Applications of the optical model to K,p interactions, 19: 39545
MARSHALL, T., Ionizing shock wave plasma diagnostics, 19: 40059
MARSHALL, Thomas C., Combination scattering of microwaves from space-charge waves in a laboratory magnetoplasma, 19: 40033
MARTIENSSEN, W., Optical absorption of Cu centers in alkali halides, 19: 40107
MARTIN, B., Influence of solid-state effects on β-γ directional correlation in ^{166}Ho, 19: 39824
MARTIN, Robert L., Irradiation evaluation of Al_2O_3-coated UO_2 fuel particles, 19: 39227 (BMI-1729)
MARTIN, Roger, Fuel loading and unloading arrangement for nuclear reactors, 19: 40145
MARTINET, A., Proximity effects under magnetic fields. I., 19: 39699
MARTINIS, M., Vector mesons and complex angular momentum, 19: 39518
MARTUCCI, G., Consequences of SU_6 for total baryon-baryon and baryon-antibaryon cross-sections, 19: 39529
MARTUCCI, G., Proton-antiproton annihilation into two mesons, 19: 39527
MARTY, N., Scattering of protons on C-12, 19: 39837
MARTZ, D. E., Observations of extremely cool stars, 19: 39347
MASEK, John G., Determination of organic residue from solvents by radioisotopic method, 19: 38538 (ADR-08-13-63.1)
MASHKOVA, E. S., Structure of energy spectra of ions scattered from

single crystals, 19: 39297
MASON, E. A., Gaseous diffusion in a temperature gradient, 19: 39291
MASON, Edward A., Gamma-radiation effects on growth of KCl crystals, 19: 38696 (MIT-2909-4)
MASON, Emerson B., Device for measuring the radioactivity of a plurality of individual samples, 19: 38799
MASSEY, H. S. H., The use of radioactive isotopes for checking production processes, 19: 39067
MASTEL, B., Electron microscope studies of second phase particles in dilute alloys of U, 19: 39092 (BNWL-SA-90)
MATHUR, P. B., Reversal of some effects of γ-irradiation by ethyl ester of gibberellic acid, 19: 38401
MATIGNON, Camille, New reaction for producing strontium, 19: 38593 (ORNL-tr-674)
MATSUDA, Kiyoshi, Preparation of uranous salt by intermediate formation of uranyl sulfide, 19: 38659
MATSUDA, Kiyoshi, Reaction between U oxides and CCl_4, 19: 38661
MATSUDA, Masanori, Production of weak bosons, 19: 39567
MATTERN, Ina E., Range of action of genes controlling radiation sensitivity in Escherichia coli, 19: 38398
MATTHEISS, L. F., Fermi surface in tungsten, 19: 40102
MATTHEWS, P. T., Covariant extension of SU(6), 19: 39555
MATTHIAS, B. T., Superconductivity of Nb_3Ge, 19: 39725
MATTHIAS, Bernd T., Vanadium–titanium composition in a superconductive device, 19: 39750
MATTOS, M. C., Total neutron cross sections of Pr, Yb, Lu, and Er, 19: 39779 (IEA-86)
MATUDA, K., Nuclear magnetic resonance of polarized ^{17}F formed through the $^{16}O(d,n)^{17}F$ reaction, 19: 39867
MATVEEV, V. V., Development of scintillation and ionization methods of radiometry and dosimetry, 19: 38995 (NP-15259)
MATVEEVA, M. D., Activity of α toxin of Cl. perfringens type A radiation mutants, 19: 38446
MATVEEVA, M. D., Radiation effects on toxin production of Cl. perfringens type A bacteria, 19: 38448
MATZNER, B., Heat transfer and hydraulic studies for SNAP-4 fuel element geometries, 19: 40249 (TID-22014)
MAURO, Francesco, Influence of post-radiational incubation conditions on x-ray survival of diploid yeast, 19: 38422
MAUSHART, R., Large-area counter for exclusive measurement of soft quanta radiation emitted by a sample, 19: 39046
MAXFIELD, B. W., Superconducting penetration depth of niobium, 19: 39726
MAY, F., Pulse shape discrimination system for $^6LiF(ZnS)$ scintillation counters, 19: 39025
MAY, R. M., Magnetohydrodynamic ionizing shock waves in a conducting medium, 19: 39267 (NP-15157)
MAY, Raoul-Michel, Differential action of x and uv rays on Macrobiotes areolatus, 19: 38373
MAYSER, B., Multi-component, stationary nonequilibrium flow in a MPD energy converter, 19: 39440
MAZAKI, H., Effect of chemical state on the decay constant of a nuclear isomer, ^{235m}U, 19: 39842
MAZIERES, Charles, Amorphous zirconia and non-stoichiometric zirconia, 19: 39190
MC CALDIN, J. O., Kev channeling and thermochemical properties of interstitial impurities, 19: 39395
MC CALDIN, J. O., The solubility of sodium in silicon, 19: 39204
MC CALL, Richard C., Reading apparatus for thermoluminescent-type radiation dosimeters, 19: 39048
MC CARTHY, I. E., Information obtainable from (p,2p) reactions, 19: 39905
MC CARTHY, K. A., Ultrasonic attenuation in copper, 19: 39249
MC CARTHY, K. A., X-ray coloration of thermally bleached γ-irradiated NaCl, 19: 40105
MC CAUGHAN, J. B. T., The density spectrum of air showers at sea level and mountain altitudes, 19: 39424
MC CLINTOCK, D. R., Fabrication and irradiation of thin-walled type 304 stainless steel clad fuel rods in the Saxton Reactor, 19: 39236 (WCAP-3269-36)
MC CLURE, J. W., Energy levels of ^{31}S and ^{19}Ne, 19: 39827
MC CLURE, Richard J., Ion beam electrography, 19: 38940
MC CONIGA, A. F., MINIMIZER–a computer code for determining minimum fuel cost, 19: 40170 (HW-71813)
MC CONIGA, A. F., Minimized fuel cycle cost for simulated pressurized water reactor. I., 19: 40114 (BNWL-104)
MC CULLOUGH, H., Application of digital recording to simultaneous collection in mass spectrometry, 19: 39023
MC CUSKER, C. B. A., The density spectrum of air showers at sea level and mountain altitudes, 19: 39424
MC DANIEL, Earl W., Collision phenomena in ionized gases, 19: 39309
MC GONIGAL, Gerard, Nuclear fuel element, 19: 40138
MC GONNAGLE, Warren J., Nondestructive assay of nuclear fuels, 19: 38547 (TID-21475)
MC GOWAN, J. William, Rotational structure at threshold in the H_2 electron-impact ionization spectrum, 19: 39413
MC GRATH, R. L., 2J + 1 dependence of total cross sections in lithium + boron reactions, 19: 39887
MC INTOSH, Gardiner, X-ray luminescence sample compartment with automatic shutter, 19: 38936
MC KEE, J. W., Experimental work in relation to the glow-plug concept, 19: 40228 (LA-3229, pp 111-15)
MC LAFFERTY, George H., Work on nuclear light bulb at UAC research laboratories, 19: 40230 (LA-3229, pp 137-47)
MC LEAN, W. L., Superconducting penetration depth of niobium, 19: 39726
MC MARTIN, Howard L., Support of new laboratory services by Division of Radiological Health, 19: 38880
MC NAMARA, P., Study of cation diffusion in UO_2 using α spectrometry, 19: 38681
MC NEIL, M. B., Calculation of activation energies for interstitial diffusion by a simple elastic model, 19: 40086
MC QUISTAN, Richmond B., Modulator materials study, 19: 38914 (SC-DC-65-1332)
MC TAGGART, F. K., Reduction of alkali and alkaline earth halides in high-frequency discharges. I., 19: 39180
MC TAGGART, F. K., Reduction of alkali and alkaline earth halides in high-frequency discharges. II., 19: 39181
MC WHAN, D. B., Effect of pressure on the magnetic properties and crystal structure of Gd, Tb, Dy, and Ho, 19: 40094
MEACHAM, S. A., Determination of oxygen in sodium metal, 19: 38539 (APDA-168)
MEASDAY, D. F., Processes for obtaining conducting areas of thin films: application ionization chambers, 19: 39135
MEHNER, A. S., Interpretation of stage I recovery after electron irradiation of Cu, 19: 39248
MEHRAN, A.-R., Radioformation of aspartic acid in aqueous solutions of alanine, 19: 38702
MEHRER, H., Recovery of Ni above room temperature, 19: 39251
MEHROTRA, R. C., Stability of Be chelates of catecholdisulphonic and chromotropic acids in aqueous solutions, 19: 38641
MEHTA, S. K., Evaluation of neutron emission, kerma, kerma equivalent, dose equivalent, and spectrum, 19: 39766 (ORNL-TM-1171)
MEIER, R. W., NRE Project—a new critical facility at the EIR for zero reactivity experiments, 19: 40266
MEIKLE, Richard W., Radiosynthesis of ^{14}C-labeled 4-dimethylamino-3,5-xylyl methylcarbamate, 19: 38748
MEISSNER, Hans, Transmission of magnetic pulses through type-II superconducting plates, 19: 39733
MELLOR, Arthur M., Prog. rpt. on combustion of metals, 7–12/64, 19: 38583 (SC-DC-65-1480)
MELTZER, C. M., Spin of the $Y_0^*(1405)$, 19: 39553
MENCL, J., Oxidative extraction separation of Ru from solutions of its compounds, 19: 38763
MENDEL, J. E., Use of U(IV) as Pu reductant in Purex Process, 19: 38751 (HW-82103)
MENZIES, D. C., Random fluctuations of DFR power, 19: 40193 (TRG-Report-921)
MERRIGAN, Joseph A., Effects of experimental parameters on (n,γ)-activated reactions of bromine with liquid cyclohexane, 19: 38713
MERRIGAN, Joseph Andrew, Evidence for bromine-82m isomeric transition activated reactions in saturated hydrocarbons and alkyl halides, 19: 38715
MERRILL, E. T., System of chained computer codes for reactor fuel cycle analysis, 19: 40149 (BNWL-SA-61)
MERRITT, Charles Jr., Irradiation damage in lipids and its effect on flavor, 19: 39068
MERRYMAN, Roy G., Thermal expansion of UC–ZrC solid solution, 19: 39200
MERZ, E., Paper electrophoretic separation of Th, Pa, and U, 19: 38775
MESERVEY, R., Superfluid flow in a venturi tube, 19: 39696
MESHCHERYAKOV, V. A., On $\gamma \to 3\pi$ and $\rho \to \pi\gamma$ interactions, 19: 39470 (JINR-P-2171)
MESHKOVSKII, A. G., Decay $f^0 \to \pi^0 + \pi^0$, 19: 39480 (NP-15247)
MESSIER, D. R., Investigation of fused-salt processes for preparation of uranium sulfides, 19: 38574 (ANL-7008)
MESTVIRISHVILI, A. N., Investigation of the energy spectra and angular particles in $K_2^0 \to \pi^2 + e\chi + \nu$ decay, 19: 39586
METHERINGHAM, A. J., Inelastic proton-deuteron scattering at 135 Mev, 19: 39579
METROPOLIS, N., Analysis of inherent errors in matrix decomposition using unnormalized arithmetic, 19: 39080 (LA-DC-7192)
METZ, Charles F., Determination of Pu in spent reactor fuels, Pu metal, alloys and compounds, 19: 38542 (LA-DC-6938)
METZLER, Allen R., Tank IV interim progress report, 19: 40288 (NVO-

98-5)
MEYER, A., Long-range interionic forces in metallic Li, 19: 39211
MEYER, F., Three years of operating experience with the Kahl nuclear power station, 19: 40201
MEYER, Peter-Juergen, Recovery of D_2O and H-3 from air of closed rooms of nuclear reactor installations, 19: 38907
MEYERHOF, W. E., Comparison of excited state of ^{4}He from two different reactions, 19: 39922
MEYEROTT, Arthur J., Observational result on x rays, 19: 39332
MEYERS, Gilbert Wayne, Nuclear reactor core arrangement, 19: 40146
MEYER-SCHUETZMEISTER, L., Search for second state in ^{20}Ne near 4.97 Mev, 19: 39809
MICHAELIS, W., Neutron sources and neutron fields, 19: 39772
MICHAELIS, W., Radiation from ^{241}Am, 19: 39946
MICHAUD, Gaston G. J., Plutonium enriched U fuel, 19: 39146
MICHEJDA, L., Results of HPD ionization measurements, 19: 38989 (CERN-65-11(p.219-27))
MICHEL, F. C., Nonthermal properties of post-shock plasma, 19: 39999
MICHEL, Louis, Group of invariance of a relativistic supermultiplet theory, 19: 39493
MICHIYOSHI, Itoro, Theoretical study of MHD power generation. III., 19: 39437
MIDDENDORF, Heinz Dieter, Structure of axisymmetric force-free magnetic fields in a dissipative plasma, 19: 40049
MIDDLETON, R., Thallium-207 states excited in the (t,α) reaction on ^{208}Pb, 19: 39852
MIGNERON, R., Index of refraction and sum rules for helium, 19: 39402
MIHALCZO, J. T., SOURCE, a neutron distribution routine for the 05R Monte Carlo code, 19: 39767 (ORNL-TM-1192)
MIKA, Janusz, Initial value problem for a slab with anisotropic scattering, 19: 39765 (INR-611/IX-A/R)
MIKHAILOV, I. N., Accuracy of calculations of collective oscillation frequency by u-v transformation method, 19: 39782 (JINR-P-2191)
MIKOSHIBA, Shigeo, Current density distributions in a coaxial plasma gun, 19: 39998
MILBOURN, G. M., Contamination of grassland with radioactive Sr. I., 19: 38332
MILLAR, C. H., Nuclear power implications of the Intense Neutron Generator, 19: 39758 (AECL-2177, Paper 5)
MILLER, Allen, Some aspects of correlation in many-particle systems, 19: 39251 (AROD-3979:2)
MILLER, B., Ionizing shock wave plasma diagnostics, 19: 40059
MILLER, D., Antiproton annihilation in H at rest. I., 19: 39462 (CU-1932-239)
MILLER, Donald H., Analysis of πp enhancements in π^- + d interactions at 3.2 Bev/c, 19: 39551
MILLER, J. F. A. P., Immunologic role of thymus in radiation chimeras, 19: 38451
MILLER, James N., Immunity in experimental syphilis. III., 19: 38380
MILLER, K. T., Effect of neutron irradiation on the liquid Na dilation of graphite, 19: 39235 (NAA-SR-11309)
MILLER, M. C., Nimbus dynamics analysis for ejection mechanism, 19: 39071 (MND-3169-68)
MILLER, Neil E., Irradiation evaluation of Al_2O_3-coated UO_2 fuel particles, 19: 39227 (BMI-1729)
MILLER, Steven Frank, Axial dispersion in liquid flow through packed beds, 19: 38812 (UCRL-11951)
MILLS, C. B., Criticality, 19: 40155 (LA-3229, pp 362-76)
MILSTED, J., Alpha half life of berkelium-247; a new long-lived isomer of berkelium-248, 19: 39807
MILTON, J. C. D., Intense Neutron Generator research facilities, 19: 39757 (AECL-2177, Paper 4)
MINAMI, Shigeo, Speculations on the meson-deuteron interaction, 19: 39564
MINARDI, E., Space charge and currents in continuous rotating plasma accelerator, 19: 39962(NP-15167)
MINART, Paul, Plant for liquid-liquid extraction by the counter-current flow process, 19: 38777
MINES, J. R., Distorted-wave Born approximation for stripping to virtual levels, 19: 39910
MINNIGERODE, B., Late changes of larynx after Ra irradiation of carcinoma of vocal cord, 19: 38519
MISENTA, R., Exponential experiment in natural U, 19: 39763 (EUR-2413.e)
MISHIMA, Masao, Isotope separation by liquid-gas chemical exchange, 19: 39075
MISHRA, L. C., Dental lesions in rat induced by radiomimetic agents, 19: 38325
MISHRA, U. C., Fission products data and its application in studying fallout from nuclear weapon tests, 19: 39774 (AEET-209)
MISTUZUMA, Yoshisuki, New alloys for reactor materials, 19: 39206
MITCHELL, M. J., HPD programming at Rutherford Lab., 19: 38986 (CERN-65-11(p.173-81))
MITCHELL III, Walter, Design and construction: Pathfinder and BONUS, 19: 40217
MITTER, H., Nonlinear quantum field theories at small distances, 19: 39655
MIYAMOTO, Tetsu, End stabilization effect in slow theta pinch, 19: 39996
MIYAZAWA, Hironori, Symmetry SU(9), 19: 39571
MIZOBUCHI, A., Nuclear magnetic resonance of polarized ^{17}F formed through the ^{16}O(d,n)^{17}F reaction, 19: 39867
MIZUSHIMA, M., Natural width of spectral lines and irreversibility, 19: 39386
MOAK, C. D., Channeling effects on the energy loss of high-energy (20-80 Mev) ^{79}Br and ^{127}I ions in gold, 19: 39370 (ORNL-P-1336)
MOAZED, C., Angular correlations for ^{9}Be(^{3}He,α)^{8}Be $\rightarrow$ 2α reaction, 19: 39916
MOAZED, C., Reaction ^{9}Be + ^{3}He $\rightarrow$ 3α, 19: 39898
MOAZED, C., Reaction ^{10}B + ^{3}He $\rightarrow$ p + 3α, 19: 39899
MOBOZ, V. I., Applicability of isobar model for Λ hyperon production in π^-p interactions, 19: 39593
MODIG, Hans, Cysteamine-induced increase of cellular glutathione level, 19: 38464
MOELLER, Dade W., Environmental behavior of nuclear debris, 19: 38857
MOENCH, L., Late bladder changes caused by radiotherapy of uterine carcinoma, 19: 38531
MOERCH, T., Use of P^{32} for the registration of changes and variations in the enamel surface. A preliminary report, 19: 38352
MOFFAT, J. W., Stimulated photon-photon scattering, 19: 39264 (CONF-796(Paper 14))
MOHAN, Radhe, Measurement of photoelectric cross section of γ rays, 19: 39376
MOHLING, Franz, Degenerate Bose system. V., 19: 39657
MOLCHANOV, V. A., Structure of energy spectra of ions scattered from single crystals, 19: 39297
MOLLWO, L., Degree of blackness and thermal radiation of homogeneous, magnetic field-free plasma, 19: 39985
MOLNAR, B., Moessbauer effect study of phase transition in ice, 19: 39715
MOLNAR, F., Decay of ^{161}Ho, 19: 39930
MONRO, J., Influence of radiation on ovarian maturation and histolysis of pupal fat body in Diptera, 19: 38406
MONRUE, C. W., Sodium void coefficient of reactivity. A review and study of analytical work, 19: 40158 (UNC-5123)
MONSTER, Jan, Ratios (^{34}S/^{32}S) for different forms of S in Orgueil meteorite and their mode of formation, 19: 39351
MOODY, F. J., Maximum two-phase vessel blowdown from pipes, 19: 38802 (APED-4827)
MOODY, J. C., Application of electron microscopy in dimensional metrology, 19: 38916 (SC-DC-65-1589)
MOORE, C. F., Reactions involving simple isobaric analog resonances, 19: 39875
MOORHEAD, W. G., CERN version of FILTER, 19: 38981 (CERN-65-11 (p.115-21))
MOORHEAD, W. G., Conference on programming for flying-spot devices, Bologna, 10/64, 19: 38971 (CERN-65-11)
MORAND, M., Automatic following of tracks in nuclear emulsions, 19: 39017
MORDARSKI, W. J., Prog. rpt. on BONUS core development, 12/64–2/65, 19: 39156 (CEND-532)
MOREAU, Claude, Hydrolysis mechanism at high temperature of UC, 19: 38606
MORGENROTH, H., Shock fronts in neutral gases and plasma. I., 19: 39984
MORGULIS, N. D., A study of the properties of a thermionic diode placed in an autonomous discharge plasma, 19: 39435 (JPRS-31048)
MORITA, Kazuo, Chemical protection against radiation. I., 19: 38458
MORITA, Tohru, Low-temperature expansion of spontaneous magnetization of Heisenberg ferromagnet, 19: 39684 (CONF-796(Paper 4))
MORNEX, R., Fixation curve of ^{131}I in thyroid in subjects treated with iodinated contrast media, 19: 38354
MOROZOV, I. V., Electrical section of the reactor at the first atomic power station, 19: 40208
MORPURGO, G., Vanishing of E2 part of $N^*_{33} \rightarrow N + \gamma$ amplitude, 19: 39536
MORRIS, D. A., Hydrology of subsurface waste disposal, national reactor testing station, Idaho. Annual Progress Report, 1964, 19: 40269 (IDO-22047-USGS)
MORRISON, David L., Postirradiation fission-product release from coated fuel particles, 19: 39228 (BMI-1734)
MORRISON, David L., Prog. rpt. on fission-product reactions with and release from fuel-element claddings, 4–6/65, 19: 39152 (BMI-X-10132)
MORRISON, G. W., SOURCE, a neutron distribution routine for the 05R

Monte Carlo code, 19: 39767 (ORNL-TM-1192)

MORRISON, J. A., Magnetic contribution to heat capacity of Nd at low temperatures, 19: 39296

MORRISON, Roderick G., Application of miniature intrinsic thermocouples for reactor transient diagnostics, 19: 38911 (LA-DC-7004)

MORSE, David L., Low-frequency instability of partially ionized plasma, 19: 40004

MOSER, Pierre, Magnetic tailing in ferromagnetic transition metals irradiated with electrons at 22°K, 19: 39239

MOSES, H. E., Transformation from a linear momentum to an angular momentum basis for relativistic particles of nonzero mass and any spin, 19: 39500

MOSHOFSKY, Raymond P., Computer codes for evaluation of space radiation hazards. IV., 19: 40062 (N64-29366)

MOSKVIN, Yu. V., Spectroscopic studies of argon jet flowing from plasmatron nozzle, 19: 40043

MOSS, Marvin, Focused heat source for x-ray diffractometer, 19: 38941

MOSTAFA, I. Y., Influence of water content on delayed effect of irradiated wheat seeds, 19: 38412

MOTEFF, John, Nuclear propulsion. Shield physics, 19: 40246 (N64-29787)

MOTSINGER, Russell E., Nuclear propulsion. Reactor system design, 19: 40247 (N64-29788)

MOTT, William E., Precision analysis with 14-Mev neutrons, 19: 38569

MOULIN, Maurice, Control apparatus for handling device, 19: 38798

MOYER, K. H., Extraction of electrolytic-grade CR Be, 19: 39140

MUEHLPFORDT, W., Europium as an alkaline earth metal, 19: 39177

MUELLER, Adolf, Effect of ionizing radiation on elementary biological objects, 19: 38365

MUELLER, D., On the applicability of a separable potential in nuclear physics, 19: 39949

MUELLER, G., Enrichment of inner components of isotope mixtures by Clusius-Dickel columns, 19: 39076

MUELLER, G., Special methods of stable isotope analysis, 19: 38559

MUELLER, Gerhard O., KER-4—the thermal analysis of cylindrical fuel rods, 19: 40171 (KAPL-M-6475)

MUELLER, Harold J. W., Relativistic potential scattering, 19: 39598

MUELLER, K.-H., Characteristic energy of pulsed subcritical assembly, 19: 40162

MUENCH, Guido, Spectra of two extremely red objects, 19: 39348

MUENNICH, F., Determination of spin of 2426-kev level in ^{82}Kr, 19: 39944

MUKHIN, A. I., Atomic capture of μ^- in chemical compounds, 19: 39366 (JINR-P-2185)

MUKOYAMA, T., Search for radiationless annihilation of positrons, 19: 39526

MUKTASIMOV, F., Decay of ^{161}Ho, 19: 39930

MULFORD, Robert N. R., The vapor pressure of plutonium, 19: 39159 (LA-DC-6926)

MULLER, F. A., Design of high field magnet coils for long pulses, 19: 38935

MULLHAUPT, J. T., Cryosorption pumping of hydrogen and helium at 20°K, 19: 39693

MULLINS, L. J., Practical application of thermodynamics to Pu process reactions at high temperature, 19: 38752 (LA-DC-6947)

MULTANI, M. S., Moessbauer effect in ferroelectric $BaTiO_3$, 19: 38651

MULY, Emil C., Energetic electron beams and cold cathode boundary conditions, 19: 38949

MURAI, Takeo, New method of integral dose measurement with plastic scintillator phantom, 19: 38893

MURAKAMI, Kazuaki, Variation of cosmic-ray intensity observed on December 23, 1957, 19: 39426

MURAMATSU, Hiroshige, Radiation-induced addition reaction of alcohols to 1,2-dichlorotetrafluorocyclobutene and 1,2-dichlorohexafluorocyclopentene, 19: 38708

MURASIK, A., Neutron diffraction study of ferromagnetic U_3P_4, 19: 40104

MURGATROYD, Robert, Improvements relating to Zr-base alloys, 19: 39223

MURPHY, Brian, Harmonic generation in a microwave discharge, 19: 39294

MURRAY, G., ft Values for ^{42}Sc, ^{46}V, and ^{56}Mn and conserved vector current hypothesis, 19: 39859

MURRAY, R. B., Preferential thermal reorientation of V_K centers in KI, 19: 40103

MURTHY, G. K., ^{90}Yttrium concentration in milk, 19: 38856

MURTHY, K. B. S., Counter for fast neutron dosimetry, 19: 38968 (AEET/HP/D-1)

MURTY, R. C., Effective atomic numbers of heterogeneous materials, 19: 40069

MURZINA, E. A., Nuclear-active high-energy particles and the accompanying cosmic-ray extensive air showers, 19: 39429

MUTA, Taizo, V-θ bound state in the Lee model, 19: 39558

MUTHUKRISHNAN, G., Counter for fast neutron dosimetry, 19: 38968 (AEET/HP/D-1)

MUZIOL, G., Decay of ^{161}Ho, 19: 39930

MYSEV, I. P., Development of scintillation and ionization methods of radiometry and dosimetry, 19: 38995 (NP-15259)

N

NACHTIGALL, D., Methods of calculation in neutron dosimetry, 19: 38897

NADLER, M. R., Thermal expansion of TaC to 3020°C, 19: 39201

NAGATA, Takesi, Seasonal dependence of SC-field in middle and low latitudes, 19: 39673

NAGAYA, Yutaka, Zinc-65 and other fallout nuclides in marine organisms of California coast, 19: 38895

NAGEL, Hans-Hellmut, Electron-photon cascades in Pb, 19: 40070

NAGY, O., Water-side experiences on Hungarian research reactor, 19: 40264 (ZFK-RN-17(p.54-67))

NAKAI, K., Nuclear magnetic resonance of polarized ^{17}F formed through the $^{16}O(d,n)^{17}F$ reaction, 19: 39867

NAKAMURA, M., Studies of radiation injury to the kidney, using radioisotope renograms, 19: 38379

NAKAMURA, Tadashi, New method of integral dose measurement with plastic scintillator phantom, 19: 38893

NAKAMURA, Yosiaki, Modification of Hamada-Johnston potential, 19: 39570

NAKANO, Yoshiei, Current density distributions in a coaxial plasma gun, 19: 39998

NAKAYAMA, Y., Search for radiationless annihilation of positrons, 19: 39526

NAMENSON, A. I., New values of neutron separation energies, 19: 39862

NAPOLI, L. S., Highly ionized dense plasma in cesium Penning arc, 19: 40023

NAPOLI, L. S., Sustained plasma oscillations near crest of moving striation, 19: 40020

NARATH, A., Nuclear spin-lattice relaxation and Knight shift in tungsten metal, 19: 39720

NASIBOV, I. O., Reactions of $A^{III}_2B^{V}_3$ La and Ga selenides, 19: 38598

NATARAJAN, A. T., Photodynamic action and post-irradiation modifying effects of methylene blue and acridine orange in barley and *Vicia faba*, 19: 38462

NATER, K. A., Utilization of mass spectrometry in nuclear science, 19: 38925

NATHAN, O., Thallium-207 states excited in the (t,α) reaction on ^{208}Pb, 19: 39852

NATHANS, Marcel W., Isotope program of Project Gnome, 19: 38787 (PNE-102F)

NATHANS, R., Measurement of the Magnon dispersion relation of iron, 19: 39213

NAUENBERG, M., Decay $\eta \to \pi^+\pi^0\pi^-$ with C violation, 19: 39528

NEDOLUHA, Alfred, Perturbation-theoretical approach to magneto-optical phenomena in the spectral region of zero absorption, 19: 40100

NEEF, W. I., System of chained computer codes for reactor fuel cycle analysis, 19: 40149 (BNWL-SA-61)

NEGOIU, M., Study of the U(VI)-pyridyl-azo-resorcinol system, 19: 38594

NEGUS, P. J., Parity of the $Y_1^*(1660)$, 19: 39540

NEIDIGH, R. V., Plasma heating by means of beam plasma interaction, 19: 39969 (ORNL-P-1373)

NEIGHBOR, J. E., Superconducting transition width in pure lead, 19: 39748

NEIL, V. Kelvin, Electron injection and E-layer build-up in Astron, 19: 39973 (UCRL-14131)

NEITZEL, Robert E., MHD induction device, 19: 39447

NELMS, J. R., Spectrochemical method for determination of U in electrolyte, 19: 38544 (MCW-1492, pp 13-19)

NELMS, J. R., Spectrochemical method for determination of impurity elements in Th compounds, 19: 38545 (MCW-1492, pp 23-8)

NELSON, R. D., Beta-α and α-β transformations in Pu under applied stresses, 19: 39153 (BNWL-33)

NELSON, R. W., A sequence for predicting waste transport by ground water, 19: 40268

NEMETH, J., Superconductive model with two kinetic energies, 19: 39687

NEMETS, O. F., Investigation of angular and energetic correlations in the Ni(d,np)Ni reaction by the neutron-proton coincidence method, 19: 39940

NEMOTO, Chyoshiro, Low-latitude whistler echoes and an estimate of electron density in the outer ionosphere, 19: 39674

NEOGY, D., Principal magnetic susceptibilities of $Dy_2(SO_4)_3 \cdot 8H_2O$ single crystal, 19: 40082

NESTOR, C. W. Jr., Long-range interionic forces in metallic Li, 19: 39211

NEUBERT, W., Three-particle isomeric state in ^{109}In, 19: 39861

NEUFELD, Jacob, Almost longitudinal instabilities in plasma-beam system, 19: 40008

NEUGEBAUER, G., Observations of extremely cool stars, 19: 39347

NEUMAN, Bruce H., Effect of processing parameters on sintering of ThO_2, 19: 39141

NEUZIL, E. F., Helium ion-induced fission of ^{194}Pt, ^{195}Pt, and ^{196}Pt at

41 and 34 Mev, 19: 39802
NEWELL, Marcia F., Isotopic composition of uranium in zircon, 19: 38849
NEWELL, Reginald E., The energy and momentum budget of the atmosphere above the tropopause, 19: 39258 (CONF-650534-1)
NEWMAN, John B., Exchange and relativistic effects on π bonding in the uranyl ion, 19: 38635
NEWSOME, Ross W. Jr., Measurements of d,pγ directional correlations in ^{20}F, 19: 39811
NEWSON, H. W., Possible doorway state in ^{209}Pb and ^{208}Pb, 19: 39847
NGUYEN DUC, X., Thermal conductivity of stabilized zirconia at high temperatures, 19: 39215
NGUYEN VAN HIEU, On the structure of vector and axial currents in broken U(12) symmetry, 19: 39467 (JINR-E-2194)
NICHOL, David, Nuclear reactor, 19: 40132 (ORNL-tr-590)
NICHOLS, C. W., Jr., Induction of neoplasms in rat thyroid glands by x irradiation of a single lobe, 19: 38367
NICHOLS, Charles R., Prog. rpt. on boiling heat transfer, 1-3/65, 19: 38807 (NYO-2404-70)
NICKSON, James J., Regional oxygenation and therapeutic response to irradiation, 19: 38374
NICULESCU-ZINCA, D., Radioactivity in thyroid and plasma of rats marked with ^{131}I and treated with vitamin B_{12}, 19: 38337
NIEDER-VAHRENHOLZ, H. G., Chemistry of niobium and tantalum. XLVII., 19: 38640
NIEHUES, K.-J., Chemistry of niobium and tantalum. XLVII., 19: 38640
NIELSEN, H. L., The $\Omega_p = \Omega_n = ½$ excitations in the odd nucleus ^{172}Tm, 19: 39822
NIEMINEN, T., Automatic application unit for intracavitary radiotherapy, 19: 38483
NIESSEN, A. K., Guided motion of vortices and anisotropic resistivity in type-II superconductors, 19: 39694
NIESSEN, A. K., Hall effect in type II superconductors, 19: 39710
NIKITIN, A. V., Applicability of isobar model for Λ hyperon production in π^-p interactions, 19: 39593
NIKL, Istvan, Measurement of radiation in traumatologic intervention, 19: 38477
NIKOL'SKII, S. I., Nuclear-active high-energy particles and the accompanying cosmic-ray extensive air showers, 19: 39429
NILSSON, Jan, Problem of combining internal- and space-time symmetries, 19: 39455 (CONF-796(Paper 19))
NISHITA, H., Effect of chelates on the movement of fission products through soil columns, 19: 38329 (TID-20471)
NISHIYAMA, Seijiro, Reaction between U oxides and CCl_4, 19: 38661
NOBLE, Robert C., Apparatus for wipe testing radioactive sources, 19: 38909
NODA, Y., Effects of various drugs on radiation damage, 19: 38456
NODWELL, R. A., High-temperature pulsed light source, 19: 38939
NOGGLE, T. S., Channeling effects on the energy loss of high-energy (20-80 Mev) ^{79}Br and ^{127}I ions in gold, 19: 39370 (ORNL-P-1336)
NORBECK, E., Reaction $2\ ^6Li \rightarrow 3\alpha$, 19: 39920
NORTON, D. S., MLBW—a multi-level Breit-Wigner computer program, 19: 39776 (AEEW-M-517)
NOTTINGHAM, W. B., Fundamentals of thermionic energy conversion, 19: 39441
NOVAK, J. K., Behavior of perlite in compression, 19: 38779 (LA-DC-7158)
NOVIKOV, D. L., Investigation of the ion motion in the central region of the fixed-field alternating-gradient cyclotron, 19: 39316 (JINR-P-2199)
NOVIKOV, P. D., Radiation stability of ion-exchange resins, 19: 38697 (ZFK-RN-17(p.139-64))
NOVIKOV, P. D., Water purification and preparation at reactors, 19: 40123 (IAE-787)
NOVOSELOVA, A. V., Research on the system LiF–ZrF_4, 19: 38610
NOVOTNY, J., Effect of ionizing radiation on glasses, 19: 39244
NOVOZHILOV, B. V., Propagation of γ quanta in matter, 19: 40071
NOWOTNY, H., Crystal structure of $ThGa_2$ and $RuIn_3$, 19: 39207
NOWOTNY, H., Crystal chemical investigations in systems (Ti, Nb, Ta, Mo, W)–(As, Sb), 19: 39209
NOWOTNY, H., The H phases: Ti_2CdC, Ti_2GaC, Ti_3GaN, Ti_2InN, Zr_2InN, and Nb_2GaC, 19: 39208
NUGENT, L. J., Time-resolved spectroscopy of europium chelates, 19: 38634
NUMANO, Masahiro, Theoretical study of MHD power generation. III., 19: 39437
NYAGU, D., Investigation of the energy spectra and angular correlations of particles in $K^+_{\beta} \rightarrow \pi^+ + e^- + \nu$ decay, 19: 39586
NYDEGGER, Raymond R., Nondestructive assay of nuclear fuels, 19: 38547 (TID-21475)
NYIRI, J., Muon decay in renormalizable vector boson theory, 19: 39489
NYITRAY, K., Radiation-induced solid-state polymerization. I., 19: 38699

O

OAKES, R. J., Structure of ^{3}He and ^{3}H from high-energy electron scattering, 19: 39909
OBEROI, R. S., Measurement of photoelectric cross section of γ rays, 19: 39376
OBRETENOVA, K., Auto-immunization and auto-allergization in guinea pigs infected with tuberculosis with preliminary x-ray treatment, 19: 38375
OBRYK, E., Possibility of uniting the Lorentz group with the unitary symmetry group, 19: 39491
O'CONNELL, R. F., Generalized conservation laws for free fields with mass, 19: 39523
O'CONNOR, J. R., Effect of Y^{+3} on the reduction of Sm^{+3} in CaF_2, 19: 38595
ODDIE, T. H., Numerical data for ^{131}I uptake measurements in rabbits, 19: 38341
ODLAND, T., Changes in plasma Fe clearance following irradiation in dogs, 19: 38388
O'DONNELL, B., The density spectrum of air showers at sea level and mountain altitudes, 19: 39424
OEPIK, E. J., Climatic change in cosmic perspective, 19: 39665
OGATA, H., Excitation of 2^+, 5^-, and 3^- states of ^{90}Zr by inelastic α-particle scattering, 19: 39844
OGAZA, S., Magnetic properties of the ^{153}Eu nucleus, 19: 39792
OGORODNIKOV, K. F., Dynamics of stellar systems, 19: 39329
OHKAWA, Tihiro, Fusion research apparatus, 19: 40060
OHNISHI, Haruyuki, End stabilization effect in slow theta pinch, 19: 39996
OHTSUKA, T., Reversible magnetocaloric effect in superconducting niobium, 19: 39703
OKABAYASHI, Takao, Behavior of composite particles, 19: 39561
OKADA, Tsutomu, 25-Mev linear accelerator in Japan, 19: 39326
OKAMOTO, Toshio, Fallout radioactivity in diet and excreta. The levels at Tokai District, Japan in 1962 to 1963, 19: 38894
OKONOV, E. O., Investigation of the energy spectra and angular correlations of particles in $K^+_{\beta} \rightarrow \pi^+ + e^- + \nu$ decay, 19: 39586
OKUMA, Y., Excitation of 2^+, 5^-, and 3^- states of ^{90}Zr by inelastic α-particle scattering, 19: 39844
OKUN, L. B., Weak interactions of colliding electron beams, 19: 39481 (NP-15248)
OKUN, P. B., Non-conservation of CP parity and nature of law $\Delta T = ½$, 19: 39476 (NP-15197)
OLINTO, A. Cesar, Quantized vortex rings in superfluid helium: a phenomenological theory, 19: 39723
OLIPHANT, T., Applications of the optical model to K,p interactions, 19: 39545
OLIVARI, A., Comparative study of radionephrography and excretion urography, 19: 38520
OLSEN, J. L., HWR power plant with 275-MW(e) PHWP and a 260-MW(e) BLWP units, 19: 40211
OLSSON, M., Baryon-baryon scattering and SU(6), 19: 39532
ONCESCU, M. Bucharest, Detection and measurement of nuclear radiations, 19: 39040
ONDOH, Tadanori, Low-latitude whistler echoes and an estimate of electron density in the outer ionosphere, 19: 39674
ONISHCHENKO, L. M., Investigation of the ion motion in the central region of the fixed-field alternating-gradient cyclotron, 19: 39316 (JINR-P-2199)
ONO, Hironori, Calculation method of flux for spherical and cylindrical sources with slab shield, 19: 40068
ONSTOTT, E. I., Kinetic studies on extraction of Eu by Li amalgam and comparison to removal by electrolysis, 19: 38753 (LA-DC-7013)
OPPENHEIM, A. K., Pressure wave generation in a fissioning gas. II. 19: 39836
OPPENHEIM, I., Nuclear spin relaxation in gases and liquids. IV., 19: 39378
OPPERMANN, W., On contamination in ^{131}I solutions (distribution after intravenous injections in rats, 19: 38351
ORANGE, John M., Precision analysis with 14-Mev neutrons, 19: 38569
ORLINOV, V., High pressure Cs thermionic converter with W cathode, 19: 39436
ORR, J. S., Computer optimization of 4-Mev treatment planning, 19: 38518
OSAKIEWICZ, W., Energy spectrum of α particles from the ^{159}Tb(n,α)^{156}Eu reaction with 14.2-Mev neutrons, 19: 39780 (INR-596/PL)
OSGOOD, Edwin E., Ordered triplet code for messenger RNA, 19: 40296 (TID-21856)
OTSUKA, Iwao, Utilization of radioisotopes, 19: 39060
OTT, Donald G., Liquid scintillators. XIII., 19: 38691
OTTER, G., Investigation of the coulomb-nuclear interference in elastic K^-p scattering at low energies, 19: 39530
OVADIA, Jacques, Intercomparison by mailed dosimeters of high-energy electron beams, 19: 38723
OWENS, R. O., Radiative capture of deuterons in ^{16}O, 19: 39830

OYOSHI, Akira, Isotope separation using inorganic ion exchanger in fused salts. I., 19: 39074
OYOSHI, Emiko, Isotope separation using inorganic ion exchanger in fused salts. I., 19: 39074
OZAWA, M., Amplification of microwaves by the interaction of an electron beam with Cs plasma, 19: 40036
OZSVATH, Istvan, All-homogeneous solutions of Einstein's field equations with incoherent matter and electromagnetic radiation, 19: 39648
OZSVATH, Istvan, Homogeneous solutions of the Einstein–Maxwell equations, 19: 39647

P

PAAKKOLA, O., Strontium-90 in the Baltic Sea, 19: 38901
PACKARD, Lyle E., Device for measuring the radioactivity of a plurality of individual samples, 19: 38799
PAGEAU, R., Radioformation of aspartic acid in aqueous solutions of alanine, 19: 38702
PAGES, A., Study of deep postradiotherapeutic digestive stenoses, 19: 38522
PAI, S. I., Nozzle flow of a fully ionized plasma based on two-fluid theory, 19: 40048
PAI, Yun-chi, Solubilities of Pr oxalate and Nd oxalate in NTA, 19: 38601
PAL, D., Anomalous stability of the $\frac{5}{2}^-$ level in ^{13}C, 19: 39848
PALCHEVSKAYA, A. E., Effect of fast neutrons on culture and morphological characteristics of Bacillus mesentericus, 19: 38449
PALMER, D. G., Four papers concerning recent work on ground motion measurements, 19: 38864 (SC-R-65-904)
PALMER, D. G., Instrumenting nuclear explosions, 19: 38919 (SC-R-65-904, pp 59-74)
PALMER, Darwin L., Purification of radioactive No o-iodohippurate, 19: 38507
PALMITER, C. C., Guides, standards and regulations from the Federal Radiation Council point of view, 19: 38886
PALMS, John M., Thermoelectric control apparatus for the fabrication of thick lithium-drifted germanium detectors, 19: 39029
PALUCH, Ilga R., Neutron measurements relating to patients treated with x rays from 70-Mev synchrotron, 19: 38517
PANY, J. E., Effect of cysteamine and AET on oxygen consumption and body temperature of mice, 19: 38469
PANZNER, R., Treatment of hemangiomas of the skin, 19: 38511
PAOLUZI, L., Double production of charged pions in hydrogen by photons of energy between 600 and 850 Mev, 19: 39519
PAPA, Robert J., Form of electron distribution function in time-varying plasma, 19: 40015
PAPACONSTANTINOU, Elias, HO_2 radicals in bleaching of dye solutions by gamma radiation, 19: 38736
PAPE, R., Effect of x irradiations of weak and moderate intensity on tumors of mice, 19: 38387
PAPROCKI, Stan J., Prog. rpt. on civilian applications, 4/65, 19: 39091 (BMI-1723(Del.))
PARILIS, E. S., Structure of energy spectra of ions scattered from single crystals, 19: 39297
PARK, J. D., High-temperature isothermal calorimeter, 19: 38675
PARK, J. F., Plutonium particle-induced neoplasia of the canine lung. I., 19: 38359 (BNWL-SA-230)
PARKASH, Om, Radiomimetic effect of irradiated DNA on Drosophila, 19: 38413
PARKE, William C., Foldy-Wouthuysen transformation in covariant spinor formulation, 19: 39630 (CONF-796(Paper 31))
PARKINSON, E. R., Proton-γ competition in the $^{63}Cu(p,2p)^{62}Ni$ reaction at 10.5 Mev, 19: 39903
PARKINSON, W. C., University of Michigan 83-inch cyclotron, 19: 39313 (COO-921-16)
PARRA, C., Radiation sensitivity of Malherbe's calcifying epithelioma, 19: 38494
PARSIGNAULT, D., Precision measurements of some γ-transition energies in the 800-kev region using a Ge(Li) detector, 19: 39866
PARTHASARADHI, K., Absolute photoelectric cross sections of 145-kev γ rays in Ta and Pt, 19: 39377
PASCARD, Roger, Process and apparatus for the preparation of U and Pu nitrides, 19: 38685
PASECHNIK, A. M., Radiation effects on antigenic and immunogenic properties of perfringens bacteria toxins. I., 19: 38447
PASECHNIK, A. M., Serological affinity of perfringens radiation mutants. I., 19: 38445
PASECHNIK, V. M., Irradiation of animals with fast neutrons and measurements of tissue doses in a nuclear reactor, 19: 38439
PASECHNIK, V. M., The use of proportional counters for neutron dosimetry, 19: 39043
PASKIN, A., Temperature dependence of generalized Ginzburg-Landau coefficient for weak- and strong-coupling superconductors, 19: 39711
PAUL, R., Concentration dependence of thermal-diffusion factor for ^3He–^4He and H_2–D_2, 19: 38633
PAVAN, C., Lethals and their suppressors in experimental populations of Drosophila willistoni, 19: 38391
PAZSIT, A., Investigation of $^{92}Mo(n,2n)^{91,91m}Mo$ reaction, 19: 39790
PEARCE, W. P., Structure and evolution of medium-mass stars. II., 19: 39334
PEARL, W. L., Corrosion of materials for nuclear superheat applications, 19: 39115 (GEAP-4760)
PEARSON, R. L., Fuel requirements for fissiochemical production, 19: 40169 (CONF-117(p.67-79))
PEARSON, R. L., Preparation and processing of fuel for fissiochemical reactors, 19: 39095 (CONF-117(p.81-97))
PEASE, M. C., Scalar invariants of rotational system in Lie algebra. II., 19: 39086
PECK, E. R., Magnetostriction of nonferromagnetic metals, 19: 39199
PECORINI, V., Comparative study of radionephrography and excretion roentgenography, 19: 38520
PEDRICK, Arthur Paul, Improvements in marine propulsion utilising energy from nuclear fission, 19: 40255
PEEBLES, R. J. E., Cosmic black-body radiation, 19: 39350
PEED, W. F., Plasma heating by means of beam plasma interaction, 19: 39969 (ORNL-P-1373)
PEEK, James M., Use of approximate functions in evaluating Born matrix element for H_2^+, 19: 39408
PELLEGRIN, J. L., External beam extraction rate for the Cosmotron, 19: 39324
PELLICCIONI, M., Ionization chambers filled with dielectric liquids for dosimetric measurements, 19: 39030
PELSER, J., Methods preventing diffusion of radioactive materials from nuclear reactors and hot laboratories, 19: 38902
PENCHEV, G. I., Interactions of 9-Bev π^- mesons with Xe nuclei, 19: 39472 (JINR-P-2178)
PENNEMAN, R. A., Alkali fluoride complexes of Pa(IV), 19: 38625
PENNEY, R., Geometric theory of neutrinos, 19: 39503
PENNOCK, P., Program for calibrating flying-spot cathode ray tube for CHLOE, 19: 38975 (CERN-65-11(p.35-41))
PENTCHEVA, E., Distribution of rare and disperse elements in subterranean Bulgarian salt water, 19: 38851
PENTZ, Michael J., Storage rings for particle physics, 19: 39325
PEPELYAEV, Yu. V., Hydrogen adsorption on Al_2O_3 during irradiation, 19: 38717
PEREL'MAN, F. M., Rubidium and cesium, 19: 38674
PERELOMOV, A. M., Polarization effects in neutrino-electron scattering, taking into account radiation corrections, 19: 39587
PEREPELKIN, S. R., Productive role of food and vitamins in radiation injuries, 19: 38457
PERETTO, Pierre, Magnetic tailing in ferromagnetic transition metals irradiated with electrons at 22°K, 19: 39239
PEREZ, R., Radioiodine and thyroid exploration, 19: 38496
PERKINS, Francis, Motion of test particle in a plasma, 19: 40006
PERKINS, G. A., Oscillating real vectors in Coulomb-bound electron fields, 19: 39390
PERKINS, Ralph H., Densities of some low-melting Pu alloys, 19: 39161 (LA-DC-6956)
PERKINS, S. T., AGN-GAM—an IBM 7090 code to calculate Army GCR spectra and multigroup constants, 19: 40176 (AGN-TM-407)
PERLOW, G. J., Moessbauer effect in Cs-133, 19: 39295
PERRET, R. G., New source of small-angle x-ray scattering, 19: 39230 (BNL-9332)
PERRET, W. R., Four papers concerning recent work on ground motion measurements, 19: 38864 (SC-R-65-904)
PERRET, W. R., Ground motion measurements, 19: 38865 (SC-R-65-904, pp 3-22)
PERUZZO, L., Study of Σ^- capture process in hydrogen, 19: 39510
PESCHKA, W., About some new aspects of photonic propulsion, 19: 39837
PESHKIN, Murray, Moessbauer line broadening in powdered crystals, 19: 39876
PESSALL, N., Critical supercurrents in niobium carbonitrides, 19: 39681
PETEC, G., Protective effect against x-ray lesions of glycine on some enzyme systems, 19: 38467
PETERS, F. G., Cylindrical geometry sputtering apparatus, 19: 38930
PETERS, Th., Arc heaters for plasma channels, 19: 38796
PETERSEN, Robert O., Incorporation of thymidine into DNA of organs of mice, 19: 38336 (TID-21106)
PETERSON, G. A., Elastic electron scattering from lead isotopes and possible dispersion effects, 19: 39860
PETERSON, Mary, Clinically useful calculations of the dose distribution from multiple radiation sources, 19: 38526
PETERSON, O. G., Rigid-tail He cryostat for x-ray-diffraction studies of

crystallized gases, 19: 38946
PETRASOVA, M., Results of radioactivity measurements of dust and rainfall in western Slovakia in 1961-1963, 19: 38881
PETROV, N. I., Investigation of the energy spectra and angular correlations of particles in $K^0_2 \rightarrow \pi^+ + e^- + \nu$ decay, 19: 39586
PETROV, R. V., Infection and immunity in irradiated animals, 19: 38434
PETROVA, L. A., Thermal hardness of β alloys of Ti–Mo–Cr–Fe–Al system, 19: 39193
PETROVA, M. M., Functional condition of G-I tract before and after I-131 treatment, 19: 38529
PETSCHEK, H. E., Production of Bev potential wells, 19: 40032
PETUSHKOV, A. A., Data on rate of air exchange in premises with powerful γ installations, 19: 38883
PETZOLD, Joachim, Problems in unstable quantum mechanical systems, 19: 39304
PFAU, Alexander, Secretion of γ radioactivity in milk in relation to contamination of feeds in spring 1962, 19: 38858
PFEIFER, V., Uranium electrolytic deposition on metals, 19: 39100 (SGAE-CH-16/1965)
PFENDER, Emil, Steadiness of a plasmajet, 19: 39975
PFIRSCH, D., Irreversibility in scope of Liouville equation, 19: 39303
PHELPS, M. E., Helium ion-induced fission of ^{194}Pt, ^{195}Pt, and ^{196}Pt at 41 and 34 Mev, 19: 39802
PHELPS, Norma J., Purification of radioactive Na o-iodohippurate, 19: 38507
PHILLIPPOT, Joseph, Hydrolysis mechanism at high temperature of UC, 19: 38606
PHILLIPS, G. C., Energy-angular correlations and sequential decay in the ^{2}H(p,2p)n and ^{1}H(d,2p)n reactions, 19: 39924
PHILLIPS, G. C., Sequential decay of ^{12}C into three α particles, 19: 39911
PHILLIPS, J. C., Spectral analysis of photoemissive yields in Si, Ge, GaAs, GaSb, InAs, and InSb, 19: 39406
PHILLIPS, J. L., Dounreay fast reactor. Sustained full power operation, 19: 40213
PHILLIPS, Mildred E., Serum protein formation of donor type in rat-into-mouse chimeras, 19: 38404
PHILLIPS, Norman E., Tungsten–platinum alloy for heater wire in calorimetry below 0.1°K, 19: 39743
PHILLIPS, T. L., Influence of AET and hypoxia on recovery from radiation injury in mice, 19: 38450 (USNRDL-TR-851)
PICNA, E. I., Treatment of x-ray-irradiated skin with local application of an anabolic steroid, 19: 38468
PICIOTTI, E., Ionization chambers filled with dielectric liquids for dosimetric measurements, 19: 39030
PICKART, S. J., Measurement of the Magnon dispersion relation of iron, 19: 39213
PICKLESIMER, M. L., Variable-gradient, electron-beam heating methods for growing Zr single crystals, 19: 39137
PIDDINGTON, J. H., Some ionospheric effects of the solar wind, 19: 39676
PIECHOWSKA, Wanda, Effect of x-rays on the dimensions of red blood cells in mice, 19: 38363
PIELAGE, H. W., Prog. rpt. on reactor control systems, 2–4/65, 19: 40122 (GEAP-4862)
PIERCE, J. F., An evaluation of a fast complementary, hybrid bistable multivibrator, 19: 38920 (TID-22019)
PIERQUIN, B., is ^{192}Ir able to replace radium?, 19: 38521
PILAWSKI, Andrzej, Effect of x-rays on dimensions of red blood cells in mice, 19: 38363
PILLOTON, R. L., Motion of particles in fluidized beds and implications for the preparation of coated nuclear fuel particles, 19: 38782 (ORNL-TM-1170)
PIPER, Arthur M., Potential applications of nuclear explosives in development and management of H_2O resources, 19: 38791 (TEI-857)
PIPER, R. D., Electrolytic preparation of U metal from UO_2 using a frozen-crust cell, 19: 39099 (MCW-1492, pp 7-11)
PIPER, Robert G., Sensitive, high-speed, d-c voltage comparator (thesis), 19: 40279 (BDX-613-72)
PIPKIN, F. M., High-energy photoproduction of ρ^0 mesons, 19: 39549
PIRNIQUE, F., Numerical data for ^{131}I uptake measurements in rabbits, 19: 38341
PITTS, S. H. Jr., Preliminary studies on reactions of burning Pu in various solvents, 19: 38879 (RFP-566)
PIVIROTTO, T. J., Separation measurements in binary species gaseous vortex flows and flow visualization studies in a water vortex, 19: 40236 (LA-3229, pp 237-50)
PLAMONDON, C., Gamma-encephalography with ^{203}Hg-neohydrin, 19: 38510
PLANO, R., Antiproton annihilation in H at rest. I., 19: 39462 (CU-1932-239)
PLESS, I., Precision encoding and pattern recognition system, 19: 38978 (CERN-65-11(p.81-90))
PLEUTHNER, R. L., Prog. rpt. on re-entry dispersal of reactor core materials, 1–3/65, 19: 39118 (SC-DC-65-1520)
PLOEGER, F., Production of nuclear fuels. II., 19: 39104
PLUMB, Geoffrey Richard, Turntable-type drier for granular material, 19: 38800
PLUMMER, G. L., Growth response of two sedges inhabiting a radioactive waste disposal area, 19: 38331
PLYUSHCHEV, V. E., Heavy lanthanide formates, 19: 38669
POCS, L., Moessbauer effect study of phase transition in ice, 19: 39715
POCS, L., The g factors of excited states in ^{192}Os, ^{192}Pt, and ^{194}Pt, 19: 39833
PODGOR, S., Calculations on uniform-field bending magnets, 19: 39317 (NRL-6248)
PODGORETSKII, M. I., Spontaneous transitions by light propagation through anisotropic media, 19: 39266 (JINR-P-2195)
POHL, Erwin, Nuclear technology in construction, 19: 38828
POHLIT, W., The mode of action of high-energy radiation, 19: 38499
POIRIER, Yves, Study of forced oscillations of a heavy, viscous, electroconductive liquid in presence of magnetic field, 19: 39281
POIZAT, J. C., Comparative study of the efficiencies of NaI(Tl), plastic, and liquid scintillators for detection of the γ of the ^{16}O isomer, 19: 39009
POLAK, L. S., Influence of the structure of hydrocarbons on formation of radicals in low-temperature γ-radiolysis in solid phase, 19: 38724
POLAK, L. S., Production of stereospecific polymers by the γ-irradiation of inclusion compounds, 19: 38725
POLAK, L. S., Radiation-thermal cracking of petroleum hydrocarbons. II., 19: 38726
POLL, R. A., Radiation effects on pressure transducer components. Final report, 19: 39055 (GA-6266)
POLLARD, E. R., Order-disorder effect on superconductivity: The Mo–Ir system, 19: 39689
POLYANOSKAYA, N. S., Electrocapillary curves of liquid gallium, 19: 39171 (IS-Trans-17)
POMRANING, G. C., A survey of several methods for computing cell cross sections, 19: 40152 (GA-6462)
POMYTKIN, V. F., Chromatographic method of determining U and Pu in air, 19: 38554
PONDROM, L., Discharge chamber sensitive time, 19: 39028
PONOSOV, A. K., Data on p,p reactions with Q = 148 Mev, 19: 39479 (NP-15216)
POPPENDIEK, H. F., Prog. rpt. on heat transfer for nuclear auxiliary power systems, 3–5/65, 19: 38811 (SAN-409-24)
POSEY, F. A., Aluminum and titanium corrosion in saline waters at elevated temperatures, 19: 39117 (ORNL-P-1430)
POSPELOVA, L. A., Acetic compounds of trivalent Ce, 19: 38666
POST, R. F., Cooperative effects in tenuous energetic plasma contained by magnetic mirror field, 19: 40017
POSTMA, H., Severe microinstability-driven losses in an energetic plasma, 19: 39967 (ORNL-P-1337)
POTA, Laszlo, Measurement of radiation in traumatologic intervention, 19: 38477
POTEKHIN, N. V., Water purification and preparation at reactors, 19: 40123 (IAE-787)
POTTER, D. L., Studies in x-ray production by proton bombardment of C, Mg, Al, Nd, Sm, Gd, Tb, Dy, and Ho, 19: 39881
POTTER, L., Status of HPD programs at BNL, 19: 38980 (CERN-65-11 (p.97-113))
POTTS, Albert M., Tracer studies on a transplantable hamster melanoma, 19: 38485
POUCHOT, Pierre, Plant for liquid-liquid extraction by the counter-current flow process, 19: 38777
POURQUIER, H., Study of deep postradiotherapeutic digestive stenoses, 19: 38522
POWELL, B. W., Automatic analysis of spark chamber pictures using the CERN HPD, 19: 38974 (CERN-65-11(p.25-33))
POWELL, B. W., Conference on programming for flying-spot devices, Bologna, 10/64, 19: 38971 (CERN-65-11)
POWELL, B. W., Getting results from an HPD system, 19: 38970 (BNL-9236)
PRADEL, J., Charge state of ultra-fine aerosols in weakly ionized media, 19: 39285
PRADHAN, T., Can massless Dirac particles have electric charge?, 19: 39513
PRASAD, K. N., Nomogram for estimation of microcuries and millimicrograms from counts per minute, 19: 38749
PREDA, G., Mandibular radionecrosis, 19: 38527
PRESCOTT, J. D., The density spectrum of air showers at sea level and mountain altitudes, 19: 39424
PRESTON, R. S., Moessbauer cross section of ^{57}Fe in iron, 19: 39877
PRETSCH, Joachim, Production of nuclear energy, 19: 40204
PRETZER, D. D., Focused slow ion beam for study of electron ejection

from solids, 19: 38937
PRICE, C. H., Critical dimensions of water reflected systems containing $^{235}U-H_2O-Zr$, 19: 40159 (WAPD-T-1774)
PRICE, J. E., Angular distributions from the $^{11}B(d,n_0)^{12}C$ and $^{11}B(d,n)^{12*}C$ reactions for deuteron energies from 1.5 to 4.7 Mev, 19: 39817
PRICE, P. B., Prog. rpt. on radiation damage in solids, final, 4/62–3/65, 19: 39226 (AFCRL-65-305)
PRICE, P. B., Tracks of charged particles in solids, 19: 39038
PRIESS, S., Irreversibility in scope of Liouville equation, 19: 39303
PRIKHOD'KO, N. E., Lanthanum germanates, 19: 38612
PRINCE, Michael John, Nuclear reactor, 19: 40139
PRINS, J. A., Conference on physics of non-crystalline solids, Delft, 7/64, 19: 40110
PROBERT, Paul, Prog. rpt. on Na-heated steam generator, 4/65, 19: 38803 (BAW-1280-26)
PRODELL, A. G., Liquid neon–hydrogen bubble chamber, 19: 39026
PROKOF'EV, A. N., Interactions of 14.1-Mev neutrons with tritium, 19: 39939
PROTASOV, V. P., Data on p,p reactions with Q = 148 Mev, 19: 39479 (NP-15216)
PRPIC, B., Assessment of average occupational exposure to ionizing radiation, 19: 38474
PTUKHA, T. P., Specific convection currents in superfluid solutions of He-3–He-4, 19: 39744
PUIG, I. P., Utilization of Rapsodie reactor for measurement of Doppler effect, 19: 40150 (CEA-R-2565)
PURDOM, C. E., Genetic effect of incorporated ^{14}C in Drosophila melanogaster, 19: 38400
PURIKA, I., Decomposition of H_2O in reactor, 19: 38698 (ZFK-RN-17 (p.199-207))
PUZYNIN, I. V., Electrostatic field of uniformly charged volumes of a cylindrical configuration, 19: 39314 (JINR-P-2131)

Q

QUAIFE, M. A., Changes in plasma Fe clearance following irradiation in dogs, 19: 38388
QUAN, Pham Mau, Relativistic magnetohydrodynamics, 19: 39279
QUITTNER, G., Pulse shape discrimination system for $^6LiF(ZnS)$ scintillation counters, 19: 39025

R

RACK, Edward P., Effects of experimental parameters on (n,γ)-activated reactions of bromine with liquid cyclohexane, 19: 38713
RACK, Edward Paul, Evidence for bromine-82m isomeric transition activated reactions in saturated hydrocarbons and alkyl halides, 19: 38715
RADEMACHER, K., Temperature profile of fading low-current arc, 19: 39986
RADEMACHER, Karl, Stationary Ar discharge of high current densities, 19: 39983
RADIK, A. P., Weak interactions of colliding electron beams, 19: 39481 (NP-15248)
RADVANYI, P., Separation of final states in reaction (p,t), 19: 39839
RAGGENBASS, Andre, Reprocessing HNO_3 solution containing compounds after extraction of U and Pu irradiated alloys, 19: 38778
RAGSDALE, Robert G., Coaxial flow research studies, 19: 40233 (LA-3229, pp 180-207)
RAIBLE, V., Narrow resonance in scattering of electrons by atomic hydrogen, 19: 39393
RAKINTZIS, Nikolaus, HO_2 radicals in bleaching of dye solutions by gamma radiation, 19: 38736
RAKOVIC, Miloslav, Application of neutron activation analysis for determining properties of organic materials, 19: 38558
RAMACCIOTTI, D., Ionization chambers filled with dielectric liquids for dosimetric measurements, 19: 39030
RAMAKRISHNA IYER, M., Maximum permissible concentrations of fission product mixtures in air and water for occupational exposures, 19: 38872 (AEET/HP/TH-15)
RAND, M. H., Thermochemical data for plutonium compounds, 19: 38677
RAND, M. H., Thermodynamic data for Pu oxides, 19: 38682
RANDOLPH, J. K., High-energy photoproduction of ρ^0 mesons, 19: 39549
RANGARAJAN, C., Fission products data and its application in studying fallout from nuclear weapon tests, 19: 39774 (AEET-209)
RANSCHOFF, M. J. A., Americium, 19: 39191
RANSOM, C. J., Density modulations in r-f plasmas, 19: 40026
RAO, P. Venugopala, L_2-L_3N Coster-Kronig transition probabilities and L-subshell fluorescence yields of Hg and Ta, 19: 39410

RAPP, Donald, Electron collision cross section plotter, 19: 38943
RAPP, Donald, Total cross sections for ionization and attachment in gases by electron impact. I., 19: 38630
RAPP, Donald, Total cross sections for ionization and attachment in gases by electron impact. II., 19: 38631
RASHID, M. A., The 572* multiplet in SU(12), 19: 39556
RASHID, Y. R., Finite element analysis of axisymmetric composite structures, 19: 40165 (GA-6303)
RASMUSSEN, J. O., Violation of Gallagher and Moszkowski's coupling rules in ^{166}Ho, 19: 39846
RAU, J., Packaging disassembled fuel elements and radioactive waste in hot cells, 19: 40270 (JUL-249-HW)
RAUB, Ch. J., Superconductivity and particle size in heterogeneous copper–lead alloys, 19: 39747
RAUB, E., Superconductivity and particle size in heterogeneous copper–lead alloys, 19: 39747
RAUH, Everett G., Vaporization, thermodynamics, and dissociation energy of LaS, 19: 38644
READ, Mildred H., New structure in Ta thin films, 19: 39179
READER, Paul D., Operation of an electron bombardment ion source with various gases, 19: 38838
REBER, L. H., Severe microinstability-driven losses in an energetic plasma, 19: 39967 (ORNL-P-1337)
REDDI, O. S., Radiation-induced translocations in mouse spermatogonia, 19: 38396
REDEMANN, Carl T., Radiosynthesis of ^{14}C-labeled 4-dimethylamino-3,5-xylyl methylcarbamate, 19: 38748
REDFIELD, J. A., CHIC-KIN–FORTRAN program for intermediate and fast transients, 19: 40160 (WAPD-TM-479)
REECE, William O., Effects of subcutaneous implantation of rare-earth metals, 19: 38334 (COO-1170-1)
REED, Robert D., Isotopic effects in liquid hydrogen, 19: 38639
REEVES III, M., Sequential emission in the reaction $^7Li(d,n)2\alpha$, 19: 39915
REICH, H. J., Rotational temperatures of H_2 determined with 15-kev electrons, 19: 39414
REICHELT, Walter H., Spectrographic investigation of the ignited mode of thermionic converter operation, 19: 39433 (LA-DC-6898)
REICHERT, E., Production of partially polarized electron beam, 19: 39892
REID, C. N., Mechanical twinning in bcc cubic metals and its relation to brittle fracture, 19: 39202
REID, G. C., Prog. rpt. on ion rocket system, 7–9/65, 19: 38834 (N64-29495)
REID, Robert C., Gamma-radiation effects on growth of KCl crystals, 19: 38696 (MIT-2909-4)
REIFFEL, Leonard, Measuring system using the resonant absorption of γ rays, 19: 38966
REITER, R., Detection of nuclear fission products from Chinese nuclear weapon test in the lower troposphere between 3000 and 700 m NN, 19: 38899
REKALO, M. P., On a possibility of determining nucleon form factors for time-like momentum transfers, 19: 39590
REKALO, M. P., Theory of interaction of high-energy elementary particles, 19: 39478 (NP-15210)
REKONEN, A., Automatic application unit for intracavitary radiotherapy, 19: 38483
REMAEV, V. V., Isomers ^{159m}Gd and ^{117m}Sb, 19: 39929
RENARD, F. M., Deuteron electrodisintegration and neutron form factors, 19: 39541
RENDIC, D., Another attempt to determine the n-n scattering length, 19: 39499
REPALOV, N. S., Longitudinal oscillations in a multi-velocity plasma beam, 19: 39964 (NP-15201)
RESHCHIKOVA, A. A., Lanthanum selenides, 19: 38614
RETZ, A., Packaging disassembled fuel elements and radioactive waste in hot cells, 19: 40270 (JUL-249-HW)
REUTER, B., Possible $N^*_{3/2}$ resonance at 1580 Mev, 19: 39548
REVESZ, Laszlo, Cysteamine-induced increase of cellular glutathione level, 19: 38464
REXER, E., Deformation, recrystallization, and welding of Mo single crystals, 19: 39139
REYNOLDS, J. M., Effect of a cylindrical boundary on the added mass of two cylinders in liquid helium, 19: 39697
REYNOLDS, William F., NMR studies of uranyl citrate in D_2O at low pD, 19: 38623
RICHARD, P., Reactions involving simple isobaric analog resonances, 19: 39875
RICHTER, F.-W., Reaction $^{11}B(p,\alpha)2\alpha$ below 675 kev, 19: 39919
RICKEY, M. E., Levels of ^{58}Ni from the reaction $^{58}Ni(p,t)^{56}Ni$ at 28 Mev, 19: 39819
RICKEY, M. E., Mass difference $^{40}Sc-^{40}Ca$ and the ^{40}Sc ground state spin, 19: 39850

RIDOUT, M. S., Hyperfine field of ^{57}Fe in Cu–Mn alloys, 19: 39212
RIEMER, F., Comparison of fallout β activity in precipitation and total β activity in milk in Greifswald District during 1963, 19: 38862
RIESE, Gretchen R., Viscosimetric studies of kinetics of thermal denaturation of DNA, 19: 40299 (LA-tr-65-12)
RIGDON, L. P., Proposed standard for titration of aqueous solutions of boron. A preliminary report, 19: 38548 (UCRL-14166-T)
RILEY, K. F., Nucleon-nucleon total cross sections between 1 and 8 Bev/c, 19: 39550
RINALDI, R., Contribution to study of radioprotective properties of 2-mercaptobenzothiazole, 19: 38466
RIOU, M., Information on nuclear structure from (p,2p) and other knock-out reactions, 19: 39904
RISSER, J. R., Angular distributions from the $^{11}B(d,n_0)^{12}C$ and $^{11}B(d,n)^{12*}C$ reactions for deuteron energies from 1.5 to 4.7 Mev, 19: 39817
RITCHIE, H., Penetration of radiation from nuclear weapons: applicability to Hiroshima and Nagasaki survey, 19: 38892
RITTNER, Walter, Separation of Sr from Y ($^{90}Sr/^{90}Y$) using anion exchanger sulfate, 19: 38774
RITZL, F., Methods for recording ^{3}H, 19: 38552
RITZMAN, Robert L., Irradiation evaluation of Al_2O_3-coated UO_2 fuel particles, 19: 39227 (BMI-1729)
RITZMAN, Robert L., Prog. rpt. on fission-fragment effects in structural materials, 4–6/65, 19: 39229 (BMI-X-10134)
ROBERT, D., Natural width of spectral lines and irreversibility, 19: 39386
ROBERTS, J. G., Calandria core weld joint development, 19: 40125 (NAA-SR-9821)
ROBERTSON, J. C., Radiative capture cross section of iodine at 24 kev and thermal energy, 19: 39816
ROBINSON, D. K., Spin of the $Y_0^*(1405)$, 19: 39553
ROBINSON, L. C., Pre-ionization and shock wave ionization in crossed-field plasma source, 19: 39961 (NP-15112)
ROBINSON, P. M., Prog. rpt. on metallic systems, annual, 1964, 19: 39168 (TID-22015)
ROBINSON, R. A., Dissociation constant of acetic acid in D_2O from 5 to 50°C, 19: 38645
ROBINSON, R. K., Tungsten fiber reinforced nickel composites, 19: 39093 (BNWL-SA-141)
ROBSON, D., Reactions involving simple isobaric analog resonances, 19: 39875
ROCKLEY, J. C., An introduction to industrial radiology, 19: 38829
ROCKWOOD, Curtis C., 4096-channel time analyzer with variable channel width, 19: 39024
ROCQUET, Consumption and inspection of water and food in event of nuclear conflict, 19: 38882
ROELAND, L. W., Design of high field magnet coils for long pulses, 19: 38935
ROERSCH, A., Location of genes controlling radiation sensitivity in Escherichia coli, 19: 38397
ROERSCH, A., Range of action of genes controlling radiation sensitivity in Escherichia coli, 19: 38398
ROESCH, W. C., Whole-body counting, 19: 38890
ROGERS, James T. Jr., Pressure tanks for nuclear reactors, 19: 40131 (ORNL-tr-585)
ROGINSKII, S. Z., Radiochromatography used in investigations of heterogeneous catalytic reactions, 19: 38718
ROIMISHVILI, N. N., Analysis of experimental data satisfying distribution of type $x^n dx$, 19: 39087
ROJO, O., General operator potential for the two-nucleon system, 19: 39504
ROLAND, C., Scattering of protons on C-12, 19: 39837
ROLL, P. G., Cosmic black-body radiation, 19: 39350
ROM, Frank E., Coaxial flow gaseous nuclear reactor concept, 19: 40232 (LA-3229, pp 177-9)
ROMAN, P., D/F ratios and baryon magnetic moments in the SV_{12} scheme, 19: 39524
ROMANO, E., First radiobiological and pharmacodynamic studies on radioprotective effect of morphine, 19: 38453
ROMANTSEV, E. F., Chemical protection against ionizing radiation, 19: 38472
ROMER, R. H., Origin of resistance in type-II superconductors, 19: 39707
ROMERO, Jacob B., Flash x-ray analysis of fluidized beds, 19: 40224 (LA-3229, pp 63-82)
RONY, Peter R., Studies of atomic hydrogen at low pressures, 19: 38590 (UCRL-16050)
ROOS, Matts, Data on particles and resonant states, 19: 39485 (UCRL-8030(Pt.I)(Mar.'65, ed.))
ROPER, L. David, Scattering phase shift equations and resonance equations, 19: 39487 (UCRL-14193)
ROSA, Richard J., Magnetohydrodynamic equipment for producing a-c power, 19: 39449
ROSA, Richard J., Nuclear propulsion schemes using MHD conversion techniques, 19: 40238 (LA-3229, pp 286-312)
ROSCHKE, E. J., Separation measurements in binary species gaseous vortex flows and flow visualization studies in a water vortex, 19: 40236 (LA-3229, pp 237-50)
ROSE, M. E., Even parity states in ^{16}O, 19: 39806
ROSE, R. M., Substructure and impurities in Nb single crystals grown by the electron-beam, floating-zone technique, 19: 39138
ROSEN, Gerald, Particle-like solutions to nonlinear scalar wave theories, 19: 39649
ROSEN, S. P., SU(6) and nonleptonic hyperon decay, 19: 39456 (CONF-796(Paper 21))
ROSENBERG, Harvey S., Postirradiation fission-product release from coated fuel particles, 19: 39228 (BMI-1734)
ROSENBERG, T. J., Association of auroral luminosity with auroral x-rays and cosmic noise absorption, 19: 39672
ROSENBLUM, M., CERN picture number finding routine, 19: 38979 (CERN-65-11(p.91-5))
ROSENBLUTH, Marshall N., Finite Larmor radius equations with nonuniform electric fields and velocities, 19: 40001
ROSENBLUTH, Marshall N., Universal instability in complex field geometries, 19: 40018
ROSENFELD, A. H., Precision encoding and pattern recognition system, 19: 38978 (CERN-65-11(p.81-90))
ROSENFELD, Arthur H., Data on particles and resonant states, 19: 39485 (UCRL-8030(Pt.1)(Mar.'65, ed.))
ROSENSON, L., Precision encoding and pattern recognition system, 19: 38978 (CERN-65-11(p.81-90))
ROSENSTEIN, Marvin, Strontium-90 measurements in milk, 19: 38556
ROSENZWEIG, Martin L., Vortices and vortex matrices, 19: 40237 (LA-3229, pp 251-85)
ROSENZWEIG, N., Brownian-motion model for eigenvalues of a random matrix, 19: 39391
ROSKIN, G. I., Influence of ionizing radiation on antitumoral effects of Krutsin antibiotic, 19: 38428
ROSS, F., Helium ion-induced fission of ^{194}Pt, ^{195}Pt, and ^{196}Pt at 41 and 34 Mev, 19: 39802
ROSSBANDER, W., Measurements of γ-dose equivalent at the body surface by means of condenser ionization chambers, 19: 39015
ROSSEEL, B., Microscopic direct-reading instrument for system of coordinates, 19: 39000
ROSSI, G., Determination of rare earths in SAP material. II., 19: 38553
ROSSOTTO, P., Strengthening of ionizing action of ^{198}Au induced by H_2O_2, 19: 38389
ROTENBERG, Manuel, Numerical spectroscopy, 19: 39642
ROTHENSTEIN, W., Code for calculation of resonance escape probability in heterogeneous reactors, 19: 40153 (IA-1001)
ROTTER, H., Three-particle isomeric state in ^{109}In, 19: 39861
ROUGE, Pierre, Fuel loading and unloading arrangement for nuclear reactors, 19: 40145
ROURNIAIRE, J., Fixation curve of ^{131}I in thyroid in subjects treated with iodinated contrast media, 19: 38354
ROUSSEL, P., Inelastic scattering of 6.35-Mev deuterons. Limit of excitation of the 3.56-Mev level (T = 1), 19: 39804
ROUVIERE, J., Application of the PERT method to the Euor Project, 19: 40265
ROWAT, D. L., Possible nuclide production in the Intense Neutron Generator, 19: 39762 (AECL-2177, Paper 9)
ROWELL, J. M., Low-level second harmonic detection system, 19: 38944
ROWLAND, F. S., Recoil tritium reactions with ethyl chloride, 19: 38704
ROXBURGH, Ian W., Effect of rotation on stability of very massive stars, 19: 39354
ROY, M., Separation of final states in reaction (p,t), 19: 39839
ROYSTON, R. J., Program for calibrating flying-spot cathode ray tube for CHLOE, 19: 38975 (CERN-65-11(p.35-41))
RUBBIA, C., Electron asymmetry in leptonic decay of polarized Λ^0, 19: 39539
RUBIN, Sidney, Brain scans in diagnosis of cerebrovascular disease: Scanning with chlormerodrin Hg-203, 19: 38501
RUBINSON, W., Yields of ^{85}Kr in thermal neutron fission of ^{235}U and ^{239}Pu, 19: 39800
RUBINSTEIN, H. R., Baryon number 2, unitary singlet as a test of one-particle-exchange dynamical models, 19: 39511
RUBY, S. L., Moessbauer effect in Cs-133, 19: 39295
RUDAKOV, N. P., Nitrate helium dosimeters of ionizing radiation, 19: 39042
RUDAKOV, N. P., Peculiarities of effects of neutron and x radiation on hematopoietic and cardiovascular systems, 19: 38441
RUDAKOV, V. P., Reaction $(^3He,\alpha)$ on ^9Be, ^{14}N and ^{16}O, 19: 39941
RUDAKOV, V. S., Variational principles for quasistationary states, 19: 39525

RUDAKOVA, G. M., Development of scintillation and ionization methods of radiometry and dosimetry, 19: 38995 (NP-15259)
RUDALI, G., Early leukemias appearing in young and young adult AkR mice exposed to x rays, 19: 38372
RUDENKO, N. P., Complex formation of Th with 8-hydroxyquinaldoxime and caproic acid, 19: 38567
RUDRA, P., Irreducible representations of space groups, 19: 40089
RUDRA, P., Projective representations of finite groups, 19: 39085
RUEDEL, R., Mechanism of the reaction $^{11}B(^{16}O,^{15}N)^{12}C$ at 30 Mev, 19: 39869
RUEHL, W., The transition temperature of various superconducting metals under the influence of very thin oxide layers, 19: 39746
RUGE, Ingolf, Density and energetic position of radioinduced agglomeration centers in Si crystals, 19: 39254
RUHGE, D. E., Rise velocity of cylindrical bubbles in inclined tubes, 19: 38808 (NYO-3114-8)
RUPERT, George N., Versatile high-temperature thermal analysis apparatus, 19: 38913 (LA-DC-7071)
RUSAKOV, V. A., Investigation of the energy spectra and angular correlations of particles in $K^+_{\pi^2} \to \pi^2 + e\tau + \nu$ decay, 19: 39586
RUSCH, W. V. T., Interaction of microwaves with an inhomogeneous and anisotropic plasma column, 19: 39994
RUSSELL, J. J., High-energy photoproduction of ρ^0 mesons, 19: 39549
RUTLEDGE, G. P., Critical dimensions of water reflected systems containing $^{235}U-H_2O-Zr$, 19: 40159 (WAPD-T-1774)
RYABOVA, E. Z., Peculiarities of effects of neutron and x radiation on hematopoietic and cardiovascular systems, 19: 38441
RYAN, K. R., Kinetic energy of fragment ions using r-f mass spectrometer, 19: 38927
RYAN, K. R., Performance of Bennett r-f mass spectrometer, 19: 38926
RYCHLIKOVA, Milena, Polyvalent tolerance in newborn and sublethally irradiated adult mice, 19: 38376
RYNDIN, R. M., Polarized proton targets for experiments with high-energy particles, 19: 39497
RYNN, N., Measurement of ion concentrations and electron temperature in Ba plasma, 19: 39958 (MATT-327)
RYNN, N., Observations on a fully ionized barium plasma, 19: 40007
RYZHIK, O. A., Electrochemical corrosion of Mo in molten chloride, 19: 39122

S

SABIN, C. M., Prog. rpt. on heat transfer for nuclear auxiliary power systems, 3–5/65, 19: 38811 (SAN-409-24)
SACH, C. I., Pulse-height measuring unit, 19: 39006
SACHS, David L., Effect of collisions on ion cyclotron waves, 19: 40021
SACHS, Mendel, Masses of elementary particles from geometry of space-time, 19: 39452 (CONF-796(Paper 13))
SACHSE, G., Natural cation exchangers for purification of radioactive wastes, 19: 40130 (ZFK-RN-17(p.165-78))
SADAGOPAN, V., Order-disorder effect on superconductivity: The Mo–Ir system, 19: 39689
SADASIVAN, S., Fission products data and its application in studying fallout from nuclear weapon tests, 19: 39774 (AEET-209)
SAFRONOV, B. S., Pulsed plasma injectors, 19: 39955 (IAE-663)
SAHA, Bijay, Improvements in hygrometric measurement of UF_6 content of gases, 19: 38573
SAKHAROV, V. N., Propagation of γ quanta in matter, 19: 40071
SAKITA, Bunji, Group of invariance of a relativistic supermultiplet theory, 19: 39493
SAKURAI, Kunitomo, Solar flare effect on the ionospheric F2 region, 19: 39675
SALANT, E. O., Spin of the $Y^*_1(1405)$, 19: 39553
SALATSKAYA, M. I., Distribution of penetrating radiation field over protective zone of 10-Bev synchrophasotron, 19: 39315 (JINR-P-2177)
SALMI, E. W., Status report on theory and experiments on heat pipes at Los Alamos, 19: 38780 (LA-DC-7206)
SALO, K., Strontium-90 content of human bones in Finland, 1960-1962, 19: 38850
SALTER, D. C., Nucleon-nucleon total cross sections between 1 and 8 Bev/c, 19: 39550
SALTER, L. S., The temperature variation of the scattering properties of crystals, 19: 39176
SAMOILOV, P. S., Development of scintillation and ionization methods of radiometry and dosimetry, 19: 38995 (NP-15259)
SAMPSON, W. B., Superconducting pseudo-Helmholtz coil, 19: 38933
SANATINA, V. N., Orthoniobates of yttrium sub-group elements, 19: 38617
SAND, H. F., Use of P^{32} for the registration of changes and variations in the enamel surface. A preliminary report, 19: 38352
SANDAGE, Allan, Photometric results of a special survey for interlopers, 19: 39349

SANDAGE, Allan R., Exploding galaxies, 19: 39362
SANDEEN, Charles R., Apparatus for wipe testing radioactive sources, 19: 38909
SANDO, Kenneth M., Dipole matrix elements for He in first-order shielding approximation, 19: 39380
SANDOVAL, Jacob, Electron microprobe data quantification, 19: 38536 (ACF-6)
SANDULESCU, A., Simplified procedure for shell model calculations of α decay rates of even-even deformed nuclei, 19: 39793
SANKARANARAYANAN, A., Covariant polarization theory of spin-one particles, 19: 39514
SANSFORD, C. S., Synthesis of DNA and nuclear protein by gonocytes in testes of normal and x-irradiated rats, 19: 38370
SANTANGELO, R., Study of Σ^- capture process in hydrogen, 19: 39510
SANTELER, Donald, Vacuum technology, 19: 38842
SANTHOLZER, Vilem, Apparatus for the collection of samples of aerosols on membrane filters, 19: 38896
SANTOS-SANCHEZ, M., Neutron-induced reactions in aromatic phosphorus compounds, 19: 38700
SAPSFORD, C. S., Effect of x rays on gonocytes in testis of rat, 19: 38369
SARAEVA, V. V., Gamma-radiolysis of methanol, 19: 38716
SASAKI, Shistuo, Electric arc reduction process for making raw metallic Nb, 19: 39133
SASLAW, Leonard D., Skin changes induced by uv-irradiated linolenic acid extract, 19: 38366
SASS, A. R., Current distribution in a thin-film superconducting strip transmission line, 19: 39692
SASTRY, P. V., X-ray coloration of thermally bleached γ-irradiated NaCl, 19: 40105
SAUCIER, Kenneth L., Stem design and shotcrete, grout, and concrete support. Project pre-schooner, 19: 38788 (PNE-501F)
SAUER, J. M., Preparation of Sr, Ca, and Mg accelerator targets, 19: 38658
SAUTERON, Jean, Bell furnace for the preparation of uranium metal by magnesiothermic reduction, 19: 39113
SAVITSKII, E. M., Constitution diagram and properties of Nb–Mo–Si alloys, 19: 39194
SAVITSKII, E. M., Solubility of certain transition metals in the V_3Si compounds and their influence of the transition of the compounds into a superconducting state, 19: 39196
SAVOCHKIN, Y. P., Electrochemical corrosion of Mo in molten chloride, 19: 39122
SAWYER, Donald C., Effect of irradiation on ferrokinetics of cross-circulated dogs, 19: 38382
SCALA, E., Field-aided electron-beam zone refining of tungsten, 19: 39111
SCARGLE, Jeffrey D., Spectra of two extremely red objects, 19: 39348
SCATTERGOOD, R. O., Prog. rpt. on metallic systems, annual, 1964, 19: 39168 (TID-22015)
SCHAARE, W., Determination of spin of 2426-kev level in ^{82}Kr, 19: 39944
SCHAEFER, H., Chemistry of niobium and tantalum. XLVII., 19: 38640
SCHAEFFER, O. A., Helium–uranium ratios for Pleistocene and Tertiary fossil aragonites, 19: 38868
SCHEARER, L. D., Nuclear spin-lattice relaxation in the presence of magnetic-field gradients, 19: 39880
SCHENK, W., Improving economy with use of standardized, movable, in-cell boxes, and decontamination of their equipment, 19: 38794 (JUL-252-RW)
SCHIFF, M., Results obtained with off-line HPD system, 19: 38988 (CERN-65-11(p.183-206))
SCHIFFMACHER, Gerard, Separation and purification of Sm distillation of the halogenides, 19: 38765
SCHILD, A., Fokker action principle for particles with charge, spin, and magnetic moment, 19: 39501
SCHINZ, H. R., Radiation protection in medical radiology, 19: 38523
SCHLEHMAN, G. J., Defect equilibria of PuO_{2-x}, 1100 to 1600°C, 19: 39221
SCHLOSSER, J. A., Fokker action principle for particles with charge, spin, and magnetic moment, 19: 39501
SCHLOSSER, K., Investigation of the coulomb-nuclear interference in elastic K^-p scattering at low energies, 19: 39530
SCHLUETER, H., Density modulations in r-f plasmas, 19: 40026
SCHMIDDEM, P. J., Disassembly of test irradiations and fuel elements in small cast iron, α-γ-cells and their subsequent handling, 19: 38795 (JUL-253-RW)
SCHMIDDEM, P. J., Packaging disassembled fuel elements and radioactive waste in hot cells, 19: 40270 (JUL-249-HW)
SCHMIDLIN, P., Influence of solid-state effects on β-γ directional correlation in ^{166}Ho, 19: 39824
SCHMIDT, B., Effects of liposoluble vitamins on Sr-90 metabolism of growing rats. I., 19: 38347
SCHMORANZER, H., Rotational temperatures of H_2 determined with 15-kev electrons, 19: 39414

SCHNEIDER, H., Measurement of the circular polarization of the 498-kev γ quanta of ^{103}Rh, 19: 39945
SCHNEIDER, I., Luminescence from ionized F-aggregate centers in alkali halide crystals, 19: 38648
SCHNERING, H. G., Chemistry of niobium and tantalum. XLVII., 19: 38640
SCHOFIELD, Philip, Improvements in C articles, 19: 38684
SCHREIBER, Franz, Electromagnetic system for movement of reactor control element, 19: 40140
SCHREUERS, J. W. H., Experimental and theoretical investigation of radiation effects in glasses, 19: 39256
SCHRIEFFER, J. R., Strongly coupled electron-phonon system in normal and superconducting metals, 19: 40073
SCHROER, B., SU_6 in relativistic particle mechanics, 19: 39459 (CONF-796(Paper 28))
SCHUETZ, Ulrich, Ion waves and ion-current waves, 19: 39988
SCHULTE-FROHLINDE, Dietrich, HO_2 radicals in bleaching of dye solutions by gamma radiation, 19: 38736
SCHULZ, J. A., Volumetric calibration of process vessels using digital computer techniques, 19: 38756 (RFP-488)
SCHULZ, W., Improving economy with use of standardized, movable, in-cell boxes, and decontamination of their equipment, 19: 38794 (JUL-252-RW)
SCHUMACHER, B. W., Review of laws for electron penetration through matter, 19: 39416
SCHUSSLER, Mortimer, Cold-workable Nb-base alloy, 19: 39224
SCHWANECKE, R., Radioprotection with neutron generators, 19: 38480
SCHWARTZ, Helmut, Mechanism of high-power-density electron-beam penetration in metal, 19: 39417
SCHWARTZ, P. E., Prog. rpt. on heat transfer for nuclear auxiliary power systems, 3–5/65, 19: 38811 (SAN-409-24)
SCHWARZ, Alexander, Radiochemical synthesis of ^{14}C-labeled trichloromethylcycloalkane, 19: 38695 (KFK-317)
SCHWILLE, W. J., Measurements of cross sections for photoproduction of π^+ on H in region of first resonance, 19: 39597
SCOPPA, P., The fluorescence of p-hydroxydiphenyl in aqueous solution, 19: 38687 (EUR-2423.e)
SCOTT, Bruce L., Analysis of the ^{6}Li(p,pd)^{4}He reaction, 19: 39907
SCOTT, William, Device for measuring the radioactivity of a plurality of individual samples, 19: 38799
SEARS, R. L., Depth of convective envelope on lower main sequence and depletion of Li, 19: 39336
SEBASTIANI, F., Double production of charged pions in hydrogen by photons of energy between 600 and 850 Mev, 19: 39519
SEBESTYEN, A., Muon decay in renormalizable vector boson theory, 19: 39489
SECREST, A. C., Preparation and evaluation of carbon-coated fuel particles, 19: 39126 (CONF-117(p.149-70))
SECREST, V. M., Preparation and evaluation of carbon-coated fuel particles, 19: 39126 (CONF-117(p.149-70))
SEDDON, W. E., The preparation and some properties of U carbonitrides, 19: 39089 (AERE-M-1389)
SEEGER, A., Recovery of Ni above room temperature, 19: 39251
SEELENTAG, W., Alloying with Na diuranate for coloring artificial teeth, 19: 38473 (NP-14923)
SEELENTAG, W., Calcium as prophylactic against uptake of Sr-90, 19: 38335 (NP-14926)
SEET, S. H., The density spectrum of air showers at sea level and mountain altitudes, 19: 39424
SEGEL, R. E., Search for second state in ^{20}Ne near 4.97 Mev, 19: 39809
SEIDLITZ, Lee, Analysis of πp enhancements in π^- + d interactions at 3.2 Bev/c, 19: 39551
SEKIGUCHI, Hiroyoshi, Measurements of fast neutron spectra by threshold detectors, 19: 39007
SELECTOR, Ya. M., Four-prong stars in π^-p interactions at 3.5 Bev, 19: 39591
SELF, M. R., Effects of nuclear radiation and various environments on a number of selected plastic, glass-laminate, and ceramo-plastic materials, 19: 39232 (FZK-227)
SELOVE, W., Final-state interaction studies at high energies, 19: 39574
SEMENENKO, E. I., Radiochronatography used in investigations of heterogeneous catalytic reactions, 19: 38718
SENGUPTA, S., Moments of inertia of asymmetric nuclei, 19: 39831
SENS, J. C., Electron asymmetry in leptonic decay of polarized Λ^0, 19: 39539
SERBER, R., Theory of atomic beam optical double resonance spectroscopy, 19: 39369 (NP-15140)
SERGEEV, F. M., Data on p,p reactions with Q = 148 Mev, 19: 39479 (NP-15216)
SERIKOV, I. N., Reaction (^{3}He,α) on ^{9}Be, ^{14}N and ^{16}O, 19: 39941
SERIN, B., Ginzburg-Landau parameter of Ta, 19: 39205
SETZER, V., Lethals and their suppressors in experimental populations of Drosophila willistoni, 19: 38391
SEVERI, M., Double production of charged pions in hydrogen by photons of energy between 600 and 850 Mev, 19: 39519
SEWELL, P. B., Observation of gas adsorption phenomena by high-energy electron diffraction, 19: 39178
SEYBOTH, P., CERN version of FILTER, 19: 38981 (CERN-65-11(p.115-21))
SEYDEL, H. Gunter, Radiation-induced changes in cytoplasmic acridine orange staining of exfoliated cells, 19: 38488
SEYERLEIN, J., Post FILTER routine of CERN HAZE, 19: 38983 (CERN-65-11(p.139-43))
SHAHIN, M. M., Ion-molecule interaction in cathode region of glow discharge, 19: 38637
SHAHINIAN, P., Effect of electron bombardment heating on surface of tungsten, 19: 39255
SHAKHBAZYAN, B. A., Applicability of isobar model for Λ hyperon production in π^-p interactions, 19: 39593
SHAKHOVA, K. I., Heat-resistance properties of Ti–Nb–Cr alloys, 19: 39192
SHAKHTAKHTINSKII, G. B., Arsenate-iodometric determination of Y, 19: 38551
SHALAMOV, Ya. Ya., Data on p,p reactions with Q = 148 Mev, 19: 39479 (NP-15216)
SHALEK, Robert J., Intercomparison by mailed dosimeters of high-energy electron beams, 19: 38723
SHANIN, L. L., Rock age of the Vindhyan system (India) according to glauconites, 19: 38853
SHANNON, J. S., Nickel-catalysed hydrogen exchange of alkylaromatic hydrocarbons and toluic acid derivatives with deuterium oxide, 19: 38688
SHAPIRO, A., Possible $N^*_{3/2}$ resonance at 1580 Mev, 19: 39548
SHAPIRO, P., Calculations on uniform-field bending magnets, 19: 39317 (NRL-6248)
SHASTRI, N. K., Reaction between U(IV) and various valence states of Np, 19: 38584 (SC-RR-65-219)
SHCHERBIN, Yu. P., Investigations of ground state of three-nucleon system, 19: 39926
SHEBANOV, V. A., Decay $f^0 \to \pi^0 + \pi^0$, 19: 39480 (NP-15247)
SHEFFIELD, James C., Ultrahigh vacuum gate valve, 19: 38841
SHEINDLIN, A. E., Niobium enthalpy between 600 and 2600°K, 19: 39217
SHELINE, G. E., Induction of neoplasms in rat thyroid glands by x irradiation of a single lobe, 19: 38367
SHELTON, H., Ion emitter studies, 19: 39164 (N64-22193)
SHEN, B. C., Observation of correlations between vector-meson and baryon-resonance decays, 19: 39542
SHEPHERD, B., Transistor ratemeter with 2μsec resolution, 19: 39004
SHEPPARD, J. C., The distribution of Am^{3+} between xylene–DBBP solutions and nitrate solutions, 19: 38750 (HW-81166)
SHERIDAN, William, Genetic effects of supra-lethal x-ray treatment of male mice, 19: 38393
SHERIDAN, William, Induction by x irradiation of dominant lethal mutations in spermatogonia of mice, 19: 38394
SHERMAN, Arthur, Engineering magnetohydrodynamics, 19: 39306
SHERMAN, Robert H., Behavior of ^{3}He in the critical region, 19: 39299
SHERMAN, Robert H., Coexistence curve of ^{3}He, 19: 39685 (LA-DC-7086)
SHERMAN, S., Cluster-star inversion and the Moebius formula, 19: 39083
SHERRILL, F. A., Observations of dislocations in Cu using Borrmann transmission topographs, 19: 39241
SHERWOOD, B. A., Momentum spectrum of positrons from muon decay, 19: 39614
SHEVCHENKO, G. V., Samarium pyrophosphates, 19: 38616
SHEVCHENKO, V. G., The energy distribution of photoprotons from ^{28}Si, 19: 39938
SHEVELEV, A. S., Mechanism of immunological unresponsiveness induced by transplantation of homologous spleen cells to sublethally irradiated animals, 19: 38454
SHEWCHUN, John, Tunneling in III-V compound p-n junctions, 19: 38931
SHIBUYA, Tai-ichi, Molecular orbitals in momentum space, 19: 39660
SHIFFMAN, C. A., Superconducting transition width in pure lead, 19: 39748
SHIM, Sun Shik, Extraction ratio and bone clearance of ^{85}Sr as a measure of effective bone blood flow, 19: 38340
SHIMA, Kazuhiso, Higher symmetry scheme of hadrons Sp(3), 19: 39565
SHIMIZU, S., Effect of chemical state on the decay constant of a nuclear isomer, ^{235m}U, 19: 39842
SHIMIZU, S., Search for radiationless annihilation of positrons, 19: 39526
SHIMOIDA, Hiroo, Transverse momentum distribution of the high-energy $p + p \to \pi^+ + d$ reaction, 19: 39569
SHIN, Ernest E. H., Born reciprocity principle and unitary symmetry, 19: 39502
SHINAGAWA, Mutsuaki, Isotope separation using inorganic ion exchanger in fused salts. I., 19: 39074
SHINOHARA, Kenichi, Radiation-induced graft copolymerization. I.,

19: 38734
SHIPMAN, J. D., Jr., Ultrafast high-voltage probe, 19: 40038
SHIRANE, G., Measurement of the Magnon dispersion relation of iron, 19: 39213
SHIRATORI, H., Potential of Pd–D/D+ electrode and ion products of HDO, 19: 38608
SHISTER, A. R., Dielectric permeability of isothermal plasma, 19: 40042
SHKLOVER, L. P., Heavy lanthanide formates, 19: 38699
SHOCKLEY, W., Study of radiation damage by using field effect, 19: 39252
SHORNIKOV, V. V., Research on the system LiF–ZrF_4, 19: 38610
SHORTER, Roy G., Labeling of human tumors with tritiated thymidine, 19: 38338
SHTUKKENBERG, Yu. M., Physics and dose measurement of penetrating radiations, 19: 38481
SHULYACHENKO, V. N., Four-prong stars in π^-p interactions at 3.5 Bev, 19: 39591
SHURAN'I, P., The problem of mass formulas in the ISL(6) theory, 19: 39466 (JINR-E-2173)
SHUR'YAN, I. M., Peculiarities of effects of neutron and x radiation on hematopoietic and cardiovascular systems, 19: 38441
SHUR'YAN, I. M., The effect of neutron radiation on some physical and chemical properties of the blood, 19: 38440
SHUSHKEVICH, S. S., Multichannel time-delay analyzer, 19: 38932
SIDEBOTHAM, Ernest William, Nuclear reactor, 19: 40139
SIEGERT, H. J., Multi-component, stationary nonequilibrium flow in a MPD energy converter, 19: 39440
SIERING, Richard, Source of radiation for measuring purposes, 19: 38905
SILK, M. G., Attempts to determine fast-neutron spectrum in thermal reactor, 19: 40256 (AERE-M-1590)
SILKER, W. B., Rapid method for determination of Pu in urine, 19: 38555
SILVESTRI, M., Characteristics and design of a co-current distillation column, 19: 38766
SIMEONOV, K., Effect of Rn inhalation on chronic diseases of nose and paranasal cavities, 19: 38528
SIMMONS, G. J., Generic classification for teaching machines, 19: 40291 (SC-R-65-923)
SIMMONS, R. O., Rigid-tail He cryostat for x-ray-diffraction studies of crystallized gases, 19: 38946
SIMON, Albert, Finite Larmor radius equations with nonuniform electric fields and velocities, 19: 40001
SIMON, Eva, Relativistic study of polarization of the electron, 19: 39582
SIMONOV, Yu. N., Phase-shift analysis of nucleon-nucleon scattering at 400 Mev, 19: 39469 (JINR-P-2170)
SIMOPOULOU, E., Possible $N^*_{7/2}$ resonance at 1580 Mev, 19: 39548
SIMPSON, James D., Photoproduction of positive pions near threshold in hydrogen (thesis), 19: 39461 (COO-1195-35)
SIMPSON, W. D., Energy-angular correlations and sequential decay in the ^{2}H(p,2p)n and ^{1}H(d,2p)n reactions, 19: 39924
SINCLAIR, W. Robert, Cylindrical geometry sputtering apparatus, 19: 38930
SIROVICH, Lawrence, On the propagation of free soundwaves in rarefied gasdynamics, 19: 39262 (BNL-8990)
SITENKO, A. G., Neutron-deuteron doublet scattering length and three-nucleon bound state with tensor forces, 19: 39585
SIVACHENKO, T. P., Effects of neutron irradiation on functional condition of thyroid, 19: 38442
SIVACHENKO, T. P., Functional state of adrenal cortex, 19: 38443
SIVACHENKO, T. P., Morphological changes in some organs of white rats due to neutron irradiation, 19: 38444
SIVINTSEV, Yu. V., Methods for surveying air contamination by radioactive aerosols, 19: 38903
SIVUKHIN, D. V., Motion of charged particles in electromagnetic fields in the drift approximation, 19: 40055
SKALAFURIS, Angelo J., Structure of shock front in atomic hydrogen. II., 19: 39280
SKIBENKO, A. I., Determination of spatial distribution of plasma density, 19: 39965 (NP-15203)
SKLAROFF, David M., Radioactive colloid treatment of malignant effusions, 19: 38515
SKLAROFF, David M., Tumor scanning with Ca-131, 19: 38508
SKREB, Yvette, Effects of γ rays on RNA and protein content of amoeba, 19: 38371
SKURNICK, I. D., Current distribution in a thin-film superconducting strip transmission line, 19: 39692
SLAUS, I., Another attempt to determine the n-n scattering length, 19: 39499
SLAUS, I., Study of (n,p) and (n,d) reactions on ^{10}B at 14.4 Mev, 19: 39798
SLEPOY, A. S. S., The effect of triiodothyroacetic acid on ^{131}I incorporation by the thyroid, 19: 38348
SLOCUM, Richard William Jr., Radiation fallout meter, 19: 39051
SLOVACEK, R. E., Asymptotic and steady state spectrum measurements in a multiplying medium, 19: 39768 (RPI-328-21)
SMART, David Lorimer, Energy transfer circuits particularly for the transfer from an inductive store to an inductive load, 19: 38960
SMART, Richard, Nuclear fuel element, 19: 40138
SMIDT, F. A. Jr., Effects of irradiation on thermally activated flow in Fe, 19: 39242
SMIRNOV, M. V., Electrochemical corrosion of Mo in molten chloride, 19: 39122
SMITH, David E., Autoradiography of the thyroid, 19: 38533
SMITH, Douglas L., Focused heat source for x-ray diffractometer, 19: 38941
SMITH, E. M., Internal dose calculation for ^{99m}Tc, 19: 38506
SMITH, Edward A., Relations between structure and properties of three graphites, 19: 39216
SMITH, Gerald A., Search for C-nonconserving decays $\phi \to \pi + \gamma$ and $\omega + \gamma$, 19: 39552
SMITH, H. I., Adhesion of polished quartz crystals under ultrahigh vacuum, 19: 38840
SMITH, H. P. Jr., Pressure wave generation in a fissioning gas. II., 19: 39836
SMITH, Hilton A., Removal of ^{3}H from ^{3}He by adsorption on charcoal, 19: 38773
SMITH, Kermit L., Observational result on x rays, 19: 39332
SMITH, Morton C., Time-dependent strengthening of graphite in tension at 2500°C, 19: 39187
SMITH, Robert M., Cesium-131 uptake and distribution in human heart, 19: 38502
SMOLINA, G. N., Mass-spectrometric study of evaporation of LaB_6 evaporation, 19: 38673
SOBELS, F. H., Role of oxygen in determining initial radiosensitivity and genesis, 19: 38463
SOBOL, N. V., Data on rate of air exchange in premises with powerful γ installations, 19: 38883
SOBOLEV, B. P., Phase composition of CaF_2–YF_3, SrF_2–YF_2, and BaF_2–YF_3, 19: 38615
SODERQUIST, Charles E., Device for measuring the radioactivity of a plurality of individual samples, 19: 38799
SODHA, Mahendra Singh, Third harmonic of current density in a plasma, 19: 40011
SOEREMARK, Rune, Concentration of some elements in enamel of (impacted) human teeth, 19: 38562
SOERENSSEN, A., Influence of electronic screening of high-energy bremsstrahlung and pair production, 19: 39389
SOFFER, J., The structure coefficients of proper self-energy parts for simple models of quantum field theory, 19: 39653
SOHL, G., Prog. rpt. on ion rocket system, 7–9/65, 19: 38834 (N64-29495)
SOKOLOV, M. V., Investigation of angular and energetic correlations in the Ni(d,np)Ni reaction by the neutron-proton coincidence method, 19: 39940
SOLLICH, W. A., Catalytic deuterium exchange reactions with organics. XII., 19: 38596
SOLLICH, W. A., Catalytic deuterium exchange reactions with organics. XIII., 19: 38597
SOLMITZ, F. T., Precision encoding and pattern recognition system, 19: 38978 (CERN-65-11(p.81-90))
SOLOMONOV, V. M., Application of scintillation granules for measuring β radiation from radioactive isotopes, 19: 38737
SOLOV'EV, L. D., On $\gamma \to 3\pi$ and $\rho \to \pi\gamma$ interactions, 19: 39470 (JINR-P-2171)
SOLZMAN, Isel I., Ventilating system for fallout shelter, 19: 38833
SONETT, C. P., Si^+–Si^- pair and interplanetary forward-reverse shock ensembles, 19: 39681
SOOD, B. S., Measurement of photoelectric cross section of γ rays, 19: 39376
SOOVIK, T. A., The concentration dependence of KI-Tl photoluminescence and radioluminescence yield, 19: 38735
SPAANDER, J., Hygienic aspects of work with ionizing radiation, 19: 38479
SPARALIS, C. W., Malleable tube clad nuclear reactor fuel element, 19: 39147
SPARROW, Nancy, Effect of oxygen pressure on radiosensitivity of Ehrlich ascites tumours at various intervals after inoculation, 19: 38402
SPEARS, J. C., Use of radioiodinated fatty acid for photoscans of the heart, 19: 38490
SPEERS, R. R., Development of fast neutron dosimetry system, 19: 38992 (COO-1226-8)
SPEISER, R. C., Prog. rpt. on ion rocket system, 7–9/65, 19: 38834 (N64-29495)
SPENCER, N. W., Behavior of the mid-latitude ionosphere from Explorer XVII, 19: 39680
SPENCER, N. W., Explorer XVII satellite, 19: 39679
SPICER B. M., Even parity states in ^{16}O, 19: 39806
SPIRN, Regina Volfovsky, Rare-earth distributions in some rocks and associated minerals of the batholith of Southern California, 19: 38848
SPITTLER, T. M., Preparation and properties of monoalkali xenates, 19: 38624

SPITZ, J., Determination of free U in UC–U and UC–U–C alloys, 19: 38540 (CEA-Note-397)
SPOKAS, J. J., Nuclear-spin-lattice relaxation of ^{51}V and ^{99}Tc in V–Tc alloys, 19: 39403
SPRUILL, Joseph L., Crater studies, Project DUGOUT, 19: 38789 (PNE-601F)
SPURLOCK, Jack M., Prog. rpt. on boiling heat transfer, 1–3/65, 19: 38807 (NYO-2404-70)
SPURNY, K., Filtration materials for respirators protecting against radioactive aerosols, 19: 38900
SPURNY, Z., Effect of ionizing radiation on glasses, 19: 39244
SPURNY, Z., Preparation of ^{35}S-labeled cystine, 19: 38747
SRAER, V., Extraction of nitrosoruthenium(III) complexes from a nitrate medium with 30% TBP. Effect of complexing reagents and acid deficiency, 19: 38764
SRINIVASAN, R., Statistical distribution of x-ray intensities in presence of pseudosymmetry. I., 19: 40067
SRINIVASAN, S. K., Novel approach to theory of shot noise, 19: 39289
SRIVASTAVA, K. D., Design of efficient flux concentrators for pulsed high magnetic fields, 19: 38934
SROUBEK, Z., ESR of NO_3^{4-} in irradiated $Ba(NO_3)_2$ single crystal, 19: 38730
STAAS, F. A., Guided motion of vortices and anisotropic resistivity in type-II superconductors, 19: 39694
STAAS, F. A., Hall effect in type II superconductors, 19: 39710
STAFFORD, G. H., Nucleon-nucleon total cross sections between 1 and 8 Bev/c, 19: 39550
STAIRS, D. G., High-energy photoproduction of ρ^0 mesons, 19: 39549
STAN, I., Fine structure of the effective mass spectrum, 19: 39583
STANCANELLI, V., Strengthening of ionizing action of ^{198}Au induced by H_2O_2, 19: 38389
STANCU, F., Simplified procedure for shell model calculations of α decay rates of even-even deformed nuclei, 19: 39793
STANIER, Margaret W., Transfer of radioactive water, urea and glycine between maternal and foetal body fluids in rabbits and pigs, 19: 38344
STANLEY, L., Prog. rpt. on reactor control systems, 2–4/65, 19: 40122 (GEAP-4862)
STARTSEV, A. A., KN scattering at low energies, 19: 39592
STAUFFER, J. L., Vaporization in LiF–BeF_2 system, 19: 38679
STEAD, Frank W., Potential applications of nuclear explosives in development and management of H_2O resources, 19: 38791 (TEI-857)
STEARNS, J. D., Effect of neutron irradiation on the liquid Na dilation of graphite, 19: 39235 (NAA-SR-11309)
STEFAN, M., Protective effect against x-ray lesions of glycine on some enzyme systems, 19: 38467
STEFANOV, B., High pressure Cs thermionic converter with W cathode, 19: 39436
STEIDL, H., Production of partially polarized electron beam, 19: 39392
STEIN, Justin J., Radiation therapy of cancer, 19: 38487
STEINBERGER, J., Antiproton annihilation in H at rest. I., 19: 39462 (CU-1932-239)
STEINSVOLL, O., Measurement of the Magnon dispersion relation of iron, 19: 39213
STEKLY, Z. J. J., 27.6 cm internal diameter superconducting magnet, 19: 39741
STELL, G., Cluster-star inversion by means of generating functionals, 19: 39084
STELL, G., Separation of interaction potential into two parts in treating many-body systems. I., 19: 39284
STELSON, P. H., Information on conversion coefficients from coulomb excitation and life-time measurements, 19: 39786 (ORNL-P-1419)
STEPHAN, W., Disassembly of test irradiations and fuel elements in small cast iron, α-γ-cells and their subsequent handling, 19: 38795 (JUL-253-RW)
STEPHAN, W., Packaging disassembled fuel elements and radioactive waste in hot cells, 19: 40270 (JUL-249-HW)
STERN, S. A., Cryosorption pumping of hydrogen and helium at 20°K, 19: 39693
STEVENS, A. L., Effect of pressure on the magnetic properties and crystal structure of Gd, Tb, Dy, and Ho, 19: 40094
STEVENS, C. A., Neutron cross sections for ^{238}U, 19: 39764 (GA-6087(Rev.))
STEVENS, C. M., Alpha half life of berkelium-247; a new long-lived isomer of berkelium-248, 19: 39807
STEVENS, L., Utilization of Rapsodie reactor for measurement of Doppler effect, 19: 40150 (CEA-R-2565)
STEWARD, K. P., Properties of cold-worked Zr–Nb fuel sheathing, 19: 39150 (AECL-2250(Pt.I))
STICHEL, P., Photoproduction of π mesons, 19: 39498
STILES, P. J., New phenomenon in semimetals and semiconductors, 19: 39734
STIRLING, W. L., Plasma heating by means of beam plasma interaction, 19: 39969 (ORNL-P-1373)
STOCK, R., The ground state of ^{40}Ca and the reactions $^{40}Ca(^3He,\alpha)^{39}Ca$, $^{42}Ca(^3He,\alpha)^{41}Ca$ and $^{40}Ca(^3He,d)^{41}Sc$, 19: 39874
STOCKSCHLAEDER, F., Disassembly and sampling of graphite ball fuel elements, 19: 38792 (JUL-250-RW)
STOCKSCHLAEDER, F., Improving economy with use of standardized, movable, in-cell boxes, and decontamination of their equipment, 19: 38794 (JUL-252-RW)
STOECKLER, H. A., Intermolecular bonding effects in ^{119m}Sn Moessbauer spectroscopy, 19: 38577 (CONF-650425-3)
STOKES, R. L., Chilldown and storage losses of large liquid hydrogen storage dewars, 19: 39686 (LA-DC-7164)
STOKES, R. W., Project Rover cryogenic evaluation laboratory, 19: 40243 (LA-DC-7169)
STONEHILL, D., Status of HPD programs at BNL, 19: 38980 (CERN-65-11 (p.97-113))
STOOPS, Robert F., Nuclear fuel consisting of very small uniformly dispersed UC particles in a uranium matrix, 19: 39127 (NCSC-2981-9)
STORBECK, I., On the behavior of Se photocells during and after irradiation with Co^{60} γ rays, 19: 39058
STORMS, Edmund K., Vapor pressure of $U_{(g)}$ and $UC_{2(g)}$ in U–C system, 19: 39160 (LA-DC-6953)
STRAIT, Bobby G., Control of nuclear rocket engines in low power-no flow region, 19: 40252
STRAND, R., Status of HPD programs at BNL, 19: 38980 (CERN-65-11 (p.97-113))
STRATTON, Frances E., Translation title list, 19: 40295 (TID-4025(Rev. 1)(Pt.1)(Suppl.4))
STRAUB, Conrad P., Environmental behavior of nuclear debris, 19: 38857
STREET, K. N., Some properties of irradiated LiF, 19: 39243
STREEVER, R. L., Nuclear resonance spin-echo study of ^{153}Eu in EuO, 19: 39840
STRELZOFF, A., Discharge chamber sensitive time, 19: 39028
STRINGER, T. E., Relationship between resistive instabilities and microinstabilities in inhomogeneous plasmas, 19: 39957 (MATT-320)
STRONGIN, M., Superconductivity in tungsten films, 19: 39708
STROUD, Agnes, Automatic analysis of photographic data in biology, 19: 38910 (CERN-65-11(p. 43-56))
STRUBLE, G. L., Violation of Gallagher and Moszkowski's coupling rules in ^{166}Ho, 19: 39846
STRUMINSKI, B. V., Group SU(12) as a generalization of the symplectic and spin symmetries, 19: 39533
STRUMINSKII, B. V., Group SU_{12} as generalization of symplectic and spin symmetries, 19: 39471 (JINR-P-2175)
STRUZHKO, B. G., Investigation of angular and energetic correlations in the Ni(d,np)Ni reaction by the neutron-proton coincidence method, 19: 39940
STUART, B. O., Non-equilibrium tissue distributions of uranium and thorium following inhalation of uranium ore by rats, 19: 38333 (BNWL-SA-226)
STUART, C., First radiobiological and pharmacodynamic studies on radioprotective effect of morphine, 19: 38453
STUCKENBERG, H.-J., ESONE—A nuclear electronics system, 19: 38924
STUETZER, Otmar M., Magnetohydrodynamic transformer, 19: 39448
STUMPF, Henry J., Gas core reactors, 19: 40235 (LA-3229, pp 222-36)
SU, Chiang, Chelating function of La and Nd with NTA, 19: 38600
SU, Chiang, Solubilities of Pr oxalate and Nd oxalate in NTA, 19: 38601
SUAREZ, Achilles A., Magnetic scattering of neutrons in ferromagnetic samples, 19: 40075 (IEA-84)
SUDAKOV, V. V., Realization of a three-dimensional unitary group by means of spherical functions, 19: 39477 (NP-15202)
SUDARSHAN, E. C. G., Concerning space-time, symmetry groups, and charge conservation, 19: 39606
SUGAHARA, Tsutomu, Effect of halogenated pyrimidines on radiosensitivity of mouse strain L cells and their radioresistant variant, 21: 38459
SUGAR, JACK, Analysis of spectrum of triply ionized Pr IV, 19: 39385
SUGAWARA, Hirotake, Symmetry SU(9), 19: 39571
SUGIMOTO, K., Nuclear magnetic resonance of polarized ^{17}F formed through the $^{16}O(d,n)^{17}F$ reaction, 19: 39867
SUJAK, B., Stress-induced variations in the spectral distribution of γ-radiation from ^{137}Cs transmitted by graphited carbon, 19: 39794
SULIMOVA, N. E., Development of scintillation and ionization methods of radiometry and dosimetry, 19: 38995 (NP-15259)
SULLIVAN, H. F., Prog. rpt. on combustion of metals, 7–12/64, 19: 38583 (SC-DC-65-1480)
SULLIVAN, R. J., Electrolysis of U carbide in fused salt using molten metal cathodes, 19: 38754 (NAA-SR-10737)
SUNDARAM, V. K., Temperature distribution in γ-active spheres, 19: 40275
SUNDERMAN, Duane N., Postirradiation fission-product release from coated fuel particles, 19: 39228 (BMI-1734)
SUNDERMAN, Duane N., Prog. rpt. on fission-product reactions with and release from fuel-element claddings, 4–6/65, 19: 39152 (BMI-X-10132)

SUNDSTROEM, I., X radiation from a flash x-ray discharge column, 19: 39305

SUNTA, C. M., Counter for fast neutron dosimetry, 19: 38968 (AEET/HP/D-1)

SUO, H., Boiling flow regimes and critical heat flux, 19: 38809 (NYO-3304-3)

SURKOV, E. L., Crossing symmetry and spiral amplitude theory, 19: 39595

SUTHERLAND, J. W., Observations on reaction of polymer carbons with CO_2, 19: 38599

SUTTON, George W., Engineering magnetohydrodynamics, 19: 39306

SVENSSON, A. G., Nuclear g factor of the 3.2-Mev 5⁻ state in the double-closed shell nucleus ^{208}Pb, 19: 39843

SWAIN, R. S., Preparation and properties of spherical particulate nuclear fuels for Pu-fueled reactors, 19: 39096 (CONF-117(p.103-26))

SWAMINARAYAN, N. S., Exact stationary solution of Einstein's equations, 19: 39663

SWAN, P., Sequential decay theory for $^{11}B(p,3\alpha)$ reaction, 19: 39895

SWARTZ, G. A., Highly ionized dense plasma in cesium Penning arc, 19: 40023

SWARTZ, G. A., Sustained plasma oscillations near crest of moving striation, 19: 40020

SWARTZ, J. M., Development of fast neutron dosimetry system, 19: 38992 (COO-1226-8)

SWEETING, J. W., α-Dehydro dimer—a major product in irradiated methyl laurate, 19: 38721

SWIDERSKI, E. F., Converter (d-c to d-c) for nuclear-thermionic energy sources, 19: 38835 (N65-27619)

SWITENDICK, A. C., Augmented plane wave calculations of band structure of Ce metal, 19: 40081 (SC-DC-65-1500)

SY, Alassane Abdoul, Research on plasmas produced in blown arcs, 19: 40037

SYKES, J. B., Dynamics of stellar systems, 19: 39329

SYMONDS, A. J., Gapless surface excitations in liquid helium, 19: 39737

SZANTO, Istvan, The role of variable parameters in the continuous x-ray diffraction analysis of structural change phenomena, 19: 38826

SZENTPETERY, I., Circular polarization of γ quanta accompanying reaction $^{10}B(d,p)^{11}B$, 19: 39937

SZILAGYI, M., Calculation of trajectory of an electron moving between coaxial tubes, 19: 39275

SZILAGYI, M., Periodic electrostatic focusing of sheet electron beams, 19: 39319

SZUCS, S., Charge spectrum of recoiling ^{216}Po in the α decay of ^{220}Rn, 19: 39884

T

TABAK, D., Code for calculation of resonance escape probability in heterogeneous reactors, 19: 40153 (IA-1001)

TABER, Richard L., Liquid scintillators. XIII., 19: 38691

TABOR, W. H., Prog. rpt. on ORR operations 1–3/65, 19: 40259 (ORNL-TM-1181)

TAFT, H. D., Precision encoding and pattern recognition system, 19: 38978 (CERN-65-11(p.81-90))

TAKADA, Yoshio, High-energy quasi-elastic proton-proton scattering, 19: 39557

TAKAMATSU, Toshiaki, Radiation-induced graft copolymerization. I., 19: 38734

TAKAMATSU, Toshiaki, Some physical properties of polyvinyl chloride–styrene graft copolymers prepared by γ-irradiation, 19: 38733

TAKEDA, Susumu, Improved microwave reflection measurement of plasmas produced by shock waves, 19: 39997

TAKEISHI, Y., Focused slow ion beam for study of electron ejection from solids, 19: 38937

TAKETANI, Kiyoaki, Oxidation of U by partially decomposed CO_2, 19: 39121

TAKEUCHI, Koichi, Atomic industry notes, 19: 39064

TALBOT, Richard B., Effects of subcutaneous implantation of rare-earth metals, 19: 38334 (COO-1170-1)

TALMONT, Xavier, Plant for liquid-liquid extraction by the counter-current flow process, 19: 38777

TALWAR, S. P., Kelvin-Helmholtz instability in an anisotropic plasma, 19: 40000

TAMAGAKI, Ryozo, Modification of Hamada-Johnston potential, 19: 39570

TAMAO, Tsutomu, Hydromagnetic radiation due to mirroring diamagnetic particles, 19: 39995

TAMASSY-LENTEI, I., Extraordinary orbitals in the united atom model, 19: 39372

TAMMINEN, V., Strontium-90 content of human bones in Finland, 1960-1962, 19: 38850

TAN, C. W., Laminar MHD channel entrance flows, 19: 39278

TAN, T. H., Antiproton annihilation in H at rest. I., 19: 39462 (CU-1932-239)

TAN, Yue-hen, Angular distribution of interactions of high-energy cosmic-ray particles with paraffin, 19: 39428

TANABE, Kosai, Higher symmetry scheme of hadrons Sp(3), 19: 39565

TANAHASHI, Goro, Energy flow of extensive air showers, 19: 39423

TANAKA, Sho, SU(3) symmetry and relation between baryons and leptons. II., 19: 39566

TANAKA, Tomoyasu, Low-temperature expansion of spontaneous magnetization of Heisenberg ferromagnet, 19: 39684 (CONF-796(Paper 4))

TANAHAEV, I. V., Investigation of yttrium chloride reactions with potassium phosphates, 19: 38620

TANANAEV, I. V., Samarium pyrophosphates, 19: 38616

TANANAEV, I. V., Yttrium phosphates, 19: 38619

TANG, Y. C., Form factors of ^3H and ^4He with repulsive-core potentials, 19: 39868

TANG, Y. C., Nonexistence of the tetraneutron, 19: 39547

TANG, Yi-Nan, Recoil tritium reactions with ethyl chloride, 19: 38704

TANNER, J. M., Solid-superfluid transition in ^4He at absolute zero, 19: 39729

TANNER, Wilmer W., Small vertebrates in U areas of upper Colorado River Basin, 19: 38330 (TID-22078)

TAPPER, R. J., Nucleon-nucleon total cross sections between 1 and 8 Bev/c, 19: 39550

TARASENKO, G. N., Thermal hardness of β alloys of Ti–Mo–Cr–Fe–Al system, 19: 39193

TARGA, H. J., Lethals and their suppressors in experimental populations of Drosophila willistoni, 19: 38391

TARJANNE, P., SU_4, 19: 39608

TARLADGIS, Basil G., Structure of the pigments of precooked irradiated meats, 19: 39065

TARUSAWA, T., Studies of radiation injury to the kidney, using radioisotope renograms, 19: 38379

TATARONIS, J. A., Plasma acoustic waves on inhomogeneous column, 19: 40028

TATARONIS, J. A., Warm magnetoplasma microinstability, 19: 40027

TATE, Raymond E., Self-diffusion studies of gamma Pu, 19: 39162 (LA-DC-6957)

TATI, Takao, On the unification of hadronic and leptonic weak interactions, 19: 39573

TATISCHEFF, B., Scattering of protons on C-12, 19: 39837

TATSII, Yu. A., Irradiation of animals with fast neutrons and measurements of tissue doses in a nuclear reactor, 19: 38439

TATSUO, Kikunori, Measurements of fast neutron spectra by threshold detectors, 19: 39007

TAYAO, Manuel S., Regional oxygenation and therapeutic response to irradiation, 19: 38374

TAYLOR, A. J., Development of the PWR for ship propulsion, 19: 40251

TAYLOR, G. N., Measurements of electron content of ionosphere during some magnetically disturbed periods in winter, 19: 39670

TAYLOR, Howard S., Many-electron-theory calculation for the Be atom, 19: 39381

TAYLOR, J. G., Existence of solutions to field equations, 19: 39627 (CONF-796(Paper 26))

TAYLOR, Louriston S., Philosophical influences on radiation protection standards, 19: 38885

TAYLOR, R., Contamination of grassland with radioactive Sr. I., 19: 38332

TAYLOR, R. I., Neutron diffraction study of antiferromagnetism in UO_2, 19: 40091

TEASDALE, W. E., Hydrology of subsurface waste disposal, National Reactor Testing Station, Idaho. Annual Progress Report, 1964, 19: 40259 (IDO-22047-USGS)

TEDMON, C. S. Jr., Substructure and impurities in Nb single crystals grown by the electron-beam, floating-zone technique, 19: 39138

TEGHTSOONIAN, E., Some properties of irradiated LiF, 19: 39243

TEICHMANN, Jiri, High-frequency containment of plasma, 19: 39982

TEMKINA, V. Ya., Complexing of 2-hydroxyethyliminodiacetic acid with rare earth elements, 19: 38671

TENENBAUM, J., High-energy photoproduction of ρ^0 mesons, 19: 39549

TENISHEVA, T. F., Infrared spectra and structure of silicates with divalent rare earth cations, 19: 38622

TERAZAWA, Osamu, Current-current interaction and nonleptonic decays of hyperons, 19: 39560

TERNOV, V. I., The effect of long-term administration of small doses of calcium-45 on certain indices of natural immunity, 19: 38362 (JPRS-30993, p.29-38)

TERRILL, James G. Jr., Public health radiation surveillance, 19: 38888

TERRY, L. E., Structure and electrical properties of vacuum-deposited CdS thin films, 19: 38585 (SC-TM-64-1677)

THACKER, T. W., Electromagnetic radii of ^3H and ^3He, 19: 39888

THARRATS, J., General operator potential for the two-nucleon system, 19: 39504
THEUS, R. B., Calculations on uniform-field bending magnets, 19: 39317 (NRL-6248)
THIEME, G. G., Computer applications in simulation, 19: 40282 (BNWL-SA-171)
THILANDER, Holger, Concentration of some elements in enamel of (impacted) human teeth, 19: 38562
THODE, H. G., Ratios ($^{34}S/^{32}S$) for different forms of S in Orgueil meteorite and their mode of formation, 19: 39351
THODE, H. G., Variations in ^{33}S, ^{34}S, and ^{36}S contents of meteorites and their relation to chemical and nuclear effects, 19: 38847
THOMAS, D. E., Low-level second harmonic detection system, 19: 38944
THOMAS, E. J., Applications of superconductivity. I., 19: 39690
THOMAS, G. E., New values of neutron separation energies, 19: 39862
THOMPSON, J. A., DIAGNOSE, a routine to debug Fortran programs, 19: 39081 (ORNL-TM-1176)
THOMPSON, W., Status of HPD programs at BNL, 19: 38980 (CERN-65-11 (p.97-113))
THOMSON, A. L., Gapless surface excitations in liquid helium, 19: 39737
THORBECKE, G. J., Serum protein formation of donor type in rat-into-mouse chimeras, 19: 38404
THORN, R. J., Thermodynamic properties and atomic transport in UO_2 phase, 19: 39219
THURBER, James K., On the propagation of free soundwaves in rarefied gasdynamics, 19: 39262 (BNL-8990)
THURSTON, M. O., Development of fast neutron dosimetry system, 19: 38992 (COO-1226-8)
TIBERGHIEN, P. Y., Application of the PERT method to the Euror Project, 19: 40265
TICHLER, P. R., HFBR containment test. April 9, 10, 1965, 19: 40258 (BNL-9237)
TICKLE, R. S., University of Michigan 83-inch cyclotron, 19: 39313 (COO-921-16)
TIELSCH, E., Evidence for isomeric states of ^{199}Po and ^{201}Po, 19: 39841
TIKHOMIROV, G. D., Decay $f^0 \rightarrow \pi^0 + \pi^0$, 19: 39480 (NP-15247)
TIKHOMIROV, L. A., Kinetics of destruction of free radicals by ionizing radiation, 19: 38719
TIMOFEEV, T. D., Radiation-thermal cracking of petroleum hydrocarbons. II., 19: 38726
TIMUSK, T., Optical absorption of Cu centers in alkali halides, 19: 40107
TISLJAR, Maria, Behavior of γ radiation in air, 19: 39483 (SGAE-PH-20/1965)
TISZA, M., Calculation of nuclear quadrupole moments, 19: 39791
TITCHENER, A. L., Prog. rpt. on metallic systems, annual, 1964, 19: 39168 (TID-22015)
TITTLE, Charles W., Radioactive well-logging method, 19: 38871
TITUS, Jack L., Labeling of human tumors with tritiated thymidine, 19: 38338
TITZE, H., Isolation of carrier-free Sr-90 and Ba-140 from irradiated U, 19: 38757 (SGAE-CH-17/1965)
TKACH, L. N., Applicability of evaporation theory to emission of multi-charged particles by heavy nuclei, 19: 39936
TKACHEV, L. G., On the structure of vector and axial currents in broken U(12) symmetry, 19: 39467 (JINR-E-2194)
TKEBUCHAVA, F. G., On $\gamma \rightarrow 3\pi$ and $\rho \rightarrow \pi\gamma$ interactions, 19: 39470 (JINR-P-2171)
TODA, H., Studies of radiation injury to the kidney, using radioisotope renograms, 19: 38379
TODOROV, I. T., Group SU_{12} as generalization of symplectic and spin symmetries, 19: 39471 (JINR-P-2175)
TODOROV, I. T., Group SU(12) as a generalization of the symplectic and spin symmetries, 19: 39533
TODOROV, I. T., Inhomogeneous group SL(6) with an extended subgroup of translations, 19: 39468 (JINR-P-2123)
TOKE, T., Present status of radioactive fallout, 19: 38861
TOLEDO, S. A., Lethals and their suppressors in experimental populations of Drosophila willistoni, 19: 38391
TOLOK, V. T., Study of a plasma bunch in motion in a toroidal magnetic field, 19: 39963 (NP-15198)
TOMAS, P., Another attempt to determine the n-n scattering length, 19: 39499
TOMAS, P., Study of (n,p) and (n,d) reactions on ^{10}B at 14.4 Mev, 19: 39798
TOMASCH, W. J., Influence of magnetic field on tunneling from type-II alloy superconductor, 19: 39718
TOMBRELLO, T. A., Capture of protons by ^7Be, 19: 39820
TOMBRELLO, T. A., Final state p-^{4}He interaction in ^{3}He(^{3}He,2p)^{4}He, 19: 39914
TOMISHIMA, Yasuo, Weizsäcker correction to the Thomas-Fermi theory of the atom, 19: 39387
TOMITA, S., Excitation of 2^+, 5^-, and 3^- states of ^{90}Zr by inelastic α-particle scattering, 19: 39844
TOMPKINS, D. R., Generalized conservation laws for free fields with mass, 19: 39523
TOMPKINS, P. C., Guides, standards and regulations from the Federal Radiation council point of view, 19: 38886
TOMUSIAK, E., The free reaction matrix as a residual interaction in finite nuclei, 19: 39815
TOOSI, Mohammad Taghi Alizadeh, Radiation effects on the physical properties of polymethyl-methacrylate (thesis), 19: 39231 (COO-1224-8)
TOPCHIEV, A. V., Radiation-thermal cracking of petroleum hydrocarbons. II., 19: 38726
TOPSCHOWSKY, M., Rotational structure in energy loss spectrum of H_2, 19: 39399
TOROPOV, N. A., Synthesis of divalent rare earth silicates, 19: 38621
TORSHINA, V. V., Mass-spectrometric study of evaporation of LaB_6 evaporation, 19: 38673
TOUSSAINT, C. J., Contribution to the quantitative x-ray spectroscopic determination of traces of elements, using direct electron excitation, 19: 38571
TOWELL, David G., Rare-earth distributions in some rocks and associated minerals of the batholith of Southern California, 19: 38848
TOWNDROW, R. G. P., Rubidium and cesium, 19: 38674
TOWNLEY, Charles W., Irradiation evaluation of Al_2O_3-coated UO_2 fuel particles, 19: 39227 (BMI-1729)
TOWNLEY, Charles W., Postirradiation fission-product release from coated fuel particles, 19: 39228 (BMI-1734)
TOYODA, Akira, Model of hadrons based on the group Sp(6), 19: 39568
TRAN THANH VAN, J., Deuteron electrodisintegration and neutron form factors, 19: 39541
TREBUKHOVSKII, Yu. V., Decay $f^0 \rightarrow \pi^0 + \pi^0$, 19: 39480 (NP-15247)
TREGO, Alan LaMar, Antiferromagnetism in dilute chromium alloys (thesis), 19: 40077 (IS-T-18)
TRICKET, Kenneth A., Pressure tanks for nuclear reactors, 19: 40131 (ORNL-tr-535)
TRILLING, G. H., Observation of correlations between vector-meson and baryon-resonance decays, 19: 39542
TROC, R., Neutron diffraction study of ferromagnetic U_3P_4, 19: 40104
TROMMER, S., Earichment of inner components of isotope mixtures by Clusius-Dickel columns, 19: 39076
TROSSI, L., Positronium in water and ice from 22° to -144°C by annihilation quanta measurements, 19: 39509
TROYAN, Yu. A., Applicability of isobar model for Λ hyperon production in π^-p interactions, 19: 39593
TROZZOLO, A. M., Moessbauer-effect study of relaxation effects in iron-dithiocarbamates, 19: 38653
TRUBNIKOV, B. A., Particle interactions in fully ionized plasma, 19: 40056
TRUCCO, R., Determination of rare earths in SAP material. II., 19: 38553
TRUSHINA, T. A., Heavy lanthanide formates, 19: 38669
TSAKADZE, J. S., Independence of the density of rotating liquid helium on the angular velocity, 19: 39714
TSAO, C. K., Nozzle flow of a fully ionized plasma based on two-fluid theory, 19: 40048
TSENG, Chin-yen, The influences of pairing force on the properties of actinide nuclei, 19: 39927
TSIRLIN, Yu. A., Application of scintillation granules for measuring β radiation from radioactive isotopes, 19: 38737
TSUBOTA, Hiroyuki, Determination of Sr in bone with ion exchange separation-flame photometric method, 19: 38345
TSUBOTA, Hiroyuki, Observation of γ-emitting nuclides with intermediate half lives in rain water, 19: 38557
TSUCHIDA, S., Radio-pyelography, 19: 38530
TSUKERMAN, I. S., Angular correlation between π mesons and leptons and determination of form factors in K decay, 19: 39482 (NP-15252)
TSURUO, Akira, Calculation method of flux for spherical and cylindrical sources with slab shield, 19: 40068
TSURUTA, Sachiko, Cooling of neutron stars, 19: 39355
TSURUTA, Sachiko, Lack of homology in the oscillations of neutron stars, 19: 39358
TSUZUKI, Toshio, Magnetic properties of intrinsic London superconductors, 19: 39721
TU, Yuan-Tsai, Applicability of isobar model for Λ hyperon production in π^-p interactions, 19: 39593
TUBIANA, M., Treatment of thyroid diseases with radioiodine, 19: 38497
TUCKER, Dorothy J., Observations on reaction of polymer carbons with CO_2, 19: 38599
TUCKER, R. F., Experimental and theoretical investigation of radiation effects in glasses, 19: 39256
TUGARINOV, A. I., Rock age of the Vindhyan system (India) according to glauconites, 19: 38853

TUKISH, E. I., Nuclear-active high-energy particles and the accompanying cosmic-ray extensive air showers, 19: 39429

TULINA, G. G., Serological affinity of perfringens radiation mutants. I., 19: 38445

TUMA, D., Synchrotron radiation from self-consistent plasma, 19: 40013

TUNNICLIFFE, P. R., The 65-mA 1-Bev proton accelerator, 19: 39755 (AECL-2177, Paper 2)

TURAEV, N. Yu., Structure of energy spectra of ions scattered from single crystals, 19: 39297

TURKIEWICZ, J., Energy spectrum of α particles from the $^{159}Tb(n,\alpha)^{156}Eu$ reaction with 14.2-Mev neutrons, 19: 39780 (INR-596/PL)

TURNILL, M. C., HPD programming at Rutherford Lab., 19: 38986 (CERN-65-11(p.173-81))

TYBOR, Vatslav, Isomagnetic interactions of Yang-Mills field, 19: 39634

TYBOR, Vatslav, Magnetic-moment-type interactions of fields with spin 1, 19: 39635

TYCKO, D., Integral FILTER technique for HPD, 19: 38985 (CERN-65-11 (p.153-72))

TYREE, Ella B., Regional oxygenation and therapeutic response to irradiation, 19: 38374

TYSON, R. F. S., Kinetics of oxidation of carbon and graphite by oxygen at 500 to 600°C, 19: 39119

TYUNINA, E. S., Effect of surrounding gas pressure on physical state of arc discharge plasma, 19: 39989

U

UCHIDA, Yutaka, Standing mode of compressional-body gravity wave in solar chromosphere, 19: 39343

UDO, F., Disintegration in flight of deuterons under the influence of nuclear fields, 19: 39901

UEDA, Teruo, Radiation-induced addition reaction of alcohols to 1,2-dichlorotetrafluorocyclobutene and 1,2-dichlorohexafluorocyclopentene, 19: 38708

UEDA, Tomiko, Catalytic isotopic isomerization of deuterated toluene-d_1 on platinum black, 19: 38693

UGLIRZH, M., On the structure of vector and axial currents in broken U(12) symmetry, 19: 39467 (JINR-E-2194)

UHLMANN, D. R., Evacuate-back fill glove box, 19: 38947

ULARIU, A., Study of the U(VI)-pyridyl-azo-resorcinol system, 19: 38594

ULLRICH, H., Disassembly and sampling of graphite ball fuel elements, 19: 38792 (JUL-250-RW)

UMEMURA, Isao, Model of hadrons based on the group Sp(6), 19: 39568

UNNERUS, C.-E., Automatic application unit for intracavitary radiotherapy, 19: 38483

UOTILA, U., Strontium-90 content of human bones in Finland, 1960-1962, 19: 38850

URIANO, G. A., Nuclear resonance spin-echo study of ^{153}Eu in EuO, 19: 39840

USKOV, V. S., Development of scintillation and ionization methods of radiometry and dosimetry, 19: 38995 (NP-15259)

V

VACLAVIK, J., Two-stream instability of radial inhomogeneous electron beams, 19: 40030

VAISLER, L., Radioactivity in thyroid and plasma of rats marked with ^{131}I and treated with vitamin B_{12}, 19: 38337

VALERINO, M. F., Noise analysis in nuclear systems, 19: 40164

VALKOVIC, V., Study of (n,p) and (n,d) reactions on ^{10}B at 14.4 Mev, 19: 39798

VAN DEN BRINK, H. A. S., Effect of oxygen pressure on radiosensitivity of Ehrlich ascites tumours at various intervals after inoculation, 19: 38402

VAN DE PUTTE, P., Location of genes controlling radiation sensitivity in Escherichia coli, 19: 38397

VAN DE WIELE, F., Color centers in CaBr single crystals irradiated at liquid-helium temperature, 19: 40098

VAN DILLEWIJN, Jeannette, Location of genes controlling radiation sensitivity in Escherichia coli, 19: 38397

VAN DONG, Nguyen, Effect of fast neutrons on thermoelectric capacity of Ge measured at low temperatures, 19: 39240

VAN GELDER, Gary, Effects of subcutaneous implantation of rare-earth metals, 19: 38334 (COO-1170-1)

VAN GURP, G. J., Measurement of noise in the resistive state of type II superconductors, 19: 39709

VAN HEYST, Hans P., Prog. rpt. on thermoelectric modules, 7/15-10/15/63, 19: 39430 (AD-426092)

VAN LINT, V. A. J., Radiation effects on pressure transducer components. Final report, 19: 39055 (GA-6266)

VAN OERTZEN, W., Mechanism of the reaction $^{11}B(^{16}O,^{15}N)^{12}C$ at 30 Mev, 19: 39869

VAN OOIJEN, D. J., Measurement of noise in the resistive state of type II superconductors, 19: 39709

VAN OSTENBURG, D. O., Nuclear-spin-lattice relaxation of ^{51}V and ^{99}Tc in V-Tc alloys, 19: 39403

VAN ROOSBROECK, W., Yield and Fano factor of electron-hole pairs generated in semiconductors by high-energy particles, 19: 39250

VAN SLUIS, C. A., Location of genes controlling radiation sensitivity in Escherichia coli, 19: 38397

VAN SUCHTELEN, J., Guided motion of vortices and anisotropic resistivity in type-II superconductors, 19: 39694

VAN TORNE, L. I., Specific electrical resistivity and interstitials in Ta crystals, 19: 39203

VAN TUYL, H. H., Promethium isotopic power data sheets, 19: 39069 (BNWL-C-45)

VAN WINDEN, Maria P., Range of action of genes controlling radiation sensitivity in Escherichia coli, 19: 38398

VARDENGA, G., An investigation of the leptonic decays of K_ξ mesons, 19: 39474 (JINR-P-2190)

VARFOLOMEEV, A. T., Nuclear photoeffect on three-particle nuclei, 19: 39809

VARNASAVANG, V., Influence of horizontal air motions on F2-region ionization, 19: 39668

VASILESCU, C., Study of the U(VI)-pyridyl-azo-resorcinol system, 19: 38594

VASIL'EVA, N. V., Four-prong stars in π^-p interactions at 3.5 Bev, 19: 39591

VASSILEV, V. N., Auto-immunization and auto-allergization in guinea pigs infected with tuberculosis with preliminary x-ray treatment, 19: 38375

VAURAMO, E., Automatic application unit for intracavitary radiotherapy, 19: 38483

VEALL, N., The partition of trace amounts of xenon between human blood and brain tissues at 37 deg C, 19: 38353

VEBERSIK, V., Work hazard and required time of hospitalization in intraperitoneal administration of colloidal Au^{198}, 19: 38476

VEDEL, J. P., Automatic following of tracks in nuclear emulsions, 19: 39017

VEDENOV, A. A., Thermodynamics of a plasma, 19: 40058

VEGNI, G., Evidence for new $\pi^+\pi^-$ resonance at 1.67 Bev, 19: 39537

VELICHKO, V. A., Device for improving stability and pulse counting in Geiger counter, 19: 39021

VELIEV, B. S., Arsenate-iodometric determination of Y, 19: 38551

VELTMAN, M., Baryon-resonance production by neutrinos, 19: 39517

VELYUKHOV, G. E., Interactions of 14.1-Mev neutrons with tritium, 19: 39939

VERDEYEN, J. T., High-frequency laser interferometry in plasma diagnostics, 19: 39993

VERDIER, Jacques, Magnetic tailing in ferromagnetic transition metals irradiated with electrons at 22°K, 19: 39239

VERDONE, Janine, Magnetic tailing in ferromagnetic transition metals irradiated with electrons at 22°K, 19: 39239

VEREBRYUSOV, V. S., Data on p,p reactions with Q = 148 Mev, 19: 39479 (NP-39479)

VERKAMP, J. P., Prog. rpt. on electromagnetic alkali metal pump, 12/27/63-3/27/64, 19: 38781 (N64-25903)

VERKHOGLYADOVA, T. S., Lanthanum silicides and their crystal structure, 19: 38613

VERKHOVSKII, B. I., The use of radioactive isotopes for checking production processes, 19: 39067

VERNON, Philippe, Photometric results of a special survey for interlopers, 19: 39349

VERTES, Paul, Bell furnace for the preparation of uranium metal by magnesiothermic reduction, 19: 39113

VESELOVSKII, G. S., Data on p,p reactions with Q = 148 Mev, 19: 39479 (NP-15216)

VEYRIE, P., Electric discharge in hydrogen and deuterium, 19: 39286

VICKERY, Austin L. Jr., Autoradiography of the thyroid, 19: 38533

VIDAURRE, Rafael, Time variations in cosmic rays and radiosonde measurements. Final technical report, 19: 39421 (NP-15154)

VIETZKE, H., Production of nuclear fuels. II., 19: 39104

VIGILEVA, E. S., Lanthanum selenides, 19: 38614

VILLA, F., Double production of charged pions in hydrogen by photons of energy between 600 and 850 Mev, 19: 39519

VILLE, M., Parity of the $Y_1^*(1660)$, 19: 39540

VISCONTI, A., The structure coefficients of proper self-energy parts for simple models of quantum field theory, 19: 39653

VISKNEVSKII, V. F., Applicability of isobar model for Λ hyperon production in π^-p interactions, 19: 39593

VITKOVA, S., Cerebral circulography with radioisotopes, 19: 38489

VITKOVITSKY, I. M., Ultrafast high-voltage probe, 19: 40038

VLASOV, I., Nuclear weaponry and protection against it, 19: 40301

VOEROES, T., New α-decay barrier penetrabilities with IGO potential, 19: 39789
VOGEL, R. S., Spectrochemical method for determination of U in electrolyte, 19: 38544 (MCW-1492, pp 13-19)
VOGEL, R. S., Spectrochemical method for determination of impurity elements in Th compounds, 19: 38545 (MCW-1492, pp 23-8)
VOIPIO, A., Strontium-90 in the Baltic Sea, 19: 38901
VOITOVICH, I. D., Superconductivity of lanthanum films, 19: 39745
VON BAECKMANN, A., Fission technetium. I., 19: 39892
VON BAEYER, H. C., Nonobservability of pseudoscalar charge density, 19: 39516
VON HAGENOW, Karl, Connection between correlations and fluctuations in plasma, 19: 40024
VON MOLNAR, S., Ferromagnetic and paramagnetic resonance in EuS, 19: 38649
VOROBEV, A. M., Chromatographic method of determining U and Pu in air, 19: 38554
VOROTNISTSKAYA, I. E., Biogenic migration of U in the lake Issyk-Kul, 19: 38855
VORTMAN, L. J., Close-in air blast from row charge in basalt, 19: 38790 (PNE-608F)
VOS, G., Contribution to the quantitative x-ray spectroscopic determination of traces of elements, using direct electron excitation, 19: 38571
VOSKRESENSKAYA, N. K., Reaction of $NaPO_3$ with Ce, Nd, and Sm oxides, 19: 38668
VOSLAMBER, D., Effect of ion-neutral collisions on plasma rotation, 19: 40052
VOUTILAINEN, Antero, Effect of x irradiation of laryngeal cancer on function of thyroid, 19: 38484
VOZENILEK, Fr., Measurement of pH value and conductivity of distilled water in primary circuit of reactor WWR-S in Rez, 19: 40263 (ZFK-RN-17 (p.32-43))
VUILLARD, Guy, Thermoelectric properties of boron carbide at high temperatures, 19: 38605
VUJNOVIC, V., Behavior of first Balmer lines in high-density plasma, 19: 39990
VULCHANOV, V. H., Auto-immunization and auto-allergization in guinea pigs infected with tuberculosis with preliminary x-ray treatment, 19: 38375
VULETIN, J., Cross sections for some (n,2n) reactions, 19: 39797
VYCHYTIL, P., A brief report on measurements of ambient radioactivity and radioactivity of food in Austria during 1963, 19: 38860
VYSOTSKY, G. L., Cluster stripping processes, 19: 39829

W

WABER, J. T., Augmented plane wave calculations of band structure of Ce metal, 19: 40081 (SC-DC-65-1500)
WACHSMANN, F., Quantity and quality of scattered x rays, 19: 38524
WADDELL III, J., Determination of depth variation in solar photosphere total photon flux, 19: 39342
WADDINGTON, C. J., Electrons, H and He nuclei in primary cosmic radiation, 1963, 19: 39420 (NP-15117)
WADDINGTON, C. J., Helium nuclei of primary cosmic radiation as studied over solar cycle of activity, 19: 39427
WADE, C. G., Nuclear spin relaxation in gases and liquids. IV., 19: 39378
WADSWOTH, B., Precision encoding and pattern recognition system, 19: 38978 (CERN-65-11(p.81-90))
WAEPPLING, R., Nuclear g factor of the 3.2-Mev 5^- state in the double-closed shell nucleus ^{208}Pb, 19: 39843
WAGGONER, M. A., Angular correlations for $^9Be(^3He,\alpha)^8Be \rightarrow 2\alpha$ reaction, 19: 39916
WAGGONER, M. A., Reaction $^9Be + {}^3He \rightarrow 3\alpha$, 19: 39898
WAGGONER, M. A., Reaction $^{10}B + {}^3He \rightarrow p + 3\alpha$, 19: 39899
WAGGONER, M. A., Reaction $^6Li + {}^3He \rightarrow p + 2\alpha$, 19: 39900
WAGGONER, M. A., Spectroscopic studies with the $^{10}B(^3He,p2\alpha)$ reaction, 19: 39917
WAHLBECK, P. G., Thermodynamics of yttrium–hydrogen system, 19: 38642
WAKASA, Akira, On the unification of hadronic and leptonic weak interactions, 19: 39573
WALDMAN, J., Prog. rpt. on metallic systems, annual, 1964, 19: 39168 (TID-22015)
WALKER, D. C., Nitrous oxide as a scavenger in the radiolysis of water, 19: 38720
WALKER, R. M., Prog. rpt. on radiation damage in solids, final, 4/62–3/65, 19: 39226 (AFCRL-65-305)
WALKER, R. M., Tracks of charged particles in solids, 19: 39038
WALL, N. S., Reaction $^{40}Ca(\alpha,2\alpha)^{36}Ar$, 19: 39902
WALLACE, A. C., Growth of mammary tumours in F_1 hybrids, 19: 38403
WALLER, Hans Dierck, Severe radioinduced hemolysis in hereditary deficiency of reduced glutathione in blood cells, 19: 38509
WALLIS, G. B., Rise velocity of cylindrical bubbles in inclined tubes, 19: 38808 (NYO-3114-8)
WALTER, Robert J., Progress in the development of refractory metals for use in nuclear rocket nozzles, 19: 40254
WALTERS, G. K., Nuclear spin-lattice relaxation in the presence of magnetic-field gradients, 19: 39880
WAND, R. H., The density spectrum of air showers at sea level and mountain altitudes, 19: 39424
WANG, C. P., Extrapolation of nucleon electromagnetic form factors, 19: 39458 (CONF-796(Paper 24))
WANSER, R., Evacuate-back fill glove box, 19: 38947
WARAVDEKAR, Vaman S., Skin changes induced by uv-irradiated linolenic acid extract, 19: 38366
WARCZEWSKI, Jerzy, Spark detectors and their uses, 19: 39019
WARD, A. G., Radio-frequency system for the Intense Neutron Generator, 19: 39759 (AECL-2177, Paper 6)
WARING, M. L., Future of nuclear power in New York City, 19: 40207
WARNER, P. C., Concrete pressure vessels for nuclear reactors, 19: 40134
WARNOCK, A. C. C., Gas laser measurements of electron density of a plasma, 19: 39978
WARNOCK, A. C. C., Time-dependent electron density measurements in a fast theta-pinch discharge, 19: 39979
WASSERMAN, R., Long interval time-to-pulse-height converter, 19: 39031
WATAGHIN, G., On a nonlocal theory, 19: 39495
WATANABE, Hironobu, Observation of γ-emitting nuclides with intermediate half lives in rain water, 19: 38557
WATANABE, Takeshi, Theoretical fitting of argon K absorption spectrum on a one-electron model, 19: 39411
WATERBURY, Glenn R., Determination of Pu in spent reactor fuels, Pu metal, alloys and compounds, 19: 38542 (LA-DC-6938)
WATSON, R. E., Nonlinear and linear shielding of rare-earth crystal-field interactions, 19: 40101
WATSON, W. W., Concentration dependence of thermal-diffusion factor for $^3He–^4He$ and $H_2–D_2$, 19: 38633
WATTS, Geoffrey P., The response of pressure transmission lines, 19: 38912 (LA-DC-7025)
WATTS, T., Precision encoding and pattern recognition system, 19: 38978 (CERN-65-11(p.81-90))
WAXMAN, Herbert J., Brain scans in diagnosis of cerebrovascular disease: Scanning with chlormerodrin Hg-203, 19: 38501
WAYMAN, C. M., Ferrous martensites, 19: 40283 (COO-1198-237)
WEAR, J. O., Reaction between U(IV) and various valence states of Np, 19: 38584 (SC-RR-65-219)
WEBB, H. P., Convenient ^{137}Cs unit for irradiating cell suspensions and small laboratory animals, 19: 38415
WEBB, R. W., Permeation of hydrogen through metals, 19: 39165 (NAA-SR-10462)
WEBER, Karl Heinz, Device for measurement of surface contamination caused by α-emitting substances, 19: 39045
WEBER, Maximilian, Contribution to the reversal of pleochroic halos, 19: 38846 (ORNL-tr-698)
WEBRE, N., Integral FILTER technique for HPD, 19: 38985 (CERN-65-11 (p.153-72))
WEBSTER, J. Wallace, Determination of neutron flux in nuclear reactors, 19: 40157 (ORNL-TM-1175)
WEDEMEYER, R. J., Measurements of cross sections for photoproduction of π^+ on H in region of first resonance, 19: 39597
WEIERSHAUSEN, Walter, Oxygen adsorption on W and Re, 19: 39103
WEIGUNY, A., Coriolis coupling in the quantum mechanical n-body problem, 19: 39948
WEIL, J. L., Reaction $^9Be(^3He,n)^{11}C$ from 1.3 to 5.4 Mev, 19: 39832
WEINSTOCK, J., Resonances in light scattered from plasma, 19: 40029
WEINSTOCK, Jacques J., Prog. rpt. on removal of metallic ions by foaming agents and suspensions, annual, 7/63–6/64, 19: 40171 (RAI-350)
WEINSTOCK, Robert, New approach to special relativity, 19: 39637
WEINTRAUB, A. A., Control of liquid hydrogen hazards at experimental facilities, 19: 38875 (HASL-160)
WEINZIERL, P., Nondestructive testing of fuel elements, 19: 38825 (NP-15176)
WEINZIERL, Peter, Pair production cross sections for 6.13 Mev γ rays, 19: 39787 (SGAE-PH-19/1965)
WEISSENBERG, Gustav, Instrument for detection of infrared radiation, 19: 39049
WEISSMAN, Stanley, Gaseous diffusion in a temperature gradient, 19: 39291
WEISSMANN, A., Fine structure of the effective mass spectrum, 19: 39583
WELLS, E. R., Production of 10^{-9} torr within a large plasma container (DCX-1), 19: 39966 (ORNL-P-1245)
WELLS, Mark B., Applications of a language for computing in combinatorics, 19: 39079 (LA-DC-7160)
WENSINK, B. L., Anelastic after-effect in electron-irradiated Mo,

19: 39247
WENZEL, Martin, Simple activity measurements of doubly-labeled substances on chromatograms, 19: 38561
WERNER, E., On the applicability of a separable potential in nuclear physics, 19: 39949
WERTZ, John E., Trapped-hole center containing F in MgO, 19: 38729
WESOLOWSKI, J. J., Energy levels of ^{21}S and ^{19}Ne, 19: 39827
WESSELDIJK, A. Th. Groot, Experiences with the use of radioactive hydrogen in industry, 19: 38355
WESTBROOK, E. A., Flame plasma seeded with SF_6, 19: 40016
WESTGARD, J. B., Spin of the $Y_1^*(1405)$, 19: 39553
WESTPHAL, D., Quality of primary circuit water in research reactors, 19: 40260 (ZFK-RN-17(p.68-74))
WESTPHAL, D., Review of work at Rossendorf research reactor, 1961, 19: 40261 (ZFK-RN-17(p.179-98))
WETZEL, L., Measurements of γ-dose equivalent at the body surface by means of condenser ionization chambers, 19: 39015
WEYMANN, Roy, Depth of convective envelope on lower main sequence and depletion of Li, 19: 39336
WHEELER, O. H., Neutron-induced reactions in aromatic phosphorus compounds, 19: 38700
WHELAN, M. J., Inelastic scattering of fast electrons by crystals. I., 19: 40083
WHELAN, M. J., Inelastic scattering of fast electrons by crystals. II., 19: 40084
WHIPPLE, Eldon C. Jr., Method and apparatus for determining satellite orientation utilizing spatial energy sources, 19: 38957
WHITAKER, H. H., Quantitative powder method for the spark source mass spectrograph, 19: 38570
WHITE, D. E., Manufacture of glass-bonded fuels for Doppler coefficient measurement, 19: 39124 (ANL-6995)
WHITE, Robert K., The effects on rat behavior of developmental aberrations induced by irradiation in utero, 19: 38361 (TID-21951)
WHITEHEAD, A. Bruce, Resolution of semiconductor detectors for fission fragments, 19: 39033
WICKMAN, H. H., Moessbauer-effect study of relaxation effects in iron-dithiocarbamates, 19: 38653
WIDEROEE, R., Radiation protection in medical radiology, 19: 38523
WIDMER, A. E., The solubility of sodium in silicon, 19: 39204
WIGHTMAN, A. S., Axiomatic field theory, 19: 39628 (CONF-796(Paper 29))
WIGINTON, C. L., Almost longitudinal instabilities in plasma-beam system, 19: 40008
WILBUR, D. W., Chemical bonding and the sulfur K-x-ray spectrum, 19: 38588 (UCRL-12496)
WILCOX, T. P., AGN-GAM—an IBM 7090 code to calculate Army GCR spectra and multigroup constants, 19: 40176 (AGN-TM-407)
WILDE, K., Enrichment of inner components of isotope mixtures by Clusius-Dickel columns, 19: 39076
WILDENTHAL, B. H., Reaction $^3He(^3He,2p)^4He$, 19: 39913
WILDERMUTH, Otliss, Case for hyperbaric oxygen radiotherapy, 19: 38500
WILEY, John S., Burnout correlations from Russian literature, 19: 38814
WILHELMI, Z., Energy spectrum of α particles from the $^{159}Tb(n,\alpha)^{156}Eu$ reaction with 14.2-Mev neutrons, 19: 39780 (INR-596/PL)
WILKENS, M., Application of electron-microscopic fine-range diffraction for the determination of the rolling texture of Cu, 19: 39175 (ORNL-tr-638)
WILKINS, J. W. H., Harwell 2000 series linear ratemeter/integrator, 19: 39005
WILKINSON, D. T., Cosmic black-body radiation, 19: 39350
WILKINSON, M. C., ENOCH, (a one-dimensional space-dependent burn-up program, 19: 40147 (AEEW-M-448)
WILLARD, H. B., Sequential emission in the reaction $^7Li(d,\alpha)2n$, 19: 39915
WILLDIG, Edward, Mass spectrometer electrostatic analysers, 19: 38963
WILLENS, R. H., Superconductivity of Nb_3Ge, 19: 39725
WILLIAMS, E. T., The $\Omega_p = \Omega_n = ½$ excitations in the odd nucleus ^{173}Tm, 19: 39822
WILLIAMS, Elinor A., Radiosynthesis of ^{14}C-labeled 4-dimethylamino-3,5-xylyl methylcarbamate, 19: 38748
WILLIAMS, I. P. G., Dental lesions in rat induced by radiomimetic agents, 19: 38325
WILLIAMS, Lawrence E., Continuum resonances in $^4He(p,p')^4He$, 19: 39886
WILLIAMS, M. W., Magnetization of current carrying cold worked NbZr superconducting wires, 19: 39749
WILLIAMS, N. L., HWR power plant with 275-MW(e) PHWP and a 260-MW(e) BLWP units, 19: 40211
WILLIAMS, Robert E., Size of a solar H II region, 19: 39340
WILLIAMS, Robert M., Tunneling in III-V compound p-n junctions, 19: 38931
WILLIAMSON, G. K., Role of crystal structure in determining mechanical properties of graphite, 19: 39237
WILLIAMSON, H. E., Examination of Zy-clad UO_2 fuel rods, 19: 39234 (GEAP-4597)
WILLIS, A., Scattering of protons on C-12, 19: 39837
WILLIS, B. T. M., Neutron diffraction study of antiferromagnetism in UO_2, 19: 40091
WILLMANN, R. B., Study of Σ^- capture process in hydrogen, 19: 39510
WILLMOTT, J. C., Excited states of ^{52}Cr, 19: 39826
WILSKY, K., The $\Omega_p = \Omega_n = ½$ excitations in the odd nucleus ^{173}Tm, 19: 39822
WILSON, B. G., The density spectrum of air showers at sea level and mountain altitudes, 19: 39424
WILSON, J. A., Spark chamber photograph analysis using LUCIOLE, 19: 38976 (CERN-65-11(p.57-69))
WILSON, J. C., Variable-gradient, electron-beam heating methods for growing Zr single crystals, 19: 39137
WILSON, M. N., Design of efficient flux concentrators for pulsed high magnetic fields, 19: 38934
WILSON, R. H., Evaluation of exposure from multiple environmental sources in the environs of the Hanford plants, 19: 38874 (BNWL-SA-53)
WIMBER, Donald E., Cell cycle of mouse embryonic tissue under continuous γ irradiation, 19: 38405
WINCHESTER, John W., Rare-earth distributions in some rocks and associated minerals of the batholith of Southern California, 19: 38848
WINKLER, E. O., Regenerative H_2O–CO_2 trap and liquid N cooled No. 2 charcoal trap assembly, 19: 40120 (GAMD-5434)
WINKLER, R., Natural cation exchangers for purification of radioactive wastes, 19: 40130 (ZFK-RN-17(p.165-78))
WINSCHE, W. E., Fuel management in the settled-bed fast reactor, 19: 40178 (BNL-9279)
WINSLOW, G. H., Thermodynamic properties and atomic transport in UO_2 phase, 19: 39219
WINTER, R. G., Radiative capture of deuterons in ^{16}O, 19: 39830
WINTERNITZ (VINTERNITTS), P., On the structure of vector and axial currents in broken U(12) symmetry, 19: 39467 (JINR-E-2194)
WINTON, John, Improvements relating to Zr-base alloys, 19: 39223
WISTOR, J. W., Extended range velocity gage for measurements in high shock environments, 19: 38917 (SC-R-65-904, pp 23-48))
WISTOR, J. W., Four papers concerning recent work on ground motion measurements, 19: 38864 (SC-R-65-904)
WISWALL, R. H. Jr., Radiation chemistry of cyclic fluorocarbons, 19: 38709
WITTELS, M. C., Observations of dislocations in Cu using Borrmann transmission topographs, 19: 39241
WITTENBERG, L. J., Prog. rpt. on reactor fuels and materials, annual, 1964, 19: 39163 (MLM-1244)
WITTIG, J., Superconductivity of germanium and silicon under high pressure, 19: 39701
WITTIG, J., Superconductivity of selenium under very high pressure, 19: 39736
WOLF, Clarence J., Recombination in γ-irradiated Si, 19: 40085
WOLFE, W. A., Some engineering problems with an Intense Neutron Generator, 19: 39760 (AECL-2177, Paper 7)
WOLFF, Sheldon, Far-red-induced mitotic delay and the apparent increase of x-ray induced chromatid aberrations in Tradescantia microspores, 19: 38416
WOLNIEWICZ, L., Variational treatment of the HeH^+ ion and the β-decay in HT, 19: 39799
WONG, C., Energy levels of ^{21}S and ^{19}Ne, 19: 39827
WONG, Chun Wa, Effect of short-range repulsion in nuclear matter. II., 19: 39814
WOO, James, Calculation of the thermal conductivity of pure superconducting lead, 19: 39732
WOOD, J. M., Prog. rpt. on chemical vapor deposition of Be from organo-beryllium compounds, final, 6/63–1/64, 19: 39102 (UCRL-13100)
WOOD, R. M., Neutrons from protons on isotopes of tin, 19: 39825
WOOLF, N. J., Mass loss and formation of white-dwarf stars, 19: 39337
WORLEY, R. D., Studies in x-ray production by proton bombardment of C, Mg, Al, Nd, Sn, Gd, Tb, Dy, and Ho, 19: 39881
WORLTON, D. C., High-voltage nondestructive test applications at Hanford, 19: 38823 (BNWL-SA-97)
WORRELL, Wayne L., Thermodynamic stabilities of Nb and Ta oxides, 19: 38586 (UCRL-11957)
WORT, D. J. H., Microwave emission from the Zeta plasma, 19: 39953 (CLM-R-40)
WORTH, Leonard V., Cesium-131 uptake and distribution in human heart, 19: 38502
WOZADLO, G. P., Corrosion of materials for nuclear superheat applications, 19: 39115 (GEAP-4760)
WOZNIAK, Jan, Effect of Co-60 radiation on vitamin content in flour, 19: 38423
WRIGHT, Harvel, Almost longitudinal instabilities in plasma-beam system, 19: 40008

WRIGHT, P. L., Life span of ovine erythrocytes as estimated from selenium-75 kinetics, 19: 38343
WU, Tsung-fan, Investigation of the energy spectra and angular correlations of particles in $K^0_2 \to \pi^+ + e^- + \nu$ decay, 19: 39586
WU, Tsung-shyh, The influences of pairing force on the properties of actinide nuclei, 19: 39927
WULFMAN, C. E., Molecular orbitals in momentum space, 19: 39660
WYBOURNE, B. G., Theoretical studies of lanthanide and actinide spectra, 19: 39383
WYLIE, A. W., Cerium tetrafluoride. I. Preparation and reactions, 19: 39182
WYLIE, A. W., Cerium tetrafluoride. II. System CeF_4–CeF_3, 19: 39183
WYLLER, Arne A., Globular clusters as remnants of quasars, 19: 39356
WYMER, R. G., Prog. rpt. on Th fuel cycle development, 10–12/63, 19: 38755 (ORNL-3611)

Y

YABE, Akira, Fallout radioactivity in diet and excreta. The levels at Tokai District, Japan in 1962 to 1963, 19: 38894
YAEGER, P., Antiproton annihilation in H at rest. I., 19: 39462 (CU-1932-239)
YAKOVLEV, V. I., Nuclear-active high-energy particles and the accompanying cosmic-ray extensive air showers, 19: 39429
YAKUBOV, I. T., State of gas behind strong shock wave, 19: 40040
YAM, Y. Y., Theory of the three-nucleon system, 19: 39923
YAMADA, Masao, Behavior of composite particles, 19: 39561
YAMADA, Masao, Bootstrap mechanism and symmetries of strong interactions, 19: 39559
YAMAGATA, N., Rapid radiochemical determination of ^{131}I in liquid milk, 19: 38560
YAMAGATA, Noboru, Geophysical variation in the total body burden of cesium-137 in Japanese people as assessed by blood analysis, 19: 38349
YAMAMOTO, Akira, New method of integral dose measurement with plastic scintillator phantom, 19: 38893
YAMAMOTO, R., Precision encoding and pattern recognition system, 19: 38978 (CERN-65-11(p.81-90))
YAMAMOTO, T., Hematological findings in those who survived in Hiroshima and Nagasaki, 19: 38378
YAMASHITA, Mikio, Observation of γ-emitting nuclides with intermediate half lives in rain water, 19: 38557
YANAGISAWA, T., Studies of radiation injury to the kidney, using radioisotope renograms, 19: 38379
YANG, Fu-yu, Studies on effect of ionizing radiation upon mitochondrial structure and function. I., 19: 38424
YANG, John Y., Radiolysis of binary paraffin-olefin solutions. II., 19: 38707
YANG, Wu-Kuang, Applicability of isobar model for Λ hyperon production in π^-p interactions, 19: 39593
YANNOPOULOS, L. N., Thermodynamics of yttrium–hydrogen system, 19: 38642
YANOVSKII, M. I., Radiochromatography used in investigations of heterogeneous catalytic reactions, 19: 38718
YANSHKEVICH, V. A., Quantitative analysis of complex γ spectra of radioactive metals and alloys, 19: 38566
YAREMBASH, E. I., Infrared absorption of $PrTe_2$, 19: 38618
YAREMBASH, E. I., Lanthanum selenides, 19: 38614
YARNELL, C. F., Nuclear spin relaxation in gases and liquids. IV., 19: 39378
YASUKAWA, Sigeru, Burn-up characteristics of pressure-tube-type D_2O-moderated power reactors, 19: 40185 (JAERI-1075)
YATSENKO, I. M., Investigation of neon plasma complex conductivity using a Q-meter, 19: 40041
YAZAKI, Koichi, Pion rescattering correction to decay rate of the hypertriton, 19: 39891
YEH, C., Interaction of microwaves with an inhomogeneous and anisotropic plasma column, 19: 39994
YEKUTIELI, G., Possible $N^*_{1/2}$ resonance at 1580 Mev, 19: 39548
YONEI, Katsumi, Weizsäcker correction to the Thomas-Fermi theory of the atom, 19: 39387
YOSHIDA, Yoshio, Studies on methodological procedures of radiation breeding. VI., 19: 38420
YOUNG, F. C., Reaction $^6Li + {}^3He \to p + 2\alpha$, 19: 39900
YOUNG, F. W. Jr., Observations of dislocations in Cu using Borrmann transmission topographs, 19: 39241
YOUNG, W. H., Long-range interionic forces in metallic Li, 19: 39211
YOUNG, Willis R., Neutron spectra from an organic scintillator, 19: 38997 (UCRL-16149)
YOUNGBLOOD, D. H., Reaction $^3He(^3He,2p)^4He$, 19: 39913
YUASA, Toshiko, Quasi-elastic (p,α) scattering in C^{13}, 19: 39908
YUREV, B. A., The energy distribution of photoprotons from ^{28}Si, 19: 39938

Z

ZAITSEVA, V. P., Behavior of Pu(V) nitrate solutions, 19: 38731
ZAITSEVA, V. P., Preparation and properties of Pu(V) nitrate solutions, 19: 38656
ZAITZEVA, T. F., Acetic compounds of trivalent Ce, 19: 38666
ZAKHAROV, V. I., K_{e4} decay and SU(3) symmetry, 19: 39589
ZAKHAROV, V. I., Strange-current vector constants in second approximation with respect to moderately strong interaction, 19: 39588
ZAKUTINSKII, D. I., Remote after-effects of ionizing radiation, 19: 38435
ZAKUTINSKII, D. I., The toxicology of radioactive substances, 19: 38357
ZAL'DOVICH, B. Ya., Non-conservation of CP parity and nature of law $\Delta T = \frac{1}{2}$, 19: 39476 (NP-15197)
ZALESKI, C. P., Utilization of Rapsodie reactor for measurement of Doppler effect, 19: 40150 (CEA-R-2565)
ZALOUBOVSKY, I. I., Investigation of $^{23}Na(d,\alpha)^{21}Ne$ reaction, 19: 39835
ZAMBERNARD, M. J., Preparation and properties of spherical particulate nuclear fuels for Pu-fueled reactors, 19: 39096 (CONF-117(p.103-26))
ZAMJA, K., Disassembly of test irradiations and fuel elements in small cast iron, α-γ-cells and their subsequent handling, 19: 38795 (JUL-253-RW)
ZANDER, Arlen R., Half life of ^{16}N, 19: 39813
ZANDER, K., ESONE—A nuclear electronics system, 19: 38924
ZANELLA, P., Automatic analysis of spark chamber pictures using the CERN HPD, 19: 38974 (CERN-65-11(p.25-33))
ZANELLA, P., Program developments in CERN-FSD spark system, 19: 38977 (CERN-65-11(p.71-9))
ZAPPA, L., Three-quantum annihilation of positrons in metals and insulators, 19: 39546
ZARKOVA, L., High pressure Cs thermionic converter with W cathode, 19: 39436
ZASLAVSKY, B., Integral FILTER technique for HPD, 19: 38985 (CERN-65-11(p.153-72))
ZAVOISKII, E. K., Turbulent heating of plasma, 19: 40047
ZDANSKY, K., ESR of NO^0_3 in irradiated $Ba(NO_3)_2$ single crystal, 19: 38730
ZETTERSTROEM, H. O., Magnetic moments of single particle states in ^{207}Pb and ^{209}Bi, 19: 39870
ZHARNOVETSKI, K., Ion-exchange filter for EWA reactor, 19: 38760 (ZFK-RN-17(p. 127-38))
ZHELEZNYKH, I. M., Covariant method for calculating cross sections and its application to some reactions induced by neutrinos, 19: 39943
ZHIGARNOVSKII, B. M., Phase composition of CaF_2–YF_3, SrF_2–YF_3, and BaF_2–YF_3, 19: 38615
ZHIROV, E. P., Complexing of 2-hydroxyethyliminodiacetic acid with rare earth elements, 19: 38671
ZHIVOPISTSEV, V. P., Complexing in Sc–diantipyrilmethane–iodide system, 19: 38670
ZHUKOVA, I. A., Niobium enthalpy between 600 and 2600°K, 19: 39217
ZHUKOVSKII, N. N., The γ spectrum of ^{152}Eu with the half life 9.2 hours, 19: 39928
ZHURAVLEVA, M., An investigation of the leptonic decays of K^0_2 mesons, 19: 39474 (JINR-P-2190)
ZICHICHI, A., Symmetries in elementary particle physics, 19: 39602
ZIEGLER, Albert, Recovery of D_2O and H-3 from air of closed rooms of nuclear reactor installations, 19: 38907
ZIEGLER, Dewey K., Brain scans in diagnosis of cerebrovascular disease: Scanning with chlormerodrin Hg-203, 19: 38501
ZIEGLER, J. F., Elastic electron scattering from lead isotopes and possible dispersion effects, 19: 39860
ZIEGLER, Max, Separation of Sr from Y ($^{90}Sr/^{90}Y$) using anion exchanger sulfate, 19: 38774
ZIMANYI, J., Circular polarization of γ quanta accompanying reaction $^{10}B(d,p)^{11}B$, 19: 39937
ZIMMERMANN, E., Viscosimetric studies of kinetics of thermal denaturation of DNA, 19: 40299 (LA-tr-65-12)
ZIMMERMANN, H. J., Prog. rpt. on electronics, 4/15/65, 19: 39270 (TID-21894)
ZINN, Walter H., Power Reactor Technology, Vol. 7, No. 3, 1964, 19: 40215
ZINOV, V. G., Atomic capture of μ^- in chemical compounds, 19: 39366 (JINR-P-2185)
ZOLIN, L. S., Distribution of penetrating radiation field over protective zone of 10-Bev synchrophasotron, 19: 39315 (JINR-P-2177)
ZOLOTAVIN, A. V., 3-hour activity of lutetium, 19: 39931
ZOMBKOVSKII, S. M., Four-prong stars in π^-p interactions at 3.5 Bev, 19: 39591
ZORINA, E. L., Infrared absorption of $PrTe_2$, 19: 38618
ZUCALI, R., Biological effects of radioactive phosphorus. An electrophoretic study of whole and denatured serum, 19: 38368
ZUMWALT, L. R., The release of condensable fission products from the GAIL III-B fuel element, 19: 39233 (GAMD-6321)

ZUPANCIC, C., Survey of simple mechanisms of three-particle reactions, 19: 39894
ZWEIG, G., Fractionally charged particles and SU_6, 19: 39607
ZWILLENBERG, Melvin, Prog. rpt. on combustion of metals, 7–12/64, 19: 38583 (SC-DC-65-1480)
ZYGIELBAUM, Joseph I., On the combination of the phase contrast process with fluorescence microscopy, 19: 38923 (UCRL-Trans-1228)
ZYKOV, V. G., Study of a plasma bunch in motion in a toroidal magnetic field, 19: 39963 (NP-15198)

SUBJECT INDEX

Main entries in this index are generally specific materials, things, and processes. These are followed by modifiers that describe the properties of, and processes applied to, the main entries.

The number preceding the colon is the *NSA* volume number, and the number following is the abstract number. The designation (R) following the abstract number indicates that the abstract is of a progress report; (P) indicates a patent; and (T) indicates a translation. Abstracts for reports other than progress reports carry no letter designation. References to report numbers, where appropriate, are included after the abstract number of the citation. Published literature (journal article or book) is identifiable by the absence of a report number.

The user should bear in mind that the ideas presented in the original literature, rather than key words, have been indexed. The indexers have tried to select what seemed the most probable and logical place to look for typical information. Since it is not possible to anticipate where a user would look for information, numerous cross references are included to assist him in his search.

Experience in using an index of this type will be the best guide in obtaining the desired information, and a consideration of synonymous or closely related terms will prove valuable.

Information must be so indexed as to be of the greatest use to the greatest number of users. This requires that a topic be indexed to headings that most specifically describe it and not ordinarily to the headings that describe its ultimate use, nor to the general class headings that include the specific headings. For example, information on the treatment of thyroid disease with I-131 would be indexed under Thyroid Diseases and under Iodine Isotopes I-131, but not necessarily under Radiotherapy. A study of the effects of x radiation on hair would be indexed under both X Radiation and Hair.

The broad, general class headings are used only for general information or for comprehensive reports or articles.

Subject Heading Styles

Generally, the direct form of subject entry is used rather than inverted headings or, in some cases, subheadings; e.g., Amino Acids rather than Acids, amino; Helium Isotopes He-4 rather than Helium — isotopes He-4 or Helium — He-4 isotopes. Note, however, that in some cases modifying terms are used parenthetically in preference to a more direct type of entry which would result in the scattering of information. Organic compounds, however, are usually entered in the index in the inverted form so that substituted compounds can be listed near the parent compound; e.g., Benzene, Bromo- rather than Bromobenzene. In general, the style of nomenclature used is that of *Chemical Abstracts*, except that some items listed in that publication as subheadings are elevated to form part of the main heading; e.g., Butyric Acid, Methyl Ester rather than Butyric Acid — methyl ester.

Alphabetization

Main headings are arranged according to the widely accepted word-by-word alphabetic system. A parenthetic qualifier following a main heading is disregarded in alphabetizing unless there are two or more headings identical except for the parenthetic qualifier, in which case the qualifier determines the order. Headings involving Greek letters are arranged as if the names of the letters were spelled out, e.g., Mesons (π), Mesons (ζ).

Nomenclature of Inorganic Compounds

Inorganic compounds are indexed in the direct form, listing cations in the order of increasing valence in the case of polycationic salts of varying valence and in alphabetic order for polycationic salts in which all cations have the same valence; e.g., Sodium Aluminum Silicates and Potassium Sodium Sulfates.

Multicomponent Systems

Multicomponent alloys, except well-known trade names, are indexed under each element in the alloy.

Example: Aluminum – Chromium Alloys are indexed

ALUMINUM ALLOYS
Al – Cr ...
CHROMIUM ALLOYS
Al – Cr ...

Well-known alloys such as Hastelloy are indexed directly. Cross references appear in the index cumulations. Multicomponent systems of elements are indexed similarly.

Example: Silicon – Tungsten Systems are indexed

SILICON SYSTEMS
Si – W ...
TUNGSTEN SYSTEMS
Si – W ...

Multicomponent systems of compounds are similarly indexed under the compound.

Physical States of Materials

Specification of the physical state of the material, if other than normal, is included in the modifying phrase.

Modifying Phrases (Subheadings)

Whenever it appears that such information would be useful, descriptive phrases (modifiers), rather than ordinary subheadings, are used under the main headings to give a better indication of the material covered in an abstract. Such phrases are written so that the idea considered most important is presented first. However, when using this index, the reader is advised to scan all modifiers under a main heading to determine whether any abstracts in addition to the most obvious should be consulted for the desired information. Many of the modifiers are designed to be read in inverted order or to be read with the main heading inserted at the position of the comma in order to obtain a meaningful phrase; e.g., Uranium – allotropic transformation temperatures of, effect of cooling rate on is read "effect of cooling rate on allotropic transformation temperatures of uranium." In many cases, the prepositions have been

omitted from such phrases provided no ambiguity results from the omission.

For entries concerned with physics, if the modifier does not indicate whether the reference is experimental or theoretical, a symbol E or T or E/T is given.

Conferences

Proceedings of conferences and conference papers are included in the Report Number Index.

A

ABSTRACTS
on nuclear materials management, 19: 39101 (TID-3315)
on plutonium technology, 19: 40281 (BNWL-113-5)
on thermionic and thermoelectric energy conversion, 19: 39434 (N64-26371)
ACCELERATORS
beam holes of, device for irradiating objects in, 19: 38831(P)
beam storage rings for, 19: 39325
beam transport systems for electron, effects of self-fields and external focusing elements on, 19: 39318 (UCRL-14194)
electrostatic field of uniformly charged cylindrical configurations in, (T), 19: 39314 (JINR-P-2131)
fermion helicity and transverse momentum in circular, (T), 19: 39320
magnets for, field calculations for bending, 19: 39317 (NRL-6248)
targets for, preparation of calcium, magnesium, and strontium, 19: 38658
use to sterilize catgut surgical bandages, pharmaceutical preparations, and blood-collecting equipment, 19: 39063
ACETAMIDE, IODO-
effects on sensitization of *E. coli* B capacity for phage T3, 19: 38455
ACETATE COMPLEXES
with cerium, preparation and properties of, 19: 38666
ACETIC ACID
dissociation in heavy water at 5 to 50°C, thermodynamics of, 19: 38645
ACETIC ACID, [(CARBOXYMETHYLIMINO)BIS(ETHYLENENITRILO)]TETRA-
effects on fission product motion in soils, 19: 38329 (TID-20471)
ACETIC ACID, (CYCLOHEPTYLENEDINITRILO)TETRA-
reactions with zirconium, stoichiometry of, 19: 38667
ACETIC ACID, (1,2-CYCLOHEXYLENEDINITRILO)TETRA-
effects on fission product motion in soils, 19: 38329 (TID-20471)
ACETIC ACID, (ETHYLENEDIIMINO)BIS(o-HYDROXYPHENYL)-
effects on fission product motion in soils, 19: 38329 (TID-20471)
ACETIC ACID, [(2-HYDROXYETHYL)IMINO]DI-
complexes with rare earths, dissociation constants, 19: 38671
ACETIC ACID, IODO-
effects on iodine-131 metabolism in thyroid, 19: 38348
ACETIC ACID, NITRILOTRI-
reactions with zirconium, stoichiometry of, 19: 38667
ACETOACETIC ACID
bromination of esters of, deuterium isotope effects on, 19: 38692
ACETYLENE
acetylene–N_2–O_2, electron density in sulfur hexafluoride seeded flame plasma of, (E), 19: 40016
ACOUSTIC WAVES
propagation in inhomogeneous plasma column, dispersion curves for, (T), 19: 40028
propagation in ionized gases, analysis of, 19: 39270(R) (TID-21894)
propagation in plasma, correlation with radar auroral reflection data, (T), 19: 39678
ACRIDINES
effects of acridine orange on radioinduced chromosome aberrations in barley and *Vicia faba*, 19: 38462
ACRYLAMIDE
acrylamide–propionamide, radioinduced solid-state polymerization of, effects of oxygen on gamma, 19: 38694 (BNL-9200)
ACRYLIC ACID, ETHYL ESTER
radioinduced grafting to chloroethylene polymers, 19: 38739(P)
ACRYLIC ACID, METHYL ESTER
radioinduced grafting to chloroethylene polymers, 19: 38739(P)
ACRYLONITRILES
radioinduced graft polymerization of vaporous, with ethylene polymers, 19: 38734
radioinduced grafting to chloroethylene polymers, 19: 38739(P)
ACTINIDES
separation from chloride solutions by ion exchange, 19: 39265(R) (IA-1021)
ACTINIUM ISOTOPES
nuclear properties of, pairing force effects on, (T), 19: 39927
ACTIVATION ANALYSIS
computer uses in, 19: 38568
gamma spectra in, equations for analysis of complex, 19: 38566
neutron sources and multipliers for use in, 19: 38565
of tooth enamel for trace elements, 19: 38562
precision of, using 14-Mev neutrons, 19: 38569
use for determination of elements and trace impurities in organic materials, 19: 38558
uses in forensic investigations, 19: 39265(R) (IA-1021)
ADHESIVES
use in fallout collection, 19: 38906(P)
ADRENAL GLANDS
radiation effects on function of rat, fast neutron, 19: 38443
radiation effects on morphology of rat, fast neutron, 19: 38444
ADRENALINE
effects on learning ability of rats, 19: 38361(R) (TID-21951)
AEROSOLS
analysis for plutonium and uranium, chromatographic, 19: 38554
charge state of ultra-fine, in weakly ionized media, 19: 39285
radioactive, filtration materials for respirators protecting against, 19: 38900
radioactivity of atmospheric, methods of measuring, 19: 38903
radioisotope content in atmospheric, apparatus for collecting and measuring, 19: 38896
AGE
effects on learning ability of rats irradiated *in utero*, 19: 38361(R) (TID-21951)
effects on radioinduced intercapillary glomerulosclerosis in mice, 19: 38409
AGE ESTIMATION
potassium–argon method of, for Vindhyan system in India, 19: 38853
uranium–helium methods of, for Pleistocene and Tertiary fossile aragonites, 19: 38868
uranium–lead method of, for zircons, errors, 19: 38849
AGING
effects on cancer susceptibility in man, epidemiology, 19: 38364
AGRICULTURE
radiobiology applications for, 19: 38327
AIR
analysis for plutonium and uranium in aerosols in, chromatographic, 19: 38554
carbon arcs in, temperature profile of low-current, (E), 19: 39986
corrosive effects on plutonium–titanium–uranium alloys, 19: 40177(R) (ANL-7046(p.1-35))
dust combustion in, ignition propagation processes for, 19: 38827
electron reactions at low energies, energy dependence of ion pair production in, 19: 39375
excitation and relaxation behind strong shock waves, equations for, (T), 19: 40040
gamma attenuation in, 19: 39483 (SGAE-PH-20/1965)
radioactivity in, maximum permissible concentrations of uranium-235 fission products in, 19: 38872 (AEET/HP/TH-15)
separation from plutonium hexafluoride by filtration, 19: 40113(R) (ANL-7071)
ALANINE
radiation effects on aspartic acid formation in aqueous solutions of, mechanism of, 19: 38702
ALANINE, PHENYL-
uptake by DNA, proteins, and RNA of L-cell nuclei, effects of tritiated thymidine on carbon-14-labeled-, 19: 38339
ALASKA
archeological survey of Ogotoruk Creek area, 19: 40289 (PNE-406)
archeological survey of Ogotoruk Creek area, 19: 40290 (PNE-407)
ALBUMINS
effects of radiophosphorus on denatured and whole, in rats, 19: 38368
labeled with iodine-131, tracer use, 19: 38525
radiation effects on sulfhydryl groups in animal blood, 19: 38427
use of iodine-131 labeled-, for photoscans of heart, 19: 38490
ALCOHOLS
reactions with phosphorus pentoxide, products of, 19: 39265(R) (IA-1021)
ALGAE
radiosensitivity of *Micrasterias truncata*, effects of illumination and darkness on, 19: 38410
uranium content in, in Lake Issyk-kul, USSR, 19: 38855
ALKALI METAL HALIDES
hydrogenation of, design of isothermal calorimeter for studying, 19: 38675
ALKALI METAL HYDROXIDES
vibration modes in, analysis of, 19: 39265(R) (IA-1021)
ALKALI METAL NITRATES
cation exchange with zeolite, 19: 39265(R) (IA-1021)
ALKALI METALS
electron-gas interactions in, one-particle Green's function for, 19: 39658
reactions of, nuclear spin effects on spin-exchange cross sections for, (T), 19: 39879
sorption on metal surfaces, bonding mechanisms of atomic, 19: 39270(R) (TID-21894)
ALKALINE EARTH HYDROXIDES
vibration modes in, analysis of, 19: 39265(R) (IA-1021)
ALKYL BROMIDES
radioinduced reactions with tin, 19: 39091(R) (BMI-1723(Del.))

ALKYL CHLORIDES
radioinduced reactions with tin, 19: 39091(R) (BMI-1723(Del.))
ALLOYS
diffusion of hydrogen through, review, 19: 39165 (NAA-SR-10462)
radiation effects on properties and structure of, 19: 39257(P)
specific heat of mixed state in superconducting, (T), 19: 39716
weight gain behavior of, in 1200°F steam, 19: 39156(R) (CEND-532)
ALPHA BEAMS
effects on cytoplasm of animal cells, 19: 38386
irradiation of single cells in tissue culture using micro-, 19: 38385
ALPHA DECAY
of even- and odd-mass nuclei, (T), 19: 39789
shell model calculations for deformed even-even nuclei, 19: 39793
ALPHA PARTICLES
angular correlations in beryllium-9 (He-3,α) reactions at 3.0 Mev, (E), 19: 39916
angular distributions and energy spectra from triton reactions (t,α) with lead-208 at 12.0 and 13.5 Mev, (E), 19: 39852
detection and measurement by liquid scintillation counting, refrigeration unit for cooling photomultiplier tube for, 19: 38546(R) (RFP-552)
detection and measurement of, design of flow counter for, 19: 39012
detection and measurement on contaminated surfaces, equipment for, 19: 39045(P)
detection using lithium-drifted position-sensitive detectors, 19: 39027
effects on luminescence of thallium-activated potassium iodide phosphors, 19: 38735
emission in deuteron reactions (d,α), spectra of, (E), 19: 39835
emission in proton reactions (p,3n) with boron-11, angular distributions, (T), 19: 39912
production in uranium-235 fission, measurement of, (E), 19: 39265(R) (IA-1021)
reactions ($\alpha,\alpha'\gamma$) with iron-56 at 22.2 Mev, (E), 19: 39865
reactions (α,2n) with silver-107 at 28 Mev, indium-109 gamma transitions from, (E), 19: 39861
reactions (α,2α) with calcium-40 at 28.7 and 30.5 Mev, angular and energy correlations, (E), 19: 39902
scattering by zirconium-90 at 34.4 Mev, excitation of 2^+, 5^-, and 3^- states by inelastic, (E), 19: 39844
spectra from beryllium-9 (He-3,$\alpha\alpha\alpha$) reactions, (E), 19: 39898
yield in lithium-6 reactions (Li-6,α) with carbon-12 at 4.0 to 5.5 Mev, (E), 19: 39853
ALPHA SOURCES
use in radiometric thickness gages, 19: 38965(P)
ALUMINATES
radiation effects on disintegration rate of solutions of, 19: 38738
ALUMINUM
analysis for trace amounts of copper, magnesium, silicon, and zinc by x-ray spectrography, 19: 38571
coating with aluminum–nickel layers by chemical deposition, 19: 39143(P)
combustion of, 19: 38583(R) (SC-DC-65-1480)
defect mobility in irradiated and tempered, (E), 19: 39246
electron inelastic scattering by crystals of, interband excitation in fast, (T), 19: 40083
electron reactions at 80 kev, transition radiation from, (E), 19: 40099
electron reactions with atomic, screening effects on bremsstrahlung and pair production in, (T), 19: 39389
electron tunneling from thin-film type-II superconducting, magnetic-field effects on, (E), 19: 39718
mercury ion reactions with ion emission in, (E), 19: 39374
neutron albedo measurement on, thermal, 19: 40065 (NP-15152)
neutron reactions (n,n'γ) at 0 to 14 Mev, energy absorption in, 19: 39769 (SC-DC-65-1544)
nuclear magnetic resonance in superconducting, spin-orbit coupling effects on Knight shift in, (T), 19: 39727
positron annihilation in, 3-quantum, (E/T), 19: 39546
proton inelastic scattering at 15 to 1900 kev, x-ray yields from, (E), 19: 39881
radiation effects on, electron, 19: 40286(R) (NAA-SR-11200)
radiation effects on, for manned space stations, 19: 40063 (NP-15125)
rare-gas ion reactions at 1 to 10 kev, secondary-electron emission in, (E), 19: 39404
separation from graphite above 1750°C in inert gases, 19: 38762
transition temperature of thin films of superconducting, effects of thin oxide layer on, (E), 19: 39746
use as threshold detectors for fast neutrons, (E), 19: 39007
ALUMINUM ALLOYS
corrosion by sodium chloride at 150°C of types 5454 and 6061, electrochemical, 19: 39117 (ORNL-P-1430)
properties for use as fuel cladding material in reactors, 19: 39206
Al–Ag, Guinier-Preston zones in, x-ray and electron microscopic studies of size of, 19: 39172(T) (ORNL-tr-633)
Al–Ag, radiation effects on, annealing electron, 19: 40286(R) (NAA-SR-11200)
Al–Ag, strain hardening of, x-ray studies of segregation zones in, 19: 39174(T) (ORNL-tr-635)
Al–Ba, cesium-133 Mossbauer effect in, 19: 39295
Al–Cr–Fe–Mo–Ti, mechanical properties and heat resistance, 19: 39193
Al–Cr–Fe–Mo–Ni–Nb–Ti, thermal response and microstructure of Inconel 718 at 1200 and 1400°F, 19: 39158 (GEAP-4751)
Al–Ge, radiation effects on, annealing electron, 19: 40286(R) (NAA-SR-11200)
Al–Mg, dislocation climb in quenched, kinetics of, 19: 39169 (UCRL-16090)
Al–Mg, radiation effects on, annealing electron, 19: 40286(R) (NAA-SR-11200)
Al–Mg, use in preparation of uranous chloride by reduction of uranyl chloride, 19: 38662
Al–Mg–Mn–Zn, plastic anisotropy of AZ31B sheet, 19: 39149 (AD-425880)
Al–Pu, thermal cycling effects on, 19: 39125(R) (BNWL-91)
Al–Sn–Ti, plastic anisotropy of alpha, 19: 39149 (AD-425880)
Al–Zn, precipitation of Guinier-Preston zones in, heat tone, 19: 39173(T) (ORNL-tr-634)
ALUMINUM CHLORIDES
reactions with thorium chlorides at high temperatures, 19: 38755(R) (ORNL-3611)
reactions with zirconium chlorides at high temperatures, 19: 38755(R) (ORNL-3611)
ALUMINUM FLUORIDES
reactions with potassium niobium fluoride to prepare niobium fluoride, 19: 38640
ALUMINUM ISOTOPES Al-28
neutron separation energy for, (E), 19: 39862
ALUMINUM OXIDES
radiation effects on coatings of, on uranium dioxide fuel particles, 19: 39227 (BMI-1729)
radiation effects on hydrogen adsorption on, 19: 38717
radiation effects on preparation from aluminate solutions, catalytic, 19: 38738
sorptive properties of gamma-phase, for metal cations in fused salts, 19: 38771
thermal conductivity, 19: 40113(R) (ANL-7071)
ALUMINUM SYSTEMS
Al–Fe–Mg–Ni–Si–Ti–Zr, coating with aluminum–nickel layers by chemical deposition, 19: 39143(P)
Al–graphite, deposition of coatings of, at 1500 to 1750°C, 19: 39144(P)
AMERICIUM
distribution between dibutylbutylphosphate–xylene and nitrate solutions, 19: 38750 (HW-81166)
properties, production, sources, and uses of, 19: 39191
separation from irradiated plutonium by solvent extraction, 19: 39265(R) (IA-1021)
separation from promethium by ion exchange, 19: 38772
AMERICIUM ISOTOPES
nuclear properties of, pairing force effects on, (T), 19: 39927
properties, production, sources, and uses of, 19: 39191
AMERICIUM ISOTOPES Am-241
alpha decay, (E), 19: 39946
alpha decay of, recoil particle charge and energy loss from, 19: 39882
detection and measurement in man using whole-body counter, 19: 38546(R) (RFP-552)
AMINO ACIDS
genetic code for, during synthesis of messenger ribonucleic acid, 19: 40296 (TID-21856)
radiation effects on bacteriophage, EPR spectra, 19: 38365
AMMONIA
diffusion in liquid, radioisotopic study of self-, 19: 38579 (JUL-238-PC)
reactions with cerium tetrafluoride at low temperatures, 19: 39182
spectra of inversion transition in, measurement of 3-3 line of, (E), 19: 39270(R) (TID-21894)
NH_3–UO_2, preparation and properties of slurries of, for fissiochemical production of hydrazine, 19: 39095 (CONF-117(p.81-97))
AMMONIUM BORATES
tetramethyl-, use as standard for titrating boron solutions, 19: 38548 (UCRL-14166-T)
AMMONIUM CHLORIDES
acoustic velocities in, effects of pressure on, 19: 39270(R) (TID-21894)
AMMONIUM COMPOUNDS, QUATERNARY
tetramethylammonium octahydrotriborate, use as standard for titrating boron solutions, 19: 38548 (UCRL-14166-T)
AMMONIUM FLUORIDES

use as electrolyte in deposition of uranium films on metals, 19: 39100 (SGAE-SH-16/1965)
AMMONIUM IRON(II) SULFATES
Mössbauer effect in ice, temperature dependence of, (E), 19: 39715
AMMONIUM NITRATES
properties in chemical radiation dosimetry, 19: 39042
AMMONIUM URANATES
thermal decomposition of, mechanism of, 19: 38660
AMOEBA
radiation effects on protein and RNA content in, 19: 38371
AMPLIFIERS
design of d-c, 19: 38961(P)
AMYLASES
radioinduced deactivation of, effects of copper on, 19: 39265(R) (IA-1021)
ANIMAL CELLS
chromosome analysis in photographs of, using flying-spot devices, (E), 19: 38910 (CERN-65-11(p.43-56))
genetic studies of, 19: 38328
radiation effects on cytoplasm of, in tissue culture, 19: 38386
radiation exposure of single, in tissue culture, using micro alpha beam, 19: 38385
radiation injury and repair in, 19: 38407
uptake of carbon-14-labeled-precursors by DNA, proteins, and RNA of L-cell nuclei, effects of tritiated thymidine on, 19: 38339
ANIMAL RESPIRATION
effects of aminoethylisothiourea in mice, 19: 38469
effects of cysteamine in mice, 19: 38469
ANIMALS
book: *Biological Effects of Neutron Radiation*, 19: 38437
metabolism and toxicology of radioisotopes in, 19: 38357(T)
population studies on, in uranium areas of Upper Colorado River Basin, Utah, 19: 38330 (TID-22078)
radiation dosimetry in tissues of, method for, 19: 38439
radiation effects on, effects of pyridoxal-5'-phosphate on, 19: 38461
radiation effects on, protective effects of chemicals against, 19: 38472(T)
radiation effects on, remote late, 19: 38435(T)
radiation sickness pathology, 19: 38426
radiation sickness effects on infection and natural immunity in, 19: 38434(T)
radiation sickness in, anatomy and pathology of, 19: 38436(T)
ANION EXCHANGE MATERIALS
sorptive properties of Dowex 1-X8 for scandium, rare earths, thorium, and uranium in nitrate solutions, tracer studies of, 19: 38770
ANODES
reaction distribution in porous, method for measuring, 19: 38591 (UCRL-16113)
ANOXIA
effects on radiosensitivity of tumors, regional, 19: 38374
protective effects against radiation injuries in mice, 19: 38450 (USNRDL-TR-851)
ANTIBARYONS
interactions with nucleons at high energy, Regge-pole hypothesis in asymptotic amplitudes for, 19: 39478 (NP-15210)
interactions with protons, U(12) symmetry for total cross sections for, 19: 39529
ANTIBIOTIC THERAPY
effects for inflammations associated with radiotherapy, 19: 38512
ANTIBIOTICS
effects of cruzine on tumor growth in mice, synergistic effects with 19: 38428
ANTIBODIES
effects of spleen cell transplants on formation of, in irradiated mice, 19: 38454
ANTIGENS
radiosensitivity of, *Cl. perfringens*, 19: 38447
structure in radioinduced mutations of *Clostridium perfringens*, 19: 38445
ANTIMONY
electric conductivity in ohmic contact with normal metal at low temperatures, (E), 19: 39734
gamma scattering by, spectra of nonresonant, (E), 19: 39265(R) (IA-1021)
magnetostriction in pure monocrystalline, 19: 39199
ANTIMONY ALLOYS
Sb–Bi, electric conductivity in ohmic contact with normal metal at low temperatures, (E), 19: 39734
Sb–Ga, spectral analysis of photoemission yields from cesiated surfaces of, 19: 39406
Sb–In, radiation effects on, electron, 19: 40286(R) (NAA-SR-11200)
Sb–Mo, crystal structure of intermetallic compounds in, 19: 39209
Sb–Nb, crystal structure of intermetallic compounds in, 19: 39209
Sb–Ta, crystal structure of intermetallic compounds in, 19: 39209
Sb–W, crystal structure of intermetallic compounds in, 19: 39209
ANTIMONY ISOTOPES Sb-116
energy level densities, (E), 19: 39825
ANTIMONY ISOTOPES Sb-117
energy level densities, (E), 19: 39825
ANTIMONY ISOTOPES Sb-118
energy level densities, (E), 19: 39825
ANTIMONY ISOTOPES Sb-120
energy level densities, (E), 19: 39825
ANTIMONY ISOTOPES Sb-121
neutron reactions (n,γ), gamma spectra of 6.25- and 15.6-ev resonance of, 19: 39781 (JAERI-1073)
ANTIMONY ISOTOPES Sb-123
neutron reactions (n,γ), gamma spectra of 21.6-ev resonance of, 19: 39781 (JAERI-1073)
ANTINEUTRINOS
interactions with nucleons, CERN experiments on, 19: 39612
production of cosmic, (T), 19: 39361
properties of, quantum laws for, (T), 19: 39661
ANTINUCLEONS
interactions with nucleons at high energy, Regge-pole hypothesis in asymptotic amplitudes for, 19: 39478 (NP-15210)
ANTIPARTICLES
interactions with elementary particles, mass-energy conversion in annihilation, (T), 19: 39554
ANTIPROTONS
interactions with protons at rest, K* production in annihilation, (E/T), 19: 39462 (CU-1932-239)
ANTIPYRINE, 4,4'-METHYLENEDI-
I–4,4'-methylenediantipyrine–Sc, complex formation in, 19: 38670
ARCHEOLOGICAL SPECIMENS
dating by analysis of charged particle tracks resulting from spontaneous uranium fission, 19: 39038
survey of, in vicinity of Cape Thompson, Alaska, 19: 40289 (PNE-406)
survey of, in vicinity of Cape Thompson, Alaska, 19: 40290 (PNE-407)
ARGON
density and temperature behind shock fronts in thermal plasma of, (T), 19: 40051
electric discharges in, at high current densities, (E), 19: 39983
electron density and temperature distribution in plasma of, optical study of, (E), 19: 40039
electron reactions at low energies, energy dependence of ion pair production in, 19: 39375
ionization cross section for, electron-impact, 19: 38630
ionization in electron-bombardment ion sources, 19: 38838
oscillations near crest of moving striation in plasma of, sustained, (E), 19: 40020
plasma of, properties of arc-jet, (E/T), 19: 40037
purification of, design of facility for, 19: 38769
radiation emission from plasma of, in gaseous core reactors, 19: 40231 (LA-3229, pp 149-76)
rubidium-vapor spin relaxation in, (E), 19: 39400
separation from nitrogen by gettering on hot titanium sponge, 19: 40177(R) (ANL-7046(p.1-35))
sorption on surfaces of vac-ion pumps, 19: 39323
temperature of jet of, from plasmatron nozzle, (E), 19: 40043
x-ray absorption spectra of, one-electron model for K, 19: 39411
ARGON IONS
reactions with metal single crystals at 1 to 10 kev, secondary-electron emission in, (E), 19: 39404
scattering by copper single crystals, energy distribution in, (E), 19: 39297
ARGON ISOTOPES Ar-36
energy levels, (E), 19: 39828
energy levels of, from calcium-40$(\alpha,2\alpha)$ reactions at 28.7 and 30.5 Mev, (E), 19: 39902
ARGON ISOTOPES Ar-40
reactions with emulsion nuclei at 10.4 Mev/nucleon, range-momentum relation for heavy recoil ions in, (E), 19: 39883
ARGON ISOTOPES Ar-41
diffusion in atmosphere, 19: 40277
performance in neutron flux monitors, 19: 40286(R) (NAA-SR-11200)
ARGON SYSTEMS
Ar–O, combustion of tantalum and zirconium in, 19: 38583(R) (SC-DC-65-1480)
Ar–H, nuclear spin lattice relaxation in, 19: 39378
Ar–H, properties of arc-jet plasma of, (E/T), 19: 40037
Ar–He, mixing at high temperatures, (E), 19: 40231 (LA-3229, pp 149-76)
Ar–N, mixing at high temperatures, (E), 19: 40231 (LA-3229, pp 149-76)
ARGONNE ADVANCED RESEARCH REACTOR

critical experiments and heat transfer in, 19: 40113(R) (ANL-7071)
development, 19: 40111(R) (ANL-7046)
development and physics studies in, 19: 40257(R) (ANL-7046(p.67-77)
ARGONNE FAST REACTOR EXPERIMENT TEST
design and development, 19: 40177(R) (ANL-7046(p.1-35))
design and development, June 1965, 19: 40113(R) (ANL-7071)
ARMY GAS COOLED REACTOR
neutron diffusion in, computer program for, 19: 40176 (AGN-TM-407)
ARMY REACTORS (ML-1)
shield design for, (E), 19: 40163
ARMY REACTORS (PM-3)
hydrogen evolution in 3A, test for, 19: 40188 (NYO-3420-2)
ARSENIC ISOTOPES As-74
use in radiodiagnosis, review on, 19: 38505
ARSENIC SYSTEMS
As–Ge–P, electric, metallurgical, and optical properties of, (E), 19: 39269(R) (SU-SEL-64-133)
As–Mo, crystal structure of compounds in, 19: 39209
As–Ti–N, crystal structure of compounds in, 19: 39209
As–W, crystal structure of compounds in, 19: 39209
ARTHROPODS
control of, preparation of methylcarbamate pesticide for, 19: 38748
radiation effects on survival of *Macrobiotes aerolatus* in active and dormant states, 19: 38373
radionuclide content in, from California waters, 19: 38895
ASCORBIC ACID
oxidation of, effects of ligands on copper-catalyzed, 19: 39265(R) (IA-1021)
radiation effects on content of, in rat adrenal glands, 19: 38443
ASPARTIC ACID
radioinduced in aqueous alanine solutions, mechanism of, 19: 38702
ASTATINE ISOTOPES At-216
alpha decay of, bismuth-212 energy levels from, (E), 19: 39796
ASTRONOMY
review, 19: 39353
ASTROPHYSICS
bibliography on nuclear, 19: 39331 (NEIC-RR-11)
book: *Dynamics of Stellar Systems*, 19: 39329(T)
cosmic ray origin in exploding galaxies, evidence of, 19: 39362
ATMOSPHERE
charge state of ultra-fine aerosols in, (T), 19: 39285
circulation energy and momentum budget above tropopause, 19: 39258 (CONF-650534-1)
contamination by cesium-137 and strontium-89 and -90, protection standards for, 19: 38877 (NP-15183)
diffusion and turbulence in, aerodyaamic effects of large reactor complex on, 19: 39259 (IDO-12041)
diffusion of argon-41 in, 19: 40277
fallout collection from, device for, 19: 38906(P)
fallout content, 1954 to 1963, 19: 38861
fallout transport in, 19: 38857
radiation monitoring of, equipment for, 19: 39050(P)
radiation transport from atomic bombs in, shielding against, 19: 38892
radioactivity in West German Republic, 19: 38904
radioactivity of Hanford area, 1964, 19: 38874 (BNWL-SA-53)
radioactivity of, methods of measuring, 19: 38903
radioactivity of, in Austria, 1963, 19: 38860
radioinduced nitrogen oxide in, 19: 38884
radioinduced ozone in, 19: 38884
radioisotope content in radioactive, apparatus for collecting and measuring, 19: 38896
scattering layers in upper, optical thickness of, 19: 39270(R) (TID-21894)
sorptive properties for cosmic and solar radiation, 19: 39363
wind turbulence in boundary layer of, analog simulation for, 19: 40282 (BNWL-SA-171)
ATMOSPHERES
processing reactor, for heavy water and tritium recovery, 19: 38907
ATOMIC BEAMS
detector for helium, performance of, 19: 39270(R) (TID-21894)
spectroscopy of, optical double resonance, (T), 19: 39369 (NP-15140)
velocity selector for hydrogen, design of magnetic, 19: 38929
ATOMIC ENERGY
bibliography of bibliographies on, June–July 1965, 19: 40294 (TID-3730)
conference on nuclear technology, France-Japan, Tokyo, Nov. 12 to 14, 1962, 19: 40302
development status in Italy, 19: 40200
review on British nuclear industry, 19: 40300
ATOMIC ENERGY, LEGAL ASPECTS
for forensic medicine, 19: 38495
ATOMIC EXPLOSIONS
effects of high-altitude, on high-frequency communication systems, 19: 38783
effects on hematology in survivors in Hiroshima and Nagasaki, 19: 38378
effects on serum proteins in Hiroshima survivors, 19: 38377
energy transport in air from, shielding against, 19: 38892
fallout from, 19: 38861
fission products from, data on, 19: 39774 (AEET-209)
instrumentation of, 19: 38919 (SC-R-65-904, pp 59-74)
isotope distribution and recovery in Gnome event, 19: 38787 (PNE-102F)
neutrons from, time-of-flight experiments with, (E), 19: 39889
protection from, 19: 40301
radiation contamination of populations from, 19: 38481(T)
use in development and management of water resources, principles of, 19: 38791 (TEI-857)
ATOMIC MODELS
correction to Thomas-Fermi inhomogeneity, (T), 19: 39387
ATOMIC PHYSICS
book: *Advances in Atomic and Molecular Physics*, 19: 39415
research, 19: 39788(R) (UCRL-12204, pp 1-27)
ATOMIC STRUCTURE
effect of shell, on bremsstrahlung and pair production, (T), 19: 39389
ATOMIC WEAPONS
effects on lesion formation in man, 19: 38478
protection from, 19: 40301
ATOMS
charge of un-ionized, determination of, 19: 39270(R) (TID-21894)
configurations for equivalent electrons, group theory for number of, 19: 39382
decay of excited, spectral shape in exponential, (T), 19: 39304
diffusion in bcc crystals, activation energy for interstitial, (T), 19: 40086
electron and x-ray scattering by, corrections for incoherent, 19: 39379
electron reactions with, screening effects on bremsstrahlung and pair production in, (T), 19: 39389
electron scattering by, exchange effects in, (T), 19: 39365 (COO-720-047)
energy calculations in Thomas-Fermi theory, inhomogeneity correction to, 19: 39387
energy level transitions in two-electron, dipole matrix elements for 2^1S-2^1P and 1^1S-2^1P, 19: 39380
energy levels of, oscillating real vectors for electron spin of, (T), 19: 39390
exciton wave packet radiation in, in crystals, (T), 19: 40087
oscillations in, statistical approximation for excitation of, 19: 39401
proton reactions with hydrogen-like, formation of excited hydrogen atoms in, (T), 19: 39398
screening functions for neutral, 19: 39265(R) (IA-1021)
sorption on metal surfaces, bonding mechanisms for alkali metal, 19: 39270(R) (TID-21894)
spectra of, Brownian-motion model for eigenvalues of random matrix for, (T), 19: 39391
spectra of, coupling in two-electron, (T), 19: 39367 (LA-DC-6548)
spectra of, time evolution of density operator for line width of, (T), 19: 39386
structure of, review on, 19: 38481(T)
AUDITORY ORGANS
motion in middle ear, research on, 19: 39270(R) (TID-21894)
radiation effects on function of vestibular organs in guinea pig, synergistic effects of vibration, 19: 38358 (AD-612660)
radiation sickness and blood loss effects on phosphorus-32 uptake by rabbit, 19: 38431
AUGER ELECTRONS
energy from, determination of total, 19: 38878 (ORNL-P-1405)
AURORAL STORMS
altitude of aurora australis, lower border, (E), 19: 39671
effects on ionospheric RF transmission, 19: 39682
luminosity of, correlation with cosmic noise absorption and x-ray intensity, (E), 19: 39672
AUSTRALIA
uranium production and uses in, in 1964, 19: 39105
AUSTRIA
fallout monitoring, 1963, 19: 38860
AUTORADIOGRAPHY
of iodine-135 and iodine-131 metabolism in thyroid, 19: 38533

B

BACTERIA
radiation effects on culture and morphology of *Bacillus mesentericus*, fast neutron, 19: 38449
BACTERIOPHAGES

radiation effects on constituents in, EPR spectra of, 19: 38365
BALANCES
calibration of thermo-, 19: 39125(R) (BNWL-91)
BALTIC SEA
strontium-90 content in, 19: 38901
BARBITURIC ACIDS
use to prevent extraction of nitrosylruthenium complexes in processing irradiated reactor fuels, 19: 38776(P)
BARIUM
content and distribution in subterranean Bulgarian salt water, 19: 38851
electron temperature and ion densities in plasma of, measurement of, 19: 39958 (MATT-327)
properties of fully ionized plasma of, (E), 19: 40007
separation from graphite above 1750°C in inert gases, 19: 38762
separation from waste water, methods for, 19: 40276
BARIUM ALLOYS
Al–Ba, cesium-133 Mossbauer effect in, 19: 39295
BARIUM BROMIDES
reduction by high-frequency hydrogen discharge to dihalide and metal, 19: 39180
BARIUM CHLORIDES
cesium-133 Mossbauer effect in, 19: 39295
reduction by high-frequency hydrogen discharge to dihalide and metal, 19: 39180
$BaCl_2$–KCl, free energy of formation of K_2BaCl_4 at 450 and 550°C, 19: 38575 (BNL-9343)
BARIUM FLUORIDES
reduction by high-frequency hydrogen discharge to dihalide and metal, 19: 39180
BaF_2–YF_2, phase studies, 19: 38615
BARIUM IODIDES
reduction by high-frequency hydrogen discharge to dihalide and metal, 19: 39180
BARIUM IONS
radiolysis of aqueous solutions of, pulse, 19: 38728
BARIUM ISOTOPES Ba-133
production in the Intense Neutron Generator, 19: 39762 (AECL-2177, Paper 9))
BARIUM ISOTOPES Ba-140
release from pyrolytic carbon-coated fuel particles, 19: 39228 (BMI-1734)
separation from irradiated uranium by ion exchange chromatography, carrier-free, 19: 38757 (SGAE-CH-17/1965)
BARIUM NITRATES
radiation effects on, nitrate ion ESR from x, 19: 38730
BARIUM TITANATES
iron-57 Mössbauer effect at 300 to 1200°K, 19: 38651
radiation effects on hysteresis loops in monocrystalline, gamma and neutron, 19: 38705
BARLEY
radiation effects on growth in seedlings of, effects of oxygen tension on gamma, 19: 38418
radioinduced chromosome aberrations in, modifying effects of acridine orange and methylene blue on, 19: 38462
radioinduced chromosome breaks in, interaction in neutron and x-ray, 19: 38399
BARYONS
decay of, leptonic, (T), 19: 39573
form factors of vector and axial currents of, in $\tilde{U}(12)$ symmetry, 19: 39467 (JINR-E-2194)
interactions with baryons, test of one-particle-exchange dynamical models for, (T), 19: 39511
interactions with mesons in SV_{12} scheme, D/F ratios for vertices of, (T), 19: 39524
interactions with protons, U(12) symmetry for total cross sections for, 19: 39529
interactions with pseudoscalar mesons, bootstrap mechanism and symmetries in, 19: 39559
magnetic moments and masses in SU_{12}, 19: 39471 (JINR-P-2175)
magnetic moments in SV_{12}, (T), 19: 39524
mass formula for, (T), 19: 39584
model for, based on three-body equation, 19: 39473 (JINR-P-2186)
model for, based on Sp(6), (T), 19: 39568
symmetry for, covariant extension of SU(6), (T), 19: 39555
symmetry for, SU(9), 19: 39571
symmetry group as test of one-particle-exchange dynamical models for, unitary singlet, (T), 19: 39511
symmetry scheme for hadrons, Sp(3), (T), 19: 39565
BARYONS, RESONANCE
decay correlations with vector-meson resonances, (E), 19: 39542
decay of N^*_{33}, nonrelativistic quark model for E2 amplitude in, (T), 19: 39536
decay of N*, meson (π) angular distribution in, (T), 19: 39517
decay of Y*, (T), 19: 39610
electromagnetic properties, (T), 19: 39563
model for, based on Sp(6), (T), 19: 39568
parity and spin of, methods for determination of, (T), 19: 39610
parity of Y^*_1, (E), 19: 39540
production in deuteron-meson interactions, (T), 19: 39564
production in neutrino-nucleon interactions, total cross sections for, (T), 19: 39517
production of isobars in nucleon interactions at high energies, 19: 39508
production of K* in antiproton-proton annihilation at rest in, (E/T), 19: 39462 (CU-1932-239)
production of $N^*_{3/2}(1580)$ in proton interactions at 5.52 Bev/c, 19: 39548
production of N* in meson (π^+)-proton interactions, peripheral, (E/T), 19: 39576
production of N*, in photon-proton interactions at 600 to 850 Mev, 19: 39519
production of N_{11} as test for properties of neutral vector mesons, (T), 19: 39572
properties of, data tabulation of, 19: 39485 (UCRL-8030(Pt.I) (Mar. '65, ed.))
spin of Y^*_1 (1405), 19: 39553
BASTNAESITES
processing of, rare earth separation from, 19: 38859
BEAMS
deflection of polyenergetic, system for, 19: 39312(P)
momentum separation of particles from, magnetic slit device for, 19: 38967(P)
BEANS
radiation effects on tritiated valine, uptake by chromosomes in *Vicia faba*, x, 19: 38417
radioinduced chromosome aberrations in, modifying effects of acridine orange and methylene blue on, 19: 38462
BEHAVIOR
radiation effects on activity of adult rats exposed *in utero*, 19: 38361(R) (TID-21951)
BENZENE
deuterium exchange with heavy water, group VIII metal catalysis of, 19: 38597
diffusion in deuterated-normal mixture, coefficients of, 19: 38646
reduction of platinic oxide by labeled, preparation of platinum oxide catalysts by, 19: 38596
BENZENE, HEXAFLUORO-
radiation effects on liquid, mechanism of electron, 19: 38709
BERKELIUM
spectra of, spark, 19: 39384
BERKELIUM ISOTOPES
nuclear properties of, pairing force effects on, (T), 19: 39927
BERKELIUM ISOTOPES Bk-247
alpha decay scheme for, 19: 39807
BERKELIUM ISOTOPES Bk-248
half life of, 19: 39807
BERYLLIUM
analysis for oxygen by activation, 19: 38546(R) (RFP-552)
bake-out time for, determination of, 19: 38546(R) (RFP-552)
deposition and properties of coatings of, by pyrolysis of di-*t*-butylberyllium, 19: 39102(R) (UCRL-13100)
electron inelastic scattering by crystals of, interband excitation in fast, (T), 19: 40083
electron reactions with atomic, screening effects on bremsstrahlung and pair production in, (T), 19: 39389
energy of atomic Sinanoglu many-electron theory for correlation, 19: 39381
extrusion of electrolytic refined, 19: 39140
production and uses, 19: 39107
properties for use as fuel cladding material in reactors, 19: 39206
BERYLLIUM CHLORIDES
reduction by high-frequency hydrogen discharge to dihalide and metal, 19: 39180
BERYLLIUM COMPLEXES
with catecholdisulfoaic and chromotropic acids, stability and formation constants, 19: 38641
BERYLLIUM, DI-*tert*-BUTYL-
pyrolysis of gaseous, for beryllium deposition, 19: 39102(R) (UCRL-13100)
BERYLLIUM FLUORIDES
BeF_2–LiF, chemistry and thermodynamics of molten, as MSRE solvent, 19: 38582 (ORNL-P-1428)
BeF_2–LiF, thermodynamic properties of, mass spectrometric studies of, 19: 38679
BERYLLIUM ISOTOPES Be-7

production in the Intense Neutron Generator, 19: 39762 (AECL-2177, Paper 9))
proton reactions (p,γ) with, models for, (T), 19: 39820
BERYLLIUM ISOTOPES Be-8
angular correlations in beryllium-9 (He-3,α) reactions at 3.0 Mev, (E), 19: 39916
BERYLLIUM ISOTOPES Be-9
gamma reactions (γ,n) with, excitation function for, (T), 19: 39805
helium-3 reactions (He-3,n) at 1.3 to 5.4 Mev, excitation functions for, (E), 19: 39832
helium-3 reactions (He-3,αnα) at 3 Mev, energy spectra of, (E), 19: 39898
helium-3 reactions (He-3,α) beryllium-8 at 3.0 Mev, angular correlations of, (E), 19: 39916
helium-3 reactions (He-3,α) with, (E), 19: 39941
neutron cross sections from 1 to 15 Mev, 19: 39775 (AEEW-M-513)
BERYLLIUM ISOTOPES Be-10
neutron separation energy for, (E), 19: 39862
BERYLLIUM MODERATED REACTORS
design of, gaseous-core criticality effects on, 19: 40155 (LA-3229, pp 362-76)
BERYLLIUM OXIDES
preparation and properties of single-crystal, 19: 40286(R) (NAA-SR-11200)
properties for use as fuel-propellant partition in gaseous fuel rocket reactors, 19: 40229 (LA-3229, pp 116-36)
radiation effects on single crystals of, 19: 40286(R) (NAA-SR-11200)
use as moderator in nuclear reactors, 19: 39107
BeO–ThO_2, preparation and properties, 19: 39091(R) (BMI-1723(Del.))
BeO–UO_2, radiation effects on clad, 19: 39091(R) (BMI-1723(Del.))
BETA PARTICLES
absorption by textiles, measurement of unevenness of fibers by, 19: 39063
absorption of, review, 19: 39416
detection and measurement of tritium, 19: 38552
detection and measurement of soft, using liquid scintillators, 19: 39002
detection and measurements of, use of scintillation granules in, 19: 38737
effects on platinum hydrogenation catalysts, 19: 38742(P)
effects on rat immunity, 19: 38362(T) (JPRS-30993, pp 29-38)
scattering of, measuring film thicknesses by, 19: 38952(P)
BETA SOURCES
for radiotherapy, energy levels of gold-198, phosphorus-32, and yttrium-90, 19: 38515
preparation of phosphorus-32 mounted on metal plates, 19: 38745 (Y-1484)
therapeutic use for cancer, 19: 38487
use in textile industry to eliminate static electricity, 19: 39063
BETA SPECTROMETERS
coincidence circuits for, scintillation design of fast β-γ, 19: 39010
magnetic characteristic curves for permanent-magnet spectrographs, (E), 19: 38998
BIBLIOGRAPHIES
of bibliographies on atomic energy literature, June–July 1965, 19: 40294 (TID-3730)
on analytical methods for plutonium in spent fuels, metal, alloy, and compounds, 19: 38542 (LA-DC-6938)
on atmospheric ozone to 40 km, properties of, 19: 39260 (LA-3328)
on boiling burnout correlations, (T), 19: 38814
on chemistry and thermodynamics of molten beryllium fluoride–lithium fluoride, 19: 38582 (ORNL-P-1428)
on control of liquid hydrogen hazards at experimental facilities, 19: 38875 (HASL-160)
on detection and measurement of nuclear radiation, 19: 39040
on determination of stable isotopes, 19: 38559
on electron penetration through matter, 19: 39416
on hydrogen permeation through metals and alloys, 19: 39165 (NAA-SR-10462)
on magnetic properties of metals, (T), 19: 40074 (CONF-796(Paper 3))
on medical radioisotope scanning, 19: 38516
on meson (π) photoproduction, 19: 39498
on neutron cross sections, 19: 39778 (BNL-9355)
on nuclear astrophysics, 19: 39331 (NEIC-RR-11)
on nuclear materials management, 19: 39101 (TID-3315)
on physics of critical assemblies, (E), 19: 40163
on plasma containment by h-f electromagnetic fields, 19: 39982
on plasma transport processes, 19: 40057(T)
on plutonium technology, 19: 40281 (BNWL-113-5)
on properties of promethium as fuel in radioisotopic power sources, 19: 39069 (BNWL-C-45)
on properties of uranium dioxide at high temperatures, 19: 39154 (BNWL-SA-54)
on properties of Zircaloy-2 and -4, 19: 39097 (GEMP-346)
on reactor fuels and materials, 19: 39163(R) (MLM-1244)
on solderability testing, 19: 40280 (BDX-613-73)
on spectra of radiation effects on elementary biological materials, 19: 38365
on thermionic and thermoelectric energy conversion, 19: 39434 (N64-26371)
on translations received by AEC Division of Technical Information Extension, 19: 40295 (TID-4025(Rev.1)(Pt.1)(Suppl.4))
on use of natural cation exchangers in waste processing, (E), 19: 40130 (ZFK-RN-17(p.165-78))
on uses of polarized proton targets, 19: 39497
BICYCLOHEXYL
perfluoro-, radiation effects on, 19: 38709
BIOLOGICAL MATERIALS
analysis for fluorides by radiometry using tantalum-182, 19: 39265(R) (IA-1021)
analysis for tritium, 19: 38552
radiation effects on living, review on, 19: 38421
radiation effects on, 19: 38432(T)
BIOLOGICAL STRESS
effects on cardiography pattern of rats irradiated *in utero*, 19: 38361(R) (TID-21951)
effects on thyroid function, 19: 38492
BIOLOGICAL SYSTEMS
for radiobiological studies, 19: 38407
BIOPHYSICS
research progress on communication, 19: 39270(R) (TID-21894)
BIOTITES
pleochroic halos produced by zircon in biotite-cordierite, reversal, 19: 38846(T) (ORNL-tr-698)
BIPHENYL
perfluoro-, radiation effects on, 19: 38709
BISMUTH
electric conductivity in ohmic contact with normal metal at low temperatures, (E), 19: 39734
gamma scattering by, spectra of nonresonant, (E), 19: 39265(R) (IA-1021)
magnetostriction in pure monocrystalline, 19: 39199
neutron reactions (n,n′γ) at 0 to 14 Mev, energy absorption in, 19: 39769 (SC-DC-65-1544)
preparation of large single crystals of, by directional freezing, 19: 39098 (INR-567/II/PS)
proton reactions (p,xn) at 1 Bev, heat production and neutron yields from, 19: 39756 (AECL-2177, Paper 3))
solvent properties for cadmium, lead, and tin in presence of tellurium, heats of solution, 19: 39168(R) (TID-22015)
BISMUTH ALLOYS
Bi–Cd, heats of fusion, 19: 39163(R) (MLM-1244)
Bi–In, heats of formation of InBi and In_2Bi, 19: 39168(R) (TID-22015)
Bi–In, tunneling and flux penetration in superimposed layers of zinc and, in magnetic fields, (E), 19: 39699
Bi–Pb, cavitation effects on materials at 500 and 1500°F, ultrasonic-induced, 19: 39116 (NP-15263)
Bi–Pb, proton reactions (p,xn) at 1 Bev, heat production and neutron yields from, 19: 39756 (AECL-2177, Paper 3))
Bi–Tl, deformation and properties of $TlBi_2$, 19: 39168(R) (TID-22015)
Bi–Tl, heat of formation of $TlBi_2$, 19: 39168(R) (TID-22015)
Sb–Bi, electric conductivity in ohmic contact with normal metal at low temperatures, (E), 19: 39734
BISMUTH BROMIDES
electric conductivity at 818°C, 19: 40286(R) (NAA-SR-11200)
BISMUTH CHLORIDES
electric conductivity at 860°C, 19: 40286(R) (NAA-SR-11200)
BISMUTH HALIDES
properties at high pressures, 19: 40286(R) (NAA-SR-11200)
BISMUTH IODIDES
thermoelectric properties of, 19: 40286(R) (NAA-SR-11200)
BISMUTH IONS
incorporation into potassium chloride crystals grown from solution, 19: 38696 (MIT-2909-4)
BISMUTH ISOTOPES Bi-206
use in radiodiagnosis, review on, 19: 38505
BISMUTH ISOTOPES Bi-208
energy levels, (T), 19: 39933
BISMUTH ISOTOPES Bi-209
energy levels of, magnetic moments of single-particle, (T), 19: 39870
BISMUTH ISOTOPES Bi-212
energy levels of, from alpha decay of astatine-216, (E), 19: 39796
BLADDER
radiation injuries after radiotherapy of uterine carcinoma, 19: 38531
radiotherapy of cancer of, using gamma sources, 19: 38504

BLOOD
cesium-137 content in, method for determining, 19: 38349
radiation effects on histamine, histaminase, and protein level in animal, 19: 38426
radiation effects on mercapto groups of animal, 19: 38427
radiation effects on chemical and physical properties of rat, fast neutron and x, 19: 38440
radiation effects on reticulocytes in peripheral, in rats, 19: 38414
radiation effects on eosinophil content in rat, neutron, 19: 38443
xenon-133 partition between human brain and, measurements on, 19: 38353
BLOOD CELLS
carbon-11 production in, during proton irradiation, 19: 38722
radiation effects on reticulocytes in peripheral blood in rats, 19: 38414
radioisotope labeling of, 19: 38493
tracer studies of life span, 19: 38493
volume of red, use of chromium-51 for determining, 19: 38346
BLOOD CIRCULATION
effects of acceleration on, in rabbit brain, 19: 38358 (AD-612660)
effects of arrest of, on radiosensitivity of tumors, 19: 38374
in brain, use of krypton-85 for determining, 19: 38491
measure in dog and rabbit bones, use of strontium-85 for, 19: 38340
radiodiagnosis of cerebral, by circulography using iodine-131, 19: 38489
tracer study of, in brain, 19: 38501
BLOOD DISEASES
radiodiagnosis, tracer techniques for, 19: 38493
BLOOD PLASMA
iodine-131 metabolism in rat, effects of vitamin B on, 19: 38337
BLOOD SERUM
radiation effects on proteins in mouse, following rat-to-mouse chimera transplants, x, 19: 38404
BLOOD VESSELS
radiation effects on rat heart, fast neutron and x, 19: 38441
BLOOD VOLUME
determination of red cell, using chromium-51, 19: 38346
tracer studies of, 19: 38525
tracer study of, 19: 38493
BODY FLUIDS
placental transfer of fetal, in rabbits and swine, tracer study, 19: 38344
BOILERS
corrosion in PWR, causes of selective, 19: 39091(R) (BMI-1723(Del.))
design for reactors, 19: 38815(P)
design for reactors, 19: 38816(P)
design for superheated-steam, 19: 38817(P)
design for waste heat from reactors, 19: 40141(P)
development and testing for NERO, 19: 40250
development of sodium-heated, 19: 38803(R) (BAW-1280-26)
fabrication for sodium components test installation, 19: 40286(R) (NAA-SR-11200)
installation of ALCO, 19: 40286(R) (NAA-SR-11200)
BOILING
burnout heat flux of water, effects of electric fields on, 19: 38807(R) (NYO-2404-70)
burnout in 19-rod bundle, effects of fluid mixing and rod spacing on, 19: 38805(R) (BNWL-C-3)
burnout in, comparisons of analyses of, 19: 38814
critical heat flux in flow regimes, 19: 38809 (NYO-3304-3)
heat transfer in transition, effects of flow disturbances on, 19: 38806(R) (GEAP-4908)
BOILING REACTORS
burnout in, comparisons of analyses of, 19: 38814
condenser system for, design of emergency, 19: 40137(P)
criticality studies in, review, (E), 19: 40163
use for providing steam for propulsion of marine vessels, 19: 40255(P)
use of heavy water moderated, in power plants, 19: 40211
BONE MARROW
radiation effects on cell nuclei in mammalian, synergistic effects of vibration, 19: 38358 (AD-612660)
radiation effects on morphology of rat, fast neutron, 19: 38444
BONES
analysis for strontium by flame photometry and ion exchange, 19: 38345
blood flow in dog and rabbit, use of strontium-85 for measure of, 19: 38340
fluoride chelation in rat, 19: 39265(R) (IA-1021)
radionecrosis of, histology and radiology of, 19: 38527
strontium-90 content of, effects of age, 19: 38850
strontium-90 content in, collected in Great Britain, 1964, 19: 38863
thorium-230 content in, after inhalation of uranium ore, in rats, 19: 38333 (BNWL-SA-226)
BORATE GLASS
radiation effects on coloration and thermoluminescence of, relation between, 19: 39244
BORAZOLE
neutron fission of gaseous, pressure wave generation in, (E), 19: 39836
BORIC ACID
corrosive effects on Inconel-600, at 600°F, 19: 40195(R) (WCAP-3269-5)
corrosive effects on boronated stainless steel at 600°F, 19: 39110
BORON
criticality effects in closed-cycle water reactors, 19: 40198(R) (WCAP-3721)
determination in water, spectrochemical, 19: 39265(R) (IA-1021)
determination, standard for titrimetric, 19: 38548 (UCRL-14166-T)
diffusion in bcc crystals, activation energy for interstitial, (T), 19: 40086
effects on cesium ion and neutral emission from hot porous tungsten, 19: 39164 (N64-22193)
hideout in reactor cooling systems, methods of detecting, 19: 40196(R) (WCAP-3269-6)
neutron absorption properties of, burnup effects on, (E), 19: 40163
preparation and properties of crystalline, 19: 39163(R) (MLM-1244)
sorption by aqueous solutions of corrosion products in autoclave tests, 19: 40197(R) (WCAP-3718)
sorption by aqueous solutions of corrosion products, 19: 40198(R) (WCAP-3721)
BORON CARBIDES
thermoelectric properties at high temperature, (E), 19: 38605
BORON FLUORIDES
analysis for boron isotopes, mass spectrometric, 19: 38541 (K-L-6057)
neutron fission of gaseous, pressure wave generation in, (E), 19: 39836
BORON ISOTOPES
determination in boron trifluoride, mass spectrometric, 19: 38541 (K-L-6057)
BORON ISOTOPES B-9
energy levels in intermediate systems in boron-10 (He-3,pααα) reactions, (E), 19: 39917
BORON ISOTOPES B-10
deuteron reactions (d,pγ) at 0.40 Mev, gamma polarization in, (E/T), 19: 39937
helium-3 reactions (He-3,pααα) at 2.45 Mev, sequential processes for, (E), 19: 39899
helium-3 reactions (He-3,pααα), intermediate states in, (E), 19: 39917
lithium-6 reactions with, total cross sections for, (E), 19: 39887
lithium-7 reactions with, total cross sections for, (E), 19: 39887
neutron fission in gases, pressure wave generation in, (E), 19: 39836
neutron reactions (n,d) and (n,p) at 14.4 Mev, differential cross sections for, (E), 19: 39798
BORON ISOTOPES B-11
deuteron reactions (d,n) at 1.5 to 4.7 Mev, distributions from, (E), 19: 39817
lithium-6 reactions with, total cross sections for, (E), 19: 39887
lithium-7 reactions with, total cross sections for, (E), 19: 39887
oxygen-16 reactions (O-16, N-15) at 30 Mev, (E), 19: 39869
proton reactions (p,3α), sequential decay theory for, (T), 19: 39895
proton reactions (p,3α), angular momenta and Pauli principle for, (T), 19: 39896
proton reactions (p,3α) at 2 to 5.64 Mev, sequential mechanism for, (E/T), 19: 39911
proton reactions (p,α)2α at 250 and 675 kev, mechanism of, (E), 19: 39919
proton reactions (p,α), direct 3α decay of carbon-12 resonance (163 kev) in, (E), 19: 39918
BORON NITRIDES
spectra of, modes of infrared reflection, (E/T), 19: 39270(R) (TID-21894)
BORON SYSTEMS
B–stainless steel, corrosion by boronated water at 600°F, 19: 39110
B–stainless steel, extrusion of fuel cladding of, 19: 39110
B–stainless steel, mechanical properties of, effects of boron content on, 19: 39110
B–stainless steel, radiation effects on mechanical properties of, fast and thermal neutron, 19: 39110
B–stainless steel, radiation effects on corrosion resistance of, fast and thermal neutron, 19: 39110
B–stainless steel, weld joint design for tubes of, 19: 39110
BOSONS
excitation spectra of many-particle system of, RPA for, 19: 39631 (IS-1111)
interactions in many-body systems of, perturbation theory and structure factor for, 19: 39261(R) (AROD-39792)
interactions of, weak-strong coupling complementarity in renormalized perturbation theory for, (T), 19: 39521
interactions with nucleons, complex angular momentum on, (T), 19: 39518
interactions with fermions, bound states in Lee model for, (T), 19: 39558
photoproduction of intermediate vector, (T), 19: 39621

production of weak vector, in electron-neutrino interactions, (T), 19: 39567
properties of intermediate vector, relation to B matter, 19: 39560
response function of degenerate system of, microscopic theory for linear, 19: 39657
spin of, quantum laws for, 19: 39661
symmetry for, SU(9), 19: 39571
thermodynamic properties of in plasma of, astrophysical relations of, (T), 19: 39339
transformations for, generalized Bogoliubov, (T), 19: 39496

BOTANY
radiobiology applications for, 19: 38327

BRAIN
blood circulation in, effects of acceleration in rabbit, 19: 38358 (AD-612660)
blood flow in, use of krypton-85 for determining, 19: 38491
oxidation in rat, effects of vibration on, 19: 38358 (AD-612660)
radiation effects on morphology of rat, fast neutron, 19: 38444
radiodiagnosis of circulation in, by circulography using iodine-131, 19: 38489
radiodiagnosis of circulatory diseases of, 19: 38501
xenon-133 partition between human blood and, measurements on, 19: 38353

BRAIN TUMORS
localization by gamma encephalography using mercury-203, 19: 38510

BRASS
gamma absorption by, effective atomic numbers for, 19: 40069

BRAZING
of copper structures for accelerators, hydrogen–oxygen furnace for, 19: 38938

BRAZING ALLOYS
corrosion by aqueous chemical shim solutions at 600°F, 19: 40198(R) (WCAP-3721)

BREEDER REACTORS
design and economics of large sodium cooled, for desalination, 19: 40190 (ORNL-TM-784)
design data for 1000 Mw(E) fast, 19: 40113(R) (ANL-7071)
design of fast split-blanket, 19: 40286(R) (NAA-SR-11200)
development of gas-cooled fast, 19: 40182 (GA-5537)

BREMSSTRAHLUNG
interactions with protons, mesons (π^+) production near threshold in, (E), 19: 39461 (COO-1195-35)
production by electrons in shielding in space, computer program for radiation dose from, 19: 40062 (N64-29366)
production by electron scattering in diamond at 1 to 40 Bev, (E/T), 19: 39622
production in electron reactions with atoms, screening effects on, (T), 19: 39389
shielding against, for manned space stations, 19: 40063 (NP-15125)

BRITTLE MATERIALS
crack formation and twinning in body-centered-cubic, 19: 39202

BROMIDES
radiolysis products of, effects of bromates and chlorates on, 19: 39265(R) (IA-1021)

BROMINE
ion reactions with emulsion nuclei of, recoil range-momentum relation for, (E), 19: 39883
neutron reactions (n,α) at 13 to 17 Mev, cross sections for, (E), 19: 39823
radioinduced reactions with cyclohexane, organic retentions of bromine-80m and -82 in, 19: 38713

BROMINE ISOTOPES Br-79
reactions with gold at 20 to 80 Mev, orientation effects on energy losses in, 19: 39370 (ORNL-P-1336)

BROMINE ISOTOPES Br-80
radiation effects on organic retentions of, in bromine-cyclohexane mixtures, 19: 38713
radiation effects on organic retentions of, in alkyl halides and hydrocarbons, 19: 38715

BROMINE ISOTOPES Br-82
decay of, spin of krypton-82 energy level (2426 kev) from, (E), 19: 39944
radiation effects on organic retentions of, in bromine-cyclohexane mixtures, 19: 38713
radiation effects on organic retentions of, in alkyl halides and hydrocarbons, 19: 38715
reactions (isomeric transition) in alkyl halides and hydrocarbons, neutron activated, 19: 38715

BROMOHYDROCARBONS
radiolysis of, effects of carbon dioxide on, 19: 39265(R) (IA-1021)

BRONZE
analysis for trace amounts of phosphorus by x-ray spectrography, 19: 38571
gamma absorption by, effective atomic numbers for, 19: 40069

BROOKHAVEN BEAM RESEARCH REACTOR
containment leak rate test, 19: 40258 (BNL-9237)

BROOKHAVEN SYNCHROTRON
beam extraction rate control for, equipment for external, 19: 39324

BROWNIAN MOVEMENT
theory of relativistic, Wiener integrals from covariant, 19: 39959 (N64-22435)

BUBBLE CHAMBERS
data processing for, computerized, 19: 38970 (BNL-9236)
data processing for, off-line global approach for, 19: 38996 (PPAD-2137-548)
development for weak neutron flux monitoring, 19: 38993 (NP-15143)
development for weak neutron flux monitoring, 19: 38994(R) (NP-15145)
operation using liquid hydrogen–neon, 19: 39026
particle track analysis in, using flying-spot devices, (E), 19: 38978 (CERN-65-11(p.81-90))
particle track analysis in, using computerized flying-spot systems, (E), 19: 38980 (CERN-65-11(p.97-113))
particle track analysis from, using flying-spot devices, (E), 19: 38982 (CERN-65-11(p. 123-37))
particle track ionization measurements in, using flying-spot devices, (E), 19: 38989 (CERN-65-11(p.219-27))
photograph identification for analysis purposes, (E), 19: 38979 (CERN-65-11(p.91-5))
use in CEA photoproduction experiments, 19: 39623
use in neutrino experiments at CERN, 19: 39612

BUBBLES
flow in liquid-core nuclear rocket, 19: 40227 (LA-3229, pp 90-110)
rise velocity in inclined tubes, 19: 38808 (NYO-2114-8)

BUILDING MATERIALS
book: *Nuclear Technology in Construction*, 19: 38828
x-ray scattering in, measurement and theory of, 19: 38524

BULBS
radiation effects on growth and reproduction of gladiolus, 19: 38430

BULGARIA
barium, cesium, lithium, rubidium, and strontium distribution in subterranean salt waters, 19: 38851

BUTADIENE, 2,3-DIMETHYL-
radioinduced polymerization of, stereospecificity in, 19: 38725(T)

BUTADIENE POLYMERS
radioinduced *cis-trans* isomerization and unsaturation loss in, 19: 38711

BUTANE, 1-BROMO-
radioinduced reactions with tin, effects of temperature on, 19: 39091(R) (BMI-1723(Del.))

BUTANE, 2,2-DIMETHYL-
radiation effects on bromine-80 and -82 retentions in, isomeric transition reaction in, 19: 38715

BUTANE, 2,3-DIMETHYL-
radiation effects on bromine-80 and -82 retentions in, isomeric transition reaction in, 19: 38715

BUTENES
dehydrogenation and isomerization of, radiochromatographical studies of action of catalysts in, 19: 38718

BUTYL PHOSPHATES
kerosene–TBP, solvent distribution of hydrochloric acid in, 19: 38563

C

CABLES
attenuation by in-core electronic, effects of frequency on, 19: 40122(R) (GEAP-4862)

CADARACHE REACTORS (RAPSODIE)
uses for Doppler-shift analysis of fast power reactors, (E/T), 19: 40150 (CEA-R-2565)

CADMIUM
determination in enamel of teeth, neutron activation, 19: 38562
heat of solution in liquid bismuth in presence of tellurium, 19: 39168(R) (TID-22015)
neutron absorption properties of, burnup effects on, (E), 19: 40163
separation from ethanolic hydrochloric acids by ion exchange, 19: 39265(R) (IA-1021)
separation from waste water, methods for, 19: 40276
use as standard for neutron soil moisture probes, 19: 38869

CADMIUM ALLOYS
Bi–Cd, heats of fusion, 19: 39163(R) (MLM-1244)
Cd–In–Ag, radiation effects on dimensions and mechanical properties of, 19: 40197(R) (WCAP-3718)
Cd–In–Ag, radiation effects on dimensions and mechanical properties of, 19: 40198(R) (WCAP-3721)

Cd–In–Ag, reactivity worths in uranium–Zircaloy-2, 19: 40196(R) (WCAP-3269-6)
Cd–In–Ag, reactivity worths of, 19: 40197(R) (WCAP-3718)
Cd–In–Ag–Sn, radiation effects on dimensions and mechanical properties of, 19: 40197(R) (WCAP-3718)
Cd–In–Ag–Sn, radiation effects on dimensions and mechanical properties of, 19: 40198(R) (WCAP-3721)
Cd–Pu, phase studies, 19: 39163(R) (MLM-1244)
CADMIUM FLUORIDES
europium-151 EPR in, (T), 19: 38664
europium-153 EPR in, (T), 19: 38664
CADMIUM IONS
radiolysis of aqueous solutions of, pulse, 19: 38728
CADMIUM ISOTOPES Cd-113
neutron reactions (n,γ), gamma spectra in 0.175-ev resonance of, 19: 39781 (JAERI-1073)
CADMIUM SULFIDES
crystal structure and electric properties of vacuum-deposited thin films, 19: 38585 (SC-TM-64-1677)
CADMIUM SYSTEMS
C–Cd–Ti, preparation and crystal structure of H-phase in, 19: 39208
CADMIUM TELLURIDES
heat of formation of, 19: 39168(R) (TID-22015)
CALCITES
carbon-13 variations in secondary, from change in isotopic composition of soil carbon dioxide, 19: 38854
CALCIUM
content in Japanese diet, 19: 38894
determination in uranium ore by x-ray-fluorescence, 19: 38543(R) (MCW-1492)
effects on cesium ion and neutral emission from hot porous tungsten, 19: 39164 (N64-22193)
effects on strontium-90 metabolism in mammals, 19: 38335 (NP-14926)
metabolism in mammals, 19: 38335 (NP-14926)
metabolism in rats, effects of vitamin D_3, 19: 38347
metabolism in rats, effects of vitamin D_3, 19: 38347
separation from graphite above 1750°C in inert gases, 19: 38762
CALCIUM ALLOYS
Ca–Eu, crystal structure of intermetallic compounds in, 19: 39177
Ca–Mg, properties of intermetallic compounds in, 19: 39177
CALCIUM BROMIDES
reduction by high-frequency hydrogen discharge to dihalide and metal, 19: 39180
CALCIUM CHLORIDES
reduction by high-frequency hydrogen discharge to dihalide and metal, 19: 39180
$CaCl_2$–KCl, free energy of formation of $KCaCl_3$ at 450 and 550°C, 19: 38575 (BNL-9343)
CALCIUM FLUORIDES
reduction by high-frequency hydrogen discharge to dihalide and metal, 19: 39180
samarium ion reduction in yttrium doped, (E), 19: 38595
CaF_2–YF_3, phase studies, 19: 38615
CALCIUM IODIDES
reduction by high-frequency hydrogen discharge to dihalide and metal, 19: 39180
CALCIUM ISOTOPES
preparation of accelerator targets of, 19: 38658
CALCIUM ISOTOPES Ca-40
alpha reactions (α,2n) at 28.7 and 30.5 Mev, angular and energy correlations in, (E), 19: 39902
energy levels, (E), 19: 39874
energy levels of, analysis of spurious states owing to center-of-mass motion, (T), 19: 39812
helium-3 reactions (He-3,t) at 37.5 Mev, calcium-40–scandium-40 mass difference from, (E), 19: 39850
helium-3 reactions (He-3,α) at 18.05 Mev, (E), 19: 39874
helium-3 reactions (He-3,d) at 18.05 Mev, (E), 19: 39874
mass difference of scandium-40 and, (E), 19: 39850
CALCIUM ISOTOPES Ca-41
energy levels, (E), 19: 39874
CALCIUM ISOTOPES Ca-42
helium-3 reactions (He-3,α) at 18.05 Mev, (E), 19: 39874
spectra of, reaction-matrix analysis of single-particle, (T), 19: 39815
CALCIUM ISOTOPES Ca-45
beta decay of, $d^3/_2$ core excitation from, 19: 39851
effects on rats of daily injection of, dose effects on, 19: 38362(T) (JPRS-30993, pp 29-38)
use in radiodiagnosis, review on, 19: 38505
CALCIUM OXIDES
radiation effects on crystalline, 19: 39265(R) (IA-1021)
CaO–SiO_2, crystal structure, 19: 38621
CaO–ThO_2, use as solid electrolyte in high-temperature cell, 19: 38586 (UCRL-11957)
CaO–UO_2–ZrO_2, densities and thermal properties, 19: 39091(R) (BMI-1723(Del.))
CALCIUM TUNGSTATES
holmium ion EPR in crystalline, 19: 38650
CALDER HALL REACTORS
design parameters of WYLFA Power Plant, 19: 40202
development and operation of Trawsfynydd, 19: 40206
development of Hinkley Point Power Plant, 19: 40199
pressure vessel design and development for Oldbury, 19: 40212
CALIBRATION
procedures for, for vessels for chemical processing of nuclear materials, 19: 38756 (RFP-488)
CALIFORNIA
radionuclide content in coastal animals of, 19: 38895
CALIFORNIUM ISOTOPES Cf-254
fission in type I supernova, spontaneous, (T), 19: 39338
CALORIMETERS
design and operation of high-temperature isothermal, 19: 38675
heater wires for, performance of platinum–tungsten alloys as, 19: 39743
CAMERAS
design of pinhole, for extreme u-v spectroscopy, 19: 38928
lens testing methods for, 19: 39270(R) (TID-21894)
CANADA
uranium production and uses in, in 1964, 19: 39105
CANDU REACTOR
fuel management in, (T), 19: 40216
CAPE THOMPSON–CAPE SEPPINGS AREA (ALASKA)
archeological survey of Ogotoruk Creek area, 19: 40290 (PNE-407)
archeological survey of Ogotoruk Creek area, 19: 40289 (PNE-406)
CAPROIC ACID
complexes with thorium in chloroform and perchlorate solutions, 19: 38567
CARBAMIC ACID, DITHIO-
iron salts, relaxation effects in, (E), 19: 38653
CARBAMIC ACID ESTERS
4-dimethylamino-3,5-xylyl methylcarbamate, carbon-14 labeling of, 19: 38748
CARBAZOLE, VINYL- POLYMERS
radiation effects on, 19: 39232 (FZK-227)
CARBON
cesium-137 gamma spectra in, stress effects on, (E), 19: 39794
chemical states in lithium and sodium, 19: 39157 (CNLM-6337)
crystal structure of pyrolytic, deposited in fluidized beds, 19: 39184
deposition of pyrolytic, on fuel particles, 19: 39126 (CONF-117(p.149-70))
deposition on ceramic fuel particles, processes for, 19: 39091(R) (BMI-1723(Del.))
deposition on fuel particles, methods for, 19: 39129(R) (ORNL-TM-1116)
determination in sodium, corrections for, 19: 40112(R) (ANL-7046 (p.36-66))
diffusion in bcc crystals, activation energy for interstitial, (T), 19: 40086
diffusion of thorium and uranium in, at high temperatures, 19: 39129(R) (ORNL-TM-1116)
effects on cesium ion and neutral emission from hot porous tungsten, 19: 39164 (N64-22193)
effects on specific electrical resistivity of tantalum crystals, 19: 39203
electron reactions with atomic, screening effects on bremsstrahlung and pair production in, (T), 19: 39389
emittance of candle soot, total hemispherical, 19: 39167 (RFP-616)
microstructure of, chemical and thermal effects on, 19: 39129(R) (ORNL-TM-1116)
neutron albedo measurement on, thermal, 19: 40065 (NP-15152)
neutron reactions (n,n′γ) at 0 to 14 Mev, energy absorption in, 19: 39769 (SC-DC-65-1544)
oxidation of, by oxygen at 500 to 600°C, kinetics of, 19: 39119
oxidation of, effects of crystal structure on, 19: 38599
porosity of, method for reducing, 19: 38684(P)
preparation by reaction of carbon dioxide with polymer carbons, 19: 38599
proton inelastic scattering at 15 to 1900 kev, x-ray yields from, (E), 19: 39881
reactions with thoria at high temperatures, 19: 38755(R) (ORNL-3611)
CARBON (ACTIVATED)
use as support for platinum metal catalyst during irradiation, 19: 38742(P)
CARBON ARCS
temperature profile of low-current, in air, (E), 19: 39986
CARBON DIOXIDES
diffusion of carbon-14-labeled from scintillation solution, method of preventing, 19: 38746
diffusion of gases of, in temperature gradients, (E), 19: 39291
ionization cross section for, electron-impact, 19: 38630

ionization cross sections for negative-ion formation, electron-impact, 19: 38631
isotopic composition in soil, effects on carbon-13 variations in secondary calcites, 19: 38854
quadrupole moments, 19: 39378
radiation effects on reactions with hydrocarbons, 19: 38727(T)
radiation effects on compatibility with uranium, 19: 39121
reactions of partially decomposed, with uranium, 19: 39121
reactions of radiolytic, 19: 39265(R) (IA-1021)
reactions with polymer carbons, production of carbon in, 19: 38599
CO_2–H, nuclear spin lattice relaxation in, 19: 39378

CARBON ISOTOPES C-10
energy levels, (E), 19: 39839

CARBON ISOTOPES C-11
production in blood cells by proton irradiation, 19: 38722

CARBON ISOTOPES C-12
decay (3α) in proton reactions with boron-11, angular distributions in, (T), 19: 39912
deuteron (d,a) reactions at 2.8 Mev, neutron polarization in, 19: 39950
electron scattering on, isospin selection rules for, (E/T), 19: 39855
energy levels (163 kev) of, 3α decay in proton reactions with boron-11, (E), 19: 39918
energy levels in intermediate systems in boron-10 (He-3,pαααα) reactions, (E), 19: 39917
gamma absorption by, with two-nucleon emission, (T), 19: 39932
lithium-6 reactions (Li-6,α) at 4.0 to 5.5 Mev, cross sections for, (E), 19: 39853
meson (π⁻) absorption by, with two-nucleon emission, (T), 19: 39932
neutron reactions at 2.5 to 5 Mev, total cross section for, 19: 40115 (CONF-650602-33)
proton inelastic scattering at 150 Mev, polarization in, (E/T), 19: 39837
proton reactions (p,γ) with, cross sections for, (T), 19: 39805
proton reactions (p,t) at 155 Mev, (E), 19: 39839
proton reactions (p,2p) at 155 Mev, angular correlations in, (T), 19: 39905
proton reactions (p,pα) at 85 Mev, angular distributions in, (E), 19: 39908
reactions with emulsion nuclei at 10.4 Mev/nucleon, range-momentum relation for heavy recoil ions in, (E), 19: 39883
reactions with rhenium-103 at 40 to 80 Mev, decay of indium-109 isomeric state from, (E), 19: 39861

CARBON ISOTOPES C-13
content in sequential stalactite layers from karst caves of Crimea Highlands, 19: 38854
deuteron (d,n) reactions at 2.8 Mev, neutron polarization in, 19: 39950
energy levels in, neutron width of ½⁻, (T), 19: 39848
neutron separation energy for, (E), 19: 39862
proton reactions (p,γ) with, cross sections for, (T), 19: 39805

CARBON ISOTOPES C-14
beta activity in carbamates in liquid scintillation mixtures, phenylethylamine carbamate, 19: 38746
content in atmosphere, 1954 to 1963, 19: 38861
determination with phosphorus-32 and tritium on chromatograms, method for, 19: 38561
genetic effects of incorporated, in *Drosophila melanogaster*, 19: 38400
incorporation in *Drosophila melanogaster*, method for, 19: 38400
incorporation in 4-dimethylamino-3,5-xylyl methylcarbamate, 19: 38748
incorporation into trichloromethylcycloalkanes, 19: 38695 (KFK-317)
use in detection of microorganisms in jet fuel, 19: 39061 (ADR-09-08a-63.1)

CARBON MONOXIDES
ionization cross section for, electron-impact, 19: 38630
ionization cross sections for negative-ion formation, electron-impact, 19: 38631
ionization of, isotope effects on Franck-Condon factors in, 19: 38632
quadrupole moments, 19: 39378
CO–H, nuclear spin lattice relaxation in, 19: 39378

CARBON STEEL
gamma absorption by, effective atomic numbers for, 19: 40069

CARBON SYSTEMS
C–Cd–Ti, preparation and crystal structure of H-phase in, 19: 39208
C–Cr–Fe–Mo–Ni, reinforcement of graphite by, 19: 39114(P)
C–Fe, martensite formation in, 19: 40283 (COO-1198-237)
C–Fe–Ni, martensite formation in, 19: 40283 (COO-1198-237)
C–Hf–Ta–W, cavitation of T-222(A) in bismuth–lead alloy at 500 and 1500°F, ultrasonic-induced, 19: 39116 (NP-15263)
C–H–U, preparation, 19: 40286(R) (NAA-SR-11200)
C–Nb–W–Zr, fabrication and properties at –325 to 3000°F, 19: 39224(P)
C–U, vapor pressure studies, 19: 39160 (LA-DC-6953)
C–U–UC, analysis for free uranium, 19: 38540 (CEA-Note-397)

CARBON TETRACHLORIDE
radiation effects on bromine-80 and -82 retentions in, isomeric transition reaction in, 19: 38715
radioinduced reactions with cycloalkenes, gamma, 19: 38695 (KFK-317)
reactions with uranium oxides, intermediate products in, 19: 38661

CARBON TETRAFLUORIDE
nuclear magnetic resonance spectra of, collision-narrowing theory of, 19: 38629

CARBONATES
radiation effects on poly-, 19: 39232 (FZK-227)

CARCINOMAS
radiation dose effects on growth of mammary, in F_1 hybrid mice, x, 19: 38403
radioinduced by inhaled plutonium-239 aerosols, in dogs, 19: 38359 (BNWL-SA-230)
radiotherapy of uterine, hemolysis induced by, 19: 38509
radiotherapy of uterine, late pathological effects, 19: 38531
radiotherapy of uterine, late pathological effects, 19: 38532
radiotherapy of vocal cord, effects on larynx from radium, 19: 38519

CARDIOGRAPHY
computer diagnosis of electrocardiograms, 19: 39269(R) (SU-SEL-64-133)
radiation effects on, in stressed rats exposed *in utero*, 19: 38361(R) (TID-21951)

CAROLINAS-VIRGINIA TUBE REACTOR
operation, May 1965, 19: 40179(R) (CVNA-236)

CARTILAGE
radiation injury and repair in rat, 19: 38407

CASCADE IMPACTORS
calibration for sampling atmospheric sodium oxide particles, 19: 40286(R) (NAA-SR-11200)

CASCADE SHOWERS
production of electron-photon, in electron reactions with lead at 100 to 1000 Mev, (T), 19: 40070

CATALASES
radioinduced deactivation of, effects of copper on, 19: 39265(R) (IA-1021)

CATALYSIS
mechanisms of, radiochromatographical method for studying, 19: 38718

CATALYSTS
radiation effects on platinum hydrogenation, 19: 38742(P)

CATHODES
design and performance of screen-mesh, for electron-beam production, 19: 38949
development for cesium ion rocket motors, 19: 38834(R) (N64-29495)

CATION EXCHANGE MATERIALS
performance in radioactive waste processing and radioactive water purification, (E), 19: 40130 (ZFK-RN-17(p.165-78))
properties of volcanic tuff, for separation of cesium and strontium from aqueous solutions, 19: 38768
radiation effects on properties of volcanic tuff, 19: 38768

CATTLE
fallout uptake by German, 1962, 19: 38858

CAVES
design and operation of high-level alpha-gamma cells, 19: 38793 (JUL-251-RW)
design and operation of small cast iron alpha-gamma cells for disassembly of test irradiations and fuel elements, 19: 38795 (JUL-253-RW)
diffusion of radioactive materials from, methods of preventing, 19: 38902
packaging of disassembled fuel elements and radioactive waste in hot cells, 19: 40270 (JUL-249-RW)
use and decontamination of standardized in-cell boxes, 19: 38794 (JUL-252-RW)

CAVITATION
ultrasonic-induced, of materials in bismuth–lead alloy at 500 and 1500°F, 19: 39116 (NP-15263)

CAVITY RESONATORS
use with reactor fuel elements for temperature measurement, 19: 40138(P)

CENTRIFUGES
scanner for ultra-, multiple-cell photoelectric, 19: 38921 (UCRL-11623)

CERAMIC MATERIALS
radiation absorption by spheres of, incorporating gamma emitters, 19: 40275
radiation effects on ceramoplastic, 19: 39232 (FZK-227)

CERIUM
densities of liquid, effects of temperature on, 19: 39163(R) (MLM-1244)
effects on superconducting transition temperature of vanadium silicide, 19: 39196
electron band structure calculations, 19: 40081 (SC-DC-65-1500)
pathological effects of subcutaneous implantations of, in mice, 19: 38334 (COO-1170-1)
phase transformations at 6 to 65 kbar, solid-liquid and solid-solid,

19: 40095
CERIUM ALLOYS
Ce–Co–Pu, densities of liquid, effects of temperature on, 19: 39163(R) (MLM-1244)
Ce–Co–Pu, density at 25 to 800°C, 19: 39161 (LA-DC-6956)
Ce–Co–Pu, viscosities of liquid, effects of composition and temperature on, 19: 39163(R) (MLM-1244)
Ce–Cu, microstructure and phase studies of, 19: 39163(R) (MLM-1244)
Ce–Fe–Pu, phase studies, 19: 39163(R) (MLM-1244)
Ce–Ir, phase studies, 19: 39163(R) (MLM-1244)
Ce–Ni–Pu, phase studies, 19: 39163(R) (MLM-1244)
Ce–Pd, phase studies, 19: 39163(R) (MLM-1244)
Ce–Pt, phase studies, 19: 39163(R) (MLM-1244)
Ce–Pu, melting point, 19: 39163(R) (MLM-1244)
Ce–Pu, viscosities of liquid, effects of composition and temperature on, 19: 39163(R) (MLM-1244)
Ce–Rh, phase studies, 19: 39163(R) (MLM-1244)
CERIUM COMPLEXES
with acetates, preparation and properties of, 19: 38666
with [(2-hydroxyethyl)imino]diacetic acid, dissociation constant of, 19: 38671
CERIUM FLUORIDES
preparation and reactions of tetravalent, 19: 39182
vapor pressure of tri-, at 1370 to 1685°K, 19: 38592 (UCRL-16150)
CeF_4–CeF_3, phase studies, 19: 39183
CERIUM IONS
crystal-field interactions of, linear and nonlinear shielding of, (E/T), 19: 40101
CERIUM ISOTOPES Ce-141
determination in rain water, 19: 38557
release from pyrolytic carbon-coated fuel particles, 19: 39228 (BMI-1734)
CERIUM ISOTOPES Ce-144
content in irradiated uranium carbide cladding, 19: 40286(R) (NAA-SR-11200)
determination in rain water, 19: 38557
motion in soil, effects of chelating agents on, 19: 38329 (TID-20471)
CERIUM OXIDES
reactions with cerium tetrafluoride, 19: 39182
reactions with sodium metaphosphate, spectra of compound formed in, 19: 38668
CeO_2–UO_2, phase studies, 19: 39222
CeO_2–UO_2, radiation effects on clad, at high burnups, 19: 39091(R) (BMI-1723(Del.))
CeO_2–UO_2, thermodynamic properties, 19: 39222
CERMETS
crystal structure and properties of nichrome–plutonia, effects of high temperatures on, 19: 39125(R) (BNWL-91)
fabrication of stainless steel–uranin, 19: 39125(R) (BNWL-91)
fabrication of stainless steel–plutonia, 19: 39125(R) (BNWL-91)
performance as thermionic diode electrode insulators, 19: 39070(R) (GEST-2046)
CESIUM
book: *Cesium and Rubidium*, 19: 38674(T)
content and distribution in subterranean Bulgarian salt water, 19: 38851
corrosive effects on thermionic diode components, 19: 39070(R) (GEST-2046)
density of plasma of, microwave diagnostics of, (E), 19: 39980
effects of plasma of, on thermionic diodes in autonomous discharges, 19: 39435(T) (JPRS-31048)
effects on electron emission from tungsten, 19: 39441
electron beam reactions with plasma of, microwave amplification by, (E), 19: 40036
feed system design and operation for ion rocket motors, 19: 38834(R) (N64-29495)
production and uses, 19: 39106
separation from aqueous solutions, properties of tuff cation exchanger for, 19: 38768
separation from waste water, methods for, 19: 40276
separation from zirconium in nitric acid solutions, 19: 38778(P)
sorption by gamma-alumina and inorganic ion exchange materials from fused salts, 19: 38771
stability of highly ionized dense plasma of, in Penning arc, (E), 19: 40023
CESIUM ALUMINUM SILICATES
separation of cesium and rubidium from, 19: 39106
CESIUM BROMIDES
radiation effects on color centers in, low-temperature x, 19: 40098
reduction by high-frequency hydrogen discharge to hydrogen halide and metal, 19: 39180
reduction by high-frequency discharge in helium, hydrogen, and nitrogen, role of electrons in, 19: 39181
CESIUM CHLORIDES
reduction by high-frequency hydrogen discharge to hydrogen halide and metal, 19: 39180
reduction by high-frequency discharge in helium, hydrogen, and nitrogen, role of electrons in, 19: 39181
CESIUM IONS
emission from tungsten, impurity effects on, 19: 39164 (N64-22193)
radiolysis of aqueous solutions of, pulse, 19: 38728
CESIUM ISOTOPES Cs-131
energy from, determination of total, 19: 38878 (ORNL-P-1405)
metabolism by tumors, differential, 19: 38508
metabolism of injected, in man, 19: 38502
metabolism of injected, in man, 19: 38503
CESIUM ISOTOPES Cs-133
Mossbauer effect in barium chloride and barium–aluminum alloys, (E), 19: 39295
CESIUM ISOTOPES Cs-137
content in animals of California coast, 19: 38895
content in atmosphere, 1954 to 1963, 19: 38861
content in diet and excreta in Japan, 19: 38894
content in German milk, 1962, 19: 38858
content in irradiated uranium carbide cladding, 19: 40286(R) (NAA-SR-11200)
content in milk, effects of atmospheric transport of fallout on, 19: 38857
determination in man, whole-blood method for, 19: 38349
gamma spectra in graphite, stress effects on, (E), 19: 39794
motion in soil, effects of chelating agents on, 19: 38329 (TID-20471)
radiation protection standards for atmospheric, 19: 38877 (NP-15183)
CESIUM PHOSPHOMOLYBDATES
precipitation from alkali solutions, 19: 38778(P)
CESIUM SYSTEMS
He–Cs, electron temperature increases in MHD cell plasma of, (T), 19: 39437
CESIUM XENATES
preparation and properties, 19: 38624
CHARGED PARTICLE BEAMS
motion through plasma, longitudinal instabilities in, (T), 19: 40008
oscillations in multivelocity plasma, longitudinal, (T), 19: 39964 (NP-15201)
use for irradiation of materials, apparatus for, 19: 38831
CHARGED PARTICLES
charge density of spin ½, nonobservability of, (T), 19: 39516
Cherenkov radiation generation in plasma, (T), 19: 39995
density in arc plasma, effect of surrounding gas pressure on, (E), 19: 39989(T)
emission by heavy nuclei, evaporation theory for, 19: 39936
flux of interplanetary, solar wind theory for, 19: 39364
interactions in plasma, kinetic effects in, 19: 40056(T)
motion in electromagnetic fields, drift approximation for, 19: 40055(T)
motion in nonadiabatic fields, analysis of, 19: 39270(R) (TID-21894)
motion in plasma, equations for, (T), 19: 40006
tracks in solids, identification after chemical etching, 19: 39038
tracks in solids, research on, 19: 39226(R) (AFCRL-65-305)
CHELATES
reactions with fluorides in bone, 19: 39265(R) (IA-1021)
CHEMICAL RADIATION DETECTORS
performance of ammonium, potassium, and sodium nitrates, 19: 39042
performance of mailed ferrous sulfate and lithium fluoride, for high energy electron beams, 19: 38723
use of chloroform-dye system as, 19: 38732
CHEMICALS AND REAGENTS
meson (μ^-) capture by, 19: 39366 (JINR-P-2185)
CHEMISTRY
heat for processes in, from power reactors, 19: 38686(P)
of molten beryllium fluoride–lithium fluoride, 19: 38582 (ORNL-P-1428)
research at IFA, 19: 40287(R) (NP-15188)
CHERENKOV DETECTORS
use in high-energy photoproduction experiments, 19: 39041
CHERENKOV RADIATION
polarization of, from electrons, (E), 19: 39599
production hydromagnetic, by charged particles in plasma, (T), 19: 39995
CHIMERAS
radiation effects on serum proteins in mice following transplants of rat-to-mouse chimeras, 19: 38404
radiation, immunologic role of thymus in, 19: 38451
CHLORIDE IONS
radiolysis of aqueous solutions of, pulse, 19: 38728
CHLORIDES
corrosive effects on 430 stainless steel, 19: 40113(R) (ANL-7071)
CHLORINE
effects on cesium ion and neutral emission from hot porous tungsten,

19: 39164 (N64-22193)
reactions with uranium tetrachloride in lithium chloride–potassium chloride melt, kinetics, 19: 38587 (UCRL-11986)
solubility in lithium chloride–potassium chloride eutectic melt, 19: 38587 (UCRL-11986)
CHLORINE FLUORIDES
use in hygrometric measurement of uranium (IV) fluorides in noncondensable gases, 19: 38573(P)
CHLORINE ISOTOPES Cl-35
proton reactions (p,γ) at 0.4 to 3.1 Mev, energy levels from, (E), 19: 39828
CHLOROFORM
chloroform-dye, properties for use as chemical dosimeter, 19: 38732
nuclear magnetic resonance spectra of, collision-narrowing theory of, 19: 38629
radioisduced reactions with cycloalkenes, gamma, 19: 38695 (KFK-317)
CHLOROPHYLLS
protective effects of cobalt-, against radiation damage in mice, 19: 38456
CHROMATE IONS
radiolysis of aqueous solutions of, pulse, 19: 38728
CHROMATOGRAPHY
radioassay of doubly labeled chromatograms, method for, 19: 38561
CHROMIUM
determination in stainless steel, electron microprobe, 19: 38536 (ACF-6)
diffusion of atoms in bcc, activation energy for interstitial, (T), 19: 40086
effects on superconducting transition temperature of vanadium silicide, 19: 39196
electric conductivity at 270 to 320°K of, effects on magnetic fields on, 19: 40077 (IS-T-18)
separation from graphite above 1750°C in inert gases, 19: 38762
CHROMIUM ALLOYS
tensile properties of René 62, 19: 39156(R) (CEND-532)
Al–Cr–Fe–Mo–Ti, mechanical properties and heat resistance, 19: 39193
Al–Cr–Fe–Mo–Ni–Nb–Ti, thermal response and microstructure of Inconel 718 at 1200 and 1400°F, 19: 39158 (GEAP-4751)
Cr–Fe, diffusion of fission products in, mechanisms of, 19: 39152(R) (BMI-X-10132)
Cr–Fe–Mo–Ni–Nb–W, tensile properties of IN-102, 19: 39156(R) (CEND-532)
Cr–Fe–Mo–Ni–Nb, thermal response and microstructure of Inconel 625 at 1200 and 1400°F, 19: 39158 (GEAP-4751)
Cr–Mn, antiferromagnetism of, at 95 to 300°K, 19: 40077 (IS-T-18)
Cr–Mn, electric conductivity and thermoelectric power of, at 4.2 to 450°K, 19: 40077 (IS-T-18)
Cr–Nb–Ti, mechanical properties for high-temperature applications, 19: 39192
Cr–Ni, reactions with plutonia at high temperatures, 19: 39125(R) (BNWL-91)
Cr–Re, aging of, effects of nitrogen on, 19: 39091(R) (BMI-1723(Del.))
Cr–Re, antiferromagnetism of, at 95 to 300°K, 19: 40077 (IS-T-18)
Cr–Re, electric conductivity and thermoelectric power of, at 4.2 to 450°K, 19: 40077 (IS-T-18)
Cr–Ti–V, mechanical properties at high temperatures, 19: 40177(R) (ANL-7046(p.1-35))
Cr–V, antiferromagnetism of, at 95 to 300°K, 19: 40077 (IS-T-18)
Cr–V, electric conductivity and thermoelectric power of, at 4.2 to 450°K, 19: 40077 (IS-T-18)
CHROMIUM IONS
radiolysis of aqueous solutions of, pulse, 19: 38728
CHROMIUM ISOTOPES Cr-51
energy from, determination of total, 19: 38878 (ORNL-P-1405)
use in determining red blood cell volumes in rabbits and sheep, 19: 38346
use in radiodiagnosis, review on, 19: 38505
CHROMIUM ISOTOPES Cr-52
proton inelastic scattering at 2.5 to 7.5 Mev, level multipolarities, parity, and spin from, (E), 19: 39826
CHROMIUM ISOTOPES Cr-54
gamma transition in, energy of, (E), 19: 39866
CHROMIUM STEEL
Cr–Mo, corrosion of Croloy 2¼ by sodium hydroxide solutions at 0 to 900°F, 19: 38803(R) (BAW-1280-26)
CHROMIUM SYSTEMS
C–Cr–Fe–Mo–Ni, reinforcement of graphite by, 19: 39114(P)
CHROMOSOMES
analysis of, uses of flying-spot devices for photographic, (E), 19: 38910 (CERN-65-11(p.43-56))
genetic code for messenger ribonucleic acid synthesis, 19: 40296 (TID-21856)
radiation effects on tritiated valine uptake by *Vicia faba*, x, 19: 38417
radioinduced aberrations in Tradescantia, 19: 38360 (TID-21695)
radioinduced aberrations in barley and *Vicia faba*, modifying effects of acridine orange and methylene blue on, 19: 38462
radioinduced aberrations in hamster, uv, 19: 38395
radioinduced aberrations in Tradescantia, synergistic infrared and x, 19: 38416
radioinduced breaks in barley, interaction in neutron and x-ray, 19: 38399
radioinduced lethals in populations of *Drosophila willistoni*, suppressors in, 19: 38391
radioinduced mutations in rat, effects of ploidy on thermal neutron, 19: 38419
CIRCUITS
analysis of lumped nonlinear, 19: 39269(R) (SU-SEL-64-133)
description and performance of compensated integrating, for ground velocities and displacements, 19: 38918 (SC-R-65-904, pp 49-58)
design and use of sensitive high-speed d-c voltage comparator, (E/T), 19: 40279 (BDX-613-72)
design for detection of fuel element failure in organic cooled reactors, 19: 40133
design for energy transfer from inductive store to inductive load, 19: 38960(P)
design for Geiger-Mueller counters, 19: 39021
design of printed, automated etching layout for, 19: 38915 (SC-DC-65-1419)
fabrication of, from metal films using electron beams, 19: 38950
performance analysis of fast complementary tunnel-diode hybrid bistable meltivibrator, (E/T), 19: 38920 (TID-22019)
theory of pulse sequential, for solid-state electronic control, 19: 40278 (AD-425879)
CIRCULATORY DISEASES
radiodiagnosis of brain, 19: 38501
radiodiagnosis of, involving blood volume, 19: 38525
CIVILIAN DEFENSE
consumption and inspection of food and water in event of nuclear conflict, 19: 38882
fallout meter design for, 19: 39051(P)
CLOSTRIDIUM
radioinduced alpha-toxin formation in, 19: 38448
radioinduced changes in antigenic and immunogenic properties of, gamma, 19: 38447
radioinduced mutations in, antigen characteristics of, 19: 38445
radioinduced mutations in, activity of alpha toxin in, 19: 38446
COATINGS
deformation of, on fuel elements, 19: 39220
deposition on fuel particles, methods for pyrolytic carbon, 19: 39129(R) (ORNL-TM-1116)
development for sodium-cooled reactor fuels, 19: 40177(R) (ANL-7046(p.1-35))
diffusion of fission products in, mechanisms of, 19: 39152(R) (BMI-X-10132)
properties of pyrolytic carbon, effects of heating on, 19: 39129(R) (ORNL-TM-1116)
radioactivity of irradiated fuel, 19: 40286(R) (NAA-SR-11200)
reactions of pylolytic carbon, with water vapor at 1000°C, 19: 39129(R) (ORNL-TM-1116)
stress on Zircaloy-2 during fuel compaction, 19: 39125(R) (BNWL-91)
thickness of, equipment for beta-backscatter measurement of, 19: 38952(P)
COAXIAL CABLES
pulse transmission by superconducting, (E), 19: 39740
radiation effects on, transient, 19: 39055 (GA-6266)
radiation effects on, 19: 39056 (N64-29558)
COBALT
determination in low-alloy steel by x-ray spectrography, 19: 38571
radiation effects on magnetic properties of, electron, (E), 19: 39239
sorption by gamma-alumina and inorganic ion exchange materials from fused salts, 19: 38771
COBALT ALLOYS
Ce–Co–Pu, densities of liquid, effects of temperature on, 19: 39163(R) (MLM-1244)
Ce–Co–Pu, density at 25 to 800°C, 19: 39161 (LA-DC-6956)
Ce–Co–Pu, viscosities of liquid, effects of composition and temperature on, 19: 39163(R) (MLM-1244)
Co–Pu, phase studies, 19: 39163(R) (MLM-1244)
COBALT(II) CHLORIDES
free energy of formation at 400 and 450°C, 19: 38575 (BNL-9343)
COBALT COMPOUNDS
protective effects of chlorophyll, against radiation damage in mice, 19: 38456
COBALT IONS
radiolysis of aqueous solutions of, pulse, 19: 38728
COBALT ISOTOPES Co-57
energy from, determination of total, 19: 38878 (ORNL-P-1405)

production in the Intense Neutron Generator, 19: 39762 (AECL-2177, Paper 9))
COBALT ISOTOPES Co-58
production in the Intense Neutron Generator, 19: 39762 (AECL-2177, Paper 9))
use in radiodiagnosis, review on, 19: 38505
COBALT ISOTOPES Co-60
design of automatic application gamma source for therapeutic use using, 19: 38483
therapeutic use for bladder cancers, 19: 38504
uses in Japan, 1950 to 1960, 19: 39060
COINCIDENCE COUNTERS
development of high- and low-energy, for helium and hydrogen isotopes in space, 19: 39419(R) (ATN-63(9219)-1)
COLLAGEN
radiation effects on viscosity of solutions of rat tail, uv, 19: 38701
COLORADO RIVER BASIN (UTAH)
population studies on plants and small vertebrates in uranium areas in, 19: 38330 (TID-22078)
COLUMBIA RIVER
radioactive waste disposal in, safety precautions for, 19: 40277
radioactivity of, 1964, 19: 38874 (BNWL-SA-53)
COMMUNICATION SYSTEMS
development of tactical, 19: 39269(R) (SU-SEL-64-133)
performance of high-frequency, in nuclear environments, 19: 38783
COMMUNICATION THEORY
research progress on statistical, 19: 39270(R) (TID-21894)
COMPUTER PROGRAMS
ACCEL, for printed circuit etching layout, 19: 38915 (SC-DC-65-1419)
AGN-GAM, for neutron spectra and multigroup constants in reactors, in FORTRAN for IBM 7090, 19: 40176 (AGN-TM-407)
CHAD, for neutron angular distribution, 19: 40286(R) (NAA-SR-11200)
CHARGE, for radiation shielding analysis, in FORTRAN, 19: 40064 (NP-15132)
CHIC-KIN, for reactivity transients in water moderated reactors, in FORTRAN, 19: 40160 (WAPD-TM-479)
development for flying-spot analysis of particle-track photographs, (E), 19: 38990 (CERN-65-11(p.229-36))
development for medical diagnosis, 19: 39270(R) (TID-21894)
development for nuclear plant environmental hazards, 19: 39265(R) (IA-1021)
development for radioactive material diffusion in sea water, 19: 39265(R) (IA-1021)
DIAGNOSE, for debugging FORTRAN programs, 19: 39081 (ORNL-TM-1176)
ENOCH, for burnup in cylindrical reactors, 19: 40147 (AEEW-M-448)
FILTER, for flying-spot analysis of particle-track photographs, (E), 19: 38981 (CERN-65-11(p.115-21))
FILTER, for particle-track analysis by flying-spot devices, (E), 19: 38983 (CERN-65-11(p.139-43))
for analysis of behavior data, for IBM 1620, 19: 38361(R) (TID-21951)
for computing in combinatorics, 19: 39079 (LA-DC-7160)
for electron bremsstrahlung radiation doses behind shielding in space, FORTRAN for IBM 7090, 19: 40062 (N64-29366)
for finding picture numbers in bubble-chamber photographs, (E), 19: 38979 (CERN-65-11(p.91-5))
for flying-spot analysis of bubble-chamber photographs, (E), 19: 38980 (CERN-65-11(p.97-113))
for flying-spot analysis of particle-track photographs, (E), 19: 38985 (CERN-65-11(p.153-72))
for flying-spot analysis of particle-track photographs, (E), 19: 38986 (CERN-65-11(p.173-81))
for flying-spot analysis of particle-track photographs, (E), 19: 38991 (CERN-65-11(p.237-58))
for neutron flux calculations in reactors, in FORTRAN for CDC 16040A, 19: 40157 (ORNL-TM-1175)
for neutron resonance absorption by mixtures, 19: 40112(R) (ANL-7046 (p.36-66))
for off-line flying-spot analysis of particle-track photographs, (E), 19: 38988 (CERN-65-11(p.183-206))
for optimization of 4 Mev radiotherapy planning, 19: 38518
for particle-track analysis by flying-spot devices, using FILTER output, (E), 19: 38983 (CERN-65-11(p. 139-43))
for particle-track following using flying-spot devices, (E), 19: 38984 (CERN-65-11(p.145-52))
for reactor fuel cycle analysis, 19: 40149 (BNWL-SA-61)
GAM-I, for ZPR-VII buckling calculations, 19: 40112(R) (ANL-7046 (p.36-66))
HAZE, for flying-spot analysis of particle-track photographs, (E), 19: 38982 (CERN-65-11(p.123-37))
HAZE, for particle-track analysis using flying-spot devices, (E), 19: 38984 (CERN-65-11(p.145-52))
HAZE, for particle-track analysis by flying-spot devices, (E), 19: 38983 (CERN-65-11(p.139-43))
KER-4, for thermal analysis of cylindrical fuel rods, FORTRAN IV for Philco 2000, 19: 40171 (KAPL-M-6475)
KINETICS I, for neutron kinetics in reactors, in FORTRAN IV for IBM 7090, 19: 40148 (BNWL-111)
LINK, analysis of particle-track data compiled by flying-spot devices, (E), 19: 38973 (CERN-65-11(p.15-23))
MC², for generation of multigroup cross sections, 19: 40112(R) (ANL-7046(p.36-66))
MINIMIZER, for reactor fuel economics, in FORTRAN for IBM 7090, 19: 40170 (HW-71813)
MLBW, for neutron cross sections of non-fissile natural elements, in FORTRAN for IBM 7090, 19: 39776 (AEEW-M-517)
NURSE-1, for nuclear rocket fission product release, 19: 40248 (NUS-180)
PERT, for design and installation phases in reactor construction, 19: 40265
PRISM, for neutron group transfer matrices, 19: 40286(R) (NAA-SR-11200)
PRTR, for one-dimensional multigroup perturbation, 19: 39265(R) (IA-1021)
SALOMON, for gamma transport calculations, in FORTRAN for IBM 7090, 19: 40066 (NP-15155)
SOURCE, for fission-neutron energy, spatial, and velocity distributions, FORTRAN 63, 19: 39767 (ORNL-TM-1192)
TEMPO, for Doppler-broadened cross sections, in FORTRAN II for IBM 7090, 19: 39777 (AEEW-M-518)
TM REP, for neutron resonance escape in thermal reactors, for Philco 2000, 19: 40153 (IA-1001)
COMPUTERS
coding for, adaptive, 19: 39269(R) (SU-SEL-64-133)
design of digital Madaline components for, 19: 39269(R) (SU-SEL-64-133)
logic circuits for, development, 19: 39269(R) (SU-SEL-64-133)
performance for bubble chamber photograph analysis, 19: 38970 (BNL-9236)
performance in studies of electron energy in thermionic diodes, 19: 39269(R) (SU-SEL-64-133)
performance of PDP-6, in system for digitized discharge planes for particle-interaction measurements, 19: 39450 (BNL-9232)
use in activation analysis, 19: 38568
use in graphical lathe part programming, 19: 40293 (SCL-DC-65-86)
use in simulation problems, 19: 40282 (BNWL-SA-171)
use in volumetric calibration of process vessels, 19: 38756 (RFP-488)
use of digital, in French power plants, 19: 40203
use of electronic digital, for calculating dose distribution from multiple radiation sources, 19: 38526
uses for control of flying-spot particle-track analyzers, (E), 19: 38987 (CERN-65-11(p.207-18))
uses for flying-spot particle-track analysis, (E), 19: 38975 (CERN-65-11(p.35-41))
uses for flying-spot analysis of spark-chamber tracks, (E), 19: 38976 (CERN-65-11(p.57-69))
uses for flying-spot analysis of spark-chamber photographs, (E), 19: 38977 (CERN-65-11(p.71-9))
uses for flying-spot analysis of bubble-chamber photographs, (E), 19: 38978 (CERN-65-11(p.81-90))
uses for flying-spot analysis of chromosome photographs, (E), 19: 38910 (CERN-65-11(p.43-56))
uses for flying-spot analysis of spark-chamber tracks, (E), 19: 38972 (CERN-65-11(p.7-13))
uses for programming flying-spot track-analyzing devices, (E), 19: 38971 (CERN-65-11)
uses with flying-spot devices for spark-chamber track analysis, (E), 19: 38974 (CERN-65-11(p.25-33))
CONCRETES
gamma absorption by, effective atomic numbers for, 19: 40069
neutron albedo measurement on, thermal, 19: 40065 (NP-15152)
neutron attenuation mechanisms in, 19: 40061 (BNWL-SA-79)
stress analysis of prestressed, finite element, 19: 40165 (GA-6303)
CONDUCTOMETRIC ANALYSIS
equipment for reactor coolant water, 19: 40262 (ZFK-RN-17(p.25-31))
CONES
pressure variation with Mach number on right circular, base and surface, (E/T), 19: 40292 (SC-TM-202-56-51)
CONFERENCES
see also introduction to Report Number Index
Electron and Ion Beam Science and Technology, First International Conference on, Toronto, May 1964, 19: 39307

Human Genetics, Cold Spring Harbor, N. Y., 1964, 19: 38328
Nuclear Fuels, Preparation and Processing of, New York, Sept. 1963, 19: 40168 (CONF-117)
Nuclear Technology, France-Japan Conference on, Tokyo, Nov. 12 to 14, 1962, 19: 40302
Spectroscopy Symposium, Fifteenth Annual Mid-America, Chicago, Illinois, June 1 to 5, 1964, 19: 38572

CONNECTORS (ELECTRIC)
radiation effects on, 19: 39056 (N64-29558)

CONTAMINATION
determination of organic residue from solvents, radioisotopic method for, 19: 38538 (ADR-08-13-63.1)

CONVERSION ELECTRONS
energy from, determination of total, 19: 38878 (ORNL-P-1405)

CONVEYERS
design for package irradiation facility, 19: 38797(P)

COPPER
argon ion scattering by single crystals of, energy distribution in, (E), 19: 39297
determination in trace amounts in aluminum by x-ray spectrography, 19: 38571
deuteron reactions (d,p) at 23 and 26 Mev, angular distribution and spectra in, (E), 19: 39901
effects on radiolytic deactivation of amylase and catalase, 19: 39265(R) (IA-1021)
electrolysis of porous, reaction distribution in acid, 19: 38591 (UCRL-16113)
electron inelastic scattering by crystals of, interband excitation in fast, (T), 19: 40083
electron reactions with atomic, screening effects on bremsstrahlung and pair production in, (T), 19: 39389
flow of plasma of, around magnetic dipole, (E), 19: 40009
gamma reactions at 6.13 Mev, electron pair production cross sections for, (E), 19: 39787 (SGAE-PH-19/1965)
radiation damage in, cross sections for atomic displacements from 1- to 3-Mev electrons, 19: 39225 (AFCRL-65-286)
radiation defects in, theory of, 19: 40286(R) (NAA-SR-11200)
radiation effects on, electron, 19: 40286(R) (NAA-SR-11200)
radiation effects on dislocations in annealed, neutron, 19: 39241
radiation effects on electric resistivity of, stage 1 annealing of electron, (E), 19: 39248
radiation effects on ultrasonic attenuation in monocrystalline, gamma, 19: 39249
rare-gas ion reactions at 1 to 10 kev, secondary-electron emission in, (E), 19: 39404
texture of rolled, from electron microscopic diffraction, 19: 39175(T) (ORNL-tr-638)
ultrasonic waves in, properties of finite-amplitude, 19: 39268 (ORNL-P-1395)
ultrasonic-wave attenuation in monocrystalline, at low temperatures, 19: 39249

COPPER ALLOYS
Ce–Cu, microstructure and phase studies of, 19: 39163(R) (MLM-1244)
Cu–Mn, iron-57 hyperfine magnetic field in, (E), 19: 39212
Cu–Pb, superconductivity of heterogeneous, particle size effects on, (E), 19: 39747
Cu–Pu, microstructure and phase studies of, 19: 39163(R) (MLM-1244)

COPPER IONS
radiation effects on optical absorption of, in potassium halides, (E), 19: 40107
radiolysis of aqueous solutions of, pulse, 19: 38728

COPPER ISOTOPES Cu-63
proton reactions (p,2p) at 10.5 Mev, relative proton-gamma emission widths in, (E), 19: 39903

CORDIERITES
pleochroic halos produced by zircon in biotite-cordierite, reversal, 19: 38846(T) (ORNL-tr-698)

CORROSION FILMS
deposition in Saxton reactor cooling system, 19: 40196(R) (WCAP-3269-6)
separation from reactor fuel elements, solutions for, 19: 40198(R) (WCAP-3721)

CORROSION LOOPS
development for reactor materials, 19: 40197(R) (WCAP-3718)
operation of chemical shim, for reactor materials, 19: 40198(R) (WCAP-3721)

CORTICOSTEROIDS
therapeutic effects for inflammations associated with radiotherapy, 19: 38512

COSMIC ELECTRONS
energy spectra, 19: 39420 (NP-15117)

COSMIC NEUTRINOS
production, (T), 19: 39361

COSMIC NEUTRONS
monitoring equipment for, 19: 39035

COSMIC PARTICLES
energy spectra in extensive air showers, (E/T), 19: 39423
energy spectra of helium nuclei at 62 to 1670 Mev, 19: 39420 (NP-15117)
energy spectrum of nuclear-active, (E), 19: 39429
intensity variation of helium, electric field modulation for, (T), 19: 39427

COSMIC PROTONS
energy spectra at 74 to 4000 Mev, 19: 39420 (NP-15117)

COSMIC RADIATION
absorption of cosmic noise, correlation with auroral luminosity, (E), 19: 39672
intensity variations with time, 19: 39421 (NP-15154)
intensity variation in, unusual diurnal, Dec. 1957, 19: 39426
nature and properties of, for space vehicle shielding, 19: 40072
origin in galactic explosions, evidence of, 19: 39362
origin of x, (T), 19: 39425
reactions with paraffin at high energies, angular distributions from, (E), 19: 39428
sorption by atmosphere and ionosphere, 19: 39363

COSMIC SHOWERS
density spectra of air showers, (E), 19: 39424
detection by atmospheric scintillation, 19: 39422(R) (TID-21895)
distribution of extensive, with primary particle energies above $3 \times 10^{\text{m}}$ ev, (E), 19: 39429
particle energy and interactions in extensive, (E/T), 19: 39423

COSMOLOGY
energy density of antineutrinos and neutrinos in universe, (T), 19: 39361
model of universe, black body radiation in, (T), 19: 39350
model of universe, singularities in homogeneous, 19: 39360

COUNTERCURRENT SEPARATION PROCESSES
design of plant for liquid-liquid, 19: 38777(P)

CRATERS
dimensions of Dugout row-charge, in basalt, 19: 38789 (PNE-601F)
Pre-Schooner experiment, stem design and shotcrete, grout, and concrete support for, 19: 38788 (PNE-501F)

CRITICAL ASSEMBLIES
buckling calculations for ZPR-VII, methods for, 19: 40112(R) (ANL-7046(p.36-66))
construction and developmental status of, compilation on, 19: 40116 (TID-8200(12th Rev.))
criticality of tungsten–uranium, effects of cadmium–indium–silver rods on, 19: 40195(R) (WCAP-3269-5)
criticality studies of LASL cavity reactor, 19: 40154 (LA-3229, pp 344-61)
criticality studies in, review, (E), 19: 40163
design for zero-reactivity experiments on heavy-water-moderated lattices, 19: 40266
development of ZPPR, 19: 40177(R) (ANL-7046(p.1-35))
neutron flux in Godiva, calculation of, 19: 40157 (ORNL-TM-1175)
neutron spectra in ZPR-VI, 19: 40113(R) (ANL-7071)
noise analysis in, (T), 19: 40164
physics measurements for closed-cycle water reactors, 19: 40197(R) (WCAP-3718)
physics measurements on ZPR-VI assembly 4Z, 19: 40177(R) (ANL-7046(p.1-35))
reactivity experiments in ZPR-IX, 19: 40113(R) (ANL-7071)
reactivity of ZPR-IX assembly 6, 19: 40177(R) (ANL-7046(p.1-35))
reactivity of ZPR-3 cores C and D, 19: 40113(R) (ANL-7071)
reactivity of ZPR-III, calculations of, 19: 39265(R) (IA-1021)

CRITICALITY STUDIES
analysis of core loadings and physics experiments in AARR, 19: 40257(R) (ANL-7046(p.67-77)

CROSS SECTIONS
method for calculating, covariant, (T), 19: 39943

CRUSTACEA
radiation effects on egg hatchability in Artemia, dose dependency of gamma, 19: 38383
radiosensitivity of eggs of Artemia, effects of moisture and temperature on gamma, 19: 38384

CRYOGENICS
hydrogen storage in large dewars, chilldown and boiloff losses, 19: 39686 (LA-DC-7164)

CRYOSTATS
design of helium, for x-ray diffraction studies of crystallized gases, 19: 38946

CRYSTAL DETECTORS
development of solid-state particle track, 19: 39038

CRYSTAL STRUCTURE

analysis of, by x-ray diffraction method, 19: 38826
exciton wave packet radiation in, (T), 19: 40088
phonon scattering by point defects, resonant, 19: 40109
CRYSTALS
brittle fracture and mechanical twinning in body-centered-cubic, 19: 39202
diffraction pattern indexing for tetragonal, hexagonal, and orthorhombic, charts for, 19: 40080 (NP-15182)
diffusion of atoms in bcc, activation energy for interstitial, (T), 19: 40086
electron inelastic scattering by, phonon excitation in fast, (T), 19: 40084
exciton wave packet radiation in atoms of, (T), 19: 40087
exciton wave-packet radiation in molecular, (T), 19: 40088
Fermi surface of, relativistic effects in, 19: 40076 (IS-1172)
galvanomagnetic phenomena in, quantum theory for, 19: 40106
lattice dipoles in, energy between induced, 19: 39265(R) (IA-1021)
light scattering in anharmonic, second sound detection by, (T), 19: 40092
neutron inelastic scattering by anharmonic, at low temperatures, (T), 19: 40093
scattering properties of, temperature variation of, (T), 19: 39176
space groups on surface of Brillouin zone of, projective representations for, 19: 40089
spectra of polar, analysis methods for infrared reflection, 19: 39270(R) (TID-21894)
spectra of powdered, Mössbauer line broadening for isomer and nuclear-multipole effects in, 19: 39876
surface vibrations of, S-matrix method for, (T), 19: 40108
thermodynamics of mass transport in ionic, 19: 38678
x-ray diffraction by, Pendelloesung fringes in, (E/T), 19: 39287
CUMENE
radiation effects on reactions with carbon dioxide, 19: 38727(T)
CURIUM
separation from irradiated plutonium by solvent extraction, 19: 39265(R) (IA-1021)
CURIUM ISOTOPES
nuclear properties of, pairing force effects on, (T), 19: 39927
CURRENT REGULATORS
design for superconducting solenoids, 19: 38945
CUTTING TOOLS
description of, for disassembly and dampling of graphite ball fuel elements, 19: 38792 (JUL-250-RW)
CYANIDE IONS
radiolysis of aqueous solutions of, pulse, 19: 38728
1-CYCLOBUTENE, 1,2-DICHLORO-3,3,4,4-TETRAFLUORO-
radioinduced reactions with methanol, ethanol, and 1- and propanol, 19: 38708
1,3-CYCLOHEXADIENE
radioinduced polymerization of, stereospecificity in, 19: 38725(T)
CYCLOHEXANE
diffusion in deuterated-normal mixture, coefficients of, 19: 38646
perfluoro-, radiation effects on, 19: 38709
radiation effects on bromine-80 and -82 retentions in, isomeric transition reaction in, 19: 38715
radioinduced reactions with chlorinated methanes, gamma, 19: 38695 (KFK-317)
radioinduced reactions with bromine, organic retentions of bromine-80m and -82 in, 19: 38713
cyclohexane–cyclohexene, radiolysis of, deuterium isotope effects on, 19: 38707
CYCLOHEXENE
radioinduced reactions with chlorinated methanes, gamma, 19: 38695 (KFK-317)
cyclohexane–cyclohexene, radiolysis of, deuterium isotope effects on, 19: 38707
cyclohexene–cyclopentane, radiolysis of, deuterium isotope effects on, 19: 38707
CYCLOPENTANE
radiolysis of liquid, yields in, 19: 38712
cyclohexene–cyclopentane, radiolysis of, deuterium isotope effects on, 19: 38707
CYCLOPENTENE
radioinduced reactions with chlorinated methanes, gamma, 19: 38695 (KFK-317)
yields in gamma radiolysis of liquid cyclopentane, 19: 38712
1,2-dichlorohexafluoro-, radioinduced reactions with methanol, ethanol, and propanol, 19: 38708
CYCLOPROPANE
yields in gamma radiolysis of liquid cyclopentane, 19: 38712
CYCLOTRON RADIATION
emission from self-consistent plasma, electron density effects on, (T), 19: 40013
CYCLOTRONS
characteristics of Karlsruhe relativistic isochronous, 19: 39322
conference on Intense Neutron Generator, 19: 39752 (AECL-2177)
development of Intense Neutron Generator, engineering problems in, 19: 39760 (AECL-2177, Paper 7))
development of Michigan 83-inch, 19: 39313 (COO-921-16)
development of separated-orbit proton, for intense neutron production, 19: 39755 (AECL-2177, Paper 2))
economics for Intense Neutron Generator, 19: 39753 (AECL-2177, Introduction)
experimental facilities of Intense Neutron Generator, 19: 39757 (AECL-2177, Paper 4)
power production in Intense Neutron Generator, nuclear, 19: 39758 (AECL-2177, Paper 5)
power supply system for Intense Neutron Generator, r-f, 19: 39759 (AECL-2177, Paper 6))
radioisotope production in the Intense Neutron Generator, 19: 39762 (AECL-2177, Paper 9))
shielding of Intense Neutron Generator, 19: 39761 (AECL-2177, Paper 8))
target development for Intense Neutron Generator, 19: 39756 (AECL-2177, Paper 3))
CYLINDERS
electron motion between coaxial conducting, (T), 19: 39275
inspection for dimensional variations, apparatus for, 19: 38830(P)
CYSTINE
labeling with sulfur-35 by neutron irradiation, 19: 38747
CYTOLOGY
of exfoliated cells from cancer patients undergoing radiotherapy, response to acridine orange stain, 19: 38488
of irradiated cells in tissue culture, 19: 38386
of irradiated single cells in tissue culture, technique for, 19: 38385
CYTOPLASM
radiation effects on, of cells in tissue culture, 19: 38386
CZECHOSLOVAKIA
radiation monitoring in dust and rainfall in, 1961 to 1963, 19: 38881

D

DATA RECORDING SYSTEMS
design for electron collision cross section measurements, 19: 38943
design of digital, for mass spectrometers, 19: 39023
development of automated, for rat maze behavior, 19: 38361(R) (TID-21951)
testing for hydrostatic pressure sensors, 19: 40288(R) (NVO-98-5)
DATA TABULATIONS
cosmic ray intensity variations, 19: 39421 (NP-15154)
elementary particles and resonant states, properties of, 19: 39485 (UCRL-8030(Pt.I)(Mar. '65, ed.))
internal conversion coefficients for plutonium, rare earth, thorium, and uranium isotopes, 19: 39786 (ORNL-P-1419)
neutron cross sections for beryllium-9 at 1 to 15 Mev, 19: 39775 (AEEW-M-513)
radiation damage atomic displacement cross sections, 1- to 3-Mev electron, 19: 39225 (AFCRL-65-286)
radioactive decay correction factors, 19: 38744 (PHS-999-RH-12)
reactivity sodium void coefficients for fast, 19: 40158 (UNC-5123)
reactor fuel costs, simulated pressurized water, 19: 40114 (BNWL-104)
use of memory-stored, in computers, 19: 40112(R) (ANL-7046(p.36-66))
DECONTAMINATING SOLUTIONS
analysis of reactor fuel element, 19: 40198(R) (WCAP-3721)
DECONTAMINATION
equipment and method for, of fluids, 19: 40119(P)
DECONTAMINATION OF EQUIPMENT
method for in-cell boxes in hot caves, 19: 38794 (JUL-252-RW)
DENSITOMETERS
calibration of radiometric, 19: 38953(P)
development for crushed oxide fuels, 19: 39125(R) (BNWL-91)
DEUTERIUM
acceleration of plasma of, by coaxial guns, 19: 39956 (LA-DC-7043)
diffusion of gases of, in temperature gradients, (E), 19: 39291
effects on bromination of acetoacetates, acetylacetones, and malonates, 19: 38692
effects on product distributions in radiolysis of paraffin-olefin solutions, 19: 38707
electric discharge in, structure of, (E), 19: 39286
exchange between heavy water and organics, group VIII metal catalysis of, 19: 38597
exchange between hydridoplatinum complex and heavy water, 19: 38627
exchange reactions in benzene, naphthalene, and *n*-octane, catalytic, 19: 38596
incorporation in *N*-methyl-4-pyridones, 19: 38689

ionization cross section for, electron-impact, 19: 38630
ionization cross sections for negative-ion formation, electron-impact, 19: 38631
isotope effects on aqueous solution radiolysis, 19: 39265(R) (IA-1021)
mass spectra of molecular, anomalous peaks in, (E), 19: 39288
motion of theta-pinch plasma of, in asymmetric fields, (E), 19: 40010
nuclear spin lattice relaxation in, 19: 39378
pinch effect in, field and impurity effects on theta, (E), 19: 40005
proton reactions (p,2p)n at 9.0 and 10.5 Mev, energy-angular correlations and sequential decay in, (E), 19: 39924
proton reactions (p,2p)n at 31 Mev, angular distributions from, (E), 19: 39925
quadrupole moments, 19: 39378
radiation effects on exchange with hydrogen ions in silica gels, 19: 38626
reactions of, with palladium electrodes, 19: 38608
thermal diffusion of, in hydrogen mixtures, at 160°K, 19: 38633
thermodynamic properties of liquid, 19: 38639
use in measurements of self-diffusion in liquid ammonia, 19: 38579 (JUL-238-PC)

DEUTERIUM HYDRIDES
ionization cross sections for negative-ion formation, electron-impact, 19: 38631
thermodynamic properties of liquid, 19: 38639

DEUTERIUM TRITIDES
thermodynamic properties of liquid, 19: 38639

DEUTERONS
emission from neutron reactions (n,p) with boron-10, angular distributions for, (E), 19: 39798
interactions with protons, cross sections for inelastic, (T), 19: 39912
interactions with electrons, nucleon form factors from, (E), 19: 39458 (CONF-796(Paper 24))
interactions with protons, resonances in, 19: 39479 (NP-15216)
interactions with mesons (π^+) at 6.0 Bev/c, $\pi^+\pi^-$ (1670) production in, (E), 19: 39537
interactions with electrons, determination of neutron form factors from, (T), 19: 39541
interactions with protons at 1 to 8 Bev/c, total cross sections for, (E), 19: 39550
interactions with mesons (π^-) at 3.2 Bev/c, enhancement at 1.0 to 1.4 Bev in, (E), 19: 39551
interactions with mesons (π^+) at 1.68 Bev/c, Y_0^0 production in, (E), 19: 39553
interactions with mesons, resonance, (T), 19: 39564
interactions with protons, inelastic cross sections for, (E/T), 19: 39577
interactions with protons at 40 Mev, Chew-Low extrapolation method for, (E), 19: 39578
interactions with protons at 135 Mev, angular distributions for inelastic, (E), 19: 39579
interactions with nucleons, (T), 19: 39585
production in proton-proton interactions at high energies, transverse momentum distribution in, (T), 19: 39569
reactions (d,α) with sodium-23 at 2.0 to 2.5 Mev, differential cross sections of, (E), 19: 39835
reactions (d,γ) with oxygen-16 at 0.4 to 3.5 Mev, cross sections for, (E), 19: 39830
reactions (d,np) with nickel at 13.6 Mev, (E), 19: 39940
reactions (d,n) with boron-11 at 1.5 to 4.7 Mev, distributions from, (E), 19: 39817
reactions (d,n) with carbon at 2.8 Mev, neutron polarization in, 19: 39950
reactions (d,n)2α with lithium-7 at 1.8 to 7.0 Mev, sequential emission in, (E), 19: 39915
reactions (d,n)2α at low energy, mechanisms of, (T), 19: 39921
reactions (d,pγ) with fluorine-19, angular correlations from, (T), 19: 39811
reactions (d,pγ) with boron-10 at 0.40 Mev, gamma polarization in, (E/T), 19: 39937
reactions (d,p) with nuclei, effects of nuclear correlations on, (T), 19: 39890
reactions (d,p) with copper and gold at 23 and 26 Mev, angular distribution and spectra in, (E), 19: 39901
reactions (d,2p)n with hydrogen at 10.5 Mev, energy-angular correlations and sequented decay in, 19: 39924
reactions with nuclei, distorted-wave Born approximation for three-body stripping, (T), 19: 39910
scattering by lithium-6 at 6.35 Mev, excitation limit of 3.56-Mev level in, (E), 19: 39804

DIAMONDS
dark current and electroluminescence in semiconducting, 19: 39265(R) (IA-1021)
electron scattering at 1 to 40 Bev by, bremsstrahlung production by, (E/T), 19: 39622
photoconductivity of 0.6- and 0.8-μ bands in type I, 19: 39265(R) (IA-1021)
photoelectric effects in insulating and semiconducting, 19: 39265(R) (IA-1021)
radiation effects on, x-ray scattering defects in neutron, 19: 39230 (BNL-9332)
thermoluminescence of insulating and semiconducting, 19: 39265(R) (IA-1021)

DIAZO COMPOUNDS
decomposition of diazonium salts, nitrogen isotope effects on, 19: 38690

DIELECTRIC BREAKDOWN
ionization function for nonuniform-field, Townsend, (T), 19: 39298

DIELECTRICS
phonon interactions in solid, thermodynamic perturbation theory for forbidden three-body, 19: 40096
positron annihilation in, 3-quantum, (E/T), 19: 39546
radiation effects on, in space environment, 19: 39059

DIET
calcium content in Japanese, 19: 38894
effects of thouracil, on iodine-131 metabolism in mice, 19: 38350
effects on recovery from radiation sickness, 19: 38457
fallout monitoring in Japanese, 19: 38894
potassium content in Japanese, 19: 38894
radioactivity of cattle, in Germany, 1962, 19: 38858

DIFFERENTIAL EQUATIONS
scalar invariants of rotational system of matrix, embedded in Lie algebra, Casimir operators from, 19: 39086
use in description of adaptive control systems, 19: 39269(R) (SU-SEL-64-133)

DIFFERENTIAL THERMAL ANALYSIS
apparatus and methods for ceramics and metals at high temperatures, 19: 39163(R) (MLM-1244)
apparatus for high-temperature, 19: 39125(R) (BNWL-91)
equipment for high-temperature, 19: 38913 (LA-DC-7071)

DIFFUSION PUMPS
traps for vacuum-system, electric discharges as, 19: 38839 (RFP-572)

DIODES
electron energies in thermionic, computer studies of, 19: 39269(R) (SU-SEL-64-133)
electron tunneling in p-n, (E), 19: 38931
performance in microwave phase shifters, 19: 40297 (UCRL-7753)
phonon absorption by aluminum-lead superconducting, transverse, (E), 19: 39713
potentials between parallel-plane electron- and ion-emitting surfaces of plasma, 19: 39269(R) (SU-SEL-64-133)
properties of thermionic, in an autonomous discharge plasma, 19: 39435(T) (JPRS-31048)
radiation effects on Shockley and Zener, 19: 39055 (GA-6266)

DIRECT ENERGY CONVERSION DEVICES
design and performance of, using ion beam interaction with electric fields, 19: 39439
development for space vehicles, (E/T), 19: 38836 (NASA-SP-79)

DISEASES
radiotherapy of chronic nose, by radon inhalation, 19: 38528

DISTILLATION APPARATUS
design and efficiency of co-current columns for, 19: 38766

DIVISION OF TECHNICAL INFORMATION EXTENSION, AEC
translation title list and cross reference guide, 19: 40295 (TID-4025 (Rev.1)(Pt.1)(Suppl.4))

DODECANE
radiolysis of solid isomers of, formation of free radicals in, 19: 38724(T)

DOGS
bone blood flow in, use of strontium-85 for measure of, 19: 38340
pathological effects of inhaled plutonium-239 aerosols in, 19: 38359 (BNWL-SA-230)
radiation effects on kidney homografts in, by local graft exposure, 19: 38425
radiation effects on erythropoiesis in cross-circulated, 19: 38382
radiation effects on hematopoietic system of, ionizing, 19: 38388

DOSIMETERS
comparison of mailed ferrous sulfate and lithium fluoride, of high energy electron beams, 19: 38723
design of thermoluminescent, 19: 39048(P)
development of silicon p-i-n fast neutron, 19: 38992 (COO-1226-8)
filter system for film badge, 19: 39052(P)
performance of glasses sensitive to radiation as, 19: 39044(P)
performance of nitrate radiochemical, 19: 39042

DOUNREAY FAST REACTOR
operation of, sustained full power, 19: 40213
reactivity fluctuations in, analysis of random, (E), 19: 40193 (TRG-

Report-921)
DROSOPHILA
effects of irradiated DNA on mutations in, 19: 38413
genetic effects of incorporated carbon-14 in, 19: 38400
genetic effects of exogenous desoxyribonucleic acid in, 19: 38408
radiation effects on, gamma, 19: 39265(R) (IA-1021)
radioinduced lethals in experimental populations of willistoni, suppressors in, 19: 38391
radioinduced mutations in male, effects of sperm maturity on frequency of, 19: 38390
radiosensitivity and recovery of spermatogenesis in, role of oxygen in determining, 19: 38463
DRY BOXES
design of evacuate-back fill, 19: 38947
development for fuel fluorination tests, 19: 40112(R) (ANL-7046(p.36-66))
DRYING APPARATUS
design of turntable-type, for granular materials, 19: 38800(P)
DUSTS
combustion of, in air, ignition propagation processes for, 19: 38827
monitoring radioactivity in, western Slovakia, 1961 to 1963, 19: 38881
DYES
chloroform-dye, properties for use as chemical dosimeter, 19: 38732
radioinduced bleaching of aqueous solutions of, effects of 2,5-dichloro-hydroquinone on, 19: 38736
DYSPROSIUM
crystal structure and magnetic properties of, pressure effects on, 19: 40094
determination of, in SAP by spectrography, 19: 38553
neutron absorption properties of, burnup effects on, (E), 19: 40163
pathological effects of subcutaneous implantations, in mice, 19: 38334 (COO-1170-1)
phase transformations at 6 to 65 kbar, solid-liquid and solid-solid, 19: 40095
proton inelastic scattering at 25 to 1700 kev, x-ray yields from, (E), 19: 39881
DYSPROSIUM COMPLEXES
with [(2-hydroxyethyl)imino]diacetic acid, dissociation constant of, 19: 38671
DYSPROSIUM IONS
crystal-field interactions of, linear and nonlinear shielding of, (E/T), 19: 40101
reduction in calcium fluoride, yttrium ion effects on, (E), 19: 38595
DYSPROSIUM ISOTOPES Dy-159
spin of ground state of, (E), 19: 39818
DYSPROSIUM ISOTOPES Dy-160
gamma transition in, energy of, (E), 19: 39866
DYSPROSIUM ISOTOPES Dy-161
energy levels, (E), 19: 39930
DYSPROSIUM ISOTOPES Dy-162
neutron reactions (n,γ), gamma spectra of 5.5-ev resonance of, 19: 39781 (JAERI-1073)
DYSPROSIUM ISOTOPES Dy-163
neutron reactions (n,γ), gamma spectra of 1.7-ev resonance of, 19: 39781 (JAERI-1073)
DYSPROSIUM NIOBATES
preparation and thermal properties, 19: 38617
DYSPROSIUM OXIDES
dysprosium-161 hyperfine interactions at 4 to 300°K in magnetic, 19: 39265(R) (IA-1021)
DYSPROSIUM SULFATES
magnetic susceptibilities of crystalline, at 80 to 300°K, 19: 40082

E

EARTH
climatic changes in, 19: 39665
ECOLOGY
of plants in waste disposal area, 19: 38331
EGGS
radiation effects on hatchability of Artemia, dose-dependency of gamma, 19: 38383
radiation effects on hatchability of Artemia, effects of moisture and temperature on gamma, 19: 38384
ELECTRIC ARCS
equilibrium in low-current, thermal, 19: 39976
equilibrium in low-current, thermal, (E), 19: 39977
ELECTRIC CONDUCTIVITY
measurement in refractory materials, apparatus for, 19: 38922(T) (AAEC/Trans-18)
theory of, in ionic solutions, 19: 38643
ELECTRIC CONDUCTORS
current distribution in thin-film superconducting strip transmission line, (T), 19: 39692
radiation effects on, 19: 39056 (N64-29558)
transmission line analysis of sectorial parallel plate, 19: 40298 (UCRL-14141)
ELECTRIC DISCHARGE
diffusion in r-f, effects of magnetic fields on, (E/T), 19: 39269(R) (SU-SEL-64-133)
electron cyclotron absorption in cesium vapor, 19: 39270(R) (TID-21894)
electron density in, measurement of, 19: 39270(R) (TID-21894)
in argon at high current densities, (E), 19: 39983
ion cyclotron resonance in r-f, 19: 39270(R) (TID-21894)
microwave harmonic generation in, (T), 19: 39294
performance as trap in diffusion-pump vacuum systems, 19: 38839 (RFP-572)
plasma turbulence studies in, device for, 19: 39270(R) (TID-21894)
reduction of alkali and alkalines earth halides in high-frequency hydrogen, 19: 39180
reduction of alkali halides by high-frequency helium, hydrogen, and nitrogen, role of electrons in, 19: 39181
ELECTRIC FIELDS
book: *Analysis and Computation of Electric and Magnetic Field Problems*, 19: 39311
effects of crossed magnetic and, on electrons, 19: 39270(R) (TID-21894)
effects on boiling burnout of water, 19: 38807(R) (NYO-2404-70)
electric breakdown in nonuniform, Townsend ionization function for, (T), 19: 39298
interactions with ion beams, direct energy conversion using, 19: 39439
use in zone refining of tungsten, 19: 39111
ELECTRIC GENERATORS
development for space vehicles, (E/T), 19: 38836 (NASA-SP-79)
ELECTRIC INSULATORS
analysis for rare earths using spark-source mass spectrograph, 19: 38570
development for thermionic cells, 19: 39070(R) (GEST-2046)
radiation effects on resistance of, in SNAP-8, 19: 39057 (NP-15022(Vol. II)(Add.))
ELECTRIC PROBES
design of ultrafast high-voltage, 19: 40038
performance of Langmuir, in plasma measurements, 19: 39270(R) (TID-21894)
ELECTROCHEMISTRY
reaction distribution in porous anodes, method for measuring, 19: 38591 (UCRL-16113)
ELECTRODES
design and performance of, for sputtering apparatus, 19: 38930
electric potential of palladium–deuterium, 19: 38608
testing copper and molybdenum, for cesium ion rocket motors, 19: 38834(R) (N64-29495)
ELECTROLYTES
analysis for uranium by spectrochemical methods, 19: 38544(R) (MCW-1492, pp 13-19)
dielectric constants of, effects of thermodynamic properties on, 19: 39265(R) (IA-1021)
Hall effect in solutions, 19: 38643
ELECTROLYTIC CELLS
use of solid-electrolyte, for high-temperature studies of niobium and tantalum oxides, 19: 38586 (UCRL-11957)
ELECTROLYTIC POLISHING
methods of, in metallography of high-melting metals, 19: 39214
ELECTROMAGNETIC FIELDS
asymptotic properties, (T), 19: 39636
charged particle motion in, drift approximation for, 19: 40055(T)
effects on electron beam trajectories, 19: 39318 (UCRL-14194)
Einstein equations for incoherent matter and, homogeneous solutions of, 19: 39648
Einstein-Maxwell equations for, homogeneous solutions of, 19: 39647
plasma containment by h-f, (T), 19: 39982
space-time model for physical phenomena description in, complex, 19: 39624 (AROD-223:60)
ELECTROMAGNETIC LENSES
design, 19: 39312(P)
ELECTROMAGNETIC PUMPS
design and evaluation for space electric power plants, 19: 38781(R) (N64-25903)
ELECTROMAGNETIC SEPARATION
of isotopes, equipment at Rome University for, 19: 39077
ELECTROMAGNETIC SEPARATION PLANT (Y-12)
reprocessing of enriched uranium scrap, nuclear material control program for, 19: 38758 (Y-KA-7)

ELECTROMAGNETIC WAVES
emission by light propagation through anisotropic media, (T), 19: 39266 (JINR-P-2195)
interactions with plasma in cavities and waveguides, 19: 39270(R) (TID-21894)
propagation in plasma, mechanisms of, 19: 39269(R) (SU-SEL-64-133)
propagation in plasma, turbulent heating in, 19: 40047
propagation in unbounded fully ionized plasma in uniform fields, (T), 19: 40021
reflection by magnetized plasma, effects of parallel plate geometry on, 19: 39270(R) (TID-21894)
stability of transverse, effects of propagation along plasma beams on, 19: 39270(R) (TID-21894)
theory in coexistence with photons in electromagnetic radiations, double solution for, (T), 19: 39640
thermodynamic properties of in plasma of, astrophysical relations of, (T), 19: 39339

ELECTROMAGNETISM
book: *Electromagnetic Theory and Geometrical Optics*, 19: 39310

ELECTRON BEAMS
conference on science and technology of, 19: 39307
dosimetry in tissues, 19: 38499
dosimetry of high energy, comparison of nailed ferrous sulfate and lithium fluoride for, 19: 38723
effects on aluminum, antimony–indium alloys, copper, and platinum, 19: 40286(R) (NAA-SR-11200)
effects on aluminum alloys, annealing of, 19: 40286(R) (NAA-SR-11200)
effects on electric resistivity of copper, stage 1 annealing of, (E), 19: 39248
effects on magnetic properties of iron, cobalt, and nickel, (E), 19: 39239
effects on molybdenum, anelastic after-effects from, (E), 19: 39247
effects on tungsten surfaces, 19: 39255
electron trajectories between coaxial conducting cylinders, (E), 19: 39275
focusing in accelerating fields, (T), 19: 39321
focusing in ionized gases, apparatus for, 19: 39269(R) (SU-SEL-64-133)
focusing of sheet, periodic electrostatic, (T), 19: 39319
interactions of colliding, at 100 to 1000 Bev, 19: 39481 (NP-15248)
interactions with plasma, effects of wave amplification on, 19: 39269(R) (SU-SEL-64-133)
interactions with plasma, heating in, 19: 39969 (ORNL-P-1373)
interactions with plasma, microwave amplification in, (E), 19: 40036
interactions with positron beams at 100 to 1000 Bev, 19: 39481 (NP-15248)
ion distribution in drift region of, (E/T), 19: 39283
monitors for, design of, 19: 39330(P)
penetration through metals, mechanism of, 19: 39417
production by screen-mesh cold cathodes, 19: 38949
production of adjustable cross section, apparatus for, 19: 38964(P)
production of polarized, by elastic scattering on mercury atomic beams, (E), 19: 39392
reactions with plasma, stability in, 19: 39972(R) (SU-IPR-17)
reactions with solenoids, current effects from, (T), 19: 39654
stability of interacting, effect of radial inhomogeneity on, (T), 19: 40030
structure of high-power-density, experimental determination of, 19: 39328
therapeutic use, 19: 38499
thermal capacity effects in, Herrmann's optical theory of, 19: 39308
trajectories of, under electromagnetic- and self-field effects, 19: 39318 (UCRL-14194)
use for cutting tracks in metal films, 19: 38950
use in crystal growing by zone melting, 19: 39138
use in crystal-growth, 19: 39137
use in micromachining by sputtering through contamination, 19: 39136
use in welding of molybdenum single crystals, 19: 39139
use in zone refining of tungsten, 19: 39111

ELECTRON MICROSCOPES
instrumentation for metallurgical uses, 19: 39125(R) (BNWL-91)

ELECTRON MICROSCOPY
of irradiated cytoplasm of cells in tissue culture, 19: 38386
of irradiated single cells in tissue culture, technique for, 19: 38385
techniques for determining particle distribution in dilute alloys of uranium, 19: 39092 (BNWL-SA-90)
use in study of plastic deformation of thin gold films by Talysurf stylus, 19: 38916 (SC-DC-65-1589)
use of diffraction in measurement of rolling texture of copper, 19: 39175(T) (ORNL-tr-638)

ELECTRON PAIRS
angular distributions from vector meson decay, (T), 19: 39451 (CALT-68-43)
photoproduction on nuclei at 6.13 Mev, cross sections for, (E), 19: 39787 (SGAE-PH-19/1965)
production in electron reactions with atoms, screening effects on, (T), 19: 39389
production in photon interactions, (E), 19: 39623

ELECTRON SHOWERS
production in electron reactions with lead at 100 to 1000 Mev, (T), 19: 40070

ELECTRON SOURCES
design for uniform irradiations of material-, 19: 38954(P)

ELECTRONIC EQUIPMENT
computer program for flying-spot analysis of particle-track photographs, (E), 19: 38981 (CERN-65-11(p. 115-21))
computer programs for use with flying-spot analyzers, (E), 19: 38980 (CERN-65-11(p.97-113))
description of flying-spot system for identifying bubble-chamber photographs, (E), 19: 38979 (CERN-65-11(p. 91-5))
design and development of Campbelling, for reactor control systems signal, 19: 40122(R) (GEAP-4862)
design and use of sensitive high-speed d-c voltage comparator, (E/T), 19: 40279 (BDX-613-72)
design of semiconductor i-r modulators, (E/T), 19: 38914 (SC-DC-65-1332)
flying-spot devices for analysis of particle-track photographs, (E), 19: 38986 (CERN-65-11(p.173-81))
flying-spot devices for analysis of particle-track photographs, (E), 19: 38987 (CERN-65-11(p.207-18))
flying-spot devices for analysis of particle-track photographs, (E), 19: 38988 (CERN-65-11(p.183-206))
flying-spot devices for ionization measurements along bubble-chamber tracks, (E), 19: 38989 (CERN-65-11(p.219-27))
flying-spot devices for analysis of particle-track photographs, (E), 19: 38990 (CERN-65-11(p.229-36))
flying-spot devices for analyzing particle-track photographs, (E), 19: 38991 (CERN-65-11(p.237-58))
noise filter design, 19: 39270(R) (TID-21894)
operation of flying-spot system for analyzing spark-chamber photographs, (E), 19: 38972 (CERN-65-11(p. 7-13))
operation of flying-spot devices for analysis of spark-chamber photographs, (E), 19: 38974 (CERN-65-11(p.25-33))
operation of flying-spot system for analysis of spark-chamber photographs, (E), 19: 38975 (CERN-65-11(p.35-41))
operation of flying-spot system for analysis of spark-chamber photographs, (E), 19: 38976 (CERN-65-11(p.57-69)
operation of flying-spot systems for analyzing spark-chamber photographs, (E), 19: 38977 (CERN-65-11(p. 71-9))
operation of PEPR flying-spot device for analyzing bubble-chamber data, (E), 19: 38978 (CERN-65-11(p. 81-90))
particle track analysis using computerized flying-spot devices, (E), 19: 38984 (CERN-65-11(p.145-52))
particle-track analysis using computerized flying-spot devices, (E), 19: 38985 (CERN-65-11(p.153-72))
performance of flying-spot systems for analyzing spark-chamber photographs, (E), 19: 38973 (CERN-65-11(p.15-23))
uses of flying-spot analyzers for chromosome-photograph analysis, (E), 19: 38910 (CERN-65-11(p.43-56))
uses of flying-spot devices for particle-track analysis, (E), 19: 38983 (CERN-65-11(p.139-43))
uses of flying-spot devices for analyzing particle-track photographs, (E), 19: 38982 (CERN-65-11(p.123-37))

ELECTRONICS
book: *Radiation and Noise in Quantum Electronics*, 19: 39664

ELECTRONS
angular distribution in leptonic decay of polarized hyperons (Λ^0), (E), 19: 39539
book: *Dose Distribution and Dose Determination in Pendulum Irradiation (200 kv at 17 Mev)*, 19: 38534
bremsstrahlung production in shielding in space by, computer program for radiation dose from, 19: 40062 (N64-29366)
charge density effects on spin direction of, in longitudinal electric field, (T), 19: 39516
Cherenkov radiation from, polarization of, (E), 19: 39599
collision cross sections for, data recording system for measuring, 19: 38943
configurations of atomic orbital, group theory for number of equivalent, 19: 39382
content in ionosphere during magnetic disturbances in winter, (E), 19: 39670
content in midlatitude ionosphere, (E), 19: 39677
correlations and fluctuations in plasma of, connection between, (T), 19: 40024
density and distribution in argon plasma, optical study of, (E), 19: 40039
density and temperature in time-varying plasma, (T), 19: 40015
density and temperature in ionosphere, measurement of Explorer XVII,

19: 39680
density in fast theta-pinch discharge, measurement of time-dependent, (E), 19: 39979
density in hydrogen plasma, measurement of, (E), 19: 39978
density in ionospheric F2 region, (T), 19: 39668
density in outer ionosphere, (E), 19: 39674
density in plasmas, measurement by coherent light, (T), 19: 40059
density in sulfur hexafluoride seeded flame plasma, 19: 40016
density in supersonic plasma at low pressures, (E), 19: 39987
density irregularities in auroral storms, (T), 19: 39678
density of slow trapped, in electron beam reactions with ions, (E/T), 19: 39283
diffusion in toroidal traps, nonadiabatic, 19: 39270(R) (TID-21894)
distribution in ionosphere, 19: 39269(R) (SU-SEL-64-133)
dosimetry behind shields, computer program for calculation of, 19: 40064 (NP-15132)
effects on aluminum, (E), 19: 39246
effects on aqueous solutions of inorganic compounds, 19: 38728
effects on deuterium–hydrogen exchange on silica gel, 19: 38626
effects on free radicals, ESR studies of, 19: 38719
effects on liquid cyclic fluorocarbons, mechanism of, 19: 38709
effects on physical properties of polymethyl methacrylate, 19: 39231 (COO-1224-8)
effects on semiconductors, 19: 40286(R) (NAA-SR-11200)
effects on silicon defect centers from, 19: 39252
effects on transistors, data re-presentation technique for, 19: 39054 (AD-607863)
emission by metal single crystals during rare-gas ion bombardment at 1 to 10 kev, (E), 19: 39404
emission from monocrystalline metal surface bombarded by high-energy ions, kinetic, (T), 19: 39405
emission from positron radiationless annihilation in lead, (E), 19: 39526
emission in decay of hyperon (Λ^0), angular correlations of, (E), 19: 39613
emission in ion reactions with solids at low energies, 19: 38937
emission of, inhomogeneous Poisson process for shot effect in, (T), 19: 39289
helicity and transverse momentum of relativistic, in circular accelerators, (T), 19: 39320
injection in Astron, (T), 19: 39973 (UCRL-14131)
interactions in atomic energy levels, two-body, (T), 19: 39367 (LA-DC-6548)
interactions of gas of, one-particle Green's function for, 19: 39658
interactions with phonons in magnetic fields, dispersion relations for, 19: 39270(R) (TID-21894)
interactions with phonons in metals, strong-coupling, (T), 19: 40073 (CONF-796(Paper 1))
interactions with phonons, Born approximation for, (T), 19: 40106
interactions with lattice imperfections, one-particle Green's function for, (T), 19: 40106
interactions with protons, Regge trajectory of photon exchange in, (E/T), 19: 39619
interactions with protons in nuclei, meson (π) production in, (E), 19: 39623
interactions with deuterons, nucleon form factors from, (E), 19: 39458 (CONF-796(Paper 24))
interactions with nucleons at high energy, Regge-pole hypothesis in asymptotic amplitudes for, 19: 39478 (NP-15210)
interactions with deuterons, determination of neutron form factors from, 19: 39541
interactions with neutrinos, weak boson production in, (T), 19: 39567
interactions with electrons, fine structure of effective mass spectrum for, 19: 39583
interactions with neutrinos, polarization effects in, (T), 19: 39587
interactions with ions in metallic lithium, (T), 19: 39211
magnetic field of, energy of interaction with solenoid field, (T), 19: 39654
magneto-optical phenomena in many-body systems of, perturbation theory for, 19: 40100
motion between coaxial conducting cylinders, (T), 19: 39275
penetration through matter, review of laws of, 19: 39416
photoemission from semiconductors at 2 to 6 ev, spectral analysis of, 19: 39406
photoproduction in upper atmosphere, measurement of, 19: 39270(R) (TID-21894)
polarization of, Darwin bispinors for relativistic study of, 19: 39582
production of plasma of, with negative electrostatic potential well, (E), 19: 40031
production of polarized, method of, 19: 39622
production, energy distribution, and solvation of secondary, tertiary, and multistage, in radiation-chemistry systems, 19: 38703
reactions with aluminum foils at 80 kev, transition radiation from, (E), 19: 40099
reactions with atoms, screening effects on bremsstrahlung and pair production in, (T), 19: 39389
reactions with gases at low energies, energy dependence of ion pair production in, 19: 39375
reactions with hydrogen molecules at 15 kev, rotational temperatures from, (E), 19: 39414
reactions with lead at 100 to 1000 Mev, electron-photon cascades in, (T), 19: 40070
reactions with metals at 1 to 3 Mev, atomic displacement cross sections for, 19: 39225 (AFCRL-65-286)
reactions with molecular hydrogen, at 30 kev, rotational spectra from, (E/T), 19: 39399
reactions with potassium iodide crystals V_K centers in, (E), 19: 40103
reactions with thick lead targets at 55 to 220 Mev, positron production cross sections in, (E), 19: 39475 (LAL-27)
role of, in reduction of alkali halides by high-frequency discharge in helium, hydrogen, and nitrogen, 19: 39181
scattering by atoms, exchange effects in, (T), 19: 39365 (COO-720-047)
scattering by carbon-12, isospin selection rules for, (E/T), 19: 39855
scattering by crystals, interband excitations in inelastic, (T), 19: 40083
scattering by crystals, phonon excitation in inelastic, (T), 19: 40084
scattering by diamond crystals at 1 to 40 Bev, bremsstrahlung production by, (E/T), 19: 39622
scattering by hydrogen, rotational excitation in, (E), 19: 39413
scattering by hydrogen atoms, narrow resonance in, (E), 19: 39393
scattering by krypton and xenon, momentum-transfer cross sections for, (T), 19: 39397
scattering by lead-207 and -208, dispersive effects in elastic, (E), 19: 39860
scattering by mercury atomic beams, electron polarization in elastic, (E), 19: 39392
scattering by nuclei, meson (π) production in, (T), 19: 39621
scattering factors of, corrections for incoherent, 19: 39379
scattering on helium-3 and tritium at 549 Mev, cross sections for inelastic, (T), 19: 39909
shielding against, for manned space stations, 19: 40063 (NP-15125)
spin of Coulomb-bound, oscillating real vectors for, (T), 19: 39390
stability in crossed electric and magnetic fields, 19: 39270(R) (TID-21894)
streaming in field-free space, equations for neutralized, 19: 39269(R) (SU-SEL-64-133)
temperature in barium plasma, determination of, 19: 39958 (MATT-327)
temperature in thermionic diode ignited mode, 19: 39433 (LA-DC-6898)
temperature in Zeta plasma, 19: 39953 (CLM-R-40)
temperature increases in MHD cell plasma, (T), 19: 39437
temperature variations in flames, (E), 19: 39282
thermodynamic properties of in plasma of, astrophysical relations of, (T), 19: 39339
transport in three-component plasmas, 19: 39270(R) (TID-21894)
tunneling in lead thallium alloys at cryogenic temperatures, (E/T), 19: 40286(R) (NAA-SR-11200)
tunneling in p-n junctions, (E), 19: 38931
velocities in plasma, measurement method for, 19: 39270(R) (TID-21894)

ELECTROSTATIC ANALYZERS
design for mass spectrometers, 19: 38963(P)

ELECTROSTATIC FIELDS
calculation for uniformly charged cylindrical configurations, 19: 39314 (JINR-P-2131)

ELEMENTARY PARTICLES
book: *Symmetries in Elementary Particle Physics*, 19: 39602
correlations in nuclear reactions, conference on, 19: 39893
coupling between two fields of, model for length scale, 19: 39652
coupling constants of, calculation of, (T), 19: 39265(R) (IA-1021)
decay of unstable, spectral shape in exponential, (T), 19: 39304
decays of, angular correlations in successive two-body, (T), 19: 39492
Dirac equations for free, Foldy-Wothuysen transformation of, 19: 39630 (CONF-796(Paper 31))
distribution functions for system of punctiform, 19: 39581
electromagnetic properties of, B(2)-symmetry model for, 19: 39490
field theory of, Lee model in, 19: 39638
field theory with mass for, generalized conservation law for, (T), 19: 39523
Green function for composite, vertex function for, (T), 19: 39561
interaction in relativistic SU(6) field theory, 19: 39459 (CONF-796 (Paper 28))
interactions at high energies, current-generated algebras of, (T), 19: 39265(R) (IA-1021)
interactions at high energy, analyses of final-state, (E/T), 19: 39574
interactions at high energy, Regge-pole hypothesis in asymptotic ampli-

tudes for, 19: 39478 (NP-15210)
interactions of many, canonical position variables in relativistic theory of, 19: 39645
interactions of scalar, spinor, and vector spin-1, (T), 19: 39635
interactions of spinor and vector, Yang-Mills, (T), 19: 39634
interactions of spin-one particles with spinless targets, covariant theory of polarization for, (T), 19: 39514
interactions of three identical, quantum-mechanical ground-state attractive, 19: 39505
interactions of 3, quantum analysis of, (T), 19: 39453 (CONF-796 (Paper 15))
interactions of, absorptive corrections to peripheral model for, (T), 19: 39522
interactions of, analyses of final-state, (T), 19: 39575
interactions of, crossing symmetry for, (T), 19: 39595
interactions of, helicity amplitudes and complex angular momentum in V-A, 19: 39618
interactions of, integration of energy variables for, (T), 19: 39512
interactions of, LSZ asymptotic condition for, 19: 39629 (CONF-796 (Paper 30))
interactions of, nonlocal theory of, 19: 39495
interactions of, N/D approach in bootstrap solutions for, (T), 19: 39463 (IC/65/62)
interactions of, properties of overlap function for, (T), 19: 39520
interactions of, peripheral production and decay correlations of resonances in, (E/T), 19: 39576
interactions of, Regge poles and scattering-amplitudes for, 19: 39618
interactions of, research on, 19: 39464(R) (ISS-64/49)
interactions of, SU(3) symmetry for weak, 19: 39605
interactions of, status of strong, electromagnetic, and weak, (T), 19: 39615
interactions of, symmetries for strong, (T), 19: 39507
interactions of, theory, 19: 39454 (CONF-796(Paper 18))
interactions of, three-body amplitudes in complex momentum, (T), 19: 39596
interactions of, vector and axial currents under first-order symmetry-breaking, 19: 39606
interactions of, with charge, magnetic moment, and spin, Fokker action principle for, 19: 39501
interactions of, weak-strong coupling complementarity in renormalized perturbation theory for, (T), 19: 39521
interactions with antiparticles, mass-energy conversion in annihilation, (T), 19: 39554
mass formulas in Schwinger model, (T), 19: 39584
mass formulas in the ISL(6) theory, 19: 39466 (JINR-E-2173)
masses of, in unified field theory, 19: 39452 (CONF-796(Paper 13))
model for three-particle systems, (T), 19: 39641
model for, based in Sp(6), (T), 19: 39568
model for, unification of Lorentz group and SU(3) group into Lie-group, 19: 39491
models for strongly interacting, ace and Sakata, 19: 39607
models for, Born reciprocity principle and unitary symmetry in, 19: 39502
models for, Heisenberg equations in rotator and symmetry, (T), 19: 39494
motion in arbitrary tensor fields, classical, 19: 39632
properties of, data tabulation of, 19: 39485 (UCRL-8030(Pt.I) (Mar. '65, ed.))
properties of, quantum laws for, (T), 19: 39661
properties of, theory of symmetries in, 19: 39455 (CONF-796(Paper 19))
representations for, SU_n, (T), 19: 39609
scattering by superposed Yukawa potentials, relativistic, (T), 19: 39598
symmetries for, Wigner's analysis of unitary representations of, 19: 39486 (UCRL-12359)
symmetry for, covariant extension of SU(6), (T), 19: 39555
symmetry for, SU(3), 19: 39604
symmetry for, SU(4), (T), 19: 39608
symmetry for, SU(9), 19: 39571
symmetry for, 572* multiplet in SU(12), 19: 39556
symmetry group for, three-dimensional unitary, 19: 39477 (NP-15202)
symmetry group SL(6) for, invariance in, 19: 39468 (JINR-P-2123)
symmetry group SU_{12} for generalization of symplectic and spin symmetries, 19: 39471 (JINR-P-2175)
symmetry group SU(12) for, generalization of symplectic and spin symmetries for, 19: 39533
symmetry groups for, charge conservation and space-time in, 19: 39506
symmetry principles for, 19: 39603
symmetry scheme for hadrons, Sp(3), (T), 19: 39565
theory of, invariance group for relativistic supermultiplet, 19: 39493
theory of, structure of G_2 multiplets in, 19: 39594
theory of, variational principles for quasi-stationary states in, 19: 39525
transformation from linear- to angular-momentum basis for relativistic nonzero-mass of arbitrary spin, 19: 39500
transitions of, axial vector coupling constants for weak, (T), 19: 39544
transport equation for relativistic, Boltzmann, 19: 39580
wave theories for, metastable finite-energy solutions for nonlinear scalar, 19: 39649

ELEMENTS
determination in organic materials by neutron activation methods, 19: 38558
determination in thorium compounds, methods for trace, 19: 38545(R) (MCW-1492, pp 23-8)

EMBRYOS
radiation effects on development of rats, 19: 38361(R) (TID-21951)
radiation effects on cell cycle duration in mouse, gamma, 19: 38405

ENDOCRINE GLANDS
radiation sickness effects on, pathology of, 19: 38433(T)

ENGLAND
radiochemical center development and operation at Amersham, 19: 39073

ENTROPY
theory of, quantum, 19: 39633

ENZYMES
radiation effects on content in animal blood, 19: 38426
radiosensitivity of, in rat liver and spleen, effects of glycine, 19: 38467

EPIDEMIOLOGY
of cancer susceptibility in man with age, 19: 38364

EQUIPMENT AND PROCEDURES
classification of teaching machines, generic, 19: 40291 (SC-R-65-923)

ERBIUM
determination of, in SAP by spectrography, 19: 38553
neutron absorption properties of, burnup effects on, (E), 19: 40163
neutron reactions at 0.0005 to 1 ev, total cross sections for, 19: 39779 (IEA-86)
neutron reactions (n,γ), gamma spectra of 0.46- and 0.58-ev resonance of, 19: 39781 (JAERI-1073)
phase transformations at 6 to 65 kbar, solid-liquid and solid-solid, 19: 40095
spectra of, atomic and ionic, 19: 39265(R) (IA-1021)

ERBIUM COMPLEXES
with [(2-hydroxyethyl)imino]diacetic acid, dissociation constant of, 19: 38671

ERBIUM IONS
crystal-field interactions of, linear and nonlinear shielding of, (E/T), 19: 40101
radiolysis of aqueous solutions of, pulse, 19: 38728

ERBIUM ISOTOPES Er-172
beta decay of, coincidence and spectral measurements of, (E), 19: 39822

ERBIUM NIOBATES
preparation and thermal properties, 19: 38617

ERYTHROCYTES
labeled with chromium-51, tracer use, 19: 38525
life span of sheep, tracer study, 19: 38343
radiation effects on rat, fast neutron and x, 19: 38440
radiation effects on size of, in mice, 19: 38363
radioinduced hemolysis after radiotherapy, 19: 38509

ERYTHROPOIESIS
tracer study of, 19: 38493

ESCHERICHIA COLI
radiation effects on capacity for phage T3, sensitization effects of iodoacetamide on, 19: 38455
radiation effects on, protective effects of ribonuclease against uv and x, 19: 38465
radiation effects on RNA synthesis in derivatives of, uv and x-ray, 19: 38381
radiosensitivity of, location of genes controlling uv, 19: 38397
radiosensitivity of, range of gene action controlling uv, 19: 38398

ETHANE
diffusion in liquid, pressure effects on self, 19: 39270(R) (TID-21894)
ionization cross section for, electron-impact, 19: 38630
yields in gamma radiolysis of liquid cyclopentane, 19: 38712

ETHANE, BROMO-
radiation effects on bromine-80 and -82 retentions in, isomeric transition reaction in, 19: 38715

ETHANE, CHLORO-
reactions of recoil tritium with, products from, 19: 38704

ETHANE, 1,2-DICHLORO-1,1,2,2-TETRAFLUORO-
vaporization lifetimes of droplets of, on oxidized and polished nickel, 19: 38811(R) (SAN-409-24)

ETHANETHIOL, 2-AMINO-
effects on glutathione and sulfhydryl group content in ascites tumor cells, 19: 38464
effects on respiration in mice, 19: 38469

protective effects of, against toxic action of liver lipids in rabbits, 19: 38429
ETHANOL
radioinduced reactions with 1,2-dichlorotetrafluorocyclobutene and 1,2-dichlorohexafluorocyclopentene, 19: 38708
ETHYLENE
yields in gamma radiolysis of liquid cyclopentane, 19: 38712
ETHYLENE, CHLORO-
dose rate determination in, absorbed, 19: 39016
ETHYLENE, CHLORO- POLYMERS
radioinduced graft polymerization with styrene, physical properties of products of, 19: 38733
radioinduced graft polymerization with acrylonitrile and styrene vapors, products of, 19: 38734
radioinduced grafting to monoethylenically unsaturated monomers, 19: 38739(P)
radioinduced grafting to styrene, 19: 38740(P)
radioinduced polymerization of monoethylenically unsaturated monomers on, production of shaped articles by, 19: 38741(P)
reactions with carbon dioxide, carbon production by, 19: 38599
use as filter material in respirator protecting against radioactive aerosols, 19: 38900
ETHYLENE, DICHLORO- POLYMERS
reactions with carbon dioxide, carbon production by, 19: 38599
ETHYLENE GLYCOL
yields from radiolysis of methanol, 19: 38716
ETHYLENE POLYMERS
radioinduced graft polymerization with acrylonitrile and styrene vapors, products of, 19: 38734
ETHYLENE, TETRAFLUORO- POLYMERS
radioinduced graft polymerization with acrylonitrile and styrene vapors, products of, 19: 38734
EUROPIUM
determination of, in SAP by spectrography, 19: 38553
europium-153 NMR in, (E), 19: 39840
neutron absorption properties of, burnup effects on, (E), 19: 40163
phase transformations at 6 to 65 kbar, solid-liquid and solid-solid, 19: 40095
properties as alkaline earth metal, 19: 39177
reactions with graphite, thermodynamics of, 19: 38680
separation from aqueous electrolytes containing gadolinium, by extraction and electrolysis using lithium amalgam, 19: 38753 (LA-DC-7013)
separation from other rare earths by distillation of bromides, 19: 38765
sorption by gamma-alumina and inorganic ion exchange materials from fused salts, 19: 38771
EUROPIUM ALLOYS
Cu–Eu, crystal structure of intermetallic compounds in, 19: 39177
Eu–Mg, properties of intermetallic compounds in, 19: 39177
EUROPIUM CARBIDES
preparation and thermodynamic properties, 19: 38680
EUROPIUM CHLORIDES
fluorescence and absorption spectra of, effects of heavy water on, 19: 38636
EUROPIUM COMPLEXES
fluoresence spectra of, stroboscopic time-resolution measurements of, 19: 38634
with [(2-hydroxyethyl)imino]diacetic acid, dissociation constant of, 19: 38671
EUROPIUM IONS
electron paramagnetic resonance and endor spectra of, in thorium dioxide, 19: 38655
energy decay from $^5D_1$ state of, relaxation time for, 19: 38634
EUROPIUM ISOTOPES Eu-151
electron paramagnetic resonance in cadmium fluorides, (T), 19: 38664
neutron reactions (n,γ), gamma spectra of 0.46-ev resonance of, 19: 39781 (JAERI-1073)
EUROPIUM ISOTOPES Eu-152
gamma spectra of isomeric, (E), 19: 39928
transfer to mouse offspring during lactation and pregnancy, 19: 39265(R) (IA-1021)
EUROPIUM ISOTOPES Eu-153
electron paramagnetic resonance in cadmium fluorides, (T), 19: 38664
nuclear magnetic properties, (T), 19: 39792
nuclear magnetic resonance in europium oxide and europium metal powders, (E), 19: 39840
EUROPIUM ISOTOPES Eu-154
transfer to mouse offspring during lactation and pregnancy, 19: 39265(R) (IA-1021)
EUROPIUM OXIDES
europium-153 NMR in, (E), 19: 39840
properties in reactor control elements, 19: 40286(R) (NAA-SR-11200)
$EuO–SiO_2$, preparation and crystal structure, 19: 38621
$EuO–SiO_2$, spectra and crystal structure of, infrared, 19: 38622
EUROPIUM SULFIDES
magnetic resonance in, ferro- and para-, 19: 38649
EXCRETORY SYSTEMS
function of calyx and renal pelvis, use of iodine-131 in radiopyelography of, 19: 38530
EXPERIMENTAL BOILING WATER REACTOR
development of, summary for May 1965, 19: 40112(R) (ANL-7046 (p.36-66))
fuels for, radiation effects on prototype, neutron, 19: 39125(R) (BNWL-91)
maintenance and performance of, 19: 40113(R) (ANL-7071)
operations and performance, (E), 19: 40267
EXPERIMENTAL BREEDER REACTOR-II
development and operation, May 1965, 19: 40177(R) (ANL-7046(p.1-35))
development and operation, June 1965, 19: 40113(R) (ANL-7071)
fuel burnup in, methods for determining, 19: 40113(R) (ANL-7071)
fuel elements for tests in, 19: 40177(R) (ANL-7046(p.1-35))
fuel processing facility development for, 19: 40177(R) (ANL-7046(p.1-35))
EXPERIMENTAL ORGANIC COOLED REACTOR
control rods for, design of pressure-balanced, (E), 19: 40135
EXPLOSIONS
electric conductivity of detonation products, time-resolved, 19: 40284 (LA-DC-6993)
EXPLOSIVES
efficiency of, low-density and low-pressure pentaerythritol tetranitrate, 19: 38589 (UCRL-14186)
use in magnetic flux compression, 19: 39300
EXPONENTIAL PILES
neutron flux distribution in subcritical sphere with central point source, (T), 19: 40162
EYE LESIONS
effects of atomic and thermonuclear weapons on, 19: 38478
radiotherapy of retinoblastoma in infant, development of cranial fibrosarcoma from, 19: 38486
EYES
motion of human, effects of vestibular system on, 19: 39270(R) (TID-21894)
movement of, effects of amplitude and velocity on saccadic, 19: 39270(R) (TID-21894)
radiodiagnosis of malignant melanomas in, 19: 38485

F

FALLOUT
collection of, adhesive for, 19: 38906(P)
content in animals of California coast, 19: 38895
content in atmosphere, 1954 to 1963, 19: 38861
content in diet and excreta in Japan, 19: 38894
data on, 19: 39774 (AEET-209)
effects on radioactivity of atmosphere in Hanford area, 19: 38874 (BNWL-SA-53)
gamma dose to man from external, 19: 38891
measurement of, design of meter for, 19: 39051(P)
measurement of, on airplane surfaces, 19: 39265(R) (IA-1021)
monitoring at IRR-1, 19: 39265(R) (IA-1021)
monitoring in Austria, 1963, 19: 38860
monitoring in Finland, 1960 to 1962, 19: 38850
monitoring in Germany, 1962, 19: 38858
monitoring in Germany, 1963, 19: 38862
monitoring in Great Britain, 1964, 19: 38863
monitoring in Hungary, 1962, 19: 38852
monitoring in U. S., program of Division of Radiological Health of the Public Health Service, 19: 38880
monitoring of, by analysis of milk for yttrium-90, 19: 38856
protection against cesium-137 and strontium-89 and -90, guides for, 19: 38877 (NP-15183)
radiation hazards to human populations, 19: 38861
strontium-90 content in, in Germany, 19: 38876 (NP-14927)
transport in atmosphere, 19: 38857
FAST REACTORS
criticality studies in, review, (E), 19: 40163
design and economics of sodium cooled breeder, for desalination, 19: 40190 (ORNL-TM-784)
design data for 1000 Mw(e) breeder, 19: 40113(R) (ANL-7071)
design of split-blanket modular, 19: 40286(R) (NAA-SR-11200)
design of 1000-Mw(e) sodium-cooled, (T), 19: 40175(R) (ACNP-63592)
development of gas-cooled breeder type, 19: 40182 (GA-5537)
fuel management in settled-bed, 19: 40178 (BNL-9279)

neutron diffusion in, parameter sets for calculation of multigroup, 19: 40161 (ZfK-TPb-11)
physics parameters of, neutron Doppler, plutonium isotope, and sodium void effects on, 19: 39265(R) (IA-1021)
reactivity of power, analysis of Doppler-shift effects on, (E/T), 19: 40150 (CEA-R-2565)
reactivity sodium void coefficients for, 19: 40158 (UNC-5123)

FATIGUE
of metals, nondestructive evaluation of, 19: 39151 (AFOSR-65-0981)

FATTY ACID ESTERS
radiation chemistry of methyl laurate, 19: 38721

FECES
fallout monitoring in Japanese, 19: 38894

FERMIONS
helicity and transverse momentum of relativistic, in circular accelerators, (T), 19: 39320
interactions of, integration of energy variables for, (T), 19: 39512
interactions with bosons, bound states in Lee model for, (T), 19: 39558
magnetization of low-temperature gases of, (T), 19: 39684
spin of, quantum laws for, 19: 39661
symmetry for, SU(9), 19: 39571
thermodynamic potential for, (T), 19: 39512

FERROMAGNETIC MATERIALS
magnetization at low temperatures, (T), 19: 39684 (CONF-796(Paper 4))

FETUSES
neutron dosage to, during radiotherapy of mother using 70 Mev synchrotron, 19: 38517
placental transfer of body fluids of, in rabbits and swine, tracer study, 19: 38344
radiation effects on development of rats, 19: 38361(R) (TID-21951)

FFAG ACCELERATORS
ion motion in central region of, (T), 19: 39316 (JINR-P-2199)

FIELD THEORY
asymptotic condition in relativistic quantum, proof of LSZ, 19: 39629 (CONF-796(Paper 30))
asymptotic properties of electromagnetic and gravitational fields, 19: 39636
Einstein field equations for empty space, 19: 39663
elementary particles in, Lee model for, 19: 39638
elementary particle masses in unified, 19: 39452 (CONF-796(Paper 13))
elementary particle interactions in, 19: 39454 (CONF-796(Paper 18))
elementary particle symmetries in, 19: 39455 (CONF-796(Paper 19))
elementary particle mechanics in relativistic SU(6), 19: 39459 (CONF-796(Paper 28))
field equations in Lagrangian, existence and uniqueness of solutions of, 19: 39627 (CONF-796(Paper 26))
fields with mass in, generalized conservation law for free, 19: 39523
Foldy-Wothuysen transformation for free particles in, covariant spinor formulation of, 19: 39630 (CONF-796(Paper 31))
gravitation in, 19: 39662
hyperon decay in SU(6), representation of nonleptonic, 19: 39456 (CONF-796(Paper 21))
interactions of scalar, spinor, and vector fields with spin 1, 19: 39635
interactions of spinor and vector fields with fixed spin, Yang-Mills, 19: 39634
invariances of, CPT, 19: 39639
models of quantum structure coefficients of proper self-energy parts in, (T), 19: 39653
momentum transfer in field interactions, (T), 19: 39543
neutrino fields on space-time curve, 19: 39639
particle motion in arbitrary tensor fields, classical, 19: 39632
Regge poles in, 19: 39618
representation of discrete symmetry operators in, 19: 39626 (CONF-796(Paper-12))
scale invariance at small distances in nonlinear quantum, asymptotic, 19: 39655
solubility of two-dimensional axiomatic, 19: 39628 (CONF-796(Paper 29))
space-time model for physical phenomena description in, complex, 19: 39624 (AROD-223:60)
wave theories in, metastable finite-energy particle-like solutions for nonlinear scalar, 19: 39649

FILMS
deposition of thin, vacuum techniques for, 19: 38842
deposition of uranium, electrolytic, 19: 39100 (SGAE-CH-16/1965)
preparation with conducting areas, methods for, 19: 39135
thickness of, equipment for beta-backscatter measurement of, 19: 38952(P)

FILTERS
development for biological studies, using charged-particle tracks, 19: 39038
materials for use in respirators protecting against radioactive aerosols, 19: 38900

FINLAND
fallout monitoring, 1960 to 1962, 19: 38850

FINNED TUBES
design for heat exchangers, 19: 38818(P)
design for heat exchangers, 19: 38819(P)

FIRES
fission product release in sodium reactor coolant, 19: 40286(R) (NAA-SR-11200)
plutonium, reactions of organic solvents in, 19: 38879 (RFP-566)

FISH
radionuclide content in, from California waters, 19: 38895
uranium content in, in Lake Issyk-kul, USSR, 19: 38855

FISSION FRAGMENTS
detection in flowing gas stream, design of flow detector for, 19: 39012
detection in semiconductor detectors, resolution of, (T), 19: 39033
distribution in pyrolytic carbon, 19: 39129(R) (ORNL-TM-1116)
effects on ionic crystals and semiconductors, (E), 19: 39245
effects on mechanical properties of Type 304 stainless steel and Zircaloy-2, 19: 39229(R) (BMI-X-10134)

FISSION PRODUCTS
activities in Saxton reactor coolant, 19: 40196(R) (WCAP-3269-6)
behavior in fluoride volatility processes, 19: 40112(R) (ANL-7046 (p.36-66))
detection and measurement of, from Chinese nuclear weapon test in lower troposphere, 19: 38899
diffusion from carbon-coated uranium carbide particles, 19: 39091(R) (BMI-1723(Del.))
diffusion from carbon-coated fuel particles, 19: 39129(R) (ORNL-TM-1116)
diffusion from irradiated stainless steel–uranium fuel rods, 19: 40197(R) (WCAP-3718)
diffusion from irradiated carbon-coated urania particles, 19: 39091(R) (BMI-1723(Del.))
diffusion from irradiated urania, effects of cladding on, 19: 39234 (GEAP-4597)
diffusion from metallic fuels, 19: 40286(R) (NAA-SR-11200)
diffusion in cladding materials, mechanisms of, 19: 39152(R) (BMI-X-10132)
diffusion in zirconium hydrides, 19: 40286(R) (NAA-SR-11200)
distribution in liquid ammonia–uranium dioxide slurry, 19: 39095 (CONF-117(p.81-97))
maximum permissible concentrations of uranium-235, in air and water, 19: 38872 (AEET/HP/TH-15)
migration in uranium dioxide at high temperatures, 19: 39154 (BNWL-SA-54)
production in atomic explosions, data on, 19: 39774 (AEET-209)
radiation doses from, effects of distance and time on, 19: 39265(R) (IA-1021)
release from irradiated alumina-coated uranium dioxide fuel particles, 19: 39227 (BMI-1729)
release from nuclear rockets, computer program for hazards of, 19: 40248 (NUS-180)
release from pyrolytic carbon-coated fuel particles, 19: 39228 (BMI-1734)
release of condensable, from GAIL III-B fuel element, 19: 39233 (GAMD-6321)
removal from in-pile loop, trapping system for, 19: 40120 (GAMD-5434)
transport in atmosphere, from nuclear explosions, 19: 38857

FISSIONABLE MATERIAL
determination in fuels, nondestructive, 19: 38547 (TID-21475)

FISSIUM
fissium–Pu–U, hydridation for cladding removal, 19: 40113(R) (ANL-7071)
fissium–Pu–U, reactions with stainless steel at high temperatures, 19: 40177(R) (ANL-7046(p.1-35))
fissium–U, radiation effects, 19: 40113(R) (ANL-7071)
fissium–U, thermal conductivity of, effects of burnup on, 19: 40112(R) (ANL-7046(p.36-66))
fissium–U–Zr, thermal conductivity of, effects of burnup on, 19: 40112(R) (ANL-7046(p.36-66))

FLAMES
electron density in sulfur hexafluoride seeded plasma of, (E), 19: 40016
electron temperature variations in, (E), 19: 39282
propagation in dust clouds, mechanisms for, 19: 38827

FLOWMETERS
design of liquid-sodium flow controller for in-pile uses, (E), 19: 40135

FLUID FLOW
boiling critical heat flux in regimes of, 19: 38809 (NYO-3304-3)
magnetohydrodynamic, thermal boundary-layer equations in, (T), 19: 39276
magnetohydrodynamic, boundary-layer compatibility condition for, (T),

19: 39277
magnetohydrodynamic, with heat addition, (T), 19: 39302
pressure drop in flow through two eccentrically positioned orifices in series, 19: 38810 (RL-SA-31)
research on, 19: 38813(R) (UCRL-12204, pp 48-59)
stability of parallel, analysis of, 19: 39270(R) (TID-21894)
two-phase, vessel blowdown from pipes, 19: 38802 (APED-4827)
FLUID FLOW (LAMINAR)
magnetohydrodynamic, channel entrance, (T), 19: 39278
FLUID FLOW (TURBULENT)
magnetohydrodynamic, inertial-range spectra of, (T), 19: 39292
FLUID FUEL REACTORS
bed densities and bubble formation in, flash x-ray analysis of, 19: 40224 (LA-3229, pp 63-82)
criticality, fuel losses, and heat transfer in, 19: 40226 (LA-3229, pp 86-8)
design and performance of rotating, for propulsion, 19: 40223 (LA-3229, pp 48-62)
design and performance of liquid core, for space propulsion, 19: 40227 (LA-3229, pp 90-110)
development for rocket propulsion, review of, 19: 40242 (LA-DC-7118)
heat transfer and material losses in rotating and static, 19: 40225 (LA-3229, pp 83-5)
FLUID PROPELLANTS
performance of hydrogen, for nuclear rockets, 19: 40243 (LA-DC-7169)
performance of hydrogen, in nuclear rockets, 19: 40244 (LA-DC-7170)
FLUIDIZATION
bed height measurement in glass apparatus, equipment for, 19: 38782 (ORNL-TM-1170)
model of, for fluidized-bed fuel particle coating studies, 19: 39129(R) (ORNL-TM-1116)
particle motion in beds, 19: 38782 (ORNL-TM-1170)
FLUIDS
decontamination of, equipment and method for, 19: 40119(P)
interaction potentials of many-body systems of, long- and short-range, 19: 39284
FLUORESCENCE
microscopy of, device for phase contrast in, 19: 38923(T) (UCRL-Trans-1228)
FLUORIDE VOLATILITY PROCESSES
development for uranium recovery, 19: 40112(R) (ANL-7046(p.36-66))
FLUORIDES
determination in biological materials and water, radiometric, 19: 39265(R) (IA-1021)
determination in plutonium metal and nitrate solutions, method for, 19: 38546(R) (RFP-552)
reactions with chelates in bones, 19: 39265(R) (IA-1021)
FLUORINE
effects on cesium ion and neutral emission from hot porous tungsten, 19: 39164 (N64-22193)
use in hygrometric measurement of uranium (IV) fluorides in noncondensable gases, 19: 38573(P)
FLUORINE ISOTOPES F-17
energy levels of, analysis of spurious states owing to center-of-mass motion, (T), 19: 39812
nuclear magnetic moment, (E), 19: 39867
FLUORINE ISOTOPES F-18
energy levels of, gamma widths for, (E), 19: 39830
FLUORINE ISOTOPES F-19
deuteron reactions (d,pγ) with, angular correlations from, (T), 19: 39811
neutron reactions (n,2n) at 14.6 Mev, total cross sections for, (E), 19: 39797
proton reactions (p,n) at 7.5 to 13.0 Mev, levels from, (E), 19: 39827
FLUORINE ISOTOPES F-21
decay and production of, 19: 39265(R) (IA-1021)
FLUOROCARBONS
radiation effects on liquid, mechanism of electron, 19: 38709
FOOD
consumption and inspection of, in event of nuclear conflict, 19: 38882
radiation processing of meats, effects on pigments, 19: 39065
radiation processing of rye flour, effects on vitamin content, 19: 38423
radioactivity in West German Republic, 19: 38904
radioactivity of, in Austria, 1963, 19: 38860
radiosterilization effects on flavor and lipids in meat, analytical methods for determining, 19: 39068
strontium-90 content in German, 19: 38876 (NP-14927)
FOOD IRRADIATION FACILITIES
survey of radiation sources available in southern U. S. for use as, 19: 39062 (TID-21710(Rev.))
FORMALDEHYDE
yields from radiolysis of methanol, 19: 38716
FORMIC ACID
reactions with lutetium, thulium, and ytterbium hydroxides, properties of formate formed by, 19: 38669
FOSSILS
age estimation of Pleistocene and Tertiary, from uranium–helium ratios, 19: 38868
dating by analysis of charged particle tracks resulting from spontaneous uranium fission, 19: 39038
FRACTURE TESTS
specimens for, double cantilever beam, 19: 38822 (BNWL-SA-2)
FRANCE
uranium production and uses in, in 1964, 19: 39105
FREE RADICALS
electron nuclear double resonance of, in solutions, 19: 38638
radioinduced destruction of, ESR studies of, 19: 38719
FREONS
organic residue from TF, radioisotopic study, 19: 38538 (ADR-08-13-63.1)
FREQUENCY MODULATION
design of semiconductor devices for i-r, (E/T), 19: 38914 (SC-DC-65-1332)
equipment for infrared, research on, 19: 39269(R) (SU-SEL-64-133)
FRUITS
radiation effects on pathogens in citrus, gamma, 19: 39265(R) (IA-1021)
radiation effects on, gamma, 19: 39265(R) (IA-1021)
radiation effects on development of apple clones, gamma, 19: 38411
radiation processing of strawberries and tomatoes to extend storage life of shipped, economic feasibility of, 19: 39062 (TID-21710(Rev.))
radiation processing of grapefruit, oranges, peaches, strawberries, and tomatoes, effects on spoilage during shipment, 19: 39062 (TID-21710(Rev.))
FUNGI
radiation effects on citrus-fruit, gamma, 19: 39265(R) (IA-1021)
FURNACES
design for sample heating in x-ray diffractometers, 19: 38941
design of bell, for reduction of tetrafluoride using magnesium, 19: 39113(P)
design of hydrogen–oxygen, for brazing copper structures, 19: 38938
uses of electron-bombardment, in metallurgy, 19: 39109
FUSED SALTS
electric conductivity of, measuring methods for, 19: 40286(R) (NAA-SR-11200)
thermodynamic properties, 19: 38683

G

GADOLINIUM
crystal structure and magnetic properties of, pressure effects on, 19: 40094
determination of, in SAP by spectrography, 19: 38553
neutron absorption properties of, burnup effects on, (E), 19: 40163
pathological effects of subcutaneous implantations of, in mice, 19: 38334 (COO-1170-1)
phase transformations at 6 to 65 kbar, solid-liquid and solid-solid, 19: 40095
proton inelastic scattering at 25 to 1700 kev, x-ray yields from, (E), 19: 39881
GADOLINIUM COMPLEXES
with [(2-hydroxyethyl)imino]diacetic acid, dissociation constant of, 19: 38671
GADOLINIUM IONS
electron paramagnetic resonance and endor spectra of, in thorium dioxide, 19: 38655
GADOLINIUM ISOTOPES Gd-153
spin of ground state of, (E), 19: 39818
GADOLINIUM ISOTOPES Gd-155
neutron capture by, gadolinium-156 Mössbauer effect following, (E), 19: 39863
GADOLINIUM ISOTOPES Gd-156
Mössbauer effect in gadolinium oxide, (E), 19: 39863
GADOLINIUM ISOTOPES Gd-157
neutron capture by, gadolinium-158 Mössbauer effect following, (E), 19: 39863
GADOLINIUM ISOTOPES Gd-158
Mössbauer effect in gadolinium metal and oxide, following neutron capture reactions, (E), 19: 39863
GADOLINIUM ISOTOPES Gd-159
production of isomeric, in proton reactions with gadolinium-160, (E), 19: 39929
GADOLINIUM ISOTOPES Gd-160
proton reactions with, isomeric gadolinium-159 from, (E), 19: 39929
GADOLINIUM NIOBATES

preparation and thermal properties, 19: 38617
GAGES
design of high-range velocity, for measurements near underground explosions, 19: 38917 (SC-R-65-904, pp 23-48)
GALAXIES
explosions of, evidence of cosmic ray origin in, 19: 39362
GALLIUM
content in solar atmosphere, (E), 19: 39345
effects on density of plutonium and iron–plutonium alloy, 19: 39161 (LA-DC-6956)
electrocapillary properties of liquid, 19: 39171(T) (IS-Trans-17)
transition temperature of thin films of superconducting, effects of thin oxide layer on, (E), 19: 39746
GALLIUM ALLOYS
Al–Ga, radiation effects on, annealing electron, 19: 40286(R) (NAA-SR-11200)
Ga–Pu, densities of liquid, effects of temperature on, 19: 39163(R) (MLM-1244)
Ga–Pu, density at 25 to 800°C, 19: 39161 (LA-DC-6956)
Ga–Pu, phase equilibria of, effects of impurities on, 19: 39163(R) (MLM-1244)
Ga–Pu, phase transformations in, latent heats of, 19: 39163(R) (MLM-1244)
Ga–Th, crystal structure of intermetallic compound $ThGa_2$ in, 19: 39207
Sb–Ga, spectral analysis of photoemission yields from cesiated surfaces of, 19: 39406
GALLIUM ARSENIDES
diffusion of zinc in, effects of partial pressures on, (E), 19: 39269(R) (SU-SEL-64-133)
electron tunneling in p-n junctions of, 19: 38931
photoelectron emission yields at 2 to 6 ev from cesiated surfaces of, spectral analysis of, 19: 39406
properties of, crystallographic and electric, (E), 19: 39269(R) (SU-SEL-64-133)
GALLIUM CARBIDES
GaC–NbC, preparation and crystal structure of H-phase in, 19: 39208
GaC–TiC, preparation and crystal structure of H-phase in, 19: 39208
GALLIUM ISOTOPES Ga-68
use in radiodiagnosis, review on, 19: 38505
GALLIUM NITRIDES
GaN–TiN, preparation and crystal structure of H-phase in, 19: 39208
GALLIUM PHOSPHIDES
electron tunneling in p-n junctions of, 19: 38931
properties of, crystallographic and electric, (E), 19: 39269(R) (SU-SEL-64-133)
properties of, electric and optical, 19: 39269(R) (SU-SEL-64-133)
GALLIUM SYSTEMS
As–Ga–P, electric, metallurgical, and optical properties of, (E), 19: 39269(R) (SU-SEL-64-133)
Ga–La–Se, chemical properties, 19: 38598
GAMMA CAMERAS
design and performance of, for clinical tracer studies, 19: 39008
GAMMA RADIATION
absorption by heterogeneous materials, effective atomic numbers for, 19: 40069
absorption by nuclei, total cross section for, (T), 19: 39873
absorption by nuclei, with two-nucleon emission, (T), 19: 39932
absorption of, measurement of velocity or related function using resonant, 19: 38966(P)
angular correlations with x radiation, relaxation effects in, 19: 39849
angular correlations in iodine-127, resonance peaks in perturbed, (E), 19: 39854
attenuation in air, 19: 39483 (SGAE-PH-20/1965)
book: *The Propagation of Gamma Quanta in Matter*, 19: 40071
detection and measurement in earth formation well-logging, 19: 38871(P)
detection and measurement of, design of gamma camera for, 19: 39008
detection and measurement of soft, design of gridded proportional counter for, 19: 39046(P)
detection of, automatic scintillation counter for, 19: 39003
detection of, scintillator efficiency for, 19: 39009
dose equivalent measurements using condenser ionization chambers, (E), 19: 39015
dose measurements of, from internally-deposited technetium-99, 19: 38506
dose to man from external fallout, 19: 38891
dosimetry of, thermoluminescence detectors for, 19: 39044(P)
dosimetry of, using radiochemical nitrate yield, 19: 39042
effects of ion exchange properties of volcanic tuff, 19: 38768
effects on addition reaction of alcohols to 1,2-dichlorotetrafluorocyclobutene and 1,2-dichlorohexafluorocyclopentene, 19: 38708
effects on algae, pathological, 19: 38410
effects on alkyl halide–tin reactions, 19: 39091(R) (BMI-1723(Del.))
effects on aluminate solutions, 19: 38738
effects on anion-exchange resins, 19: 38697 (ZFK-RN-17(p.139-64))
effects on annealing and deformation behavior of lithium fluorides, 19: 39243
effects on aspartic acid formation in aqueous alanine solutions, mechanism of, 19: 38702
effects on *Callosobruchus maculatus*, 19: 39265(R) (IA-1021)
effects on cell cycle duration in tail tissues of mouse embryos, 19: 38405
effects on central nervous system, synergistic effects of acceleration and vibration during space flight, 19: 38358 (AD-612660)
effects on ceramic spheres, from incorporated radioisotopes, 19: 40275
effects on *cis-trans* isomerization and unsaturation loss in polybutadiene, 19: 38711
effects on citrus fruit, 19: 39265(R) (IA-1021)
effects on citrus-fruit fungi, 19: 39265(R) (IA-1021)
effects on *Cl. perfringens*, alpha toxin formation in, 19: 38446
effects on *Cl. perfringens* alpha toxin formation, 19: 38447
effects on coloration and thermoluminescence of borate glasses, relation between, 19: 39244
effects on crystal structure of silicon, microplasm studies of, 19: 39254
effects on culture and morphology of *Bacillus mesentericus*, 19: 38449
effects on decomposition of water in reactor, 19: 36898 (ZFK-RN-17 (p.199-207))
effects on degradation of desoxyribonucléic acid, 19: 38408
effects on deuterium–hydrogen exchange on silica gel, 19: 38626
effects on development of apple clones, 19: 38411
effects on dye solutions, 19: 38736
effects on egg hatchability in Artemia, dose dependency of, 19: 38383
effects on electric cables, 19: 39056 (N64-29558)
effects on formation of free radicals in solid hydrocarbons, ESR studies of, 19: 38724(T)
effects on free radical density in polymethylmethacrylate, 19: 38706
effects on fruit pathogens, 19: 39265(R) (IA-1021)
effects on fused metal halides, 19: 39265(R) (IA-1021)
effects on graft polymerization of polyvinyl chloride with styrene, 19: 38733
effects on growth of potassium chloride crystals from aqueous solutions, 19: 38696 (MIT-2909-4)
effects on growth in cereal seedlings, effects of oxygen tension on inhibitory, 19: 38418
effects on growth and reproduction of gladiolus bulbs, 19: 38430
effects on hatchability in Artemia, effects of moisture and temperature on, 19: 38384
effects on heavy water, acidity effects on yields in, 19: 38710
effects on hemolysin production in rabbit liver, 19: 38429
effects on histolysis of pupal fat-bodies in Dacus, 19: 38406
effects on hydrogen adsorption on aluminum oxide, 19: 38717
effects on hysteresis loops in monocrystalline barium titanates, 19: 38705
effects on infectiousness and motility of *Treponema pallidum*, 19: 38380
effects on lethal induction in *Drosophila willistoni* populations, suppressors in, 19: 38391
effects on liquid cyclopentane, yields in, 19: 38712
effects on Mediterranean fruit flies, 19: 39265(R) (IA-1021)
effects on metabolism and respiration in rat tumors, synergistic effects of hydrogen peroxide, 19: 38389
effects on methanol, 19: 38716
effects on methyl laurate, 19: 38721
effects on mutation induction in Dahlbominus oogonia, 19: 38392
effects on neutron spectra measurement, 19: 40122(R) (GEAP-4862)
effects on ovarian development in Dacus, 19: 38406
effects on particle size in monodisperse colloidal sulfur, 19: 38714
effects on petroleum hydrocarbons in uniform temperature and dose field at 1 to 30 atm, 19: 38726(T)
effects on plastic, glass-laminate, and ceramoplastic materials, 19: 39232 (FZK-227)
effects on potato sprouting and tomato ripening, effects of gibberellic acid on, 19: 38401
effects on pressure transducer components, transient and permanent, 19: 39055 (GA-6266)
effects on production of stereospecific polymers from inclusion compounds, 19: 38725(T)
effects on properties of alloys, 19: 39257(P)
effects on proton content and RNA in amoeba, 19: 38371
effects on reactions of chlorinated methanes with cycloalkenes, 19: 38695 (KFK-317)
effects on reactions of hydrocarbons with carbon dioxide, 19: 38727(T)
effects on recombination in silicon, (E), 19: 40085
effects on reticulocytes in peripheral blood in rats, 19: 38414
effects on selenium photoelectric cells, (E), 19: 39058
effects on silicate glass, (E/T), 19: 39256
effects on silicon semiconductors, 19: 39269(R) (SU-SEL-64-133)

effects on structure of pigments in cooked meats, 19: 39065
effects on toxin formation by *Cl. perfringens*, 19: 38448
effects on ultrasonic attenuation in monocrystalline copper, 19: 39249
effects on vestibular organs in guinea pigs, synergistic effects of vibration, 19: 38358 (AD-612660)
effects on vitamin content in rye flour, 19: 38423
effects on wheat seeds, effects of water content on, 19: 38412
emission by quasar 3C286, low-energy, (E), 19: 39357
emission from rhodium-103, circular polarization of, (E), 19: 39945
emission from type I supernova, (T), 19: 39338
interactions with protons at 600 to 850 Mev, double meson (π) production in, (E), 19: 39519
measurement using scintillation counters, efficiency of well-type crystals for, 19: 39039
monitoring in industrial buildings, 19: 38884
photoelectric cross section at 662 kev, method for measuring K-shell, 19: 39376
polymerization of acrylamide–propionamide solid solutions induced by, effects of oxygen on, 19: 38694 (BNL-9200)
reactions (γ,α) with light nuclei, (T), 19: 39934
reactions (γ,n) with beryllium-9, excitation functions for, (T), 19: 39805
reactions (γ,n) and (γ,p) with helium-3, cross sections, 19: 39808
reactions with copper, nickel, and silver at 6.13 Mev, electron pair production cross sections for, (E), 19: 39787 (SGAE-PH-19/1965)
reactions with tantalum and platinum at 145 kev, photoelectric cross sections of, 19: 39377
reactions with water, nitrous oxide scavanging of products of, 19: 38720
scattering by nuclei, spectra of nonresonant and resonant, (E), 19: 39265(R) (IA-1021)
therapeutic effects for calcifying epithelioma, 19: 38494
therapeutic use for tumors of vagina, effects on thyroid function, 19: 38492
transport in air from atomic bombs, shielding against, 19: 38892
transport in one-dimensional plane geometries, computer program for, 19: 40066 (NP-15155)
use in well logging for determination of heavy metal ores, 19: 38867

GAMMA SOURCES
design of automatic application intercavitary cobalt-60, for therapeutic use, 19: 38483
design of cesium-137, for cell suspensions and small animals, 19: 38415
for radiotherapy, energy level of gold-198, 19: 38515
installation in IRR-1, 19: 39265(R) (IA-1021)
therapeutic use for cancer, 19: 38487
use in well logging for determination of heavy metal ores, 19: 38867
use of cobalt-60 and radium for therapy of bladder cancers, 19: 38504
ventilation of rooms containing, 19: 38883

GAMMA SPECTRA
analysis of complex, in activation analysis, equations for, 19: 38566

GAMMA SPECTROMETERS
design and performance for reactor fuel burnup determination, 19: 38825 (NP-15176)

GAMMA SPECTROSCOPY
method for determining gamma emitters in rain water, 19: 38557

GARIGLIANO POWER REACTOR
fuel management in, (T), 19: 40216

GARNETS
magnetic properties of rare earth iron, theory of, 19: 39265(R) (IA-1021)

GAS ANALYZERS
design for measuring uranium (IV) fluoride in noncondensable gas stream, 19: 38573(P)

GAS COOLED REACTORS
contamination from cooling system of, method and apparatus for removal of, 19: 40119(P)
design and performance of liquid core, for space propulsion, 19: 40227 (LA-3229, pp 90-110)
development of fast breeder, 19: 40182 (GA-5537)
fuel processing for high-temperature, costs of, 19: 39129(R) (ORNL-TM-1116)
heat exchanger design for, waste-heat, 19: 40141(P)
loading device for graphite moderated, 19: 40145(P)
pressure vessel design for, 19: 40131(T) (ORNL-tr-585)

GAS FLOW
boundary layer of MGD, in crossed electric and magnetic fields, (T), 19: 40044
in gaseous-core reactors, dynamics and heat transfer of coaxial, 19: 40233 (LA-3229, pp 180-207)
in gaseous-core reactors, heat transfer in coaxial, 19: 40234 (LA-3229, pp 208-21)
in gaseous-core reactors, vortex matrix for, 19: 40237 (LA-3229, pp 251-85)
in gaseous-core rocket reactors, vortex, 19: 40236 (LA-3229, pp 237-50)
velocity past right circular cone, effects on base and surface pressure of, (E/T), 19: 40292 (SC-TM-202-56-51)

GASEOUS FUEL REACTORS
criticality studies, (T), 19: 40239 (LA-3229, pp 315-43)
design of coaxial flow, for propulsion, 19: 40232 (LA-3229, pp 177-9)
design of, criticality effects on, 19: 40155 (LA-3229, pp 362-76)
development for rocket propulsion, review of, 19: 40242 (LA-DC-7118)
fuel containment and heat deposition in, for propulsion, 19: 40235 (LA-3229, pp 222-36)
fuel material partition from propellant in rockets, glow-plug concept for, 19: 40228 (LA-3229, pp 111-15)
fuel material partition from propellant in, light bulb concept for, 19: 40230 (LA-3229, pp 137-47)
fuel material partition from propellant in rocket reactors, 19: 40229 (LA-3229, pp 116-36)
fuel vortex flow in, matrix for, 19: 40237 (LA-3229, pp 251-85)
fuel vortex flow study in, 19: 40236 (LA-3229, pp 237-50)
fuel-propellant energy exchange using MHD cells, 19: 40238 (LA-3229, pp 286-312)
fuel-propellant flow in, dynamics and heat transfer of coaxial, 19: 40233 (LA-3229, pp 180-207)
gas interactions in, high-temperature, (E), 19: 40231 (LA-3229, pp 149-76)
heat transfer in coaxial flow, 19: 40234 (LA-3229, pp 208-21)

GASES
analysis for uranium (IV) fluoride, 19: 38573(P)
Boltzmann equation for, statistical equivalent to, (T), 19: 39396
book: *Collision Phenomena in Ionized Gases*, 19: 39309
determination using double focusing mass spectrometer, 19: 38546(R) (RFP-552)
electric discharge in, harmonic generation in microwave, (T), 19: 39294
excitation and relaxation behind strong shock waves, equations for, (T), 19: 40040
interactions in gaseous-core reactors, high-temperature, (E), 19: 40231 (LA-3229, pp 149-76)
ionization in nonuniform electric fields, Townsend function for, (T), 19: 39298
magnetization of low-temperature Fermi, (T), 19: 39684 (CONF-796 (Paper 4))
neutron thermalization in, Van Hove theory for relaxation times in, 19: 39773
nuclear spin relaxation in, 19: 39378
particle correlation functions for, antinormalization properties of, (T), 19: 39290
pseudopotentials of hard-sphere, (T), 19: 39651
separation of mixtures of, by diffusion through porous barriers, 19: 38767
shock wave structure in neutral, (T), 19: 39984
sound propagation in weakly ionized, longitudinal, (T), 19: 39293
soundwave propagation in rarefied, kinetic theory of, 19: 39262 (BNL-8990)
theory of, Liouville equation in, 19: 39303
thermodynamic properties of, astrophysical relations of, (T), 19: 39339
x-ray diffraction studies of crystallized, helium cryostat for, 19: 38946

GASTROINTESTINAL TRACT
radiation effects on morphology of rat, fast neutron, 19: 38444
radiation sickness effects on, pathology of, 19: 38433(T)
treatment of disorders of, using iodine-131, 19: 38529

GENES
location of, controlling radiosensitivity of *E. coli*, 19: 38397
range of action of, controlling uv radiosensitivity of *E. coli*, 19: 38398

GENETICS
code for messenger ribonucleic acid synthesis, 19: 40296 (TID-21856)
effects of exogenous desoxyribonucleic acid in Drosophila, 19: 38408
human, 19: 38328

GEOLOGY
of Cuzco-Anta-Urubamba area, Cuzco Department, Peru, 19: 38845 (RME-4584)

GEOMAGNETIC STORMS
commencement effects on ionospheric F2 region, sudden, (T), 19: 39669
effects on lower ionosphere at low latitudes, 19: 39667
production by interplanetary shock waves, 19: 39681
properties of, seasonal dependence of, 19: 39673

GEOPHYSICS
shock wave studies in, 19: 39274(T) (JPRS-30799)
upper atmosphere observations using optical radar, 19: 39270(R) (TID-21894)

GERMANIUM
electron and x-ray scattering by, corrections to incoherent, 19: 39379
fabrication and performance of lithium-drifted, for gamma detectors, 19: 39018

fission-fragment damage in, (E), 19: 39245
helium ion channeling reactions at 209 ev, thermochemical properties for, (T), 19: 39395
neutron reactions (n,n´γ) at 0 to 14 Mev, energy absorption in, 19: 39769 (SC-DC-65-1544)
photoelectron emission yields at 2 to 6 ev from cesiated surfaces of, spectral analysis of, 19: 39406
radiation effects on thermoelectric capacity at low temperatures, fast neutron, (E), 19: 39240
superconductivity under high pressure, (E), 19: 39701
ultrasonic waves in, properties of finite-amplitude, 19: 39268 (ORNL-P-1395)

GERMANIUM ALLOYS
Ge–La, preparation, properties, and structure of intermetallic compounds $LaGe_2$, LaGe, and La_5Ge_3, 19: 39195
Ge–Nb, superconductivity of Nb_3Ge, (E), 19: 39725

GERMANIUM JUNCTIONS
performance as i-r modulators, (E/T), 19: 38914 (SC-DC-65-1332)

GERMANIUM OXIDES
GeO_2–La_2O_3, preparation, phase studies, and properties, 19: 38612

GERMANIUM SULFIDES
spectra of, microwave rotational, (E), 19: 38663

GERMANIUM SYSTEMS
Ge–Si, properties for thermocouples, 19: 39430(R) (AD-426092)

GERMANY
fallout content of milk in, 1962, 19: 38858
fallout monitoring, 1963, 19: 38862
radioactivity of atmosphere, food, soil, and water in Federal Republic of, 19: 38904
strontium-90 content in fallout, food, human skeleton, milk, soil, and water in, 19: 38876 (NP-14927)

GIBBERELLIC ACID
ethyl ester, radiosensitivity effects on potato sprouting and tomato ripening, 19: 38401

GLACIERS
production during ice ages, 19: 39665

GLASS
charged particle tracks in, identification after chemical etching, 19: 39038
radiation effects on, (E/T), 19: 39256
radioinduced thermoluminescence in, dosimetric use of, 19: 39044(P)

GLAUCONITES
age estimation of, in Vindhyan system in India, 19: 38853

GLEEP
neutron spectra determination by lithium-6 and helium-3 semiconductor spectrometers, fast, 19: 40256 (AERE-M-1590)

GLOBULIN
effects of radiophosphorus on denatured and whole, in rats, 19: 38368

GLOW DISCHARGES
ion-molecule reactions in cathode region of, 19: 38637

GLUCURONIC ACID
protective effects against radiation damage in mice, 19: 38456

GLUTATHIONE
content in ascites tumor cells, effects of cysteamine on, 19: 38464
radiation effects on metabolism of, in blood, 19: 38509

GLYCINE
placental transfer in rabbits and swine, tracer study, 19: 38344
protective effects of, against radiation injury of enzyme systems in rat liver and spleen, 19: 38467

GLYOXIME, DIMETHYL-
analytical use for spectrophotometric determination of nickel, 19: 38546(R) (RFP-552)

GOLD
analysis for impurities by mass spectrometry, 19: 38546(R) (RFP-552)
annealing of cold-worked, kinetics, 19: 39168(R) (TID-22015)
bromine-79 and iodine-127 reactions at 20 to 80 Mev, orientation effect on energy losses from, 19: 39370 (ORNL-P-1336)
determination in enamel of teeth, neutron activation, 19: 38562
determination in minerals by activation, 19: 39265(R) (IA-1021)
deuteron reactions (d,p) at 23 and 26 Mev, angular distribution and spectra in, (E), 19: 39901
deuteron reactions at 26 Mev, neutron-proton correlations from deuteron breakup in, (E), 19: 39901
electron inelastic scattering by crystals of, phonon excitation in fast, (T), 19: 40084
plastic deformation of thin films of, by Talysurf stylus, 19: 38916 (SC-DC-65-1589)
radiation damage in, cross sections for atomic displacements from 1- to 3-Mev electrons, 19: 39225 (AFCRL-65-286)

GOLD ALLOYS
Au–Zn, heat of formation of AuZn, 19: 39168(R) (TID-22015)

GOLD ISOTOPES Au-197
neutron Doppler effect and resonance integrals of, (E), 19: 40286(R) (NAA-SR-11200)
neutron reactions (n,γ), gamma spectra of 4.9-ev resonance in, 19: 39781 (JAERI-1073)

GOLD ISOTOPES Au-198
colloids, use in treatment of malignant effusions, energy levels for, 19: 38515
effects of injected, on metabolism and respiration in tumors, synergistic effects of hydrogen peroxide in rats, 19: 38389
excretion by rat kidneys, morphology of, 19: 38342
radiation hazards of colloidal, 19: 38476
use in radiodiagnosis, review on, 19: 38505

GONADS
radiation effects on gonocytes in testes of rats, 19: 38369
radiation effects on DNA and nucleoprotein synthesis in rat testes, 19: 38370
radiation effects on development of Dacus ovarian, gamma, 19: 38406
radiation effects on morphology of rat, fast neutron, 19: 38444

GRAPHITE
analysis for trace amounts of sodium by x-ray spectrography, 19: 38571
cesium-137 gamma spectra in, stress effects on, (E), 19: 39794
crystal structure of, formed by decomposition of silicon carbide, 19: 39185
densification of powdered, effects of fine-particle metals on, 19: 39091(R) (BMI-1723(Del.))
fabrication of pyrolytic, 19: 39142(P)
mechanical properties of, effects of crystal structure on, 19: 39237
oxidation of, by oxygen at 500 to 600°C, kinetics of, 19: 39119
preparation of expanded pyrolytic, 19: 39112(P)
properties of, mechanical and physical, 19: 39216
radiation effects on liquid sodium dilation of, 19: 39235 (NAA-SR-11309)
radiation effects on mechanical properties, 19: 39237
radiation effects on tensile fracture strain of, at 25, 550, and 600°C, 19: 39238
reactions with borides to 2200°C, 19: 38654
reactions with europium, thermodynamics of, 19: 38680
reinforcement using deposited fused metals, 19: 39114(P)
separation of metallic impurities from, at temperatures above 1750°C in high-pressure inert gases, 19: 38762
tensile properties of polycrystalline, under compression up to fracture, 19: 39186
tensile properties at 2500°C time-dependent strengthening of, 19: 39187
tensile properties of H4LM, at –269 to 500°C, 19: 39188

GRAPHITE (IMPREGNATED)
radiation effects on, neutron, 19: 39129(R) (ORNL-TM-1116)

GRAPHITE MODERATED REACTORS
contamination of core of, method and apparatus for removal of, 19: 40119(P)
criticality studies in, review, (E), 19: 40163
design of, gaseous-core criticality effects on, 19: 40155 (LA-3229, pp 362-76)
loading device for gas cooled, 19: 40145(P)

GRAPHITE SYSTEMS
Al–graphite, deposition of coatings of, at 1500 to 1750°C, 19: 39144(P)
graphite–Th, deposition of coatings of, at 1500 to 1750°C, 19: 39144(P)
graphite–V, deposition of coatings of, at 1500 to 1750°C, 19: 39144(P)
graphite–U, deposition of coatings of, at 1500 to 1750°C, 19: 39144(P)

GRASS
radioactivity in Germany, 1962, 19: 38858
strontium-89 contamination of, retention and loss of, 19: 38332

GRAVITATION
asymptotic properties of gravitational fields, (T), 19: 39636
collapse of quasi-stellar radio sources, 19: 39359
Einstein-Maxwell equations for electromagnetic fields and, homogeneous solutions of, 19: 39647
elementary particle masses in unified field theory, 19: 39452 (CONF-796(Paper 13))
energy of field of, relativity theory for negative, 19: 39656
theory of, field, 19: 39662
theory of, Hoyle-Narlikar, 19: 39659
theory of, research programs on, 19: 39270(R) (TID-21894)

GREAT BRITAIN
fallout monitoring, 1964, 19: 38863
leukemia epidemiology in children of, 19: 38326

GROUND
motion measurements, meeting on, 19: 38864 (SC-R-65-904)
motion measurements during large explosion, instrumentation for, 19: 38865 (SC-R-65-904, pp 3-22)
velocity and displacement measurement, electronic integrators for,

19: 38918 (SC-R-65-904, pp 49-58)
velocity measurement near underground explosions, gage for, 19: 38917 (SC-R-65-904, pp 23-48)
GROUND WATERS
barium, cesium, lithium, rubidium, and strontium distribution in subterranean salt, in Bulgaria, 19: 38851
hydrology at National Reactor Testing Station, 19: 40269(R) (IDO-22047-USGS)
waste transport in soils by, analysis, 19: 40268 (BNWL-63)
GROWTH
radiation dose effects on tumor, in F_1 hybrid mice, 19: 38403
radioinduced inhibition of cereal seedling, effects of oxygen tension on gamma, 19: 38418
GUINEA PIGS
radiation effects on vestibular organs in, synergistic effects of vibration on, 19: 38358 (AD-612660)
radiation effects on immune reactions to tuberculosis infections in, 19: 38375

H

HAFNIUM
neutron absorption properties of, burnup effects on, (E), 19: 40163
production and uses, 19: 39108
separation from zirconium, 19: 39108
HAFNIUM ALLOYS
Hf–Ta, development and properties of, 19: 39123
Hf–Ta, oxidation resistance of, to 4000°F, 19: 39123
Hf–Ta–W, cavitation of T-111 in bismuth–lead alloy at 500 and 1500°F, ultrasonic-induced, 19: 39116 (NP-15263)
HAFNIUM BORIDES
reactions with graphite to 2200°C, 19: 38654
HAFNIUM ISOTOPES Hf-176
internal conversion, (E), 19: 39931
HAFNIUM ISOTOPES Hf-177
internal conversion from, 321-kev level of, E1 K, (E), 19: 39947
neutron reactions (n,γ), gamma spectra of 1.1-ev resonance of, 19: 39781 (JAERI-1073)
HAFNIUM ISOTOPES Hf-178
neutron reactions (n,γ), gamma spectra of 7.8-ev resonance of, 19: 39781 (JAERI-1073)
HAFNIUM OXIDES
production and uses in control rods of nuclear reactors, 19: 39108
HAFNIUM SYSTEMS
C–Hf–Ta–W, cavitation of T-222(A) in bismuth–lead alloy at 500 and 1500°F, ultrasonic-induced, 19: 39116 (NP-15263)
HALDEN BOILING REACTOR
noise analysis in, (E), 19: 40164
HALL EFFECT
calculation of, in ionic solutions, 19: 38643
measurement in semiconductors, methods for, 19: 39269(R) (SU-SEL-64-133)
HALLAM POWER REACTOR
fuel element performance in, 19: 40286(R) (NAA-SR-11200)
moderator design and development, 19: 40286(R) (NAA-SR-11200)
HAMBURG ELECTRON SYNCHROTRON
construction status of, 19: 39327
HAMSTERS
radioinduced chromosome aberrations in, uv, 19: 38395
HANDBOOKS AND MANUALS
for SALOMON program use, 19: 40066 (NP-15155)
on operation of SRE, 19: 40286(R) (NAA-SR-11200)
HANDLING AND STORAGE
of plutonium, measurement problems in, 19: 38535 (RFP-508)
HANFORD AREA (WASH.)
monitoring of environs, 1964, 19: 38874 (BNWL-SA-53)
stratigraphy of late basalt flows, Ellensburg Formation, and lower Ringold Formation, 19: 38843 (BNWL-SA-135)
stratigraphy of post-basalt sediments, 19: 38844 (BNWL-SA-140)
HANFORD PRODUCTION REACTORS (N)
containment system for, design of vented, (E), 19: 40220
design characteristics and uses, 19: 40191 (RL-SA-42)
performance for desalination, 19: 40219 (RL-SA-21)
performance of, analog simulation for, 19: 40282 (BNWL-SA-171)
HARMONIC ANALYSIS
numerical continuation backward-in-time of Laplace equation, (T), 19: 38804 (BNL-8185)
HASTELLOY F
thermal response and microstructure at 1400°F, 19: 39158 (GEAP-4751)
HASTELLOY RZ35
properties as cladding material for SNAP hydride reactors, 19: 39166 (NAA-SR-Memo-11149)
HASTELLOY X
corrosion by steam at 1050 and 1150°F of, isothermal, 19: 39115 (GEAP-4760)
corrosion by steam of, at 800 to 1410°F with heat transfer, 19: 39115 (GEAP-4760)
properties as cladding material for SNAP hydride reactors, 19: 39166 (NAA-SR-Memo-11149)
tensile properties of, on aging at 1000 and 2000°F in steam, 19: 39156(R) (CEND-532)
thermal response and microstructure at 1400°F, 19: 39158 (GEAP-4751)
HEALTH PHYSICS
analytical radiochemical techniques for, 19: 38889
HEART
distribution of injected cesium-131 in normal, 19: 38502
photoscans of, use of iodine-131-labeled albumin for, 19: 38490
radiation effects on blood vessels in rat, fast neutron and x, 19: 38441
radiation sickness effects on, pathology of, 19: 38433(T)
HEART DISEASES
radiodiagnosis, using injected cesium-131, 19: 38502
radiodiagnosis, using injected cesium-131, 19: 38503
radiotherapy of cardiac failure using iodine-131, 19: 38497
HEAT
conversion to electricity, fundamentals of thermionic, 19: 39441
HEAT EXCHANGERS
design for liquid metals, 19: 38821(P)
design for waste heat from reactors, 19: 40141(P)
design of finned-tube, 19: 38818(P)
design of finned-tube, 19: 38819(P)
design of multitubed cylindrical, 19: 38820(P)
HEAT TRANSFER
equations for, numerical continuation backward-in-time of, (T), 19: 38804 (BNL-8185)
from fuel particles to reactor coolant, analysis of, 19: 40113(R) (ANL-7071)
from zirconium in simulated reentry tests, 19: 39118(R) (SC-DC-65-1520)
in double-pipe heat exchangers, calculation of, 19: 40113(R) (ANL-7071)
in fluidized bed reactors, 19: 40225 (LA-3229, pp 83-5)
in fluidized bed reactors, 19: 40226 (LA-3229, pp 86-8)
in gaseous-core, coaxial flow reactors, 19: 40233 (LA-3229, pp 180-207)
in gaseous-core, coaxial flow type reactors, 19: 40234 (LA-3229, pp 208-21)
in liquid-core nuclear rocket, 19: 40227 (LA-3229, pp 90-110)
in transition boiling, effects of flow disturbances on, 19: 38806(R) (GEAP-4908)
HEAT TRANSFER SYSTEMS
development of heat pipes, survey, 19: 38780 (LA-DC-7206)
HEATERS
tubes for, method of fabricating, 19: 39145(P)
HEAVY WATER REACTORS
construction of Essor, use of PERT method for design and installation phases in, 19: 40265
criticality studies in, review, (E), 19: 40163
criticality studies on spectral-shift, review, (E), 19: 40163
design of, gaseous-core criticality effects on, 19: 40155 (LA-3229, pp 362-76)
fuel burnup in pressure-tube power, (E/T), 19: 40185 (JAERI-1075)
use in nuclear power plants, 19: 40211
HELIUM
content in primary radiation, solar activity effects on, (T), 19: 39427
cylinders in liquid, boundary effects on added mass of, (T), 19: 39697
density and temperature behind shock fronts in thermal plasma of, (T), 19: 40051
density of rotating liquid II, dependence on angular velocity, (E), 19: 39714
electron free energy in, (E/T), 19: 39722
energy level transitions in, shielding approximation for dipole matrix elements for 2^1S-2^1P and 1^1S-2^1P transitions, 19: 39380
helium ion reactions at 20 to 120 kev, electron capture in, (E), 19: 39407
ionization cross section for, electron-impact, 19: 38630
ionization in electron-bombardment ion sources, 19: 38838
phase transition of superfluid II, determination of superconducting lead transition by, (E), 19: 39691
phonon interactions in liquid II, thermodynamic perturbation theory for forbidden three-body, 19: 40096
potentials near lambda point, effective interatomic, (T), 19: 39731
pumping at 20 to 40°K cryosorption, (E), 19: 39693
reduction of alkali halides by high-frequency electric discharge in, role of electrons in, 19: 39181
refraction index and sum rules at 2700 to 600 Å, (T), 19: 39402
rubidium-vapor spin relaxation in, (E), 19: 39400

spectra of liquid II, linear response function of degenerate Bose system for, (T), 19: 39657
surface excitations in superfluid, gapless, (E), 19: 39737
thermal conductivity length dependence in liquid II, (E), 19: 39730
vortex rings in superfluid, quantized, (T), 19: 39723
HELIUM HYDRIDES
energy levels of ions of, variational method for calculating, 19: 39799
HELIUM IONS
reactions with germanium and silicon at 209 ev, thermochemical properties for, (T), 19: 39395
reactions with helium, nitrogen, and oxygen at 20 to 120 kev, electron capture in, (E), 19: 39407
reactions with platinum-194, -195, and -196 at 34 and 41 Mev, fission, (E), 19: 39802
HELIUM ISOTOPES
detection and measurement in space, development of counter telescopes for, 19: 39419(R) (ATN-63(9219)-1)
HELIUM ISOTOPES He-3
charge and magnetic-moment structure of, model for, (T), 19: 39888
Coulomb energy, (T), 19: 39868
electron inelastic scattering at 549 Mev, cross sections for, (T), 19: 39909
gamma reactions (γ,n) and (γ,p) with, cross sections, 19: 39808
helium-3 reactions (He-3,2p) at 4.9 Mev, energy spectra of, (E), 19: 39913
helium-3 reactions (He-3,2p) at 3 to 18 Mev, energy spectra of, (E), 19: 39914
magnetization at low temperatures, (T), 19: 39684 (CONF-796(Paper 4))
nuclear magnetic resonance in liquid, (E/T), 19: 39728
nuclear spin-lattice relaxation in, in magnetic-field gradients, (T), 19: 39880
performance in fast neutron spectrometers for determination of GLEEP neutron spectra, 19: 40256 (AERE-M-1590)
properties in critical region, (E), 19: 39299
properties of liquid, coexistence curve of, 19: 39685 (LA-DC-7086)
reactions (He-3,α) with calcium-40 and calcium-42 at 18.05 Mev, (E), 19: 39874
reactions (He-3,αnn) with beryllium-9 at 3 Mev, energy spectra of, (E), 19: 39898
reactions (He-3,α) beryllium-8 at 3.0 Mev, angular correlations of, (E), 19: 39916
reactions (He-3,α) with beryllium-9, nitrogen-14, and oxygen-16, (E), 19: 39941
reactions (He-3,d) with calcium-40 at 18.05 Mev, (E), 19: 39874
reactions (He-3,n) with beryllium-9 at 1.3 to 5.4 Mev, excitation functions for, (E), 19: 39832
reactions (He-3,pαα) with lithium-6, rescattering effects in, (T), 19: 39897
reactions (He-3,pααn) with boron-10 at 2.45 Mev, sequential processes for, (E), 19: 39899
reactions (He-3,pα) with lithium-6 at 2.7 Mev, energy spectra of, (E/T), 19: 39900
reactions (He-3,pααn) with boron-10, intermediate states in, (E), 19: 39917
reactions (He-3,t) with calcium-40 at 37.5 Mev, calcium-40–scandium-40 mass difference from, (E), 19: 39850
reactions (He-3,2p) with helium-3 at 4.9 Mev, energy spectra of, (E), 19: 39913
reactions (He-3,2p) with helium-3 at 3 to 18 Mev, energy spectra of, (E), 19: 39914
scattering by nuclei, DWBA analysis of inelastic, (T), 19: 39885
separation of tritium from, by adsorption on activated charcoal, (E), 19: 38773
thermal-diffusion of, in helium-4 mixtures, at 160°K, 19: 38633
He-3–He-4, convection currents in superfluid, (E), 19: 39744
HELIUM ISOTOPES He-4
energy levels of, from deuterium–tritium and deuterium–helium-3 reactions, (E/T), 19: 39922
form factors of, calculation using repulsive-core potentials, (T), 19: 39868
phase transitions at absolute zero, solid-superfluid, (T), 19: 39729
proton inelastic scattering at 40 Mev, continuum resonances in, (E), 19: 39886
thermal diffusion of, in helium-3 mixtures, at 160°K, 19: 38633
He-3–He-4, convection currents in superfluid, (E), 19: 39744
HELIUM SYSTEMS
Ar–He, mixing at high temperatures, (E), 19: 40231 (LA-3229, pp 149-76)
He–Cs, electron temperature increases in MHD cell plasma of, (T), 19: 39437
He–H, nuclear spin lattice relaxation in, 19: 39378
HEMATOLOGY
effects of atomic bombing on, in survivors in Hiroshima and Nagasaki, 19: 38378
tracer techniques for, 19: 38493
use of radioisotopes in, review on, 19: 38356
HEMATOPOIETIC SYSTEM
radiation effects on rat, fast neutron and x, 19: 38441
radiation effects on dog, ionizing, 19: 38388
radiation sickness effects on, pathology of, 19: 38433(T)
HEMOGLOBIN
genetic code for synthesis in mammals, 19: 40296 (TID-21856)
HEMOLYSIN
radioinduced in rabbit liver, 19: 38429
HEMOLYSIS
radioinduced by radiotherapy, 19: 38509
HEMORRHAGE
radiation sickness effects on, pathology of, 19: 38433(T)
HEPTANE
diffusion in deuterated-normal mixture, coefficients of, 19: 38646
radiation effects on reactions with carbon dioxide, 19: 38727(T)
HEXAMETHYLENETETRAMINE
use of resin of, with phenol in production of carbon with reduced porosity, 19: 38684(P)
HEXANE
radiation effects on bromine-80 and -82 retentions in, isomeric transition reaction in, 19: 38715
HIGH-ALTITUDE EXPLOSIONS
fission products in troposphere from Chinese, 19: 38899
HIGH ENERGY INJECTION DEVICES
magnetic coil operation and maintenance for DCX-2, 19: 39971 (ORNL-P-1438)
plasma currents and space charge distribution in continuous, 19: 39962 (NP-15167)
vacuum techniques for operation of DCX-1, 19: 39966 (ORNL-P-1245)
HIGH TEMPERATURE GAS COOLED REACTOR EXPERIMENT
development of Dragon project, 19: 40210
HIGH-TEMPERATURE REACTIONS
thermodynamics for plutonium processing at high temperatures, 19: 38752 (LA-DC-6947)
HIGH TEMPERATURE SEPARATION PROCESSES
development for irradiated plutonium and uranium carbides, 19: 40113(R) (ANL-7071)
HIPPURIC ACID, *o*-IODO-, SODIUM SALTS
purification of iodine-131 labeled, ion exchange, 19: 38507
HIROSHIMA
bombing effects on hematology in survivors in, 19: 38378
radiation effects on serum proteins in survivors of atomic bombing in, 19: 38377
HISTAMINE
radiation effects on content in animal blood, 19: 38426
HISTIDINE
complexes with copper, catalytic properties of, 19: 39265(R) (IA-1021)
HOLMIUM
crystal structure and magnetic properties of, pressure effects on, 19: 40094
holmium-166 decay in, solid state effects on β-γ directional correlation in, (E), 19: 39824
neutron absorption properties of, burnup effects on, (E), 19: 40163
phase transformations at 6 to 65 kbar, solid-liquid and solid-solid, 19: 40095
proton inelastic scattering at 25 to 1700 kev, x-ray yields from, (E), 19: 39881
HOLMIUM CHLORIDES
holmium-166 decay in, solid state effects on β-γ directional correlation in, (E), 19: 39824
HOLMIUM COMPLEXES
with [(2-hydroxyethyl)imino]diacetic acid, dissociation constant of, 19: 38671
HOLMIUM IONS
crystal-field interactions of, linear and nonlinear shielding of, (E/T), 19: 40101
electron paramagnetic resonance in calcium tungstate crystals, 19: 38650
radiolysis of aqueous solutions of, pulse, 19: 38728
HOLMIUM ISOTOPES Ho-161
decay, (E), 19: 39930
HOLMIUM ISOTOPES Ho-166
beta decay of, solid state effects on β-γ directional correlation in, (E), 19: 39824
energy levels in, coupling rules for, 19: 39846
HOLMIUM NIOBATES
preparation and thermal properties, 19: 38617
HOLMIUM OXIDES
holmium-166 decay in, solid state effects on β-γ directional correlation

in, (E), 19: 39824
HOSPITALS
radiation hazards to nurses in radiodiagnoses, 19: 38482
HUMIDITY
radiosensitivity effects on egg hatchability in Artemia, gamma, 19: 38384
HUNGARY
fallout monitoring, 1962, 19: 38852
HYDRAZINE
production in reactors, slurries for, 19: 39095 (CONF-117(p.81-97))
N_2H_4–uranium(IV), use as partitioning agent in Purex process, 19: 38751 (HW-82103)
HYDROAROMATIC COMPOUNDS
exchange reactions between deuterium oxide and hydrogen in, nickel-catalyzed, 19: 38688
HYDROBROMIC ACID
reactions with uranium trioxide at –20 and 250°C, 19: 38603
HYDROCARBONS
radiation-thermal cracking of, at 1 to 30 atm in uniform temperature and dose field, gamma, 19: 38726(T)
reaction with halides at 1500 to 1750°C to deposit alloys containing pyrolytic graphite, 19: 39144(P)
yields from radiation-thermal cracking of petroleum at 450 to 600°C and 1 to 30 atm, 19: 38726(T)
HYDROCHLORIC ACID
effects on yields of atomic hydrogen from electric discharge in low-pressure hydrogen, 19: 38590 (UCRL-16050)
ionization of, isotope effects on Franck-Condon factors in, 19: 38632
solvent distribution in kerosene–TBP system, 19: 38563
sorption by ion exchange materials, 19: 39265(R) (IA-1021)
HYDRODYNAMICS
research on, 19: 38813(R) (UCRL-12204, pp 48-59)
HYDROGEN
containment of plasma of, by magnetic mirrors, (E), 19: 40017
crystal structure near 1.5°K, (E), 19: 39738
density and temperature behind shock fronts in thermal plasma of, (T), 19: 40051
density modulations in r-f plasma of, (E), 19: 40026
deuteron reactions (d,2p)n at 10.5 Mev, energy-angular correlations and sequential decay in, (E), 19: 39924
diffusion in bcc crystals, activation energy for interstitial, (T), 19: 40086
diffusion of gases of, in temperature gradients, (E), 19: 39291
diffusion through metals and alloys, review, 19: 39165 (NAA-SR-10462)
effects on calibration of neutron moisture meters, 19: 38948
effects on stellar convective core vanishing, (T), 19: 39334
electric discharge in, structure of, (E), 19: 39286
electron density in plasma of, (E), 19: 39978
electron density in fast theta pinch discharge, (E), 19: 39979
electron reactions at low energies, energy dependence of ion pair production in, 19: 39375
electron reactions at 30 kev with molecular, rotational spectra from, (E/T), 19: 39399
electron reactions at 15 kev, rotational temperatures from, (E), 19: 39414
electron scattering by atoms of, narrow resonance in, (E), 19: 39393
electron scattering by, rotational excitation in, (E), 19: 39413
energy level cross-over signals in, 19: 39371 (TID-22044)
energy levels of, quantum laws for, (T), 19: 39661
exchange reactions with deuterium oxide in alkylaromatic hydrocarbons and toluic acid derivatives, nickel-catalyzed, 19: 38688
fluorescence in, resonance, 19: 39371 (TID-22044)
injection of atomic, into electron-cyclotron plasma, 19: 39970 (ORNL-P-1374)
ion losses in plasma of, microinstability driven, (E), 19: 39967 (ORNL-P-1337)
ionization cross section for, electron-impact, 19: 38630
ionization cross sections for negative-ion formation, electron-impact, 19: 38631
ionization in electron-bombardment ion sources, 19: 38838
ionization of plasma of, by crossed-fields, 19: 39961 (NP-15112)
ionization of solar, size of H II region of, (T), 19: 39340
ionization of, isotope effects on Franck-Condon factors in, 19: 38632
isotope effects on radiolytic, from aqueous solutions, 19: 39265(R) (IA-1021)
magnetic fields in dissipative plasma of, structure of axisymmetric force-free, (T), 19: 40049
mass spectra of molecular, anomalous peaks in, (E), 19: 39288
neutron reactions (n,n′γ) at 0 to 14 Mev, energy absorption in, 19: 39769 (SC-DC-65-1544)
nuclear spin relaxation in, effects of ortho and para concentrations on, 19: 39378
performance of liquid, for nuclear rocket propellant, 19: 40243 (LA-DC-7169)
performance of liquid, for nuclear rocket propellant, 19: 40244 (LA-DC-7170)
photoionization cross section of atomic, at 850.6 Å, (E), 19: 39388
population densities of excited atoms in stationary plasma of, (T), 19: 40053
production of excited atoms of, by proton reactions with hydrogen-like atoms, (T), 19: 39398
production within containment in PM-type plants, test for, 19: 40188 (NYO-3420-2)
pumping at 20 to 40°K cryosorption, (E), 19: 39693
quadrupole moments, 19: 39378
radiation effects on adsorption of, on aluminum oxide, 19: 38717
reactions of, with palladium electrodes, 19: 38608
recombination kinetics of atomic, at low pressures, 19: 38590 (UCRL-16050)
reduction of alkali and alkaline earth halides by high-frequency electric discharge in, 19: 39180
reduction of alkali halides by high-frequency electric discharge in, role of electrons in, 19: 39181
safety hazards of liquid, control at experimental facilities, 19: 38875 (HASL-160)
shock front structure in atomic, in internal relaxation region, (T), 19: 39280
spectra of high-density plasma of, Balmer line characteristics in, (T), 19: 39990
spectra of molecular, rotational structure in energy loss, (E/T), 19: 39399
storage of liquid, in large dewars, 19: 39686 (LA-DC-7164)
thermal diffusion of, in deuterium mixtures, at 160°K, 19: 38633
thermodynamic properties of liquid, isotopic effects on, 19: 38639
velocity selector for atomic beams of, design of magnetic, 19: 38929
yields from radiolysis of methanol, 19: 38716
yields in gamma radiolysis of liquid cyclopentane, 19: 38712
yields of atomic, from a microwave or electrodeless discharge at 75 mtorr, 19: 38590 (UCRL-16050)
HYDROGEN IONS
electron orbitals for molecular, in united atom model, (T), 19: 39372
energy level transitions in molecular, Born matrix elements for, (T), 19: 39408
HYDROGEN ISOTOPES
detection and measurement in space, development of counter telescopes for, 19: 39419(R) (ATN-63(9219)-1)
HYDROGEN PEROXIDES
effects on radiosensitivity of tumors, 19: 38374
energy levels and wave functions of, calculation of, 19: 39265(R) (IA-1021)
synergistic effects with gamma radiation on tumor metabolism and respiration in rats, 19: 38389
HYDROGEN SULFIDES
reactions with uranyl salt, preparation of uranous chloride or sulfate by, 19: 38659
HYDROGEN SYSTEMS
Ar–H, nuclear spin lattice relaxation in, 19: 39378
Ar–H, properties of arc-jet plasma of, (E/T), 19: 40037
C–H–U, preparation, 19: 40286(R) (NAA-SR-11200)
CO_2–H, nuclear spin lattice relaxation in, 19: 39378
CO–H, nuclear spin lattice relaxation in, 19: 39378
H–chlorotrifluoromethane, vortex flow in gaseous, 19: 40236 (LA-3229, pp 237-50)
He–H, nuclear spin lattice relaxation in, 19: 39378
H–N, nuclear spin lattice relaxation in, 19: 39378
H–Ne, nuclear spin lattice relaxation in, 19: 39378
H–Ne, use in bubble chambers, 19: 39026
H–NO, nuclear spin lattice relaxation in, 19: 39378
H–N_2O, nuclear spin lattice relaxation in, 19: 39378
H–O, nuclear spin lattice relaxation in, 19: 39378
H–Y, thermodynamic properties at 250 to 350 and 650 to 950°C, 19: 38642
HYDROGEN TRITIDES
tritium beta decay in, theory of, 19: 39799
HYDROGENATION
radiation effects on platinum catalysts for, 19: 38742(P)
HYDROLOGY
measurement of deep-water Tsunami-like waves, 19: 40288(R) (NYO-98-5)
HYDROMAGNETIC WAVES
excitation in plasma in interplanetary space, (T), 19: 36983
stability of finite amplitude ion cyclotron, in plasma, (T), 19: 40022
HYDROQUINONE
2,5-dichloro-, effects on radioinduced bleaching of dye solutions, 19: 38736
HYGROMETERS

design of dew-point, for measuring the uranium (IV) content of gases, 19: 38573(P)
HYPERFRAGMENTS
decay of $_{\Lambda}H^{3}$, meson (π) rescattering corrections to rate of, (T), 19: 39891
hyperon (Λ) binding energy for $_{\Lambda}He^{7}$, (T), 19: 39834
production in lithium-6 reactions with mesons (K⁻), (E/T), 19: 39265(R) (IA-1021)
HYPERONS
beta decay of, vector constants for, (T), 19: 39588
decay of, SU(6) representation of nonleptonic, 19: 39456 (CONF-796 (Paper 21))
decays of, current-current interaction in nonleptonic, (T), 19: 39560
HYPERONS (Λ)
interactions with protons at low energies, elastic, (E/T), 19: 39460 (CONF-650410-3)
interactions with protons, SU(6) predictions for, 19: 39532
production in meson (π^-) reactions with xenon at 9 Bev/c, cross sections for, 19: 39472 (JINR-P-2178)
production in meson (π^-)-proton interactions, isobar model for, (T), 19: 39593
HYPERONS (Λ^0)
decay of polarized, electron angular distribution in leptonic, (E), 19: 39539
decay of, electron angular correlations in, (E), 19: 39613
production in photon-proton interactions, polarization in, (E), 19: 39620
HYPERONS (Σ^-)
interactions with protons at low energies, absorption properties of, (E/T), 19: 39460 (CONF-650410-3)
interactions with protons, hyperon (Σ^0) production rate for, 19: 39510
HYPERONS (Σ^0)
decay of, time reversal invariance in, (E), 19: 39484 (TID-22038)
production in hyperon (Σ^-)-proton interactions, rate for, (E), 19: 39510
HYPERONS (Σ^+)
interactions with protons at low energies, elastic, (E/T), 19: 39460 (CONF-650410-3)
interactions with protons, SU(6) predictions for, 19: 39532

I

ICE
Mössbauer effect for iron salts in, temperature dependence of, (E), 19: 39715
phase transition in, (E), 19: 39715
positronium production in, (E/T), 19: 39509
IMAGE BRIGHTNESS INTENSIFIERS
development for neutrons, 19: 40112(R) (ANL-7046(p.36-66))
IMMUNE REACTIONS
effects of spleen cell transplants on, in irradiated mice, 19: 38454
effects on course of intercapillary glomerulosclerosis in mice, 19: 38409
radiation effects on, to tuberculosis infection in guinea pigs, 19: 38375
role of thymus in radiation mouse chimera, 19: 38451
IMMUNITY
radiation effects on rat, beta, 19: 38362(T) (JPRS-30993, pp 29-38)
radiation sickness effects on natural, in animals, 19: 38434(T)
radiosensitivity of, *Cl. perfringens*, 19: 38447
IMPACT SHOCK
absorption of control rod, device for, 19: 40142(P)
IMPEDANCE BRIDGES
analysis of lossless, 19: 39270(R) (TID-21894)
IN-PILE LOOPS
fission product release from fuel element in General Atomic, 19: 39233 (GAMD-6321)
fission product trapping system for General Atomic, 19: 40120 (GAMD-5434)
INCOLOY
composition of commercial type 800, 19: 39152(R) (BMI-X-10132)
corrosion by steam of types 800 and 825, at 800 to 1410°F with heat transfer, 19: 39115 (GEAP-4760)
corrosion by steam of type 800, at 1050 and 1150°F, isothermal, 19: 39115 (GEAP-4760)
corrosion by steam at 1050°F of type 800, effects of surface preparation on, 19: 39115 (GEAP-4760)
diffusion of fission products in 800, mechanisms of, 19: 39152(R) (BMI-X-10132)
tensile properties of 800, on aging at 1000 and 2000°F in steam, 19: 39156(R) (CEND-532)
thermal response and microstructure of 800, 801, 804, and 825, at 1200 and 1400°F, 19: 39158 (GEAP-4751)
INCONEL
corrosion by aqueous chemical shim solutions at 600°F, 19: 40198(R) (WCAP-3721)
corrosion by steam of type 600, at 800 to 1410°F with heat transfer, 19: 39115 (GEAP-4760)
corrosion by steam of types 600 and 625, at 1050 and 1150°F, isothermal, 19: 39115 (GEAP-4760)
corrosion by steam at 1050°F of type 600, effects of surface preparation on, 19: 39115 (GEAP-4860)
corrosion of type 600, by aqueous reactor shim solutions at 600°F, 19: 40196(R) (WCAP-3269-6)
corrosion of 600, by aqueous boric acid at 600°F, 19: 40195(R) (WCAP-3269-5)
tensile properties of 625, on aging at 1000 and 2000°F in steam, 19: 39156(R) (CEND-532)
tensile properties of 600, on aging at 1000 and 2000°F in steam, 19: 39156(R) (CEND-532)
thermal response and microstructure of 625 and 718, at 1200 and 1400°F, 19: 39158 (GEAP-4751)
welding of 600 and Zircaloy-2 plates with flat and contoured surfaces, explosive, 19: 39156(R) (CEND-532)
INCONEL X
corrosion by aqueous chemical shim solutions at 600°F, 19: 40198(R) (WCAP-3721)
INDIA
uranium production and uses in, in 1964, 19: 39105
INDIAN POINT POWER REACTOR
operations and performance, (E), 19: 40267
INDIUM
content in solar atmosphere, (E), 19: 39345
energy gap in superconducting, dependence on transport current, (E), 19: 39735
neutron absorption properties of, burnup effects on, (E), 19: 40163
superconducting critical currents in films of, (E), 19: 39724
transition temperature of thin films of superconducting, effects of thin oxide layer on, (E), 19: 39746
use as threshold detectors for fast neutrons, (E), 19: 39007
INDIUM ALLOYS
Bi–In, heats of formation of InBi and In_2Bi, 19: 39168(R) (TID-22015)
Bi–In, tunneling and flux penetration in superimposed layers of zinc and, in magnetic fields, (E), 19: 39699
Cd–In–Ag, radiation effects on dimensions and mechanical properties of, 19: 40197(R) (WCAP-3718)
Cd–In–Ag, radiation effects on dimensions and mechanical properties of, 19: 40198(R) (WCAP-3721)
Cd–In–Ag, reactivity worths in uranium–Zircaloy-2, 19: 40196(R) (WCAP-3269-6)
Cd–In–Ag, reactivity worths of, 19: 40197(R) (WCAP-3718)
Cd–In–Ag–Sn, radiation effects on dimensions and mechanical properties of, 19: 40197(R) (WCAP-3718)
Cd–In–Ag–Sn, radiation effects on dimensions and mechanical properties of, 19: 40198(R) (WCAP-3721)
In–Pb, magnetic pulse transmission through superconducting plates of, (E), 19: 39733
In–Ru, crystal structure of intermetallic compound $RuIn_3$ in, 19: 39207
Sb–In, radiation effects on, electron, 19: 40286(R) (NAA-SR-11200)
Sb–In, spectral analysis of photoemission yields from cesiated surfaces of, 19: 39406
INDIUM ARSENIDES
photoelectron emission yields at 2 to 6 ev from cesiated surfaces of, spectral analysis of, 19: 39406
solvent properties for zinc, measurement by Hall coefficient, 19: 39269(R) (SU-SEL-64-133)
INDIUM ISOTOPES In-109
gamma transitions of three-particle isomeric state of, (E), 19: 39861
INDIUM ISOTOPES In-113
neutron reactions (n,γ), gamma spectra in 14.7-ev resonance of, 19: 39781 (JAERI-1073)
INDIUM ISOTOPES In-115
neutron reactions (n,γ), gamma spectra in 9.1-, 3.86-, and 1.46-ev resonance of, 19: 39781 (JAERI-1073)
INDIUM NITRIDES
InN–TiN, preparation and crystal structure of H-phase in, 19: 39208
InN–ZrN, preparation and crystal structure of H-phase in, 19: 39208
INDIUM PHOSPHIDES
electron tunneling in p-n junctions of, 19: 38931
INDOLE
derivatives of, ionization ratio of, 19: 39265(R) (IA-1021)
INDUCTORS
energy transfer from, circuit for, 19: 38960(P)
INDUSTRIAL HYGIENE
for tritium users, 19: 38355
ventilation in building containing radiation sources, 19: 38884

ventilation of rooms containing gamma sources, 19: 38883
INDUSTRIAL MANAGEMENT
teaching machines, generic classification of, 19: 40291 (SC-R-65-923)
INFECTIONS
radiation effects on immune reactions to tuberculosis, in guinea pigs, 19: 38375
radiation sickness effects on, in animals, 19: 38434(T)
INFLAMMATION
during radiotherapy, therapy using antibiotics and corticosteroids, 19: 38512
INFORMATION RETRIEVAL SYSTEMS
design of automated tumor registry, 19: 39270(R) (TID-21894)
development, 19: 39265(R) (IA-1021)
INFRARED IMAGE TUBES
design using thermoluminescence, 19: 39049(P)
INFRARED RADIATION
detection of, using thermoluminescence, 19: 39049(P)
effects on chromosomes in Tradescantia, synergism with x radiation on aberrant, 19: 38416
effects on mitotis in Tradescantia, synergism with x radiation, 19: 38416
modulation of, design of semiconductor devices for, (E/T), 19: 38914 (SC-DC-65-1332)
properties of cosmic black body radiation, (T), 19: 39350
INFRARED SPECTRA
reflection by polar crystals, analysis methods for, 19: 39270(R) (TID-21894)
INOR-8
properties as cladding material for SNAP hydride reactors, 19: 39166 (NAA-SR-Memo-11149)
INSECTS
radiation effects on *Callosobruchus maculatus*, gamma, 19: 39265(R) (IA-1021)
radiation effects on ovarian development in Dacus, gamma, 19: 38406
radiation effects on histolysis of pupal fat-bodies in Dacus, 19: 38406
radioinduced mutations in Dahlbominum oogonia, gamma and x-ray, 19: 38392
INSPECTION AND CONTROL
equipment for cylindrical bodies, 19: 38830(P)
INSTRUMENTATION
design of nuclear explosion, 19: 38919 (SC-R-65-904, pp 59-74)
development for reactor control, 19: 40122(R) (GEAP-4862)
development of, ESONE electrical and mechanical reference parameters for, 19: 38924
INSTRUMENTS
calibration and testing for deep-ocean measurements, 19: 40288(R) (NVO-98-5)
design of fast-closing light shutter, 19: 38942
development of superconducting, 19: 39690
INTERFEROMETERS
diagnostic use for plasma electron density measurements, (E), 19: 39979
performance of h-f laser, in plasma diagnostics, (E/T), 19: 39993
INTERMETALLIC COMPOUNDS
metallography of high-melting, 19: 39214
INTERNAL CONVERSION
coefficients for plutonium, rare earth, thorium, and uranium isotopes, (E/T), 19: 39786 (ORNL-P-1419)
INTESTINE
iodine-131 metabolism in mouse, effects of thiouracil diet on, 19: 38350
radiation effects on stenoses of, from therapy of gynecologic tumors, 19: 38522
IODIDES
radiolysis products of, effects of bromates and chlorates on, 19: 39265(R) (IA-1021)
IODINE
separation from waste water, methods for, 19: 40276
with cyclodextrin, Mössbauer effect in, 19: 39265(R) (IA-1021)
IODINE ISOTOPES I-125
diagnostic use for thyroid diseases, 19: 38496
thyroid metabolism of, autoradiographic study, 19: 38533
IODINE ISOTOPES I-127
gamma-gamma angular correlations in, resonance peaks in perturbed, (E), 19: 39854
neutron reactions (n,γ) at 0.025 ev and 24 kev, cross sections, (E), 19: 39816
reactions with gold at 20 to 80 Mev, orientation effects on energy losses in, 19: 39370 (ORNL-P-1336)
IODINE ISOTOPES I-129
Mössbauer effect in cyclodextrin complexes with, 19: 39265(R) (IA-1021)
IODINE ISOTOPES I-131
determination in milk, radiochemical, 19: 38560
diagnostic use for thyroid diseases, 19: 38496
distribution in man, computer simulation for, 19: 40282 (BNWL-SA-171)
metabolism by thyroid gland, effects of use of iodinated contrast media for diagnostic radiography on, 19: 38354
metabolism in mice, effects of thiouracil diet on, 19: 38350
metabolism in rats, effects of vitamin B on, 19: 38337
metabolism in thyroid gland, effects of triiodothyroacetic acid, 19: 38348
release from pyrolytic carbon-coated fuel particles, 19: 39228 (BMI-1734)
specific activity of, determination without carrier isotope, 19: 38609
therapeutic use for hyperthyroidism, 19: 38497
therapeutic use for heart failure, 19: 38497
thyroid metabolism of, autoradiographic study, 19: 38533
treatment of gastrointestinal tract disorders in patients with thyrotoxicosis, 19: 38529
uptake by rabbit thyroid, procedures for measuring, 19: 38341
uptake by rat liver, lungs, and thyroid from sodium solution, effects of colloid formation on, 19: 38351
use in albumin for photoscans of heart, 19: 38490
use in cerebral circulography in man, 19: 38489
use in radiodiagnosis, review on, 19: 38505
use in radiopyelography of calyx and renal pelvis excretion, 19: 38530
uses in Japan, 1950 to 1960, 19: 39060
IODINE ISOTOPES I-132
diagnostic use for thyroid diseases, 19: 38496
IODINE SYSTEMS
I–4,4'-methylenediantipyrine–Sc, complex formation in, 19: 38670
ION BEAMS
conference on science and technology of, 19: 39307
focusing of low-energy, lens system for, 19: 38937
interactions with electric fields, direct energy conversion using, 19: 39439
trajectories of, under electromagnetic- and self-field effects, 19: 39318 (UCRL-14194)
ION EXCHANGE
analytical use for determining strontium in bones, 19: 38345
ION EXCHANGE MATERIALS
performance in coolant circuits of water-cooled reactors, (E), 19: 40128 (ZFK-RN-17(p.75-94))
performance in filters for reactor water purification, 19: 38759 (ZFK-RN-17(p.95-117))
sorptive properties for hydrochloric acid, 19: 39265(R) (IA-1021)
sorptive properties for metal cations in fused salts, 19: 38771
ION EXCHANGERS
operation of filter, for EWA research reactor, 19: 38760 (ZFK-RN-17 (p.127-38))
ION PAIR PRODUCTION
energy dependence of, in low-energy reactions of electrons in gases, 19: 39375
ION SOURCES
performance of electron-bombardment, with various gases, 19: 38838
testing of, mass spectrometric, 19: 39265(R) (IA-1021)
IONIZATION
measurement along bubble-chamber tracks, using flying-spot devices, (E), 19: 38989 (CERN-65-11(p.219-27))
IONIZATION CHAMBERS
design and development for reactor control systems, 19: 40122(R) (GEAP-4862)
design of dielectric-filled, for dosimetry, 19: 39030
discharge mechanisms in bromine-quenched argon, 19: 39036
plate preparation with conducting areas for, 19: 39135
use of condenser, in gamma dose equivalent measurements, (E), 19: 39015
IONOSPHERE
auroral luminosity association with auroral x radiation and cosmic noise absorption, (E), 19: 39672
current system instabilities in, auroral echoes from, (T), 19: 39678
electron and ion density and temperature in, measurement of, 19: 39680
electron content and equivalent slab thickness of midlatitude, (E), 19: 39677
electron content during magnetic disturbances in winter, (E), 19: 39670
electron densities in, 19: 39269(R) (SU-SEL-64-133)
electron density in outer, (E), 19: 39674
frequency variations of F2 layer of, geomagnetic storm effects on critical, 19: 39669
geomagnetic storm effects on lower, at low-latitudes, 19: 39667
ionization layers in, formation of F1 and F2, 19: 39666
ionization of F2 region, effects of horizontal air motion on, (T), 19: 39668
radio wave transmission in, factors influencing, 19: 39682
satellites in, electromagnetic effects near, (T), 19: 39683
solar flare effects on F2 region of, 19: 39675
solar-wind effects on, (T), 19: 39676

sorptive properties for cosmic and solar radiation, 19: 39363
IONS
collector for, design of mass spectrometer, 19: 38962(P)
density and temperature in ionosphere, measurement of Explorer XVII, 19: 39680
density distribution in drift region of electron beams, (E/T), 19: 39283
density in barium plasma, determination of, 19: 39958 (MATT-327)
density profiles in thermionic diode ignited mode, 19: 39433 (LA-DC-6898)
diffusion coefficient and mobility measurement using radioisotopes, 19: 38665
effects of metallic, on iodine depletion in rat thyroxine, 19: 39265(R) (IA-1021)
emission in mercury ion reactions with aluminum and magnesium, (E), 19: 39374
fixation on monodispersed aerosols as function of intensity of, (T), 19: 39285
kinetic energy in dissociation of molecular, measurement using r-f mass spectrometer, (E/T), 19: 38927
motion in FFAG cyclotrons, (T), 19: 39316 (JINR-P-2199)
motion in plasma, wave dispersion of, 19: 39972(R) (SU-IPR-17)
reactions with monocrystalline metal surfaces at high energy, electron emission in, (T), 19: 39405
reactions with solids at low energies, electron emission in, 19: 38937
scattering by single crystals, energy distribution in, (E), 19: 39297
streaming in field-free space, equations for neutralized, 19: 39269(R) (SU-SEL-64-133)
IRIDIUM
catalytic properties in deuterium exchange reactions, 19: 38597
performance as emitter in thermionic converters, 19: 39431(R) (AD-608554)
radiation damage in, cross sections for atomic displacements from 1- to 3-Mev electrons, 19: 39225 (AFCRL-65-286)
IRIDIUM ALLOYS
Ce–Ir, phase studies, 19: 39163(R) (MLM-1244)
Ir–Mo, superconductivity of, order-disorder effects on, (E), 19: 39689
IRIDIUM ISOTOPES Ir-192
use in radiotherapy in place of radium, 19: 38521
IRON
determination in plutonium, spectrophotometric, 19: 38546(R) (RFP-552)
determination in stainless steel, electron microprobe, 19: 38536 (ACF-6)
diffusion of atoms in bcc, activation energy for interstitial, (T), 19: 40086
electron reactions with atomic, screening effects on bremsstrahlung and pair production in, (T), 19: 39389
gamma resonant absorption of iron-57 in, Mössbauer cross section for, 19: 39877
magnon dispersion relation of, (E), 19: 39213
neutron albedo measurement on, thermal, 19: 40065 (NP-15152)
neutron scattering in hydrogenated, magnetic, 19: 40075 (IEA-84)
radiation effects on magnetic properties of, electron, (E), 19: 39239
radiation effects on thermally activated flow stress in, fast-neutron, 19: 39242
radiation effects on metabolism of, in cross-circulated dogs, 19: 38382
radioinduced reduction of, in porphyrins of cooked meats, 19: 39065
reactions with plutonia at high temperatures, 19: 39125(R) (BNWL-91)
separation from graphite above 1750°C in inert gases, 19: 38762
sorption by gamma-alumina and inorganic ion exchange materials from fused salts, 19: 38771
thermal diffusivity of Armco ingot, 19: 39163(R) (MLM-1244)
tracer study of metabolism in man, 19: 38493
use as threshold detectors for fast neutrons, (E), 19: 39007
IRON ALLOYS
Al–Cr–Fe–Mo–Ti, mechanical properties and heat resistance, 19: 39193
Al–Cr–Fe–Mo–Ni–Nb–Ti, thermal response and microstructure of Inconel 718 at 1200 and 1400°F, 19: 39158 (GEAP-4751)
Ce–Fe–Pu, phase studies, 19: 39163(R) (MLM-1244)
Cr–Fe, diffusion of fission products in, mechanisms, 19: 39152(R) (BMI-X-10132)
Cr–Fe–Mo–Ni–Nb–W, tensile properties of IN-102, 19: 39156(R) (CEND-532)
Cr–Fe–Mo–Ni–Nb, thermal response and microstructure of Inconel 625 at 1200 and 1400°F, 19: 39158 (GEAP-4751)
Fe–Ni, martensite formation in, 19: 40283 (COO-1198-237)
Fe–Pu, density at 25 to 800°C, 19: 39161 (LA-DC-6956)
Fe–Pu, phase studies, 19: 39163(R) (MLM-1244)
IRON CHLORIDES
corrosive effects on Zircaloy-4 at 68°F, 19: 40196(R) (WCAP-3269-6)
Mössbauer effect in ice, temperature dependence of, (E), 19: 39715
$FeCl_3$–$FeSO_4$, Mössbauer effect in frozen aqueous, 19: 39265(R) (IA-1021)
IRON COMPOUNDS
Mössbauer parameters for organic, 19: 38576 (CONF-650425-2)
IRON IONS
incorporation into potassium chloride crystals grown from solution, 19: 38696 (MIT-2909-4)
radiolysis of aqueous solutions of, pulse, 19: 38728
IRON ISOTOPES Fe-56
alpha reactions ($\alpha,\alpha'\gamma$) at 22.2 Mev, (E), 19: 39865
helium-3 inelastic scattering by, DWBA analysis of, (T), 19: 39885
IRON ISOTOPES Fe-57
displacement in polycrystalline zinc lattice, Mössbauer-effect measurements of, 19: 40097
gamma resonant absorption in iron, Mössbauer cross section for, 19: 39877
magnetic field in copper–manganese alloys, hyperfine, (E), 19: 39212
magnetic moment of, electron-nuclear double resonance for nuclear, (E), 19: 39878
Mössbauer effect in barium titanates at 300 to 1200°K, 19: 38651
neutron separation energy for, (E), 19: 39862
IRON ISOTOPES Fe-58
helium-3 inelastic scattering by, DWBA analysis of, (T), 19: 39885
IRON ISOTOPES Fe-59
incorporation in potassium ferrocyanide, 19: 38743 (NP-15262)
use in radiodiagnosis, review on, 19: 38505
IRON SALTS
dithiocarbamates, relaxation effects in, (E), 19: 38653
Mössbauer effect in ice, temperature dependence of, (E), 19: 39715
IRON SULFATES
Mössbauer effect in ice, temperature dependence of, (E), 19: 39715
IRON(II) SULFATES
performance of mailed dosimeters of, for high energy electron beams, 19: 38723
$FeCl_3$–$FeSO_4$, Mössbauer effect in frozen aqueous, 19: 39265(R) (IA-1021)
IRON SYSTEMS
Al–Fe–Mg–Ni–Si–Ti–Zr, coating with aluminum–nickel layers by chemical deposition, 19: 39143(P)
C–Cr–Fe–Mo–Ni, reinforcement of graphite by, 19: 39114(P)
C–Fe, martensite formation in, 19: 40283 (COO-1198-237)
C–Fe–Ni, martensite formation in, 19: 40283 (COO-1198-237)
Fe–Ni–WC, internal friction of, effects on composition on, 19: 39170(P) (FTD-TT-64-1001)
Fe–WC, internal friction of, effects of composition on, 19: 39170(T) (FTD-TT-64-1001)
IRRADIATION FACILITIES
conveyor system for package, 19: 38797(P)
design for electron radiation of materials, 19: 38954(P)
design for use with accelerator, 19: 38831(P)
design of cesium-137, for cell suspensions and small animals, 19: 38415
IRRADIATION TECHNIQUES
for alloys to increase the degree of order, 19: 39257(P)
ISOTOPE EFFECTS
of deuterium on bromination of acetoacetates, acetylacetones, and malonates, 19: 38692
of deuterium on radiolysis of binary paraffin-olefin solutions, 19: 38707
on ionization efficiencies of light and heavy molecules, 19: 38632
on thermodynamic properties of liquid hydrogen, 19: 38639
ISOTOPES
concentration in polynary mixtures by thermal diffusion in Clusius-Dickel columns, (E/T), 19: 39076
determination of stable, methods for, 19: 38559
distribution and recovery in Gnome project, 19: 38787 (PNE-102F)
separation by gas-liquid chemical exchange, 19: 39075
separation of, equipment at Rome University for electromagnetic, 19: 39077
ISOTOPIC EXCHANGE
of deuterium between hydridoplatinum complex and heavy water, 19: 38627
of deuterium between deuterated toluene and water, 19: 38693
radiation effects on deuterium–hydrogen, on silica gel surfaces, 19: 38626
ITALY
nuclear energy development in, 19: 40200

J

JAPAN
calcium and potassium content in diet in, 19: 38894
cesium-137 body burdens in, whole-blood method for determining, 19: 38349
fallout content in diet and excreta in, 19: 38894
nuclear industry development in, 19: 39064

radioisotope uses in, 1950 to 1960, 19: 39060
JAPANESE POWER DEMONSTRATION REACTOR
kinetics models for core of, development and testing of, (E/T), 19: 40186 (JAERI-1076)
JAWS
radionecrosis of, histology and radiology of, 19: 38527
JET ENGINE FUELS
analysis for microorganisms, tracer method for, 19: 39061 (ADR-09-08a-63.1)

K

KEROSENE
kerosene–TBP, solvent distribution of hydrochloric acid in, 19: 38563
KIDNEYS
gold-198 excretion by rat, morphology of, 19: 38342
radiation effects on homografts of dog, by local graft exposure, 19: 38425
radiation effects on rabbit, renograms of, 19: 38379
radiation effects on function of, in mice, 19: 38409
radiation sickness effects on, pathology of, 19: 38433(T)
radiodiagnosis of human, relation between excretory urography and radioisotope renography, 19: 38520
radiodiagnosis of excretion in, by radiopyelography using iodine-131, 19: 38530
uranium content in, after inhalation of ore particles, in rats, 19: 38333 (BNWL-SA-226)
KRYPTON
diffusion of gases of, in temperature gradients, (E), 19: 39291
electron elastic scattering by, momentum-transfer cross sections for slow, (T), 19: 39397
ionization cross section for, electron-impact, 19: 38630
ionization in electron-bombardment ion sources, 19: 38838
rubidium-vapor spin relaxation in, (E), 19: 39400
sorption by tungsten, energy of interatomic, 19: 39265(R) (IA-1021)
KRYPTON IONS
reactions with metal single crystals at 1 to 10 kev, secondary-electron emission in, (E), 19: 39404
KRYPTON ISOTOPES Kr-82
energy levels in, spin of 2426-kev, (E), 19: 39944
KRYPTON ISOTOPES Kr-85
use in determining cerebral blood flow, 19: 38491
yields in thermal-neutron fission of plutonium-239 and uranium-235, (E), 19: 39800

L

LABORATORIES
design and operation of NASA Space Radiation Effects Laboratory, 19: 39059
design of, and equipment for, for therapeutic use of radon baths, 19: 38498
LABORATORY EQUIPMENT
design for measuring radioactivity of samples, 19: 38799(P)
LAMINATES
fabrication and strength of tungsten-fiber-reinforced nickel composites, 19: 39093 (BNWL-SA-141)
radiation effects on glass-reinforced diallyl phthalate, 19: 39232 (FZK-227)
LANGUAGE
research programs at MIT on, 19: 39270(R) (TID-21894)
LANTHANUM
effects on superconducting transition temperature of vanadium silicide, 19: 39196
phase transformations at 6 to 65 kbar, solid-liquid and solid-solid, 19: 40095
properties of, position in periodic table from, 19: 39373
separation from waste water, methods for, 19: 40276
superconductivity of films of, (E), 19: 39745
LANTHANUM ALLOYS
Ge–La, preparation, properties, and structure of intermetallic compounds $LaGe_2$, LaGe, and La_5Ge_3, 19: 39195
LANTHANUM BORATES
preparation and chemical properties, 19: 38611
LANTHANUM BORIDES
evaporation of, mass spectrometric study of, 19: 38673
LANTHANUM COMPLEXES
with [(2-hydroxyethyl)imino]diacetic acid, dissociation constant of, 19: 38671
with *N,N'*-dimethyl-*N,N'*-dinitrosoterephthalamide, mechanism of formation of, 19: 38600
LANTHANUM IONS
radiolysis of aqueous solutions of, pulse, 19: 38728
LANTHANUM OXIDES
reactions with silicon to prepare lanthanum silicides, 19: 38613
GeO_2–La_2O_3, preparation, phase studies, and properties, 19: 38612
LANTHANUM SELENIDES
preparation, semiconducting properties, and structure of, 19: 38614
LANTHANUM SILICIDES
crystal structure and phase studies, 19: 38613
LANTHANUM SULFIDES
properties of, dissociation energy, thermodynamic, and vaporization of, 19: 38644
LANTHANUM SYSTEMS
Ga–La–Se, chemical properties, 19: 38598
LARYNX
radiation effects on, from radium therapy of carcinoma of vocal cord, 19: 38519
radiotherapy of cancer of, effects on thyroid function, 19: 38484
LATINA POWER REACTOR
operation, 19: 40181(R) (EUR-2429.i)
LAURIC ACID
methyl ester, radiation chemistry of, 19: 38721
LEAD
electron reactions at 100 to 1000 Mev, electron-photon cascades in, (T), 19: 40070
electron reactions with atomic, screening effects on bremsstrahlung and pair production in, (T), 19: 39389
gamma reactions with, method for measuring photoelectric cross sections for K-shell in, 19: 39376
heat of solution in liquid bismuth in presence of tellurium, 19: 39168(R) (TID-22015)
neutron albedo measurement on, thermal, 19: 40065 (NP-15152)
photon interactions in, meson (π^0) production in, (E), 19: 39620
positron annihilation at 300 kev in, radiationless, (E), 19: 39526
positron annihilation in, 3-quantum, (E/T), 19: 39546
proton reactions (p,xn) at 1 Bev, heat production and neutron yields from, 19: 39756 (AECL-2177, Paper 3)
sorption by gamma-alumina and inorganic ion exchange materials from fused salts, 19: 38771
superconducting transition region of determination by phase transition of superfluid helium II, (E), 19: 39691
superconducting transition width in, 19: 39748
thermal conductivity of pure superconducting, (T), 19: 39732
transition temperature of thin films of superconducting, effects of thin oxide layer on, (E), 19: 39746
LEAD ALLOYS
Bi–Pb, cavitation effects on materials at 500 and 1500°F, ultrasonic-induced, 19: 39116 (NP-15263)
Bi–Pb, proton reactions (p,xn) at 1 Bev, heat production and neutron yields from, 19: 39756 (AECL-2177, Paper 3))
Cu–Pb, superconductivity of heterogeneous, particle size effects on, (E), 19: 39747
In–Pb, magnetic pulse transmission through superconducting plates of, (E), 19: 39733
Pb–Tl, electron tunneling in, at cryogenic temperatures, (E/T), 19: 40286(R) (NAA-SR-11200)
Pb–Tl, magnetic fields of superconducting, (E), 19: 40286(R) (NAA-SR-11200)
Pb–Tl, magnetic-field effects on tunneling from superconducting, (E), 19: 39718
LEAD CHLORIDES
$PbCl_2$–UCl_4, phase studies, 19: 39265(R) (IA-1021)
LEAD IONS
incorporation into potassium chloride crystals grown from solution, 19: 38696 (MIT-2909-4)
radiolysis of aqueous solutions of, pulse, 19: 38728
LEAD ISOTOPES Pb-200
nuclear gyromagnetic ratio of first 4+ state of, 19: 39810
LEAD ISOTOPES Pb-202
nuclear gyromagnetic ratio of first 4+ state of, 19: 39810
LEAD ISOTOPES Pb-204
nuclear gyromagnetic ratio of first 4+ state of, 19: 39810
LEAD ISOTOPES Pb-206
neutron reactions (n,γ), radiative transitions in, 19: 39783 (ORNL-P-1345)
neutron total cross sections of, resonances in, (E/T), 19: 39847
nuclear gyromagnetic ratio of first 4+ state of, 19: 39810
LEAD ISOTOPES Pb-207
electron elastic scattering by, dispersive effects in, (E), 19: 39860
energy levels of, from lead-206 (n,γ) reactions, 19: 39783 (ORNL-P-1345)
energy levels of, magnetic moments of single-particle, (T), 19: 39870

neutron reactions (n,γ), radiative transitions in, 19: 39783 (ORNL-P-1345)
neutron total cross sections of, resonances in, (E/T), 19: 39847
LEAD ISOTOPES Pb-208
electron elastic scattering by, dispersive effects in, (E), 19: 39860
energy levels in, from neutron reactions with lead-207, (E/T), 19: 39847
energy levels of, from lead-207 (n,γ) reactions, 19: 39783 (ORNL-P-1345)
magnetic moment of 3.2 Mev S-state in, (E/T), 19: 39843
neutron scattering at 0.5 to 4 Mev, phase shifts analyses for, (E), 19: 39785 (ORNL-P-1356)
neutron total cross sections of, resonances in, (E/T), 19: 39847
triton reactions (t,α) at 12.0 and 13.5 Mev, thallium-207 energy levels from, (E), 19: 39852
LEAD ISOTOPES Pb-209
energy levels in, from neutron reactions with lead-208, (E/T), 19: 39847
LEAD TELLURIDES
heat of formation of, 19: 39168(R) (TID-22015)
LECTURES
book: *Symmetries in Elementary Particle Physics*, 19: 39602
on reactor system design for nuclear propulsion, 19: 40247 (N64-29788)
on shield physics for nuclear propulsion, 19: 40246 (N64-29787)
LEPTONS
coupling between two fields of, model for length scale, 19: 39652
interactions in SU(3), moderately strong, 19: 39566
interactions of, unification of weak, 19: 39573
mass formulas and quantum numbers for, (T), 19: 39562
pair production by neutrinos in nuclear fields, (T), 19: 39943
pair production in vector meson decay, angular distributions for, (T), 19: 39451 (CALT-68-43)
LEUKEMIA
epidemiology of, in children in Great Britain, 19: 38326
radioinduced in mice, 19: 38372
susceptibility of man as function of age to, epidemiology of, 19: 38364
LEVEL INDICATORS
development of radiometric, in Hungary, 19: 39063
LIGHT
modulation of microwave, methods for, 19: 39269(R) (SU-SEL-64-133)
propagation through anisotropic media, electromagnetic wave emission from, (T), 19: 39266 (JINR-P-2195)
reactions with semiconductors at 2 to 6 ev, spectral analysis of electron-emission yields in, 19: 39406
scattering by plasma, resonances in, (T), 19: 40029
scattering by plasma, second harmonic, (T), 19: 40050
scattering from plasma, stimulated incoherent, (T), 19: 40012
scattering in anharmonic crystals, second sound detection by, (T), 19: 40092
LIGHT SOURCES
design for absorption spectroscopy in plasma, 19: 38939
design using radioisotopes and luminescent materials, 19: 38951(P)
LIGHT SPECTRA
measurement of theta-pinch plasma, light shutter for, 19: 38942
LINEAR ACCELERATORS
beam energies of, apparatus for continuously determining, 19: 39330(P)
design and performance of Japanese 25-Mev, 19: 39326
operation of Orsay, 19: 39327
storage rings for electron, 19: 39622
LINOLEIC ACID
effects of ultraviolet-irradiated, on skin of mice, 19: 38366
LIPIDS
radiation effects on, in rabbit liver, 19: 38429
radiosterilization effects on meat, analytical methods for determining, 19: 39068
LIQUID FLOW
boiling burnout in water, comparisons of analyses of, (T), 19: 38814
magnetohydrodynamic, forced oscillations of heavy, viscous electro-conductive, (E), 19: 39281
magnetohydrodynamic, with ignorable coordinate, (T), 19: 39301
through packed beds, axial dispersion in, 19: 38812 (UCRL-11951)
LIQUID METAL COOLED REACTORS
cooling systems for sodium-cooled, flow controllers for, (E), 19: 40135
design and economics of sodium cooled fast breeder reactor for desalination, 19: 40190 (ORNL-TM-784)
design of fast split-blanket, 19: 40286(R) (NAA-SR-11200)
design of 1000-Mw(e) sodium-cooled fast, (T), 19: 40175(R) (ACNP-63592)
development, 19: 40111(R) (ANL-7046)
heat transfer in sodium, 19: 40286(R) (NAA-SR-11200)
reactivity sodium void coefficients for, 19: 40158 (UNC-5123)
tube joints in calandria cores of large sodium–graphite, equipment for cutting and rewelding bottom of process, 19: 40125 (NAA-SR-9821)
LIQUIDS
neutron thermalization in, Van Hove theory for relaxation times in, 19: 39773
thermodynamic properties of ionic, 19: 38683
ultrasonic waves in, properties of finite-amplitude, 19: 39268 (ORNL-P-1395)
LITHIUM
chemical states of carbon, nitrogen, and oxygen in, 19: 39157 (CNLM-6337)
content and distribution in subterranean Bulgarian salt water, 19: 38851
content in lower main sequence stars, depletion of, (T), 19: 39336
content in sun, (E), 19: 39346
corrosive effects on molybdenum and tantalum, effects of nitrogen on, 19: 40112(R) (ANL-7046(p.36-66))
electron inelastic scattering by crystals of, interband excitation in fast, (T), 19: 40083
electron reactions with atomic, screening effects on bremsstrahlung and pair production in, (T), 19: 39389
electron scattering by atomic, exchange effects in, (T), 19: 39365 (COO-720-047)
ion interactions in metallic, long-range, (T), 19: 39211
neutron absorption properties of, burnup effects on, (E), 19: 40163
LITHIUM ALLOYS
Li–Hg, use in removing europium from aqueous electrolytes by extraction and electrolysis, 19: 38753 (LA-DC-7013)
LITHIUM BROMIDES
reduction by high-frequency hydrogen discharge to hydrogen halide and metal, 19: 39180
reduction by high-frequency discharges in helium, hydrogen, and nitrogen, role of electrons in, 19: 39181
LITHIUM CHLORIDES
reduction by high-frequency hydrogen discharge to hydrogen halide and metal, 19: 39180
reduction by high-frequency discharges in helium, hydrogen, and nitrogen, role of electrons in, 19: 39181
LiCl–KCl, chlorination of uranium tetrachloride in fused eutectics of, kinetics, 19: 38587 (UCRL-11986)
LITHIUM COOLED REACTOR EXPERIMENT
cooling system of, design of pumps for primary, (E), 19: 40135
LITHIUM FLUORIDES
heat of sublimation at 1000°K, 19: 38679
performance of mailed dosimeters of, for high energy electron beams, 19: 38723
radiation effects on annealing and deformation behavior of, gamma, 19: 39243
reduction by high-frequency hydrogen discharge to hydrogen halide and metal, 19: 39180
reduction by high-frequency discharges in helium, hydrogen, and nitrogen, role of electrons in, 19: 39181
BeF_2–LiF, chemistry and thermodynamics of molten, as MSRE solvent, 19: 38582 (ORNL-P-1428)
BeF_2–LiF, thermodynamic properties of, mass spectrometric studies of, 19: 38679
LiF–ZrF, phase studies, 19: 38610
LITHIUM IODIDES
reduction by high-frequency discharges in helium, hydrogen, and nitrogen, role of electrons in, 19: 39181
reduction by high-frequency hydrogen discharge to hydrogen halide and metal, 19: 39180
LITHIUM ISOTOPES Li-6
deuteron inelastic scattering at 6.35 Mev, excitation limit of 3.56-Mev level in, (E), 19: 39804
helium-3 reactions (He-3,pαα), reacattering effects in, (T), 19: 39897
helium-3 reactions (He-3,pαα) at 2.7 Mev, energy spectra of, (E/T), 19: 39900
lithium-6 reactions (Li-6,3α) with, angular correlations in, (E), 19: 39920
meson (K⁻), reactions with, hyperfragments from, (E/T), 19: 39265(R) (IA-1021)
performance in fast neutron spectrometers for determination of GLEEP neutron spectra, 19: 40256 (AERE-M-1590)
proton reactions (p,pd) with, analysis of quasifree scattering in, (T), 19: 39906
proton reactions (p,pd) at 30.5 and 155 Mev, analysis of angular correlations in, (T), 19: 39907
reactions (Li-6,α) with carbon-12 at 4.0 to 5.5 Mev, cross sections for, (E), 19: 39853
reactions (Li-6,3α) with lithium-6, angular correlations in, (E), 19: 39920
reactions with boron-10 and boron-11, total cross sections for, (E), 19: 39887
LITHIUM ISOTOPES Li-7
deuteron reactions (d,n)2α at low energy, mechanisms of, (T), 19: 39921

deuteron reactions (d,n) 2α, at 1.8 to 7.0 Mev, sequential emission in, (E), 19: 39915
neutron reactions (n,n) and (n,γ) with, cross sections for, (T), 19: 39820
reactions with boron-10 and boron-11, total cross sections for, (E), 19: 39887
LITHIUM NITRATES
$LiNO_3$–KNO_3, properties for metal cation ion exchange from fused, 19: 38771
LITHIUM TUNGSTATES
thorium-dioxide monocrystal growth in solvent of, 19: 38628
LIVER
iodine-131 metabolism in mouse, effects of thiouracil diet on, 19: 38350
iodine-131 uptake by rat, effects of colloid formation in iodine solution on, 19: 38351
radiation effects on mitochondria function and structure in mouse, 19: 38424
radiation effects on serum proteins in mouse, following rat chimera transplant, 19: 38404
radiation effects on morphology of rat, fast neutron, 19: 38444
radiation injuries of enzyme systems in rat, protective effects of glycine, 19: 38467
radiation sickness effects on, pathology of, 19: 38433(T)
radioinduced hemolysins in rabbit, 19: 38429
thorium-230 content in, after inhalation of uranium ore, in rats, 19: 38333 (BNWL-SA-226)
LOOPS
boiling heat transfer in, effects of flow disturbances on, 19: 38806(R) (GEAP-4908)
development for TREAT, 19: 39090(R) (ANL-7046(p.78-82))
development of niobium–zirconium, for liquid metals, 19: 40112(R) (ANL-7046(p.36-66))
fabrication for high-temperature sodium, 19: 40113(R) (ANL-7071)
fabrication of TREAT, 19: 40113(R) (ANL-7071)
heat transfer from two-phase sodium, 19: 40286(R) (NAA-SR-11200)
LUMINESCENCE
measurement of radioinduced, in phosphors, 19: 38936
LUMINESCENT MATERIALS
use with radioactive isotope as light source in light projector, 19: 38951(P)
LUNGS
iodine-131 uptake by rat, effects of colloid formation in iodine solution on, 19: 38351
radiation effects on morphology of rat, fast neutron, 19: 38444
LUTETIUM
neutron absorption properties of, burnup effects on, (E), 19: 40163
neutron reactions at 0.0005 to 1 ev, total cross sections for, 19: 39779 (IEA-86)
phase transformations at 6 to 65 kbar, solid-liquid and solid-solid, 19: 40095
LUTETIUM COMPLEXES
with [(2-hydroxyethyl)imino]diacetic acid, dissociation constant of, 19: 38671
LUTETIUM HYDROXIDES
reactions with formic acid, properties of formate formed by, 19: 38669
LUTETIUM ISOTOPES Lu-176
production of isomeric, in proton reactions with tantalum at 660 Mev, (E), 19: 39931
LUTETIUM NIOBATES
preparation and thermal properties, 19: 38617
LYMPH SYSTEM
radiation effects on morphology of rat, fast neutron, 19: 38444
LYSINES
uptake by DNA, proteins, and RNA of L-cell nuclei, effects of tritiated thymidine on carbon-14-labeled-, 19: 38339

M

MACHINE TOOLS
design for remote cutting of process tube joints in sodium–graphite reactors, 19: 40125 (NAA-SR-9821)
lathe part programming, graphical computer system for, 19: 40293 (SCL-DC-65-86)
MACHINING
method for micro-, by sputtering through mask of contamination, 19: 39136
MAGNESIUM
determination in trace amounts in aluminum by x-ray spectrography, 19: 38571
mercury ion reactions with ion emission in, (E), 19: 39374
proton inelastic scattering at 15 to 1900 kev, x-ray yields from, (E), 19: 39881
reduction of uranium tetrafluoride, design of bell furnace for, 19: 39113(R)
separation from graphite above 1750°C in inert gases, 19: 38762
use as threshold detector for fast neutrons, (E), 19: 39007
MAGNESIUM ALLOYS
properties for use as fuel cladding material in reactors, 19: 39206
Al–Mg, dislocation climb in quenched, kinetics of, 19: 39169 (UCRL-16090)
Al–Mg, radiation effects on, annealing electron, 19: 40286(R) (NAA-SR-11200)
Al–Mg, use in preparation of uranous chloride by reduction of uranyl chloride, 19: 38662
Al–Mg–Mn–Zn, plastic anisotropy of AZ31B sheet, 19: 39149 (AD-425880)
Ca–Mg, properties of intermetallic compounds in, 19: 39177
Eu–Mg, properties of intermetallic compounds in, 19: 39177
Mg–Ag, annealing of deformed AgMg, 19: 39168(R) (TID-22015)
Mg–Ag, heats of formation of silver-rich solid solutions, 19: 39168(R) (TID-22015)
Mg–misch metal–Zn, plastic anisotropy of ZE10A sheet, 19: 39149 (AD-425880)
Mg–Sr, properties of intermetallic compounds in, 19: 39177
Mg–Th–Zr, plastic anisotropy of HK31A sheet, 19: 39149 (AD-425880)
MAGNESIUM CHLORIDES
reduction by high-frequency hydrogen discharge to dihalide and metal, 19: 39180
$MgCl_2$–KCl, free energy of formation of $KMgCl_3$ at 450°C, 19: 38575 (BNL-9343)
MAGNESIUM ISOTOPES
preparation of accelerator targets of, 19: 38658
MAGNESIUM ISOTOPES Mg-25
neutron separation energy for, (E), 19: 39862
MAGNESIUM ISOTOPES Mg-26
neutron separation energy for, (E), 19: 39862
MAGNESIUM ISOTOPES Mg-27
neutron separation energy for, (E), 19: 39862
MAGNESIUM OXIDES
fission-fragment damage in, (E), 19: 39245
properties for use as fuel-propellant partition in gaseous fuel rocket reactors, 19: 40229 (LA-3229, pp 116-36)
radioinduced trapped hole center containing fluorine in crystalline, 19: 38729
MAGNESIUM SYSTEMS
Al–Fe–Mg–Ni–Si–Ti–Zr, coating with aluminum–nickel layers by chemical deposition, 19: 39143(P)
MAGNET COILS
design for production of strong pulsed fields, 19: 38935
field distribution along axis of superconducting, (E), 19: 38933
MAGNETIC FIELDS
book: *Analysis and Computation of Electric and Magnetic Field Problems*, 19: 39311
calculation for uniform-field bending magnets, 19: 39317 (NRL-6248)
distribution along axis of superconducting coils, (E), 19: 38933
effects of crossed electric and, on electrons, 19: 39270(R) (TID-21894)
effects on diffusion in r-f discharges, (E/T), 19: 39269(R) (SU-SEL-64-133)
effects on nuclear spin-lattice relaxation, (T), 19: 39880
flux penetration in superconductors, (T), 19: 39712
intensity reduction in expandable superconducting enclosure, 19: 39742
interactions with plasma bunches, research on, 19: 39955 (IAE-663)
measurement of, using gamma resonant absorption, 19: 38966(P)
penetration depth in superconducting niobium, (E/T), 19: 39726
plasma compressional heating by, effect of frequency on, (T), 19: 39991
plasma containment in multipole, (E), 19: 39954(R) (COO-1233-20)
plasma diffusion in, stability criteria for, 19: 39968 (ORNL-P-1338)
plasma flow around dipole, (E), 19: 40009
plasma motion in asymmetry, theta-pinch, (E), 19: 40010
plasma universal instability in complex, (T), 19: 40018
production of megagauss, by explosive flux compression, 19: 39300
production of pulsed strong, flux concentrator for, 19: 38934
structure of axisymmetric force-free, in dissipative plasma, (T), 19: 40049
structure of interplanetary, 19: 39364
MAGNETIC MATERIALS
properties for electromagnetic pumps, 19: 38781(R) (N64-25903)
properties of metals, survey, (T), 19: 40074 (CONF-796(Paper 3))
properties of square-loop, 19: 39269(R) (SU-SEL-64-133)
MAGNETIC MIRROR MACHINES
plasma diffusion in Q-1 device, Bohm, (T), 19: 40014
MAGNETIC MIRRORS
plasma containment by, cooperative effects in tenuous energetic, (E),

19: 40017
plasma containment by, high-temperature, 19: 40045
plasma containment in, 19: 40046
MAGNETIC PROBES
diagnostic use for plasma, 19: 40059
MAGNETIC PROPERTIES
of metals, survey, (T), 19: 40074 (CONF-796(Paper 3))
MAGNETIC SEPARATORS
design of momentum analyzing slit device for particle beams, 19: 38967(P)
MAGNETOHYDRODYNAMIC CELLS
analysis of laminar-flow induction, 19: 39270(R) (TID-21894)
design for producing a-c power, 19: 39449(P)
design of a-c, with rotating magnetic field, 19: 39447(P)
electron temperature increases in plasma of, (T), 19: 39437
performance for linear induction, (T), 19: 39432 (JUL-256-TP)
performance for space vehicles, 19: 39442
performance in rocket reactors for fuel-propellant energy exchange, 19: 40238 (LA-3229, pp 286-312)
plasma flow in, kinetic equations for non-equilibrium, (E/T), 19: 39440
plasma ionization in, nonequilibrium, (T), 19: 39438
use in MHD transformers, 19: 39448(P)
MAGNETOHYDRODYNAMICS
book: *Engineering Magnetohydrodynamics*, 19: 39306
conductivity and Hall effects on flow stability, 19: 39270(R) (TID-21894)
flow of conducting gas in crossed fields, laminar boundary layer of, (T), 19: 40044
fluid flow in, boundary-layer compatibility conditions for, (T), 19: 39277
fluid flow in, inertial-range spectra of turbulent, (T), 19: 39292
fluid flow in, thermal boundary-layer equations in, (T), 19: 39276
fluid flow with heat addition in, quasi-one-dimensional, (T), 19: 39302
fluid flow with ignorable coordinate, steady incompressible viscous, (T), 19: 39301
fluid flows in, closed-form analytic solutions for laminar channel entrance, (T), 19: 39278
friction factor measurements for liquid-metal channel flows, 19: 39270(R) (TID-21894)
liquid flow in, forced oscillations of heavy, viscous electroconductive, (E), 19: 39281
shock wave propagation in conducting media, ionizing, 19: 39267 (NP-15157)
theory of relativistic, 19: 39279
MAGNETOSPHERE
stability of boundary of, (T), 19: 40000
MAGNETS
design and testing of superconducting, 19: 39741
design for cesium ion rocket motors, 19: 38834(R) (N64-29495)
field calculations for accelerator beam bending, 19: 39317 (NRL-6248)
use in positioning reactor control rods, 19: 40140(P)
MAGNOX ALLOYS
deformation of, as fuel element cladding, 19: 39220
MALONIC ACID, ESTERS
bromination of, deuterium isotope effects on, 19: 38692
MAMMALS
genetic code for hemoglobin synthesis in, 19: 40296 (TID-21856)
radiation effects on cell nuclei in bone marrow, synergistic effects of vibration, 19: 38358 (AD-612660)
strontium-90 metabolism in, effects of calcium, phosphates, and stable strontium on, 19: 38335 (NP-14926)
MAMMARY GLAND
radiation dose effects on tumor growth in F_1 hybrid mouse, 19: 38403
MAN
analysis for americium-241 and plutonium-239 in, using whole-body counter, 19: 38546(R) (RFP-552)
cesium-131 metabolism in, 19: 38502
cesium-131 metabolism in, 19: 38503
cesium-137 content in blood of, method for determining, 19: 38349
fallout content in diet and excreta of Japanese, 19: 38894
gamma dose to, from fallout, 19: 38891
genetic studies of, 19: 38328
metabolism of tritium in, 19: 38355
radiation dose from fallout, 1954 to 1963, 19: 38861
radiation effects on, effects of pyridoxal-5'-phosphate on, 19: 38461
radiation protection on space stations, shielding requirements for, 19: 40063 (NP-15125)
radiation sickness in, development, symptoms, and treatment of, 19: 38471(T)
radioactivity in, whole-body counting of, 19: 38890
radiodiagnosis of, relation between excretory urography and radioisotope renography, 19: 38520
radioisotope distribution in, computer simulation of, 19: 40282 (BNWL-SA-171)
radiotherapy of carcinoma of vocal cord in, effects on larynx from radium, 19: 38519
susceptibility to cancer as function of age, epidemiology of, 19: 38364
tolerance to hyperbaric oxygen of, 19: 38500
MANGANATE IONS
radiolysis of aqueous solutions of, pulse, 19: 38728
MANGANESE
determination in enamel of teeth, neutron activation, 19: 38562
effects on expansion of cerium–cobalt–plutonium alloys on freezing, 19: 39161 (LA-DC-6956)
effects on superconducting transition temperature of vanadium silicide, 19: 39196
energy levels of mesic (μ) atoms of, quadrupolar effects on, (T), 19: 39368 (NP-15089)
MANGANESE ALLOYS
Al–Mg–Mn–Zn, plastic anisotropy of AZ31B sheet, 19: 39149 (AD-425880)
Cr–Mn, antiferromagnetism of, at 95 to 300°K, 19: 40077 (IS-T-18)
Cr–Mn, electric conductivity and thermoelectric power of, at 4.2 to 450°K, 19: 40077 (IS-T-18)
Cu–Mn, iron-57 hyperfine magnetic field in, (E), 19: 39212
MANGANESE IONS
radiolysis of aqueous solutions of, pulse, 19: 38728
MANGANESE ISOTOPES Mn-50
beta decay of, conserved vector current hypothesis and ft values for, (E/T), 19: 39859
MANGANESE ISOTOPES Mn-54
content in animals of California coast, 19: 38895
decay of, gamma transitions in, (E), 19: 39866
MARITIME PRESSURIZED WATER REACTOR
core structures for, characteristics of Zircaloy, (E), 19: 40218
noise analysis in, (E), 19: 40164
MARITIME REACTORS
design of boiling water, with steam jet propulsion system, 19: 40255(P)
development of PWR, 19: 40251
steam generator development and testing for NERO, 19: 40250
MARTENSITES
structure in, fine, 19: 40283 (COO-1198-237)
MASERS (OPTICAL)
beam interactions from, detection of photon-photon, (E), 19: 39264 (CONF-796(Paper 14))
diagnostic use for plasma electron densities, (E), 19: 39978
diagnostic use for plasma electron density measurements, (E), 19: 39979
diagnostic use for plasma, 19: 40059
frequency mixing in, photoelectric, 19: 39269(R) (SU-SEL-64-133)
light from, production of sideband, 19: 39269(R) (SU-SEL-64-133)
light scattering from, Brillouin, 19: 39273(R) (UCRL-12204, pp 60-5)
operation of xenon, 5d-6p transitions from pulsed, (E), 19: 39394
performance of, h-f, as interferometer in plasma diagnostics, (E/T), 19: 39993
spectra of rare earth-doped zinc sulfide, emission, 19: 39269(R) (SU-SEL-64-133)
use studies on, 19: 39269(R) (SU-SEL-64-133)
MASS SPECTROGRAPHY
method for determining boron isotopes in boron trifluoride, 19: 38541 (K-L-6057)
uses in nuclear science, 19: 38925
MASS SPECTROMETERS
data display system for fast-scanning, 19: 39022
data recording system for, design of digital, 19: 39023
description, 19: 38925
design producing fluctuating component in ion stream, 19: 38958(P)
electrostatic analysis design for, 19: 38963(P)
ion charge distribution in, measurement using Mylar films, (E), 19: 38940
ion collector design with a secondary particle collecting electrode for, 19: 38962(P)
performance of r-f, (E), 19: 38926
use of double focusing, for gas determinations, 19: 38546(R) (RFP-552)
use of r-f, in measurement of fragment-ion kinetic energies, (E/T), 19: 38927
MASS TRANSFER
processes of, in solids subjected to temperature gradient, 19: 38678
MATERIALS TESTING
book: *Nuclear Technology in Construction*, 19: 38828
nondestructive evaluation of metal fatigue, 19: 39151 (AFOSR-65-0981)
nondestructive methods for thin-walled tubing and automatic fuel inspection, 19: 38823 (BNWL-SA-97)
nondestructive methods for, development of, 19: 40113(R) (ANL-7071)
nondestructive radiological methods of, book, 19: 38829

radiometric coin identification, apparatus for, 19: 38956(P)
MATHEMATICS
analysis of $x^n dx$ data distributions, method for, 19: 39087
convex sets in, applications of, 19: 39082 (TID-22032)
discrimination of curves, method of experiment planning for, 19: 39088
groups in, algebra of projective representations at finite, 19: 39085
matrix decomposition, inherent error analysis in, 19: 39080 (LA-DC-7192)
models of linear dynamic systems, 19: 39269(R) (SU-SEL-64-133)
nomograms for calculation of ventilation parameters for rooms containing gamma sources, 19: 38883
representations of G_2 algebra, irreducible, (T), 19: 39594
MATTER
Einstein equations for electromagnetic fields and incoherent, homogeneous solutions of, 19: 39648
thermodynamic properties of, research on, 19: 39272(R) (UCRL-12204, pp 27-48)
MEATS
radiation processing of cooked beef, lamb, pork, and veal, effects on color, 19: 39065
MECHANICS
cluster-star equations in classical statistical, Möbius formula for inversion of, 19: 39083
cluster-star equations in classical statistical, generating functionals for inversion of, 19: 39084
MEDICAL SUPPLIES
radiosterilization of, use of electron accelerators in, 19: 39063
MEDICINE
book: *Radiation Medicine*, 19: 38470(T)
radiation dosimetry of personnel in accident clinic, 19: 38477
radiation exposure problems of forensic, 19: 38495
use of radioisotopes in diagnostic, review on, 19: 38505
MEMBRANE FILTERS
use for collection of radioactive aerosols, 19: 38896
MEMORY DEVICES
operation with defective storage elements, methods for, 19: 39269(R) (SU-SEL-64-133)
MERCAPTO GROUP
content in ascites tumor cells of non-protein bound, effects of cysteamine on, 19: 38464
radiation effects on animal blood levels, 19: 38427
MERCURY
effects of plasma of, on thermionic diodes in autonomous discharges, 19: 39435(T) (JPRS-31048)
electron elastic scattering by atomic beams of, electron polarization in, (E), 19: 39392
nuclear magnetic resonance in superconducting, spin-orbit coupling effects on Knight shift in, (T), 19: 39727
separation from ethanolic hydrochloric acids by ion exchange, 19: 39265(R) (IA-1021)
use as threshold detector for fast neutrons, (E), 19: 39007
x-ray spectra of, Coster-Kronig transition probabilities from, (E), 19: 39410
MERCURY ALLOYS
Li–Hg, use in removing europium from aqueous electrolytes by extraction and electrolysis, 19: 38753 (LA-DC-7013)
MERCURY BROMIDES
separation from fused salts by solvent extraction using polyphenyls, 19: 39265(R) (IA-1021)
spectra in benzene and water, uv, 19: 39265(R) (IA-1021)
MERCURY IODIDES
solubilities in organic solvents, 19: 39265(R) (IA-1021)
spectra in benzene and water, uv, 19: 39265(R) (IA-1021)
MERCURY IONS
incorporation into potassium chloride crystals grown from solution, 19: 38696 (MIT-2909-4)
reactions with aluminum and magnesium, ion emission in, (E), 19: 39374
MERCURY ISOTOPES Hg^{-197}
energy from, determination of total, 19: 38878 (ORNL-P-1405)
MERCURY ISOTOPES Hg^{-203}
tracer use for measurement of blood circulation in brain, 19: 38501
use in gamma encephalography, 19: 38510
MESONS
decay of vector, amplitudes for radiative, 19: 39471
decay of, leptonic, (T), 19: 39573
interaction amplitudes of vector, Regge behavior of, 19: 39618
interactions with nucleons, complex angular momentum in, (T), 19: 39518
interactions with baryons in SV_{12} scheme, D/F ratios for vertices of, (T), 19: 39524
interactions with baryons, bootstrap mechanism and symmetries in, 19: 39559
mass formula for, (T), 19: 39584
model for, based on Sp(6), (T), 19: 39568
production in proton pair annihilation, amplitudes for, (T), 19: 39527
production of vector, in photon-proton interactions, (T), 19: 39621
symmetry for, covariant extension of SU(6), (T), 19: 39555
symmetry for, SU(9), 19: 39571
symmetry scheme for hadrons, Sp(3), (T), 19: 39565
MESONS, RESONANCE
decay correlations of vector, with baryon resonances, (E), 19: 39542
decay of vector, angular distributions of lepton pairs from, (T), 19: 39451 (CALT-68-43)
electromagnetic properties, (T), 19: 39563
production in deuteron-meson (π^-) interactions at 3.2 Bev/c, (E), 19: 39551
production of K^{*+} in meson (K^+)-proton interactions, peripheral, (E/T), 19: 39576
production of non-K^*, in proton pair annihilation, 19: 39534
production of $\pi^+\pi^-$ (1670) in meson (π^+)-deuteron and meson (π^-)-proton interactions, (E), 19: 39537
properties of, data tabulation of, 19: 39485 (UCRL-8030(Pt.I) (Mar. '65, ed.))
MESONS (D)
production in proton pair annihilations at 1.2 Bev/c, (E), 19: 39535
MESONS (η)
decay and production in photon interactions with protons, (E), 19: 39620
decay of, C-violation in 3π, (T), 19: 39528
decay of, vector interaction constant in, (T), 19: 39589
interactions with deuterons resonance, (T), 19: 39564
MESONS (P)
decay of, branching ratio for 2π, (E), 19: 39480 (NP-15247)
spin, (E), 19: 39480 (NP-15247)
MESONS (K)
decay of, four-body leptonic, (T), 19: 39589
interactions with deuterons resonance, (T), 19: 39564
interactions with nucleons, peripheral production and decay of K^* in, (E/T), 19: 39576
interactions with nucleons at low energies, model for, (T), 19: 39592
MESONS (K^-)
interactions with protons at low energies, Coulomb-nuclear interference in, (E/T), 19: 39530
interactions with protons, optical model analysis of elastic, (T), 19: 39545
interactions with protons at 2.1 to 2.7 Bev/c, meson (ϕ) production in, (E), 19: 39552
reactions with lithium-6, hyperfragments from, (E/T), 19: 39265(R) (IA-1021)
MESONS (K^0)
decay into two charged mesons (π), analysis of CP-nonconserving, 19: 39457 (CONF-796(Paper 23))
decay of (K^0_2), CP-nonconserving, 19: 39476 (NP-15197)
decay of K^0_2, CP invariance breakdown in, (T), 19: 39265(R) (IA-1021)
decay of K^0_2, leptonic, (E), 19: 39474 (JINR-P-2190)
decay of K^0_2, three-body, (E), 19: 39586
decay of K^0_2, CP violation in 2π, 19: 39601
production in meson (π^-) reactions with xenon at 9 Bev/c, cross sections for, 19: 39472 (JINR-P-2178)
MESONS (K^+)
interactions with protons, peripheral production and decay of K^* in, 19: 39576
MESONS (K_{e3})
decay, (E), 19: 39474 (JINR-P-2190)
MESONS ($K_{\pi\pi}$)
decay of, meson (π) final-state interactions in, (T), 19: 39515
decay of, vector interaction contribution to, 19: 39589
MESONS ($K_{\mu 3}$)
decay, (E), 19: 39474 (JINR-P-2190)
decay of, form factors for angular distributions of leptons and mesons (π), 19: 39482 (NP-15252)
MESONS ($K^+_{\pi 2}$)
decay of, energy spectra for modes of, 19: 39488 (UCRL-16058)
MESONS (μ)
decay in renormalizable vector boson theory, 19: 39489
production in photon interactions, (E), 19: 39623
MESONS (μ^-)
capture by chemical compounds, atomic, 19: 39366 (JINR-P-2185)
capture by manganese atoms, quadrupolar effects on energy levels in, (T), 19: 39368 (NP-15089)
decay of, electron momentum spectra in, (E), 19: 39614
MESONS (μ^+)
decay of, positron momentum spectrum in, (E), 19: 39614

MESONS (ω)
interactions of, effects on nucleon form factors, (E/T), 19: 39458 (CONF-796(Paper 24))
properties of, test for, (T), 19: 39572
MESONS (ω^0)
decay of, angular distributions of electron pairs from, (T), 19: 39451 (CALT-68-43)
MESONS (ϕ)
decay of, branching ratios for, (E), 19: 39531
decay of, upper limits for C-nonconserving, (E), 19: 39552
interactions of, effects on nucleon form factors, (E/T), 19: 39458 (CONF-796(Paper 24))
properties of, test for, (T), 19: 39572
MESONS (π)
interactions in meson ($K^+_{\mu 4}$) decay, (T), 19: 39515
interactions with protons, phase shift and resonance equations for elastic, 19: 39487 (UCRL-14193)
interactions with nucleons at high energy, Regge-pole hypothesis in asymptotic amplitudes for, 19: 39478 (NP-15210)
interactions with deuterons, resonance, (T), 19: 39564
interactions with nucleons, peripheral production and decay of mesons (ρ) in, (E/T), 19: 39576
interactions with photons in SU(3) and SU(6), 19: 39470 (JINR-P-2171)
interactions with nucleons at high energies, analyses of final-state, (E/T), 19: 39574
photoproduction, (T), 19: 39498
photoproduction at 0.300 to 1.5 Bev, meson (ρ) production in pair, (E), 19: 39549
production in electron scattering by nuclei, (T), 19: 36921
production in electron-proton interactions, (E), 19: 39623
production in mesons (η), decay, C-violation in, 19: 39528
MESONS (π^-)
absorption by nuclei, with two-nucleon emission, (T), 19: 39932
interactions with protons at 7 to 17 Bev/c, Regge pole analysis of, (E/T), 19: 39619
interactions with protons at 2.8 Bev/c, angular distribution analysis of, (E), 19: 39480 (NP-15247)
interactions with protons at 8.0 Bev/c, $\pi^+\pi^-$ (1670) production in, (E), 19: 39537
interactions with protons at 1.68 Bev/c, Y^*_0 production in, (E), 19: 39553
interactions with protons, determination of nucleon form factors from, (T), 19: 39590
interactions with protons at 3.5 Bev/c, four-prong events in, (E), 19: 39591
interactions with protons, isobar model for hyperon (Λ) production in, (T), 19: 39593
interactions with deuterons at 3.2 Bev/c, enhancement at 1.0 to 1.4 Bev in, (E), 19: 39551
production in photon-proton interactions at 600 to 850 Mev, double, (E), 19: 39519
reactions with xenon at 9 Bev/c, hyperons (Λ) and mesons (K^0) cross sections from, 19: 39472 (JINR-P-2178)
MESONS (π^0)
production in photon-proton interactions, cross sections for, (E), 19: 39620
production in photon-proton interactions, (E), 19: 39623
MESONS (π^+)
interactions with nucleons, amplitudes for elastic, (T), 19: 39621
interactions with deuterons at 6.0 Bev/c, $\pi^+\pi^-$(1670) production in, (E), 19: 39537
interactions with deuterons at 1.68 Bev/c, Y^*_0 production in, (E), 19: 39553
interactions with protons, peripheral production and decay of mesons (ρ) and N^* resonance in, (E/T), 19: 39576
photoproduction of, (T), 19: 39621
photoproduction on protons near threshold, cross sections for, (E), 19: 39461 (COO-1195-35)
photoproduction on protons near first resonance, (E), 19: 39597
MESONS (ρ)
decay to π and γ in SU(3) and SU(6), 19: 39470 (JINR-P-2171)
interactions of, effects on nucleon form factors, (E/T), 19: 39458 (CONF-796(Paper 24))
production in meson (π)-nucleon interactions, analyses of, (E/T), 19: 39574
production in meson (π) interactions with nucleons, peripheral, (E/T), 19: 39576
MESONS (ρ^0)
decay of, angular distributions of electron pairs from, (T), 19: 39451 (CALT-68-43)
production from meson (π) pair photoproduction, 19: 39549
MESONS (X)
decay of, branching ratios for, (E), 19: 39531
METABOLISM
of radioisotopes in animals, 19: 38357(T)
radiation sickness effects on, pathology of, 19: 38433(T)
METALLIC FILMS
plastic deformation of thin gold, by Talysurf stylus, 19: 38916 (SC-DC-65-1589)
track formation in thin, by electron beams, 19: 38950
METALLOGRAPHY
of intermetallic-high-melting metals, 19: 39214
METALLURGY
heat for processes in, from power reactors, 19: 38686(P)
research at IFA, 19: 40287(R) (NP-15188)
uses of electron-bombardment furnaces in, 19: 39109
METALS
combustion of, temperature of flame during, 19: 38583(R) (SC-DC-65-1480)
diffusion of hydrogen through, review, 19: 39165 (NAA-SR-10462)
electron-beam penetration through, mechanism of, 19: 39417
electron-gas interactions in, one-particle Green's function for, 19: 39658
fatigue, nondestructive evaluation of, 19: 39151 (AFOSR-65-0981)
Fermi surface of, relativistic effects in, 19: 40076 (IS-1172)
ion reactions with monocrystalline surfaces of, electron emission in high-energy, (T), 19: 39405
machining of, by sputtering through mask of contamination, 19: 39136
magnetic flux permeability and tunneling in superimposed layers of superconductors and, in magnetic fields, (T), 19: 39700
magnetic properties of, survey, (T), 19: 40074 (CONF-796(Paper 3))
metallography of high-melting, 19: 39214
positron annihilation in, 3-quantum, (E/T), 19: 39546
properties of, effects of electron-phonon interactions on, (T), 19: 40073 (CONF-796(Paper 1))
pump development for liquid, 19: 38781(R) (N64-25903)
purification using electron-bombardment furnaces, 19: 39109
thermodynamics of mass transport in, 19: 38678
x-ray scattering in, measurement and theory of, 19: 38524
METEORITES
dating by analysis of charged particle tracks resulting from spontaneous uranium fission, 19: 39038
sulfur isotope content of, (E), 19: 38847
sulfur-34 to sulfur-32 ratio in Orgueil, 19: 39351
METHACRYLIC ACID, ESTERS
radioinduced polymerization of cetyl, at 60 to −195°C, kinetics of, 19: 38699
METHACRYLIC ACID, METHYL ESTER
radioinduced grafting to chloroethylene polymers, 19: 38739(P)
METHACRYLIC ACID, METHYL ESTER POLYMERS
gamma absorption by, effective atomic numbers for, 19: 40069
radiation effects on physical properties of, 19: 39231 (COO-1224-8)
radiation effects on free radical density, gamma and x, 19: 38706
METHANE
ionization cross section for, electron-impact, 19: 38630
yields from radiolysis of methanol, 19: 38716
yields in gamma radiolysis of liquid cyclopentane, 19: 38712
METHANE, BROMOTRICHLORO-
radiation effects on bromine-80 and -82 retentions in, isomeric transition reaction in, 19: 38715
METHANE, CHLOROTRIFLUORO-
H–chlorotrifluoromethane, vortex flow in gaseous, 19: 40236 (LA-3229, pp 237-50)
METHANE, DICHLORO-
radioinduced reactions with cycloalkenes, gamma, 19: 38695 (KFK-317)
METHANE, DIFLUORO-
nuclear magnetic resonance spectra of, collision-narrowing theory of, 19: 38629
METHANE, FLUORO-
nuclear magnetic resonance spectra of, collision-narrowing theory of, 19: 38629
METHANE, IODO-
preparation of iodine-isotope labeled, effects of diluent gases on, 19: 39265(R) (IA-1021)
METHANE, NITRO-
electric conductivity of detonation products of, 19: 40284 (LA-DC-6993)
METHANOL
radioinduced reactions with 1,2-dichlorotetrafluorocyclobutene and 1,2-dichlorohexafluorocyclopentene, 19: 38708
radiolysis of, product yields from gamma, 19: 38716
METHYL ETHER
yields from radiolysis of methanol, 19: 38716
METHYLENE BLUE
effects on radioinduced chromosome aberrations in barley and *Vicia faba*, 19: 38462

METROLOGY
electron microscopic study of plastic deformation of thin gold films by Talysurf stylus, 19: 38916 (SC-DC-65-1589)
MICE
effects of ultraviolet-irradiated linolenic acid extract on skin of, 19: 38366
europium isotope effects on, 19: 39265(R) (IA-1021)
iodine-131 metabolism in, effects of thiouracil diet on, 19: 38350
metabolism of desoxyribonucleic acid in, tracer study using tritiated thymidine, 19: 38336 (TID-21106)
pathological effects of subcutaneous rare earth metal implants in, 19: 38334 (COO-1170-1)
radiation chimeras in, immunologic role of thymus in, 19: 38451
radiation effects on erythrocyte size in, 19: 38363
radiation effects on, protective effects of spleen cell induced immunological unresponsiveness against, 19: 38454
radiation effects on, protective effects of cobalt–chlorophyll and glucuronic acid against whole-body, 19: 38456
radiation effects on, protective effects of orotic acid against, x, 19: 38458
radiation effects on mitochondria function and structure in liver of, 19: 38424
radiation effects on growth of transplanted tumors in, synergistic effects of cruzine, 19: 38428
radiation effects on erythrocyte size in, 19: 38363
radiation effects with spleen cell transplants on polyvalent tolerance in adult and newborn, 19: 38376
radiation effects on growth of transplanted tumors in, 19: 38387
radiation effects on Ehrlich ascites tumors in, at various times following inoculation, 19: 38402
radiation effects on serum proteins in, following rat-to-mouse chimera transplants, 19: 38404
radiation effects on cell cycle duration in tail tissues of embryonic, gamma, 19: 38405
radiation effects on kidney function in, 19: 38409
radiation injuries, effects of chemical radioprotective compounds, 19: 38452
radiation injuries, protective effects of morphine, 19: 38453
radiation injuries, protective effects of 2-mercaptobenzothiazole, 19: 38466
radiation injuries, protective effects of anoxia, 19: 38450 (USNRDL-TR-851)
radiation injuries, protective effects of aminoethylisothiouranium, 19: 38450 (USNRDL-TR-851)
radioinduced dominant lethal mutations in spermatogonia in, 19: 38394
radioinduced leukemia in, 19: 38372
radioinduced mutations in male, superlethal, 19: 38393
radioinduced translocations in spermatogonia in, 19: 38396
respiration in, effects of cysteamine, 19: 38469
respiration in, effects of aminoethylisothiouren, 19: 38469
MICROORGANISMS
detection in jet fuel, tracer method for, 19: 39061 (ADR-09-08a-63.1)
radiation effects on fruit pathogenic, gamma, 19: 39265(R) (IA-1021)
radiation effects on infectiousness and motility of *Treponema pallidum*, 19: 38380
MICROSCOPES
design for measuring particle lengths in nuclear emulsions, 19: 39000
MICROSCOPY
fluorescence, device for phase contrast in, 19: 38923(T) (UCRL-Trans-1228)
MICROWAVE EQUIPMENT
magnetohydrodynamic waveguides, experiments with liquid metal, 19: 39270(R) (TID-21894)
performance of multimode cylindrical, 19: 39269(R) (SU-SEL-64-133)
phase shifter for, varactor diodes utilization in, 19: 40297 (UCRL-7753)
MICROWAVES
amplification in electron beam interactions with cesium plasma, (E), 19: 40036
diagnostic use for plasma density spatial distribution, (E/T), 19: 39965 (NP-15203)
diagnostic use for thermally ionized alkali plasmas, (E), 19: 39980
emission from atmospheric oxygen, measurement of, 19: 39270(R) (TID-21894)
emission from Zeta plasma, 19: 39953 (CLM-R-40)
interactions with inhomogeneous anisotropic plasma column, in axial magnetic field, (T), 19: 39994
propagation in multimode waveguides, 19: 39269(R) (SU-SEL-64-133)
propagation in plasma, transient, (T), 19: 40034
propagation in warm magnetoplasma, (T), 19: 40027
reactions with isotropic collisionless plasma, transient phenomena in, (T), 19: 40035
reflection of, diagnostics of shock-produced plasma by, (E), 19: 39997
scattering by magneto plasma waves, (E), 19: 40033
MILK
analysis for iodine-131, radiochemical, 19: 38560
analysis for strontium-90, 19: 38556
analysis for yttrium-90, 19: 38856
radioactivity of effects of atmospheric transport of fallout on, 19: 38857
radioactivity of German, 1962, 19: 38858
strontium-90 content in German, 19: 38876 (NP-14927)
MINERAL METABOLISM
effects of vitamin D_3, in rats, 19: 38347
MINERALS
analysis for gold and silver, activation, 19: 39265(R) (IA-1021)
analysis for silver, spectrochemical, 19: 39265(R) (IA-1021)
charged particle tracks in, identification after chemical etching, 19: 39038
rare-earth contents of, from batholith of Southern California, (E), 19: 38848
MISCH METAL
Mg–misch metal–Zn, plastic anisotropy of ZE10A sheet, 19: 39149 (AD-425880)
MITOCHONDRIA
radiation effects on function and structure of, in mouse liver, 19: 38424
MITOMYCINS
effects on RNA synthesis in derivatives of *E. coli*, 19: 38381
MITOSIS
radiation effects on, in gonocytes in testes of rats, 19: 38369
radiation effects on duration in mouse embryos, gamma, 19: 38405
radiation effects on Tradescantia, synergistic infrared and x, 19: 38416
MOLDING MATERIALS
analysis of thermosetting diallyl phthalate powders for *tert*-butyl perbenzoate, 19: 40285 (MLM-1284)
MOLECULAR BEAMS
nuclear magnetic resonance of, collision-narrowing theory of, 19: 38629
MOLECULES
book: *Advances in Atomic and Molecular Physics*, 19: 39415
condensation and equilibria in solar nebula and cool stellar atmosphere, (T), 19: 39352
electron orbitals in united atom model, (T), 19: 39372
exciton wave-packet radiation in, in crystals, (T), 19: 40088
Jahn-Teller effect in, energy values of, 19: 39265(R) (IA-1021)
wave functions for, in momentum space, (T), 19: 39660
MOLLUSKS
control of, preparation of methylcarbamate pesticide for, 19: 38748
radionuclide content in, from California waters, 19: 38895
MOLTEN SALT REACTOR EXPERIMENT
operation safety limits of, 19: 40189 (ORNL-TM-733(Rev.))
solvent for, chemistry and thermodynamics of beryllium fluoride–lithium fluoride as, 19: 38582 (ORNL-P-1428)
MOLYBDENUM
corrosion by lithium at high temperatures, effects of nitrogen on, 19: 40112(R) (ANL-7046(p.36-66))
corrosion by molten chlorides, electrochemical, 19: 39122
deformation, recrystallization, and welding of single crystals of, effects of orientation on, 19: 39139
diffusion of atoms in bcc, activation energy for interstitial, (T), 19: 40086
diffusion of oxygen at 1500 to 1800°C, 19: 39072(R) (NP-15187)
diffusion rate of oxygen in, at 1500 to 1800°C, 19: 39070(R) (GEST-2046)
effects on superconducting transition temperature of vanadium silicide, 19: 39196
electron reactions with atomic, screening effects on bremsstrahlung and pair production in, (T), 19: 39389
fabrication for impaction testing of particulate materials, 19: 39125(R) (BNWL-91)
gamma scattering by, spectra of resonant, (E), 19: 39265(R) (IA-1021)
magnetostriction in pure monocrystalline, 19: 39199
performance as collector in a thermionic converter, 19: 39431(R) (AD-608554)
potassium-ion thermionic emission from, at 30 to 1100°C, 19: 39197
radiation effects on, anelastic after-effects from electron, (E), 19: 39247
rare-gas ion reactions at 1 to 10 kev, secondary-electron emission in, (E), 19: 39404
reactions with sodium at 2100 to 2400°C, 19: 39090(R) (ANL-7046(p.78-82))
separation from zirconium in nitric acid solutions, 19: 38778(P)
MOLYBDENUM ALLOYS
Al–Cr–Fe–Mo–Ti, mechanical properties and heat resistance, 19: 39193
Al–Cr–Fe–Mo–Ni–Nb–Ti, thermal response and microstructure of Inconel 718 at 1200 and 1400°F, 19: 39158 (GEAP-4751)
Cr–Fe–Mo–Ni–Nb–W, tensile properties of IN-102, 19: 39156(R) (CEND-532)

Cr–Fe–Mo–Ni–Nb, thermal response and microstructure of Inconel 625 at 1200 and 1400°F, 19: 39158 (GEAP-4751)
Ir–Mo, superconductivity of, order-disorder effects on, (E), 19: 39689
Mo–Re, elastic properties of, determination by ultrasonics, 19: 40112(R) (ANL-7046(p.36-66))
Mo–Ti, cavitation in bismuth–lead alloy at 500 and 1500°F, ultrasonic-induced, 19: 39116 (NP-15263)
Mo–Ti–Zr, properties of TZM as cladding material for SNAP hydride reactors, 19: 39166 (NAA-SR-Memo-11149)
Mo–U, performance in HNPF, 19: 40286(R) (NAA-SR-11200)
Sb–Mo, crystal structure of intermetallic compounds in, 19: 39209

MOLYBDENUM BORIDES
reactions with graphite to 2200°C, 19: 38654

MOLYBDENUM COUPLES
Mo/UO_2, uranium diffusion rate at 1600 to 1800°C, 19: 39070(R) (GEST-2046)

MOLYBDENUM ISOTOPES Mo-91
production of isomeric, in neutron reactions (n,2a) with molybdenum-92, (E), 19: 39790

MOLYBDENUM ISOTOPES Mo-92
neutron reactions (n,2n) at 14.8 Mev, isomer production in, (E), 19: 39790

MOLYBDENUM ISOTOPES Mo-103
half life, 19: 39892

MOLYBDENUM ISOTOPES Mo-105
half life, 19: 39892

MOLYBDENUM STEEL
Cr–Mo, corrosion of Croloy 2¼ by sodium hydroxide solutions at 0 to 900°F, 19: 38803(R) (BAW-1280-26)

MOLYBDENUM SYSTEMS
As–Mo, crystal structure of compounds in, 19: 39209
C–Cr–Fe–Mo–ni, reinforcement of graphite by, 19: 39114(P)
Mo–Nb–Si, phase studies and properties of, 19: 39194

MOMENTS
calculation of nuclear quadrupole, (T), 19: 39791
theory for asymmetric nuclei inertial, 19: 39831

MONAZITES
processing of, rare earth separation from, 19: 38859

MONEL
gamma absorption by, effective atomic numbers for, 19: 40069

MONTE CARLO METHOD
neutron flux distribution in subcritical sphere with central point source, (T), 19: 40162
use for neutron resonance escape calculations, 19: 40153 (IA-1001)

MORPHINES
protective effects against radiation injuries in mice, 19: 38453

MOSSBAUER EFFECT
detection of, spectrometer for, 19: 39032
diagnostic use for surface studies, 19: 40078 (NP-15111)
experiments using, 19: 39795
in aqueous metal salts, 19: 39265(R) (IA-1021)
in iodine-129 complexes, 19: 39265(R) (IA-1021)
in iron dithiocarbamates, relaxation studies by, (E), 19: 38653
in organic iron and tin compounds, 19: 38576 (CONF-650425-2)
in organo-tin compounds, effects of intermolecular bonding on, 19: 38577 (CONF-650425-3)
iron-57 spectra in copper–manganese alloys, (E), 19: 39212
use for measuring isomer and nuclear-multipole spectral effects on powdered crystals, 19: 39876

MULTIPLICATION FACTOR
calculation of Doppler coefficient of reactivity, basis for, 19: 40286(R) (NAA-SR-11200)
determination of, pulsed source techniques for, (T), 19: 40151 (EIR-79)
measurement for fertile and fissile isotopes, methods of, 19: 40286(R) (NAA-SR-11200)

MUSCLES
iodine-131 metabolism in mouse, effects of thiouracil diet on, 19: 38350

MUTATIONS
effects of incorporated carbon-14 on, in *Drosophila melanogaster*, 19: 38400
effects of irradiated DNA on, in *Drosophila melanogaster*, 19: 38413
genetic code for messenger ribonucleic acid for induction of, 19: 40296 (TID-21856)
induced by exogenous desoxyribonucleic acid in Drosophila, 19: 38408
radioinduced dominant lethal, in mouse spermatogonia, 19: 38394
radioinduced in *Cl. perfringens*, 19: 38445
radioinduced in *Cl. perfringens*, 19: 38446
radioinduced in Dahlbominum oogonia, gamma and x-ray, 19: 38392
radioinduced in male Drosophila, effects of sperm maturity on frequency of, 19: 38390
radioinduced in male mice, superlethal, 19: 38393
radioinduced in oats, effects of ploidy on thermal neutron, 19: 38419
radioinduced in plants, agricultural importance of, 19: 38327
radioinduced, theoretical bases for methods of producing, 19: 38420

N

NAGASAKI
bombing effects on hematology in survivors in, 19: 38378

NAPHTHALENE
deuterium exchange with heavy water, group VIII metal catalysis of, 19: 38597
reduction of platinic oxide by labeled, preparation of platinum oxide catalysts by, 19: 38596

NAPHTHALENE, DECAHYDRO-
perfluoro-, radiation effects on, 19: 38709

2,7-NAPHTHALENEDISULFONIC ACID, 4,5-DIHYDROXY-
complex formation with beryllium in aqueous solutions, 19: 38641

NATIONAL REACTOR TESTING STATION
atmospheric turbulence and diffusion at, effects of MTR-ETR complex on, 19: 39259 (IDO-12041)
hydrology of subsurface waste disposal at, 19: 40269(R) (IDO-22047-USGS)

NAVAL VESSELS
propulsion systems for, nuclear, 19: 40255(P)

NEBULAE
molecular condensation and equilibria in solar, (T), 19: 39352

NECK
radiotherapy of cancer of larynx, effects on thyroid function, 19: 38484

NEODYMIUM
fluorescence conversion efficiency of glasses of, 19: 40090
phase transformations at 6 to 65 kbar, solid-liquid and solid-solid, 19: 40095
proton inelastic scattering at 25 to 1700 kev, x-ray yields from, (E), 19: 39881
separation from promethium by ion exchange, 19: 38772
thermal capacity at low temperature, magnetic contribution to, (T), 19: 39296

NEODYMIUM COMPLEXES
with [(2-hydroxyethyl)imino]diacetic acid, dissociation constant of, 19: 38671
with *N,N'*-dimethyl-*N,N'*-dinitrosoterephthalamide, mechanism of formation of, 19: 38600

NEODYMIUM ISOTOPES Nd-147
release from pyrolytic carbon-coated fuel particles, 19: 39228 (BMI-1734)

NEODYMIUM OXALATES
solubility in *N,N'*-dimethyl-*N,N'*-dinitrosoterephthalamide at 25°C, 19: 38601

NEODYMIUM OXIDES
reactions with sodium metaphosphate, spectra of compound formed in, 19: 38668

NEON
electric conductivity of positive-column discharge plasma of, (E), 19: 40041
electron and x-ray scattering by, corrections to incoherent, 19: 39379
electron inelastic scattering by crystals of, interband excitation in fast, (T), 19: 40083
ionization cross section for, electron-impact, 19: 38630
rubidium-vapor spin relaxation in, (E), 19: 39400

NEON IONS
reactions with metal single crystals at 1 to 10 kev, secondary-electron emission in, (E), 19: 39404

NEON ISOTOPES Ne-19
energy levels, (E), 19: 39827

NEON ISOTOPES Ne-20
energy levels of, search for 4.97-Mev doublet, (E), 19: 39809
reactions with emulsion nuclei at 10.4 Mev/nucleon, range-momentum relation for heavy recoil ions in, (E), 19: 39883

NEON SYSTEMS
H–Ne, nuclear spin lattice relaxation in, 19: 39378
H–Ne, use in bubble chambers, 19: 39026

NEPTUNIUM
determination in neptunium–plutonium alloys, spectrophotometric, 19: 38546(R) (RFP-552)
neutron capture cross sections at 20 kev, 19: 38786 (LA-DC-7111)

NEPTUNIUM ALLOYS
Np–Pu, spectrophotometric analysis for plutonium, 19: 38546(R) (RFP-552)

NEPTUNIUM IONS
reduction of different valence states of, by uranium(IV) in chloride and perchlorate solutions, 19: 38584 (SC-RR-65-219)

NEPTUNIUM ISOTOPES

nuclear properties of, pairing force effects on, (T), 19: 39927
NEPTUNIUM ISOTOPES Np-237
energy levels, (E), 19: 39946
NERVES
response inhibition of auditory, effects of acoustic intensity on, 19: 39270(R) (TID-21894)
NERVOUS SYSTEM
radiation effects on function of, synergistic effects of acceleration and vibration during space flight, 19: 38358 (AD-612660)
radiation sickness effects on, pathology of, 19: 38433(T)
NEUROLOGY
research programs on, 19: 39270(R) (TID-21894)
NEUTRINOS
charge acquisition in minimal interactions of, (T), 19: 39513
experiments at CERN on, bubble and spark chamber, 19: 39612
field theory of, 19: 39639
geometric theory of, 19: 39503
interactions of high-energy, review on, 19: 39611
interactions with nucleons, resonance production in, (T), 19: 39517
interactions with electrons, weak boson production in, (T), 19: 39567
interactions with electrons, polarization effects in, (T), 19: 39587
properties of, quantum laws for, (T), 19: 39661
reactions with nuclei, cross sections for, (T), 19: 39943
NEUTRON CAPTURE CROSS SECTIONS
measurement in nuclear explosions, 19: 38786 (LA-DC-7111)
NEUTRON CROSS SECTIONS
bibliography on, 19: 39778 (BNL-9355)
calculation for natural non-fissile elements, computer program for, 19: 39776 (AEEW-M-517)
calculation for reactor cells, methods for, 19: 40152 (GA-6462)
calculations of Doppler broadened, computer program for, 19: 39777 (AEEW-M-518)
library for fast reactor analysis, 19: 40286(R) (NAA-SR-11200)
library of multigroup, for reactor materials, 19: 40286(R) (NAA-SR-11200)
measurement using neutrons from nuclear detonation, (E), 19: 39889
NEUTRON SHIELDING
neutron transport in, removal-diffusion theory for, 19: 39751 (AE-185)
NEUTRON SOURCES
conference on Intense Neutron Generator, 19: 39752 (AECL-2177)
design of portable, 19: 39770
development of Intense Neutron Generator, engineering problems in, 19: 39760 (AECL-2177, Paper 7))
development of separated-orbit cyclotron as, 19: 39755 (AECL-2177, Paper 2))
dose and energy distributions from americium–beryllium, americium–boron, plutonium–beryllium, and polonium–beryllium, 19: 39766 (ORNL-TM-1171)
economics for Intense Neutron Generator, 19: 39753 (AECL-2177, Introduction)
experimental facilities of Intense Neutron Generator, 19: 39757 (AECL-2177, Paper 4)
flux intensification, 19: 39754 (AECL-2177, Paper 1))
performance of pulsed, for reactor studies, (T), 19: 40151 (EIR-79)
power production in Intense Neutron Generator, nuclear, 19: 39758 (AECL-2177, Paper 5))
power supply system for Intense Neutron Generator, r-f, 19: 39759 (AECL-2177, Paper 6))
properties and spectra of, 19: 39772
radiation hazards from, 19: 38480
radioisotope production in the Intense Neutron Generator, 19: 39762 (AECL-2177, Paper 9))
shielding of Intense Neutron Generator, 19: 39761 (AECL-2177, Paper 8))
use in activation analysis, 19: 38565
use of pulsed, in well logging, 19: 38871(P)
NEUTRON SPECTRA
calculation in reactors, computer program for, 19: 40176 (AGN-TM-407)
measurement of, effects of gamma radiation on, 19: 40122(R) (GEAP-4862)
NEUTRON SPECTROMETERS
performance for GLEEP fast neutron spectra determination, 19: 40256 (AERE-M-1590)
NEUTRONS
absorption by mixtures, computer program for resonance, 19: 40112(R) (ANL-7046(p.36-66))
absorption by poisoning materials, burnup effects on, (E), 19: 40163
attenuation in concretes, mechanisms of, 19: 40061 (BNWL-SA-79)
book: *Biological Effects of Neutron Radiation*, 19: 38437
book: *Nuclear Technology in Construction*, 19: 38828
capture by gadolinium-155 and -157, gadolinium-156 and -157 Mössbauer effect following, (E), 19: 39863
decay of non-oriented, polarization in, 19: 39582
detection and measurement of, monitor for, 19: 40286(R) (NAA-SR-11200)
detection and measurement using bubble chamber, 19: 38993 (NP-15143)
detection and measurement using bubble chamber, 19: 38994(R) (NP-15145)
detection and measurement of, electronic circuit and equivalent proportional counters for, 19: 39001
detection of, efficiency of long shielded counters for, 19: 39034
diffraction by uranium dioxide, magnetic structure determination by, (E), 19: 40091
diffusion in cylinders, methods of calculating, 19: 40286(R) (NAA-SR-11200)
diffusion in fast reactors, multigroup calculations for, 19: 40161 (ZfK-TPh-11)
diffusion in reactors, computer program for, 19: 40176 (AGN-TM-407)
dosimetry in 10-Bev synchrophasotron, 19: 39315 (JINR-P-2177)
dosimetry of, calculational methods in, 19: 38897
dosimetry of, using radiochemical nitrate yields, 19: 39042
effects on alumina-coated uranium dioxide fuel particles, 19: 39227 (BMI-1729)
effects on anion-exchange resins, 19: 38697 (ZFK-RN-17(p.139-64))
effects on carbon-coated fuel particles, 19: 39129(R) (ORNL-TM-1116)
effects on chromosome break induction in barley, interaction in, 19: 38399
effects on *Cl. perfringens*, alpha toxin, 19: 38446
effects on diamond crystals, small-angle x-ray scattering from defects in, 19: 39230 (BNL-9332)
effects on EBWR fuel rods, 19: 39125(R) (BNWL-91)
effects on electric cables, 19: 39056 (N64-29558)
effects on fueled graphite, 19: 39129(R) (ORNL-TM-1116)
effects on graphite mechanical properties, 19: 39237
effects on hysteresis loops in monocrystalline barium titanates, 19: 38705
effects on liquid sodium dilation of graphite, 19: 39235 (NAA-SR-11309)
effects on mechanical properties of cladding materials for SNAP hydride reactors, 19: 39166 (NAA-SR-Memo-11149)
effects on nickel crystals, recovery above room temperature, 19: 39251
effects on plastic, glass-laminate, and ceramoplastic materials, 19: 39232 (FZK-227)
effects on plutonium nitride–uranium nitride fuels, 19: 39125(R) (BNWL-91)
effects on plutonia–urania fuels, 19: 39125(R) (BNWL-91)
effects on pressure transducer components, transient and permanent, 19: 39055 (GA-6266)
effects on reactions between bromine and cyclohexane, organic retentions of bromine-80m and -82 in, 19: 38713
effects on reactor materials, method for studying, 19: 38822 (BNWL-SA-2)
effects on silicon defect centers from, 19: 39252
effects on stainless steel and Zircaloy-2, 19: 40286(R) (NAA-SR-11200)
effects on tensile fracture strain of graphite, at 25, 550, and 600°C, 19: 39238
effects on toxin formation by *Cl. perfringens*, 19: 38448
effects on uranía, 19: 39125(R) (BNWL-91)
effects on 347 stainless steel, 19: 39091(R) (BMI-1723(Del.))
energy spectra in multiplying medium, asymptotic and steady-state, (E), 19: 39768 (RPI-328-21)
existence of tetra-, (T), 19: 39547
flux and spectrum of, cancer therapy using 70 Mev synchrotron, 19: 38517
flux distribution in subcritical sphere with central point source, (T), 19: 40162
flux distributions in reactor cells, space-energy, (T), 19: 40152 (GA-6462)
flux in reactors, computer programs for calculating, 19: 40157 (ORNL-TM-1175)
form factors of, determination from deuteron-electron interactions, (T), 19: 39541
interactions of, scattering-length correction to, (T), 19: 39499
interactions with protons, gamma asymmetry and circular polarization in, (T), 19: 39538
kinetics in coupled KIWI cores, models for, 19: 40240 (LA-3263)
kinetics in reactors, computer program for calculation of, 19: 40148 (BNWL-111)
monitoring in industrial buildings, 19: 38884
polarization by reflection from cobalt–iron mirrors, facility for, 19: 39265(R) (IA-1021)
polarization in deuteron reactions (d,n) with carbon at 2.8 Mev, 19: 39950
reactions (n,α) with terbium-159 at 14.2 Mev, alpha energy spectrum of, (E), 19: 39780 (INR-596/PL)
reactions (n,α) with osmium-192 at 14 Mev, production of tungsten-189 in, (E), 19: 39801
reactions (n,α) and (n,p) with rubidium at 13 to 17 Mev, cross sections

for, (E), 19: 39823
reactions (n,α) with bromine at 13 to 17 Mev, cross sections for, (E), 19: 39823
reactions (n,d) and (n,p) with boron-10 at 14.4 Mev, differential cross sections for, (E), 19: 39798
reactions (n,γ) with tin-118, -120, and -124, p-wave resonances of, 19: 39784 (ORNL-P-1352)
reactions (n,γ) with rhenium-185 and -187 at 4 kev to 6 Mev, cross sections for, (E), 19: 40112(R) (ANL-7046(p.36-66))
reactions (n,γ) with nuclei, gamma spectra of resonances of, (E), 19: 39781 (JAERI-1073)
reactions (n,γ) with iodine-127 at 0.025 ev and 24 kev, cross sections, (E), 19: 39816
reactions (n,n′γ) with nuclei at 0 to 14 Mev, energy absorption in, 19: 39769 (SC-DC-65-1544)
reactions (n,n) and (n,γ) with lithium-7, cross sections for, (T), 19: 39820
reactions (n,xn) with tritium at 14.1 Mev, charged-particle spectra in, (E), 19: 39939
reactions (n,2n) with molybdenum-92 at 14.8 Mev, isomer production in, (E), 19: 39790
reactions (n,2n) with fluorine-19 and nitrogen-14 at 14.6 Mev, total cross sections for, (E), 19: 39797
reactions with boron-10 in gases, pressure wave generation in fission, (E), 19: 39836
reactions with carbon-12 at 2.5 to 5 Mev, total cross section for, 19: 40115 (CONF-650602-33)
reactions with plutonium and uranium isotopes, cross sections for fission, (E), 19: 39889
reactions with rare earths at 0.0005 to 1 ev, total cross sections for, 19: 39779 (IEA-86)
reactions with thorium-232 at 0.56 Mev, differential cross section for, 19: 40115 (CONF-650602-33)
reactions with uranium-238 from 0.001 ev to 15.0 Mev, cross sections for, 19: 39764 (GA-6087(Rev.))
resonance escape probabilities in thermal reactors, computer program for, 19: 40153 (IA-1001)
scattering by anharmonic crystals at low temperatures, inelastic, (T), 19: 40093
scattering by crystals, incoherent, (T), 19: 39176
scattering by lead-208 and oxygen-16 at 0.5 to 4 Mev, phase shift analysis of, (E), 19: 39785 (ORNL-P-1356)
scattering by moisture in soils, use of cadmium for calibration of probes for measuring, 19: 38869
scattering in slabs, initial value problem for anisotropic, 19: 39765 (INR-611/IX-A/R)
separation energies for nuclei, (E), 19: 39862
slowing down in reactor shields, method for prediction of, 19: 40156 (NP-15161)
spectra in natural uranium, measurement of exponential, (E), 19: 39763 (EUR-2413.e)
spectra in reactor cores, effects of temperature on, 19: 40122(R) (GEAP-4862)
thermalization in gases, liquids, and solids, Van Hove theory for relaxation times in, 19: 39773
transport in air from atomic bombs, shielding against, 19: 38892
transport in homogeneous plane slabs, (T), 19: 39771
transport in shielding, removal-diffusion theory for, 19: 39751 (AE-185)
use of 14-Mev, for activation analysis, precision in, 19: 38569

NEUTRONS, EPITHERMAL
scattering by hydrogenated iron, magnetic, 19: 40075 (IEA-84)

NEUTRONS, FAST
detection by organic scintillators, (T), 19: 38997 (UCRL-16149)
dosimetry in animal tissue, method for, 19: 38439
dosimetry of, development of semiconductor devices for, 19: 38992 (COO-1226-8)
dosimetry of, proton recoil proportional counter for, 19: 38968 (AEET/HP/D-1)
dosimetry of, use of proportional detectors for, 19: 39043
effects on adrenal cortex function in rats, 19: 38443
effects on cardiovascular and hematopoietic system of rats, 19: 38441
effects on chemical and physical properties of rat blood, 19: 38440
effects on corrosion resistance of boronated stainless steel, 19: 39110
effects on culture and morphology of *Bacillus mesentericus*, 19: 38449
effects on decomposition of water in reactor, 19: 38698 (ZFK-RN-17 (p.199-207))
effects on dislocations in annealed copper, 19: 39241
effects on mechanical properties of Type 304 stainless steel and Zircaloy-2, 19: 39229(R) (BMI-X-10134)
effects on mechanical properties of boronated stainless steel, 19: 39110
effects on morphology of organs in rats, 19: 38444
effects on mortality of rats in different positions, RBE of, 19: 38438
effects on thermally activated flow stress in iron, 19: 39242
effects on thermoelectric capacity of germanium at low temperatures, (E), 19: 39240
effects on thyroid function in rats, 19: 38442
radiation effects on ductility of type 304 stainless steel, 19: 39236 (WCAP-3269-36)
reactions (n,p) with oxygen-16 at 12 to 17 Mev, cross sections, (E), 19: 40163
spectra in ZPR-VI assembly 4Z, 19: 40113(R) (ANL-7071)
spectra of, measuring using threshold detectors, (E), 19: 39007

NEUTRONS, FISSION
energy, spatial, and velocity distributions of, computer program for, 19: 39767 (ORNL-TM-1192)

NEUTRONS, THERMAL
effects on corrosion resistance of boronated stainless steel, 19: 39110
effects on mechanical properties of boronated stainless steel, 19: 39110
effects on oats, effects of ploidy on frequency of mutagenic, 19: 38419
effects on organic retentions of bromine-80 and -82 in alkyl halides and hydrocarbons, 19: 38715
reactions (n,γf) with transuranic nuclei, (T), 19: 39864
reactions with aromatic phosphorus compounds, phosphorus-32 formation in, 19: 38700
reactions with plutonium-239 and uranium-235, yields of krypton-85 in fission, (E), 19: 39800
scattering by hydrogenated nickel-palladium alloy, magnetic, 19: 40075 (IEA-84)
scattering by shielding materials, albedo measurements on, 19: 40065 (NP-15152)

NEW YORK
radiation protection program of, 19: 38887

NICKEL
catalytic effects on hydrogen exchange of alkylaromatic hydrocarbons and toluic acid derivatives with deuterium oxide, 19: 38688
catalytic properties in deuterium exchange reactions, 19: 38597
determination in plutonium using dimethylglyoxime, spectrophotometric, 19: 38546(R) (RFP-552)
determination in stainless steel, electron microprobe, 19: 38536 (ACF-6)
deuteron reactions (d,np) at 13.6 Mev, (E), 19: 39940
gamma reactions at 6.13 Mev, electron pair production cross sections for, (E), 19: 39787 (SGAE-PH-19/1965)
nickel-61 nuclear magnetic resonance in, 19: 39418
oxygen sorption on, high-energy electron diffraction studies of, 19: 39178
radiation effects on magnetic properties of, electron, (E), 19: 39239
radiation effects on, recovery from neutron, 19: 39251
rare-gas ion reactions at 1 to 10 kev, secondary-electron emission in, (E), 19: 39404
reactions with sodium at high temperatures, 19: 39090(R) (ANL-7046 (p.78-82))
reinforcing by tungsten fibers in pneumatically compacted plates, 19: 39093 (BNWL-SA-141)
sorption by gamma-alumina and inorganic ion exchange materials from fused salts, 19: 38771

NICKEL ALLOYS
tensile properties of René 62, 19: 39156(R) (CEND-532)
Al–Cr–Fe–Mo–Ni–Nb–Ti, thermal response and microstructure of Inconel 718 at 1200 and 1400°F, 19: 39158 (GEAP-4751)
Ce–Ni–Pu, phase studies, 19: 39163(R) (MLM-1244)
Cr–Fe–Mo–Ni–Nb–W, tensile properties of IN-102, 19: 39156(R) (CEND-532)
Cr–Fe–Mo–Ni–Nb, thermal response and microstructure of Inconel 625 at 1200 and 1400°F, 19: 39158 (GEAP-4751)
Cr–Ni, reactions with plutonia at high temperatures, 19: 39125(R) (BNWL-91)
Fe–Ni, martensite formation in, 19: 40283 (COO-1198-237)
Ni–Pd, neutron magnetic scattering in hydrogenated, 19: 40075 (IEA-84)
Ni–Pu, phase studies, 19: 39163(R) (MLM-1244)

NICKEL CHLORIDES
free energy of formation at 400 and 450°C, 19: 38575 (BNL-9343)
thermal decomposition mechanisms, 19: 39265(R) (IA-1021)

NICKEL IONS
radiolysis of aqueous solutions of, pulse, 19: 38728

NICKEL ISOTOPES Ni-56
energy levels of, detection using (p,t) reactions with nickel-58, (E), 19: 39819

NICKEL ISOTOPES Ni-58
helium-3 inelastic scattering by, DWBA analysis of, (T), 19: 39885
proton reactions (p,t) at 28 Mev, energy levels from, (E), 19: 39819

NICKEL ISOTOPES Ni-61
nuclear magnetic resonance in metallic nickel, 19: 39418

NICKEL SYSTEMS

Al–Fe–Mg–Ni–Si–Ti–Zr, coating with aluminum–nickel layers by chemical deposition, 19: 39143(P)
C–Cr–Fe–Mo–Ni, reinforcement of graphite by, 19: 39114(P)
C–Fe–Ni, martensite formation in, 19: 40283 (COO-1198-237)
Fe–Ni–WC, internal friction of, effects of composition on, 19: 39170(T) (FTD-TT-64-1001)
Ni–PuC–UC, thermal diffusivities of, 19: 39163(R) (MLM-1244)
Ni–ThO_2, properties of TD nickel as cladding material for SNAP hydride reactors, 19: 39166 (NAA-SR-Memo-11149)
Ni–UC, thermal diffusivities of, calculations of, 19: 39163(R) (MLM-1244)
Ni–WC, internal friction of, effects of composition on, 19: 39170(T) (FTD-TT-64-1001)

NIOBIUM
determination by x-ray fluorescence spectroscopy, 19: 38549
diffusion of atoms in bcc, activation energy for interstitial, (T), 19: 40086
effects on superconducting transition temperature of vanadium silicide, 19: 39196
enthalpy and heat capacity at 273 to 2740°K, (E/T), 19: 39217
magnetic field penetration in superconducting, radial velocity of, (E), 19: 39702
magnetic field penetration depth in superconducting, (E/T), 19: 39726
magnetocalorie effects in superconducting, reversible, (E), 19: 39703
magnetostriction in pure monocrystalline, 19: 39199
preparation and properties of single crystals of, 19: 39138
preparation of, electric arc reduction process for, 19: 39133
properties for use as fuel cladding material in reactors, 19: 39206
pulse transmission by coaxial cables of superconducting, (E), 19: 39740
reactions with plutonia at high temperatures, 19: 39125(R) (BNWL-91)
reactions with sodium at 2100 to 2400°C, 19: 39090(R) (ANL-7046(p. 78-82))
separation from waste water, methods for, 19: 40276

NIOBIUM ALLOYS
properties for use as fuel cladding material in reactors, 19: 39206
Al–Cr–Fe–Mo–Ni–Nb–Ti, thermal response and microstructure of Inconel 718 at 1200 and 1400°F, 19: 39158 (GEAP-4751)
Cr–Fe–Mo–Ni–Nb–W, tensile properties of IN-102, 19: 39156(R) (CEND-532)
Cr–Fe–Mo–Ni–Nb, thermal response and microstructure of Inconel 625 at 1200 and 1400°F, 19: 39158 (GEAP-4751)
Cr–Nb–Ti, mechanical properties for high-temperature applications, 19: 39192
Ge–Nb, superconductivity of Nb_3Ge, (E), 19: 39625
Nb–Ta, Hall effect in superconducting, (E), 19: 39710
Nb–Zr, analysis of, gamma spectra measurements in activation, 19: 38566
Nb–Zr, cavitation in bismuth–lead alloy at 500 and 1500°F, ultrasonic-induced, 19: 39116 (NP-15263)
Nb–Zr, magnetic field penetration in superconducting, radial velocity of, (E), 19: 39702
Nb–Zr, paramagnetism in cold-worked superconducting wires of, 19: 39749
Nb–Zr, properties for liquid metal loops, 19: 40112(R) (ANL-7046 (p.36-66))
Nb–Zr, properties of cold-worked fuel sheathing tubes of, 19: 39150 (AECL-2250(Pt.I))
Nb–Zr, pulse transmission by coaxial cables of superconducting, (E), 19: 39740
Nb–Zr, reactions with sodium at 2100 to 2400°C, 19: 39090(R) (ANL-7046(p.78-82))
Nb–Zr, strengthening by oxygen addition and quenching, 19: 39223(P)
Nb–Zr, superconductivity, 19: 39695
Sb–Nb, crystal structure of intermetallic compounds in, 19: 39209

NIOBIUM BORIDES
reactions with graphite to 2200°C, 19: 38654

NIOBIUM CARBIDES
GaC–NbC, preparation and crystal structure of H-phase in, 19: 39208
NbC–NbN, critical supercurrents in, (E), 19: 39688
Nb_2O_5–NbC, reduction of, electric arc method for, 19: 39133

NIOBIUM FLUORIDES
preparation and crystal structure, 19: 38640

NIOBIUM ISOTOPES Nb-95
content in diet and excreta in Japan, 19: 38894
determination in rain water, 19: 38557

NIOBIUM NITRIDES
NbC–NbN, critical supercurrents in, (E), 19: 39688

NIOBIUM OXIDES
thermodynamic stability at 1030 to 1300°K, 19: 38586 (UCRL-11957)
Nb_2O_5–NbC, reduction of, electric arc method for, 19: 39133

NIOBIUM SYSTEMS
C–Nb–W–Zr, fabrication and properties at –325 to 3000°F, 19: 39224(P)
Mo–Nb–Si, phase studies and properties of, 19: 39194

NITRATE COMPLEXES
with rare earths in aqueous and organic solutions, 19: 38578 (IA-1014)

NITRATE IONS
electron spin resonance in irradiated barium nitrate crystals, 19: 38730
production in tetrabutyl ammonium, 19: 39265(R) (IA-1021)
reactions with rare earths in solutions, 19: 39265(R) (IA-1021)

NITRITE IONS
radiolysis of aqueous solutions of, pulse, 19: 38728

NITROGEN
charged-particle density in plasma of, effects of surrounding gas pressure on, (E), 19: 39989(T)
chemical states in lithium and sodium, 19: 39157 (CNLM-6337)
determination in stainless steel, method for, 19: 38537 (ACF-7)
diffusion in bcc crystals, activation energy for interstitial, (T), 19: 40086
diffusion in uranium dioxide, model for, 19: 39219
diffusion of gases of, in temperature gradients, (E), 19: 39291
effect on specific electrical resistivity of tantalum crystals, 19: 39203
effects on yields of atomic hydrogen from electric discharge in low-pressure hydrogen, 19: 38590 (UCRL-16050)
electron reactions at low energies, energy dependence of ion pair production in, 19: 39375
helium ion reactions at 20 to 120 kev, electron capture in, (E), 19: 39407
ionization cross section for, electron-impact, 19: 38630
ionization in electron-bombardment ion sources, 19: 38838
ionization of, isotope effects on Franck-Condon factors in, 19: 38632
neutron reactions (n,n′γ) at 0 to 14 Mev, energy absorption in, 19: 39769 (SC-DC-65-1544)
quadrupole moments, 19: 39378
reactions with nitrogen ions in cathode region of glow discharge, 19: 38637
reduction of alkali halides by high-frequency electric discharge in, role of electrons in, 19: 39181
separation from nitrogen by gettering on hot titanium sponge, 19: 40177(R) (ANL-7046(p.1-35))
spectral line shifts and Stark width measurements in plasma of, 19: 39952 (AFCRL-65-348)

NITROGEN IONS
reactions with nitrogen molecules in cathode region of glow discharge, 19: 38637

NITROGEN ISOTOPES N-13
neutron separation energy for, (E), 19: 39862

NITROGEN ISOTOPES N-14
effects on fractional decomposition of diazonium salts, 19: 38690
energy levels in, isospin selection rules for transitions of 5.10 Mev, (T), 19: 39856
helium-3 reactions (He-3,α) with, (E), 19: 39941
neutron reactions (n,2n) at 14.6 Mev, total cross sections for, (E), 19: 39797
scattering by zirconium-90 and zirconium-96 at 44 Mev, Coulomb energy-level excitation in, (E), 19: 39942

NITROGEN ISOTOPES N-15
effects on fractional decomposition of diazonium salts, 19: 38690
energy levels of, analysis of spurious states owing to center-of-mass motion, (T), 19: 39812
proton reactions (p,α_0) and (p,γ_0) with, theory for, 19: 39805
use in measurements of self-diffusion in liquid ammonia, 19: 38579 (JUL-238-PC)

NITROGEN ISOTOPES N-16
half life, (E), 19: 39813

NITROGEN MUSTARDS
effects on induction of dental lesions in rats, mechanism of, 19: 38325

NITROGEN OXIDES
ionization cross section for, electron-impact, 19: 38630
ionization cross sections for negative-ion formation, electron-impact, 19: 38631
ionization of, isotope effects on Franck-Condon factors in, 19: 38632
properties as scavenger of water radiolysis products, 19: 38720
quadrupole moments, 19: 39378
radioinduced in atmospheres of industrial radiation facilities, 19: 38884
radiolysis of, effects of transition metal cations on, 19: 39265(R) (IA-1021)
H–NO, nuclear spin lattice relaxation in, 19: 39378
H–N_2O, nuclear spin lattice relaxation in, 19: 39378

NITROGEN SYSTEMS
acetylene–N_2–O_2, electron density in sulfur hexafluoride seeded flame plasma of, (E), 19: 40016
Ar–N, mixing at high temperatures, (E), 19: 40231 (LA-3229, pp 149-76)
H–N, nuclear spin lattice relaxation in, 19: 39378

NOISE
filters for electronic, optimization of, 19: 39270(R) (TID-21894)

NOMOGRAPHS
for estimation of microcuries and millimicrograms from counts per minute, 19: 38749
NONANE
radiation effects on reactions with carbon dioxide, 19: 38727(T)
NOSE
radiation sickness and blood loss effects on phosphorus-32 uptake by rabbit, 19: 38431
radiotherapy of chronic diseases of, by radon inhalation, 19: 38528
NOZZLES
plasma flow in, one-dimensional fully ionized, (T), 19: 40048
NUCLEAR BATTERIES
properties of promethium as fuel in, summary, 19: 39069 (BNWL-C-45)
NUCLEAR EMULSIONS
ion reactions at 10.4 Mev/nucleon, range-momentum relation for heavy recoil ions in, (E), 19: 39883
particle track length measurement in, design of micrometer for microscope with optical, 19: 39000
particle tracks in, device for automatic following of, 19: 39017
NUCLEAR ENGINEERING
conference on nuclear technology, France-Japan, Tokyo, Nov. 12 to 14, 1962, 19: 40302
NUCLEAR MAGNETIC RESONANCE
detection at low temperatures, equipment for, 19: 39011
NUCLEAR MATERIALS MANAGEMENT
bibliography on, annotated, 19: 39101 (TID-3315)
control of uranium fuel element fabrication, systems for, 19: 39130 (RFP-507)
control program for reprocessing enriched uranium scrap, 19: 38758 (Y-KA-7)
fuel assay, feasibility of nondestructive methods for, 19: 38547 (TID-21475)
materials management processing methods for fast reactor fuels, 19: 40177(R) (ANL-7046(p.1-35))
plutonium determination in spent fuels, metal, alloys, and compounds, review of methods for, 19: 38542 (LA-DC-6938)
plutonium handling and shipping, measurement problems in, 19: 38535 (RFP-508)
process vessel calibration for, 19: 38756 (RFP-488)
processing methods for irradiated fuels, 19: 40112(R) (ANL-7046 (p.36-66))
thorium fuel cycle process development, 19: 38755(R) (ORNL-3611)
NUCLEAR MODELS
alpha decay rates of deformed even-even nuclei in, (T), 19: 39793
potentials in, effects of short-range repulsive forces on, 19: 39814
reaction cross section calculations in, method for, (T), 19: 39935
NUCLEAR MODELS (SHELL)
energy levels in, jj-coupling model for spurious, (T), 19: 39812
even parity energy levels in oxygen-16 in jj-coupling, 19: 39806
NUCLEAR PHYSICS
book: *Concepts of Nuclear Physics*, 19: 39951
research, 19: 39788(R) (UCRL-12204, pp 1-27)
NUCLEAR POWER
development in Germany, 19: 40204
development status in Italy, 19: 40200
growth of civilian, estimated, 19: 40194 (WASH-1055)
review on British nuclear industry, 19: 40300
NUCLEAR POWER PLANTS
design of marine, using steam jet propulsion, 19: 40255(P)
design using heavy water moderated reactors, 19: 40211
development for space vehicles, (E/T), 19: 38836 (NASA-SP-79)
development in Japan, 19: 39064
feasibility of, in heavily populated areas, 19: 40207
use in digital computers in French, 19: 40203
NUCLEAR REACTIONS
analysis of (p,2p) and other knockout, for nuclear structure, (E), 19: 39904
analysis of stripping, using distorted-wave Born approximation, (T), 19: 39910
cross sections for, calculation in optical model, (T), 19: 39935
mechanisms of three-particle, (T), 19: 39894
particle correlations in, conference on, 19: 39893
resonances in, isobaric analog, (E/T), 19: 39875
theory for cluster stripping, distorted wave, 19: 39829
theory of, using few-level approximations, 19: 39805
NUCLEAR SPIN
effects in extracting alkali spin-exchange cross sections from Zeeman optical-pumping signals, (T), 19: 39879
relaxation in gases, 19: 39378
NUCLEAR STRUCTURE
analysis using (p,2p) and other knock-out reactions, (E), 19: 39904
NUCLEAR THEORY
potentials in, effects of short-range repulsive forces on, 19: 39814
reactions in, using few-level approximations, 19: 39805
t-matrix formalism in, 19: 39871
NUCLEI
alpha decay of even- and odd-mass, (T), 19: 39789
alpha decay rates of deformed even-even, shell model calculations of, (T), 19: 39793
charged-particle emission by heavy, evaporation theory for, 19: 39936
decay of radioactive, spectral shape in exponential, (T), 19: 39304
deuteron stripping reactions on, distorted-wave Born approximation for three-body, (T), 19: 39910
electron scattering by, meson (π) production in, (T), 19: 39621
energy gap for soft core potentials of, (T), 19: 39857
energy levels of, effects of temperature on, (T), 19: 40112(R) (ANL-7046(p.36-66))
energy levels of, analysis of spurious states owing to center-of-mass motion, (T), 19: 39812
gamma absorption by, total cross section for, (T), 19: 39873
gamma reactions (γ,α) with light, (T), 19: 39934
gamma spectra in powdered crystals, Mössbauer line broadening for measuring, 19: 39876
helium-3 inelastic scattering by, DWBA analysis of, (T), 19: 39885
inertial moments of asymmetric, (T), 19: 39831
model for, superfluid, (T), 19: 39687
neutrino reactions with, cross sections for, 19: 39943
nucleon pairing correlations in, effect of nuclear rotation on, (T), 19: 39858
nucleon-nucleon interaction in, tensor, (T), 19: 39872
particle elastic scattering by, formal theory for, 19: 39821
potentials of, effects of short-range repulsive forces on, (T), 19: 39814
proton reactions (p,2p) with, nuclear structure from, (E), 19: 39904
pseudopotentials of hard-sphere, (T), 19: 39651
quadrupole moments, (T), 19: 39791
structure of light, (T), 19: 39932
NUCLEI (CELLS)
chromosome analysis in photographs of, using flying-spot devices, (E), 19: 38910 (CERN-65-11(p.43-56))
radiation dosimetry of labeled DNA in, beta, 19: 38873 (BNL-9331)
radiation effects on, beta, 19: 38873 (BNL-9331)
radiation effects on bone marrow, synergistic effects of vibration, 19: 38358 (AD-612660)
NUCLEIC ACIDS
radiation effects on bacteriophage, EPR spectra, 19: 38365
NUCLEONS
binding energy of three-body system of, (T), 19: 39926
electromagnetic form factors of, extrapolation of, (E/T), 19: 39458 (CONF-796(Paper 24))
form factors of, determination for time-like momentum transfer, (T), 19: 39590
interactions at high energy, Regge-pole hypothesis in asymptotic amplitudes for, 19: 39478 (NP-15210)
interactions at high energies, isobar production in, (T), 19: 39508
interactions in nuclei, t-matrix formalism for, (T), 19: 39871
interactions in nuclei, tensor, (T), 19: 39872
interactions of, effects of short-range repulsions on nuclear potentials, (T), 19: 39814
interactions of, Hamada-Johnston potential for bound-state, (T), 19: 39570
interactions with antineutrinos, CERN experiments on, 19: 39612
interactions with deuterons, (T), 19: 39585
interactions with mesons (π^+) amplitudes for elastic, (T), 19: 39621
interactions with nucleons at 400 Mev, phase shift analysis for, (T), 19: 39469 (JINR-P-2170)
interactions with photons, meson (π) production in, (T), 19: 39498
interactions with nucleons, general operator potential for, 19: 39504
interactions with neutrinos, resonance production in, (T), 19: 39517
interactions with vector mesons, complex angular momentum in, (T), 19: 39518
interactions with nucleons, SU(6) predictions for, 19: 39532
interactions with mesons (π), peripheral production and decay of mesons (ρ) in, (E/T), 19: 39576
interactions with mesons (K), peripheral production and decay of K^* in, (E/T), 19: 39576
interactions with mesons (K) at low energies, model for, (T), 19: 39592
interactions with mesons (π) at high energies, analyses of final-state, (E/T), 19: 39574
interactions with vector bosons, complex angular momentum in, (T), 19: 39518
many-body problem in quantum mechanics, Coriolis coupling in, (E), 19: 39948

pairing correlations in nuclei, effects of nuclear rotation on, (T), 19: 38858
theory of three-body system of, (T), 19: 39923
NUCLEOPROTEINS
radiation effects on synthesis of, by gonocytes in rat testes, 19: 38370
NUCLEOSIDES
radiation effects on bacteriophage, EPR spectra, 19: 38365
NUCLEOTIDES
genetic code for, during synthesis of messenger ribonucleic acid, 19: 40296 (TID-21856)
radiation effects on bacteriophage, EPR spectra, 19: 38365

O

OATS
radioinduced mutations in, effects of ploidy on frequency of thermal neutron, 19: 38419
OCEANOGRAPHY
measurement of deep-water Tsunami-like waves, 19: 40288(R) (NVO-98-5)
OCTANE
deuterium exchange with heavy water, group VIII metal catalysis of, 19: 38597
diffusion in deuterated-normal mixture, coefficients of, 19: 38646
reduction of platinic oxide by labeled, preparation of platinum oxide catalysts by, 19: 38596
OHMMETERS
design for reactor coolant analysis, 19: 40262 (ZFK-RN-17(p.25-31))
OILS
analysis for sodium by neutron activation methods, 19: 38550
OOGENESIS
radioinduced mutations in Dahlbominus, gamma and x-ray, 19: 38392
OPTICAL SYSTEMS
book: *Electromagnetic Theory and Geometrical Optics*, 19: 39310
computer program for flying-spot analysis of particle-track photographs, (E), 19: 38981 (CERN-65-11(p.115-21))
computer programs for use with flying-spot analyzers, (E), 19: 38980 (CERN-65-11(p.97-113))
description of flying-spot system for identifying bubble-chamber photographs, (E), 19: 38979 (CERN-65-11(p.91-5))
design of modulating, temperature effects on, 19: 39269(R) (SU-SEL-64-133)
flying-spot devices for analysis of particle-track photographs, (E), 19: 38986 (CERN-65-11(p.173-81))
flying-spot devices for analysis of particle-track photographs, (E), 19: 38987 (CERN-65-11(p.207-18))
flying-spot devices for analysis of particle-track photographs, (E), 19: 38988 (CERN-65-11(p.183-206))
flying-spot devices for ionization measurements along bubble-chamber tracks, 19: 38989 (CERN-65-11(p.219-27))
flying-spot devices for analysis of particle-track photographs, (E), 19: 38990 (CERN-65-11(p.229-36))
flying-spot devices for analyzing particle-track photographs, (E), 19: 38991 (CERN-65-11(p.237-58))
operation of flying-spot system for analyzing spark-chamber photographs, (E), 19: 38972 (CERN-65-11(p.7-13))
operation of flying-spot devices for analysis of spark-chamber photographs, (E), 19: 38974 (CERN-65-11(p.25-33))
operation of flying-spot system for analysis of spark-chamber photographs, (E), 19: 38975 (CERN-65-11(p.35-41))
operation of flying-spot system for analysis of spark-chamber photographs, (E), 19: 38976 (CERN-65-11(p.57-69))
operation of flying-spot systems for analyzing spark-chamber photographs, (E), 19: 38977 (CERN-65-11(p.71-9))
operation of PEPR flying-spot device for analyzing bubble-chamber data, (E), 19: 38978 (CERN-65-11(p.81-90))
particle track analysis using computerized flying-spot devices, (E), 19: 38984 (CERN-65-11(p.145-52))
particle-track analysis using computerized flying-spot devices, (E), 19: 38985 (CERN-65-11(p.153-72))
performance of flying-spot systems for analyzing spark-chamber photographs, (E), 19: 38973 (CERN-65-11(p.15-23))
uses of flying-spot analyzers for chromosome-photograph analysis, (E), 19: 38910 (CERN-65-11(p.43-56))
uses of flying-spot devices for particle-track analysis, (E), 19: 38983 (CERN-65-11(p.139-43))
uses of flying-spot devices for analyzing particle-track photographs, (E), 19: 38982 (CERN-65-11(p.123-37))
ORGANIC COMPOUNDS
analysis for elements and trace impurities by neutron activation methods, 19: 38558
determination of gaseous, in vacuum systems, 19: 38564
radioinduced bromination in aqueous solutions of, mechanisms of, 19: 39265(R) (IA-1021)
ORGANIC COMPOUNDS, METALLO-
Mössbauer parameters for iron and tin, 19: 38576 (CONF-650425-2)
tin-119 Mössbauer effects in, 19: 38577 (CONF-650425-3)
ORGANIC COOLED REACTORS
construction of Essor, use of PERT method for design and installation phases in, 19: 40265
fuel element failure in, circuits for detecting, 19: 40133
materials evaluation for, (E), 19: 40218
ORGANIC MODERATED REACTOR EXPERIMENT
fuel element design and fabrication, 19: 40187 (NAA-SR-Memo-7753)
ORGANISMS
uranium content in benthos, in Lake Issyk-kul, USSR, 19: 38855
ORIFICES
flow through series of two eccentrically positioned, pressure drop characteristics, 19: 38810 (RL-SA-31)
ORNL RESEARCH REACTOR
operation of, Jan.–Mar. 1965, 19: 40259(R) (ORNL-TM-1181)
OROTIC ACID
radiosensitivity effects on mice, x, 19: 38458
OSCILLATORS
interactions with wave fields, transitions in, 19: 39270(R) (TID-21894)
OSCILLOGRAPHS
fabrication of computer-operated, 19: 39269(R) (SU-SEL-64-133)
OSMIUM ISOTOPES Os-192
energy levels of, g factors of excited, (E), 19: 39833
neutron reactions (n,α) at 14 Mev, tungsten-189 production in, (E), 19: 39801
OXIDATION
in rat brain, effects of vibration on, 19: 38358 (AD-612660)
OXIMES
8-hydroxyquinaldic, complexes with thorium in chloroform and perchlorate solutions, 19: 38567
OXYGEN
chemical states in lithium and sodium, 19: 39157 (CNLM-6337)
determination in beryllium by activation, 19: 38546(R) (RFP-552)
determination in earth formations by pulsed neutron activation, well-logging method for, 19: 38871(P)
determination in sodium, 19: 38539 (APDA-168)
diffusion in bcc crystals, activation energy for interstitial, (T), 19: 40086
diffusion in molybdenum and tungsten at 1500 to 1800°C, 19: 39072(R) (NP-15187)
diffusion in uranium dioxide, model for, 19: 39219
diffusion rate through molybdenum and tungsten at 1500 to 1800°C, 19: 39070(R) (GEST-2046)
effect on specific electrical resistivity of tantalym crystals, 19: 39203
effects on cesium ion and neutral emission from hot porous tungsten, 19: 39164 (N64-22193)
effects on radioinduced polymerization of acrylamide–propionamide solid solutions, 19: 38694 (BNL-9200)
effects on radiosensitivity and recovery in Drosophila spermatogenesis, 19: 38463
effects on radiosensitivity of tumors, 19: 38374
effects on strength of zirconium-base alloys, 19: 39223(P)
effects on vapor pressure of plutonium, 19: 39159 (LA-DC-6926)
effects on yields of atomic hydrogen from electric discharge in low-pressure hydrogen, 19: 38590 (UCRL-16050)
helium ion reactions at 20 to 120 kev, electron capture in, (E), 19: 39407
hyperbaric, effects on results of radiotherapy of cancers, 19: 38500
ionization cross section for, electron-impact, 19: 38630
ionization cross sections for negative-ion formation, electron-impact, 19: 38631
ionization of, isotope effects on Franck-Condon factors in, 19: 38632
microwave emission from atmospheric, measurement of, (E/T), 19: 39270(R) (TID-21894)
migration in uranium dioxide at high temperatures, 19: 39154 (BNWL-SA-54)
neutron reactions (n,n´γ) at 0 to 14 Mev, energy absorption in, 19: 39769 (SC-DC-65-1544)
oxidative effects on hafnium–tantalum alloys, 19: 39123
quadrupole moments, 19: 39378
radiosensitivity effects on growth in cereal seedlings, 19: 38418
radiosensitivity effects on Ehrlich ascites tumors at various intervals following inoculation into mice, x, 19: 38402
reactions with carbon and graphite at 500 to 600°C, kinetics of, 19: 39119
reactions with single-crystal uranium carbide at 900°C, 19: 40286(R) (NAA-SR-11200)
sorption by liquid sodium from stainless steel containers, 19: 40177(R) (ANL-7046(p.1-35))

sorption on nickel, high-energy electron diffraction studies of, 19: 39178
sorption on rhenium and tungsten, (E/T), 19: 39103
OXYGEN ISOTOPES O-15
energy levels of, analysis of spurious states owing to center-of-mass motion, (T), 19: 39812
OXYGEN ISOTOPES O-16
deuteron reactions (d,γ) at 0.4 to 3.5 Mev, cross sections for, (E), 19: 39830
energy levels in, jj-coupling shell model analysis of even-parity, 19: 39806
energy levels of, analysis of spurious states owing to center-of-mass motion, (T), 19: 39812
gamma absorption by, with two-nucleon emission, (T), 19: 39932
helium-3 reactions (He-3,α) with, (E), 19: 39941
meson (π^-) absorption by, with two-nucleon emission, (T), 19: 39932
neutron reactions (n,p) at 12 to 17 Mev, cross sections, (E), 19: 40163
neutron scattering at 0.5 to 4 Mev, phase shifts analyses for, (E), 19: 39785 (ORNL-P-1356)
reactions (O-16, N-15) with boron-11 at 30 Mev, (E), 19: 39869
OXYGEN ISOTOPES O-17
energy levels of, analysis of spurious states owing to center-of-mass motion, (T), 19: 39812
OXYGEN ISOTOPES O-18
spectra of, reaction-matrix analysis of single-particle, (T), 19: 39815
OXYGEN SYSTEMS
acetylene–N_2–O_2, electron density in sulfur hexafluoride seeded flame plasma of, (E), 19: 40016
As–O, combustion of tantalum and zirconium in, 19: 38583(R) (SC-DC-65-1480)
H–O, nuclear spin lattice relaxation in, 19: 39378
O–U, phase studies, 19: 39125(R) (BNWL-91)
OZONE
bibliography on atmospheric, 19: 39260 (LA-3328)
radioinduced in atmospheres of industrial radiation facilities, 19: 38884
OZONOSPHERE
properties of, bibliography on, 19: 39260 (LA-3328)

P

PACKAGING
of disassembled fuel elements and radioactive waste in hot cells, 19: 40270 (JUL-249-RW)
PACKED COLUMNS
liquid flow through beds, axial dispersion in, 19: 38812 (UCRL-11951)
PAINTS
development of luminous, 19: 39265(R) (IA-1021)
PALLADIUM
catalytic properties in deuterium exchange reactions, 19: 38597
effects on superconducting transition temperature of vanadium silicide, 19: 39196
electric potential of electrodes of, in water-heavy water solutions, 19: 38608
radiation damage in, cross sections for atomic displacements from 1- to 3-Mev electrons, 19: 39225 (AFCRL-65-286)
PALLADIUM ALLOYS
Ce–Pd, phase studies, 19: 39163(R) (MLM-1244)
Ni–Pd, neutron magnetic scattering in hydrogenated, 19: 40075 (IEA-84)
PAPER
weight per unit surface of, radiometric methods of measuring, 19: 39063
PARABIOSIS
radiation effects on erythropoiesis in cross-circulated dogs, 19: 38382
PARAFFIN
cosmic particle reactions at high energies, angular distributions from, (E), 19: 39428
neutron albedo measurement on, thermal, 19: 40065 (NP-15152)
paraffin–UO_2–ZrO_2, neutron spectra in, asymptotic and steady-state, (E), 19: 39768 (RPI-328-21)
PARTICLE TRACKS
analysis in spark chambers, using flying-spot devices, (E), 19: 38973 (CERN-65-11(p.15-23))
analysis of bubble chamber, computer utilization for, 19: 38970 (BNL-9236)
analysis of bubble-chamber, using flying-spot devices, (E), 19: 38978 (CERN-65-11(p. 81-90))
analysis of bubble-chamber, using computerized flying-spot systems, (E), 19: 38980 (CERN-65-11(p.97-113))
analysis of bubble-chamber, using flying-spot devices, (E), 19: 38982 (CERN-65-11(p.123-37))
analysis of spark-chamber, using flying-spot system, (E), 19: 38972 (CERN-65-11(p.7-13))
analysis of spark-chamber, using flying-spot devices, (E), 19: 38974 (CERN-65-11(p.25-33))
analysis of spark-chamber, using flying-spot devices, (E), 19: 38976 (CERN-65-11(p. 57-69))
analysis of spark-chamber, using flying-spot devices, (E), 19: 38977 (CERN-65-11(p.71-9))
analysis of, computer programs for flying-spot, (E), 19: 38981 (CERN-65-11(p.115-21))
analysis of, using programmed flying-spot devices, (E), 19: 38987 (CERN-65-11(p.207-18))
analysis of, using programmed flying-spot devices, (E), 19: 38990 (CERN-65-11(p.229-36))
analysis using Chloe flying-spot system, (E), 19: 38975 (CERN-65-11 (p. 35-41))
analysis using computerized flying-spot devices, (E), 19: 38983 (CERN-65-11(p.139-43))
analysis using computerized flying-spot devices, (E), 19: 38984 (CERN-65-11(p.145-52))
analysis using computerized flying-spot devices, (E), 19: 38985 (CERN-65-11(p. 153-72))
analysis using flying-spot devices, (E), 19: 38971 (CERN-65-11)
analysis using flying-spot devices, (E), 19: 38988 (CERN-65-11 (p.183-206))
analysis using programmed flying-spot devices, (E), 19: 38986 (CERN-65-11(p.173-81))
analysis using programmed flying-spot devices, (E), 19: 38991 (CERN-65-11(p.237-58))
formation, detection, and uses in solids, research on, 19: 39226(R) (AFCRL-65-305)
identification in solids by chemical etching, 19: 39038
ionization measurements in bubble-chamber, using flying-spot devices, (E), 19: 38989 (CERN-65-11(p.219-27))
measurement in nuclear emulsions, design of equipment for, 19: 39000
PARTICLES
interaction potentials of classical many-body systems of, long- and short-range, 19: 39284
interactions of many, canonical position variables in relativistic theory of, 19: 39645
motion in fluidized beds, 19: 38782 (ORNL-TM-1170)
radiation monitoring of airborne, equipment for, 19: 39050(P)
scattering by nuclei, formal theory for elastic, 19: 39821
size analyzer calibration for, 19: 40286(R) (NAA-SR-11200)
PATHOLOGY
of radiation sickness, 19: 38433(T)
of radiation sickness in animals, 19: 38436(T)
PEACH BOTTOM POWER REACTOR
criticality studies at zero power, 19: 40183(R) (GA-5924)
development and testing at zero power, 19: 40184(R) (GA-6406)
PEBBLE BED REACTORS
fuel management in fast, 19: 40178 (BNL-9279)
PENTAERYTHRITOL TETRANITRATE
electric conductivity of detonation products of, 19: 40284 (LA-DC-6993)
properties as low-density and low-pressure solid explosive, 19: 38589 (UCRL-14186)
PENTANE, 2,4-DIMETHYL-
radiolysis G values and products of, 19: 40286(R) (NAA-SR-11200)
PENTANE, 2-METHYL-
radiation effects on bromine-80 and -82 retentions in, isomeric transition reaction in, 19: 38715
PENTANE, 3-METHYL-
radiation effects on bromine-80 and -82 retentions in, isomeric transition reaction in, 19: 38715
2,4-PENTANEDIONE
bromination of, deuterium isotope effects on, 19: 38692
PENTANES
radiolysis of, effects of tetrachloroethylene on, 19: 39265(R) (IA-1021)
yields in gamma radiolysis of liquid cyclopentane, 19: 38712
1-PENTENE
yields in gamma radiolysis of liquid cyclopentane, 19: 38712
PENTOSES
radiation effects on bacteriophage, EPR spectra, 19: 38365
PEPTIDES
radiation effects on bacteriophage, EPR spectra, 19: 38365
PERCHLORATE IONS
radiolysis of aqueous solutions of, pulse, 19: 38728
PERLITE
compaction in large dewars by thermal cycling, 19: 38779 (LA-DC-7158)
PEROXIDES
determination of *tert*-butyl perbenzoate in thermosetting molding powders, 19: 40285 (MLM-1284)
PEROXYBENZOIC ACIDS
determination of *tert*-butyl ester of, in thermosetting molding powders,

19: 40285 (MLM-1284)
PERSONNEL
instruction of, classification of teaching machines for, 19: 40291 (SC-R-65-923)
radiation dosimetry of medical, in accident clinic, 19: 38477
radiation exposure of medical, assessment of occupational, 19: 38474
radiation protection of, clothing, materials, and methods for individual, 19: 38475
radiation protection of, policies for external and internal, 19: 38479
radiation protection of medical, during therapeutic use of brachycurie sources, 19: 38514
PERTURBATION THEORY
energy eigenvalues in Schrödinger, inhomogeneous-equation and partitioning techniques for, 19: 39650
energy variables in graphs of, interaction of, (T), 19: 39512
for many-boson system, structure factor for, 19: 39261(R) (AROD-3979:2)
formalism for magneto-optical phenomena in many-electron systems, 19: 40100
formalism for weak-strong coupling complementarity in renormalized, 19: 39521
PERU
geology of Cuzco-Anta-Urubamba area, Cuzco Department, 19: 38845 (RME-4584)
PESTICIDES
synthesis of carbon-14 labeled 4-dimethylamino-3,5-xylyl methylcarbamate, 19: 38748
PETROLEUM
radiation processing, 19: 39066
radiation-thermal cracking of, at 1 to 30 atm in uniform temperature and dose field, gamma, 19: 38726(T)
PHANTOMS
plastic scintillator, integral dose measurement using, 19: 38893
PHARMACEUTICALS
purification of iodine-131 labeled sodium *o*-iodohippurate for intravenous use, ion exchange, 19: 38507
radiosterilization of, use of electron accelerators in, 19: 39063
technetium-99 labeled, radiation dose measurements for internally deposited, 19: 38506
PHENANTHRENE
radiation effects on, x-ray scattering from defects in neutron, 19: 39230 (BNL-9332)
PHENETHYLAMINE
carbamate, carbon-14 activity in, in liquid scintillation mixtures, 19: 38746
PHENOBARBITAL
effects on learning ability of rats, 19: 38361(R) (TID-21951)
PHENOL
radiostability of ion-exchange resins based on, (E), 19: 40129 (ZFK-RN-17(p.114-26))
use of resin of, with hexamethylenetetramine in production of carbon with reduced porosity, 19: 38684(P)
PHENOL, *p*-PHENYL-
fluorescence in aqueous solution, 19: 38687 (EUR-2423.e)
PHENOTHIAZINE, 2-CHLORO-10-(3-DIMETHYLAMINOPROPYL)-
effects on learning ability of rats, 19: 38361(R) (TID-21951)
PHONONS
absorption of transverse, by aluminum-lead superconducting diodes, (E), 19: 39713
interactions of, thermodynamic perturbation theory for forbidden three-body, 19: 40096
interactions with electrons in magnetic fields, dispersion relations for, 19: 39270(R) (TID-21894)
interactions with electrons in metals, strong-coupling, (T), 19: 40073 (CONF-796(Paper 1))
interactions with electrons, Born approximation for, (T), 19: 40106
propagation in quartz, incoherent, (E/T), 19: 39270(R) (TID-21894)
scattering by point defects, resonant, 19: 40109
PHOSPHATE GLASS
radiation effects on, (E/T), 19: 39256
PHOSPHATES
effects on strontium-90 metabolism in mammals, 19: 38335 (NP-14926)
PHOSPHINE
triphenyl-, neutron reactions with, chemical properties of phosphorus-32 formed in, 19: 38700
PHOSPHINE OXIDE, TRIPHENYL-
neutron reactions with, chemical properties of phosphorus-32 formed in, 19: 38700
PHOSPHONATES
di-sec-butylphenyl-, solvent properties for uranium, 19: 38755(R) (ORNL-3611)
PHOSPHONIC ACID, BUTYL, DIBUTYL ESTER
dibutylbutylphosphonate–xylene, solvent properties for americium from nitrate solutions, 19: 38750 (HW-81166)
PHOSPHONIUM CHLORIDES
tetraphenyl-, neutron reactions with, chemical properties of phosphorus-32 formed in, 19: 38700
PHOSPHORIC ACID, BIS(2-ETHYLHEXYL) ESTERS
solvent properties for beryllium, 19: 39107
PHOSPHORS
performance in scintillation detectors, review of, 19: 38995 (NP-15259)
radioinduced luminescence of, sample compartment for measuring x, 19: 38936
radioluminescence of thallium-activated potassium iodide, effects of activator concentration on, 19: 38735
scintillation properties of polyphenyl, effects of steric inhibition of resonance on, 19: 38691
stability of carbon-14-labeled phenylethylamine carbamate in liquid, 19: 38746
use of plastic, in integral dose determination, 19: 38893
PHOSPHORUS
determination in bronze by x-ray spectrography, 19: 38571
effects of radioactive, on denatured and whole serum in rats, 19: 38368
separation from waste water, methods for, 19: 40276
PHOSPHORUS COMPOUNDS
organic, synthesis of, 19: 39265(R) (IA-1021)
PHOSPHORUS ISOTOPES P-31
proton reactions (p,n) at 7.5 to 13.0 Mev, levels from, (E), 19: 39827
PHOSPHORUS ISOTOPES P-32
adhesion to metal plates as beta sources, 19: 38745 (Y-1484)
colloids, use in treatment of malignant effusions, energy levels for, 19: 38515
determination with carbon-14 on chromatograms, method for, 19: 38561
radiation sickness and blood loss effects on uptake of, by ear, nose, and throat in rabbits, 19: 38431
use in studies on enamel surface on teeth, 19: 38352
yields from neutron reactions with triphenylphosphine, triphenylphosphine oxide, and tetraphenylphosphonium chloride, 19: 38700
PHOSPHORUS OXIDES
reactions with alcohols, products of, 19: 39265(R) (IA-1021)
PHOSPHORUS SYSTEMS
As–Ga–P, electric, metallurgical, and optical properties of, (E), 19: 39269(R) (SU-SEL-64-133)
PHOTOELECTRIC CELLS
radiation effects on selenium, gamma, (E), 19: 39058
PHOTOELECTRIC EFFECT
cross sections for gamma radiation at 662 kev, method of measuring K-shell, 19: 39376
PHOTOGRAPHIC FILM
identification systems for bubble-chamber, computerized, (E), 19: 38979 (CERN-65-11(p.91-5))
particle track analysis on, using flying-spot devices, (E), 19: 38981 (CERN-65-11(p.115-21))
particle track analysis in, using flying-spot devices, (E), 19: 38982 (CERN-65-11(p.123-37))
particle track analysis on, using flying-spot devices, (E), 19: 38983 (CERN-65-11(p.139-43))
particle track analysis in, using computerized flying-spot devices, (E), 19: 38984 (CERN-65-11(p.145-52))
particle track analysis in, using computerized flying-spot devices, (E), 19: 38985 (CERN-65-11(p.153-72))
particle track analysis in, using programmed flying-spot devices, (E), 19: 38986 (CERN-65-11(p.173-81))
particle track analysis in, using flying-spot devices, (E), 19: 38987 (CERN-65-11(p.207-18))
particle track analysis in, using flying-spot devices, (E), 19: 38988 (CERN-65-11(p.183-206))
particle track analysis in, using flying-spot devices, (E), 19: 38989 (CERN-65-11(p.219-27))
particle track analysis in, using programmed flying-spot devices, (E), 19: 38990 (CERN-65-11(p.229-36))
particle track analysis in, using programmed flying-spot devices, (E), 19: 38991 (CERN-65-11(p.237-58))
particle-track analysis in, using Chloe flying-spot systems, (E), 19: 38975 (CERN-65-11(p.35-41))
PHOTOGRAPHIC FILM DETECTORS
filter system for badge, 19: 39052(P)
PHOTOMETRY
analytical use of flame, for determining strontium in bone, 19: 38345
PHOTOMULTIPLIER TUBES
performance for detecting cosmic showers using atmospheric fluorescence, 19: 39422(R) (TID-21895)
refrigeration unit for cooling, for alpha counting by liquid scintillation,

19: 38546(R) (RFP-552)
PHOTON SHOWERS
production in electron reactions with lead at 100 to 1000 Mev, (T), 19: 40070
PHOTONS
charge acquisition in minimal interactions of, (T), 19: 39513
detection methods for interactions of, 19: 39041
emission in elementary particle decays, rate of, (T), 19: 39620
flux of solar, variation with depth in photosphere, (T), 19: 39342
interactions in Bev range, 19: 39616
interactions in lead, meson (π^0) production in, (E), 19: 39620
interactions of, detection of stimulated, (E), 19: 39264 (CONF-796 (Paper 14))
interactions with protons, meson (η) production and decay in, (E), 19: 39620
interactions with protons, meson (K^+) production in, (E), 19: 39620
interactions with protons, production of vector mesons in, (T), 19: 39621
interactions with protons, meson (π^0) production in, 19: 39623
interactions with mesons (π) in SU(3) and SU(6), 19: 39470 (JINR-P-2171)
interactions with nucleons at high energy, Regge-pole hypothesis in asymptotic amplitudes for, 19: 39478 (NP-15210)
interactions with nucleons, meson (π) production in, (T), 19: 39498
interactions with protons, meson (π^+) production near first resonance, (E), 19: 39597
interactions with protons, cross sections and angular distributions for mesons (π^0) and (π^+) production in, (E), 19: 39620
production of polarized, method of, 19: 39622
properties of, quantum laws for, (T), 19: 39661
reactions with semiconductors at 2 to 6 ev, spectral analysis of electron-emission yields in, 19: 39406
theory in coexistence with waves in electromagnetic radiations, double solution for, (T), 19: 39640
thermodynamic properties of in plasma of, astrophysical relations of, (T), 19: 39339
PHOTOPROTONS
energy distribution from silicon-28, (E), 19: 39938
PHYSICS
research, 19: 39271(R) (UCRL-12204)
research at IFA, 19: 40287(R) (NP-15188)
shock wave studies in, 19: 39274(T) (JPRS-30799)
PHYSIOLOGY
conference on simulation in space technology, 19: 38784
effects of space flight conditions on, of mammals, 19: 38358 (AD-612660)
radiation effects on, of rats exposed *in utero*, 19: 38361(R) (TID-21951)
research programs on neuro-, 19: 39270(R) (TID-21894)
PIEZOELECTRIC CRYSTALS
radiation effects on quartz, transient, 19: 39055 (GA-6266)
PIGMENTS
radiation effects on structure of, in cooked meats, 19: 39065
PINCH DEVICES
plasma stability in slow theta, (E), 19: 39996
PINCH EFFECT
plasma electron densities in theta, (E), 19: 39978
plasma electron density in fast theta, measurement of time-dependent, (E), 19: 39979
plasma motion in asymmetric fields in theta, (E), 19: 40010
plasma rotation in theta, (T), 19: 39974
plasma stability in theta, field and impurity effects on, (E), 19: 40005
PIPES
development of heat, survey, 19: 38780 (LA-DC-7206)
flow from, two-phase blowdown transients, 19: 38802 (APED-4827)
rupture of, program for study of, 19: 38824 (GEAP-4474)
PIQUA POWER REACTOR
core II and fuel elements for, design of, 19: 40286(R) (NAA-SR-11200)
PITUITARY GLAND
radiation effects on morphology of rat, fast neutron, 19: 38444
PLACENTA
permeability of rabbits and swine, tracer study, 19: 38344
PLANETS
spectra of Venus at 1-cm wavelength, (E/T), 19: 39270(R) (TID-21894)
PLANKTON
uranium content in, in Lake Issyk-kul, USSR, 19: 38855
PLANTS
population studies on, in uranium areas of Upper Colorado River Basin, Utah, 19: 38330 (TID-22078)
radiation effects on growth of sedges, 19: 38331
radiation effects on growth and reproduction of gladiolus, 19: 38430
radiation effects on reproduction of gladiolus, 19: 38430
radiation effects on, theoretical bases for mutagenic, 19: 38420
transpiration in, tracer studies of reverse, 19: 39265(R) (IA-1021)
uranium content in, in Lake Issyk-kul, USSR, 19: 38855
PLASMA
acceleration, by coaxial guns, 19: 39956 (LA-DC-7043)
acoustic wave properties in, correlation with radar auroral reflection data, (T), 19: 39678
atom injection at 20 kev in hydrogen, 19: 39970 (ORNL-P-1374)
book: *Reviews of Plasma Physics*. Vol. I., 19: 40054(T)
Brownian motion in relativistic, Wiener integrals from, (T), 19: 39959 (N64-22435)
charged-particle beam motion through, longitudinal instabilities in, (T), 19: 40008
charged-particle density in, effect of surrounding gas pressure on, (E), 19: 39989(T)
charged-particle motion in, equations for, (T), 19: 40006
Cherenkov radiation generation by charged particles in, (T), 19: 39995
containment at ion cyclotron resonances, r-f, 19: 39270(R) (TID-21894)
containment by h-f electromagnetic fields, (T), 19: 39982
containment by magnetic mirrors, cooperative effects in, (E), 19: 40017
containment in creep-geometry, apparatus for, 19: 40060(P)
containment in magnetic-mirror traps, 19: 40046
containment in multipole magnetic fields, (E), 19: 39954(R) (COO-1233-20)
containment of high-temperature, in magnetic mirrors, 19: 40045
containment of, design of stuffed-cusp facility for, 19: 39270(R) (TID-21894)
containment using electrostatic potential wells, (T), 19: 40032
correlations and fluctuations in, connection between, (T), 19: 40024
current density in, third harmonic of, (T), 19: 40011
current distribution and space-charge in, 19: 39962 (NP-15167)
cyclotron wave propagation and instabilities in warm magneto-, (T), 19: 40027
density modulations in r-f, (E), 19: 40026
density of electron-cyclotron resonance-discharge, oscillations of, 19: 39270(R) (TID-21894)
density spatial distribution of, microwave-refraction determination of, (E/T), 19: 39965 (NP-15203)
diagnostics of arc, by Thompson scattering, 19: 39270 (TID-21894)
diagnostics of low-temperature, spectroscopic method for, 19: 39960(R) (N64-33202)
diagnostics of shock-produced, using microwave reflection, (E), 19: 39997
diagnostics of thermally ionized alkali, microwave, (E), 19: 39980
diagnostics of, electron beam, 19: 39972(R) (SU-IPR-17)
diagnostics of, h-f laser interferometry in, (E/T), 19: 39993
diagnostics of, probe for, 19: 40038
diagnostics of, using Langmuir probes, 19: 39270(R) (TID-21894)
dielectric permeability tensor of isothermal, complex, (T), 19: 40042
diffusion in Q-1 device, Bohm, (T), 19: 40014
dispersion diagrams for hot-electron, 19: 39270(R) (TID-21894)
effects on thermionic diode in autonomous discharges, 19: 39435(T) (JPRS-31048)
electric conductivity of neon positive-column discharge, (E), 19: 40041
electric current density distribution in coaxial gun, (E), 19: 39998
electric current flow in, effects of binary collisions on, 19: 39269(R) (SU-SEL-64-133)
electron beam interactions with, stability in, 19: 39972(R) (SU-IPR-17)
electron beam reactions with, microwave amplification by, (E), 19: 40036
electron cyclotron absorption in cesium, 19: 39270(R) (TID-21894)
electron density and temperature distribution in argon, optical study of, (E), 19: 40039
electron density in hydrogen, (E), 19: 39978
electron density in fast theta pinch discharge, (E), 19: 39979
electron density in supersonic, at low pressures, (E), 19: 39987
electron density in sulfur hexafluoride seeded flame, (E), 19: 40016
electron distribution function in time-varying, form of, (T), 19: 40015
electron E-layer formation in Astron, (T), 19: 39973 (UCRL-14131)
electron temperature and ion densities in barium, measurement of, 19: 39958 (MATT-327)
electron temperature increases in MHD cell, (T), 19: 39437
electron transport in three-component, 19: 39270(R) (TID-21894)
electron velocities in, measurement method for, 19: 39270(R) (TID-21894)
electrostatic waves in, gaps in spectra of, (T), 19: 40025
equilibrium in low-current arcs, thermal, 19: 39976
equilibrium in low-current arcs, (E), 19: 39977
equilibrium of toroidal, with finite inertia and resistivity, (T), 19: 40003
explosion bubble expansion and retardation of cold, multiple bounce theory for, (T), 19: 39344
flow around magnetic dipole, (E), 19: 40009
flow in magnetohydrodynamic cells, kinetic equations for non-equilibrium, (E/T), 19: 39440

flow of fully ionized, steady-channel one-dimensional nozzle, (T), 19: 40048
flux of interplanetary, solar wind theory for, 19: 39364
heating by electron beams, 19: 39969 (ORNL-P-1373)
heating by magnetic field compression of, (T), 19: 39991
heating by shock waves, turbulent, 19: 40047
injectors of pulsed, research on coaxial and end-type, 19: 39955 (IAE-663)
interactions of bunches of, with magnetic fields, research on, 19: 39955 (IAE-663)
interactions with electron beams, effects of beam wave amplification on, 19: 39269(R) (SU-SEL-64-133)
interactions with electromagnetic waves in cavities and waveguides, 19: 39270(R) (TID-21894)
ion cyclotron waves in, collision effects on, (T), 19: 40021
ion cyclotron waves in, stability of finite amplitude, (T), 19: 40022
ion losses in energetic hydrogen, microinstability driven, (E), 19: 39967 (ORNL-P-1337)
ion wave propagation in, 19: 39972(R) (SU-IPR-17)
ion waves in, (E), 19: 39988
ionization degree of, formula for, 19: 40058(T)
ionization development in crossed-field hydrogen, 19: 39961 (NP-15112)
ionization in MHD cells, nonequilibrium, (T), 19: 39438
light emission from argon, spectra intensity of, 19: 39270(R) (TID-21894)
light scattering by, resonances in, (T), 19: 40029
light scattering by, second harmonic, (T), 19: 40050
light scattering from, stimulated incoherent, (T), 19: 40012
light spectra of theta-pinch, light shutter for measuring, 19: 38942
magnetic field measurements, (T), 19: 40059
magnetic fields in dissipative, structure of axisymmetric force-free, (T), 19: 40049
microwave emission from Zeta, electron density and temperature from, (E), 19: 39953 (CLM-R-40)
microwave interactions in inhomogeneous anisotropic column of, in magnetic field, (T), 19: 39994
microwave propagation in, transient, (T), 19: 40034
microwave scattering by space-charge waves of magneto-, (E), 19: 40033
microwave transient phenomena in isotopic collisionless, (T), 19: 40035
models of beam-generated, computer analyses of, 19: 39269(R) (SU-SEL-64-133)
motion of theta-pinch, in asymmetric fields, (E), 19: 40010
noise generation in, mechanisms of, 19: 39269(R) (SU-SEL-64-133)
oscillations in multivelocity beam of, longitudinal, (T), 19: 39964 (NP-15201)
oscillations in, research on, 19: 39972(R) (SU-IPR-17)
oscillations near crest of moving striation in, sustained, (E), 19: 40020
particle flux near body moving in interplanetary space, (T), 19: 39683
particle interactions in fully ionized, kinetic effects in, 19: 40056(T)
pinch effect in, field and impurity effects on theta, (E), 19: 40005
polarization of cluster of, moving in toroidal magnetic field, (E), 19: 39963 (NP-15198)
population densities of excited atoms in stationary hydrogen, (T), 19: 40053
production by lasers, 19: 39273(R) (UCRL-12204, pp 60-5)
production of electron, with negative electrostatic potential well, (E), 19: 40031
properties, 19: 39992
properties of arc-jet, (E/T), 19: 40037
properties of fully ionized barium, (E), 19: 40007
properties of post-shock, nonthermal, (T), 19: 39999
radiation in anisotropic, effects of ray refractive index on, 19: 39270(R) (TID-21894)
rotation in magnetically confined, mechanisms for, (T), 19: 39974
rotation in, effect of ion-neutral collisions on, 19: 40052
shock propagation in thermal, density and temperature behind, (T), 19: 40051
shock wave structure in, (T), 19: 39984
spectra of high-density hydrogen, Balmer line characteristics in, (T), 19: 39990
spectral line shifts in nitrogen, Stark width measurements, 19: 39952 (AFCRL-65-348)
spectroscopy of, light source for absorption, 19: 38939
stability in complex field geometries, universal, (T), 19: 40018
stability in inhomogeneous, theory for micro- and resistive, 19: 39957 (MATT-320)
stability in magnetic traps, anomalous diffusion of, 19: 39968 (ORNL-P-1338)
stability in slow theta pinch, (E), 19: 39996
stability of anisotropic, Kelvin-Helmholtz, (T), 19: 40000
stability of highly ionized dense cesium, in Penning arc, (E), 19: 40023
stability of magnetoactive, h-f velocity space, (T), 19: 40019
stability of partially ionized, low-frequency, (T), 19: 40004
stability of resistive, inhomogeneous, universal, (T), 19: 40002
stability of, effects of finite Larmor radius and nonuniform rotation on, (T), 19: 40001
synchrotron radiation from self-consistent, electron density effects on, (T), 19: 40013
temperature of supersonic, at low pressures, (E), 19: 39987
thermal radiation from homogeneous, near plasma frequency, (T), 19: 39985
thermodynamic functions of, computation of, 19: 40058(T)
thermodynamic properties of, astrophysical relations of, (T), 19: 39339
transition forms in, equations for ambipolar, 19: 39270(R) (TID-21894)
transport processes in, (T), 19: 40057(T)
wave excitation in, in interplanetary space, (T), 19: 39683
wave propagation in, detection of, 19: 39269(R) (SU-SEL-64-133)
wave propagation in inhomogeneous column of, dispersion curves for acoustic, (T), 19: 40028

PLASMA JETS
development of coaxial gun, 19: 39956 (LA-DC-7043)
Hall current and coherent oscillations in linear Hall, correlation of, (T), 19: 39981
performance of, fluctuating mode of arc in, (E), 19: 39975
production in wind tunnels, arc heaters for, 19: 38796
temperature of argon, spectroscopic studies of, (E), 19: 40043

PLASTICS
phantoms of, method for integral dose measurement using scintillating, 19: 38893
radiation effects on, in air and vacuum, 19: 39232 (FZK-227)
radiation processing, 19: 39066

PLATINUM
catalytic properties in deuterium exchange reactions, 19: 38597
gamma reactions at 145 kev, photoelectric cross sections in, 19: 39377
radiation damage in, cross sections for atomic displacements from 1- to 3-Mev electrons, 19: 39225 (AFCRL-65-286)
radiation effects on, electron, 19: 40286(R) (NAA-SR-11200)
radiation effects on catalytic properties of, beta, 19: 38742(P)
tin-119 Mössbauer effect in monolayer on, (E), 19: 39210

PLATINUM ALLOYS
Ce–Pt, phase studies, 19: 39163(R) (MLM-1244)
Pt–Pu, phase studies, 19: 39163(R) (MLM-1244)
Pt–W, performance as heater wire in calorimetry below 0.1°K, 19: 39743

PLATINUM CATALYSTS
effects on isotopic isomerization of deuterated toluene, 19: 38693

PLATINUM COMPLEXES
deuterium exchange between hydrido-, and heavy water, 19: 38627

PLATINUM ISOTOPES Pt-192
energy levels of, g factors of excited, (E), 19: 39833

PLATINUM ISOTOPES Pt-194
energy levels of, g factors of excited, (E), 19: 39833
helium–ion fission at 34 and 41 Mev, 19: 39802

PLATINUM ISOTOPES Pt-195
helium–ion fission at 34 and 41 Mev, 19: 39802
neutron reactions (n,γ), gamma spectra of 12-ev resonance of, 19: 39781 (JAERI-1073)

PLATINUM ISOTOPES Pt-196
helium–ion fission at 34 and 41 Mev, 19: 39802

PLATINUM OXIDES
preparation of catalysts of, by reduction using labeled organic compound, 19: 38596

PLOWSHARE PROJECT
archeological survey of vicinity of Cape Thompson, Alaska, 19: 40289 (PNE-406)
archeological survey of vicinity of Cape Thompson, Alaska, 19: 40290 (PNE-407)
blast from Dugout row-charge cratering experiment, measurements of close-in air, 19: 38790 (PNE-608F)
crater dimensions in Dogout row-charge event, 19: 38789 (PNE-601F)
isotope distribution and recovery in Gnome event, 19: 38787 (PNE-102F)
stem design and shotcrete, grout, and concrete support for Pre-Schooner, 19: 38788 (PNE-501F)

PLUTONIUM
analysis for fluoride, method for, 19: 38546(R) (RFP-552)
analysis for impurities, spectrographic, 19: 38546(R) (RFP-552)
analysis for iron, spectrophotometric, 19: 38546(R) (RFP-552)
analysis for nickel using dimethylglyoxime, spectrophotometric, 19: 38546(R) (RFP-552)
bibliography on technology of, 19: 40281 (BNWL-113-5)
density at 25 to 800°C, 19: 39161 (LA-DC-6956)
determination in air in presence of uranium, chromatographic, 19: 38554
determination in plutonium fluoride, volumetric, 19: 38546(R) (RFP-552)

determination in spent fuels, metal, alloys, and compounds, review of methods for, 19: 38542 (LA-DC-6938)
determination in urine, radiometric, 19: 38555
diffusion in gamma, studies of self-, 19: 39162 (LA-DC-6957)
emittance of polished, effects of oxidation on total hemispherical, 19: 39167 (RFP-616)
handling and shipping of, measurement problems in, 19: 38535 (RFP-508)
phase transformations in, effects of applied stresses on beta–alpha and alpha–beta, 19: 39153 (BNWL-33)
phase transformations in high-purity, latent heats of, 19: 39163(R) (MLM-1244)
processing of, thermodynamics of high-temperature reactions for, 19: 38752 (LA-DC-6947)
reactions of burning, with organic solvents, 19: 38879 (RFP-566)
reactions with uranium trichlorides to 1200°C, mechanisms in, 19: 40177(R) (ANL-7046(p.1-35))
reduction in Purex process by uranium(IV)-hydrazine, 19: 38751 (HW-82103)
separation from actinides in urine by ion exchange, 19: 38546(R) (RFP-552)
separation from americium and curium by solvent extraction, 19: 39265(R) (IA-1021)
separation from irradiated fuels by fluoride volatility processes, 19: 40113(R) (ANL-7071)
separation from irradiated reactor fuels by TBP extraction, 19: 38776(P)
separation from spent fuel by halide slagging, 19: 40177(R) (ANL-7046(p.1-35))
separation from urine, ion-exchange, 19: 38555
solvent extraction of tetravalent, from nitric acid solutions by tertiary amines, 19: 38761(T) (CEA-tr-A-1809)
solvent properties for tantalum and tungsten, evaluation of sampling methods for determination of, 19: 38680 (LA-3303)
thermionic work function of, device for measuring, 19: 39125(R) (BNWL-91)
vapor pressure at 1100 to 1800°K, 19: 39159 (LA-DC-6926)

PLUTONIUM ALLOYS
phase studies of multicomponent, methods for, 19: 39163(R) (MLM-1244)
Al–Pu, thermal cycling effects on, 19: 39125(R) (BNWL-91)
Cd–Pu, phase studies, 19: 39163(R) (MLM-1244)
Ce–Co–Pu, densities of liquid, effects of temperature on, 19: 39163(R) (MLM-1244)
Ce–Co–Pu, density at 25 to 800°C, 19: 39161 (LA-DC-6956)
Ce–Co–Pu, viscosities of liquid, effects of composition and temperature on, 19: 39163(R) (MLM-1244)
Ce–Fe–Pu, phase studies, 19: 39163(R) (MLM-1244)
Ce–Ni–Pu, phase studies, 19: 39163(R) (MLM-1244)
Ce–Pu, melting point, 19: 39163(R) (MLM-1244)
Ce–Pu, viscosities of liquid, effects of composition and temperature on, 19: 39163(R) (MLM-1244)
Co–Pu, phase studies, 19: 39163(R) (MLM-1244)
Cu–Pu, microstructure and phase studies of, 19: 39163(R) (MLM-1244)
Fe–Pu, density at 25 to 800°C, 19: 39161 (LA-DC-6956)
Fe–Pu, phase studies, 19: 39163(R) (MLM-1244)
fissium–Pu–U, hydridation for cladding removal, 19: 40113(R) (ANL-7071)
fissium–Pu–U, reactions with stainless steel at high temperatures, 19: 40177(R) (ANL-7046(p.1-35))
Ga–Pu, densities of liquid, effects of temperature on, 19: 39163(R) (MLM-1244)
Ga–Pu, density at 25 to 800°C, 19: 39161 (LA-DC-6956)
Ga–Pu, phase equilibria of, effects of impurities on, 19: 39163(R) (MLM-1244)
Ga–Pu, phase transformations in, latent heats of, 19: 39163(R) (MLM-1244)
Ni–Pu, phase studies, 19: 39163(R) (MLM-1244)
Np–Pu, spectrophotometric analysis for plutonium, 19: 38546(R) (RFP-552)
Pt–Pu, phase studies, 19: 39163(R) (MLM-1244)
Pu–Ti–U, corrosion by air, 19: 40177(R) (ANL-7046(p.1-35))
Pu–Ti–U, phase studies, 19: 40177(R) (ANL-7046(p.1-35))
Pu–Ti–U, reactions with stainless steel at high temperatures, 19: 40177(R) (ANL-7046(p.1-35))
Pu–U–Zr, phase studies, 19: 40177(R) (ANL-7046(p.1-35))
Pu–U–Zr, reactions with stainless steel at high temperatures, 19: 40177(R) (ANL-7046(p.1-35))

PLUTONIUM CARBIDES
radiation effects on clad, 19: 40113(R) (ANL-7071)
thermochemical properties, 19: 38677
Ni–PuC–UC, thermal diffusivities of, 19: 39163(R) (MLM-1244)
PuC–UC, fabrication by compaction, 19: 40177(R) (ANL-7046(p.1-35))
PuC–UC, thermal diffusivities of, 19: 39163(R) (MLM-1244)

PLUTONIUM COMPOUNDS
entropies of, thermochemical calculations of, 19: 38677

PLUTONIUM FLUORIDES
analysis for plutonium, volumetric, 19: 38546(R) (RFP-552)

PLUTONIUM(VI) FLUORIDES
separation from air by hydrolysis, 19: 40112(R) (ANL-7046(p.36-66))
separation from air by filtration, 19: 40113(R) (ANL-7071)

PLUTONIUM ISOTOPES
nuclear properties of, pairing force effects on, (T), 19: 39927

PLUTONIUM ISOTOPES Pu-239
content in atmosphere, methods of measuring, 19: 38903
detection and measurement in man using whole-body counter, 19: 38546(R) (RFP-552)
determination in contaminated wounds, development of miniature counters for, 19: 38546(R) (RFP-552)
determination in urine, radiometric, 19: 39265(R) (IA-1021)
neutron fission cross sections at 1 kev to 1 Mev, 19: 39889
neutron fission of, yields of krypton-85 in thermal, (E), 19: 39800
neutron reactions (n,γf) with, thermal, (T), 19: 39864
pathological effects of inhaled aerosols of, in dogs, 19: 38359 (BNWL-SA-230)

PLUTONIUM ISOTOPES Pu-240
internal conversion coefficients for, (E/T), 19: 39786 (ORNL-P-1419)

PLUTONIUM ISOTOPES Pu-241
neutron fission cross sections at 1 kev to 1 Mev, 19: 39889
neutron reactions (n,γf) with, thermal, (T), 19: 39864

PLUTONIUM NITRATES
analysis for fluoride, method for, 19: 38546(R) (RFP-552)
preparation and properties of pentavalent, 19: 38656
stability of solutions of pentavalent, radiolysis and temperature effects on, 19: 38731

PLUTONIUM NITRIDES
preparation of massive, process and apparatus for, 19: 38685(P)
PuN–ThN, preparation for high-temperature fuel evaluation, 19: 39091(R) (BMI-1723(Del.))
PuN–TiN, preparation for high-temperature fuel evaluation, 19: 39091(R) (BMI-1723(Del.))
PuN–UN, radiation effects on, neutron, 19: 38125(R) (BNWL-91)

PLUTONIUM OXIDES
crystal structure and oxygen content at 1100 to 1600°C, 19: 39221
electric conductivity of, effects of oxygen content on, 19: 39221
phase diagram at 25 to 900°C, 19: 38682
thermodynamic properties at 700 to 1140°C, 19: 38682

PLUTONIUM(IV) OXIDES
fabrication into glass-bonded fuel rods, 19: 39124 (ANL-6995)
fabrication of microspheres of, 19: 39125(R) (BNWL-91)
fabrication of recycle, by remote equipment, 19: 39125(R) (BNWL-91)
preparation and properties of spherical fuel particles containing, 19: 39096 (CONF-117(p.103-26))
preparation and properties of microspheres of, 19: 39163(R) (MLM-1244)
reactions with chromium–nickel alloys at high temperatures, 19: 39125(R) (BNWL-91)
reactions with iron, niobium, and silicon at high temperatures, 19: 39125(R) (BNWL-91)
BeO–ThO_2, preparation and properties, 19: 39091(R) (BMI-1723(Del.))
PuO_2–stainless steel, fabrication into pins, 19: 39125(R) (BNWL-91)
PuO_2–UO_2, distributions and phases in, 19: 39125(R) (BNWL-91)
PuO_2–UO_2, fabrication for plutonium recycle experiments, 19: 40112(R) (ANL-7046(p.36-66))
PuO_2–UO_2, fabrication into glass-bonded fuel rods, 19: 39124 (ANL-6995)
PuO_2–UO_2, fabrication for use as reactor fuel, 19: 39146(P)
PuO_2–UO_2, processing by fluorination, 19: 40112(R) (ANL-7046 (p.36-66))
PuO_2–UO_2, radiation effects on, neutron, 19: 39125(R) (BNWL-91)

PLUTONIUM RECYCLE TEST REACTOR
fuel elements for, radiation effects on, 19: 39125(R) (BNWL-91)
fuel fabrication for, variables in, 19: 39125(R) (BNWL-91)
operations and performance, (E), 19: 40267
performance of, simulation for, 19: 40282 (BNWL-SA-171)

POLONIUM CHLORIDES
corrosive effects on molybdenum, electrochemical, 19: 39122

POLONIUM ISOTOPES
alpha decay of, energies and half lives of, (E), 19: 39841

POLONIUM ISOTOPES Po-197
alpha decay, (E), 19: 39838

POLONIUM ISOTOPES Po-198
alpha decay, (E), 19: 39838

POLONIUM ISOTOPES Po-199
alpha decay, (E), 19: 39838
alpha decay of isometric, (E), 19: 39841

POLONIUM ISOTOPES Po-200
alpha decay, (E), 19: 39838
POLONIUM ISOTOPES Po-201
alpha decay, (E), 19: 39838
alpha decay of isometric, (E), 19: 39841
POLONIUM ISOTOPES Po-202
alpha decay, (E), 19: 39838
POLONIUM ISOTOPES Po-210
alpha decay of, recoil particle charge and energy loss from, 19: 39882
content in atmosphere, methods of measuring, 19: 38903
POLONIUM ISOTOPES Po-216
electric charge in alpha decay of radon-220, (E), 19: 39884
POLYMERIZATION
radioinduced, 19: 39066
POLYMERS
charged particle tracks in, identification after chemical etching, 19: 39038
radiation effects on, in space environment, 19: 39059
radioinduced production of stereospecific, from inclusion compounds, 19: 38725(T)
radioinduced reactions, 19: 39066
POLYPHENYLS
scintillation properties of, effects of steric inhibition of resonance on, 19: 38691
solvent properties for mercury bromides, 19: 39265(R) (IA-1021)
POPULATIONS
genetic factors in human, 19: 38328
of plants and small vertebrates in uranium areas of Upper Colorado River Basin, Utah, 19: 38330 (TID-22078)
radiation body burden in, in West German Federal Republic, 19: 38904
radiation hazards to, fallout, 19: 38861
PORPHYRINS
radioinduced reduction of iron of, in cooked meats, 19: 39065
PORTUGAL
uranium production and uses in, in 1964, 19: 39105
POSITRON BEAMS
focusing in accelerating fields, (T), 19: 39321
interactions with electron beams at 100 to 1000 Bev, 19: 39481 (NP-15248)
POSITRONIUM
decay in ice and water, (E/T), 19: 39509
decay in insulators and metals, 3-quantum, (E/T), 19: 39546
production in ice and water at 22 to −144°C, (E/T), 19: 39509
POSITRONS
annihilation in insulators and metals, 3-quantum, (E/T), 19: 39546
annihilation in lead at 300 kev, radiationless, (E), 19: 39526
emission in decay of manganese-50, scandium-42, and vanadium-46, ft values for, 19: 39859
production cross sections on thick targets by electrons at 55 to 220 Mev, (E), 19: 39475 (LAL-27)
POTASSIUM
boiling heat conductance measurements, accuracy of forced-flow, 19: 38811(R) (SAN-409-24)
content in Japanese diet, 19: 38894
effects on liquid sodium dilation of graphite, 19: 39235 (NAA-SR-11309)
electric properties of vaporous, effects of electric and magnetic fields on, 19: 39270(R) (TID-21894)
vaporization lifetimes of droplets of, on tantalum, 19: 38811(R) (SAN-409-24)
POTASSIUM ACID PHOSPHATES
energy levels of, measurement of, 19: 39265(R) (IA-1021)
POTASSIUM BROMIDES
color centers in, luminescence from ionized F-aggregate, (E), 19: 38648
radiation effects on optical absorption of copper centers in, x, (E), 19: 40107
reduction by high-frequency discharge in helium, hydrogen, and nitrogen, role of electrons in, 19: 38181
reduction by high-frequency hydrogen discharge to hydrogen halide and metal, 19: 39180
POTASSIUM CHLORIDES
color centers in, luminescence from ionized F-aggregate, (E), 19: 38648
corrosive effects on molybdenum, electrochemical, 19: 39122
crystal growth from aqueous solutions, effects of irradiation and additives on, 19: 38696 (MIT-2909-4)
radiation effects on optical absorption of copper centers in, x, (E), 19: 40107
reduction by high-frequency hydrogen discharge to hydrogen halide and metal, 19: 39180
reduction by high-frequency discharge in helium, hydrogen, and nitrogen, role of electrons in, 19: 39181
$BaCl_2$–KCl, free energy of formation of K_2BaCl_4 at 450 and 550°C, 19: 38575 (BNL-9343)
$CaCl_2$–KCl, free energy of formation of $KCaCl_2$ at 450 and 550°C, 19: 38575 (BNL-9343)
KCl–NaCl, use of fused, in attempts to prepare uranium sulfide, 19: 38574 (ANL-7008)
KCl–$SrCl_2$, free energy of formation of K_2SrCl_4 and KSr_2Cl_5 at 450 and 550°C, 19: 38575 (BNL-9343)
LiCl–KCl, chlorination of uranium tetrachloride in fused eutectics of, 19: 38587 (UCRL-11986)
$MgCl_2$–KCl, free energy of formation of $KMgCl_3$ at 450°C, 19: 38575 (BNL-9343)
POTASSIUM FERROCYANIDES
labeling with iron-59, 19: 38743 (NP-15262)
POTASSIUM FLUORIDES
reduction by high-frequency hydrogen discharge to hydrogen halide and metal, 19: 39180
reduction by high-frequency discharge in helium, hydrogen, and nitrogen, role of electrons in, 19: 39181
POTASSIUM IODIDES
radiation effects on optical absorption of copper centers in, x, (E), 19: 40107
radioinduced color centers in, preferential thermal reorientation of electron and x, (E), 19: 40103
radioluminescence of thallium-activated, effects of activator concentration on, 19: 38735
reduction by high-frequency discharges in helium, hydrogen, and nitrogen, role of electrons in, 19: 39181
reduction by high-frequency hydrogen discharge to hydrogen halide and metal, 19: 39180
POTASSIUM IONS
emission from molybdenum ribbon at 30 to 1100°C, thermionic, 19: 39197
radiolysis of aqueous solutions of, pulse, 19: 38728
POTASSIUM ISOTOPES
separation on zirconyl phosphate ion exchanger in fused potassium nitrate, 19: 39074
POTASSIUM ISOTOPES K-42
use in radiodiagnosis, review on, 19: 38505
POTASSIUM NICKEL FLUORIDES
spectra of, modes of infrared reflection, (E/T), 19: 39270(R) (TID-21894)
POTASSIUM NIOBIUM FLUORIDES
reactions with aluminum fluoride to prepare niobium fluoride, 19: 38640
POTASSIUM NITRATES
properties in chemical radiation dosimetry, 19: 39042
KNO_3–$NaNO_2$, use in preparation of aluminum–nickel coatings, 19: 39143(P)
$LiNO_3$–KNO_3, properties for metal cation ion exchange from fused, 19: 38771
POTASSIUM NITRITES
KNO_2–$NaNO_3$, use in preparation of aluminum–nickel coatings, 19: 39143(P)
POTASSIUM PERCHLORATES
effects on iodine-131 uptake by rabbit thyroid, 19: 38341
POTASSIUM PHOSPHATES
reactions with yttrium chlorides at 25°C, 19: 38620
POTASSIUM XENATES
preparation and properties, 19: 38624
POTATOES
radiation effects on sprouting in, effects of gibberellic acid on gamma, 19: 38401
POWER PLANTS
pump development for space, 19: 38781(R) (N64-25903)
use of digital computers in French, 19: 40203
POWER REACTORS
construction and developmental status of, compilation on, 19: 40116 (TID-8200(12th Rev.))
design of 1000-Mw(e) sodium-cooled fast (T), 19: 40175(R) (ACNP-63592)
development of, survey, 19: 40215
electrical systems of first Russian, operation of, 19: 40208
fuel burnup in pressure-tube heavy-water, (E/T), 19: 40185 (JAERI-1075)
fuel management in, (T), 19: 40216
material demands for, economics, 19: 40180 (DL-56)
reactivity of fast, analysis of Doppler-shift effects on, (E/T), 19: 40150 (CEA-R-2565)
site selection for Israeli, 19: 39265(R) (IA-1021)
use of heat produced in, chemical-metallurigical processes, 19: 38686(P)
water purification in water-cooled, performance of resins for, (E), 19: 40128 (ZFK-RN-17(p.75-94))
POWER SUPPLIES
design of transistorized regulated high-voltage, for portable radiation detectors, 19: 39053(P)

development for space vehicles, (E/T), 19: 38836 (NASA-SP-79)
PRASEODYMIUM
neutron reactions at 0.0005 to 1 ev, total cross sections for, 19: 39779 (IEA-86)
pathological effects of subcutaneous implantations of, in mice, 19: 38334 (COO-1170-1)
phase transformations at 6 to 65 kbar, solid-liquid and solid-solid, 19: 40095
PRASEODYMIUM COMPLEXES
with [(2-hydroxyethyl)imino]diacetic acid, dissociation constant of, 19: 38671
PRASEODYMIUM IONS
radiolysis of aqueous solutions of, pulse, 19: 38728
spectra of trivalent, energy levels from, (E), 19: 39385
PRASEODYMIUM OXALATES
solubility in *N,N'*-dimethyl-*N,N'*-dinitrosoterephthalamide at 25°C, 19: 38601
PRASEODYMIUM TELLURIDES
spectra of, infrared absorption, 19: 38618
PRESSURE
measurement of deep-ocean, instrumentation for, 19: 40288(R) (NVO-98-5)
PRESSURE DROP
in flow through two eccentrically positioned orifices in series, 19: 38810 (RL-SA-31)
in foam-carrying pipes and tubes, 19: 40271(R) (RAI-350)
PRESSURE TRANSMITTERS
response of, comparison of calculated and experimental, 19: 38912 (LA-DC-7025)
PRESSURE VESSELS
closure design for reactor, 19: 40136(P)
design of concrete, for reactors, 19: 40134
design with internal insulation and external cooling, for gas-cooled reactors, 19: 40131(T) (ORNL-tr-585)
PRESSURIZED WATER REACTORS
boiler corrosion in, causes of selective, 19: 39091(R) (BMI-1723(Del.))
design for power or testing, 19: 40167(P)
development, 19: 40196(R) (WCAP-3269-6)
development, 19: 40197(R) (WCAP-3718)
development, 19: 40198(R) (WCAP-3721)
development of maritime, 19: 40251
fuel costs for simulated, minimized, 19: 40114 (BNWL-104)
PRODUCTION REACTORS
construction and developmental status of, compilation on, 19: 40116 (TID-8200(12th Rev.))
PROMETHIUM
phase transformations at 6 to 65 kbar, solid-liquid and solid-solid, 19: 40095
properties as fuel in radioisotopic power sources, summary, 19: 39069 (BNWL-C-45)
separation from americium, neodymium, and samarium by ion exchange, 19: 38772
PROMETHIUM ISOTOPES Pm-147
determination in urine, radiometric, 19: 39265(R) (IA-1021)
luminous properties in paints, 19: 39265(R) (IA-1021)
motion in soil, effects of chelating agents on, 19: 38329 (TID-20471)
preparation of pure, 19: 38772
PROMETHIUM ISOTOPES Pm-148
spin of ground state of, (E), 19: 39818
PROPANE
yields in gamma radiolysis of liquid cyclopentane, 19: 38712
PROPANE, 1-BROMO-
radiation effects on bromine-80 and -82 retentions in, isomeric transition reaction in, 19: 38715
1-PROPANOL
radioinduced reactions with 1,2-dichlorotetrafluorocyclobutene and 1,2-dichlorohexafluorocyclopentene, 19: 38708
2-PROPANOL
radioinduced reactions with 1,2-dichlorotetrafluorocyclobutene and 1,2-dichlorohexafluorocyclopentene, 19: 38708
PROPENE
yields in gamma radiolysis of liquid cyclopentane, 19: 38712
PROPIONAMIDE
acrylamide–propionamide, radioinduced solid-state polymerization of, effects of oxygen on gamma, 19: 38694 (BNL-9200)
PROPORTIONAL DETECTORS
design and performance of gas-flow, 19: 38543(R) (MCW-1492)
design for measuring alpha particles or fission fragments in flowing gas stream, 19: 39012
design of large-area gridded, for soft gamma and x rays, 19: 39046(P)
design of proton recoil, for fast neutron dosimetry, 19: 38968 (AEET/HP/D-1)
sample changer for windowless gas-flow, design of, 19: 39037
use for fast neutron dosimetry, 19: 39043
use in measurement of alpha contaminated surfaces, 19: 39045(P)
PROPULSION
ion thruster for space, d-c to d-c converters for power system of, 19: 38835 (N65-27619)
nuclear development for space vehicles, (E/T), 19: 38836 (NASA-SP-79)
nuclear reactor system design for, 19: 40247 (N64-29788)
nuclear, advanced concepts on, 19: 40242 (LA-DC-7118)
nuclear, conference on, 19: 40221 (LA-3229)
systems for space, photonic, 19: 38837
PROTACTINIUM
neutron capture cross sections at 20 kev, 19: 38786 (LA-DC-7111)
separation from thorium and uranium by paper electrophoresis, 19: 38775
PROTACTINIUM COMPLEXES
composition and formation constants of pentavalent and tetravalent, 19: 38602
PROTACTINIUM(IV) FLUORIDES
PaF_4–RbF, preparation and crystal structure of complex compound in, 19: 38625
PROTACTINIUM ISOTOPES
nuclear properties of, pairing force effects on, (T), 19: 39927
PROTECTIVE CLOTHING
improvised, 19: 38475
PROTECTIVE OINTMENTS
effectiveness of anabolic steroid, for radiodermatitis, 19: 38468
PROTEINS
genetic control of human, 19: 38328
radiation effects on blood serum, in animal, 19: 38426
radiation effects on bacteriophage, EPR spectra, 19: 38365
radiation effects on content of, in amoeba, 19: 38371
radiation effects on serum, in Hiroshima bomb survivors, 19: 38377
radiation effects on mouse serum, following rat-to-mouse chimera transplants, x, 19: 38404
synthesis of, genetic control by desoxyribonucleic acid, 19: 40299(T) (LA-tr-65-12)
uptake of carbon-14-labeled precursors by L-cell nuclei, effects of tritiated thymidine on, 19: 38339
PROTON BEAMS
therapeutic use, 19: 38499
PROTON PAIRS
annihilation at 1.2 Bev/c, meson (D) production in, (E), 19: 39535
annihilation into two mesons, amplitudes for, (T), 19: 39527
annihilation of, non-K* resonances in, 19: 39534
PROTONS
detection using lithium-drifted position-sensitive detectors, 19: 39027
dosimetry behind shields, computer program for calculation of, 19: 40064 (NP-15132)
emission from neutron reactions (n,p) with boron-10, angular distributions for, (E), 19: 39798
interactions with protons, digitized discharge planes for automatic measurement of inelastic, (E), 19: 39450 (BNL-9232)
interactions with hyperons at low energies, elastic, (E/T), 19: 39460 (CONF-650410-3)
interactions with antiprotons at rest, K* production in annihilation, (E/T), 19: 39462 (CU-1932-239)
interactions with mesons (π), phase shift and resonance equations for elastic, 19: 39487 (UCRL-14193)
interactions with bremsstrahlung, meson (π^+) production near threshold in, (E), 19: 39461 (COO-1195-35)
interactions with deuterons, cross sections for inelastic, (T), 19: 39912
interactions with protons at 6.78 to 19.6 Bev/c, Regge pole analysis of, (E/T), 19: 39619
interactions with electrons, Regge trajectory of photon exchange in, (E/T), 19: 39619
interactions with photons, cross sections and angular distributions for mesons (π^0) and (π^+) production in, (E), 19: 39620
interactions with photons, meson (η) production and decay in, (E), 19: 39620
interactions with photons, meson (K^+) production in, (E), 19: 39620
interactions with photons, production of vector mesons in, (T), 19: 39621
interactions with electrons, meson (π) production in, (E), 19: 39623
interactions with photons, meson (π^0) production in, (E), 19: 39623
interactions with protons, resonances in, 19: 39479 (NP-15216)
interactions with deuterons, resonances in, 19: 39479 (NP-15216)
interactions with mesons (π^-) at 2.8 Bev-c, angular distribution analysis of, (E), 19: 39480 (NP-15247)

interactions with photons at 600 to 850 Mev, double meson (π) production in, (E), 19: 39519
interactions with antibaryons and baryons, U(12) symmetry for total cross sections for, 19: 39529
interactions with mesons (K^-) at low energies, Coulomb-nuclear interference in, (E/T), 19: 39530
interactions with hyperons (Λ), SU(6) predictions for, 19: 39532
interactions with hyperons (Σ^*), SU(6) predictions for, 19: 39532
interactions with neutrons, gamma asymmetry and circular polarization in, (T), 19: 39538
interactions with mesons (K^-), optical model analysis of elastic, (T), 19: 39545
interactions with protons at 5.52 Bev/c, N^*_{33} resonance in, 19: 39548
interactions with mesons (K^-) at 2.1 to 2.7 Bev/c, meson (ϕ) production in, (E), 19: 39552
interactions with mesons (π^-) at 1.68 Bev/c, Y^*_0 production in, (E), 19: 39553
interactions with protons, modified peripheral model for, (T), 19: 39557
interactions with protons, transverse momentum distribution in deuteron-producing, (T), 19: 39569
interactions with mesons (π^+) peripheral production and decay of mesons (ρ) and N^* resonance in, (E/T), 19: 39576
interactions with mesons (K^+), peripheral production and decay of K^* in, 19: 39576
interactions with deuterons, inelastic cross sections for, (E/T), 19: 39577
interactions with deuterons at 40 Mev, Chew-Low extrapolation method for, (E), 19: 39578
interactions with deuterons at 135 Mev, angular distributions for inelastic, (E), 19: 39579
interactions with mesons (π^-), determination of nucleon form factors from, (T), 19: 39590
interactions with mesons (π^-) at 3.5 Bev/c, four-prong events in, (E), 19: 39591
interactions with mesons (π^-), isobar model for hyperon (Λ) production in, (T), 19: 39593
interactions with mesons (π^-) at 8.0 Bev/c, $\pi^+\pi^-$ (1670) production in, (E), 19: 39537
interactions with deuterons and protons at 1 to 8 Bev/c, total cross sections for, (E), 19: 39550
interactions with photons, meson (π^+) production near first resonance, (E), 19: 39597
interactions with hyperons (Σ^-), hyperon (Σ^0) production rate for, (E), 19: 39510
photoproduction on silicon-28, energy distribution for, (E), 19: 39938
reactions (p,a_0) and (p,γ_0) with nitrogen-15, theory for, 19: 39805
reactions (p,a)2a at 250 and 675 kev, mechanism of, (E), 19: 39919
reactions (p,a) with boron-11, direct 3a decay of carbon-12 resonance (163 kev) in, (E), 19: 39918
reactions (p,d) with nuclei, effects of nuclear correlations on, (T), 19: 39890
reactions (p,γ) with carbon-12 and -13, cross sections for, (T), 19: 39805
reactions (p,γ) with beryllium-7, models for, (T), 19: 39820
reactions (p,γ) with chlorine-35 at 0.4 to 3.1 Mev, energy levels from, (E), 19: 39828
reactions (p,n) with tin isotopes at 7 to 14 Mev, angular and energy distributions from, (E), 19: 39825
reactions (p,n) with fluorine-19 and phosphorus-31 at 7.5 to 13.0 Mev, levels from, (E), 19: 39827
reactions (p,pa) with carbon-12 at 85 Mev, angular distributions in, (E), 19: 39908
reactions (p,pd) with lithium-6, analysis of quasifree scattering in, (T), 19: 39906
reactions (p,pd) with lithium-6 at 30.5 and 155 Mev, analysis of angular correlations in, (T), 19: 39907
reactions (p,t) with nickel-58 at 28 Mev, energy levels from, (E), 19: 39819
reactions (p,t) with carbon-12 at 155 Mev, (E), 19: 39839
reactions (p,xn) with tin isotopes, isomeric tin-117 from, (E), 19: 39929
reactions (p,xn) with bismuth and lead at 1 Bev, heat production and neutron yields from, 19: 39756 (AECL-2177, Paper 3))
reactions (p,2p) with copper-63 at 10.5 Mev, relative proton-gamma emission widths in, (E), 19: 39903
reactions (p,2p) with nuclei, analysis of nuclear structure from, (E), 19: 39904
reactions (p,2p) with carbon-12 at 155 Mev, angular correlations in, (T), 19: 39905
reactions (p,2p)n with deuterium at 9.0 and 10.5 Mev, energy-angular correlations and sequential decay in, (E), 19: 39924
reactions (p,2p)n with deuterium at 31 Mev, angular distributions from, (E), 19: 39925
reactions (p,3a) with boron-11, sequential decay theory for, (T), 19: 39895
reactions (p,3a) with boron-11, angular momenta and Pauli principle for, (T), 19: 39896
reactions (p,3a) with boron-11 at 2 to 5.64 Mev, sequential mechanism for, (E/T), 19: 39911
reactions in blood, carbon-11 production in, 19: 38722
reactions with gadolinium-160, isomeric gadolinium-159 from, (E), 19: 39929
reactions with hydrogen-like atoms, formation of excited hydrogen atoms in, (T), 19: 39398
reactions with tantalum at 660 Mev, isomeric lutetium-176 from, (E), 19: 39931
reactions with tungsten at 50 to 225 kev, electron emission in, (E), 19: 39409
scattering by carbon-12 at 150 Mev, polarization in inelastic, (E/T), 19: 39837
scattering by chromium-52 at 2.5 to 7.5 Mev, level multipolarities, parity, and spin from, (E), 19: 39826
scattering by helium-4 at 40 Mev, continuum resonances in inelastic, (E), 19: 39886
scattering by nuclei at 15 to 1900 kev, x-ray yields from inelastic, (E), 19: 39881
shielding against, for manned space stations, 19: 40063 (NP-15125)
uses of polarized targets of, in high-energy particle experiments, 19: 39497

PSEUDOUREA, 2-(2-AMINOETHYL)-2-THIO-
effects on respiration in mice, 19: 38469
protective effects against radiation injuries in mice, 19: 38450 (USNRDL-TR-851)

PSYCHOLOGY
radiation effects on learning ability of adult rats exposed *in utero*, 19: 38361(R) (TID-21951)

PUERTO RICO POWER REACTOR
construction and design features, (E), 19: 40217
development and performance of, advanced-core, 19: 39156(R) (CEND-532)
fuel element design for, superheater, 19: 39156(R) (CEND-532)

PULMONARY ABSORPTION
of thorium-230, from inhaled uranium ore particles, 19: 38333 (BNWL-SA-226)
of uranium ore particles, 19: 38333 (BNWL-SA-226)

PULSE ANALYZERS
design and performance of pulse height measuring unit, 19: 39006
design of pulse shape discriminator for scintillation counters, 19: 39025
design of time-to-pulse height converter for, 19: 39031
design of 4096-channel time analyzer with variable channel width, 19: 39024

PUMPS
design of fluid-driven mechanical, for integral type reactor, 19: 40139(P)
testing manually operated punkah, for shelter ventilation, 19: 38832 (ORNL-TM-1155)

PUMPS (LIQUID METAL)
design of primary-coolant, for LCRE, (E), 19: 40135

PUPAE
radiation effects on fat-body histolysis in Dacus, gamma, 19: 38406

PUREX PROCESS
partitioning agent in, use of uranium(IV)-hydrazine as, 19: 38751 (HW-82103)

4-PYRIDONE, 1-METHYL-
labeling with deuterium, 19: 38689

PYRIDOXINE
effects on radiation effects in animals and man, 19: 38461

PYRIMIDINES
halogenated, radiosensitivity effects on mouse L cells, 19: 38459

Q

QUALITY CONTROL
inspection of parts having cylindrical bodies, apparatus for, 19: 38830(P)

QUANTUM ELECTRODYNAMICS
electromagnetic form factors in, 19: 39617
equations of, finite nonperturbative solutions for, 19: 39646
length scale in, without bare mass, 19: 39652

QUANTUM MECHANICS
asymptotic condition in relativistic, proof of LSZ, 19: 39629 (CONF-796(Paper 30))
book: *Radiation and Noise in Quantum Electronics*, 19: 39664
elementary particle masses in unified field theory, 19: 39452 (CONF-796(Paper 13))
elementary particle 3-body interactions in, 19: 39453 (CONF-796

(Paper 15))
energy eigenvalues in Schrödinger perturbation, inhomogeneous-equation and partitioning techniques for, 19: 39650
expectation values in, trace formalism for, 19: 39644
field equations in, existence and uniqueness of solutions of Lagrangian, 19: 39627 (CONF-796(Paper 26))
Foldy-Wothuysen transformation for free particles in, covariant spinor formulation of, 19: 39639 (CONF-796(Paper 31))
gases in, pseudopotentials of hard-sphere, (T), 19: 39651
many-body problem in, Coriolis coupling in, (T), 19: 39948
many-body problem in, (T), 19: 39263 (CONF-796)
mass spectrum for electron-electron interactions, fine structure of effective, 19: 39583
measurements in, processes in, 19: 39265(R) (IA-1021)
model for three-particle systems, (T), 19: 39641
representation of discrete symmetry operators in, 19: 39626 (CONF-796(Paper 22))
Schroedinger equation in, procedure for solving time-dependent, 19: 39642
space-time properties in macroscopic regime, 19: 39625 (CONF-796 (Paper 12))
theory for stochastic processes, 19: 39661
theory of entropy, 19: 39633
wave functions for molecules, momentum-space, (T), 19: 39660
wave theories in, metastable finite-energy particle-like solutions for nonlinear scalar, 19: 39649

QUARTZ
adhesion of polished monocrystalline, at ultrahigh vacuum, 19: 38840
phonon propagation in, incoherent, (E/T), 19: 39270(R) (TID-21894)
properties for use as fuel-propellant partition in gaseous fuel rocket reactors, 19: 40229 (LA-3229, pp 116-36)

QUINALDIC ACID
8-hydroxy-, complexes of oxime of, with thorium in chloroform and perchlorate solutions, 19: 38567

R

RABBITS
blood circulation in brain of, effects of acceleration, 19: 38358 (AD-612660)
bone blood flow in, use of strontium-85 for measure of, 19: 38340
iodine-131 uptake by thyroid in, procedures for measuring, 19: 38341
placental transfer of glycine, urea, and water in, 19: 38344
radiation effects on mercapto groups in blood, 19: 38427
radiation effects on kidneys in, renograms of, 19: 38379
radiation sickness and blood loss effects on phosphorus-32 uptake by ear, nose, and throat in, 19: 38431
radiodiagnosis of malignant melanomas of eye, 19: 38485
radioinduced hemolysins in liver of, 19: 38429
radiosensitivity of carcinoma in, effects of regional oxygenation, 19: 38374
zinc-65 metabolism in, 19: 39265(R) (IA-1021)

RADAR
reflection during auroral storms, correlation with acoustic wave theory, 19: 39678

RADIATION
background calculations, method for, 19: 40112(R) (ANL-7046(p.36-66))
book: *Detection and Measurement of Nuclear Radiations*, 19: 39040
book: *The Use of Radioactive Isotopes For Checking Production Processes*, 19: 39067(T)
chimeras, immunologic role of thymus in mouse, 19: 38451
dose accumulation in medical personnel, occupational, 19: 38474
dosimetry and physics of penetrating, 19: 38481(T)
dosimetry of medical personnel in accident clinic, 19: 38477
dosimetry of, ionization chambers for, 19: 39030
dosimetry using scintillating plastic phantoms, 19: 38893
effects on animals and man, effects of pyridoxal-5'-phosphate on, 19: 38461
effects on animals, remote late, 19: 38435(T)
effects on biological materials, 19: 38432(T)
effects on ceramic fuel elements, 19: 39234 (GEAP-4597)
effects on compatibility of carbon dioxide with uranium, 19: 39121
effects on constituents in bacteriophages, EPR spectra of, 19: 38365
effects on graft polymerization of ethylene polymers with acrylonitrile and styrene vapors, 19: 38734
effects on grafting of monoethylenically unsaturated monomers on polyvinylchloride, 19: 38741(P)
effects on living structures, review on, 19: 38421
effects on mercapto group in animal blood, 19: 38427
effects on mice, protective effects of spleen cell induced immunological unresponsiveness against, 19: 38454
effects on mutations in *Drosophila melanogaster* by DNA exposure, 19: 38413
effects on plants, theoretical bases for mutagenic, 19: 38420
effects on space vehicles, 19: 39059
effects on stability of pentavalent plutonium nitrate solutions, 19: 38731
effects with spleen cell transplants on polyvalent tolerance in adult and newborn mice, 19: 38376
hazards from fission-product, computer program for, 19: 40248 (NUS-180)
hazards from neutron sources, 19: 38480
hazards to nurses in diagnoses, 19: 38482
industrial uses of, 19: 39265(R) (IA-1021)
industrial uses of, review of Japanese, 19: 39064
interactions with matter, 19: 38499
propagation in upper atmosphere, mathematical analysis of, 19: 39270(R) (TID-21894)
radiative transfer of, matrix formulation for polarization effects on, 19: 39270(R) (TID-21894)
use in coin identification device, 19: 38956(P)

RADIATION CHEMISTRY
electron production, energy distribution, and solvation in, 19: 38703
industrial aspects of, review of, 19: 39066

RADIATION DETECTION INSTRUMENTS
design for cosmic neutron monitoring, 19: 39035
design for fallout measurement, 19: 39051(P)
evaluation for beta particles, 19: 38552
track analysis in, using flying spot devices, (E), 19: 38971 (CERN-65-11)

RADIATION DETECTION INSTRUMENTS (PULSE TYPE)
circuit design for Geiger-Mueller counter, 19: 39021
design for narrow-band x radiation, 19: 39047(P)
design for neutron detection and measurement, 19: 39001
design of automatic, for measuring liquid or powdered radioactive materials, 19: 39020
design of whole-body, 19: 38999
efficiency of long shielded, for neutrons, 19: 39034
pulse pile-up distortion in, (T), 19: 38969 (ANL-6949)
pulse shape discriminator for, design of, 19: 39025

RADIATION DETECTORS
design for reactor control systems, 19: 40122(R) (GEAP-4862)
development of gamma-insensitive, for neutrons, 19: 40286(R) (NAA-SR-11200)
evaluation for beta particles, 19: 38552
gamma effects on out-of-core neutron, 19: 40122(R) (GEAP-4862)
power supply for portable, design of high-voltage, 19: 39053(P)
sample changers for, automatic, 19: 39013

RADIATION INJURIES
book: *Radiation Medicine*, 19: 38470(T)
evaluation of, forensic, 19: 38495
of bladder, after radiotherapy of cancer of uterus, 19: 38531
pathology of, induced by inhaled plutonium-239 aerosols in dogs, 19: 38359 (BNWL-SA-230)
protection against, effectiveness of chemical radioprotective agents, 19: 38452
protection against, effects of morphine in mice, 19: 38453
protection against, effects of 2-mercaptobenzothiazole in mice, 19: 38466
protection against, effects of glycine on rat enzyme systems, 19: 38467
protection against skin, effects of anabolic steroid ointment, 19: 38468
protection against, effects of aminoethylisothiouranium in mice, 19: 38450 (USNRDL-TR-851)
protection against, effects of anoxia in mice, 19: 38450 (USNRDL-TR-851)
recovery from, in rat growth cartilage, 19: 38407

RADIATION MONITORING
equipment for atmospheric, 19: 39050(P)
equipment for cosmic neutron, 19: 39035
program at CVTR, 19: 40179(R) (CVNA-236)
Public Health Service program in U. S., 19: 38888

RADIATION PROTECTION
book: *Radiation Medicine*, 19: 38470(T)
clothing, materials, and methods for individual, 19: 38475
during diagnostic radiography, 19: 38523
effects of chemical compounds for, 19: 38472(T)
guides for, New York State, 19: 38887
guides, standards, and regulations of Federal Radiation Council, 19: 38886
in radiotherapy departments using brachycurie sources, 19: 38514
maximum permissible levels for external and internal, policies for, 19: 38479
measures for neutron source, 19: 38480
methods for, in handling gaseous, liquid, and solid wastes, 19: 38902
philosophy, 19: 38885
regulations for, 19: 38898

standards for, development of, 19: 38885
standards of, for atmospheric contamination by cesium-137 and strontium-89 and -90, 19: 38877 (NP-15183)
systems for closed-cycle water reactors, 19: 40197(R) (WCAP-3718)
ventilation of rooms containing gamma sources, 19: 38883
RADIATION SICKNESS
anatomy and pathology of, in animals, 19: 38436(T)
book: *Radiation Medicine*, 19: 38470(T)
development, symptoms, and treatment of, 19: 38471(T)
dietary factors affecting recovery of dogs and rats from, 19: 38457
effects combined with blood loss on phosphorus-32 uptake by ear, nose, and throat in rabbits, 19: 38431
effects on infection and natural immunity in animals, 19: 38434(T)
pathology in animals, 19: 38426
pathology of, 19: 38433(T)
protective effects of chemicals against, in animals, 19: 38472(T)
symptoms of, in rats, 19: 38444
RADIATION SOURCES
design of small, portable, 19: 38905(P)
dose distribution from multiple, use of digital computer for calculating, 19: 38526
flux from cylindrical and spherical, with slab shield, 19: 40068
industrial applications in Hungary, 19: 39063
leak testing enclosed, apparatus for, 19: 38909(P)
ventilation for industrial buildings containing, 19: 38884
RADIATION TARGETS
development for Intense Neutron Generator cyclotron, 19: 39756 (AECL-2177, Paper 3))
preparation of calcium, magnesium, and strontium, for accelerators, 19: 38658
uses of polarized proton, in high-energy physics, 19: 39497
RADIO WAVES
transmission in ionosphere, factors influencing, 19: 39682
RADIOACTIVE CONTAMINATION
measurement of alpha, equipment for, 19: 39045(P)
of fluid streams, method and apparatus for removal of, 19: 40119(P)
of soil, effects on plant ecology, 19: 38331
of soils, movement patterns in, 19: 40274
RADIOACTIVE MATERIALS
activities of, device for automatic measurement by scintillation counting, 19: 39020
activity measurement of, automatic sample changers for, 19: 39013
diffusion from laboratories and reactors, methods of preventing, 19: 38902
diffusion in sea water, computer program for, 19: 39265(R) (IA-1021)
drying apparatus for, 19: 38800(P)
monitoring atmospheric, equipment for, 19: 39050(P)
processing of, volumetric calibration of vessels for, 19: 38756 (RFP-488)
radioactivity of, equipment for measuring, 19: 38799(P)
use with luminescent materials as light source in light projector, 19: 38951(P)
RADIOACTIVITY
monitoring atmosphere, food, soil, and water for, in West German Republic, 19: 38904
monitoring dust and rainfall, in western Slovakia, 1961 to 1963, 19: 38881
RADIOAPPLICATORS
radiation protection during therapeutic use of brachycurie sources, 19: 38514
RADIOBIOLOGY
book: *Biological Effects of Neutron Radiation*, 19: 38437
botanical applications of, 19: 38327
RADIOCHEMICAL PROCESSING PLANTS
description of, at The Hague, 19: 40273
design and development for thorium–uranium fuel cycles, 19: 38755(R) (ORNL-3611)
design and operation for radioisotope production at Amersham, England, 19: 39073
nuclear material control program for reprocessing enriched uranium scrap, 19: 38758 (Y-KA-7)
RADIOCHEMISTRY
estimation of microcuries and millimicrograms from counts per minute, 19: 38749
RADIODERMATITIS
therapy using anabolic steroid ointment, 19: 38468
RADIODIAGNOSIS
hazards to nurses in, 19: 38482
of blood dyscrasias, 19: 38493
of brain tumors by gamma encephalography using mercury-203, 19: 38510
of calyx and renal pelvis excretion by radiopyelography using iodine-131, 19: 38530
of cerebral circulation in man by circulography using iodine-131, 19: 38489
of circulatory diseases of brain, using chlormerodrin–mercury-203 and external counting, 19: 38501
of diseases involving blood volume, 19: 38525
of heart diseases using cesium-131 and external counting, 19: 38503
of heart infarction using cesium-131 and external counting, 19: 38502
of heart using iodine-131-labeled albumin, 19: 38490
of kidneys in man, relation between excretory urography and radioisotope renography, 19: 38520
of malignant melanomas of eye, 19: 38485
of thyroid diseases using iodine isotopes, 19: 38496
of thyroid diseases using iodine-131, 19: 38497
of tumors, using cesium-131 and external counting, 19: 38508
radiation climate in rooms for, 19: 38524
radiation injuries during, legal aspects, 19: 38495
use of radioisotopes in, review on, 19: 38505
use of radioisotopes in, review on, 19: 38516
use of technetium-99 as tracer for, 19: 38506
RADIOFREQUENCY SPECTROMETERS
design of Mössbauer, using piezoelectric bar in resonant oscillation, 19: 39032
development of NMR, 19: 39011
RADIOGRAPHY
book: *An Introduction to Industrial Radiology*, 19: 38829
radiation protection during diagnostic, 19: 38523
use of iodinated contrast media for diagnostic, effects on iodine-131 metabolism in thyroid, 19: 38354
RADIOISOTOPES
activity of beta-emitting, liquid scintillators for measuring, 19: 39002
beta activity of, use of scintillation granules for measuring, 19: 38737
book: *Radiation Medicine*, 19: 38470(T)
book: *The Use of Radioactive Isotopes For Checking Production Processes*, 19: 39067(T)
decay correction factors for, data tabulations of, 19: 38744 (PHS-999-RH-12)
distribution in man, computer simulation for, 19: 40282 (BNWL-SA-171)
gamma spectra of, in IRR-1 pool-water, 19: 39265(R) (IA-1021)
half life of gaseous, design of flow detector for measuring, 19: 39012
incorporation of gamma-emitting, in ceramic spheres, temperature distributions from, 19: 40275
industrial applications in Hungary, 19: 39063
industrial uses of, review of Japanese, 19: 39064
injection into soils, probe for rapid, 19: 38870
metabolism, properties, and toxicology of, in animals, 19: 38357(T)
production in Amersham, England, 19: 39073
production in the Intense Neutron Generator, 19: 39762 (AECL-2177, Paper 9))
production of, for industrial uses, 19: 39066
separation from waste water, review of methods for, 19: 40276
use in diagnostic applications, review on, 19: 38505
use in diagnostic radiology, review on, 19: 38516
use in hematology, review on, 19: 38356
use in measurement of ion diffusion coefficients and mobility, 19: 38665
uses in Japan, 1950 to 1960, 19: 39060
RADIOLOGY
book: *An Introduction to Industrial Radiology*, 19: 38829
RADIOMETRIC ANALYSIS
estimation of microcuries and millimicrograms from counts per minute, 19: 38749
results of, reproducibility of, 19: 38556
techniques for, 19: 38889
uses of whole-body, 19: 38890
RADIOMIMETIC SUBSTANCES
effects on desoxyribonucleic acid content of intestinal wall of rats, 19: 38460
RADIOPROTECTIVE COMPOUNDS
effectiveness of chemical, 19: 38452
effectiveness of morphine, in mice, 19: 38453
effects on desoxyribonucleic acid content of intestinal wall in rats after administration of radiomimetic substances, 19: 38460
properties of, 19: 38472(T)
reaction mechanisms of cysteamine in mice, 19: 38469
reaction mechanisms of aminoethylisothiourea in mice, 19: 38469
RADIOSENSITIVITY
of algae, effects of illumination and darkness on, 19: 38410
of carcinoma in rabbits, effects of regional anoxia, 19: 38374
of Drosophila spermatogenesis, role of oxygen in determining, 19: 38463
of *E. coli*, location of genes controlling uv, 19: 38397
of *E. coli*, range of gene action controlling uv, 19: 38398
of Ehrlich ascites tumors at various invervals following inoculation,

oxygen effects on mouse x, 19: 38402
RADIOSTERILIZATION
of fruits, economic feasibility in southern U. S., 19: 39062 (TID-21710(Rev.))
of fruits, effects on spoilage during shipment, 19: 39062 (TID-21710(Rev.))
of meat, effects on flavor and lipids, 19: 39068
of meats, effects on color, 19: 39065
of rye flour, effects on vitamin content, 19: 38423
RADIOTHERAPY
book: *Dose Distribution and Dose Determination in Pendulum Irradiation (200 kv at 17 Mev)*, 19: 38534
design of automatic application intercavitary cobalt-60 source for, 19: 38483
development of high-energy sources for, 19: 38499
effects on mandibular necrosis induction, 19: 38527
inflammatory complications during, therapy using antibiotics and corticosteroids, 19: 38512
methods and equipment for, using radium and radon, 19: 38498
of cancer of bladder using gamma sources, 19: 38504
of cancer of larynx, effects on thyroid function, 19: 38484
of cancer using 70 Mev synchrotron, neutron flux and spectrum in, 19: 38517
of cancer, review, 19: 38487
of cancers, effects of hyperbaric oxygen on results, 19: 38500
of carcinoma of cervix, use of digital computer for calculating dose distribution in radium, 19: 38526
of carcinoma of uterus, hemolysis induced by, 19: 38509
of carcinoma of uterus, late pathological effects, 19: 38531
of carcinoma of uterus, late pathological effects, 19: 38532
of carcinomas of vocal cord, effects on larynx from radium, 19: 38519
of epithelioma, 19: 38494
of gynecologic tumors, digestive stenoses induction by, 19: 38522
of heart failure using iodine-131, 19: 38497
of hemangiomas of skin, contra-indications, 19: 38511
of hyperthyroidism using iodine-131, 19: 38497
of nose diseases by radon inhalation, 19: 38528
of retinoblastoma in infant, development of cranial fibrosarcoma from, 19: 38486
of thyroid tumors using iodine-131, 19: 38497
of tumors of vagina, effects on thyroid function, 19: 38492
of tumors, computer optimization of 4 Mev, 19: 38518
of tumors, evaluation by acridine orange staining of exfoliated cells, 19: 38488
radiation injuries during, legal aspects, 19: 38495
radiation protection during use of brachycurie sources, 19: 38514
radiocolloid treatment of malignant effusions, 19: 38515
ulcers of skin induced by, etiology, pathology, and therapy, 19: 38513
use of colloidal gold-198 for, hazards of, 19: 38476
use of iridium-192 in place of radium in, 19: 38521
RADIUM
dosimetry of dose distribution from therapy using, use of digital computer for calculating, 19: 38526
therapeutic use for tumors of vagina, effects on thyroid function, 19: 38492
therapeutic use for bladder cancers, 19: 38504
therapeutic uses of, equipment and laboratory for, 19: 38498
RADIUM ISOTOPES Ra-226
content in atmosphere, methods of measuring, 19: 38903
RADON
therapeutic effects of inhaled, for chronic nose diseases, 19: 38528
therapeutic uses of, equipment and laboratory for, 19: 38498
RADON ISOTOPES Rn-220
alpha decay of, polonium-216 charge in, (E), 19: 39884
charge state of ultra-fine aerosols of, in weakly ionized media, (T), 19: 39285
half life of, design of flow detector for measuring, 19: 39012
RAIN WATER
analysis for gamma sources, 19: 38557
analysis for strontium-89, 19: 38852
analysis for strontium-90, 19: 38852
monitoring radioactivity in, western Slovakia, 1961 to 1963, 19: 38881
radioactivity in Germany, 1962, 19: 38858
radioactivity of, in Austria, 1963, 19: 38860
RARE EARTH ALLOYS
study of CsCl-type intermediate phases in binary, 19: 39155 (CALT-221-11)
RARE EARTH COMPLEXES
with nitrate ions in aqueous and organic solutions, 19: 38578 (IA-1014)
RARE EARTH ISOTOPES
energy level collective oscillation frequency in, calculation by u-v transformation method, 19: 39782 (JINR-P-2191)
internal conversion coefficients for, (E/T), 19: 39786 (ORNL-P-1419)
RARE EARTH NITRATES
electric potential in liquid alkali nitrate cells, 19: 39265(R) (IA-1021)
RARE EARTHS
contents in minerals and rocks of batholith of Southern California, (E), 19: 38848
determination in electric insulators using spark-source mass spectrograph, 19: 38570
determination of, in SAP by spectrography, 19: 38553
energy levels of, (T), 19: 39383
pathological effects of subcutaneous implantations of, in mice, 19: 38334 (COO-1170-1)
phase transformations at 6 to 65 kbar, solid-liquid and solid-solid, 19: 40095
production and uses, 19: 38859
reactions with nitrate ions in solutions, 19: 39265(R) (IA-1021)
separation by ion exchange in nitrate solutions, 19: 38770
separation from chloride solutions by ion exchange, 19: 39265(R) (IA-1021)
separation from europium by distillation of bromides, 19: 38765
RATE METERS
design and performance of linear integrator, 19: 39005
design and performance of random pulse, 19: 39004
RATS
calcium metabolism in, 19: 38347
effects of nitrogen mustards on induction of dental lesions in, mechanism of, 19: 38325
effects of radiomimetic substances on content of desoxyribonucleic acid in intestinal wall of, 19: 38460
effects of radiophosphorus on denatured and whole serum in, 19: 38368
gold-198 excretion by kidneys in, morphology of, 19: 38342
iodine-131 metabolism in, effects of vitamin B on, 19: 38337
iodine-131 uptake by liver, lungs, and thyroid in, effects of colloid formation in iodine solution on, 19: 38351
oxidation in brain of, effects of vibration, 19: 38358 (AD-612660)
radiation effects in, of exposure *in utero*, psychological, 19: 38361(R) (TID-21951)
radiation effects on cardiovascular and hematopoietic systems in, fast neutron and x, 19: 38441
radiation effects on gonocytes in testes of, 19: 38369
radiation effects on DNA and nucleoprotein synthesis in by gonocytes in rat testes, 19: 38370
radiation effects on reticulocytes in peripheral blood in, 19: 38414
radiation effects on thyroid function in, neutron, 19: 38442
radiation effects on adrenal cortex function in, fast neutron, 19: 38443
radiation effects on chemical and physical properties of blood in, fast neutron and x, 19: 38440
radiation effects on morphology of organs in, fast neutron, 19: 38444
radiation effects on mortality of, RBE of fast neutron, 19: 38438
radiation effects on, dose effects on chronic calcium-45, 19: 38362(T) (JPRS-30993, pp 29-38)
radiation injuries of enzyme systems in liver and spleen, protective effects of glycine, 19: 38467
radiation injury and repair in cartilage in, 19: 38407
radioinduced neoplasms in thyroid of, after exposure of single lobe, 19: 38367
strontium-90 metabolism in, 19: 38347
thorium-230 metabolism in, after inhalation of uranium ore particles, 19: 38333 (BNWL-SA-226)
uranium metabolism, after inhalation of ore particles, 19: 38333 (BNWL-SA-226)
REACTION MECHANISMS
in molten beryllium fluoride--lithium fluoride, 19: 38582 (ORNL-P-1428)
REACTOR COMPONENTS
design of auxiliary, for closed-cycle water reactors, 19: 40197(R) (WCAP-3718)
design of auxiliary, for closed-cycle water reactors, 19: 40198(R) (WCAP-3721)
design of control elements, flow regulators, and pumps, (E), 19: 40135
development for large sodium graphite reactors, 19: 40286(R) (NAA-SR-11200
development of heat-transfer, for sodium-cooled reactors, 19: 40286(R) (NAA-SR-11200)
effects of operation on SRE, 19: 40286(R) (NAA-SR-11200)
testing facility for sodium-cooled, 19: 40286(R) (NAA-SR-11200)
REACTOR CONTROL ELEMENTS
burnup effects on worths of, (E), 19: 40163
movement of, electromagnetic system for, 19: 40140(P)
REACTOR CONTROL RODS
actuators for, using primary coolant water, (E), 19: 40135

design and development for large sodium graphite reactors, 19: 40286(R) (NAA-SR-11200
design of pressure-balanced, with fueled follower, (E), 19: 40135
development, 19: 40197(R) (WCAP-3718)
development, 19: 40198(R) (WCAP-3721)
development for LSGR, 19: 40126 (NAA-SR-11327)
drive mechanism for, 19: 40132(T) (ORNL-tr-590)
reactivity effects of, relations with core position, 19: 40195(R) (WCAP-3269-5)
reactivity worths of cadmium–indium–silver, 19: 40197(R) (WCAP-3718)
shock-absorbing device for, 19: 40142(P)
worths of cadmium–indium–silver, in tungsten–uranium lattices, 19: 40195(R) (WCAP-3269-5)

REACTOR CONTROL SYSTEMS
actuators in, using primary coolant water, (E), 19: 40135
design and development of full-range, 19: 40122(R) (GEAP-4862)
design for shut-down, 19: 40143(P)
development of chemical shim, for closed-cycle water reactors, 19: 40195(R) (WCAP-3269-5)
development of chemical shim for closed-cycle water reactors, 19: 40196(R) (WCAP-3269-6)
development of chemical shim, for closed-cycle reactors, 19: 40197(R) (WCAP-3718)

REACTOR COOLANTS
fission product activities in Saxton reactor, 19: 40196(R) (WCAP-3269-6)
pressure pulses in locally-heated sodium, 19: 39090(R) (ANL-7046(p.78-87))
radioactivity of Saxton, effects of defected fuel elements on, 19: 40195(R) (WCAP-3269-5)

REACTOR COOLING SYSTEMS
boiling burnout in water, comparisons of analyses of, (T), 19: 38814
coolant purification in primary, ion-resin methods for water, 19: 40123 (IAE-787)
coolant purity monitoring in primary loops of, standardization of water, 19: 40124 (IAE-789)
corrosion product deposition in Saxton reactor, 19: 40196(R) (WCAP-3269-6)
design for closed-cycle water reactors, 19: 40197(R) (WCAP-3718)
design for closed-cycle water reactors, 19: 40198(R) (WCAP-3721)
pipe failures in, survey of, 19: 40121 (GEAP-4574)
pipe rupture, program for study of, 19: 38824 (GEAP-4474)
water pH in, problems in measurement of, (E), 19: 40127 (ZFK-RN-17 (p.9-23))
water problems in, conference, (E/T), 19: 40117 (ZFK-RN-17)
water purification in, performance of resins for, (E), 19: 40128 (ZFK-RN-17(p.75-94))

REACTOR ENGINEERING
research on closed-cycle water reactors, 19: 40196(R) (WCAP-3269-6)
research programs on, 19: 40111(R) (ANL-7046)
startup preparations for power-expanded SRE, 19: 40286(R) (NAA-SR-11200)
stress analysis for prestressed-concrete vessels, finite element, 19: 40165 (GA-6303)
vessel blowdown from pipes, theory of two-phase, 19: 38802 (APED-4827)

REACTOR FUEL ALLOYS
development, 19: 39125(R) (BNWL-91)
development and testing, 19: 40177(R) (ANL-7046(p.1-35))
development of plutonium–uranium for ZPPR and ZPR-6 critical experiments, 19: 40177(R) (ANL-7046(p.1-35))
hydridation for removal of cladding, 19: 40113(R) (ANL-7071)
performance in HNPF, 19: 40286(R) (NAA-SR-11200)
processing by fluoride volatility, 19: 40112(R) (ANL-7046(p.36-66))
processing irradiated, by fluoride volatility, 19: 40113(R) (ANL-7071)

REACTOR FUEL ELEMENTS
boiling burnout of water-cooled rod clusters, comparisons of analyses of, (T), 19: 38814
cladding deformation on, effects of diffusion and stresses on, 19: 39220
cladding for, welding of SAP, 19: 39131
design of finned sheathed, in graphite sleeve, 19: 40173(P)
detection of failed, in Saxton reactor, 19: 40196(R) (WCAP-3269-6)
development and fabrication for SEFOR critical experiments, 19: 40177(R) (ANL-7046(p.1-35))
development and fabrication of canless prototype, 19: 40195(R) (WCAP-3269-5)
development for gas-cooled fast breeder, 19: 40182 (GA-5537)
development of advanced RCC canless, 19: 40196(R) (WCAP-3269-6)
diffusion of fission products from clad, mechanisms of, 19: 39152(R) (BMI-X-10132)
end closures for, design and evaluation of, (E), 19: 40172
fabrication of sheathed pellet type, to prevent movement between fuels and sheath, 19: 39148(P)
fabrication of uranium, nuclear materials management control system for, 19: 39130 (RFP-507)
failure detection in organic cooled reactors, circuits for, 19: 40133 (GAMD-6321)
fission product release from GAIL III-B, condensable, 19: 39233
packaging of disassembled, in hot cells, 19: 40270 (JUL-249-RW)
performance of PRTR, under reactor conditions, 19: 39125(R) (BNWL-91)
processing for high-temperature gas-cooled reactors, costs of, 19: 39129(R) (ORNL-TM-1116)
radiation effects on Saxton prototype, 19: 40195(R) (WCAP-3269-5)
radiation effects on Saxton in-pile defect test assemblies, 19: 40196(R) (WCAP-3269-6)
sheathing for, properties of cold-worked niobium–zirconium alloy, 19: 39150 (AECL-2250(Pt.I))
spacers for, to insure correct positioning, 19: 40174(P)
storage of irradiated, container for, 19: 38908(P)
temperature measurement in, acoustic resonator for, 19: 40138(P)
testing in pulsed water flows, vibration, 19: 40198(R) (WCAP-3721)
testing of, equipment for vibration, 19: 40197(R) (WCAP-3718)
testing of, nondestructive methods for automatic, 19: 38823 (BNWL-SA-97)

REACTOR FUEL ELEMENTS (CERAMIC)
fabrication for plutonium recycle experiments, 19: 40112(R) (ANL-7046 (p.36-66))
fabrication of "annular multitube" uranium-dioxide, (E), 19: 40172
fabrication of recycle PRTR, by remote equipment, 19: 39125(R) (BNWL-91)
fabrication of thoria–urania, by vibratory compaction, 19: 38755(R) (ORNL-3611)
fabrication of uranium-dioxide rods, (E), 19: 40172
radiation effects on clad urania, at high burnups, 19: 39234 (GEAP-4597)

REACTOR FUEL ELEMENTS (DISPERSION)
fabrication and properties of cermets of very small uranium carbide particles in uranium matrix, 19: 39127 (NCSC-2981-9)
fabrication of stainless-steel-clad stainless steel–urania, (E), 19: 40172

REACTOR FUEL PINS
fabrication of stainless steel-cerania, 19: 39125(R) (BNWL-91)
fabrication of stainless steel–plutonia, 19: 39125(R) (BNWL-91)

REACTOR FUEL RODS
boiling burnout of water-cooled rod clusters, comparisons of analyses of, (T), 19: 38814
end cap cracking on EBWR, effects of thermal cycling on, 19: 39125(R) (BNWL-91)
fabrication of glass-bonded plutonium-containing, for Doppler coefficient measurements, 19: 39124 (ANL-6995)
fabrication of prototype RCC, 19: 40195(R) (WCAP-3269-5)
fabrication of uranium dioxide, (E), 19: 40172
fabrication of Zircaloy-4-clad, 19: 40196(R) (WCAP-3269-6)
inspection for dimensional variations, apparatus for, 19: 38830(P)
production of thoria–urania in the Kilorod facility, flowsheets for, 19: 38755(R) (ORNL-3611)
radiation effects on stainless steel–urania prototype, 19: 40197(R) (WCAP-3718)
radiation effects on uranium carbide, at high burnups and temperatures, 19: 40286(R) (NAA-SR-11200)
radiation effects on clad uranium carbide, in TREAT transient heating, 19: 40286(R) (NAA-SR-11200)
radiation effects on EBWR-prototype, neutron, 19: 39125(R) (BNWL-91)
radiation effects on EBR-II, 19: 40113(R) (ANL-7071)
radiation effects on FR2, in-pile, (E), 19: 39253
repair of EBWR plutonium, 19: 39125(R) (BNWL-91)
separation from corrosion films, methods for, 19: 40198(R) (WCAP-3721)
thermal analysis of cylindrical, computer program for, 19: 40171 (KAPL-M-6475)

REACTOR FUEL SPHERES
disassembly and sampling of graphite-ball, equipment for, 19: 38792 (JUL-250-RW)
fabrication of graphite, 19: 39129(R) (ORNL-TM-1116)
radiation effects on graphite, neutron, 19: 39129(R) (ORNL-TM-1116)

REACTOR FUEL TUBES
boiling burnout of water-cooled, comparisons of analyses of, (T), 19: 38814
fabrication of "annular multitube" uranium-dioxide, (E), 19: 40172
fabrication of stainless-steel-clad stainless steel–urania, (E), 19: 40172
fabrication of stainless steel fuel cans for AGR, 19: 39134

REACTOR FUELS
analysis for fissionable material, nondestructive, 19: 38547 (TID-21475)
burnup determination by Compton recoil spectrometry, 19: 38825 (NP-15176)

burnup in pressure-tube heavy-water power reactors, (E/T), 19: 40185 (JAERI-1075)
burnup in SCE core, computer analysis of, 19: 40195(R) (WCAP-3269-5)
burnup of EBR-II, methods for determining, 19: 40113(R) (ANL-7071)
burnup of, computer program for, 19: 40147 (AEEW-M-448)
coating of particles, study of particle motion in fluidized-bed, 19: 38782 (ORNL-TM-1170)
coating of particulate, methods for pyrolytic carbon, 19: 39129(R) (ORNL-TM-1116)
conference on preparation and processing of particulate, 19: 40168 (CONF-117)
costs of, computer code for minimizing, 19: 40170 (HW-71813)
costs of, for simulated pressurized water reactor, 19: 40114 (BNWL-104)
cycle analysis of, chained computer codes for, 19: 40149 (BNWL-SA-61)
development and testing, 19: 39091(R) (BMI-1723(Del.))
evaluation for fissiochemical reactor, 19: 40169 (CONF-117(p.67-79))
fabrication and processing of uranium dioxide–plutonium dioxide, 19: 39146(P)
fission product release from irradiated pyrolytic carbon-coated particles, 19: 39228 (BMI-1734)
preparation and evaluation of carbon-coated particles, 19: 39126 (CONF-117(p.149-70))
preparation and properties of spherical plutonium-based particles, 19: 39096 (CONF-117(p.103-26))
preparation of uranium dioxide–yttrium oxide–zirconium oxide powders, 19: 39094 (CONF-117(p.11-19))
processing for plutonium and uranium recovery using TBP, 19: 38776(P)
processing of irradiated, methods for, 19: 40113(R) (ANL-7071)
processing of irradiated, description of The Hague Center for, 19: 40273
processing of thorium–uranium, fuel cycle facility for, 19: 38755(R) (ORNL-3611)
properties and structure of, 19: 39163(R) (MLM-1244)
radiation effects on alumina-coated uranium dioxide particles, 19: 39227 (BMI-1729)

REACTOR MATERIALS
development and testing, 19: 39091(R) (BMI-1723(Del.))
development for organic-cooled reactors, (E), 19: 40218
neutron economy and thermal efficiency demands of, 19: 40180 (DL-56)
properties and structure of, 19: 39163(R) (MLM-1244)
radiation damage in, small specimens for measurement of, 19: 38822 (BNWL-SA-2)

REACTOR MATRICES
critical experiments in uranium–Zircaloy-4, 19: 40196(R) (WCAP-3269-6)
critical facility for zero-reactivity experiments on heavy-water-moderated, 19: 40266
criticality measurements in proposed advanced SGR, 19: 40286(R) (NAA-SR-11200)
performance of 395 Mw(e), hydraulic and thermal, 19: 40198(R) (WCAP-3721)
power distribution in SCE, computer analysis of, 19: 40195(R) (WCAP-3269-5)

REACTOR MODERATORS
chemistry of water, problems in pH measurements, (E), 19: 40127 (ZFK-RN-17(p.9-23))
design and development for HNPF, 19: 40286(R) (NAA-SR-11200)

REACTOR SAFETY
coolant injection system design for San Onofre plant, 19: 40195(R) (WCAP-3269-5)
coolant water expulsion studies, 19: 40113(R) (ANL-7071)
hazard analyses for closed-cycle water reactors, 19: 40198(R) (WCAP-3721)
hazards analyses for closed-cycle water reactors, 19: 40197(R) (WCAP-3718)
tests for fast, development of, 19: 40286(R) (NAA-SR-11200)

REACTOR SAFETY EXPERIMENTS
operation of TREAT, 19: 40111(R) (ANL-7046)
operations in TREAT, 19: 39090(R) (ANL-7046(p.78-82))
operations in TREAT, June 1965, 19: 40113(R) (ANL-7071)

REACTOR SHIELDING
development for nuclear rockets, 19: 40246 (N64-29787)
neutron slowing down in, method for prediction of, 19: 40156 (NP-15161)
neutron transport in, removal-diffusion theory for, 19: 39751 (AE-185)

REACTOR SIMULATORS
performance of analog, 19: 40282 (BNWL-SA-171)

REACTOR SLURRIES
requirements for fissiochemical production, 19: 40169 (CONF-117 (p.67-79))

REACTOR TUBES
development for large sodium graphite reactors, 19: 40286(R) (NAA-SR-11200)
failure of primary coolant, survey of, 19: 40121 (GEAP-4574)
inspection of CVTR, sonic, 19: 40179(R) (CVNA-236)
replacement of process, in calandria cores of large sodium–graphite reactors, 19: 40125 (NAA-SR-9821)

REACTORS
atmospheres of, deuterium oxide and tritium separation from, 19: 38907
control rod movement in, electromagnetic system for, 19: 40140(P)
control rod shock-absorbing device for, 19: 40142(P)
coolant channel deformation under fuel expansion, hydraulic, and thermal loads, 19: 40118 (WAPD-T-1782)
core design with movable and fixed control rods for, 19: 40146(P)
criticality studies on zirconium-hydride moderated, review, (E), 19: 40163
design with fluid coolant flowing through fuel magazines, 19: 40166(P)
diffusion of radioactive materials from, methods of preventing, 19: 38902
effects of large complex of, on atmospheric turbulence and diffusion, 19: 39259 (IDO-12041)
fuel burnup studies in cylindrical, computer program for, 19: 40147 (AEEW-M-448)
fuel cladding materials for, 19: 39206
instrumentation for, ESONE electrical and mechanical reference parameters for, 19: 38924
loading device for, design, 19: 40144(P)
neutron cross sections for cells of calculational methods for, 19: 40152 (GA-6462)
neutron flux in, computer programs for calculating, 19: 40157 (ORNL-TM-1175)
neutron pulsed source technique for, modified, (T), 19: 40151 (EIR-79)
noise analysis in, (T), 19: 40164
pressure vessels for, concrete, 19: 40134
pumps design, fluid-driven mechanical, 19: 40139(P)
research at IFA, 19: 40287(R) (NP-15188)

RECTIFIERS
radiation effects on silicon-controlled, 19: 39055 (GA-6266)

REFLECTOR MODERATED REACTORS
criticality studies of LASL cavity reactor, 19: 40154 (LA-3229, pp 344-61)
design of coaxial flow gaseous, for propulsion, 19: 40232 (LA-3229, pp 177-9)
design of, gaseous-core criticality effects on, 19: 40155 (LA-3229, pp 362-76)
fuel containment and heat deposition in gaseous core, 19: 40235 (LA-3229, pp 222-36)
fuel-propellant flow in gaseous-core, for propulsion, 19: 40233 (LA-3229, pp 180-207)
heat transfer in coaxial flow gaseous core, 19: 40234 (LA-3229, pp 208-21)

REFRACTORY MATERIALS
electric conductivity of, apparatus for measurement of, 19: 38922(T) (AAEC/Tmns-18)

RELATIVITY THEORY
Einstein field equations for empty space, 19: 39663
Einstein field equations for incoherent matter and electromagnetic fields, 19: 39648
elementary particle masses in unified field theory, 19: 39452 (CONF-796(Paper 13))
field equations in, solution of Einstein, 19: 39273(R) (UCRL-12204, pp 60-5)
formalism for special, principle for inertial frames applied to mechanical phenomena in, (T), 19: 39637
Lorentz transformation matrix in Minkowski space, decomposition into skew-symmetric tensors, 19: 39643
mass equivalent of potential energy in, (T), 19: 39554
particle interactions in, canonical position variables in many-body, 19: 39645
space-time properties in macroscopic regime, 19: 39625 (CONF-796 (Paper 12))
transformation of Lorentz group, from linear- to angular momentum basis for nonzero-mass arbitrary-spin particles, 19: 39500

REMOTE-CONTROL EQUIPMENT
control device with safety program for, 19: 38798(P)
design and development for thorium fuel cycle program, 19: 38755(R) (ORNL-3611)
design for cutting and rewelding bottom process tube joints in large sodium–graphite reactors, 19: 40125 (NAA-SR-9821)

RENE-41
properties as cladding material for SNAP hydride reactors, 19: 39166 (NAA-SR-Memo-11149)

RESEARCH REACTORS
construction and developmental status of, compilation on, 19: 40116 (TID-8200(12th Rev.))

construction of Essor, use of PERT method for design and installation phases in, 19: 40265
coolant characteristics in Hungarian, (E), 19: 40264 (ZFK-RN-17 (p.54-67))
coolant purification using ion exchange materials, water, 19: 38759 (ZFK-RN-17(p.95-117))
coolant water decomposition rate in, 19: 38698 (ZFK-RN-17(p.199-207))
coolant water of Soviet RPT, conductometer for dissolved salts in, 19: 40262 (ZFK-RN-17(p.25-31))
design of Zero Power Plutonium Reactor, 19: 40113(R) (ANL-7071)
neutron flux distributions in, intensification of, 19: 39754 (AECL-2177, Paper 1))
operation of WWR-C, at Rossendorf, Germany, (E), 19: 40261 (ZFK-RN-17(p.179-98))
radiation effects on fuel elements of FR2, in-pile, 19: 39253
water characteristics in primary circuits of, (E), 19: 40260 (ZKF-RN-17(p.68-74))
water chemistry measurements in Czech WWR-S, (E), 19: 40263 (ZFK-RN-17(p.32-43))
water purification in water-cooled, performance of resins for, (E), 19: 40128 (ZFK-RN-17(p.75-94))
water purification in EWA Polish, ion-exchange filter for, 19: 38760 (ZFK-RN-17(p.127-38))
RESINS
elastic properties of epoxy, determination by ultrasonics, 19: 40112(R) (ANL-7046(p.36-66))
performance of ion-exchange, in filter for EWA research reactor, 19: 38760 (ZFK-RN-17(p.127-38))
radiation stability of anion-exchange, reactor, 19: 38697 (ZFK-RN-17 (p.139-64))
radiostability of synthetic, used in radioactive-water purification, (E), 19: 40129 (ZFK-RN-17(p.114-26))
β-RESORCYLIC ACID
complexes with uranyl ions, spectra of, absorption, 19: 38607
RESPIRATORS
filtration materials for, protecting against radioactive aerosols, 19: 38900
RESPIRATORY TRACTS
radiation sickness effects on, pathology of, 19: 38433(T)
thorium-230 content in, after inhalation of uranium ore, in rats, 19: 38333 (BNWL-SA-226)
RHENIUM
effects on superconducting transition temperature of vanadium silicide, 19: 39196
elastic properties of, determination by ultrasonics, 19: 40112(R) (ANL-7046(p.36-66))
performance as emitter in thermionic converters, 19: 39431(R) (AD-608554)
sorptive properties for oxygen, (E/T), 19: 39103
RHENIUM ALLOY COUPLES
Re–W/Re–W, emf measurements, (E), 19: 40177(R) (ANL-7046(p.1-35))
RHENIUM ALLOYS
Cr–Re, aging of, effects of nitrogen on, 19: 39091(R) (BMI-1723(Del.))
Cr–Re, antiferromagnetism of, at 95 to 300°K, 19: 40077 (IS-T-18)
Cr–Re, electric conductivity and thermoelectric power of, at 4.2 to 450°K, 19: 40077 (IS-T-18)
Mo–Re, elastic properties of, determination by ultrasonics, 19: 40112(R) (ANL-7046(p.36-66))
Re–W, fabrication of seamless tubing of, 19: 39128(R) (NMI-1267)
RHENIUM ISOTOPES Re-185
neutron reactions (n,γ) at 4 kev to 2.6 Mev, cross sections for, (E), 19: 40112(R) (ANL-7046(p.36-66))
RHENIUM ISOTOPES Re-187
neutron reactions (n,γ) at 4 kev to 2.6 Mev, cross sections for, (E), 19: 40112(R) (ANL-7046(p.36-66))
RHODIUM
catalytic properties in deuterium exchange reactions, 19: 38597
radiation damage in, cross sections for atomic displacements from 1- to 3-Mev electrons, 19: 39225 (AFCRL-65-286)
RHODIUM ALLOYS
Ce–Rh, phase studies, 19: 39163(R) (MLM-1244)
Rh–Zr, specific heat at 0.9 to 12°K, (E), 19: 39218
RHODIUM ISOTOPES Rh-103
carbon-12 reactions at 40 to 80 Mev, decay of indium-109 isomeric state from, (E), 19: 39861
energy levels in, polarization determination of spin of, (E), 19: 39945
gamma transitions in, circular polarization of 498-kev, (E), 19: 39945
RHODIUM ISOTOPES Rh-106
determination in rain water, 19: 38557
RIBONUCLEASE
radiation effects on synthesis in rat spleen and thymus, x, 19: 39265(R) (IA-1021)
radiosensitivity effects on *E. coli*, 19: 38465
RIBONUCLEIC ACID
genetic code for messenger, 19: 40296 (TID-21856)
radiation effects on content of, in amoeba, 19: 38371
radiation effects on synthesis of, in derivatives of *E. coli*, 19: 38381
uptake of carbon-14-labeled precursors by L-cell nuclei, effects of tritiated thymidine on, 19: 38339
RIBONUCLEIC ACID, DESOXY-
denaturation of, thermal, 19: 40299(T) (LA-tr-65-12)
effects of irradiated, on mutations in *Drosophila melanogaster*, 19: 38413
effects of radiomimetic substances on content of, in intestinal wall of rats, 19: 38460
genetic properties of exogenous, in Drosophila, 19: 38408
genetic role of, in protein synthesis, 19: 40299(T) (LA-tr-65-12)
metabolism in mice, tracer study using tritiated thymidine, 19: 38336 (TID-21106)
radiation dosimetry of tritium-labeled, 19: 38873 (BNL-9331) (IA-1021)
radiation effects on synthesis in rat spleen and thymus, x, 19: 39265(R)
radiation effects on synthesis of, by gonocytes in rat testes, 19: 38370
radioinduced degradation of, effects on genetic properties in Drosophila, 19: 38408
sorption by water, tracer study of mechanisms of, 19: 39265(R) (IA-1021)
uptake of carbon-14-labeled precursors by L-cell nuclei, effects of tritiated thymidine on, 19: 38339
uptake of halogenated pyrimidines by L cell, radiosensitivity effects of, 19: 38459
viscosity of, effects of temperature, 19: 42099(T) (LA-tr-65-12)
ROCKET MOTOR NOZZLES
development for rocket reactors, using refractory metals, 19: 40254
ROCKET MOTORS
development and operation of cesium ion, 19: 38834(R) (N64-29495)
ROCKET REACTORS
conference, 19: 40221 (LA-3229)
criticality studies of gaseous-core, (T), 19: 40239 (LA-3229, pp 315-43)
design and performance of fluidized bed, 19: 40223 (LA-3229, pp 48-62)
design and performance of liquid core, 19: 40227 (LA-3229, pp 90-110)
design of coaxial flow gaseous core, 19: 40232 (LA-3229, pp 177-9)
development, 19: 40247 (N64-29788)
flow development of, review of, 19: 40242 (LA-DC-7118)
fuel containment and heat deposition in gaseous core, 19: 40235 (LA-3229, pp 222-36)
fuel material partition from propellant in gaseous fuel, glow-plug concept for, 19: 40228 (LA-3229, pp 111-15)
fuel material partition from propellant in gaseous core, 19: 40229 (LA-3229, pp 116-36)
fuel material partition from propellant in gaseous fuel, light bulb concept for, 19: 40230 (LA-3229, pp 137-47)
fuel vortex flow in gaseous-core, 19: 40236 (LA-3229, pp 237-50)
fuel vortex flows in gaseous-core, 19: 40237(LA-3229, pp 251-85)
fuel-propellant coaxial flow in, 19: 40233 (LA-3229, pp 180-207)
fuel-propellant energy exchange using MHD cells, 19: 40238 (LA-3229, pp 286-312)
heat transfer in coaxial flow gaseous core, 19: 40234 (LA-3229, pp 208-21)
power production using MHD cells, 19: 39442
properties for space travel, 19: 40222 (LA-3229, pp 10-47)
radiation hazards from, computer program for, 19: 40248 (NUS-180)
shielding physics for, lectures on, 19: 40246 (N64-29787)
ROCKET REACTORS (KIWI)
control system for NERVA in low power, no flow region, 19: 40252
neutron kinetics in coupled, models for pulsed, 19: 40240 (LA-3263)
propellant testing in, liquid hydrogen, 19: 40244 (LA-DC-7170)
radiation-level measurements from ground test of B-4, (E), 19: 40253
temperature transfer function of B4E, measurement of power-to-core, 19: 40241 (LA-DC-6845)
testing of RIFT stages, plans for captive, 19: 40245 (N64-23519)
ROCKETS
properties for space travel, 19: 40222 (LA-3229, pp 10-47)
propulsion of nuclear, liquid hydrogen for, 19: 40243 (LA-DC-7169)
ROCKS
age estimation of, in Vindhyan system in India, by potassium–argon method, 19: 38853
crater formation in basalt by Dugout row-charge explosion, 19: 38789 (PNE-601F)
rare-earth contents of, from batholith of Southern California, (E), 19: 38848
RODS
boiling burnout in 19-rod bundle, effects of fluid mixing and rod spacing on, 19: 38805(R) (BNWL-C-3)

ROENTGEN UNITS
energy equivalent for vinyl chloride, 19: 39016
RUBIDIUM
book: *Cesium and Rubidium*, 19: 38674(T)
content and distribution in subterranean Bulgarian salt water, 19: 38851
determination in enamel of teeth, neutron activation, 19: 38562
neutron reactions (n,α) and (n,p) at 13 to 17 Mev, cross sections for, (E), 19: 39823
production and uses, 19: 39106
sorption by gamma-alumina and inorganic ion exchange materials from fused salts, 19: 38771
spin relaxation of optically pumped vapor of, in rare gases, (E), 19: 39400
RUBIDIUM FLUORIDES
PaF_4–RbF, preparation and crystal structure of complex compound in, 19: 38625
RUBIDIUM XENATES
preparation and properties, 19: 38624
RUPTURE
reactor pipe, program for study of, 19: 38824 (GEAP-4474)
RUSSIAN REACTORS
water chemistry measurements in Czech WWR-S, (E), 19: 40263 (ZFK-RN-17(p.32-43))
RUTHENIUM
catalytic properties in deuterium exchange reactions, 19: 38597
performance as collector and emitter in a thermionic converter, 19: 39431(R) (AD-608554)
separation from plutonium and uranium by TBP extraction, 19: 38776(P)
separation from solutions of its compounds by oxidation and extraction, 19: 38763
separation from uranyl nitrate solutions by solvent extraction using TBP, 19: 38764
RUTHENIUM ALLOYS
In–Ru, crystal structure of intermetallic compound $RuIn_3$ in, 19: 39207
RUTHENIUM COMPOUNDS
separation of ruthenium from solutions of, by oxidation and extraction, 19: 38763
RUTHENIUM ISOTOPES Ru-103
content in diet and excreta in Japan, 19: 38894
determination in rain water, 19: 38557
RUTHENIUM ISOTOPES Ru-106
content in diet and excreta in Japan, 19: 38894
determination in rain water, 19: 38557
motion in soil, effects of chelating agents on, 19: 38329 (TID-20471)
RUTHENIUM NITROSYLS
solvent extraction from nitric acid solutions by tertiary amines, 19: 38761(T) (CEA-tr-A-1809)
RYE
radiation effects on growth in seedlings of, effects of oxygen tension on gamma, 19: 38418

S

SAFETY
regulations for protection from ionizing radiations, 19: 38898
SAFETY HAZARDS
control of liquid hydrogen, at experimental facilities, 19: 38875 (HASL-160)
radiation exposure, assessment of occupational, 19: 38474
SALT DEPOSITS
waste disposal in, problems in, 19: 40272
SAMARIUM
determination of, in SAP by spectrography, 19: 38553
neutron absorption properties of, burnup effects on, (E), 19: 40163
phase transformations at 6 to 65 kbar, solid-liquid and solid-solid, 19: 40095
proton inelastic scattering at 25 to 1700 kev, x-ray yields from, (E), 19: 39881
separation from europium by distillation of bromides, 19: 38765
separation from promethium by ion exchange, 19: 38772
SAMARIUM COMPLEXES
with [(2-hydroxyethyl)imino]diacetic acid, dissociation constant of, 19: 38671
SAMARIUM FERRATES
samarium-149 hyperfine interactions in, 19: 39265(R) (IA-1021)
SAMARIUM IONS
reduction in calcium fluoride, yttrium ion effects on, (E), 19: 38595
SAMARIUM ISOTOPES Sm-147
neutron reactions (n,γ), gamma spectra of 3.4-ev resonance of, 19: 39781 (JAERI-1073)
SAMARIUM ISOTOPES Sm-148
energy levels in, negative parity, (T), 19: 39845
SAMARIUM ISOTOPES Sm-149
hyperfine interactions of ground- and 22-kev-state in samarium ferrites, 19: 39265(R) (IA-1021)
neutron reactions (n,γ), gamma spectra of 0.096- and 0.89-ev resonance of, 19: 39781 (JAERI-1073)
SAMARIUM ISOTOPES Sm-152
energy levels, (E), 19: 39928
neutron reactions (n,γ), gamma spectra of 8.2-ev resonance of, 19: 39781 (JAERI-1073)
SAMARIUM OXIDES
reactions with sodium metaphosphate, spectra of compound formed in, 19: 38668
SmO–SiO_2, preparation and crystal structure, 19: 38621
SmO–SiO_2, spectra and crystal structure of, infrared, 19: 38622
SAMARIUM PYROPHOSPHATES
preparation and properties, 19: 38616
SAMPLING
equipment for graphite ball fuel elements, 19: 38792 (JUL-250-RW)
methods for solubility of elements in liquid plutonium, evaluation, 19: 38580 (LA-3303)
SAN ONOFRE POWER REACTOR
coolant injection system for, 19: 40195(R) (WCAP-3269-5)
xenon oscillations in, calculations of, 19: 40195(R) (WCAP-3269-5)
SAP (SINTERED ALUMINUM PRODUCTS)
analysis for rare earths, spectrographic, 19: 38553
fabrication into reactor fuel cladding, (E), 19: 40172
performance in organic-cooled reactors, (E), 19: 40218
properties for use as fuel cladding material in reactors, 19: 39206
welding of, for use for nuclear fuel cladding, 19: 39131
SAPPHIRES
properties for use as fuel-propellant partition in gaseous fuel rocket reactors, 19: 40229 (LA-3229, pp 116-36)
SARCOMAS
radiation effects on development of cranial, from therapy of retinoblastoma, 19: 38486
SATELLITES
design and performance of Explorer XVII, 19: 39679
motion in interplanetary space and ionosphere, electromagnetic effects from, (T), 19: 39683
orientation in space, determination of, 19: 38957(P)
power generator ejection from NIMBUS-B, dynamic analysis of mechanism for SNAP-19, 19: 39071 (MND-3169-68)
radiation effects on, 19: 39059
SAVANNAH RIVER COMPONENTS TEST REACTOR
operations and performance, (E), 19: 40267
SAXTON POWER REACTOR
coolant fission product activity levels in, 19: 40196(R) (WCAP-3269-6)
fuel assemblies for, design of removable, 19: 40198(R) (WCAP-3721)
fuel elements for, fabrication of, 19: 39125(R) (BNWL-91)
noise analysis in, (E), 19: 40164
reactivity of, effects of coolant heat transfer and radioactive corrosion products on, 19: 40196(R) (WCAP-3269-6)
SCANDIUM
separation from thorium and uranium by ion exchange in nitrate solutions, 19: 38770
separation from waste water, methods for, 19: 40276
SCANDIUM CARBONATES
compound formation with oxalate, electric conductivity and structure of, 19: 38672
SCANDIUM ISOTOPES Sc-40
beta decay of, ground state spin from, (E), 19: 39850
mass difference of calcium-40 and, (E), 19: 39850
SCANDIUM ISOTOPES Sc-41
energy levels, (E), 19: 39874
SCANDIUM ISOTOPES Sc-42
beta decay of, conserved vector current hypothesis and ft values for, (E/T), 19: 39859
SCANDIUM ISOTOPES Sc-46
decay of, gamma transitions in, (E), 19: 39866
SCANDIUM OXALATES
compound formation with carbonate, electric conductivity and structure of, 19: 38672
SCANDIUM SYSTEMS
1–4,4'-methylenediantipyrine–Sc, complex formation in, 19: 38670
SCATTERING
amplitudes for three-body, in complex momentum, (T), 19: 39596
amplitudes in, N/D approach in bootstrap solutions for, 19: 39463 (IC/65/62)
bound states in multichannel and single-channel, (T), 19: 39600

Feynman graphs in, asymptotic behavior of, 19: 39465 (JINR-E-2125)
of particles by superposed Yukawa potentials, relativistic, (T), 19: 39598
phase shift and resonance equations for elastic, 19: 39487 (UCRL-14193)
potential, momentum transfer in, (T), 19: 39543
potentials in, separable, (T), 19: 39949
theory of elastic, derivation of formal, 19: 39821
theory of phonon, by point defects, 19: 40109
SCINTILLATION DETECTORS
design and performance of automatic gamma, 19: 39003
development of liquid, of soft beta-particles, 19: 39002
efficiency crystal, liquid, and plastic, for gamma radiation, 19: 39009
efficiency of well-type crystals in, for gamma measurements, 19: 39039
performance for beta particles, effects of discrimination and dead times on, 19: 39014
performance of, review of, 19: 38995 (NP-15259)
response of organic, to fast neutrons, (T), 19: 38997 (UCRL-16149)
use in measurement of alpha contaminated surfaces, 19: 39045(P)
SEA WATER
contamination by accidents at IRR-1, estimates of, 19: 39265(R) (IA-1021)
desalination of, design and economics of sodium cooled fast breeder reactor for, 19: 40190 (ORNL-TM-784)
desalination of, performance of NPR for, 19: 40219 (RL-SA-21)
radioactive waste disposal in, safety precautions for, 19: 40277
SEALS AND GLANDS
design for coaxial tubes, 19: 38785(P)
development of ceramic-to-metal, for thermionic cells, 19: 39070(R) (GEST-2046)
SEDIMENTARY DEPOSITS
age estimation of pelagic, from uranium-234/uranium-238 ratio, (E/T), 19: 38866
SEED
radiation effects on wheat, effects of water content on, 19: 38412
SEEDLINGS
radioinduced growth inhibition in cereal, effects of oxygen tension on gamma, 19: 38418
SEISMOMETERS
array design, information theory uses in, 19: 39269(R) (SU-SEL-64-133)
SELENIUM
superconductivity under high pressure, (E), 19: 39736
SELENIUM ISOTOPES Se-75
energy from, determination of total, 19: 38878 (ORNL-P-1405)
SELENIUM SYSTEMS
Ge–La–Se, chemical properties, 19: 38598
SEMICONDUCTOR DETECTORS
development of silicon p-i-n fast neutron dosimeters, 19: 38992 (COO-1226-8)
fabrication and performance of windowless lithium-drifted germanium, 19: 39018
fabrication of lithium-drifted position-sensitive, 19: 39027
fabrication of lithium-drifted germanium, temperature control system for, 19: 39029
resolution for fission fragments, (T), 19: 39033
SEMICONDUCTORS
current-voltage characteristics of tunnel junctions of, second harmonic detection system for, 19: 38944
electric conductivity in ohmic contact with normal metal at low temperatures, (E), 19: 39734
fission-fragment damage in, (E), 19: 39245
light detection by, research on, 19: 39269(R) (SU-SEL-64-133)
radiation effects on, electron, 19: 40286(R) (NAA-SR-11200)
radiation effects on silicon, gamma, 19: 39269(R) (SU-SEL-64-133)
radiation effects on, in space environment, 19: 39059
radiation effects on, electron-hole pair production in high-energy particle, (T), 19: 39250
transport properties of n-type, theory of high-field, 19: 39269(R) (SU-SEL-64-133)
SENA POWER REACTOR
design and development, Jan.–Mar. 1965, 19: 40192(R) (TID-22003)
design, construction, and improvements, 19: 40209
SEPARATION PROCESSES
distillation column design and efficiency for, 19: 38766
SEPARATORS
development of horizontal and upcomer, for steam, 19: 38801(R) (ACNP-65004)
SERUMS
effects of radiophosphorus on denatured and whole, in rats, 19: 38368
radiation effects on proteins of, in Hiroshima bomb survivors, 19: 38377
SEX
effects on behavior and learning ability of rats irradiated *in utero*, 19: 38361(R) (TID-21951)
SF MATERIALS ACCOUNTING
control of uranium fuel element fabrication, systems for, 19: 39130 (RFP-507)
SHEEP
erythrocyte life span in, tracer study, 19: 38343
SHELTERS
ventilating system for fallout, 19: 38833(P)
ventilation of, durability tests of punkah-pump for, 19: 38832 (ORNL-TM-1155)
SHIELDED CONTAINERS
design for radiation sources, 19: 38905(P)
design for temporary storage of irradiated fuel elements, 19: 38908(P)
drop tests on Types F and G, 19: 38546(R) (RFP-552)
SHIELDING
book: *The Propagation of Gamma Quanta in Matter*, 19: 40071
data on, against radiation transport in air from atomic explosions, 19: 38893
development for Intense Neutron Generator, 19: 39761 (AECL-2177, Paper 8))
development for manned space vehicles, 19: 40063 (NP-15125)
electron dose rates behind spherical multilayer, computer program for calculation of, 19: 40064 (NP-15132)
electron reactions in space vehicle, bremsstrahlung from, 19: 40062 (N64-29366)
problems in space-vehicle, 19: 40072
proton dose rates behind spherical multilayer, computer program for calculation of, 19: 40064 (NP-15132)
radiation flux from cylindrical and spherical sources with slab, 19: 40068
SHIELDING MATERIALS
book: *Nuclear Technology in Construction*, 19: 38828
gamma absorption by heterogeneous, effective atomic numbers for, 19: 40069
neutron albedo measurement on, thermal, 19: 40065 (NP-15152)
SHIPPING
containers for, drop tests on Types F and G, 19: 38546(R) (RFP-552)
of plutonium, measurement problems in, 19: 38535 (RFP-508)
SHOCK WAVES
blast from Dugout row-charge cratering experiment, measurements of close-in air, 19: 38790 (PNE-608F)
effects of interplanetary, on sudden impulse pairs in magnetic storms, 19: 39681
gas state behind strong, excitation and relaxation of, (T), 19: 40040
propagation in plasma, turbulent heating in, 19: 40047
propagation in thermal plasmas, density and temperature behind, (T), 19: 40051
propagation parameters of MHD ionizing, in a conducting media, 19: 39267 (NP-15157)
structure in atomic hydrogen in internal relaxation region, (T), 19: 39280
structure in neutral gases and plasma, (T), 19: 39984
use in high-pressure physics, 19: 39274(T) (JPRS-30799)
SILICON
determination in trace amounts in aluminum by x-ray spectrography, 19: 38571
effects on cesium ion and neutral emission from hot porous tungsten, 19: 39164 (N64-22193)
fission-fragment damage in, (E), 19: 39245
helium ion channeling reactions at 209 ev, thermochemical properties for, (T), 19: 39395
neutron reactions (n,n′γ) at 0 to 14 Mev, energy absorption in, 19: 39769 (SC-DC-65-1544)
photoelectron emission yields at 2 to 6 ev from cesiated surfaces of, spectral analysis of, 19: 39406
radiation damage detection by field effect, (T), 19: 39252
radiation effects on recombination in, gamma, (E), 19: 40085
radiation effects on, electron-hole pair production in high-energy particle, (T), 19: 39250
radiation effects on crystal structure of, microplasm studies of, 19: 39254
reactions with lanthanum and lanthanum oxides to prepare lanthanum silicides, 19: 38613
reactions with plutonia at high temperatures, 19: 39125(R) (BNWL-91)
reactions with strontia at 1200°C, 19: 38593(T) (ORNL-tr-674)
separation from graphite above 1750°C in inert gases, 19: 38762
solvent properties for sodium at 800°C, 19: 39204
superconductivity under high pressure, (E), 19: 39701
x-ray diffraction by single crystals of, Pendelloesung fringes in, (E/T), 19: 39287
SILICON CARBIDES
decomposition of, crystal structure of graphite formed in, 19: 39185
SILICON FLUORIDES

nuclear magnetic resonance spectra of, collision-narrowing theory of, 19: 38629

SILICON ISOTOPES Si-28
bremsstrahlung reactions (γp) with, proton energy distribution in, (E), 19: 39938

SILICON JUNCTIONS
performance as i-r modulators, (E/T), 19: 38914 (SC-DC-65-1332)
radiation effects, gamma, 19: 39269(R) (SU-SEL-64-133)

SILICON OXIDES
performance for thermal energy transfer in gaseous fuel rocket reactors, 19: 40230 (LA-3229, pp 137-47)
radiation effects on deuterium–hydrogen exchange on surfaces of colloidal, 19: 38626
CeO–SiO_2, crystal structure, 19: 38621
EuO–SiO_2, preparation and crystal structure, 19: 38621
EuO–SiO_2, spectra and crystal structure of, infrared, 19: 38622
SiO_2–SrO, crystal structure, 19: 38621
SiO_2–YbO, preparation and crystal structure, 19: 38621
SiO_2–YbO, spectra and crystal structure of, infrared, 19: 38622
SmO–SiO_2, preparation and crystal structure, 19: 38621
SmO–SiO_2, spectra and crystal structure of, infrared, 19: 38622

SILICON SYSTEMS
Al–Fe–Mg–Ni–Si–Ti–Zr, coating with aluminum–nickel layers by chemical deposition, 19: 39143(P)
Ge–Si, properties for thermocouples, 19: 39430(R) (AD-426092)
Mo–Nb–Si, phase studies and properties of, 19: 39194

SILTS
uranium content in, in water of Lake Issyk-kul, USSR, 19: 38855

SILVER
content in solar atmosphere, (E), 19: 39345
determination in minerals, spectrochemical, 19: 39265(R) (IA-1021)
determination in minerals by activation, 19: 39265(R) (IA-1021)
gamma reactions at 6.13 Mev, electron pair production cross sections for, (E), 19: 39787 (SGAE-PH-19/1965)
ion reactions with emulsion nuclei of, recoil range-momentum relation for, (E), 19: 39883
neutron absorption properties of, burnup effects on, (E), 19: 40163
rare-gas ion reactions at 1 to 10 kev, secondary-electron emission in, (E), 19: 39404

SILVER ALLOYS
Al–Ag, Guinier-Preston zones in, x-ray and electron microscopic studies of size of, 19: 39172(T) (ORNL-tr-633)
Al–Ag, radiation effects on, annealing electron, 19: 40286(R) (NAA-SR-11200)
Al–Ag, strain hardening of, x-ray studies of segregation zones in, 19: 39174(T) (ORNL-tr-635)
Cd–In–Ag, radiation effects on dimensions and mechanical properties of, 19: 40197(R) (WCAP-3718)
Cd–In–Ag, radiation effects on dimensions and mechanical properties of, 19: 40198(R) (WCAP-3721)
Cd–In–Ag, reactivity worths in uranium–Zircaloy-2, 19: 40196(R) (WCAP-3269-6)
Cd–In–Ag, reactivity worths of, 19: 40197(R) (WCAP-3718)
Cd–In–Ag–Sn, radiation effects on dimensions and mechanical properties of, 19: 40197(R) (WCAP-3718)
Cd–In–Ag–Sn, radiation effects on dimensions and mechanical properties of, 19: 40198(R) (WCAP-3721)
Mg–Ag, annealing of deformed AgMg, 19: 39168(R) (TID-22015)
Mg–Ag, heats of formation of silver-rich solid solutions, 19: 39168(R) (TID-22015)

SILVER IONS
radiolysis of aqueous solutions of, pulse, 19: 38728

SILVER ISOTOPES Ag-107
alpha reactions (α,2n) at 28 Mev, indium-109 gamma transitions from, (E), 19: 39861
neutron reactions (n,γ), gamma spectra in 16.6-ev resonance of, 19: 39781 (JAERI-1073)

SILVER ISOTOPES Ag-109
neutron reactions (n,γ), gamma spectra in 5.2-ev resonance of, 19: 39781 (JAERI-1073)

SILVER ISOTOPES Ag-111
release from pyrolytic carbon-coated fuel particles, 19: 39228 (BMI-1734)

SINGLE CRYSTALS
development for mixing infrared and visible laser output, 19: 39269(R) (SU-SEL-64-133)
ion scattering by, energy distribution in, (E), 19: 39297
lattice dynamics of one-dimensional, with free ends, (T), 19: 40079 (NP-15114)

SIOUX FALLS POWER REACTOR
construction and design features, (E), 19: 40217
control rod drive for, design of prototype, (E), 19: 40135

SKELETON
strontium-90 content in human, in Germany, 19: 38876 (NP-14927)

SKIN
effects of ultraviolet-irradiated linolenic acid extract on mouse, 19: 38366
radiosensitivity of, effects of anabolic steroid ointment, 19: 38468

SKIN DISEASES
radiotherapy of hemangiomas, contra-indications, 19: 38511
therapy of hemangiomas using frozen carbon dioxide or surgery, 19: 38511

SKIN GRAFTING
radiation effects with spleen cell transplants on tolerance to, in adult and newborn mice, 19: 38376

SKIN LESIONS
radioinduced ulcers, etiology, pathology, and therapy, 19: 38513

SLURRIES
drying apparatus for, 19: 38800(P)

SODIUM
analysis for carbon, corrections for, 19: 40112(R) (ANL-7046(p.36-66))
analysis for oxygen, 19: 38539 (APDA-168)
chemical states of carbon, nitrogen, and oxygen in, 19: 39157 (CNLM-6337)
combustion of reactor coolant, fission product release in, 19: 40286(R) (NAA-SR-11200)
corrosive effects on titanium–vanadium alloys at 650°C, 19: 40177(R) (ANL-7046(p.1-35))
corrosive effects on zirconium at 540°C, 19: 40112(R) (ANL-7046 (p.36-66))
corrosive effects of vaporous, on zirconium, 19: 40113(R) (ANL-7071)
determination in enamel of teeth, neutron activation, 19: 38562
determination in graphite by x-ray spectrography, 19: 38571
determination in heavy fuel oils by neutron-activated analysis, 19: 38550
fission product retention in reactor-coolant, 19: 40286(R) (NAA-SR-11200)
flow of liquid, design of in-pile controller for, (E), 19: 40135
oxygen pickup from stainless steel containers, 19: 40177(R) (ANL-7046(p.1-35))
pressure pulses in locally-heated channels of, 19: 39090(R) (ANL-7046 (p.78-82))
reactions with cladding materials at high temperatures, 19: 39090(R) (ANL-7046(p.78-82))
reactions with water in steam generators, analysis, 19: 38803(R) (BAW-1280-26)
reactor criticality effects of, void coefficients for, 19: 40158 (UNC-5123)
sampling liquid, methods for, 19: 40112(R) (ANL-7046(p.36-66))
solubility in silicon crystals at 800°C, 19: 39204
sorption by gamma-alumina and inorganic ion exchange materials from fused salts, 19: 38771

SODIUM BROMIDES
reduction by high-frequency hydrogen discharge to hydrogen halide and metal, 19: 39180
reduction by high-frequency discharges in helium, hydrogen, and nitrogen, role of electrons in, 19: 39181

SODIUM CHLORIDES
corrosive effects on types 5454 and 6061 aluminum alloys at 150°C, electrochemical, 19: 39117 (ORNL-P-1430)
corrosive effects on titanium alloys at 100 and 200°C, electrochemical, 19: 39117 (ORNL-P-1430)
radioinduced coloration in gamma irradiated, x, (E), 19: 40105
reduction by high-frequency hydrogen discharge to hydrogen halide and metal, 19: 39180
reduction by high-frequency discharges in helium, hydrogen, and nitrogen, role of electrons in, 19: 39181
KCl–NaCl, use of fused, in attempts to prepare uranium sulfide, 19: 38574 (ANL-7008)

SODIUM FLUORIDES
reduction by high-frequency hydrogen discharge to hydrogen halide and metal, 19: 39180
reduction by high-frequency discharges in helium, hydrogen, and nitrogen, role of electrons in, 19: 39181

SODIUM GRAPHITE REACTORS
calandria core for large, development of, 19: 40286(R) (NAA-SR-11200)
control rod development for LSGR, 19: 40126 (NAA-SR-11327)
design and development of 1000-Mw(e), 19: 40286(R) (NAA-SR-11200)

SODIUM HYDROXIDES
corrosive effects of solutions of, on Croloy 2¼ at 0 to 900°F, 19: 38803(R) (BAW-1280-26)

SODIUM IODIDES
gamma absorption by, effective atomic numbers for, 19: 40069
reduction by high-frequency hydrogen discharge to hydrogen halide and metal, 19: 39180
reduction by high-frequency discharges in helium, hydrogen, and nitrogen,

role of electrons in, 19: 39181
scintillation efficiencies of crystals of, for gamma radiation, 19: 39009
SODIUM IONS
radiolysis of aqueous solutions of, pulse, 19: 38728
SODIUM ISOTOPES Na-23
deuteron reactions (d,α) at 2.0 to 2.5 Mev, differential cross sections of, (E), 19: 39835
SODIUM ISOTOPES Na-24
use in radiodiagnosis, review on, 19: 38505
SODIUM NITRATES
properties in chemical radiation dosimetry, 19: 39042
KNO_3–$NaNO_3$, use in preparation of aluminum–nickel coatings, 19: 39143(P)
SODIUM NITRITES
KNO_3–$NaNO_2$, use in preparation of aluminum–nickel coatings, 19: 39143(P)
SODIUM OXIDES
production and dispersion in fires, 19: 40286(R) (NAA-SR-11200)
SODIUM PHOSPHATES
reactions with cerium neodymium, and samarium oxides, spectra of compounds formed in, 19: 38668
reactions with yttrium chlorides, 19: 38619
SODIUM REACTOR EXPERIMENT
components of, operation effects on, 19: 40286(R) (NAA-SR-11200)
development for power expansion, 19: 40286(R) (NAA-SR-11200)
SODIUM SYSTEMS
Na–UC, corrosive effects on stainless steel, 19: 40113(R) (ANL-7071)
Na–UN, corrosive effects on stainless steel, 19: 40113(R) (ANL-7071)
Na–UO_2, corrosive effects on stainless steel, 19: 40113(R) (ANL-7071)
SODIUM URANATES
radiation hazards from use of, as coloring agent for artificial teeth, 19: 38473 (NP-14923)
SODIUM XENATES
preparation and properties, 19: 38624
SODIUM ZIRCONATES
preparation and uses, 19: 38647
SOILS
carbon dioxide isotopic composition in, effects on carbon-13 variations in secondary calcites, 19: 38854
fission product motion in, effects of chelating agents on, 19: 38329 (TID-20471)
moisture content determination by neutron scattering, cadmium standards for probes for, 19: 38869
radioactive contamination of, effects on plant ecology, 19: 38331
radioactive contamination of, movement patterns in, 19: 40274
radioactivity in West German Republic, 19: 38904
radioactivity of German, 1962, 19: 38858
radioactivity of, in Austria, 1963, 19: 38860
radioisotope injection into probe for rapid, 19: 38870
strontium-89 contamination of, retention and loss of, 19: 38332
strontium-90 content in German, 19: 38876 (NP-14927)
waste transport by ground water in, analysis, 19: 40268 (BNWL-63)
water content in, effects of bulk density and hydrogen form on calibration of meter for measuring, 19: 38948
SOLAR BATTERIES
design of converter for, 19: 39443(P)
radiation effects on, in space environment, 19: 39059
SOLAR FLARES
effects on ionospheric F2 region, 19: 39675
effects on ionospheric RF transmission, 19: 39682
SOLAR RADIATION
effects of solar wind on ionosphere, (T), 19: 39676
effects on geomagnetic storms, 19: 39673
effects on sudden impulse pairs in magnetic storms, 19: 39681
energy spectra of x, below 60 Å, (E), 19: 39333
flux in interplanetary space, 19: 39364
flux of photon, variation with depth in photosphere, (T), 19: 39342
sorption by atmosphere and ionosphere, 19: 39363
SOLDERING
testing of solderability, review, 19: 40280 (BDX-613-73)
SOLENOIDS
current regulators for superconducting, design of, 19: 38945
electron beam reactions with, current effects from, (T), 19: 39654
SOLIDS
book: *Physics of Non-Crystalline Solids*, 19: 40110
charged particle tracks in, identification after chemical etching, 19: 39038
magneto-optical phenomena in many-electron systems in, perturbation theory for, 19: 40100
mass transfer along temperature gradient in, 19: 38678
neutron thermalization in, Van Hove theory for relaxation times in, 19: 39773
radiation damage tracks in, research on, 19: 39226(R) (AFCRL-65-305)
theory, 19: 39263 (CONF-796)
ultrasonic waves in, properties of finite-amplitude, 19: 39268 (ORNL-P-1395)
SOLVENT EXTRACTION PROCESSES
design for reactor fuels processing using TBP, 19: 38776(P)
SOLVENTS
analysis for organic residue from, radioisotopic method for, 19: 38538 (ADR-08-13-63.1)
effects of organic, on mercury iodide, 19: 39265(R) (IA-1021)
reactions of organic, with burning plutonium, 19: 38879 (RFP-566)
SONIC INSPECTION
methods for irradiated ceramic fuel elements, 19: 39234 (GEAP-4597)
SOUND
propagation in rarefied gases, kinetic theory of, 19: 39262 (BNL-8990)
propagation in weakly ionized gases, longitudinal, (T), 19: 39293
SPACE
electron bremsstrahlung radiation doses in, computer program for, 19: 40062 (N64-29366)
helium and hydrogen isotope measurement in, development of counter telescopes for, 19: 39419(R) (ATN-63(9219)-1)
satellite orientation in, determination of, 19: 38957(P)
satellites in, electromagnetic effects near, (T), 19: 39683
simulation of, development of vacuum techniques for, 19: 38842
SPACE FLIGHT
conference on simulation in space technology, 19: 38784
physiological effects of acceleration, radiation, and vibration during, 19: 38358 (AD-612660)
propulsion development for, 19: 40222 (LA-3229, pp 10-47)
propulsion systems for, photonic, 19: 38837
SPACE VEHICLES
conference on simulation in space technology, 19: 38784
electron bremsstrahlung radiation doses in, computer program for, 19: 40062 (N64-29366)
motion in interplanetary space and ionosphere, electromagnetic effects from, (T), 19: 39683
power plant pump development for, 19: 38781(R) (N64-25903)
power plants for, development, (E/T), 19: 38836 (NASA-SP-79)
power supplies for, magnetohydrodynamic generators for, 19: 39442
radiation effects on, simulation of, 19: 39059
shielding of manned, 19: 40063 (NP-15125)
shielding of, problems in, 19: 40072
SPAIN
uranium production and uses in, in 1964, 19: 39105
SPARK CHAMBERS
design of digitized, for automatic measurement of particle interactions, 19: 39450 (BNL-9232)
particle track analysis in, using flying-spot devices, (E), 19: 38976 (CERN-65-11(p. 57-69))
particle track analysis in, using flying-spot devices, (E), 19: 38977 (CERN-65-11(p.71-9))
performance of controlled-discharge, (E), 19: 39028
properties and uses, review, 19: 39019
track analysis from, using flying-spot system, (E), 19: 38972 (CERN-65-11(p.7-13))
track analysis in, using flying-spot devices, (E), 19: 38973 (CERN-65-11(p.15-23))
track analysis in, using flying-spot devices, (E), 19: 38974 (CERN-65-11(p.25-33))
use for detection in photon interactions, 19: 39041
use in neutrino experiments at CERN using deuterium targets, 19: 39612
SPECTRA
line width of atomic, time evolution of density operator for, (T), 19: 39386
SPECTROMETERS
performance of combination time-of-flight proton-recoil, 19: 39265(R) (IA-1021)
SPECTROSCOPY
book: *Developments in Applied Spectroscopy*, 19: 38572
diagnostic use for plasma property studies, 19: 39960(R) (N64-33202)
numerical, for solving time-dependent Schroedinger equation, 19: 39642
theory of atomic beam optical double resonance, 19: 39369 (NP-15140)
SPERM
effects of maturity of, on radioinduced mutation frequency in male Drosophila, 19: 38390
radioinduced dominant lethal mutations in mouse, 19: 38394
radioinduced translocations in mouse, 19: 38396
SPERMATOGENESIS
radiosensitivity and recovery of Drosophila, role of oxygen in determining, 19: 38463

SPINAL CORD
radiation effects on reflex arc of, whole-body gamma, 19: 38358 (AD-612660)
SPLEEN
effects with radiation on polyvalent tolerance in adult and newborn mice, 19: 38376
protective effects of immunological unresponsiveness induction against radiation effects in mice, 19: 38454
radiation effects on DNA ribonuclease in, x, 19: 39265(R) (IA-1021)
radiation effects on serum proteins in mouse, following rat chimera transplant, 19: 38404
radiation effects on morphology of rat, fast neutron, 19: 38444
radiation injuries of enzyme systems in rat, protective effects of glycine, 19: 38467
SPUTTERING
equipment for, design and performance of, 19: 38930
micromachining by, through mask of contamination, 19: 39136
STACK DISPOSAL
effects on radioactivity of atmosphere in Hanford area, 19: 38874 (BNWL-SA-53)
STAINING
of cells from cancer patients with acridine orange, effects of radiotherapy, 19: 38488
STAINLESS STEEL
analysis for chromium, iron, and nickel, electron microprobe, 19: 38536 (ACF-6)
analysis for nitrogen, method for, 19: 38537 (ACF-7)
cavitation of Types 304 and 316 in bismuth–lead alloy at 500 and 1500°F, ultrasonic-induced, 19: 39116 (NP-15263)
composition of commercial type 304, 19: 39152(R) (BMI-X-10132)
corrosion by aqueous chemical shim solutions at 600°F, 19: 40198(R) (WCAP-3721)
corrosion by ceramic uranium–sodium pastes, 19: 40113(R) (ANL-7071)
corrosion by steam of type-300 series, at 800 to 1410°F with heat transfer, 19: 39115 (GEAP-4760)
corrosion by steam of types 304 and 406, at 1050 and 1150°F, isothermal, 19: 39115 (GEAP-4760)
corrosion by steam at 1050°F of type 304, effects of surface preparation on, 19: 39115 (GEAP-4760)
corrosion of type 430, by metal chlorides at high temperatures, 19: 40113(R) (ANL-7071)
creep and stress rupture of 304 and 316, effects of grain-size and temperature on, 19: 40286(R) (NAA-SR-11200)
deformation of, as fuel element cladding, 19: 39220
diffusion of fission products in 304, mechanisms of, 19: 39152(R) (BMI-X-10132)
fabrication for reactor fuel tubes containing uranium dioxide pellets, 19: 39147(P)
fabrication of fuel cans of, for AGR, 19: 39134
mechanical properties of austenitic, effects of pressure and temperature on, 19: 40286(R) (NAA-SR-11200)
mechanical properties of 347, effects of heat treatments on, 19: 39091(R) (BMI-1723(Del.))
performance as cladding for ceramic and cermet fuels, (E), 19: 40172
properties for use as fuel cladding material in reactors, 19: 39206
radiation effects on 304, neutron, 19: 40286(R) (NAA-SR-11200)
radiation effects on 347, neutron, 19: 39091(R) (BMI-1723(Del.))
radiation effects on mechanical properties of Type 304, fission-fragment and neutron, 19: 39229(R) (BMI-X-10134)
radiation effects on ductility of type 304, fast neutron, 19: 39236 (WCAP-3269-36)
reactions with plutonium–uranium fuels at high temperatures, 19: 40177(R) (ANL-7046(p.1-35))
reactions with sodium at high temperatures, 19: 39090(R) (ANL-7046 (p.78-82))
stress-rupture of 304, effects of carburization on, 19: 40286(R) (NAA-SR-11200)
tensile properties of type 406, on aging at 1000 and 2000°F in steam, 19: 39156(R) (CEND-532)
thermal response and microstructure of Type 310, at 1400°F, 19: 39158 (GEAP-4751)
B–stainless steel, corrosion by boronated water at 600°F, 19: 39110
B–stainless steel, extrusion of fuel cladding of, 19: 39110
B–stainless steel, mechanical properties of, effects of boron content on, 19: 39110
B–stainless steel, radiation effects on mechanical properties of, fast and thermal neutron, 19: 39110
B–stainless steel, radiation effects on corrosion resistance of, fast and thermal neutron, 19: 39110
B–stainless steel, weld joint design for tubes of, 19: 39110
PuO_2–stainless steel, fabrication into pins, 19: 39125(R) (BNWL-91)
stainless steel-UO_2, fabrication into pins, 19: 39125(R) (BNWL-91)
STANFORD LINEAR ACCELERATOR
beam switching system for, 19: 39327
STARK EFFECT
measurement in nitrogen plasma, ion line shifts, 19: 39952 (AFCRL-65-348)
STARS
book: *Dynamics of Stellar Systems*, 19: 39329(T)
convective envelope depth in lower main sequence, lithium depletion effects on, (T), 19: 39336
cooling of neutron, composite equations of state with nuclear forces for, (T), 19: 39355
energy of quasi-stellar radio sources, 19: 39359
explosions of supernova, multiple bounce theory for cold plasma bubble in, (T), 19: 39344
formation of white-dwarf, mass loss in, 19: 39337
gamma emission from quasar 3C286, low-energy, (E), 19: 39357
model for globular-cluster formation, quasars as prototypes in, (T), 19: 39356
models for mass of vanishing convective core, (T), 19: 39334
molecular condensation and equilibria in atmosphere of, (T), 19: 39352
neutrino emission from, (T), 19: 39361
nuclear reactions in, theory for, 19: 39805
oscillations of neutron, (T), 19: 39358
properties of extremely red, in 0.68 to 0.92 and 2.01 to 2.41 μ range, (E), 19: 39347
properties of ultraviolet quasi-stellar radio sources, (E), 19: 39349
radiation from, Schwarzschild metric for, 19: 39273(R) (UCRL-12204, pp 60-5)
radiation pressure in interior of, (T), 19: 39335
radioactivity in type I supernova, (T), 19: 39338
spectra of extremely red, (E), 19: 39348
stability of very massive, effect of rotation on gravitational, (T), 19: 39354
thermodynamic properties, (T), 19: 39339
x-ray emission at 0.2 to 20 kev, rocket detection of, 19: 39332
STATISTICS
cluster-star equations in, generating functionals for inversion of, 19: 39084
cluster-star equations in, Möbius formula for inversion of, 19: 39083
quantum many-body problem in, (T), 19: 39263 (CONF-796)
theory for multivariable systems, pseudo-random binary sequences in, 19: 39078
uses in communication theory, 19: 39270(R) (TID-21894)
uses in processing and transmission of information, 19: 39270(R) (TID-21894)
STEAM
corrosive effects on Hastelloy-X, heat transfer and isothermal, 19: 39115 (GEAP-4860)
corrosive effects on stainless steel, heat transfer and isothermal, 19: 39115 (GEAP-4760)
corrosive effects on Incoloy-800 and Inconel-600, effects of surface preparation on, 19: 39115 (GEAP-4760)
corrosive effects on type 304 stainless steel, effects of surface preparation on, 19: 39115 (GEAP-4760)
corrosive effects on Inconel-600 and -625, heat transfer and isothermal, 19: 39115 (GEAP-4760)
corrosive effects on Incoloy-800 and -825, heat transfer and isothermal, 19: 39115 (GEAP-4760)
separation from water, development of devices for, 19: 38801(R) (ACNP-65004)
steam–water, two-phase vessel blowdown from pipes, theory, 19: 38802 (APED-4827)
STEAM GENERATING HEAVY WATER MODERATED REACTOR
design and development, 19: 40205
safety of, computer model for studying, 19: 40214
STEEL
analysis for trace amounts of cobalt by x-ray spectrography, 19: 38571
radiation effects on type 4340, 19: 40112(R) (ANL-7046(p.36-66))
reactions with sodium at high temperatures, 19: 39090(R) (ANL-7046 (p.78-82))
STEROIDS, 17-KETO-
radiation effects on content of, in rat urine, 19: 38443
STRAIN GAGES
radiation effects on, transient, 19: 39055 (GA-6266)
STRESS ANALYSIS
finite element, of axisymmetric composite structures, 19: 40165 (GA-6303)
stress-strain relationships of polycrystalline graphite under compression up to fracture, 19: 39186
STRONTIUM

content and distribution in subterranean Bulgarian salt water, 19: 38851
determination in bone, method using flame photometry and ion exchange for, 19: 38345
determination in enamel of teeth, neutron activation, 19: 38562
determination in water, spectrochemical, 19: 39265(R) (IA-1021)
effects on strontium-90 metabolism in mammals, 19: 38335 (NP-14926)
production by decomposition of strontia by silicon, 19: 38593(T) (ORNL-tr-674)
separation from aqueous solutions, properties of tuff cation exchanger for, 19: 38768
separation from graphite above 1750°C in inert gases, 19: 38762
separation from waste water, methods for, 19: 40276
separation from yttrium by ion exchange, 19: 38774
STRONTIUM ALLOYS
Mg–Sr, properties of intermetallic compounds in, 19: 39177
STRONTIUM CHLORIDES
KCl–$SrCl_2$, free energy of formation of K_2SrCl_4 and KSr_2Cl_5 at 450 and 550°C, 19: 38575 (BNL-9343)
STRONTIUM FLUORIDES
SrF_2–YF_2, phase studies, 19: 38615
STRONTIUM ISOTOPES
preparation of accelerator targets of, 19: 38658
STRONTIUM ISOTOPES Sr-85
energy from, determination of total, 19: 38878 (ORNL-P-1405)
motion in soil, effects of chelating agents on, 19: 38329 (TID-20471)
use as measure of effective bone blood flow in dogs and rabbits, 19: 38340
STRONTIUM ISOTOPES Sr-87
energy from, determination of total, 19: 38878 (ORNL-P-1405)
STRONTIUM ISOTOPES Sr-89
contamination, retention, and loss of, in grass, 19: 38332
determination in rainwater, 19: 38852
radiation protection standards for atmospheric, 19: 38877 (NP-15183)
release from pyrolytic carbon-coated fuel particles, 19: 39228 (BMI-1734)
STRONTIUM ISOTOPES Sr-90
content in atmosphere, 1954 to 1963, 19: 38861
content in Baltic Sea, 19: 38901
content in bone samples, Great Britain, 1964, 19: 38863
content in bones, effects of age, 19: 38850
content in diet and excreta in Japan, 19: 38894
content in fallout, food, human skeleton, milk, soil, and water in Germany, 19: 38876 (NP-14927)
content in food in Austria, 1963, 19: 38860
content in German milk, 1962, 19: 38858
content in milk, effects of atmospheric transport of fallout on, 19: 38857
determination in milk, 19: 38556
determination in milk, 19: 38856
determination in rainwater, 19: 38852
metabolism in mammals, effects of calcium on, 19: 38335 (NP-14926)
metabolism in rats, effects of vitamin D_3, 19: 38347
motion in soil, effects on chelating agents on, 19: 38329 (TID-20471)
radiation protection standards for atmospheric, 19: 38877 (NP-15183)
separation from irradiated uranium by ion exchange chromatography, carrier-free, 19: 38757 (SGAE-CH-17/1965)
uses in Japan, 1950 to 1960, 19: 39060
STRONTIUM OXIDES
radiation effects on crystalline, 19: 39265(R) (IA-1021)
reactions with silicon at 1200°C, 19: 38593(T) (ORNL-tr-674)
SiO_2–SrO, crystal structure, 19: 38621
STYRENE
radioinduced graft polymerization with polyvinyl chloride, physical properties of products of, 19: 38733
radioinduced graft polymerization of vaporous, with ethylene polymers, 19: 38734
radioinduced grafting to chloroethylene polymers, 19: 38740(P)
radiostability of ion-exchange resins based on, (E), 19: 40129 (ZFK-RN-17(p.114-26))
STYRENE POLYMERS
properties as scintillator for beta detection, 19: 38737
SULFATE IONS
radiolysis of aqueous solutions of, pulse, 19: 38728
SULFONIC ACIDS
catecholdi-, complex formation with beryllium in aqueous solutions, 19: 38641
SULFUR
chemical bonding in K-x-ray spectra of sulfur compounds, 19: 38588 (UCRL-12496)
radiolysis of monodisperse colloidal, effects on particle size, 19: 38714
SULFUR COMPOUNDS
spectra of, chemical bonding in K-x-ray, 19: 38588 (UCRL-12496)
SULFUR FLUORIDES
effects on electron density in flame plasma, (E), 19: 40016
ionization cross section for, electron-impact, 19: 38630
ionization cross sections for negative-ion formation, electron-impact, 19: 38631
nuclear magnetic resonance spectra of, collision-narrowing theory of, 19: 38629
SULFUR ISOTOPES
content ratios in meteorites, variations in, (E), 19: 38847
SULFUR ISOTOPES S-31
energy levels, (E), 19: 39827
SULFUR ISOTOPES S-32
content ratio with sulfur-34 in Orgueil meteorite, 19: 39351
SULFUR ISOTOPES S-33
content in meteorites, variations in, (E), 19: 38847
SULFUR ISOTOPES S-34
content in meteorites, variations in, (E), 19: 38847
content ratio to sulfur-32 in Orgueil meteorite, 19: 39351
SULFUR ISOTOPES S-35
incorporation in cystine by neutron irradiation, 19: 38747
use to determine optimum amount of material carried by viscose fibers, 19: 39063
SULFUR ISOTOPES S-36
content in meteorites, variations in, (E), 19: 38847
SULFURIC ACID
reactions with uranium oxides, effects on composition and structure, 19: 38657
use in solvent extraction of uranium tetrachloride by kerosene–TBP system, 19: 38563
SUN
coronal streamers from, stability of, (T), 19: 40000
coronal temperature from Lyman α profile width, (T), 19: 39341
element abundances in atmosphere of, (E), 19: 39345
gravitation and mass variations of, (T), 19: 39665
gravity waves in chromosphere of, standing mode of compressional body, (T), 19: 39343
ionization of surrounding gas, size of H II region of, (T), 19: 39340
lithium content in, (E), 19: 39346
molecular condensation and equilibria in nebula of, (T), 19: 39352
photon flux from, variation with depth in photosphere, (T), 19: 39342
spot cycle variation effects on midlatitude ionosphere, (E), 19: 39677
ultraviolet radiation scattering by free electrons in corona of, profiles of Lyman-alpha, (T), 19: 39341
SUPERCONDUCTIVITY
of lanthanum films, (E), 19: 39745
of selenium under high pressure, (E), 19: 39736
uses, 19: 39690
SUPERCONDUCTORS
critical currents in niobium carbide–niobium nitride systems, (E), 19: 39688
critical currents in indium film, (E), 19: 39724
critical fields for strong- and weak-coupling, two-fluid model for, 19: 39711
current distribution in thin-film strip transmission-line, (T), 19: 39692
current regulators for solenoids of, design of, 19: 38945
current-voltage characteristics of tunnel junctions of, second harmonic detection system for, 19: 38944
design and testing of magnets of, 19: 39741
design using titanium–vanadium alloy, 19: 39750(P)
development of instruments using, 19: 39690
electric conductivity of type II, in mixed state, (T), 19: 39698
electric conductivity in type-II, origin of, (T), 19: 39707
energy gap in, dependence on transport current, (E), 19: 39735
Knight shift due to spin-orbit coupling in, magnetic field dependence of, (T), 19: 39739
Knight shift in, magnetic field dependence of, (T), 19: 39705
magnetic field penetration depth in niobium, (E/T), 19: 39726
magnetic field reduction in expandable enclosures of, 19: 39742
magnetic flux movement in type II, (T), 19: 39704
magnetic flux penetration in, (T), 19: 39712
magnetic flux permeability and tunneling in superimposed layers of normal metal and, in magnetic fields, (T), 19: 39700
magnetic properties of intrinsic London, near transition point, (T), 19: 39721
magnetic pulse transmission through plates of type-II, (E), 19: 39733
model for, with two kinetic energies, (T), 19: 39687
nuclear magnetic resonance in nontransition-metal, spin-orbit coupling effects on Knight shift in, (T), 19: 39727
power losses by alternating current in, 19: 39695
properties of copper–lead heterogeneous alloys, particle size effects on, (E), 19: 39747
properties of germanium–niobium alloys, (E), 19: 39725

properties of, effects of electron-phonon interactions on, (T), 19: 40073 (CONF-796(Paper 1))
properties of, magnetic and thermal, 19: 40286(R) (NAA-SR-11200)
pulse transmission by coaxial cables of high-field, (E), 19: 39740
specific heat of mixed state in alloy, (T), 19: 39716
spectral shift at zero temperature, magnetic-field dependence of NMR Knight, (T), 19: 39719
surface sheaths of type II, 19: 40286(R) (NAA-SR-11200)
thermal conductivity of pure lead, (T), 19: 39732
transition region determination by superfluid phase transition, (E), 19: 39691
transition temperature of, containing paramagnetic impurities, gap-anisotropy effects on, (T), 19: 39717
voltages in, guided motion of vortices for transversal, 19: 39694
SUPERFLUIDITY
flow in Venturi tubes, (T), 19: 39696
surface excitation in helium, gapless, (E), 19: 39737
vortex rings in helium, quantized, (T), 19: 39723
SUPERHEATERS (NUCLEAR)
boiler design for, 19: 38817(P)
SURFACE-ACTIVE AGENTS
evaluation of biodegradable, for foam separation treatment of wastes, 19: 40271(R) (RAI-350)
SURFACE WATERS
flow rates of, analog simulation for, 19: 40282 (BNWL-SA-171)
SURFACES
contamination of, equipment for measuring alpha, 19: 39045(P)
properties of, Mössbauer effect for studies of, 19: 40078 (NP-15111)
vibration modes from impurities adsorbed on, S-matrix method for, (T), 19: 40108
SURGERY
use for radioinduced ulcers of skin, 19: 38513
SWIMMING POOL REACTORS
accidents at IRR-1, sea water contamination by, 19: 39265(R) (IA-1021)
operation of IRR-1, 19: 39265(R) (IA-1021)
SWINE
placental transfer of glycine, urea, and water in, 19: 38344
radiation effects on mercapto groups in blood, 19: 38427
SYNCHROTRONS
construction status of Frascati electron, 19: 39327
development of Cornell 10-Bev strong-focusing electron, 19: 39327
development of Lund 4-Bev strong-focusing electron, 19: 39327
development of University of Glasgow 4-Bev strong-focusing electron, 19: 39327
magnet design for Cornell electron, 19: 39327
neutron dosimetry on 10-Bev, 19: 39315 (JINR-P-2177)
operation of Tokyo electron, 19: 39327
performance of Lund electron, 19: 39327
use in cancer therapy, neutron flux and spectrum in, 19: 38517
SYSTEMS FOR NUCLEAR AUXILIARY POWER
cladding material property data for hydride reactors, 19: 39166 (NAA-SR-Memo-11149)
development for space vehicles, (E/T), 19: 38836 (NASA-SP-79)
SYSTEMS FOR NUCLEAR AUXILIARY POWER (SNAP-4)
fuel element geometries of, heat transfer and hydraulic studies in, 19: 40249 (TID-22014)
SYSTEMS FOR NUCLEAR AUXILIARY POWER (SNAP-8)
radiation effects on electric insulator resistance in, 19: 39057 (NP-15022(Vol.II)(Add.))
SYSTEMS FOR NUCLEAR AUXILIARY POWER (SNAP-19)
ejection from NIMBUS-B, dynamic analysis of mechanism for, 19: 39071 (MND-3169-68)

T

TANTALUM
combustion in argon–oxygen mixtures, 19: 38583(R) (SC-DC-65-1480)
corrosion by lithium at high temperatures, effects of nitrogen on, 19: 40112(R) (ANL-7046(p.36-66))
crystal structure of beta, 19: 39179
determination by x-ray fluorescence spectroscopy, 19: 38549
diffusion of atoms in bcc, activation energy for interstitial, (T), 19: 40086
electric conductivity of superconducting, magnetic field dependence of surface, (E), 19: 39706
electric conductivity of crystals of, effects of interstitial carbon, nitrogen, and oxygen on, 19: 39203
electron reactions with atomic, screening effects on bremsstrahlung and pair production in, (T), 19: 39389
gamma reactions at 145 kev, photoelectric cross sections in, 19: 39377
magnetostriction in pure monocrystalline, 19: 39199
neutron reactions (n,n′γ) at 0 to 14 Mev, energy absorption in, 19: 39769 (SC-DC-65-1544)
potassium droplet vaporization on heated surfaces of, 19: 38811(R) (SAN-409-24)
proton reactions at 660 Mev, isomeric lutetium-176 from, (E), 19: 39931
radiation damage in, cross sections for atomic displacements from 1- to 3-Mev electrons, 19: 39225 (AFCRL-65-286)
reactions with sodium at 2100 to 2400°C, 19: 39090(R) (ANL-7046(p.78-82))
solubility in liquid plutonium, evaluation of sampling methods for determination of, 19: 38580 (LA-3303)
superconducting properties of, Ginzburg-Landau parameter for, 19: 39205
x-ray spectra of, Coster-Kronig transition probabilities from, (E), 19: 39410
TANTALUM ALLOYS
Hf–Ta, development and properties of, 19: 39123
Hf–Ta, oxidation resistance of, to 4000°F, 19: 39123
Hf–Ta–W, cavitation of T-111 in bismuth–lead alloy at 500 and 1500°F, ultrasonic-induced, 19: 39116 (NP-15263)
Nb–Ta, Hall effect in superconducting, (E), 19: 39710
Sb–Ta, crystal structure of intermetallic compounds in, 19: 39209
TANTALUM BORIDES
reactions with graphite to 2200°C, 19: 38654
TANTALUM CARBIDES
thermal expansion of, at 21 to 3020°C in argon at 20 psig, 19: 39201
TANTALUM ISOTOPES Ta-181
neutron reactions (n,γ), gamma spectra of 4.8-ev resonance of, 19: 39781 (JAERI-1073)
TANTALUM OXIDES
thermodynamic stability at 1030 to 1300°K, 19: 38586 (UCRL-11957)
TANTALUM SYSTEMS
C–Hf–Ta–W, cavitation of T-222(A) in bismuth–lead alloy at 500 and 1500°F, ultrasonic-induced, 19: 39116 (NP-15263)
TARTARIC ACID COMPLEXES
with uranyl ions, thermal decomposition of, 19: 38660
TECHNETIUM ALLOYS
Tc–V, nuclear spin-lattice relaxation time of technetium-99 and vanadium-51 in, (E), 19: 39403
TECHNETIUM ISOTOPES Tc-99
energy from, determination of total, 19: 38878 (ORNL-P-1405)
nuclear spin-lattice relaxation time in technetium–vanadium alloys, temperature variations of, (E), 19: 39403
radiation dose from internally deposited, 19: 38506
TECHNETIUM ISOTOPES Tc-103
half life, 19: 39892
TECHNETIUM ISOTOPES Tc-105
half life, 19: 39892
TECHNETIUM ISOTOPES Tc-106
half life, 19: 39892
TECHNETIUM ISOTOPES Tc-107
half life, 19: 39892
TECHNICAL REPORTS
bibliography of Israeli, 19: 39265(R) (IA-1021)
TEETH
analysis for trace elements in enamel of, neutron activation, 19: 38562
artificial, radiation hazards from use of sodium uranate as coloring agent for, 19: 38473 (NP-14923)
effects of nitrogen mustards on induction of lesions in rat, mechanism of, 19: 38325
enamel surface changes on, use of phosphorus-32 for determining, 19: 38352
TELEMETERING SYSTEMS
design for instrumentation of nuclear explosions, 19: 38919 (SC-R-65-904, pp 59-74)
TELLURIUM
effects on heats of solution of cadmium, lead, and tin in liquid bismuth, 19: 39168(R) (TID-22015)
gamma scattering by, spectra of resonant, (E), 19: 39265(R) (IA-1021)
TELLURIUM ISOTOPES Te-132
release from pyrolytic carbon-coated fuel particles, 19: 39228 (BMI-1734)
TEMPERATURE
effects on stability of pentavalent plutonium nitrate solutions, 19: 38731
in fabrication of lithium-drifted germanium detectors, system for, 19: 39029
measurement in reactor fuel element sheaths, device for, 19: 40138(P)
measurement in simulated reentry tests, methods for, 19: 39118(R) (SC-DC-65-1520)
radiosensitivity effects on egg hatchability in Artemia, gamma, 19: 38384
TERBIUM
crystal structure and magnetic properties of, pressure effects on, 19: 40094
phase transformations at 6 to 65 kbar, solid-liquid and solid-solid,

19: 40095
proton inelastic scattering at 25 to 1700 kev, x-ray yields from, (E), 19: 39881
TERBIUM COMPLEXES
with [(2-hydroxyethyl)imino]diacetic acid, dissociation constant of, 19: 38671
TERBIUM IONS
crystal-field interactions of, linear and nonlinear shielding of, (E/T), 19: 40101
electron paramagnetic resonance and endor spectra of, in thorium dioxide, 19: 38655
radiolysis of aqueous solutions of, pulse, 19: 38728
TERBIUM ISOTOPES Tb-159
neutron reactions (n,α) at 14.2 Mev, alpha energy spectrum of, (E), 19: 39780 (INR-596/PL)
TEREPHTHALAMIDE, *N,N'*-DIMETHYL-*N,N'*-DINITROSO-
complexes with lanthanum and neodymium, mechanism of formation of, 19: 38600
solvent properties for neodymium and praseodymium oxalates, 19: 38601
TEREPHTHALIC ACID, ETHYLENE POLYMER ESTERS
use in measurement of ion charge distributions in mass spectrometers, (E), 19: 38940
TEXTILES
beta absorption by, to measure unevenness of fibers, 19: 39063
radiation processing, 19: 39066
THALLIUM
gamma scattering at 7.64 Mev, cross section and self-absorption ratio of, (E), 19: 39265(R) (IA-1021)
gamma scattering by, spectra of resonant, (E), 19: 39265(R) (IA-1021)
sorption by gamma-alumino and inorganic ion exchange materials from fused salts, 19: 38771
transition temperature of thin films of superconducting, effects of thin oxide layer on, (E), 19: 39746
THALLIUM ALLOYS
Bi–Tl, deformation and properties of $TlBi_2$, 19: 39168(R) (TID-22015)
Bi–Tl, heat of formation of $TlBi_2$, 19: 39168(R) (TID-22015)
Pb–Tl, electron tunneling in, at cryogenic temperatures, (E/T), 19: 40286(R) (NAA-SR-11200)
Pb–Tl, magnetic fields of superconducting, (E), 19: 40286(R) (NAA-SR-11200)
Pb–Tl, magnetic-field effects on tunneling from superconducting, (E), 19: 39718
THALLIUM BROMIDES
electric conductivity at 450 to 1600°C, 19: 40286(R) (NAA-SR-11200)
THALLIUM CHLORIDES
electric conductivity at 450 to 1600°C, 19: 40286(R) (NAA-SR-11200)
THALLIUM IODIDES
electric conductivity at 450 to 1600°C, 19: 40286(R) (NAA-SR-11200)
THALLIUM ISOTOPES Tl-207
energy levels from triton reactions (t,α) reactions with lead-208 at 12.0 and 13.5 Mev, (E), 19: 39852
THALLIUM ISOTOPES Tl-208
energy levels, (T), 19: 39933
THAMES RIVER
radioactive waste disposal in, safety precautions for, 19: 40277
THERMAL CONDUCTIVITY
measurement in ceramics, method for, 19: 40113(R) (ANL-7071)
THERMAL INSULATION
compaction of perlite, in large dewars by thermal cycling, 19: 38779 (LA-DC-7158)
THERMAL RADIATION
emission from homogeneous plasma near plasma frequency, (T), 19: 39985
THERMAL REACTORS
neutron resonance escape probabilities in, computer program for calculation of, 19: 40153 (IA-1001)
shutdown xenon control in, (T), 19: 39265(R) (IA-1021)
THERMIONIC CELLS
bibliography, 19: 39434 (N64-26371)
collector and emitter performance for, 19: 39431(R) (AD-608554)
design, 19: 39446(P)
design of energy converter including a plurality of, connected in series, 19: 39445(P)
design of high-vacuum, 19: 39444(P)
design of solar, 19: 39443(P)
development and operation, 19: 40113(R) (ANL-7071)
development of uranium dioxide fueled, 19: 39072(R) (NP-15187)
development of uranium dioxide-fueled, 19: 39070(R) (GEST-2046)
electron temperature and ion density profiles in ignited mode, 19: 39433 (LA-DC-6898)
performance of high-pressure cesium, with tungsten cathode, 19: 39436
performance of 30 kw d-c to d-c in series, for electric propulsion, 19: 38835 (N65-27619)
properties of diode, in autonomous discharge plasma, 19: 39435(T) (JPRS-31048)
research on fundamentals of, review, 19: 39441
THERMOCOUPLES
performance of germanium–silicon, in thermoelectric cells, (E), 19: 39430(R) (AD-426092)
performance of rhenium–tungsten alloy, 19: 40177(R) (ANL-7046(p.1-35))
use for reactor transient diagnostics, miniature intrinsic, 19: 38911 (LA-DC-7004)
THERMODYNAMICS
of molten beryllium fluoride–lithium fluoride, 19: 38582 (ORNL-P-1428)
particle systems in, interaction potentials of classical many-body, 19: 39284
quantum many-body problem in, (T), 19: 39263 (CONF-796)
research on properties of matter, 19: 39272(R) (UCRL-12204, pp 27-48)
THERMOELECTRIC CELLS
bibliography, 19: 39434 (N64-26371)
development and operation of germanium–silicon, (E), 19: 39430(R) (AD-426092)
THERMOLUMINESCENT DETECTORS
design for infrared radiation, 19: 39049(P)
design of dosimeters of, 19: 39048(P)
development for dosimetry, 19: 39044(P)
THERMONUCLEAR EXPLOSIONS
fallout from, 19: 38861
fallout transport in atmosphere from, 19: 38857
neutron capture in, production of heavy nuclides in, 19: 38786 (LA-DC-7111)
protection from, 19: 40301
THERMONUCLEAR REACTIONS
development of multipole-field, (E), 19: 39954(R) (COO-1233-20)
THERMONUCLEAR REACTORS
plasma density and electron temperature in Zeta, (E), 19: 39953 (CLM-R-40)
plasma E-layer formation in Astron, (T), 19: 39973 (UCRL-14131)
THERMONUCLEAR WEAPONS
protection from, 19: 40301
THIAZOLES
protective effects against radiation injuries in mice, 19: 38466
THICKNESS GAGES
design of alpha-radiometric, 19: 38965(P)
design of beta-backscatter, for thin films, 19: 38952(P)
film deformation by Talysurf stylus, 19: 38916 (SC-DC-65-1589)
mount for radiometric, design of movable, 19: 38959(P)
THORIUM
diffusion in pyrolytic carbon at high temperatures, 19: 39129(R) (ORNL-TM-1116)
fission effects in, 19: 40286(R) (NAA-SR-11200)
neutron resonance integral, (E), 19: 40163
production and use as nuclear fuel, 19: 38859
separation from protactinium and uranium by paper electrophoresis, 19: 38775
separation from scandium by ion exchange in nitrate solutions, 19: 38770
separation from uranium by solvent extraction using di-sec-butylphenyl phosphonate, 19: 38755(R) (ORNL-3611)
sorption by gamma-alumina and inorganic ion exchange materials from fused salts, 19: 38771
THORIUM ALLOYS
Ga–Th, crystal structure of intermetallic compound $ThGa_2$ in, 19: 39207
Mg–Th–Zr, plastic anisotropy of HK31A sheet, 19: 39149 (AD-425880)
Th–U, radiation effects on, 19: 38755(R) (ORNL-3611)
Th–U–Zr, radiation effects on, 19: 38755(R) (ORNL-3611)
Th–Zr, mechanical properties at high temperatures, 19: 38755(R) (ORNL-3611)
THORIUM CARBIDES
microstructure of, 19: 39129(R) (ORNL-TM-1116)
preparation by sol-gel process, 19: 38755(R) (ORNL-3611)
processing irradiated, pyrochemical, 19: 40113(R) (ANL-7071)
production by carbon–thoria reactions, 19: 38755(R) (ORNL-3611)
reactions of carbon-coated particulate, with water vapor at 1000°C, 19: 39129(R) (ORNL-TM-1116)
ThC_2–UC_2, preparation by sol-gel process, 19: 38755(R) (ORNL-3611)
ThC_2–UC_2, preparation and properties of carbon-coated particulate, 19: 39129(R) (ORNL-TM-1116)
ThC_2–UC_2, processing of irradiated, costs of, 19: 39129(R) (ORNL-TM-1116)
ThC_2–UC_2, radiation effects on, effects of coatings, matrix materials, and temperatures on, 19: 39091(R) (BMI-1723(Del.))
ThC_2–UO_2, radiation effects on carbon-coated particulate, neutron, 19: 39129(R) (ORNL-TM-1116)

THORIUM CHLORIDES
reactions with zirconium chlorides at high temperatures, 19: 38755(R) (ORNL-3611)
THORIUM(IV) CHLORIDES
reactions with aluminum chloride at high temperatures, 19: 38755(R) (ORNL-3611)
THORIUM COMPLEXES
with caproic acid and 8-hydroxyquinaldoxime in chloroform and perchlorate solutions, 19: 38567
THORIUM COMPOUNDS
analysis for trace impurities by spectrochemical methods, 19: 38545(R) (MCW-1492, pp 23-8)
THORIUM ISOTOPES
nuclear properties of, pairing force effects on, (T), 19: 39927
THORIUM ISOTOPES Th-230
metabolism of, from inhaled uranium ore, 19: 38333 (BNWL-SA-226)
THORIUM ISOTOPES Th-232
internal conversion coefficients for, (E/T), 19: 39786 (ORNL-P-1419)
neutron reactions at 0.56 Mev, differential cross section for, 19: 40115 (CONF-650602-33)
THORIUM NITRIDES
PuN–ThN, preparation for high-temperature fuel evaluation, 19: 39091(R) (BMI-1723(Del.))
THORIUM OXIDES
neutron resonance integral, (E), 19: 40163
preparation of monocrystals of, from lithium ditungstate solvent, 19: 38628
THORIUM(IV) OXIDES
conversion to thorium carbide, 19: 39129(R) (ORNL-TM-1116)
density of sintered, effects of presintering variables on, 19: 39141
electron paramagnetic resonance and endor spectra of, containing europium, gadolinium, or terbium ions, 19: 38655
properties of carbon-coated particulate, effects of heating on, 19: 39129(R) (ORNL-TM-1116)
reactions with carbon at high temperatures, 19: 38755(R) (ORNL-3611)
BeO–ThO_2, preparation and properties, 19: 39091(R) (BMI-1723(Del.))
CaO–ThO_2, use as solid electrolyte in high-temperature cell, 19: 38586 (UCRL-11957)
Ni–ThO_2, properties of TD nickel as cladding material for SNAP hydride reactors, 19: 39166 (NAA-SR-Memo-11149)
ThO_2–UO_2, preparation of carbon-coated particulate, for radiation effects testing, 19: 39091(R) (BMI-1723(Del.))
ThO_2–UO_2, preparation and properties of carbon-coated particulate, 19: 39129(R) (ORNL-TM-1116)
ThO_2–UO_2 production by sol-gel process using vibratory compaction, 19: 38755(R) (ORNL-3611)
ThO_2–UO_2, properties of sol-gel processed, 19: 38755(R) (ORNL-3611)
ThO_2–UO_2, radiation effects on, 19: 38755(R) (ORNL-3611)
ThO_2–Y_2O_3, use as solid electrolyte in high-temperature cell, 19: 38586 (UCRL-11957)
THORIUM SYSTEMS
graphite–Th, deposition of coatings of, at 1500 to 1750°C, 19: 39144(P)
THRESHOLD DETECTORS
use in measurement of fast-neutron spectra, (E), 19: 39007
THULIUM
neutron absorption properties of, burnup effects on, (E), 19: 40163
phase transformations at 6 to 65 kbar, solid-liquid and solid-solid, 19: 40095
THULIUM COMPLEXES
with [(2-hydroxyethyl)imino]diacetic acid, dissociation constant of, 19: 38671
THULIUM ETHYL SULFATES
spectra of, absorption, 19: 38652
THULIUM HYDROXIDES
reactions with formic acid, properties of formate formed by, 19: 38669
THULIUM IONS
crystal-field interactions of, linear and nonlinear shielding of, (E/T), 19: 40101
reduction in calcium fluoride, yttrium ion effects on, (E), 19: 38595
THULIUM ISOTOPES Tm-169
neutron reactions (n,γ), gamma spectra of 3.9-ev resonance of, 19: 39781 (JAERI-1073)
THULIUM ISOTOPES Tm-172
energy levels of, parity and spin of, (E), 19: 39822
THYMIDINE
effects of tritiated, on uptake of carbon-14-labeled precursors by DNA, proteins, and RNA of L-cell nuclei, 19: 38339
incorporated of tritiated, by human tumor cells, 19: 38338
metabolism in desoxyribonucleic acid of mouse tissues, tracer study, 19: 38336 (TID-21106)
uptake by DNA, proteins, and RNA of L-cell nuclei, effects of tritiated thymidine on carbon-14-labeled-, 19: 38339
THYMUS
immunologic role of, in mouse radiation chimeras, 19: 38451
radiation effects on DNA ribonuclease in, x, 19: 39265(R) (IA-1021)
THYROID DISEASES
effects of thyrotoxicosis on gastrointestinal tract, use of iodine-131 for treatment of, 19: 38529
radiodiagnosis using iodine isotopes, 19: 38496
radiodiagnosis using iodine-131, 19: 38497
radiotherapy of hyperthyroidism using iodine-131, 19: 38497
THYROID GLAND
function tests using iodine-131, 19: 38497
function, effects of age and stress, 19: 38492
histology of surgically removed, 19: 38533
iodine-125 metabolism in, autoradiographic studies, 19: 38533
iodine-131 metabolism in, autoradiographic studies, 19: 38533
iodine-131 metabolism in rat, effects of vitamin B on, 19: 38337
iodine-131 metabolism in, effects of use of iodinated contrast media for diagnostic radiography on, 19: 38354
iodine-131 uptake by rat, effects of colloid formation in iodine solution on, 19: 38351
iodine-131 uptake by rabbit, procedures for measuring, 19: 38341
metabolism of iodine-131 in, effects of thyroid hormones on, 19: 38348
radiation effects on function of, x, 19: 38484
radiation effects on function of rat, neutron, 19: 38442
radiation effects on morphology of rat, fast neutron, 19: 38444
radioinduced neoplasms in rat, after exposure of single lobe, 19: 38367
THYRONINE, TRIIODO-
effects on iodine-131 metabolism in thyroid, 19: 38348
THYROXINE
deiodination in humans, effects of thyroid function on, 19: 39265(R) (IA-1021)
deiodination in rats, effects of metal ions and tumors on, 19: 39265(R) (IA-1021)
TIMING CIRCUITS
design of 4096-channel time analyzer with variable channel width, 19: 39024
review on multichannel time analyzers, 19: 38932
TIN
electron reactions with atomic, screening effects on bremsstrahlung and pair production in, (T), 19: 39389
energy gap in superconducting, dependence on transport current, (E), 19: 39735
heat of solution in liquid bismuth in presence of tellurium, 19: 39168(R) (TID-22015)
nuclear magnetic resonance in superconducting, spin-orbit coupling effects on Knight shift in, (T), 19: 39727
radioinduced reactions with alkyl halides, 19: 39091(R) (BMI-1723(Del.))
transition temperature of thin films of superconducting, effects of thin oxide layer on, (E), 19: 39746
TIN ALLOYS
Al–Sn–Ti, plastic anisotropy of alpha, 19: 39149 (AD-425880)
Cd–In–Ag–Sn, radiation effects on dimensions and mechanical properties of, 19: 40197(R) (WCAP-3718)
Cd–In–Ag–Sn, radiation effects on dimensions and mechanical properties of, 19: 40198(R) (WCAP-3721)
Sn–V, preparation and crystal structure of intermetallic compound V_2Sn_3 in, 19: 39189
TIN COMPOUNDS
Mössbauer parameters for organic, 19: 38576 (CONF-650425-2)
tin-119 Mössbauer effect in, 19: 38577 (CONF-650425-3)
TIN ISOTOPES
proton reactions (p,xn) with, isomeric tin-117 from, (E), 19: 39929
TIN ISOTOPES Sn-112
nuclear gyromagnetic ratio of first 5⁻ state of, 19: 39810
proton reactions (p,n) at 7 to 14 Mev, angular and energy distributions from, (E), 19: 39825
TIN ISOTOPES Sn-114
nuclear gyromagnetic ratio of first 5⁻ state of, 19: 39810
TIN ISOTOPES Sn-116
nuclear gyromagnetic ratio of first 5⁻ state of, 19: 39810
proton reactions (p,n) at 7 to 14 Mev, angular and energy distributions from, (E), 19: 39825
TIN ISOTOPES Sn-117
production of isomeric, in proton reactions (p,xn) with tin isotopes, (E), 19: 39929
proton reactions (p,n) at 7 to 14 Mev, angular and energy distributions from, (E), 19: 39825
TIN ISOTOPES Sn-118
neutron reactions (n,γ), p-wave resonances of, 19: 39784 (ORNL-P-1352)
nuclear gyromagnetic ratio of first 5⁻ state of, 19: 39810

proton reactions (p,n) at 7 to 14 Mev, angular and energy distributions from, (E), 19: 39825
TIN ISOTOPES Sn-119
Mössbauer effect in, effects of intermetallic bonding on, 19: 38577 (CONF-650425-3)
Mössbauer effect in monolayer on platinum, (E), 19: 39210
proton reactions (p,n) at 7 to 14 Mev, angular and energy distributions from, (E), 19: 39825
TIN ISOTOPES Sn-120
neutron reactions (n,γ), p-wave resonances of, 19: 39784 (ORNL-P-1352)
nuclear gyromagnetic ratio of first 5⁻ state of, 19: 39810
proton reactions (p,n) at 7 to 14 Mev, angular and energy distributions from, (E), 19: 39825
TIN ISOTOPES Sn-122
nuclear gyromagnetic ratio of first 5⁻ state of, 19: 39810
proton reactions (p,n) at 7 to 14 Mev, angular and energy distributions from, (E), 19: 39825
TIN ISOTOPES Sn-124
neutron reactions (n,γ), p-wave resonances of, 19: 39784 (ORNL-P-1352)
nuclear gyromagnetic ratio of first 5⁻ state of, 19: 39810
proton reactions (p,n) at 7 to 14 Mev, angular and energy distributions from, (E), 19: 39825
TIN ISOTOPES Sn-127
half life of isomeric, (E), 19: 39803
TIN TELLURIDES
heat of formation of, 19: 39168(R) (TID-22015)
TISSUE CULTURES
ascites tumor cell, effects of cysteamine on glutathione and sulfhydryl group content in, 19: 38464
genetic studies of human cells in, 19: 38328
radiation effects on mouse L cell, protective effects of halogenated pyrimidines against, 19: 38459
radiation effects on cytoplasm of cells in, 19: 38386
radiation exposure of single cells in, technique for, 19: 38385
TISSUES
radiation dosimetry in animal, method for fast neutron, 19: 38439
TITANIUM
combustion of particles of, in air, 19: 38827
effects on superconducting transition temperature of vanadium silicide, 19: 39196
electron reactions with atomic, screening effects on bremsstrahlung and pair production in, (T), 19: 39389
plastic anisotropy of sheet of, 19: 39149 (AD-425880)
separation from graphite above 1750°C in inert gases, 19: 38762
TITANIUM ALLOYS
corrosion by sodium chloride at 100 and 200°C, electrochemical, 19: 39117 (ORNL-P-1430)
Al–Cr–Fe–Mo–Ti, mechanical properties and heat resistance, 19: 39193
Al–Cr–Fe–Mo–Ni–Nb–Ti, thermal response and microstructure of Inconel 718 at 1200 and 1400°F, 19: 39158 (GEAP-4751)
Al–Sn–Ti, plastic anisotropy of alpha, 19: 39149 (AD-425880)
Cr–Nb–Ti, mechanical properties for high-temperature applications, 19: 39192
Cr–Ti–V, mechanical properties at high temperatures, 19: 40177(R) (ANL-7046(p.1-35))
Mo–Ti, cavitation in bismuth–lead alloy at 500 and 1500°F, ultrasonic-induced, 19: 39116 (NP-15263)
Mo–Ti–Zr, properties of TZM as cladding material for SNAP hydride reactors, 19: 39166 (NAA-SR-Memo-11149)
Pu–Ti–U, corrosion by air, 19: 40177(R) (ANL-7046(p.1-35))
Pu–Ti–U, phase studies, 19: 40177(R) (ANL-7046(p.1-35))
Pu–Ti–U, reactions with stainless steel at high temperatures, 19: 40177(R) (ANL-7046(p.1-35))
Ti–V, corrosion by sodium at 650°C, 19: 40177(R) (ANL-7046(p.1-35))
Ti–V, fabrication into tubes by extrusion, 19: 40177(R) (ANL-7046 (p.1-35))
Ti–V, mechanical properties at high temperatures, 19: 40177(R) (ANL-7046(p.1-35))
Ti–V, preparation for superconductor magnetic field measurements, 19: 40286(R) (NAA-SR-11200)
Ti–V, properties as fuel cladding, 19: 40113(R) (ANL-7071)
Ti–V, removal from fuel pins by hydrogen-induced swelling, 19: 40113(R) (ANL-7071)
Ti–V, superconducting properties and uses, 19: 39750(P)
TITANIUM CARBIDES
GaC–TiC, preparation and crystal structure of H-phase in, 19: 39208
TITANIUM CHLORIDES
corrosive effects on molybdenum, electrochemical, 19: 39122
TITANIUM HYDRIDES
TiH–TiN, preparation of stoichiometric, 19: 40286(R) (NAA-SR-11200)
TITANIUM IONS
incorporation into potassium chloride crystals grown from solution, 19: 38696 (MIT-2909-4)
TITANIUM ISOTOPES Ti-46
gamma transitions in, energies of, (E), 19: 39866
TITANIUM NITRIDES
GaN–TiN, preparation and crystal structure of H-phase in, 19: 39208
InN–TiN, preparation and crystal structure of H-phase in, 19: 39208
PuN–TiN, preparation for high-temperature fuel evaluation, 19: 39091(R) (BMI-1723(Del.))
TiH–TiN, preparation of stoichiometric, 19: 40286(R) (NAA-SR-11200)
TITANIUM SYSTEMS
Al–Fe–Mg–Ni–Si–Ti–Zr, coating with aluminum–nickel layers by chemical deposition, 19: 39143(P)
As–Ti–N, crystal structure of compounds in, 19: 39209
C–Cd–Ti, preparation and crystal structure of H-phase in, 19: 39208
TOLUENE
isotopic exchange of deuterated, with water, 19: 38693
isotopic isomerization of deuterated, effects of platinum catalyst on, 19: 38693
TOLUENE, TRINITRO-
electric conductivity of detonation products of, 19: 40284 (LA-DC-6993)
TOLUIC ACID
exchange reactions between deuterium oxide and hydrogen in, nickel-catalyzed, 19: 38688
exchange reactions between deuterium oxide and hydrogen in, nickel-catalyzed, 19: 38688
TOMATOES
radioinduced ripening in, effects of gibberellic acid on gamma, 19: 38401
TOPOLOGY
convex sets in, applications of, 19: 39082 (TID-22032)
TOXICOLOGY
of radioisotopes in animals, 19: 38357(T)
TOXINS
radiation effects on formation of, by *Cl. perfringens*, 19: 38448
radioinduced in *Cl. perfringens*, activity of, 19: 38446
radioinduced in *Cl. perfringens*, 19: 38447
TRACER TECHNIQUES
estimation of microcuries and millimicrograms from counts per minute, 19: 38749
for detecting microorganisms in jet fuel, 19: 39061 (ADR-09-08a-63.1)
industrial uses of, 19: 39265(R) (IA-1021)
uses in Hungarian industry, 19: 39063
zinc-65 diffusion in gallium arsenide, 19: 39269(R) (SU-SEL-64-133)
TRACER TECHNIQUES (AGRICULTURE)
equipment for rapid placement of radioisotopes in soil for, 19: 38870
TRACER TECHNIQUES (BIOLOGY)
preparation of carbon-11-labeled blood cells, 19: 38722
TRACER TECHNIQUES (CHEMISTRY)
for determining organic residue from solvents, 19: 38538 (ADR-08-13-63.1)
performance of tantalum-182 in fluoride determination, 19: 39265(R) (IA-1021)
TRACER TECHNIQUES (MEDICINE)
for blood volume measurements, 19: 38525
for brain circulation measurements, using chlormerodrin–mercury-203 and external counting, 19: 38501
for diagnosis of blood dyscrasias, 19: 38493
for diagnosis of cardiac infarcts, 19: 38502
for diagnosis of cardiac infarcts, 19: 38503
for diagnosis of thyroid diseases, 19: 38496
for diagnosis of thyroid diseases, 19: 38497
for iodine metabolism in thyroid, 19: 38533
for radiodiagnosis using technetium-99 as tracer, 19: 38506
for tumor diagnosis, using cesium-131 and external counting, 19: 38508
gamma camera design and performance for, 19: 39008
purification of iodine-131 labeled sodium *o*-iodohippurate for intravenous use, ion exchange, 19: 38507
TRADESCANTIA
chromosome pattern of native populations, 19: 38360 (TID-21695)
pattern in Tradescantia, 19: 38360 (TID-21695)
radiation effects on mitosis in, synergistic infrared and x, 19: 38416
radiation effects on chromosomes in, aberrant infrared and x, 19: 38416
TRANSDUCERS
development and testing of pressure, 19: 40288(R) (NVO-98-5)
radiation effects on components, 19: 39055 (GA-6266)
temperature effects on zirconate titanate, 19: 39270(R) (TID-21894)
TRANSFORMERS
design of magnetohydrodynamic, 19: 39448(P)
TRANSISTORS
radiation effects on, data re-presentation technique for electron, 19: 39054 (AD-607863)

TRANSITION METALS
transitions in ionic crystals of, optical, 19: 39265(R) (IA-1021)
TRANSURANIC ELEMENTS
production in nuclear explosions, 19: 38786 (LA-DC-7111)
TRAPS
design of regenerative H_2O–CO_2 and charcoal, for fission products in in-pile loop, 19: 40120 (GAMD-5434)
TRIDODECYLAMINE
solvent properties for ruthenium nitrosyls, plutonium(IV), uranium(IV), and zirconium from nitric acid solutions, 19: 38761(T) (CEA-tr-A-1809)
TRIISOOCTYLAMINE
lanthanide-citrate complexes in, 19: 38578 (IA-1014)
solvent properties for ruthenium nitrosyls, plutonium(IV), uranium(IV), and zirconium from nitric acid solutions, 19: 38761(T) (CEA-tr-A-1809)
TRITIUM
charge and magnetic-moment structure of, model for, (T), 19: 39888
decay in hydrogen tritide, theory of beta, 19: 39799
determination and measurement of, radiometric, 19: 38552
determination with carbon-14 on chromatograms, method for, 19: 38561
dosimetry of thymidine-incorporated, in nuclear DNA, 19: 38873 (BNL-9331)
effects on cell nuclei, 19: 38873 (BNL-9331)
electron inelastic scattering at 549 Mev, cross sections for, (T), 19: 39909
form factors of, calculation using repulsive-core potentials, (T), 19: 39868
labeling of human tumors using, in thymidine, 19: 38338
metabolism of inhaled or percutaneously absorbed, in man, 19: 38355
neutron reactions (n,xn) at 14.1 Mev, charged-particle spectra in, (E), 19: 39939
reactions of recoil, with cloroethane, products from, 19: 38704
separation from air at reactor installations, 19: 38907
separation from helium-3 by adsorption on activated charcoal, (E), 19: 38773
thermodynamic properties of liquid, 19: 38639
use in determining organic residue from solvents, 19: 38538 (ADR-08-13-63.1)
uses in Japan, 1950 to 1960, 19: 39060
TRITONS
binding energy, (T), 19: 39926
reactions (t,α) with lead-208 at 12.0 and 13.5 Mev, thallium-207 energy levels from, (E), 19: 39852
TROPOSPHERE
radioactivity from fission products in, from Chinese nuclear weapon test, 19: 38899
TUBERCULOSIS
radiation effects on immune reactions to, in guinea pigs, 19: 38375
TUBES
bubble rise velocity in inclined, 19: 38808 (NYO-3114-8)
fabrication of electric heater, with embedded resistor, 19: 39145(P)
performance of reactor-fuel-cladding, evaluation of, (E), 19: 40172
properties of cold-worked niobium–zirconium alloy fuel sheathing, 19: 39150 (AECL-2250(Pt.I))
sealing means for coaxial, 19: 38785(P)
superfluid flow in Venturi, (T), 19: 39696
testing of thin-walled, nondestructive methods for, 19: 38823 (BNWL-SA-97)
TUMORS
cesium-131 metabolism by, differential, 19: 38508
effects of atomic and thermonuclear weapons on, 19: 38478
effects on iodine depletion in rat thyroxine, 19: 39265(R) (IA-1021)
induced by rare earth metal subcutaneous implants in mice, 19: 38334 (COO-1170-1)
labeling of human, by tritiated thymidine, 19: 38338
radiation dose effects on growth of mammary, in F_1 hybrid mice, x, 19: 38403
radiation effects on growth of transplanted mouse, synergistic effects of cruzine, 19: 38428
radiation effects on growth of transplanted, in mice, 19: 38387
radiation effects on metabolism and respiration in rat, synergistic effects of hydrogen peroxide, 19: 38389
radiocolloid treatment of malignant effusions, 19: 38515
radiodiagnosis of malignant melanomas of eye, 19: 38485
radiodiagnosis of, using cesium-131 and external counting, 19: 38508
radioinduced in rat thyroid after exposure of single lobe, 19: 38367
radiosensitivity of, effects of regional oxygenation in rabbits, 19: 38374
radiosensitivity of Ehrlich ascites, at various times following inoculation, 19: 38402
radiotherapy of bladder using gamma sources, 19: 38504
radiotherapy of calcifying epithelioma, 19: 38494
radiotherapy of gynecologic, digestive stenoses induction by, 19: 38522
radiotherapy of hemangiomas of skin, contra-indications, 19: 38511
radiotherapy of thyroid using iodine-131, 19: 38497
radiotherapy of vagina, effects on thyroid function, 19: 38492
radiotherapy of, computer optimization of 4 Mev, 19: 38518
radiotherapy of, review, 19: 38487
radiotherapy using high-energy sources, 19: 38499
radiotherapy, design of automatic application intercavitary cobalt-60 source for, 19: 38483
radiotherapy, effects of hyperbaric oxygen on results, 19: 38500
radiotherapy, evaluation by acridine orange staining of exfoliated cells, 19: 38488
therapy of hemangiomas of skin using frozen carbon dioxide or surgery, 19: 38511
TUNGSTEN
cesium ion emission from hot porous, impurity effects on, 19: 39164 (N64-22193)
diffusion of atoms in bcc, activation energy for interstitial, (T), 19: 40086
diffusion of oxygen at 1500 to 1800°C, 19: 39072(R) (NP-15187)
diffusion rate of oxygen in, at 1500 to 1800°C, 19: 39070(R) (GEST-2046)
elastic properties of polycrystalline, dynamic, 19: 39198
electron emission from effects of cesium on, 19: 39441
electron-beam effects on surfaces of, 19: 39255
Fermi surface in, (T), 19: 40102
magnetostriction in pure monocrystalline, 19: 39199
proton reactions at 50 to 225 kev, electron emission in, (E), 19: 39409
purification by field-aided electron-beam zone refining, 19: 39111
radiation damage in, cross sections for atomic displacements from 1- to 3-Mev electrons, 19: 39225 (AFCRL-65-286)
separation from waste water, methods for, 19: 40276
solubility in liquid plutonium, evaluation of sampling methods for determination of, 19: 38580 (LA-3303)
sorptive properties for krypton, 19: 39265(R) (IA-1021)
sorptive properties for oxygen, (E/T), 19: 39103
superconducting transition temperatures in films of, (E), 19: 39708
tungsten-183 spin-lattice relaxation and Knight shift in, (E), 19: 39720
use of fibers of, for reinforcing nickel, 19: 39093 (BNWL-SA-141)
TUNGSTEN ALLOY COUPLES
Re–W/Re–W, emf measurements, (E), 19: 40177(R) (ANL-7046(p.1-35))
TUNGSTEN ALLOYS
Cr–Fe–Mo–Ni–Nb–W, tensile properties of IN-102, 19: 39156(R) (CEND-532)
Hf–Ta–W, cavitation of T-111 in bismuth–lead alloy at 500 and 1500°F, ultrasonic-induced, 19: 39116 (NP-15263)
Pt–W, performance as heater wire in calorimetry below 0.1°K, 19: 39743
Re–W, fabrication of seamless tubing of, 19: 39128(R) (NMI-1267)
Sb–W, crystal structure of intermetallic compounds in, 19: 39209
TUNGSTEN BORIDES
reactions with graphite to 2200°C, 19: 38654
TUNGSTEN CARBIDES
Fe–Ni–WC, internal friction of, effects of composition on, 19: 39170(T) (FTD-TT-64-1001)
Fe–WC, internal friction of, effects of composition on, 19: 39170(T) (FTD-TT-64-1001)
Ni–WC, internal friction of, effects of composition on, 19: 39170(T) (FTD-TT-64-1001)
TUNGSTEN COUPLES
W/UO_2, uranium diffusion rate at 1800 to 2200°C, 19: 39070(R) (GEST-2046)
TUNGSTEN ISOTOPES W-183
spin-lattice relaxation time and Knight shift in tungsten at 1.1 to 4.0°K, (E), 19: 39720
TUNGSTEN ISOTOPES W-189
beta decay and gamma spectra, (E), 19: 39801
production in reactions (n,α) with osmium-192, (E), 19: 39801
TUNGSTEN SYSTEMS
As–Ti–N, crystal structure of compounds in, 19: 39209
As–W, crystal structure of compounds in, 19: 39209
C–Hf–Ta–W, cavitation of T-222(A) in bismuth–lead alloy at 500 and 1500°F, ultrasonic-induced, 19: 39116 (NP-15263)
C–Nb–W–Zr, fabrication and properties at –325 to 3000°F, 19: 39224(P)

U

ULCERS
radioinduced skin, etiology, pathology, and therapy of, 19: 38513
ULTRASONICS
attenuation in monocrystalline copper at low temperatures, 19: 39249
cavitation by, of materials in bismuth–lead alloy at 500 and 1500°F, 19: 39116 (NP-15263)
use for nondestructive testing of bonds in welds, 19: 38546(R) (RFP-552)

ULTRAVIOLET RADIATION
effects on aluminate solutions, 19: 38738
effects on chromosome aberration induction in hamster cells, 19: 38395
effects on *E. coli*, protective effects of ribonuclease against, 19: 38465
effects on linolenic acid extract effects on mouse skin, 19: 38366
effects on RNA synthesis in derivatives of *E. coli*, 19: 38381
effects on survival of *Macrobiotes areolatus* in active and dormant states, 19: 38373
effects on viscosity of rat tail collagen in solution, 19: 38701
reactions with atomic hydrogen at 850.6 Å, ionization cross section for, (E), 19: 39388
refraction by helium at 2700 to 600 Å, index and sum rules for, (T), 19: 39402
ULTRAVIOLET SPECTROSCOPY
camera for extreme, design of pinhole, 19: 38928
UNDERGROUND EXPLOSIONS
blast from Dugout row-charge cratering experiment, measurements of close-in air, 19: 38790 (PNE-608F)
crater dimensions in Dugout row-charge event, 19: 38789 (PNE-601F)
ground motion measurements during large, instrumentation for, 19: 38865 (SC-R-65-904, pp 3-22)
ground velocity measurements near, high-range gage for, 19: 38917 (SC-R-65-904, pp 23-48)
isotope distribution and recovery in Gnome event, 19: 38787 (PNE-102F)
neutrons from, time-of-flight experiments with, (E), 19: 39889
stem design and shotcrete, grout, and concrete support for Pre-Schooner, 19: 38788 (PNE-501F)
use in development and management of water resources, principles of, 19: 38791 (TEI-857)
UNION OF SOUTH AFRICA
uranium production and uses in, in 1964, 19: 39105
UNITED STATES
fallout monitoring in, program of Division of Radiological Health of the Public Health Service, 19: 38880
radiation monitoring program of Public Health Service, 19: 38888
uranium production and uses in, in 1964, 19: 39105
URACIL, 2-THIO-
effects on iodine-131 metabolism in mice, 19: 38350
URANIUM
analysis for impurities by mass spectrometry, 19: 38546(R) (RFP-552)
biogenic migration of, in Lake Issyk-kul, USSR, 19: 38855
deposition from fused salt into liquid metal cathodes, electrolytic, 19: 38754 (NAA-SR-10737)
deposition on metals of films of, electrolytic, 19: 39100 (SGAE-CH-16/1965)
determination by x-ray fluorescence spectroscopy, 19: 38549
determination in air in presence of plutonium, chromatographic, 19: 38554
determination in electrolytes by spectrochemical methods, 19: 38544(R) (MCW-1492, pp 13-19)
determination of free, in carbon–uranium–uranium carbide systems, 19: 38540 (CEA-Note-397)
diffusion in molybdenum and tungsten at 1600 to 1800°C, 19: 39070(R) (GEST-2046)
diffusion in pyrolytic carbon at high temperatures, 19: 39129(R) (ORNL-TM-1116)
electron reactions with atomic, screening effects on bremsstrahlung and pair production in, (T), 19: 39389
fission effects in, 19: 40286(R) (NAA-SR-11200)
neutron capture cross sections at 20 kev, 19: 38786 (LA-DC-7111)
neutron spectra in natural, measurement of exponential, (E), 19: 39763 (EUR-2413.e)
oxidation by partially decomposed carbon dioxide, 19: 39121
preparation of uranium-235 enriched fuels of, 19: 39104
production and uses of, in 1964, 19: 39105
production by tetrafluoride reduction using magnesium, design of bell furnaces for, 19: 39113(P)
production from urania by electrolysis in fluorides, 19: 39099 (MCW-1492, pp 7-11)
radiation effects on compatibility with carbon dioxide, 19: 39121
reprocessing of unirradiated enriched scrap, nuclear material control program for, 19: 38758 (Y-KA-7)
separation from fuels by fluoride volatility processing, 19: 40112(R) (ANL-7046(p.36-66))
separation from irradiated fuels by fluoride volatility processes, 19: 40113(R) (ANL-7071)
separation from irradiated reactor fuels by TBP extraction, 19: 38776(P)
separation from melt-refining crucibles, 19: 40177(R) (ANL-7046 (p.1-35))
separation from melt refining skulls, flowsheet for, 19: 40113(R) (ANL-7071)
separation from protactinium and thorium by paper electrophoresis, 19: 38775
separation from scandium by ion exchange in nitrate solutions, 19: 38770
separation from spent fuel by halide slagging, 19: 40177(R) (ANL-7046(p.1-35))
separation of barium-140 and strontium-90 from irradiated, by ion exchange chromatography, 19: 38757 (SGAE-CH-17/1965)
sintering behavior of powdered, (E), 19: 39132
solvent extraction of tetravalent, for nitric acid solutions by tertiary amines, 19: 38761(T) (CEA-tr-A-1809)
vapor pressure over uranium–carbon systems, 19: 39160 (LA-DC-6953)
x-ray isotope shift in, K, (E), 19: 39412
URANIUM ALLOYS
precipitated particles in dilute, electron microscopic techniques for determining distribution of, 19: 39092 (BNWL-SA-90)
fissium–Pu–U, hydridation for cladding removal, 19: 40113(R) (ANL-7071)
fissium–U, radiation effects, 19: 40113(R) (ANL-7071)
fissium–Pu–U, reactions with stainless steel at high temperatures, 19: 40177(R) (ANL-7046(p.1-35))
fissium–U–Zr, thermal conductivity of, effects of burnup on, 19: 40112(R) (ANL-7046(p.36-66))
fissium–U, thermal conductivity of, effects of burnup on, 19: 40112(R) (ANL-7046(p.36-66))
Mo–U, performance in HNPF, 19: 40286(R) (NAA-SR-11200)
Pu–Ti–U, corrosion by air, 19: 40177(R) (ANL-7046(p.1-35))
Pu–Ti–U, phase studies, 19: 40177(R) (ANL-7046(p.1-35))
Pu–Ti–U, reactions with stainless steel at high temperatures, 19: 40177(R) (ANL-7046(p.1-35))
Pu–U–Zr, phase studies, 19: 40177(R) (ANL-7046(p.1-35))
Pu–U–Zr, reactions with stainless steel at high temperatures, 19: 40177(R) (ANL-7046(p.1-35))
Th–U, radiation effects on, 19: 38755(R) (ORNL-3611)
Th–U–Zr, radiation effects on, 19: 38755(R) (ORNL-3611)
URANIUM CARBIDES
diffusion in, self, 19: 40286(R) (NAA-SR-11200)
diffusion of fission products from carbon-coated, 19: 39091(R) (BMI-1723 (Del.))
electrolysis in fused salt using molten metal cathodes, 19: 38754 (NAA-SR-10737)
hardness at high temperatures, 19: 40286(R) (NAA-SR-11200)
hydrolysis at high temperature, mechanism of, (E), 19: 38606
hydrolysis of, kinetics at 30 to 86°C, 19: 38581 (NAA-SR-11401)
mechanical properties of, effects of temperature on, 19: 40286(R) (NAA-SR-11200)
oxidation of single-crystal, at 900°C, 19: 40286(R) (NAA-SR-11200)
performance in HNPF, 19: 40286(R) (NAA-SR-11200)
preparation and properties of carbon-coated particulate, 19: 39129(R) (ORNL-TM-1116)
preparation of single-crystal, 19: 40286(R) (NAA-SR-11200)
preparation properties and structure of tungsten-doped, 19: 40286(R) (NAA-SR-11200)
processing irradiated, pyrochemical, 19: 40113(R) (ANL-7071)
production process for, 19: 40286(R) (NAA-SR-11200)
radiation effects on stainless steel-clad, at 1800°F and high burnups, 19: 40286(R) (NAA-SR-11200)
radiation effects on, under transient heating in TREAT, 19: 40286(R) (NAA-SR-11200)
radiation effects on, effects of coatings, matrix materials, and temperature on, 19: 39091(R) (BMI-1723(Del.))
radiation effects on carbon-coated particulate, neutron, 19: 39129(R) (ORNL-TM-1116)
reactions of carbon-coated particulate, with water vapor at 1000°C, 19: 39129(R) (ORNL-TM-1116)
vapor pressure of di-, over uranium–carbon systems, 19: 39160 (LA-DC-6953)
C–U–UC, analysis for free uranium, 19: 38540 (CEA-Note-397)
Na–UC, corrosive effects on stainless steel, 19: 40113(R) (ANL-7071)
Ni–PuC–UC, thermal diffusivities of, 19: 39163(R) (MLM-1244)
Ni–UC, thermal diffusivities of, calculations of, 19: 39163(R) (MLM-1244)
PuC–UC, fabrication by compaction, 19: 40177(R) (ANL-7046(p.1-35))
PuC–UC, thermal diffusivities of, 19: 39163(R) (MLM-1244)
ThC_2–UC_2, preparation by sol-gel process, 19: 38755(R) (ORNL-3611)
ThC_2–UC_2, preparation and properties of carbon-coated particulate, 19: 39129(R) (ORNL-TM-1116)
ThC_2–UC_2, processing of irradiated coats of, 19: 39129(R) (ORNL-TM-1116)
ThC_2–UC_2, radiation effects on, effects of coatings, matrix materials, and temperatures on, 19: 39091(R) (BMI-1723(Del.))
ThC_2–UC_2, radiation effects on carbon-coated particulate, neutron, 19: 39129(R) (ORNL-TM-1116)

U–UC, fabrication and properties of cermets of, 19: 39127 (NCSC-2981-9)
UC–ZrC, thermal expansion of polycrystalline solid solution of, at 25 to 1000°C, 19: 39200
URANIUM CARBONITRIDES
preparation and properties of, 19: 39089 (AERE-M-1389)
URANIUM(III) CHLORIDES
reactions with plutonium to 1200°C, mechanisms in, 19: 40177(R) (ANL-7046(p.1-35))
URANIUM(IV) CHLORIDES
chlorination in lithium chloride–potassium chloride melt, kinetics, 19: 38587 (UCRL-11986)
conversion to sulfide in fused salt, 19: 38574 (ANL-7008)
preparation by reduction of uranyl chloride using aluminum–magnesium alloy, 19: 38662
preparation from uranyl salt by reaction with alkali sulfide or hydrogen sulfide, 19: 38659
separation by solvent extraction using kerosene–TBP, acid effects in, 19: 38563
$PbCl_2$–UCl_4, phase studies, 19: 39265(R) (IA-1021)
URANIUM COMPLEXES
formation and stability in pridyl-azo-resorcinol system, 19: 38594
with β-resorcylic acid, spectra of, absorption, 19: 38607
URANIUM DEPOSITS (UTAH)
population studies on plants and vertebrates in, of Upper Colorado River Basin, 19: 38330 (TID-22078)
URANIUM(IV) FLUORIDES
conversion to sulfide in fused salt, 19: 38574 (ANL-7008)
determination in gases using dew-point hygrometer, 19: 38573(P)
reduction using magnesium, design of bell furnace for, 19: 39113(P)
URANIUM(VI) FLUORIDES
conversion of uranium-235 enriched, into nuclear fuel, 19: 39104
URANIUM IONS
diffusion in uranium dioxide, alpha spectrometric studies of, 19: 38681
oxidation of tetravalent, by diffraction neptunium valence states in chloride and perchlorate solutions, 19: 38584 (SC-RR-65-219)
N_2H_4–uranium(IV), use as partitioning agent in Purex process, 19: 38751 (HW-82103)
URANIUM ISOTOPES
nuclear properties of, pairing force effects on, (T), 19: 39927
URANIUM ISOTOPES U-233
neutron reactions (n,γf) with, thermal, (T), 19: 39864
separation from thorium by solvent extraction using di-*sec*-butylphenyl phosphonate, 19: 38755(R) (ORNL-3611)
URANIUM ISOTOPES U-234
content in zircons, 19: 38849
internal conversion coefficients for, (E/T), 19: 39786 (ORNL-P-1419)
use in age estimation of pelagic sediments, (E/T), 19: 38866
URANIUM ISOTOPES U-235
concentration in nuclear fuels, methods for, 19: 39104
content in zircons, 19: 38849
critical concentrations in simple and complex geometries, 19: 40155 (LA-3229, pp 362-76)
decay of isomeric, effect of chemical state on, 19: 39842
fission of, alpha particle production in, (E), 19: 39265(R) (IA-1021)
maximum permissible concentrations of fission products of, in air and water, 19: 38872 (AEET/HP/TH-15)
neutron fission cross sections at 10 to 25 ev, (E), 19: 39889
neutron fission of, yields of krypton-85 in thermal, (E), 19: 39800
neutron reactions (n,γf) with, thermal, (T), 19: 39864
reactivity of, temperature effects on, 19: 40286(R) (NAA-SR-11200)
U-235–H_2O–Zr, critical bucklings and extrapolation distance for, (T), 19: 40159 (WAPD-T-1774)
URANIUM ISOTOPES U-236
internal conversion coefficients for, (E/T), 19: 39786 (ORNL-P-1419)
URANIUM ISOTOPES U-238
content in zircons, 19: 38849
internal conversion coefficients for, (E/T), 19: 39786 (ORNL-P-1419)
neutron cross sections from 0.001 ev to 15.0 Mev, 19: 39764 (GA-6087(Rev.))
neutron resonance integral, (E), 19: 40163
reactivity of, effects of neutron spectra and temperature on, 19: 40286(R) (NAA-SR-11200)
URANIUM NITRIDES
preparation of carbon-coated particulate, for radiation effects testing, 19: 39091(R) (BMI-1723(Del.))
preparation of massive, process and apparatus for, 19: 38685(P)
Na–UN, corrosive effects on stainless steel, 19: 40113(R) (ANL-7071)
PuN–UN, radiation effects on, neutron, 19: 38125(R) (BNWL-91)
UN–UP, phase studies and properties, 19: 40112(R) (ANL-7046(p.36-66))
URANIUM ORES
analysis for calcium by x-ray-fluorescence, 19: 38543(R) (MCW-1492)
metabolism of inhaled particles in rats, 19: 38333 (BNWL-SA-226)
URANIUM OXIDE SLURRIES
preparation and properties of ammonia–uranium dioxide, for fissiochemical production of hydrazine, 19: 39095 (CONF-117(p.81-97))
requirements for fissiochemical production, 19: 40169 (CONF-117 (p.67-79))
URANIUM OXIDES
mechanical properties of, effects of oxygen–uranium ratios on, 19: 40113(R) (ANL-7071)
URANIUM(IV) OXIDES
coating with stainless steel, 19: 39147(P)
density of powdered, 19: 39125(R) (BNWL-91)
diffusion of nitrogen and oxygen in, model for, 19: 39219
diffusion of uranium ions in, alpha spectrometric studies of, 19: 38681
elastic modulus of, effects of atomic ratio and density on, 19: 40112(R) (ANL-7046(p.36-66))
elastic properties of, determination by ultrasonics, 19: 40112(R) (ANL-7046(p.36-66))
electric conductivity of single-crystal, at high temperatures, 19: 39125(R) (BNWL-91)
electrolysis in fluorides for production of uranium, 19: 39099 (MCW-1492, pp 7-11)
enrichment using plutonium wires, 19: 39125(R) (BNWL-91)
etching of, cathodic, 19: 39125(R) (BNWL-91)
fabrication into "annular multitube" fuel elements, (E), 19: 40172
fabrication into pellet and powder fuel elements, economics of, (E), 19: 40172
neutron diffraction by, magnetic structure determination by, (E), 19: 40091
oxidation in air, mechanism of, 19: 38660
preparation and properties of carbon-coated particulate, 19: 39129(R) (ORNL-TM-1116)
preparation and properties of microspheres of, 19: 39163(R) (MLM-1244)
preparation of carbon-coated particulate, for radiation effects testing, 19: 39091(R) (BMI-1723(Del.))
preparation of uranium-235 enriched fuels of, 19: 39104
processing irradiated, by low-decontamination methods, 19: 40286(R) (NAA-SR-11200)
properties at high temperatures, ionic diffusion in, 19: 39154 (BNWL-SA-54)
properties of carbon-coated particulate, effects of heating on, 19: 39129(R) (ORNL-TM-1116)
radiation effects on carbon-coated particulate, 19: 39091(R) (BMI-1723 (Del.))
radiation effects on, effects of coatings, matrix materials, and temperature on, 19: 39091(R) (BMI-1723(Del.))
radiation effects on microstructure and electric properties of, neutron, 19: 39125(R) (BNWL-91)
radiation effects on carbon-coated particulate, neutron, 19: 39129(R) (ORNL-TM-1116)
radiation effects on Zircaloy-clad, neutron, 19: 39125(R) (BNWL-91)
radiation effects on alumina-coated particles of, 19: 39227 (BMI-1729)
radiation effects on Zircaloy-clad, at high burnups, 19: 39234 (GEAP-4597)
radioinduced swelling in encapsulated, 19: 40195(R) (WCAP-3269-5)
radioinduced swelling of stainless steel- and Zircaloy-clad, 19: 40196(R) (WCAP-3269-6)
reactions with carbon tetrachloride, 19: 38661
reactions with sulfuric acid, composition and structure changes in, 19: 38657
thermodynamic properties of, correlation of atomic transport with, 19: 39219
uranium-238 resonance integral in, (E), 19: 40163
BeO–UO_2, radiation effects on clad, 19: 39091(R) (BMI-1723(Del.))
CaO–UO_2–ZrO_2, densities and thermal properties, 19: 39091(R) (BMI-1723(Del.))
CeO_2–UO_2, phase studies, 19: 39222
CeO_2–UO_2, radiation effects on clad, at high burnups, 19: 39091(R) (BMI-1724(Del.))
CeO_2–UO_2, thermodynamic properties, 19: 39222
Mo/UO_2, uranium diffusion rate at 1600 to 1800°C, 19: 39070(R) (GEST-2046)
Na–UO_2, corrosive effects on stainless steel, 19: 40113(R) (ANL-7071)
NH_3–UO_2, preparation and properties of slurries of, for fissiochemical production of hydrazine, 19: 39095 (CONF-117(p.81-97))
paraffin–UO_2–ZrO_2, neutron spectra in, asymptotic and steady-state, (E), 19: 39768 (RPI-328-21)
PuO_2–UO_2, distributions and phases in, 19: 39125(R) (BNWL-91)
PuO_2–UO_2, fabrication for plutonium recycle experiments, 19: 40112(R) (ANL-7046(p.36-66))
PuO_2–UO_2, fabrication into glass-bonded fuel rods, 19: 39124 (ANL-6995)

PuO_2–UO_2, fabrication for use as reactor fuel, 19: 39146(P)
PuO_2–UO_2, processing by fluorination, 19: 40112(R) (ANL-7046 (p.36-66))
PuO_2–UO_2, radiation effects on, neutron, 19: 39125(R) (BNWL-91)
stainless steel–UO_2, fabrication into pins, 19: 39125(R) (BNWL-91)
ThO_2–UO_2, preparation of carbon-coated particulate, for radiation effects testing, 19: 39091(R) (BMI-1723(Del.))
ThO_2–UO_2, preparation and properties of carbon-coated particulate, 19: 39129(R) (ORNL-TM-1116)
ThO_2–UO_2 production by sol-gel process using vibratory compaction, 19: 38755(R) (ORNL-3611)
ThO_2–UO_2, properties of sol-gel processed, 19: 38755(R) (ORNL-3611)
ThO_2–UO_2, radiation effects on, 19: 38755(R) (ORNL-3611)
UO_2–Y_2O_3–ZrO_2, preparation of solid solution powders of, for use as reactor fuel, 19: 39094 (CONF-117(p.11-19))
UO_2–ZrO_2, partial pressures of, 19: 39091(R) (BMI-1723(Del.))
UO_2–ZrO_2, radiation effects on calcia-stabilized, at high burnups, 19: 39091(R) (BMI-1723(Del.))
UO_2–ZrO_2, radiation effects on clad, 19: 39091(R) (BMI-1723(Del.))
W/UO_2, diffusion of uranium at 1800 to 2200°C, 19: 39070(R) (GEST-2046)

URANIUM(IV-VI) OXIDES
gas evolution from, at 1000°C, 19: 39125(R) (BNWL-91)
reactions with carbon tetrachloride, intermediate products in, 19: 38661
reactions with sulfuric acid, composition and structure changes in, 19: 38657
U_3O_8–UO_3, thermodynamic properties, 19: 38676

URANIUM(VI) OXIDES
heat of solution in nitric acid, 19: 38676
reactions with carbon tetrachloride, intermediate products in, 19: 38661
reactions with hydrobromic acid at –20 and 250°C, 19: 38603
thermal decomposition of, mechanism of, 19: 38660
U_3O_8–UO_3, thermodynamic properties, 19: 38676

URANIUM OXYSULFIDES
preparation of, using fused salt processes, 19: 38574 (ANL-7008)

URANIUM PEROXIDES
thermodynamic properties, 19: 38676

URANIUM PHOSPHIDES
magnetic structure of, from neutron diffraction, (E), 19: 40104
mechanical and physical properties, 19: 40113(R) (ANL-7071)
properties of, mechanical and thermal, 19: 40112(R) (ANL-7046 (p.36-66))
UN–UP, phase studies and properties, 19: 40112(R) (ANL-7046(p.36-66))

URANIUM(IV) SULFATES
preparation from uranyl salt by reaction with alkali sulfide or hydrogen sulfide, 19: 38659

URANIUM SULFIDES
mechanical and physical properties, 19: 40113(R) (ANL-7071)
preparation of, using fused salt processes, 19: 38574 (ANL-7008)
properties of, mechanical and thermal, 19: 40112(R) (ANL-7046 (p.36-66))

URANIUM SYSTEMS
C–H–U, preparation, 19: 40286(R) (NAA-SR-11200)
C–U, vapor pressure studies, 19: 39160 (LA-DC-6953)
C–U–UC, analysis for free uranium, 19: 38540 (CEA-Note-397)
graphite–U, deposition of coatings of, at 1500 to 1750°C, 19: 39144(P)
O–U, phase studies, 19: 39125(R) (BNWL-91)
U–UC, fabrication and properties of cermets of, 19: 39127 (NCSC-2981-9)

URANYL ACETATES
thermal decomposition of, mechanism of, 19: 38660

URANYL BROMIDES
preparation and properties, 19: 38603

URANYL CHLORIDES
reduction by aluminum–magnesium chlorides, preparation of uranous chloride by, 19: 38662
thermodynamic properties, 19: 38676

URANYL CITRATE COMPLEXES
nuclear magnetic resonance spectra of, in heavy water, 19: 38623

URANYL IONS
formation complex with β resorcylic acid, 19: 38607
heat of formation, 19: 38676
pi bonding in, exchange and relativistic effects on, 19: 38635
radiolysis of aqueous solutions of, pulse, 19: 38728
sorption by gamma-alumina and inorganic ion exchange materials from fused salts, 19: 38771

URANYL NITRATES
separation of ruthenium from, by solvent extraction using TBP, 19: 38764
thermal decomposition of, mechanism of, 19: 38660
thermodynamic properties, 19: 38676

URANYL OXALATES
thermal decomposition of, mechanism of, 19: 38660

URANYL SULFATES
thermal decomposition of, mechanism of, 19: 38660

UREA
placental transfer in rabbits and swine, tracer study, 19: 38344

UREA, [3-(CHLOROMERCURI)-2-METHOXYPROPYL]-
synthesis of mercury-197 labeled, 19: 39265(R) (IA-1021)

URIDINE
uptake by DNA, proteins, and RNA of L-cell nuclei, effects of tritiated thymidine on carbon-14-labeled-, 19: 38339

URINARY TRACT
radioinduced injuries of, after radiotherapy of carcinomas of uterus, 19: 38532

URINE
analysis for plutonium, radiometric, 19: 38555
analysis for plutonium-239 and promethium-147, radiometric, 19: 39265(R) (IA-1021)
fallout monitoring in Japanese, 19: 38894
radiation effects on content of 17-ketosteroids in rat, neutron, 19: 38443
separation of plutonium from actinides in, by ion exchange, 19: 38546(R) (RFP-552)

UTERUS
radiotherapy of carcinoma of, hemolysis induced by, 19: 38509
radiotherapy of carcinoma of, late pathological effects, 19: 38531
radiotherapy of carcinomas of, late pathological effects, 19: 38532

V

VACUUM PUMPS
argon sorption on surfaces of vac-ion, 19: 39323

VACUUM SYSTEMS
description of pyrex ultrahigh, for observation of adhesion between quartz crystal surfaces, 19: 38840
organic vapor measurements in, polymer film formation for, 19: 38564
traps for diffusion-pump, electric discharges as, 19: 38839 (RFP-572)

VACUUM TECHNIQUES
development of, for space simulation and deposition of thin films, 19: 38842

VACUUM VALVES
design for ultrahigh vacuum systems, 19: 38841

VAK REACTOR
operation of, review of 3-year's, 19: 40201

VALINE
radiation effects on uptake by *Vicia faba* chromosomes of tritiated, x, 19: 38417

VALLECITOS BOILING WATER REACTOR
noise analysis in, (E), 19: 40164

VALVES
design of liquid-sodium flow controller for in-pile uses, (E), 19: 40135

VANADIUM
diffusion of atoms in bcc, activation energy for interstitial, (T), 19: 40086
electric potential fluctuations in mixed state of superconducting, (E), 19: 39709
magnetostriction in pure monocrystalline, 19: 39199
properties for use as fuel cladding material in reactors, 19: 39206
radiation damage in, cross sections for atomic displacements from 1- to 3-Mev electrons, 19: 39225 (AFCRL-65-286)
separation from graphite above 1750°C in inert gases, 19: 38762

VANADIUM ALLOYS
Cr–Ti–V, mechanical properties at high temperatures, 19: 40177(R) (ANL-7046(p.1-35))
Cr–V, antiferromagnetism of, at 95 to 300°K, 19: 40077 (IS-T-18)
Cr–V, electric conductivity and thermoelectric power of, at 4.2 to 450°K, 19: 40077 (IS-T-18)
Sn–V, preparation and crystal structure of intermetallic compound V_2Sn_3 in, 19: 39189
Tc–V, nuclear spin-lattice relaxation time of technetium-99 and vanadium-51 in, (E), 19: 39403
Ti–V, corrosion by sodium at 650°C, 19: 40177(R) (ANL-7046(p.1-35))
Ti–V, fabrication into tubes by extrusion, 19: 40177(R) (ANL-7046 (p.1-35))
Ti–V, mechanical properties at high temperatures, 19: 40177(R) (ANL-7046(p.1-35))
Ti–V, preparation for superconductor magnetic field measurements, 19: 40286(R) (NAA-SR-11200)
Ti–V, properties as fuel cladding, 19: 40113(R) (ANL-7071)
Ti–V, removal from fuel pins by hydrogen-induced swelling, 19: 40113(R) (ANL-7071)
Ti–V, superconducting properties and uses, 19: 39750(P)

VANADIUM ISOTOPES V-46
beta decay of, conserved vector current hypothesis and ft values for, (E/T), 19: 39859

VANADIUM ISOTOPES V-51
nuclear spin-lattice relaxation time in technetium–vanadium alloys, temperature variations of, (E), 19: 39403
VANADIUM SILICIDES
superconductive properties of, effects on transition metals on, 19: 39196
VANADIUM SYSTEMS
graphite–V, deposition of coatings of, at 1500 to 1750°C, 19: 39144(P)
VELOCITY
measurement near underground explosions, gage for, 19: 38917 (SC-R-65-904, pp 23-48)
measurement of, using gamma resonant absorption, 19: 38966(P)
VENTILATION
of rooms containing gamma sources, 19: 38883
pumps for shelter, durability tests of punkah, 19: 38832 (ORNL-TM-1155)
standards for, radiation industrial buildings, 19: 38884
system for fallout shelter, 19: 38833(P)
VESSELS
chilldown and boiloff losses of large liquid hydrogen storage dewars, 19: 39686 (LA-DC-7164)
insulation compaction in large dewars by thermal cycling, study of perlite, 19: 38779 (LA-DC-7158)
VIBRATIONS
effects on oxidation in rat brain, 19: 38358 (AD-612660)
effects on vestibular organs in guinea pigs, synergistic effects of radiation, 19: 38358 (AD-612660)
VINYL COMPOUNDS
dehydrogenation and isomerization of, radiochromatographical studies of action of catalysts in, 19: 38718
VIRUSES
genetic code for spontaneous and chemically-induced mutations of, 19: 40296 (TID-21856)
VITAMIN B
effects on metabolism of iodine-131, in rats, 19: 38337
VITAMIN B_{12}
tracer study of metabolism in man, 19: 38493
VITAMIN D
effects on calcium metabolism in rats, 19: 38347
effects on strontium-90 metabolism in rats, 19: 38347
VITAMINS
effects on recovery from radiation sickness, 19: 38457
radiation effects on content of, in rye flour, 19: 38423

W

WASHINGTON
stratigraphy of late basalt flows, Ellensburg Formation, and lower Ringold Formation in south-central, 19: 38843 (BNWL-SA-135)
stratigraphy of post-basalt sediments in south-central, 19: 38844 (BNWL-SA-140)
WASTE DISPOSAL
burial, temperature distributions in gamma-active ceramic spheres for, 19: 40275
effects on radioactivity of Columbia River below Hanford, 19: 38874 (BNWL-SA-53)
ground, development for EBR-II waste, 19: 40113(R) (ANL-7071)
ground, hydrology at National Reactor Testing Station, 19: 40269(R) (IDO-22047-USGS)
ground, method for analyzing transport by water, 19: 40268 (BNWL-63)
methods for gaseous, 19: 38902
packaging in hot cells, 19: 40270 (JUL-249-RW)
safety in, to atmosphere and water, 19: 40277
salt deposit, problems in, 19: 40272
WASTE PROCESSING
foam separation treatment of low-activity wastes at ORNL, 19: 40271(R) (RAI-350)
ion-exchange, uses of natural cation exchangers in, (E), 19: 40130 (ZFK-RN-17(p.165-78))
methods of, review of, 19: 40276
plant for, description of, at The Hague, 19: 40273
WASTE SOLUTIONS
separation of radioisotopes from, by precipitation filtration, lime and soda treatment, and ion exchange, 19: 40276
treatment of, economics and problems in, 19: 40274
WATER
analysis for boron and strontium, spectrochemical, 19: 39265(R) (IA-1021)
analysis for fluorides by radiometry using tantalum-182, 19: 39265(R) (IA-1021)
boiling burnout in, comparisons of analyses of, (T), 19: 38814
boiling burnout, effects of electric fields on, 19: 38807(R) (NYO-2404-70)
content in soils, effects of bulk density and hydrogen form on calibration of meter for measuring, 19: 38948
determination in soils by neutron scattering, cadmium standards for, 19: 38869
effects on radiation effects on wheat seeds, 19: 38412
effects on yields of atomic hydrogen from electric discharge in low-pressure hydrogen, 19: 38590 (UCRL-16050)
flow of, dynamics of vortex, 19: 40236 (LA-3229, pp 237-50)
flow through two eccentrically positioned orifices in series, pressure drop characteristics, 19: 38810 (RL-SA-31)
isotopic exchange of deuterated toluene, 19: 38693
leakage from pipes, detection by sodium-24 tracer, 19: 39265(R) (IA-1021)
oxygen-17 NMR absorption in, effects of electrolytes on, 19: 39265(R) (IA-1021)
placental transfer in rabbits and swine, tracer study, 19: 38344
positronium production in, (E/T), 19: 39509
purification of radioactive, effects of radiostability of exchange resins on, (E), 19: 40129 (ZFK-RN-17(p.114-26))
purification of reactor primary-coolant, ion-resin methods for, 19: 40123 (IAE-787)
purification of reactor coolant, ion exchange materials for, 19: 38759 (ZFK-RN-17(p.95-117))
purity monitoring in reactor primary coolant loops, standardization of, 19: 40124 (IAE-789)
radioactive waste disposal in, safety precautions for, 19: 40277
radioactivity in, maximum permissible concentrations of uranium-235 fission products in, 19: 38872 (AEET/HP/TH-15)
radiolysis in PM-3A spent core storage tank, hydrogen evolution in, 19: 40188 (NYO-3420-2)
radiolysis in reactors, rate of, 19: 38698 (ZFK-RN-17(p.199-207))
radiolysis of, nitrous oxide as scavenger in, 19: 38720
reactions with sodium in steam generators, analysis, 19: 38803(R) (BAW-1280-26)
reactions with uranium carbide at 30 to 86°C, kinetics, 19: 38581 (NAA-SR-11401)
reactions with zirconium at high temperatures, 19: 40195(R) (WCAP-3269-5)
separation from steam, development of devices for, 19: 38801(R) (ACNP-65004)
steam–water, two-phase vessel blowdown from pipes, theory, 19: 38802 (APED-4827)
U-235–H_2O–Zr, critical bucklings and extrapolation distance for, (T), 19: 40159 (WAPD-T-1774)
WATER-*d*
ion products of, 19: 38608
WATER-d_2
analysis of CVTR, 19: 40179(R) (CVNA-236)
deuterium exchange with organics, group VIII metal catalysis of, 19: 38597
deuterium exchange between, and hydridoplatinum complex, 19: 38627
effects on fluorescence and absorption spectra of europium chloride solutions, 19: 38636
effects on palladium–deuterium electrode potential, 19: 38608
exchange reactions with hydrogen in alkylaromatic hydrocarbons and toluic acid derivatives, nickel-catalyzed, 19: 38688
nuclear magnetic resonance spectra of uranyl citrate complexes in, 19: 38623
radiolysis of, acidity effects on yields in gamma, 19: 38710
separation from air at reactor installations, 19: 38907
WATER COOLED REACTORS
contamination from cooling system of, method and apparatus for removal of, 19: 40119(P)
coolant characteristics in Hungarian research, (E), 19: 40264 (ZFK-RN-17(p.54-67))
coolant purification in, ion-resin methods for primary, 19: 40123 (IAE-787)
coolant purity monitoring in primary loops of, standardization of, 19: 40124 (IAE-789)
core components for chemically shimmed, design of, 19: 40198(R) (WCAP-3721)
development of large closed-cycle, 19: 40195(R) (WCAP-3269-5)
operation of WWR-C, at Rossendorf, Germany, (E), 19: 40261 (ZFK-RN-17(p.179-98))
reactivity modulator for, design for parameter measurements, 19: 40197(R) (WCAP-3718)
reactivity modulator for, design for parameter measurements, 19: 40198(R) (WCAP-3721)
water characteristics in primary circuits of research, (E), 19: 40260 (ZFK-RN-17(p.68-74))
water chemistry measurements in Czech WWR-S, (E), 19: 40263 (ZFK-RN-17(p.32-43))

water pH in, problems in measurement of, (E), 19: 40127 (ZFK-RN-17 (p.9-23))
water problems in, conference, (E/T), 19: 40117 (ZFK-RN-17)
water purification in, performance of resins for, (E), 19: 40128 (ZFK-RN-17(p.75-94))
water purification equipment for, performance of ion-exchange, (E), 19: 40130 (ZFK-RN-17(p.165-78))
WATER MODERATED REACTORS
coolant characteristics in Hungarian research, (E), 19: 40264 (ZFK-RN-17(p.54-67))
criticality studies in, review, (E), 19: 40163
criticality studies on spectral-shift, review, (E), 19: 40163
operation of WWR-C, at Rossendorf, Germany, (E), 19: 40261 (ZFK-RN-17(p.179-98))
reactivity transients in, computer program for calculation of, 19: 40160 (WAPD-TM-479)
water chemistry measurements in Czech WWR-S, (E), 19: 40263 (ZFK-RN-17(p.32-43))
water pH in, problems in measurement of, (E), 19: 40127 (ZFK-RN-17 (p.9-23))
water problems in, conference, (E/T), 19: 40117 (ZFK-RN-17)
WATER PURIFICATION EQUIPMENT
performance of ion-exchange, for reactors, (E), 19: 40128 (ZFK-RN-17 (p.75-94))
performance of ion-exchange, using natural cations, (E), 19: 40130 (ZFK-RN-17(p.165-78))
performance of synthetic-resin, in radioactive circuits, (E), 19: 40129 (ZFK-RN-17(p.114-26))
WATER SUPPLIES
consumption and inspection of, in event of nuclear conflict, 19: 38882
development and management of, use of nuclear explosions in, 19: 38791 (TEI-857)
radioactivity in West German Republic, 19: 38904
radioactivity of Hanford area, 1964, 19: 38874 (BNWL-SA-53)
radioactivity of, in Austria, 1963, 19: 38860
strontium-90 content in German, 19: 38876 (NP-14927)
WATER VAPOR
reactions with cerium tetrafluoride, 19: 39182
reactions with pyrolytic carbon fuel particle coatings at 1000°C, 19: 39129(R) (ORNL-TM-1116)
WATER WAVES
measurement of deep Tsunami-like, instrumentation for, 19: 40288(R) (NVO-98-5)
WELDING
equipment for remote rewelding of process tube joints in sodium–graphite reactors, 19: 40125 (NAA-SR-9821)
WELDS
bonding in, ultrasonic method for testing, 19: 38546(R) (RFP-552)
WELL LOGGING
equipment design and method for determination of oxygen in earth formations, 19: 38871(P)
method for gamma, 19: 38867
WHEAT
radiation effects on seeds of, effects of water content on, 19: 38412
WHISTLERS
propagation of echoes of, in low latitudes, (E), 19: 39674
WHITE OAK CREEK
ecology of plants, 19: 38331
WHITESHELL REACTOR NO. 1
design parameters for, (E), 19: 40218
WIND
turbulence in boundary layer of atmosphere, analog simulation for, 19: 40282 (BNWL-SA-171)
WIND TUNNELS
plasma jet production in, arc heaters for, 19: 38796
WINDOWS
radiation effects on optical transmission properties of, in space environment, 19: 39059
WINDSCALE ADVANCED GAS COOLED REACTOR
fuel cans for, fabrication of stainless steel, 19: 39134
WOUNDS
analysis for plutonium-239, development of miniature counters for, 19: 38546(R) (RFP-552)

X

X RADIATION
absorption by argon, one-electron model for spectra of K, 19: 39411
angular correlations with gamma radiation, relaxation effects in, 19: 39849
biological effects in yeast, effects of incubation time on, 19: 38422
book: *Dose Distribution and Dose Determination in Pendulum Irradiation (200 kv at 17 Mev)*, 19: 38534
detection and measurement of soft, design of gridded proportional counter for, 19: 39046(P)
detection of narrow band, apparatus for, 19: 39047(P)
detection of soft stellar, rocket, 19: 39332
diffraction by crystals, Pendelloesung fringes in, (E/T), 19: 39287
dose rate determination in vinyl chloride, absorbed, 19: 39016
dosimetry in tissues, 19: 38499
dosimetry of, thermoluminescence detectors for, 19: 39044(P)
dosimetry using scintillating phantoms, 19: 38893
effects in mice, pathological, 19: 38450 (USNRDL-TR-851)
effects on aluminate solutions, 19: 38738
effects on barium nitrate crystals, nitrate ion ESR from, 19: 38730
effects on cardiovascular and hematopoietic system of rats, 19: 38441
effects on cell nuclei in bone marrow, synergistic effects of vibration, whole-body, 19: 38358 (AD-612660)
effects on cesium-bromide color centers at low temperature, 19: 40098
effects on chemical and physical properties of rat blood, 19: 38440
effects on chromosome aberrations in barley and *Vicia faba*, modifying effects of acridine orange and methylene blue on, 19: 38462
effects on chromosome break induction in barley interaction in, 19: 38399
effects on chromosomes in Tradescantia, synergism with infrared radiation on aberrant, 19: 38416
effects on *Cl. perfringens*, genetic, 19: 38445
effects on coloration and thermoluminescence of borate glasses, relation between, 19: 39244
effects on course of intercapillary glomerulosclerosis in mice, 19: 38409
effects on DNA and nucleoprotein synthesis in rat testes, 19: 38370
effects on dominant lethal mutation induction in mouse spermatogonia, 19: 38394
effects on *E. coli* B capacity for phage T3, sensitization effects of iodoacetamide on, 19: 38455
effects on *E. coli*, protective effects of ribonuclease against, 19: 38465
effects on Ehrlich ascites tumors at various times following inoculation into mice, 19: 38402
effects on erythropoiesis in cross-circulated dogs, 19: 38382
effects on free radical density in polymethylmethacrylate, 19: 38706
effects on gamma-irradiated sodium chloride, coloration from, 19: 40105
effects on gonocytes in testes of rats, 19: 38369
effects on growth of tumor transplants in mice, 19: 38387
effects on immune reactions to tuberculosis infection in guinea pigs, 19: 38375
effects on induction of neoplasms in rat thyroid, by exposure of single lobe, 19: 38367
effects on induction of mutations in male mice, superlethal, 19: 38393
effects on kidney homografts in dogs by local graft exposure, 19: 38425
effects on mice, protective effects of cobalt–chlorophyll and glucuronic acid against whole-body, 19: 38456
effects on mice, protective effects of orotic acid against, 19: 38458
effects on mitochondria function and structure in mouse liver, 19: 38424
effects on mitosis in Tradescantia, synergism with infrared radiation, 19: 38416
effects on mouse L cell cultures, protective effects of halogenated pyrimidines against, 19: 38459
effects on mutation induction in male Drosophila, effects of sperm maturity on frequency of, 19: 38390
effects on mutation induction in Dahlbominum oogonia, 19: 38392
effects on optical absorption of copper centers in potassium halides, (E), 19: 40107
effects on phosphate glass, (E/T), 19: 39256
effects on physical properties of polymethyl methacrylate, 19: 39231 (COO-1224-8)
effects on plasma iron clearance in dogs, 19: 38388
effects on rabbit kidneys, renograms of, 19: 38379
effects on reactions of hydrocarbons with carbon dioxide, 19: 38727(T)
effects on RNA synthesis in derivatives of *E. coli*, 19: 38381
effects on serum proteins in mice following transplants of rat-to-mouse chimeras, 19: 38404
effects on spleen and thymus, 19: 39265(R) (IA-1021)
effects on survival of *Macrobiotes areolatus* in active and dormant states, 19: 38373
effects on survival and recovery of rat growth cartilage, 19: 38407
effects on translocation induction in mouse spermatogonia, 19: 38396
effects on tritiated valine uptake by *Vicia faba* chromosomes, 19: 38417
effects on tumor growth in mice, synergistic effects of cruzine, 19: 38428
effects on tumor growth in rabbits, effects of regional oxygenation, 19: 38374
effects on tumor growth in F_1 hybrid mice, dose dependence of, 19: 38403

emission from spark-triggered discharge, (E), 19: 39305
energy from, determination of total, 19: 38878 (ORNL-P-1405)
energy spectra of solar, (E), 19: 39333
genetic effects in Tradescantia, 19: 38360 (TID-21695)
intensity distribution in presence of structure pseudosymmetry, statistical, 19: 40067
intensity of auroral, correlation with auroral luminosity, (E), 19: 39672
leukemogenic effects in mice, 19: 38372
origin of cosmic, (T), 19: 39425
physiological effects of exposure *in utero* in rats, 19: 38361(R) (TID-21951)
psychological effects of exposure *in utero* in rats, 19: 38361(R) (TID-21951)
reactions with potassium iodide crystals V_K centers in, (E), 19: 40103
scattering by diamond crystal defects, small-angle, 19: 39230 (BNL-9332)
scattering factors of, corrections for incoherent, 19: 39379
scattering in matter, measurement and theory of, 19: 38524
therapeutic effects for calcifying epitheliona, 19: 38494
therapeutic use, 19: 38499
therapeutic use for cancer, 19: 38487
therapeutic use for cancer of larynx, effects on thyroid function, 19: 38484
yields from proton inelastic scattering by nuclei at 15 to 1900 kev, (E), 19: 39881

X-RAY DIFFRACTION ANALYSIS
equipment for crystallized gas, cryostat, 19: 38946
of structural change phenomena, effects of time on, 19: 38826
pattern indexing for tetragonal, hexagonal, and orthorhombic crystals, charts for, 19: 40080 (NP-15182)

X-RAY DIFFRACTOMETERS
sample heating in, furnace for, 19: 38941

X-RAY EQUIPMENT
design of serialograph with movable cassettes, 19: 38955(P)
performance for fluidized-bed reactor analysis, 19: 40224 (LA-3229, pp 63-82)

X-RAY SOURCES
design with adjustable electron beam cross section, 19: 38964(P)
x-ray emission from spark-triggered discharge, (E), 19: 39305

X-RAY SPECTROSCOPY
sensitivity improvements for determining traces of elements using direct electron excitation, 19: 38571

XENON
electron elastic scattering by, momentum-transfer cross sections for slow, (T), 19: 39397
ionization cross section for, electron-impact, 19: 38630
laser oscillations in, 5d-6p transitions from pulsed, (E), 19: 39394
mesons (π^-) reactions at 9 Bev/c, cross sections for hyperons (Λ) and (K^0) from, 19: 39472 (JINR-P-2178)
rubidium-vapor spin relaxation in, (E), 19: 39400

XENON IONS
reactions with metal single crystals at 1 to 10 kev, secondary-electron emission in, (E), 19: 39404

XENON ISOTOPES Xe-133
diffusion from irradiated uranium carbonitride, 19: 39089 (AERE-M-1389)
partition between human blood and brain tissues at 37°C, measurements on, 19: 38353
release from pyrolytic carbon-coated fuel particles, 19: 39228 (BMI-1734)

XYLENE
dibutylbutylphosphonate–xylene, solvent properties for americium from nitrate solutions, 19: 38750 (HW-81166)

Y

YEASTS
radiation effects on survival of, effects of incubation, 19: 38422

YTTERBIUM
neutron absorption properties of, burnup effects on, (E), 19: 40163
neutron reactions at 0.0005 to 1 ev, total cross sections for, 19: 39779 (IEA-86)
pathological effects of subcutaneous implantations, in mice, 19: 38334 (COO-1170-1)
phase transformations at 6 to 65 kbar, solid-liquid and solid-solid, 19: 40095

YTTERBIUM COMPLEXES
with [(2-hydroxyethyl)imino]diacetic acid, dissociation constant of, 19: 38671

YTTERBIUM HYDROXIDES
reactions with formic acid, properties of formate formed by, 19: 38669

YTTERBIUM IONS
crystal-field interactions of, linear and nonlinear shielding of, (E/T), 19: 40101
radiolysis of aqueous solutions of, pulse, 19: 38728

YTTERBIUM NIOBATES
preparation and thermal properties, 19: 38617

YTTERBIUM OXIDES
SiO_2–YbO, preparation and crystal structure, 19: 38621
SiO_2–YbO, spectra and crystal structure of, infrared, 19: 38622

YTTRIUM
content in minerals and rocks of batholith of Southern California, (E), 19: 38848
determination by arsenate-iodometric method, 19: 38551
pathological effects of subcutaneous implantations of, in mice, 19: 38334 (COO-1170-1)
separation from strontium by ion exchange, 19: 38774
separation from waste water, methods for, 19: 40276

YTTRIUM CHLORIDES
reaction with sodium phosphates, 19: 38619
reactions with potassium chlorides at 25°C, 19: 38620

YTTRIUM COMPLEXES
with [(2-hydroxyethyl)imino]diacetic acid, dissociation constant of, 19: 38671

YTTRIUM FLUORIDES
BaF_2–YF_2, phase studies, 19: 38615
CaF_2–YF_3, phase studies, 19: 38615
SrF_2–YF_2, phase studies, 19: 38615

YTTRIUM IONS
effects on reduction of rare earth ions in calcium fluoride, (E), 19: 38595
radiolysis of aqueous solutions of, pulse, 19: 38728

YTTRIUM ISOTOPES Y-90
colloids, use in treatment of malignant effusions, energy levels for, 19: 38515
determination in milk, 19: 38856

YTTRIUM ISOTOPES Y-91
motion in soil, effects of chelating agents on, 19: 38329 (TID-20471)

YTTRIUM OXIDES
ThO_2–Y_2O_3, use as solid electrolyte in high-temperature cell, 19: 38586 (UCRL-11957)
UO_2–Y_2O_3–ZrO_2, preparation of solid solution powders of, for use as reactor fuel, 19: 39094 (CONF-117(p.11-19))

YTTRIUM PHOSPHATES
preparation and properties, 19: 38619
preparation of hydrated, 19: 38620

YTTRIUM SYSTEMS
H–Y, thermodynamic properties at 250 to 350 and 650 to 950°C, 19: 38642

Z

ZINC
determination in enamel of teeth, neutron activation, 19: 38562
determination in trace amounts in aluminum by x-ray spectrography, 19: 38571
diffusion in gallium arsenide, effects of partial pressures on, (E), 19: 39269(R) (SU-SEL-64-133)
iron-57 displacement in lattice of polycrystalline, Mössbauer-effect measurements of, 19: 40097
magnetic flux penetration and tunneling in superimposed layers of indium–bismuth alloys and, in magnetic fields, (E), 19: 39699
separation from ethanolic hydrochloric acids by ion exchange, 19: 39265(R) (IA-1021)
solubility in indium arsenide, determination by Hall coefficient, 19: 39269(R) (SU-SEL-64-133)
use as threshold detector for fast neutrons, (E), 19: 39007
vapor pressure of liquid, effects of temperature on, 19: 39163(R) (MLM-1244)

ZINC ALLOYS
Al–Mg–Mn–Zn, plastic anisotropy of AZ31B sheet, 19: 39149 (AD-425880)
Al–Zn, precipitation of Guinier-Preston zones in, heat tone, 19: 39173(T) (ORNL-ts-634)
Au–Zn, heat of formation of AuZn, 19: 39168(R) (TID-22015)
Mg–misch metal–Zn, plastic anisotropy of ZE10A sheet, 19: 39149 (AD-425880)

ZINC CHLORIDES
radiation effects on fused, gamma, 19: 39265(R) (IA-1021)

ZINC IONS
radiolysis of aqueous solutions of, pulse, 19: 38728

ZINC ISOTOPES Zn-65
content in animals of California coast, 19: 38895
metabolism in rabbits, 19: 39265(R) (IA-1021)
motion in soil, effects of chelating agents on, 19: 38329 (TID-20471)

ZINC SULFIDES
spectra of dysprosium-doped crystalline, emission, (E), 19: 39269(R) (SU-SEL-64-133)
spectra of terbium-doped crystalline, emission, (E), 19: 39269(R) (SU-SEL-64-133)
ZIRCALOY-2
bibliography on properties on, 19: 39097 (GEMP-346)
corrosion by water at high temperatures, 19: 39234 (GEAP-4597)
growth of single crystals of, using electron-beam heating, 19: 39137
mechanical properties of, summary of, 19: 39097 (GEMP-346)
properties of, as core structure for N.S. *Savannah* reactor, (E), 19: 40218
properties of, summary of corrosion, hydridation, and oxidation, 19: 39097 (GEMP-346)
radiation effects on, neutron, 19: 40286(R) (NAA-SR-11200)
radiation effects on properties of, summary of, 19: 39097 (GEMP-346)
radiation effects on mechanical properties of, fission-fragment and neutron, 19: 39229(R) (BMI-X-10134)
radiation effects on mechanical properties of, 19: 39234 (GEAP-4597)
stresses on tubular, during fuel compaction in, 19: 39125(R) (BNWL-91)
uses in nuclear reactors, 19: 39108
welding with Inconel 600 to flat and contoured surfaces, explosive, 19: 39156(R) (CEND-532)
ZIRCALOY-4
bibliography on properties of, 19: 39097 (GEMP-346)
composition of commercial, 19: 39152(R) (BMI-X-10132)
corrosion by aqueous chemical shim solutions at 600°F, 19: 40198(R) (WCAP-3721)
corrosion by pressurized water, 19: 40195(R) (WCAP-3269-5)
corrosion by water at 680°F, effects of heat transfer on, 19: 40196(R) (WCAP-3269-6)
corrosion by water at high temperatures, 19: 39234 (GEAP-4597)
diffusion of fission products in, mechanisms of, 19: 39152(R) (BMI-X-10132)
fatigue limits for, 19: 40196(R) (WCAP-3269-6)
fatigue of cold-worked, mechanisms of, 19: 40195(R) (WCAP-3269-5)
mechanical properties of tubular, at 500 to 680°F, 19: 40195(R) (WCAP-3269-5)
mechanical properties at 750 to 800°F, 19: 40196(R) (WCAP-3269-6)
mechanical properties of, summary of, 19: 39097 (GEMP-346)
properties of, summary of corrosion, hydridation, and oxidation, 19: 39097 (GEMP-346)
radiation effects on mechanical properties of, 19: 40195(R) (WCAP-3269-5)
radiation effects on properties of, summary of, 19: 39097 (GEMP-346)
radiation effects on mechanical properties of, 19: 39234 (GEAP-4597)
stress corrosion by aqueous ferric chloride at 68°F, 19: 40196(R) (WCAP-3269-6)
ZIRCONIUM
bonding to zirconium, effects of interatomic forces on pressure, 19: 39091(R) (BMI-1723(Del.))
combustion in argon–oxygen mixtures, 19: 38583(R) (SC-DC-65-1480)
corrosion by sodium vapor, 19: 40113(R) (ANL-7071)
corrosion by sodium at 540°C, 19: 40112(R) (ANL-7046(p.36-66))
diffusion of fission products in, mechanisms of, 19: 39152(R) (BMI-X-10132)
effects on superconducting transition temperature of vanadium silicide, 19: 39196
gamma scattering by, spectra of nonresonant, (E), 19: 39265(R) (IA-1021)
growth of single crystals of, using electron-beam heating, 19: 39137
melting and oxidation in simulated reentry tests, 19: 39118(R) (SC-DC-65-1520)
oxidation of oriented thin layers of, in air and oxygen, 19: 39120
production and uses in nuclear reactors, 19: 39108
properties for use as fuel cladding material in reactors, 19: 39206
reactions with complexing agents, stoichiometry of, 19: 38667 (p.78-82))
reactions with sodium at high temperatures, 19: 39090(R) (ANL-7046
reactions with water at high temperatures, 19: 40195(R) (WCAP-3269-5)
separation from cesium and molybdenum by precipitation from nitric acid solutions, 19: 38778(P)
separation from hafnium, 19: 39108
separation from waste water, methods for, 19: 40276
solvent extraction from nitric acid solutions by tertiary amines, 19: 38761(T) (CEA-tr-A-1809)
ZIRCONIUM ACETATES
preparation and uses, 19: 38647
ZIRCONIUM ALLOYS
performance in organic-cooled reactors, (E), 19: 40218
properties for use as fuel cladding material in reactors, 19: 39206
fissium–U–Zr, thermal conductivity of, effects of burnup on, 19: 40112(R) (ANL-7046(p.36-66))
Mg–Th–Zr, plastic anisotropy of HK31A sheet, 19: 39149 (AD-425880)
Mo–Ti–Zr, properties of TZM as cladding material for SNAP hydride reactors, 19: 39166 (NAA-SR-Memo-11149)
Nb–Zr, analysis of, gamma spectra measurements in activation, 19: 38566
Nb–Zr, cavitation in bismuth–lead alloy at 500 and 1500°F, ultrasonic-induced, 19: 39116 (NP-15263)
Nb–Zr, magnetic field penetration in superconducting, radial velocity of, (E), 19: 39702
Nb–Zr, paramagnetism in cold-worked superconducting wires of, 19: 39749
Nb–Zr, properties for liquid metal loops, 19: 40112(R) (ANL-7046 (p.36-66))
Nb–Zr, properties of cold-worked fuel sheathing tubes of, 19: 39150 (AECL-2250(Pt.I))
Nb–Zr, pulse transmission by coaxial cables of superconducting, (E), 19: 39740
Nb–Zr, reactions with sodium at 2100 to 2400°C, 19: 39090(R) (ANL-7046(p.78-82))
Nb–Zr, strengthening by oxygen addition and quenching, 19: 39223(P)
Nb–Zr, superconductivity, 19: 39695
Pu–U–Zr, phase studies, 19: 40177(R) (ANL-7046(p.1-35))
Pu–U–Zr, reactions with stainless steel at high temperatures, 19: 40177(R) (ANL-7046(p.1-35))
Rb–Zr, specific heat at 0.9 to 12°K, (E), 19: 39218
Th–U–Zr, radiation effects on, 19: 38755(R) (ORNL-3611)
Th–Zr, mechanical properties at high temperatures, 19: 38755(R) (ORNL-3611)
ZIRCONIUM BORIDES
reactions with graphite to 2200°C, 19: 38654
ZIRCONIUM CARBIDES
UC–ZrC, thermal expansion of polycrystalline solid solution of, at 25 to 1000°C, 19: 39200
ZIRCONIUM CHLORIDES
reactions with aluminum chlorides at high temperatures, 19: 38755(R) (ORNL-3611)
reactions with thorium chlorides at high temperatures, 19: 38755(R) (ORNL-3611)
ZIRCONIUM COMPOUNDS
preparation and uses, 19: 38647
ZIRCONIUM FLUORIDES
LiF–ZrF, phase studies, 19: 38610
ZIRCONIUM HYDRIDES
diffusion in, self, 19: 40286(R) (NAA-SR-11200)
diffusion of fission products in, 19: 40286(R) (NAA-SR-11200)
ZIRCONIUM ISOTOPES Zr-90
alpha inelastic scattering at 34.4 Mev, excitation of 2^+, 5^-, and 3^- states by, (E), 19: 39844
energy levels of, Coulomb excitation in nitrogen-14 inelastic scattering, (E), 19: 39942
ZIRCONIUM ISOTOPES Zr-95
content in diet and excreta in Japan, 19: 38894
content in irradiated uranium carbide cladding, 19: 40286(R) (NAA-SR-11200)
determination in rain water, 19: 38557
ZIRCONIUM ISOTOPES Zr-96
energy levels of, Coulomb excitation in nitrogen-14 inelastic scattering, (E), 19: 39942
ZIRCONIUM NITRIDES
InN–ZrN, preparation and crystal structure of H-phase in, 19: 39208
ZIRCONIUM OXIDES
electrotransport in, color variation during, (E), 19: 38604
oxidation of, color variations during, 19: 38604
phase transformation in, on heating in vacuum and in air, 19: 39190
preparation and uses, 19: 38647
thermal conductivity at high temperatures, (E), 19: 39215
$CaO–UO_2–ZrO_2$, densities and thermal properties, 19: 39091(R) (BMI-1723(Del.))
paraffin–$UO_2–ZrO_2$, neutron spectra in, asymptotic and steady-state, (E), 19: 39768 (RPI-328-21)
$UO_2–Y_2O_3–ZrO_2$, preparation of solid solution powders of, for use as reactor fuel, 19: 39094 (CONF-117(p.11-19))
$UO_2–ZrO_2$, partial pressures of, 19: 39091(R) (BMI-1723(Del.))
$UO_2–ZrO_2$, radiation effects on calcia-stabilized, at high burnups, 19: 39091(R) (BMI-1723(Del.))
$UO_2–ZrO_2$, radiation effects on clad, 19: 39091(R) (BMI-1723(Del.))
ZIRCONIUM SYSTEMS
Al–Fe–Mg–Ni–Si–Ti–Zr, coating with aluminum–nickel layers by chemical deposition, 19: 39143(P)
C–Nb–W–Zr, fabrication and properties at −325 to 3000°F, 19: 39224(P)
U-235–H_2O–Zr, critical bucklings and extrapolation distance for, (T), 19: 40159 (WAPD-T-1774)

ZIRCONIUM TITANATES
temperature effects on transducers of, 19: 39270(R) (TID-21894)
ZIRCONS
age estimation of, errors in uranium–lead method of, 19: 38849
pleochroic halos produced in biotite-cordierite by, reversal, 19: 38846(T) (ORNL-tr-698)
uranium-234, uranium-235, and uranium-238 contents and ratios in, 19: 38849
ZIRCONYL CHLORIDES
preparation and uses, 19: 38647
ZIRCONYL PHOSPHATES
properties as ion exchanger for potassium isotope separation in fused potassium nitrate, 19: 39074
ZIRCONYL SULFATES
preparation and uses, 19: 38647

REPORT NUMBER INDEX

Reports, conference papers and proceedings, numbered translations, and patents abstracted during the period are included in this index. Each item is listed by report number; this is followed by the abstract number and a brief notation regarding public availability. The index entries show, when known, which reports are on file in the depository libraries, which reports have been published in open-literature journals (journal citation given), and which reports can be purchased (source and price). Whenever a report is identified by more than one number, cross references from secondary to primary report numbers are cited.

The report number codes apply to AEC reports unless designated otherwise. Non-AEC reports are identified by parenthetical notes after the report codes; e.g., (non-AEC), (British), (Canadian), (French). The note (Misc.) identifies those codes used for both USAEC and non-AEC reports. Patents are listed under the heading "PATENTS"; the country of origin is included in parentheses.

A comprehensive listing of both AEC and non-AEC report codes is contained in TID-85(3rd Rev.), *Report Number Series Used by the Division of Technical Information in Cataloging Reports.* This information is also included in the Cumulative Report Number Index (issued annually).

Public Availability of USAEC Reports

All USAEC reports abstracted in *NSA* are available to the public through one or more of the following sources:

(1) Depository libraries in the United States, in other countries, and in international agencies. A list of these depositories appears on the inside covers of each issue of *NSA*.

(2) Scientific and technical journals or other publications.

(3) Microcard Editions, Inc., in Microcard and micronegative form. Orders and inquiries should be sent to: Accounting and Shipping Department, West Salem, Wisconsin 54669.

(4) Clearinghouse for Federal Scientific and Technical Information, U. S. Department of Commerce, Springfield, Virginia 22151.

(5) Superintendent of Documents, U. S. Government Printing Office, Washington, D. C. 20402.

Public Availability of Non-AEC Reports

U. S. Reports. Many reports of U. S. Government agencies are available to the public from the Clearinghouse for Federal Scientific and Technical Information (CFSTI). This availability is given when known. Such reports should be ordered by AD number or NASA-N number. If availability is not shown, inquiries may be directed to CFSTI. In the case of NP numbers, inquiries should be by title and author.

Non-U. S. Reports. Many reports of atomic energy establishments of other countries are deposited in the libraries listed on the inside covers of each issue of *NSA*.

Additionally, the following countries have made their reports available as indicated.

AUSTRALIA

Australian Atomic Energy Commission Research Establishment. Available upon request from the Library, Australian Atomic Research Establishment, Private Mail Bag, Sutherland, New South Wales, Australia.

BELGIUM

Centre d'Étude de l'Énergie Nucléaire. Available upon request to individuals and organizations, from the Centre d'Étude de l'Énergie Nucléaire (CEN), 31, Rue Belliard, Bruxelles, Belgium.

CANADA

Atomic Energy of Canada Limited. For sale by the Technical Information Officer, Atomic Energy of Canada Limited, Chalk River, Ontario, Canada. Copies are also deposited in libraries in the United Kingdom.

National Research Council of Canada. Available from the National Research Council of Canada, Ottawa 2, Ontario, Canada.

DENMARK

Atomic Energy Commission Research Establishment, Risø. Available on exchange from the Library, Danish Atomic Energy Commission, Risø, Roskilde, Denmark. Also for sale by Jul. Gjellerup, Booksellers, 87 Sölvgade, København K., Denmark.

Danatom. Available on loan from Research Establishment, Risø, Roskilde, Denmark. Copies are available from Danatom, Aurehøjvej 2, Hellerup, Denmark.

FRANCE

Commissariat à l'Énergie Atomique. Inquiries for reports numbered 1-2199 should be addressed to Commissariat à l'Énergie Atomique, Service Central de Documentation, Centre d'Études Nucléaires de Saclay, Boite Postale No. 2, Gif-sur-Yvette (S. et O.), France. Reports numbered 2200 and above are available from La Documentation Francaise, 16 Rue Lord-Byron, Paris VIII, France.

Service Central de Protection contre les Rayonnements Ionisants. Copies are available from Ministère de la Santé Publique, Service Central de Protection contre les Rayonnements Ionisants, B. P. n° 35—LE VESINET (S. et O.), France.

GERMANY

Deutsches Elektronen-Synchrotron DESY. Copies are available from Deutsches Elektronen-Synchrotron Desy, Dokumentation, 2000 Hamburg-Gr. Flottbek 1, Notkestieg 1, Germany.

Kernforschungsanlage. Copies may be ordered from Zentralbibliothek der Kernforschungsanlage Jülich, Jülich, Bundesrepublik Deutschland.

Hahn-Meitner-Institute für Kernforschung. Available without charge from Hahn-Meitner-Institute für Kernforschung Berlin, Bibliothek, Glienicker Strasse 100, 1 Berlin 39, Germany. Copies are deposited in many national nuclear centers in the world.

Johann-Wolfgang-Goethe Universität, Frankfurt Am Main, Institut für Kernphysik, (IKF). Copies are available from Gmelin Institut, 40-42 Varrentrappstrasse, Frankfurt (Main), West Germany.

ISRAEL

Israel Atomic Energy Commission. Available without charge from Ministry of Defence/Atomic Energy Com-

mission, Soreq Research Establishment, Yavne, Israel. Copies are deposited in libraries in Israel and in other countries.

ITALY

Centro Informazioni Studi Esperienze (CISE). For sale at CISE Press Office, Casella Postale 3986, Milano, Italy. Copies are deposited in libraries in Italy.

Comitato Nazionale per l'Energia Nucleare. Copies are available from Comitato Nazionale per l'Energia Nucleare, Divisione Affari Internazionali e Studi Economici, Ufficio Pubblicazioni, Via Belisario, 15, Roma, Italy.

JAPAN

Japan Atomic Energy Research Institute (JAERI). Available from the Staff Supply Cooperative of Japan Atomic Energy Research Institute (JAERI), 1-1 Tamura-Cho, Shiba, Minato-Ku, Tokyo, Japan. Copies are deposited in depositories in Tokyo, Nagoya, and Osaka.

Nagoya University. Copies are available from Research Information Center, Institute of Plasma Physics, Nagoya University, Nagoya, Japan.

University of Tokyo. Available free of charge from Institute for Nuclear Study, University of Tokyo, Tanashi-Machi, Kitatama-gun, Tokyo, Japan.

NETHERLANDS

Reactor Centrum Nederland. For sale by Reactor Centrum Nederland, 112 Scheveningseweg, 's-Gravenhage, The Netherlands. Copies are deposited in university libraries in Holland and in many national nuclear centers in the world.

NEW ZEALAND

Institute of Nuclear Sciences. Copies are available from Librarian, Institute of Nuclear Sciences, D.S.I.R., Private Bag, Lower Hutt, New Zealand. Copies are deposited in other countries.

NORWAY

Forsvarets Forskningsinstitutt. Copies available from Norwegian Defence Research Establishment, Library, P. O. Box 25, Kjeller, Norway.

Institutt for Atomenergi. "KR" reports are available on an exchange basis from the Library, Institutt for Atomenergi, Box 40, Kjeller, Norway. Other series are not generally available to the public.

Norwegian Reactor School. Copies are available from The Library, Institutt for Atomenergi, P. O. Box 40, Kjeller, Norway.

PAKISTAN

Atomic Energy Center. Copies are available from Atomic Energy Center, P. O. Box 658, Lahore, (West Pakistan).

POLAND

Reports of the Polish nuclear institutes are published by the Nuclear Energy Information Center of the Government Commissioner for Use of Nuclear Energy. Copies are available from Ośrodek Informacji o Energii Jądrowej, Warszawa, PKiN, Poland.

SPAIN

Junta de Energia Nuclear. "JEN" reports are available without charge from Servicio de Documentation, Junta de Energia Nuclear, Ciudad Universitaria, Madrid (3), Spain.

SWEDEN

Aktiebolaget Atomenergi. "AE" reports are for sale from Aktiebolaget Atomenergi, Library Section, Box 43041, Stockholm 43, Sweden. Bibliographies and literature surveys of the VDDIT- series may be obtained from Aktiebolaget Atomenergi, Information Office, Scientific and Technical Information, Box 43041, Stockholm 43, Sweden. Other series are not generally available to the public. Organizations in the atomic energy field may obtain copies from Aktiebolaget Atomenergi. Microcopy of AE reports is available from the International Documentation Centre, Tumba, Sweden.

SWITZERLAND

CERN European Organization for Nuclear Research. Available without charge from CERN European Organization for Nuclear Research, Geneva 23, Switzerland. Copies are deposited in libraries in 13 countries.

Eidgenössisches Institut für Reaktorforschung. "EIR" reports are available from Eidgenössiches Institut für Reaktorforschung, c/o Bibliothek, Würenlingen/Ag, Switzerland.

TURKEY

Turkish Atomic Energy Commission. Copies are available free of charge from T.A.E.C., Çekmece Nuclear Research Center, P. O. Box 1, Airport, Istanbul, Turkey.

UNITED KINGDOM

United Kingdom Atomic Energy Authority. Some reports are for sale in the United States by the British Information Service (BIS), 845 Third Avenue, New York, N. Y. 10022. United Kingdom reports generally may be purchased from Her Majesty's Stationery Office, London. Copies not for sale by Her Majesty's Stationery Office may be purchased in microcopy form from Micro Methods Limited, East Ardsley, Wakefield, Yorks, England. Report copies are deposited in a large number of libraries in England.

Conferences

Published conference proceedings as well as individual unpublished papers from conferences are included in this index. A CONF number is assigned to the conference if published proceedings are received and also if only a single paper is received. The base number used is year-month-sequence. Thus, the number CONF-650101 would indicate that the conference was held in 1965, in January, and that this was the first January 1965 conference so received. This number would be assigned to complete published proceedings, or if individual papers are received, the base number would be extended to include a paper number, i.e., CONF-650101-1. As additional papers are received, they will be assigned consecutive numbers in the series, CONF-650101-1, 2, 3, 4, etc. This numbering system ensures that all papers received from a conference will be associated with that conference in this index.

If published proceedings are received after the receipt of individual papers, the complete proceedings will be abstracted and the abstract number will appear in this index with the base CONF number.

Abbreviations Used in Availability Column

AECL	For sale by Atomic Energy of Canada Ltd., Chalk River, Ontario, Canada.
BIS	For sale by British Information Service, 845 Third Avenue, New York, N. Y. 10022
CFSTI	For sale by the Clearinghouse for Federal Scientific and Technical Information, U. S. Department of Commerce, Springfield, Virginia 22151. The symbol "cy" indicates that the format of the item sold may be either a printed document or a photographic reproduction (two-thirds of original size) depending upon the availability of printed stock. The indicated price is for either format. The symbol "mn" is used to indicate

that copy is available in the form of micronegatives (microfiche). The number preceding the "mn" symbol indicates the number of micronegatives in the set. Micronegatives are available at the following prices: One micronegative, $0.50; each additional micronegative of the set, $0.25. For additional micronegative copies of the same report requested at the time of the original order, $0.25 per micronegative. Prices are reduced on micronegatives if subscription distribution is purchased.

Dep. AEC reports: Full-size copy is on deposit in the depository libraries both inside and outside the United States. These reports are also for sale by Microcard Editions, Inc., Accounting and Shipping Department, West Salem, Wisconsin 54669.

Non-AEC reports: Full-size copy on deposit in the depository libraries in the United States only.

Dep.(mn) Same as for Dep., except copy is in micronegative (microfiche) form.

DSIR For sale by the National Lending Library for Science and Technology (D.S.I.R.), Boston Spa, Yorkshire, England.

DTI Extension Available from the U. S. Atomic Energy Commission, Division of Technical Information Extension, P. O. Box 62, Oak Ridge, Tennessee 37831.

EM Blueprints and Microcopy of AEC engineering drawings are available from Clearinghouse for Federal Scientific and Technical Information, U. S. Department of Commerce, Springfield, Virginia 22151. Current prices of the CAPE- packages may be obtained from this address. TID-4100, available from the Division of Technical Information Extension, P. O. Box 62, Oak Ridge, Tennessee 37831, contains information on all the CAPE- packages for sale.

Gmelin Available at a nominal charge and under the AED- number shown from Atomic Energy Documentation Center, Gmelin Institute, 40-42 Varrentrappstrasse, Frankfurt (Main), West Germany.

GPO For sale by the Superintendent of Documents, Government Printing Office, Washington, D. C. 20402.

HMSO Her Majesty's Stationery Office, London.

IAEA Available from the International Atomic Energy Agency, Vienna, Austria, and from its sales agencies in various countries throughout the world. A list of these agencies is found in each STI/DOC and STI/PUB publication.

JCL For sale by the Special Libraries Association Translation Center, John Crerar Library, 35 West 33rd Street, Chicago, Illinois 60616.

LC For sale by the Library of Congress, Photoduplication Service, Washington, D. C. 20540.

NAS National Academy of Sciences, National Research Council, Washington, D. C. 20418.

NRC For sale by the National Research Council of Canada, Ottawa, Ontario, Canada.

ORINS Available on interlibrary loan from the Library, Oak Ridge Institute of Nuclear Studies, Post Office Box 117, Oak Ridge, Tennessee 37831.

UKAEA, London Available from United Kingdom Atomic Energy Authority, 11 Charles II Street, London, S. W. 1.

UN United Nations Bookshop, United Nations Headquarters, New York, New York.

USGS Available free of charge from the U. S. Geological Survey, Washington, D. C. 20242.

[The symbols "ph," "mf," and "fs" are used to designate that copy is available only in photostat, microfilm, or facsimile form. The symbol "mn" is used to designate that copy is available in micronegative (microfiche) form. The symbol "cy" is used to designate full size or photographically enlarged copy (two-thirds of original size).]

Report No.	Abstract No.	Availability
NUMERICAL	**(Misc.)**	
65APE4	19-38802	See APED-4827
AAEC-Trans–	**(Australian)**	
18	19-38922	Dep. mn; CFSTI, $1.00 cy, $0.50 mn; JCL, $1.10 fs, $0.80 mf
ACF–		
6	19-38536	Dep.(mn); $1.00(cy), 1(mn) CFSTI
7	19-38537	Dep. mn; CFSTI, $1.00 cy, $0.50 mn
413-244	19-38536	See ACF-6
ACNP–	**(Misc.)**	
63592	19-40175	Dep.(mn); $1.00(cy), 1(mn) CFSTI
65004	19-38801	Dep. mn; CFSTI, $3.00 cy, $0.75 mn
AD–	**(Misc.)**	
425879	19-40278	CFSTI, $1.60 cy
425880	19-39149	CFSTI, $5.60 cy
426092	19-39430	CFSTI, $2.60 cy
607863	19-39054	CFSTI, $4.00 cy, $1.00 mn
608554	19-39431	CFSTI, $3.00 cy, $0.75 mn
612660	19-38358	$1.00(CFSTI)
ADR–	**(Non-AEC)**	
08-13-63.1	19-38538	
09-08a-63.1	19-39061	
AE–	**(Non-AEC)**	
185	19-39751	Dep.(mn)
AECL–	**(Canadian)**	
1939	19-39066	Trans. Eng. Inst. Can., 7: E-2(1964)
2177	19-39752	Dep.; AECL, $2.00 cy
2236	19-40180	See DL-56
2250(Pt.1)	19-39150	Dep.; AECL, $1.00 cy
AEET–	**(Indian)**	
209	19-39774	Dep. mn
AEET-HP–	**(Indian)**	
D-1	19-38968	
TH-15	19-38872	Dep. mn
AEEW-M–	**(British)**	
448	19-40147	Dep.; BIS, $0.90; HMSO, 4s. 6d.
507	19-39078	Dep.; BIS, $0.40; HMSO, 2s
513	19-39775	Dep.; BIS, $0.40; HMSO, 2s.
517	19-39776	Dep.; BIS, $0.40; HMSO, 2s. 0d.
518	19-39777	Dep.; BIS, $0.40; HMSO, 2s. 0d.
AERE-M–	**(British)**	
1389	19-39089	Dep. mn
1590	19-40256	Dep.; BIS, $0.70; HMSO, 3s. 6d.
AERE-R–	**(British)**	
4676	19-39005	Electron. Eng., 37: 456-9(1965)
AFCRL–	**(Non-AEC)**	
65-286	19-39225	
65-305	19-39226	
65-348	19-39952	
AFOSR–	**(Misc.)**	
65-0981	19-39151	
AFWL-TR–	**(Non-AEC)**	
65-40	19-39232	See FZK-227
65-49	19-39055	See GA-6266
AGN-TM–		
407	19-40176	Dep. mn; CFSTI, $3.00 cy, $1.00 mn
AHL–		
6949	19-38969	Dep. mn; CFSTI, $2.00 cy, $0.50 mn
6995	19-39124	Dep. mn; CFSTI, $2.00 cy, $0.50 mn
7008	19-38574	Dep. mn; CFSTI, $1.00 cy, $0.50 mn
7046	19-40111	Dep.(mn); $3.00(cy), 2(mn) CFSTI
7071	19-40113	Dep. mn; CFSTI, $3.00 cy, $0.75 mn
APDA–	**(Misc.)**	
168	19-38539	Dep. mn; CFSTI, $2.00 cy, $0.50 mn
APED–	**(Misc.)**	
4827	19-38802	
AROD–	**(Misc.)**	
223:60	19-39624	
3979:2	19-39261	
ATN–	**(Non-AEC)**	
63(9219)-1	19-39419	
BAW–	**(Misc.)**	
1280-26	19-38803	Dep. mn; CFSTI, $3.00 cy, $0.50 mn
BDX–		
613-72	19-40279	Dep. mn; CFSTI, $4.00 cy, $0.75 mn
613-73	19-40280	Dep. mn; CFSTI, $2.00 cy, $0.50 mn
BMI–	**(Misc.)**	
1723(Del.)	19-39091	Dep. mn; CFSTI, $1.00 cy, $0.50 mn
1729	19-39227	Dep. mn; CFSTI, $0.50 cy, $0.50 mn
1734	19-39228	Dep. mn; CFSTI, $1.25 cy, $0.50 mn
BMI-X–		
10132	19-39152	Dep. mn; CFSTI, $1.00 cy, $0.50 mn
10134	19-39229	Dep. mn; CFSTI, $1.00 cy, $0.50 mn
BNL–		
8185	19-38804	Dep.(mn); $2.00(cy), 1(mn) CFSTI
8483	19-38749	J. Nucl. Med., 6: 297-9(1965)
8511	19-39894	Rev. Mod. Phys., 37: 330-5(1965)
8555	19-39800	J. Inorg. Nucl. Chem., 27: 1447-50(1965)
8659	19-38709	J. Phys. Chem., 69: 2526-30(1965)
8791	19-38417	Radiation Botany, 5: 299-305(1965)
8866	19-39026	Rev. Sci. Instr., 36: 1174-5(1965)
8920	19-39773	Phys. Rev., 139: 981-90(1965)
8939	19-38868	Science, 149: 312-17(1965)
8974	19-39324	Rev. Sci. Instr., 36: 1339-40(1965)
8990	19-39262	Dep.(mn); $2.00(cy), 1(mn) CFSTI
9130	19-38933	Rev. Sci. Instr., 36: 1081-3(1965)
9200	19-38694	Dep. mn; CFSTI, $1.00 cy, $0.50 mn
9232	19-39450	Dep.(mn); $1.00(cy), 1(mn) CFSTI
9236	19-38970	Dep.(mn); $2.00(cy), 1(mn) CFSTI
9237	19-40258	Dep. mn; CFSTI, $2.00 cy, $0.50 mn
9279	19-40178	Dep.(mn); $1.00(cy), 1(mn) CFSTI
9331	19-38873	Dep. mn; CFSTI, $2.00 cy, $0.50 mn
9332	19-39230	Dep. mn; CFSTI, $1.00 cy, $0.50 mn
9343	19-38575	Dep. mn; CFSTI, $1.00 cy, $0.50 mn
9355	19-39778	Dep. mn; CFSTI, $1.00 cy, $0.50 mn
BNWL–		
33	19-39153	Dep. mn; CFSTI, $2.00 cy, $0.50 mn
63	19-40268	Dep. mn; CFSTI, $1.00 cy, $0.50 mn
91	19-39125	Dep. mn; CFSTI, $4.00 cy, $1.00 mn
104	19-40114	Dep. mn; CFSTI, $3.00 cy, $0.75 mn
111	19-40148	Dep. mn; CFSTI, $1.00 cy, $0.50 mn
113-5	19-40281	Dep. mn; CFSTI, $2.00 cy, $0.50 mn
BNWL-C–		
3	19-38805	Dep. mn; CFSTI, $1.00 cy, $0.50 mn
45	19-39069	Dep. mn; CFSTI, $1.00 cy, $0.50 mn
BNWL-SA–		
2	19-38822	Dep. mn; CFSTI, $1.00 cy, $0.50 mn
53	19-38874	Dep.(mn); $1.00(cy), 1(mn) CFSTI
54	19-39154	Dep. mn; CFSTI, $1.00 cy, $0.50 mn
61	19-40149	Dep.(mn); $2.00(cy), 1(mn) CFSTI
79	19-40061	Dep.(mn); $2.00(cy), 1(mn) CFSTI
90	19-39092	Dep.(mn); $1.00(cy), 1(mn) CFSTI
97	19-38823	Dep.(mn); $2.00(cy), 1(mn) CFSTI
135	19-38843	Dep.(mn); $1.00(cy), 1(mn) CFSTI
140	19-38844	Dep.(mn); $1.00(cy), 1(mn) CFSTI
141	19-39093	Dep.(mn); $1.00(cy), 1(mn) CFSTI
171	19-40282	Dep.(mn); $1.00(cy), 1(mn) CFSTI
226	19-38333	Dep. mn; CFSTI, $1.00 cy, $0.50 mn
230	19-38359	Dep.(mn); $1.00(cy), 1(mn) CFSTI
CALT–		

Report No.	Abstract No.	Availability
68-43	19-39451	Dep. mn; CFSTI, $2.00 cy, $0.50 mn
221-11	19-39155	Dep. mn; CFSTI, $3.00 cy, $0.75 mn
CEA-Note–	(French)	
397	19-38540	Dep.(mn)
CEA-R–	(French)	
2565	19-40150	Dep.(mn)
CEA-tr–	(French)	
A-1809	19-38761	Dep.(mn); $1.10(fn), $0.80(mf) JCL
CEND–	(Misc.)	
532	19-39156	Dep.(mn); $6.00(cy), 4(mn) CFSTI
CERN–	(European Organization for Nuclear Research)	
65-11	19-38971	Dep.(mn)
CLM-R–	(British)	
40	19-39953	Dep.; BIS, $0.90; HMSO, 4s. 6d.
CNLM–	(Misc.)	
6337	19-39157	Dep.(mn); $1.00(cy), 1(mn) CFSTI
CONF-117–	19-40168	(American Chemical Society 145th National Meeting, New York, Sept. 1963)
CONF-407–	19-39307	(Electro Chemical Society, Toronto, May 1964)
CONF-550–		(The International Conference on High-Energy Physics, Dubna, Aug. 5–15, 1964)
98	19-38978	See CERN-65-11(p.81-90)
CONF-651–		(9th International Conference on Low Temperature Physics, Columbus, Ohio, Aug. 31–Sept. 4, 1964)
89	19-39748	Gmelin, AED-CONF-64-140-113
CONF-654–		(American Nuclear Society Meeting, San Francisco, Nov. 30–Dec. 3, 1964) Proceedings
92	19-39110	Gmelin, AED-CONF-64-219-110
CONF-729–		(International Conference on Beryllium, Philadelphia, Oct. 1964)
24	19-39140	Gmelin, AED-CONF-64-247-28
CONF-758–		(American Physical Society Meeting, New York, Jan. 22–25, 1965)
26	19-39631	See IS-1111
32	19-39749	Gmelin, AED-CONF-65-003-73
CONF-796–	19-39263	(3rd Eastern Theoretical Physics Conference, College Park, Md., Oct. 30–31, 1964)
CONF-803–		(International Symposium on the Dosimetry of Irradiations from External Sources, Paris, Nov. 23–27, 1964)
6	19-38968	See AEET/HP/D-1
CONF-620402–	19-40117	(International Symposium on Water Problems in Nuclear Reactors, Rossendorf, Germany, Apr. 25–27, 1962) See ZFK-RN-17
CONF-621102–	19-40302	(France-Japan Conference on Nuclear Technology, Tokyo, Nov. 12–14, 1962)
CONF-631104–		(Meeting on the Utilization of Research Reactors, Sao Paulo, Brazil, Nov. 4–8, 1963)
2	19-40075	See IEA-84
3	19-39779	See IEA-86
CONF-640207–		(American Society for Testing Materials Conference, Philadelphia, Feb. 3–6, 1964)
1	19-40180	See DL-56
CONF-640410–	19-40221	(Advanced Nuclear Propulsion Symposium, Los Alamos, N. Mex., Apr. 1964)
CONF-640612–	19-38572	(15th Annual Mid-America Symposium on Spectroscopy, Chicago, June 2–5, 1964)
CONF-640622–	19-38328	(Symposia on Quantitative Biology, Cold Spring Harbor, N. Y., June 5–11, 1964)
CONF-640704–		(4th International Symposium on Rarefied Gasdynamics, Toronto, July 1964)
1	19-39262	See BNL-8990
CONF-640708–	19-40110	(International Conference on Physics of Non-Crystalline Solids, Delft, Netherlands, July 1964. (Complete proceedings as pub. lit.))
CONF-640806– (Pts.A,B,C,D)	19-38784	(Conference on the Role of Simulation in Space Technology, Blacksburg, Va., Aug. 17–21, 1964)
CONF-641004–		(American Physical Society, Chicago, Oct. 23–24, 1964)
13	19-39418	Gmelin, AED-CONF-64-220-37
CONF-641005–	19-39893	(Correlation of Particles Emitted in Nuclear Reactions, Gatlinburg, Tenn., Oct. 15–17, 1964)
CONF-641023–	19-38971	(Programming for Flying Spot Devices Conference, Bologna, Oct. 7–9, 1964) See CERN-65-11
CONF-650114–		(American Society for Testing Materials Meeting, Washington, D. C., Jan. 12, 1965)
1	19-38822	See BNWL-SA-2
CONF-650203–		(National AIME Meeting, Chicago, Feb. 14–18, 1965)
9	19-39123	Gmelin, AED-CONF-65-005-8
CONF-650302–		(IAEA Symposium on Personnel Dosimetry for Accidental High-Level Exposure to External and Internal Radiation, Vienna, Mar. 1965)
23	19-38873	See BNL-9331
CONF-650311–		(Conference on Analytical Chemistry and Applied Spectroscopy, Pittsburgh, Mar. 5, 1965)
2	19-38570	Gmelin, AED-CONF-65-025-10
4	19-38571	Gmelin, AED-CONF-65-025-6
CONF-650313–		(Symposium on Nuclear Medicine, Philadelphia, Mar. 19–20, 1965)
3	19-38878	See ORNL-P-1405
CONF-650401–		(American Chemical Society, Detroit, Apr. 4–9, 1965)
10	19-39068	Gmelin, AED-CONF-65-041-31
CONF-650405–		(International Conference on Modern Trends in Activation Analysis, College Station, Tex., Apr. 19–22, 1965)
6	19-38569	Gmelin, AED-CONF-65-040-15
12	19-38568	Gmelin, AED-CONF-65-040-7
CONF-650410–		(American Physical Society, Washington, D. C., Apr. 26–29, 1965)
3	19-39460	Dep.(mn); $2.00(cy), 1(mn) CFSTI
CONF-650411–		(Joint NASA–AEC Liquid Metals Corrosion Meeting, Gatlinburg, Tenn., Apr. 21–23, 1965)
5	19-39157	See CNLM-6337
CONF-650414–		(19th Metallographic Group Meeting, Oak Ridge, Tenn., Apr. 20–22, 1965)
4	19-39092	See BNWL-SA-90
CONF-650416–		(4th Symposium on Advanced Propulsion Concepts, Palo Alto, Calif., Apr. 26–28, 1965)
2	19-39442	ORINS
6	19-40059	ORINS
CONF-650419–		(Meeting of Refractory Composites Working Group, Atlanta, Apr. 12–14, 1965)
2	19-39093	See BNWL-SA-141

Report No.	Abstract No.	Availability
CONF-650425–		(Panel on the Uses of the Mössbauer Effect in Chemistry and Solid State Physics, Vienna, Apr. 26–30, 1965)
2	19-38576	Dep. nn; CFSTI, $2.00 cy, $0.50 mn
3	19-38577	Dep. nn; CFSTI, $1.00 cy, $0.50 mn
CONF-650428–		(Conference on Phenomena in the Neighborhood of the Critical Point, Washington, D. C., Apr. 5–8, 1965)
1	19-39685	See LA-DC-7086
CONF-650432–		(53rd General Conference of Pacific-Northwest Trade Assn., Portland, Oreg., Apr. 12, 1965)
2	19-38844	See BNWL-SA-140
3	19-38843	See BNWL-SA-135
CONF-650433–	19-39752	(AECL Symposium on the Generation of Intense Neutron Fluxes, Chalk River, Ont., Apr. 22–23, 1965) Proceedings. See AECL-2177
CONF-650438–		(Analytical Chemistry Conference, Albuquerque, N. Mex., Apr. 28–29, 1965)
1	19-38537	See ACF-7
CONF-650501–		(The Application of Computing Methods to Reactor Problems, Argonne, Ill., May 17–19, 1965)
14	19-40149	See BNWL-SA-61
CONF-650504–		(IAEA Symposium on Pulsed Neutron Methods, Karlsruhe, Germany, May 10–14, 1965)
43	19-39765	See INR-611/IX-A/R
CONF-650505–		(IFIP Congress 1965 Meeting, New York, May 24–29, 1965)
4	19-39080	See LA-DC-7192
5	19-39079	See LA-DC-7160
CONF-650509–		(IAEA Symposium on Nondestructive Testing in Nuclear Technology, Bucharest, May 17–21, 1965)
5	19-38823	See BNWL-SA-97
CONF-650510–		(Purdue Conference on Instrumentation for High Energy Physics, Lafayette, Indiana, May 11–15, 1965)
10	19-38970	See BNL-9236
11	19-38996	See PPAD-2137-548
12	19-39450	See BNL-9232
CONF-650512–	19-37944	(Symposium on Engineering Problems of Controlled Thermonuclear Research, Livermore, Calif., May 4–7, 1965)
2	19-39966	See ORNL-P-1245
4	19-39971	See ORNL-P-1438
CONF-650513–		(American Ceramic Society, Annual Meeting, Philadelphia, May 4, 1965)
8	19-39141	Gmelin, AED-CONF-65-092-1
CONF-650524–		(European Nuclear Energy Agency and Atomic Energy Commission Seminar, Upton, N. Y., May 3–7, 1965)
3	19-39778	See BNL-9355
CONF-650525–		(International Conference on the Internal Conversion Process, Nashville, Tenn., May 10–13, 1965)
5	19-39786	See ORNL-P-1419
CONF-650534–		(6th International Space Science Symposium, Buenos Aires, May 17, 1965)
1	19-39258	Dep. nn; CFSTI, $2.00 cy, $0.50 mn
CONF-650537–		(Conference on the Physical Metallurgy of Bainite and Martensite, Scarborough, England, May 10–12, 1965)
1	19-40283	See COO-1198-237
CONF-650542–		(Midwest Theoretical Conference, Columbus, May 14–15, 1965)
1	19-40076	See IS-1172
CONF-650548–		(National Society for Programmed Instruction, 3rd Annual Convention, Philadelphia, May 5–8, 1965)
1	19-40291	See SC-R-65-923
CONF-650602–		(American Nuclear Society 11th Annual Meeting, Gatlinburg, Tenn., June 20–24, 1965)
3	19-40219	See RL-SA-21
16	19-38911	See LA-DC-7004
29	19-40178	See BNL-9279
33	19-40115	Dep. nn; CFSTI, $1.00 cy, $0.50 mn
35	19-40118	See WAPD-T-1782
36	19-40159	See WAPD-T-1774
38	19-40061	See BNWL-SA-79
39	19-40191	See RL-SA-42
CONF-650610–		(American Institute of Aeronautics and Astronautics, Propulsion Joint Specialists Conference, Colorado Springs, Colo., June 14–18, 1965)
11	19-40253	ORINS
12	19-40252	ORINS
16	19-40254	ORINS
19	19-40241	See LA-DC-6845
CONF-650611–		(Symposium on Heat Flow Below 100°K and Its Technological Applications, Grenoble, France, June 9–11, 1965)
3	19-40244	See LA-DC-7170
CONF-650616–		(Health Physics Society, Annual Meeting, Los Angeles, June 14–17, 1965)
4	19-38874	See BNWL-SA-53
CONF-650624–		(2nd International Conference on Lung Tumors in Animals, Perugia, Italy, June 24–29, 1965)
2	19-38359	See BNWL-SA-230
CONF-650627–		(Conference on Electromagnetic Isotope Separators and Related Ion Accelerators, and Their Applications to Physics, Aarhus, Denmark, June 14–18, 1965)
1	19-39370	See ORNL-P-1336
CONF-650629–		(Conference on Small-Angle X-Ray Scattering, Syracuse, N. Y., June 24–26, 1965)
2	19-39230	See BNL-9332
CONF-650639–		(Analytical Chemistry Conference, Lewiston, N. Y., June 8–9, 1965)
1	19-38548	See UCRL-14166-T
CONF-650702–		(American Electroplater's Convention, New York, July 12–15, 1965)
2	19-40280	See BDX-613-73
CONF-650704–		(IAEA Symposium on Thermodynamics, Vienna, July 22–27, 1965)
3	19-39159	See LA-DC-6926
4	19-39162	See LA-DC-6957
5	19-38586	See UCRL-11957
6	19-38582	See ORNL-P-1428
7	19-39154	See BNWL-SA-54
8	19-39161	See LA-DC-6956
9	19-38752	See LA-DC-6947
10	19-39160	See LA-DC-6953
11	19-38575	See BNL-9343
12	19-39222	ORINS
14	19-38676	ORINS
17	19-38679	ORINS
18	19-38678	ORINS
19	19-38677	ORINS
20	19-38682	ORINS
21	19-39220	ORINS
23	19-38681	ORINS
24	19-38680	ORINS
27	19-39221	ORINS
28	19-39219	ORINS
30	19-38683	ORINS
31	19-38675	ORINS
CONF-650706–		(International Conference on the Study of Nuclear Structure with Neutrons, Antwerp, July 19–23, 1965)
3	19-39785	See ORNL-P-1356
6	19-38783	See ORNL-P-1345
8	19-39784	See ORNL-P-1352
18	19-38786	See LA-DC-7111

Report No.	Abstract No.	Availability
CONF-650707–		**(IEEE Annual Conference on Nuclear and Space Radiation Effects, Ann Arbor, Mich., July 12–15, 1965)**
2	19-39769	See SC-DC-65-1544
CONF-650711–		**(AIAA 2nd Annual Meeting and Technical Demonstration, San Francisco, July 26–29, 1965)**
2	19-40242	See LA-DC-7118
CONF-650802–		**(Cryogenic Engineering Conference, Houston, Tex., Aug. 23–25, 1965)**
2	19-40243	See LA-DC-7169
3	19-39686	See LA-DC-7164
4	19-38779	See LA-DC-7158
CONF-650803–		**(IAEA Symposium on Nuclear Materials Management, Vienna, Aug. 30–Sept. 3, 1965)**
3	19-38758	See Y-KA-7
4	19-39130	See RFP-507
5	19-38535	See RFP-508
6	19-38542	See LA-DC-6938
CONF-650804–		**(5th Rare Earth Research Conference, Ames, Iowa, Aug. 30–Sept. 1, 1965)**
4	19-38753	See LA-DC-7013
5	19-40081	See SC-DC-65-1500
CONF-650810–		**(Annual Conference on Applications of X-Ray Analysis, Denver, Aug. 25–27, 1965)**
1	19-38588	See UCRL-12496
CONF-650906–		**(2nd International Symposium on Inhaled Particles and Vapours, Cambridge, England, Sept. 27–30, 1965)**
3	19-38333	See BNWL-SA-226
CONF-650908–		**(International Conference on Thermionic Electrical Power Generation, London, Sept. 20–25, 1965)**
1	19-38780	See LA-DC-7206
2	19-39433	See LA-DC-6898
CONF-650910–		**(International Congress on Acoustics, Liege, Sept. 7–14, 1965)**
1	19-39268	See ORNL-P-1395
CONF-650911–		**(2nd Conference on Plasma Physics and Controlled Nuclear Fusion Research, Abingdon, Berks., England, Sept. 6–10, 1965)**
2	19-39970	See ORNL-P-1374
3	19-39969	See ORNL-P-1373
4	19-39968	See ORNL-P-1338
7	19-39973	See UCRL-14131
8	19-39967	See ORNL-P-1337
9	19-39956	See LA-DC-7043
CONF-650914–		**(1st International Conference on Thermal Analysis, Aberdeen, Scotland, Sept. 6–9, 1965)**
1	19-38913	See LA-DC-7071
CONF-651002–		**(Instrument Society of America, 20th Annual Conference, Los Angeles, Oct. 4–7, 1965)**
3	19-38916	See SC-DC-65-1589
5	19-38912	See LA-DC-7025
CONF-651003–		**(4th Symposium on Detonation, Silver Spring, Md., Oct. 13–15, 1965)**
2	19-40284	See LA-DC-6993
CONF-651004–		**(9th Conference on Analytical Chemistry in Nuclear Technology, Gatlinburg, Tenn., Oct. 12, 1965)**
1	19-38541	See K-L-6057
CONF-651005–		**(1st International Symposium on Water Desalination, Washington, D. C., Oct. 3–9, 1965)**
1	19-39117	See ORNL-P-1430
COO–		
7-354	19-39825	Nucl. Phys., 71: 529-45(1965)
720-047	19-39365	Dep.(mn); $3.00(cy), 2(mn) CFSTI
881-52	19-39532	Phys. Letters, 17: 340-2(1965)
921-16	19-39313	Dep.(mn); $1.00(cy), 1(mn) CFSTI
1029-5	19-38642	J. Phys. Chem., 69: 2510-15(1965)
1170-1	19-38334	Dep. mn; CFSTI, $1.00 cy, $0.50 mn
1195-35	19-39461	Dep. mn; CFSTI, $3.00 cy, $0.50 mn
1198-237	19-40283	Dep. mn; CFSTI, $2.00 cy, $0.50 mn
1198-250	19-38946	Rev. Sci. Instr., 36: 1316-18(1965)
1224-8	19-39231	Dep. mn; CFSTI, $3.00 cy, $0.75 mn
1226-8	19-38992	Dep.(mn); $2.00(cy), 1(mn) CFSTI
1233-20	19-39954	Dep.(mn); $1.00(cy), 1(mn) CFSTI
1371-14	19-39871	Phys. Letters, 18: 51-4(1965)
CR–	**(Misc.)**	
74	19-39420	See NP-15117
CU–	**(Misc.)**	
4-65-AMC-00099(E)Phy.	19-39369	See NP-15140
239	19-39462	See CU-1932-239
1932-239	19-39462	Dep.(mn); $2.00(cy), 1(mn) CFSTI
CVNA–	**(Misc.)**	
236	19-40179	Dep. mn; CFSTI, $2.00 cy, $0.50 mn
D–	**(Misc.)**	
2-90418-4	19-40062	See N64-29366
DL–	**(Canadian)**	
56	19-40180	Dep.; AECL, $0.50 cy
DUBNA REPORTS	**(Russian)**	
See JINR (Russian)		
EDR–	**(Misc.)**	
3969	19-39960	See N64-33202
EIR–	**(Swiss)**	
79	19-40151	Dep.(mn)
EOS–	**(Non-AEC)**	
4920-Q-2	19-38834	See N64-29495
ER–	**(Misc.)**	
14	19-39961	See NP-15112
7591(Add.)	19-39057	See NP-15022(Vol.II)(Add.)
EUR–	**(European Atomic Energy Community)**	
2233.f	19-40150	See CEA-R-2565
2413.e	19-39763	Dep.(mn)
2423.e	19-38687	Dep. mn
2429.i	19-40181	Dep.(mn)
EURAEC–		
1412	19-39127	See NCSC-2981-9
1416	19-38808	See NYO-3114-8
1417	19-38801	See ACNP-65004
1426	19-39229	See BMI-X-10134
1427	19-39152	See BMI-X-10132
1443	19-38806	See GEAP-4908
FTD-TT–	**(Non-AEC)**	
64-1001	19-39170	CFSTI
FZK–	**(Non-AEC)**	
227	19-39232	CFSTI
GA–	**(Misc.)**	
5163	19-39184	Carbon, 3: 17-29(1965)
5537	19-40182	Dep. mn; CFSTI, $6.00 cy, $1.50 mn
5924	19-40183	Dep.(mn); $1.00(cy), 1(mn) CFSTI
6087(Rev.)	19-39764	
6266	19-39055	CFSTI
6303	19-40165	Dep. mn; CFSTI, $3.00 cy, $0.75 mn
6406	19-40184	Dep. mn; CFSTI, $1.00 cy, $0.50 mn
6462	19-40152	Dep. mn; CFSTI, $3.00 cy, $0.50 mn
GAMD–	**(Misc.)**	
5434	19-40120	Dep. mn; CFSTI, $3.00 cy, $0.50 mn
6321	19-39233	Dep. mn; CFSTI, $1.00 cy, $0.50 mn
GEAP–	**(Misc.)**	
4474	19-38824	Dep. mn; CFSTI, $3.00 cy, $0.75 mn
4574	19-40121	Dep. mn; CFSTI, $5.00 cy, $1.25 mn

Report No.	Abstract No.	Availability
4597	19-39234	Dep. mn; CFSTI, $6.00 cy, $1.50 mn
4751	19-39158	Dep. mn; CFSTI, $3.00 cy, $0.75 mn
4760	19-39115	Dep. mn; CFSTI, $4.00 cy, $0.75 mn
4862	19-40122	Dep. mn; CFSTI, $3.00 cy, $0.75 mn
4908	19-38806	Dep. mn; CFSTI, $2.00 cy, $0.50 mn
GEMP–	**(Misc.)**	
190d	19-40246	See N64-29787
190e	19-40247	See N64-29788
346	19-39097	Dep. mn; CFSTI, $3.00 cy, $0.75 mn
GEST–	**(Misc.)**	
2046	19-39070	
HASL–		
160	19-38875	Dep. mn; CFSTI, $6.00 cy, $1.25 mn
HW–		
71813	19-40170	Dep. mn; CFSTI, $3.00 cy, $0.75 mn
81166	19-38750	Dep. mn; CFSTI, $1.00 cy, $0.50 mn
82103	19-38751	Dep. mn; CFSTI, $1.00 cy, $0.50 mn
HW-SA–		
3601	19-38890	Health Phys., 11: 945-8(1965)
3737	19-39238	Carbon, 3: 94-6(1965)
3752	19-39242	J. Appl. Phys., 36: 2317-18(1965)
3760	19-38555	Health Phys., 11: 965-6(1965)
IA–	**(Non-AEC)**	
1001	19-40153	Dep. mn
1014	19-38578	Dep. mn
1021	19-39265	Dep. mn
IAE–	**(Non-AEC)**	
663	19-39955	Dep. mn
787	19-40123	Dep. mn
789	19-40124	Dep. mn
IC–	**(Misc.)**	
65/14	19-39556	Proc. Roy. Soc. (London), Ser. A, 286: 412-14(1965)
65/62	19-39463	Dep. mn
IDO–		
12041	19-39259	Dep. mn; CFSTI, $2.00 cy, $0.50 mn
22047-USGS	19-40269	Dep. mn; CFSTI, $7.00 cy, $1.50 mn
IEA–	**(Brazilian)**	
84	19-40075	Dep. mn
86	19-39779	Dep. mn
INR–	**(Polish)**	
567/II/PS	19-39098	Dep.
596/PL	19-39780	Dep.
611/IX-A/R	19-39765	Dep.
IS–		
1077	19-39514	Nuovo Cimento (10), 38: 889-906(1965)
1111	19-39631	Dep. mn; CFSTI, $1.00 cy, $0.50 mn; Gmelin, AED-CONF-65-003-64
1172	19-40076	Dep. mn; CFSTI, $1.00 cy, $0.50 mn
IS-T–		
18	19-40077	Dep. mn; CFSTI, $4.00 cy, $0.75 mn
IS-Trans–		
17	19-39171	Dep. mn; CFSTI, $1.00 cy, $0.50 mn; JCL, $1.10 fs, $0.80 mf
ISS–	**(Italian)**	
84/49	19-39464	Dep. mn
JAERI–	**(Japanese)**	
1073	19-39781	Dep. mn
1075	19-40185	Dep.(mn)
1076	19-40186	Dep.(mn)
JINR–	**(Russian)**	
E-2125	19-39465	Dep. mn
E-2173	19-39466	Dep. mn
E-2194	19-39467	Dep. mn
P-2123	19-39468	Dep. mn
P-2131	19-39314	Dep. mn
P-2170	19-39469	Dep. mn
P-2171	19-39470	Dep. mn
P-2175	19-39471	Dep. mn
P-2177	19-39315	Dep. mn
P-2178	19-39472	Dep. mn
P-2185	19-39366	Dep. mn
P-2186	19-39473	Dep. mn
P-2190	19-39474	Dep. mn
P-2191	19-39782	Dep. mn
P-2195	19-39266	Dep. mn
P-2199	19-39316	Dep. mn
JPRS–	**(Non-AEC)**	
30799	19-39274	CFSTI, $3.00 cy
30993	19-38324	CFSTI, $2.00 cy
31048	19-39435	CFSTI, $1.00 cy
JüL–	**(German)**	
238-PC	19-38579	Dep.(mn)
249-RW	19-40270	Dep. mn
250-RW	19-38792	Dep. mn
251-RW	19-38793	Dep. mn
252-RW	19-38794	Dep. mn
253-RW	19-38795	Dep. mn
256-TP	19-39432	Dep.(mn)
K-L–		
6057	19-38541	Dep. mn; CFSTI, $1.00 cy, $0.50 mn
KAPL-M–		
6475	19-40171	Dep. mn; CFSTI, $1.00 cy, $0.50 mn
KFK–	**(German)**	
317	19-38695	Dep.(mn)
LA–		
3229	19-40221	Dep.(mn); $7.00(cy), 7(mn) CFSTI
3263	19-40240	Dep. mn; CFSTI, $1.00 cy, $0.50 mn
3303	19-38580	Dep. mn; CFSTI, $1.00 cy, $0.50 mn
3328	19-39260	Dep. mn; CFSTI, $2.00 cy, $0.50 mn
LA-DC–		
6521	19-39029	Rev. Sci. Instr., 36: 1209-13(1965)
6548	19-39367	Dep.(mn); $3.00(cy), 2(mn) CFSTI
6845	19-40241	Dep. mn; CFSTI, $1.00 cy, $0.50 mn
6873	19-39187	Carbon, 3: 96-7(1965)
6898	19-39433	Dep. mn; CFSTI, $1.00 cy, $0.50 mn
6915	19-40025	Phys. Fluids, 8: 1568-70(1965)
6926	19-39159	Dep. mn; CFSTI, $1.00 cy, $0.50 mn
6938	19-38542	Dep. mn; CFSTI, $2.00 cy, $0.50 mn
6947	19-38752	Dep. mn; CFSTI, $1.00 cy, $0.50 mn
6948	19-38942	Rev. Sci. Instr., 36: 1256-7(1965)
6953	19-39160	Dep. mn; CFSTI, $3.00 cy, $0.50 mn
6956	19-39161	Dep. mn; CFSTI, $1.00 cy, $0.50 mn
6957	19-39162	Dep. mn; CFSTI, $1.00 cy, $0.50 mn
6993	19-40284	Dep. mn; CFSTI, $1.00 cy, $0.50 mn
7004	19-38911	Dep. mn; CFSTI, $1.00 cy, $0.50 mn
7013	19-38753	Dep. mn; CFSTI, $1.00 cy, $0.50 mn
7025	19-38912	Dep. mn; CFSTI, $1.00 cy, $0.50 mn
7043	19-39956	Dep. mn; CFSTI, $2.00 cy, $0.50 mn
7053	19-39188	Carbon, 3: 97-8(1965)
7071	19-38913	Dep. mn; CFSTI, $1.00 cy, $0.50 mn
7084	19-39200	J. Chem. Phys., 43: 1736-8(1965)
7086	19-39585	Dep. mn; CFSTI, $1.00 cy, $0.50 mn
7090	19-39201	J. Chem. Phys., 43: 1739-42(1965)
7111	19-38786	Dep. mn; CFSTI, $1.00 cy, $0.50 mn
7118	19-40242	Dep. mn; CFSTI, $2.00 cy, $0.75 mn
7122	19-39889	Phys. Today, 18: 17-23(1965)
7144	19-38625	J. Am. Chem. Soc., 87: 3518(1965)
7158	19-38779	Dep. mn; CFSTI, $1.00 cy, $0.50 mn
7160	19-39079	Dep. mn; CFSTI, $1.00 cy, $0.50 mn
7164	19-39686	Dep. mn; CFSTI, $1.00 cy, $0.50 mn
7169	19-40243	Dep. mn; CFSTI, $2.00 cy, $0.50 mn
7170	19-40244	Dep. mn; CFSTI, $2.00 cy, $0.50 mn
7179	19-38691	J. Heterocycl. Chem., 2: 181-7(1965)
7192	19-39080	Dep. mn; CFSTI, $1.00 cy, $0.50 mn
7206	19-38780	Dep. mn; CFSTI, $1.00 cy, $0.50 mn

Report No.	Abstract No.	Availability
LA-tr-		
65-12	19-40299	Dep. mn; JCL, $1.60 fs, $0.80 mf
LAL-	**(French)**	
27	19-39475	Dep.(mn)
MATT-		
271	19-39344	Astrophys. J., 142: 369-82(1965)
311	19-40002	Phys. Fluids, 8: 1323-33(1965)
316	19-40007	Phys. Fluids, 8: 1368-74(1965)
320	19-39957	Dep. mn; CFSTI, $2.00 cy, $0.50 mn
327	19-39958	Dep. mn; CFSTI, $2.00 cy, $0.50 mn
MCW-		
1492	19-38543	Dep. mn; CFSTI, $1.00 cy, $0.50 mn
MIT-	**(Misc.)**	
2098-81	19-39902	Rev. Mod. Phys., 37: 369-71(1965)
2098-129	19-39655	Nuovo Cimento (10), 38: 1040-6(1965)
2098-139	19-39723	Phys. Rev., 139: A1441-51(1965)
2909-4	19-38696	Dep. mn; CFSTI, $7.77 cy, $2.00 mn
MLM-		
1244	19-39163	Dep. mn; CFSTI, $3.00 cy, $0.50 mn
1284	19-40285	Dep. mn; CFSTI, $1.00 cy, $0.50 mn
MND-	**(Misc.)**	
3169-68	19-39071	Dep. mn; CFSTI, $3.00 cy, $0.75 mn
3177	19-39431	See AD-608554
N-	**(Misc.)**	
64-22193	19-39164	CFSTI, $8.10 cy
64-22435	19-39959	
64-23519	19-40245	CFSTI, $11.00 cy
64-25903	19-38781	CFSTI, $10.10 cy
64-26371	19-39434	CFSTI, $16.50 cy
64-29366	19-40062	CFSTI, $4.60 cy
64-29495	19-38834	CFSTI, $6.60 cy
64-29558	19-39056	CFSTI, $6.60 cy
64-29787	19-40246	CFSTI, $6.60 cy
64-29788	19-40247	CFSTI, $7.60 cy
64-33202	19-39960	CFSTI, $2.00 cy, $0.50 mn
65-27619	19-38835	CFSTI, $5.00 cy, $1.00 mn
NAA-SR-		
9821	19-40125	Dep. mn; CFSTI, $1.25 cy, $0.50 mn
10462	19-39165	Dep. mn; CFSTI, $2.00 cy, $0.50 mn
10737	19-38754	Dep. mn; CFSTI, $2.00 cy, $0.50 mn
11200	19-40286	Dep.(mn); $6.00(cy), 5(mn) CFSTI
11309	19-39235	Dep. mn; CFSTI, $2.00 cy, $0.50 mn
11327	19-40126	Dep. mn; CFSTI, $2.00 cy, $0.50 mn
11401	19-38581	Dep. mn; CFSTI, $1.00 cy, $0.50 mn
NAA-SR-Memo-		
7753	19-40187	Dep. mn; CFSTI, $2.00 cy, $0.50 mn
11149	19-39166	Dep. mn; CFSTI, $1.00 cy, $0.50 mn
NASA-CR-	**(Misc.)**	
52957	19-40247	See N64-29788
52958	19-40246	See N64-29787
54026	19-38834	See N64-29495
54036	19-38781	See N64-25903
54045	19-39164	See N64-22193
54290(Rev.)	19-39764	See GA-6087(Rev.)
54415	19-38835	See N65-27619
56561	19-40245	See N64-23519
56779	19-39056	See N64-29558
58125	19-39434	See N64-26371
58295	19-40062	See N64-29366
58969	19-39960	See N64-33202
NASA-SP-	**(Misc.)**	
79	19-38836	$1.00(CFSTI)
NCSC-	**(Misc.)**	
2981-9	19-39127	Dep. mn; CFSTI, $2.00 cy, $0.50 mn
NEIC-RR-	**(Polish)**	
11	19-39331	Dep.
NEVIS-	**(Misc.)**	
133	19-39462	See CU-1932-239
NMI-	**(Misc.)**	
1267	19-39128	Dep. mn; CFSTI, $4.00 cy, $0.75 mn
NP-	**(AEC File No. for Non-AEC Reports)**	
14923	19-38473	Dep. mn
14926	19-38335	Dep. mn
14927	19-38876	Dep. mn
15022(Vol.II) (Add.)	19-39057	
15089	19-39368	Dep.(mn)
15111	19-40078	
15112	19-39961	Dep. mn
15114	19-40079	
15117	19-39420	
15125	19-40063	
15132	19-40064	
15133	19-38877	GPO, $0.30 cy
15140	19-39369	
15143	19-38993	Dep. mn
15145	19-38994	Dep. mn
15152	19-40065	CFSTI, $2.00 cy
15154	19-39421	
15155	19-40066	Dep. mn
15157	19-39267	Dep. mn
15161	19-40156	Dep. mn
15167	19-39962	Dep. mn
15176	19-38825	Dep. mn
15182	19-40080	
15187	19-39072	
15188	19-40287	Dep. mn
15197	19-39476	Dep. mn
15198	19-39963	Dep. mn
15201	19-39964	Dep. mn
15202	19-39477	
15203	19-39965	Dep. mn
15210	19-39478	Dep. mn
15216	19-39479	Dep. mn
15247	19-39480	Dep. mn
15248	19-39481	Dep. mn
15252	19-39482	Dep. mn
15259	19-38995	Dep. mn
15262	19-38743	Dep. mn
15263	19-39116	
NRL-	**(Misc.)**	
6248	19-39317	
NSP-	**(Non-AEC)**	
64-24	19-40245	See N64-23519
64-25	19-39056	See N64-29558
NUS-	**(Misc.)**	
180	19-40248	Dep. mn; CFSTI, $6.00 cy, $1.50 mn
NYO-		
98-5	19-40288	Dep. mn; CFSTI, $3.00 cy, $0.75 mn
NYO-		
2404-70	19-38807	Dep. mn; CFSTI, $2.00 cy, $0.50 mn
3114-8	19-38808	Dep. mn; CFSTI, $2.00 cy, $0.50 mn
3304-3	19-38809	Dep. mn; CFSTI, $4.00 cy, $0.75 mn
3399-02	19-39506	J. Math. Phys. (N. Y.), 6: 1329-31(1965)
3420-2	19-40188	Dep. mn; CFSTI, $3.00 cy, $0.75 mn
ORNL-		
3611	19-38755	Dep.(mn); $5.00(cy), 4(mn) CFSTI
ORNL-P-		
417	19-40008	Phys. Fluids, 8: 1375-84(1965)
461	19-38416	Radiation Botany, 5: 293-8(1965)
699	19-38628	J. Appl. Phys., 36: 2143-5(1965)
760	19-39241	J. Appl. Phys., 36: 2225-30(1965)
886	19-39915	Rev. Mod. Phys., 37: 437-41(1965)
908	19-38399	Mutation Res., 2: 149-55(1965)
929	19-38690	J. Chem. Phys., 43: 1688-91(1965)
1225	19-40099	Phys. Rev., 139: A1455-8(1965)
1245	19-39966	Dep.(mn); $2.00(cy), 1(mn) CFSTI

Report No.	Abstract No.	Availability
1282	19-40103	Phys. Rev. Letters, 15: 198-200(1965)
1336	19-39370	Dep. mn; CFSTI, $1.00 cy, $0.50 mn
1337	19-39967	Dep.(mn); $1.00(cy), 1(mn) CFSTI
1338	19-39968	Dep. mn; CFSTI, $1.00 cy, $0.50 mn
1345	19-39783	Dep.(mn); $1.00(cy), 1(mn) CFSTI
1352	19-39784	Dep.(mn); $1.00(cy), 1(mn) CFSTI
1356	19-39785	Dep.(mn); $1.00(cy), 1(mn) CFSTI
1359	19-38626	J. Am. Chem. Soc., 87: 3521-2(1965)
1373	19-39969	Dep. mn; CFSTI, $2.00 cy, $0.50 mn
1374	19-39970	Dep. mn; CFSTI, $2.00 cy, $0.50 mn
1405	19-38878	Dep.(mn); $1.00(cy), 1(mn) CFSTI
1419	19-39786	Dep.(mn); $1.00(cy), 1(mn) CFSTI
1428	19-38582	Dep. mn; CFSTI, $2.00 cy, $0.50 mn
1430	19-39117	Dep. mn; CFSTI, $2.00 cy, $0.50 mn
1438	19-39971	Dep.(mn); $1.00(cy), 1(mn) CFSTI
1441	19-39211	Phys. Letters, 18: 10-11(1965)
ORNL-TM–		
733(Rev.)	19-40189	Dep. mn; CFSTI, $1.00 cy, $0.50 mn
784	19-40190	Dep. mn; CFSTI, $3.00 cy, $0.75 mn
1116	19-39129	Dep. mn; CFSTI, $4.00 cy, $0.75 mn
1155	19-38832	Dep.(mn); $1.00(cy), 1(mn) CFSTI
1170	19-38782	Dep. mn; CFSTI, $2.00 cy, $0.50 mn
1171	19-39766	Dep.(mn); $5.00(cy), 3(mn) CFSTI
1175	19-40157	Dep. mn; CFSTI, $2.00 cy, $0.50 mn
1176	19-39081	Dep. mn; CFSTI, $2.00 cy, $0.50 mn
1181	19-40259	Dep.(mn); $2.00(cy), 1(mn) CFSTI
1192	19-39767	Dep. mn; CFSTI, $1.00 cy, $0.50 mn
ORNL-tr–		
535	19-40131	Dep. mn; JCL, $1.60 fs, $0.80 mf
590	19-40132	Dep. mn; JCL, $1.60 fs, $0.80 mf
633	19-39172	Dep. mn; JCL, $1.60 fs, $0.80 mf
634	19-39173	Dep. mn; JCL, $1.60 fs, $0.80 mf
635	19-39174	Dep. mn; JCL, $2.60 fs, $1.04 mf
638	19-39175	Dep. mn; JCL, $1.60 fs, $0.80 mf
674	19-38593	Dep. mn; JCL, $1.10 fs, $0.80 mf
698	19-38846	Dep. mn; JCL, $1.10 fs, $0.80 mf
PATENTS	**(British)**	**(3s. 6d. each, U. K. Patent Office)**
989,078	19-39044	
990,665	19-38905	
990,675	19-38951	
991,516	19-38830	
991,581	19-39112	
991,681	19-39142	
991,714	19-40119	
991,817	19-39143	
991,911	19-38815	
991,912	19-38816	
991,913	19-38817	
992,021	19-40166	
992,030	19-40136	
992,033	19-40137	
992,047	19-39144	
992,085	19-38684	
996,458	19-38573	
996,508	19-38785	
996,512	19-40138	
996,641	19-38739	
996,642	19-38740	
996,643	19-38741	
996,775	19-38797	
996,777	19-38952	
996,784	19-40139	
996,816	19-39113	
996,859	19-39114	
996,864	19-38906	
996,946	19-39145	
997,064	19-38798	
997,423	19-38776	
997,432	19-39443	
997,446	19-38685	
997,579	19-38953	
997,629	19-40173	
997,664	19-38818	
997,665	19-38819	
997,712	19-38777	
997,738	29-40255	
997,761	19-39223	

Report No.	Abstract No.	Availability
PATENTS	**(Canadian)**	
696,525	19-39146	
702,595	19-39147	
PATENTS	**(German)**	
1,188,085	19-40141	
1,188,225	19-38831	
1,189,536	19-38778	
1,190,117	19-40140	
1,192,329	19-38799	
1,192,331	19-39045	
1,193,617	19-39046	
1,194,074	19-40142	
1,194,994	19-38686	
1,194,995	19-38907	
PATENTS	**(U. S.)**	**($0.25 each, U. S. Patent Office)**
3,176,129	19-38954	
3,176,130	19-39047	
3,176,133	19-39048	
3,176,164	19-39444	
3,176,165	19-39445	
3,176,166	19-39446	
3,176,169	19-39447	
3,179,243	19-38908	
3,179,804	19-39330	
3,179,824	19-39448	
3,179,873	19-39449	
3,183,969	19-38820	
3,184,598	19-38871	
3,187,807	19-38821	
3,188,207	19-39224	
3,188,466	19-38955	
3,188,467	19-39049	
3,188,471	19-38956	
3,188,472	19-38957	
3,188,530	19-39750	
3,189,560	19-38742	
3,189,742	19-39050	
3,191,027	19-38958	
3,191,033	19-39051	
3,191,034	19-38959	
3,191,037	19-38909	
3,191,074	19-38960	
3,191,126	19-38961	
3,191,517	19-38833	
3,192,123	19-40143	
3,192,383	19-38962	
3,192,384	19-38963	
3,192,425	19-38964	
3,192,621	19-39148	
3,193,678	19-39257	
3,193,680	19-38965	
3,193,683	19-38966	
3,193,945	19-38800	
3,194,739	19-40060	
3,194,740	19-40167	
3,194,741	19-40144	
3,194,742	19-40145	
3,194,743	19-40146	
3,201,585	19-38967	
3,202,817	19-39312	
3,202,821	19-39052	
3,202,902	19-39053	
PHS–	**(Non-AEC)**	
999-RH-12	19-38744	Free(Public Health Service, Washington, D. C.)
PNE–		
102F	19-38787	Dep. mn; CFSTI, $4.00 cy, $0.75 mn
406	19-40289	Dep.(mn); $3.00(cy), 1(mn) CFSTI
407	19-40290	Dep.(mn); $3.00(cy), 2(mn) CFSTI
501F	19-38788	Dep. mn; CFSTI, $0.50 cy, $0.50 mn
601F	19-38789	Dep. mn; CFSTI, $3.00 cy, $0.75 mn
608F	19-38790	Dep. mn; CFSTI, $3.00 cy, $0.75 mn
PPAD–		
2137-548	19-38996	Dep.(mn); $1.00(cy), 1(mn) CFSTI

Report No.	Abstract No.	Availability
R–	**(Misc.)**	
377	19-40065	See NP-15152
501	19-39462	See CU-1932-239
RAI–	**(Misc.)**	
350	19-40271	Dep. mn; CFSTI, $2.00 cy, $0.50 mn
RFP–		
488	19-38756	Dep. mn; CFSTI, $3.00 cy, $0.75 mn
507	19-39130	Dep.(mn); $3.00(cy), 2(mn) CFSTI
508	19-38535	Dep. mn; CFSTI, $2.00 cy, $0.50 mn
552	19-38546	Dep. mn; CFSTI, $1.00 cy, $0.50 mn
566	19-38879	Dep. mn; CFSTI, $1.00 cy, $0.50 mn
572	19-38839	Dep. mn; CFSTI, $1.00 cy, $0.50 mn
616	19-39167	Dep. mn; CFSTI, $1.00 cy, $0.50 mn
RL-SA–		
21	19-40219	Dep. mn; CFSTI, $1.00 cy, $0.50 mn
31	19-38810	Dep. mn; CFSTI, $3.00 cy, $0.75 mn
42	19-40191	Dep. mn; CFSTI, $1.00 cy, $0.50 mn
RLO–		
1921-1	19-39410	Phys. Rev., 139: A1926-9(1965)
RME–		
4584	19-38845	Dep. mn; CFSTI, $3.00 cy, $0.75 mn
RPI–	**(Misc.)**	
328-21	19-39768	Dep. mn; CFSTI, $1.00 cy, $0.50 mn
SAN–		
409-24	19-38811	Dep. mn; CFSTI, $1.00 cy, $0.50 mn
SC-DC–		
65-1332	19-38914	Dep.(mn); $3.00(cy), 2(mn) CFSTI
65-1419	19-38915	Dep. mn; CFSTI, $1.00 cy, $0.50 mn
65-1480	19-38583	Dep. mn; CFSTI, $2.00 cy, $0.50 mn
65-1500	19-40081	Dep.(mn); $1.00(cy), 1(mn) CFSTI
65-1520	19-39118	Dep. mn; CFSTI, $2.00 cy, $0.50 mn
65-1544	19-39769	Dep.(mn); $1.00(cy), 1(mn) CFSTI
65-1589	19-38916	Dep. mn; CFSTI, $1.00 cy, $0.50 mn
SC-R–		
65-904	19-38864	Dep. mn; CFSTI, $3.00 cy, $0.75 mn
65-923	19-40291	Dep. mn; CFSTI, $1.00 cy, $0.50 mn
SC-RR–		
65-219	19-38584	Dep. mn; CFSTI, $3.00 cy, $0.75 mn
SC-TM–		
64-1677	19-38585	Dep. mn; CFSTI, $2.00 cy, $0.50 mn
202-56-51	19-40292	Dep. mn; CFSTI, $1.00 cy, $0.50 mn
SCL-DC–		
65-86	19-40293	Dep. mn; CFSTI, $3.00 cy, $0.75 mn
SGAE-CH–	**(Austrian)**	
16/1965	19-39100	Dep.(mn)
17/1965	19-38757	Dep.(mn)
SGAE-PH–	**(Austrian)**	
16/1965	19-39025	Rev. Sci. Instr., 36: 1167-9(1965)
19/1965	19-39787	Dep.(mn)
20/1965	19-39483	Dep.(mn)
SM–	**(Misc.)**	
66/65	19-39162	See LA-DC-6957
66/73	19-39161	See LA-DC-6956
67/33	19-38542	See LA-DC-6938
46335	19-40064	See NP-15132
SU-IPR–		
17	19-39972	Dep. mn; CFSTI, $2.00 cy, $0.50 mn
SU-SEL–	**(Misc.)**	
64-133	19-39269	Dep.(mn); $5.00(cy), 3(mn) CFSTI
TEI–		
857	19-38791	Dep. mn; CFSTI, $4.00 cy, $1.00 mn
TID–		
3315	19-39101	Dep. mn; CFSTI, $5.00 cy, $1.00 mn
3730	19-40294	Free(DTI Extension)
4025(Rev.1)(Pt.1) (Suppl.4)	19-40295	Dep. mn; CFSTI, $7.00 cy, $1.50 mn
8200(12th Rev.)	19-40116	Dep. mn; CFSTI, $1.00 cy, $0.50 mn
20471	19-38329	Dep. mn; CFSTI, $2.00 cy, $0.50 mn
21106	19-38336	Dep.(mn); $2.00(cy), 1(mn) CFSTI
21475	19-38547	Dep. mn; $3.00 cy, $0.75 mn
21508	19-39832	Nucl. Phys., 71: 641-61(1965)
21637	19-38773	Rev. Sci. Instr., 36: 1250-1(1965)
21695	19-38360	Dep.(mn); $1.00(cy), 1(mn) CFSTI
21710(Rev.)	19-39062	Dep. mn; CFSTI, $4.00 cy, $0.75 mn
21729	19-38646	J. Phys. Chem., 69: 2782-3(1965)
21730	19-40088	J. Chem. Phys., 43: 1675-9(1965)
21731	19-40087	J. Chem. Phys., 43: 1662-75(1965)
21732	19-39817	Nucl. Phys., 71: 433-40(1965)
21856	19-40296	Dep.(mn); $1.00(cy), 1(mn) CFSTI
21894	19-39270	Dep.(mn); $7.36(cy), 7(mn) CFSTI
21895	19-39422	Dep.(mn); $1.00(cy), 1(mn) CFSTI
21951	19-38361	Dep. mn; CFSTI, $7.00 cy, $1.75 mn
21965	19-39032	Rev. Sci. Instr., 36: 1344-6(1965)
22003	19-40192	Dep.(mn); $2.00(cy), 1(mn) CFSTI
22014	19-40249	Dep. mn; CFSTI, $1.00 cy, $0.50 mn
22015	19-39168	Dep. mn; CFSTI, $1.00 cy, $0.50 mn
22019	19-38920	Dep. mn; CFSTI, $3.00 cy, $0.75 mn
22032	19-39082	Dep. mn; CFSTI, $5.00 cy, $1.00 mn
22038	19-39484	Dep.(mn); $1.00(cy), 1(mn) CFSTI
22044	19-39371	Dep.(mn); $6.00(cy), 4(mn) CFSTI
22078	19-38330	Dep.(mn); $2.00(cy), 1(mn) CFSTI
TR–	**(Misc.)**	
17	19-39267	See NP-15157
1185	19-40278	See AD-425879
TRG-Report–	**(British)**	
921	19-40193	Dep.; $0.60(BIS); 3s. (HMSO)
TT–	**(Canadian)**	
65-31343	19-39274	See JPRS-30799
65-31491	19-38324	See JPRS-30993
65-31546	19-39435	See JPRS-31048
UCRL–		
7753	19-40297	Dep.(mn); $1.00(cy), 1(mn) CFSTI
8030(Pt.I) (Mar. '65, ed.)	19-39485	Dep. mn; CFSTI, $2.00 cy, $0.50 mn
11407(Rev.1)	19-40021	Phys. Fluids, 8: 1520-30(1965)
11623	19-38921	Dep. mn; CFSTI, $4.00 cy, $1.00 mn
11814	19-39879	Phys. Rev., 139: A1374-91(1965)
11837	19-39818	Nucl. Phys., 71: 441-8(1965)
11951	19-38812	Dep. mn; CFSTI, $2.00 cy, $0.50 mn
11957	19-38586	Dep.(mn); $1.00(cy), 1(mn) CFSTI
11986	19-38587	Dep. mn; CFSTI, $4.00 cy, $0.75 mn
12034	19-40017	Phys. Fluids, 8: 1472-88(1965)
12204	19-39271	Dep.(mn); $3.00(cy), 2(mn) CFSTI
12274	19-39384	J. Opt. Soc. Am., 55: 1029-30(1965)
12333	19-39018	Phys. Letters, 17: 279-80(1965)
12358	19-39827	Nucl. Phys., 71: 586-92(1965)
12359	19-39486	Dep. mn; CFSTI, $3.00 cy, $0.75 mn
12496	19-38588	Dep. mn; CFSTI, $1.00 cy, $0.50 mn
13100	19-39102	Dep. mn; CFSTI, $1.00 cy, $0.50 mn
14107	19-39881	Phys. Rev., 139: A1735-46(1965)
14131	19-39973	Dep.(mn); $1.00(cy), 1(mn) CFSTI
14141	19-40298	Dep. mn; CFSTI, $2.00 cy, $0.50 mn
14166-T	19-38548	Dep. mn; CFSTI, $1.00 cy, $0.50 mn
14186	19-38589	Dep. mn; CFSTI, $1.00 cy, $0.50 mn
14193	19-39487	Dep. mn; CFSTI, $2.00 cy, $0.50 mn
14194	19-39318	Dep. mn; CFSTI, $1.00 cy, $0.50 mn
14234	19-39398	Phys. Letters, 17: 263-4(1965)
16050	19-38590	Dep. mn; CFSTI, $6.00 cy, $1.25 mn
16058	19-39488	Dep.(mn); $2.00(cy), 1(mn) CFSTI
16090	19-39169	Dep. mn; CFSTI, $2.00 cy, $0.50 mn
16102	19-39846	Phys. Letters, 17: 283-6(1965)
16113	19-38591	Dep. mn; CFSTI, $3.00 cy, $0.75 mn
16149	19-38997	Dep. mn; CFSTI, $3.00 cy, $0.75 mn
16150	19-38592	Dep.(mn); $2.00(cy), 1(mn) CFSTI
16201	19-39542	Phys. Letters, 18: 76-80(1965)
UCRL-Trans–		

Report No.	Abstract No.	Availability
1226	19-38923	Dep. mn; JCL, $1.60 fs, $0.80 mf
UNC–	(Misc.)	
5123	19-40158	Dep. mn; CFSTI, $4.00 cy, $1.00 mn
USNRDL-TR–	(Misc.)	
851	19-38450	
WAED–	(Non-AEC)	
65.28E	19-38835	See N65-27619
WAL-TR–	(Non-AEC)	
834.12/2-3	19-39149	See AD-425880
WAPD-T–		
1774	19-40159	Dep. mn; CFSTI, $1.00 cy, $0.50 mn
1782	19-40118	Dep. mn; CFSTI, $1.00 cy, $0.50 mn
WAPD-TM–	(Misc.)	
479	19-40160	Dep. mn; CFSTI, $4.00 cy, $1.00 mn
WASH–		
1065	19-40194	Dep.; GPO, $0.20 cy
WCAP–	(Misc.)	
3269-5	19-40195	Dep. mn; CFSTI, $4.00 cy, $1.00 mn
3269-6	19-40196	Dep. mn; CFSTI, $4.00 cy, $0.75 mn
3269-36	19-39236	Dep. mn; CFSTI, $3.00 cy, $0.50 mn
3718	19-40197	Dep. mn; CFSTI, $3.00 cy, $0.75 mn
3721	19-40198	Dep. mn; CFSTI, $3.00 cy, $0.75 mn
Y–		
1484	19-38745	Dep. mn; CFSTI, $1.00 cy, $0.50 mn
Y-KA–		
7	19-38758	Dep. mn; CFSTI, $1.00 cy, $0.50 mn
ZFK-RN–	(German)	
17	19-40117	Dep.(mn)
ZFK-TPH–	(German)	
11	19-40161	Dep.(mn)

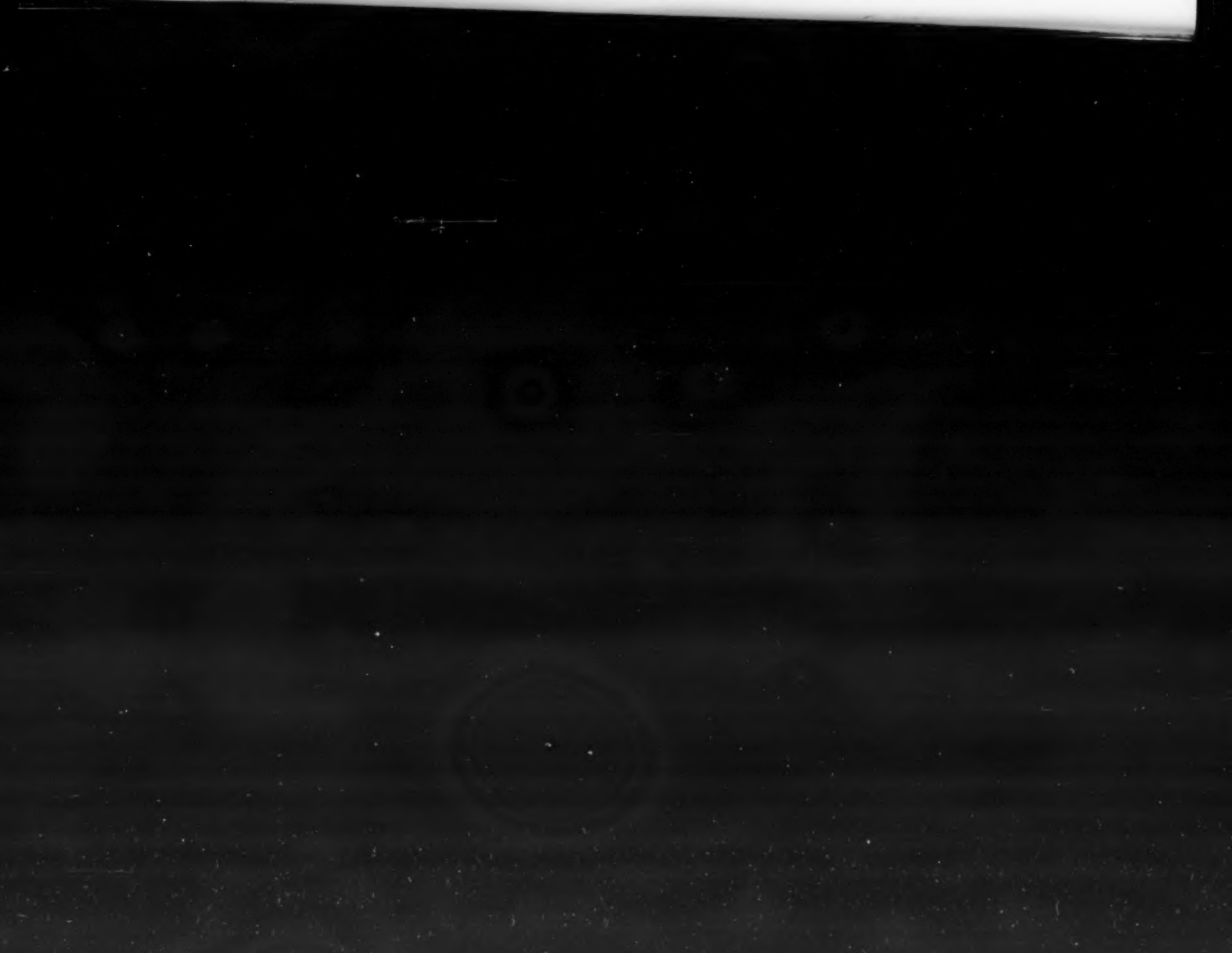

DEPOSITORIES OF USAEC REPORTS

In Countries Other than the U.S.

ARGENTINA
Buenos Aires, Comisión Nacional de Energía Atómica
AUSTRALIA
Canberra, Australian National Library
Sutherland, New South Wales, Australian Atomic Energy Commission
AUSTRIA
Vienna, Zentral Bibliothek der Physikalischen Institute der Universität
BELGIUM
Mol-Donk, Centre d'Etude de l'Energie Nucleaire
BOLIVIA
La Paz, Comisión Nacional de Energia Nuclear
BRAZIL
Rio de Janeiro, Instituto Brasileiro de Bibliografia e Documentacao
São Paulo, Instituto de Energia Atomica, Cidade Universitaria São Paulo
BURMA
Rangoon, Union of Burma Applied Research Institute, Atomic Energy Center Library
CANADA
Hamilton, McMaster University
Ottawa, National Research Council Library
Vancouver, University of British Columbia
CEYLON
Colombo, University of Ceylon
CHILE
Santiago, Instituto de Fisica y Matematicas, Universidad de Chile
CHINA
Hsinchu, Taiwan, Free China, National Tsing Hua University
COLOMBIA
Bogota, Instituto De Asuntos Nucleares
COSTA RICA
San Pedro, University of Costa Rica Library
DENMARK
Risö, Danish Atomic Energy Commission
ECUADOR
Quito, Escuela Politécnica Nacional
EL SALVADOR
San Salvador, Universidad de El Salvador, Biblioteca de Energia Nuclear
FINLAND
Helsinki, Teknillisen Korkeakoulun Kirjasto
FRANCE
Gif-sur-Yvette, Centre d'Etudes Nucléaires de Saclay
Paris, Académie des Sciences
GERMANY
Berlin, Hahn-Weitner-Institut für Kernforschun Berlin
Frankfurt/Main, Gmelin-Institut
Munich, Technische Hochschule, Bibliothek
GHANA
Accra, University College of Ghana
GREECE
Athens, Nuclear Research Center "Democritus"
GUATEMALA
Guatemala, Comisión Nacional de Energía Nuclear
HAITI
Port au Prince, University of Haiti
ICELAND
Reykjavik, University of Iceland, Atomic Energy Library
INDIA
Bombay, Department of Atomic Energy
INDONESIA
Bandung, Java, Bandung Institute of Technology
Djogjakarta, Java, Science Faculty, Gadjah Mada University
IRAN
Tehran, Tehran University Nuclear Centre
IRAQ
Baghdad, Iraqi Atomic Energy Commission
IRELAND
Dublin, University College
ISRAEL
Rehovoth, Israel Atomic Energy Commission
ITALY
Rome, Centro di Studi Nucleari della Casaccia
Rome, Comitato Nazionale per l'Energia Nucleare
JAPAN
Tokyo, National Diet Library
KOREA
Seoul, Office of Atomic Energy
LEBANON
Beirut, Lebanese National Council for Scientific Research
LUXEMBOURG
Luxembourg, Ministry of Transport and Electricity
MALAYSIA
Kuala Lumpur, University of Malaysia
MEXICO
Mexico, D.F., Comisión Nacional de Energía Nuclear
NETHERLANDS
The Hague, Reactor Centrum Nederland
NEW ZEALAND
Lower Hutt, Institute of Nuclear Sciences
NIGERIA
Ibadan, University of Ibadan
NORWAY
Lillestrom, Institutt för Atomenergi
PAKISTAN
Lahore, West Pakistan, Atomic Energy Centre
PERU
Lima, Junta de Control de Energia Atomica
PHILIPPINE REPUBLIC
Manila, Philippine Atomic Energy Commission
POLAND
Warsaw, Biura Pelnomocnika Rzadu do Spraw Wykorzystania Energii Jadrowej
PORTUGAL
Sacavem, Junta de Energía Nuclear
REPUBLIC OF SOUTH AFRICA
Pretoria, Atomic Energy Board Library
REPUBLIC OF THE CONGO
Leopoldville, Université Lovanium
SPAIN
Madrid, Junta de Energía Nuclear, Biblioteca Documentación y Publicaciones, Ciudad Universitaria
SWEDEN
Nyköping, Aktiebolaget Atomenergi
SWITZERLAND
Zürich, Eidgenössische Technische Hochschule, Bibliothek
THAILAND
Bangkok, Office of the Thai Atomic Energy Commission, Department of Science
TURKEY
Ankara, Turkish Atomic Energy Commission, Atomic Energy Library
UNITED ARAB REPUBLIC
Cairo, Atomic Energy Commission
UNITED KINGDOM
Belfast, City Library
Birmingham, Central Library
Boston Spa, National Lending Library for Science and Technology
Bristol, Central Library
Glasgow, Mitchell Library
Kingston upon Hull, Central Library
Leeds, Central Library
Liverpool, Central Library
London, Central Library, Acton
London, Science Museum Library, South Kensington
Manchester, Central Library
Newcastle upon Tyne, Central Library
Nottingham, Central Library
Sheffield, Central Library
URUGUAY
Montevideo, Comision Nacional de Energia Atomica
VENEZUELA
Caracas, Instituto Venezolano de Investigaciones Científicas
VIET-NAM
Saigon, Atomic Energy Office
YUGOSLAVIA
Belgrade, Federal Commission for Nuclear Energy

In International Agencies

AUSTRIA
Vienna, International Atomic Energy Agency
BELGIUM
Brussels, La Bibliotheque EURATOM
FRANCE
Paris, European Nuclear Energy Agency, O.E.C.D.
ITALY
Ispra, EURATOM Research Center
SWITZERLAND
Geneva, United Nations Library

UNITED STATES
ATOMIC ENERGY COMMISSION
P. O. BOX 62
OAK RIDGE, TENNESSEE 37831

OFFICIAL BUSINESS

POSTAGE AND FEES PAID
U. S. ATOMIC ENERGY COMMISSION

POSTAGE AND FEES PAID
U.S. GOVERNMENT PRINTING OFFICE

MIAMI UNIVERSITY LIBRARY 1
PERIODICAL RECORD
OXFORD, OHIO 45056

MIAMI UNIVERSITY LIBRARY